Higher-Order Corrections in Perturbative Quantum Field Theory – Concepts, Techniques, and Applications –

HABILITATIONSSCHRIFT

vorgelegt von
Dr. sc. nat. Tobias Huber

eingereicht bei der Naturwissenschaftlich-Technischen Fakultät
der Universität Siegen
Siegen 2016

Contents

Abstract 1

I. Quark Flavour Physics 17

Heavy-to-light currents at NNLO in SCET and semi-inclusive $\bar{B} \to X_s \ell^+ \ell^-$ decay 19

Master integrals for the two-loop penguin contribution in non-leptonic B-decays 53

Two-loop current-current operator contribution to the non-leptonic QCD penguin amplitude 95

Two-loop master integrals for non-leptonic heavy-to-heavy decays 103

Four-body contributions to $\bar{B} \to X_s \gamma$ at NLO 135

The $(Q_7, Q_{1,2})$ contribution to $\bar{B} \to X_s \gamma$ at $\mathcal{O}(\alpha_s^2)$ 171

Inclusive $\bar{B} \to X_s \ell^+ \ell^-$: complete angular analysis and a thorough study of collinear photons 209

II. Collider Physics 271

Calculation of the quark and gluon form factors to three loops in QCD 273

The quark and gluon form factors to three loops in QCD through to $\mathcal{O}(\epsilon^2)$ ... 337

III. Supersymmetric Gauge Theories 351

The three-loop form factor in $\mathcal{N} = 4$ super Yang-Mills 353

Systematics of the cusp anomalous dimension 389

The four-loop cusp anomalous dimension in $\mathcal{N} = 4$ super Yang-Mills and analytic integration techniques for Wilson line integrals 421

Acknowledgments 451

Abstract

The quest for the fundamental constituents of matter, as well as the interactions between them, has a long tradition in science in general, and in physics in particular. Already the ancient Greeks pursued the idea that macroscopic matter should be made up of tiny building blocks which cannot be subdivided any further. They referred to them as "atoms" (from "$\alpha\tau o\mu o\zeta$", impartible), a notion which is still present in our modern language. This concept was fuelled anew in the 17th, 18th, and 19th century by discoveries related to thermodynamics and the kinetic theory of gases, as well as to chemical reactions. To mention two examples, the ideal gas law (and special cases thereof such as the law of Boyle-Mariotte) can be explained by assuming numerous collisions of tiny particles with each other and with the walls of the container. Later, Dalton used the concept of atoms to explain why in chemical reactions elements react with each other always in proportions of small integer numbers, the so-called "law of multiple proportions", which became one of the foundations of stoichiometry.

Since the late 19th and early 20th century we know that atoms are not impartible, but have a substructure. The discovery of the electron, the phenomenon of radioactivity, Rutherford's scattering experiment and the resulting atomic model, and the formulation of relativity and quantum mechanics are among the early milestones towards the era of subatomic physics.

The search for the fundamental building blocks of matter is inherently related to the problem of resolving smaller and smaller length scales. Since the resolution power of any analysing apparatus is of the order of the deployed *wavelength* λ, the problem is equivalent to creating smaller and smaller wavelengths. For instance, an optical microscope, which uses visible light, can resolve structures down to $\sim$ 500nm. Decreasing the wavelength further leads to X-rays, which are used to analyse cristals with a lattice spacing of several angstroms ($1\mathring{A} = 0.1$nm). A further reduction of wavelengths is obtained by using matter waves. According to de Broglie, every particle of momentum p can be assigned a wavelength $\lambda = h/p$, where h is Planck's constant. Electron microscopes use this principle to reach resolutions which are several orders of magnitude better compared to ordinary light microscopes.

By further increasing the momentum (or, equivalently, the energy) of a particle, one can obtain a resolution of structures in the region of pico- or even femtometers. For this purpose, particle accelerators have been developed since the middle of the last century. Their main benefit is the possibility to study particle reactions in a laboratory environment. Elementary particles get accelerated either in a straight line (linear colliders) or in storage rings. Afterwards, the particles are brought to collision, either by letting particles from two oppositely moving beams collide, or by sending fast particles onto a target at rest (fixed target experiment). The particle energies achieved at an accelerator entail several important consequences. First, since the energies reach or, in many cases, exceed the rest energy, relativistic kinematics has to be applied according to Einstein's relation between a particle's energy E, its momentum p and its rest mass m,

$$E^2 = m^2c^4 + p^2c^2 \ , \tag{1}$$

where c denotes the speed of light. Second, particle number is not conserved in this type of reactions. Though particle reactions obey the fundamental conservation laws of nature

such as overall energy, momentum, or charge conservation, particles can be created and annihilated. One major consequence of this feature is the possibility to create heavy particles from energetic light ones, which becomes clear by looking at eq. (1). The produced heavy particles are usually not stable, but decay within a fraction of a second. The decay products leave tracks and are thereby identified and measured in a detector, which is built around the collision point. Third, the result of a *single* reaction cannot be predicted with absolute certainty. The reaction of two particles t_1 and t_2 or the decay of a heavy particle T can – according to quantum mechanics – result in different final states X_n and one can only give a *probability* p_n for each of the X_n to occur. These probabilities are determined at particle accelerators by measuring *cross sections* and *decay rates*, respectively. One therefore needs a multitude of collisions in order to determine each of the p_n accurately.

In this way, and by means of a close interplay between theory and experiment, many new particles have been discovered and symmetry principles established. To mention a few examples, in 1928 Dirac's relativistic quantum theory of an elementary spin-1/2 particle predicted the existence of anti-particles, whose first representative was discovered in 1932 in form of the positron, the electron's anti-particle. Later, in 1970, after the quarks had been accepted as physical degrees of freedom and the three species u, d, and s were known, the existence of a fourth quark (charm) was predicted by Glashow, Iliopoulos, and Maiani [1] in order to explain the tiny decay width in flavour-changing neutral current decays such as $K_L \to \mu^+ \mu^-$. The charm quark was discovered four years later in the J/ψ resonance independently by two experiments. Another example is related to discrete symmetries. The violation of the CP symmetry, the combined transformation of charge conjugation (C) and parity (P), was observed in 1964 by Fitch and Cronin in decays of neutral Kaons. In 1973, Kobayashi and Maskawa [2] suggested a third generation of fermions as one possibility to explain this phenomenon. The first members of the third generation, the τ-lepton and the bottom (b)-quark, were found in 1974 and 1977, respectively. Their partners, the τ-neutrino and the top (t)-quark, were discovered in 2000 and 1995, respectively. However, even before its discovery via direct production at the Tevatron, the effects of the top quark were already seen in B-meson oscillations at the ARGUS experiment at DESY Hamburg in 1987. From the value of the oscillation frequency one could already infer that the top quark is very heavy. We will come back to this point below. This list of examples of interplay between theory and experiment is by far not exhaustive and could be extended almost arbitrarily. One of the latest examples is the discovery of the Higgs boson at the LHC in 2012 [3, 4], which was already predicted in the 1960's by Brout, Englert [5], Higgs [6–8] and others [9, 10] to give masses to vector bosons in gauge theories via spontaneous symmetry breaking.

On the theoretical side, the concepts of special relativity and quantum mechanics were combined to formulate *quantum field theory* (QFT). Early breakthroughs in quantizing a relativistically covariant theory were achieved in the field of quantum electrodynamics (QED) by Feynman [11], Schwinger [12, 13], and Tomonaga [14]. Later on, the concept of non-abelian gauge theories was introduced by Yang and Mills [15], and their quantization was achieved by Faddeev and Popov [16], as well as by Becchi, Rouet, Stora, and Tyutin [17–19]. The ideas of the spontaneous breaking of global and local symmetries, initially put forward by Goldstone [20], Nambu [21], Jona-Lasinio [22, 23] and the aforementioned persons related to the Higgs mechanism, marked additional milestones in the formulation of modern particle theory. The *unification* of the electromagnetic and weak interaction by Glashow [24], Salam [25], and Weinberg [26], as well as the formulation of Quantum Chromodynamics (QCD) [27] and the phenomenon of asymptotic freedom [28, 29] paved the road towards the

Standard Model of Particle Physics, a theory that comprises all currently known elementary particles, as well as their interactions, with the exception of gravity. The Standard Model (SM) is a spontaneously broken, non-abelian local gauge theory. This kind of theory was shown to be *renormalisable* by 't Hooft and Veltman [30]. Together with the insights on the renormalisation group by Wilson [31, 32], this guarantees the predictive power of the theory also beyond the Born level. Besides, the development of renormalisation group techniques also triggered the development of *effective field theories* (EFTs), which are applicable to physical problems with widely separated scales $S_H \gg S_L$. The EFT serves to efficiently describe processes at scales of order S_L, and can be formulated in terms of the pertinent degrees of freedom. Among the most prominent representatives of EFTs are Chiral Perturbation Theory (ChPT) [33–37] (for reviews, see [38, 39]), Heavy-Quark Effective Theory [40–44] (for reviews, see [45, 46]), Soft-Collinear Effective Theory (SCET) [47–50] (for a review see [51]), and the Effective Weak Hamiltonian [52]. Recently, also the complete dimension-six Lagrangian for the SM was formulated in [53–61], (see also [62, 63]), building on earlier work from [64]. Many EFTs allow to formulate factorization theorems and serve as precision tools in contemporary particle physics phenomenology. Many excellent textbooks on QFT, the SM of particle physics, and EFTs can be found on the market (see, e.g. [65–72]).

The particle content of the SM consists of six *quarks* (u, d, c, s, t, b) and six *leptons* (ν_e, e, ν_μ, μ, ν_τ, τ), all of which are spin-1/2 fermions and constitute the matter content of the SM. They can be classified into three *families* or *generations*, where $\{u, d, \nu_e, e\}$, $\{c, s, \nu_\mu, \mu\}$, and $\{t, b, \nu_\tau, \tau\}$ make up the first, second, and third generation, respectively. Moreover, each fermion has a corresponding anti-particle. The interactions between them are based on a local $SU(3)_C \times SU(2)_L \times U(1)_Y$ gauge symmetry, which gets spontaneously broken via the Higgs mechanism to $SU(3)_C \times U(1)_{\rm em}$, where $U(1)_{\rm em}$ is the gauge symmetry of QED. The corresponding spin-1 *gauge bosons* (or force carriers) are the gluons g, associated with the colour group $SU(3)_C$ of the strong interaction, the $W^\pm$ and Z^0 bosons associated with the weak interaction, and the photon γ which mediates the electromagnetic force. The three generations of quarks and leptons differ only by their (highly hierarchical) masses, but have otherwise identical couplings to gauge bosons. Finally, the Higgs boson H is the only currently-known elementary spin-0 particle.

The dynamics of the SM particles is encoded in a Lagrangian density which can be subdivided into a gauge (or kinetic) part that contains all terms with field strength tensors and covariant derivatives and therefore the gauge fields, into a Higgs part which contains the Higgs potential, and into a Yukawa part which contains the couplings of scalars to fermions. After diagonalisation of the Yukawa matrices residual terms remain in the kinetic terms of the fermions which are non-diagonal in familiy space. This *mixing* of the different quark species ("flavours") is encoded in the unitary Cabibbo-Kobayashi-Maskawa (CKM) matrix [2, 73] [1]. The quark mixing pattern via the CKM matrix allows for flavour transitions via the weak interaction and entails a plethora of interesting applications, the most prominent ones being neutral meson mixing and the phenomenon of CP violation. The quark flavour sector of the SM has been subject to numerous experimental and theoretical studies in recent years. In particular, the experiments at the B-factories at SLAC in Stanford (California, USA) and at KEK in Tsukuba (Japan), but also at DAFNE in Frascati (Italy), the BEPC in Beijing (China), the Tevatron in Batavia (Illinois, USA) and recently at the LHC in Geneva (Switzerland), have performed precision tests of various flavour observables and confirm the

[1] Due to the non-zero neutrino masses, there occurs also mixing in the lepton sector, described by the PMNS matrix.

CKM mechanism as the correct description of quark flavour physics. Since the area of quark flavour physics is a very active field of reserach, about half of the papers accumulated in the present thesis are on this topic.

The SM is also extremely successful in describing all phenomena up to the highest accessible energies in the gauge and the Higgs sector. But despite the tremendous success of the SM, there is consensus that most likely it is not the ultimate theory of nature. A few prominent shortcomings and open questions related to the SM are:

- Why do the masses of the fermions span more than ten orders of magnitude? Why do we observe three generations?
- What is the origin of the large hierarchy between the electroweak and the Planck scale?
- Are there new particles, new interactions or other new degrees of freedom (e.g. Supersymmetry, axions, additional spatial dimensions)?
- What is Dark Matter made of? What is Dark Energy?
- Why is there a matter-antimatter asymmetry in our Universe? What is the mechanism of baryo- and leptogenesis? Are there additional sources of CP violation?
- Are neutrinos Dirac or Majorana particles, i.e. are they their own anti-particles?
- Do the strong and electroweak interaction get unified at some high scale?
- Can gravity be embedded into the theory?

Again, this list is not exhaustive. Owing to these open questions, one expects new effects (new particles and/or interations) at yet unexplored scales, so-called *Physics beyond the SM*, or *New Physics*. There are essentially two approaches to search for New Physics: *Direct* searches via the on-shell production of new particles at colliders, and *indirect* searches via virtual effects in low-energy processes, mostly in flavour physics, just like the aforementioned effects of the heavy top quark in B-meson oscillations. In both approaches, *precision* in theoretical predictions and in experimental measurements is an indispensable ingredient for testing the SM, and for the quest of finding effects beyond it. Since interacting quantum field theories lead to expressions that are non-linear in the fields, expressions for cross sections and decay rates cannot be written down in closed form, but they can be organised in a power series in the coupling constants, the *perturbative expansion*. Via the knowledge of higher orders in the perturbative expansion, the perturbative uncertainty can be reduced order by order. The computation of higher-order perturbative corrections is therefore of crucial relevance [74], and besides improved theory predictions it has also been responsible for tremendous progress in computational techniques. The present thesis accumulates papers that contain perturbative calculations from different fields of high-energy physics, such as quark flavour physics, collider physics, and supersymmetric gauge theories. Moreover, they address technical and conceptual issues, as well as results of phenomenological analyses.

Unfortunately, except for some tensions which are statistically not significant, there is currently no definite evidence for physics beyond the SM, neither in direct nor indirect searches. On the experimental side, current and future facilities such as the LHC, the planned Belle-II experiment, and experiments related to the charged lepton and the neutrino sector will try to shed light on the open questions related to particle physics, the fundamental constituents of matter and their interactions, and will also contribute to technological progress. On the theory side, the concepts of EFTs, precision calculations, and model building will be among the main pillars to make the most of the experimental data and to suggest new measurements and observables.

The present thesis consists of three parts, with a total of twelve scientific articles [75–86]. The first part contains work that is related to the quark flavour sector of the Standard Model [75–81]. The second part deals with higher-order corrections in perturbative QCD to two particular quantities which have numerous applications in collider physics, namely the quark and gluon form factors [82, 83]. Finally, the third part consists of calculations in supersymmetric gauge theories, in particular $\mathcal{N} = 4$ super Yang-Mills theory [84–86]. In the following I will summarize the papers in the different parts in turn and in the end comment on my personal contributions to the various articles.

The **first part** "Quark Flavour Physics" contains papers from two sub-areas of this field of research. Rare and radiative B-decays [75,79–81], as well as non-leptonic B-decays [76–78]. These topics also constitute two of the main pillars of the DFG Research Unit "Quark Flavour Physics and Effective Field Theories", where the author is principal investigator of the project on non-leptonic B-decays and participating researcher in the project on rare and radiative B-decays. The Research Unit was established in 2013 in Siegen and Dortmund, and recently got extended until the end of 2018.

The first part of the thesis starts with the paper "Heavy-to-light currents at NNLO in SCET and semi-inclusive $\bar{B} \to X_s \ell^+ \ell^-$ decay" [75], which already got completed before the start of the Research Unit. It contains the matching calculation from QCD onto SCET for the complete set of Dirac structures at next-to-next-to-leading order (NNLO), i.e. $\mathcal{O}(\alpha_s^2)$. In order to determine the matching coefficients at this order, a two-loop computation is required, which is carried out by means of Passarino-Veltman reduction of tensor integrals [87], followed by Laporta-reduction [88, 89] to so-called master integrals via integration-by-parts identities [90, 91], and finally the evaluation of the master integrals. These techniques have become standard in the field of loop computations and will be applied in all following papers which deal with the evaluation of loop integrals. The master integrals have been known analytically from earlier calculations such as the two-loop matching of the vector current [92–96], and NNLO corrections to non-leptonic B-decays [97–99]. The size of the NNLO correction to the matching coefficients depends on the momentum transfer q^2 of the heavy-to-light decay, and one can identify regions in q^2 where the NNLO correction is sizable (see Figure 1 of [75]). However, the perturbative corrections are always small enough such that this does not indicate a breakdown of perturbation theory. With the matching coefficients at NNLO at hand we discuss three physical applications: Heavy-to-light form factor ratios, exclusive radiative B-decays, and the semi-inclusive $\bar{B} \to X_s \ell^+ \ell^-$ decay. In the context of heavy-to-light form factor ratios we discuss relations between different QCD form factors $F_i^{B\to M}(E)$ (M denotes a light meson and E its energy), which contain short-distance coefficients that are expressible in terms of the heavy-to-light matching coefficients. For M being a pseudoscalar or vector meson, there are in total five independent short-distance coefficients (Eq. (54) of [75]). And in the physical form factor scheme, there are only three non-trivial ratios thereof (Eq. (58) of [75]), which we discuss in detail. In these ratios, the size of the NNLO corrections is moderate, and in general smaller than the next-to-leading order (NLO) terms (see Figures 2 – 4 of [75]). Moreover, their scale dependence decreases, as expected when adding another term in the perturbative expansion (see Figure 2 of [75]). The exclusive radiative B-decays then make use of the form factor ratios at maximum recoil. The inclusive decay $\bar{B} \to X_s \ell^+ \ell^-$ was measured by the B-factories [100–103]. In order to reduce background coming from $b \to c\, \ell^- \bar{\nu}_\ell \to s\, \ell^+ \ell^- \nu_\ell \bar{\nu}_\ell$, a cut on the invariant mass m_X of the X_s system is imposed. Babar chooses $m_X = 1.8$ GeV, whereas Belle takes $m_X = 2.0$ GeV. In our third application, we compute the zero-crossing q_0^2 of the forward-backward asymmetry in semi-inclusive

$\bar{B} \to X_s \ell^+ \ell^-$, i.e. in the presence of a cut on m_X. Our result $q_0^2 = 3.40^{+0.22}_{-0.25}$ GeV^2 for $m_X = 1.8$ GeV ($q_0^2 = 3.34^{+0.22}_{-0.25}$ GeV^2 for $m_X = 2.0$ GeV) is considerably smaller than in the exclusive $\bar{B} \to K^* \ell^+ \ell^-$ case [104,105], but in the same region as in the inclusive case [81,106].

The two following papers in the first part deal with the penguin amplitudes at two-loop order in the QCD factorisation approach [107–110] to non-leptonic decays of B-mesons. The QCD factorisation approach disentangles short and long distances (corresponding to perturbative and non-perturbative quantities, respectively) in the decay amplitude systematically, and the established factorisation formula is valid to all orders in α_s and to leading order in $\Lambda_{\rm QCD}/m_b$. The first work "Master integrals for the two-loop penguin contribution in non-leptonic B-decays" [76] contains the result of the most difficult part of the two-loop calculation, namely the analytic evaluation of the master integrals. This task is complicated due to the fact that it is a genuine two-loop, two-scale problem, the two scales being the momentum fraction of the quark in one of the final-state mesons, and the quark-mass ratio m_c^2/m_b^2. A common method to solve this kind of master integrals are differential equations in the kinematic invariants [111, 112]. This method got recently refined in the sense that if a particularly suitable basis of master integrals is chosen the dependence on the kinematic invariants in the differential equations is factorised from that on the number of space-time dimensions [113]. A basis that exhibits this property is referred to as *canonical basis*. In our work, we identify the canonical basis of master integrals for the two-loop penguin amplitudes, and subsequently give analytic results for all of them in terms of iterated integrals with rational weight functions. Our work is the first application of this method to the case of two different internal masses (m_c and m_b). There are multiple benefits of choosing a canonical basis. First, the system of differential equations disentangles order by order in the dimensional resularisation parameter ϵ. Second the solution can be written in terms of iterated integrals whose weight is uniform within a certain power in the ϵ-expansion. Third, if the basis of master integrals is chosen unhandily, one might have to include terms in individual integrals which are of higher weight than what can appear in the final expression of the QCD amplitude. These fake higher weights will cancel once the contributions of all master integrals are summed up since the expression for the QCD amplitude is independent of the basis that one chooses for the master integrals. If, one the other hand, a canonical basis of master integrals is chosen, fake higher weights are absent by construction at any stage of the calculation. Fourth, the expression of the QCD amplitude as a linear combination of pre-factors times master integrals looks much simpler in a canonical basis, especially the denominators of the pre-factors of the master integrals. Finally, and indeed most importantly, finding analytic results by means of the method of differential equations in a canonical basis catalyses the convolution with the light-cone distribution amplitude of the light meson, which in turn enables us to obtain the leading penguin amplitudes at two loops in QCD factorisation almost completely analytically. The computation and the results of these amplitudes is the subject of the next paper "Two-loop current-current operator contribution to the non-leptonic QCD penguin amplitude" [77]. The main motivation to calculate the penguin amplitudes at two-loop order are the direct CP asymmetries. They vanish at leading order (LO) since the amplitude is real, which is a consequence of the fact that in the QCD factorisation framework strong phases are generated perturbatively or via power corrections. Hence, our NNLO correction is only the first perturbative correction, so NNLO is in fact NLO for the direct CP asymmetries. In our work [77], we focus on the contribution from the current-current operators $Q_{1,2}$ from the effective weak Hamiltonian, since these insertions already render the bulk of the contribution at NLO, and, moreover,

only a subset of about two dozens of diagrams (out of a total of ~ 70) has to be evaluated. After the calculation of the bare two-loop amplitude, ultra-violet (UV) renormalisation and infra-red (IR) subtraction (via matching onto SCET) is carried out in order to cancel all poles in the dimensional regularisation parameter ϵ. With the NNLO contribution at hand, we study its impact on the leading penguin amplitudes a_4^p (with $p = u, c$) and provide a first estimate of NNLO CP asymmetries in penguin-dominated $b \to s$ transitions. One observes that the new correction is rather large, see eqs. (13), (14) and Figure 2 in [77]. However, this does not imply a breakdown of the perturbative expansion, as we will argue below. Next, we study the dependence of the amplitudes on the renormalisation scale μ, which is usually considered as a measure of the accuracy of the approximation at a given order in perturbation theory. This is shown in Figure 3 of [77]. One observes a considerable stabilization of the scale dependence for the real part, but less for the imaginary part. The reason for this feature is the fact that the imaginary part vanishes at LO. We also study ratios of penguin amplitudes over the sum of colour-allowed and colour-suppressed tree-amplitudes (see Figure 4 in [77]), as well as estimates of the direct CP asymmetries, including suitably chosen linear combinations of asymmetries (see Table 1 in [77]). Comparing the NLO and NNLO predictions of direct CP asymmetries, one observes that the large NNLO correction of the penguin amplitudes gets diluted in the physical observables, for several reasons. First, in most of the channels also the tree amplitudes enter. Second, there is the contribution from the power-suppressed but chirally enhanced scalar penguin amplitude $r_\chi^{M_2}\, a_6^p(M_1 M_2)$, which is small when meson M_2 is a vector meson, but larger than the leading-power amplitude for pseudoscalar M_2. It interferes constructively if M_1 is pseudoscalar, and destructively if M_1 is a vector meson. It follows from this brief discussion that the impact of the NNLO correction to a_4^p is always diluted in the full penguin amplitude. In the third column of Table 1 in [77] we give the predictions for the CP asymmetries once the power-corrections from weak annihilation is added on top. These power-corrections are parametrised in the annihilation model via a magnitude and a phase. They have a large impact on the central values, and give rise to sizable uncertainties, which, however, are partially tamed in the linear combinations $\delta(M_1 M_2)$ and $\Delta(M_1 M_2)$. This discussion clearly shows the need to better understand the power-suppressed terms in QCD factorisation.

The next paper in the first part, "Two-loop master integrals for non-leptonic heavy-to-heavy decays" [78], is the last one on non-leptonic B-decays. It deals with heavy-to-heavy decays like, for example, $B \to D\pi$. These decays are interesting on their own grounds, and address – at least indirectly – the aforementioned lack of understanding of power-corrections in QCD factorisation. In the QCD factorisation framework, the decay $B \to D\pi$ at leading power is very clean. There is neither a colour-suppressed tree amplitude nor penguin contributions, and spectator scattering and weak annihilation are power-suppressed [108]. One therefore only has the vertex kernels to the colour-allowed tree amplitude. Hence, a precise theory prediction of this single contribution, together with comparison to experimental data, might give a reliable estimate of the size of power corrections in QCD factorisation. We aim at computing the short-distance part of the $B \to D\pi$ amplitude to NNLO. The NNLO corrections may be significant in size since the contribution at NLO is colour suppressed and appears alongside small Wilson coefficients. The calculation again amounts to the evaluation of ~ 70 two-loop diagrams, whose reduction to master integrals is performed along the same lines as in previous works. The paper [78] then constitutes another non-trivial application for finding a canonical basis for two-loop master integrals in a genuine two-scale problem. The results are given as linear combinations of Goncharov polylogarithms. Again, the solu-

tion takes a convenient form for a subsequent convolution with the light meson's light-cone distribution amplitude in the QCD factorisation approach. Comparing the integrals in [78] to those in [76], one observes both, similarities and differences. Both are two-loop problems with the same two scales (momentum fraction u and quark-mass ratio z_c). The integrals in [78] are a bit less involved compared to those in [76], in a sense that the linear combinations that form a canonical master integral are shorter, the occurring weights are fewer, and the choice of kinematic invariants is less complicated. The main reason for this is that in [78] the external kinematics of the final state contains also the second internal mass, notably m_c. On the other hand, the only five-line integral in [76], a two-point function (M_{22}), is in fact a one-scale integral, whereas in [78] we encountered several five-line integrals with four external legs which are genuine two-scale functions. Moreover, most of the integrals in [78] are needed to order $\mathcal{O}(\epsilon^4)$, whereas in [76] all but two integrals were required only to order $\mathcal{O}(\epsilon^3)$. Putting the computation of master integrals in a canonical basis on more general grounds, it will be interesting to investigate how the canonical basis depends on the number of loops, legs, scales, space-time dimensions, and on the external kinematics. Every representative therefore sharpens our understanding of the patterns that such bases follow. We hope that our examples will contribute to the development of an algorithm for the automated construction of canonical bases.

The project of NNLO corrections to $B \to D\pi$ in QCD factorisation was done in collaboration with the Ph.D. student Susanne Kränkl, who did the calculation under my supervision. Every step was carried out and cross-checked by both of us. The master integrals already got published in [78]. The QCD amplitude, the phenomenological analysis of $B \to D\pi$ decays, and the interpretation of the results are in preparation.

The next two papers in the first part deal with the inclusive radiative decay $\bar{B} \to X_s\gamma$, which is still a paradigm for precision tests of the Standard Model in quark flavour physics. The first estimate to NNLO in QCD was given in 2006 [114], where certain contributions – which in part even count as NLO – were not included since they were assumed to be negligible. A major part of these unknown pieces are four-body contributions corresponding to the partonic process $b \to s\bar{q}q\gamma$ at NLO, which we address in the paper "Four-body contributions to $\bar{B} \to X_s\gamma$ at NLO" [79]. The smallness of the Wilson coefficients of penguin operators and CKM-suppression of current-current operators suggests that this contribution should be small. However, only an explicit calculation can turn this estimate into a firm statement. The calculation arises from tree and one-loop Feynman diagrams, but it involves the four-body phase-space integration in dimensional regularisation, which makes the calculation non-trivial owing to the appearance of higher transcendental functions such as hypergeometric functions. Moreover, the cancellation of poles in the dimensional regularisation parameter ϵ is only achieved after proper UV and IR renormalisation. The latter gives rise to logarithms $\ln(m_b/m_q)$ when turning the dimensional into a mass regulator. These logarithms stem from the phase space region of energetic collinear photon radiation off light quarks in the final state. They are of the same physical origin as the collinear logarithms $\ln(m_b/m_\ell)$ in inclusive $\bar{B} \to X_s\ell^+\ell^-$ [115], and are computed with the splitting function technique. We perform an exhaustive numerical analysis. We find a pronounced reduction of the scale uncertainty compared to the corresponding LO [116] contribution (Figure 7 in [79]). In addition, we study the dependence on the photon energy cut and the quark-mass ratio m_c^2/m_b^2 (Figure 8 in [79]). We find that the contribution of the four-body NLO correction to the total rate in the Standard Model is below the 1% level. This statement even holds true once we vary the input parameters such as the charm mass, the photon energy cut, the masses of the light

quarks, or the renormalisation and matching scales.

The second paper on $\bar{B} \to X_s\gamma$, "The $(Q_7, Q_{1,2})$ contribution to $\bar{B} \to X_s\gamma$ at $\mathcal{O}(\alpha_s^2)$" [80], addresses the interference of the magnetic dipole operator Q_7 with the current-current operators $Q_{1,2}$ at $\mathcal{O}(\alpha_s^2)$. This contribution was considered in [117] in the limit $m_c \gg m_b/2$ and then extrapolated to physical charm masses. In [80] we computed this interference for $m_c = 0$, and use both limits for an interpolation in m_c. The calculation amounts to the evaluation of more than 800 four-loop Feynman diagrams of which two-, three-, and four-particle cuts need to be taken. Besides the bare calculation at $\mathcal{O}(\alpha_s^2)$ we also provide all necessary counter-terms and a master formula (Eq. (2.10) of [80]) which shows how the renormalised matrix elements are constructed. Further, we investigate the impact of the interpolation in m_c (Figures 4 and 5 [80]). In the phenomenological study we also include all those contributions that have become available since 2006. Their sum amounts to a shift of +6.4%, and the updated prediction for the CP- and isospin-averaged branching ratio in the Standard Model reads $\mathcal{B}_{s\gamma}^{\rm SM} = (3.36 \pm 0.23) \times 10^{-4}$ for a photon energy cut of $E_\gamma > 1.6\,\text{GeV}$. It agrees very well with the current experimental world average $\mathcal{B}_{s\gamma}^{\rm exp} = (3.43 \pm 0.21 \pm 0.07) \times 10^{-4}$ and allows to put stringent constraints on many extensions of the Standard Model, e.g. on the mass of the charged Higgs boson in type-II two-Higgs doublet models [118].

The final paper of the first part, "Inclusive $\bar{B} \to X_s\ell^+\ell^-$: complete angular analysis and a thorough study of collinear photons" [81], deals with the rare inclusive decay $\bar{B} \to X_s\ell^+\ell^-$. We compute logarithmically enhanced electromagnetic corrections to the entire set of angular observables. The logarithmic enhancement stems from the region in phase space where an energetic photon is radiated collinearly off a final state lepton [115]. We observe that the structure of the double differential decay rate is modified in the presence of QED corrections. The simple second-order polynomial in the angular variable z (Eq. (1.4) in [81]) is replaced by a complicated functional dependence (Eq. (3.28) in [81]). We therefore propose a procedure how to project onto the individual observables, and in addition identify new observables which vanish if only QCD corrections are taken into account. We then give the Standard Model predictions of all (conventional and newly identified) observables for different bins in the lepton invariant-mass squared q^2, thereby taking all available NNLO QCD, NLO QED and power corrections into account. To supplement our analytic calculation we carry out a dedicated Monte Carlo study on the treatment of collinear photons. We investigate how the electromagnetic logarithms are treated correctly in the presence of angular and energy cuts. We find that our analytical predictions can be directly applied, with the exception of the electron channel at BaBar, where our numbers have to be modified by a few percent (Eqs. (7.1) and (7.2) in [81]). Finally we investigate the sensitivity of the observables to New Physics in a model-independent way. We give all observables in terms of ratios of high-scale Wilson coefficients, which we assume to be altered by new interactions. We also study correlations between different observables, bins and channels, and extrapolate to the final Belle II data set of 50 ab^{-1}. We find that the inclusive $\bar{B} \to X_s\ell^+\ell^-$ decay can constrain the ratios of high-scale Wilson coefficients significantly, and gives additional and in part complementary information compared to exclusive $b \to s\ell^+\ell^-$ transitions. Last but not least, we study the experimental sensitivity to the newly identified observables at Belle II.

The **second part** of the thesis discusses the quark and gluon form factors to three loops in perturbative QCD, and contains the articles [82] and [83]. The quark form factor is the coupling of a virtual photon to a massless quark-antiquark pair, while the gluon form factor is the coupling of a Higgs boson to a pair of gluons in an effective Lagrangian where the top quark is heavy and has been integrated out [119, 120]. These form factors are the simplest

objects containing infrared divergences at higher orders in massless quantum field theory, and therefore are of particular interest in many respects. They appear, for instance, as virtual higher-order corrections in coefficient functions for the inclusive Drell-Yan process, in deep-inelastic scattering, and in the inclusive Higgs production cross section (for recent updates including all currently available corrections, see [121, 122]). In these observables, the infrared poles of the form factors cancel against infrared singularities from real radiation corrections. The computation of perturbative QCD corrections to the quark and gluon form factor has a rather long history. The one- and two-loop contributions were already completed several years ago [123–127]. In [127] closed expressions valid to all orders in the dimensional regularisation parameter ϵ were provided. At the three-loop order, the pole terms in ϵ can be inferred from the three-loop calculation of the splitting functions [128–131]. Numerical values for the finite pieces were first obtained in [132]. In our work [82] we give analytic results for the three-loop quark and gluon form factors through to the finite terms, thereby confirming the ones from [132]. In addition, we provide results for certain subleading terms in the ϵ-expansion. The form factors are obtained by applying projection operators on the three-loop amplitudes (equations (2.1) and (2.2) in [82]). Afterwards, the calculation again amounts to a Laporta reduction to master integrals, followed by the computation of the latter. Both steps are highly non-trivial. The system of linear equations that is generated during the course of the Laporta reduction reaches almost a million equations, and the run-time to solve them is of the order of several weeks to a few months. In total, one obtains 22 master integrals, 14 of which are genuine three-loop vertex functions. Their analytic evaluation proved to be a major technical challenge, which was completed only in several steps [133–136]. Having analytic results through to three loops at hand, one can use them for several applications, two of which are discussed in our work [82]. First, by general arguments about the infrared pole structure of QCD amplitudes one can extract the cusp and collinear anomalous dimensions to three loops. We confirm all results obtained previously in the literature [130, 131, 137, 138]. Moreover, in this context we derive the pole structure of the four-loop result, assuming Casimir scaling of the cusp anomalous dimension. As a second application, we derive the matching coefficients onto SCET up to three loops.

In the second article of part II of the thesis [83], we extend the results of [82] to two more orders in the ϵ-expansion. The master integrals became available analytically to this order in [139]. We confirmed these results partially analytically and numerically to better than one per-mille for the remaining coefficients, and subsequently used them to derive the three-loop quark and gluon form factors to $\mathcal{O}(\epsilon^2)$. These contributions are relevant in the study of the infrared singularity structure at four loops. In particular, the $\mathcal{O}(\epsilon)$ terms of the three-loop form factors are required for the extraction of the four-loop quark and gluon collinear anomalous dimensions. The $\mathcal{O}(\epsilon^2)$ terms contribute to the finite part of the infrared-subtraction of the form factors at four loops. It is this infrared-subtracted finite part which is relevant for the study of the next-to-next-to-next-to-next-to-leading ($\mathrm{N^4LO}$) Drell-Yan and Higgs production processes. In particular, the $\mathcal{O}(\epsilon^2)$ three-loop contributions represent a finite ingredient to these processes at four-loops. In this context, one also needs the $\mathcal{O}(\epsilon^6)$ and $\mathcal{O}(\epsilon^4)$ results of the one- and two-loop form factors, respectively. Since all-order expressions for these quantities exist (see e.g. [127]) it is very simple to obtain them.

The **third part** of the thesis contains the articles [84–86], and is devoted to multi-loop calculations in supersymmetric gauge theories, in particular $\mathcal{N} = 4$ super Yang-Mills (SYM) theory. $\mathcal{N} = 4$ SYM is not realised in nature in the unbroken way in which it is written down in the Lagrangian [140], but due to its large symmetry content is ideally suited as a testing

ground for properties of many observables in realistic theories such as QCD. It is a conformal theory and as such has vanishing β-function. For pedagogical introductions to $\mathcal{N} = 4$ SYM, see [141, 142]. In recent years, scattering amplitudes in $\mathcal{N} = 4$ SYM have been intensively studied, and many properties such as dual conformal invariance have been investigated in order to exploit the beauty and simplicity that scattering amplitudes in $\mathcal{N} = 4$ SYM exhibit (for a review, see [143]). Form factors, on the other hand, were so far only marginally studied in $\mathcal{N} = 4$ SYM. The Sudakov form factor for instance has been known to two loops only, and its calculation dates back to 1986 [144]. Compared to scattering amplitudes, form factors are, on one hand, simpler because they do not depend on Mandelstam variables like s or t, but have trivial kinematic dependence. On the other hand, form factors are more complicated than scattering amplitudes since even at leading colour they have contributions from non-planar diagrams. Expressing the latter statement in the context of the unitarity approach, it means that form factors are sensitive to subleading double trace terms of scattering amplitudes. The main motivation for our work [84] was therefore to see how much of the simplicity of scattering amplitudes carries over to form factors, and to extend the calculation [144] to one higher loop. We construct the Sudakov form factor from unitarity cuts, and were surprised to see that at one, two and three loops, the form factor can be written as a linear combination of, respectively, one, two and eight integrals only. They are not master integrals in the sense of a Laporta reduction, but instead have the beautiful property that each coefficient of the Laurent expansion about $\epsilon = 0$ is of uniform transcendental weight. For the derivation of this result, our preliminary work [82, 83] proved to be of essential relevance. From the result we can make a number of further interesting observations. First, a nice manifestation of the leading transcendentality principle [145] is revealed by specifying the QCD quark and gluon form factors to a supersymmetric Yang-Mills theory containing a bosonic and fermionic degree of freedom in the same colour representation. By doing so, the leading transcendentality pieces of the quark and gluon form factor become equal, and coincide, up to a normalisation factor, with the coefficients of the Sudakov form factor in $\mathcal{N} = 4$ SYM. Second, the cusp and collinear anomalous dimension can be inferred from the logarithm of the form factor. Finally, we investigate the UV behaviour of the form factor, which is UV-finite in $D = 4$ dimensions. The question in which dimension D_c – the so-called *critical* dimension – it first develops UV-divergent parts, is of theoretical interest, can give useful cross-checks on calculations, and constrains the appearance of certain diagrams. We find that $D_c = 6$ for the one-, two-, and three-loop form factor.

The second article of this part of the thesis [85] deals with the angle-dependent cusp-anomalous dimension in supersymmetric Yang-Mills theory. In a previous paper [146], a scaling limit was identified in which the ladder diagrams are dominant and are mapped onto a one-dimensional Schrödinger problem. In our article [85] we show how to solve the latter in perturbation theory and provide an algorithm to compute the solution at any loop order. The answer is written in terms of harmonic polylogarithms, which at L loops are of homogeneous weight $2L - 1$. Moreover, we give evidence for two curious properties of the result. First, we observe that the result can be written using the subset of harmonic polylogarithms with non-negative indices only, which we confirm to six loops. Second, we show that in the light-like limit, only single zeta values and products thereof appear in the asymptotic expansion, although multiple zeta values of depth ≥ 2 would be allowed in principle. Again, we verify this feature explicitly up to six loops. We then extend the analysis of the scaling limit to systematically include subleading terms. This leads to a Schrödinger-type equation, but with an inhomogeneous term. We show how its solution can be computed in perturbation theory,

in a way similar to the leading order case. Finally, we analyse the strong coupling limit of these subleading contributions and find that they are in agreement with the corresponding string theory answer.

The final article of the thesis [86] is the computation of the angle-dependent cusp-anomalous dimension in $\mathcal{N} = 4$ SYM at the four-loop order. Besides the usual leading colour factor N_c^L at L loops, there appears, due to the advent of the quartic Casimir, for the first time a subleading colour factor N_c^2, which renders this loop-order particularly interesting. There have been conjectures based on factorisation theorems [138] that this subleading colour piece vanishes in the light-like limit. In our work [86] we compute the complete planar contribution of N_c^4, and the subleading, non-planar contribution in the aforementioned scaling limit. The result can again be written in terms of harmonic polylogarithms of weight $2L - 1$ with non-negative indices.We study several applications of our result. First we take certain limits, such as the light-like limit, or the limits of small and large cusp angles. Finally, we use the available perturbative data, as well as insight from AdS/CFT [147], in order to extrapolate the leading order values at strong coupling. The latter agree within two percent with the corresponding string theory result, over a wide range of parameters.

Let me finally make a few comments on my personal contribution to the various articles. I would like to emphasize that listing my achievements does not mean that I am the only person who performed these steps, but the size and complexity of the calculations require a cross check by at least two people. This automatically means that in all two-author papers (i.e. [76, 78, 85, 86]) all steps were carried out and cross-checked by both authors, and an explicit listing of my personal contributions becomes obsolete. For all other papers, I list my contribution in the following. In [75] I performed the entire two-loop calculation and the derivation of the matching coefficients. Moreover, I implemented the form factor ratios and performed the phenomenology related to the zero of the forward-backward asymmetry. In [77] I performed the entire two-loop calculation, including the reduction to master integrals and the analytic evaluation of the latter (separately published in [76]). Moreover I performed the convolution with the light-cone distribution amplitude of the bare amplitude and the counterterms, and verified the cancellation of all poles to obtain the NNLO contribution to the topological QCD penguin amplitude. In [79] I computed the matrix elements of all necessary interferences, including the phase space integration, UV renormalisation and splitting function contribution. I derived all formulas of the final result, and performed a small part of the numerics. In [80] I evaluated analytically all master integrals for the boundary conditions. Moreover, I checked that all formulas consistently add up to the final result (eq. (2.11)), and provided some of the new relations in Appendix B. In [81] I derived the entire set of formulas for the logarithmically enhanced QED corrections, implemented all master formulas, and did the entire phenomenological analysis in the SM. I also derived and implemented the New Physics formulas in terms of ratios of high-scale Wilson coefficients. In [82] and [83] I did part of the Laporta reduction, computed all genuine three-loop vertex master integrals (see also [133–136]), checked that all formulas consistently make up the form factors, and from the final result derived the cusp and collinear anomalous dimensions and the SCET matching coefficients. Finally, in [84] I wrote down the linear combination of homogeneous integrals that builds the form factor, derived the momentum routing invariances based on graph symmetries, and carried out all calculations related to the logarithm of the form factor and its UV behaviour in higher dimensions. Besides calculating, I also did a major part of the write-up of all papers. These statements show that I contributed in a significant and leading manner to all papers.

References

[1] S. L. Glashow, J. Iliopoulos and L. Maiani, Phys. Rev. D **2** (1970) 1285.

[2] M. Kobayashi and T. Maskawa, Prog. Theor. Phys. **49** (1973) 652.

[3] G. Aad *et al.* [ATLAS Collaboration], Phys. Lett. B **716** (2012) 1 [arXiv:1207.7214 [hep-ex]].

[4] S. Chatrchyan *et al.* [CMS Collaboration], Phys. Lett. B **716** (2012) 30 [arXiv:1207.7235 [hep-ex]].

[5] F. Englert and R. Brout, Phys. Rev. Lett. **13** (1964) 321.

[6] P. W. Higgs, Phys. Lett. **12** (1964) 132.

[7] P. W. Higgs, Phys. Rev. Lett. **13** (1964) 508.

[8] P. W. Higgs, Phys. Rev. **145** (1966) 1156.

[9] G. S. Guralnik, C. R. Hagen and T. W. B. Kibble, Phys. Rev. Lett. **13** (1964) 585.

[10] T. W. B. Kibble, Phys. Rev. **155** (1967) 1554.

[11] R. P. Feynman, Phys. Rev. **76** (1949) 769.

[12] J. S. Schwinger, Phys. Rev. **74** (1948) 1439.

[13] J. S. Schwinger, Phys. Rev. **75** (1948) 651.

[14] S. Tomonaga, Prog. Theor. Phys. **1** (1946) 27.

[15] C. N. Yang and R. L. Mills, Phys. Rev. **96** (1954) 191.

[16] L. D. Faddeev and V. N. Popov, Phys. Lett. B **25** (1967) 29.

[17] C. Becchi, A. Rouet and R. Stora, Commun. Math. Phys. **42** (1975) 127.

[18] C. Becchi, A. Rouet and R. Stora, Annals Phys. **98** (1976) 287.

[19] I. V. Tyutin, arXiv:0812.0580 [hep-th].

[20] J. Goldstone, Nuovo Cim. **19** (1961) 154.

[21] Y. Nambu, Phys. Rev. Lett. **4** (1960) 380.

[22] Y. Nambu and G. Jona-Lasinio, Phys. Rev. **122** (1961) 345.

[23] Y. Nambu and G. Jona-Lasinio, Phys. Rev. **124** (1961) 246.

[24] S. L. Glashow, Nucl. Phys. **22** (1961) 579.

[25] A. Salam, Conf. Proc. C **680519** (1968) 367.

[26] S. Weinberg, Phys. Rev. Lett. **19** (1967) 1264.

[27] H. Fritzsch, M. Gell-Mann and H. Leutwyler, Phys. Lett. B **47** (1973) 365.

[28] D. J. Gross and F. Wilczek, Phys. Rev. Lett. **30** (1973) 1343.

[29] H. D. Politzer, Phys. Rev. Lett. **30** (1973) 1346.

[30] G. 't Hooft and M. J. G. Veltman, Nucl. Phys. B **44** (1972) 189.

[31] K. G. Wilson and J. B. Kogut, Phys. Rept. **12** (1974) 75.

[32] K. G. Wilson, Rev. Mod. Phys. **47** (1975) 773.

[33] S. Weinberg, Phys. Rev. **166** (1968) 1568.

[34] S. R. Coleman, J. Wess and B. Zumino, Phys. Rev. **177** (1969) 2239.

[35] S. Weinberg, Physica A **96** (1979) 327.

[36] J. Gasser and H. Leutwyler, Annals Phys. **158** (1984) 142.

[37] J. Gasser and H. Leutwyler, Nucl. Phys. B **250** (1985) 465.

[38] S. Scherer, Adv. Nucl. Phys. **27** (2003) 277 [hep-ph/0210398].

[39] B. Kubis, hep-ph/0703274 [HEP-PH].

[40] N. Isgur and M. B. Wise, Phys. Lett. B **232** (1989) 113.

[41] N. Isgur and M. B. Wise, Phys. Lett. B **237** (1990) 527.

[42] B. Grinstein, Nucl. Phys. B **339** (1990) 253.

[43] H. Georgi, Phys. Lett. B **240** (1990) 447.

[44] A. F. Falk, H. Georgi, B. Grinstein and M. B. Wise, Nucl. Phys. B **343** (1990) 1.

[45] M. Neubert, Phys. Rept. **245** (1994) 259 [hep-ph/9306320].

[46] T. Mannel, Rept. Prog. Phys. **60** (1997) 1113.

[47] C. W. Bauer, S. Fleming, D. Pirjol and I. W. Stewart, Phys. Rev. D **63** (2001) 114020 [hep-ph/0011336].

[48] C. W. Bauer, D. Pirjol and I. W. Stewart, Phys. Rev. D **65** (2002) 054022 [hep-ph/0109045].

[49] M. Beneke, A. P. Chapovsky, M. Diehl and T. Feldmann, Nucl. Phys. B **643** (2002) 431 [hep-ph/0206152].

[50] M. Beneke and T. Feldmann, Phys. Lett. B **553** (2003) 267 [hep-ph/0211358].

[51] T. Becher, A. Broggio and A. Ferroglia, arXiv:1410.1892 [hep-ph].

[52] G. Buchalla, A. J. Buras and M. E. Lautenbacher, Rev. Mod. Phys. **68** (1996) 1125 [hep-ph/9512380].

[53] B. Grzadkowski, M. Iskrzynski, M. Misiak and J. Rosiek, JHEP **1010** (2010) 085 [arXiv:1008.4884 [hep-ph]].

[54] E. E. Jenkins, A. V. Manohar and M. Trott, JHEP **1310** (2013) 087 [arXiv:1308.2627 [hep-ph]].

[55] E. E. Jenkins, A. V. Manohar and M. Trott, JHEP **1401** (2014) 035 [arXiv:1310.4838 [hep-ph]].

[56] R. Alonso, E. E. Jenkins, A. V. Manohar and M. Trott, JHEP **1404** (2014) 159 [arXiv:1312.2014 [hep-ph]].

[57] G. Buchalla and O. Cata, JHEP **1207** (2012) 101 [arXiv:1203.6510 [hep-ph]].

[58] G. Buchalla, O. Cata and C. Krause, Nucl. Phys. B **880** (2014) 552 [arXiv:1307.5017 [hep-ph]].

[59] G. Buchalla, O. Cat and C. Krause, Phys. Lett. B **731** (2014) 80 [arXiv:1312.5624 [hep-ph]].

[60] J. Elias-Miro, J. R. Espinosa, E. Masso and A. Pomarol, JHEP **1311** (2013) 066 [arXiv:1308.1879 [hep-ph]].

[61] A. Pomarol and F. Riva, JHEP **1401** (2014) 151 [arXiv:1308.2803 [hep-ph]].

[62] G. F. Giudice, C. Grojean, A. Pomarol and R. Rattazzi, JHEP **0706** (2007) 045 [hep-ph/0703164].

[63] J. A. Aguilar-Saavedra, Nucl. Phys. B **843** (2011) 638 Erratum: [Nucl. Phys. B **851** (2011) 443] [arXiv:1008.3562 [hep-ph]].

[64] W. Buchmuller and D. Wyler, Nucl. Phys. B **268** (1986) 621.

[65] S. Weinberg, "The Quantum theory of fields. Vol. 1 and 2," Cambridge University Press, (1995)

[66] M. E. Peskin and D. V. Schroeder, "An Introduction to quantum field theory," Westview Press (1995)

[67] C. Itzykson and J. B. Zuber, "Quantum Field Theory," McGraw-Hill, New York, USA (1980)

[68] J. F. Donoghue, E. Golowich and B. R. Holstein, "Dynamics of the standard model," Cambridge University Press (1992)

[69] A. V. Manohar and M. B. Wise, "Heavy quark physics," Cambridge University Press (2000)

[70] A. G. Grozin, "Heavy quark effective theory," Springer Tracts Mod. Phys. **201** (2004) 1.

[71] W. Kilian, "Electroweak symmetry breaking: The bottom-up approach," Springer Tracts Mod. Phys. **198** (2003) 1.

[72] A. A. Petrov and A. E. Blechman, "Effective Field Theories," World Scientific (2016)

[73] N. Cabibbo, Phys. Rev. Lett. **10** (1963) 531.

[74] J. Blumlein, PoS RADCOR **2011** (2011) 048 [arXiv:1205.4991 [hep-ph]].

[75] G. Bell, M. Beneke, T. Huber and X. Q. Li, Nucl. Phys. B **843** (2011) 143 [arXiv:1007.3758 [hep-ph]].

[76] G. Bell and T. Huber, JHEP **1412** (2014) 129 [arXiv:1410.2804 [hep-ph]].

[77] G. Bell, M. Beneke, T. Huber and X. Q. Li, Phys. Lett. B **750** (2015) 348 [arXiv:1507.03700 [hep-ph]].

[78] T. Huber and S. Kränkl, JHEP **1504** (2015) 140 [arXiv:1503.00735 [hep-ph]].

[79] T. Huber, M. Poradziǹski and J. Virto, JHEP **1501** (2015) 115 [arXiv:1411.7677 [hep-ph]].

[80] M. Czakon, P. Fiedler, T. Huber, M. Misiak, T. Schutzmeier and M. Steinhauser, JHEP **1504** (2015) 168 [arXiv:1503.01791 [hep-ph]].

[81] T. Huber, T. Hurth and E. Lunghi, JHEP **1506** (2015) 176 [arXiv:1503.04849 [hep-ph]].

[82] T. Gehrmann, E. W. N. Glover, T. Huber, N. Ikizlerli and C. Studerus, JHEP **1006** (2010) 094 [arXiv:1004.3653 [hep-ph]].

[83] T. Gehrmann, E. W. N. Glover, T. Huber, N. Ikizlerli and C. Studerus, JHEP **1011** (2010) 102 [arXiv:1010.4478 [hep-ph]].

[84] T. Gehrmann, J. M. Henn and T. Huber, JHEP **1203** (2012) 101 [arXiv:1112.4524 [hep-th]].

[85] J. M. Henn and T. Huber, JHEP **1211** (2012) 058 [arXiv:1207.2161 [hep-th]].

[86] J. M. Henn and T. Huber, JHEP **1309** (2013) 147 [arXiv:1304.6418 [hep-th]].

[87] G. Passarino and M. J. G. Veltman, Nucl. Phys. B **160** (1979) 151.

[88] S. Laporta and E. Remiddi, Phys. Lett. B **379** (1996) 283 [hep-ph/9602417].

[89] S. Laporta, Int. J. Mod. Phys. A **15** (2000) 5087 [hep-ph/0102033].

[90] F. V. Tkachov, Phys. Lett. B **100** (1981) 65.

[91] K. G. Chetyrkin and F. V. Tkachov, Nucl. Phys. B **192** (1981) 159.

[92] R. Bonciani and A. Ferroglia, JHEP **0811** (2008) 065 [arXiv:0809.4687 [hep-ph]].

[93] H. M. Asatrian, C. Greub and B. D. Pecjak, Phys. Rev. D **78** (2008) 114028 [arXiv:0810.0987 [hep-ph]].

[94] M. Beneke, T. Huber and X.-Q. Li, Nucl. Phys. B **811** (2009) 77 [arXiv:0810.1230 [hep-ph]].

[95] G. Bell, Nucl. Phys. B **812** (2009) 264 [arXiv:0810.5695 [hep-ph]].

[96] T. Huber, JHEP **0903** (2009) 024 [arXiv:0901.2133 [hep-ph]].

[97] G. Bell, Nucl. Phys. B **795** (2008) 1 [arXiv:0705.3127 [hep-ph]].

[98] G. Bell, Nucl. Phys. B **822** (2009) 172 [arXiv:0902.1915 [hep-ph]].

[99] M. Beneke, T. Huber and X. Q. Li, Nucl. Phys. B **832** (2010) 109 [arXiv:0911.3655 [hep-ph]].

[100] B. Aubert *et al.* [BaBar Collaboration], Phys. Rev. Lett. **93** (2004) 081802 [hep-ex/0404006].

[101] M. Iwasaki *et al.* [Belle Collaboration], Phys. Rev. D **72** (2005) 092005 [hep-ex/0503044].

[102] J. P. Lees *et al.* [BaBar Collaboration], Phys. Rev. Lett. **112** (2014) 211802 [arXiv:1312.5364 [hep-ex]].

[103] Y. Sato *et al.* [Belle Collaboration], Phys. Rev. D **93** (2016) 3, 032008 [arXiv:1402.7134 [hep-ex]].

[104] M. Beneke, T. Feldmann and D. Seidel, Nucl. Phys. B **612** (2001) 25 [hep-ph/0106067].

[105] M. Beneke, T. Feldmann and D. Seidel, Eur. Phys. J. C **41** (2005) 173 [hep-ph/0412400].

[106] T. Huber, T. Hurth and E. Lunghi, Nucl. Phys. B **802** (2008) 40 [arXiv:0712.3009 [hep-ph]].

[107] M. Beneke, G. Buchalla, M. Neubert and C. T. Sachrajda, Phys. Rev. Lett. **83** (1999) 1914 [hep-ph/9905312].

[108] M. Beneke, G. Buchalla, M. Neubert and C. T. Sachrajda, Nucl. Phys. B **591** (2000) 313 [hep-ph/0006124].

[109] M. Beneke, G. Buchalla, M. Neubert and C. T. Sachrajda, Nucl. Phys. B **606** (2001) 245 [hep-ph/0104110].

[110] M. Beneke and M. Neubert, Nucl. Phys. B **675** (2003) 333 [hep-ph/0308039].

[111] A. V. Kotikov, Phys. Lett. B **254** (1991) 158.

[112] A. V. Kotikov, Phys. Lett. B **267** (1991) 123.

[113] J. M. Henn, Phys. Rev. Lett. **110** (2013) 251601 [arXiv:1304.1806 [hep-th]].

[114] M. Misiak *et al.*, Phys. Rev. Lett. **98** (2007) 022002 [hep-ph/0609232].

[115] T. Huber, E. Lunghi, M. Misiak and D. Wyler, Nucl. Phys. B **740** (2006) 105 [hep-ph/0512066].

[116] M. Kaminski, M. Misiak and M. Poradziňski, Phys. Rev. D **86** (2012) 094004 [arXiv:1209.0965 [hep-ph]].

[117] M. Misiak and M. Steinhauser, Nucl. Phys. B **764** (2007) 62 [hep-ph/0609241].

[118] M. Misiak *et al.*, Phys. Rev. Lett. **114** (2015) no.22, 221801 [arXiv:1503.01789 [hep-ph]].

[119] M. Krämer, E. Laenen and M. Spira, Nucl. Phys. B **511** (1998) 523 [hep-ph/9611272].

[120] K. G. Chetyrkin, B. A. Kniehl and M. Steinhauser, Phys. Rev. Lett. **79** (1997) 353 [hep-ph/9705240].

[121] C. Anastasiou, C. Duhr, F. Dulat, E. Furlan, T. Gehrmann, F. Herzog, A. Lazopoulos and B. Mistlberger, arXiv:1602.00695 [hep-ph].

[122] M. Bonvini, S. Marzani, C. Muselli and L. Rottoli, arXiv:1603.08000 [hep-ph].

[123] G. Kramer and B. Lampe, Z. Phys. C **34** (1987) 497 Erratum: [Z. Phys. C **42** (1989) 504].

[124] T. Matsuura and W. L. van Neerven, Z. Phys. C **38** (1988) 623.

[125] T. Matsuura, S. C. van der Marck and W. L. van Neerven, Nucl. Phys. B **319** (1989) 570.

[126] R. V. Harlander, Phys. Lett. B **492** (2000) 74 [hep-ph/0007289].

[127] T. Gehrmann, T. Huber and D. Maitre, Phys. Lett. B **622** (2005) 295 [hep-ph/0507061].

[128] S. Moch, J. A. M. Vermaseren and A. Vogt, Nucl. Phys. B **688** (2004) 101 [hep-ph/0403192].

[129] A. Vogt, S. Moch and J. A. M. Vermaseren, Nucl. Phys. B **691** (2004) 129 [hep-ph/0404111].

[130] S. Moch, J. A. M. Vermaseren and A. Vogt, JHEP **0508** (2005) 049 [hep-ph/0507039].

[131] S. Moch, J. A. M. Vermaseren and A. Vogt, Phys. Lett. B **625** (2005) 245 [hep-ph/0508055].

[132] P. A. Baikov, K. G. Chetyrkin, A. V. Smirnov, V. A. Smirnov and M. Steinhauser, Phys. Rev. Lett. **102** (2009) 212002 [arXiv:0902.3519 [hep-ph]].

[133] T. Gehrmann, G. Heinrich, T. Huber and C. Studerus, Phys. Lett. B **640** (2006) 252 [hep-ph/0607185].

[134] G. Heinrich, T. Huber and D. Maitre, Phys. Lett. B **662** (2008) 344 [arXiv:0711.3590 [hep-ph]].

[135] G. Heinrich, T. Huber, D. A. Kosower and V. A. Smirnov, Phys. Lett. B **678** (2009) 359 [arXiv:0902.3512 [hep-ph]].

[136] R. N. Lee, A. V. Smirnov and V. A. Smirnov, JHEP **1004** (2010) 020 [arXiv:1001.2887 [hep-ph]].

[137] T. Becher, M. Neubert and B. D. Pecjak, JHEP **0701** (2007) 076 [hep-ph/0607228].

[138] T. Becher and M. Neubert, JHEP **0906** (2009) 081 Erratum: [JHEP **1311** (2013) 024] [arXiv:0903.1126 [hep-ph]].

[139] R. N. Lee and V. A. Smirnov, JHEP **1102** (2011) 102 [arXiv:1010.1334 [hep-ph]].

[140] R. Grimm, M. Sohnius and J. Wess, Nucl. Phys. B **133** (1978) 275.

[141] E. D'Hoker and D. H. Phong, hep-th/9912271.

[142] E. D'Hoker and D. Z. Freedman, hep-th/0201253.

[143] R.Roiban, M. Spradlin and A. Volovich (eds.), J. Phys. A **44**, number 45, (2011) 450301 doi:10.1088/1751-8113/44/45/450301

[144] W. L. van Neerven, Z. Phys. C **30** (1986) 595.

[145] A. V. Kotikov, L. N. Lipatov, A. I. Onishchenko and V. N. Velizhanin, Phys. Lett. B **595** (2004) 521 Erratum: [Phys. Lett. B **632** (2006) 754] [hep-th/0404092].

[146] D. Correa, J. Henn, J. Maldacena and A. Sever, JHEP **1205** (2012) 098 [arXiv:1203.1019 [hep-th]].

[147] J. M. Maldacena, Int. J. Theor. Phys. **38** (1999) 1113 [Adv. Theor. Math. Phys. **2** (1998) 231] [hep-th/9711200].

Part I

Quark Flavour Physics

Author's personal copy

Available online at www.sciencedirect.com
ScienceDirect
Nuclear Physics B 843 (2011) 143–176
NUCLEAR PHYSICS B
www.elsevier.com/locate/nuclphysb

Heavy-to-light currents at NNLO in SCET and semi-inclusive $\bar{B} \to X_s \ell^+ \ell^-$ decay

G. Bell [a], M. Beneke [b], T. Huber [c], Xin-Qiang Li [d,e,*]

[a] *Albert Einstein Center for Fundamental Physics, Institute for Theoretical Physics, University of Bern, Sidlerstrasse 5, 3012 Bern, Switzerland*
[b] *Institut für Theoretische Teilchenphysik und Kosmologie, RWTH Aachen University, D-52056 Aachen, Germany*
[c] *Theoretische Physik 1, Fachbereich 7, Universität Siegen, D-57068 Siegen, Germany*
[d] *Department of Physics, Henan Normal University, Xinxiang, Henan 453007, PR China*
[e] *Institute of Theoretical Physics, Chinese Academy of Science, Beijing 100190, PR China*

Received 27 July 2010; accepted 29 September 2010

Available online 7 October 2010

Abstract

We perform the two-loop matching calculation for heavy-to-light currents from QCD onto soft-collinear effective theory for the complete set of Dirac structures. The newly obtained matching coefficients enter several phenomenological applications, of which we discuss heavy-to-light form factor ratios and exclusive radiative decays, as well as the semi-inclusive decay $\bar{B} \to X_s \ell^+ \ell^-$. For this decay, we observe a significant shift of the forward–backward asymmetry zero and find $q_0^2 = (3.34^{+0.22}_{-0.25})\ \mathrm{GeV}^2$ for an invariant mass cut $m_X^{\mathrm{cut}} = 2.0$ GeV.
© 2010 Elsevier B.V. All rights reserved.

1. Introduction

The flavour-changing quark currents $\bar{q}\Gamma_i b$, with $\Gamma_i = \{1, \gamma_5, \gamma^\mu, \gamma_5\gamma^\mu, i\sigma^{\mu\nu}\}$, govern the hadronic dynamics in semi-leptonic and radiative B decays. The matrix elements of the currents, usually parameterized by several transition form factors, are also important inputs to the factorization formulae for non-leptonic B decays [1]. In the kinematic region where the hadronic final state has small invariant mass but large energy, soft-collinear effective theory (SCET) [2,3] is the appropriate theoretical framework, with which transparent factorization formulae for the

* Corresponding author at: Department of Physics, Henan Normal University, Xinxiang, Henan 453007, PR China.
E-mail address: xqli@itp.ac.cn (X.-Q. Li).

0550-3213/$ – see front matter © 2010 Elsevier B.V. All rights reserved.
doi:10.1016/j.nuclphysb.2010.09.022

Author's personal copy

heavy-to-light form factors have been derived [4] (see also [5,6]). Thus, the accurate representation of the heavy-to-light currents in SCET is of particular interest.

The LO and NLO matching coefficients for heavy-to-light currents from QCD onto SCET for an arbitrary Dirac matrix have been worked out a few years ago [2,7,8]. The coefficients for V–A currents have recently been determined to NNLO in the context of inclusive semi-leptonic B decays [9–12] in the shape-function region. In this paper we complete the NNLO calculation by computing the remaining matching coefficients of the tensor currents. The tensor matching coefficients enter several phenomenological applications, of which we shall discuss heavy-to-light form factor ratios and exclusive radiative decays, as well as the semi-inclusive decay $\bar{B} \to X_s \ell^+ \ell^-$.

The paper is organized as follows. In Section 2 we first set up notation and then briefly recapitulate the techniques applied and the necessary ingredients for the two-loop calculation. In Section 3 the two-loop calculation of the QCD form factors and the corresponding matching coefficients are presented in detail. Three interesting phenomenological applications of our results to heavy-to-light form factor ratios, exclusive radiative decays, as well as the inclusive decay $\bar{B} \to X_s \ell^+ \ell^-$ are discussed in Sections 4 and 5. We conclude in Section 6. The lengthy analytic expressions for the coefficient functions can be found in Appendices A and B.

2. NNLO calculation

2.1. Set-up of the matching calculation

A generic heavy-to-light current $\bar{q}\Gamma_i b$ is represented in SCET by a set of non-local "two-body" and "three-body" [3–6] operators,

$$[\bar{q}\Gamma_i b](0) = \sum_j \int ds\, \tilde{C}_i^j(s)[\bar{\xi} W_{hc}](sn_+)\Gamma_j' h_v(0) + \sum_j \int ds_1\, ds_2\, \tilde{C}_{i\mu}^{(B1)j}(s_1, s_2) O_i^{(B1)j\mu}(s_1, s_2) + \cdots, \tag{1}$$

where h_v is the static heavy quark field defined in HQET, whereas ξ and W_{hc} are the hard-collinear light quark field and a hard-collinear Wilson line from SCET, respectively. In this paper we are concerned with the calculation of the matching coefficients in the first line of (1). The three-body operators $O_i^{(B1)j\mu}(s_1, s_2)$ in the second line are $1/m_b$-suppressed but relevant at leading power for exclusive transitions and form factors due to the matrix element suppression of the leading term. Their one-loop matching coefficients are known from [8,13] and this suffices to work out their contribution to the exclusive transitions at $\mathcal{O}(\alpha_s^2)$. We refer to [14] for the details of the calculation of these spectator-scattering terms. In the current work we consider the missing $\mathcal{O}(\alpha_s^2)$ matching coefficients of the two-body operators $[\bar{\xi} W_{hc}](sn_+)\Gamma_j' h_v(0)$ and adopt the momentum space representation, which follows from

$$C_i^j(n_+ p) = \int ds\, e^{isn_+ p} \tilde{C}_i^j(s). \tag{2}$$

We decompose the heavy-to-light currents in the basis from [14] (summarized in Table 1) with two reference vectors v and n_- that fulfill $v = (n_- + n_+)/2$, $n_\pm^2 = 0$ and $n_+ n_- = 2$. The matching calculation involves 12 coefficient functions C_i^j, which are not independent in a renormalization scheme with anti-commuting γ_5 due to the chiral symmetry of QCD. In the NDR

Author's personal copy

Table 1
Matching coefficients C_i^j according to the decomposition in (1) ($a^{[\mu}b^{\nu]} \equiv a^\mu b^\nu - a^\nu b^\mu$).

Γ_i	1	γ_5	γ^μ			$\gamma_5\gamma^\mu$			$i\sigma^{\mu\nu}$			
Γ'_j	1	γ_5	γ^μ	v^μ	n_-^μ	$\gamma_5\gamma^\mu$	$v^\mu\gamma_5$	$n_-^\mu\gamma_5$	$\gamma^{[\mu}\gamma^{\nu]}$	$v^{[\mu}\gamma^{\nu]}$	$n_-^{[\mu}\gamma^{\nu]}$	$n_-^{[\mu}v^{\nu]}$
C_i^j	C_S	C_P	C_V^1	C_V^2	C_V^3	C_A^1	C_A^2	C_A^3	C_T^1	C_T^2	C_T^3	C_T^4

scheme adopted in this work, this translates into the constraints $C_P = C_S$ and $C_A^i = C_V^i$, while similar relations hold between the matching coefficients of the tensor and the pseudotensor current. As the latter is reducible in four space–time dimensions, we obtain the additional constraints $C_T^2 = C_T^4 = 0$ in four dimensions. We nevertheless keep the more general basis from Table 1, since we work in dimensional regularization and obtain intermediate results that are valid in $d = 4 - 2\epsilon$ dimensions, where C_T^2 and C_T^4 are of $\mathcal{O}(\epsilon)$ but non-vanishing.

It is convenient to perform the matching calculation with on-shell quarks and to use dimensional regularization to regularize ultraviolet (UV) and infrared (IR) singularities. The SCET diagrams are then scaleless and vanish and the computation essentially amounts to a two-loop calculation in QCD. We, in particular, introduce an analogous tensor decomposition to (1) and parameterize the QCD result in terms of 12 form factors,

$$\langle q(p)|\bar{q}\Gamma_i b|b(p_b)\rangle = \sum_j F_i^j(q^2)\bar{u}(p)\Gamma'_j u(p_b), \tag{3}$$

where $p_b = m_b v$ is the momentum of the heavy quark, $p = u m_b n_-/2$ the momentum of the light quark and $q^2 = (p_b - p)^2 = (1-u)m_b^2$ denotes the momentum transfer. Due to the absence of loop contributions on the effective theory side, the SCET matrix elements are given by the tree level matrix elements multiplied by a universal renormalization factor Z_J of the SCET current $[\bar{\xi} W_{hc}]\Gamma'_j h_v$. There is thus a one-to-one correspondence between the matching coefficients C_i^j and the form factors F_i^j,

$$C_i^j = Z_J^{-1} F_i^j. \tag{4}$$

As the form factors are, however, in general IR-divergent, there exists no analogous relation on the form factor level to the four-dimensional constraints $C_T^2 = C_T^4 = 0$.

The purpose of our analysis consists in the computation of the matching coefficients C_i^j (and the respective form factors F_i^j) to NNLO in QCD. Whereas the NLO corrections have been worked out in [2,7,8], the coefficients C_V^i and C_A^i have recently been determined to NNLO in the context of inclusive semi-leptonic B decays [9–12]. In the current work we complete the NNLO calculation by computing the remaining matching coefficients C_S, C_P and C_T^i. The four-dimensional constraints mentioned above, will serve as a non-trivial check of our calculation.

2.2. Technical aspects of the calculation

We organize the calculation along the strategy that we used in our previous works on the V–A current [11,12]. The calculation is based on an automated reduction algorithm, which uses integration-by-parts techniques [15] and the Laporta algorithm [16] to express the two-loop diagrams (shown in Fig. 1 of [11]) in terms of a small set of scalar master integrals. The required master integrals are already known from the computations in [9–11,17,18].

Author's personal copy

Our results will be given in terms of the following set of harmonic polylogarithms (HPLs) [19],

$$\begin{aligned}
&H(0;x)=\ln(x), && H(0,0,1;x)=\mathrm{Li}_3(x),\\
&H(1;x)=-\ln(1-x), && H(0,1,1;x)=\mathrm{S}_{1,2}(x),\\
&H(-1;x)=\ln(1+x), && H(0,0,0,1;x)=\mathrm{Li}_4(x),\\
&H(0,1;x)=\mathrm{Li}_2(x), && H(0,0,1,1;x)=\mathrm{S}_{2,2}(x),\\
&H(0,-1;x)=-\mathrm{Li}_2(-x), && H(0,1,1,1;x)=\mathrm{S}_{1,3}(x),\\
&H(-1,0,1;x)\equiv\mathcal{H}_1(x), && H(0,-1,0,1;x)\equiv\mathcal{H}_2(x),
\end{aligned} \tag{5}$$

where we introduced a shorthand notation for the last two HPLs. Whereas the first one can be written in a compact form [20],

$$\mathcal{H}_1(x)=\ln(1+x)\mathrm{Li}_2(x)+\frac{1}{2}\mathrm{S}_{1,2}\big(x^2\big)-\mathrm{S}_{1,2}(x)-\mathrm{S}_{1,2}(-x), \tag{6}$$

the second one, $\mathcal{H}_2(x)=\int_0^x dx'\,\mathcal{H}_1(x')/x'$, cannot be expressed in terms of Nielsen Polylogarithms and has to be evaluated numerically.

The charm quark enters the matching calculation at the two-loop level through the gluon self energy which contains closed fermion loops. Our analytical results from Sections 3.1 and 3.2 are valid for massless charm quark, but we also show some numerical results in Section 3.2 that include charm mass effects. In this case we formally keep m_c/m_b fixed in the heavy-quark expansion, so the coefficients depend non-trivially on the quark mass ratio (see Section 5 of [12]).

The pure two-loop calculation yields bare form factors F_i^j that are UV- and IR-divergent. The UV-divergences are subtracted in a standard renormalization procedure, which has been described in detail in our previous works [11,12]. We, in particular, renormalize the strong coupling constant in the $\overline{\mathrm{MS}}$-scheme, whereas the quark wave-functions and the b-quark mass are renormalized in the on-shell scheme. The only difference in the current calculation consists in the fact that the scalar and the tensor current have non-vanishing anomalous dimensions in contrast to the vector current considered in [11,12]. This gives rise to an additional multiplicative counterterm Z_i^{-1} $(i=S,T)$. We expand the inverse

$$Z_i=1+\sum_{k=1}^{\infty}\left(\frac{\alpha_s^{(5)}}{4\pi}\right)^k Z_i^{(k)} \tag{7}$$

in terms of the renormalized coupling constant of a theory with five active quark flavours. In the $\overline{\mathrm{MS}}$-scheme the respective NLO coefficients are then given by $Z_S^{(1)}=3C_F/\epsilon$ and $Z_T^{(1)}=-C_F/\epsilon$ for the scalar and the tensor current, respectively. At NNLO the counterterms can be inferred from [21],

$$\begin{aligned}
Z_S^{(2)}&=C_F\left\{\left[\frac{9}{2}C_F-\frac{11}{2}C_A+2n_fT_F\right]\frac{1}{\epsilon^2}+\left[\frac{3}{4}C_F+\frac{97}{12}C_A-\frac{5}{3}n_fT_F\right]\frac{1}{\epsilon}\right\},\\
Z_T^{(2)}&=C_F\left\{\left[\frac{1}{2}C_F+\frac{11}{6}C_A-\frac{2}{3}n_fT_F\right]\frac{1}{\epsilon^2}+\left[\frac{19}{4}C_F-\frac{257}{36}C_A+\frac{13}{9}n_fT_F\right]\frac{1}{\epsilon}\right\},
\end{aligned} \tag{8}$$

where $n_f=5$ denotes the number of active quark flavours.

Author's personal copy

3. Results

3.1. Renormalized form factors

We first present our results for the renormalized form factors F_i^j, which are UV-finite but IR-divergent. It will be convenient to decompose the form factors according to

$$F_i^j = \sum_{k=0}^{\infty} \left(\frac{\alpha_s^{(5)}}{4\pi}\right)^k F_i^{j,(k)}, \qquad F_i^{j,(k)} = \sum_l F_{i,l}^{j,(k)} \epsilon^l. \tag{9}$$

In this normalization the form factors become at tree level

$$\begin{aligned} &F_S^{(0)} = -2F_T^{1,(0)} = 1, \\ &F_T^{2,(0)} = F_T^{3,(0)} = F_T^{4,(0)} = 0. \end{aligned} \tag{10}$$

Here and below we do not quote our results for the pseudoscalar and the (axial) vector current, since the former are equal to those of the scalar current in the NDR scheme, while the latter have already been computed before and can be found in [9–12].

One-loop form factors. At NLO we compute the form factors up to terms of $\mathcal{O}(\epsilon^2)$. Our results are given in terms of a set of coefficient functions $g_i(u)$, which we list in Appendix A. The scalar form factor is IR-divergent and becomes (with $q^2 = \bar{u}m_b^2$, $\bar{u} = 1-u$ and $L = \ln \mu^2/m_b^2$),

$$\begin{aligned} F_{S,-2}^{(1)}(u) &= -C_F, \\ F_{S,-1}^{(1)}(u) &= C_F\big(g_0(u) - L\big), \\ F_{S,0}^{(1)}(u) &= C_F\left(g_1(u) + \big[g_0(u)+3\big]L - \frac{1}{2}L^2\right), \\ F_{S,1}^{(1)}(u) &= C_F\left(g_2(u) + g_1(u)L + \frac{1}{2}\big[g_0(u)+3\big]L^2 - \frac{1}{6}L^3\right), \\ F_{S,2}^{(1)}(u) &= C_F\left(g_3(u) + g_2(u)L + \frac{1}{2}g_1(u)L^2 + \frac{1}{6}\big[g_0(u)+3\big]L^3 - \frac{1}{24}L^4\right). \end{aligned} \tag{11}$$

The first tensor form factor is also IR-divergent and given by

$$\begin{aligned} F_{T,-2}^{1,(1)}(u) &= \frac{C_F}{2}, \\ F_{T,-1}^{1,(1)}(u) &= -\frac{C_F}{2}\big(g_0(u) - L\big), \\ F_{T,0}^{1,(1)}(u) &= -\frac{C_F}{2}\left(g_4(u) + \big[g_0(u)-1\big]L - \frac{1}{2}L^2\right), \\ F_{T,1}^{1,(1)}(u) &= -\frac{C_F}{2}\left(g_5(u) + g_4(u)L + \frac{1}{2}\big[g_0(u)-1\big]L^2 - \frac{1}{6}L^3\right), \\ F_{T,2}^{1,(1)}(u) &= -\frac{C_F}{2}\left(g_6(u) + g_5(u)L + \frac{1}{2}g_4(u)L^2 + \frac{1}{6}\big[g_0(u)-1\big]L^3 - \frac{1}{24}L^4\right), \end{aligned} \tag{12}$$

whereas the other tensor form factors are IR-finite at NLO and read

Author's personal copy

$$
\begin{aligned}
F_{T,0}^{2,(1)}(u) &= 0,\\
F_{T,1}^{2,(1)}(u) &= C_F g_7(u),\\
F_{T,2}^{2,(1)}(u) &= C_F\big(g_8(u) + g_7(u)L\big),
\end{aligned}
\tag{13}
$$

$$
\begin{aligned}
F_{T,0}^{3,(1)}(u) &= C_F g_9(u),\\
F_{T,1}^{3,(1)}(u) &= C_F\big(g_{10}(u) + g_9(u)L\big),\\
F_{T,2}^{3,(1)}(u) &= C_F\left(g_{11}(u) + g_{10}(u)L + \frac{1}{2}g_9(u)L^2\right),
\end{aligned}
\tag{14}
$$

$$
\begin{aligned}
F_{T,0}^{4,(1)}(u) &= 0,\\
F_{T,1}^{4,(1)}(u) &= C_F g_{12}(u),\\
F_{T,2}^{4,(1)}(u) &= C_F\big(g_{13}(u) + g_{12}(u)L\big).
\end{aligned}
\tag{15}
$$

Two-loop form factors. At NNLO the IR-divergent parts of the form factors can be expressed in terms of the one-loop coefficient functions $g_i(u)$. The divergent terms of the scalar form factor read

$$
\begin{aligned}
F_{S,-4}^{(2)}(u) &= \frac{1}{2}C_F^2,\\
F_{S,-3}^{(2)}(u) &= C_F^2\big(L - g_0(u)\big) + \frac{11}{4}C_A C_F - n_l T_F C_F,\\
F_{S,-2}^{(2)}(u) &= C_F^2\left[L^2 - \big(2g_0(u) + 3\big)L + \frac{1}{2}g_0(u)^2 - g_1(u)\right] + \frac{4}{3}LT_F C_F\\
&\quad + C_A C_F\left[\frac{11}{6}\big(L - g_0(u)\big) - \frac{67}{36} + \frac{\pi^2}{12}\right] + n_l T_F C_F\left[\frac{5}{9} - \frac{2}{3}\big(L - g_0(u)\big)\right],\\
F_{S,-1}^{(2)}(u) &= C_F^2\left[\frac{2}{3}L^3 - \left(2g_0(u) + \frac{9}{2}\right)L^2 - \big(2g_1(u) - g_0(u)^2 - 3g_0(u)\big)L\right.\\
&\quad \left. + g_0(u)g_1(u) - g_2(u) - \frac{3}{8} + \frac{\pi^2}{2} - 6\zeta_3\right]\\
&\quad + C_A C_F\left[\left(\frac{\pi^2}{6} - \frac{67}{18}\right)\big(L - g_0(u)\big) + \frac{461}{216} - \frac{17\pi^2}{24} + \frac{11}{2}\zeta_3\right]\\
&\quad + n_l T_F C_F\left[\frac{10}{9}\big(L - g_0(u)\big) - \frac{25}{54} + \frac{\pi^2}{6}\right]\\
&\quad + T_F C_F\left[2L^2 - \frac{4}{3}g_0(u)L + \frac{\pi^2}{9}\right],
\end{aligned}
\tag{16}
$$

and for the first tensor form factor we get

$$
\begin{aligned}
F_{T,-4}^{1,(2)}(u) &= -\frac{1}{4}C_F^2,\\
F_{T,-3}^{1,(2)}(u) &= -\frac{1}{2}C_F^2\big(L - g_0(u)\big) - \frac{11}{8}C_A C_F + \frac{1}{2}n_l T_F C_F,\\
F_{T,-2}^{1,(2)}(u) &= -\frac{1}{2}C_F^2\left[L^2 - \big(2g_0(u) - 1\big)L + \frac{1}{2}g_0(u)^2 - g_4(u)\right] - \frac{2}{3}LT_F C_F
\end{aligned}
$$

Author's personal copy

$$
\begin{aligned}
&-\frac{1}{2}C_A C_F\left[\frac{11}{6}\big(L-g_0(u)\big)-\frac{67}{36}+\frac{\pi^2}{12}\right]-\frac{1}{2}n_l T_F C_F\left[\frac{5}{9}-\frac{2}{3}\big(L-g_0(u)\big)\right],\\
F^{1,(2)}_{T,-1}(u)=&-\frac{1}{2}C_F^2\left[\frac{2}{3}L^3-\left(2g_0(u)-\frac{3}{2}\right)L^2-\big(2g_4(u)-g_0(u)^2+g_0(u)\big)L\right.\\
&\left.+g_0(u)g_4(u)-g_5(u)-\frac{3}{8}+\frac{\pi^2}{2}-6\zeta_3\right]\\
&-\frac{1}{2}C_A C_F\left[\left(\frac{\pi^2}{6}-\frac{67}{18}\right)\big(L-g_0(u)\big)+\frac{461}{216}-\frac{17\pi^2}{24}+\frac{11}{2}\zeta_3\right]\\
&-\frac{1}{2}n_l T_F C_F\left[\frac{10}{9}\big(L-g_0(u)\big)-\frac{25}{54}+\frac{\pi^2}{6}\right]\\
&-\frac{1}{2}T_F C_F\left[2L^2-\frac{4}{3}g_0(u)L+\frac{\pi^2}{9}\right].
\end{aligned}
\tag{17}
$$

The IR-divergent parts of the other tensor form factors are given by

$$
F^{2,(2)}_{T,-1}(u)=-C_F^2 g_7(u),
\tag{18}
$$

and

$$
\begin{aligned}
F^{3,(2)}_{T,-2}(u)&=-C_F^2 g_9(u),\\
F^{3,(2)}_{T,-1}(u)&=C_F^2\big(g_0(u)g_9(u)-g_{10}(u)-2g_9(u)L\big),
\end{aligned}
\tag{19}
$$

and

$$
F^{4,(2)}_{T,-1}(u)=-C_F^2 g_{12}(u).
\tag{20}
$$

The finite parts of the two-loop form factors involve a new set of coefficient functions $h_i(u)$, which we specify in Appendix B. We find

$$
\begin{aligned}
F^{(2)}_{S,0}(u)=&\,C_F^2\left[\frac{1}{3}L^4-\left(\frac{4}{3}g_0(u)+\frac{7}{2}\right)L^3-\left(2g_1(u)-g_0(u)^2-\frac{9}{2}g_0(u)-\frac{9}{2}\right)L^2\right.\\
&\left.-\left(2g_2(u)-2g_1(u)g_0(u)-3g_1(u)-\frac{3}{4}-\pi^2+12\zeta_3\right)L+h_1(u)\right]\\
&+C_A C_F\left[-\frac{11}{18}L^3+\left(\frac{11}{6}g_0(u)+\frac{16}{9}+\frac{\pi^2}{6}\right)L^2\right.\\
&\left.+\left(\frac{11}{3}g_1(u)+\left(\frac{67}{9}-\frac{\pi^2}{3}\right)g_0(u)+\frac{2207}{108}-\frac{17\pi^2}{12}+11\zeta_3\right)L+h_2(u)\right]\\
&+n_l T_F C_F\left[\frac{2}{9}L^3-\left(\frac{2}{3}g_0(u)+\frac{8}{9}\right)L^2-\left(\frac{4}{3}g_1(u)+\frac{20}{9}g_0(u)+\frac{115}{27}-\frac{\pi^2}{3}\right)L\right.\\
&\left.-\frac{4}{3}g_2(u)-\frac{20}{9}g_1(u)-\left(\frac{20}{27}+\frac{\pi^2}{3}\right)g_0(u)-\frac{541}{324}-\frac{13\pi^2}{18}+\frac{10}{3}\zeta_3\right]\\
&+T_F C_F\left[\frac{14}{9}L^3-\big(2g_0(u)+2\big)L^2\right.\\
&\left.-\left(\frac{4}{3}g_1(u)+\frac{10}{3}-\frac{2\pi^2}{9}\right)L+h_3(u)\right],
\end{aligned}
\tag{21}
$$

Author's personal copy

and

$$\begin{aligned}
F_{T,0}^{1,(2)}(u) = &-\frac{1}{2}C_F^2\Bigg[\frac{1}{3}L^4 - \left(\frac{4}{3}g_0(u) - \frac{7}{6}\right)L^3 - \left(2g_4(u) - g_0(u)^2 + \frac{3}{2}g_0(u) - \frac{1}{2}\right)L^2 \\
&- \left(2g_5(u) - 2g_4(u)g_0(u) + g_4(u) - \frac{35}{4} - \pi^2 + 12\zeta_3\right)L + h_4(u)\Bigg] \\
&- \frac{1}{2}C_A C_F\Bigg[-\frac{11}{18}L^3 + \left(\frac{11}{6}g_0(u) - \frac{50}{9} + \frac{\pi^2}{6}\right)L^2 \\
&+ \left(\frac{11}{3}g_4(u) + \left(\frac{67}{9} - \frac{\pi^2}{3}\right)g_0(u) - \frac{1081}{108} - \frac{17\pi^2}{12} + 11\zeta_3\right)L + h_5(u)\Bigg] \\
&- \frac{1}{2}n_l T_F C_F\Bigg[\frac{2}{9}L^3 - \left(\frac{2}{3}g_0(u) - \frac{16}{9}\right)L^2 \\
&- \left(\frac{4}{3}g_4(u) + \frac{20}{9}g_0(u) - \frac{53}{27} - \frac{\pi^2}{3}\right)L \\
&- \frac{4}{3}g_5(u) - \frac{20}{9}g_4(u) - \left(\frac{20}{27} + \frac{\pi^2}{3}\right)g_0(u) + h_6(u)\Bigg] \\
&- \frac{1}{2}T_F C_F\Bigg[\frac{14}{9}L^3 - \left(2g_0(u) - \frac{2}{3}\right)L^2 \\
&- \left(\frac{4}{3}g_4(u) - \frac{26}{9} - \frac{2\pi^2}{9}\right)L + h_7(u)\Bigg],
\end{aligned} \tag{22}$$

and

$$F_{T,0}^{2,(2)}(u) = C_F^2\big(g_0(u)g_7(u) - g_8(u) - 2g_7(u)L\big), \tag{23}$$

and

$$\begin{aligned}
F_{T,0}^{3,(2)}(u) = &\, C_F^2\big[-2g_9(u)L^2 + \big(2g_0(u)g_9(u) - g_9(u) - 2g_{10}(u)\big)L + h_8(u)\big] \\
&+ C_A C_F\left[\frac{11}{3}g_9(u)L + h_9(u)\right] + T_F C_F\left[-\frac{4}{3}g_9(u)L + h_{10}(u)\right] \\
&+ n_l T_F C_F\left[-\frac{4}{3}g_9(u)L - \frac{4}{3}g_{10}(u) - \frac{8}{9}g_9(u) + \frac{4u}{3\bar{u}^2}\ln(u) + \frac{4u}{3\bar{u}}\right],
\end{aligned} \tag{24}$$

and

$$F_{T,0}^{4,(2)}(u) = C_F^2\big(g_0(u)g_{12}(u) - g_{13}(u) - 2g_{12}(u)L\big). \tag{25}$$

3.2. Matching coefficients

The matching coefficients C_i^j follow from the above expressions for the renormalized form factors F_i^j after multiplication with the inverse of the renormalization factor of the SCET current Z_J, cf. (4). To this end one has to keep in mind that the form factors have been computed in QCD with five active quark flavours, while Z_J is usually given in SCET with four active flavours. We thus have

$$Z_J = 1 + \sum_{k=1}^{\infty}\left(\frac{\alpha_s^{(4)}}{4\pi}\right)^k Z_J^{(k)}, \tag{26}$$

Author's personal copy

with NLO coefficient [2],

$$Z_J^{(1)} = C_F\left\{-\frac{1}{\epsilon^2} - \frac{1}{\epsilon}\left(\ln\frac{\mu^2}{u^2 m_b^2} + \frac{5}{2}\right)\right\}. \tag{27}$$

The two-loop anomalous dimension can be deduced from [22] (see also [10])

$$\begin{aligned} Z_J^{(2)} = C_F\Bigg\{&\frac{C_F}{2\epsilon^4} + \left[\left(\ln\frac{\mu^2}{u^2 m_b^2} + \frac{5}{2}\right)C_F + \frac{11}{4}C_A - n_l T_F\right]\frac{1}{\epsilon^3} \\ &+ \left[\frac{1}{2}\left(\ln\frac{\mu^2}{u^2 m_b^2} + \frac{5}{2}\right)^2 C_F + \left(\frac{\pi^2}{12} - \frac{67}{36} + \frac{11}{6}\left(\ln\frac{\mu^2}{u^2 m_b^2} + \frac{5}{2}\right)\right)C_A \right. \\ &\left. + \left(\frac{5}{9} - \frac{2}{3}\left(\ln\frac{\mu^2}{u^2 m_b^2} + \frac{5}{2}\right)\right)n_l T_F\right]\frac{1}{\epsilon^2} + \left[\left(\frac{\pi^2}{2} - \frac{3}{8} - 6\zeta_3\right)C_F \right. \\ &+ \left(\frac{461}{216} - \frac{17\pi^2}{24} + \frac{11}{2}\zeta_3 + \left(\frac{\pi^2}{6} - \frac{67}{18}\right)\left(\ln\frac{\mu^2}{u^2 m_b^2} + \frac{5}{2}\right)\right)C_A \\ &\left. + \left(\frac{\pi^2}{6} - \frac{25}{54} + \frac{10}{9}\left(\ln\frac{\mu^2}{u^2 m_b^2} + \frac{5}{2}\right)\right)n_l T_F\right]\frac{1}{\epsilon}\Bigg\}, \end{aligned} \tag{28}$$

where $n_l = n_f - 1 = 4$ is the number of active quark flavours in the effective theory.

We now expand the matching coefficients in terms of the coupling constant of the four-flavour theory as

$$C_i^j = \sum_{k=0}^{\infty}\left(\frac{\alpha_s^{(4)}}{4\pi}\right)^k C_i^{j,(k)}, \tag{29}$$

and rewrite (4) up to NNLO, which yields

$$\begin{aligned} C_i^{j,(0)} &= F_i^{j,(0)}, \\ C_i^{j,(1)} &= F_i^{j,(1)} - Z_J^{(1)} F_i^{j,(0)}, \\ C_i^{j,(2)} &= F_i^{j,(2)} + \delta\alpha_s^{(1)} F_i^{j,(1)} - Z_J^{(1)}\left(F_i^{j,(1)} - Z_J^{(1)} F_i^{j,(0)}\right) - Z_J^{(2)} F_i^{j,(0)}. \end{aligned} \tag{30}$$

Notice that the last relation implies a term which stems from the conversion of the five-flavour to the four-flavour coupling constant,

$$\alpha_s^{(5)} = \alpha_s^{(4)}\left[1 + \frac{\alpha_s^{(4)}}{4\pi}\delta\alpha_s^{(1)} + \mathcal{O}\left(\alpha_s^2\right)\right] \tag{31}$$

with (see also [11,12] for further details)

$$\begin{aligned} \delta\alpha_s^{(1)} = T_F\Bigg[&\frac{4}{3}\ln\frac{\mu^2}{m_b^2} + \left(\frac{2}{3}\ln^2\frac{\mu^2}{m_b^2} + \frac{\pi^2}{9}\right)\epsilon + \left(\frac{2}{9}\ln^3\frac{\mu^2}{m_b^2} + \frac{\pi^2}{9}\ln\frac{\mu^2}{m_b^2} - \frac{4}{9}\zeta_3\right)\epsilon^2 \\ &+ \mathcal{O}\left(\epsilon^3\right)\Bigg]. \end{aligned} \tag{32}$$

At LO the matching coefficients then become

$$\begin{aligned} C_S^{(0)} &= -2C_T^{1,(0)} = 1, \\ C_T^{2,(0)} &= C_T^{3,(0)} = C_T^{4,(0)} = 0. \end{aligned} \tag{33}$$

Author's personal copy

At NLO the matching coefficients are given by the finite terms of the one-loop form factors,

$$\begin{aligned} C_S^{(1)}(u) &= F_{S,0}^{(1)}(u), \\ C_T^{1,(1)}(u) &= F_{T,0}^{1,(1)}(u), \\ C_T^{3,(1)}(u) &= F_{T,0}^{3,(1)}(u), \end{aligned} \tag{34}$$

and, in particular, $C_T^{2,(1)} = F_{T,0}^{2,(1)} = 0$ and $C_T^{4,(1)} = F_{T,0}^{4,(1)} = 0$ in accordance with the four-dimensional constraints for the tensor coefficients that we mentioned in Section 2.1. Here and in the following we provide the expressions for the matching coefficients in the limit $\epsilon \to 0$, since the $\mathcal{O}(\epsilon)$ terms are not relevant in two-loop applications.

At NNLO the matching coefficients are no longer given by the finite terms of the respective form factors alone. We now find

$$\begin{aligned} C_S^{(2)}(u) = {} & F_{S,0}^{(2)}(u) \\ & + T_F C_F \left[\frac{4}{9}\zeta_3 + \frac{\pi^2}{9} g_0(u) + \frac{2}{9}\big(6g_1(u) - \pi^2\big)L + \big(2g_0(u) + 4\big)L^2 - \frac{14}{9}L^3 \right] \\ & + C_F^2 \Big[g_3(u) - g_0(u)g_2(u) + \big(2g_2(u) - g_0(u)g_1(u)\big)L \\ & + \frac{1}{2}\big(3g_1(u) - g_0(u)^2 - 3g_0(u)\big)L^2 + \left(\frac{5}{6}g_0(u) + 2\right)L^3 - \frac{5}{24}L^4 \Big], \end{aligned} \tag{35}$$

and

$$\begin{aligned} C_T^{1,(2)}(u) = {} & F_{T,0}^{1,(2)}(u) - \frac{1}{2} T_F C_F \left[\frac{4}{9}\zeta_3 + \frac{\pi^2}{9} g_0(u) + \frac{2}{9}\big(6g_4(u) - \pi^2\big)L \right. \\ & \left. + \left(2g_0(u) - \frac{4}{3}\right)L^2 - \frac{14}{9}L^3 \right] \\ & - \frac{1}{2} C_F^2 \Big[g_6(u) - g_0(u)g_5(u) + \big(2g_5(u) - g_0(u)g_4(u)\big)L \\ & + \frac{1}{2}\big(3g_4(u) - g_0(u)^2 + g_0(u)\big)L^2 + \left(\frac{5}{6}g_0(u) - \frac{2}{3}\right)L^3 - \frac{5}{24}L^4 \Big], \end{aligned} \tag{36}$$

and

$$\begin{aligned} C_T^{3,(2)}(u) = {} & F_{T,0}^{3,(2)}(u) + T_F C_F \left[\frac{4}{3} g_9(u) L \right] \\ & + C_F^2 \left[g_{11}(u) - g_0(u)g_{10}(u) + \big(2g_{10}(u) - g_0(u)g_9(u)\big)L + \frac{3}{2} g_9(u) L^2 \right]. \end{aligned} \tag{37}$$

The other tensor coefficients are again found to fulfill the four-dimensional constraints

$$\begin{aligned} C_T^{2,(2)}(u) &= F_{T,0}^{2,(2)}(u) - C_F^2\big[g_0(u)g_7(u) - g_8(u) - 2g_7(u)L\big] = 0, \\ C_T^{4,(2)}(u) &= F_{T,0}^{4,(2)}(u) - C_F^2\big[g_0(u)g_{12}(u) - g_{13}(u) - 2g_{12}(u)L\big] = 0, \end{aligned} \tag{38}$$

which provides a non-trivial cross check of our calculation.

As a further check of our NNLO results we verified that the matching coefficients obey the renormalization group equation,

Author's personal copy

$$\frac{d}{d\ln\mu}C_i^j(u;\mu)=\left[\Gamma_{\rm cusp}\left(\alpha_s^{(4)}\right)\ln\frac{um_b}{\mu}+\gamma'\left(\alpha_s^{(4)}\right)+\gamma_i\left(\alpha_s^{(5)}\right)\right]C_i^j(u;\mu), \tag{39}$$

which consists of a universal piece related to the renormalization properties of the SCET current with

$$\Gamma_{\rm cusp}\left(\alpha_s^{(4)}\right)=\sum_{k=1}^{\infty}\left(\frac{\alpha_s^{(4)}}{4\pi}\right)^k\Gamma_{\rm cusp}^{(k)},\qquad \gamma'\left(\alpha_s^{(4)}\right)=\sum_{k=1}^{\infty}\left(\frac{\alpha_s^{(4)}}{4\pi}\right)^k\gamma'^{(k)}, \tag{40}$$

and a second term that contains the anomalous dimension of the QCD current with

$$\gamma_i\left(\alpha_s^{(5)}\right)=\sum_{k=1}^{\infty}\left(\frac{\alpha_s^{(5)}}{4\pi}\right)^k\gamma_i^{(k)}. \tag{41}$$

The one- and two-loop coefficients needed for the check read $\Gamma_{\rm cusp}^{(1)}=4C_F$, $\gamma'^{(1)}=-5C_F$,

$$\begin{aligned}\Gamma_{\rm cusp}^{(2)}&=C_AC_F\left[\frac{268}{9}-\frac{4\pi^2}{3}\right]-\frac{80}{9}n_lT_FC_F,\\ \gamma'^{(2)}&=C_F^2\left[2\pi^2-\frac{3}{2}-24\zeta_3\right]+C_AC_F\left[22\zeta_3-\frac{1549}{54}-\frac{7\pi^2}{6}\right]\\ &\quad+n_lT_FC_F\left[\frac{250}{27}+\frac{2\pi^2}{3}\right],\end{aligned} \tag{42}$$

and

$$\begin{aligned}\gamma_S^{(1)}&=6C_F,\qquad \gamma_S^{(2)}=C_F\left[3C_F+\frac{97}{3}C_A-\frac{20}{3}(n_l+1)T_F\right],\\ \gamma_T^{(1)}&=-2C_F,\qquad \gamma_T^{(2)}=C_F\left[19C_F-\frac{257}{9}C_A+\frac{52}{9}(n_l+1)T_F\right].\end{aligned} \tag{43}$$

The twofold structure of (39) can be used to distinguish the scale μ, that governs the renormalization group evolution in SCET, from a second scale ν, that is related to the non-conservation of the scalar/tensor current in QCD. More explicitly the distinction between the scales μ and ν can be accounted for by writing

$$C_i^j(u;\mu,\nu)=C_i^j(u;\mu)+\delta C_i^j(u;\mu,\nu), \tag{44}$$

where the first term on the right-hand side refers to the above expressions for the matching coefficients, $C_i^j(u;\mu)\equiv C_i^j(u)$, while the latter captures the dependence on $\ln(\nu/\mu)$, which vanishes when the two scales are not distinguished. Expanding the new contribution as

$$\delta C_i^j=\sum_{k=1}^{\infty}\left(\frac{\alpha_s^{(4)}(\mu)}{4\pi}\right)^k\delta C_i^{j,(k)}, \tag{45}$$

we find

$$\delta C_i^{j,(1)}(u;\mu,\nu)=\gamma_i^{(1)}C_i^{j,(0)}\ln\frac{\nu}{\mu} \tag{46}$$

in NLO, and

Author's personal copy

$$\delta C_i^{j,(2)}(u;\mu,\nu) = \left[\frac{\gamma_i^{(1)2}}{2} - \gamma_i^{(1)}\beta_0^{(5)}\right] C_i^{j,(0)} \ln^2\frac{\nu}{\mu} + \left[\left(\gamma_i^{(2)} + \frac{4}{3}T_F\gamma_i^{(1)}\ln\frac{\mu^2}{m_b^2}\right)C_i^{j,(0)} + \gamma_i^{(1)}C_i^{j,(1)}(u;\mu)\right]\ln\frac{\nu}{\mu} \tag{47}$$

in NNLO. (Here $\beta_0^{(5)} = 11C_A/3 - 4/3T_F n_f$ refers to the QCD beta-function with $n_f = n_l + 1$ flavours.) Our final results for the matching coefficients with the two scales μ and ν distinct from each other are provided in electronic form in [23].

The matching coefficients with the SCET and QCD scale distinct from each other can be used for additional cross-checks. The scalar coefficient is not independent but can be related to the vector coefficients by means of the equations of motion, yielding [13]

$$C_V^1(u;\mu) + \left(1 - \frac{u}{2}\right)C_V^2(u;\mu) + C_V^3(u;\mu) = \frac{\overline{m}_b(\nu)}{m_b}C_S(u;\mu,\nu), \tag{48}$$

where $\overline{m}_b(\nu)$ is the $\overline{\text{MS}}$ renormalized mass in five-flavour QCD. Due to the conservation of the vector current the left-hand side of (48), which happens to be just the coefficient $C_{f_0}^{(A0)}$ from (54) below, is free of ν. Hence the QCD scale must also drop out of the right-hand side. We checked that our results satisfy (48). An equivalent formulation of (48) was given in [9] in terms of a Ward-identity. Also the tensor coefficients at $u = 1$, corresponding to $q^2 = 0$, can be checked against existing results in the literature, since they enter the $b \to s\gamma$ process. From [24] (see also [25]) one can infer the combinations

$$-2F_T^1(u=1) + \frac{1}{2}F_T^2(u=1) + F_T^3(u=1) \tag{49}$$

and

$$-2C_T^1(u=1;\mu,\nu) + C_T^3(u=1;\mu,\nu). \tag{50}$$

The latter equation can again be checked for distinct μ and ν, and both (49) and (50) agree with the formulas in [24]. Note that (50) is just the coefficient $C_{T_1}^{(A0)}$ from (54) at $u = 1$.

In Fig. 1 we evaluate the matching coefficients for $\mu = \nu = m_b$ and $\alpha_s^{(4)}(m_b) = 0.22$. For completeness we show the full set of matching coefficients C_i^j that we introduced in Table 1. We see that the NNLO corrections are in general moderate and add in each case constructively to the NLO corrections. In Fig. 1 we also show the effect of a finite charm quark mass, which is generally rather small, typically modifying the NNLO correction by about 10–20%.

4. Exclusive semi-leptonic and radiative B decays

With the two-loop matching coefficients C_i^j at hand, we explore several applications to B meson decays in this and the following section. For the numerical study we use the following input parameters: the b-quark pole mass $m_b = 4.8$ GeV; the renormalization scale of the QCD scalar and tensor currents $\nu = m_b$; the hard scale $\mu = m_b$. The strong coupling constant is obtained from $\alpha_s^{(4)}(m_b) = 0.215$ by employing three-loop running ($\Lambda_{\overline{\text{MS}}}^{(n_f=4)} = 290.9$ MeV), which gives $\alpha_s^{(4)}(1.5\text{ GeV}) = 0.349$. When we add the hard spectator-scattering contribution from [14] as required for exclusive processes, we need further parameters (such as moments of light-cone distribution amplitudes), for which we use the same values as [14] including the hard-collinear scale $\mu_{hc} = 1.5$ GeV.

Author's personal copy

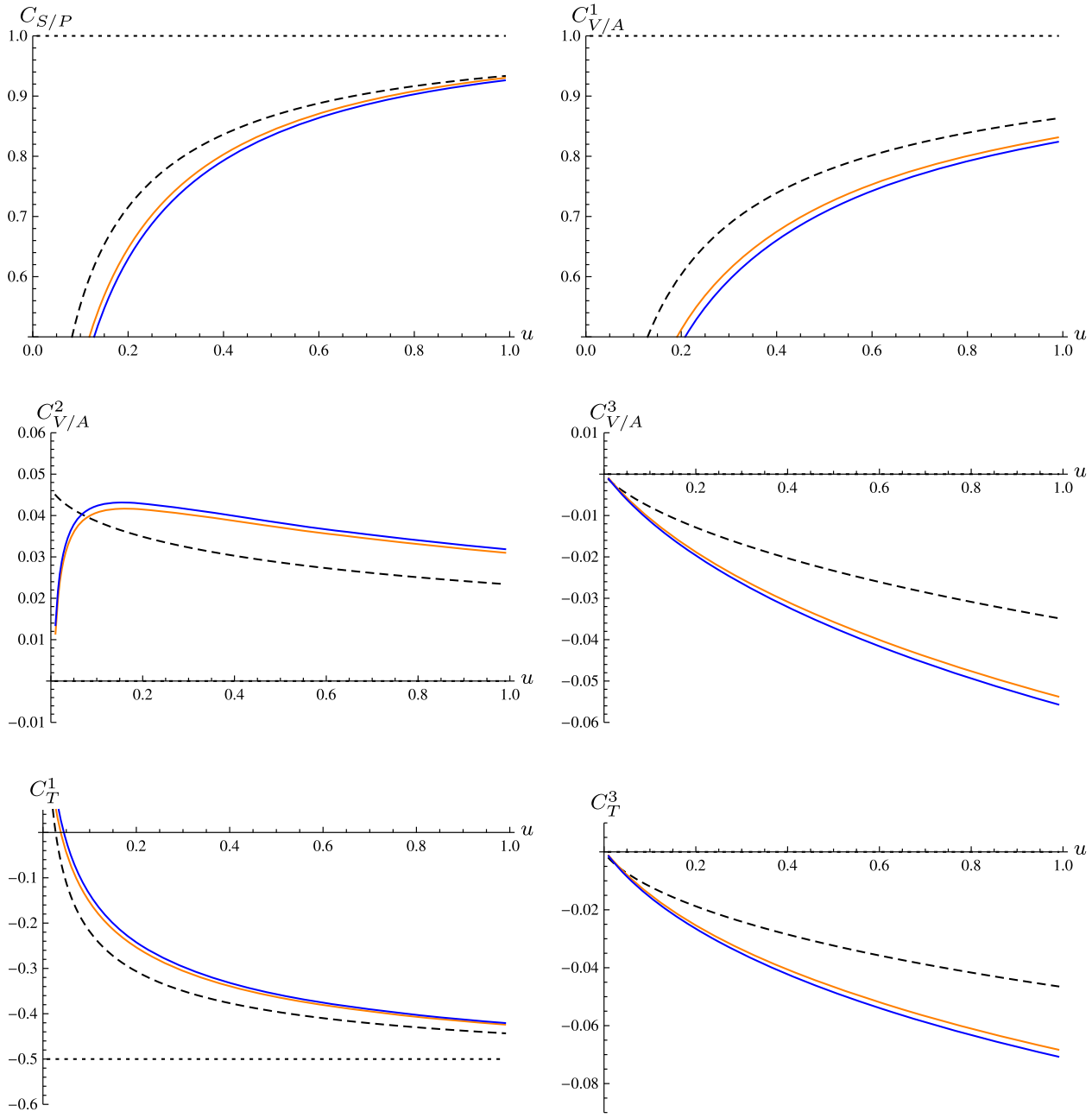

Fig. 1. Matching coefficients C_i^j at the scale $\mu = \nu = m_b$ as a function of u (the momentum transfer is given by $q^2 = (1-u)m_b^2$). The dotted horizontal lines show the tree level results, the dashed lines the one-loop approximation and the solid lines the two-loop approximation with massless charm quarks (orange/light grey) and massive charm quarks with $m_c/m_b = 0.3$ (blue/dark grey).

4.1. Heavy-to-light form factor ratios

The heavy-to-light form factors in the large-recoil regime, where the light meson momentum is parametrically of order of the heavy-quark mass, take the following factorization formula [4,7]

$$F_i^{B\to M}(E) = C_i(E)\xi_a(E) + \int_0^\infty \frac{d\omega}{\omega} \int_0^1 dv\, T_i(E; \ln\omega, v)\phi_{B+}(\omega)\phi_M(v), \tag{51}$$

Author's personal copy

where E denotes the energy of the light meson M, $\xi_a(E)$ is the single non-perturbative form factor (one of two when M is a vector meson), and ϕ_X the light-cone distribution amplitudes of the B meson and the light meson. The short-distance coefficients C_i and the spectator-scattering kernel T_i can be calculated in perturbation theory. The two terms in the above equation correspond to the matrix elements of the two terms in the operator matching equation (1). In particular, the two-loop results from the previous section enter the coefficients $C_i(E)$ of the first term. The spectator-scattering kernels T_i have been calculated at $\mathcal{O}(\alpha_s)$ in [7], and at $\mathcal{O}(\alpha_s^2)$ in [13,14].

In the following we discuss relations between different QCD form factors $F_i^{B\to M}(E)$ that can be deduced from the factorization formula (51). Adopting the same conventions and notations as [14], we can express the three independent $B \to P$ form factors as

$$\begin{aligned}
f_+(E) &= C_{f_+}^{(A0)}(E)\xi_P(E) + \int d\tau\, C_{f_+}^{(B1)}(E,\tau)\Xi_P(\tau,E),\\
\frac{m_B}{2E} f_0(E) &= C_{f_0}^{(A0)}(E)\xi_P(E) + \int d\tau\, C_{f_0}^{(B1)}(E,\tau)\Xi_P(\tau,E),\\
\frac{m_B}{m_B+m_P} f_T(E) &= C_{f_T}^{(A0)}(E)\xi_P(E) + \int d\tau\, C_{f_T}^{(B1)}(E,\tau)\Xi_P(\tau,E),
\end{aligned} \tag{52}$$

and the seven independent $B \to V$ form factors as

$$\begin{aligned}
\frac{m_B}{m_B+m_V} V(E) &= C_V^{(A0)}(E)\xi_\perp(E) + \int d\tau\, C_V^{(B1)}(E,\tau)\Xi_\perp(\tau,E),\\
\frac{m_V}{E} A_0(E) &= C_{f_0}^{(A0)}(E)\xi_\parallel(E) + \int d\tau\, C_{f_0}^{(B1)}(E,\tau)\Xi_\parallel(\tau,E),\\
\frac{m_B+m_V}{2E} A_1(E) &= C_V^{(A0)}(E)\xi_\perp(E) + \int d\tau\, C_V^{(B1)}(E,\tau)\Xi_\perp(\tau,E),\\
\frac{m_B+m_V}{2E} A_1(E) - \frac{m_B-m_V}{m_B} A_2(E) &= C_{f_+}^{(A0)}(E)\xi_\parallel(E) + \int d\tau\, C_{f_+}^{(B1)}(E,\tau)\Xi_\parallel(\tau,E),\\
T_1(E) &= C_{T_1}^{(A0)}(E)\xi_\perp(E) + \int d\tau\, C_{T_1}^{(B1)}(E,\tau)\Xi_\perp(\tau,E),\\
\frac{m_B}{2E} T_2(E) &= C_{T_1}^{(A0)}(E)\xi_\perp(E) + \int d\tau\, C_{T_1}^{(B1)}(E,\tau)\Xi_\perp(\tau,E),\\
\frac{m_B}{2E} T_2(E) - T_3(E) &= C_{f_T}^{(A0)}(E)\xi_\parallel(E) + \int d\tau\, C_{f_T}^{(B1)}(E,\tau)\Xi_\parallel(\tau,E).
\end{aligned} \tag{53}$$

Here m_B represents the B meson mass, m_P and m_V refer to the pseudoscalar and vector light meson masses, respectively. The coefficient functions $C_F^{(A0)}$ and $C_F^{(B1)}$ are defined as linear combinations of the matching coefficients of two- ("A0-type") and three-body ("B-type") SCET operators, while $\Xi_a(\tau,E)$ denotes the matrix elements of the three-body operators $O_i^{(B1)j\mu}(s_1,s_2)$, see (1). In terms of the coefficients C_i^j introduced in previous sections, the five independent A0-coefficients are given by

$$\begin{aligned}
C_{f_+}^{(A0)} &= C_V^1(u;\mu) + \frac{u}{2} C_V^2(u;\mu) + C_V^3(u;\mu),\\
C_{f_0}^{(A0)} &= C_V^1(u;\mu) + \left(1-\frac{u}{2}\right) C_V^2(u;\mu) + C_V^3(u;\mu),\\
C_{f_T}^{(A0)} &= -2C_T^1(u;\mu,\nu) + C_T^2(u;\mu,\nu) - C_T^4(u;\mu,\nu),
\end{aligned}$$

Author's personal copy

$$C_V^{(A0)} = C_V^1(u;\mu),$$
$$C_{T_1}^{(A0)} = -2C_T^1(u;\mu,\nu) + \left(1-\frac{u}{2}\right)C_T^2(u;\mu,\nu) + C_T^3(u;\mu,\nu). \tag{54}$$

Recall that in $D=4$ dimensions one has $C_T^2 = C_T^4 = 0$. The variable E used in (52) and (53) is related to u through $u = 2E/m_B$. The five independent B-coefficients are given in Appendix A2 of [14].

From (52) and (53), we have the following two identities

$$\frac{m_B}{m_B+m_V}V(E) = \frac{m_B+m_V}{2E}A_1(E), \qquad T_1(E) = \frac{m_B}{2E}T_2(E) \tag{55}$$

up to power corrections [26]. In the physical form factor scheme [7,14], where the $\mathrm{SCET_I}$ form factors $\xi_a(E)$ are defined in terms of three QCD form factors,

$$\xi_P^{\mathrm{FF}} \equiv f_+, \qquad \xi_\perp^{\mathrm{FF}} \equiv \frac{m_B}{m_B+m_V}V, \qquad \xi_\parallel^{\mathrm{FF}} \equiv \frac{m_B+m_V}{2E}A_1 - \frac{m_B-m_V}{m_B}A_2, \tag{56}$$

the five remaining form factors read

$$\frac{m_B}{2E}f_0 = R_0\xi_P^{\mathrm{FF}} + \left(C_{f_0}^{(B1)} - C_{f_+}^{(B1)}R_0\right)\star\Xi_P,$$
$$\frac{m_B}{m_B+m_P}f_T = R_T\xi_P^{\mathrm{FF}} + \left(C_{f_T}^{(B1)} - C_{f_+}^{(B1)}R_T\right)\star\Xi_P,$$
$$T_1 = R_\perp\xi_\perp^{\mathrm{FF}} + \left(C_{T_1}^{(B1)} - C_V^{(B1)}R_\perp\right)\star\Xi_\perp,$$
$$\frac{m_V}{E}A_0 = R_0\xi_\parallel^{\mathrm{FF}} + \left(C_{f_0}^{(B1)} - C_{f_+}^{(B1)}R_0\right)\star\Xi_\parallel,$$
$$\frac{m_B}{2E}T_2 - T_3 = R_T\xi_\parallel^{\mathrm{FF}} + \left(C_{f_T}^{(B1)} - C_{f_+}^{(B1)}R_T\right)\star\Xi_\parallel. \tag{57}$$

In this scheme there are only three non-trivial ratios R and three non-trivial combinations of B-coefficients, defined, respectively, as

$$\begin{aligned}
R_0(u) \equiv \frac{C_{f_0}^{(A0)}}{C_{f_+}^{(A0)}} &= 1 + \frac{\alpha_s^{(4)}}{4\pi}C_F\left[2+g_9(u)\right]\left[1+\frac{\alpha_s^{(4)}}{4\pi}\beta_0^{(4)}L_\mu\right] \\
&\quad + \left(\frac{\alpha_s^{(4)}}{4\pi}\right)^2\left\{C_F^2 j_1(u) + C_F C_A j_2(u) + C_F n_l T_F j_3(u) + C_F T_F j_4(u)\right\} + \mathcal{O}\left(\alpha_s^3\right), \\
R_T(u) \equiv \frac{C_{f_T}^{(A0)}}{C_{f_+}^{(A0)}} &= 1 + \frac{\alpha_s^{(4)}}{4\pi}C_F\left[-L_\nu - g_9(u)\right]\left[1+\frac{\alpha_s^{(4)}}{4\pi}\beta_0^{(4)}L_\mu\right] \\
&\quad + \left(\frac{\alpha_s^{(4)}}{4\pi}\right)^2\left\{C_F^2\left[\frac{L_\nu^2}{2} + \left(\frac{19}{2}+g_9(u)\right)L_\nu + j_5(u)\right]\right. \\
&\quad + C_F C_A\left[\frac{11L_\nu^2}{6} - \frac{257L_\nu}{18} + j_6(u)\right] \\
&\quad + C_F n_l T_F\left[-\frac{2L_\nu^2}{3} + \frac{26L_\nu}{9} + j_7(u)\right] \\
&\quad \left. + C_F T_F\left[-\frac{2L_\nu^2}{3} + \frac{26L_\nu}{9} + j_8(u)\right]\right\} + \mathcal{O}\left(\alpha_s^3\right),
\end{aligned}$$

Author's personal copy

$$
\begin{aligned}
R_\perp(u) \equiv \frac{C_{T_1}^{(A0)}}{C_V^{(A0)}} &= 1 + \frac{\alpha_s^{(4)}}{4\pi} C_F \left[-L_\nu + \frac{1}{2} g_9(u) \right] \left[1 + \frac{\alpha_s^{(4)}}{4\pi} \beta_0^{(4)} L_\mu \right] \\
&+ \left(\frac{\alpha_s^{(4)}}{4\pi} \right)^2 \left\{ C_F^2 \left[\frac{L_\nu^2}{2} + \left(\frac{19}{2} - \frac{1}{2} g_9(u) \right) L_\nu - \frac{1}{2} j_5(u) + j_9(u) \right] \right. \\
&+ C_F C_A \left[\frac{11 L_\nu^2}{6} - \frac{257 L_\nu}{18} - \frac{1}{2} j_6(u) + j_{10}(u) \right] \\
&+ C_F n_l T_F \left[-\frac{2L_\nu^2}{3} + \frac{26 L_\nu}{9} - \frac{1}{2} j_7(u) + \frac{2\pi^2}{3} + \frac{205}{36} \right] \\
&\left. + C_F T_F \left[-\frac{2L_\nu^2}{3} + \frac{26 L_\nu}{9} - \frac{1}{2} j_8(u) - \frac{4\pi^2}{3} + \frac{421}{36} \right] \right\} + \mathcal{O}(\alpha_s^3),
\end{aligned}
\tag{58}
$$

and

$$
\begin{aligned}
C_{0+}^{(B1)}(\tau, E) &= C_{f_0}^{(B1)}(\tau, E) - C_{f_+}^{(B1)}(\tau, E) R_0(E), \\
C_{T+}^{(B1)}(\tau, E) &= C_{f_T}^{(B1)}(\tau, E) - C_{f_+}^{(B1)}(\tau, E) R_T(E), \\
C_{T_1 V}^{(B1)}(\tau, E) &= C_{T_1}^{(B1)}(\tau, E) - C_V^{(B1)}(\tau, E) R_\perp(E).
\end{aligned}
\tag{59}
$$

We denote $L_\mu = \ln(\mu^2/m_b^2)$, $L_\nu = \ln(\nu^2/m_b^2)$, and $\beta_0^{(4)} = 11/3 C_A - 4/3 T_F n_l$. The functions $j_i(u)$ can be found in Appendix B. One recognizes the relatively simple structure of the ratios R_X in the physical form factor scheme. Compared to the matching coefficients, where we encounter up to the fourth power of logarithms, the ratios R_X have logarithmic dependences that are at most quadratic, since the universal Sudakov logarithms cancel in the ratios.

As expected in any perturbative QCD calculation, the higher-order correction is necessary to eliminate scale ambiguities. While the A0-coefficients $C_X^{(A0)}$ depend on the hard scale μ (which is cancelled by the corresponding dependence of the $\mathrm{SCET_I}$ form factors $\xi_a(E)$), the μ dependence of the ratios R_X $(X = 0, T, \perp)$ arises only from the scale-dependence of $\alpha_s(\mu)$ and should be reduced after including the higher-order correction. In Fig. 2, we show the dependence of the three ratios R_X on the scale μ at $u = 0.85$ (corresponding to the light-meson energy $E = u m_B/2 = 2.24$ GeV or momentum transfer $q^2 = 4.18$ GeV^2) and fixed renormalization scale $\nu = m_b$ of the QCD tensor current. In the absence of radiative and power corrections, all these coefficients equal 1 (dotted lines). We observe that the scale dependence is reduced at the two-loop order for the ratios $R_{0,T}$, but not for $R_\perp$, which receives a large two-loop correction.

Since the A0-type coefficients $C_X^{(A0)}$ and hence the ratios R_X also depend on the momentum transfer q^2, we show in Fig. 3 these coefficients as a function of u (related to light-meson energy $E = u m_B/2$ or momentum transfer $q^2 = (1-u) m_B^2$), with the scales fixed at $\nu = \mu = m_b$. As illustrated in Fig. 3, the NNLO correction to all the five coefficients $C_X^{(A0)}$ is quite similar and adds in each case constructively to the NLO result; among the three ratios R_X, the two-loop correction to $R_\perp$, i.e. to the ratio of the tensor and vector form factor, T_1/V, is most significant.

To further investigate these two-loop corrections to the form factor ratios, following [14] we also take the $B \to \pi$ and $B \to \rho$ transitions as examples. Seven ratios among the total of ten pion and ρ meson form factors can be obtained from the two identities (55), which do not receive any perturbative corrections, and the five relations that follow from (57) by dividing through the appropriate ξ_a^{FF}. The q^2 dependence of these form factor ratios are shown in Fig. 4. As in [14] the q^2-dependence of the ξ_a^{FF} in the normalization of the spectator-scattering correction is taken from

Author's personal copy

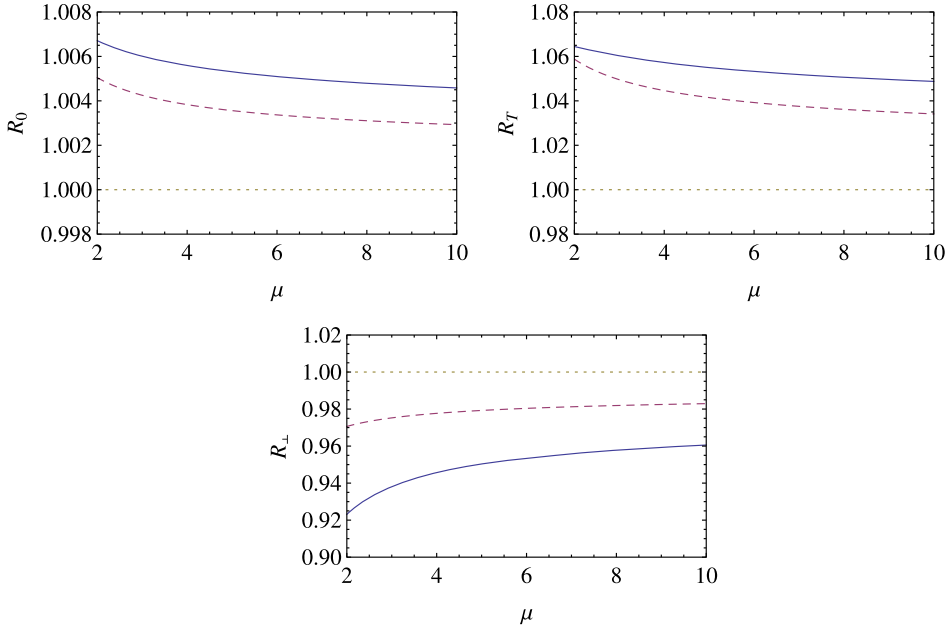

Fig. 2. Dependence of the ratios R_X ($X = 0, T, \perp$) defined in (58) on the scale μ, with $u = 0.85$ (corresponding to the light-meson energy $E = um_B/2 = 2.24$ GeV or momentum transfer $q^2 = 4.18$ GeV^2) and $\nu = m_b$ (the renormalization scale of the QCD tensor current). All of them equal 1 in the absence of radiative and power corrections (dotted line). The solid and dashed lines denote the NNLO and NLO results, respectively.

the QCD sum rule calculation. The ratios are normalized such that in absence of any radiative and power corrections they equal 1 for all q^2. Our final results, including both R_X and the spectator-scattering term to order α_s^2, are shown as solid dark grey (blue in colour) curves, while the results with R_X evaluated only at NLO as solid light grey (orange in colour) ones. One can see that the radiative correction always enhances the symmetry-breaking effect, and the NNLO term is generally quite moderate; the most significant effect from the two-loop correction is on the ratio T_1/V (through the ratio $R_\perp$). To see the relative size of the two terms in the factorization formula (51), we also show the result without the spectator-scattering term (dashed curves with blue/dark grey and orange/light grey denoting the NNLO and NLO results, respectively). Comparing the solid with the dashed curves, one can see that the radiative correction from the A0-coefficients $C_X^{(A0)}$ is always smaller than the spectator-scattering contribution.

To compare our results with the QCD sum rule calculations [27], the sum rule predictions for these form factor ratios are shown as dash-dotted curves in Fig. 4. One notices that, while the sum rule calculation generally satisfies the symmetry relations better than predicted on the basis of the heavy-quark limit corrected by radiative and spectator-scattering effects, see for instance the lower right panel of Fig. 4, there are also significant differences concerning the sign of the correction, which might be due to $1/m_b$ power corrections or ununderstood systematics of the sum rule calculations; further detailed discussions could be found in [7,14,28]. The new two-loop correction does not affect the conclusions on this point.

4.2. Exclusive radiative B decays

As factorization calculations of exclusive radiative and hadronic B decays involving only light mesons make use of the heavy-to-light form factors at maximal recoil, it is of interest to investigate the short-distance corrections at $u = 1$, i.e. $E = m_B/2$ or $q^2 = 0$. In this subsection we shall consider the following two ratios [14]

Author's personal copy

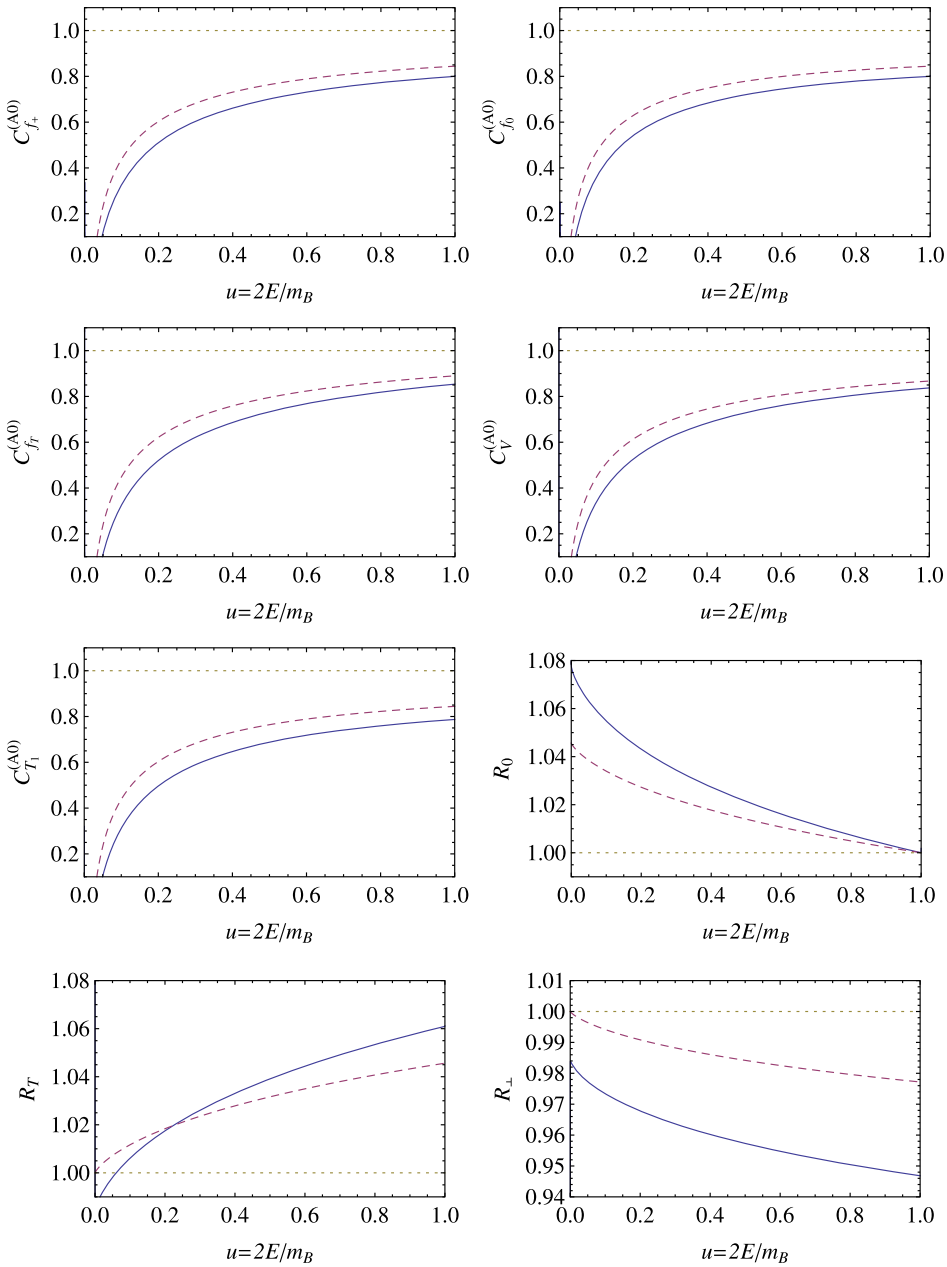

Fig. 3. The A0-type coefficients $C_X^{(A0)}$ and the ratios R_X $(X = 0, T, \perp)$ defined in (58) as a function of u (related to light-meson energy $E = um_B/2$ or momentum transfer $q^2 = (1-u)m_B^2$), with the scales fixed at $\nu = \mu = m_b$. The legend is the same as in Fig. 2.

$$\mathcal{R}_1(E) \equiv \frac{m_B}{m_B + m_P}\frac{f_T(E)}{f_+(E)} = R_T(E) + \int_0^1 d\tau\, C_{T+}^{(B1)}(\tau, E)\frac{\Xi_P(\tau, E)}{f_+(E)},$$

$$\mathcal{R}_2(E) \equiv \frac{m_B + m_V}{m_B}\frac{T_1(E)}{V(E)} = R_\perp(E) + \frac{m_B + m_V}{m_B}\int_0^1 d\tau\, C_{T_1V}^{(B1)}(\tau, E)\frac{\Xi_\perp(\tau, E)}{V(E)}, \tag{60}$$

defined in the physical form factor scheme. Note that in this scheme the above expressions for the form factor ratios are valid independent of the size of the second term, which arises from the

Author's personal copy

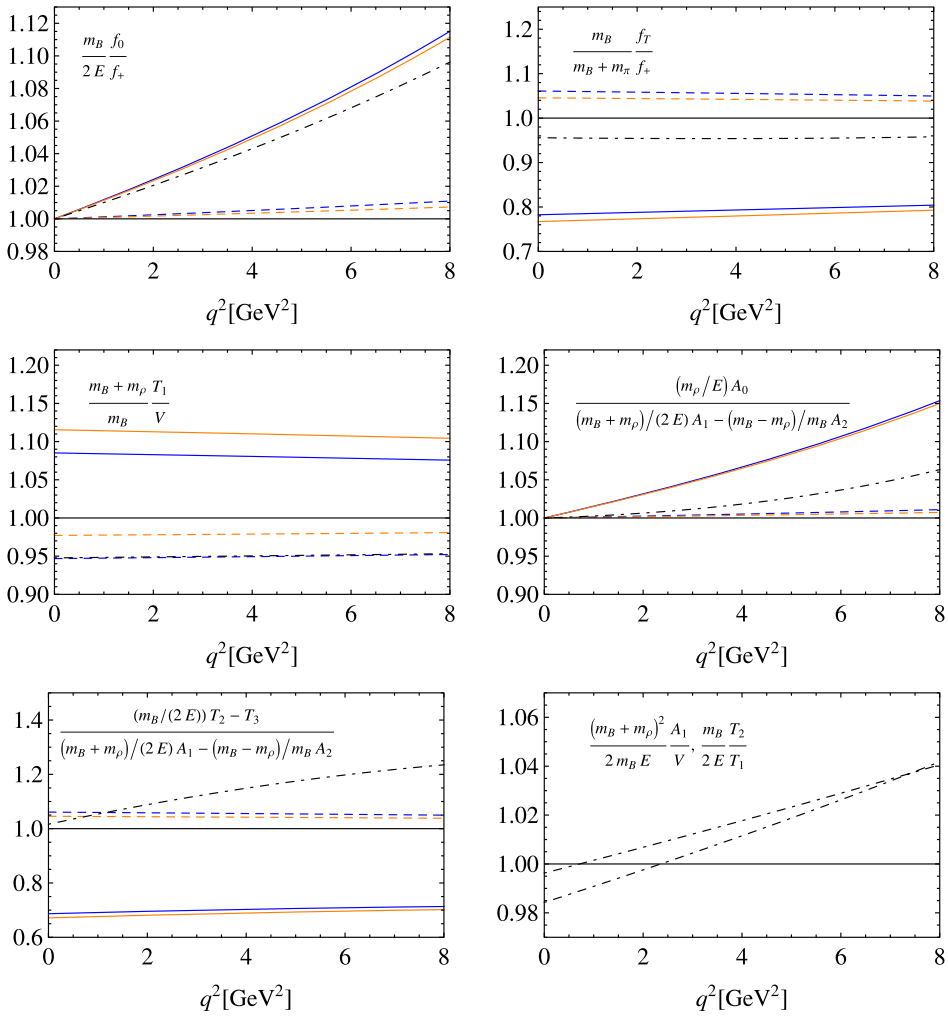

Fig. 4. Corrections to the $B \to \pi$ and $B \to \rho$ form factor ratios as a function of momentum transfer q^2. All the ratios equal 1 in the absence of radiative corrections. Solid curves: full results with R_X evaluated at NNLO (blue/dark grey) and NLO (orange/light grey), including the spectator-scattering term; dashed: results without the spectator-scattering contribution; dash-dotted: results from QCD sum rule calculation. The lower right panel shows the two form factor ratios that equal 1 at leading power. For comparison, the QCD sum rule results for these two ratios are also shown (upper line refers to A_1/V, lower line to T_2/T_1).

spectator-scattering term in (51), relative to the first one. Thus, the issue of whether the spectator contribution should be counted as $\mathcal{O}(\alpha_s)$ or rather $\mathcal{O}(1)$ debated in [29] has no bearing on (60).

At $u = 1$ and assuming the asymptotic form for the light-meson distribution amplitude $\phi_M(v) = 6v\bar{v}$, the analytic expressions for these two ratios simplify considerably, even at NNLO. As the spectator-scattering contribution is already given by Eq. (124) in [14], here we give only the expressions for the ratios $R_{T,\perp}$ at $u = 1$ (as a consequence of the equations of motion, we have $R_0(u = 1) \equiv 1$),

$$R_T(u=1) = 1 + \frac{\alpha_s^{(4)}}{4\pi}\left[\frac{8}{3} - \frac{4}{3}L_\nu\right] + \left(\frac{\alpha_s^{(4)}}{4\pi}\right)^2\left[-\frac{100}{9}L_\mu L_\nu + \frac{200}{9}L_\mu + 6L_\nu^2 - \frac{922}{27}L_\nu - \frac{16}{3}\zeta(3) + \frac{10}{3}\pi^4 - \frac{952}{27}\pi^2 + \frac{8047}{162} + \frac{128}{27}\pi^2\ln 2\right],$$

$$R_\perp(u=1) = 1 + \frac{\alpha_s^{(4)}}{4\pi}\left[-\frac{4}{3} - \frac{4}{3}L_\nu\right] + \left(\frac{\alpha_s^{(4)}}{4\pi}\right)^2\left[-\frac{100}{9}L_\mu L_\nu - \frac{100}{9}L_\mu + 6L_\nu^2 - \frac{778}{27}L_\nu\right.$$

Author's personal copy

$$+4\zeta(3)-\frac{5}{3}\pi^4+\frac{428}{27}\pi^2-\frac{13\,013}{162}-\frac{88}{27}\pi^2\ln 2\Big], \tag{61}$$

with $L_\mu=\ln(\mu^2/m_b^2)$, $L_\nu=\ln(\nu^2/m_b^2)$, and $n_l=4$ has been used. Using the three-loop running coupling and specifying to the pion ($\mathcal{R}_1$) and ρ meson ($\mathcal{R}_2$), numerically we obtain (setting $\nu=\mu=m_b$)

$$\begin{aligned}
\mathcal{R}_1(E_{\max}) &= 1+\big[0.046(\text{NLO})+0.015(\text{NNLO})\big](R_T)\\
&\quad -0.160\big\{1+0.524(\text{NLO spec.})-0.002\big(\delta_{\log}^{\|}\big)\big\}\\
&= 0.817,\\
\mathcal{R}_2(E_{\max}) &= 1-\big[0.023(\text{NLO})+0.030(\text{NNLO})\big](R_\perp)\\
&\quad +0.084\big\{1+0.406(\text{NLO spec.})+0.032\big(\delta_{\log}^{\|}\big)\big\}\\
&= 1.067.
\end{aligned} \tag{62}$$

In these expressions we separated the symmetry-conserving (first number, normalized to 1), A0- and B-type corrections (denoted by $R_{T,\perp}$ and the remaining terms, respectively). The parameter $\delta_{\log}^{\|}$ denotes the small effect from renormalization-group summation and has the same meaning as in Eq. (124) of [14]. We observe that the A0-type and spectator-scattering corrections always have opposite sign, but the latter are larger (though not $\mathcal{O}(1)$) and determine the sign of the deviation from the symmetry limit. We also notice that the two-loop correction to $R_\perp$ is more significant than to R_T. The small numerical difference of spectator-scattering contribution relative to Eq. (124) in [14] is due to the fact that now the three-loop running coupling is used. For comparison the QCD sum rule calculation [27] gives $\mathcal{R}_1=0.955$ and $\mathcal{R}_2=0.947$. For the tensor-to-vector ratio $\mathcal{R}_2$, one notices that the sign of the symmetry-breaking correction between these two methods is opposite. Since the form factor ratio T_1/V is important for radiative and electroweak penguin decays (see the discussion in Section 5.2 of [14]), the discrepancy between the SCET and QCD sum rules results for $\mathcal{R}_2$ suggests that a dedicated analysis of symmetry breaking corrections to form factors (rather than the form factors themselves) with the QCD sum rule method should be performed.

5. Semi-inclusive $\bar{B}\to X_s\ell^+\ell^-$ decays

Rare inclusive B-meson decays induced by the quark level transition $b\to s\ell^+\ell^-$ are highly sensitive to new physics. Due to the presence of two extra operators $(\bar{\ell}\ell)_{V,A}(\bar{s}b)_{V-A}$ in the effective Hamiltonian and the availability of additional kinematical observables, such as the dilepton invariant mass (q^2) spectrum and the forward–backward asymmetry, the $b\to s\ell^+\ell^-$ decay provides complementary information relative to the radiative $b\to s\gamma$ process.

The exclusive decay process $B\to K^*\ell^+\ell^-$ has been studied in great detail, both with respect to its QCD dynamics [30] and to the sensitivity of various observables to new physics [31], because it can be measured relatively easily at hadron colliders. Also on the inclusive decay process $\bar{B}\to X_s\ell^+\ell^-$ dedicated work exists on higher order radiative corrections (see [32] for recent reviews), power corrections [33,34], and on the identification of additional kinematic observables [35].

The low dilepton invariant mass region, $1\ \text{GeV}^2\leqslant q^2\leqslant 6\ \text{GeV}^2$ is particularly interesting, since it benefits from smaller theoretical uncertainties and a higher rate. At somewhat higher q^2 the spectrum is dominated by charmonium resonances (which also determine the integrated

Author's personal copy

decay rate, see the discussion in [36]). On the other hand, for $q^2 < 1\ \mathrm{GeV}^2$, the branching ratio is determined largely by the contribution from almost real intermediate photons, and hence contains essentially the same information as the $b \to s\gamma$ transition.

In the following we discuss semi-inclusive $\bar{B} \to X_s \ell^+ \ell^-$ decay, where the hadronic final state X_s is constrained to have small invariant mass m_X and q^2 is in the range from 1 GeV^2 to 6 GeV^2. In this kinematic region (the so-called "shape function region"), the outgoing hadronic state is jet-like and the relevant degrees of freedom are hard-collinear and soft modes. The semi-inclusive decay rates can be calculated by matching the effective weak interaction Hamiltonian to soft-collinear effective theory. At the leading order in the $\Lambda_{\mathrm{QCD}}/m_b$ expansion, the decay rates can be factorized into process-dependent hard functions $h^{[0]}$, related to physics at the hard scale $\mu \sim m_b$ and above, a universal jet function J, related to physics at the intermediate hard-collinear scale $\mu_{hc} \sim \sqrt{m_b \Lambda_{\mathrm{QCD}}}$, as well as a universal non-perturbative shape function S, describing the internal soft dynamics of the B meson, with the following schematic form [37,38]

$$\mathrm{d}\Gamma^{[0]} = h^{[0]} \times J \otimes S, \tag{63}$$

a result already applied extensively to inclusive $\bar{B} \to X_u \ell \bar{\nu}$ and $\bar{B} \to X_s \gamma$ decays in the shape-function region. The two-loop matching coefficients of the tensor currents calculated in the present paper provide further input to reaching NNLO (α_s^2) accuracy in $h^{[0]}$ and the entire differential decay rate $\mathrm{d}\Gamma^{[0]}$. Compared to exclusive decays mediated by the $b \to s\ell^+\ell^-$ transition [30] the semi-inclusive case has the advantage that the theoretically less certain spectator-scattering contributions to the currents that enter the exclusive form factors are power-suppressed and can be dropped.

In the following we will be mainly interested in the forward–backward asymmetry of the differential rate integrated up to an invariant mass m_X^{cut} in the final state. We briefly review the theoretical description of this quantity, adopting the same conventions and notation as [38], to which we also refer for further details. The short-distance coefficients $h^{[0]}$ at the hard matching scale μ are composed of products of two factors, since the hadronic part of the effective weak interaction Hamiltonian is first matched to two QCD (rather than SCET) currents,

$$J_9^\mu = \bar{s}\gamma^\mu P_L b, \qquad J_7^\mu = \frac{2m_b}{q^2} \bar{s} i q_\rho \sigma^{\rho\mu} P_R b \bigg|_{\nu = m_b}, \tag{64}$$

with coefficients $C_i^{\mathrm{incl}}(q^2, \mu)$ and $P_{L,R} = (1 \mp \gamma_5)/2$. Moreover, m_b in J_7^μ refers to the bottom quark pole mass. The QCD currents are then related to the corresponding SCET currents,

$$\begin{aligned} J_9^\mu &= \sum_{i=1,2,3} c_i^9(u,\mu)[\bar{\xi} W_{hc}] \Gamma_{9,i}^\mu h_v, \\ J_7^\mu &= \frac{2m_b}{q^2} \sum_{i=1,2} c_i^7(u,\mu)[\bar{\xi} W_{hc}] \Gamma_{7,i}^\mu h_v. \end{aligned} \tag{65}$$

These equations represent the momentum space versions of (1). The variable u is related to the kinematics of the process by $u = p^-/m_b$, where

$$p^- = n_+ p = m_b - \frac{q^2}{m_B - p_X^+}, \tag{66}$$

and $p_X^+ = n_- p_X \ll m_B$ is the small light-cone component of the hadronic final state's momentum. The basis of Dirac structures is chosen as

Author's personal copy

$$\Gamma^{\mu}_{9,i} = P_R\{\gamma^\mu, v^\mu, q^\mu\},$$
$$\Gamma^{\mu}_{7,i} = P_R\{iq_\nu\sigma^{\nu\mu}, q_\nu(q^\nu v^\mu - q^\mu v^\nu)\}. \tag{67}$$

As noted in [38], the choice of q^μ instead of n_-^μ for $\Gamma^{\mu}_{9,3}$ is convenient here as it makes explicit the constraint from lepton current conservation, which implies that for massless leptons c_3^9 does not contribute, while for $\Gamma^{\mu}_{7,i}$ there are only two independent coefficients. Transforming the basis (67) to our operator basis listed in Table 1, the matching coefficients c_i^9 and c_i^7 are given, respectively, as

$$\begin{aligned}
c_1^9(u,\mu) &= C_V^1(u;\mu),\\
c_2^9(u,\mu) &= C_V^2(u;\mu) + \frac{2}{u}C_V^3(u;\mu),\\
c_3^9(u,\mu) &= -\frac{2}{um_b}C_V^3(u;\mu),\\
c_1^7(u,\mu) &= -2C_T^1(u;\mu,\nu=m_b) + C_T^3(u;\mu,\nu=m_b),\\
c_2^7(u,\mu) &= -\frac{2}{um_b}C_T^3(u;\mu,\nu=m_b).
\end{aligned} \tag{68}$$

The two-loop matching coefficients c_i^9 for the vector current have become available in the context of inclusive semi-leptonic B decays [9–12]. The results of this paper allow us to compute also the matching coefficients c_i^7 at NNLO. As a consequence the factor in $h^{[0]}$ related to the QCD current matching is now complete at NNLO, while the other factor related to $C_i^{\text{incl}}(q^2,\mu)$ is known at the next-to-next-to-leading logarithmic (NNLL) order, since the three-loop $\mathcal{O}(\alpha_s^2)$ matrix elements of the current–current operators (giving rise to charm-loop diagrams) are not available.

In Fig. 5 we show these matching coefficients as a function of u in the one- (dashed) and two-loop (solid) approximation, evaluated at $\mu = m_b = 4.8$ GeV (blue/dark grey curves) and at $\mu = 1.5$ GeV (orange/light grey curves), respectively. The difference between these two different choices of the IR factorization scale μ is compensated by the corresponding scale dependence of the convolution $J \otimes S$ such that the differential rate (63) is μ-independent. Note that, while we show the entire range of u, Eq. (66) implies that the relevant values of u for $b \to s\ell^+\ell^-$ in the q^2 region of interest are above $u \approx 0.75$. In the lower right panel of Fig. 5, we also show the ratio c_1^7/c_1^9, which equals the quantity $R_\perp$ defined earlier in (58) at $\nu = m_b$, and plays an important role for the forward–backward asymmetry as discussed below. Note that $R_\perp$ is μ-independent, except for the truncation of the perturbative series. In evaluating this ratio to a given order in α_s, we expand the denominator and truncate the expanded expression.

Comparing the dashed (one-loop approximation) and solid (two-loop approximation) curves of the same colour in Fig. 5, we observe that the two-loop corrections are generally moderate in the large u (low q^2) region, whereas the large correction in the region of small u is due to the fact that increasing powers of large logarithms take over in this region. However, the correction is amplified in the ratio $R_\perp$, where the two-loop correction exceeds the one-loop term. This leads to a considerable residual μ-dependence (difference of blue/dark grey and orange/light grey curves) as can also be seen in Fig. 2. Since the infrared physics drops out from the ratio c_1^7/c_1^9 the natural scale is of order of the hard scale m_b.

The differential decay rate (63) can be written as

$$\frac{d^3\Gamma}{dq^2\,dp_X^+\,d\cos\theta} = \frac{3}{8}\big[(1+\cos^2\theta)H_T(q^2,p_X^+) + 2(1-\cos^2\theta)H_L(q^2,p_X^+)$$

Author's personal copy

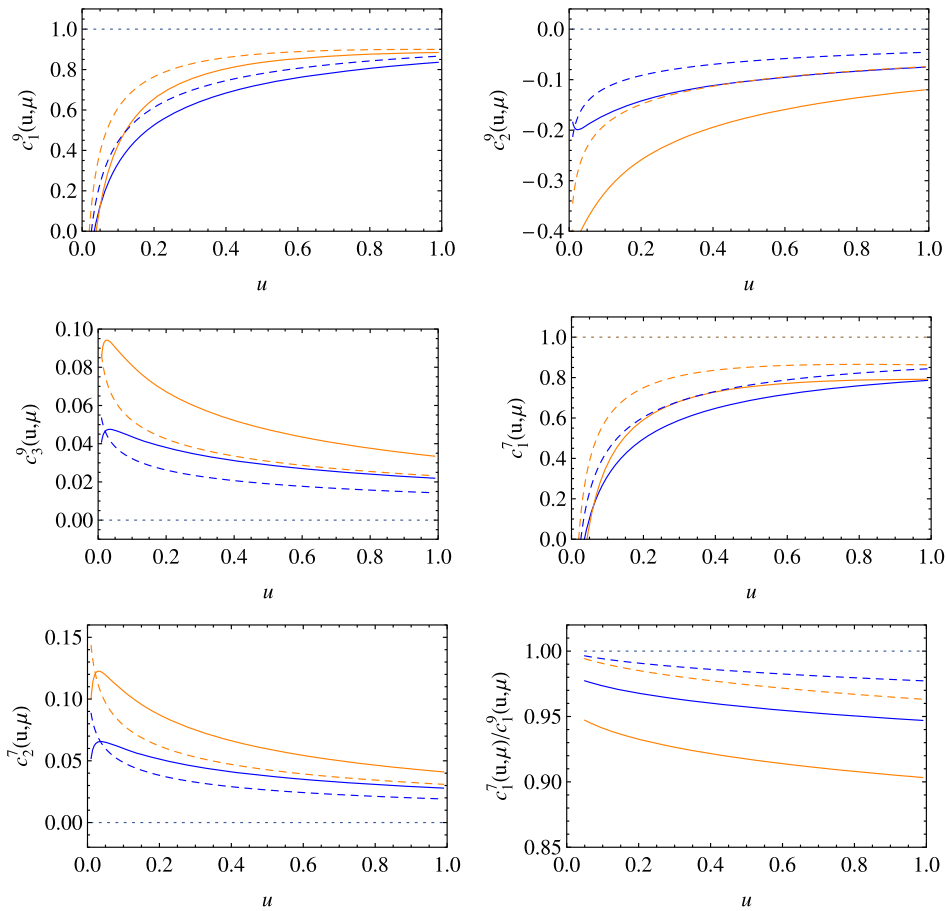

Fig. 5. The matching coefficients $c_i^9(u,\mu)$ and $c_i^7(u,\mu)$ as a function of u (related to the dilepton invariant mass $q^2 = (1-u)m_b^2$) in the one-loop (dashed) and two-loop (solid) approximation. The blue/dark grey curves refer to $\mu = m_b = 4.8$ GeV, and the orange/light grey ones to $\mu = 1.5$ GeV.

$$+ 2\cos\theta\, H_A\big(q^2, p_X^+\big)\Big], \tag{69}$$

where for $\bar{B}$ decay, θ denotes the angle between the positively charged lepton and the $\bar{B}$ meson in the centre-of-mass frame of the $\ell^+\ell^-$ pair. For fixed p_X^+, the forward–backward asymmetry in θ therefore vanishes for a particular q_0^2 at which $H_A(q_0^2, p_X^+) = 0$. Integrating over the invariant mass of the hadronic final state up to the cut m_X^{cut}, the asymmetry zero occurs at

$$\begin{aligned} 0 &= \int_0^{p_X^{+\text{cut}}} dp_X^+\, H_A\big(q_0^2, p_X^+\big) \\ &= \text{const} \times \int_0^{p_X^{+\text{cut}}} dp_X^+\, h_A^{[0]}\big(q_0^2, p_X^+\big) \frac{(q_{0+} - q_{0-})^2}{q_{0+}} q_0^2 \int d\omega\, p^- J\big(p^-\omega\big) S\big(p_X^+ - \omega\big), \end{aligned} \tag{70}$$

where [38] $q_+ = m_B - p_X^+$, $q_- = q^2/q_+$,

$$p_X^{+\text{cut}} = \frac{1}{2m_B}\Big[m_B^2 + \big(m_X^{\text{cut}}\big)^2 - q^2 - \sqrt{\big(m_B^2 + \big(m_X^{\text{cut}}\big)^2 - q^2\big)^2 - 4m_B^2\big(m_X^{\text{cut}}\big)^2}\,\Big], \tag{71}$$

Author's personal copy

and

$$h_A^{[0]}(q^2, p_X^+) = 2\mathcal{C}_{10} c_1^9(u)\,\mathrm{Re}\left[C_9^{\mathrm{incl}}(q^2)c_1^9(u) + \frac{2m_b}{q_-}C_7^{\mathrm{incl}}(q^2)c_1^7(u)\right]. \tag{72}$$

We now observe that $h_A^{[0]}(q_0^2, p_X^+)$ depends on p_X^+ only through the definition of u in (66) and the kinematic factor $2m_b/q_-$. For typical m_X^{cut} of 2 GeV this dependence is very weak, since then $p_X^+ \sim 1$ GeV $\ll m_B$. Thus, p_X^+ appears only as a small correction to $m_B - p_X^+$, and in the definition of u in a term that is additionally suppressed by q^2/m_B relative to m_b, see (66). This results in a very small variation of u of about 0.02 over the entire p_X^+ integration region. We may therefore pull the slowly varying function $h_A^{[0]}(q_0^2, p_X^+)$ in front of the p_X^+ integration in (70) thereby replacing p_X^+ in the argument by an average value which we assume to be $\langle p_X^+\rangle = p_X^{+\mathrm{cut}}/2$. The remaining integral over the jet and soft function is different from zero, thus the forward–backward asymmetry zero is determined by $h_A^{[0]}(q_0^2, \langle p_X^+\rangle) = 0$. Using (72) this is equivalent to the condition

$$\frac{q_0^2}{2m_b(m_B - \langle p_X^+\rangle)} = -\frac{\mathrm{Re}[C_7^{\mathrm{incl}}(q_0^2)]}{\mathrm{Re}[C_9^{\mathrm{incl}}(q_0^2)]}\frac{c_1^7(u_0)}{c_1^9(u_0)} \tag{73}$$

with $u_0 \equiv 1 - q_0^2/(m_b(m_B - \langle p_X^+\rangle))$. This result leads to the important conclusion that *the QCD dynamics that determines the location of the asymmetry zero is to a very good approximation independent of the long-distance physics below the scale m_b contained in the jet function and the non-perturbative shape function*. It also depends only very weakly on the value of the invariant mass cut through the dependence of $\langle p_X^+\rangle$ on m_X^{cut}. The bulk dependence of q_0^2 on the invariant mass cut m_X^{cut} enters through the kinematical factor $m_B - \langle p_X^+\rangle$ on the left-hand side of (73). This conclusion is in agreement with the study [37] where the near-independence of q_0^2 on the value of m_X^{cut} has been noted.

We are now in the position to quantify the impact of the two-loop calculation of $R_\perp(u_0, \nu = m_b) = c_1^7(u_0)/c_1^9(u_0)$ on q_0^2. In [38] the asymmetry zero has been determined by keeping the full NNLL expression for $\mathrm{Re}[C_7^{\mathrm{incl}}(q^2)]/\mathrm{Re}[C_9^{\mathrm{incl}}(q^2)]$ but setting $R_\perp = 1$. In this approximation, and excluding $1/m_b$-suppressed shape function effects for the moment, the zero is found to be

$$q_0^2|_{R_\perp=1} = (3.62\ldots3.69)\ \mathrm{GeV}^2 \quad \text{for } m_X^{\mathrm{cut}} = (2.0\ldots1.8)\ \mathrm{GeV}. \tag{74}$$

As indicated the lowest value corresponds to $m_X^{\mathrm{cut}} = 2.0$ GeV and the highest one to $m_X^{\mathrm{cut}} = 1.8$ GeV. Our value is somewhat larger than what can be extracted from Fig. 4 of [38], because we expand the factor $\overline{m}_b(\mu)/m_b^{\mathrm{pole}}$ that accompanies C_7 in α_s. Moreover, the variation of the zero when changing m_X^{cut} from 1.8 GeV to 2.0 GeV is about twice as large compared to what can be read off from Fig. 4 of [38], which is likely due to our approximation of pulling the slowly varying function $h_A^{[0]}(q_0^2, p_X^+)$ out of the integral in (70). However, our approximation is still justified since even the increased sensitivity of the zero on m_X^{cut} is only ± 0.03 GeV^2 and hence below 1%. Taking into account $R_\perp$ at the NLO, we find for the position of the zero

$$q_0^2|_{R_\perp\mathrm{NLO}} = (3.55\ldots3.61)\ \mathrm{GeV}^2 \quad \text{for } m_X^{\mathrm{cut}} = (2.0\ldots1.8)\ \mathrm{GeV}. \tag{75}$$

The impact of the NLO correction to $R_\perp$ is to shift the zero by -2.2%. As we already stated before, and as can also be seen from Figs. 2 and 5, the size of the NNLO correction to $R_\perp$ is significant. It amounts to a shift of the NLO zero in (75) by another -3% and hence is larger than the NLO shift. The total shift induced by $R_\perp$ through NNLO therefore amounts to -5%.

Author's personal copy

Table 2
Numerical inputs that we use in the phenomenological analysis of the forward–backward asymmetry zero.

$\alpha_s(M_Z) = 0.1180$	$\lambda_2 \simeq \frac{1}{4}(m_{B^*}^2 - m_B^2) \simeq 0.12\ \text{GeV}^2$
$\sin^2\theta_W = 0.23122$	$m_t^{\text{pole}} = 171.4\ \text{GeV}$
$M_W = 80.426\ \text{GeV}$	$m_c^{\text{pole}} = (1.5 \pm 0.1)\ \text{GeV}$
$M_Z = 91.1876\ \text{GeV}$	$m_b^{\text{PS}}(2\ \text{GeV}) = (4.6 \pm 0.1)\ \text{GeV}$

Before proceeding to our final result we briefly comment on the rôle of power corrections. The authors of [38] performed a thorough study of $1/m_b$-suppressed shape function effects which result in a shift of the zero of $-0.05\ \text{GeV}^2$ to $-0.1\ \text{GeV}^2$. This shift is more strongly dependent on the invariant mass cut and the theoretical error increases when m_X^{cut} is chosen smaller. In the following we take the larger value as an estimate for the shift and also for the associated uncertainty. However, the study of power corrections in [38] does not cover all such corrections and applies a rather crude treatment to those arising from soft gluon attachments to the charm-loop diagrams by absorbing the $1/m_c^2$ non-perturbative power corrections into the C_i^{incl}, which is justified only in the absence of invariant mass cuts. In the semi-inclusive region, the matrix element of (29) in [34] cannot, due to the presence of a soft gluon, be expressed in terms of a short-distance coefficient times a local matrix element, since the soft gluon attached to the charm loop affects the invariant mass of an energetic hadronic final state by a relevant amount $\sqrt{m_b \Lambda_{\text{QCD}}}$, which must be accounted for by a subleading shape function. By treating this correction as in the inclusive case, the authors of [38] implicitly assumed that this shape function somehow factorizes into the local heavy-quark effective theory matrix element λ_2 and the leading-power shape function. It is not clear to us how this simplification can be justified and it is likely not even parametrically correct. Nevertheless, in the absence of better information we follow the treatment of [38] and include the $1/m_c^2$ power corrections into the C_i^{incl}. This results in a shift of the asymmetry zero by $+0.07\ \text{GeV}^2$, which is included in (74), (75), and below in (76). To be conservative we assign another $0.1\ \text{GeV}^2$ uncertainty to this estimate and add it in quadrature with the other power correction uncertainty.

We are now in the position to present our final NNLO result based on the numerical input parameters and their respective intervals as specified in Table 2. We then find

$$\begin{aligned} q_0^2 &= \left[(3.34\ldots3.40)^{+0.04}_{-0.13\mu} \pm 0.08_{m_b}{}^{+0.05}_{-0.04 m_c} \pm 0.14_{\text{SF}} \pm 0.14_{\langle p_X^+\rangle}\right]\text{GeV}^2 \\ &= \left[(3.34\ldots3.40)^{+0.22}_{-0.25}\right]\text{GeV}^2 \quad \text{for } m_X^{\text{cut}} = (2.0\ldots1.8)\ \text{GeV}. \end{aligned} \tag{76}$$

The error estimate is computed as follows: The range of scale variation is taken to be $2.3\ \text{GeV} < \mu < 9.2\ \text{GeV}$, and we vary the scale in the C_i^{incl} and in $R_\perp$ independently to account conservatively for the absence of the $\mathcal{O}(\alpha_s^2)$ correction to the C_i^{incl}. The input quark mass is the bottom mass in the potential-subtracted (PS) scheme [39], see Table 2. The pole mass and $\overline{\text{MS}}$ mass used in intermediate expressions are computed using the one-loop conversion factors resulting in $m_b^{\text{pole}} = 4.78\ \text{GeV}$ and $\overline{m}(m_b^{\text{PS}}) = 4.36\ \text{GeV}$, respectively, when $m_b^{\text{PS}}(2\ \text{GeV}) = 4.6\ \text{GeV}$. The dependence on the charm quark mass enters through the matrix elements of the current–current operators. The error labelled "SF" is connected with the subleading shape function effects as discussed above. Finally we have added an uncertainty estimate for the approximation made by pulling out the slowly varying function $h_A^{[0]}(q_0^2, p_X^+)$ out of the p_X^+ integral in (70). We estimate

Author's personal copy

this error rather generously by varying $\langle p_X^+ \rangle$ from $p_X^{\rm cut}/4$ to $3p_X^{\rm cut}/4$. The total error is obtained by adding all these uncertainties in quadrature.

We note that the value of the asymmetry zero in semi-inclusive $b \to s\ell^+\ell^-$ decay is significantly smaller than for the exclusive case [30], where spectator scattering is responsible for a positive shift as is the fact that in this case $\langle p_X^+ \rangle = 0$ in (73). On the other hand the semi-inclusive zero is in the same region as in the inclusive case [40], where virtual effects together with hard gluon bremsstrahlung encoded in functions ω_{710} and ω_{910} [41] also induce a negative shift on the zero.

6. Conclusion

In this paper we completed the two-loop matching calculation for heavy-to-light currents from QCD onto SCET for the complete set of Dirac structures. These matching coefficients enter several phenomenological applications, of which we have discussed their effects on heavy-to-light form factor ratios, exclusive radiative and semi-leptonic decays, as well as the inclusive decay $\bar{B} \to X_s\ell^+\ell^-$ in the shape-function region. The two-loop corrections are generally relatively small, in the few percent range. However, one ratio, $R_\perp = c_1^7(u,\mu)/c_1^9(u,\mu)$, which is also the most important for phenomenology, since it enters the comparison of radiative and semi-leptonic decays as well as the forward–backward asymmetry in exclusive and semi-inclusive $b \to s\ell^+\ell^-$ transition, exhibits a two-loop correction that is larger than the one-loop term. The two-loop term alone shifts the location of the asymmetry zero by about -0.1 GeV^2, comparable to the effect of $1/m_b$ suppressed shape functions estimated in [38]. We showed that the location of the asymmetry zero in semi-inclusive $\bar{B} \to X_s\ell^+\ell^-$ with an invariant mass cut is to a very good approximation independent of the long-distance physics below the scale m_b contained in the jet function and the non-perturbative shape function, and obtain $q_0^2 = (3.34^{+0.22}_{-0.25})$ GeV^2 for an invariant mass cut $m_X^{\rm cut} = 2.0$ GeV as our best estimate for the asymmetry zero. Moreover, we confirm the discrepancy between QCD sum rule and SCET results for the form factor ratio T_1/V in the low q^2 region discussed in [14] and suggest that a dedicated QCD sum rules analysis of deviations from the symmetry limit (rather than the form factors themselves) should be done to clarify the situation.

Acknowledgements

We would like to thank F. Tackmann and M. Misiak for useful correspondence. This work was supported in part by the DFG Sonderforschungsbereich/Transregio 9 “Computergestützte Theoretische Teilchenphysik” (G.B., M.B.), the Helmholtz alliance “Physics at the Terascale” (T.H.), the Alexander-von-Humboldt Stiftung (X.-Q. Li), and the National Natural Science Foundation under contract No. 11005032 (X.-Q. Li). X.-Q. Li acknowledges hospitality from the Institute of Theoretical Physics, Chinese Academy of Science, where part of this work was performed.

Appendix A. NLO coefficient functions

In Section 3.1 we introduced the following set of one-loop coefficient functions,

$$g_0(u) = -\frac{5}{2} + 2\ln(u),$$

$$g_1(u) = -\frac{\pi^2}{12} + \frac{2}{\bar{u}}\ln(u) - 2\ln^2(u) - 2\mathrm{Li}_2(\bar{u}),$$

Author's personal copy

$$
\begin{aligned}
g_2(u) &= \frac{\pi^2}{24} + \frac{1}{3}\zeta_3 + \frac{12(1+\bar{u}) + \pi^2\bar{u}}{6\bar{u}}\ln(u) - \frac{2}{\bar{u}}\big(\ln^2(u) + \mathrm{Li}_2(\bar{u})\big) + \frac{4}{3}\ln^3(u) \\
&\quad + 4\ln(u)\mathrm{Li}_2(\bar{u}) - 2\mathrm{Li}_3(\bar{u}) + 4\mathrm{S}_{1,2}(\bar{u}), \\
g_3(u) &= -\frac{\pi^4}{160} - \frac{1}{6}\zeta_3 + \frac{48(1+\bar{u}) + 2\pi^2 - 8\bar{u}\zeta_3}{12\bar{u}}\ln(u) - \frac{2}{3}\ln^4(u) - 4\ln^2(u)\mathrm{Li}_2(\bar{u}) \\
&\quad - \frac{12(1+\bar{u}) + \pi^2\bar{u}}{6\bar{u}}\big(\ln^2(u) + \mathrm{Li}_2(\bar{u})\big) - 8\ln(u)\mathrm{S}_{1,2}(\bar{u}) \\
&\quad + 4\ln(u)\mathrm{Li}_3(\bar{u}) - 2\mathrm{Li}_4(\bar{u}) \\
&\quad + \frac{2}{\bar{u}}\left(\frac{2}{3}\ln^3(u) + 2\ln(u)\mathrm{Li}_2(\bar{u}) - \mathrm{Li}_3(\bar{u}) + 2\mathrm{S}_{1,2}(\bar{u})\right) - 8\mathrm{S}_{1,3}(\bar{u}) + 4\mathrm{S}_{2,2}(\bar{u}), \\
g_4(u) &= g_1(u) - 6 - \frac{4u}{\bar{u}}\ln(u), \\
g_5(u) &= g_2(u) - 10 - \frac{\pi^2}{3} - \frac{2u}{\bar{u}}\big(3\ln(u) - 2\ln^2(u) - 2\mathrm{Li}_2(\bar{u})\big), \\
g_6(u) &= g_3(u) - 18 - \frac{\pi^2}{2} + \frac{4}{3}\zeta_3 \\
&\quad - \frac{2u}{\bar{u}}\left(\frac{30+\pi^2}{6}\ln(u) - 3\ln^2(u) - 3\mathrm{Li}_2(\bar{u}) + \frac{4}{3}\ln^3(u)\right. \\
&\quad \left. + 4\ln(u)\mathrm{Li}_2(\bar{u}) - 2\mathrm{Li}_3(\bar{u}) + 4\mathrm{S}_{1,2}(\bar{u})\right), \\
g_7(u) &= -\frac{2}{\bar{u}} - \frac{2u}{\bar{u}^2}\ln(u), \\
g_8(u) &= -\frac{6}{\bar{u}} - \frac{2u}{\bar{u}^2}\big(2\ln(u) - \ln^2(u) - \mathrm{Li}_2(\bar{u})\big), \\
g_9(u) &= \frac{2u}{\bar{u}}\ln(u), \\
g_{10}(u) &= \frac{u(1+4\bar{u})}{\bar{u}^2}\ln(u) + \frac{u}{\bar{u}}\big(1 - 2\ln^2(u) - 2\mathrm{Li}_2(\bar{u})\big), \\
g_{11}(u) &= \frac{6u(2+7\bar{u}) + \pi^2 u\bar{u}}{6\bar{u}^2}\ln(u) - \frac{u(1+4\bar{u})}{\bar{u}^2}\big(\ln^2(u) + \mathrm{Li}_2(\bar{u})\big) \\
&\quad + \frac{u}{\bar{u}}\left(3 + \frac{4}{3}\ln^3(u) + 4\ln(u)\mathrm{Li}_2(\bar{u}) - 2\mathrm{Li}_3(\bar{u}) + 4\mathrm{S}_{1,2}(\bar{u})\right), \\
g_{12}(u) &= g_7(u) + 2, \\
g_{13}(u) &= g_8(u) + 6 + \frac{2u}{\bar{u}}\ln(u).
\end{aligned} \tag{77}
$$

Appendix B. NNLO coefficient functions

The finite parts of the two-loop form factors involve the following coefficient functions,

$$
\begin{aligned}
h_1(u) &= -\frac{2(7 - 2\bar{u} + 3\bar{u}^2)}{u^2}\mathrm{Li}_4(\bar{u}) - \frac{4(11 + 2\bar{u} + 3\bar{u}^2)}{u^2}\mathrm{S}_{2,2}(\bar{u}) \\
&\quad + 8\mathrm{S}_{1,3}(\bar{u}) - 8\ln(u)\mathrm{Li}_3(\bar{u})
\end{aligned}
$$

Author's personal copy

$$
\begin{aligned}
&+\frac{2(3+\bar{u}^2)}{u^2}\mathrm{Li}_2(\bar{u})^2+16\ln(u)\mathrm{S}_{1,2}(\bar{u})+\frac{16}{3}\ln^4(u)+16\ln^2(u)\mathrm{Li}_2(\bar{u})\\
&-\frac{6+47\bar{u}-5\bar{u}^2}{3u\bar{u}}\mathrm{Li}_3(\bar{u})-\frac{2(42-29\bar{u})}{9\bar{u}}\ln^3(u)+\frac{2(6-115\bar{u}+13\bar{u}^2)}{3u\bar{u}}\mathrm{S}_{1,2}(\bar{u})\\
&-\frac{2(12+\bar{u}+11\bar{u}^2)}{3u\bar{u}}\ln(u)\mathrm{Li}_2(\bar{u})+\frac{36-87\bar{u}-250\bar{u}^2+18\pi^2\bar{u}^2}{9\bar{u}^2}\ln^2(u)\\
&-\left(\frac{33+109\bar{u}-322\bar{u}^2}{9u\bar{u}}-\frac{(7-2\bar{u}+3\bar{u}^2)\pi^2}{u^2}\right)\mathrm{Li}_2(\bar{u})+\frac{(2815+353\bar{u})\pi^2}{432u}\\
&+\left(\frac{1173+241\bar{u}}{27\bar{u}}-\frac{(9+46\bar{u}+17\bar{u}^2)\pi^2}{9u\bar{u}}-\frac{56}{3}\zeta_3\right)\ln(u)\\
&-\frac{(509+278\bar{u}+77\bar{u}^2)\pi^4}{720u^2}+\frac{76}{9}\zeta_3+\frac{30\,331}{1296}-2h_2(u),\\
h_2(u)=&\frac{2(1+\bar{u})^2}{3u\bar{u}}\big(12\mathcal{H}_1(\bar{u})+\pi^2\ln(2-u)\big)+\frac{1}{3}\big(24\mathcal{H}_2(\bar{u})-2\pi^2\mathrm{Li}_2(-\bar{u})\big)\\
&-\frac{8}{u^2}\mathrm{S}_{2,2}(\bar{u})-\frac{2}{u^2}\mathrm{Li}_4(\bar{u})-8\ln(u)\mathrm{Li}_3(\bar{u})-\frac{(u-\bar{u})(3-2\bar{u})}{u^2}\mathrm{Li}_2(\bar{u})^2\\
&-\frac{40-56\bar{u}+7\bar{u}^2}{3u^2}\mathrm{Li}_3(\bar{u})+\frac{14-40\bar{u}+17\bar{u}^2}{3u^2}\mathrm{S}_{1,2}(\bar{u})+\frac{29-35\bar{u}}{3u}\ln(u)\mathrm{Li}_2(\bar{u})\\
&+\frac{44}{9}\ln^3(u)-\left(\frac{66+122\bar{u}-89\bar{u}^2}{9u\bar{u}}-\frac{(7-8\bar{u}+4\bar{u}^2)\pi^2}{3u^2}\right)\mathrm{Li}_2(\bar{u})\\
&-\frac{78+223\bar{u}-12\pi^2\bar{u}}{18\bar{u}}\ln^2(u)+\frac{(13-62\bar{u}+31\bar{u}^2)\pi^4}{120u^2}\\
&+\left(\frac{2(354+121\bar{u})}{27\bar{u}}-\frac{(24-71\bar{u}+65\bar{u}^2)\pi^2}{18u\bar{u}}-14\zeta_3\right)\ln(u)\\
&+\frac{3(2-\bar{u})^2}{u^2}\left(\mathrm{Li}_3(-u)-\ln(u)\mathrm{Li}_2(-u)-\frac{\ln^2(u)+\pi^2}{2}\ln(1+u)\right)+\frac{5405}{1296}\\
&+\frac{(877+239\bar{u})\pi^2}{216u}+\frac{469-73\bar{u}}{18u}\zeta_3-\frac{2(3+\bar{u})\pi^2}{u}\ln(2),\\
h_3(u)=&\frac{8}{3}\mathrm{Li}_3(\bar{u})+\frac{8(1+\bar{u})(3+11\bar{u}-11\bar{u}^2+5\bar{u}^3)}{9u^3\bar{u}}\mathrm{Li}_2(\bar{u})\\
&-\frac{2(96+208\bar{u}-224\bar{u}^2+112\bar{u}^3+3\bar{u}u^2\pi^2)}{27u^2\bar{u}}\ln(u)+\frac{3773-4954\bar{u}+2333\bar{u}^2}{81u^2}\\
&-\frac{(265-315\bar{u}+219\bar{u}^2-41\bar{u}^3)\pi^2}{54u^3}-\frac{28}{9}\zeta_3,\\
h_4(u)=&h_1(u)+2h_2(u)+\frac{12(1+\bar{u})^2}{u^3}\left(8\mathrm{S}_{2,2}(\bar{u})+2\mathrm{Li}_4(\bar{u})-\mathrm{Li}_2(\bar{u})^2+\frac{3\pi^4}{20}\right)\\
&+\frac{4(1+\bar{u})(1+10\bar{u}+\bar{u}^2)}{u^2\bar{u}}\mathrm{Li}_3(\bar{u})+\frac{56u}{3\bar{u}}\ln^3(u)\\
&-\frac{8(1-31\bar{u}-13\bar{u}^2-5\bar{u}^3)}{u^2\bar{u}}\mathrm{S}_{1,2}(\bar{u})
\end{aligned}
$$

Author's personal copy

$$
\begin{aligned}
&+\frac{8(2+\bar{u}+10\bar{u}^2-\bar{u}^3)}{u^2\bar{u}}\ln(u)\mathrm{Li}_2(\bar{u})\\
&-\frac{4(3-4\bar{u}-46\bar{u}^2+11\bar{u}^3)}{3u\bar{u}^2}\ln^2(u)\\
&+\left(\frac{4(4+3\bar{u}-72\bar{u}^2-7\bar{u}^3)}{3u^2\bar{u}}-\frac{12(1+\bar{u})^2\pi^2}{u^3}\right)\mathrm{Li}_2(\bar{u})\\
&-\frac{(359+362\bar{u}+143\bar{u}^2)\pi^2}{18u^2}\\
&-\left(\frac{611-251\bar{u}}{9\bar{u}}-\frac{2(3+32\bar{u}+35\bar{u}^2+2\bar{u}^3)\pi^2}{3u^2\bar{u}}\right)\ln(u)\\
&-\frac{4}{3}\zeta_3-\frac{3050}{27}-2h_5(u),
\end{aligned}
$$

$$
\begin{aligned}
h_5(u)=\;&h_2(u)-\frac{4(1+\bar{u})}{3\bar{u}}\big(12\mathcal{H}_1(\bar{u})+\pi^2\ln(2-u)\big)\\
&+\frac{4(12-21\bar{u}+18\bar{u}^2-8\bar{u}^3)}{3u^3}\mathrm{Li}_3(\bar{u})\\
&+\frac{2(1+3\bar{u}^2)}{u^3}\left(8\mathrm{S}_{2,2}(\bar{u})+2\mathrm{Li}_4(\bar{u})-\mathrm{Li}_2(\bar{u})^2+\frac{3\pi^4}{20}\right)\\
&+\frac{16(1+\bar{u}+\bar{u}^2)}{3u^2}\ln(u)\mathrm{Li}_2(\bar{u})\\
&+\frac{4(14+15\bar{u}-24\bar{u}^2-6\bar{u}^3)}{3u^3}\mathrm{S}_{1,2}(\bar{u})-\left(\frac{472u}{9\bar{u}}-\frac{8(1-2\bar{u}+4\bar{u}^2)\pi^2}{3u^2\bar{u}}\right)\ln(u)\\
&+\left(\frac{4(11-21\bar{u}+4\bar{u}^2-5\bar{u}^3)}{3u^2\bar{u}}-\frac{2(1+3\bar{u}^2)\pi^2}{u^3}\right)\mathrm{Li}_2(\bar{u})\\
&-\frac{4(2-\bar{u})(5-8\bar{u}+2\bar{u}^2)}{3u^3}\Big(\mathrm{Li}_3(-u)-\ln(u)\mathrm{Li}_2(-u)\\
&-\frac{\ln^2(u)+\pi^2}{2}\ln(1+u)\Big)\\
&+\frac{2(13-18\bar{u}+16\bar{u}^2)}{3u\bar{u}}\ln^2(u)-\frac{2(13+4\bar{u}+16\bar{u}^2)\pi^2}{9u^2}-\frac{16}{u}\zeta_3-\frac{5219}{54},
\end{aligned}
$$

$$
h_6(u)=-\frac{8u}{3\bar{u}}\ln(u)+\frac{10}{3}\zeta_3+\frac{11\pi^2}{18}-\frac{1381}{324},
$$

$$
\begin{aligned}
h_7(u)=\;&h_3(u)-\frac{16(1+\bar{u})^3}{3u^2\bar{u}}\mathrm{Li}_2(\bar{u})+\frac{128(1+\bar{u}+\bar{u}^2)}{9u\bar{u}}\ln(u)+\frac{32(1+\bar{u})\pi^2}{9u^2}\\
&-\frac{2(251+325\bar{u})}{27u},
\end{aligned}
$$

$$
\begin{aligned}
h_8(u)=\;&-\frac{2(3+20\bar{u}+13\bar{u}^2)}{u^3}\left(8\mathrm{S}_{2,2}(\bar{u})+2\mathrm{Li}_4(\bar{u})-\mathrm{Li}_2(\bar{u})^2+\frac{3\pi^4}{20}\right)-\frac{28u}{3\bar{u}}\ln^3(u)\\
&-\frac{2(1+17\bar{u}+51\bar{u}^2+3\bar{u}^3)}{u^2\bar{u}}\mathrm{Li}_3(\bar{u})+\frac{4(1-43\bar{u}-93\bar{u}^2-9\bar{u}^3)}{u^2\bar{u}}\mathrm{S}_{1,2}(\bar{u})
\end{aligned}
$$

Author's personal copy

$$
\begin{aligned}
&- \frac{8(1+2\bar{u}+15\bar{u}^2)}{u^2\bar{u}}\ln(u)\mathrm{Li}_2(\bar{u}) + \frac{9+13\bar{u}-209\bar{u}^2-29\bar{u}^3}{3u\bar{u}^2}\ln^2(u) \\
&+ \left(\frac{3-14\bar{u}-84\bar{u}^2+402\bar{u}^3+125\bar{u}^4}{3u^2\bar{u}^2} + \frac{2(3+20\bar{u}+13\bar{u}^2)\pi^2}{u^3}\right)\mathrm{Li}_2(\bar{u}) \\
&- \left(\frac{81-539\bar{u}+242\bar{u}^2}{18\bar{u}^2} + \frac{(1+17\bar{u}+51\bar{u}^2+3\bar{u}^3)\pi^2}{u^2\bar{u}}\right)\ln(u) \\
&+ \frac{2(14+77\bar{u}+17\bar{u}^2)\pi^2}{3u^2} - \frac{11-3\bar{u}}{2\bar{u}} - 2h_9(u), \\
h_9(u) = {} & \frac{1}{2}h_2(u) - \frac{1}{2}h_5(u) - \frac{2\bar{u}(1+3\bar{u})}{u^3}\left(8\mathrm{S}_{2,2}(\bar{u}) + 2\mathrm{Li}_4(\bar{u}) - \mathrm{Li}_2(\bar{u})^2 + \frac{3\pi^4}{20}\right) \\
&- \frac{2(3+21\bar{u}-24\bar{u}^2+2\bar{u}^3)}{3u^3}\mathrm{Li}_3(\bar{u}) - \frac{4(1+7\bar{u}+4\bar{u}^2)}{3u^2}\ln(u)\mathrm{Li}_2(\bar{u}) \\
&- \frac{2(1+69\bar{u}-48\bar{u}^2-24\bar{u}^3)}{3u^3}\mathrm{S}_{1,2}(\bar{u}) + \left(4 + \frac{2(1-11\bar{u}-2\bar{u}^2)\pi^2}{3u^2}\right)\ln(u) \\
&- \left(\frac{2(9-13\bar{u}-18\bar{u}^2)}{3u^2} - \frac{2\bar{u}(1+3\bar{u})\pi^2}{u^3}\right)\mathrm{Li}_2(\bar{u}) - \frac{7+15\bar{u}}{3u}\ln^2(u) \\
&- \frac{2(1-3\bar{u}+6\bar{u}^2-2\bar{u}^3)}{3u^3}\left(\mathrm{Li}_3(-u) - \ln(u)\mathrm{Li}_2(-u) - \frac{\ln^2(u)+\pi^2}{2}\ln(1+u)\right) \\
&+ \frac{(11+17\bar{u}+38\bar{u}^2)\pi^2}{9u^2} + \frac{4(3-\bar{u})}{u}\zeta_3 - 4\pi^2\ln(2) - \frac{5435}{108}, \\
h_{10}(u) = {} & \frac{1}{2}h_3(u) - \frac{1}{2}h_7(u) - \frac{8\pi^2}{9} + \frac{181}{27}.
\end{aligned} \tag{78}
$$

Moreover, for the ratios R_X in (58) we need the following auxiliary functions,

$$
\begin{aligned}
j_1(u) = {} & \frac{4(u-2)(u^2+2u-2)}{3u^2\bar{u}}s_1(u) + \frac{16\bar{u}}{3u^3}s_2(u) + \frac{8(2u-7)\bar{u}}{3u^3}s_3(u) - \frac{4u}{3\bar{u}}s_4(u) \\
&+ \frac{2(u+3)(u^2-1)}{u^3}s_5(u) - \frac{16(2u-3)\bar{u}\mathrm{Li}_4(\bar{u})}{u^3} - \frac{4(u^2-36u+25)\mathrm{Li}_2(\bar{u})}{u^2} \\
&+ \frac{4(4u^3-8u^2+5u+3)(\mathrm{Li}_3(\bar{u})-\zeta(3))}{u^3} + \frac{4(7u^3+85u^2-111u+3)\mathrm{Li}_3(u)}{u^3} \\
&+ \frac{8\pi^2(6u-17)\bar{u}\mathrm{Li}_2(\bar{u})}{3u^3} + \frac{6u\mathrm{Li}_2(\bar{u})}{\bar{u}} - \frac{4(5u^3+63u^2-83u+3)\mathrm{Li}_2(u)\ln(u)}{u^3} \\
&- \frac{2\pi^4(20u-33)\bar{u}}{45u^3} - \frac{8(u^2+51u-62)\zeta(3)}{u^2} - \frac{2\pi^2(9u^2-73u+59)}{3u^2} \\
&- \frac{32\pi^2(5u-6)\ln(u)}{3u^2} - \frac{2(3u^3+41u^2-55u+3)\ln^2(u)\ln(\bar{u})}{u^3} \\
&+ \frac{4(2u-1)^2\ln^2(u)}{\bar{u}^2} + \frac{(9u-4)\ln(u)}{\bar{u}} - \frac{2(11u-25)\ln^2(u)}{u} - 1, \\
j_2(u) = {} & -\frac{2(u-2)(u^2+2u-2)}{3u^2\bar{u}}s_1(u) - \frac{8\bar{u}}{3u^3}s_2(u) + \frac{2(4u-7)\bar{u}}{3u^3}s_3(u) \\
&- \frac{(u+3)(u^2-1)}{u^3}s_5(u) + \frac{2\pi^2(12u-29)\bar{u}\mathrm{Li}_2(\bar{u})}{3u^3} - \frac{4(4u-15)\bar{u}\mathrm{Li}_4(\bar{u})}{u^3}
\end{aligned}
$$

Author's personal copy

$$
\begin{aligned}
&- \frac{2(25u^2-99u+51)\mathrm{Li}_2(\bar{u})}{3u^2} - \frac{2(3u^3+29u^2-37u+3)(\mathrm{Li}_3(\bar{u})-\zeta(3))}{u^3} \\
&- \frac{2(11u^3-63u^2+57u+3)\mathrm{Li}_3(u)}{u^3} + \frac{2(8u^3-48u^2+43u+3)\mathrm{Li}_2(u)\ln(u)}{u^3} \\
&- \frac{22\mathrm{Li}_2(\bar{u})}{3\bar{u}} - \frac{4\pi^4(5u-18)\bar{u}}{45u^3} \\
&+ \frac{2(7u^2-83u+86)\zeta(3)}{u^2} - \frac{\pi^2(8u^2-69u+67)}{3u^2} \\
&+ \frac{4\pi^2(2u^2-17u+18)\ln(u)}{3u^2} + \frac{(5u^3-33u^2+29u+3)\ln^2(u)\ln(\bar{u})}{u^3} \\
&- \frac{13\ln^2(u)}{3\bar{u}} - \frac{4\pi^2\ln(u)}{3\bar{u}} + \frac{203\ln(u)}{9\bar{u}} - \frac{(8u-51)\ln^2(u)}{3u} - \frac{257\ln(u)}{9} + \frac{269}{9},
\end{aligned}
$$

$$
j_3(u) = -\frac{26}{9}g_9(u) + \frac{8u}{3\bar{u}}\left[\ln^2(u) + \mathrm{Li}_2(\bar{u})\right] - \frac{76}{9},
$$

$$
\begin{aligned}
j_4(u) = {} & \frac{32\pi^2(u+2)\bar{u}}{9u^2} + \frac{32\bar{u}(\mathrm{Li}_3(\bar{u})-\zeta(3))}{u^3} - \frac{8(u-2)(u^2+2u-2)\mathrm{Li}_2(\bar{u})}{3u^2\bar{u}} \\
& - \frac{52u\ln(u)}{9\bar{u}} - \frac{104}{3u} + \frac{80\ln(u)}{3u} + \frac{236}{9},
\end{aligned}
$$

$$
\begin{aligned}
j_5(u) = {} & -\frac{4(u-2)(u^2-2u+2)}{3u^2\bar{u}}s_1(u) + \frac{16\bar{u}}{3u^3}s_2(u) - \frac{8(2u^2-12u+11)}{3u^3}s_3(u) \\
& + \frac{4}{3\bar{u}}s_4(u) - \frac{2(u+1)(u^2+2u+7)}{3u^3}s_5(u) + \frac{16(2u^2-8u+7)\mathrm{Li}_4(\bar{u})}{u^3} \\
& - \frac{2(51u^2-328u+250)\mathrm{Li}_2(\bar{u})}{3u^2} - \frac{4(u^3+48u^2-69u-7)(\mathrm{Li}_3(\bar{u})-\zeta(3))}{3u^3} \\
& + \frac{4(3u^3+315u^2-519u+7)\mathrm{Li}_3(u)}{3u^3} \\
& - \frac{8\pi^2(6u^2-32u+29)\mathrm{Li}_2(\bar{u})}{3u^3} - \frac{2\mathrm{Li}_2(\bar{u})}{\bar{u}} \\
& + \frac{4(2u^3-237u^2+387u-7)\mathrm{Li}_2(u)\ln(u)}{3u^3} + \frac{2\pi^4(20u^2-83u+73)}{45u^3} \\
& + \frac{8(4u^2-183u+306)\zeta(3)}{3u^2} - \frac{\pi^2(11u^2-206u+218)}{3u^2} \\
& + \frac{8\pi^2(u^2-72u+120)\ln(u)}{9u^2} \\
& + \frac{2(7u^3-159u^2+255u-7)\ln^2(u)\ln(\bar{u})}{3u^3} + \frac{4\ln^2(u)}{\bar{u}} + \frac{\ln(u)}{\bar{u}} - 13\ln(u) \\
& - \frac{2(27u-125)\ln^2(u)}{3u} - 8\pi^2\ln(2) + \frac{563}{24},
\end{aligned}
$$

$$
\begin{aligned}
j_6(u) = {} & \frac{2(u-2)(u^2-2u+2)}{3u^2\bar{u}}s_1(u) - \frac{8\bar{u}}{3u^3}s_2(u) - \frac{2(7u^2-17u+11)}{3u^3}s_3(u) \\
& + \frac{(u+1)(u^2+2u+7)}{3u^3}s_5(u) + \frac{4(7u^2-25u+19)\mathrm{Li}_4(\bar{u})}{u^3}
\end{aligned}
$$

Author's personal copy

$$
\begin{aligned}
&- \frac{2(35u^2 - 133u + 73)\mathrm{Li}_2(\bar{u})}{3u^2} + \frac{2(7u^3 - 99u^2 + 129u - 7)(\mathrm{Li}_3(\bar{u}) - \zeta(3))}{3u^3} \\
&- \frac{2(45u^3 - 273u^2 + 273u + 7)\mathrm{Li}_3(u)}{3u^3} \\
&- \frac{2\pi^2(21u^2 - 59u + 41)\mathrm{Li}_2(\bar{u})}{3u^3} + \frac{22\mathrm{Li}_2(\bar{u})}{3\bar{u}} \\
&+ \frac{2(28u^3 - 204u^2 + 207u + 7)\mathrm{Li}_2(u)\ln(u)}{3u^3} + \frac{\pi^4(35u^2 - 122u + 92)}{45u^3} \\
&+ \frac{2(40u^2 - 369u + 378)\zeta(3)}{3u^2} - \frac{\pi^2(68u^2 - 279u + 267)}{9u^2} \\
&+ \frac{4\pi^2(8u^2 - 75u + 78)\ln(u)}{9u^2} \\
&+ \frac{(11u^3 - 135u^2 + 141u + 7)\ln^2(u)\ln(\bar{u})}{3u^3} + \frac{13\ln^2(u)}{3\bar{u}} - \frac{269\ln(u)}{9\bar{u}} \\
&+ \frac{4\pi^2\ln(u)}{3\bar{u}} + \frac{215\ln(u)}{9} - \frac{(40u - 73)\ln^2(u)}{3u} \\
&+ 4\pi^2\ln(2) - \frac{4421}{216}, \\
j_7(u) &= \frac{38}{9}g_9(u) - \frac{8u}{3\bar{u}}\left[\ln^2(u) + \mathrm{Li}_2(\bar{u})\right] + \frac{4\pi^2}{9} + \frac{205}{54}, \\
j_8(u) &= -\frac{8\pi^2(u^2 + 8u - 16)}{9u^2} + \frac{32\bar{u}(\mathrm{Li}_3(\bar{u}) - \zeta(3))}{u^3} + \frac{8(u-2)(u^2 - 10u + 10)\mathrm{Li}_2(\bar{u})}{3u^2\bar{u}} \\
&+ \frac{76\ln(u)}{9\bar{u}} - \frac{232}{3u} - \frac{4(19u - 156)\ln(u)}{9u} + \frac{1429}{54}, \\
j_9(u) &= -\frac{5\pi^2(5u + 4)}{6u} - \frac{16\bar{u}(\mathrm{Li}_3(\bar{u}) - \zeta(3))}{u^2} - \frac{2(u-2)\mathrm{Li}_2(\bar{u})}{u} + \frac{u^2\ln^2(u)}{\bar{u}^2} \\
&- 12\ln(u) - 6\zeta(3) + 4\pi^2\ln(2) + \frac{563}{16}, \\
j_{10}(u) &= \frac{4\pi^2(u+1)}{3u} + \frac{8\bar{u}(\mathrm{Li}_3(\bar{u}) - \zeta(3))}{u^2} + 4\ln(u) + 3\zeta(3) - 2\pi^2\ln(2) - \frac{5141}{144},
\end{aligned}
\tag{79}
$$

with

$$
\begin{aligned}
s_1(u) &= 12\mathcal{H}_1(\bar{u}) + \pi^2\ln(2-u), \\
s_2(u) &= 12\mathcal{H}_2(\bar{u}) - \pi^2\mathrm{Li}_2(-\bar{u}), \\
s_3(u) &= 3\mathrm{Li}_2^2(\bar{u}) - 24\mathrm{S}_{2,2}(\bar{u}) - \frac{17\pi^4}{60}, \\
s_4(u) &= 6\mathrm{Li}_3(u) - 3\mathrm{Li}_2(u)\ln(u) + 3\mathrm{Li}_3(\bar{u}) - 2\pi^2\ln(u) - 6\zeta(3), \\
s_5(u) &= -2\mathrm{Li}_3(-u) + 2\mathrm{Li}_2(-u)\ln(u) + \ln(u+1)\ln^2(u) + \pi^2\ln(u+1).
\end{aligned}
\tag{80}
$$

References

[1] M. Beneke, G. Buchalla, M. Neubert, C.T. Sachrajda, Phys. Rev. Lett. 83 (1999) 1914, hep-ph/9905312;
M. Beneke, G. Buchalla, M. Neubert, C.T. Sachrajda, Nucl. Phys. B 591 (2000) 313, hep-ph/0006124.

Author's personal copy

[2] C.W. Bauer, S. Fleming, D. Pirjol, I.W. Stewart, Phys. Rev. D 63 (2001) 114020, hep-ph/0011336;
C.W. Bauer, D. Pirjol, I.W. Stewart, Phys. Rev. D 65 (2002) 054022, hep-ph/0109045.
[3] M. Beneke, A.P. Chapovsky, M. Diehl, T. Feldmann, Nucl. Phys. B 643 (2002) 431, hep-ph/0206152;
M. Beneke, T. Feldmann, Phys. Lett. B 553 (2003) 267, hep-ph/0211358.
[4] M. Beneke, T. Feldmann, Nucl. Phys. B 685 (2004) 249, hep-ph/0311335.
[5] C.W. Bauer, D. Pirjol, I.W. Stewart, Phys. Rev. D 67 (2003) 071502, hep-ph/0211069.
[6] B.O. Lange, M. Neubert, Nucl. Phys. B 690 (2004) 249, hep-ph/0311345;
B.O. Lange, M. Neubert, Nucl. Phys. B 723 (2005) 201, Erratum.
[7] M. Beneke, T. Feldmann, Nucl. Phys. B 592 (2001) 3, hep-ph/0008255.
[8] M. Beneke, Y. Kiyo, D.s. Yang, Nucl. Phys. B 692 (2004) 232, hep-ph/0402241.
[9] R. Bonciani, A. Ferroglia, JHEP 0811 (2008) 065, arXiv:0809.4687 [hep-ph].
[10] H.M. Asatrian, C. Greub, B.D. Pecjak, Phys. Rev. D 78 (2008) 114028, arXiv:0810.0987 [hep-ph].
[11] M. Beneke, T. Huber, X.Q. Li, Nucl. Phys. B 811 (2009) 77, arXiv:0810.1230 [hep-ph].
[12] G. Bell, Nucl. Phys. B 812 (2009) 264, arXiv:0810.5695 [hep-ph].
[13] R.J. Hill, T. Becher, S.J. Lee, M. Neubert, JHEP 0407 (2004) 081, hep-ph/0404217.
[14] M. Beneke, D. Yang, Nucl. Phys. B 736 (2006) 34, hep-ph/0508250.
[15] F.V. Tkachov, Phys. Lett. B 100 (1981) 65;
K.G. Chetyrkin, F.V. Tkachov, Nucl. Phys. B 192 (1981) 159.
[16] S. Laporta, Int. J. Mod. Phys. A 15 (2000) 5087, hep-ph/0102033.
[17] G. Bell, Nucl. Phys. B 795 (2008) 1, arXiv:0705.3127 [hep-ph];
G. Bell, PhD thesis, LMU München, arXiv:0705.3133 [hep-ph], 2006;
G. Bell, Nucl. Phys. B 822 (2009) 172, arXiv:0902.1915 [hep-ph].
[18] T. Huber, JHEP 0903 (2009) 024, arXiv:0901.2133 [hep-ph];
M. Beneke, T. Huber, X.Q. Li, Nucl. Phys. B 832 (2010) 109, arXiv:0911.3655 [hep-ph].
[19] E. Remiddi, J.A.M. Vermaseren, Int. J. Mod. Phys. A 15 (2000) 725, hep-ph/9905237.
[20] J. Blumlein, S. Kurth, Phys. Rev. D 60 (1999) 014018, hep-ph/9810241.
[21] D.V. Nanopoulos, D.A. Ross, Nucl. Phys. B 157 (1979) 273;
R. Tarrach, Nucl. Phys. B 183 (1981) 384;
D.J. Broadhurst, A.G. Grozin, Phys. Rev. D 52 (1995) 4082, hep-ph/9410240.
[22] T. Becher, M. Neubert, Phys. Lett. B 633 (2006) 739, hep-ph/0512208;
T. Becher, M. Neubert, Phys. Lett. B 637 (2006) 251, hep-ph/0603140.
[23] An electronic file containing all coefficients is attached to the arXiv submission of the present work, and can be obtained from the authors upon request.
[24] A. Ali, B.D. Pecjak, C. Greub, Eur. Phys. J. C 55 (2008) 577, arXiv:0709.4422 [hep-ph].
[25] H.M. Asatrian, A. Hovhannisyan, V. Poghosyan, T. Ewerth, C. Greub, T. Hurth, Nucl. Phys. B 749 (2006) 325, hep-ph/0605009.
[26] G. Burdman, G. Hiller, Phys. Rev. D 63 (2001) 113008, hep-ph/0011266.
[27] P. Ball, R. Zwicky, Phys. Rev. D 71 (2005) 014015, hep-ph/0406232;
P. Ball, R. Zwicky, Phys. Rev. D 71 (2005) 014029, hep-ph/0412079.
[28] F. De Fazio, T. Feldmann, T. Hurth, Nucl. Phys. B 733 (2006) 1, hep-ph/0504088;
F. De Fazio, T. Feldmann, T. Hurth, Nucl. Phys. B 800 (2008) 405, Erratum;
F. De Fazio, T. Feldmann, T. Hurth, JHEP 0802 (2008) 031, arXiv:0711.3999 [hep-ph].
[29] C.W. Bauer, D. Pirjol, I.Z. Rothstein, I.W. Stewart, Phys. Rev. D 70 (2004) 054015, hep-ph/0401188;
M. Beneke, G. Buchalla, M. Neubert, C.T. Sachrajda, Phys. Rev. D 72 (2005) 098501, hep-ph/0411171.
[30] M. Beneke, T. Feldmann, D. Seidel, Nucl. Phys. B 612 (2001) 25, hep-ph/0106067;
M. Beneke, T. Feldmann, D. Seidel, Eur. Phys. J. C 41 (2005) 173, hep-ph/0412400.
[31] C. Bobeth, G. Hiller, G. Piranishvili, JHEP 0807 (2008) 106, arXiv:0805.2525 [hep-ph];
U. Egede, T. Hurth, J. Matias, M. Ramon, W. Reece, JHEP 0811 (2008) 032, arXiv:0807.2589 [hep-ph];
U. Egede, T. Hurth, J. Matias, M. Ramon, W. Reece, arXiv:1005.0571 [hep-ph];
W. Altmannshofer, P. Ball, A. Bharucha, A.J. Buras, D.M. Straub, M. Wick, JHEP 0901 (2009) 019, arXiv:0811.1214 [hep-ph];
A. Bharucha, W. Reece, arXiv:1002.4310 [hep-ph].
[32] T. Hurth, Int. J. Mod. Phys. A 22 (2007) 1781, hep-ph/0703226;
M. Artuso, et al., Eur. Phys. J. C 57 (2008) 309, arXiv:0801.1833 [hep-ph];
T. Hurth, M. Nakao, arXiv:1005.1224 [hep-ph].
[33] A.F. Falk, M.E. Luke, M.J. Savage, Phys. Rev. D 49 (1994) 3367, hep-ph/9308288;

Author's personal copy

A. Ali, G. Hiller, L.T. Handoko, T. Morozumi, Phys. Rev. D 55 (1997) 4105, hep-ph/9609449;
G. Buchalla, G. Isidori, Nucl. Phys. B 525 (1998) 333, hep-ph/9801456.
[34] G. Buchalla, G. Isidori, S.J. Rey, Nucl. Phys. B 511 (1998) 594, hep-ph/9705253.
[35] K.S.M. Lee, Z. Ligeti, I.W. Stewart, F.J. Tackmann, Phys. Rev. D 75 (2007) 034016, hep-ph/0612156.
[36] M. Beneke, G. Buchalla, M. Neubert, C.T. Sachrajda, Eur. Phys. J. C 61 (2009) 439, arXiv:0902.4446 [hep-ph].
[37] K.S.M. Lee, I.W. Stewart, Phys. Rev. D 74 (2006) 014005, hep-ph/0511334;
K.S.M. Lee, Z. Ligeti, I.W. Stewart, F.J. Tackmann, Phys. Rev. D 74 (2006) 011501, hep-ph/0512191.
[38] K.S.M. Lee, F.J. Tackmann, Phys. Rev. D 79 (2009) 114021, arXiv:0812.0001 [hep-ph].
[39] M. Beneke, Phys. Lett. B 434 (1998) 115, hep-ph/9804241.
[40] T. Huber, T. Hurth, E. Lunghi, Nucl. Phys. B 802 (2008) 40, arXiv:0712.3009 [hep-ph].
[41] H.M. Asatrian, K. Bieri, C. Greub, A. Hovhannisyan, Phys. Rev. D 66 (2002) 094013, hep-ph/0209006.

Published for SISSA by Springer

Received: October 22, 2014
Accepted: December 3, 2014
Published: December 18, 2014

Master integrals for the two-loop penguin contribution in non-leptonic B-decays

Guido Bell[a] **and Tobias Huber**[b]

[a] *Rudolf Peierls Centre for Theoretical Physics, University of Oxford, 1 Keble Road, Oxford OX1 3NP, U.K.*

[b] *Theoretische Physik 1, Naturwissenschaftlich-Technische Fakultät, Universität Siegen, Walter-Flex-Straße 3, D-57068 Siegen, Germany*

E-mail: guido.bell@physics.ox.ac.uk, huber@tp1.physik.uni-siegen.de

Abstract: We compute the master integrals that arise in the calculation of the leading penguin amplitudes in non-leptonic B-decays at two-loop order. The application of differential equations in a canonical basis enables us to give analytic results for all master integrals in terms of iterated integrals with rational weight functions. It is the first application of this method to the case of two different internal masses.

Keywords: B-Physics, QCD, Heavy Quark Physics, CP violation

ArXiv ePrint: 1410.2804

Open Access, © The Authors.
Article funded by SCOAP[3].

doi:10.1007/JHEP12(2014)129

JHEP12(2014)129

Contents

1 Introduction **1**

2 Definitions and notation **3**
2.1 Kinematics 3
2.2 Iterated integrals 4

3 Canonical basis **5**

4 Results **9**
4.1 M_1 9
4.2 M_2 10
4.3 M_3 and M_4 11
4.4 M_5 12
4.5 M_6 and M_7 12
4.6 M_8 and M_9 13
4.7 M_{10} and M_{11} 14
4.8 M_{12} – M_{14} 15
4.9 M_{15} – M_{17} 18
4.10 M_{18} – M_{21} 18
4.11 M_{22} 21
4.12 M_{23} – M_{25} 21
4.13 M_{26} and M_{27} 24
4.14 M_{28} and M_{29} 25

5 Checks and validation **27**

6 Conclusion and outlook **27**

A Matrices $\tilde{A}_k$ **28**

B Auxiliary integrals **33**

C $\tilde{M}_{18} + \tilde{M}_{19}$ to $\mathcal{O}(\epsilon^4)$ **35**

1 Introduction

The study of flavour-changing quark transitions provides an important indirect probe to search for new heavy particles as well as to test the CKM mechanism of flavour mixing and CP violation. One prominent class of such transitions are non-leptonic B-meson decays,

JHEP12(2014)129

which offer a rich and interesting phenomenology including many CP-violating asymmetries. Non-leptonic two-body decays therefore play a central role at current and future B-physics experiments. The extraction of the underlying decay amplitudes is, however, complicated by the strong-interaction dynamics of the purely hadronic environment. A systematic formalism to compute the hadronic matrix elements arises in the heavy-quark limit [1–3]. Schematically,

$$\begin{aligned}\langle M_1 M_2 | Q_i | \bar{B} \rangle \simeq\; & F^{BM_1} \int du\, T_i^I(u)\, \phi_{M_2}(u) \\ & + \int d\omega\, dv\, du\, T_i^{II}(\omega, v, u)\, \phi_B(\omega)\, \phi_{M_1}(v)\, \phi_{M_2}(u)\,, \end{aligned} \tag{1.1}$$

where $M_{1,2}$ are light (charmless) pseudo-scalar or vector mesons and Q_i is a generic operator of the effective weak Hamiltonian. The hadronic dynamics in the above factorisation formula is encoded in a form factor F and in light-cone distribution amplitudes ϕ. The hard-scattering kernels T, on the other hand, can be computed to all orders in perturbation theory in a partonic calculation. In the last few years, the perturbative corrections have been worked out to next-to-next-to-leading order (NNLO) accuracy. While the full set of $\mathcal{O}(\alpha_s^2)$ corrections to the spectator-scattering kernels T_i^{II} is known [4–8], NNLO corrections to the kernels T_i^I have to date only been determined for the topological tree amplitudes [9–11].

The missing NNLO ingredient consists of a two-loop calculation of the hard-scattering kernels T_i^I in the penguin sector. The calculation involves various types of operator insertions, for details we refer to a future publication [12]. The one-loop contribution of the magnetic dipole operator has been computed in [13]. The most difficult part of the calculation consists in the computation of massive two-loop penguin diagrams like the ones shown in figure 1. Whereas the integrals that entered the two-loop tree calculation [14, 15] can be expressed in terms of Harmonic Polylogarithms (HPLs) [16], the massive propagator in the penguin loop introduces an additional scale and complicates the calculation. In the present paper we give analytic results for the master integrals that arise in this calculation.

A convenient technique for the calculation of multi-scale integrals is the method of differential equations [17–19]. In combination with integration-by-parts identities [20, 21] and Laporta's reduction algorithm [22], the master integrals are computed by solving a set of differential equations where the derivatives are taken with respect to the external scales of the process. It has recently been pointed out that the solution simplifies considerably if the basis of master integrals is chosen appropriately [23]. We will discuss the properties of such a *canonical basis* in detail below. The method has been successfully applied to compute various massless as well as massive two-loop and three-loop integrals [24–33]. The present calculation is the first application of the method in which the integrals have two different internal masses.

Our paper is organised as follows. We first discuss the kinematics of the process and introduce a generalisation of the HPLs in section 2. The canonical basis of master integrals is defined in section 3, and analytic results for all master integrals are given in section 4. We comment on several cross-checks of our calculation in section 5, before we conclude in

JHEP12(2014)129

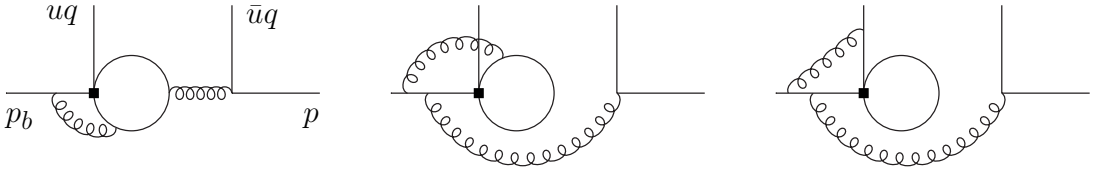

Figure 1. Sample diagrams that arise in the two-loop calculation of the leading penguin amplitudes. The black square denotes an insertion of an operator from the effective weak Hamiltonian. The line to the left of the square is the incoming b-quark with momentum $p_b = q + p$. The quark in the penguin loop can either be massless (up, down, strange) or massive (charm, bottom). The momenta of the massless final state quarks are outgoing.

section 6. The paper is complemented by three appendices with various technical details, as well as an electronic file that contains the analytic results of all master integrals and is attached to the arXiv submission of the present work.

2 Definitions and notation

2.1 Kinematics

The kinematics of the process is depicted in figure 1. We write $p_b = q+p$ with $p_b^2 = m_b^2$ and $p^2 = q^2 = 0$. The momentum q of the emitted final state meson is split up into two parallel momenta $q_1 = uq$ and $q_2 = (1-u)q \equiv \bar{u}q$ of the quark and anti-quark, respectively, where $u \in [0,1]$ is the convolution variable that enters the first term of eq. (1.1). The quark in the penguin loop can either be massless in the case of up, down and strange quarks, or massive of mass m_c or m_b in the case of charm or bottom. For massless quarks, the master integrals are already known from the calculation of the two-loop tree amplitudes in [14, 15]. We therefore only consider the situation with a massive quark in the penguin loop in the following. The problem then depends on two dimensionless variables, which we choose as the momentum fraction $\bar{u}$ of the anti-quark and the mass ratio $z_f \equiv m_f^2/m_b^2$, with $f = c, b$. The analytic continuation is done via $z_f \to z_f - i\eta$, with infinitesimally small $\eta > 0$.

In order to express the solution to the master integrals in terms of iterated integrals with rational weights, it will be convenient to trade the variables $\bar{u}$ and z_f for other sets of variables. Our default choice is the set (r, s) with

$$r \equiv \sqrt{1-4z_f}\,, \qquad s \equiv \sqrt{1-\frac{4z_f}{\bar{u}}}\,, \tag{2.1}$$

which, when solved for the original variables, implies

$$\bar{u} = \frac{1-r^2}{1-s^2}\,, \qquad z_f = \frac{1-r^2}{4}\,. \tag{2.2}$$

Let us have a look at the possible values of s. When $\bar{u}$ runs from $0 \to 1$, the variable s for $4z_f > 1$ runs from $+i\infty \to r$ along the imaginary axis. For $4z_f < 1$, s runs from $+i\infty \to 0$ along the imaginary axis, followed by $0 \to r$ along the real axis. In this case the threshold at $\bar{u} = 4z_f$ is mapped onto $s = 0$.

JHEP12(2014)129

Another convenient choice of variables will be the set (r, s_1), with

$$s_1 \equiv \sqrt{1 - \frac{4z_b}{\bar{u}}} \tag{2.3}$$

and $z_b = 1 - i\eta$. The variable s_1 runs from $+i\infty \to +i\sqrt{3}$ along the imaginary axis once we let $\bar{u}$ run from $0 \to 1$.

A third choice of variables consists of the set (r, p) with

$$p \equiv \frac{1 - \sqrt{u^2 + 4\bar{u}z_f}}{\bar{u}} \,. \tag{2.4}$$

When solved for the original variable $\bar{u}$ one obtains

$$\bar{u} = \frac{r^2 + 1 - 2p}{1 - p^2} \,. \tag{2.5}$$

When $\bar{u}$ runs from $0 \to 1$, the variable p runs from $1 - 2z_f \to 1 - 2\sqrt{z_f}$.

2.2 Iterated integrals

One of the classical examples of iterated integrals are HPLs [16]. They are generalisations of ordinary polylogarithms and appear in many calculations of higher-order corrections in perturbative Quantum Field Theory. The HPLs are defined by

$$H_{a_1,a_2,\ldots,a_n}(x) = \int_0^x dt\, f_{a_1}(t)\, H_{a_2,\ldots,a_n}(t) \,, \tag{2.6}$$

where the parameters a_i can take the values 0 or ± 1, and n is called the *weight* of the HPL. In the special case that all indices are zero, one defines $H_{\vec{0}_n}(x) = \frac{1}{n!}\ln^n(x)$. The weight functions $f_{a_i}(x)$ are given by

$$f_1(x) = \frac{1}{1-x} \,, \qquad f_0(x) = \frac{1}{x} \,, \qquad f_{-1}(x) = \frac{1}{1+x} \,. \tag{2.7}$$

In addition one assigns the weight k to numbers like π^k, $\ln^k(2)$ and the Riemann zeta function ζ_k, and one uses that the product of two expressions of weights k_1 and k_2 has weight $k_1 + k_2$.

These definitions were generalised in [34] by introducing linear combinations of $f_1(x)$ and $f_{-1}(x)$, the so-called "+" and "−"-weights, according to

$$f_+(x) = f_1(x) + f_{-1}(x) = \frac{2}{1-x^2} \,, \tag{2.8}$$

$$f_-(x) = f_1(x) - f_{-1}(x) = \frac{2x}{1-x^2} \,. \tag{2.9}$$

In the present work we further generalise the weights by allowing more generic expressions to appear in the weight functions. For any expression $w \neq 0$ we define

$$f_w(x) = \frac{1}{w-x} \,, \qquad f_{-w}(x) = \frac{1}{w+x} \,, \tag{2.10}$$

JHEP12(2014)129

and accordingly

$$f_{w^+}(x) = f_w(x) + f_{-w}(x) = \frac{2w}{w^2 - x^2}\,, \tag{2.11}$$

$$f_{w^-}(x) = f_w(x) - f_{-w}(x) = \frac{2x}{w^2 - x^2}\,. \tag{2.12}$$

Also with these newly introduced weight functions we define a general HPL by means of eq. (2.6), but we also allow the weights (2.10) – (2.12) to enter the integrand. In the current calculation, we encounter the following expressions for w,

$$\begin{aligned} w_1 &= 1\,, & w_4 &= 1 + \sqrt{1-r^2}\,, \\ w_2 &= r\,, & w_5 &= 1 - \sqrt{1-r^2}\,. \\ w_3 &= \frac{r^2+1}{2}\,, \end{aligned} \tag{2.13}$$

We will refer to $w_1 - w_5$ as *rational weights*, since any of the w_i is rational either in r or m_f, given that $\sqrt{1-r^2} = 2\sqrt{z_f} = 2m_f/m_b$ is free of any square roots.

As a matter of fact, the generalised HPLs are closely related to Goncharov polylogarithms [35], which are defined by

$$G_{a_1,a_2,\ldots,a_n}(x) = \int_0^x \frac{dt}{t-a_1}\, G_{a_2,\ldots,a_n}(t) \tag{2.14}$$

and $G_{\vec{0}_n}(x) = H_{\vec{0}_n}(x)$. We can therefore always write a generalised HPL as a linear combination of Goncharov polylogarithms, for example

$$H_{w_2^+}(x) = G_{-r}(x) - G_r(x)\,, \tag{2.15}$$

and similarly for higher weights.

The structure of the differential equations in the subsequent sections reveals that the results of the master integrals are most compactly written in terms of HPLs with generalised weights. For their numerical evaluation described in section 5, however, we prefer the notation in terms of Goncharov polylogarithms.

3 Canonical basis

Within dimensional regularisation where space-time is analytically continued to $D = 4-2\epsilon$ dimensions, integration-by-parts identities [20, 21] provide non-trivial relations between different loop integrals. It has now become a standard tool to use automated reduction algorithms to express complicated multi-loop calculations in terms of a much smaller set of irreducible master integrals. The choice of the master integrals is, however, not unique. Henn recently conjectured that the set $\vec{M}$ of master integrals can always be chosen in a way such that the set of differential equations assumes the form [23]

$$\frac{\partial}{\partial x_m}\,\vec{M}(\epsilon, x_n) = \epsilon\, A_m(x_n)\,\vec{M}(\epsilon, x_n)\,, \tag{3.1}$$

JHEP12(2014)129

where x_n are dimensionless kinematic variables and $A_m(x_n)$ is a matrix which does not depend on ϵ. In this form the system of differential equations decouples order-by-order in the ϵ-expansion. The system (3.1) can be written as a total differential,

$$d\,\vec{M}(\epsilon, x_n) = \epsilon\, d\tilde{A}(x_n)\, \vec{M}(\epsilon, x_n)\ . \tag{3.2}$$

The matrix $\tilde{A}$ contains the relevant information about the structure of the occurring weight functions. Together with suitably chosen boundary conditions, this entirely fixes the solution. As an additional feature, the solutions to the master integrals contain functions that are of uniform weight at each order in ϵ, and the weight increases by unit steps as one goes from one power to the next one in the ϵ-expansion. As a consequence, by assigning the weight -1 to ϵ and multiplying the master integrals by an appropriate power of ϵ, one can achieve that the total weight of each master integral is zero to all orders in ϵ. Integrals with the latter property and a system of differential equations of the form (3.2) will be referred to as a *canonical basis*.

At present there does not exist a systematic algorithm to find a canonical basis of master integrals. The construction therefore requires some level of experimentation, for some guidelines cf. the discussions in [24, 27, 29, 31, 32]. In the current calculation we mainly used explicit integral representations to find the canonical basis. The basis consists of 29 master integrals which we denote by M_{1-29}. In terms of the integrals I_{1-34} defined in figure 2, they are given by

$$M_1(r,s) = \epsilon\, \bar{u}\, s\, I_1(\bar{u}, z_f)\,, \tag{3.3}$$

$$M_2(\bar{u}) = \epsilon^2 u\, I_2(\bar{u})\,, \tag{3.4}$$

$$M_3(r,s) = \epsilon^2 \bar{u}\, I_3(\bar{u}, z_f)\,, \tag{3.5}$$

$$M_4(r,s) = \epsilon^2 \bar{u}\, s \Big(I_3(\bar{u}, z_f) + 2I_4(\bar{u}, z_f)\Big)\,, \tag{3.6}$$

$$M_5(r) = \epsilon^2 r \Big(I_5(z_f) + 2I_6(z_f)\Big)\,, \tag{3.7}$$

$$M_6(r,s) = \epsilon^3 \bar{u}\, I_7(u, z_f)\,, \tag{3.8}$$

$$M_7(r,s) = \frac{\epsilon^2 \bar{u}\, s}{2m_b^2} \Big(2um_b^2\, I_8(u, z_f) - I_3(1, z_f) - 2I_4(1, z_f)\Big)\,, \tag{3.9}$$

$$M_8(r,s) = \epsilon^3 u\, I_9(u, z_f)\,, \tag{3.10}$$

$$M_9(r,s) = \frac{\epsilon^2 \bar{u}\, s}{2m_b^2} \Big(2um_b^2\, I_{10}(u, z_f) - I_5(z_f) - 2I_6(z_f)\Big)\,, \tag{3.11}$$

$$M_{10}(r,s) = \epsilon^3 u\, I_{11}(\bar{u}, z_f)\,, \tag{3.12}$$

$$M_{11}(r,s) = \epsilon^2 \bar{u}\, s \Big(I_{12}(\bar{u}, z_f) + 2I_{13}(\bar{u}, z_f)\Big)\,, \tag{3.13}$$

$$M_{12}(r,s) = \epsilon^3 u\, I_{14}(\bar{u}, z_f)\,, \tag{3.14}$$

$$M_{13}(r,s) = \epsilon^3 u\, I_{15}(\bar{u}, z_f)\,, \tag{3.15}$$

JHEP12(2014)129

$$M_{14}(r,s) = \frac{\epsilon^2 s}{(1+r^2)m_b^2}\Big\{4z_f m_b^2\big(1-\bar{u}+\bar{u}z_f\big)\big(I_{16}(\bar{u},z_f)+I_{17}(\bar{u},z_f)\big) + 3I_3(1,z_f) + 2\epsilon\big(1-\bar{u}+2\bar{u}z_f\big)\big(I_{15}(\bar{u},z_f)+2I_{14}(\bar{u},z_f)\big)\Big\}, \tag{3.16}$$

$$M_{15}(r,s) = \epsilon^3\bar{u}\, I_{18}(\bar{u},z_f), \tag{3.17}$$

$$M_{16}(r,s) = \epsilon^3\bar{u}\, I_{19}(\bar{u},z_f), \tag{3.18}$$

$$M_{17}(r,s) = \frac{\epsilon^2\bar{u}\, s}{m_b^2}\Big(2z_f m_b^2\, I_{20}(\bar{u},z_f) + \epsilon\, I_{19}(\bar{u},z_f) + 2\epsilon\, I_{18}(\bar{u},z_f)\Big), \tag{3.19}$$

$$M_{18}(r,s) = \epsilon^3 u\, I_{21}(\bar{u},z_f), \tag{3.20}$$

$$M_{19}(r,s) = \epsilon^3 u\, I_{22}(\bar{u},z_f), \tag{3.21}$$

$$M_{20}(r,s) = -\frac{\epsilon^2\bar{u}\, s}{2m_b^2}\Big\{u m_b^2\big(I_{23}(\bar{u},z_f)+I_{24}(\bar{u},z_f)\big) + I_5(z_f) + 2I_6(z_f)\Big\}, \tag{3.22}$$

$$M_{21}(r,s) = \frac{\epsilon^2}{\bar{u}m_b^2}\Big\{2m_b^2\big((1+\bar{u})^2 z_f - \bar{u}^2\big)I_{25}(\bar{u},z_f) + 2z_f(1+\bar{u})\big(I_5'(z_f)+2I_4'(z_f)\big) + \big(\bar{u}^2 - 2(1+\bar{u})z_f\big)\big(I_5(z_f)+2I_6(z_f)\big) + 2\epsilon\, u\bar{u}\,\big(I_{21}(\bar{u},z_f)+I_{22}(\bar{u},z_f)\big) - \bar{u}m_b^2(1+\bar{u})(\bar{u}-4z_f)\big(I_{23}(\bar{u},z_f)+I_{24}(\bar{u},z_f)\big) + 2\bar{u}\, I_4'(z_f)\Big\}, \tag{3.23}$$

$$M_{22}(r,s) = \epsilon^3(1-2\epsilon)\,\bar{u}\, I_{26}(\bar{u},z_f), \tag{3.24}$$

$$M_{23}(r,s_1) = \epsilon^3\, u\, I_{27}(\bar{u},z_f), \tag{3.25}$$

$$M_{24}(r,s_1) = \frac{2\epsilon^2(1+s_1)}{(1-s_1)^2 m_b^2}\sqrt{1+\frac{8z_f(1-s_1)}{(1+s_1)^2}}\Big\{m_b^2\,(1-s_1)\,\big(I_{28}(\bar{u},z_f)+2\,I_{29}(\bar{u},z_f)\big) - 2m_b^2\,(1+s_1)\,I_{30}(\bar{u},z_f) + (1-s_1)\,\big(I_5'(z_f)+2I_4'(z_f)\big)\Big\}, \tag{3.26}$$

$$M_{25}(r,s_1) = \frac{2\epsilon^2(1-s_1)}{(1+s_1)^2 m_b^2}\sqrt{1+\frac{8z_f(1+s_1)}{(1-s_1)^2}}\Big\{m_b^2\,(1+s_1)\,\big(I_{28}(\bar{u},z_f)+2\,I_{29}(\bar{u},z_f)\big) - 2m_b^2\,(1-s_1)\,I_{30}(\bar{u},z_f) + (1+s_1)\,\big(I_5'(z_f)+2I_4'(z_f)\big)\Big\}, \tag{3.27}$$

$$M_{26}(s_1) = \epsilon^3 u\, I_{31}(\bar{u}), \tag{3.28}$$

$$M_{27}(s_1) = -\frac{2\epsilon^2 s_1}{(1-s_1^2)m_b^2}\Big(m_b^2\, I_{32}(\bar{u}) + 3\epsilon\, I_{31}(\bar{u})\Big), \tag{3.29}$$

$$M_{28}(r,p) = \epsilon^3 u\, I_{33}(\bar{u},z_f), \tag{3.30}$$

$$M_{29}(r,p) = \frac{\epsilon^2}{2m_b^2}\Big\{2u\big(1-\bar{u}p\big)m_b^2 I_{34}(\bar{u},z_f) - \big(\bar{u}p - 1 + 2\sqrt{z_f}\big)\big(I_5'(z_f)+2I_4'(z_f)\big)\Big\}. \tag{3.31}$$

The variables r, s, s_1 and p have been introduced in section 2.1, and the definition of the integrals $I'_{4,5}(z_f)$ can be found in appendix B. In addition there are seven auxiliary integrals, labeled M'_{1-7}, which are already known from previous calculations but which are needed in order to close the system of differential equations.

JHEP12(2014)129

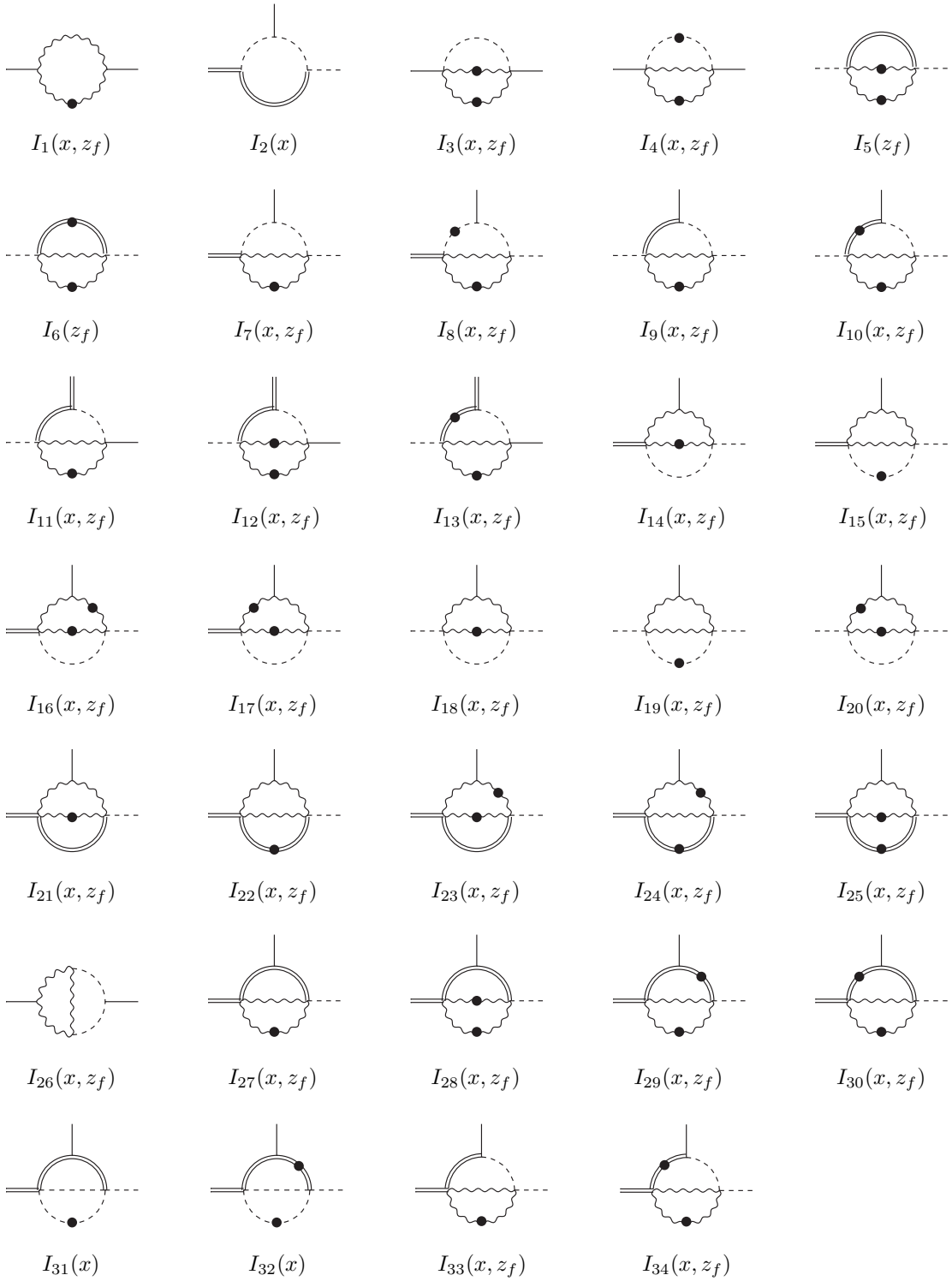

Figure 2. Integrals required to define the basis integrals in (3.3)–(3.31). Dashed/wavy/double internal lines denote propagators with mass $0/\sqrt{z_f}m_b/m_b$. Dashed/solid/double external lines correspond to virtualities $0/xm_b^2/m_b^2$. Dotted propagators are taken to be squared.

JHEP12(2014)129

In the given integral basis the system of differential equations takes the form (3.2). Instead of one large matrix $\tilde{A}$, we solve each topology separately and in turn get several smaller matrices $\tilde{A}_k$. We give the solution to the basis integrals M_{1-29} in the next section, together with the relevant boundary conditions. The solution to the auxiliary integrals M'_{1-7} can be found in appendix B.

4 Results

We write the results for the master integrals in the form

$$M = i^L \, S_\Gamma^L \, \left(m_b^2\right)^{L\,D/2-N} \, \tilde{M} \,, \tag{4.1}$$

with the number of loops L and an integer N which denotes the sum of all propagator powers. The integral $\tilde{M}$ is therefore dimensionless. Our integration measure per loop is $\int d^D k/(2\pi)^D$ and the pre-factor S_Γ reads

$$S_\Gamma = \frac{1}{(4\pi)^{D/2}\,\Gamma(1-\epsilon)} \,. \tag{4.2}$$

Once the differential equations are set up, the only missing ingredient are the boundary conditions. It turns out that the following conditions — almost all of which describe the vanishing of an integral in a particular kinematic point — are sufficient to write down the entire solution to an integral. We find that $M_{1,3,4,6,7,9,11,14-17,20-22}(r,s)$ and $M_{27}(s_1)$ vanish in $\bar{u}=0$, corresponding to $s=+i\infty$ or $s_1=+i\infty$. Furthermore, $M_{8,10,12,13,18,19}(r,s)$, $M_2(\bar{u})$, $M_{23}(r,s_1)$, $M_{26}(s_1)$, and $M_{28,29}(r,p)$ vanish in $\bar{u}=1$, corresponding to $s=r$, $s_1=+i\sqrt{3}$ or $p=1-2\sqrt{z_f}$. Moreover, $M_5(r)$ vanishes in $r=0$. Finally, the integrals $M_{24,25}(r,s_1)$ fulfill

$$\tilde{M}_{24,25}(r,s_1=+i\infty) = 4\,\tilde{M}_{23}(r,s_1=+i\infty) \,-\, 4\,\tilde{M}'_4(z_f) \,, \tag{4.3}$$

which can be derived using the Laporta reduction algorithm [22]. All these considerations lead to the full set of solutions which we list below.

4.1 M_1

As a warm-up exercise and to demonstrate how the method of differential equations in the canonical basis works, we consider the one-loop integral

$$M_1(r,s) = \int \frac{d^D k}{(2\pi)^D} \, \frac{\epsilon\,\bar{u}\,s}{[(k+p-uq)^2 - z_f m_b^2][k^2 - z_f m_b^2]^2} \,. \tag{4.4}$$

The auxiliary integral

$$M'_1(z_f) = \int \frac{d^D k}{(2\pi)^D} \, \frac{\epsilon}{[k^2 - z_f m_b^2]^2} \tag{4.5}$$

appears as a subtopology and has to be taken into account in order to make the system of differential equations complete. The solution to the auxiliary integral $M'_1(z_f)$ is elementary and can be found in appendix B.

JHEP12(2014)129

In terms of the variables r and s, the system of differential equations becomes

$$\frac{\partial \tilde{M}_1(r,s)}{\partial s} = -\frac{2\,\epsilon\,\tilde{M}_1(r,s)}{s\,(1-s^2)} + \frac{2\,\epsilon\,\tilde{M}_1'(z_f)}{1-s^2}\,, \tag{4.6}$$

$$\frac{\partial \tilde{M}_1'(z_f)}{\partial s} = 0\,, \tag{4.7}$$

and

$$\frac{\partial \tilde{M}_1(r,s)}{\partial r} = \frac{2\,\epsilon\,r\,\tilde{M}_1(r,s)}{1-r^2}\,, \tag{4.8}$$

$$\frac{\partial \tilde{M}_1'(z_f)}{\partial r} = \frac{2\,\epsilon\,r\,\tilde{M}_1'(z_f)}{1-r^2}\,. \tag{4.9}$$

The system of differential equations can be brought into the canonical form (3.2), with $\vec{M} = \{\tilde{M}_1(r,s), \tilde{M}_1'(z_f)\}$ and

$$\tilde{A}_1(r,s) = \begin{pmatrix} \ln(1-s^2) - 2\ln(s) - \ln(1-r^2) & \ln\left(\frac{1+s}{1-s}\right) \\ 0 & -\ln(1-r^2) \end{pmatrix}. \tag{4.10}$$

Solving eqs. (4.6) and (4.8) together with the aforementioned boundary condition gives

$$\begin{aligned}
\tilde{M}_1(r,s) = z_f^{-\epsilon} \Big\{ & \epsilon\,[H_{w_1^+}(s) - i\pi] \\
& + \epsilon^2\,[\pi^2 + 2\,i\pi\,H_0(s) + i\pi\,H_{w_1^-}(s) - 2\,H_{0,w_1^+}(s) - H_{w_1^-,w_1^+}(s) + 2\,i\pi\,\ln(2)] \\
& + \epsilon^3 \Big[\frac{i\pi^3}{6} - 2\pi^2 H_0(s) - \pi^2 H_{w_1^-}(s) + \frac{\pi^2}{6} H_{w_1^+}(s) - 4\,i\pi H_{0,0}(s) - 2\,i\pi H_{0,w_1^-}(s) \\
& - 2i\pi H_{w_1^-,0}(s) - i\pi H_{w_1^-,w_1^-}(s) + 4H_{0,0,w_1^+}(s) + 2H_{0,w_1^-,w_1^+}(s) + 2H_{w_1^-,0,w_1^+}(s) \\
& + H_{w_1^-,w_1^-,w_1^+}(s) - 2\pi^2\ln(2) - 4i\pi H_0(s)\ln(2) - 2i\pi H_{w_1^-}(s)\ln(2) - 2i\pi\ln^2(2) \Big] \\
& + \mathcal{O}(\epsilon^4) \Big\}\,.
\end{aligned} \tag{4.11}$$

The solution can also be obtained from the following closed form,

$$\tilde{M}_1(r,s) = z_f^{-\epsilon}\,\frac{2\,\epsilon\,s\,\Gamma(1-\epsilon)\,\Gamma(1+\epsilon)}{s^2-1}\;{}_2F_1\left(1, 1+\epsilon;\, \frac{3}{2};\, \frac{1}{1-s^2}\right)\,, \tag{4.12}$$

by expanding the hypergeometric function e.g. with `HypExp` [36, 37].

4.2 M_2

From now on, we will not give the explicit form of the differential equations anymore, but only the corresponding matrices $\tilde{A}_k$ and the final solution to the integrals. The integral

JHEP12(2014)129

M_2 only depends on one kinematic variable, which we choose to be $\bar{u}$. The set of integrals is now given by $\vec{M} = \left\{\tilde{M}_2(\bar{u}), \tilde{M}_1'(z_f = 1), \tilde{M}_2'(\bar{u})\right\}$, and we have

$$\tilde{A}_2(\bar{u}) = \begin{pmatrix} 2\ln(1-\bar{u}) - 2\ln(\bar{u}) & -\ln(\bar{u}) & -\ln(\bar{u}) \\ 0 & 0 & 0 \\ 0 & 0 & -\ln(\bar{u}) \end{pmatrix} . \tag{4.13}$$

The solution reads

$$\begin{aligned} \tilde{M}_2(\bar{u}) = & \epsilon^2 \left[i\pi\, H_0(\bar{u}) - H_{0,0}(\bar{u}) \right] \\ & + \epsilon^3 \Big[-\frac{i\pi^3}{3} - \frac{2}{3}\pi^2 H_0(\bar{u}) - 3\, i\pi H_{0,0}(\bar{u}) - i\pi H_{w_1^-,0}(\bar{u}) - i\pi H_{w_1^+,0}(\bar{u}) + 3\, H_{0,0,0}(\bar{u}) \\ & + H_{w_1^-,0,0}(\bar{u}) + H_{w_1^+,0,0}(\bar{u}) - 2\,\zeta_3 \Big] + \mathcal{O}(\epsilon^4) . \end{aligned} \tag{4.14}$$

Also in this case the solution can be obtained from an expression containing hypergeometric functions,

$$\begin{aligned} \tilde{M}_2(\bar{u}) = & \frac{(1-\bar{u})\,\epsilon\,\Gamma(1-\epsilon)\,\Gamma(1+\epsilon)}{\Gamma(2-2\epsilon)} \left\{ \Gamma(1-2\epsilon)\, {}_2F_1\left(1,1\,;\,2-2\epsilon\,;\,1-\bar{u}\right) \right. \\ & \left. - \Gamma^2(1-\epsilon)\, e^{i\pi\epsilon}\, \bar{u}^{-\epsilon}\, {}_2F_1\left(1,1-\epsilon\,;\,2-2\epsilon\,;\,1-\bar{u}\right) \right\} . \end{aligned} \tag{4.15}$$

4.3 M_3 and M_4

In this topology we have the set of integrals $\vec{M} = \left\{\tilde{M}_3(r,s), \tilde{M}_4(r,s), \left[\tilde{M}_1'(z_f)\right]^2\right\}$, together with the corresponding matrix $\tilde{A}_{3,4}(r,s)$. Since the expressions for the matrices $\tilde{A}_k$ become more and more involved, we from now on relegate them to appendix A. The solution to $M_3(r,s)$ and $M_4(r,s)$ reads

$$\begin{aligned} \tilde{M}_3(r,s) = & z_f^{-2\epsilon} \Big\{ \epsilon^2 \left[-\pi^2 - 2\, i\pi\, H_{w_1^+}(s) + 2\, H_{w_1^+,w_1^+}(s) \right] \\ & + \epsilon^3 \Big[-\pi^2\, H_{w_1^-}(s) + 6\,\pi^2\, H_{w_1^+}(s) - 2\, i\pi\, H_{w_1^-,w_1^+}(s) + 12\, i\pi\, H_{w_1^+,0}(s) \\ & + 8\, i\pi\, H_{w_1^+,w_1^-}(s) + 2\, H_{w_1^-,w_1^+,w_1^+}(s) - 12\, H_{w_1^+,0,w_1^+}(s) - 8\, H_{w_1^+,w_1^-,w_1^+}(s) \\ & - 2\,\pi^2\, \ln(2) + 16\, i\pi\, H_{w_1^+}(s)\, \ln(2) - 21\,\zeta_3 \Big] + \mathcal{O}(\epsilon^4) \Big\} , \end{aligned} \tag{4.16}$$

$$\begin{aligned} \tilde{M}_4(r,s) = & z_f^{-2\epsilon} \Big\{ \epsilon \left[2\, i\pi - 2\, H_{w_1^+}(s) \right] \\ & + \epsilon^2 \Big[12\, H_{0,w_1^+}(s) + 8 H_{w_1^-,w_1^+}(s) - 12\, i\pi H_0(s) - 8\, i\pi H_{w_1^-}(s) - 16\, i\pi \ln(2) - 6\pi^2 \Big] \\ & + \epsilon^3 \Big[-4\, i\pi^3 + 36\,\pi^2\, H_0(s) + 24\,\pi^2\, H_{w_1^-}(s) - \frac{20}{3}\pi^2\, H_{w_1^+}(s) + 72\, i\pi\, H_{0,0}(s) \\ & + 48\, i\pi\, H_{0,w_1^-}(s) + 48\, i\pi\, H_{w_1^-,0}(s) + 32\, i\pi\, H_{w_1^-,w_1^-}(s) - 12\, i\pi\, H_{w_1^+,w_1^+}(s) \\ & - 72\, H_{0,0,w_1^+}(s) - 48\, H_{0,w_1^-,w_1^+}(s) - 48\, H_{w_1^-,0,w_1^+}(s) - 32\, H_{w_1^-,w_1^-,w_1^+}(s) \\ & + 12\, H_{w_1^+,w_1^+,w_1^+}(s) + 48\,\pi^2\, \ln(2) + 96\, i\pi\, H_0(s)\, \ln(2) \\ & + 64\, i\pi\, H_{w_1^-}(s)\, \ln(2) + 64\, i\pi\, \ln^2(2) \Big] + \mathcal{O}(\epsilon^4) \Big\} . \end{aligned} \tag{4.17}$$

JHEP12(2014)129

A closed form of these integrals is given by

$$\tilde{M}_3(r,s) = z_f^{-2\epsilon}\,\frac{\Gamma^2(1-\epsilon)\,\Gamma^2(1+\epsilon)}{2\,s^2\,(\epsilon-1)}\,\Big\{(\epsilon-1)\,(s^2+1) \tag{4.18}$$
$$+\,(1-2\epsilon)\,(3-s^2)\,{}_3F_2\left(1,\epsilon,2\epsilon\,;\,2-\epsilon,\frac{1}{2}+\epsilon\,;\,\frac{1}{1-s^2}\right)$$
$$-\,(2-3\epsilon)\,(1-s^2)\,{}_3F_2\left(1,\epsilon,2\epsilon-1\,;\,2-\epsilon,\frac{1}{2}+\epsilon\,;\,\frac{1}{1-s^2}\right)\Big\}\,,$$

$$\tilde{M}_4(r,s) = z_f^{-2\epsilon}\,\frac{\Gamma^2(1-\epsilon)\,\Gamma(1+\epsilon)\,\Gamma(\epsilon-1)}{4\,s^3}\Big\{(\epsilon-1)\,\left[\epsilon(4s^4-6s^2+6)-(s^2-1)^2\right] \tag{4.19}$$
$$-\,(1-2\epsilon)(3+s^2)\,\left[\epsilon\left(4s^2-6\right)-s^2+1\right]\,{}_3F_2\left(1,\epsilon,2\epsilon\,;\,2-\epsilon,\frac{1}{2}+\epsilon\,;\,\frac{1}{1-s^2}\right)$$
$$-\,(2-3\epsilon)(1-s^2)\,\left[\epsilon\left(4s^2+6\right)-s^2-1\right]\,{}_3F_2\left(1,\epsilon,2\epsilon-1\,;\,2-\epsilon,\frac{1}{2}+\epsilon\,;\,\frac{1}{1-s^2}\right)\Big\}.$$

4.4 M_5

In this case the set of integrals consists of $\vec{M} = \left\{\tilde{M}_5(r), \left[\tilde{M}_1'(z_f)\right]^2, \tilde{M}_1'(z_f)\,\tilde{M}_1'(z_f=1)\right\}$. The matrix $\tilde{A}_5(r)$ can be found in appendix A, and the solution becomes

$$\tilde{M}_5(r) = \epsilon^2\,[-2\,H_{w_1^+,w_1^-}(r) - 4\,H_{w_1^+}(r)\,\ln(2)]$$
$$+\,\epsilon^3\Big[4\,H_{0,w_1^+,w_1^-}(r) - 6\,H_{w_1^+,w_1^-,w_1^-}(r) + 8\,H_{0,w_1^+}(r)\,\ln(2) - 12\,H_{w_1^+,w_1^-}(r)\,\ln(2)$$
$$-\,12\,H_{w_1^+}(r)\,\ln^2(2)\Big] + \mathcal{O}(\epsilon^4)\,, \tag{4.20}$$

which can also be obtained from the expansion of

$$\tilde{M}_5(r) = \frac{4^{1+\epsilon}\,\epsilon\,r\,\Gamma^2(1-\epsilon)\Gamma^2(1+\epsilon)}{1+2\epsilon} \tag{4.21}$$
$$\times\left\{(1-r^2)^{-\epsilon}\,{}_2F_1\left(1,\frac{1}{2}\,;\,\frac{3}{2}+\epsilon\,;\,r^2\right) - 4^{\epsilon}(1-r^2)^{-2\epsilon}\,{}_2F_1\left(1,\frac{1}{2}-\epsilon\,;\,\frac{3}{2}+\epsilon\,;\,r^2\right)\right\}.$$

4.5 M_6 and M_7

Here the topology consists of six integrals

$$\vec{M} = \left\{\tilde{M}_6(r,s), \tilde{M}_7(r,s), \tilde{M}_3(r,s=r), \tilde{M}_4(r,s=r), \tilde{M}_1'(z_f)\tilde{M}_2'(u), \left[\tilde{M}_1'(z_f)\right]^2\right\}\,, \tag{4.22}$$

and the corresponding matrix is $\tilde{A}_{6,7}(r,s)$. The solutions to the integrals reads

$$\tilde{M}_6(r,s) = \epsilon^3\Big[-\frac{i\pi^3}{2} + \pi^2\,H_0(r) + \frac{\pi^2}{2}\,H_{w_1^-}(s) + i\pi H_{w_1^-}(s)\,H_{w_1^+}(r) - \frac{\pi^2}{2}\,H_{w_2^-}(s)$$
$$-\,i\pi H_{w_1^+}(r)\,H_{w_2^-}(s) + 2\,i\pi H_{0,w_1^+}(r) - H_{w_1^-}(s)\,H_{w_1^+,w_1^+}(r) + H_{w_2^-}(s)\,H_{w_1^+,w_1^+}(r)$$
$$+\,i\pi H_{w_1^+,w_1^+}(s) - 2\,H_0(r)\,H_{w_1^+,w_1^+}(s) - H_{w_1^-}(r)\,H_{w_1^+,w_1^+}(s) - i\pi H_{w_1^+,w_2^+}(s)$$
$$+\,H_{w_1^+}(r)\,H_{w_1^+,w_2^+}(s) - 2\,H_{0,w_1^+,w_1^+}(r) - H_{w_1^+,w_1^+,w_1^-}(s) + H_{w_1^+,w_1^+,w_2^-}(s)$$
$$-\,2\,H_{w_1^+,w_1^+}(s)\,\ln(2) + \frac{7}{2}\,\zeta_3\Big] + \mathcal{O}(\epsilon^4)\,, \tag{4.23}$$

JHEP12(2014)129

$$
\begin{aligned}
\tilde{M}_7(r,s) = \epsilon^2 \Big[& - i\pi H_{w_1^+}(s) + 2\, H_0(r)\, H_{w_1^+}(s) + H_{w_1^-}(r)\, H_{w_1^+}(s) + i\pi H_{w_2^+}(s) \\
& - H_{w_1^+}(r)\, H_{w_2^+}(s) + H_{w_1^+,w_1^-}(s) - H_{w_1^+,w_2^-}(s) + 2\, H_{w_1^+}(s)\, \ln(2) \Big] \\
& + \epsilon^3 \Big[\frac{13}{6}\, \pi^2\, H_{w_1^+}(s) + 2\, i\pi H_0(r)\, H_{w_1^+}(s) - i\pi H_{w_1^-}(r)\, H_{w_1^+}(s) - 3\, \pi^2\, H_{w_2^+}(s) \\
& + 3 i\pi H_{w_1^+}(r)\, H_{w_1^+}(s) - 6 i\pi H_0(r) H_{w_2^+}(s) - 2 i\pi H_{w_1^-}(r)\, H_{w_2^+}(s) + H_{w_2^-,w_1^+,w_1^-}(s) \\
& - 4 H_{w_1^+}(s)\, H_{0,0}(r) + 2\, H_{w_1^+}(s) H_{0,w_1^-}(r) + 6 H_{w_2^+}(s)\, H_{0,w_1^+}(r) + 4\, i\pi H_{0,w_1^+}(s) \\
& - 8\, H_0(r)\, H_{0,w_1^+}(s) - 4\, H_{w_1^-}(r)\, H_{0,w_1^+}(s) - 4\, i\pi H_{0,w_2^+}(s) + 4\, H_{w_1^+}(r)\, H_{0,w_2^+}(s) \\
& + 2\, H_{w_1^+}(s)\, H_{w_1^-,0}(r) + 3\, H_{w_1^+}(s)\, H_{w_1^-,w_1^-}(r) + 2\, H_{w_2^+}(s)\, H_{w_1^-,w_1^+}(r) \\
& - H_{w_1^+,w_2^-,w_2^-}(s) + 3\, i\pi H_{w_1^-,w_1^+}(s) - 6\, H_0(r)\, H_{w_1^-,w_1^+}(s) - 3\, H_{w_1^-}(r)\, H_{w_1^-,w_1^+}(s) \\
& - 3 i\pi H_{w_1^-,w_2^+}(s) + 3 H_{w_1^+}(r) H_{w_1^-,w_2^+}(s) - 2 H_{w_2^+}(s)\, H_{w_1^+,w_1^-}(r) + i\pi H_{w_1^+,w_1^-}(s) \\
& - 2 H_0(r)\, H_{w_1^+,w_1^-}(s) + H_{w_1^-}(r) H_{w_1^+,w_1^-}(s) - 3 H_{w_1^+}(s) H_{w_1^+,w_1^+}(r) - i\pi H_{w_1^+,w_2^-}(s) \\
& + 2\, H_0(r)\, H_{w_1^+,w_2^-}(s) - H_{w_1^-}(r)\, H_{w_1^+,w_2^-}(s) - i\pi H_{w_2^-,w_1^+}(s) + 2\, H_0(r)\, H_{w_2^-,w_1^+}(s) \\
& + H_{w_1^-}(r)\, H_{w_2^-,w_1^+}(s) + i\pi H_{w_2^-,w_2^+}(s) - H_{w_1^+}(r)\, H_{w_2^-,w_2^+}(s) - 4\, H_{0,w_1^+,w_1^-}(s) \\
& + 4\, H_{0,w_1^+,w_2^-}(s) - 3\, H_{w_1^-,w_1^+,w_1^-}(s) + 3\, H_{w_1^-,w_1^+,w_2^-}(s) - H_{w_1^+,w_1^-,w_1^-}(s) \\
& + H_{w_1^+,w_1^-,w_2^-}(s) + H_{w_1^+,w_2^-,w_1^-}(s) - H_{w_2^-,w_1^+,w_2^-}(s) - 2\, i\pi H_{w_1^+}(s)\, \ln(2) \\
& + 4\, H_0(r)\, H_{w_1^+}(s)\, \ln(2) + 6\, H_{w_1^-}(r)\, H_{w_1^+}(s)\, \ln(2) - 4\, i\pi H_{w_2^+}(s)\, \ln(2) \\
& - 4\, H_{w_1^+}(r)\, H_{w_2^+}(s)\, \ln(2) - 8\, H_{0,w_1^+}(s)\, \ln(2) - 6\, H_{w_1^-,w_1^+}(s)\, \ln(2) \\
& + 2\, H_{w_1^+,w_1^-}(s)\, \ln(2) - 2\, H_{w_1^+,w_2^-}(s)\, \ln(2) + 2\, H_{w_2^-,w_1^+}(s)\, \ln(2) \\
& + 6\, H_{w_1^+}(s)\, \ln^2(2) \Big] + \mathcal{O}(\epsilon^4)\,. \qquad (4.24)
\end{aligned}
$$

4.6 M_8 and M_9

Also here the topology consists of six integrals, namely

$$
\vec{M} = \left\{ \tilde{M}_8(r,s), \tilde{M}_9(r,s), \tilde{M}_5(r), \tilde{M}_1'(z_f)\tilde{M}_3'(u), \left[\tilde{M}_1'(z_f)\right]^2, \tilde{M}_1'(z_f)\tilde{M}_1'(z_f=1) \right\}\,, \qquad (4.25)
$$

and the matrix $\tilde{A}_{8,9}(r,s)$. Owing to simple boundary conditions, the result is quite short,

$$
\begin{aligned}
\tilde{M}_8(r,s) = \epsilon^3 \, & [-H_{w_1^+,w_1^+,w_1^-}(r) + H_{w_1^+,w_1^+,w_1^-}(s) - 2\, H_{w_1^+,w_1^+}(r)\, \ln(2) \\
& + 2\, H_{w_1^+,w_1^+}(s)\, \ln(2)] + \mathcal{O}(\epsilon^4)\,, \qquad (4.26) \\
\tilde{M}_9(r,s) = \epsilon^2 \, & [H_{w_1^+,w_1^-}(s) + 2\, H_{w_1^+}(s)\, \ln(2)] \\
& + \epsilon^3 \, [-2\, H_{w_1^+}(s)\, H_{0,w_1^-}(r) - H_{w_1^+}(s)\, H_{w_1^-,w_1^-}(r) + H_{w_2^+}(s)\, H_{w_1^+,w_1^-}(r) \\
& + 2\, H_{w_1^-}(r)\, H_{w_1^+,w_1^-}(s) + H_{w_1^-}(r)\, H_{w_1^+,w_2^-}(s) - 4\, H_{0,w_1^+,w_1^-}(s) - 3\, H_{w_1^-,w_1^+,w_1^-}(s) \\
& - H_{w_1^+,w_1^-,w_1^-}(s) - H_{w_1^+,w_2^-,w_1^-}(s) - H_{w_2^-,w_1^+,w_1^-}(s) + 4\, H_{w_1^-}(r)\, H_{w_1^+}(s)\, \ln(2)
\end{aligned}
$$

JHEP12(2014)129

$$+ 2\, H_{w_1^+}(r)\, H_{w_2^+}(s)\, \ln(2) - 8\, H_{0,w_1^+}(s)\, \ln(2) - 6\, H_{w_1^-,w_1^+}(s)\, \ln(2)$$
$$+ 2\, H_{w_1^+,w_1^-}(s)\, \ln(2) - 2\, H_{w_2^-,w_1^+}(s)\, \ln(2) + 6\, H_{w_1^+}(s)\, \ln^2(2)] + \mathcal{O}(\epsilon^4)\,. \qquad (4.27)$$

4.7 M_{10} and M_{11}

This topology consists of seven integrals

$$\vec{M} = \Big\{ \tilde{M}_{10}(r,s), \tilde{M}_{11}(r,s), \tilde{M}_3(r,s), \tilde{M}_4(r,s), \tilde{M}_5(r), \big[\tilde{M}_1'(z_f)\big]^2, \tilde{M}_1'(z_f)\tilde{M}_1'(z_f=1) \Big\}, \quad (4.28)$$

and the matrix $\tilde{A}_{10,11}(r,s)$. The result is rather long since we need functions up to weight four in $M_{10}(r,s)$,

$$\begin{aligned}
\tilde{M}_{10}(r,s) = \epsilon^3 \Big[& -\frac{\pi^2}{2} H_{w_1^-}(r) + \frac{\pi^2}{2} H_{w_1^-}(s) - i\,\pi H_{w_1^-}(r)\, H_{w_1^+}(s) + i\,\pi H_{w_1^-,w_1^+}(s) \\
& + i\,\pi H_{w_1^+,w_1^-}(s) + H_{w_1^-}(r)\, H_{w_1^+,w_1^+}(s) - H_{w_1^-,w_1^+,w_1^+}(s) - H_{w_1^+,w_1^-,w_1^+}(s) \\
& - H_{w_1^+,w_1^+,w_1^-}(r) - 2\, H_{w_1^+,w_1^+}(r)\, \ln(2) + 2\, H_{w_1^+,w_1^+}(s)\, \ln(2) \Big] \\
& + \epsilon^4 \Big[3\,\pi^2\, H_{w_1^-}(r)\, H_{w_1^+}(s) + \pi^2\, H_{w_1^-}(r)\, H_{w_2^-}(s) - 4\, i\pi H_{w_1^+}(s)\, H_{0,w_1^-}(r) \\
& - \frac{3}{2}\pi^2\, H_{w_1^-,w_1^-}(r) - 5\, i\pi H_{w_1^+}(s)\, H_{w_1^-,w_1^-}(r) + \frac{3}{2}\pi^2\, H_{w_1^-,w_1^-}(s) - 3\,\pi^2\, H_{w_1^-,w_1^+}(s) \\
& - \pi^2\, H_{w_1^-,w_2^-}(r) + 6\, i\pi H_{w_1^-}(r)\, H_{w_1^+,0}(s) - 3\,\pi^2\, H_{w_1^+,w_1^-}(s) \\
& + 5\, i\pi H_{w_1^-}(r)\, H_{w_1^+,w_1^-}(s) + 3\, H_{w_1^-,w_1^-}(r)\, H_{w_1^+,w_1^+}(s) + 2\, i\pi H_{w_1^-}(r)\, H_{w_1^+,w_2^-}(s) \\
& + 2\, H_{w_1^+,w_1^-}(r)\, H_{w_1^+,w_2^+}(s) - \pi^2\, H_{w_2^-,w_1^-}(s) + 2\, i\pi H_{w_1^-}(r)\, H_{w_2^-,w_1^+}(s) \\
& + 4\, i\pi H_{0,w_1^-,w_1^+}(r) + 4\, i\pi H_{0,w_1^+,w_1^-}(r) + 2\, i\pi H_{w_1^-,w_1^-,w_1^+}(r) + 3\, i\pi H_{w_1^-,w_1^-,w_1^+}(s) \\
& - 6\, i\pi H_{w_1^-,w_1^+,0}(s) + 2\, i\pi H_{w_1^-,w_1^+,w_1^-}(r) - 2\, i\pi H_{w_1^-,w_1^+,w_1^-}(s) - 2\, i\pi H_{w_1^-,w_1^+,w_2^-}(r) \\
& - 2\, i\pi H_{w_1^-,w_2^-,w_1^+}(r) + 4\, i\pi H_{w_1^+,0,w_1^-}(r) - 6\, i\pi H_{w_1^+,0,w_1^-}(s) \\
& - 6\, H_{w_1^-}(r)\, H_{w_1^+,0,w_1^+}(s) - 6\, i\pi H_{w_1^+,w_1^-,0}(s) + 2\, i\pi H_{w_1^+,w_1^-,w_1^-}(r) \\
& - 7\, i\pi H_{w_1^+,w_1^-,w_1^-}(s) - 5\, H_{w_1^-}(r)\, H_{w_1^+,w_1^-,w_1^+}(s) - 2\, i\pi H_{w_1^+,w_1^-,w_2^-}(r) \\
& - 2\, H_{w_1^-}(s)\, H_{w_1^+,w_1^+,w_1^-}(r) + 2\, H_{w_2^-}(s)\, H_{w_1^+,w_1^+,w_1^-}(r) - 2\, i\pi H_{w_1^+,w_2^-,w_1^-}(s) \\
& - 2\, H_{w_1^-}(r)\, H_{w_1^+,w_2^-,w_1^+}(s) - 2\, i\pi H_{w_2^-,w_1^-,w_1^+}(s) - 2\, i\pi H_{w_2^-,w_1^+,w_1^-}(s) \\
& - 2\, H_{w_1^-}(r)\, H_{w_2^-,w_1^+,w_1^+}(s) - 3\, H_{w_1^-,w_1^-,w_1^+,w_1^+}(s) + 6\, H_{w_1^-,w_1^+,0,w_1^+}(s) \\
& + 2\, H_{w_1^-,w_1^+,w_1^-,w_1^+}(s) - H_{w_1^-,w_1^+,w_1^+,w_1^-}(r) + 2\, H_{w_1^-,w_1^+,w_2^-,w_1^+}(r) \\
& + 2 H_{w_1^-,w_2^-,w_1^+,w_1^+}(r) + 6 H_{w_1^+,0,w_1^-,w_1^+}(s) + 6 H_{w_1^+,0,w_1^+,w_1^-}(r) + 6 H_{w_1^+,w_1^-,0,w_1^+}(s) \\
& + 7\, H_{w_1^+,w_1^-,w_1^-,w_1^+}(s) + 4\, H_{w_1^+,w_1^-,w_1^+,w_1^-}(r) - 2\, H_{w_1^+,w_1^-,w_1^+,w_2^+}(r) \\
& + 2\, H_{w_1^+,w_1^-,w_2^-,w_1^+}(r) + H_{w_1^+,w_1^+,w_1^-,w_1^-}(r) - 2\, H_{w_1^+,w_1^+,w_1^-,w_2^-}(r) \\
& - 4\, H_{w_1^+,w_1^+,w_1^-,w_2^+}(r) - 2\, H_{w_1^+,w_1^+,w_2^-,w_1^-}(r) - 4\, H_{w_1^+,w_1^+,w_2^+,w_1^-}(r)
\end{aligned}$$

JHEP12(2014)129

$$
\begin{aligned}
&+ 2\, H_{w_1^+,w_2^-,w_1^-,w_1^+}(s) - 2\, H_{w_1^+,w_2^+,w_1^+,w_1^-}(r) + 2\, H_{w_2^-,w_1^-,w_1^+,w_1^+}(s) \\
&+ 2\, H_{w_2^-,w_1^+,w_1^-,w_1^+}(s) - 3\,\pi^2\, H_{w_1^-}(r)\, \ln(2) + 3\,\pi^2\, H_{w_1^-}(s)\, \ln(2) \\
&+ 4\, i\pi H_{w_1^-}(r)\, H_{w_1^+}(s)\, \ln(2) - 4\, i\pi H_{w_1^-,w_1^+}(s)\, \ln(2) - 4\, i\pi H_{w_1^+,w_1^-}(s)\, \ln(2) \\
&- 4\, H_{w_1^-}(s)\, H_{w_1^+,w_1^+}(r)\, \ln(2) + 4\, H_{w_2^-}(s)\, H_{w_1^+,w_1^+}(r)\, \ln(2) \\
&+ 6 H_{w_1^-}(r)\, H_{w_1^+,w_1^+}(s) \ln(2) + 4 H_{w_1^+}(r) H_{w_1^+,w_2^+}(s) \ln(2) - 2 H_{w_1^-,w_1^+,w_1^+}(r) \ln(2) \\
&+ 12\, H_{w_1^+,0,w_1^+}(r)\, \ln(2) - 12\, H_{w_1^+,0,w_1^+}(s) \ln(2) + 8\, H_{w_1^+,w_1^-,w_1^+}(r)\, \ln(2) \\
&- 10\, H_{w_1^+,w_1^-,w_1^+}(s)\, \ln(2) - 2\, H_{w_1^+,w_1^+,w_1^-}(r)\, \ln(2) - 4\, H_{w_1^+,w_1^+,w_2^-}(r)\, \ln(2) \\
&- 8\, H_{w_1^+,w_1^+,w_2^+}(r)\, \ln(2) - 4\, H_{w_1^+,w_2^-,w_1^+}(s)\, \ln(2) - 4\, H_{w_1^+,w_2^+,w_1^+}(r)\, \ln(2) \\
&- 4\, H_{w_2^-,w_1^+,w_1^+}(s)\, \ln(2) - 6\, H_{w_1^+,w_1^+}(r)\, \ln^2(2) + 6\, H_{w_1^+,w_1^+}(s)\, \ln^2(2) \\
&- \frac{21}{2}\, H_{w_1^-}(r)\, \zeta_3 + \frac{21}{2}\, H_{w_1^-}(s)\, \zeta_3 \Big] + \mathcal{O}(\epsilon^5)\,,
\end{aligned}
\tag{4.29}
$$

$$
\begin{aligned}
\tilde{M}_{11}(r,s) =& \epsilon\, [H_{w_1^+}(s) - i\pi] \\
&+ \epsilon^2 \Big[3\,\pi^2 + 6\, i\pi H_0(s) - i\,\pi H_{w_1^-}(r) + 3\, i\pi H_{w_1^-}(s) + H_{w_1^-}(r)\, H_{w_1^+}(s) \\
&- 6\, H_{0,w_1^+}(s) - 3\, H_{w_1^-,w_1^+}(s) + 4\, i\pi \ln(2) + 2\, H_{w_1^+}(s)\, \ln(2) \Big] \\
&+ \epsilon^3 \Big[2\, i\pi^3 - 18\,\pi^2\, H_0(s) + 3\,\pi^2\, H_{w_1^-}(r) + 6\, i\pi H_0(s)\, H_{w_1^-}(r) - 9\,\pi^2\, H_{w_1^-}(s) \\
&+ 3\, i\pi H_{w_1^-}(r)\, H_{w_1^-}(s) + \frac{10}{3}\,\pi^2\, H_{w_1^+}(s) - 2\, i\pi H_{w_1^-}(r)\, H_{w_2^-}(s) - 36\, i\pi H_{0,0}(s) \\
&+ 4\, i\pi H_{0,w_1^-}(r) - 18\, i\pi H_{0,w_1^-}(s) - 6\, H_{w_1^-}(r)\, H_{0,w_1^+}(s) - 18\, i\pi H_{w_1^-,0}(s) \\
&+ i\,\pi H_{w_1^-,w_1^-}(r) + H_{w_1^+}(s)\, H_{w_1^-,w_1^-}(r) - 9\, i\pi H_{w_1^-,w_1^-}(s) - 3\, H_{w_1^-}(r)\, H_{w_1^-,w_1^+}(s) \\
&- 2 H_{w_2^+}(s) H_{w_1^+,w_1^-}(r) + 6 i\pi H_{w_1^+,w_1^+}(s) + 2 i\pi H_{w_2^-,w_1^-}(s) + 2 H_{w_1^-}(r) H_{w_2^-,w_1^+}(s) \\
&+ 36\, H_{0,0,w_1^+}(s) + 18\, H_{0,w_1^-,w_1^+}(s) + 18\, H_{w_1^-,0,w_1^+}(s) + 9\, H_{w_1^-,w_1^-,w_1^+}(s) \\
&- 6\, H_{w_1^+,w_1^+,w_1^+}(s) - 2\, H_{w_2^-,w_1^-,w_1^+}(s) - 12\,\pi^2\, \ln(2) - 24\, i\pi H_0(s)\, \ln(2) \\
&+ 4\, i\pi H_{w_1^-}(r)\, \ln(2) - 12\, i\pi H_{w_1^-}(s)\, \ln(2) + 2\, H_{w_1^-}(r)\, H_{w_1^+}(s)\, \ln(2) \\
&- 4\, H_{w_1^+}(r)\, H_{w_2^+}(s)\, \ln(2) - 12\, H_{0,w_1^+}(s)\, \ln(2) - 6\, H_{w_1^-,w_1^+}(s)\, \ln(2) \\
&+ 4\, H_{w_2^-,w_1^+}(s)\, \ln(2) - 8\, i\pi \ln^2(2) + 2\, H_{w_1^+}(s)\, \ln^2(2) \Big] + \mathcal{O}(\epsilon^4)\,.
\end{aligned}
\tag{4.30}
$$

4.8 $M_{12} - M_{14}$

Again we need seven integrals to complete the system of differential equations. They are

$$
\vec{M} = \Big\{ \tilde{M}_{12}(r,s), \tilde{M}_{13}(r,s), \tilde{M}_{14}(r,s), \tilde{M}_3(r,r), \tilde{M}_4(r,r), \big[\tilde{M}_1'(z_f)\big]^2, \tilde{M}_1(r,s)\tilde{M}_1'(z_f) \Big\}, \tag{4.31}
$$

together with the matrix $\tilde{A}_{12-14}(r,s)$. The results are

JHEP12(2014)129

$$
\begin{aligned}
\tilde{M}_{12}(r,s) = \epsilon^3 \Big[& \pi^2 H_{w_1^-}(r) - \pi^2 H_{w_1^-}(s) - 2\pi^2 H_{w_1^+}(r) - 2i\pi H_{w_1^-}(s)\, H_{w_1^+}(r) + 2\pi^2 H_{w_1^+}(s) \\
& + 4\, i\pi H_0(r)\, H_{w_1^+}(s) + 2i\pi H_{w_1^-}(r)\, H_{w_1^+}(s) - \frac{3}{4}\pi^2 H_{w_3^-}(r) + \frac{3}{4}\pi^2 H_{w_3^-}(s) \\
& + 2i\pi H_{w_1^+}(r)\, H_{w_3^-}(s) + \pi^2 H_{w_3^+}(r) - \pi^2 H_{w_3^+}(s) - 2i\pi H_0(r)\, H_{w_3^+}(s) \\
& - i\pi H_{w_1^-}(r)\, H_{w_3^+}(s) - 4\, i\pi H_{0,w_1^+}(r) + 2i\pi H_{0,w_3^+}(r) + i\pi H_{w_1^-,w_3^+}(r) \\
& - 4\, i\pi H_{w_1^+,0}(r) - i\pi H_{w_1^+,w_1^-}(r) + i\pi H_{w_1^+,w_1^-}(s) + 2H_{w_1^-}(s)\, H_{w_1^+,w_1^+}(r) \\
& - 2H_{w_3^-}(s)\, H_{w_1^+,w_1^+}(r) - 2i\pi H_{w_1^+,w_3^-}(r) + 2i\pi H_{w_1^+,w_2^-}(r) - 2i\pi H_{w_1^+,w_2^-}(s) \\
& - 2i\pi H_{w_1^+,w_2^+}(r) + 2i\pi H_{w_1^+,w_2^+}(s) - 2H_{w_1^+}(r)\, H_{w_1^+,w_2^+}(s) - \frac{3}{2}\, i\pi H_{w_3^-,w_1^+}(r) \\
& - \frac{1}{2}\, i\pi H_{w_3^-,w_1^+}(s) + 2i\pi H_{w_3^+,0}(r) + \frac{3}{2}\, i\pi H_{w_3^+,w_1^-}(r) - \frac{1}{2}\, i\pi H_{w_3^+,w_1^-}(s) \\
& - i\pi H_{w_3^+,w_2^-}(r) + i\pi H_{w_3^+,w_2^-}(s) + i\pi H_{w_3^+,w_2^+}(r) - i\pi H_{w_3^+,w_2^+}(s) \\
& + H_{w_1^+}(r)\, H_{w_3^+,w_2^+}(s) - 2H_{w_1^-,w_1^+,w_1^+}(r) - H_{w_1^+,w_1^-,w_1^+}(r) - H_{w_1^+,w_1^-,w_1^+}(s) \\
& - 2H_{w_1^+,w_1^+,w_1^-}(r) + 2H_{w_1^+,w_1^+,w_3^-}(r) + 4\, H_{w_1^+,w_1^+,w_2^+}(r) + 2H_{w_1^+,w_3^-,w_1^+}(r) \\
& - H_{w_1^+,w_3^+,w_2^+}(r) - 2H_{w_1^+,w_2^-,w_1^+}(r) + 2H_{w_1^+,w_2^-,w_1^+}(s) + 2H_{w_1^+,w_2^+,w_1^+}(r) \\
& + \frac{3}{2}\, H_{w_3^-,w_1^+,w_1^+}(r) + \frac{1}{2}\, H_{w_3^-,w_1^+,w_1^+}(s) - \frac{1}{2}\, H_{w_3^+,w_1^-,w_1^+}(r) + \frac{1}{2}\, H_{w_3^+,w_1^-,w_1^+}(s) \\
& - H_{w_3^+,w_1^+,w_2^+}(r) + H_{w_3^+,w_2^-,w_1^+}(r) - H_{w_3^+,w_2^-,w_1^+}(s) - H_{w_3^+,w_2^+,w_1^+}(r) \\
& - 2i\pi H_{w_1^+}(r)\, \ln(2) + 2i\pi H_{w_1^+}(s)\, \ln(2) + i\pi H_{w_3^+}(r)\, \ln(2) - i\pi H_{w_3^+}(s)\, \ln(2) \Big] \\
& + \mathcal{O}(\epsilon^4)\,, \qquad (4.32)
\end{aligned}
$$

$$
\begin{aligned}
\tilde{M}_{13}(r,s) = \epsilon^2 & \Big[i\pi H_{w_1^+}(r) - i\pi H_{w_1^+}(s) - H_{w_1^+,w_1^+}(r) + H_{w_1^+,w_1^+}(s) \Big] \\
& + \epsilon^3 \Big[-\frac{1}{2}\pi^2 H_{w_1^-}(r) + \frac{1}{2}\pi^2 H_{w_1^-}(s) - \pi^2 H_{w_1^+}(r) + \pi^2 H_{w_1^+}(s) + \frac{3}{4}\pi^2 H_{w_3^-}(r) \\
& - 2i\pi H_{w_1^-}(r)\, H_{w_1^+}(s) - \frac{3}{4}\pi^2 H_{w_3^-}(s) - 2i\pi H_{w_1^+}(r)\, H_{w_3^-}(s) - \pi^2 H_{w_3^+}(r) \\
& + \pi^2 H_{w_3^+}(s) + 2i\pi H_0(r)\, H_{w_3^+}(s) + i\pi H_{w_1^-}(r)\, H_{w_3^+}(s) + 2i\pi H_{w_1^+}(r)\, H_{w_2^-}(s) \\
& - 2i\pi H_{0,w_3^+}(r) + i\pi H_{w_1^-,w_1^+}(r) + i\pi H_{w_1^-,w_1^+}(s) - i\pi H_{w_1^-,w_3^+}(r) - 2i\pi H_{w_1^+,0}(r) \\
& + 2i\pi H_{w_1^+,0}(s) + i\pi H_{w_1^+,w_1^-}(r) + i\pi H_{w_1^+,w_1^-}(s) + 2H_{w_3^-}(s)\, H_{w_1^+,w_1^+}(r) \\
& - 2H_{w_2^-}(s)\, H_{w_1^+,w_1^+}(r) + 2H_{w_1^-}(r)\, H_{w_1^+,w_1^+}(s) + 2i\pi H_{w_1^+,w_3^-}(r) - 2i\pi H_{w_1^+,w_2^-}(r) \\
& + \frac{3}{2}\, i\pi H_{w_3^-,w_1^+}(r) + \frac{1}{2}\, i\pi H_{w_3^-,w_1^+}(s) - 2i\pi H_{w_3^+,0}(r) - \frac{3}{2}\, i\pi H_{w_3^+,w_1^-}(r) \\
& + \frac{1}{2}\, i\pi H_{w_3^+,w_1^-}(s) + i\pi H_{w_3^+,w_2^-}(r) - i\pi H_{w_3^+,w_2^-}(s) - i\pi H_{w_3^+,w_2^+}(r) \\
& + i\pi H_{w_3^+,w_2^+}(s) - H_{w_1^+}(r)\, H_{w_3^+,w_2^+}(s) - 2i\pi H_{w_2^-,w_1^+}(s) - H_{w_1^-,w_1^+,w_1^+}(r) \\
& - H_{w_1^-,w_1^+,w_1^+}(s) + 2H_{w_1^+,0,w_1^+}(r) - 2H_{w_1^+,0,w_1^+}(s) - H_{w_1^+,w_1^-,w_1^+}(r)
\end{aligned}
$$

JHEP12(2014)129

$$
\begin{aligned}
&- H_{w_1^+,w_1^-,w_1^+}(s) - 2H_{w_1^+,w_1^+,w_1^-}(r) - 2H_{w_1^+,w_1^+,w_3^-}(r) + 2H_{w_1^+,w_1^+,w_2^-}(r) \\
&- 2H_{w_1^+,w_3^-,w_1^+}(r) + H_{w_1^+,w_3^+,w_2^+}(r) + 2H_{w_1^+,w_2^-,w_1^+}(r) - \frac{3}{2}\, H_{w_3^-,w_1^+,w_1^+}(r) \\
&- \frac{1}{2}\, H_{w_3^-,w_1^+,w_1^+}(s) + \frac{1}{2}\, H_{w_3^+,w_1^-,w_1^+}(r) - \frac{1}{2}\, H_{w_3^+,w_1^-,w_1^+}(s) + H_{w_3^+,w_1^+,w_2^+}(r) \\
&- H_{w_3^+,w_2^-,w_1^+}(r) + H_{w_3^+,w_2^-,w_1^+}(s) + H_{w_3^+,w_2^+,w_1^+}(r) + 2H_{w_2^-,w_1^+,w_1^+}(s) \\
&+ 2i\pi H_{w_1^+}(r)\, \ln(2) - 2i\pi H_{w_1^+}(s)\, \ln(2) - i\pi H_{w_3^+}(r)\, \ln(2) + i\pi H_{w_3^+}(s)\, \ln(2) \\
&- 4\, H_{w_1^+,w_1^+}(r)\, \ln(2) + 4\, H_{w_1^+,w_1^+}(s)\, \ln(2)\Big] + \mathcal{O}(\epsilon^4)\,,
\end{aligned}
\tag{4.33}
$$

$$
\begin{aligned}
\tilde{M}_{14}(r,s) = \epsilon^2 \Big[&- 2\pi^2 - 4i\pi H_0(r) - 2i\pi H_{w_1^-}(r) - i\pi H_{w_1^-}(s) + 2i\pi H_{w_2^-}(s) - 2i\pi H_{w_2^+}(s) \\
&+ 2H_{w_1^+}(r)\, H_{w_2^+}(s) + H_{w_1^-,w_1^+}(s) - 2H_{w_2^-,w_1^+}(s) - 2i\pi \ln(2)\Big] \\
&+ \epsilon^3 \Big[- \frac{11}{3}\, i\pi^3 - 2\pi^2 H_{-1}(r^2) + 12\pi^2 H_0(r) + 4\pi^2 H_0(s) + 8\, i\pi H_0(r)\, H_0(s) \\
&+ 4i\pi H_0(s)\, H_{w_1^-}(r) + 5\, \pi^2 H_{w_1^-}(s) + 8\, i\pi H_0(r)\, H_{w_1^-}(s) + 2i\pi H_{w_1^-}(r)\, H_{w_1^-}(s) \\
&- \frac{3}{2}\, \pi^2 H_{w_1^+}(s) - 4i\pi H_{w_1^+}(r)\, H_{w_1^+}(s) + \pi^2 H_{w_3^-}(s) + 2i\pi H_0(r)\, H_{w_3^-}(s) \\
&+ i\pi H_{w_1^-}(r)\, H_{w_3^-}(s) - \frac{3}{4}\, \pi^2 H_{w_3^+}(s) - 2i\pi H_{w_1^+}(r)\, H_{w_3^+}(s) - 6\, \pi^2 H_{w_2^-}(s) \\
&- 8\, i\pi H_0(r)\, H_{w_2^-}(s) + 6\, \pi^2 H_{w_2^+}(s) + 12i\pi H_0(r)\, H_{w_2^+}(s) + 4i\pi H_{w_1^-}(r)\, H_{w_2^+}(s) \\
&- 2i\pi H_{-1,0}(r^2) - 2i\pi H_{-1,1}(r^2) + 16\, i\pi H_{0,0}(r) + 2i\pi H_{0,w_1^-}(s) \\
&- 12H_{w_2^+}(s)\, H_{0,w_1^+}(r) - 4i\pi H_{0,w_2^-}(s) + 4i\pi H_{0,w_2^+}(s) - 4H_{w_1^+}(r)\, H_{0,w_2^+}(s) \\
&- 4i\pi H_{w_1^-,0}(r) + 2i\pi H_{w_1^-,0}(s) - 6\, i\pi H_{w_1^-,w_1^-}(r) + 3\, i\pi H_{w_1^-,w_1^-}(s) \\
&- 4H_{w_2^+}(s)\, H_{w_1^-,w_1^+}(r) + 2H_{w_1^-}(r)\, H_{w_1^-,w_1^+}(s) - 4i\pi H_{w_1^-,w_2^-}(s) + 4i\pi H_{w_1^-,w_2^+}(s) \\
&- 4H_{w_1^+}(r)\, H_{w_1^-,w_2^+}(s) + 4H_{w_2^+}(s)\, H_{w_1^+,w_1^-}(r) + 4H_{w_1^+}(s)\, H_{w_1^+,w_1^+}(r) \\
&+ 2H_{w_3^+}(s)\, H_{w_1^+,w_1^+}(r) + i\pi H_{w_1^+,w_1^+}(s) + \frac{1}{2}\, i\pi H_{w_3^-,w_1^-}(s) - i\pi H_{w_3^-,w_2^-}(s) \\
&+ i\pi H_{w_3^-,w_2^+}(s) - H_{w_1^+}(r)\, H_{w_3^-,w_2^+}(s) + \frac{1}{2}\, i\pi H_{w_3^+,w_1^+}(s) - 4i\pi H_{w_2^-,0}(s) \\
&- 4i\pi H_{w_2^-,w_1^-}(s) - 4H_{w_1^-}(r)\, H_{w_2^-,w_1^+}(s) + 4i\pi H_{w_2^-,w_2^-}(s) - 4i\pi H_{w_2^-,w_2^+}(s) \\
&+ 4H_{w_1^+}(r)\, H_{w_2^-,w_2^+}(s) - 2H_{0,w_1^-,w_1^+}(s) + 4H_{0,w_2^-,w_1^+}(s) - 2H_{w_1^-,0,w_1^+}(s) \\
&- 3\, H_{w_1^-,w_1^-,w_1^+}(s) + 4H_{w_1^-,w_2^-,w_1^+}(s) - H_{w_1^+,w_1^+,w_1^+}(s) - \frac{1}{2}\, H_{w_3^-,w_1^-,w_1^+}(s) \\
&+ H_{w_3^-,w_2^-,w_1^+}(s) - \frac{1}{2}\, H_{w_3^+,w_1^+,w_1^+}(s) + 4H_{w_2^-,0,w_1^+}(s) + 4H_{w_2^-,w_1^-,w_1^+}(s) \\
&- 4H_{w_2^-,w_2^-,w_1^+}(s) + 2\pi^2 \ln(2) - 2i\pi H_{-1}(r^2)\, \ln(2) + 4i\pi H_0(s)\, \ln(2) \\
&- 6\, i\pi H_{w_1^-}(r)\, \ln(2) + 2i\pi H_{w_1^-}(s)\, \ln(2) + i\pi H_{w_3^-}(s)\, \ln(2) + 8\, i\pi H_{w_2^+}(s)\, \ln(2) \\
&+ 8H_{w_1^+}(r)\, H_{w_2^+}(s)\, \ln(2) + 4H_{w_1^-,w_1^+}(s)\, \ln(2) - 8H_{w_2^-,w_1^+}(s) \ln(2) - 2i\pi \ln^2(2)\Big] \\
&+ \mathcal{O}(\epsilon^4)\,.
\end{aligned}
\tag{4.34}
$$

JHEP12(2014)129

4.9 $M_{15} - M_{17}$

The integrals in this topology only depend on one non-trivial scale ratio, and their solution can be written in terms of ordinary HPLs. The topology involves five integrals,

$$\vec{M} = \left\{\tilde{M}_{15}(r,s), \tilde{M}_{16}(r,s), \tilde{M}_{17}(r,s), \left[\tilde{M}_1'(z_f)\right]^2, \tilde{M}_1(r,s)\tilde{M}_1'(z_f)\right\}, \tag{4.35}$$

and the matrix $\tilde{A}_{15-17}(r,s)$. The result reads

$$\tilde{M}_{15}(r,s) = z_f^{-2\epsilon}\left\{\epsilon^3\left[-i\pi H_{w_1^+,w_1^-}(s) + H_{w_1^+,w_1^-,w_1^+}(s) - 2i\pi H_{w_1^+}(s)\,\ln(2) - 7\,\zeta_3\right] + \mathcal{O}(\epsilon^4)\right\}, \tag{4.36}$$

$$\begin{aligned}\tilde{M}_{16}(r,s) = z_f^{-2\epsilon}\Bigg\{&\epsilon^2\left[\frac{\pi^2}{2} + i\pi H_{w_1^+}(s) - H_{w_1^+,w_1^+}(s)\right]\\ &+\epsilon^3\Bigg[-\frac{\pi^2}{2}H_{w_1^-}(s) - \pi^2 H_{w_1^+}(s) - i\pi H_{w_1^-,w_1^+}(s) - 2i\pi H_{w_1^+,0}(s) - i\pi H_{w_1^+,w_1^-}(s)\\ &+ H_{w_1^-,w_1^+,w_1^+}(s) + 2H_{w_1^+,0,w_1^+}(s) + H_{w_1^+,w_1^-,w_1^+}(s) - \pi^2\ln(2) - 2i\pi H_{w_1^+}(s)\ln(2)\\ &+\frac{21}{2}\zeta_3\Bigg] + \mathcal{O}(\epsilon^4)\Bigg\},\end{aligned} \tag{4.37}$$

$$\begin{aligned}\tilde{M}_{17}(r,s) = z_f^{-2\epsilon}\Bigg\{&\epsilon^2[i\pi H_{w_1^-}(s) - H_{w_1^-,w_1^+}(s) + 2i\pi\ln(2)]\\ &+\epsilon^3\Bigg[\frac{i\pi^3}{6} - \pi^2 H_{w_1^-}(s) - \frac{\pi^2}{2}H_{w_1^+}(s) - 2i\pi H_{0,w_1^-}(s) - 2i\pi H_{w_1^-,0}(s)\\ &- 3\,i\pi H_{w_1^-,w_1^-}(s) - i\pi H_{w_1^+,w_1^+}(s) + 2H_{0,w_1^-,w_1^+}(s) + 2H_{w_1^-,0,w_1^+}(s)\\ &+ 3\,H_{w_1^-,w_1^-,w_1^+}(s) + H_{w_1^+,w_1^+,w_1^+}(s) - 2\pi^2\ln(2) - 4i\pi H_0(s)\,\ln(2)\\ &- 6\,i\pi H_{w_1^-}(s)\,\ln(2) - 6\,i\pi\ln^2(2)\Bigg] + \mathcal{O}(\epsilon^4)\Bigg\}.\end{aligned} \tag{4.38}$$

4.10 $M_{18} - M_{21}$

This is the largest topology with eleven integrals,

$$\begin{aligned}\vec{M} = \Big\{&\tilde{M}_{18}(r,s), \tilde{M}_{19}(r,s), \tilde{M}_{20}(r,s), \tilde{M}_{21}(r,s), \tilde{M}_5(r), \left[\tilde{M}_1'(z_f)\right]^2, \tilde{M}_1'(z_f)\tilde{M}_1'(z_f=1),\\ &\tilde{M}_1'(z_f)\tilde{M}_1(r,s), \tilde{M}_1'(z_f=1)\tilde{M}_1(r,s), \tilde{M}_4'(z_f), \tilde{M}_5'(z_f)\Big\},\end{aligned} \tag{4.39}$$

and the matrix $\tilde{A}_{18-21}(r,s)$. It turns out that we need the combination $\tilde{M}_{18}(r,s)+\tilde{M}_{19}(r,s)$ up to functions of weight four. This very coefficient fills several pages and is relegated to appendix C. The results up to functions of weight three are

$$\begin{aligned}\tilde{M}_{18}(r,s) = \epsilon^3\Bigg[&-\frac{\pi^2}{6}H_{w_1^-}(r) + \frac{\pi^2}{6}H_{w_1^-}(s) - \frac{\pi^2}{12}H_{w_3^-}(r) + \frac{\pi^2}{12}H_{w_3^-}(s) - i\pi H_{w_1^-}(r)H_{w_3^+}(s)\\ &+ H_{w_1^-}(s)H_{w_1^-,w_1^-}(r) - H_{w_3^-}(s)H_{w_1^-,w_1^-}(r) + i\pi H_{w_1^-,w_3^+}(r) - i\pi H_{w_1^+,w_1^-}(r)\\ &+ i\pi H_{w_1^+,w_1^-}(s) - \frac{1}{2}i\pi H_{w_3^-,w_1^+}(r) + \frac{1}{2}i\pi H_{w_3^-,w_1^+}(s) + \frac{1}{2}i\pi H_{w_3^+,w_1^-}(r)\end{aligned}$$

JHEP12(2014)129

$$
\begin{aligned}
&+\frac{1}{2}i\pi H_{w_3^+,w_1^-}(s)+H_{w_1^-}(r)H_{w_3^+,w_1^+}(s)-3H_{w_1^-,w_1^-,w_1^-}(r)+H_{w_1^-,w_1^-,w_3^-}(r)\\
&+H_{w_1^-,w_3^-,w_1^-}(r)-H_{w_1^-,w_3^+,w_1^+}(r)+H_{w_1^+,w_1^-,w_1^+}(r)-H_{w_1^+,w_1^-,w_1^+}(s)\\
&+H_{w_3^-,w_1^-,w_1^-}(r)+\frac{1}{2}H_{w_3^-,w_1^+,w_1^+}(r)-\frac{1}{2}H_{w_3^-,w_1^+,w_1^+}(s)-\frac{1}{2}H_{w_3^+,w_1^-,w_1^+}(r)\\
&-\frac{1}{2}H_{w_3^+,w_1^-,w_1^+}(s)-H_{w_3^+,w_1^+,w_1^-}(r)+2H_{w_1^-}(r)H_{w_1^-}(s)\ln(2)-2i\pi H_{w_1^+}(r)\ln(2)\\
&+2i\pi H_{w_1^+}(s)\ln(2)-2H_{w_1^-}(r)H_{w_3^-}(s)\ln(2)+i\pi H_{w_3^+}(r)\ln(2)\\
&-i\pi H_{w_3^+}(s)\ln(2)-4H_{w_1^-,w_1^-}(r)\ln(2)+2H_{w_1^-,w_3^-}(r)\ln(2)+2H_{w_3^-,w_1^-}(r)\ln(2)\\
&-2H_{w_3^+,w_1^+}(r)\ln(2)+2H_{w_3^+,w_1^+}(s)\ln(2)-2H_{w_1^-}(r)\ln^2(2)+2H_{w_1^-}(s)\ln^2(2)\\
&+2H_{w_3^-}(r)\ln^2(2)-2H_{w_3^-}(s)\ln^2(2)-H_{w_1^-}(r)\mathrm{Li}_2(1-z_f)+H_{w_1^-}(s)\mathrm{Li}_2(1-z_f)\\
&+H_{w_3^-}(r)\mathrm{Li}_2(1-z_f)-H_{w_3^-}(s)\mathrm{Li}_2(1-z_f)\Big]+\mathcal{O}(\epsilon^4),
\end{aligned}
\tag{4.40}
$$

$$
\begin{aligned}
\tilde{M}_{19}(r,s)=\epsilon^3\Big[&-\frac{\pi^2}{3}H_{w_1^-}(r)+\frac{\pi^2}{3}H_{w_1^-}(s)-i\pi H_{w_1^-}(r)H_{w_1^+}(s)+\frac{\pi^2}{12}H_{w_3^-}(r)-\frac{\pi^2}{12}H_{w_3^-}(s)\\
&+i\pi H_{w_1^-}(r)H_{w_3^+}(s)-H_{w_1^-}(s)H_{w_1^-,w_1^-}(r)+H_{w_3^-}(s)H_{w_1^-,w_1^-}(r)+i\pi H_{w_1^-,w_1^+}(s)\\
&-i\pi H_{w_1^-,w_3^+}(r)+i\pi H_{w_1^+,w_1^-}(r)+H_{w_1^-}(r)H_{w_1^+,w_1^+}(s)+\frac{1}{2}i\pi H_{w_3^-,w_1^+}(r)\\
&-\frac{1}{2}i\pi H_{w_3^-,w_1^+}(s)-\frac{1}{2}i\pi H_{w_3^+,w_1^-}(r)-\frac{1}{2}i\pi H_{w_3^+,w_1^-}(s)-H_{w_1^-}(r)H_{w_3^+,w_1^+}(s)\\
&+3H_{w_1^-,w_1^-,w_1^-}(r)-H_{w_1^-,w_1^-,w_3^-}(r)-H_{w_1^-,w_1^+,w_1^+}(s)-H_{w_1^-,w_3^-,w_1^-}(r)\\
&+H_{w_1^-,w_3^+,w_1^+}(r)-H_{w_1^+,w_1^-,w_1^+}(r)-H_{w_1^+,w_1^+,w_1^-}(r)-H_{w_3^-,w_1^-,w_1^-}(r)\\
&-\frac{1}{2}H_{w_3^-,w_1^+,w_1^+}(r)+\frac{1}{2}H_{w_3^-,w_1^+,w_1^+}(s)+\frac{1}{2}H_{w_3^+,w_1^-,w_1^+}(r)+\frac{1}{2}H_{w_3^+,w_1^-,w_1^+}(s)\\
&+H_{w_3^+,w_1^+,w_1^-}(r)-2H_{w_1^-}(r)H_{w_1^-}(s)\ln(2)+2i\pi H_{w_1^+}(r)\ln(2)\\
&-2i\pi H_{w_1^+}(s)\ln(2)+2H_{w_1^-}(r)H_{w_3^-}(s)\ln(2)-i\pi H_{w_3^+}(r)\ln(2)\\
&+i\pi H_{w_3^+}(s)\ln(2)+4H_{w_1^-,w_1^-}(r)\ln(2)-2H_{w_1^-,w_3^-}(r)\ln(2)-2H_{w_1^+,w_1^+}(r)\ln(2)\\
&+2H_{w_1^+,w_1^+}(s)\ln(2)-2H_{w_3^-,w_1^-}(r)\ln(2)+2H_{w_3^+,w_1^+}(r)\ln(2)\\
&-2H_{w_3^+,w_1^+}(s)\ln(2)+2H_{w_1^-}(r)\ln^2(2)-2H_{w_1^-}(s)\ln^2(2)-2H_{w_3^-}(r)\ln^2(2)\\
&+2H_{w_3^-}(s)\ln^2(2)+H_{w_1^-}(r)\mathrm{Li}_2(1-z_f)-H_{w_1^-}(s)\mathrm{Li}_2(1-z_f)\\
&-H_{w_3^-}(r)\mathrm{Li}_2(1-z_f)+H_{w_3^-}(s)\mathrm{Li}_2(1-z_f)\Big]+\mathcal{O}(\epsilon^4),
\end{aligned}
\tag{4.41}
$$

$$
\begin{aligned}
\tilde{M}_{20}(r,s)=\epsilon^2\Big[&-i\pi H_{w_1^-}(r)+i\pi H_{w_1^-}(s)+H_{w_1^-}(r)H_{w_1^+}(s)-H_{w_1^-,w_1^+}(s)+2H_{w_1^+}(s)\ln(2)\Big]\\
+\epsilon^3\Big[&\pi^2H_{w_1^-}(r)+2i\pi H_0(s)H_{w_1^-}(r)-\pi^2H_{w_1^-}(s)+3i\pi H_{w_1^-}(r)H_{w_1^-}(s)\\
&-2i\pi H_{w_1^-}(r)H_{w_5^-}(s)-\frac{\pi^2}{6}H_{w_5^+}(s)-2i\pi H_{w_1^-}(r)H_{w_4^-}(s)+\frac{11}{6}\pi^2H_{w_4^+}(s)
\end{aligned}
$$

JHEP12(2014)129

$$
\begin{aligned}
&- \frac{2}{3}\pi^2 H_{w_1^+}(s) + i\pi H_{w_1^-}(r) H_{w_3^-}(s) - \frac{\pi^2}{12} H_{w_3^+}(s) + 2i\pi H_{w_1^-}(r) H_{w_2^-}(s) \\
&- 2i\pi H_{-1,1}(r^2) + 4i\pi H_{0,w_1^-}(r) - 2i\pi H_{0,w_1^-}(s) - 2H_{w_1^-}(r) H_{0,w_1^+}(s) \\
&- 2i\pi H_{w_1^-,0}(s) - 3i\pi H_{w_1^-,w_1^-}(r) - H_{w_5^+}(s) H_{w_1^-,w_1^-}(r) - H_{w_4^+}(s) H_{w_1^-,w_1^-}(r) \\
&+ 2H_{w_1^+}(s) H_{w_1^-,w_1^-}(r) + H_{w_3^+}(s) H_{w_1^-,w_1^-}(r) - 3i\pi H_{w_1^-,w_1^-}(s) \\
&- 3H_{w_1^-}(r) H_{w_1^-,w_1^+}(s) + 2i\pi H_{w_5^-,w_1^-}(s) + 2H_{w_1^-}(r) H_{w_5^-,w_1^+}(s) + 2i\pi H_{w_5^+,w_1^+}(s) \\
&+ 2i\pi H_{w_4^-,w_1^-}(s) + 2H_{w_1^-}(r) H_{w_4^-,w_1^+}(s) + 2i\pi H_{w_4^+,w_1^+}(s) \\
&- 2H_{w_5^+}(s) H_{w_1^+,0}(\sqrt{z_f}) + 2H_{w_4^+}(s) H_{w_1^+,0}(\sqrt{z_f}) + 2H_{w_2^+}(s) H_{w_1^+,w_1^-}(r) \\
&- i\pi H_{w_1^+,w_1^+}(s) - \frac{1}{2} i\pi H_{w_3^-,w_1^-}(s) - H_{w_1^-}(r) H_{w_3^-,w_1^+}(s) - \frac{1}{2} i\pi H_{w_3^+,w_1^+}(s) \\
&- 2i\pi H_{w_2^-,w_1^-}(s) - 2H_{w_1^-}(r) H_{w_2^-,w_1^+}(s) + 2H_{0,w_1^-,w_1^+}(s) + 2H_{w_1^-,0,w_1^+}(s) \\
&+ 3H_{w_1^-,w_1^-,w_1^+}(s) - 2H_{w_5^-,w_1^-,w_1^+}(s) - 2H_{w_5^+,w_1^+,w_1^+}(s) - 2H_{w_4^-,w_1^-,w_1^+}(s) \\
&- 2H_{w_4^+,w_1^+,w_1^+}(s) + H_{w_1^+,w_1^+,w_1^+}(s) + \frac{1}{2} H_{w_3^-,w_1^-,w_1^+}(s) + \frac{1}{2} H_{w_3^+,w_1^+,w_1^+}(s) \\
&+ 2H_{w_2^-,w_1^-,w_1^+}(s) - 2i\pi H_{-1}(r^2)\ln(2) - 2i\pi H_{w_1^-}(r)\ln(2) \\
&- 2H_{w_1^-}(r) H_{w_5^+}(s)\ln(2) - 2H_{w_1^-}(r) H_{w_4^+}(s)\ln(2) + 4H_{w_1^-}(r) H_{w_1^+}(s)\ln(2) \\
&+ i\pi H_{w_3^-}(s)\ln(2) + 2H_{w_1^-}(r) H_{w_3^+}(s)\ln(2) + 4H_{w_1^+}(r) H_{w_2^+}(s)\ln(2) \\
&- 4H_{0,w_1^+}(s)\ln(2) - 6H_{w_1^-,w_1^+}(s)\ln(2) + 4H_{w_5^-,w_1^+}(s)\ln(2) + 4H_{w_4^-,w_1^+}(s)\ln(2) \\
&- 2H_{w_3^-,w_1^+}(s)\ln(2) - 4H_{w_2^-,w_1^+}(s)\ln(2) - 2H_{w_5^+}(s)\ln^2(2) - 2H_{w_4^+}(s)\ln^2(2) \\
&+ 4H_{w_1^+}(s)\ln^2(2) + 2H_{w_3^+}(s)\ln^2(2) - H_{w_5^+}(s)\mathrm{Li}_2(1-z_f) - H_{w_4^+}(s)\mathrm{Li}_2(1-z_f) \\
&- H_{w_1^+}(s)\mathrm{Li}_2(1-z_f) + H_{w_3^+}(s)\mathrm{Li}_2(1-z_f)\Big] + \mathcal{O}(\epsilon^4)\,, \qquad (4.42)
\end{aligned}
$$

$$
\begin{aligned}
\tilde{M}_{21}(r,s) =& \epsilon^2\Big[-\pi^2 - 2i\pi H_{w_1^+}(s) + 2H_{w_1^+,w_1^+}(s)\Big] \\
&+ \epsilon^3\Big[-4\pi^2 H_0\left(\tfrac{1}{1+2\sqrt{z_f}}\right) - \pi^2 H_{w_1^-}(r) + \frac{8}{3}\pi^2 H_{w_1^-}(s) + \frac{\pi^2}{3} H_{w_5^-}(s) \\
&+ 4i\pi H_{w_1^-}(r) H_{w_5^+}(s) - \frac{11}{3}\pi^2 H_{w_4^-}(s) + 4i\pi H_{w_1^-}(r) H_{w_4^+}(s) + 2\pi^2 H_{w_1^+}(s) \\
&- 8i\pi H_{w_1^-}(r) H_{w_1^+}(s) + \frac{\pi^2}{6} H_{w_3^-}(s) - 2i\pi H_{w_1^-}(r) H_{w_3^+}(s) - 2H_{w_1^-}(s) H_{w_1^-,w_1^-}(r) \\
&+ 2H_{w_5^-}(s) H_{w_1^-,w_1^-}(r) + 2H_{w_4^-}(s) H_{w_1^-,w_1^-}(r) - 2H_{w_3^-}(s) H_{w_1^-,w_1^-}(r) \\
&+ 6i\pi H_{w_1^-,w_1^+}(s) - 4i\pi H_{w_5^-,w_1^+}(s) - 4i\pi H_{w_5^+,w_1^-}(s) - 4H_{w_1^-}(r) H_{w_5^+,w_1^+}(s) \\
&- 4i\pi H_{w_4^-,w_1^+}(s) - 4i\pi H_{w_4^+,w_1^-}(s) - 4H_{w_1^-}(r) H_{w_4^+,w_1^+}(s) + 4i\pi H_{w_1^+,0}(s) \\
&+ 4H_{w_5^-}(s) H_{w_1^+,0}(\sqrt{z_f}) - 4H_{w_4^-}(s) H_{w_1^+,0}(\sqrt{z_f}) + 6i\pi H_{w_1^+,w_1^-}(s) \\
&+ 8H_{w_1^-}(r) H_{w_1^+,w_1^+}(s) + i\pi H_{w_3^-,w_1^+}(s) + i\pi H_{w_3^+,w_1^-}(s) + 2H_{w_1^-}(r) H_{w_3^+,w_1^+}(s) \\
&+ 16H_{0,w_1^+,0}\left(\tfrac{1}{1+2\sqrt{z_f}}\right) - 8H_{0,w_1^+,w_1^-}(1-2\sqrt{z_f}) + 8H_{0,w_1^+,w_1^-}\left(\tfrac{1}{1+2\sqrt{z_f}}\right)
\end{aligned}
$$

JHEP12(2014)129

$$
\begin{aligned}
&+ 2H_{0,w_1^+,w_1^-}(1-2z_f) - 8H_{0,w_1^+,w_1^+}(1-2\sqrt{z_f}) + 8H_{0,w_1^+,w_1^+}\left(\tfrac{1}{1+2\sqrt{z_f}}\right) \\
&+ 2H_{0,w_1^+,w_1^+}(1-2z_f) - 6H_{w_1^-,w_1^+,w_1^+}(s) + 4H_{w_5^-,w_1^+,w_1^+}(s) + 4H_{w_5^+,w_1^-,w_1^+}(s) \\
&+ 4H_{w_4^-,w_1^+,w_1^+}(s) + 4H_{w_4^+,w_1^-,w_1^+}(s) - 4H_{w_1^+,0,w_1^+}(s) - 6H_{w_1^+,w_1^-,w_1^+}(s) \\
&- H_{w_3^-,w_1^+,w_1^+}(s) - H_{w_3^+,w_1^-,w_1^+}(s) - 3\pi^2\ln(2) - 4H_{w_1^-}(r)H_{w_1^-}(s)\ln(2) \\
&+ 4H_{w_1^-}(r)H_{w_5^-}(s)\ln(2) + 4H_{w_1^-}(r)H_{w_4^-}(s)\ln(2) - 4i\pi H_{w_1^+}(s)\ln(2) \\
&- 4H_{w_1^-}(r)H_{w_3^-}(s)\ln(2) - 2i\pi H_{w_3^+}(s)\ln(2) - 16H_{0,w_1^+}(1-2\sqrt{z_f})\ln(2) \\
&+ 16H_{0,w_1^+}\left(\tfrac{1}{1+2\sqrt{z_f}}\right)\ln(2) + 4H_{0,w_1^+}(1-2z_f)\ln(2) \\
&- 8H_{w_5^+,w_1^+}(s)\ln(2) - 8H_{w_4^+,w_1^+}(s)\ln(2) + 16H_{w_1^+,w_1^+}(s)\ln(2) \\
&+ 4H_{w_3^+,w_1^+}(s)\ln(2) - 4H_{w_1^-}(s)\ln^2(2) + 4H_{w_5^-}(s)\ln^2(2) + 4H_{w_4^-}(s)\ln^2(2) \\
&- 4H_{w_3^-}(s)\ln^2(2) - 2H_{w_1^-}(s)\mathrm{Li}_2(1-z_f) + 2H_{w_5^-}(s)\mathrm{Li}_2(1-z_f) \\
&+ 2H_{w_4^-}(s)\mathrm{Li}_2(1-z_f) - 2H_{w_3^-}(s)\mathrm{Li}_2(1-z_f) + 14\zeta_3\Big] + \mathcal{O}(\epsilon^4)\,. \qquad (4.43)
\end{aligned}
$$

4.11 M_{22}

This is the only integral with five lines. However, since it is essentially a one-scale integral its result can be written in terms of ordinary HPLs. The topology consists of seven integrals,

$$
\begin{aligned}
\vec{M} = \Big\{&\tilde{M}_{22}(r,s), \tilde{M}_3(r,s), \tilde{M}_4(r,s), \tilde{M}_1'(z_f)\tilde{M}_2'(\bar{u}), \left[\tilde{M}_1'(z_f)\right]^2, \\
&\tilde{M}_1(r,s)\tilde{M}_1'(z_f), \tilde{M}_1(r,s)\tilde{M}_2'(\bar{u})\Big\}, \qquad (4.44)
\end{aligned}
$$

and the matrix $\tilde{A}_{22}(r,s)$. The result reads

$$
\begin{aligned}
\tilde{M}_{22}(r,s) = z_f^{-2\epsilon}\Big\{\epsilon^3\Big[&-\frac{i\pi^3}{2} - \pi^2\, H_{w_1^-}(s) + \pi^2\, H_{w_1^+}(s) - 2\,i\pi\, H_{w_1^-,w_1^+}(s) + i\pi\, H_{w_1^+,w_1^-}(s) \\
&+ i\pi\, H_{w_1^+,w_1^+}(s) + 2H_{w_1^-,w_1^+,w_1^+}(s) - H_{w_1^+,w_1^-,w_1^+}(s) - 2\pi^2\ln(2) - H_{w_1^+,w_1^+,w_1^-}(s) \\
&+ 2\,i\pi\, H_{w_1^+}(s)\,\ln(2) - 2\,H_{w_1^+,w_1^+}(s)\,\ln(2) + \frac{21}{2}\,\zeta_3\Big] + \mathcal{O}(\epsilon^4)\Big\}\,. \qquad (4.45)
\end{aligned}
$$

4.12 $M_{23} - M_{25}$

Also this topology is quite large and we need nine integrals

$$
\begin{aligned}
\vec{M} = \Big\{&\tilde{M}_{23}(r,s_1), \tilde{M}_{24}(r,s_1), \tilde{M}_{25}(r,s_1), \tilde{M}_5(r), \left[\tilde{M}_1'(z_f)\right]^2, \tilde{M}_1'(z_f)\tilde{M}_1'(z_f=1), \\
&\tilde{M}_4'(z_f), \tilde{M}_5'(z_f), \tilde{M}_1'(z_f)\tilde{M}_1(r=i\sqrt{3},s_1)\Big\}\,, \qquad (4.46)
\end{aligned}
$$

where $r = i\sqrt{3}$ corresponds to $z_f = 1$. Here we choose the set of variables (r, s_1). The fact that the number of integrals is large is not the only complication of this topology. As can be seen from the matrix $\tilde{A}_{23-25}(r,s_1)$ in eq. (A.11), many factors appear in the differential

JHEP12(2014)129

equations which are irrational in both r and s_1. For example,

$$\frac{\partial \tilde{M}_{23}(r,s_1)}{\partial s_1} = \frac{2\epsilon\, \tilde{M}_{23}(r,s_1)\, s_1 \left(5-s_1^2\right)}{\left(1-s_1^2\right)\,\left(3+s_1^2\right)} - \frac{\epsilon\, \tilde{M}_{24}(r,s_1)\,\left(3-s_1\right)}{4(1-s_1^2)\sqrt{1+\frac{2(1-r^2)(1-s_1)}{(1+s_1)^2}}} + \frac{\epsilon\, \tilde{M}_{25}(r,s_1)\,\left(3+s_1\right)}{4\left(1-s_1^2\right)\sqrt{1+\frac{2(1-r^2)(1+s_1)}{(1-s_1)^2}}} + \frac{2\epsilon\, \tilde{M}_4'(z_f)\, s_1}{1-s_1^2}\,. \tag{4.47}$$

Fortunately, we can still find a form of the differential equations which allows us to apply the formulas for iterated integrals from section 2. There are two reasons why this is possible. First, there exist variable transformations which rationalise either of the square roots, namely

$$t = \frac{1-s_1}{2} + \frac{1+s_1}{2}\sqrt{1+\frac{2(1-r^2)(1-s_1)}{(1+s_1)^2}} \quad \Longrightarrow \quad s_1 = \frac{2t^2-2t-1+r^2}{r^2-2t+1}\,, \tag{4.48}$$

and

$$v = \frac{1+s_1}{2} + \frac{1-s_1}{2}\sqrt{1+\frac{2(1-r^2)(1+s_1)}{(1-s_1)^2}} \quad \Longrightarrow \quad s_1 = -\frac{2v^2-2v-1+r^2}{r^2-2v+1}\,. \tag{4.49}$$

For later convenience we also define

$$\begin{aligned} t_0 &= e^{\frac{i\pi}{3}}\, r + e^{-\frac{i\pi}{3}}\,, \\ v_0 &= e^{-\frac{i\pi}{3}}\, r + e^{\frac{i\pi}{3}}\,, \end{aligned} \tag{4.50}$$

which correspond to the limit $s_1 \to +i\sqrt{3}$ of t and v, respectively. Second, it turns out that we only need the lowest order in the ϵ-expansion for each of the integrals M_{23-25}. This ensures that M_{24} appears only in combination with t, whereas M_{25} appears only with v, without any admixture of the respective other variable. This does not hold at higher orders in ϵ, which can be concluded for instance from the appearance of the logarithm L_{15} in $\tilde{A}_{23-25}(r,s_1)$ in eq. (A.11) which contains both t and v. Having said this, we find

$$\begin{aligned} \tilde{M}_{23}(r,s_1) = \epsilon^3 \Big[& f^{(1)}(t) + f^{(2)}(t) + f^{(1)}(v) - f^{(2)}(v) + f^{(3)}(v) \\ & - f^{(1)}(t_0) - f^{(2)}(t_0) - f^{(1)}(v_0) + f^{(2)}(v_0) - f^{(3)}(v_0) + (H_{w_1^-}(s_1) + 2\ln(2)) \\ & \times \left(-\frac{\pi^2}{12} - \frac{1}{2} H_{w_1^-,w_1^-}(r) - H_{w_1^-}(r)\,\ln(2) - \ln^2(2) - \frac{1}{2}\,\mathrm{Li}_2(1-z_f) \right) \Big] + \mathcal{O}(\epsilon^4)\,, \end{aligned} \tag{4.51}$$

$$\tilde{M}_{24}(r,s_1) = \epsilon^2 [f^{(4)}(t) + f^{(5)}(t)] + \mathcal{O}(\epsilon^3)\,, \tag{4.52}$$

$$\tilde{M}_{25}(r,s_1) = \epsilon^2 [f^{(4)}(v) - f^{(5)}(v) + f^{(6)}(v)] + \mathcal{O}(\epsilon^3)\,, \tag{4.53}$$

with

$$\begin{aligned} f^{(1)}(x) = & -\frac{5\pi^2}{12} H_{w_1^+}(x) - \frac{5\pi^2}{24} H_{w_3^-}(x) - \frac{5\pi^2}{24} H_{w_3^+}(x) + H_{w_1^+}(x)\, H_{-1,0}(r^2) \\ & + \frac{1}{2} H_{w_3^-}(x)\, H_{-1,0}(r^2) + \frac{1}{2} H_{w_3^+}(x)\, H_{-1,0}(r^2) + 2 H_{w_1^+}(x)\, H_{w_1^-,0}(r) \\ & + H_{w_3^-}(x)\, H_{w_1^-,0}(r) + H_{w_3^+}(x)\, H_{w_1^-,0}(r) + \frac{1}{2} H_{w_1^+}(x)\, H_{w_1^-,w_1^-}(r) \end{aligned}$$

JHEP12(2014)129

$$
\begin{aligned}
&+\frac{1}{4}\,H_{w_3^-}(x)\,H_{w_1^-,w_1^-}(r)+\frac{1}{4}\,H_{w_3^+}(x)\,H_{w_1^-,w_1^-}(r)-2H_0(r)\,H_{w_1^+,w_1^+}(x)\\
&-H_{w_1^-}(r)\,H_{w_1^+,w_1^+}(x)-H_0(r)\,H_{w_1^+,w_3^-}(x)-H_0(r)\,H_{w_1^+,w_3^+}(x)-H_0(r)\,H_{w_3^-,w_1^+}(x)\\
&-\frac{1}{2}\,H_{w_1^-}(r)\,H_{w_3^-,w_1^+}(x)-\frac{1}{2}\,H_0(r)\,H_{w_3^-,w_3^-}(x)-\frac{1}{2}\,H_0(r)\,H_{w_3^-,w_3^+}(x)\\
&-H_0(r)\,H_{w_3^+,w_1^+}(x)-\frac{1}{2}\,H_{w_1^-}(r)\,H_{w_3^+,w_1^+}(x)-\frac{1}{2}\,H_0(r)\,H_{w_3^+,w_3^-}(x)\\
&-\frac{1}{2}\,H_0(r)\,H_{w_3^+,w_3^+}(x)-H_{w_1^+,w_1^+,w_1^-}(x)+\frac{1}{2}\,H_{w_1^+,w_1^+,w_5^-}(x)+\frac{1}{2}\,H_{w_1^+,w_1^+,w_5^+}(x)\\
&+\frac{1}{2}\,H_{w_1^+,w_1^+,w_4^-}(x)+\frac{1}{2}\,H_{w_1^+,w_1^+,w_4^+}(x)-\frac{1}{2}\,H_{w_1^+,w_3^-,w_1^-}(x)+\frac{1}{4}\,H_{w_1^+,w_3^-,w_5^-}(x)\\
&+\frac{1}{4}\,H_{w_1^+,w_3^-,w_5^+}(x)+\frac{1}{4}\,H_{w_1^+,w_3^-,w_4^-}(x)+\frac{1}{4}\,H_{w_1^+,w_3^-,w_4^+}(x)-\frac{1}{2}\,H_{w_1^+,w_3^+,w_1^-}(x)\\
&+\frac{1}{4}\,H_{w_1^+,w_3^+,w_5^-}(x)+\frac{1}{4}\,H_{w_1^+,w_3^+,w_5^+}(x)+\frac{1}{4}\,H_{w_1^+,w_3^+,w_4^-}(x)+\frac{1}{4}\,H_{w_1^+,w_3^+,w_4^+}(x)\\
&-\frac{1}{2}\,H_{w_3^-,w_1^+,w_1^-}(x)+\frac{1}{4}\,H_{w_3^-,w_1^+,w_5^-}(x)+\frac{1}{4}\,H_{w_3^-,w_1^+,w_5^+}(x)+\frac{1}{4}\,H_{w_3^-,w_1^+,w_4^-}(x)\\
&+\frac{1}{4}\,H_{w_3^-,w_1^+,w_4^+}(x)-\frac{1}{4}\,H_{w_3^-,w_3^-,w_1^-}(x)+\frac{1}{8}\,H_{w_3^-,w_3^-,w_5^-}(x)+\frac{1}{8}\,H_{w_3^-,w_3^-,w_5^+}(x)\\
&+\frac{1}{8}\,H_{w_3^-,w_3^-,w_4^-}(x)+\frac{1}{8}\,H_{w_3^-,w_3^-,w_4^+}(x)-\frac{1}{4}\,H_{w_3^-,w_3^+,w_1^-}(x)+\frac{1}{8}\,H_{w_3^-,w_3^+,w_5^-}(x)\\
&+\frac{1}{8}\,H_{w_3^-,w_3^+,w_5^+}(x)+\frac{1}{8}\,H_{w_3^-,w_3^+,w_4^-}(x)+\frac{1}{8}\,H_{w_3^-,w_3^+,w_4^+}(x)-\frac{1}{2}\,H_{w_3^+,w_1^+,w_1^-}(x)\\
&+\frac{1}{4}\,H_{w_3^+,w_1^+,w_5^-}(x)+\frac{1}{4}\,H_{w_3^+,w_1^+,w_5^+}(x)+\frac{1}{4}\,H_{w_3^+,w_1^+,w_4^-}(x)+\frac{1}{4}\,H_{w_3^+,w_1^+,w_4^+}(x)\\
&-\frac{1}{4}\,H_{w_3^+,w_3^-,w_1^-}(x)+\frac{1}{8}\,H_{w_3^+,w_3^-,w_5^-}(x)+\frac{1}{8}\,H_{w_3^+,w_3^-,w_5^+}(x)+\frac{1}{8}\,H_{w_3^+,w_3^-,w_4^-}(x)\\
&+\frac{1}{8}\,H_{w_3^+,w_3^-,w_4^+}(x)-\frac{1}{4}\,H_{w_3^+,w_3^+,w_1^-}(x)+\frac{1}{8}\,H_{w_3^+,w_3^+,w_5^-}(x)+\frac{1}{8}\,H_{w_3^+,w_3^+,w_5^+}(x)\\
&+\frac{1}{8}\,H_{w_3^+,w_3^+,w_4^-}(x)+\frac{1}{8}\,H_{w_3^+,w_3^+,w_4^+}(x)+H_{w_1^-}(r)\,H_{w_1^+}(x)\,\ln(2)\\
&+\frac{1}{2}\,H_{w_1^-}(r)\,H_{w_3^-}(x)\,\ln(2)+\frac{1}{2}\,H_{w_1^-}(r)\,H_{w_3^+}(x)\,\ln(2)-2H_{w_1^+,w_1^+}(x)\,\ln(2)\\
&-H_{w_3^-,w_1^+}(x)\,\ln(2)-H_{w_3^+,w_1^+}(x)\,\ln(2)+H_{w_1^+}(x)\,\ln^2(2)+\frac{1}{2}\,H_{w_3^-}(x)\,\ln^2(2)\\
&+\frac{1}{2}\,H_{w_3^+}(x)\,\ln^2(2)+\frac{1}{2}\,H_{w_1^+}(x)\,\mathrm{Li}_2(1-z_f)+\frac{1}{4}\,H_{w_3^-}(x)\,\mathrm{Li}_2(1-z_f)\\
&+\frac{1}{4}\,H_{w_3^+}(x)\,\mathrm{Li}_2(1-z_f)\,,
\end{aligned}
\tag{4.54}
$$

$$
\begin{aligned}
f^{(2)}(x)=&\,i\pi\Big[-H_{-1}(r^2)\,H_{w_1^+}(x)-H_{w_1^-}(r)\,H_{w_1^+}(x)-\frac{1}{2}\,H_{-1}(r^2)\,H_{w_3^-}(x)\\
&-\frac{1}{2}\,H_{w_1^-}(r)\,H_{w_3^-}(x)-\frac{1}{2}\,H_{-1}(r^2)\,H_{w_3^+}(x)-\frac{1}{2}\,H_{w_1^-}(r)\,H_{w_3^+}(x)+H_{w_1^+,w_1^+}(x)\\
&+\frac{1}{2}\,H_{w_1^+,w_3^-}(x)+\frac{1}{2}\,H_{w_1^+,w_3^+}(x)+\frac{1}{2}\,H_{w_3^-,w_1^+}(x)+\frac{1}{4}\,H_{w_3^-,w_3^-}(x)+\frac{1}{4}\,H_{w_3^-,w_3^+}(x)\\
&+\frac{1}{2}\,H_{w_3^+,w_1^+}(x)+\frac{1}{4}\,H_{w_3^+,w_3^-}(x)+\frac{1}{4}\,H_{w_3^+,w_3^+}(x)\Big]\,,
\end{aligned}
\tag{4.55}
$$

JHEP12(2014)129

$$
\begin{aligned}
f^{(3)}(x) =& \left[\frac{1}{4}H_0(r^4) - H_0(r)\right] \times \Big[4H_{-1}(r^2)\, H_{w_1^+}(x) + 4H_{w_1^-}(r)\, H_{w_1^+}(x) \\
&+ 2H_{-1}(r^2)\, H_{w_3^-}(x) + 2H_{w_1^-}(r)\, H_{w_3^-}(x) + 2H_{-1}(r^2)\, H_{w_3^+}(x) + 2H_{w_1^-}(r)\, H_{w_3^+}(x) \\
&- 4H_{w_1^+,w_1^+}(x) - 2H_{w_1^+,w_3^-}(x) - 2H_{w_1^+,w_3^+}(x) - 2H_{w_3^-,w_1^+}(x) - H_{w_3^-,w_3^-}(x) \\
&- H_{w_3^-,w_3^+}(x) - 2H_{w_3^+,w_1^+}(x) - H_{w_3^+,w_3^-}(x) - H_{w_3^+,w_3^+}(x)\Big]\,, \qquad (4.56)
\end{aligned}
$$

$$
\begin{aligned}
f^{(4)}(x) =& \frac{5\,\pi^2}{3} + 8\, H_0(r)\, H_{w_1^+}(x) + 4H_{w_1^-}(r)\, H_{w_1^+}(x) + 4H_0(r)\, H_{w_3^-}(x) + 4H_0(r)\, H_{w_3^+}(x) \\
&- 4H_{-1,0}(r^2) - 8\, H_{w_1^-,0}(r) - 2H_{w_1^-,w_1^-}(r) + 4H_{w_1^+,w_1^-}(x) - 2H_{w_1^+,w_5^-}(x) \\
&- 2H_{w_1^+,w_5^+}(x) - 2H_{w_1^+,w_4^-}(x) - 2H_{w_1^+,w_4^+}(x) + 2H_{w_3^-,w_1^-}(x) - H_{w_3^-,w_5^-}(x) \\
&- H_{w_3^-,w_5^+}(x) - H_{w_3^-,w_4^-}(x) - H_{w_3^-,w_4^+}(x) + 2H_{w_3^+,w_1^-}(x) - H_{w_3^+,w_5^-}(x) - H_{w_3^+,w_5^+}(x) \\
&- H_{w_3^+,w_4^-}(x) - H_{w_3^+,w_4^+}(x) - 4H_{w_1^-}(r)\, \ln(2) + 8\, H_{w_1^+}(x)\, \ln(2) - 4\ln^2(2) \\
&- 2\mathrm{Li}_2(1 - z_f)\,, \qquad (4.57)
\end{aligned}
$$

$$
f^{(5)}(x) = i\pi\left[4H_{-1}(r^2) + 4H_{w_1^-}(r) - 4H_{w_1^+}(x) - 2H_{w_3^-}(x) - 2H_{w_3^+}(x)\right], \qquad (4.58)
$$

$$
f^{(6)}(x) = 2\left[4H_0(r) - H_0(r^4)\right]\left[2H_{-1}(r^2) + 2H_{w_1^-}(r) - 2H_{w_1^+}(x) - H_{w_3^-}(x) - H_{w_3^+}(x)\right]. \qquad (4.59)
$$

For numerical cross-checks, we also present two-fold integral representations over ordinary Feynman parameters. For the relevant coefficients of the ϵ-expansion of $M_{23-25}(r, s_1)$, they read ($\bar{x} = 1 - x$, $\hat{x} = 1 + x$)

$$
\begin{aligned}
\tilde{M}_{23}(r, s_1) &= \int_0^1 dt_1 \int_0^1 dt_2\, \frac{\epsilon^3\left(s_1^2 + 3\right)\bar{t}_2\, \ln\left[\frac{\left(1-s_1^2\right)\left(t_1^2 t_2 \bar{t}_2 + \bar{t}_1 z_f\right)}{t_2\bar{t}_2\left((1-2t_1)^2 - s_1^2\right)}\right]}{t_2\bar{t}_2\left(\left(s_1^2+3\right)t_1 + s_1^2 - 1\right) + \left(1 - s_1^2\right) z_f} + \mathcal{O}(\epsilon^4)\,, \\
\tilde{M}_{24}(r, s_1) &= \int_0^1 dt_1 \int_0^1 dt_2\, \frac{\epsilon^2 \hat{s}_1 \sqrt{1 + \frac{8\bar{s}_1 z_f}{\hat{s}_1^2}}}{\hat{s}_1^2 t_2 \bar{t}_2 + 2\bar{s}_1 z_f}\left[\frac{2\left(\hat{s}_1 t_1 t_2 \bar{t}_2 - 2z_f\right)}{t_1^2 t_2 \bar{t}_2 + \bar{t}_1 z_f} + \frac{4 s_1 \hat{s}_1}{s_1^2 - (1-2t_1)^2}\right] + \mathcal{O}(\epsilon^3)\,, \\
\tilde{M}_{25}(r, s_1) &= \tilde{M}_{24}(r, -s_1)\,. \qquad (4.60)
\end{aligned}
$$

4.13 M_{26} and M_{27}

This topology consists of four integrals, $\vec{M} = \left\{\tilde{M}_{26}(s_1), \tilde{M}_{27}(s_1), \tilde{M}_6', \tilde{M}_7'\right\}$, and the matrix $\tilde{A}_{26,27}(s_1)$. The integrals in this topology depend on a single variable and we only need functions up to weight two. The solution reads

$$
\tilde{M}_{26}(s_1) = \epsilon^2\left[-\frac{4\pi^2}{3} - 3\, i\pi H_{w_1^+}(s_1) + 3\, H_{w_1^+,w_1^+}(s_1)\right] + \mathcal{O}(\epsilon^3)\,, \qquad (4.61)
$$

$$
\begin{aligned}
\tilde{M}_{27}(s_1) =& \epsilon\left[-H_{w_1^+}(s_1) + i\pi\right] \\
&+ \epsilon^2\left[\frac{1}{2}\, H_{w_1^-,w_1^+}(s_1) + 2\, H_{0,w_1^+}(s_1) - \frac{i\pi}{2}\, H_{w_1^-}(s_1) - 2\, i\pi\, H_0(s_1) - \pi^2 - i\pi\ln(2)\right] \\
&+ \mathcal{O}(\epsilon^3)\,. \qquad (4.62)
\end{aligned}
$$

JHEP12(2014)129

4.14 M_{28} and M_{29}

The integrals in this topology already appeared in the two-loop calculation of the tree amplitudes [9–11], where explicit Mellin-Barnes (MB) representations have been used for their numerical evaluation (for a convenient parameterisation cf. also the appendix of [38]). With the current techniques, we are now in the position to compute these integrals analytically.

For this topology, it will be convenient to use the variables (r,p) defined in section 2. We need seven integrals,

$$\vec{M} = \left\{ \tilde{M}_{28}(r,p), \tilde{M}_{29}(r,p), \tilde{M}_1'(z_f)\tilde{M}_3'(\bar{u}), \left[\tilde{M}_1'(z_f)\right]^2, \tilde{M}_1'(z_f)\tilde{M}_1'(z_f=1), \tilde{M}_4'(z_f), \tilde{M}_5'(z_f) \right\} \tag{4.63}$$

and the matrix $\tilde{A}_{28,29}(r,p)$. The integral M_{28} is required up to functions of weight three, but M_{29} is only needed up to weight two. The solution is again lengthy, and we introduce a short-hand notation for $p_0 = 1 - 2\sqrt{z_f}$. We find

$$\tilde{M}_{28}(r,p) = \epsilon^3 \left[f^{(7)}(p) - f^{(7)}(p_0) \right] + \mathcal{O}(\epsilon^4)\,, \tag{4.64}$$

$$\tilde{M}_{29}(r,p) = \epsilon^2 [f^{(8)}(p) - f^{(8)}(p_0)] + \mathcal{O}(\epsilon^3)\,, \tag{4.65}$$

with

$$\begin{aligned}
f^{(7)}(x) = &- i\pi H_{w_1^+}(x)H_{w_1^+}(p_0) + 2H_0(r)H_{w_1^+}(x)H_{w_1^+}(p_0) + H_{w_1^-}(r)H_{w_1^+}(x)H_{w_1^+}(p_0) \\
&- \frac{\pi^2}{6}H_{w_3^-}(x) - \frac{i\pi}{2}H_{w_1^+}(p_0)H_{w_3^-}(x) + H_0(r)H_{w_1^+}(p_0)H_{w_3^-}(x) - \frac{\pi^2}{6}H_{w_1^-}(x) \\
&+ \frac{1}{2}H_{w_1^-}(r)H_{w_1^+}(p_0)H_{w_3^-}(x) - \frac{i\pi}{2}H_{w_1^+}(x)H_{w_3^-}(p_0) - H_{w_1^-}(r)H_{w_1^+,w_1^+}(x) \\
&+ H_0(r)H_{w_1^+}(x)H_{w_3^-}(p_0) - \frac{i\pi}{4}H_{w_3^-}(x)H_{w_3^-}(p_0) + \frac{1}{2}H_0(r)H_{w_3^-}(x)H_{w_3^-}(p_0) \\
&- \frac{\pi^2}{6}H_{w_3^+}(x) - \frac{i\pi}{2}H_{w_1^+}(p_0)H_{w_3^+}(x) + H_0(r)H_{w_1^+}(p_0)H_{w_3^+}(x) - \frac{\pi^2}{2}H_{w_1^+}(x) \\
&+ \frac{1}{2}H_{w_1^-}(r)H_{w_1^+}(p_0)H_{w_3^+}(x) - \frac{i\pi}{4}H_{w_3^-}(p_0)H_{w_3^+}(x) + \frac{1}{2}H_0(r)H_{w_3^-}(p_0)H_{w_3^+}(x) \\
&- \frac{i\pi}{2}H_{w_1^+}(x)H_{w_3^+}(p_0) + H_0(r)H_{w_1^+}(x)H_{w_3^+}(p_0) - H_0(r)H_{w_1^+,w_3^-}(x) \\
&- \frac{i\pi}{4}H_{w_3^-}(x)H_{w_3^+}(p_0) + \frac{1}{2}H_0(r)H_{w_3^-}(x)H_{w_3^+}(p_0) - \frac{i\pi}{4}H_{w_3^+}(x)H_{w_3^+}(p_0) \\
&+ \frac{1}{2}H_0(r)H_{w_3^+}(x)H_{w_3^+}(p_0) - 2H_{w_1^-}(x)H_{0,0}(\sqrt{z_f}) + H_{w_3^-}(x)H_{0,0}(\sqrt{z_f}) \\
&+ H_{w_3^+}(x)H_{0,0}(\sqrt{z_f}) + \frac{1}{2}H_{w_3^-}(x)H_{w_1^-,0}(\sqrt{z_f}) + \frac{1}{2}H_{w_3^+}(x)H_{w_1^-,0}(\sqrt{z_f}) \\
&- H_{w_1^+}(x)H_{w_1^+,0}(\sqrt{z_f}) - \frac{1}{2}H_{w_3^-}(x)H_{w_1^+,0}(\sqrt{z_f}) - H_{w_1^-}(x)H_{w_1^-,0}(\sqrt{z_f}) \\
&- \frac{1}{2}H_{w_3^+}(x)H_{w_1^+,0}(\sqrt{z_f}) + H_{w_1^+}(x)H_{w_1^+,w_1^-}(p_0) + \frac{1}{2}H_{w_3^-}(x)H_{w_1^+,w_1^-}(p_0) \\
&+ \frac{1}{2}H_{w_3^+}(x)H_{w_1^+,w_1^-}(p_0) - \frac{1}{2}H_{w_1^+}(x)H_{w_1^+,w_5^-}(p_0) - \frac{1}{4}H_{w_3^-}(x)H_{w_1^+,w_5^-}(p_0) \\
&- \frac{1}{4}H_{w_3^+}(x)H_{w_1^+,w_5^-}(p_0) - \frac{1}{2}H_{w_1^+}(x)H_{w_1^+,w_5^+}(p_0) - \frac{1}{4}H_{w_3^-}(x)H_{w_1^+,w_5^+}(p_0)
\end{aligned}$$

JHEP12(2014)129

$$
\begin{aligned}
&-\frac{1}{4}H_{w_3^+}(x)H_{w_1^+,w_5^+}(p_0)-\frac{1}{2}H_{w_1^+}(x)H_{w_1^+,w_4^-}(p_0)-\frac{1}{4}H_{w_3^-}(x)H_{w_1^+,w_4^-}(p_0)\\
&-\frac{1}{4}H_{w_3^+}(x)H_{w_1^+,w_4^-}(p_0)-\frac{1}{2}H_{w_1^+}(x)H_{w_1^+,w_4^+}(p_0)-\frac{1}{4}H_{w_3^-}(x)H_{w_1^+,w_4^+}(p_0)\\
&-\frac{1}{4}H_{w_3^+}(x)H_{w_1^+,w_4^+}(p_0)+i\pi H_{w_1^+,w_1^+}(x)-2H_0(r)H_{w_1^+,w_1^+}(x)+\frac{i\pi}{2}H_{w_1^+,w_3^-}(x)\\
&+\frac{1}{2}H_{w_1^+}(x)H_{w_3^-,w_1^-}(p_0)+\frac{1}{4}H_{w_3^-}(x)H_{w_3^-,w_1^-}(p_0)+\frac{1}{4}H_{w_3^+}(x)H_{w_3^-,w_1^-}(p_0)\\
&-\frac{1}{4}H_{w_1^+}(x)H_{w_3^-,w_5^-}(p_0)-\frac{1}{8}H_{w_3^-}(x)H_{w_3^-,w_5^-}(p_0)-\frac{1}{8}H_{w_3^+}(x)H_{w_3^-,w_5^-}(p_0)\\
&-\frac{1}{4}H_{w_1^+}(x)H_{w_3^-,w_5^+}(p_0)-\frac{1}{8}H_{w_3^-}(x)H_{w_3^-,w_5^+}(p_0)-\frac{1}{8}H_{w_3^+}(x)H_{w_3^-,w_5^+}(p_0)\\
&-\frac{1}{4}H_{w_1^+}(x)H_{w_3^-,w_4^-}(p_0)-\frac{1}{8}H_{w_3^-}(x)H_{w_3^-,w_4^-}(p_0)-\frac{1}{8}H_{w_3^+}(x)H_{w_3^-,w_4^-}(p_0)\\
&-\frac{1}{4}H_{w_1^+}(x)H_{w_3^-,w_4^+}(p_0)-\frac{1}{8}H_{w_3^-}(x)H_{w_3^-,w_4^+}(p_0)-\frac{1}{8}H_{w_3^+}(x)H_{w_3^-,w_4^+}(p_0)\\
&+\frac{i\pi}{2}H_{w_3^-,w_1^+}(x)-H_0(r)H_{w_3^-,w_1^+}(x)-\frac{1}{2}H_{w_1^-}(r)H_{w_3^-,w_1^+}(x)+\frac{i\pi}{4}H_{w_3^-,w_3^+}(x)\\
&+\frac{i\pi}{4}H_{w_3^-,w_3^-}(x)-\frac{1}{2}H_0(r)H_{w_3^-,w_3^-}(x)+\frac{i\pi}{2}H_{w_1^+,w_3^+}(x)-H_0(r)H_{w_1^+,w_3^+}(x)\\
&-\frac{1}{2}H_0(r)H_{w_3^-,w_3^+}(x)+\frac{1}{2}H_{w_1^+}(x)H_{w_3^+,w_1^-}(p_0)+\frac{1}{4}H_{w_3^-}(x)H_{w_3^+,w_1^-}(p_0)\\
&+\frac{1}{4}H_{w_3^+}(x)H_{w_3^+,w_1^-}(p_0)-\frac{1}{4}H_{w_1^+}(x)H_{w_3^+,w_5^-}(p_0)-\frac{1}{8}H_{w_3^-}(x)H_{w_3^+,w_5^-}(p_0)\\
&-\frac{1}{8}H_{w_3^+}(x)H_{w_3^+,w_5^-}(p_0)-\frac{1}{4}H_{w_1^+}(x)H_{w_3^+,w_5^+}(p_0)-\frac{1}{8}H_{w_3^-}(x)H_{w_3^+,w_5^+}(p_0)\\
&-\frac{1}{8}H_{w_3^+}(x)H_{w_3^+,w_5^+}(p_0)-\frac{1}{4}H_{w_1^+}(x)H_{w_3^+,w_4^-}(p_0)-\frac{1}{8}H_{w_3^-}(x)H_{w_3^+,w_4^-}(p_0)\\
&-\frac{1}{8}H_{w_3^+}(x)H_{w_3^+,w_4^-}(p_0)-\frac{1}{4}H_{w_1^+}(x)H_{w_3^+,w_4^+}(p_0)-\frac{1}{8}H_{w_3^-}(x)H_{w_3^+,w_4^+}(p_0)\\
&-\frac{1}{8}H_{w_3^+}(x)H_{w_3^+,w_4^+}(p_0)+\frac{i\pi}{2}H_{w_3^+,w_1^+}(x)-H_0(r)H_{w_3^+,w_1^+}(x)+\frac{i\pi}{4}H_{w_3^+,w_3^-}(x)\\
&-\frac{1}{2}H_{w_1^-}(r)H_{w_3^+,w_1^+}(x)-\frac{1}{2}H_0(r)H_{w_3^+,w_3^-}(x)+\frac{i\pi}{4}H_{w_3^+,w_3^+}(x)-\frac{1}{2}H_0(r)H_{w_3^+,w_3^+}(x)\\
&+\frac{1}{2}H_{w_1^+,w_1^+,w_5^-}(x)+\frac{1}{2}H_{w_1^+,w_1^+,w_5^+}(x)-\frac{1}{2}H_{w_3^-,w_1^+,w_1^-}(x)-H_{w_1^+,w_1^+,w_1^-}(x)\\
&+\frac{1}{2}H_{w_1^+,w_1^+,w_4^-}(x)+\frac{1}{2}H_{w_1^+,w_1^+,w_4^+}(x)-\frac{1}{2}H_{w_1^+,w_3^-,w_1^-}(x)+\frac{1}{4}H_{w_1^+,w_3^-,w_5^-}(x)\\
&+\frac{1}{4}H_{w_1^+,w_3^-,w_5^+}(x)+\frac{1}{4}H_{w_1^+,w_3^-,w_4^-}(x)+\frac{1}{4}H_{w_1^+,w_3^-,w_4^+}(x)-\frac{1}{2}H_{w_1^+,w_3^+,w_1^-}(x)\\
&+\frac{1}{4}H_{w_1^+,w_3^+,w_5^-}(x)+\frac{1}{4}H_{w_1^+,w_3^+,w_5^+}(x)+\frac{1}{4}H_{w_1^+,w_3^+,w_4^-}(x)+\frac{1}{4}H_{w_1^+,w_3^+,w_4^+}(x)\\
&+\frac{1}{4}H_{w_3^-,w_1^+,w_5^-}(x)+\frac{1}{4}H_{w_3^-,w_1^+,w_5^+}(x)+\frac{1}{4}H_{w_3^-,w_1^+,w_4^-}(x)+\frac{1}{4}H_{w_3^-,w_1^+,w_4^+}(x)\\
&-\frac{1}{4}H_{w_3^-,w_3^-,w_1^-}(x)+\frac{1}{8}H_{w_3^-,w_3^-,w_5^-}(x)+\frac{1}{8}H_{w_3^-,w_3^-,w_5^+}(x)+\frac{1}{8}H_{w_3^-,w_3^-,w_4^-}(x)\\
&+\frac{1}{8}H_{w_3^-,w_3^-,w_4^+}(x)-\frac{1}{4}H_{w_3^-,w_3^+,w_1^-}(x)+\frac{1}{8}H_{w_3^-,w_3^+,w_5^-}(x)+\frac{1}{8}H_{w_3^-,w_3^+,w_5^+}(x)
\end{aligned}
$$

JHEP12(2014)129

$$
\begin{aligned}
&+\frac{1}{8}H_{w_3^-,w_3^+,w_4^-}(x)+\frac{1}{8}H_{w_3^-,w_3^+,w_4^+}(x)-\frac{1}{2}H_{w_3^+,w_1^+,w_1^-}(x)+\frac{1}{4}H_{w_3^+,w_1^+,w_5^-}(x)\\
&+\frac{1}{4}H_{w_3^+,w_1^+,w_5^+}(x)+\frac{1}{4}H_{w_3^+,w_1^+,w_4^-}(x)+\frac{1}{4}H_{w_3^+,w_1^+,w_4^+}(x)-\frac{1}{4}H_{w_3^+,w_3^-,w_1^-}(x)\\
&+\frac{1}{8}H_{w_3^+,w_3^-,w_5^-}(x)+\frac{1}{8}H_{w_3^+,w_3^-,w_5^+}(x)+\frac{1}{8}H_{w_3^+,w_3^-,w_4^-}(x)+\frac{1}{8}H_{w_3^+,w_3^-,w_4^+}(x)\\
&-\frac{1}{4}H_{w_3^+,w_3^+,w_1^-}(x)+\frac{1}{8}H_{w_3^+,w_3^+,w_5^-}(x)+\frac{1}{8}H_{w_3^+,w_3^+,w_5^+}(x)+\frac{1}{8}H_{w_3^+,w_3^+,w_4^-}(x)\\
&+\frac{1}{8}H_{w_3^+,w_3^+,w_4^+}(x)+2H_{w_1^+}(x)H_{w_1^+}(p_0)\ln(2)-H_{w_3^-,w_1^+}(x)\ln(2)-H_{w_3^+,w_1^+}(x)\ln(2)\\
&+H_{w_1^+}(p_0)H_{w_3^-}(x)\ln(2)+H_{w_1^+}(p_0)H_{w_3^+}(x)\ln(2)-2H_{w_1^+,w_1^+}(x)\ln(2)\,, \qquad (4.66)
\end{aligned}
$$

$$
\begin{aligned}
f^{(8)}(x)=\;&i\pi H_{w_1^+}(x)-2H_0(r)\,H_{w_1^+}(x)-H_{w_1^-}(r)\,H_{w_1^+}(x)+\frac{i\pi}{2}\,H_{w_3^-}(x)-H_0(r)\,H_{w_3^-}(x)\\
&+\frac{i\pi}{2}\,H_{w_3^+}(x)-H_0(r)\,H_{w_3^+}(x)-H_{w_1^+,w_1^-}(x)+\frac{1}{2}\,H_{w_1^+,w_5^-}(x)+\frac{1}{2}\,H_{w_1^+,w_4^-}(x)\\
&+\frac{1}{2}\,H_{w_1^+,w_5^+}(x)+\frac{1}{2}\,H_{w_1^+,w_4^+}(x)-\frac{1}{2}\,H_{w_3^-,w_1^-}(x)+\frac{1}{4}\,H_{w_3^-,w_5^-}(x)+\frac{1}{4}\,H_{w_3^-,w_4^-}(x)\\
&+\frac{1}{4}\,H_{w_3^-,w_5^+}(x)+\frac{1}{4}\,H_{w_3^-,w_4^+}(x)-\frac{1}{2}\,H_{w_3^+,w_1^-}(x)+\frac{1}{4}\,H_{w_3^+,w_5^-}(x)+\frac{1}{4}\,H_{w_3^+,w_4^-}(x)\\
&+\frac{1}{4}\,H_{w_3^+,w_5^+}(x)+\frac{1}{4}\,H_{w_3^+,w_4^+}(x)-2H_{w_1^+}(x)\,\ln(2)\,. \qquad (4.67)
\end{aligned}
$$

5 Checks and validation

We performed several cross checks of the analytic results presented in the previous section. First of all, we evaluated the generalised HPLs numerically by rewriting them in terms of Goncharov polylogarithms and evaluating them both with the GiNaC-library [39, 40] and an in-house `Mathematica` routine. We also derived MB representations for most of the integrals, where the `AMBRE`-package [41] proved to be useful. Their numerical evaluation with the `MB`-package [42], however, turned out to be difficult due to highly oscillating integrands related to the presence of the threshold. We therefore used the MB representations to derive ordinary Feynman parameter representations, similar to the ones given in (4.60). Another purely numerical method is sector decomposition, where we used both the `SecDec`-package [43, 44] as well a `Mathematica`-based in-house routine. For the most complicated coefficients the numerical evaluations confirm the analytic results at the level of 10^{-4}, and for the simpler coefficients the agreement is several orders of magnitude better.

6 Conclusion and outlook

We computed the master integrals that arise in the computation of the two-loop correction to the vertex kernel of the leading penguin amplitudes in non-leptonic B-decays. The calculation is complicated by the presence of two non-trivial scales ($\bar{u}$ and $z_f = m_f^2/m_b^2$), as well as the kinematic threshold at $\bar{u} = 4z_f$. We computed the master integrals in a recently advocated canonical basis, which enabled us to derive analytic results for all

JHEP12(2014)129

master integrals in terms of generalised HPLs. The results are given up to the relevant order in the ϵ-expansion that is needed to obtain the finite terms of the penguin amplitudes. Our calculation is the first application of a canonical basis to integrals with two different internal masses. Apart from the integral basis, we find that the choice of the kinematic variables is of utmost importance since it renders the logarithms in the matrices $\tilde{A}_k$ rational and therefore makes the formulas for iterated integrals applicable.

The results of this paper form the basis to derive fully analytic expressions for the hard-scattering kernels T_i^I in the factorisation formula (1.1). In phenomenological applications, one has to integrate over the product of the kernels and the Gegenbauer expansion of the light-cone distribution amplitudes. The presence of the charm threshold makes the numerical evaluation of the convolutions delicate. The threshold is much easier to handle in an analytic approach, and the convolutions can now be computed to very high precision.

The integrals presented here are also relevant for other applications such as rare or radiative B-meson decays. For example, the two-loop QCD correction to the matrix elements of current-current operators in inclusive $\bar{B} \to X_s \ell^+ \ell^-$ decays have to date only been computed numerically [45] or as expansions in the lepton-invariant mass q^2 [46, 47]. With the present results, one can now obtain completely analytical expressions for any value of q^2. In exclusive $\bar{B} \to K^{(*)} \ell^+ \ell^-$ decays, one can study non-factorisable corrections to charm-loop effects.

Acknowledgments

We thank Sophia Borowka and Gudrun Heinrich for assistance on the program SecDec and for performing cross-checks on some of the integrals. We thank Claude Duhr, Johannes Henn, Andreas von Manteuffel and Stefan Weinzierl for useful discussions. The work of TH is supported by DFG research unit FOR 1873 "Quark Flavour Physics and Effective Field Theories". GB gratefully acknowledges the support of a University Research Fellowship by the Royal Society.

A Matrices $\tilde{A}_k$

In this appendix we list the matrices $\tilde{A}_k$ for the different subtopologies. To this end, we define the following logarithms,

$$L_1^x = \ln(x)\,, \qquad L_{11}^x = \ln\left(\frac{1-\sqrt{1-r^2}+x}{1-\sqrt{1-r^2}-x}\right)\,,$$

$$L_2^x = \ln(1-x^2)\,, \qquad L_{12} = \ln\left(\frac{2+\sqrt{1-r^2}}{2-\sqrt{1-r^2}}\right)\,,$$

$$L_3^x = \ln\left(\frac{1+x}{1-x}\right)\,, \qquad L_{13}^x = \ln\left(\frac{x^2+3}{4}\right)\,,$$

$$L_4^x = \ln(r^2-x^2)\,, \qquad L_{14}^x = \ln\left(x^2 - x\left(r^2+1\right)+1\right)\,,$$

$$L_5^x = \ln\left(\frac{r+x}{r-x}\right)\,, \qquad L_{15} = \ln\left((1-s_1)(1-t)-(1+s_1)(1-v)\right)\,,$$

JHEP12(2014)129

$$
\begin{aligned}
L_6^x &= \ln\left(\left(\frac{r^2+1}{2}\right)^2 - x^2\right), & L_{16} &= \ln\left((1+s_1)(1+r) - 2(1-t)\right), \\
L_7^x &= \ln\left(\frac{r^2+2x+1}{r^2-2x+1}\right), & L_{17} &= \ln\left((1-s_1)(1+r) - 2(1-v)\right), \\
L_8^x &= \ln\left(\left(1+\sqrt{1-r^2}\right)^2 - x^2\right), & L_{18} &= \ln\left(\sqrt{1-r^2} - 2t + (1-s_1)(1+\frac{1}{2}\sqrt{1-r^2})\right), \\
L_9^x &= \ln\left(\frac{1+\sqrt{1-r^2}+x}{1+\sqrt{1-r^2}-x}\right), & L_{19} &= \ln\left(\sqrt{1-r^2} - 2v + (1+s_1)(1+\frac{1}{2}\sqrt{1-r^2})\right). \\
L_{10}^x &= \ln\left(\left(1-\sqrt{1-r^2}\right)^2 - x^2\right),
\end{aligned}
\tag{A.1}
$$

The matrices $\tilde{A}_k$ now assume a compact form,

$$
\tilde{A}_{3,4} = \begin{pmatrix} -L_2^s - 2L_2^r & -L_3^s & 0 \\ 6L_3^s & -6L_1^s + 4L_2^s - 2L_2^r & -2L_3^s \\ 0 & 0 & -2L_2^r \end{pmatrix}, \tag{A.2}
$$

$$
\tilde{A}_5 = \begin{pmatrix} -2L_1^r & -2L_3^r & 2L_3^r \\ 0 & -2L_2^r & 0 \\ 0 & 0 & -L_2^r \end{pmatrix}, \tag{A.3}
$$

$$
\tilde{A}_{6,7} = \begin{pmatrix} -L_2^s - L_2^r - L_4^s & -L_3^s & \frac{L_2^s}{2} - \frac{L_4^s}{2} & 0 & 0 & 0 \\ 3L_3^s & -4L_1^s + 3L_2^s - L_2^r - L_4^s & -\frac{3L_3^s}{2} & \frac{L_5^s}{2} & L_3^s & L_3^s \\ 0 & 0 & -3L_2^r & -L_3^r & 0 & 0 \\ 0 & 0 & 6L_3^r & 2L_2^r - 6L_1^r & 0 & -2L_3^r \\ 0 & 0 & 0 & 0 & L_2^s - L_2^r - L_4^s & 0 \\ 0 & 0 & 0 & 0 & 0 & -2L_2^r \end{pmatrix} \tag{A.4}
$$

$$
\tilde{A}_{8,9} = \begin{pmatrix} -L_2^s - 3L_2^r + L_4^s & L_3^s & \frac{L_3^r}{2} & 0 & 0 & 0 \\ -3L_3^s & -4L_1^s + 3L_2^s - 3L_2^r + L_4^s & -\frac{L_5^s}{2} & L_3^s & L_3^s & -L_3^s \\ 0 & 0 & -2L_1^r & 0 & -2L_3^r & 2L_3^r \\ 0 & 0 & 0 & L_2^s - 3L_2^r + L_4^s & 0 & L_2^r - L_2^s \\ 0 & 0 & 0 & 0 & -2L_2^r & 0 \\ 0 & 0 & 0 & 0 & 0 & -L_2^r \end{pmatrix} \tag{A.5}
$$

$$
\tilde{A}_{10,11} = \begin{pmatrix} -2L_2^s - 3L_2^r + 2L_4^s & -L_3^s & \frac{L_2^s}{2} - \frac{L_2^r}{2} \\ 6L_3^s & -6L_1^s + 3L_2^s - 3L_2^r + 2L_4^s & -3L_3^s \\ 0 & 0 & -L_2^s - 2L_2^r \\ 0 & 0 & 6L_3^s \\ 0 & 0 & 0 \\ 0 & 0 & 0 \\ 0 & 0 & 0 \end{pmatrix}
$$

JHEP12(2014)129

$$
\begin{matrix}
-\frac{L_3^s}{2} & \frac{L_3^r}{2} & 0 & 0 \\
L_4^s - L_2^r & L_5^s & 0 & L_3^s \\
-L_3^s & 0 & 0 & 0 \\
-6L_1^s + 4L_2^s - 2L_2^r & 0 & -2L_3^s & 0 \\
0 & -2L_1^r & -2L_3^r & 2L_3^r \\
0 & 0 & -2L_2^r & 0 \\
0 & 0 & 0 & -L_2^r
\end{matrix}
\Bigg) \tag{A.6}
$$

$$
\tilde{A}_{12-14} = \Bigg(
\begin{matrix}
-L_2^s - 2L_2^r + 2L_4^s - L_6^s & L_2^r - \frac{L_6^s}{2} & \frac{L_7^s}{2} - L_3^s \\
L_2^s - 2L_4^s + L_6^s & L_2^s - L_2^r - 2L_4^s + \frac{L_6^s}{2} & -\frac{L_7^s}{2} \\
L_3^s - L_7^s & -L_3^s - \frac{L_7^s}{2} & -2L_1^s + 2L_2^s - L_2^r - 2L_4^s + \frac{L_6^s}{2} \\
0 & 0 & 0 \\
0 & 0 & 0 \\
0 & 0 & 0 \\
0 & 0 & 0
\end{matrix}
\begin{matrix}
-L_2^s - \frac{L_2^r}{2} + \frac{3L_6^s}{4} & 0 & 0 & 0 \\
\frac{L_2^s}{2} + L_2^r - \frac{3L_6^s}{4} & \frac{L_3^r}{2} & 0 & L_3^s \\
\frac{3L_3^s}{2} + \frac{3L_7^s}{4} & -L_5^s & 0 & -L_2^s - 2L_2^r + 2L_4^s \\
-3L_2^r & -L_3^r & 0 & 0 \\
6L_3^r & 2L_2^r - 6L_1^r & -2L_3^r & 0 \\
0 & 0 & -2L_2^r & 0 \\
0 & 0 & L_3^s & -2L_1^s + L_2^s - 2L_2^r
\end{matrix}
\Bigg) \tag{A.7}
$$

$$
\tilde{A}_{15-17} = \begin{pmatrix}
-L_2^s - 2L_2^r & 0 & -L_3^s & 0 & 0 \\
L_2^s & L_2^s - 2L_2^r & 0 & 0 & -L_3^s \\
L_3^s & -L_3^s & -2L_1^s + 2L_2^s - 2L_2^r & 0 & L_2^s \\
0 & 0 & 0 & -2L_2^r & 0 \\
0 & 0 & 0 & L_3^s & -2L_1^s + L_2^s - 2L_2^r
\end{pmatrix}, \tag{A.8}
$$

$$
\tilde{A}_{18-21} = \Bigg(
\begin{matrix}
-L_2^s - 2L_2^r + 2L_4^s - L_6^s & 0 \\
L_6^s - L_2^s & -2L_2^s - L_2^r + 2L_4^s \\
-3L_3^s - L_7^s + 2L_9^s + 2L_{11}^s & -2L_3^s + 2L_9^s + 2L_{11}^s \\
-10L_2^s + 4L_4^s - 2L_6^s + 4L_8^s + 4L_{10}^s & -12L_2^s + 4L_4^s + 4L_8^s + 4L_{10}^s \\
0 & 0 \\
0 & 0 \\
0 & 0 \\
0 & 0 \\
0 & 0 \\
0 & 0 \\
0 & 0
\end{matrix}
$$

JHEP12(2014)129

$$
\begin{array}{cccc}
L_3^s+\frac{L_7^s}{2} & \frac{L_6^s}{4}-\frac{L_2^r}{2} & L_3^r & 0 \\
-\frac{L_7^s}{2} & \frac{L_2^s}{2}-\frac{L_6^s}{4} & -\frac{L_3^r}{2} & 0 \\
-2L_1^s+2L_2^s-L_2^r+2L_4^s+\frac{L_6^s}{2}-2L_8^s-2L_{10}^s & \frac{L_3^s}{2}+\frac{L_7^s}{4}-L_9^s-L_{11}^s & -L_5^s & L_3^s \\
4L_3^s+L_7^s-4L_9^s-4L_{11}^s & 3L_2^s-L_2^r+\frac{L_6^s}{2}-2L_8^s-2L_{10}^s & 0 & 0 \\
0 & 0 & -2L_1^r & -2L_3^r \\
0 & 0 & 0 & -2L_2^r \\
0 & 0 & 0 & 0 \\
0 & 0 & 0 & L_3^s \\
0 & 0 & 0 & 0 \\
0 & 0 & 0 & \frac{L_2^r}{2}-\frac{L_{13}^r}{2} \\
0 & 0 & 0 & \frac{L_{12}}{2}
\end{array}
$$

$$
\left.
\begin{array}{ccccc}
0 & \frac{L_7^s}{2}-L_3^s & L_3^s-\frac{L_7^s}{2} & 2L_2^s+2L_2^r-2L_6^s & 0 \\
0 & L_3^s-\frac{L_7^s}{2} & \frac{L_7^s}{2}-L_3^s & -2L_2^s-2L_2^r+2L_6^s & 0 \\
-L_3^s & \frac{L_6^s}{2}-L_2^r & L_2^s-\frac{L_6^s}{2} & 2L_3^s-2L_7^s+2L_9^s+2L_{11}^s & 2L_{11}^s-2L_9^s \\
0 & 2L_3^s+L_7^s & -L_7^s & -4L_2^s-4L_6^s+4L_8^s+4L_{10}^s & 4L_{10}^s-4L_8^s \\
2L_3^r & 0 & 0 & 0 & 0 \\
0 & 0 & 0 & 0 & 0 \\
-L_2^r & 0 & 0 & 0 & 0 \\
0 & -2L_1^s+L_2^s-2L_2^r & 0 & 0 & 0 \\
L_3^s & 0 & -2L_1^s+L_2^s-L_2^r & 0 & 0 \\
\frac{L_{13}^r}{2}-\frac{L_2^r}{2} & 0 & 0 & -3L_{13}^r & -L_{12} \\
-\frac{L_{12}}{2} & 0 & 0 & 3L_{12} & L_{13}^r-2L_2^r
\end{array}
\right)
\tag{A.9}
$$

$$
\tilde{A}_{22}=\begin{pmatrix}
L_2^s & -L_2^s & 0 & 0 & 0 & -L_3^s & -L_3^s \\
0 & -L_2^s & -L_3^s & 0 & 0 & 0 & 0 \\
0 & 6L_3^s & 4L_2^s-6L_1^s & 0 & -2L_3^s & 0 & 0 \\
0 & 0 & 0 & L_2^s & 0 & 0 & 0 \\
0 & 0 & 0 & 0 & 0 & 0 & 0 \\
0 & 0 & 0 & 0 & L_3^s & L_2^s-2L_1^s & 0 \\
0 & 0 & 0 & L_3^s & 0 & 0 & 2L_2^s-2L_1^s
\end{pmatrix}-2L_2^r\mathbb{1}_{7\times 7}\,, \tag{A.10}
$$

$$
\tilde{A}_{23-25}=\begin{pmatrix}
-L_2^{s_1}-3L_2^r+2L_{13}^{s_1} & -\frac{L_3^t}{4}-\frac{L_2^r}{4}+\frac{L_6^t}{8}-\frac{L_7^t}{8} \\
12L_3^t+12L_2^r-6L_6^t+6L_7^t & -L_1^{s_1}+\frac{L_2^{s_1}}{2}-\frac{5L_3^{s_1}}{2}+L_2^r+L_{13}^{s_1}+2L_6^t-2L_7^t-4L_{14}^t \\
12L_3^v+12L_2^r-6L_6^v+6L_7^v & -L_1^{s_1}-L_2^r-L_{13}^{s_1}+2L_{15} \\
0 & 0 \\
0 & 0 \\
0 & 0 \\
0 & 0 \\
0 & 0 \\
0 & 0
\end{pmatrix}
$$

JHEP12(2014)129

$$
\begin{array}{ccccccc}
-\frac{L_3^v}{4}-\frac{L_2^r}{4}+\frac{L_6^v}{8}-\frac{L_7^v}{8} & -\frac{L_3^r}{2} & 0 & 0 & 0 & 0 & 0 \\
-L_1^{s_1}-L_2^r-L_{13}^{s_1}+2L_{15} & 2L_2^r+2L_{13}^{s_1}-4L_{16} & 4L_3^t+2L_2^r-2L_{13}^r & -4L_2^{s_1}-4L_3^{s_1}-4L_{13}^r+8L_{18} & 0 & 0 & 0 \\
-L_1^{s_1}+\frac{L_2^{s_1}}{2}+\frac{5L_3^{s_1}}{2}+L_2^r+L_{13}^{s_1}+2L_6^v-2L_7^v-4L_{14}^v & 2L_2^r+2L_{13}^{s_1}-4L_{17} & 4L_3^v+2L_2^r-2L_{13}^r & -4L_3^v-2L_2^r+2L_{13}^r & 12L_3^v+6L_6^v-6L_7^v-12L_{13}^r & -4L_2^{s_1}+4L_3^{s_1}-4L_{13}^r+8L_{19} & 0 \\
0 & -2L_1^r & -2L_3^r & 2L_3^r & 0 & 0 & 0 \\
0 & 0 & -2L_2^r & 0 & 0 & 0 & 0 \\
0 & 0 & 0 & -L_2^r & 0 & 0 & 0 \\
0 & 0 & \frac{L_2^r}{2}-\frac{L_{13}^r}{2} & \frac{L_{13}^r}{2}-\frac{L_2^r}{2} & -3L_{13}^r & -L_{12} & 0 \\
0 & 0 & \frac{L_{12}}{2} & -\frac{L_{12}}{2} & 3L_{12} & L_{13}^r-2L_2^r & 0 \\
0 & 0 & 0 & L_3^{s_1} & 0 & 0 & -2L_1^{s_1}+L_2^{s_1}-L_2^r
\end{array}
\Bigg), \qquad \text{(A.11)}
$$

$$
\tilde{A}_{26,27}=\begin{pmatrix}
2L_{13}^{s_1}-\frac{5L_2^{s_1}}{2} & -3L_3^{s_1} & \frac{L_2^{s_1}}{4} & -L_2^{s_1} \\
-\frac{9L_3^{s_1}}{4} & \frac{L_2^{s_1}}{2}-2L_1^{s_1} & \frac{5L_3^{s_1}}{8} & \frac{3L_3^{s_1}}{2} \\
0 & 0 & 0 & 0 \\
0 & 0 & 0 & 0
\end{pmatrix}, \qquad \text{(A.12)}
$$

JHEP12(2014)129

$$
\tilde{A}_{28,29} = \begin{pmatrix}
-L_2^p - 3L_2^r - \frac{L_6^p}{2} + \frac{L_7^p}{2} + L_8^p - L_9^p + L_{10}^p - L_{11}^p & L_3^p + L_2^r - \frac{L_6^p}{2} + \frac{L_7^p}{2} & 0 & 0 & 0 & -L_3^p - L_2^r + \frac{L_6^p}{2} - \frac{L_7^p}{2} & -L_2^p + \frac{L_6^p}{2} - \frac{L_7^p}{2} & 0 & 0 & -L_3^p - \frac{L_2^r}{2} - \frac{L_{12}}{2} + \frac{L_{13}^r}{2} & L_3^p + \frac{L_2^r}{2} + \frac{L_{12}}{2} - \frac{L_{13}^r}{2} & -L_2^p + \frac{L_6^p}{2} - \frac{L_7^p}{2} \\
-3L_3^p - 3L_2^r + \frac{3L_6^p}{2} - \frac{3L_7^p}{2} & 3L_2^p + L_2^r + \frac{3L_6^p}{2} - \frac{3L_7^p}{2} - L_8^p + L_9^p - L_{10}^p + L_{11}^p - 4L_{14}^p & -L_3^p - L_2^r + \frac{L_6^p}{2} - \frac{L_7^p}{2} & 0 & 0 & 0 & L_2^p - L_2^r + \frac{L_6^p}{2} - \frac{L_7^p}{2} - L_8^p + L_9^p - L_{10}^p + L_{11}^p & 0 & 0 & 0 & 0 & -L_2^p + \frac{L_8^p}{2} - \frac{L_9^p}{2} + \frac{L_{10}^p}{2} - \frac{L_{11}^p}{2} & 0 & -3L_3^p - \frac{3L_6^p}{2} + \frac{3L_7^p}{2} - 3L_{12} + 3L_{13}^r \\
0 & 0 & 0 & 0 & 0 & 0 & 0 & 0 & 0 & -2L_2^r & 0 & 0 \\
0 & 0 & 0 & 0 & 0 & 0 & 0 & 0 & 0 & 0 & -L_2^r & 0 \\
0 & 0 & 0 & 0 & 0 & 0 & 0 & 0 & 0 & \frac{L_2^r}{2} - \frac{L_{13}^r}{2} & \frac{L_{13}^r}{2} - \frac{L_2^r}{2} & -3L_{13}^r \\
0 & 0 & 0 & 0 & 0 & 0 & 0 & 0 & 0 & \frac{L_{12}}{2} & -\frac{L_{12}}{2} & 3L_{12} \\
L_3^p + L_2^r - \frac{L_6^p}{2} + \frac{L_7^p}{2} & 3L_2^p + 3L_2^r + \frac{3L_6^p}{2} - \frac{3L_7^p}{2} - 2L_8^p + 2L_9^p + L_{12} - L_{13}^r - 4L_{14}^p & 0 & 0 & 0 & -L_{12} & L_{13}^r - 2L_2^r
\end{pmatrix}. \quad \text{(A.13)}
$$

B Auxiliary integrals

Here we collect the results of the integrals that are already known from previous calculations, but which appear as subtopologies of the master integrals discussed in the main text and are needed in order to make the system of differential equations complete. In terms of

JHEP12(2014)129

the integrals defined in figure 3, they read

$$M_1'(z_f) = \epsilon\, I_1'(z_f)\,, \qquad M_5'(z_f) = \epsilon^2 \sqrt{z_f}\left(I_5'(z_f) + 2I_4'(z_f)\right), \tag{B.1}$$

$$M_2'(x) = \epsilon\, x\, I_2'(x)\,, \qquad M_6' = \epsilon^2\left(I_6' + 2I_7'\right), \tag{B.2}$$

$$M_3'(x) = \epsilon\, x\, I_3'(x)\,, \qquad M_7' = \epsilon^2\, I_8'\,. \tag{B.3}$$

$$M_4'(z_f) = \epsilon^2\, I_4'(z_f)\,, \tag{B.4}$$

Normalizing these integrals according to the definition in (4.1), the results become

$$\tilde{M}_1'(z_f) = z_f^{-\epsilon}\,\Gamma(1-\epsilon)\,\Gamma(1+\epsilon)\,, \tag{B.5}$$

$$\tilde{M}_2'(x) = -\,e^{i\pi\epsilon}\,x^{-\epsilon}\,\frac{\Gamma^3(1-\epsilon)\Gamma(1+\epsilon)}{\Gamma(1-2\epsilon)}\,, \tag{B.6}$$

$$\begin{aligned}\tilde{M}_3'(x) &= -\,\frac{\epsilon\, x}{1-\epsilon}\,\Gamma(1-\epsilon)\,\Gamma(1+\epsilon)\;{}_2F_1\left(1, 1+\epsilon\,;\, 2-\epsilon\,;\, x\right)\\ &= \epsilon\,\ln(1-x) - \epsilon^2\left[\mathrm{Li}_2(x) + \ln^2(1-x)\right] + \epsilon^3\Big[-2\,\mathrm{Li}_3(1-x) - \mathrm{Li}_3(x)\\ &\quad + \frac{2}{3}\,\ln^3(1-x) - \ln(x)\ln^2(1-x) + \frac{1}{2}\,\pi^2\ln(1-x) + 2\zeta_3\Big] + \mathcal{O}(\epsilon^4)\,,\end{aligned} \tag{B.7}$$

$$\begin{aligned}\tilde{M}_4'(z_f) &= \epsilon^2\left[-\frac{\pi^2}{12} - \frac{1}{2}\,H_{w_1^-,w_1^-}(r) - H_{w_1^-}(r)\,\ln(2) - \ln^2(2) - \frac{1}{2}\,\mathrm{Li}_2(1-z_f)\right]\\ &\quad + \epsilon^3\Big[\frac{\pi^2}{2}\,H_{w_1^+}(\sqrt{z_f}) - \frac{3}{2}\,H_{w_1^-,w_1^-,w_1^-}(r) + H_{w_1^+,w_1^+,0}(\sqrt{z_f}) - 3\,H_{w_1^-,w_1^-}(r)\,\ln(2)\\ &\quad - 3\,H_{w_1^-}(r)\,\ln^2(2) - 2\ln^3(2) + \frac{\pi^2}{4}\,\ln(1-z_f) + \frac{3}{2}\,\mathrm{Li}_3(1-z_f) - \frac{7}{2}\,\zeta_3\Big] + \mathcal{O}(\epsilon^4)\,,\end{aligned} \tag{B.8}$$

$$\begin{aligned}\tilde{M}_5'(z_f) &= \epsilon^2\left[-\frac{\pi^2}{2} - H_{w_1^+,0}(\sqrt{z_f})\right] + \epsilon^3\Big[2\pi^2 H_0(\sqrt{z_f}) + \frac{\pi^2}{2}\,H_{w_1^-}(\sqrt{z_f}) - \frac{\pi^2}{2}\,H_{w_1^+}(\sqrt{z_f})\\ &\quad +\; 4H_{0,w_1^+,0}(\sqrt{z_f}) + H_{w_1^-,w_1^+,0}(\sqrt{z_f}) - 3\,H_{w_1^+,w_1^-,0}(\sqrt{z_f}) + 4\pi^2\ln(2)\Big] + \mathcal{O}(\epsilon^4)\,,\end{aligned} \tag{B.9}$$

$$\tilde{M}_6' = -\,\Gamma^3(1-\epsilon)\,\Gamma(1+\epsilon)\,\Gamma(1+2\epsilon)\,, \tag{B.10}$$

$$\tilde{M}_7' = -\,\frac{\Gamma(1-4\epsilon)\,\Gamma^4(1-\epsilon)\,\Gamma(1+\epsilon)\,\Gamma(1+2\epsilon)}{4\,\Gamma(1-3\epsilon)\,\Gamma(1-2\epsilon)}\,. \tag{B.11}$$

JHEP12(2014)129

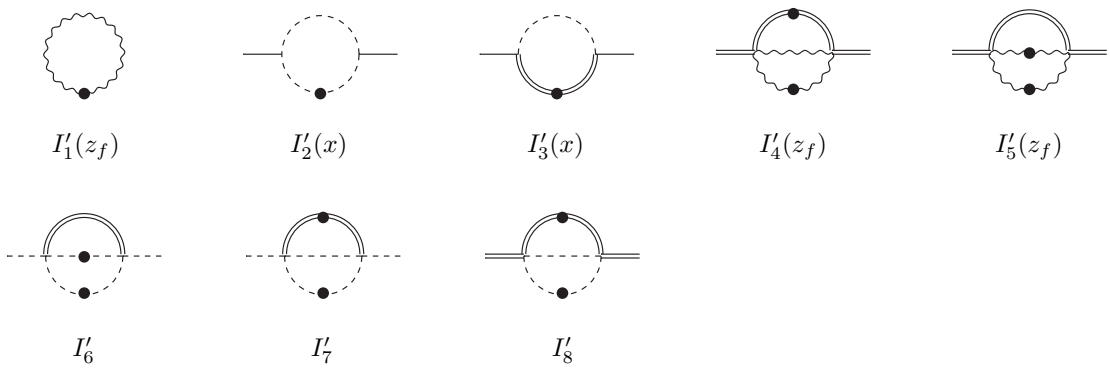

Figure 3. Integrals required to define the auxiliary integrals in (B.1)–(B.4). The notation has been introduced in the caption of figure 2.

C $\tilde{M}_{18} + \tilde{M}_{19}$ to $\mathcal{O}(\epsilon^4)$

Here we present the result of $\tilde{M}_{18}(r,s) + \tilde{M}_{19}(r,s)$ to $\mathcal{O}(\epsilon^4)$. This result is needed in the final result of the QCD amplitude, but due to its length it was relegated to this appendix.

$$
\begin{aligned}
&\tilde{M}_{18}(r,s) + \tilde{M}_{19}(r,s)\big|_{\epsilon^4} = -2\pi^2 H_0\left(\tfrac{1}{1+2\sqrt{z_f}}\right) H_{w_1^-}(r) + 2\pi^2 H_0\left(\tfrac{1}{1+2\sqrt{z_f}}\right) H_{w_1^-}(s) \\
&-\frac{\pi^2}{2} H_{w_1^-}(r)\, H_{w_1^-}(s) + \pi^2 H_{w_1^-}(r)\, H_{w_1^+}(s) + \pi^2 H_{w_1^-}(r)\, H_{w_2^-}(s) + 2i\pi H_{w_1^+}(r)\, H_{-1,1}(r^2) \\
&-2i\pi H_{w_1^+}(s)\, H_{-1,1}(r^2) + 4i\pi H_{w_1^+}(s)\, H_{0,w_1^-}(r) + \frac{4}{3}\pi^2 H_{w_1^-,w_1^-}(r) \\
&-3\, i\pi H_{w_1^+}(s)\, H_{w_1^-,w_1^-}(r) - \frac{\pi^2}{3} H_{w_1^-,w_1^-}(s) + H_{w_1^-,w_1^-}(r)\, H_{w_1^-,w_1^-}(s) + \frac{\pi^2}{6} H_{w_1^-,w_5^-}(r) \\
&-\frac{\pi^2}{6} H_{w_1^-,w_5^-}(s) - H_{w_1^-,w_1^-}(r)\, H_{w_1^-,w_5^-}(s) - 2i\pi H_{w_1^-}(r)\, H_{w_1^-,w_5^+}(s) - \frac{11}{6}\pi^2 H_{w_1^-,w_4^-}(r) \\
&+\frac{11}{6}\pi^2 H_{w_1^-,w_4^-}(s) - H_{w_1^-,w_1^-}(r)\, H_{w_1^-,w_4^-}(s) - 2i\pi H_{w_1^-}(r)\, H_{w_1^-,w_4^+}(s) - \pi^2 H_{w_1^-,w_1^+}(s) \\
&+2i\pi H_{w_1^-}(r)\, H_{w_1^-,w_1^+}(s) + \frac{\pi^2}{12} H_{w_1^-,w_3^-}(r) - \frac{\pi^2}{12} H_{w_1^-,w_3^-}(s) + H_{w_1^-,w_1^-}(r)\, H_{w_1^-,w_3^-}(s) \\
&+i\pi H_{w_1^-}(r)\, H_{w_1^-,w_3^+}(s) - \pi^2 H_{w_1^-,w_2^-}(r) + 2i\pi H_{w_1^-}(r)\, H_{w_1^+,0}(s) \\
&+2H_{w_1^-,w_5^-}(r)\, H_{w_1^+,0}(\sqrt{z_f}) - 2H_{w_1^-,w_5^-}(s)\, H_{w_1^+,0}(\sqrt{z_f}) - 2H_{w_1^-,w_4^-}(r)\, H_{w_1^+,0}(\sqrt{z_f}) \\
&+2H_{w_1^-,w_4^-}(s)\, H_{w_1^+,0}(\sqrt{z_f}) - \pi^2 H_{w_1^+,w_1^-}(s) + 3\, i\pi H_{w_1^-}(r)\, H_{w_1^+,w_1^-}(s) \\
&-2i\pi H_{w_1^-}(r)\, H_{w_1^+,w_5^-}(s) + \frac{\pi^2}{6} H_{w_1^+,w_5^+}(r) + 2H_{w_1^+,0}(\sqrt{z_f})\, H_{w_1^+,w_5^+}(r) - \frac{\pi^2}{6} H_{w_1^+,w_5^+}(s) \\
&-H_{w_1^-,w_1^-}(r)\, H_{w_1^+,w_5^+}(s) - 2H_{w_1^+,0}(\sqrt{z_f})\, H_{w_1^+,w_5^+}(s) - 2i\pi H_{w_1^-}(r)\, H_{w_1^+,w_4^-}(s) \\
&-\frac{11}{6}\pi^2 H_{w_1^+,w_4^+}(r) - 2H_{w_1^+,0}(\sqrt{z_f})\, H_{w_1^+,w_4^+}(r) + \frac{11}{6}\pi^2 H_{w_1^+,w_4^+}(s) \\
&-H_{w_1^-,w_1^-}(r)\, H_{w_1^+,w_4^+}(s) + 2H_{w_1^+,0}(\sqrt{z_f})\, H_{w_1^+,w_4^+}(s) + \frac{2}{3}\pi^2 H_{w_1^+,w_1^+}(r) - \frac{2}{3}\pi^2 H_{w_1^+,w_1^+}(s) \\
&+2H_{w_1^-,w_1^-}(r)\, H_{w_1^+,w_1^+}(s) + i\pi H_{w_1^-}(r)\, H_{w_1^+,w_3^-}(s) + \frac{\pi^2}{12} H_{w_1^+,w_3^+}(r) - \frac{\pi^2}{12} H_{w_1^+,w_3^+}(s)
\end{aligned}
$$

JHEP12(2014)129

$$
\begin{aligned}
&+H_{w_1^-,w_1^-}(r)\,H_{w_1^+,w_3^+}(s)+2i\pi H_{w_1^-}(r)\,H_{w_1^+,w_2^-}(s)+2H_{w_1^+,w_1^-}(r)\,H_{w_1^+,w_2^+}(s)\\
&-\pi^2 H_{w_2^-,w_1^-}(s)+2i\pi H_{w_1^-}(r)\,H_{w_2^-,w_1^+}(s)-4i\pi H_{0,w_1^-,w_1^+}(r)\\
&+8\,H_{w_1^-}(r)\,H_{0,w_1^+,0}\left(\tfrac{1}{1+2\sqrt{z_f}}\right)-8\,H_{w_1^-}(s)\,H_{0,w_1^+,0}\left(\tfrac{1}{1+2\sqrt{z_f}}\right)-4i\pi H_{0,w_1^+,w_1^-}(r)\\
&-4H_{w_1^-}(r)\,H_{0,w_1^+,w_1^-}(1-2\sqrt{z_f})+4H_{w_1^-}(s)\,H_{0,w_1^+,w_1^-}(1-2\sqrt{z_f})\\
&+4H_{w_1^-}(r)\,H_{0,w_1^+,w_1^-}\left(\tfrac{1}{1+2\sqrt{z_f}}\right)-4H_{w_1^-}(s)\,H_{0,w_1^+,w_1^-}\left(\tfrac{1}{1+2\sqrt{z_f}}\right)\\
&+H_{w_1^-}(r)\,H_{0,w_1^+,w_1^-}(1-2z_f)-H_{w_1^-}(s)\,H_{0,w_1^+,w_1^-}(1-2z_f)\\
&-4H_{w_1^-}(r)\,H_{0,w_1^+,w_1^+}(1-2\sqrt{z_f})+4H_{w_1^-}(s)\,H_{0,w_1^+,w_1^+}(1-2\sqrt{z_f})\\
&+4H_{w_1^-}(r)\,H_{0,w_1^+,w_1^+}\left(\tfrac{1}{1+2\sqrt{z_f}}\right)-4H_{w_1^-}(s)\,H_{0,w_1^+,w_1^+}\left(\tfrac{1}{1+2\sqrt{z_f}}\right)\\
&+H_{w_1^-}(r)\,H_{0,w_1^+,w_1^+}(1-2z_f)-H_{w_1^-}(s)\,H_{0,w_1^+,w_1^+}(1-2z_f)+4i\pi H_{w_1^-,w_1^-,w_5^+}(r)\\
&+4i\pi H_{w_1^-,w_1^-,w_4^+}(r)-i\pi H_{w_1^-,w_1^-,w_1^+}(s)-2i\pi H_{w_1^-,w_1^-,w_3^+}(r)-2i\pi H_{w_1^-,w_5^-,w_1^+}(r)\\
&+2i\pi H_{w_1^-,w_5^-,w_1^+}(s)+2i\pi H_{w_1^-,w_5^+,w_1^-}(s)+2H_{w_1^-}(r)\,H_{w_1^-,w_5^+,w_1^+}(s)-2i\pi H_{w_1^-,w_4^-,w_1^+}(r)\\
&+2i\pi H_{w_1^-,w_4^-,w_1^+}(s)+2i\pi H_{w_1^-,w_4^+,w_1^-}(s)+2H_{w_1^-}(r)\,H_{w_1^-,w_4^+,w_1^+}(s)-2i\pi H_{w_1^-,w_1^+,0}(s)\\
&-i\pi H_{w_1^-,w_1^+,w_1^-}(r)-i\pi H_{w_1^-,w_1^+,w_1^-}(s)+2i\pi H_{w_1^-,w_1^+,w_5^-}(r)+2i\pi H_{w_1^-,w_1^+,w_4^-}(r)\\
&-2H_{w_1^-}(r)\,H_{w_1^-,w_1^+,w_1^+}(s)-i\pi H_{w_1^-,w_1^+,w_3^-}(r)-2i\pi H_{w_1^-,w_1^+,w_2^-}(r)+\frac{1}{2}\,i\pi H_{w_1^-,w_3^-,w_1^+}(r)\\
&-\frac{1}{2}\,i\pi H_{w_1^-,w_3^-,w_1^+}(s)-\frac{1}{2}\,i\pi H_{w_1^-,w_3^+,w_1^-}(r)-\frac{1}{2}\,i\pi H_{w_1^-,w_3^+,w_1^-}(s)-H_{w_1^-}(r)\,H_{w_1^-,w_3^+,w_1^+}(s)\\
&-2i\pi H_{w_1^-,w_2^-,w_1^+}(r)-4i\pi H_{w_1^+,0,w_1^-}(r)-2i\pi H_{w_1^+,0,w_1^-}(s)-2H_{w_1^-}(r)\,H_{w_1^+,0,w_1^+}(s)\\
&-2i\pi H_{w_1^+,w_1^-,0}(s)-3\,i\pi H_{w_1^+,w_1^-,w_1^-}(s)+2i\pi H_{w_1^+,w_1^-,w_5^-}(r)+2i\pi H_{w_1^+,w_1^-,w_4^-}(r)\\
&-3\,H_{w_1^-}(r)\,H_{w_1^+,w_1^-,w_1^+}(s)-i\pi H_{w_1^+,w_1^-,w_3^-}(r)-2i\pi H_{w_1^+,w_1^-,w_2^-}(r)+2i\pi H_{w_1^+,w_5^-,w_1^-}(s)\\
&+2H_{w_1^-}(r)\,H_{w_1^+,w_5^-,w_1^+}(s)-2i\pi H_{w_1^+,w_5^+,w_1^+}(r)+2i\pi H_{w_1^+,w_5^+,w_1^+}(s)+2i\pi H_{w_1^+,w_4^-,w_1^-}(s)\\
&+2H_{w_1^-}(r)\,H_{w_1^+,w_4^-,w_1^+}(s)-2i\pi H_{w_1^+,w_4^+,w_1^+}(r)+2i\pi H_{w_1^+,w_4^+,w_1^+}(s)\\
&-2H_{w_1^-}(s)\,H_{w_1^+,w_1^+,w_1^-}(r)+2H_{w_2^-}(s)\,H_{w_1^+,w_1^+,w_1^-}(r)+i\pi H_{w_1^+,w_1^+,w_1^+}(r)\\
&-i\pi H_{w_1^+,w_1^+,w_1^+}(s)-\frac{1}{2}\,i\pi H_{w_1^+,w_3^-,w_1^-}(r)-\frac{1}{2}\,i\pi H_{w_1^+,w_3^-,w_1^-}(s)-H_{w_1^-}(r)\,H_{w_1^+,w_3^-,w_1^+}(s)\\
&+\frac{1}{2}\,i\pi H_{w_1^+,w_3^+,w_1^+}(r)-\frac{1}{2}\,i\pi H_{w_1^+,w_3^+,w_1^+}(s)-2i\pi H_{w_1^+,w_2^-,w_1^-}(s)-2H_{w_1^-}(r)\,H_{w_1^+,w_2^-,w_1^+}(s)\\
&-2i\pi H_{w_2^-,w_1^-,w_1^+}(s)-2i\pi H_{w_2^-,w_1^+,w_1^-}(s)-2H_{w_1^-}(r)\,H_{w_2^-,w_1^+,w_1^+}(s)-6\,H_{w_1^-,w_1^-,w_1^-,w_1^-}(r)\\
&+3\,H_{w_1^-,w_1^-,w_1^-,w_5^-}(r)+3\,H_{w_1^-,w_1^-,w_1^-,w_4^-}(r)-3\,H_{w_1^-,w_1^-,w_1^-,w_3^-}(r)+2H_{w_1^-,w_1^-,w_5^-,w_1^-}(r)\\
&-4H_{w_1^-,w_1^-,w_5^+,w_1^+}(r)+2H_{w_1^-,w_1^-,w_4^-,w_1^-}(r)-4H_{w_1^-,w_1^-,w_4^+,w_1^+}(r)+H_{w_1^-,w_1^-,w_1^+,w_5^+}(r)\\
&+H_{w_1^-,w_1^-,w_1^+,w_4^+}(r)+H_{w_1^-,w_1^-,w_1^+,w_1^+}(r)+H_{w_1^-,w_1^-,w_1^+,w_1^+}(s)-H_{w_1^-,w_1^-,w_1^+,w_3^+}(r)\\
&-2H_{w_1^-,w_1^-,w_3^-,w_1^-}(r)+2H_{w_1^-,w_1^-,w_3^+,w_1^+}(r)+H_{w_1^-,w_5^-,w_1^-,w_1^-}(r)+2H_{w_1^-,w_5^-,w_1^+,w_1^+}(r)\\
&-2H_{w_1^-,w_5^-,w_1^+,w_1^+}(s)-2H_{w_1^-,w_5^+,w_1^-,w_1^+}(s)-2H_{w_1^-,w_5^+,w_1^+,w_1^-}(r)+H_{w_1^-,w_4^-,w_1^-,w_1^-}(r)\\
&+2H_{w_1^-,w_4^-,w_1^+,w_1^+}(r)-2H_{w_1^-,w_4^-,w_1^+,w_1^+}(s)-2H_{w_1^-,w_4^+,w_1^-,w_1^+}(s)-2H_{w_1^-,w_4^+,w_1^+,w_1^-}(r)\\
&+2H_{w_1^-,w_1^+,0,w_1^+}(s)+H_{w_1^-,w_1^+,w_1^-,w_5^+}(r)+H_{w_1^-,w_1^+,w_1^-,w_4^+}(r)+2H_{w_1^-,w_1^+,w_1^-,w_1^+}(r)\\
&+H_{w_1^-,w_1^+,w_1^-,w_1^+}(s)-H_{w_1^-,w_1^+,w_1^-,w_3^+}(r)-2H_{w_1^-,w_1^+,w_5^-,w_1^+}(r)+H_{w_1^-,w_1^+,w_5^+,w_1^-}(r)
\end{aligned}
$$

JHEP12(2014)129

$$
\begin{aligned}
&-2H_{w_1^-,w_1^+,w_4^-,w_1^+}(r)+H_{w_1^-,w_1^+,w_4^+,w_1^-}(r)+2H_{w_1^-,w_1^+,w_1^+,w_1^-}(r)+H_{w_1^-,w_1^+,w_3^-,w_1^+}(r)\\
&-H_{w_1^-,w_1^+,w_3^+,w_1^-}(r)+2H_{w_1^-,w_1^+,w_2^-,w_1^+}(r)-H_{w_1^-,w_3^-,w_1^-,w_1^-}(r)-\frac{1}{2}H_{w_1^-,w_3^-,w_1^+,w_1^+}(r)\\
&+\frac{1}{2}H_{w_1^-,w_3^-,w_1^+,w_1^+}(s)+\frac{1}{2}H_{w_1^-,w_3^+,w_1^-,w_1^+}(r)+\frac{1}{2}H_{w_1^-,w_3^+,w_1^-,w_1^+}(s)+H_{w_1^-,w_3^+,w_1^+,w_1^-}(r)\\
&+2H_{w_1^-,w_2^-,w_1^+,w_1^+}(r)+2H_{w_1^+,0,w_1^-,w_1^+}(s)+2H_{w_1^+,0,w_1^+,w_1^-}(r)+2H_{w_1^+,w_1^-,0,w_1^+}(s)\\
&+H_{w_1^+,w_1^-,w_1^-,w_5^+}(r)+H_{w_1^+,w_1^-,w_1^-,w_4^+}(r)+H_{w_1^+,w_1^-,w_1^-,w_1^+}(r)+3H_{w_1^+,w_1^-,w_1^-,w_1^+}(s)\\
&-H_{w_1^+,w_1^-,w_1^-,w_3^+}(r)-2H_{w_1^+,w_1^-,w_5^-,w_1^+}(r)+H_{w_1^+,w_1^-,w_5^+,w_1^-}(r)-2H_{w_1^+,w_1^-,w_4^-,w_1^+}(r)\\
&+H_{w_1^+,w_1^-,w_4^+,w_1^-}(r)+3H_{w_1^+,w_1^-,w_1^+,w_1^-}(r)-2H_{w_1^+,w_1^-,w_1^+,w_2^+}(r)+H_{w_1^+,w_1^-,w_3^-,w_1^+}(r)\\
&-H_{w_1^+,w_1^-,w_3^+,w_1^-}(r)+2H_{w_1^+,w_1^-,w_2^-,w_1^+}(r)-2H_{w_1^+,w_5^-,w_1^-,w_1^+}(s)-2H_{w_1^+,w_5^-,w_1^+,w_1^-}(r)\\
&+H_{w_1^+,w_5^+,w_1^-,w_1^-}(r)+2H_{w_1^+,w_5^+,w_1^+,w_1^+}(r)-2H_{w_1^+,w_5^+,w_1^+,w_1^+}(s)-2H_{w_1^+,w_4^-,w_1^-,w_1^+}(s)\\
&-2H_{w_1^+,w_4^-,w_1^+,w_1^-}(r)+H_{w_1^+,w_4^+,w_1^-,w_1^-}(r)+2H_{w_1^+,w_4^+,w_1^+,w_1^+}(r)-2H_{w_1^+,w_4^+,w_1^+,w_1^+}(s)\\
&+2H_{w_1^+,w_1^+,w_1^-,w_1^-}(r)-2H_{w_1^+,w_1^+,w_1^-,w_2^-}(r)-4H_{w_1^+,w_1^+,w_1^-,w_2^+}(r)-H_{w_1^+,w_1^+,w_1^+,w_1^+}(r)\\
&+H_{w_1^+,w_1^+,w_1^+,w_1^+}(s)-2H_{w_1^+,w_1^+,w_2^-,w_1^-}(r)-4H_{w_1^+,w_1^+,w_2^+,w_1^-}(r)+\frac{1}{2}H_{w_1^+,w_3^-,w_1^-,w_1^+}(r)\\
&+\frac{1}{2}H_{w_1^+,w_3^-,w_1^-,w_1^+}(s)+H_{w_1^+,w_3^-,w_1^+,w_1^-}(r)-H_{w_1^+,w_3^+,w_1^-,w_1^-}(r)-\frac{1}{2}H_{w_1^+,w_3^+,w_1^+,w_1^+}(r)\\
&+\frac{1}{2}H_{w_1^+,w_3^+,w_1^+,w_1^+}(s)+2H_{w_1^+,w_2^-,w_1^-,w_1^+}(s)-2H_{w_1^+,w_2^+,w_1^+,w_1^-}(r)+2H_{w_2^-,w_1^-,w_1^+,w_1^+}(s)\\
&+2H_{w_2^-,w_1^+,w_1^-,w_1^+}(s)-\frac{3}{2}\pi^2H_{w_1^-}(r)\ln(2)+\frac{3}{2}\pi^2H_{w_1^-}(s)\ln(2)\\
&+2i\pi H_{-1}(r^2)H_{w_1^+}(r)\ln(2)-2i\pi H_{-1}(r^2)H_{w_1^+}(s)\ln(2)-2i\pi H_{w_1^-}(r)H_{w_1^+}(s)\ln(2)\\
&-8H_{w_1^-}(r)H_{0,w_1^+}(1-2\sqrt{z_f})\ln(2)+8H_{w_1^-}(s)H_{0,w_1^+}(1-2\sqrt{z_f})\ln(2)\\
&+8H_{w_1^-}(r)H_{0,w_1^+}\left(\tfrac{1}{1+2\sqrt{z_f}}\right)\ln(2)-8H_{w_1^-}(s)H_{0,w_1^+}\left(\tfrac{1}{1+2\sqrt{z_f}}\right)\ln(2)\\
&+2H_{w_1^-}(r)H_{0,w_1^+}(1-2z_f)\ln(2)-2H_{w_1^-}(s)H_{0,w_1^+}(1-2z_f)\ln(2)\\
&+2H_{w_1^-}(r)H_{w_1^-,w_1^-}(s)\ln(2)-2H_{w_1^-}(r)H_{w_1^-,w_5^-}(s)\ln(2)-2H_{w_1^-}(r)H_{w_1^-,w_4^-}(s)\ln(2)\\
&+2i\pi H_{w_1^-,w_1^+}(s)\ln(2)+2H_{w_1^-}(r)H_{w_1^-,w_3^-}(s)\ln(2)-i\pi H_{w_1^-,w_3^+}(r)\ln(2)\\
&+i\pi H_{w_1^-,w_3^+}(s)\ln(2)+2i\pi H_{w_1^+,w_1^-}(r)\ln(2)-2H_{w_1^-}(r)H_{w_1^+,w_5^+}(s)\ln(2)\\
&-2H_{w_1^-}(r)H_{w_1^+,w_4^+}(s)\ln(2)-4H_{w_1^-}(s)H_{w_1^+,w_1^+}(r)\ln(2)+4H_{w_2^-}(s)H_{w_1^+,w_1^+}(r)\ln(2)\\
&+4H_{w_1^-}(r)H_{w_1^+,w_1^+}(s)\ln(2)-i\pi H_{w_1^+,w_3^-}(r)\ln(2)+i\pi H_{w_1^+,w_3^-}(s)\ln(2)\\
&+2H_{w_1^-}(r)H_{w_1^+,w_3^+}(s)\ln(2)+4H_{w_1^+}(r)H_{w_1^+,w_2^+}(s)\ln(2)-6H_{w_1^-,w_1^-,w_1^-}(r)\ln(2)\\
&+4H_{w_1^-,w_1^-,w_5^-}(r)\ln(2)+4H_{w_1^-,w_1^-,w_4^-}(r)\ln(2)-4H_{w_1^-,w_1^-,w_3^-}(r)\ln(2)\\
&+2H_{w_1^-,w_5^-,w_1^-}(r)\ln(2)-4H_{w_1^-,w_5^+,w_1^+}(r)\ln(2)+4H_{w_1^-,w_5^+,w_1^+}(s)\ln(2)\\
&+2H_{w_1^-,w_4^-,w_1^-}(r)\ln(2)-4H_{w_1^-,w_4^+,w_1^+}(r)\ln(2)+4H_{w_1^-,w_4^+,w_1^+}(s)\ln(2)\\
&+2H_{w_1^-,w_1^+,w_5^+}(r)\ln(2)+2H_{w_1^-,w_1^+,w_4^+}(r)\ln(2)+4H_{w_1^-,w_1^+,w_1^+}(r)\ln(2)\\
&-4H_{w_1^-,w_1^+,w_1^+}(s)\ln(2)-2H_{w_1^-,w_1^+,w_3^+}(r)\ln(2)-2H_{w_1^-,w_3^-,w_1^-}(r)\ln(2)\\
&+2H_{w_1^-,w_3^+,w_1^+}(r)\ln(2)-2H_{w_1^-,w_3^+,w_1^+}(s)\ln(2)+4H_{w_1^+,0,w_1^+}(r)\ln(2)\\
&-4H_{w_1^+,0,w_1^+}(s)\ln(2)+2H_{w_1^+,w_1^-,w_5^+}(r)\ln(2)+2H_{w_1^+,w_1^-,w_4^+}(r)\ln(2)
\end{aligned}
$$

JHEP12(2014)129

$$
\begin{aligned}
&+6\,H_{w_1^+,w_1^-,w_1^+}(r)\,\ln(2) - 6\,H_{w_1^+,w_1^-,w_1^+}(s)\,\ln(2) - 2H_{w_1^+,w_1^-,w_3^+}(r)\,\ln(2)\\
&-4H_{w_1^+,w_5^-,w_1^+}(r)\,\ln(2) + 4H_{w_1^+,w_5^-,w_1^+}(s)\,\ln(2) + 2H_{w_1^+,w_5^+,w_1^-}(r)\,\ln(2)\\
&-4H_{w_1^+,w_4^-,w_1^+}(r)\,\ln(2) + 4H_{w_1^+,w_4^-,w_1^+}(s)\,\ln(2) + 2H_{w_1^+,w_4^+,w_1^-}(r)\,\ln(2)\\
&-4H_{w_1^+,w_1^+,w_2^-}(r)\,\ln(2) - 8\,H_{w_1^+,w_1^+,w_2^+}(r)\,\ln(2) + 2H_{w_1^+,w_3^-,w_1^+}(r)\,\ln(2)\\
&-2H_{w_1^+,w_3^-,w_1^+}(s)\,\ln(2) - 2H_{w_1^+,w_3^+,w_1^-}(r)\,\ln(2) - 4H_{w_1^+,w_2^-,w_1^+}(s)\,\ln(2)\\
&-4H_{w_1^+,w_2^+,w_1^+}(r)\,\ln(2) - 4H_{w_2^-,w_1^+,w_1^+}(s)\,\ln(2) - 2H_{w_1^-,w_1^-}(r)\,\ln^2(2)\\
&+2H_{w_1^-,w_1^-}(s)\,\ln^2(2) + 2H_{w_1^-,w_5^-}(r)\,\ln^2(2) - 2H_{w_1^-,w_5^-}(s)\,\ln^2(2) + 2H_{w_1^-,w_4^-}(r)\,\ln^2(2)\\
&-2H_{w_1^-,w_4^-}(s)\,\ln^2(2) - 2H_{w_1^-,w_3^-}(r)\,\ln^2(2) + 2H_{w_1^-,w_3^-}(s)\,\ln^2(2) + 2H_{w_1^+,w_5^+}(r)\,\ln^2(2)\\
&-2H_{w_1^+,w_5^+}(s)\,\ln^2(2) + 2H_{w_1^+,w_4^+}(r)\,\ln^2(2) - 2H_{w_1^+,w_4^+}(s)\,\ln^2(2) - 4H_{w_1^+,w_1^+}(r)\,\ln^2(2)\\
&+4H_{w_1^+,w_1^+}(s)\,\ln^2(2) - 2H_{w_1^+,w_3^+}(r)\,\ln^2(2) + 2H_{w_1^+,w_3^+}(s)\,\ln^2(2) - H_{w_1^-,w_1^-}(r)\,\mathrm{Li}_2(1-z_f)\\
&+H_{w_1^-,w_1^-}(s)\,\mathrm{Li}_2(1-z_f) + H_{w_1^-,w_5^-}(r)\,\mathrm{Li}_2(1-z_f) - H_{w_1^-,w_5^-}(s)\,\mathrm{Li}_2(1-z_f)\\
&+H_{w_1^-,w_4^-}(r)\,\mathrm{Li}_2(1-z_f) - H_{w_1^-,w_4^-}(s)\,\mathrm{Li}_2(1-z_f) - H_{w_1^-,w_3^-}(r)\,\mathrm{Li}_2(1-z_f)\\
&+H_{w_1^-,w_3^-}(s)\,\mathrm{Li}_2(1-z_f) + H_{w_1^+,w_5^+}(r)\,\mathrm{Li}_2(1-z_f) - H_{w_1^+,w_5^+}(s)\,\mathrm{Li}_2(1-z_f)\\
&+H_{w_1^+,w_4^+}(r)\,\mathrm{Li}_2(1-z_f) - H_{w_1^+,w_4^+}(s)\,\mathrm{Li}_2(1-z_f) + H_{w_1^+,w_1^+}(r)\,\mathrm{Li}_2(1-z_f)\\
&-H_{w_1^+,w_1^+}(s)\,\mathrm{Li}_2(1-z_f) - H_{w_1^+,w_3^+}(r)\,\mathrm{Li}_2(1-z_f) + H_{w_1^+,w_3^+}(s)\,\mathrm{Li}_2(1-z_f)\\
&+7\,H_{w_1^-}(r)\,\zeta_3 - 7\,H_{w_1^-}(s)\,\zeta_3\,. \qquad \text{(C.1)}
\end{aligned}
$$

Open Access. This article is distributed under the terms of the Creative Commons Attribution License (CC-BY 4.0), which permits any use, distribution and reproduction in any medium, provided the original author(s) and source are credited.

References

[1] M. Beneke, G. Buchalla, M. Neubert and C.T. Sachrajda, *QCD factorization for $B \to \pi\pi$ decays: Strong phases and CP-violation in the heavy quark limit*, *Phys. Rev. Lett.* **83** (1999) 1914 [hep-ph/9905312] [INSPIRE].

[2] M. Beneke, G. Buchalla, M. Neubert and C.T. Sachrajda, *QCD factorization for exclusive, nonleptonic B meson decays: General arguments and the case of heavy light final states*, *Nucl. Phys.* **B 591** (2000) 313 [hep-ph/0006124] [INSPIRE].

[3] M. Beneke, G. Buchalla, M. Neubert and C.T. Sachrajda, *QCD factorization in $B \to \pi K$, $\pi\pi$ decays and extraction of Wolfenstein parameters*, *Nucl. Phys.* **B 606** (2001) 245 [hep-ph/0104110] [INSPIRE].

[4] M. Beneke and S. Jager, *Spectator scattering at NLO in non-leptonic b decays: Tree amplitudes*, *Nucl. Phys.* **B 751** (2006) 160 [hep-ph/0512351] [INSPIRE].

[5] N. Kivel, *Radiative corrections to hard spectator scattering in $B \to \pi\pi$ decays*, *JHEP* **05** (2007) 019 [hep-ph/0608291] [INSPIRE].

[6] M. Beneke and S. Jager, *Spectator scattering at NLO in non-leptonic B decays: Leading penguin amplitudes*, *Nucl. Phys.* **B 768** (2007) 51 [hep-ph/0610322] [INSPIRE].

JHEP12(2014)129

[7] A. Jain, I.Z. Rothstein and I.W. Stewart, *Penguin Loops for Nonleptonic B-Decays in the Standard Model: Is there a Penguin Puzzle?*, arXiv:0706.3399 [INSPIRE].

[8] V. Pilipp, *Hard spectator interactions in $B \to \pi\pi$ at order α_s^2*, *Nucl. Phys.* **B 794** (2008) 154 [arXiv:0709.3214] [INSPIRE].

[9] G. Bell, *NNLO vertex corrections in charmless hadronic B decays: Imaginary part*, *Nucl. Phys.* **B 795** (2008) 1 [arXiv:0705.3127] [INSPIRE].

[10] G. Bell, *NNLO vertex corrections in charmless hadronic B decays: Real part*, *Nucl. Phys.* **B 822** (2009) 172 [arXiv:0902.1915] [INSPIRE].

[11] M. Beneke, T. Huber and X.-Q. Li, *NNLO vertex corrections to non-leptonic B decays: Tree amplitudes*, *Nucl. Phys.* **B 832** (2010) 109 [arXiv:0911.3655] [INSPIRE].

[12] G. Bell, M. Beneke, T. Huber and X.-Q. Li, in preparation.

[13] C.S. Kim and Y.W. Yoon, *Order α_s^2 magnetic penguin correction for B decay to light mesons*, *JHEP* **11** (2011) 003 [arXiv:1107.1601] [INSPIRE].

[14] G. Bell, *Higher order QCD corrections in exclusive charmless B decays*, arXiv:0705.3133 [INSPIRE].

[15] T. Huber, *On a two-loop crossed six-line master integral with two massive lines*, *JHEP* **03** (2009) 024 [arXiv:0901.2133] [INSPIRE].

[16] E. Remiddi and J.A.M. Vermaseren, *Harmonic polylogarithms*, *Int. J. Mod. Phys.* **A 15** (2000) 725 [hep-ph/9905237] [INSPIRE].

[17] A.V. Kotikov, *Differential equations method: New technique for massive Feynman diagrams calculation*, *Phys. Lett.* **B 254** (1991) 158 [INSPIRE].

[18] A.V. Kotikov, *Differential equation method: The Calculation of N point Feynman diagrams*, *Phys. Lett.* **B 267** (1991) 123 [INSPIRE].

[19] E. Remiddi, *Differential equations for Feynman graph amplitudes*, *Nuovo Cim.* **A 110** (1997) 1435 [hep-th/9711188] [INSPIRE].

[20] F.V. Tkachov, *A Theorem on Analytical Calculability of Four Loop Renormalization Group Functions*, *Phys. Lett.* **B 100** (1981) 65 [INSPIRE].

[21] K.G. Chetyrkin and F.V. Tkachov, *Integration by Parts: The Algorithm to Calculate β-functions in 4 Loops*, *Nucl. Phys.* **B 192** (1981) 159 [INSPIRE].

[22] S. Laporta, *High precision calculation of multiloop Feynman integrals by difference equations*, *Int. J. Mod. Phys.* **A 15** (2000) 5087 [hep-ph/0102033] [INSPIRE].

[23] J.M. Henn, *Multiloop integrals in dimensional regularization made simple*, *Phys. Rev. Lett.* **110** (2013) 251601 [arXiv:1304.1806] [INSPIRE].

[24] J.M. Henn, A.V. Smirnov and V.A. Smirnov, *Analytic results for planar three-loop four-point integrals from a Knizhnik-Zamolodchikov equation*, *JHEP* **07** (2013) 128 [arXiv:1306.2799] [INSPIRE].

[25] J.M. Henn and V.A. Smirnov, *Analytic results for two-loop master integrals for Bhabha scattering I*, *JHEP* **11** (2013) 041 [arXiv:1307.4083] [INSPIRE].

[26] J.M. Henn, A.V. Smirnov and V.A. Smirnov, *Evaluating single-scale and/or non-planar diagrams by differential equations*, *JHEP* **03** (2014) 088 [arXiv:1312.2588] [INSPIRE].

JHEP12(2014)129

[27] M. Argeri et al., *Magnus and Dyson Series for Master Integrals*, *JHEP* **03** (2014) 082 [arXiv:1401.2979] [INSPIRE].

[28] J.M. Henn, K. Melnikov and V.A. Smirnov, *Two-loop planar master integrals for the production of off-shell vector bosons in hadron collisions*, *JHEP* **05** (2014) 090 [arXiv:1402.7078] [INSPIRE].

[29] T. Gehrmann, A. von Manteuffel, L. Tancredi and E. Weihs, *The two-loop master integrals for $q\bar{q} \to VV$*, *JHEP* **06** (2014) 032 [arXiv:1404.4853] [INSPIRE].

[30] F. Caola, J.M. Henn, K. Melnikov and V.A. Smirnov, *Non-planar master integrals for the production of two off-shell vector bosons in collisions of massless partons*, *JHEP* **09** (2014) 043 [arXiv:1404.5590] [INSPIRE].

[31] M. Höschele, J. Hoff and T. Ueda, *Adequate bases of phase space master integrals for $gg \to h$ at NNLO and beyond*, *JHEP* **09** (2014) 116 [arXiv:1407.4049] [INSPIRE].

[32] S. Di Vita, P. Mastrolia, U. Schubert and V. Yundin, *Three-loop master integrals for ladder-box diagrams with one massive leg*, *JHEP* **09** (2014) 148 [arXiv:1408.3107] [INSPIRE].

[33] A. von Manteuffel, R.M. Schabinger and H.X. Zhu, *The two-loop soft function for heavy quark pair production at future linear colliders*, arXiv:1408.5134 [INSPIRE].

[34] D. Maître, *Extension of HPL to complex arguments*, *Comput. Phys. Commun.* **183** (2012) 846 [hep-ph/0703052] [INSPIRE].

[35] A.B. Goncharov, *Multiple polylogarithms, cyclotomy and modular complexes*, *Math. Res. Lett.* **5** (1998) 497 [arXiv:1105.2076] [INSPIRE].

[36] T. Huber and D. Maître, *HypExp: A Mathematica package for expanding hypergeometric functions around integer-valued parameters*, *Comput. Phys. Commun.* **175** (2006) 122 [hep-ph/0507094] [INSPIRE].

[37] T. Huber and D. Maître, *HypExp 2, Expanding Hypergeometric Functions about Half-Integer Parameters*, *Comput. Phys. Commun.* **178** (2008) 755 [arXiv:0708.2443] [INSPIRE].

[38] G. Bell, *NNLO corrections to inclusive semileptonic B decays in the shape-function region*, *Nucl. Phys.* **B 812** (2009) 264 [arXiv:0810.5695] [INSPIRE].

[39] C.W. Bauer, A. Frink and R. Kreckel, *Introduction to the GiNaC framework for symbolic computation within the C++ programming language*, *J. Symb. Comput.* **33** (2002) 1.

[40] J. Vollinga and S. Weinzierl, *Numerical evaluation of multiple polylogarithms*, *Comput. Phys. Commun.* **167** (2005) 177 [hep-ph/0410259] [INSPIRE].

[41] J. Gluza, K. Kajda and T. Riemann, *AMBRE: A Mathematica package for the construction of Mellin-Barnes representations for Feynman integrals*, *Comput. Phys. Commun.* **177** (2007) 879 [arXiv:0704.2423] [INSPIRE].

[42] M. Czakon, *Automatized analytic continuation of Mellin-Barnes integrals*, *Comput. Phys. Commun.* **175** (2006) 559 [hep-ph/0511200] [INSPIRE].

[43] J. Carter and G. Heinrich, *SecDec: A general program for sector decomposition*, *Comput. Phys. Commun.* **182** (2011) 1566 [arXiv:1011.5493] [INSPIRE].

[44] S. Borowka, J. Carter and G. Heinrich, *Numerical Evaluation of Multi-Loop Integrals for Arbitrary Kinematics with SecDec 2.0*, *Comput. Phys. Commun.* **184** (2013) 396 [arXiv:1204.4152] [INSPIRE].

JHEP12(2014)129

[45] A. Ghinculov, T. Hurth, G. Isidori and Y.P. Yao, *The Rare decay $B \to X_s\ \ell^+\ell^-$ to NNLL precision for arbitrary dilepton invariant mass*, *Nucl. Phys.* **B 685** (2004) 351 [hep-ph/0312128] [INSPIRE].

[46] H.H. Asatryan, H.M. Asatrian, C. Greub and M. Walker, *Calculation of two loop virtual corrections to $b \to s\ \ell^+\ell^-$ in the standard model*, *Phys. Rev.* **D 65** (2002) 074004 [hep-ph/0109140] [INSPIRE].

[47] C. Greub, V. Pilipp and C. Schupbach, *Analytic calculation of two-loop QCD corrections to $b \to s\ \ell^+\ell^-$ in the high Q^2 region*, *JHEP* **12** (2008) 040 [arXiv:0810.4077] [INSPIRE].

JHEP12(2014)129

Physics Letters B 750 (2015) 348–355

Contents lists available at ScienceDirect

Physics Letters B

www.elsevier.com/locate/physletb

Two-loop current–current operator contribution to the non-leptonic QCD penguin amplitude

G. Bell [a], M. Beneke [b], T. Huber [c], Xin-Qiang Li [d,e,*]

[a] Rudolf Peierls Centre for Theoretical Physics, University of Oxford, 1 Keble Road, Oxford OX1 3NP, United Kingdom
[b] Physik Department T31, Technische Universität München, James-Franck-Straße 1, D-85748 Garching, Germany
[c] Theoretische Physik 1, Naturwissenschaftlich-Technische Fakultät, Universität Siegen, Walter-Flex-Strasse 3, D-57068 Siegen, Germany
[d] Institute of Particle Physics and Key Laboratory of Quark and Lepton Physics (MOE), Central China Normal University, Wuhan, Hubei 430079, PR China
[e] State Key Laboratory of Theoretical Physics, Institute of Theoretical Physics, Chinese Academy of Sciences, Beijing 100190, PR China

ARTICLE INFO

Article history:
Received 17 July 2015
Accepted 15 September 2015
Available online 24 September 2015
Editor: B. Grinstein

ABSTRACT

The computation of direct CP asymmetries in charmless B decays at next-to-next-to-leading order (NNLO) in QCD is of interest to ascertain the short-distance contribution. Here we compute the two-loop penguin contractions of the current–current operators $Q_{1,2}$ and provide a first estimate of NNLO CP asymmetries in penguin-dominated $b \to s$ transitions.

© 2015 The Authors. Published by Elsevier B.V. This is an open access article under the CC BY license (http://creativecommons.org/licenses/by/4.0/). Funded by SCOAP³.

1. Introduction

Non-leptonic exclusive decays of B mesons play a crucial role in studying the CKM mechanism of quark flavour mixing and in quantifying the phenomenon of CP violation. Direct CP violation is related to the rate difference of $\bar{B} \to f$ decay and its CP-conjugate and arises if the decay amplitude is composed of at least two partial amplitudes with different re-scattering ("strong") phases, which are multiplied by different CKM matrix elements. Very often useful information on the CKM parameters including the CP-violating phase can be obtained from combining different decay modes, whose partial amplitudes are related by the approximate flavour symmetries of the strong interaction [1], which are then determined from data.

The direct computation of the partial amplitudes is a complicated strong interaction problem, which can, however, be addressed in the heavy-quark limit. The QCD factorization approach [2–4] employs soft-collinear factorization in this limit to express the hadronic matrix elements in terms of form factors and convolutions of perturbative objects (hard-scattering kernels) with non-perturbative light-cone distribution amplitudes (LCDAs). At leading order in Λ/m_b,

$$\begin{aligned}\langle M_1 M_2 | Q_i | \bar{B}\rangle = i m_B^2 \Bigg\{ & f_+^{BM_1}(0) \int_0^1 du\, T_i^I(u)\, f_{M_2}\phi_{M_2}(u) \\ & + (M_1 \leftrightarrow M_2) \\ & + \int_0^\infty d\omega \int_0^1 du dv\, T_i^{II}(\omega, v, u)\, \hat{f}_B \phi_B(\omega) \\ & \times f_{M_1}\phi_{M_1}(v)\, f_{M_2}\phi_{M_2}(u) \Bigg\}, \end{aligned} \tag{1}$$

where Q_i is a generic operator from the effective weak Hamiltonian. At this order the re-scattering phases are generated at the scale m_b only, and reside in the loop corrections to the hard-scattering kernels. Beyond the leading order factorization does not hold, and re-scattering occurs at all scales. The leading contributions to the strong phases are therefore of order $\alpha_s(m_b)$ or/and Λ/m_b. It is of paramount importance for the predictivity of the approach for the direct CP asymmetries to know whether the short-distance or long-distance contribution dominates in practice, since apart from being parametrically small, both could be numerically of similar size.

The short-distance contribution to the direct CP asymmetries is fully known only to the first non-vanishing order (that is, $\mathcal{O}(\alpha_s)$) through the one-loop computations of the vertex kernels T_i^I performed long ago [2,4,5]. A reliable result presumably requires the next-to-next-to-leading order $\mathcal{O}(\alpha_s^2)$ hard-scattering kernels, at least their imaginary parts. For the spectator-scattering kernels T_i^{II}

* Corresponding author at: Institute of Particle Physics and Key Laboratory of Quark and Lepton Physics (MOE), Central China Normal University, Wuhan, Hubei 430079, PR China.
E-mail address: xqli@itp.ac.cn (X.-Q. Li).

http://dx.doi.org/10.1016/j.physletb.2015.09.037
0370-2693/© 2015 The Authors. Published by Elsevier B.V. This is an open access article under the CC BY license (http://creativecommons.org/licenses/by/4.0/). Funded by SCOAP³.

this task is already completed, both for the tree [6–8] and penguin [9,10] amplitudes, but for the so-called form factor term(s) in the first two lines of (1) an important piece is still missing, which is the focus of this Letter.

We recall that due to CKM unitarity, the amplitude for a $\bar{B}$ decay governed by the $b \to D$ $(D = d, s)$ transition can always be written in the form

$$A(\bar{B} \to f) = \lambda_u^{(D)} [T + \ldots] + \lambda_c^{(D)} [P_c + \ldots], \tag{2}$$

where $\lambda_p^{(D)} = V_{pD}^* V_{pb}$. It is generic that the first CKM structure is dominated by the colour-allowed or colour-suppressed topological tree amplitude, both denoted by T here, corresponding to the flavour quantum numbers of a $b \to u\bar{u}D$ transition, while the second is dominated by the topological QCD penguin amplitude of the $b \to \sum_{q=u,d,s} q\bar{q}D$ transition. The first is typically larger than the second for $D = d$ and vice-versa for the $D = s$ case, which therefore refers to the penguin-dominated decays such as $\bar{B} \to \pi K$ and related. In the notation of [5,9], P_c corresponds to the quantity $\alpha_4^c(M_1 M_2)$.[1]

The vertex kernels T_i^I have been computed at the two-loop $\mathcal{O}(\alpha_s^2)$ order only for the topological tree amplitudes T [11–13]. However, direct CP asymmetries can only be non-zero due to the interference of the two terms in (2), hence the penguin amplitude P_c is also needed. Only the one-loop $\mathcal{O}(\alpha_s^2)$ contribution from the chromomagnetic dipole operator Q_{8g} to P_c has been considered in the past [14], while the dominant, genuine two-loop contributions remain to be computed. This calculation is technically very involved since it requires the computation of massive two-loop penguin diagrams – a genuine two-loop, two-scale problem. One step towards this goal was recently achieved in [15], where analytic results of all occurring master integrals were derived.

At this point it is important to note that the topological tree and penguin amplitudes are not in one-to-one correspondence with the tree (or current–current) operators $Q_{1,2}^p$ and QCD penguin operators Q_{3-6} of the weak effective Hamiltonian. By contracting the $p\bar{p}$ fields of the operators $Q_{1,2}^p$ (see (5) below), they contribute to the QCD penguin amplitude starting from the one-loop order. Since these "penguin contractions" of the current–current operators come with the large short-distance coefficients $C_{1,2}$, we may argue that they constitute the largest contribution to the penguin amplitude at any given loop order.[2] At *next-to-leading order* we find for the penguin contractions (including the chromomagnetic dipole operator Q_{8g})

$$\begin{aligned} a_4^u(\pi\bar{K})_{|\mathrm{NLO}} &= (-0.0087 - 0.0172i)_{|Q_{1,2}} \\ &\quad + (0.0042 + 0.0041i)_{|Q_{3-6}} + 0.0083_{|Q_{8g}}, \\ a_4^c(\pi\bar{K})_{|\mathrm{NLO}} &= (-0.0131 - 0.0102i)_{|Q_{1,2}} \\ &\quad + (0.0042 + 0.0041i)_{|Q_{3-6}} + 0.0083_{|Q_{8g}}, \end{aligned} \tag{3}$$

where we separated the contributions from the current–current and the other operators. While there is a cancellation for the real part, the imaginary part from $Q_{1,2}^p$ is clearly dominant. If we add the vertex contractions at leading (LO) and next-to-leading order (NLO) and consider the entire form factor contribution to $a_4^p(M_1 M_2)$ at NLO, the second term changes to $(-0.0266 + 0.0032i)_{|Q_{3-6}}$ in both expressions, and the imaginary part from $Q_{1,2}^p$ is still by far dominant. Thus, at NLO, the short-distance direct CP asymmetries are mainly determined by the one-loop penguin contractions of the current–current operators. It is reasonable to assume that the insertion of $Q_{1,2}^{u,c}$ at two loops also captures the bulk of the yet unknown NNLO form factor contribution T_i^I to the penguin amplitudes $a_4^{u,c}$. In this Letter we report the result of this computation together with a few phenomenological implications. We shall provide more technical details together with the remaining contributions from the QCD penguin operators Q_{3-6}, which require additional work on infrared subtractions not present for $Q_{1,2}^p$, in a future publication.

2. Outline of the calculation

The effective weak Hamiltonian for $b \to D$ transitions $(D = d, s)$ is given by

$$\mathcal{H}_{\mathrm{eff}} = \frac{4G_F}{\sqrt{2}} \sum_{p=u,c} V_{pD}^* V_{pb} \left(C_1 Q_1^p + C_2 Q_2^p + \ldots \right) + \mathrm{h.c.}. \tag{4}$$

Here and in the following we give explicitly only the definitions pertinent to the current–current operators relevant to our calculation. We adopt the Chetyrkin–Misiak–Münz (CMM) operator basis [16], where the current–current operators are defined as

$$\begin{aligned} Q_1^p &= (\bar{p}_L \gamma^\mu T^A b_L)(\bar{D}_L \gamma_\mu T^A p_L), \\ Q_2^p &= (\bar{p}_L \gamma^\mu b_L)(\bar{D}_L \gamma_\mu p_L), \end{aligned} \tag{5}$$

in terms of left-chiral quark fields $q_L = \frac{1}{2}(1 - \gamma_5)q$. In dimensional regularization the operator basis has to be supplemented by evanescent (vanishing in $D = 4$ dimensions) operators, for which we adopt the convention of [17].

At the two-loop level about 70 diagrams contribute to the QCD penguin amplitude, but only a subset of two dozens (shown in Fig. 1) are non-vanishing for the insertion of the current–current operators $Q_{1,2}^p$. The quark in the fermion loop can either be massless (for $p = u$) or massive (for $p = c$). In the massless case the problem involves one non-trivial scale, the momentum fraction $\bar{u} = 1 - u$ of the anti-quark in meson M_2, and the structure is similar to the NNLO calculation of the tree amplitudes [11–13]. In the massive case, however, we are dealing with a genuine two-loop, two-scale problem since the hard-scattering kernels depend in addition on the mass ratio $s_c = m_c^2/m_b^2$. As we have already elaborated extensively on the kinematics in [15], we shall not repeat those formulae here.

The calculation is performed in dimensional regularization with $D = 4 - 2\epsilon$, where ultraviolet (UV) and infrared (soft and collinear) divergences manifest themselves as poles in ϵ. The CMM basis ensures that the NDR scheme with a fully anti-commuting γ_5 can be adopted. The amplitude of the diagrams is then computed using standard multi-loop techniques. After a Passarino–Veltman [18] decomposition of the tensor integrals, the scalar integrals are reduced to a small set of master integrals by means of integration-by-parts techniques [19,20] and the Laporta algorithm [21,22]. To this end, we use the program AIR [23] as well as an in-house routine.

For the massless up-type operator insertions, the diagrams can be expressed in terms of the master integrals that appeared in our former calculations [11–13]. For the massive charm-type insertions, on the other hand, we find 29 new master integrals. The computation of the master integrals constitutes the main technical challenge of the calculation. Analytic results for all master integrals have recently been derived in [15], based on a differential

[1] $\alpha_4^u(M_1 M_2)$ refers to a generically sub-leading penguin contribution to the term multiplied by the CKM factor $\lambda_u^{(D)}$. We also note that $\alpha_4^p(M_1 M_2)$ consists of a leading-power term a_4^p and a power-suppressed term a_6^p [5]. The calculation reported here concerns the leading-power contribution a_4^p.

[2] Since the contribution from $Q_{1,2}^p$ alone is not renormalization-group invariant, this statement cannot be true in arbitrary schemes nor at arbitrary renormalization scales. What we mean is that the statement holds in the conventional $\overline{\mathrm{MS}}$ scheme and with a reasonable choice $\mathcal{O}(m_b)$ of scale.

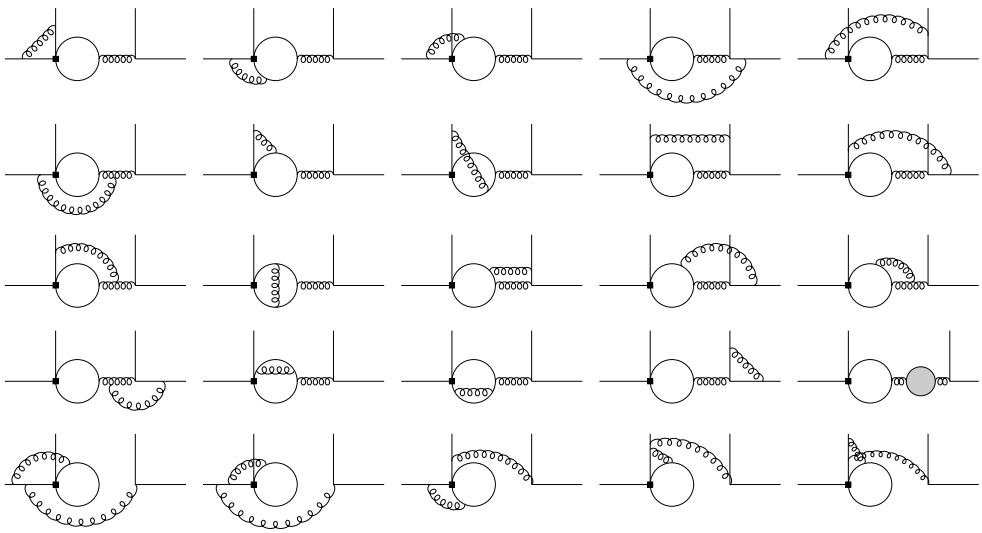

Fig. 1. Two-loop penguin diagrams that contribute to the insertion of the operators $Q_{1,2}^{u,c}$ (black square). The gray filled circle denotes the one-loop gluon self-energy.

equation approach in a canonical basis [24]. The canonical basis, together with suitably chosen kinematic variables, also catalyses the convolution of the hard-scattering kernels with the LCDA.

After the computation of the bare QCD two-loop amplitude, the hard-scattering kernels are extracted from a matching calculation onto soft-collinear effective theory (SCET). The main conceptual challenge in this context is the consistent treatment of evanescent and Fierz-equivalent operators in SCET, for which we follow the method employed in [13]. The SCET operators have the flavour structure $\sum_q(\bar{\chi}_D\chi_q)(\bar{\xi}_q h_v)$ where χ and ξ denote collinear light-quark fields moving in opposite directions. The two-loop diagrams relevant to the penguin amplitude a_4^p are all of the "wrong-insertion" type (see [13]) and hence lead to operators where the fermion indices are contracted in the form $\sum_q(\bar{\xi}_q\chi_q)(\bar{\chi}_D h_v)$. In Fig. 1 the $(\bar{\xi}_q\chi_q)$ fermion lines correspond to the solid line on the right side of the diagram. In the following we omit the sum over q and the flavour labels on the fields. In the CMM basis the fermion line that corresponds to $(\bar{\xi}\chi)$ carries no γ_5 matrix. This suggests that we use the following basis for the SCET operators:

$$O_1 = \bar{\chi}\,\frac{\not{n}_-}{2}(1-\gamma_5)\chi\;\bar{\xi}\not{n}_+(1-\gamma_5)h_v\,,$$
$$\tilde{O}_n = \bar{\xi}\,\gamma_\perp^\alpha\gamma_\perp^{\mu_1}\gamma_\perp^{\mu_2}\cdots\gamma_\perp^{\mu_{2n-2}}\chi \times \bar{\chi}(1+\gamma_5)\gamma_{\perp\alpha}\gamma_{\perp\mu_{2n-2}}\gamma_{\perp\mu_{2n-3}}\cdots\gamma_{\perp\mu_1}h_v\,, \tag{6}$$

where we need n up to 2 (strings with three γ matrices in each bilinear). The operator O_1 is the only physical SCET operator. It is the same as in [13], whereas the $\tilde{O}_n$ differ by the absence of the $1-\gamma_5$ factor to the left of χ. The operators $\tilde{O}_n$ are evanescent for $n>1$. $\tilde{O}_1$ is Fierz-equivalent to $O_1/2$ in four dimensions, so we add $\tilde{O}_1 - O_1/2$ as another evanescent operator. We also recall that the SCET operators are non-local on the light-cone [13].

After operator matching the hard-scattering kernels follow from the bare QCD amplitudes plus subtraction terms from UV counterterms of the operators Q_i and the SCET operators. The master formulae at LO, NLO, and NNLO read, respectively,

$$\widetilde{T}_i^{(0)} = \widetilde{A}_{i1}^{(0)}\,, \tag{7}$$
$$\widetilde{T}_i^{(1)} = \widetilde{A}_{i1}^{(1)\mathrm{nf}} + Z_{ij}^{(1)}\,\widetilde{A}_{j1}^{(0)} + \ldots\,, \tag{8}$$
$$\widetilde{T}_i^{(2)} = \widetilde{A}_{i1}^{(2)\mathrm{nf}} + Z_{ij}^{(1)}\,\widetilde{A}_{j1}^{(1)} + Z_{ij}^{(2)}\,\widetilde{A}_{j1}^{(0)} + Z_\alpha^{(1)}\,\widetilde{A}_{i1}^{(1)\mathrm{nf}} + (-i)\,\delta m^{(1)}\,\widetilde{A}_{i1}^{\prime(1)\mathrm{nf}} + Z_{ext}^{(1)}\left[\widetilde{A}_{i1}^{(1)\mathrm{nf}} + Z_{ij}^{(1)}\,\widetilde{A}_{j1}^{(0)}\right] - \widetilde{T}_i^{(1)}\left[C_{FF}^{(1)} + \widetilde{Y}_{11}^{(1)}\right] + \ldots\,. \tag{9}$$

The symbols have the same meaning as in Eq. (29) of [13]. The ellipses denote further terms that do not contribute to the kernels $i=1,2$ of the current–current operators. The matrices $Z_{ij}^{(1)}$ and $Z_{ij}^{(2)}$ contain the UV counterterms from operator mixing. Compared to the calculation of the tree amplitudes, they have to be extended by the mixing with the penguin operators including the correspondent evanescent operators [17]. This implies, in particular, that the one-loop amplitudes $\widetilde{A}_{j1}^{(1)}$ must be computed including the $\mathcal{O}(\epsilon)$ terms for all operators Q_j, which mix with the current–current operators. Finally, one has to convolute the hard-scattering kernels with the LCDA, for which we adopt the conventional Gegenbauer expansion.

3. The topological QCD penguin amplitude

In this section we give the numerical results of the penguin amplitudes a_4^u and a_4^c and discuss the size and scale dependence of the new contribution. At LO, the penguin amplitude coefficients are given in the CMM basis by ($N_c=3$, $C_F=4/3$)

$$a_{4,\mathrm{LO}}^p = \frac{1}{N_c}\left[C_3 + C_F C_4 + 16(C_5 + C_F C_6)\right]. \tag{10}$$

They are identical for $p=u,c$ and independent of the LCDA. At NLO we have ($L=\ln\mu^2/m_b^2$, $s_p=m_p^2/m_b^2$, $\bar{u}=1-u$)

$$a_{4,\mathrm{NLO}}^p\big|_{C_{1,2}} = \frac{\alpha_s}{4\pi}\frac{C_F}{N_c}\left(C_2 - \frac{C_1}{2N_c}\right) \times \int_0^1 du\left[-\frac{2}{3}L + \frac{2}{3} - G(s_p - i\epsilon,\bar{u})\right]\phi_{M_2}(u), \tag{11}$$

where we show only the terms from the current–current operators to illustrate the structure of the result. Here

$$G(s,u) = \frac{2(12s+5u-3u\ln s)}{9u} - \frac{2\xi(2s+u)}{3u}\ln\frac{\xi+1}{\xi-1} \tag{12}$$

is the one-loop penguin function with $\xi=\sqrt{1-4s/u}$. In practice, one then inserts the Gegenbauer expansion of $\phi_{M_2}(u)$ truncated at the second order to perform the integral. The result is finally expressed in terms of Wilson coefficients, quark masses and the Gegenbauer moments $a_{1,2}^{M_2}$.

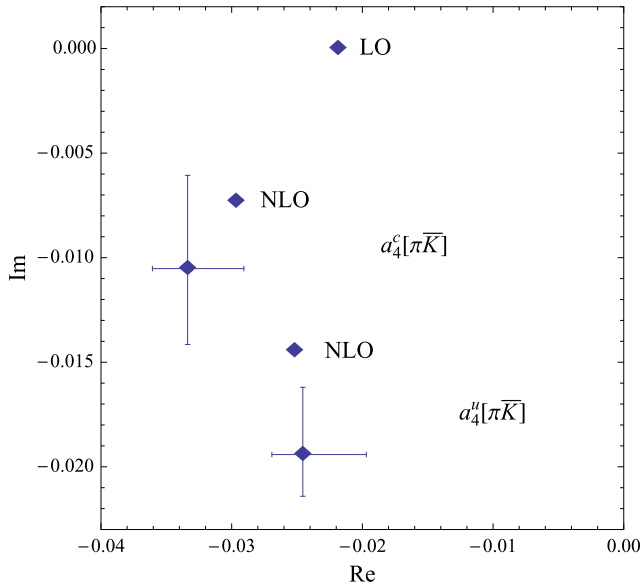

Fig. 2. The LO, NLO and NNLO values of $a_4^u(\pi\bar{K})$ and $a_4^c(\pi\bar{K})$ in the complex plane. The NNLO point includes a theoretical error estimate.

At NNLO the explicit expressions are involved, and we postpone the details to a future publication. Our final numerical predictions for the leading QCD penguin amplitudes $a_4^{u,c}(\pi\bar{K})$ are given as (for input parameters, see Section 4):

$$\begin{aligned} a_4^u(\pi\bar{K})/10^{-2} &= -2.87 - [0.09 + 0.09i]_{V_1} \\ &\quad + [0.49 - 1.32i]_{P_1} - [0.32 + 0.71i]_{P_2} \\ &\quad + \left[\frac{r_{sp}}{0.434}\right]\Big\{[0.13]_{LO} + [0.14 + 0.12i]_{HV} \\ &\quad - [0.01 - 0.05i]_{HP} + [0.07]_{tw3}\Big\} \\ &= (-2.46^{+0.49}_{-0.24}) + (-1.94^{+0.32}_{-0.20})i\,, \end{aligned} \tag{13}$$

$$\begin{aligned} a_4^c(\pi\bar{K})/10^{-2} &= -2.87 - [0.09 + 0.09i]_{V_1} \\ &\quad + [0.05 - 0.62i]_{P_1} - [0.77 + 0.50i]_{P_2} \\ &\quad + \left[\frac{r_{sp}}{0.434}\right]\Big\{[0.13]_{LO} + [0.14 + 0.12i]_{HV} \\ &\quad + [0.01 + 0.03i]_{HP} + [0.07]_{tw3}\Big\} \\ &= (-3.34^{+0.43}_{-0.27}) + (-1.05^{+0.45}_{-0.36})i\,. \end{aligned} \tag{14}$$

In both equations the third and fourth lines represent the spectator-scattering term, which for $r_{sp} = 0.434$ makes only a small contribution to a_4^p. In the respective first and second lines, the number without brackets is the LO contribution, which has no imaginary part, the following two numbers are the vertex and penguin NLO terms, and the new two-loop NNLO contribution from the current–current operators $Q_{1,2}^p$ is the number labelled P_2. We observe that the new correction is rather large. It amounts approximately to 40% (15%) of the imaginary (real) part of $a_4^u(\pi\bar{K})$, and 50% (25%) in the case of $a_4^c(\pi\bar{K})$. Graphical representations of $a_4^p(\pi\bar{K})$ are shown in Fig. 2 at LO, NLO and NNLO, where the NNLO point includes the theoretical error estimate.[3] The larger uncertainty of the imaginary part of $a_4^c(\pi\bar{K})$ is a consequence of the sensitivity to the charm-quark (pole) mass, for which we adopt the conservative range $m_c = 1.3 \pm 0.2$ GeV.

The values (13), (14) depend on the renormalization scale due to the truncation of the perturbative expansion and on hadronic parameters. The dependence on the renormalization scale μ may be considered as a measure of the accuracy of the approximation at a given order in perturbation theory. This is shown in Fig. 3 for the form factor term contribution to $a_4^p(\pi\bar{K})$ up to NNLO. We observe a considerable stabilization of the scale dependence for the real part, but less for the imaginary part. This is explained by the fact that the imaginary part vanishes at LO. Hence only the first correction is now available and is, moreover, large.

4. Phenomenology – direct CP asymmetries

We now consider the new contribution to a_4^p in the context of the full QCD penguin amplitude and provide first results for some direct CP asymmetries. We defer the discussion of branching fractions to the more complete treatment including the two-loop matrix elements of the penguin operators Q_{3-6}.

We recall that in the QCD factorization approach the full QCD penguin amplitude consists of the parameters a_4^p, a_6^p, and the penguin annihilation amplitude β_3^p in the combination [5]

$$\hat{\alpha}_4^p(M_1M_2) = a_4^p(M_1M_2) \pm r_\chi^{M_2} a_6^p(M_1M_2) + \beta_3^p(M_1M_2), \tag{15}$$

where the plus (minus) sign applies to the decays where M_1 is a pseudoscalar (vector) meson. The first term, $a_4^p(M_1M_2)$, is the only leading-power contribution. Its real part is of order −0.03. The annihilation term is $1/m_b$ suppressed and cannot be calculated in the factorization framework. Estimates based on the model defined in [4] suggest that its modulus is also of order 0.03. While the magnitude of these two terms is largely independent of the spin of the final state mesons, the contribution from the power-suppressed scalar penguin amplitude $r_\chi^{M_2} a_6^p(M_1M_2)$ is very small when M_2 is a vector meson, but larger than the leading-power amplitude for pseudoscalar M_2. It interferes constructively for the *PP* final state, and destructively for *VP*. It follows from this brief discussion that the impact of a correction to a_4^p is always diluted in the full penguin amplitude. When $M_2 = V$, the computation of a_4^p ascertains the short-distance contribution to the amplitude, and hence the direct CP asymmetry, but there is an uncertain annihilation contribution of similar size. When $M_2 = P$, there is another NNLO short-distance contribution from a_6^p, which is difficult though not impossible to calculate, since it is power-suppressed. These features will be clearly seen in the analysis below.

In the following we adopt the same values for the Standard Model, meson and form factor parameters as in Table 1 of [13] with the exception of $|V_{ub}/V_{cb}| = 0.085 \pm 0.015$, $\tau_{B_d} = 1.52$ ps, $m_s(2\text{ GeV}) = (90 \pm 10)$ MeV, and $f_{B_d} = (190 \pm 10)$ MeV. The decay constants, Gegenbauer moments and form factors involving kaons coincide with [9], those involving K^* mesons with [5], except for $A_0^{BK^*}(0) = 0.39 \pm 0.06$. We note that the B-meson LCDA parameter λ_B is not important here, since the leading spectator-scattering contribution to the QCD penguin amplitude is colour-suppressed.

In Fig. 4 we show the QCD penguin amplitude $\hat{\alpha}_4^c(M_1M_2)$ normalized to the sum of colour-allowed and colour-suppressed tree amplitude $\alpha_1(\pi\pi) + \alpha_2(\pi\pi)$,[4] as was shown before in [5,9], but now includes the NNLO computation for numerator and denominator. The NNLO result is represented by the dark point with error

[3] The LO and NLO numbers here as in the subsequent figure are not the same as (13), (14) truncated to LO and NLO, because they employ Wilson coefficients C_i at LO and NLO, respectively. Moreover, consistent with previous LO and NLO calculations, they are computed in the operator basis as defined in [25]. On the other hand, in (13), (14) NNLO Wilson coefficients in the CMM basis are used throughout.

[4] For $M_1M_2 = \pi\bar{K}, \pi\bar{K}^*$. For $M_1M_2 = \rho\bar{K}, \rho\bar{K}^*$ we use the $\rho\rho$ final state instead. Also, for $\rho\bar{K}^*$ and $\rho\rho$, only the longitudinal polarization amplitude is considered in the following.

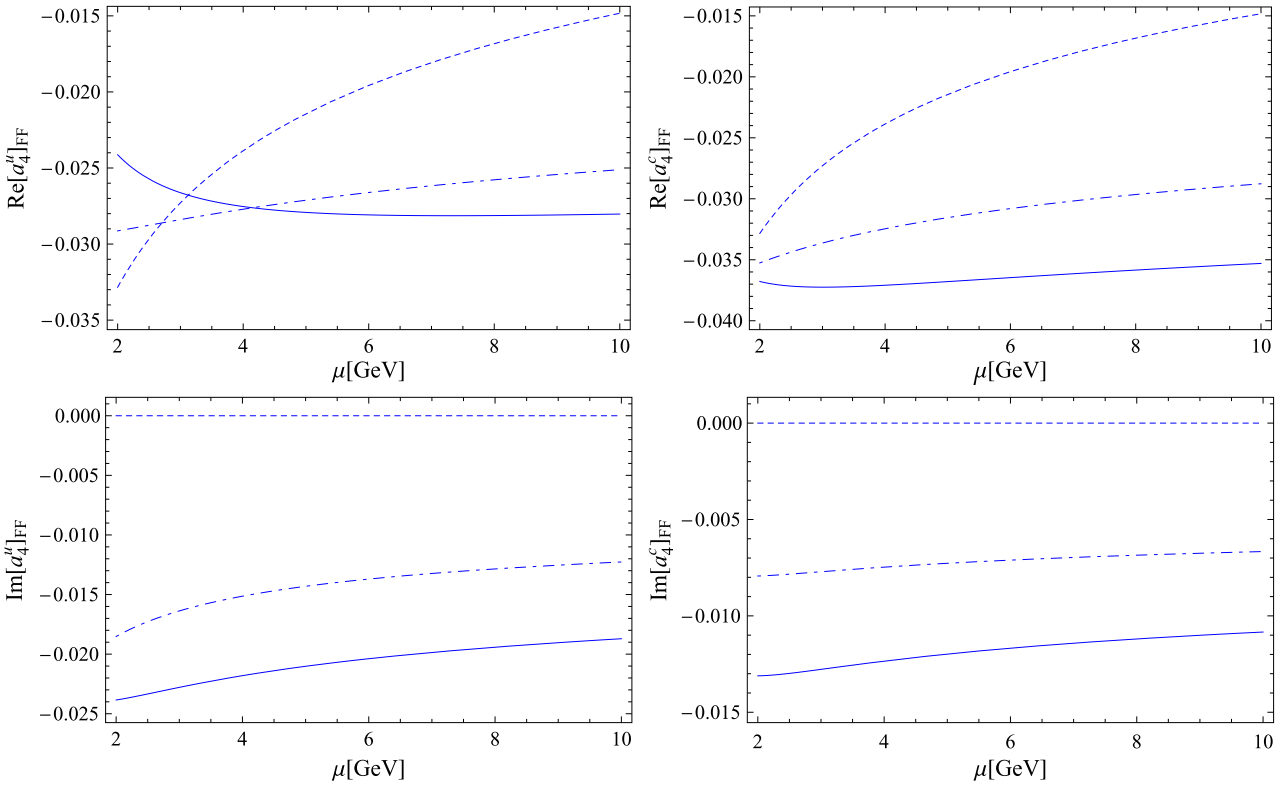

Fig. 3. The dependence of the leading QCD penguin amplitudes $a_4^p(\pi\bar{K})$ on the hard renormalization scale μ (form factor term only). Dashed, dashed–dotted and solid lines represent LO, NLO, and NNLO, respectively.

bars and corresponds to setting $\varrho_A = 0$ in the annihilation model, which implies a small value of β_3^c. The nearly circular contours around this point show the variation of the theoretical prediction when the phase of the annihilation model is varied from 0 to 2π for fixed $\varrho_A = 1, 2, 3$ (inner to outer circles). The radius of the circle for $\varrho_A = 1$ leads to the estimate $|\beta_3^c| \approx 0.03$ mentioned above. The LO and NLO results are marked by diamonds without error bars. Despite the sizable NNLO correction to a_4^c as shown in Fig. 2, the difference between NNLO and NLO is small. This is a consequence of the "dilution" discussed above and a partial cancellation in the ratio of amplitudes.

The theoretical prediction can be compared to data, since the amplitude ratio can be related to CP-averaged decay rates Γ and direct CP asymmetries. We discuss this for the *PP* case, from which the others can be inferred by obvious replacements. First, to very good approximation [5]

$$\left|\frac{\hat{\alpha}_4^c(\pi\bar{K})}{\alpha_1(\pi\pi)+\alpha_2(\pi\pi)}\right| = \left|\frac{V_{ub}}{V_{cb}}\right| \frac{f_\pi}{f_K}\left[\frac{\Gamma_{\pi^-\bar{K}^0}}{2\Gamma_{\pi^-\pi^0}}\right]^{1/2}, \tag{16}$$

which determines the gray rings around the origin. The darker rings are due to the experimental errors in the branching fractions and the lighter ones include also the uncertainty of $|V_{ub}/V_{cb}|$ (added linearly). To obtain the wedges we define ψ to be the phase of the amplitude ratio shown in the figure, and

$$\mathcal{R} = \frac{\alpha_1(\pi\bar{K}) + \hat{\alpha}_4^u(\pi\bar{K})}{\alpha_1(\pi\pi)+\alpha_2(\pi\pi)}. \tag{17}$$

We then find

$$-\sin\psi + \frac{\operatorname{Im}\mathcal{R}}{\operatorname{Re}\mathcal{R}}\cos\psi = \frac{1}{2\sin\gamma\operatorname{Re}\mathcal{R}}\left|\frac{V_{cs}}{V_{us}}\right|\frac{f_\pi}{f_K}\frac{\Gamma_{\pi^+K^-}}{\sqrt{2\Gamma_{\pi^-\pi^0}\Gamma_{\pi^-\bar{K}^0}}}A_{\mathrm{CP}}(\pi^+K^-). \tag{18}$$

In previous discussions [5,9] the experimental error on the observables on the right-hand side and the error on γ combined was large, so that it was justified to assume that $\mathcal{R}$ is real and to neglect the theoretical uncertainty on $\operatorname{Re}\mathcal{R}$, which mainly stems from the colour-suppressed tree amplitude $\alpha_2(\pi\pi)$. This is no longer the case. The outer wedge now includes the theoretical uncertainty on $\mathcal{R}$ and γ, which is added linearly to the purely experimental uncertainties (inner wedge). The middle wedge includes the uncertainty from γ only. Note that (18) has two solutions as shown in the figure, but the wedge that does not match the theoretical prediction is excluded by $\Gamma_{\pi^+K^-}/\Gamma_{\pi^-\bar{K}^0} < 1$.

Since the NNLO correction to the amplitude ratio turned out to be small, we can reaffirm the conclusions from [9] in the light of significantly improved data. The different magnitude of the *PP* penguin amplitude vs. *PV*, *VP* and *VV* is clearly reflected in the data as predicted. There is reasonable quantitative agreement as indicated by the error bars and the small onion-shaped regions corresponding to $\varrho_A = 1$. An annihilation contribution of 0.02 to 0.03 seems to be required, except for the longitudinal *VV* final states. The red square in the first three plots of Fig. 4 corresponds to the theoretical prediction with $\varrho_A = 1$ and the phase $\phi_A = -55°$ (*PP*), $\phi_A = -45°$ (*PV*), $\phi_A = -50°$ (*VP*) (see [4] for the definition of these quantities), which is similar to the favoured parameter set S4 of [5]. Only the CP asymmetry of the πK final state now appears to require a value larger than $\varrho_A = 1$ for a perfect fit. More general parametrizations of the power corrections with a non-universal value for ρ_A can in principle be adopted, at the price of losing predictive power.

Moving to the observables themselves, we show in Table 1 the theoretical predictions for direct CP asymmetries, defined as the rate asymmetry between $\bar{B}$ and B decays, together with the world average of experimental data (last column), compiled from HFAG [26]. We focus on the penguin-dominated $b \to s$ transitions of non-

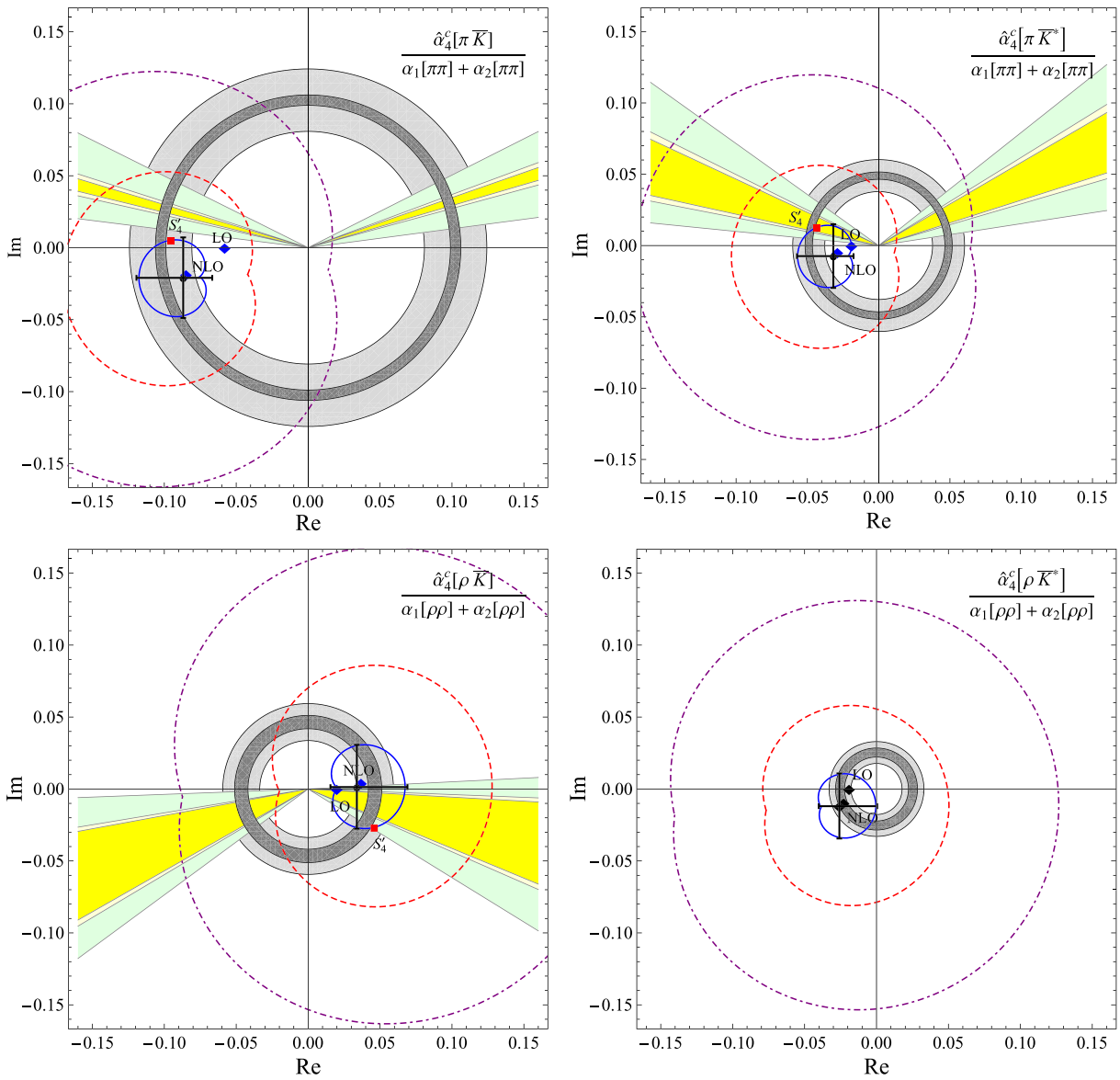

Fig. 4. The QCD penguin amplitude $\hat{\alpha}_4^c(M_1M_2)$ for the $PP = \pi K$ final state and its PV, VP, and VV relatives. The VV case refers to the longitudinal polarization amplitude only. Shown are the theoretical predictions for the ratios $\hat{\alpha}_4^c(M_1M_2)/(\alpha_1(\pi\pi)+\alpha_2(\pi\pi))$ ($\rho\rho$ instead of $\pi\pi$ in the lower row) and a comparison of extractions of the modulus (rings) and phase (wedges) from data. Note there is no data for the CP asymmetry in the rate of the longitudinally polarized ρ^+K^{*-} final state. See text for further explanations. (For interpretation of the references to color in this figure, the reader is referred to the web version of this article.)

strange B mesons to πK final states and their PV and VP relatives. We also show the CP asymmetry difference

$$\delta(\pi\bar{K}) = A_{\rm CP}(\pi^0K^-) - A_{\rm CP}(\pi^+K^-) \tag{19}$$

and the asymmetry "sum rule"

$$\Delta(\pi\bar{K}) = A_{\rm CP}(\pi^+K^-) + \frac{\Gamma_{\pi^-\bar{K}^0}}{\Gamma_{\pi^+K^-}} A_{\rm CP}(\pi^-\bar{K}^0) - \frac{2\Gamma_{\pi^0K^-}}{\Gamma_{\pi^+K^-}} A_{\rm CP}(\pi^0K^-) - \frac{2\Gamma_{\pi^0\bar{K}^0}}{\Gamma_{\pi^+K^-}} A_{\rm CP}(\pi^0\bar{K}^0)\,. \tag{20}$$

The latter quantity is expected to be small [27], since the leading CP-violating interference of QCD penguin and tree amplitudes cancels out in the sum. In order to focus on the effect of the new NNLO correction on the perturbatively calculable short-distance part of the CP asymmetry, the columns labelled "NLO" and "NNLO" give the respective results, when the long-distance, power-suppressed terms are set to zero. This means that we set β_3^p to zero, as well as power-suppressed spectator-scattering terms. However, we keep the short-distance dominated, but power-suppressed scalar penguin contributions. The column labelled "NNLO+LD" adds the previously neglected terms back. The main effect is from weak annihilation, for which we adopt the S4-like scenario (S_4') marked by the red square in Fig. 4.

Focusing first on the "NLO" and "NNLO" results, we note that for the PP final states the change is minor, since, as discussed above, a_4^c represents only part of the short-distance penguin amplitude. The situation is different for the πK^* final states where the a_6^c contribution is small, and for the ρK final states where due to the opposite sign of a_4^c and a_6^c a cancellation occurs. In these cases, we observe a large modification for the π^0K^{*-}, π^+K^{*-} and the corresponding ρK final states, for which the CP asymmetry arises predominantly from the imaginary part of $\hat{\alpha}_4^c/\alpha_1$. These modifications are a reflection of the sizable corrections seen in Fig. 2. The effect is much less pronounced in the remaining modes, where the asymmetry is due to interference with $\hat{\alpha}_4^u$ (in case of

Table 1
Direct CP asymmetries in percent for the πK, πK^*, and ρK final states. The theoretical errors shown correspond to the uncertainties due to the CKM and hadronic parameters, respectively. The errors on the experimental values of δ and Δ are computed from those of the individual observables appearing in (20) ignoring possible correlations.

f	NLO	NNLO	NNLO+LD	Exp
$\pi^-\bar{K}^0$	$0.71^{+0.13}_{-0.14}{}^{+0.21}_{-0.19}$	$0.77^{+0.14}_{-0.15}{}^{+0.23}_{-0.22}$	$0.10^{+0.02}_{-0.02}{}^{+1.24}_{-0.27}$	-1.7 ± 1.6
$\pi^0 K^-$	$9.42^{+1.77}_{-1.76}{}^{+1.87}_{-1.88}$	$10.18^{+1.91}_{-1.90}{}^{+2.03}_{-2.62}$	$-1.17^{+0.22}_{-0.22}{}^{+20.00}_{-6.62}$	4.0 ± 2.1
$\pi^+ K^-$	$7.25^{+1.36}_{-1.36}{}^{+2.13}_{-2.58}$	$8.08^{+1.52}_{-1.51}{}^{+2.52}_{-2.65}$	$-3.23^{+0.61}_{-0.61}{}^{+19.17}_{-3.36}$	-8.2 ± 0.6
$\pi^0\bar{K}^0$	$-4.27^{+0.83}_{-0.77}{}^{+1.48}_{-2.23}$	$-4.33^{+0.84}_{-0.78}{}^{+3.29}_{-2.32}$	$-1.41^{+0.27}_{-0.25}{}^{+5.54}_{-6.10}$	1 ± 10
$\delta(\pi\bar{K})$	$2.17^{+0.40}_{-0.40}{}^{+1.39}_{-0.74}$	$2.10^{+0.39}_{-0.39}{}^{+1.40}_{-2.86}$	$2.07^{+0.39}_{-0.39}{}^{+2.76}_{-4.55}$	12.2 ± 2.2
$\Delta(\pi\bar{K})$	$-1.15^{+0.21}_{-0.22}{}^{+0.55}_{-0.84}$	$-0.88^{+0.16}_{-0.17}{}^{+1.31}_{-0.91}$	$-0.48^{+0.09}_{-0.09}{}^{+1.09}_{-1.15}$	-14 ± 11
$\pi^-\bar{K}^{*0}$	$1.36^{+0.25}_{-0.26}{}^{+0.60}_{-0.47}$	$1.49^{+0.27}_{-0.29}{}^{+0.69}_{-0.56}$	$0.27^{+0.05}_{-0.05}{}^{+3.18}_{-0.67}$	-3.8 ± 4.2
$\pi^0 K^{*-}$	$13.85^{+2.40}_{-2.70}{}^{+5.84}_{-5.86}$	$18.16^{+3.11}_{-3.52}{}^{+7.79}_{-10.57}$	$-15.81^{+3.01}_{-2.83}{}^{+69.35}_{-15.39}$	-6 ± 24
$\pi^+ K^{*-}$	$11.18^{+2.00}_{-2.15}{}^{+9.75}_{-10.62}$	$19.70^{+3.37}_{-3.80}{}^{+10.54}_{-11.42}$	$-23.07^{+4.35}_{-4.05}{}^{+86.20}_{-20.64}$	-23 ± 6
$\pi^0\bar{K}^{*0}$	$-17.23^{+3.33}_{-3.00}{}^{+7.59}_{-12.57}$	$-15.11^{+2.93}_{-2.65}{}^{+12.34}_{-10.64}$	$2.16^{+0.39}_{-0.42}{}^{+17.53}_{-36.80}$	-15 ± 13
$\delta(\pi\bar{K}^*)$	$2.68^{+0.72}_{-0.67}{}^{+5.44}_{-4.30}$	$-1.54^{+0.45}_{-0.58}{}^{+4.60}_{-9.19}$	$7.26^{+1.21}_{-1.34}{}^{+12.78}_{-20.65}$	17 ± 25
$\Delta(\pi\bar{K}^*)$	$-7.18^{+1.38}_{-1.28}{}^{+3.38}_{-5.35}$	$-3.45^{+0.67}_{-0.59}{}^{+9.48}_{-4.95}$	$-1.02^{+0.19}_{-0.18}{}^{+4.32}_{-7.86}$	-5 ± 45
$\rho^-\bar{K}^0$	$0.38^{+0.07}_{-0.07}{}^{+0.16}_{-0.27}$	$0.22^{+0.04}_{-0.04}{}^{+0.19}_{-0.17}$	$0.30^{+0.06}_{-0.06}{}^{+2.28}_{-2.39}$	-12 ± 17
$\rho^0 K^-$	$-19.31^{+3.42}_{-3.61}{}^{+13.95}_{-8.96}$	$-4.17^{+0.75}_{-0.80}{}^{+19.26}_{-19.52}$	$43.73^{+7.07}_{-7.62}{}^{+44.00}_{-137.77}$	37 ± 11
$\rho^+ K^-$	$-5.13^{+0.95}_{-0.97}{}^{+6.38}_{-4.02}$	$1.50^{+0.29}_{-0.27}{}^{+8.69}_{-10.36}$	$25.93^{+4.43}_{-4.90}{}^{+25.40}_{-75.63}$	20 ± 11
$\rho^0\bar{K}^0$	$8.63^{+1.59}_{-1.65}{}^{+2.31}_{-1.69}$	$8.99^{+1.66}_{-1.71}{}^{+3.60}_{-7.44}$	$-0.42^{+0.08}_{-0.08}{}^{+19.49}_{-8.78}$	6 ± 20
$\delta(\rho\bar{K})$	$-14.17^{+2.80}_{-2.96}{}^{+7.98}_{-5.39}$	$-5.67^{+0.96}_{-1.01}{}^{+10.86}_{-9.79}$	$17.80^{+3.15}_{-3.01}{}^{+19.51}_{-62.44}$	17 ± 16
$\Delta(\rho\bar{K})$	$-8.75^{+1.62}_{-1.66}{}^{+4.78}_{-6.48}$	$-10.84^{+1.98}_{-2.09}{}^{+11.67}_{-9.09}$	$-2.43^{+0.46}_{-0.42}{}^{+4.60}_{-19.43}$	-37 ± 37

$\pi^-\bar{K}^{*0}$, $\rho^-\bar{K}^0$) or α_2 (in case of $\pi^0\bar{K}^{*0}$, $\rho^0\bar{K}^0$), and the effect of the NNLO correction cancels to a certain extent in the ratio of interfering amplitudes. Despite these large modifications of some of the *PV* and *VP* modes' asymmetries, the long-distance annihilation contribution is always more important numerically, and usually required to obtain a satisfactory description of the data. The modelling of the long-distance contribution also determines the final theoretical uncertainty, which can become very large. Given that the short-distance contribution is now known to NNLO and given the large amount of experimental data, it becomes imperative to better determine the annihilation amplitude, presumably through fits to data.

5. Conclusion

The computation of direct CP asymmetries in charmless B decays at next-to-next-to-leading order in QCD has been a long-standing issue. The long- and short-distance contributions can in principle be of the same order and a NNLO calculation is required to ascertain the perturbative part. In this paper we computed the two-loop contributions of the current–current operators $Q^p_{1,2}$ to the QCD penguin amplitude, which are expected to constitute the dominant contribution, at least to the imaginary part, which is required for observing CP violation. We find a sizable correction to the short-distance part of the direct CP asymmetry, the effect of which is, however, tempered by power-suppressed short- and long-distance terms. Our preliminary conclusion is that the NNLO correction does not help resolving the πK CP asymmetry puzzle, nor does it render the poorly known annihilation terms redundant. The final analysis should, however, include the penguin operator matrix elements, as well as the one from the chromomagnetic operator considered in [14]. The corresponding calculations are in progress.

Acknowledgements

This work was supported in part by the NNSFC of China under contract Nos. 11005032 and 11435003 (XL), by DFG Forschergruppe FOR 1873 "Quark Flavour Physics and Effective Field Theories" (TH) and by the DFG Sonderforschungsbereich/Transregio 9 "Computergestützte Theoretische Teilchenphysik" (MB). GB gratefully acknowledges the support of a University Research Fellowship by the Royal Society. XL is also supported in part by the SRF for ROCS, SEM, by the Open Project Program of SKLTP, ITP, CAS (No. Y4KF081CJ1), and by the self-determined research funds of CCNU from the colleges' basic research and operation of MOE (CCNU15A02037). MB and XL acknowledge the hospitality of the Munich Institute for Astro- and Particle Physics (MIAPP) of the DFG cluster of excellence "Origin and Structure of the Universe", where this work was finalized.

References

[1] D. Zeppenfeld, Z. Phys. C 8 (1981) 77.
[2] M. Beneke, G. Buchalla, M. Neubert, C.T. Sachrajda, Phys. Rev. Lett. 83 (1999) 1914, arXiv:hep-ph/9905312.
[3] M. Beneke, G. Buchalla, M. Neubert, C.T. Sachrajda, Nucl. Phys. B 591 (2000) 313, arXiv:hep-ph/0006124.
[4] M. Beneke, G. Buchalla, M. Neubert, C.T. Sachrajda, Nucl. Phys. B 606 (2001) 245, arXiv:hep-ph/0104110.
[5] M. Beneke, M. Neubert, Nucl. Phys. B 675 (2003) 333, arXiv:hep-ph/0308039.
[6] M. Beneke, S. Jäger, Nucl. Phys. B 751 (2006) 160, arXiv:hep-ph/0512351.
[7] N. Kivel, J. High Energy Phys. 0705 (2007) 019, arXiv:hep-ph/0608291.
[8] V. Pilipp, Nucl. Phys. B 794 (2008) 154, arXiv:0709.3214 [hep-ph].
[9] M. Beneke, S. Jäger, Nucl. Phys. B 768 (2007) 51, arXiv:hep-ph/0610322.
[10] A. Jain, I.Z. Rothstein, I.W. Stewart, arXiv:0706.3399 [hep-ph].
[11] G. Bell, Nucl. Phys. B 795 (2008) 1, arXiv:0705.3127 [hep-ph].
[12] G. Bell, Nucl. Phys. B 822 (2009) 172, arXiv:0902.1915 [hep-ph].
[13] M. Beneke, T. Huber, X.Q. Li, Nucl. Phys. B 832 (2010) 109, arXiv:0911.3655 [hep-ph].
[14] C.S. Kim, Y.W. Yoon, J. High Energy Phys. 1111 (2011) 003, arXiv:1107.1601 [hep-ph].

[15] G. Bell, T. Huber, J. High Energy Phys. 1412 (2014) 129, arXiv:1410.2804 [hep-ph].
[16] K.G. Chetyrkin, M. Misiak, M. Münz, Nucl. Phys. B 520 (1998) 279, arXiv:hep-ph/9711280.
[17] M. Gorbahn, U. Haisch, Nucl. Phys. B 713 (2005) 291, arXiv:hep-ph/0411071.
[18] G. Passarino, M.J.G. Veltman, Nucl. Phys. B 160 (1979) 151.
[19] F.V. Tkachov, Phys. Lett. B 100 (1981) 65.
[20] K.G. Chetyrkin, F.V. Tkachov, Nucl. Phys. B 192 (1981) 159.
[21] S. Laporta, E. Remiddi, Phys. Lett. B 379 (1996) 283, arXiv:hep-ph/9602417.
[22] S. Laporta, Int. J. Mod. Phys. A 15 (2000) 5087, arXiv:hep-ph/0102033.
[23] C. Anastasiou, A. Lazopoulos, J. High Energy Phys. 0407 (2004) 046, arXiv:hep-ph/0404258.
[24] J.M. Henn, Phys. Rev. Lett. 110 (2013) 251601, arXiv:1304.1806 [hep-th].
[25] G. Buchalla, A.J. Buras, M.E. Lautenbacher, Rev. Mod. Phys. 68 (1996) 1125, arXiv:hep-ph/9512380.
[26] Y. Amhis, et al., Heavy Flavor Averaging Group Collaboration, arXiv:1412.7515 [hep-ex], and update at http://www.slac.stanford.edu/xorg/hfag/.
[27] M. Gronau, Phys. Lett. B 627 (2005) 82, arXiv:hep-ph/0508047.

Published for SISSA by Springer

Received: March 6, 2015
Accepted: April 4, 2015
Published: April 24, 2015

Two-loop master integrals for non-leptonic heavy-to-heavy decays

Tobias Huber and Susanne Kränkl

Theoretische Physik 1, Naturwissenschaftlich-Technische Fakultät, Universität Siegen, Walter-Flex-Straße 3, D-57068 Siegen, Germany

E-mail: huber@physik.uni-siegen.de, kraenkl@physik.uni-siegen.de

Abstract: We compute the two-loop master integrals for non-leptonic heavy-to-heavy decays analytically in a recently-proposed canonical basis. For this genuine two-loop, two-scale problem we first derive a basis for the master integrals that disentangles the kinematics from the space-time dimension in the differential equations, and subsequently solve the latter in terms of iterated integrals up to weight four. The solution constitutes another valuable example of the finding of a canonical basis for two-loop master integrals that have two different internal masses, and assumes a form that is ideally suited for a subsequent convolution with the light-cone distribution amplitude in the framework of QCD factorisation.

Keywords: B-Physics, Heavy Quark Physics, QCD

ArXiv ePrint: 1503.00735

Open Access, © The Authors.
Article funded by SCOAP[3].

doi:10.1007/JHEP04(2015)140

JHEP04(2015)140

Contents

1 Introduction **1**

2 Kinematics **3**

3 Iterated integrals and Goncharov polylogarithms **4**

4 The canonical basis **5**

5 Boundary conditions **10**

6 Results **13**
- 6.1 $C_1 - C_{12}$ 14
- 6.2 $C_{13} - C_{15}$ 18
- 6.3 $C_{16} - C_{22}$ 18
- 6.4 $C_{23} - C_{27}$ 19
- 6.5 $C_{28} - C_{32}$ 21
- 6.6 C_{33} and C_{34} 22
- 6.7 C_{35} 22
- 6.8 C_{36} and C_{37} 23
- 6.9 C_{38} and C_{39} 24

7 Checks **24**

8 Conclusion **25**

A The matrices $\tilde{A}$ **26**

JHEP04(2015)140

1 Introduction

Non-leptonic B-decays are interesting for a number of phenomenological applications like the extraction of CKM elements and the study of CP asymmetries. Their study has already entered the area of precision physics, both on the experimental [1] and on the theoretical side. However, their theoretical description is complicated by the purely hadronic environment, entailing QCD effects from many widely separated scales. The two main approaches to non-leptonic B-decays are flavour symmetries of the light quarks [2] and factorisation frameworks such as pQCD [3] and QCD factorisation (QCDF) [4–6]. In the latter framework, next-to-leading order (NLO) corrections to both, heavy-to-heavy [5] and heavy-to-light [4, 7] transitions have been known since more than a decade. More recently, also next-to-next-to-leading order (NNLO) results for heavy-to-light decays have become

available [8–12]. In the present article, we consider NNLO corrections also to the heavy-to-heavy decays such as $B \to D\pi$ in the framework of QCDF [13]. In the heavy-quark limit, the decay amplitude for $\bar{B}^0 \to D^+\pi^-$ is given by [5]

$$\langle D^+\pi^-|\mathcal{O}_i|\bar{B}^0\rangle = \sum_j F_j^{B\to D}(m_\pi^2) \int_0^1 du\, T_{ij}(u)\Phi_\pi(u)\,, \tag{1.1}$$

where $\mathcal{O}_i$ are the operators from the effective Hamiltonian that describe the underlying weak decay. The $F_j^{B\to D}$ form factors and the pion light-cone distribution amplitude (LCDA) $\Phi_\pi(u)$, with momentum fractions u and $1-u$ shared among the pion constituents, are the non-perturbative inputs. The hard-scattering kernels $T_{ij}(u)$, on the other hand, can be evaluated in a perturbative expansion in the strong coupling, and are known in QCD to NLO accuracy [5]. Yet it is interesting to go beyond NLO in $B \to D\pi$ transitions: since the contribution at NLO is colour suppressed and appears alongside small Wilson coefficients, the NNLO corrections may be significant in size. Moreover, since there is neither a colour-suppressed tree amplitude nor penguin contributions, and spectator scattering and weak annihilation are power-suppressed [5], we have only the vertex kernels to the colour-allowed tree amplitude. A precise theory prediction of this single contribution, together with comparison to experimental data, might give a reliable estimate of the size of power corrections in the QCDF framework.

The evaluation of Feynman diagrams that contribute to the NNLO hard-scattering kernel amounts to the computation of ~ 70 two-loop diagrams. By using contemporary techniques to evaluate multi-loop integrals, the two-loop Feynman diagrams are reduced to a small set of a few dozens of master integrals. A powerful method to evaluate the latter analytically are differential equations [14–16]. This method was recently refined by Henn [17]. Considering that the basis of master integrals is not unique, Henn discovered that in a suitably chosen basis — denoted as *canonical basis* — the differential equations can be cast into a form that factorises the dependence on the kinematic variables from that on the number of space-time dimensions D. In this case, the solution is expressed in terms of iterated integrals. This method was recently applied to a number of problems for loop [11, 18–26] and phase-space [27, 28] integrals.

To the present day, the construction of the canonical basis is mostly based on experience or experimentation, rather than on a systematic procedure, although developments in this direction have recently become available [21, 29, 30]. In the future it would be most desirable to have a general algorithm for finding a canonical basis for arbitrary external kinematics and numbers of loops, legs, scales, and space-time dimensions. Therefore, every non-trivial example of a canonical basis is most valuable, and our results contribute towards finding a general algorithm for constructing the canonical basis.

Last but not least, if the master integrals that enter the hard-scattering kernels $T_{ij}(u)$ are written in terms of iterated integrals, the convolution with the pion LCDA in (1.1) simplifies to a large extent. Our results therefore catalyse the steps necessary to obtain the decay amplitudes considerably, and constitute an important step towards the phenomenology of $B \to D\pi$ decays at NNLO in QCDF.

JHEP04(2015)140

This paper is organized as follows. In section 2 we introduce the kinematics of the two-body decay and present the generic form of the differential equations with respect to the kinematic variables. We proceed by defining Goncharov polylogarithm in section 3, which are a class of iterated integrals suited to describe the solutions to the differential equations. In section 4 the canonical basis is defined and the expressions for the master integrals in this basis are presented. We also elaborate on strategies to find a canonical basis. The boundary conditions for the integrals are discussed in section 5 and the results are presented in section 6. In section 7 we comment on the performed cross-checks before concluding in section 8. In appendix A we collect the matrices that contain all relevant information on the differential equations. The analytic results of all master integrals are also available electronically [31].

2 Kinematics

We consider the kinematics of the decay $\bar{B}^0 \to D^+\pi^-$, which emerges from the underlying weak transition $b \to c\bar{u}d$. A sample of Feynman diagrams contributing to the two-loop hard-scattering kernels is given in figure 1. The complete set of diagrams consists of those shown in figures 15 and 16 of [5], supplemented by gluon self-energy insertions in one-loop diagrams. All external momenta are taken to be incoming throughout this work. q_4 and q_3 denote the external momenta of the b and the c quark, respectively, which fulfill the on-shell constraints $q_{4,3}^2 = m_{b,c}^2$. The constituents of the pion share the momentum q with $q_1 = uq$ and $q_2 = (1-u)q \equiv \bar{u}q$, where $u \in [0,1]$ is the momentum fraction of the quarks inside the pion entering eq. (1.1) in a convolution of the hard-scattering kernel with the pion LCDA. We consider the pion to be massless, i.e. $q^2 = q_{1,2}^2 = 0$. Due to the linear dependence of the momenta, $q_1 + q_2 = q = -q_3 - q_4$, the kinematics is completely determined by two of the on-shell conditions and one additional kinematic invariant, for instance

$$q_4^2 = m_b^2\,, \quad q_3^2 = m_c^2\,, \quad q_3 q_4 = -\frac{1}{2}(m_b^2 + m_c^2)\,. \tag{2.1}$$

We apply commonly used multi-loop techniques which include integration-by-parts identities [32, 33] and the Laporta algorithm [34], and reduce the two-loop Feynman diagrams to master integrals [35, 36]. Furthermore, we construct the differential equation of the latter with respect to kinematic variables. In the derivation of eq. (1.1) the charm quark was assumed to be heavy. Hence, the ratio m_c/m_b remains fixed in the heavy-quark limit and our master integrals depend on two scales: the momentum fraction u and the ratio of the heavy quark masses $z \equiv m_c^2/m_b^2$. They are further functions of the kinematic invariants (2.1)

$$C(u,z) = C(u, q_3^2(z), (q_4 q_3)(z), q_4^2(z), z)\,. \tag{2.2}$$

Thus, the total derivative of a generic master integral C with respect to u is given by

$$\frac{dC}{du} = \frac{\partial C}{\partial u}\,, \tag{2.3}$$

whereas the one in z reads

$$\frac{dC}{dz} = \frac{\partial C}{\partial z} + \frac{\partial C}{\partial q_3^2}\frac{dq_3^2}{dz} + \frac{\partial C}{\partial (q_3 q_4)}\frac{d(q_3 q_4)}{dz} + \frac{\partial C}{\partial q_4^2}\frac{dq_4^2}{dz}\,. \tag{2.4}$$

JHEP04(2015)140

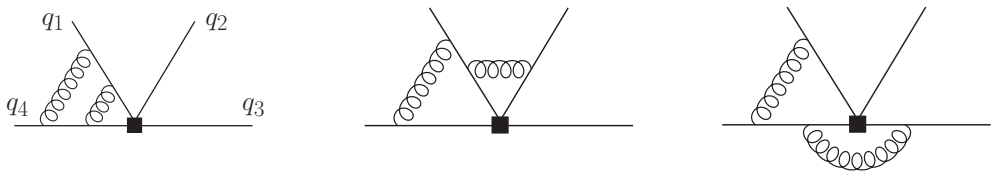

Figure 1. Sample of Feynman diagrams: q_4 and q_3 are the momenta of the quark lines with masses m_b and m_c, respectively. $q_1 = uq$ and $q_2 = \bar{u}q$ are the momenta of the light quark and anti-quark, respectively. $q = q_1 + q_2$ is the momentum of the pion. All momenta are incoming. The black square denotes an operator insertion from the weak effective Hamiltonian.

The computation of $\partial C/\partial z$ is straightforward. The partial derivatives of C with respect to the kinematics on the r.h.s. of eq. (2.4) can be expressed in terms of partial derivatives with respect to the momenta $q_{3,\mu}$ and $q_{4,\mu}$ [37], which can be easily carried out. Note that the last term on the r.h.s. vanishes since $dq_4^2/dz = 0$. We finally obtain

$$\frac{dC}{dz} = \frac{\partial C}{\partial z} - \frac{1}{1-z}\left(q_{3,\mu}\frac{\partial C}{\partial q_{3,\mu}} + q_{4,\mu}\frac{\partial C}{\partial q_{3,\mu}}\right) . \tag{2.5}$$

This is the differential equation with respect to z valid for a generic master integral $C(u, z)$.

3 Iterated integrals and Goncharov polylogarithms

The classical example of iterated integrals is given by the harmonic polylogarithms (HPLs) [38]. They generalise the ordinary polylogarithms and are defined by

$$H_{a_1,a_2,\ldots,a_n}(x) = \int_0^x dt\; f_{a_1}(t)\, H_{a_2,\ldots,a_n}(t)\,, \tag{3.1}$$

where the parameters a_i can be 0 or ± 1, and n is the weight of the HPL. The integral (3.1) diverges for HPLs with trailing zeroes. In order to handle HPLs in such cases, one defines $H_{\vec{0}_n}(x) = \frac{1}{n!}\ln^n(x)$. The weight functions $f_{a_i}(x)$ are simply

$$f_1(x) = \frac{1}{1-x}\,, \qquad f_0(x) = \frac{1}{x}\,, \qquad f_{-1}(x) = \frac{1}{1+x}\,. \tag{3.2}$$

The HPLs fulfil a Hopf algebra according to

$$H_{\vec{a}}(x)H_{\vec{b}}(x) = \sum_{\vec{c}\in\vec{a}\uplus\vec{b}} H_{\vec{c}}(x)\,, \tag{3.3}$$

where $\vec{a}\uplus\vec{b}$ are all possibilities of arranging the elements of $\vec{a}$ and $\vec{b}$ such that the internal order of the elements of $\vec{a}$ and $\vec{b}$ is preserved individually (cf. also [39]). Hence the product of two HPLs of weights w_1 and w_2 has weight $w_1 + w_2$. The Hopf algebra can also be used to extract singular behaviour near $x = 0$ or $x = 1$. Due to the relation

$$H_{0,\ldots,0,1}(1) = \zeta_k \tag{3.4}$$

with $k-1$ zeroes and $k > 1$, one also assigns the weight k to numbers like ζ_k and π^k.

JHEP04(2015)140

A generalisation of the HPLs are the Goncharov polylogarithms [40], whose definition reads

$$G_{a_1,a_2,\ldots,a_n}(x) = \int_0^x \frac{dt}{t-a_1}\, G_{a_2,\ldots,a_n}(t) \tag{3.5}$$

and $G_{\vec{0}_n}(x) = H_{\vec{0}_n}(x)$. They fulfil a Hopf algebra that has the same structure as (3.3), and allow for more general weights a_i than just 0 or ± 1. In particular, in multi-scale problems the argument x can be represented by one scale, and the remaining scales are comprised in the weights a_i. In our problem at hand, it is most convenient to choose u as the argument of the Goncharov polylogarithm whenever there is a dependence on this scale, bearing in mind that this choice simplifies a subsequent convolution with the light-cone distribution amplitude, which in a Gegenbauer expansion is a u-dependent polynomial. In this case the weights are either integer $(0, \pm 1)$ or one of the following six z-dependent weights,[1]

$$\begin{aligned} a_1 &= \frac{1}{1-z}\,, & a_3 &= \frac{1}{1-\sqrt{z}}\,, & a_5 &= \frac{\sqrt{z}}{\sqrt{z}-1}\,, \\ a_2 &= \frac{z}{z-1}\,, & a_4 &= \frac{1}{1+\sqrt{z}}\,, & a_6 &= \frac{\sqrt{z}}{\sqrt{z}+1}\,. \end{aligned} \tag{3.6}$$

Goncharov polylogarithms that do not depend on u are written in terms of integer weights and argument z or $\sqrt{z}$. Products of Goncharov polylogarithms of the same argument are expanded by means of the Hopf algebra.

4 The canonical basis

We work in dimensional regularisation with $D = 4-2\epsilon$ and evaluate the two-loop, two-scale master integrals by applying the method proposed by Henn [17]. Considering a specific power in the ϵ-expansion of a master integral, the associated function is called uniform if each summand has the same weight. Moreover, a uniform function is called pure, if its derivative with respect to any one of its arguments yields a uniform function whose weight is lowered by one unit.

The proposal in [17] now states that a basis $\vec{C}$ of master integrals can be found such that the system of differential equations in the kinematic variables x_j is given by

$$d_i \vec{C}(x_j, \epsilon) = \epsilon\, A_i(x_j) \vec{C}(x_j, \epsilon)\,, \tag{4.1}$$

where $d_i \equiv d/dx_i$. The $\vec{C}(x_j, \epsilon)$ denote the N master integrals and $A_i(x_j)$ are $N \times N$ matrices which are independent of ϵ. It turns out that eq. (4.1) can be expressed in a compact form

$$d\vec{C}(x_j, \epsilon) = \epsilon \left(d\, \tilde{A}(x_j)\right) \vec{C}(x_j, \epsilon)\,, \tag{4.2}$$

with the function $\tilde{A}$ determined by the differential $d_i \tilde{A} = A_i$. We note that $\tilde{A}$, together with the boundary conditions, completely determines the solution to a master integral. The

[1] The analytic results in section 6 contain only $a_1 - a_4$. The results of the "mass-flipped" integrals (see section 6 and [31]) contain also a_5 and a_6.

JHEP04(2015)140

master integrals in such a basis have in turn several pleasant features: first, the solution decouples order-by-order in the ϵ-expansion. Second, it is given by pure functions to all orders in ϵ. Consequently, assigning a weight -1 to each power of the expansion parameter ϵ and multiplying each master integral by an appropriate power of ϵ renders the total weight of the master integral to be zero to all orders. Third, the solution can be expressed in terms of iterated integrals. If the coefficients $A_i(x_j)$ are rational functions of the x_j, the Goncharov polylogarithms discussed above represent a suitable class of iterated integrals to describe the master integrals. We will refer to such a basis as a *canonical basis*.

In the absence of a completely general algorithm for the systematic construction of the canonical basis, the procedure of finding such a basis requires a certain amount of experience and experimentation. In our case, we start from a "traditional" basis that consists of undotted and singly-dotted integrals, and compute them up to terms that involve functions of weight two. For this task, alternative approaches like Feynman parameters or Mellin-Barnes representations [41, 42] have to be used. Afterwards one plugs these expressions into seemingly more complicated integrals like the ones in figures 2 and 3 and investigates if the resulting expressions are uniform or even pure. This method is mostly based on trial and error, but has proven to be successful as we show below.

In the case at hand, many master integrals can be adopted from several $B \to \pi\pi$ calculations [8–10, 43]. In order to describe the yet unknown ones in the canonical basis, a set of 39 integrals is needed. We obtain the following expressions for the canonical master integrals C_{1-39} in terms of the integrals I_{1-42}, which are defined in figures 2 and 3 ($\bar{x} = 1 - x$).

$$C_1(u,z) = \epsilon^3\, u\bar{z}\, I_1(u,z)\,, \tag{4.3}$$

$$C_2(u,z) = \epsilon^3\, u(z-1)z\, I_2(u,z)\,, \tag{4.4}$$

$$C_3(u,z) = \epsilon^3\, \bar{u}\bar{z}\, I_3(u,z)\,, \tag{4.5}$$

$$C_4(u,z) = \epsilon^3\, \bar{u}\bar{z}\, I_4(u,z)\,, \tag{4.6}$$

$$C_5(u,z) = \epsilon^3\, \bar{u}(z-1)\, I_5(u,z)\,, \tag{4.7}$$

$$C_6(u,z) = \epsilon^3\, \bar{u}(z-1)\, I_6(u,z)\,, \tag{4.8}$$

$$C_7(z) = \epsilon\,(1-\epsilon)\bar{z}\, I_7(z)\,, \tag{4.9}$$

$$C_8(u,z) = \epsilon^2\,(\bar{u} + uz)\, I_8(u,z)\,, \tag{4.10}$$

$$C_9(u,z) = \epsilon^2\, u\bar{z}\Big(I_9(u,z) + 2I_8(u,z)\Big)\,, \tag{4.11}$$

$$C_{10}(u,z) = \epsilon^2\,(u + \bar{u}z)\, I_{10}(u,z)\,, \tag{4.12}$$

$$C_{11}(u,z) = \epsilon^2\, u(z-1)\Big(I_{11}(u,z) + 2I_{10}(u,z)\Big)\,, \tag{4.13}$$

$$C_{12}(z) = \epsilon^2\, I_{12}(z)\,, \tag{4.14}$$

$$C_{13}(u,z) = \epsilon^4\, u\bar{z}\, I_{13}(u,z)\,, \tag{4.15}$$

$$C_{14}(z) = \epsilon^3\, \bar{z}\, I_{14}(z)\,, \tag{4.16}$$

JHEP04(2015)140

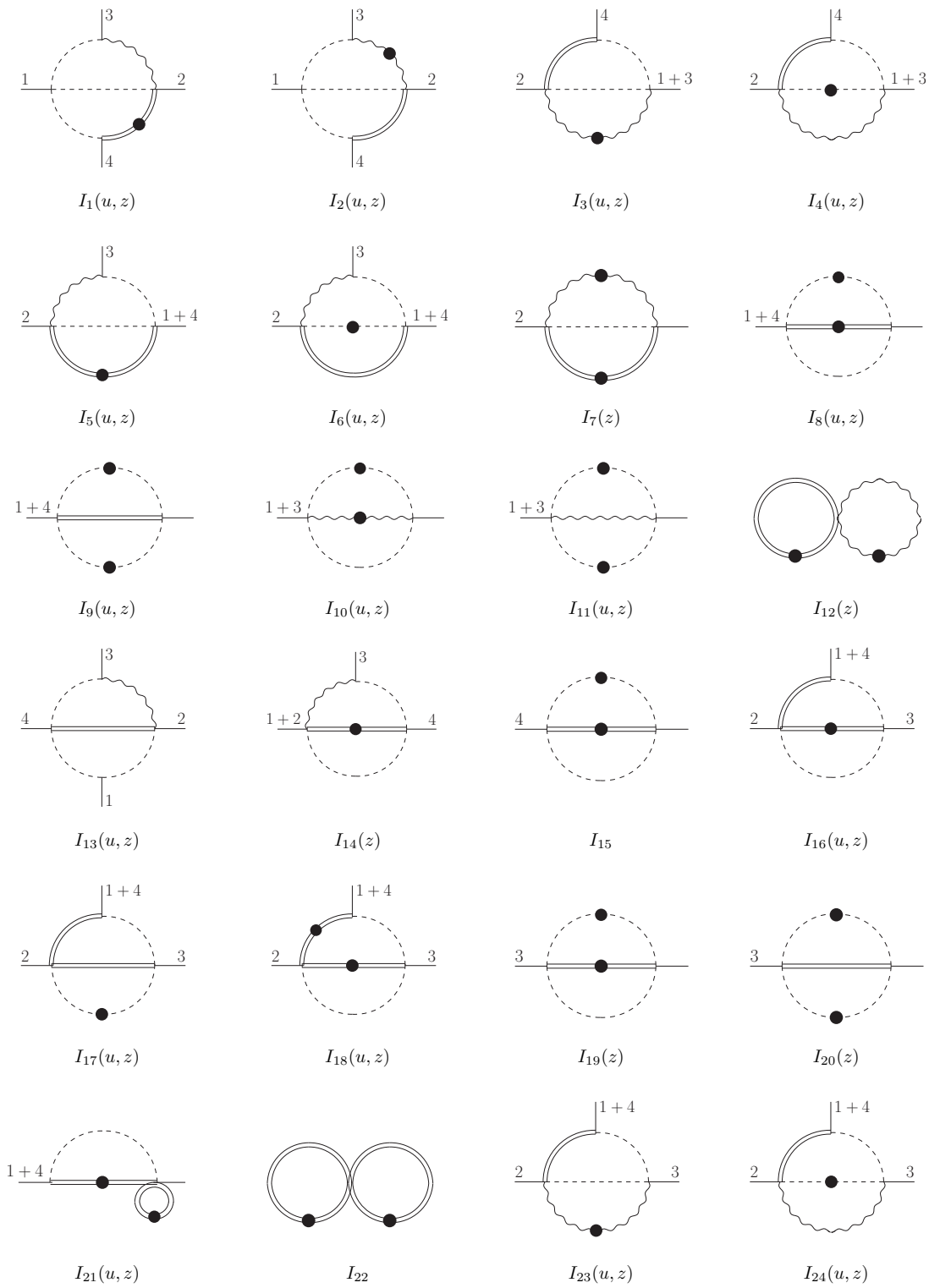

Figure 2. Part I of the basic integrals needed in the construction of the canonical basis: $1,\ldots,4$ denote the incoming momenta $q_1,\ldots,q_4$. The double/curly/dashed line represents a propagator with mass $m_b/m_c/0$. The dot on a line indicates a squared propagator.

JHEP04(2015)140

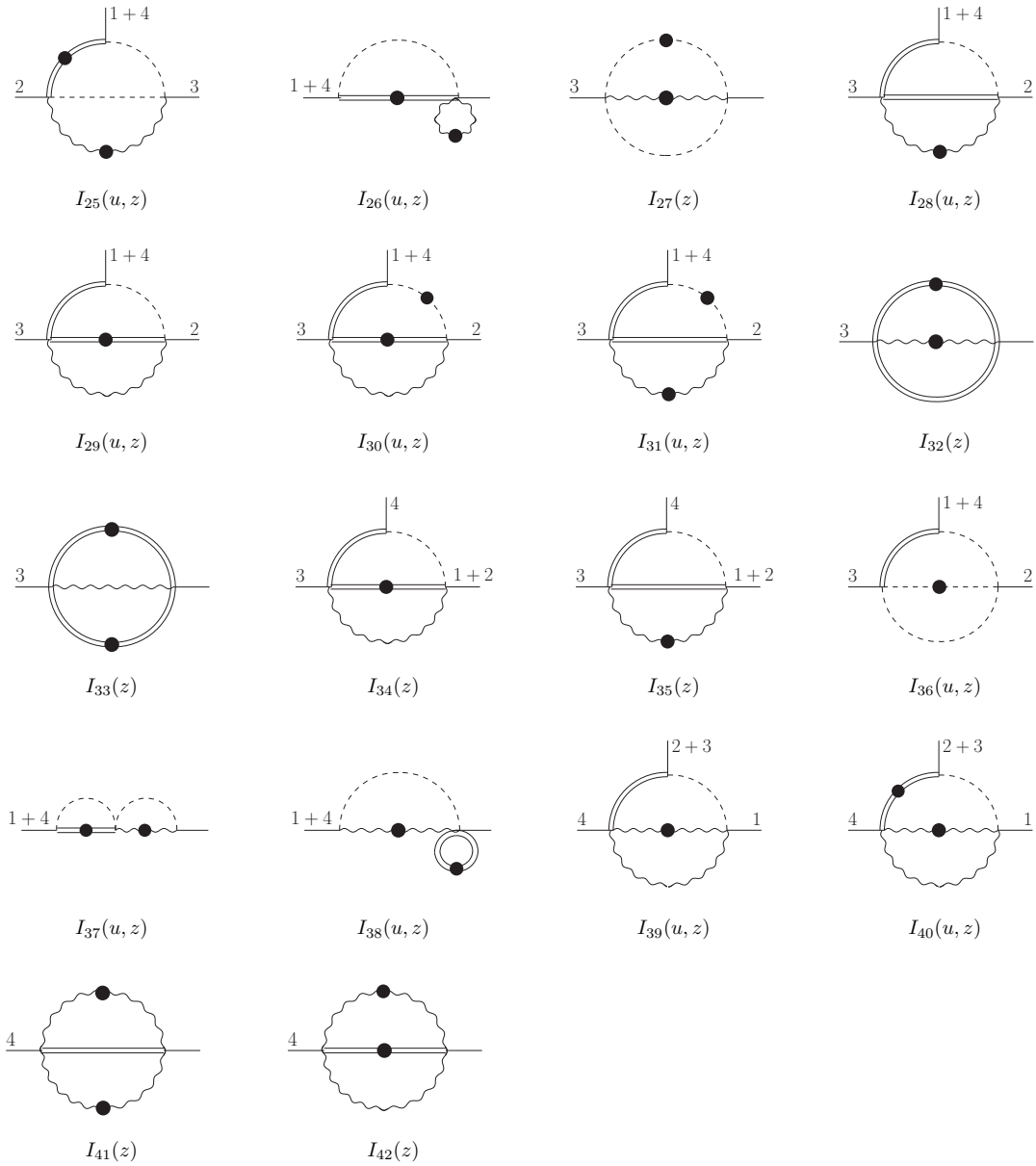

Figure 3. Part II of the basic integrals needed in the construction of the canonical basis. All symbols have the same meaning as in figure 2.

$$C_{15} = \epsilon^2 \, I_{15} \, , \tag{4.17}$$

$$C_{16}(u,z) = \epsilon^3 \, \bar{u}\bar{z} \, I_{16}(u,z) \, , \tag{4.18}$$

$$C_{17}(u,z) = \epsilon^3 \, \bar{u}\bar{z} \, I_{17}(u,z) \, , \tag{4.19}$$

$$C_{18}(u,z) = \epsilon^2 \, (1-\bar{u}\bar{z}) \left(I_{18}(u,z) + \frac{\epsilon}{m_b^2} I_{17}(u,z) + \frac{2\epsilon}{m_b^2} I_{16}(u,z) \right) \, , \tag{4.20}$$

$$C_{19}(z) = \epsilon^2 \, z \, I_{19}(z) \, , \tag{4.21}$$

JHEP04(2015)140

$$C_{20}(z) = \epsilon^2\, \bar{z} \left(I_{20}(z) + 2I_{19}(z) \right), \tag{4.22}$$

$$C_{21}(u,z) = \epsilon^2\, (1-u\bar{z})\, I_{21}(u,z)\,, \tag{4.23}$$

$$C_{22} = \epsilon^2\, I_{22}\,, \tag{4.24}$$

$$C_{23}(u,z) = \epsilon^3\, \bar{u}\bar{z}\, I_{23}(u,z)\,, \tag{4.25}$$

$$C_{24}(u,z) = \epsilon^3\, \bar{u}\bar{z}\, I_{24}(u,z)\,, \tag{4.26}$$

$$C_{25}(u,z) = \epsilon^2\, (1-\bar{u}\bar{z}) \left(I_{25}(u,z) + \frac{\epsilon}{m_b^2} I_{24}(u,z) + \frac{2\epsilon}{m_b^2} I_{23}(u,z) \right), \tag{4.27}$$

$$C_{26}(u,z) = \epsilon^2\, (1-u\bar{z})\, I_{26}(u,z)\,, \tag{4.28}$$

$$C_{27}(z) = \epsilon^2\, z\, I_{27}(z)\,, \tag{4.29}$$

$$C_{28}(u,z) = \epsilon^3\, \bar{u}\bar{z}\, I_{28}(u,z)\,, \tag{4.30}$$

$$C_{29}(u,z) = \epsilon^3\, \bar{u}\bar{z}\, I_{29}(u,z)\,, \tag{4.31}$$

$$C_{30}(u,z) = \frac{1}{2}\epsilon^2\, u\bar{u}\bar{z}^2 \left(I_{31}(u,z) + I_{30}(u,z) - \frac{1-\epsilon}{\epsilon} \frac{1}{m_b^2 u\bar{z}} I_7(z) \right), \tag{4.32}$$

$$C_{31}(z) = \epsilon^2\, z\, I_{32}(z)\,, \tag{4.33}$$

$$C_{32}(z) = \epsilon^2\, \sqrt{z} \left(I_{33}(z) + 2I_{32}(z) \right), \tag{4.34}$$

$$C_{33}(z) = \epsilon^3\, \bar{z}\, I_{34}(z)\,, \tag{4.35}$$

$$C_{34}(z) = \epsilon^3\, \bar{z}\, I_{35}(z)\,, \tag{4.36}$$

$$C_{35}(u,z) = \epsilon^3\, \bar{u}\bar{z}\, I_{36}(u,z)\,, \tag{4.37}$$

$$C_{36}(u,z) = \epsilon^2\, (1-u\bar{z})^2\, I_{37}(u,z)\,, \tag{4.38}$$

$$C_{37}(u,z) = \epsilon^2\, (1-u\bar{z})\, I_{38}(u,z)\,, \tag{4.39}$$

$$C_{38}(u,z) = \epsilon^3\, u\bar{z}\, I_{39}(u,z)\,, \tag{4.40}$$

$$\begin{aligned} C_{39}(u,z) = \epsilon^2 \Bigg\{ & u\bar{z}\, \left[1-(1-u\bar{z})p\right] I_{40}(u,z) \\ & - \frac{1}{m_b^2} \left(\sqrt{z} - \frac{1-(1-u\bar{z})p}{2} \right) \left(I_{41}(z) + 2I_{42}(z) \right) \Bigg\}, \end{aligned} \tag{4.41}$$

with

$$p = \frac{1-\sqrt{(2-u\bar{z})^2 - 4\bar{z}(1-u\bar{z})}}{1-u\bar{z}}\,. \tag{4.42}$$

Note that the master integrals have to be evaluated to $\mathcal{O}(\epsilon^4)$ since the two-loop amplitude contains poles up to $1/\epsilon^4$ stemming from the infrared and ultraviolet regions. A few exceptions are $C_{26,38}$ and C_{39} which only enter the hard-scattering kernel to order $\mathcal{O}(\epsilon^3)$ and $\mathcal{O}(\epsilon^2)$, respectively.

JHEP04(2015)140

5 Boundary conditions

Before we present the differential equations, we specify the boundary conditions that are used to completely fix the solution. In the simplest cases, the master integrals vanish in a specific kinematic point. This is the case for $C_{13,38,39}$, which vanish in $u = 0$, whereas $C_{3,4,5,6,16,17,23,24,28,29,30,35}$ vanish in $u = 1$. Moreover, $C_{19,31,32}$ vanish in $z = 0$, whereas $C_{7,14,33,34}$ vanish in $z = 1$. In other cases we find special relations between integrals, that hold either in general, or in certain kinematic points, and can be used as boundary conditions. Examples are the relation $C_{26} = z^{-\epsilon} C_{21}$, or the following relations that hold in $u = 1$,

$$\begin{aligned} C_8 &\xrightarrow{u\to 1} C_{19}\,, & C_{10} &\xrightarrow{u\to 1} C_{19}^{\leftrightarrow}\,, \\ C_9 &\xrightarrow{u\to 1} C_{20}\,, & C_{11} &\xrightarrow{u\to 1} C_{20}^{\leftrightarrow}\,, \end{aligned} \tag{5.1}$$

where the symbol "$\leftrightarrow$" is used for the corresponding "mass-flipped" integral, in which $m_c \leftrightarrow m_b$ and $q_3 \leftrightarrow q_4$, see section 6 for more details. Hence, the integrals $C_{19,20}^{\leftrightarrow}$ can be easily obtained from $C_{19,20}$ or from [31]. Relations that have a similar structure than (5.1) hold in $z = 1$ for

$$C_{12} \xrightarrow{z\to 1} C_{22}\,, \qquad C_{27} \xrightarrow{z\to 1} C_{15}\,. \tag{5.2}$$

For the remaining integrals we either use that they assume simple, closed forms that are valid to all orders in the ϵ-expansion, or asymptotic forms as $u \to 0$ or $z \to 0$. Examples of the former type are (see below in section 6 for the precise definition of $\tilde{C}_i$)

$$\begin{aligned} \tilde{C}_{15} &= -\frac{\Gamma^4(1-\epsilon)\Gamma(1-4\epsilon)\Gamma(1+\epsilon)\Gamma(1+2\epsilon)}{4\Gamma(1-3\epsilon)\Gamma(1-2\epsilon)}\,, \\ \tilde{C}_{22} &= \Gamma^2(1-\epsilon)\Gamma^2(1+\epsilon)\,, \\ \tilde{C}_{36} &= \left[-\frac{\epsilon\,(1-u\bar{z})}{(1-\epsilon)}\,\Gamma(1-\epsilon)\,\Gamma(1+\epsilon)\;{}_2F_1\left(1,1+\epsilon\,;\,2-\epsilon\,;\,\bar{u}+uz\right)\right] \\ &\quad\times\left[-\frac{\epsilon\,z^{-\epsilon}\,(1-u\bar{z})}{(1-\epsilon)z}\,\Gamma(1-\epsilon)\,\Gamma(1+\epsilon)\;{}_2F_1\left(1,1+\epsilon\,;\,2-\epsilon\,;\,u+\frac{\bar{u}}{z}\right)\right]\,, \end{aligned} \tag{5.3}$$

where for C_{36} we give the result for each loop separately, such that also the boundary conditions for $C_{21,37}$ can be read off. Asymptotic expansions as $u \to 0$ or $z \to 0$ were derived by means of `MBasymptotics.m` [44] for

$$\begin{aligned} \tilde{C}_{20} &\overset{z\to 0}{=} -1 - \frac{2\pi^2}{3}\epsilon^2 + 2\zeta_3\epsilon^3 - \frac{5\pi^4}{18}\epsilon^4 + \mathcal{O}(\epsilon^5, z), \\ \tilde{C}_1 &\overset{u\to 0}{=} \frac{1}{24} + \epsilon\left[-\frac{1}{6}\ln(u) + \frac{1}{8}G_0(z) - \frac{1}{6}G_1(z) + \frac{1}{4}i\pi\right] \\ &\quad + \epsilon^2\left[\frac{1}{3}\ln^2(u) + \left(\frac{2}{3}G_1(z) - \frac{1}{2}G_0(z) - i\pi\right)\ln(u) + \frac{3}{4}i\pi G_0(z) - i\pi G_1(z) + \frac{3}{8}G_{0,0}(z)\right. \\ &\quad \left. - \frac{1}{2}G_{0,1}(z) - \frac{1}{2}G_{1,0}(z) + \frac{2}{3}G_{1,1}(z) - \frac{37\pi^2}{72}\right] \end{aligned}$$

JHEP04(2015)140

$$
\begin{aligned}
&+\epsilon^3\Big[-\frac{4}{9}\ln^3(u)+(G_0(z)-\frac{4}{3}G_1(z)+2i\pi)\ln^2(u)+\Big(4i\pi G_1(z)-3i\pi G_0(z)\\
&-\frac{3}{2}G_{0,0}(z)+2G_{0,1}(z)+2G_{1,0}(z)-\frac{8}{3}G_{1,1}(z)+\frac{37\pi^2}{18}\Big)\ln(u)-\frac{37\pi^2}{24}G_0(z)\\
&+\frac{37\pi^2}{18}G_1(z)+\frac{5}{4}i\pi G_{0,0}(z)-3i\pi G_{0,1}(z)-2i\pi G_{1,0}(z)+4i\pi G_{1,1}(z)+\frac{1}{8}G_{0,0,0}(z)\\
&-\frac{3}{2}G_{0,0,1}(z)-\frac{3}{2}G_{0,1,0}(z)+2G_{0,1,1}(z)-\frac{1}{2}G_{1,0,0}(z)+2G_{1,0,1}(z)+2G_{1,1,0}(z)\\
&-\frac{8}{3}G_{1,1,1}(z)-\frac{17}{6}\zeta_3-\frac{7}{12}i\pi^3\Big]\\
&+\epsilon^4\Big[\frac{4}{9}\ln^4(u)+\Big(\frac{16}{9}G_1(z)-\frac{4}{3}G_0(z)-\frac{8}{3}i\pi\Big)\ln^3(u)+\Big(6i\pi G_0(z)-8i\pi G_1(z)\\
&+3G_{0,0}(z)-4G_{0,1}(z)-4G_{1,0}(z)+\frac{16}{3}G_{1,1}(z)-\frac{37\pi^2}{9}\Big)\ln^2(u)+\Big(\frac{37\pi^2}{6}G_0(z)\\
&-\frac{74\pi^2}{9}G_1(z)-5i\pi G_{0,0}(z)+12i\pi G_{0,1}(z)+8i\pi G_{1,0}(z)-16i\pi G_{1,1}(z)+\frac{34}{3}\zeta_3\\
&-\frac{1}{2}G_{0,0,0}(z)+6G_{0,0,1}(z)+6G_{0,1,0}(z)-8G_{0,1,1}(z)+2G_{1,0,0}(z)-8G_{1,0,1}(z)\\
&-8G_{1,1,0}(z)+\frac{32}{3}G_{1,1,1}(z)+\frac{7}{3}i\pi^3\Big)\ln(u)-\frac{17}{12}i\pi^3G_0(z)+2i\pi^3G_1(z)-8G_{1,0,1,1}(z)\\
&-\frac{35\pi^2}{24}G_{0,0}(z)+\frac{37\pi^2}{6}G_{0,1}(z)+3\pi^2G_{1,0}(z)-\frac{74\pi^2}{9}G_{1,1}(z)+\frac{3}{4}i\pi G_{0,0,0}(z)\\
&-5i\pi G_{0,0,1}(z)-4i\pi G_{0,1,0}(z)+12i\pi G_{0,1,1}(z)-2i\pi G_{1,0,0}(z)+8i\pi G_{1,0,1}(z)\\
&+6i\pi G_{1,1,0}(z)-16i\pi G_{1,1,1}(z)+\frac{3}{8}G_{0,0,0,0}(z)-\frac{1}{2}G_{0,0,0,1}(z)-\frac{3}{2}G_{0,0,1,0}(z)\\
&+6G_{0,0,1,1}(z)+\frac{1}{2}G_{0,1,0,0}(z)+6G_{0,1,0,1}(z)+6G_{0,1,1,0}(z)-8G_{0,1,1,1}(z)+\frac{82\pi^4}{135}\\
&-\frac{1}{2}G_{1,0,0,0}(z)+2G_{1,0,0,1}(z)+3G_{1,0,1,0}(z)-8G_{1,1,0,1}(z)-8G_{1,1,1,0}(z)\\
&+\frac{32}{3}G_{1,1,1,1}(z)-\frac{17}{2}G_0(z)\zeta_3+\frac{34}{3}G_1(z)\zeta_3-12i\pi\zeta_3\Big]+\mathcal{O}(\epsilon^5,u),
\end{aligned}
\tag{5.4}
$$

$$
\begin{aligned}
\tilde{C}_2 \overset{u\to 0}{=}\ & \frac{1}{24}+\epsilon\Big[-\frac{1}{6}\ln(u)-\frac{1}{24}G_0(z)-\frac{1}{6}G_1(z)-\frac{1}{12}i\pi\Big]\\
&+\epsilon^2\Big[\frac{1}{3}\ln^2(u)+(\frac{1}{6}G_0(z)+\frac{2}{3}G_1(z)+\frac{1}{3}i\pi)\ln(u)+\frac{1}{12}i\pi G_0(z)+\frac{1}{3}i\pi G_1(z)\\
&+\frac{1}{24}G_{0,0}(z)+\frac{1}{6}G_{0,1}(z)+\frac{1}{6}G_{1,0}(z)+\frac{2}{3}G_{1,1}(z)+\frac{11\pi^2}{72}\Big]\\
&+\epsilon^3\Big[-\frac{4}{9}\ln^3(u)+\Big(-\frac{1}{3}G_0(z)-\frac{4}{3}G_1(z)-\frac{2}{3}i\pi\Big)\ln^2(u)+\Big(-\frac{1}{3}i\pi G_0(z)-\frac{4}{3}i\pi G_1(z)\\
&-\frac{1}{6}G_{0,0}(z)-\frac{2}{3}G_{0,1}(z)-\frac{2}{3}G_{1,0}(z)-\frac{8}{3}G_{1,1}(z)-\frac{11\pi^2}{18}\Big)\ln(u)-\frac{11\pi^2}{72}G_0(z)\\
&-\frac{11\pi^2}{18}G_1(z)-\frac{1}{12}i\pi G_{0,0}(z)-\frac{1}{3}i\pi G_{0,1}(z)+\frac{2}{3}i\pi G_{1,0}(z)-\frac{4}{3}i\pi G_{1,1}(z)
\end{aligned}
$$

JHEP04(2015)140

$$
\begin{aligned}
&-\frac{1}{24}G_{0,0,0}(z)-\frac{1}{6}G_{0,0,1}(z)-\frac{1}{6}G_{0,1,0}(z)-\frac{2}{3}G_{0,1,1}(z)+\frac{5}{6}G_{1,0,0}(z)-\frac{2}{3}G_{1,0,1}(z)\\
&-\frac{2}{3}G_{1,1,0}(z)-\frac{8}{3}G_{1,1,1}(z)-\frac{17}{6}\zeta_3-\frac{1}{4}i\pi^3\Big]\\
&+\epsilon^4\Big[\frac{4}{9}\ln^4(u)+\Big(\frac{4}{9}G_0(z)+\frac{16}{9}G_1(z)+\frac{8}{9}i\pi\Big)\ln^3(u)+\Big(\frac{2}{3}i\pi G_0(z)+\frac{8}{3}i\pi G_1(z)\\
&+\frac{1}{3}G_{0,0}(z)+\frac{4}{3}G_{0,1}(z)+\frac{4}{3}G_{1,0}(z)+\frac{16}{3}G_{1,1}(z)+\frac{11\pi^2}{9}\Big)\ln^2(u)+\Big(\frac{11\pi^2}{18}G_0(z)\\
&+\frac{22\pi^2}{9}G_1(z)+\frac{1}{3}i\pi G_{0,0}(z)+\frac{4}{3}i\pi G_{0,1}(z)-\frac{8}{3}i\pi G_{1,0}(z)+\frac{16}{3}i\pi G_{1,1}(z)\\
&+\frac{1}{6}G_{0,0,0}(z)+\frac{2}{3}G_{0,0,1}(z)+\frac{2}{3}G_{0,1,0}(z)+\frac{8}{3}G_{0,1,1}(z)-\frac{10}{3}G_{1,0,0}(z)+\frac{8}{3}G_{1,0,1}(z)\\
&+\frac{8}{3}G_{1,1,0}(z)+\frac{32}{3}G_{1,1,1}(z)+\frac{34}{3}\zeta_3+i\pi^3\Big)\ln(u)+\frac{1}{4}i\pi^3G_0(z)+\frac{2}{3}i\pi^3G_1(z)\\
&+\frac{11\pi^2}{72}G_{0,0}(z)+\frac{11\pi^2}{18}G_{0,1}(z)-\frac{5\pi^2}{9}G_{1,0}(z)+\frac{22\pi^2}{9}G_{1,1}(z)+\frac{1}{12}i\pi G_{0,0,0}(z)\\
&+\frac{1}{3}i\pi G_{0,0,1}(z)-\frac{2}{3}i\pi G_{0,1,0}(z)+\frac{4}{3}i\pi G_{0,1,1}(z)+\frac{10}{3}i\pi G_{1,0,0}(z)-\frac{8}{3}i\pi G_{1,0,1}(z)\\
&-\frac{14}{3}i\pi G_{1,1,0}(z)+\frac{16}{3}i\pi G_{1,1,1}(z)+\frac{1}{24}G_{0,0,0,0}(z)+\frac{1}{6}G_{0,0,0,1}(z)+\frac{1}{6}G_{0,0,1,0}(z)\\
&+\frac{2}{3}G_{0,0,1,1}(z)-\frac{5}{6}G_{0,1,0,0}(z)+\frac{2}{3}G_{0,1,0,1}(z)+\frac{2}{3}G_{0,1,1,0}(z)+\frac{8}{3}G_{0,1,1,1}(z)-\frac{4}{3}i\pi\zeta_3\\
&+\frac{19}{6}G_{1,0,0,0}(z)-\frac{10}{3}G_{1,0,0,1}(z)-\frac{7}{3}G_{1,0,1,0}(z)+\frac{8}{3}G_{1,0,1,1}(z)-\frac{16}{3}G_{1,1,0,0}(z)+\frac{49\pi^4}{135}\\
&+\frac{8}{3}G_{1,1,0,1}(z)+\frac{8}{3}G_{1,1,1,0}(z)+\frac{32}{3}G_{1,1,1,1}(z)+\frac{17}{6}G_0(z)\zeta_3+\frac{34}{3}G_1(z)\zeta_3\Big]+\mathcal{O}(\epsilon^5,u),
\end{aligned}
\tag{5.5}
$$

$$
\begin{aligned}
\tilde{C}_{18}\overset{u\to 0}{=}{}&\epsilon^2[G_1(z)\ln(u)-G_{0,1}(z)+G_{1,1}(z)]\\
&+\epsilon^3\Big[(G_{0,1}(z)-6G_{1,1}(z))\ln(u)-G_1(z)\ln^2(u)+\frac{\pi^2}{6}G_1(z)+5G_{0,1,1}(z)-6G_{1,1,1}(z)\Big]\\
&+\epsilon^4\Big[\frac{2}{3}\ln^3(u)G_1(z)+(6G_{1,1}(z)-G_{0,1}(z))\ln^2(u)+\Big(\frac{2\pi^2}{3}G_1(z)+G_{0,0,1}(z)\\
&-6G_{0,1,1}(z)-4G_{1,0,1}(z)+28G_{1,1,1}(z)\Big)\ln(u)+5\zeta_3G_1(z)-\frac{5\pi^2}{6}G_{0,1}(z)\\
&+\frac{\pi^2}{3}G_{1,1}(z)-G_{0,0,0,1}(z)+G_{0,0,1,1}(z)+4G_{0,1,0,1}(z)-22G_{0,1,1,1}(z)+4G_{1,0,0,1}(z)\\
&-4G_{1,0,1,1}(z)+2G_{1,1,0,1}(z)+28G_{1,1,1,1}(z)\Big]+\mathcal{O}(\epsilon^5,u),
\end{aligned}
\tag{5.6}
$$

$$
\begin{aligned}
\tilde{C}_{25}\overset{u\to 0}{=}{}&\epsilon^2\Big[\frac{\ln^2(u)}{2}+(G_1(z)-G_0(z))\ln(u)+G_{0,0}(z)-G_{0,1}(z)-G_{1,0}(z)+G_{1,1}(z)+\frac{\pi^2}{2}\Big]\\
&+\epsilon^3\Big[-\ln^3(u)+\Big(\frac{3}{2}G_0(z)-3G_1(z)\Big)\ln^2(u)+(3G_{0,1}(z)+2G_{1,0}(z)-6G_{1,1}(z)
\end{aligned}
$$

JHEP04(2015)140

$$
\begin{aligned}
&- \pi^2) \ln(u) - \frac{\pi^2}{2} G_0(z) - \frac{7\pi^2}{6} G_1(z) - 3G_{0,0,0}(z) + G_{0,1,0}(z) + 3G_{0,1,1}(z) \\
&+ 2G_{1,0,1}(z) + 2G_{1,1,0}(z) - 6G_{1,1,1}(z) \Big] \\
&+ \epsilon^4 \Big[\frac{7}{6} \ln^4(u) + \left(\frac{14}{3} G_1(z) - \frac{5}{3} G_0(z) \right) \ln^3(u) + \Big(\frac{1}{2} G_{0,0}(z) - 5G_{0,1}(z) - 3G_{1,0}(z) \\
&+ 14G_{1,1}(z) + \frac{7\pi^2}{3} \Big) \ln^2(u) + \Big(5\pi^2 G_1(z) - \frac{5\pi^2}{3} G_0(z) - G_{0,0,0}(z) + G_{0,0,1}(z) \\
&- 10G_{0,1,1}(z) + 2G_{1,0,0}(z) - 6G_{1,0,1}(z) - 4G_{1,1,0}(z) + 28G_{1,1,1}(z) + 6\zeta_3 \Big) \ln(u) \\
&- 6\zeta_3 G_0(z) + 3\zeta_3 G_1(z) + \frac{19\pi^2}{6} G_{0,0}(z) - \frac{3\pi^2}{2} G_{0,1}(z) - \frac{5\pi^2}{3} G_{1,0}(z) + \frac{16\pi^2}{3} G_{1,1}(z) \\
&+ 10G_{0,0,0,0}(z) - G_{0,0,0,1}(z) - 3G_{0,0,1,0}(z) + G_{0,0,1,1}(z) - 2G_{0,1,0,0}(z) - 2G_{0,1,1,0}(z) \\
&- 10G_{0,1,1,1}(z) - 2G_{1,0,0,0}(z) + 2G_{1,0,0,1}(z) + 2G_{1,0,1,0}(z) - 6G_{1,0,1,1}(z) \\
&+ 2G_{1,1,0,0}(z) - 4G_{1,1,0,1}(z) - 4G_{1,1,1,0}(z) + 28G_{1,1,1,1}(z) + \frac{16\pi^4}{15} \Big] + \mathcal{O}(\epsilon^5, u). \qquad (5.7)
\end{aligned}
$$

6 Results

In order to facilitate the presentation of the results we write the master integrals as

$$
C = - S_\Gamma^2 \left(m_b^2\right)^{D-n} \tilde{C}\,, \qquad (6.1)
$$

with an integer n that denotes the sum of all propagator powers, such that the integral $\tilde{C}$ is dimensionless. Our integration measure is $\int d^D k/(2\pi)^D$ per loop and we use the pre-factor

$$
S_\Gamma = \frac{1}{(4\pi)^{D/2}\, \Gamma(1-\epsilon)}\,. \qquad (6.2)
$$

Besides the integrals defined in section 4, the QCD amplitude also contains the same set of integrals but with $m_c \leftrightarrow m_b$ and $q_3 \leftrightarrow q_4$. We will refer to these as "mass-flipped" integrals and denote them as $C^{\leftrightarrow}$, see section 5. However, we note here that in order to define $\tilde{C}^{\leftrightarrow}$ we factor out an appropriate power of m_b, rather than m_c.

As stated earlier the QCD amplitude requires terms of order $\mathcal{O}(\epsilon^4)$ for most of the integrals. However, in order to keep the paper at a reasonable length, we only give terms up to order $\mathcal{O}(\epsilon^3)$ explicitly below. If desired, terms of weight four can be derived from the $\tilde{A}$ and the boundary condition, which we actually give to weight four. Moreover, we refrain from presenting the "mass-flipped" integrals explicitly. They can be obtained by letting $z \to 1/z$, keeping in mind that analytic continuation is done via $z \to z - i\eta$, with infinitesimal $\eta > 0$. We provide the results to all integrals, including the "mass-flipped" ones, to order $\mathcal{O}(\epsilon^4)$ in electonic form in [31].

Last but not least, instead of dealing with one large 39×39 system of equations, we solve each topology separately and therefore deal with several, smaller matrices $\tilde{A}_i$ which we collect in appendix A. This finally puts us in the position to present the analytic results to the C_{1-39}.

JHEP04(2015)140

6.1 $C_1 - C_{12}$

We start right away with the largest topology, which contains twelve integrals,

$$\vec{C} = \left\{\tilde{C}_1, \tilde{C}_2, \tilde{C}_3, \tilde{C}_4, \tilde{C}_5, \tilde{C}_6, \tilde{C}_7, \tilde{C}_8, \tilde{C}_9, \tilde{C}_{10}, \tilde{C}_{11}, \tilde{C}_{12}\right\} . \tag{6.3}$$

The corresponding matrix is $\tilde{A}_{1-12}$. Taking into account the boundary conditions specified in the previous section, the solution to the twelve integrals reads

$$\begin{aligned}
\tilde{C}_1 =& \frac{1}{24} + \epsilon\Big[-\frac{1}{6}G_0(u) + \frac{1}{8}G_0(z) - \frac{1}{6}G_1(z) + \frac{1}{4}i\pi\Big] \\
&+ \epsilon^2\Big[-\frac{1}{2}G_0(z)G_0(u) + \frac{2}{3}G_1(z)G_0(u) - i\pi G_0(u) + \frac{3}{4}i\pi G_0(z) - i\pi G_1(z) \\
&+ \frac{1}{2}G_0(z)G_{a_2}(u) - \frac{1}{2}G_1(z)G_{a_2}(u) + \frac{1}{2}i\pi G_{a_2}(u) + \frac{2}{3}G_{0,0}(u) + \frac{3}{8}G_{0,0}(z) - \frac{1}{2}G_{0,1}(z) \\
&- \frac{1}{2}G_{1,0}(z) + \frac{2}{3}G_{1,1}(z) - \frac{1}{2}G_{a_2,0}(u) - \frac{37\pi^2}{72}\Big] \\
&+ \epsilon^3\Big[-3i\pi G_0(z)G_0(u) + 4i\pi G_1(z)G_0(u) - \frac{3}{2}G_{0,0}(z)G_0(u) + 2G_{0,1}(z)G_0(u) \\
&+ 2G_{1,0}(z)G_0(u) - \frac{8}{3}G_{1,1}(z)G_0(u) + \frac{37\pi^2}{18}G_0(u) - \frac{37\pi^2}{24}G_0(z) + i\pi G_0(z)G_1(u) \\
&+ \frac{37\pi^2}{18}G_1(z) + \frac{1}{2}i\pi G_0(z)G_{a_2}(u) - 2i\pi G_1(z)G_{a_2}(u) - \frac{13\pi^2}{12}G_{a_2}(u) + 2G_0(z)G_{0,0}(u) \\
&- \frac{8}{3}G_1(z)G_{0,0}(u) + 4i\pi G_{0,0}(u) + G_1(u)G_{0,0}(z) - G_{a_2}(u)G_{0,0}(z) + \frac{5}{4}i\pi G_{0,0}(z) \\
&- \frac{1}{2}G_{a_2}(u)G_{0,1}(z) - 3i\pi G_{0,1}(z) - 2G_0(z)G_{0,a_2}(u) + 2G_1(z)G_{0,a_2}(u) - 2i\pi G_{0,a_2}(u) \\
&- \frac{1}{2}G_{a_2}(u)G_{1,0}(z) - 2i\pi G_{1,0}(z) + 2G_{a_2}(u)G_{1,1}(z) + 4i\pi G_{1,1}(z) - G_1(z)G_{1,a_1}(u) \\
&+ G_0(z)G_{1,a_2}(u) - G_1(z)G_{1,a_2}(u) + i\pi G_{1,a_2}(u) - \frac{1}{2}G_0(z)G_{a_2,0}(u) + 2G_1(z)G_{a_2,0}(u) \\
&- 2i\pi G_{a_2,0}(u) - \frac{1}{2}G_0(z)G_{a_2,a_2}(u) + \frac{1}{2}G_1(z)G_{a_2,a_2}(u) - \frac{1}{2}i\pi G_{a_2,a_2}(u) - \frac{8}{3}G_{0,0,0}(u) \\
&+ \frac{1}{8}G_{0,0,0}(z) - \frac{3}{2}G_{0,0,1}(z) - \frac{3}{2}G_{0,1,0}(z) + 2G_{0,1,1}(z) + 2G_{0,a_2,0}(u) - \frac{1}{2}G_{1,0,0}(z) \\
&+ 2G_{1,0,1}(z) + 2G_{1,1,0}(z) - \frac{8}{3}G_{1,1,1}(z) - G_{1,a_1,0}(u) - G_{1,a_2,0}(u) + 2G_{a_2,0,0}(u) \\
&+ \frac{1}{2}G_{a_2,a_2,0}(u) - \frac{17}{6}\zeta_3 - \frac{7}{12}i\pi^3\Big] + \mathcal{O}(\epsilon^4),
\end{aligned} \tag{6.4}$$

$$\begin{aligned}
\tilde{C}_2 =& \frac{1}{24} + \epsilon\Big[-\frac{1}{6}G_0(u) - \frac{1}{24}G_0(z) - \frac{1}{6}G_1(z) - \frac{1}{12}i\pi\Big] \\
&+ \epsilon^2\Big[\frac{1}{6}G_0(z)G_0(u) + \frac{2}{3}G_1(z)G_0(u) + \frac{1}{3}i\pi G_0(u) + \frac{1}{12}i\pi G_0(z) + \frac{1}{3}i\pi G_1(z) \\
&- \frac{1}{2}G_1(z)G_{a_1}(u) + \frac{2}{3}G_{0,0}(u) + \frac{1}{24}G_{0,0}(z) + \frac{1}{6}G_{0,1}(z) + \frac{1}{6}G_{1,0}(z) + \frac{2}{3}G_{1,1}(z) \\
&- \frac{1}{2}G_{a_1,0}(u) + \frac{11\pi^2}{72}\Big]
\end{aligned}$$

JHEP04(2015)140

$$
\begin{aligned}
&+\epsilon^3\Big[-\frac{1}{3}i\pi G_0(z)G_0(u)-\frac{4}{3}i\pi G_1(z)G_0(u)-\frac{1}{6}G_{0,0}(z)G_0(u)-\frac{2}{3}G_{0,1}(z)G_0(u)\\
&-\frac{2}{3}G_{1,0}(z)G_0(u)-\frac{8}{3}G_{1,1}(z)G_0(u)-\frac{11\pi^2}{18}G_0(u)-\frac{11\pi^2}{72}G_0(z)+i\pi G_0(z)G_1(u)\\
&-\frac{11\pi^2}{18}G_1(z)-\frac{\pi^2}{12}G_{a_1}(u)-\frac{2}{3}G_0(z)G_{0,0}(u)-\frac{8}{3}G_1(z)G_{0,0}(u)-\frac{4}{3}i\pi G_{0,0}(u)\\
&+G_1(u)G_{0,0}(z)-\frac{1}{12}i\pi G_{0,0}(z)-\frac{1}{2}G_{a_1}(u)G_{0,1}(z)-\frac{1}{3}i\pi G_{0,1}(z)+2G_1(z)G_{0,a_1}(u)\\
&-\frac{1}{2}G_{a_1}(u)G_{1,0}(z)+\frac{2}{3}i\pi G_{1,0}(z)+2G_{a_1}(u)G_{1,1}(z)-\frac{4}{3}i\pi G_{1,1}(z)-G_1(z)G_{1,a_1}(u)\\
&+G_0(z)G_{1,a_2}(u)-G_1(z)G_{1,a_2}(u)+i\pi G_{1,a_2}(u)-\frac{1}{2}G_0(z)G_{a_1,0}(u)+2G_1(z)G_{a_1,0}(u)\\
&+\frac{1}{2}G_1(z)G_{a_1,a_1}(u)-\frac{8}{3}G_{0,0,0}(u)-\frac{1}{24}G_{0,0,0}(z)-\frac{1}{6}G_{0,0,1}(z)-\frac{1}{6}G_{0,1,0}(z)\\
&-\frac{2}{3}G_{0,1,1}(z)+2G_{0,a_1,0}(u)+\frac{5}{6}G_{1,0,0}(z)-\frac{2}{3}G_{1,0,1}(z)-\frac{2}{3}G_{1,1,0}(z)-\frac{8}{3}G_{1,1,1}(z)\\
&-G_{1,a_1,0}(u)-G_{1,a_2,0}(u)+2G_{a_1,0,0}(u)+\frac{1}{2}G_{a_1,a_1,0}(u)-\frac{17}{6}\zeta_3-\frac{1}{4}i\pi^3\Big]+\mathcal{O}(\epsilon^4),
\end{aligned}
\tag{6.5}
$$

$$
\begin{aligned}
\tilde{C}_3=&\epsilon^3\Big[i\pi G_{a_2}(u)G_0(z)-G_{a_2,0}(u)G_0(z)+2G_{a_2,a_2}(u)G_0(z)+\frac{\pi^2}{2}G_0(z)+\frac{\pi^2}{3}G_{a_2}(u)\\
&+2G_{a_2}(u)G_{0,0}(z)-G_{a_2}(u)G_{0,1}(z)-G_{a_2}(u)G_{1,0}(z)-2G_1(z)G_{a_2,a_2}(u)\\
&+2i\pi G_{a_2,a_2}(u)+G_{0,0,0}(z)-G_{0,1,0}(z)-2G_{a_2,a_2,0}(u)+2\zeta_3\Big]+\mathcal{O}(\epsilon^4),
\end{aligned}
\tag{6.6}
$$

$$
\begin{aligned}
\tilde{C}_4=&\epsilon^2\Big[G_0(u)G_0(z)-G_{a_2}(u)G_0(z)-i\pi G_0(z)+G_1(z)G_{a_2}(u)-i\pi G_{a_2}(u)-G_{0,0}(z)\\
&+G_{0,1}(z)+G_{a_2,0}(u)+\frac{\pi^2}{6}\Big]\\
&+\epsilon^3\Big[4i\pi G_0(z)G_0(u)+3G_{0,0}(z)G_0(u)-4G_{0,1}(z)G_0(u)-2G_{1,0}(z)G_0(u)\\
&-\frac{\pi^2}{3}G_0(u)+\frac{3\pi^2}{2}G_0(z)-2i\pi G_0(z)G_1(u)+\frac{\pi^2}{3}G_1(u)-\frac{\pi^2}{3}G_1(z)\\
&-3i\pi G_0(z)G_{a_2}(u)+4i\pi G_1(z)G_{a_2}(u)+\frac{3\pi^2}{2}G_{a_2}(u)-4G_0(z)G_{0,0}(u)\\
&-2G_1(u)G_{0,0}(z)-2G_{a_2}(u)G_{0,0}(z)-3i\pi G_{0,0}(z)+2G_1(u)G_{0,1}(z)\\
&+3G_{a_2}(u)G_{0,1}(z)+4i\pi G_{0,1}(z)+4G_0(z)G_{0,a_2}(u)-4G_1(z)G_{0,a_2}(u)+4i\pi G_{0,a_2}(u)\\
&+2G_0(z)G_{1,0}(u)+3G_{a_2}(u)G_{1,0}(z)+2i\pi G_{1,0}(z)-4G_{a_2}(u)G_{1,1}(z)+2G_{1,0,0}(z)\\
&-2G_0(z)G_{1,a_2}(u)+2G_1(z)G_{1,a_2}(u)-2i\pi G_{1,a_2}(u)+3G_0(z)G_{a_2,0}(u)\\
&-4G_1(z)G_{a_2,0}(u)+4i\pi G_{a_2,0}(u)-3G_0(z)G_{a_2,a_2}(u)+3G_1(z)G_{a_2,a_2}(u)\\
&-3i\pi G_{a_2,a_2}(u)-2G_{0,0,0}(z)+3G_{0,0,1}(z)+3G_{0,1,0}(z)-4G_{0,1,1}(z)-4G_{0,a_2,0}(u)\\
&-2G_{1,0,1}(z)+2G_{1,a_2,0}(u)-4G_{a_2,0,0}(u)+3G_{a_2,a_2,0}(u)-\zeta_3+\frac{1}{3}i\pi^3\Big]+\mathcal{O}(\epsilon^4),
\end{aligned}
\tag{6.7}
$$

JHEP04(2015)140

$$\tilde{C}_5 = \epsilon^3 \Big[G_{a_1,0}(u)G_0(z) - \frac{\pi^2}{6}G_0(z) + \frac{\pi^2}{3}G_{a_1}(u) + G_{a_1}(u)G_{0,1}(z) + G_{a_1}(u)G_{1,0}(z) - 2G_1(z)G_{a_1,a_1}(u) - G_{0,1,0}(z) - 2G_{a_1,a_1,0}(u) + 2\zeta_3 \Big] + \mathcal{O}(\epsilon^4), \tag{6.8}$$

$$\begin{aligned}\tilde{C}_6 =& \epsilon^2 \Big[- G_0(u)G_0(z) + G_1(z)G_{a_1}(u) - G_{0,1}(z) + G_{a_1,0}(u) - \frac{\pi^2}{6} \Big] \\ &+ \epsilon^3 \Big[G_{0,0}(z)G_0(u) + 4G_{0,1}(z)G_0(u) + 2G_{1,0}(z)G_0(u) + \frac{\pi^2}{3}G_0(u) + \frac{\pi^2}{2}G_0(z) \\ &- \frac{\pi^2}{3}G_1(u) + \frac{\pi^2}{3}G_1(z) - \frac{\pi^2}{2}G_{a_1}(u) + 4G_0(z)G_{0,0}(u) - 2G_1(u)G_{0,1}(z) \\ &- G_{a_1}(u)G_{0,1}(z) - 4G_1(z)G_{0,a_1}(u) - 2G_0(z)G_{1,0}(u) - G_{a_1}(u)G_{1,0}(z) \\ &- 4G_{a_1}(u)G_{1,1}(z) + 2G_1(z)G_{1,a_1}(u) - G_0(z)G_{a_1,0}(u) - 4G_1(z)G_{a_1,0}(u) \\ &+ 3G_1(z)G_{a_1,a_1}(u) + G_{0,0,1}(z) + G_{0,1,0}(z) + 4G_{0,1,1}(z) - 4G_{0,a_1,0}(u) + 2G_{1,0,1}(z) \\ &+ 2G_{1,a_1,0}(u) - 4G_{a_1,0,0}(u) + 3G_{a_1,a_1,0}(u) - \zeta_3 \Big] + \mathcal{O}(\epsilon^4),\end{aligned} \tag{6.9}$$

$$\begin{aligned}\tilde{C}_7 =& \epsilon G_0(z) + \epsilon^2 \Big[- G_{0,0}(z) - 2G_{1,0}(z) + \frac{\pi^2}{3} \Big] \\ &+ \epsilon^3 \Big[\frac{\pi^2}{3}G_0(z) - \frac{2\pi^2}{3}G_1(z) + G_{0,0,0}(z) + 2G_{1,0,0}(z) + 4G_{1,1,0}(z) - 2\zeta_3 \Big] + \mathcal{O}(\epsilon^4),\end{aligned} \tag{6.10}$$

$$\begin{aligned}\tilde{C}_8 =& \epsilon[-G_0(u) - G_1(z)] \\ &+ \epsilon^2 \Big[4G_0(u)G_1(z) - G_{a_1}(u)G_1(z) + 4G_{0,0}(u) + 4G_{1,1}(z) - G_{a_1,0}(u) + \frac{\pi^2}{6} \Big] \\ &+ \epsilon^3 \Big[- 16G_{1,1}(z)G_0(u) - \frac{5\pi^2}{3}G_0(u) - \frac{5\pi^2}{3}G_1(z) + \frac{\pi^2}{6}G_{a_1}(u) - 16G_1(z)G_{0,0}(u) \\ &+ 6G_1(z)G_{0,a_1}(u) + 4G_{a_1}(u)G_{1,1}(z) + 4G_1(z)G_{a_1,0}(u) - G_1(z)G_{a_1,a_1}(u) - 7\zeta_3 \\ &- 16G_{0,0,0}(u) + 6G_{0,a_1,0}(u) - 16G_{1,1,1}(z) + 4G_{a_1,0,0}(u) - G_{a_1,a_1,0}(u) \Big] + \mathcal{O}(\epsilon^4),\end{aligned} \tag{6.11}$$

$$\begin{aligned}\tilde{C}_9 =& -1 + \epsilon[4G_0(u) + 4G_1(z)] \\ &+ \epsilon^2 \Big[- 16G_0(u)G_1(z) + 6G_{a_1}(u)G_1(z) - 16G_{0,0}(u) - 16G_{1,1}(z) + 6G_{a_1,0}(u) - \frac{5\pi^2}{3} \Big] \\ &+ \epsilon^3 \Big[64G_{1,1}(z)G_0(u) + \frac{20\pi^2}{3}G_0(u) + \frac{20\pi^2}{3}G_1(z) - \pi^2 G_{a_1}(u) + 64G_1(z)G_{0,0}(u) \\ &- 24G_1(z)G_{0,a_1}(u) - 24G_{a_1}(u)G_{1,1}(z) - 24G_1(z)G_{a_1,0}(u) + 6G_1(z)G_{a_1,a_1}(u) + 20\zeta_3 \\ &+ 64G_{0,0,0}(u) - 24G_{0,a_1,0}(u) + 64G_{1,1,1}(z) - 24G_{a_1,0,0}(u) + 6G_{a_1,a_1,0}(u) \Big] + \mathcal{O}(\epsilon^4),\end{aligned} \tag{6.12}$$

JHEP04(2015)140

$$
\begin{aligned}
\tilde{C}_{10} =& \epsilon[-G_0(u) + G_0(z) - G_1(z) + i\pi] \\
&+ \epsilon^2\Big[- 2G_0(z)G_0(u) + 4G_1(z)G_0(u) - 4i\pi G_0(u) + 2i\pi G_0(z) - 4i\pi G_1(z) \\
&+ G_0(z)G_{a_2}(u) - G_1(z)G_{a_2}(u) + i\pi G_{a_2}(u) + 4G_{0,0}(u) - 2G_{0,1}(z) - 2G_{1,0}(z) \\
&+ 4G_{1,1}(z) - G_{a_2,0}(u) - \frac{11\pi^2}{6}\Big] \\
&+ \epsilon^3\Big[- 8i\pi G_0(z)G_0(u) + 16i\pi G_1(z)G_0(u) - 4G_{0,0}(z)G_0(u) + 8G_{0,1}(z)G_0(u) \\
&+ 8G_{1,0}(z)G_0(u) - 16G_{1,1}(z)G_0(u) + \frac{19\pi^2}{3}G_0(u) - \frac{8}{3}\pi^2 G_0(z) + \frac{19\pi^2}{3}G_1(z) \\
&+ 2i\pi G_0(z)G_{a_2}(u) - 4i\pi G_1(z)G_{a_2}(u) - \frac{11\pi^2}{6}G_{a_2}(u) + 8G_0(z)G_{0,0}(u) \\
&- 16G_1(z)G_{0,0}(u) + 16i\pi G_{0,0}(u) + 4i\pi G_{0,0}(z) - 2G_{a_2}(u)G_{0,1}(z) - 8i\pi G_{0,1}(z) \\
&- 6G_0(z)G_{0,a_2}(u) + 6G_1(z)G_{0,a_2}(u) - 6i\pi G_{0,a_2}(u) - 2G_{a_2}(u)G_{1,0}(z) - 8i\pi G_{1,0}(z) \\
&+ 4G_{a_2}(u)G_{1,1}(z) + 16i\pi G_{1,1}(z) - 2G_0(z)G_{a_2,0}(u) + 4G_1(z)G_{a_2,0}(u) + 4G_{0,0,0}(z) \\
&- 4i\pi G_{a_2,0}(u) + G_0(z)G_{a_2,a_2}(u) - G_1(z)G_{a_2,a_2}(u) + i\pi G_{a_2,a_2}(u) - 16G_{0,0,0}(u) \\
&- 4G_{0,0,1}(z) - 4G_{0,1,0}(z) + 8G_{0,1,1}(z) + 6G_{0,a_2,0}(u) - 4G_{1,0,0}(z) + 8G_{1,0,1}(z) \\
&+ 8G_{1,1,0}(z) - 16G_{1,1,1}(z) + 4G_{a_2,0,0}(u) - G_{a_2,a_2,0}(u) - 7\zeta_3 - i\pi^3\Big] + \mathcal{O}(\epsilon^4), \qquad (6.13)
\end{aligned}
$$

$$
\begin{aligned}
\tilde{C}_{11} =& -1 + \epsilon[4G_0(u) - 2G_0(z) + 4G_1(z) - 4i\pi] \\
&+ \epsilon^2\Big[8G_0(z)G_0(u) - 16G_1(z)G_0(u) + 16i\pi G_0(u) - 8i\pi G_0(z) + 16i\pi G_1(z) \\
&- 6G_0(z)G_{a_2}(u) + 6G_1(z)G_{a_2}(u) - 6i\pi G_{a_2}(u) - 16G_{0,0}(u) - 4G_{0,0}(z) + 8G_{0,1}(z) \\
&+ 8G_{1,0}(z) - 16G_{1,1}(z) + 6G_{a_2,0}(u) + \frac{19\pi^2}{3}\Big] \\
&+ \epsilon^3\Big[32i\pi G_0(z)G_0(u) - 64i\pi G_1(z)G_0(u) + 16G_{0,0}(z)G_0(u) - 32G_{0,1}(z)G_0(u) \\
&- 32G_{1,0}(z)G_0(u) + 64G_{1,1}(z)G_0(u) - \frac{76\pi^2}{3}G_0(u) + \frac{38\pi^2}{3}G_0(z) - \frac{76\pi^2}{3}G_1(z) \\
&- 12i\pi G_0(z)G_{a_2}(u) + 24i\pi G_1(z)G_{a_2}(u) + 11\pi^2 G_{a_2}(u) - 32G_0(z)G_{0,0}(u) \\
&+ 64G_1(z)G_{0,0}(u) - 64i\pi G_{0,0}(u) - 16i\pi G_{0,0}(z) + 12G_{a_2}(u)G_{0,1}(z) + 32i\pi G_{0,1}(z) \\
&+ 24G_0(z)G_{0,a_2}(u) - 24G_1(z)G_{0,a_2}(u) + 24i\pi G_{0,a_2}(u) + 12G_{a_2}(u)G_{1,0}(z) \\
&+ 32i\pi G_{1,0}(z) - 24G_{a_2}(u)G_{1,1}(z) - 64i\pi G_{1,1}(z) + 12G_0(z)G_{a_2,0}(u) + 64G_{0,0,0}(u) \\
&- 24G_1(z)G_{a_2,0}(u) + 24i\pi G_{a_2,0}(u) - 6G_0(z)G_{a_2,a_2}(u) + 6G_1(z)G_{a_2,a_2}(u) \\
&- 6i\pi G_{a_2,a_2}(u) - 8G_{0,0,0}(z) + 16G_{0,0,1}(z) + 16G_{0,1,0}(z) - 32G_{0,1,1}(z) \\
&- 24G_{0,a_2,0}(u) + 16G_{1,0,0}(z) - 32G_{1,0,1}(z) - 32G_{1,1,0}(z) + 64G_{1,1,1}(z) \\
&- 24G_{a_2,0,0}(u) + 6G_{a_2,a_2,0}(u) + 20\zeta_3 + 4i\pi^3\Big] + \mathcal{O}(\epsilon^4), \qquad (6.14)
\end{aligned}
$$

$$
\tilde{C}_{12} = 1 - \epsilon G_0(z) + \epsilon^2\Big[G_{0,0}(z) + \frac{\pi^2}{3}\Big] + \epsilon^3\Big[- \frac{\pi^2}{3}G_0(z) - G_{0,0,0}(z)\Big] + \mathcal{O}(\epsilon^4). \qquad (6.15)
$$

JHEP04(2015)140

6.2 $C_{13} - C_{15}$

The new integrals in this topology are $C_{13} - C_{15}$. However, in order to close the system of differential equations nine integrals are needed which we order as follows,

$$\vec{C} = \left\{\tilde{C}_{13}, \tilde{C}_5, \tilde{C}_6, \tilde{C}_7, \tilde{C}_{14}, \tilde{C}_8, \tilde{C}_9, \tilde{C}_{15}, \tilde{C}_{12}\right\}. \tag{6.16}$$

The corresponding matrix is $\tilde{A}_{13-15}$. The solution to the $C_{13} - C_{15}$ reads

$$\tilde{C}_{13} = \epsilon^3\left[G_1(z)G_{1,a_1}(u) + G_{1,a_1,0}(u) - G_{0,1}(z)G_1(u) - \frac{\pi^2}{6}G_1(u) - G_0(z)G_{1,0}(u)\right] + \mathcal{O}(\epsilon^4), \tag{6.17}$$

$$\tilde{C}_{14} = \epsilon^3\left[\frac{\pi^2}{6}G_0(z) + G_{0,1,0}(z) - 2\zeta_3\right] + \mathcal{O}(\epsilon^4), \tag{6.18}$$

$$\tilde{C}_{15} = -\frac{1}{4} - \epsilon^2\frac{\pi^2}{4} - \epsilon^3 2\zeta_3 + \mathcal{O}(\epsilon^4). \tag{6.19}$$

6.3 $C_{16} - C_{22}$

This topology has seven integrals, none of which has appeared in previous subsections. They are ordered according to

$$\vec{C} = \left\{\tilde{C}_{16}, \tilde{C}_{17}, \tilde{C}_{18}, \tilde{C}_{19}, \tilde{C}_{20}, \tilde{C}_{21}, \tilde{C}_{22}\right\}. \tag{6.20}$$

The corresponding matrix is $\tilde{A}_{16-22}$. The solution reads

$$\begin{aligned}\tilde{C}_{16} =& \epsilon^3[G_{a_1}(u)G_{0,1}(z) - G_{a_2}(u)G_{0,1}(z) + G_{a_1}(u)G_{1,1}(z) + G_{a_2}(u)G_{1,1}(z)\\ &+ G_1(z)G_{a_1,0}(u) - G_1(z)G_{a_1,a_1}(u) + G_1(z)G_{a_2,0}(u) - 2G_{0,0,1}(z) + G_{a_1,1,0}(u)\\ &- G_{a_1,a_1,0}(u) + G_{a_2,1,0}(u) - 2\zeta_3] + \mathcal{O}(\epsilon^4),\end{aligned} \tag{6.21}$$

$$\begin{aligned}\tilde{C}_{17} =& \epsilon^2\left[-G_1(z)G_{a_1}(u) + G_{0,1}(z) - G_{a_1,0}(u) + \frac{\pi^2}{6}\right]\\ &+ \epsilon^3\left[-2G_{0,1}(z)G_1(u) - \frac{\pi^2}{3}G_1(u) - \frac{\pi^2}{3}G_1(z) + \frac{\pi^2}{6}G_{a_1}(u) + G_{a_1}(u)G_{0,1}(z)\right.\\ &+ G_{a_2}(u)G_{0,1}(z) + 3G_{a_1}(u)G_{1,1}(z) - G_{a_2}(u)G_{1,1}(z) + 2G_1(z)G_{1,a_1}(u) - G_{a_2,1,0}(u)\\ &+ 3G_1(z)G_{a_1,0}(u) - 2G_1(z)G_{a_1,a_1}(u) - G_1(z)G_{a_2,0}(u) + 3G_{0,0,1}(z) - 4G_{0,1,1}(z)\\ &\left.- 2G_{1,0,1}(z) + 2G_{1,a_1,0}(u) + 2G_{a_1,0,0}(u) + G_{a_1,1,0}(u) - 2G_{a_1,a_1,0}(u) + 3\zeta_3\right] + \mathcal{O}(\epsilon^4),\end{aligned} \tag{6.22}$$

JHEP04(2015)140

$$\tilde{C}_{18} = \epsilon^2[G_0(u)G_1(z) - G_{0,1}(z) + G_{1,0}(u) + G_{1,1}(z)]$$
$$+ \epsilon^3\Big[- G_{0,1}(z)G_1(u) + \frac{\pi^2}{6}G_1(u) + \frac{\pi^2}{6}G_1(z) - 2G_1(z)G_{0,0}(u) + G_0(u)G_{0,1}(z)$$
$$+ G_1(z)G_{0,a_1}(u) - 4G_1(z)G_{1,0}(u) - 6G_0(u)G_{1,1}(z) + G_1(z)G_{1,a_1}(u) - 2G_{0,1,0}(u)$$
$$+ 5G_{0,1,1}(z) + G_{0,a_1,0}(u) - 2G_{1,0,0}(u) - 2G_{1,1,0}(u) - 6G_{1,1,1}(z) + G_{1,a_1,0}(u)\Big] + \mathcal{O}(\epsilon^4), \tag{6.23}$$

$$\tilde{C}_{19} = -\epsilon G_1(z) + \epsilon^2[4G_{1,1}(z) - G_{0,1}(z)] \tag{6.24}$$
$$+ \epsilon^3\Big[- \frac{2\pi^2}{3}G_1(z) - G_{0,0,1}(z) + 4G_{0,1,1}(z) + 6G_{1,0,1}(z) - 16G_{1,1,1}(z)\Big] + \mathcal{O}(\epsilon^4),$$

$$\tilde{C}_{20} = -1 + \epsilon 4G_1(z) + \epsilon^2\Big[6G_{0,1}(z) - 16G_{1,1}(z) - \frac{2\pi^2}{3}\Big] \tag{6.25}$$
$$+ \epsilon^3\Big[\frac{8\pi^2}{3}G_1(z) + 6G_{0,0,1}(z) - 24G_{0,1,1}(z) - 24G_{1,0,1}(z) + 64G_{1,1,1}(z) + 2\zeta_3\Big] + \mathcal{O}(\epsilon^4),$$

$$\tilde{C}_{21} = \epsilon[G_0(u) + G_1(z)] \tag{6.26}$$
$$+ \epsilon^2\Big[- 2G_0(u)G_1(z) + G_{a_1}(u)G_1(z) - 2G_{0,0}(u) - 2G_{1,1}(z) + G_{a_1,0}(u) - \frac{\pi^2}{6}\Big]$$
$$+ \epsilon^3\Big[4G_{1,1}(z)G_0(u) + \frac{2\pi^2}{3}G_0(u) + \frac{2\pi^2}{3}G_1(z) - \frac{\pi^2}{6}G_{a_1}(u) + 4G_1(z)G_{0,0}(u)$$
$$- 2G_1(z)G_{0,a_1}(u) - 2G_{a_1}(u)G_{1,1}(z) - 2G_1(z)G_{a_1,0}(u) + G_1(z)G_{a_1,a_1}(u)$$
$$+ 4G_{0,0,0}(u) - 2G_{0,a_1,0}(u) + 4G_{1,1,1}(z) - 2G_{a_1,0,0}(u) + G_{a_1,a_1,0}(u) + \zeta_3\Big] + \mathcal{O}(\epsilon^4),$$

$$\tilde{C}_{22} = 1 + \epsilon^2\frac{\pi^2}{3} + \mathcal{O}(\epsilon^4). \tag{6.27}$$

6.4 $C_{23} - C_{27}$

This topology has also seven integrals, of which $C_{23} - C_{27}$ are new. The entire topology reads

$$\vec{C} = \left\{\tilde{C}_{23}, \tilde{C}_{24}, \tilde{C}_{25}, \tilde{C}_7, \tilde{C}_{26}, \tilde{C}_{27}, \tilde{C}_{12}\right\}. \tag{6.28}$$

The corresponding matrix is $\tilde{A}_{23-27}$. The solution reads

$$\tilde{C}_{23} = \epsilon^3\Big[- G_{a_2,0}(u)G_0(z) + \frac{\pi^2}{2}G_0(z) + \frac{\pi^2}{6}G_{a_1}(u) + \frac{\pi^2}{2}G_{a_2}(u) + G_{a_2}(u)G_{0,0}(z)$$
$$- G_{a_2}(u)G_{0,1}(z) - G_{a_2}(u)G_{1,0}(z) + G_{a_1}(u)G_{1,1}(z) + G_{a_2}(u)G_{1,1}(z) + G_1(z)G_{a_1,0}(u)$$
$$- G_1(z)G_{a_1,a_1}(u) + G_1(z)G_{a_2,0}(u) + G_{0,0,0}(z) - G_{0,1,0}(z) + G_{a_1,0,0}(u) - G_{a_1,a_1,0}(u)$$
$$+ G_{a_2,0,0}(u) + 2\zeta_3\Big] + \mathcal{O}(\epsilon^4), \tag{6.29}$$

JHEP04(2015)140

$$
\begin{aligned}
\tilde{C}_{24} =& \epsilon^2\Big[G_0(u)G_0(z) - G_1(z)G_{a_1}(u) + G_{0,1}(z) - G_{a_1,0}(u) + \frac{\pi^2}{6}\Big] \\
&+ \epsilon^3\Big[- G_{0,0}(z)G_0(u) - 4G_{0,1}(z)G_0(u) - 2G_{1,0}(z)G_0(u) - \frac{\pi^2}{3}G_0(u) - \pi^2 G_0(z) \\
&+ \frac{\pi^2}{3}G_1(u) - \frac{\pi^2}{3}G_1(z) + \frac{\pi^2}{3}G_{a_1}(u) - \frac{\pi^2}{2}G_{a_2}(u) - 4G_0(z)G_{0,0}(u) - G_{a_2}(u)G_{0,0}(z) \\
&+ 2G_1(u)G_{0,1}(z) + G_{a_1}(u)G_{0,1}(z) + G_{a_2}(u)G_{0,1}(z) + 4G_1(z)G_{0,a_1}(u) - 2G_{a_1,a_1,0}(u) \\
&+ 2G_0(z)G_{1,0}(u) + G_{a_1}(u)G_{1,0}(z) + G_{a_2}(u)G_{1,0}(z) + 3G_{a_1}(u)G_{1,1}(z) - G_{a_2,0,0}(u) \\
&- G_{a_2}(u)G_{1,1}(z) - 2G_1(z)G_{1,a_1}(u) + G_0(z)G_{a_1,0}(u) + 3G_1(z)G_{a_1,0}(u) + 3G_{a_1,0,0}(u) \\
&- 2G_1(z)G_{a_1,a_1}(u) + G_0(z)G_{a_2,0}(u) - G_1(z)G_{a_2,0}(u) - G_{0,0,0}(z) - G_{0,0,1}(z) \\
&- 4G_{0,1,1}(z) + 4G_{0,a_1,0}(u) - 2G_{1,0,1}(z) - 2G_{1,a_1,0}(u) - \zeta_3\Big] + \mathcal{O}(\epsilon^4),
\end{aligned} \tag{6.30}
$$

$$
\begin{aligned}
\tilde{C}_{25} =& \epsilon^2\Big[G_0(u)(G_1(z) - G_0(z)) + G_{0,0}(u) + G_{0,0}(z) - G_{0,1}(z) - G_{1,0}(z) + G_{1,1}(z) + \frac{\pi^2}{2}\Big] \\
&+ \epsilon^3\Big[3G_{0,1}(z)G_0(u) + 2G_{1,0}(z)G_0(u) - 6G_{1,1}(z)G_0(u) - \pi^2 G_0(u) - \frac{\pi^2}{2}G_0(z) \\
&- \frac{\pi^2}{6}G_1(u) - \frac{7\pi^2}{6}G_1(z) + 3G_0(z)G_{0,0}(u) - 6G_1(z)G_{0,0}(u) - G_1(u)G_{0,1}(z) \\
&+ G_1(z)G_{0,a_1}(u) - G_0(z)G_{1,0}(u) + G_1(z)G_{1,a_1}(u) - 6G_{0,0,0}(u) - 3G_{0,0,0}(z) \\
&+ G_{0,1,0}(z) + 3G_{0,1,1}(z) + G_{0,a_1,0}(u) + 2G_{1,0,1}(z) + 2G_{1,1,0}(z) - 6G_{1,1,1}(z) \\
&+ G_{1,a_1,0}(u)\Big] + \mathcal{O}(\epsilon^4),
\end{aligned} \tag{6.31}
$$

$$
\begin{aligned}
\tilde{C}_{26} =& \epsilon[G_0(u) + G_1(z)] \\
&+ \epsilon^2\Big[- G_0(u)G_0(z) - 2G_0(u)G_1(z) + G_1(z)G_{a_1}(u) - 2G_{0,0}(u) - G_{0,1}(z) - G_{1,0}(z) \\
&- 2G_{1,1}(z) + G_{a_1,0}(u) - \frac{\pi^2}{6}\Big] \\
&+ \epsilon^3\Big[G_{0,0}(z)G_0(u) + 2G_{0,1}(z)G_0(u) + 2G_{1,0}(z)G_0(u) + 4G_{1,1}(z)G_0(u) + \frac{2\pi^2}{3}G_0(u) \\
&+ \frac{\pi^2}{6}G_0(z) + \frac{2\pi^2}{3}G_1(z) - \frac{\pi^2}{6}G_{a_1}(u) + 2G_0(z)G_{0,0}(u) + 4G_1(z)G_{0,0}(u) + G_{1,0,0}(z) \\
&- G_{a_1}(u)G_{0,1}(z) - 2G_1(z)G_{0,a_1}(u) - G_{a_1}(u)G_{1,0}(z) - 2G_{a_1}(u)G_{1,1}(z) + 2G_{1,0,1}(z) \\
&- G_0(z)G_{a_1,0}(u) - 2G_1(z)G_{a_1,0}(u) + G_1(z)G_{a_1,a_1}(u) + 4G_{0,0,0}(u) + G_{0,0,1}(z) \\
&+ G_{0,1,0}(z) + 2G_{0,1,1}(z) - 2G_{0,a_1,0}(u) + 2G_{1,1,0}(z) + 4G_{1,1,1}(z) - 2G_{a_1,0,0}(u) \\
&+ G_{a_1,a_1,0}(u) + \zeta_3\Big] + \mathcal{O}(\epsilon^4),
\end{aligned} \tag{6.32}
$$

$$
\tilde{C}_{27} = -\frac{1}{4} + \epsilon\frac{1}{2}G_0(z) + \epsilon^2\Big[- G_{0,0}(z) - \frac{\pi^2}{4}\Big] + \epsilon^3\Big[\frac{\pi^2}{2}G_0(z) + 2G_{0,0,0}(z) - 2\zeta_3\Big] + \mathcal{O}(\epsilon^4). \tag{6.33}
$$

JHEP04(2015)140

6.5 $C_{28} - C_{32}$

This topology has ten integrals, of which the five integrals $C_{28} - C_{32}$ are new. They are embedded in the topology as follows

$$\vec{C} = \left\{\tilde{C}_{28}, \tilde{C}_{29}, \tilde{C}_{30}, \tilde{C}_{7}, \tilde{C}_{26}, \tilde{C}_{21}, \tilde{C}_{22}, \tilde{C}_{31}, \tilde{C}_{32}, \tilde{C}_{12}\right\}. \tag{6.34}$$

The corresponding matrix is $\tilde{A}_{28-32}$. The solution reads

$$\begin{aligned}\tilde{C}_{28} =& \epsilon^3\Big[-G_{1,0}(u)G_0(z) + \frac{\pi^2}{6}G_0(z) - \frac{\pi^2}{6}G_1(u) - \frac{\pi^2}{6}G_{a_1}(u) - G_1(u)G_{0,1}(z) \\ &- G_1(z)G_{0,a_1}(u) + G_1(z)G_{1,a_1}(u) + G_1(z)G_{a_1,a_1}(u) - G_{0,a_1,0}(u) + G_{1,a_1,0}(u) \\ &+ G_{a_1,a_1,0}(u)\Big] + \mathcal{O}(\epsilon^4),\end{aligned} \tag{6.35}$$

$$\begin{aligned}\tilde{C}_{29} =& \epsilon^3\Big[G_{0,1}(z)G_1(u) + \frac{\pi^2}{6}G_1(u) - \frac{\pi^2}{6}G_{a_1}(u) - G_{a_1}(u)G_{0,1}(z) + G_1(z)G_{0,a_1}(u) \\ &+ G_0(z)G_{1,0}(u) - G_{a_1}(u)G_{1,0}(z) - G_1(z)G_{1,a_1}(u) - G_0(z)G_{a_1,0}(u) + G_1(z)G_{a_1,a_1}(u) \\ &+ G_{0,1,0}(z) + G_{0,a_1,0}(u) - G_{1,a_1,0}(u) + G_{a_1,a_1,0}(u) - 2\zeta_3\Big] + \mathcal{O}(\epsilon^4),\end{aligned} \tag{6.36}$$

$$\begin{aligned}\tilde{C}_{30} =& \epsilon^2\Big[-G_0(u)G_0(z) + G_1(z)G_{a_1}(u) - G_{0,1}(z) + G_{a_1,0}(u) - \frac{\pi^2}{6}\Big] \\ &+ \epsilon^3\Big[2G_{0,0}(u)G_0(z) - 3G_{1,0}(u)G_0(z) - 2G_{a_1,0}(u)G_0(z) + 2G_{a_3,0}(u)G_0(z) \\ &+ 2G_{a_4,0}(u)G_0(z) + \frac{\pi^2}{6}G_0(z) - \frac{\pi^2}{2}G_1(u) + \frac{\pi^2}{3}G_1(z) - \frac{2\pi^2}{3}G_{a_1}(u) + \frac{2\pi^2}{3}G_{a_3}(u) \\ &+ \frac{2\pi^2}{3}G_{a_4}(u) - 2G_{a_3}(u)G_{-1,0}(\sqrt{z}) + 2G_{a_4}(u)G_{-1,0}(\sqrt{z}) + G_0(u)G_{0,0}(z) - G_{0,a_1,0}(u) \\ &+ 2G_0(u)G_{0,1}(z) - 3G_1(u)G_{0,1}(z) - 2G_{a_1}(u)G_{0,1}(z) + 2G_{a_3}(u)G_{0,1}(z) + G_{0,1,0}(z) \\ &+ 2G_{a_4}(u)G_{0,1}(z) - G_1(z)G_{0,a_1}(u) + 2G_{a_3}(u)G_{1,0}(\sqrt{z}) - 2G_{a_4}(u)G_{1,0}(\sqrt{z}) \\ &+ 2G_0(u)G_{1,0}(z) - 2G_{a_1}(u)G_{1,0}(z) + G_{a_3}(u)G_{1,0}(z) + G_{a_4}(u)G_{1,0}(z) + G_{0,0,1}(z) \\ &- 2G_{a_1}(u)G_{1,1}(z) + 3G_1(z)G_{1,a_1}(u) - 2G_1(z)G_{a_1,0}(u) + 4G_1(z)G_{a_1,a_1}(u) + \zeta_3 \\ &- 4G_1(z)G_{a_3,a_1}(u) - 4G_1(z)G_{a_4,a_1}(u) + 2G_{0,1,1}(z) + 2G_{1,0,1}(z) - 4G_{a_4,a_1,0}(u) \\ &+ 3G_{1,a_1,0}(u) - 2G_{a_1,0,0}(u) + 4G_{a_1,a_1,0}(u) - 4G_{a_3,a_1,0}(u)\Big] + \mathcal{O}(\epsilon^4),\end{aligned} \tag{6.37}$$

$$\begin{aligned}\tilde{C}_{31} =& -\epsilon^2\frac{1}{2}G_{1,0}(z) + \epsilon^3\Big[-G_{-1,-1,0}(\sqrt{z}) + G_{-1,1,0}(\sqrt{z}) - \frac{1}{2}G_{0,1,0}(z) + G_{1,-1,0}(\sqrt{z}) \\ &+ \frac{1}{2}G_{1,0,0}(z) - G_{1,1,0}(\sqrt{z}) + \frac{3}{2}G_{1,1,0}(z)\Big] + \mathcal{O}(\epsilon^4),\end{aligned} \tag{6.38}$$

JHEP04(2015)140

$$\begin{aligned}\tilde{C}_{32} =& \epsilon^2[G_{-1,0}(\sqrt{z}) - G_{1,0}(\sqrt{z})] \\ &+ \epsilon^3\Big[-2G_{-1,-1,0}(\sqrt{z}) - 2G_{-1,0,0}(\sqrt{z}) - 4G_{-1,1,0}(\sqrt{z}) - 2G_{0,-1,0}(\sqrt{z}) \\ &+ 2G_{0,1,0}(\sqrt{z}) + 4G_{1,-1,0}(\sqrt{z}) + 2G_{1,0,0}(\sqrt{z}) + 2G_{1,1,0}(\sqrt{z})\Big] + \mathcal{O}(\epsilon^4). \end{aligned} \tag{6.39}$$

6.6 C_{33} and C_{34}

This topology has seven integrals, of which only C_{33} – C_{34} have not yet appeared in the previous topologies. The integrals are ordered as

$$\vec{C} = \left\{\tilde{C}_{33}, \tilde{C}_{34}, \tilde{C}_7, \tilde{C}_{22}, \tilde{C}_{31}, \tilde{C}_{32}, \tilde{C}_{12}\right\}. \tag{6.40}$$

The corresponding matrix is $\tilde{A}_{33,34}$. The solution to $\mathcal{O}(\epsilon^3)$ is very short

$$\tilde{C}_{33} = \epsilon^3[G_{0,1,0}(z) - 2\zeta_3] + \mathcal{O}(\epsilon^4), \tag{6.41}$$

$$\tilde{C}_{34} = \epsilon^3\frac{\pi^2}{6}G_0(z) + \mathcal{O}(\epsilon^4). \tag{6.42}$$

At order $\mathcal{O}(\epsilon^4)$ the solution requires also Goncharov polylogarithms of argument $\sqrt{z}$.

6.7 C_{35}

This topology has three integrals, and only C_{35} is new. The integrals are ordered as

$$\vec{C} = \left\{\tilde{C}_{35}, \tilde{C}_{19}, \tilde{C}_{20}\right\}. \tag{6.43}$$

The corresponding matrix is $\tilde{A}_{35}$. The solution reads

$$\begin{aligned}\tilde{C}_{35} =& \epsilon\frac{1}{2}G_0(u) + \epsilon^2\Big[-2G_0(u)G_1(z) + G_{a_1}(u)G_1(z) - \frac{3}{2}G_{0,0}(u) - G_{0,1}(z) - \frac{1}{2}G_{1,0}(u) \\ &+ G_{a_1,0}(u) - \frac{\pi^2}{12}\Big] \\ &+ \epsilon^3\Big[8G_{1,1}(z)G_0(u) + \frac{7\pi^2}{12}G_0(u) + \frac{\pi^2}{12}G_1(u) + \frac{\pi^2}{3}G_1(z) - \frac{\pi^2}{6}G_{a_1}(u) + \frac{9}{2}G_{0,0,0}(u) \\ &+ 6G_1(z)G_{0,0}(u) + G_1(u)G_{0,1}(z) - G_{a_1}(u)G_{0,1}(z) - 3G_1(z)G_{0,a_1}(u) - 3G_{0,a_1,0}(u) \\ &+ 2G_1(z)G_{1,0}(u) - 4G_{a_1}(u)G_{1,1}(z) - G_1(z)G_{1,a_1}(u) - 4G_1(z)G_{a_1,0}(u) + 4G_{1,0,1}(z) \\ &+ 2G_1(z)G_{a_1,a_1}(u) - G_{0,0,1}(z) + \frac{3}{2}G_{0,1,0}(u) + 4G_{0,1,1}(z) + \frac{3}{2}G_{1,0,0}(u) + \frac{1}{2}G_{1,1,0}(u) \\ &- G_{1,a_1,0}(u) - 3G_{a_1,0,0}(u) - G_{a_1,1,0}(u) + 2G_{a_1,a_1,0}(u) + \zeta_3\Big] + \mathcal{O}(\epsilon^4). \end{aligned} \tag{6.44}$$

JHEP04(2015)140

6.8 C_{36} and C_{37}

This topology has four integrals, of which C_{36} and C_{37} are new. The integrals are

$$\vec{C} = \left\{\tilde{C}_{36}, \tilde{C}_{37}, \tilde{C}_{26}, \tilde{C}_{12}\right\}. \tag{6.45}$$

The corresponding matrix is $\tilde{A}_{36,37}$. The solution reads

$$\begin{aligned}
\tilde{C}_{36} =& \epsilon^2[-G_0(z)G_0(u) + G_1(z)G_0(u) - i\pi G_0(u) + G_1(u)G_1(z) - i\pi G_1(z) \\
&+ G_{0,1}(u) - G_{0,1}(z) + G_{1,0}(u) - G_{1,0}(z) + 2G_{1,1}(z)] \\
&+ \epsilon^3\Big[4i\pi G_1(z)G_0(u) + G_{0,0}(z)G_0(u) + 2G_{0,1}(z)G_0(u) + 3G_{1,0}(z)G_0(u) \\
&- 6G_{1,1}(z)G_0(u) + \frac{2\pi^2}{3}G_0(u) + \frac{\pi^2}{6}G_0(z) - \frac{\pi^2}{6}G_1(u) + 2i\pi G_1(u)G_1(z) + \frac{\pi^2}{2}G_1(z) \\
&- 2i\pi G_1(z)G_{a_1}(u) + 2G_0(z)G_{0,0}(u) - 2G_1(z)G_{0,0}(u) + 2i\pi G_{0,0}(u) + G_0(z)G_{0,1}(u) \\
&- 4G_1(z)G_{0,1}(u) + 2i\pi G_{0,1}(u) + G_1(u)G_{0,1}(z) - 2G_{a_1}(u)G_{0,1}(z) - G_0(z)G_{0,a_1}(u) \\
&+ G_1(z)G_{0,a_1}(u) - i\pi G_{0,a_1}(u) + G_0(z)G_{1,0}(u) - 4G_1(z)G_{1,0}(u) + 2i\pi G_{1,0}(u) \\
&+ G_1(u)G_{1,0}(z) - 2G_{a_1}(u)G_{1,0}(z) - 2G_1(z)G_{1,1}(u) - 6G_1(u)G_{1,1}(z) + 6i\pi G_{1,1}(z) \\
&+ 4G_{a_1}(u)G_{1,1}(z) + G_1(z)G_{1,a_1}(u) - 2G_0(z)G_{a_1,0}(u) + 2G_1(z)G_{a_1,0}(u) + 3G_{1,0,1}(z) \\
&- 2i\pi G_{a_1,0}(u) + 2G_1(z)G_{a_1,1}(u) - 2G_{0,0,1}(u) + G_{0,0,1}(z) - 2G_{0,1,0}(u) - 2G_{1,0,1}(u) \\
&- 2G_{0,1,1}(u) + 2G_{0,1,1}(z) + G_{0,a_1,1}(u) - 2G_{1,0,0}(u) + G_{1,0,0}(z) + G_{0,1,0}(z) - 2G_{1,1,0}(u) \\
&+ 4G_{1,1,0}(z) - 12G_{1,1,1}(z) + G_{1,a_1,0}(u) + 2G_{a_1,0,1}(u) + 2G_{a_1,1,0}(u) + \frac{1}{6}i\pi^3\Big] + \mathcal{O}(\epsilon^4),
\end{aligned} \tag{6.46}$$

$$\begin{aligned}
\tilde{C}_{37} =& \epsilon[-G_0(z) + G_1(u) + G_1(z) - i\pi] \\
&+ \epsilon^2\Big[G_0(z)G_1(u) - 2G_1(z)G_1(u) + 2i\pi G_1(u) + 2i\pi G_1(z) - G_0(z)G_{a_1}(u) + G_{a_1,1}(u) \\
&+ G_1(z)G_{a_1}(u) - i\pi G_{a_1}(u) + G_{0,0}(z) + G_{1,0}(z) - 2G_{1,1}(u) - 2G_{1,1}(z) + \frac{2\pi^2}{3}\Big] \\
&+ \epsilon^3\Big[-2G_{1,1}(u)G_0(z) + 2G_{1,a_1}(u)G_0(z) + G_{a_1,1}(u)G_0(z) - G_{a_1,a_1}(u)G_0(z) \\
&- \frac{\pi^2}{3}G_0(z) - \pi^2 G_1(u) - 4i\pi G_1(u)G_1(z) - \pi^2 G_1(z) + 2i\pi G_1(z)G_{a_1}(u) + 4G_{1,1,1}(z) \\
&+ \frac{2\pi^2}{3}G_{a_1}(u) - G_1(u)G_{0,0}(z) + G_{a_1}(u)G_{0,0}(z) - 2G_1(u)G_{1,0}(z) + G_{a_1}(u)G_{1,0}(z) \\
&+ 4G_1(z)G_{1,1}(u) - 4i\pi G_{1,1}(u) + 4G_1(u)G_{1,1}(z) - 2G_{a_1}(u)G_{1,1}(z) - 4i\pi G_{1,1}(z) \\
&- 2G_1(z)G_{1,a_1}(u) + 2i\pi G_{1,a_1}(u) - 2G_1(z)G_{a_1,1}(u) + 2i\pi G_{a_1,1}(u) + G_1(z)G_{a_1,a_1}(u) \\
&- i\pi G_{a_1,a_1}(u) - G_{0,0,0}(z) - G_{1,0,0}(z) - 2G_{1,1,0}(z) + 4G_{1,1,1}(u) - 2G_{1,a_1,1}(u) \\
&- 2G_{a_1,1,1}(u) + G_{a_1,a_1,1}(u) + 2\zeta_3\Big] + \mathcal{O}(\epsilon^4).
\end{aligned} \tag{6.47}$$

JHEP04(2015)140

6.9 C_{38} and C_{39}

These integrals arise from diagrams with a massive quark loop inside a gluon propagator. They appeared in a slightly different version already in the calculation of the two-loop tree amplitudes in $B \to \pi\pi$ [9, 10], and analytic results were recently derived in [11] as $M_{28,29}$. It turns out that the results of $C_{38,39}$ can be obtained from the latter reference if one adjusts the kinematics to the present problem. To be precise, one has to replace

$$u \to u\,(1-z) \tag{6.48}$$

in the expressions in [11]. That is, in the definition of the canonical basis (cf. (3.30) and (3.31) of [11] and (4.40), (4.41) of the present article), and also in the solution, eqs. (4.64) and (4.65) of [11]. In particular, the kinematic variable p changes to ($\bar{z} = 1 - z$)

$$p = \frac{1 - \sqrt{(2-u\bar{z})^2 - 4\bar{z}(1-u\bar{z})}}{1-u\bar{z}}\,. \tag{6.49}$$

7 Checks

In order to validate the analytic results presented above, we performed several checks of analytic and numeric nature. Those integrals that possess a closed form in terms of hypergeometric functions were analytically expanded in ϵ using `HypExp` [45, 46]. Subsequently, we re-wrote the resulting polylogarithms and HPLs in terms of Goncharov polylogarithms and compared to the results obtained by the differential equation method.

For the numerical checks we used a dozen points in the $u - z$ plane. We first evaluated the Goncharov polylogarithms that appear in our analytic results numerically with the GiNaC-library [47, 48]. We also derived Mellin-Barnes (MB) representations, partially using the `AMBRE`-package [49]. The analytic continuation to $\epsilon = 0$ and subsequent numerical integration was carried out by `MB.m` [50]. This worked for almost all cases, even in the presence of kinematic thresholds, and yielded agreement to the GiNaC results to $5 \cdot 10^{-10}$ or better. There are, however, a few cases in which the Monte-Carlo integration implemented in `MB.m` failed due to highly oscillating integrands, notably for the integrals C_{28-30}, and their "mass-flipped" counterparts (where $m_c \leftrightarrow m_b$ and $q_3 \leftrightarrow q_4$). In these cases, we relied on the sector decomposition method implemented in `SecDec` [51, 52], which yielded agreement with GiNaC at the level of $8 \cdot 10^{-7}$ for the highest ϵ-coefficients in C_{28-30}, and at the level of $6 \cdot 10^{-4}$ for the highest ϵ-coefficients of their "mass-flipped" counterparts. The agreement is several orders of magnitude better for the lower coefficients in the ϵ-expansion.

Another important point to mention is the fact that the GiNaC results were obtained in the canonical basis, whereas most of the MB representations and the `SecDec` results were derived in an "ordinary" basis of un-dotted and singly-dotted master integrals. The change of basis was then performed using the Laporta reduction. Having calculated the numerics in two different integral bases constitutes another non-trivial check of our results.

JHEP04(2015)140

8 Conclusion

We obtained analytic results to all two-loop master integrals that are necessary for the description of the non-leptonic decay $B \to D\pi$ at NNLO in QCD factorisation. They are expressed in terms of Goncharov polylogarithms of argument u and weights that are either integer numbers (0 or ± 1), or contain the second kinematic varible, z. It is remarkable that six z-dependent weights are sufficient for writing down the entire set of solutions, including the "mass-flipped" integrals.

With the master integrals at hand, the bare two-loop part of the hard-scattering kernels $T_{ij}(u)$ in (1.1) is complete. The remaining task consists of renormalising the ultraviolet divergences and subtracting infrared divergences via matching from QCD onto soft-collinear effective theory. Steps towards this goal are outlined in [13]. Having the hard-scattering kernels $T_{ij}(u)$ written in terms of iterated integrals is an optimal choice for carrying out the convolution integral with the pion LCDA in (1.1), and it might be feasible to obtain the NNLO topological tree amplitude in analytic form. In any case our results constitute an important step towards the phenomenology of $B \to D\pi$ decays at NNLO in QCD factorisation.

Let us compare the integrals in the present work to those recently obtained in [11] during the evaluation of the two-loop penguin amplitude. Both are two-loop problems with scales u and z. The present integrals are a bit less involved compared to those in [11], in a sense that the linear combinations that form a canonical master integral are shorter, the occurring weights are fewer, and the choice of kinematic invariants is less complicated. The main reason for this is that in the present work the external kinematics of the final state contains also the second internal mass, notably m_c. On the other hand, the only five-line integral in [11], a two-point function (M_{22}), is in fact a one-scale integral, whereas here we encountered several five-line integrals with four external legs which are genuine two-scale functions. Moreover, most of our integrals are needed to order $\mathcal{O}(\epsilon^4)$, whereas in [11] all but two integrals were required only to order $\mathcal{O}(\epsilon^3)$.

On more general grounds, it will be interesting to investigate how the canonical basis depends on the number of loops, legs, scales, space-time dimensions, and on the external kinematics. Every example therefore sharpens our understanding of the patterns that such bases follow, with the goal of eventually developing an algorithm for their automated construction.

Acknowledgments

We would like to thank A. Smirnov for useful correspondence on `FIRE` [36]. This work is supported by DFG research unit FOR 1873 "Quark Flavour Physics and Effective Field Theories".

JHEP04(2015)140

A The matrices $\tilde{A}$

Here we list the matrices $\tilde{A}$ for the different topologies. Their entries can all be expressed in terms of the following nine logarithms,

$$
\begin{aligned}
L_1 &= \ln(u)\,, & L_6 &= \ln(z+u(1-z))\,,\\
L_2 &= \ln(1-u)\,, & L_7 &= \ln\left(1-u\left(1-\sqrt{z}\right)\right)\,,\\
L_3 &= \ln(z)\,, & L_8 &= \ln\left(1-u\left(1+\sqrt{z}\right)\right)\,,\\
L_4 &= \ln(1-z)\,, & L_9 &= \ln\left(\frac{1-\sqrt{z}}{1+\sqrt{z}}\right)\,.\\
L_5 &= \ln(1-u(1-z))\,,
\end{aligned}
\tag{A.1}
$$

The matrices $\tilde{A}$ now assume the following compact form,

$$
\tilde{A}_{1-12} = \left(\begin{array}{cccccccccccccc}
-4L_1-L_4 & 3L_3-3L_4 & -2L_2-\frac{L_3}{2}-\frac{L_4}{2}+L_6 & -L_2+\frac{L_3}{2}-L_4+\frac{L_6}{2} & L_2+\frac{L_3}{2}-\frac{L_4}{2} & -L_2+L_3-L_4 & \frac{L_3}{4}-\frac{L_6}{4} & 0 & \frac{L_3}{4}-\frac{L_4}{4} & \frac{3L_6}{2}-\frac{3L_3}{2} & -\frac{L_3}{2}+\frac{L_4}{4}+\frac{L_6}{4} & \frac{L_6}{4}-\frac{L_3}{4}\\
-3L_4 & -4L_1-L_3-L_4 & L_2-\frac{L_4}{2} & -L_2-L_4 & -2L_2-\frac{L_4}{2}+L_5 & -L_2-L_4+\frac{L_5}{2} & \frac{L_5}{4} & \frac{3L_5}{2} & \frac{L_4}{4}+\frac{L_5}{4} & 0 & -\frac{L_4}{4} & \frac{L_5}{4}\\
0 & 0 & 2L_2-L_3+2L_4-2L_6 & L_3-L_6 & 0 & 0 & \frac{L_6}{2} & 0 & 0 & -2L_6 & -\frac{L_6}{2} & -\frac{L_6}{2}\\
0 & 0 & -2L_1-2L_4+2L_6 & -4L_1+2L_2-2L_4+L_6 & 0 & 0 & L_1-\frac{L_6}{2} & 0 & 0 & L_6 & \frac{L_6}{2} & \frac{L_6}{2}\\
0 & 0 & 0 & 0 & 2L_2-L_3+2L_4-2L_5 & -L_5 & \frac{L_3}{2}-\frac{L_5}{2} & 2L_3-2L_5 & \frac{L_3}{2}-\frac{L_5}{2} & 0 & 0 & \frac{L_3}{2}-\frac{L_5}{2}\\
0 & 0 & 0 & 0 & -2L_1-2L_4+2L_5 & -4L_1+2L_2-L_3-2L_4+L_5 & -L_1-\frac{L_3}{2}+\frac{L_5}{2} & L_5-L_3 & \frac{L_5}{2}-\frac{L_3}{2} & 0 & 0 & \frac{L_5}{2}-\frac{L_3}{2}\\
0 & 0 & 0 & 0 & 0 & 0 & -2L_4 & 0 & 0 & 0 & 0 & L_3\\
0 & 0 & 0 & 0 & 0 & 0 & 0 & L_5 & L_1+L_4 & 0 & 0 & 0\\
0 & 0 & 0 & 0 & 0 & 0 & 0 & -6L_5 & -4L_1-4L_4 & 0 & 0 & 0\\
0 & 0 & 0 & 0 & 0 & 0 & 0 & 0 & 0 & L_6-3L_3 & L_1-L_3+L_4 & 0\\
0 & 0 & 0 & 0 & 0 & 0 & 0 & 0 & 0 & 6L_3-6L_6 & -4L_1+2L_3-4L_4 & 0\\
0 & 0 & 0 & 0 & 0 & 0 & 0 & 0 & 0 & 0 & 0 & -L_3
\end{array}\right),
\tag{A.2}
$$

$$
\tilde{A}_{13-15} = \left(\begin{array}{ccccc}
-2L_4 & L_3-L_4 & L_2 & 0 & L_3-L_4\\
0 & 2L_2-L_3+2L_4-2L_5 & -L_5 & \frac{L_3}{2}-\frac{L_5}{2} & 0\\
0 & -2L_1-2L_4+2L_5 & -4L_1+2L_2-L_3-2L_4+L_5 & -L_1-\frac{L_3}{2}+\frac{L_5}{2} & 0\\
0 & 0 & 0 & -2L_4 & 0\\
0 & 0 & 0 & -\frac{L_3}{2} & 2L_4-L_3\\
0 & 0 & 0 & 0 & 0\\
0 & 0 & 0 & 0 & 0\\
0 & 0 & 0 & 0 & 0\\
0 & 0 & 0 & 0 & 0
\end{array}\right)
$$

JHEP04(2015)140

$$
\begin{pmatrix}
2L_4-2L_3 & \frac{L_4}{2}-\frac{L_3}{2} & 2L_3-2L_4 & 0 \\
2L_3-2L_5 & \frac{L_3}{2}-\frac{L_5}{2} & 0 & \frac{L_3}{2}-\frac{L_5}{2} \\
L_5-L_3 & \frac{L_5}{2}-\frac{L_3}{2} & 0 & \frac{L_5}{2}-\frac{L_3}{2} \\
0 & 0 & 0 & L_3 \\
0 & 0 & -2L_3 & -\frac{L_3}{2} \\
L_5 & L_1+L_4 & 0 & 0 \\
-6L_5 & -4L_1-4L_4 & 0 & 0 \\
0 & 0 & 0 & 0 \\
0 & 0 & 0 & -L_3
\end{pmatrix}, \tag{A.3}
$$

$$
\tilde{A}_{16-22} = \begin{pmatrix}
2L_2-2L_3+2L_4+L_5 & L_5-L_3 & -L_3+L_5+L_6 & 2L_5-2L_3 & \frac{L_5}{2}-\frac{L_3}{2} & 0 & \frac{L_5}{2}-\frac{L_3}{2} \\
-2L_2+2L_3-2L_4+L_5 & -2L_2+L_3-2L_4+L_5 & L_3+L_5-L_6 & L_3+2L_5 & \frac{L_3}{2}+\frac{L_5}{2} & -L_5 & \frac{L_3}{2}+\frac{L_5}{2} \\
-2L_1-3L_2+2L_3-5L_4 & -L_1+L_3-L_4 & -2L_1-2L_2+L_3-4L_4 & -3L_1-3L_2+3L_3-6L_4 & -\frac{L_1}{2}-L_2+\frac{L_3}{2}-\frac{3L_4}{2} & L_2+L_4 & -\frac{L_1}{2}-L_2+\frac{L_3}{2}-\frac{3L_4}{2} \\
0 & 0 & 0 & L_3 & L_4 & 0 & 0 \\
0 & 0 & 0 & -6L_3 & -4L_4 & 0 & 0 \\
0 & 0 & 0 & 0 & 0 & -2L_1-2L_4+L_5 & L_1+L_4 \\
0 & 0 & 0 & 0 & 0 & 0 & 0
\end{pmatrix}, \tag{A.4}
$$

$$
\tilde{A}_{23-27} = \begin{pmatrix}
2L_2-3L_3+2L_4+L_5 & L_5 & -L_3+L_5+L_6 & \frac{L_3}{2}-\frac{L_5}{2} & 0 & 2L_5-2L_3 & \frac{L_5}{2}-\frac{L_3}{2} \\
-2L_1-L_3-2L_4+L_5 & -4L_1+2L_2-2L_3-2L_4+L_5 & -L_3+L_5-L_6 & L_1+\frac{L_3}{2}-\frac{L_5}{2} & L_3-L_5 & 2L_5-2L_3 & \frac{L_5}{2}-\frac{L_3}{2} \\
-3L_1-2L_2+3L_3-5L_4 & -L_2-L_4 & -4L_1+L_3-4L_4 & \frac{L_1}{2}-\frac{L_3}{2}+\frac{L_4}{2} & L_1-L_3+L_4 & -6L_1+6L_3-6L_4 & -\frac{3L_1}{2}+\frac{3L_3}{2}-\frac{3L_4}{2} \\
0 & 0 & 0 & -2L_4 & 0 & 0 & L_3 \\
0 & 0 & 0 & 0 & -2L_1-L_3-2L_4+L_5 & 0 & L_1+L_4 \\
0 & 0 & 0 & 0 & 0 & -2L_3 & 0 \\
0 & 0 & 0 & 0 & 0 & 0 & -L_3
\end{pmatrix}, \tag{A.5}
$$

JHEP04(2015)140

$$\tilde{A}_{28-32} = \left(\begin{array}{cccc}
L_2-L_3-L_5 & L_2-2L_3+2L_4 & -L_1+L_2-L_3+L_5 & -\frac{L_1}{2} \\
L_2+2L_4-L_5 & L_2 & L_1-L_2+L_5 & \frac{L_1}{2} \\
-L_2-3L_5+2L_7+2L_8 & L_2-2L_7-2L_8 & -L_1+3L_2-2L_4+3L_5-4L_7-4L_8 & -\frac{L_1}{2} \\
0 & 0 & 0 & -2L_4 \\
0 & 0 & 0 & 0 \\
0 & 0 & 0 & 0 \\
0 & 0 & 0 & 0 \\
0 & 0 & 0 & 0 \\
0 & 0 & 0 & 0 \\
0 & 0 & 0 & 0
\end{array}\right.$$

$$\left.\begin{array}{cccccc}
L_1+L_3-L_5 & -L_1-L_3+L_5 & \frac{L_1}{2} & 2L_5-2L_3 & 0 & -\frac{L_1}{2} \\
-L_1 & L_1 & -\frac{L_1}{2} & 2L_5-2L_3 & 0 & \frac{L_1}{2} \\
-L_1-L_3-L_5+2L_7+2L_8 & L_1+2L_5-2L_7-2L_8 & -\frac{L_1}{2} & 6L_5-6L_7-6L_8 & 2L_8-2L_7 & \frac{L_1}{2} \\
0 & 0 & 0 & 0 & 0 & L_3 \\
-2L_1-L_3-2L_4+L_5 & 0 & 0 & 0 & 0 & L_1+L_4 \\
0 & -2L_1-2L_4+L_5 & L_1+L_4 & 0 & 0 & 0 \\
0 & 0 & 0 & 0 & 0 & 0 \\
0 & 0 & -\frac{L_4}{2} & L_3-3L_4 & L_9 & \frac{L_4}{2} \\
0 & 0 & -\frac{L_9}{2} & -3L_9 & L_4-L_3 & \frac{L_9}{2} \\
0 & 0 & 0 & 0 & 0 & -L_3
\end{array}\right), \tag{A.6}$$

$$\tilde{A}_{33,34} = \begin{pmatrix}
0 & 2L_4 & 0 & 0 & -2L_3 & 0 & 0 \\
2L_4-2L_3 & -L_3 & \frac{L_3}{2} & -\frac{L_3}{2} & -2L_3 & 0 & \frac{L_3}{2} \\
0 & 0 & -2L_4 & 0 & 0 & 0 & L_3 \\
0 & 0 & 0 & 0 & 0 & 0 & 0 \\
0 & 0 & 0 & -\frac{L_4}{2} & L_3-3L_4 & L_9 & \frac{L_4}{2} \\
0 & 0 & 0 & -\frac{L_9}{2} & -3L_9 & L_4-L_3 & \frac{L_9}{2} \\
0 & 0 & 0 & 0 & 0 & 0 & -L_3
\end{pmatrix}, \tag{A.7}$$

$$\tilde{A}_{35} = \begin{pmatrix}
-3L_1-L_2-4L_4+2L_5 & L_3-L_5 & -\frac{L_1}{2} \\
0 & L_3 & L_4 \\
0 & -6L_3 & -4L_4
\end{pmatrix}, \tag{A.8}$$

$$\tilde{A}_{36,37} = \begin{pmatrix}
2L_5-2L_1-2L_2-4L_4 & L_1+L_4 & L_2-L_3+L_4 & 0 \\
0 & L_5-2L_2-2L_4 & 0 & L_2-L_3+L_4 \\
0 & 0 & L_5-2L_1-L_3-2L_4 & L_1+L_4 \\
0 & 0 & 0 & -L_3
\end{pmatrix}. \tag{A.9}$$

Open Access. This article is distributed under the terms of the Creative Commons Attribution License (CC-BY 4.0), which permits any use, distribution and reproduction in any medium, provided the original author(s) and source are credited.

JHEP04(2015)140

References

[1] LHCb collaboration, *Letter of Intent for the LHCb Upgrade*, CERN-LHCC-2011-001, LHCC-I-018 (2011).

[2] D. Zeppenfeld, SU(3) *Relations for B Meson Decays*, *Z. Phys.* **C 8** (1981) 77 [INSPIRE].

[3] Y.-Y. Keum, H.-n. Li and A.I. Sanda, *Fat penguins and imaginary penguins in perturbative QCD*, *Phys. Lett.* **B 504** (2001) 6 [hep-ph/0004004] [INSPIRE].

[4] M. Beneke, G. Buchalla, M. Neubert and C.T. Sachrajda, *QCD factorization for $B \to \pi\pi$ decays: Strong phases and CP-violation in the heavy quark limit*, *Phys. Rev. Lett.* **83** (1999) 1914 [hep-ph/9905312] [INSPIRE].

[5] M. Beneke, G. Buchalla, M. Neubert and C.T. Sachrajda, *QCD factorization for exclusive, nonleptonic B meson decays: general arguments and the case of heavy light final states*, *Nucl. Phys.* **B 591** (2000) 313 [hep-ph/0006124] [INSPIRE].

[6] M. Beneke, G. Buchalla, M. Neubert and C.T. Sachrajda, *QCD factorization in $B \to \pi K, \pi\pi$ decays and extraction of Wolfenstein parameters*, *Nucl. Phys.* **B 606** (2001) 245 [hep-ph/0104110] [INSPIRE].

[7] M. Beneke and M. Neubert, *QCD factorization for $B \to PP$ and $B \to PV$ decays*, *Nucl. Phys.* **B 675** (2003) 333 [hep-ph/0308039] [INSPIRE].

[8] G. Bell, *NNLO vertex corrections in charmless hadronic B decays: Imaginary part*, *Nucl. Phys.* **B 795** (2008) 1 [arXiv:0705.3127] [INSPIRE].

[9] G. Bell, *NNLO vertex corrections in charmless hadronic B decays: Real part*, *Nucl. Phys.* **B 822** (2009) 172 [arXiv:0902.1915] [INSPIRE].

[10] M. Beneke, T. Huber and X.-Q. Li, *NNLO vertex corrections to non-leptonic B decays: tree amplitudes*, *Nucl. Phys.* **B 832** (2010) 109 [arXiv:0911.3655] [INSPIRE].

[11] G. Bell and T. Huber, *Master integrals for the two-loop penguin contribution in non-leptonic B-decays*, *JHEP* **12** (2014) 129 [arXiv:1410.2804] [INSPIRE].

[12] G. Bell, M. Beneke, T. Huber and X.-Q. Li, *Two-loop current-current operator contribution to the non-leptonic QCD penguin amplitude*, in preparation.

[13] T. Huber and S. Kränkl, *Towards NNLO corrections in $B \to D\pi$*, arXiv:1405.5911 [INSPIRE].

[14] A.V. Kotikov, *Differential equations method: new technique for massive Feynman diagrams calculation*, *Phys. Lett.* **B 254** (1991) 158 [INSPIRE].

[15] A.V. Kotikov, *Differential equation method: the calculation of N point Feynman diagrams*, *Phys. Lett.* **B 267** (1991) 123 [INSPIRE].

[16] E. Remiddi, *Differential equations for Feynman graph amplitudes*, *Nuovo Cim.* **A 110** (1997) 1435 [hep-th/9711188] [INSPIRE].

[17] J.M. Henn, *Multiloop integrals in dimensional regularization made simple*, *Phys. Rev. Lett.* **110** (2013) 251601 [arXiv:1304.1806] [INSPIRE].

[18] J.M. Henn, A.V. Smirnov and V.A. Smirnov, *Analytic results for planar three-loop four-point integrals from a Knizhnik-Zamolodchikov equation*, *JHEP* **07** (2013) 128 [arXiv:1306.2799] [INSPIRE].

JHEP04(2015)140

[19] J.M. Henn and V.A. Smirnov, *Analytic results for two-loop master integrals for Bhabha scattering I*, *JHEP* **11** (2013) 041 [arXiv:1307.4083] [INSPIRE].

[20] J.M. Henn, A.V. Smirnov and V.A. Smirnov, *Evaluating single-scale and/or non-planar diagrams by differential equations*, *JHEP* **03** (2014) 088 [arXiv:1312.2588] [INSPIRE].

[21] M. Argeri et al., *Magnus and Dyson Series for Master Integrals*, *JHEP* **03** (2014) 082 [arXiv:1401.2979] [INSPIRE].

[22] J.M. Henn, K. Melnikov and V.A. Smirnov, *Two-loop planar master integrals for the production of off-shell vector bosons in hadron collisions*, *JHEP* **05** (2014) 090 [arXiv:1402.7078] [INSPIRE].

[23] T. Gehrmann, A. von Manteuffel, L. Tancredi and E. Weihs, *The two-loop master integrals for $q\bar{q} \to VV$*, *JHEP* **06** (2014) 032 [arXiv:1404.4853] [INSPIRE].

[24] F. Caola, J.M. Henn, K. Melnikov and V.A. Smirnov, *Non-planar master integrals for the production of two off-shell vector bosons in collisions of massless partons*, *JHEP* **09** (2014) 043 [arXiv:1404.5590] [INSPIRE].

[25] S. Di Vita, P. Mastrolia, U. Schubert and V. Yundin, *Three-loop master integrals for ladder-box diagrams with one massive leg*, *JHEP* **09** (2014) 148 [arXiv:1408.3107] [INSPIRE].

[26] A. von Manteuffel, R.M. Schabinger and H.X. Zhu, *The two-loop soft function for heavy quark pair production at future linear colliders*, arXiv:1408.5134 [INSPIRE].

[27] M. Höschele, J. Hoff and T. Ueda, *Adequate bases of phase space master integrals for $gg \to h$ at NNLO and beyond*, *JHEP* **09** (2014) 116 [arXiv:1407.4049] [INSPIRE].

[28] H.X. Zhu, *On the calculation of soft phase space integral*, *JHEP* **02** (2015) 155 [arXiv:1501.00236] [INSPIRE].

[29] R.N. Lee, *Reducing differential equations for multiloop master integrals*, arXiv:1411.0911 [INSPIRE].

[30] J.M. Henn, *Lectures on differential equations for Feynman integrals*, *J. Phys.* **A 48** (2015) 153001 [arXiv:1412.2296] [INSPIRE].

[31] Analytic results to order $\mathcal{O}(\epsilon^4)$ of all integrals, including their mass-flipped counterparts, are attached in electronic form to the arXiv submission of the present article.

[32] F.V. Tkachov, *A Theorem on Analytical Calculability of Four Loop Renormalization Group Functions*, *Phys. Lett.* **B 100** (1981) 65 [INSPIRE].

[33] K.G. Chetyrkin and F.V. Tkachov, *Integration by Parts: The Algorithm to Calculate β-functions in 4 Loops*, *Nucl. Phys.* **B 192** (1981) 159 [INSPIRE].

[34] S. Laporta, *High precision calculation of multiloop Feynman integrals by difference equations*, *Int. J. Mod. Phys.* **A 15** (2000) 5087 [hep-ph/0102033] [INSPIRE].

[35] C. Anastasiou and A. Lazopoulos, *Automatic integral reduction for higher order perturbative calculations*, *JHEP* **07** (2004) 046 [hep-ph/0404258] [INSPIRE].

[36] A.V. Smirnov, *Algorithm FIRE – Feynman Integral REduction*, *JHEP* **10** (2008) 107 [arXiv:0807.3243] [INSPIRE].

[37] M. Argeri and P. Mastrolia, *Feynman Diagrams and Differential Equations*, *Int. J. Mod. Phys.* **A 22** (2007) 4375 [arXiv:0707.4037] [INSPIRE].

JHEP04(2015)140

[38] E. Remiddi and J.A.M. Vermaseren, *Harmonic polylogarithms*, *Int. J. Mod. Phys.* **A 15** (2000) 725 [hep-ph/9905237] [INSPIRE].

[39] D. Maître, *HPL, a mathematica implementation of the harmonic polylogarithms*, *Comput. Phys. Commun.* **174** (2006) 222 [hep-ph/0507152] [INSPIRE].

[40] A.B. Goncharov, *Multiple polylogarithms, cyclotomy and modular complexes*, *Math. Res. Lett.* **5** (1998) 497 [arXiv:1105.2076] [INSPIRE].

[41] V.A. Smirnov, *Analytical result for dimensionally regularized massless on shell double box*, *Phys. Lett.* **B 460** (1999) 397 [hep-ph/9905323] [INSPIRE].

[42] J.B. Tausk, *Nonplanar massless two loop Feynman diagrams with four on-shell legs*, *Phys. Lett.* **B 469** (1999) 225 [hep-ph/9909506] [INSPIRE].

[43] T. Huber, *On a two-loop crossed six-line master integral with two massive lines*, *JHEP* **03** (2009) 024 [arXiv:0901.2133] [INSPIRE].

[44] M. Czakon, http://mbtools.hepforge.org/.

[45] T. Huber and D. Maître, *HypExp: A Mathematica package for expanding hypergeometric functions around integer-valued parameters*, *Comput. Phys. Commun.* **175** (2006) 122 [hep-ph/0507094] [INSPIRE].

[46] T. Huber and D. Maître, *HypExp 2, Expanding Hypergeometric Functions about Half-Integer Parameters*, *Comput. Phys. Commun.* **178** (2008) 755 [arXiv:0708.2443] [INSPIRE].

[47] C.W. Bauer, A. Frink and R. Kreckel, *Introduction to the GiNaC framework for symbolic computation within the C++ programming language*, *J. Symb. Comput.* **33** (2002) 1.

[48] J. Vollinga and S. Weinzierl, *Numerical evaluation of multiple polylogarithms*, *Comput. Phys. Commun.* **167** (2005) 177 [hep-ph/0410259] [INSPIRE].

[49] J. Gluza, K. Kajda and T. Riemann, *AMBRE: A Mathematica package for the construction of Mellin-Barnes representations for Feynman integrals*, *Comput. Phys. Commun.* **177** (2007) 879 [arXiv:0704.2423] [INSPIRE].

[50] M. Czakon, *Automatized analytic continuation of Mellin-Barnes integrals*, *Comput. Phys. Commun.* **175** (2006) 559 [hep-ph/0511200] [INSPIRE].

[51] J. Carter and G. Heinrich, *SecDec: a general program for sector decomposition*, *Comput. Phys. Commun.* **182** (2011) 1566 [arXiv:1011.5493] [INSPIRE].

[52] S. Borowka, J. Carter and G. Heinrich, *Numerical Evaluation of Multi-Loop Integrals for Arbitrary Kinematics with SecDec 2.0*, *Comput. Phys. Commun.* **184** (2013) 396 [arXiv:1204.4152] [INSPIRE].

JHEP04(2015)140

Published for SISSA by Springer

Received: December 3, 2014
Accepted: January 1, 2015
Published: January 21, 2015

Four-body contributions to $\bar{B} \to X_s\gamma$ at NLO

Tobias Huber,[a] **Michał Poradziński**[a,b] **and Javier Virto**[a]

[a] *Theoretische Physik 1, Naturwissenschaftlich-Technische Fakultät, Universität Siegen, D-57068 Siegen, Germany*

[b] *Faculty of Physics, University of Warsaw, PL-00-681 Warsaw, Poland*

E-mail: huber@physik.uni-siegen.de, michal.poradzinski@fuw.edu.pl, virto@physik.uni-siegen.de

Abstract: Ongoing efforts to reduce the perturbative uncertainty in the $\bar{B} \to X_s\gamma$ decay rate have resulted in a theory estimate to NNLO in QCD. However, a few contributions from multi-parton final states which are formally NLO are still unknown. These are parametrically small and included in the estimated error from higher order corrections, but must be computed if one is to claim complete knowledge of the $\bar{B} \to X_s\gamma$ rate to NLO. A major part of these unknown pieces are four-body contributions corresponding to the partonic process $b \to s\bar{q}q\gamma$. We compute these NLO four-body contributions to $\bar{B} \to X_s\gamma$, and confirm the corresponding tree-level leading-order results. While the NLO contributions arise from tree-level and one-loop Feynman diagrams, the four-body phase-space integrations make the computation non-trivial. The decay rate contains collinear logarithms arising from the mass regularization of collinear divergences. We perform an exhaustive numerical analysis, and find that these contributions are positive and amount to no more than $\sim 1\%$ of the total rate in the Standard Model, thus confirming previous estimates of the perturbative uncertainty.

Keywords: Rare Decays, B-Physics, QCD, Effective field theories

ArXiv ePrint: 1411.7677

Open Access, © The Authors.
Article funded by SCOAP[3].

doi:10.1007/JHEP01(2015)115

Contents

1 Introduction **1**

2 Details of the calculation **5**
- 2.1 Operator identities 5
  - 2.1.1 Color 5
  - 2.1.2 Insertions to the right of the cut 6
  - 2.1.3 Insertions to the left of the cut 7
- 2.2 Set of diagrams 9
- 2.3 Other details 12
  - 2.3.1 Irrelevance of evanescent terms to the right of the cut 12
  - 2.3.2 Cancellation of $i\epsilon_{\mu\nu\rho\sigma}k_1^\mu k_2^\nu k_3^\rho k_4^\sigma$ terms 12
- 2.4 Phase-space integration 13
- 2.5 Renormalization 16
- 2.6 Collinear divergences and splitting functions 17

3 Results **18**

4 Numerical analysis **20**

5 Conclusions **23**

A Intermediate results **24**
- A.1 (P_7, P_i) interference 24
- A.2 (P_8, P_i) interference 24
- A.3 (P_i, P_j) interference 25

1 Introduction

The inclusive radiative B meson decay $\bar{B} \to X_s\gamma$ is the paradigm for precision tests of the Standard Model (SM) in quark flavor physics. Its branching ratio is measured with a precision of $\sim 7\%$ [1–8],[1]

$$\mathcal{B}(\bar{B} \to X_s\gamma)^{\text{exp}}_{E_\gamma > 1.6\,\text{GeV}} = (3.43 \pm 0.22) \cdot 10^{-4} \,. \tag{1.1}$$

To match this experimental precision, a theory calculation to next-to-next-to-leading order (NNLO) accuracy is necessary. This program has been carried out during the last

[1] The semi-inclusive measurement in reference [2] has recently been superseded by a new, more precise one — see refs. [9, 10]. However, this new measurement is not yet taken into account in the HFAG average of eq. (1.1).

JHEP01(2015)115

two decades and it is almost – but not quite – finished. The current theory estimate results in the following value [11]:

$$\mathcal{B}(\bar{B} \to X_s\gamma)^{\rm SM}_{E_\gamma > 1.6\,{\rm GeV}} = (3.15 \pm 0.23) \cdot 10^{-4}\,, \tag{1.2}$$

where the total $\pm 7\%$ uncertainty is due to non-perturbative (5%), parametric (3%), higher orders (3%) and m_c-interpolation ambiguity (3%) [11].

The calculation can be divided into: 1. Matching conditions [12–20], 2. Anomalous dimensions [21–30], and 3. Matrix elements [31–50]. Matching conditions and anomalous dimensions are complete up to NNLO since a long time. Missing pieces include m_c-dependent matrix elements at NNLO [43, 51], as well as next-to-leading-order (NLO) matrix elements proportional to penguin or CKM-suppressed current-current operators. The latter are formally NLO but are suppressed by very small Wilson coefficients, and should indeed be rather small, fitting within the estimated $\sim 3\%$ uncertainty from higher orders [11, 52]. However, only a full calculation can provide precise knowledge of their true effect, and we intend to do that here. This work constitutes part of an ongoing effort to reduce the perturbative uncertainty down to a negligible level.

The $\bar{B} \to X_s\gamma$ rate is given by the inclusive partonic rate of the b quark, up to non-perturbative effects that, for a photon energy cut $E_0 = 1.6\,{\rm GeV}$, are estimated at the level of $\sim 5\%$ [53],

$$\Gamma(\bar{B} \to X_s\gamma)_{E_\gamma > E_0} = \Gamma(b \to X_s^{\rm parton}\gamma)_{E_\gamma > E_0} + \mathcal{O}(1/m_b) \tag{1.3}$$

where $b \to X_s^{\rm parton}\gamma$ denotes the partonic decay of the b quark into any number of particles with an overall strangeness $S = -1$, plus a hard photon with $E_\gamma > E_0$, and *excluding* charm:

$$\Gamma(b \to X_s^{\rm parton}\gamma) = \Gamma(b \to s\gamma) + \Gamma(b \to sg\gamma) + \Gamma(b \to sq\bar{q}\gamma) + \cdots\,, \tag{1.4}$$

with $q = u, d, s$. Each individual rate is an interference of different amplitudes, computed as matrix elements of local operators in the effective Lagrangian:

$$\mathcal{L}_{\rm eff} = \mathcal{L}_{\rm QED+QCD} + \frac{4G_F}{\sqrt{2}} V_{ts}^* V_{tb} \left[\sum_{i=1}^{2} (\mathcal{C}_i^u P_i^u + \mathcal{C}_i^c P_i^c) + \sum_{i=3}^{8} \mathcal{C}_i P_i \right] + h.c.\,, \tag{1.5}$$

where the operators P_i are defined as [24]:

$$\begin{aligned}
P_1^q &= (\bar{s}_L\gamma_\mu T^a q_L)(\bar{q}_L\gamma^\mu T^a b_L)\,, & P_2^q &= (\bar{s}_L\gamma_\mu q_L)(\bar{q}_L\gamma^\mu b_L)\,,\\
P_3 &= (\bar{s}_L\gamma_\mu b_L)\textstyle\sum_q(\bar{q}\gamma^\mu q)\,, & P_4 &= (\bar{s}_L\gamma_\mu T^a b_L)\textstyle\sum_q(\bar{q}\gamma^\mu T^a q)\,,\\
P_5 &= (\bar{s}_L\gamma_\mu\gamma_\nu\gamma_\rho b_L)\textstyle\sum_q(\bar{q}\gamma^\mu\gamma^\nu\gamma^\rho q)\,, & P_6 &= (\bar{s}_L\gamma_\mu\gamma_\nu\gamma_\rho T^a b_L)\textstyle\sum_q(\bar{q}\gamma^\mu\gamma^\nu\gamma^\rho T^a q)\,,\\
P_7 &= (e/16\pi^2) m_b(\bar{s}_L\sigma^{\mu\nu} b_R) F_{\mu\nu}\,, & P_8 &= (g_s/16\pi^2) m_b(\bar{s}_L\sigma^{\mu\nu} T^a b_R) G^a_{\mu\nu}\,.
\end{aligned} \tag{1.6}$$

With this notation, $\mathcal{C}_{1,2}^q$ contain CKM phases: $\mathcal{C}_{1,2}^q = -\lambda_q C_{1,2}$, with $\lambda_q \equiv V_{qs}^* V_{qb}/V_{ts}^* V_{tb}$ and $C_{1,2}$ defined in the usual way, e.g. ref. [24]. We will also use the notation $\mathcal{C}_{1u} \equiv \mathcal{C}_1^u$ etc. The other Wilson coefficients are simply $\mathcal{C}_{3,\ldots,8} = C_{3,\ldots,8}$ as in ref. [24].

JHEP01(2015)115

For more than two final state particles, the rate involves integration over phase space; the photon spectrum opens up, and the rate depends on the photon-energy cut. The perturbative contribution can be written, in the notation of ref. [40], as:

$$\Gamma(b \to X_s^{\rm parton}\gamma)_{E_\gamma > E_0} = \Gamma_0 \sum_{i,j} \mathcal{C}_i^{\rm eff}(\mu_b)^* \, \mathcal{C}_j^{\rm eff}(\mu_b) \, \widetilde{G}_{ij}(\mu_b, \delta) \, , \tag{1.7}$$

summed over $i, j = 1u, 2u, 3, \ldots, 6, 1c, 2c, 7, 8$, and with the normalization

$$\Gamma_0 = \frac{G_F^2 m_b^5 \alpha_e |V_{ts}^* V_{tb}|^2}{32\pi^4} \, . \tag{1.8}$$

The "effective" Wilson coefficients are $\mathcal{C}^{\rm eff}_{1q,2q,3,\ldots,6} = \mathcal{C}_{1q,2q,3,\ldots,6}$, $\mathcal{C}_7^{\rm eff} = \mathcal{C}_7 - \frac{1}{3}\mathcal{C}_3 - \frac{4}{3}\mathcal{C}_4 - \frac{20}{3}\mathcal{C}_5 - \frac{80}{9}\mathcal{C}_6$ and $\mathcal{C}_8^{\rm eff} = \mathcal{C}_8 + \mathcal{C}_3 - \frac{1}{6}\mathcal{C}_4 + 20\mathcal{C}_5 - \frac{10}{3}\mathcal{C}_6$. Throughout the paper we use the NDR-$\overline{\rm MS}$ scheme with fully anti-commuting γ_5.

The objects $\widetilde{G}_{ij}$ arise from the interference of operators P_i and P_j in the squared matrix elements, integrated over phase space. They depend on the photon energy cut through the variable $\delta \equiv 1 - 2E_0/m_b$. In the notation of ref. [43], where normalization to the inclusive semileptonic $b \to u$ rate is used, $K_{ij} = \widetilde{G}_{ij}/G_u$, with $G_u = 1 + C_F\left(\frac{25}{2} - 12\zeta_2\right)\frac{\alpha_s}{4\pi} + \mathcal{O}(\alpha_s^2)$ [54].

In this paper we focus on the four-body contributions to $\Gamma(b \to X_s^{\rm parton}\gamma)_{E_\gamma > E_0}$, corresponding to $\Gamma(b \to s\bar{q}q\gamma)$:

$$\Gamma(b \to s\bar{q}q\gamma)_{E_\gamma > E_0} = \Gamma_0 \sum_{i,j} \mathcal{C}_i^{\rm eff}(\mu_b)^* \, \mathcal{C}_j^{\rm eff}(\mu_b) \, G_{ij}(\mu_b, \delta) \, , \tag{1.9}$$

where we define G_{ij} as the $b \to s\bar{q}q\gamma$ contribution to $\widetilde{G}_{ij}$. In addition, we expand G_{ij} as:

$$G_{ij}(\mu, \delta) = G_{ij}^{(0)}(\delta) + \frac{\alpha_s(\mu)}{4\pi} G_{ij}^{(1)}(\mu, \delta) + \mathcal{O}(\alpha_s^2) \, . \tag{1.10}$$

There is a hierarchy in the size of the Wilson coefficients of the operators in eq. (1.6), which can be divided into two classes:

$$A = \{P_1^c, P_2^c, P_7, P_8\} \; ; \quad B = \{P_1^u, P_2^u, P_3, P_4, P_5, P_6\} \, . \tag{1.11}$$

Operators in class A have large Wilson coefficients, whereas class-B operators have either very small Wilson coefficients or are CKM-suppressed. Among the four-body leading and next-to leading contributions we distinguish four groups:

- Tree-level (B, B) interference (figure 1.a). These are the leading-order (LO) contributions and provide the complete matrix $G^{(0)}(\delta)$. This matrix has been computed in ref. [50].

- Tree-level (A, B) interference (figures 1.b and 1.c). These are NLO and provide the matrix elements $G_{7j}^{(1)}$ and $G_{8j}^{(1)}$, with $j = 1u, 2u, 3, \ldots, 6$.

- One-loop (A, B) interference (figure 1.d). These are NLO and provide the matrix elements $G_{ij}^{(1)}$, with $i = 1c, 2c$ and $j = 1u, 2u, 3, \ldots, 6$.

JHEP01(2015)115

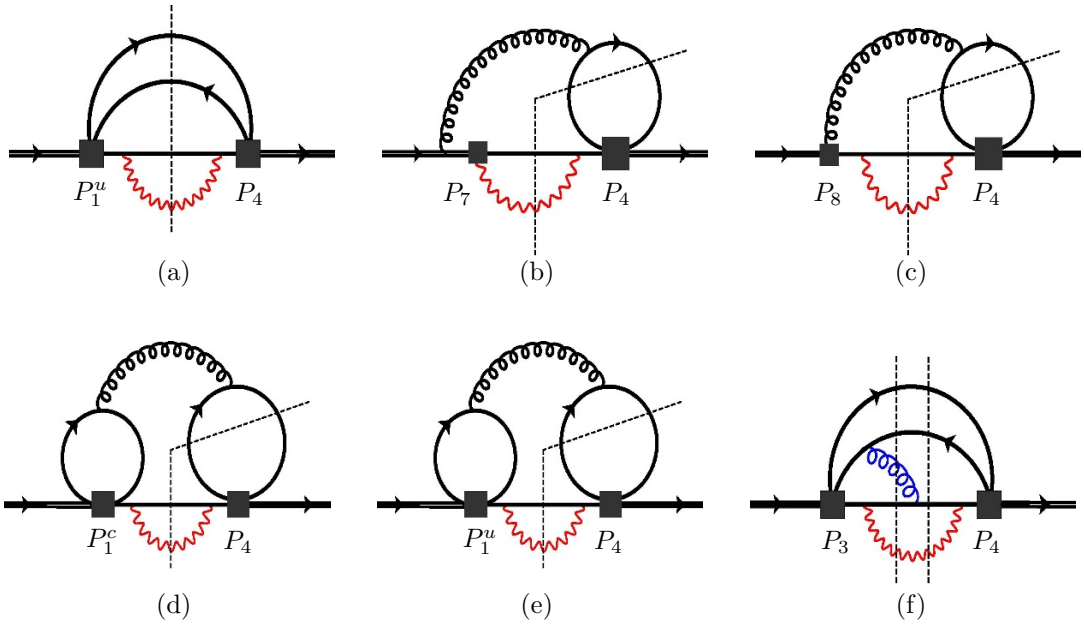

Figure 1. Sample cut-diagrams contributing to LO and NLO four-body matrix elements. In our calculation we include all contributions but those from panel (f). See the text for details.

- One-loop (B, B) interference (figures 1.e and 1.f). The ones in panel (e) can be obtained from the ones in panel (d) as discussed in section 2.1, and provide the matrix elements $G_{ij}^{(1)}$, with $i, j = 1u, 2u, 3, \ldots, 6$. The ones in panel (f) include five-particle cuts since the one-loop four-body diagrams must be complemented with the five-body gluon-bremsstrahlung correction $b \to s\bar{q}q\gamma + g$. We therefore leave the contributions from panel (f) aside from the present four-body calculation.

We note that NLO (A, B) interference terms are presumably as large as the (B, B) interference at the LO since $\mathcal{C}_{1u,2u,3,\ldots,6} \sim \alpha_s/\pi\, \mathcal{C}_{1c,2c,7,8}$. For the same reason, the partly neglected (B, B) interference terms at the NLO are expected to be much smaller than the (A, B) interferences that we calculate in a complete manner. As a final comment, we note that four-body NNLO contributions of the type $b \to sgg\gamma$ are part of the calculation in ref. [51], and do not interfere with our results.

The structure of the paper is the following. In section 2 we discuss the details of our calculation and the structure of the different contributions, including the set of diagrams needed, the UV renormalization, and the treatment of collinear divergences. In section 3 we collect the final results. In section 4 we perform a numerical study of all the evaluated interferences. Section 5 contains our conclusions. In appendix A we collect some intermediate results of the calculation, where analytic cancellation of UV and collinear divergences can be explicitly checked.

JHEP01(2015)115

2 Details of the calculation

The NLO calculation is performed in 4 steps:

1. Evaluation of the cut-diagrams shown in figures 2, 3, 4. We use the Cutkosky rules for cut (on-shell) propagators, accounting for spin and color sums for all external particles. The result of each diagram is a contribution to the differential decay rate $\mathcal{K}(s_{ij})$, a scalar function of the momentum invariants s_{ij}, $i, j = 1, \ldots, 4$, with $i \neq j$ (see sections 2.4 and 2.3.2).

2. Integration over the four-particle phase-space. This step is described in section 2.4.

3. Renormalization: this requires the evaluation of the tree-level diagrams with counterterms shown in figure 5, and the corresponding phase-space integration. As a bonus, this step allows one to check the LO result for $G^{(0)}_{ij}$ of ref. [50]. This step is described in section 2.5.

4. Collinear logarithms: having regularized collinear divergences in dimensional regularization, we use the method of splitting functions [50, 55–58] to transform $1/\epsilon_{\rm coll}$ poles into collinear logarithms of the form $\log(m_q/m_b)$. This requires the computation of the corresponding $b \to s\bar{q}q$ corrections with subsequent photon emission $q' \to q'\gamma$ (with $q' = q, s$), by evaluation of the diagrams shown in figure 6, the convolution with the splitting function, and the three-particle phase-space integration. This step is described in section 2.6.

We note that every diagram has to be computed inserting all the operators $P_{1u,2u,3,\ldots,6}$ to the right of the cut, and $P_{1u,2u,1c,2c,3,\ldots,8}$ to the left (see e.g. figure 1), leading to all the different interference terms in the matrix $G^{(1)}_{ij}$. In section 2.1 we argue that most of the elements of this matrix can be obtained from a reduced set by the use of different operator relations and Fierz identities. In addition, this spells out transparently the dependence of the full result on the Wilson coefficients before any calculation is performed. We will see that — with one exception discussed at the end of section 2.1.3 — only diagrams with $P_{7,8,1c}$ to the left of the cut and P_4 to the right must be considered. This simplifies the calculation considerably.

Finally, for each diagram in figures 2–6, there is the corresponding mirror image. These "mirror" contributions are just obtained by complex conjugation, and ensure that the rate is real, i.e. $G^{(1)}_{ij}$ is hermitian. We disregard these mirror contributions in the calculation, but at the end we substitute $G^{(1)}_{ij} \to G^{(1)}_{ij} + G^{(1)\,*}_{ji}$.

2.1 Operator identities

2.1.1 Color

Diagrams with insertion of the color octet operators $P_{4,6}$ are related to the ones with insertion of color singlet operators $P_{3,5}$ by a simple color factor, which can be obtained just

JHEP01(2015)115

from the color structure of the gluon penguin:

("straight") 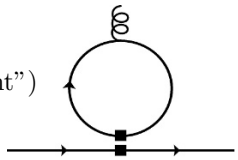 $\longrightarrow \begin{cases} tr(T^a) = 0 & \text{color singlet} \\ tr(T^b T^a) T^b = \frac{1}{2} T^a & \text{color octet} \end{cases}$ (2.1)

("crossed") 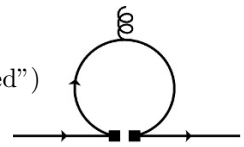 $\longrightarrow \begin{cases} T^a & \text{color singlet} \\ T^b T^a T^b = -\frac{1}{2N_c} T^a & \text{color octet} \end{cases}$ (2.2)

This leads to the rule that $P_{3,5}$ can always be replaced by:

$$P_{3,5} \to 0 \qquad \text{(straight insertion)}\,, \tag{2.3}$$

$$P_{3,5} \to -6\, P_{4,6} \qquad \text{(crossed insertion)}\,. \tag{2.4}$$

For the same reason, one can always put $P_2^q \to -6P_1^q$, meaning that $\mathcal{C}_{1,2}^q$ always come in the combination $(\mathcal{C}_1^q - 6\,\mathcal{C}_2^q)$.

2.1.2 Insertions to the right of the cut

We restrict ourselves here to the insertion of operators to the *right* of the cut. Using the 4D identity $\gamma^\mu\gamma^\nu\gamma^\lambda = g^{\mu\nu}\gamma^\lambda + g^{\nu\lambda}\gamma^\mu - g^{\mu\lambda}\gamma^\nu + i\epsilon^{\mu\nu\lambda\alpha}\gamma_\alpha\gamma_5$ we find:

$$P_6 = 10P_4 - 6\widetilde{P}_4 + \mathcal{O}(\epsilon)\,, \tag{2.5}$$

where $\widetilde{P}_4 = \sum_q (\bar{s}_L\gamma^\mu T^a b_L)(\bar{q}\gamma_\mu\gamma_5 T^a q)$. We now consider the following "crossed" insertion of $\widetilde{P}_4$ into a massless fermion loop with an arbitrary number of *vector* currents:

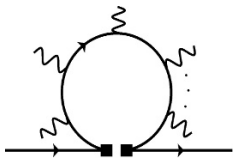

$$= \cdots \gamma_\mu P_L \cdot \underbrace{\gamma^{\mu_1}\gamma^{\mu_2}\cdots\gamma^{\mu_N}\cdot\gamma^\mu}_{\text{even \# of } \gamma\text{'s}}\gamma_5 \cdots = \tag{2.6}$$

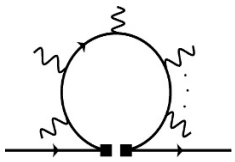

$\widetilde{P}_4$ $\qquad$ $-P_4$

There is always an even number of gamma matrices to the left of γ_5, which can be moved besides the projector P_L. After that, the relationship $P_L\gamma_5 = -P_L$ provides the given negative sign.

The "straight" insertion of $\widetilde{P}_4$ does not vanish in general but does not contribute in our case: in the situation where *one* vector current is attached to the loop (figure 2), the result is proportional to $\mathrm{Tr}[\gamma^\mu\gamma^\nu\gamma^\rho\gamma^\lambda\gamma_5] \sim \epsilon^{\mu\nu\rho\lambda}$, but there are not enough independent momenta to be contracted with the antisymmetric tensor, so this contribution vanishes. This is true also in the case where the photon couples twice to the quark loop (figure 4). In the case of *two* current insertions (figure 3) the result is non-zero, but summing over u, d, s quarks in the loop the result is proportional to $Q_u + Q_d + Q_s = 0$.

JHEP01(2015)115

Summing up, in the diagrams with a P_6 insertion one can always substitute:

$$\begin{aligned} P_6 &\to 10P_4 + \mathcal{O}(\epsilon) \qquad \text{(straight insertion)}\,, \\ P_6 &\to 16P_4 + \mathcal{O}(\epsilon) \qquad \text{(crossed insertion)}\,. \end{aligned} \tag{2.7}$$

The replacement rules (2.7) combined with eqs. (2.3) and (2.4) imply that the full contribution from $P_{3,4,5,6}$ can be obtained from the terms proportional to $\mathcal{C}_4^*$:

$$\text{Result}(P_{3,4,5,6},\text{straight}) = (\mathcal{C}_4^* + 10\,\mathcal{C}_6^*) \times \text{Result}(P_4,\text{straight}), \tag{2.8}$$

$$\text{Result}(P_{3,4,5,6},\text{crossed}) = (-6\,\mathcal{C}_3^* + \mathcal{C}_4^* - 96\,\mathcal{C}_5^* + 16\,\mathcal{C}_6^*) \times \text{Result}(P_4,\text{crossed}). \tag{2.9}$$

Since this is based on a 4D identity, it is in principle only true up to evanescent terms. Below we show that up to the needed order in ϵ these terms do not contribute. We have also checked this by direct computation.

The (crossed) insertion of the operators $P_{1,2}^u$ can also be obtained from P_4 by an argument almost identical to that of eq. (2.6). In this case one must pay attention to the case where the photon couples to the loop, where the P_4 and $P_{1,2}^u$ contributions are proportional to different charge factors.

2.1.3 Insertions to the left of the cut

We have shown that we only need to compute diagrams with an insertion of P_4 to the right of the cut. To the *left* of the cut we must insert $P_{7,8}$ as well as $P_{3,4,5,6}$ and $P_{1,2}^{u,c}$. As before, $P_{2,3,5}$ contributions are related to $P_{1,4,6}$ by a simple color factor. In addition, the contribution from P_1^u is obtained from the P_1^c insertion with the replacement $m_c \to 0$. We now show that insertions of $P_{4,6}$ are also known from the insertions of P_7, P_8 and P_1^c.

First we consider the case of the photon penguin, where the gluon does not couple to the fermion loop to the left of the cut. By direct inspection be find that:

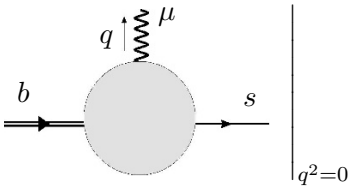

$$= -\frac{ie}{(4\pi)^2}(\mathcal{C}_7^{\text{eff}} + \mathcal{O}(\epsilon))m_b[\not{q}, \gamma^\mu]P_R + X\not{q}q^\mu P_L\,, \tag{2.10}$$

where $\mathcal{C}_7^{\text{eff}} = \mathcal{C}_7 - \mathcal{C}_3/3 - 4\,\mathcal{C}_4/3 - 20\,\mathcal{C}_5/3 - 80\,\mathcal{C}_6/9$ is the usual "effective" Wilson coefficient [25], which includes the contributions from b-quark loops. The $\mathcal{O}(\epsilon)$ corrections are irrelevant to our calculation as the contributions from P_7 are finite. The term $X\not{q}q^\mu$ denotes the contribution from four-quark operators proportional to the structure $[\not{q}q^\mu - q^2\gamma^\mu]$. This last term does not contribute in our case. To see this, consider the insertion of $P_{1,2}$ into the full diagram:

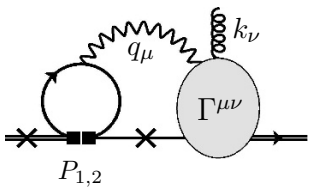

$$\sim \cdots \Gamma^{\mu\nu} \cdots (\not{q}q_\mu - q^2\gamma_\mu)P_L \cdots = 0\,. \tag{2.11}$$

JHEP01(2015)115

Here the gluon is attached to either '×'. Since we cut the photon propagator, the photon is on-shell but there is no q^2 denominator, and therefore the q^2 term cancels. The term $\not{q} q_\mu$ also cancels due to the Ward identity $q_\mu \Gamma^{\mu\nu} = 0$. Note that non-zero contributions to the Ward identity vanish since they either involve a massless fermion tadpole, or if the gluon couples to the loop then it does not depend on the incoming/outgoing quark momenta. We have also checked this result by explicit computation, and indeed the different sets of diagrams satisfying the Ward identity vanish identically.

To summarize: all contributions from photon penguins to the left of the cut are obtained from the diagrams with insertion of P_7 by the replacement $\mathcal{C}_7 \to \mathcal{C}_7^{\rm eff}$.

Next, we consider the case of the gluon penguin, where the photon does not couple to the fermion loop to the left of the cut. We find:

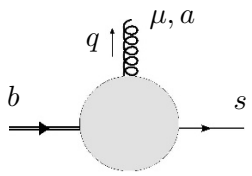

$$= -\frac{i g_s}{(4\pi)^2}\Big[(\mathcal{C}_8^{\rm eff} + \mathcal{O}(\epsilon)) m_b T^a [\not{q}, \gamma^\mu] P_R + X T^a (\not{q} q^\mu - q^2 \gamma^\mu) P_L\Big]\,, \tag{2.12}$$

where $\mathcal{C}_8^{\rm eff} = \mathcal{C}_8 + \mathcal{C}_3 - \mathcal{C}_4/6 + 20\,\mathcal{C}_5 - 10\,\mathcal{C}_6/3$, as usual (e.g. ref. [37]). As before, $\mathcal{O}(\epsilon)$ corrections to the chromomagnetic contribution are irrelevant for our calculation because contributions from P_8 are UV-finite (collinear divergences are inconsequential here). In the last term, the quantity X is given by:

$$\begin{aligned} X = -\frac{1}{6}\Big[&(\mathcal{C}_1^c - 6\,\mathcal{C}_2^c)\, g(m_c) + (\mathcal{C}_1^u - 6\,\mathcal{C}_2^u)\, g(0) + (\mathcal{C}_4 - 6\,\mathcal{C}_3)[g(0) + g(m_b)] \\ &+(4\,\mathcal{C}_6 - 24\,\mathcal{C}_5)(4 - \epsilon - \epsilon^2)\,[g(0) + g(m_b)] \\ &-\frac{6\,\mathcal{C}_4 + (60 - 36\epsilon)\mathcal{C}_6}{1-\epsilon}\,[n_\ell\, g(0) + g(m_c) + g(m_b)]\Big]\,, \end{aligned} \tag{2.13}$$

where $n_\ell = 3$ is the number of light flavors and

$$g(m) = \frac{2}{3}(1-\epsilon)\mu^{2\epsilon} e^{\epsilon\gamma_E} m^{-2\epsilon}\,\Gamma(\epsilon)\,{}_2F_1(\epsilon, 2; 5/2; q^2/4m^2) \tag{2.14}$$

is the loop integral to all orders in ϵ. Therefore, all contributions from gluon penguins to the left of the cut are known from the contribution of P_8 and P_1^c.

Now we consider the case in which both the photon and the gluon couple to the loop:

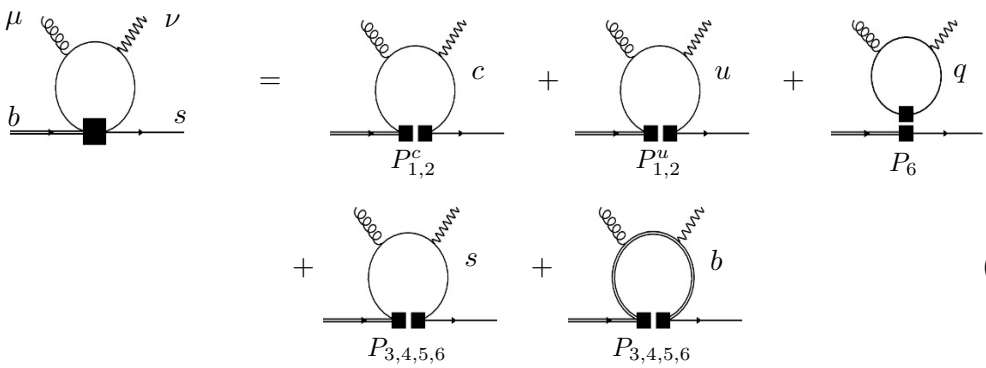

(2.15)

JHEP01(2015)115

When inserted into the full diagrams, these contributions are both UV-finite and collinear safe,[2] and we can use 4D identities. The first term in the right-hand side of eq. (2.15) can be written as $Q_u(\mathcal{C}_1^c - 6\mathcal{C}_2^c)h^{\mu\nu}(m_c)$, which defines the function $h^{\mu\nu}(m)$. The second term can be obtained from the first term by the replacement $m_c \to 0$: $Q_u(\mathcal{C}_1^u - 6\mathcal{C}_2^u)h^{\mu\nu}(0)$. The third term ($q = u, d, s, c, b$) contains only the insertion of P_6, because $P_{3,5}$ insertions are zero due to color, while the insertion of P_4 vanishes due to Furry's theorem. For P_6 we can make use of the Fierz identity:[3]

$$P_1^q = -\frac{4}{27}P_3^q + \frac{1}{9}P_4^q + \frac{1}{27}P_5^q - \frac{1}{36}P_6^q + \mathcal{O}(\epsilon)\,, \tag{2.16}$$

which implies that we can trade the straight insertion of P_6^q with the crossed insertion of $-36P_1^q$. Note also that the contributions from $q = u, d, s$ add up to zero in the massless limit due to electric charge: $Q_u + Q_d + Q_s = 0$. This means that the third term in eq. (2.15) is given by $-36\,\mathcal{C}_6(Q_u h^{\mu\nu}(m_c) + Q_d h^{\mu\nu}(m_b))$.

The fourth term can be obtained from the first one using the identities in eqs. (2.5) and (2.6), leading to: $Q_d(-6\,\mathcal{C}_3 + \mathcal{C}_4 - 96\,\mathcal{C}_5 + 16\,\mathcal{C}_6)h^{\mu\nu}(0)$. The fifth term cannot be completely determined from the insertion of P_1 due to the chirality structure. Using the Fierz identity (2.5) we can trade $P_6^b \to 4P_4^b + 12P_1^b$. The second piece, together with the corresponding contribution from P_5, results in $Q_d(-72\,\mathcal{C}_5 + 12\,\mathcal{C}_6)h^{\mu\nu}(m_b)$. The rest will provide a term $Q_d(-6\,\mathcal{C}_3 + \mathcal{C}_4 - 24\,\mathcal{C}_5 + 4\,\mathcal{C}_6)\widetilde{h}^{\mu\nu}(m_b)$, where $\widetilde{h}^{\mu\nu} \neq h^{\mu\nu}$. Altogether, the right-hand side of eq. (2.15) can be written as:

$$\begin{aligned}
&Q_u(\mathcal{C}_1^c - 6\mathcal{C}_2^c)h^{\mu\nu}(m_c) + Q_u(\mathcal{C}_1^u - 6\mathcal{C}_2^u)h^{\mu\nu}(0) - 36\,\mathcal{C}_6 Q_u h^{\mu\nu}(m_c)\\
&-Q_d(72\,\mathcal{C}_5 + 24\,\mathcal{C}_6)h^{\mu\nu}(m_b) + Q_d(-6\,\mathcal{C}_3 + \mathcal{C}_4 - 96\,\mathcal{C}_5 + 16\,\mathcal{C}_6)h^{\mu\nu}(0)\\
&+Q_d(-6\,\mathcal{C}_3 + \mathcal{C}_4 - 24\,\mathcal{C}_5 + 4\,\mathcal{C}_6)\widetilde{h}^{\mu\nu}(m_b)\ .
\end{aligned} \tag{2.17}$$

Therefore only diagrams with insertions of the operators $P_{7,8}$ and P_1^c to the left of the cut need to be calculated, plus the extra contribution from $\widetilde{h}^{\mu\nu}(m_b)$. All these relationships shape the structure of the full results displayed below in the following sections.

2.2 Set of diagrams

There are three types of diagrams:

Type (i). The photon does not couple to the cut fermion loop (figure 2): in this case crossed and straight diagrams contribute. In addition, straight diagrams contain a factor n_ℓ. All in all, the contribution from these diagrams is:

$$\mathcal{D}_{(i)}^k = Q_d\left[n_\ell\,(\mathcal{C}_4^* + 10\,\mathcal{C}_6^*)\langle P_4\rangle_{(i)}^{s,k} + (\mathcal{C}_1^{u*} - 6\,\mathcal{C}_2^{u*} - 6\,\mathcal{C}_3^* + \mathcal{C}_4^* - 96\,\mathcal{C}_5^* + 16\,\mathcal{C}_6^*)\langle P_4\rangle_{(i)}^{\times,k}\right], \tag{2.18}$$

where $\langle P_4\rangle_{(J)}^{s,k}$ and $\langle P_4\rangle_{(J)}^{\times,k}$ denote the contributions to (P_k, P_4) interference terms from straight and crossed insertions of the operator P_4 to the right of the cut, to diagrams of type (J), respectively.

[2] We consider always the sum of the two diagrams obtained by swapping the gluon and photon insertions.
[3] Here we use the notation $P_3^u = (\bar{s}_L\gamma_\mu b_L)(\bar{u}\gamma^\mu u)$, etc.

JHEP01(2015)115

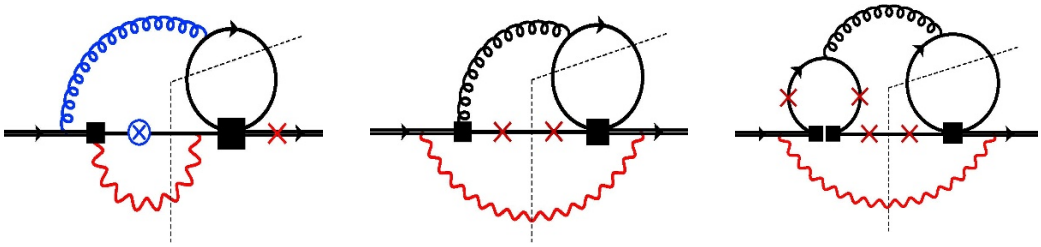

Figure 2. Diagrams of type (i). Crosses denote alternative insertions of the photon vertex (always one vertex at each side of the cut). Circle-cross denotes the alternative insertion of the gluon vertex.

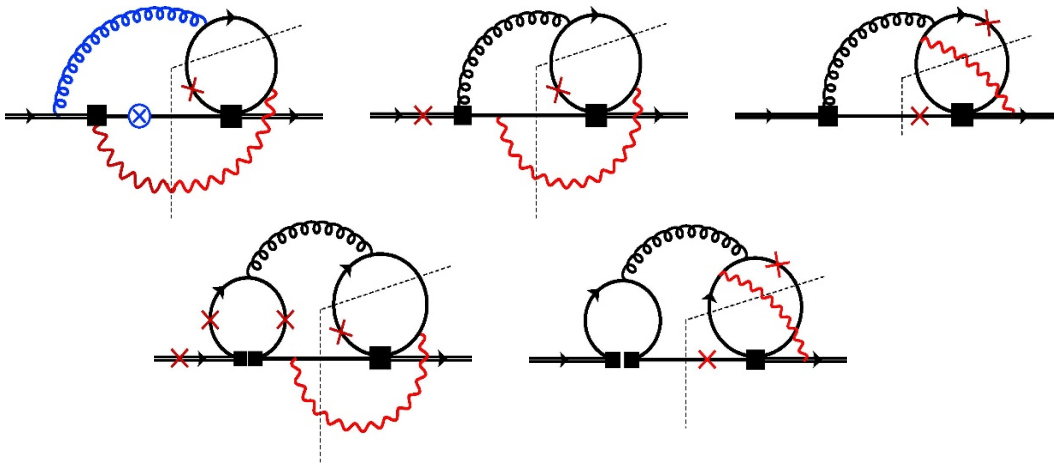

Figure 3. Diagrams of type (ii). Crosses denote alternative insertions of the photon vertex (always one vertex at each side of the cut). Circle-cross denotes the alternative insertion of the gluon vertex.

Type (ii). The photon couples to the cut fermion loop once (figure 3): in this case the straight diagrams are proportional to $Q_u + Q_d + Q_s = 0$ and need not be considered. The $P^u_{1,2}$ contributions are proportional to Q_u. Therefore the total contribution from these diagrams is:

$$\mathcal{D}^k_{(ii)} = \Big[Q_d\,\big(-6\,\mathcal{C}^*_3 + \mathcal{C}^*_4 - 96\,\mathcal{C}^*_5 + 16\,\mathcal{C}^*_6\big) + Q_u\,(\mathcal{C}^{u*}_1 - 6\,\mathcal{C}^{u*}_2)\Big]\langle P_4\rangle^{\times,k}_{(ii)}\,. \tag{2.19}$$

Type (iii). The photon couples to the cut fermion loop twice (figure 4): in this case crossed diagrams are proportional to $Q_s^2 = Q_d^2$ (or Q_u^2 in the case of $P^u_{1,2}$) and straight diagrams to $Q_u^2 + Q_d^2 + Q_s^2 = Q_u^2 + 2Q_d^2$. We have:

$$\begin{aligned}\mathcal{D}^k_{(iii)} &= [Q_u^2 + 2Q_d^2]\big(\mathcal{C}^*_4 + 10\,\mathcal{C}^*_6\big)\langle P_4\rangle^{s,k}_{(iii)} \\ &\quad + \Big[Q_d^2\,\big(-6\,\mathcal{C}^*_3 + \mathcal{C}^*_4 - 96\,\mathcal{C}^*_5 + 16\,\mathcal{C}^*_6\big) + Q_u^2\,(\mathcal{C}^{u*}_1 - 6\,\mathcal{C}^{u*}_2)\Big]\langle P_4\rangle^{\times,k}_{(iii)}\,.\end{aligned} \tag{2.20}$$

We assume that the objects $\langle P_4\rangle^{I,k}_{(J)}$ are phase-space-integrated matrix elements containing no prefactors or couplings, such that:

$$\sum_{\substack{i=3,\ldots,8,1q,2q\\ j=3,\ldots,6,1u,2u}} \mathcal{C}^*_i\,\mathcal{C}_j\,G^{(1)}_{ij} = \sum_{J=i,ii,iii}\Big[\mathcal{D}^C_{(J)} + \sum_{k=3,\ldots,8,1q,2q}\mathcal{D}^k_{(J)}\Big] \tag{2.21}$$

JHEP01(2015)115

in the notation of eq. (1.9). In eq. (2.21), $\mathcal{D}^C_{(J)}$ denotes the UV counterterms, and both $\mathcal{D}^C_{(J)}, \mathcal{D}^k_{(J)}$ include the relevant collinear counterterms. Both are discussed below in sections 2.5 and 2.6. The structure of the objects $\langle P_4\rangle^{(s,\times),k}_{(J)}$ can be deduced from the discussion in section 2.1.3. In the case of $P_{7,8}$ we have:

$$\begin{aligned}
\langle P_4\rangle^{I,7}_{(J)} &= \mathcal{C}_7^{\rm eff}\,\mathcal{F}^{I,7}_{(J)}(\delta) && \text{for} \quad (I,J) = (s,i),(\times,i),(\times,ii)\,,\\
\langle P_4\rangle^{I,8}_{(J)} &= \mathcal{C}_8^{\rm eff}\,Q_d\,\hat{\mathcal{F}}^{I,8}_{(J)}(\delta) && \text{for} \quad (I,J) = (s,i),(\times,i),(\times,ii)\,,\\
\langle P_4\rangle^{I,8}_{(J)} &= \mathcal{C}_8^{\rm eff}\,\hat{\mathcal{F}}^{I,8}_{(J)}(\delta) && \text{for} \quad I = s,\times \;\text{ and }\; J = iii\,.
\end{aligned} \tag{2.22}$$

For $P^{(u)}_{1,2}$ we have:

$$\begin{aligned}
\sum_{k=1,2}\langle P_4\rangle^{I,k}_{(J)} &= (\mathcal{C}_1^c - 6\,\mathcal{C}_2^c)\left[Q_d\hat{\mathcal{F}}^{I,1}_{(J)}(z_c,\delta) + Q_u\widetilde{\mathcal{F}}^{I,1}_{(J)}(z_c,\delta)\right]\\
&\qquad\qquad \text{for} \quad (I,J) = (s,i),(\times,i),(\times,ii)\,,\\
\sum_{k=1,2}\langle P_4\rangle^{I,k}_{(J)} &= (\mathcal{C}_1^c - 6\,\mathcal{C}_2^c)\,\hat{\mathcal{F}}^{I,1}_{(J)}(z_c,\delta) \qquad \text{for} \quad I = s,\times \;\text{ and }\; J = iii\,,
\end{aligned} \tag{2.23}$$

$$\begin{aligned}
\sum_{k=1u,2u}\langle P_4\rangle^{I,k}_{(J)} &= (\mathcal{C}_1^u - 6\,\mathcal{C}_2^u)\left[Q_d\hat{\mathcal{F}}^{I,1}_{(J)}(0,\delta) + Q_u\widetilde{\mathcal{F}}^{I,1}_{(J)}(0,\delta)\right]\\
&\qquad\qquad \text{for} \quad (I,J) = (s,i),(\times,i),(\times,ii)\,,\\
\sum_{k=1u,2u}\langle P_4\rangle^{I,k}_{(J)} &= (\mathcal{C}_1^u - 6\,\mathcal{C}_2^u)\,\hat{\mathcal{F}}^{I,1}_{(J)}(0,\delta) \qquad \text{for} \quad I = s,\times \;\text{ and }\; J = iii\,,
\end{aligned} \tag{2.24}$$

where $z_c \equiv m_c^2/m_b^2$. The contributions with penguin operators to the left of the cut are given by:

$$\begin{aligned}
\sum_{k=3\ldots6}\langle P_4\rangle^{I,k}_{(J)} &= (\mathcal{C}_4 - 6\,\mathcal{C}_3)\,Q_d\left[\hat{\mathcal{F}}^{I,1}_{(J)}(0,\delta) + \hat{\mathcal{F}}^{I,1}_{(J)}(1,\delta) + \widetilde{\mathcal{F}}^{I,1}_{(J)}(0,\delta)\right]\\
&\quad +4(\mathcal{C}_6 - 6\,\mathcal{C}_5)\,Q_d\left[(4-\epsilon)\big(\hat{\mathcal{F}}^{I,1}_{(J)}(0,\delta) + \hat{\mathcal{F}}^{I,1}_{(J)}(1,\delta)\big) + 4\,\widetilde{\mathcal{F}}^{I,1}_{(J)}(0,\delta)\right]\\
&\quad -\frac{6\,\mathcal{C}_4 + (60-36\epsilon)\,\mathcal{C}_6}{1-\epsilon}\,Q_d\left[n_\ell\,\hat{\mathcal{F}}^{I,1}_{(J)}(0,\delta) + \hat{\mathcal{F}}^{I,1}_{(J)}(z_c,\delta) + \hat{\mathcal{F}}^{I,1}_{(J)}(1,\delta)\right]\\
&\quad -36\,\mathcal{C}_6\,Q_u\,\widetilde{\mathcal{F}}^{I,1}_{(J)}(z_c,\delta) - 24(3\,\mathcal{C}_5 + \mathcal{C}_6)Q_d\,\widetilde{\mathcal{F}}^{I,1}_{(J)}(1,\delta)\\
&\quad +(-6\,\mathcal{C}_3 + \mathcal{C}_4 - 24\,\mathcal{C}_5 + 4\,\mathcal{C}_6)\,Q_d\,\widetilde{\mathcal{F}}^{I,4}_{(J)}(\delta)\\
&\qquad\qquad \text{for} \quad (I,J) = (s,i),(\times,i),(\times,ii)\,,\\
\sum_{k=3\ldots6}\langle P_4\rangle^{I,k}_{(J)} &= \left[(\mathcal{C}_4 - 6\,\mathcal{C}_3) + 4(4-\epsilon)(\mathcal{C}_6 - 6\,\mathcal{C}_5)\right]\left[\hat{\mathcal{F}}^{I,1}_{(J)}(0,\delta) + \hat{\mathcal{F}}^{I,1}_{(J)}(1,\delta)\right]\\
&\quad -\frac{6\,\mathcal{C}_4 + (60-36\epsilon)\,\mathcal{C}_6}{1-\epsilon}\left[n_\ell\,\hat{\mathcal{F}}^{I,1}_{(J)}(0,\delta) + \hat{\mathcal{F}}^{I,1}_{(J)}(z_c,\delta) + \hat{\mathcal{F}}^{I,1}_{(J)}(1,\delta)\right]\\
&\qquad\qquad \text{for} \quad I = s,\times \;\text{ and }\; J = iii\,.
\end{aligned} \tag{2.25}$$

JHEP01(2015)115

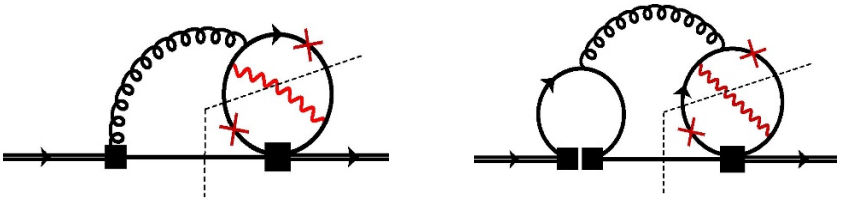

Figure 4. Diagrams of type (iii). Crosses denote alternative insertions of the photon vertex (always one vertex at each side of the cut).

The functions $\hat{\mathcal{F}}^{I,k}_{(J)} = \mathcal{F}^{I,k}_{(J)} + \mathcal{F}^{I,k}_{\text{coll}(J)}$ include the collinear regulators discussed in section 2.6. The functions $\widetilde{\mathcal{F}}^{I,1}_{(J)}$ and $\widetilde{\mathcal{F}}^{I,4}_{(J)}$ are related to diagrams where the photon couples to the left-hand quark loop, corresponding respectively to the terms with $h^{\mu\nu}$ and $\widetilde{h}^{\mu\nu}$ in eq. (2.17). Explicit results for all these functions are collected in appendix A.

2.3 Other details

2.3.1 Irrelevance of evanescent terms to the right of the cut

In the case of (P_7, P_i) interference, there are no UV or collinear divergences, and therefore evanescent structures are irrelevant for the $\mathcal{O}(\epsilon^0)$ result.

In the case of (P_8, P_i) interference, collinear divergences appear which combined with evanescent terms give finite contributions in the dimensionally regularized result. However these finite terms cancel when we express the dimensional regulators in terms of logarithms of masses, via the splitting-function approach (see section 2.6):

$$\frac{d\Gamma}{dx} = \frac{d\Gamma_\epsilon}{dx} + \frac{d\Gamma_{\text{shift}}}{dx} + \epsilon\left(\frac{d\Gamma^{\text{Ev}}_\epsilon}{dx} + \frac{d\Gamma^{\text{Ev}}_{\text{shift}}}{dx}\right) = \frac{d\Gamma_{\text{mass reg.}}}{dx} + \mathcal{O}(\epsilon) \tag{2.26}$$

since the $1/\epsilon$ terms cancel in both 4D and evanescent terms separately.

In the case of $(P_{1,2}, P_i)$ interference, UV and collinear divergences are nested inside dimensionally regularized expressions. However all UV divergences cancel against counterterm diagrams, including finite terms from evanescent operators:

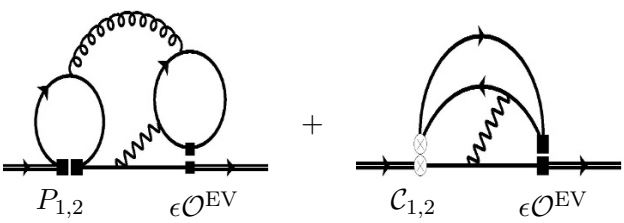

$$+ \qquad = \epsilon\left(\frac{1}{\epsilon_{\text{coll}}} + \text{UV finite}\right) \tag{2.27}$$

All "finite" terms from collinear divergences now disappear when going to mass regularization, as in the case with P_8.

2.3.2 Cancellation of $i\epsilon_{\mu\nu\rho\sigma}k_1^\mu k_2^\nu k_3^\rho k_4^\sigma$ terms

Traces with γ_5 will introduce terms proportional to $i\epsilon_{\mu\nu\rho\sigma}k_1^\mu k_2^\nu k_3^\rho k_4^\sigma$ in the differential decay rate. Here we show that these terms always cancel if we perform a full angular integration over phase-space.

JHEP01(2015)115

Consider fixing all double invariants $k_i \cdot k_j$. Then all k_i are fixed only up to an Euler rotation *and* an orientation. To see this go to the rest frame of the b-quark. Momentum conservation fixes all the energies (since $k_i \cdot p_b$ are fixed). This implies that $\vec{k}_i \cdot \vec{k}_j$ are also fixed. We can rotate the frame to put $\vec{k}_1$ along the positive z axis, and $\vec{k}_2$ in the (y, z) plane. Then $\vec{k}_3$ is fixed only up to a two-fold ambiguity (an orientation), given by the sign of its x component. Once this sign is chosen k_4 is also fixed. This proves that $i\epsilon_{\mu\nu\rho\sigma}k_1^\mu k_2^\nu k_3^\rho k_4^\sigma$ is fixed by $k_i \cdot k_j$ up to a sign, which is given by the orientation of $(\vec{k}_1, \vec{k}_2, \vec{k}_3)$.

Now consider phase-space integration. Terms in the integrand of the form $F(k_i \cdot k_j)$ do not depend on the Euler rotation nor the orientation, and the angular integral over $d\Omega_3 d\Omega_2 d\Omega_1$ can always be performed trivially, giving a factor $16\pi^2$. Terms of the form $F(k_i \cdot k_j)\epsilon_{\mu\nu\rho\sigma}k_1^\mu k_2^\nu k_3^\rho k_4^\sigma$, however, change sign under change of orientation, and vanish upon integration over $d\Omega_1$. Obviously parity-odd terms cancel out in parity-even observables. Therefore we drop these terms from the beginning in the calculation of the integrated decay rate.

2.4 Phase-space integration

The phase-space measure for a $(1 \to 4)$ decay of a particle of mass M into four massless particles with momenta $k_{1,2,3,4}$ is given in terms of kinematic invariants by [59]:

$$\begin{aligned} dPS_4 = {} & \tilde{\mu}^{6\epsilon}\, 2^{5-5d}\pi^{4-3d}M^{3d-8}\,(-\Delta_4)^{\frac{d-5}{2}}\,\delta(1 - s_{12} - s_{13} - s_{14} - s_{23} - s_{24} - s_{34}) \\ & \times \Theta(-\Delta_4)\, d\Omega_{d-1}\, d\Omega_{d-2}\, d\Omega_{d-3}\, ds_{12}\, ds_{13}\, ds_{14}\, ds_{23}\, ds_{24}\, ds_{34}\,, \end{aligned} \tag{2.28}$$

where $s_{ij} = 2k_i \cdot k_j/M^2$ $(0 \le s_{ij} \le 1)$, and Δ_4 is the Gram determinant:

$$+\Delta_4 = s_{12}^2 s_{34}^2 + s_{13}^2 s_{24}^2 + s_{14}^2 s_{23}^2 - 2s_{12}s_{34}s_{13}s_{24} - 2s_{12}s_{34}s_{14}s_{23} - 2s_{13}s_{24}s_{14}s_{23}\,. \tag{2.29}$$

The unpolarized decay rate is given by the phase-space integral:

$$\Gamma = \frac{1}{2M}\frac{1}{2N_c}\int \sum |\mathcal{M}|^2 dPS_4 \tag{2.30}$$

where the sum runs over the spins and color of all particles (we assume the parent is a color triplet). $\sum|\mathcal{M}|^2$ depends only on s_{ij}: $\sum|\mathcal{M}|^2 \equiv \mathcal{K}(s_{ij})$, so the angular integrations can be performed trivially:

$$\int d\Omega_{d-1}\, d\Omega_{d-2}\, d\Omega_{d-3} = \frac{8\pi^{\frac{3d-6}{2}}}{\Gamma(\frac{d-1}{2})\Gamma(\frac{d-2}{2})\Gamma(\frac{d-3}{2})}\,, \tag{2.31}$$

and the general formula for the decay rate becomes

$$\Gamma = \frac{\tilde{\mu}^{6\epsilon}\, 2^{8-5d}\,\pi^{1-3d/2}M^{3d-9}}{4N_c\Gamma(\frac{d-1}{2})\Gamma(\frac{d-2}{2})\Gamma(\frac{d-3}{2})}\int [ds_{ij}]\,\delta(1 - \textstyle\sum s_{ij})\mathcal{K}(s_{ij})(-\Delta_4)^{\frac{d-5}{2}}\,\Theta(-\Delta_4)\,. \tag{2.32}$$

This integral might contain soft and/or collinear divergences associated to regions of phase space where some particles are soft or collinear. These divergences can be regularized in dimensional regularization by setting $d = 4 - 2\epsilon$. If we insist on integrating over these

JHEP01(2015)115

regions, one must include virtual corrections to cancel the divergences. Otherwise, the regulator must be traded by a physical cutoff at a later stage.

We now specify to the $b \to q(k_1)\bar{q}(k_2)s(k_3)\gamma(k_4)$ case. We consider a cut on the photon energy $E_\gamma > E_0 \equiv \frac{m_b}{2}(1-\delta)$ (in the b quark rest frame), which defines the parameter δ. This translates into the constraint $s_{14}+s_{24}+s_{34} > 1-\delta$, which can be included in the phase-space integral in the following way. We include a delta function $\delta(1-z-s_{14}-s_{24}-s_{34})$ in the integrand, and we integrate over the new variable z from 0 to δ:

$$\int_0^\delta dz \int_0^1 [ds_{ij}]\, \delta(1-z-s_{14}-s_{24}-s_{34})\delta(z-s_{12}-s_{23}-s_{13})\mathcal{K}(s_{ij})(-\Delta_4)^{\frac{d-5}{2}}\,\Theta(-\Delta_4)\,. \quad (2.33)$$

The delta functions can be used to integrate over two invariants, e.g. s_{13} and s_{24}:

$$\Gamma_{E_\gamma>E_0} = N(d)\int_0^\delta dz \int_0^{\bar{z}} ds_{34} \int_0^{\bar{z}-s_{34}} ds_{14} \int_0^z ds_{12} \int_0^{z-s_{12}} ds_{23}\, \mathcal{K}(s_{ij})(-\Delta_4)^{\frac{d-5}{2}}\,\Theta(-\Delta_4)\Big|_{s_{13},s_{24}} \quad (2.34)$$

where $\bar{z} \equiv 1-z$, and $N(d)$ is given by the prefactor in eq. (2.32), and the substitution rule $X|_{s_{13},s_{24}}$ corresponds to $s_{13} \to z - s_{12} - s_{23}$ and $s_{24} \to \bar{z} - s_{14} - s_{34}$. The next integration can be performed over an invariant that appears only polynomially in $\mathcal{K}$ (see e.g. [60]). It is easy to see that s_{23} always satisfies this criterion by checking the uncut propagators in figures 2, 3, 4 and the loop functions. Upon substitution of s_{13}, s_{24}, the Gram determinant remains quadratic in s_{23}: $-\Delta_4 = (\bar{z}-s_{34})^2(a^+ - s_{23})(s_{23}-a^-)$, where $a^\pm$ are complicated functions of the rest of the invariants:

$$(\bar{z}-s_{34})^2 a^\pm = (\bar{z}-s_{34})[z(\bar{z}-s_{34})(1-s_{14}) - s_{12}(\bar{z}-s_{14})(\bar{z}+s_{34})] \pm 2\sqrt{\Xi}\,, \quad (2.35)$$

$$\Xi = s_{12}s_{14}s_{34}(s_{14}+s_{34}-\bar{z})[zs_{34} - \bar{z}(z-s_{12})]\,. \quad (2.36)$$

Thus, $-\Delta_4$ is positive only if $a^\pm$ are real (happening only if $s_{34} < \bar{z}(z-s_{12})/z < \bar{z}$), and for $a^- < s_{23} < a^+$. In addition, $a^- > 0$. This sets the integration limits for s_{23} and s_{34} imposed by the Θ-function, which can then be dropped:

$$\Gamma_{E_\gamma>E_0} = N(d)\int_0^\delta dz \int_0^z ds_{12} \int_0^{\bar{z}(z-s_{12})/z} ds_{34} \int_0^{\bar{z}-s_{34}} ds_{14} \int_{a^-}^{a^+} ds_{23}\, \mathcal{K}(s_{ij})(-\Delta_4)^{\frac{d-5}{2}}\Big|_{s_{13},s_{24}}\,. \quad (2.37)$$

Now it is convenient to perform the following changes of variables:

$$\begin{aligned} s_{12} &= zvw & s_{34} &= \bar{z}\bar{v} \\ s_{14} &= \bar{z}vx & s_{23} &= (a^+ - a^-)u + a^- \end{aligned} \quad (2.38)$$

where u, v, w, x are integrated independently from 0 to 1, and

$$(a^+ - a^-) = 4z(\bar{v}w\bar{w}x\bar{x})^{1/2}\,, \quad (2.39)$$

$$a^- = z\big[\bar{v}wx + \bar{w}\bar{x} - 2(\bar{v}w\bar{w}x\bar{x})^{-1/2}\big]\,. \quad (2.40)$$

This gives

$$\begin{aligned} \Gamma_{E_\gamma>E_0} &= N(d)\int_0^\delta dz\, z\, \bar{z}^{d-3} \int_0^1 du\, dv\, dw\, dx\, (u\bar{u})^{\frac{d-5}{2}} v^{d-3}(a^+-a^-)^{d-4}\,\mathcal{K} \\ &= N(d)\, 4^{d-4}\int_0^\delta dz\, (z\bar{z})^{d-3} \int_0^1 du\, dv\, dw\, dx\, (u\bar{u})^{\frac{d-5}{2}} v^{d-3}(\bar{v}w\bar{w}x\bar{x})^{\frac{d-4}{2}}\,\mathcal{K}\,. \end{aligned} \quad (2.41)$$

JHEP01(2015)115

In the following we must consider the kernel $\mathcal{K}(u,v,w,x,z)$. As mentioned above, $\mathcal{K}$ is polynomial in s_{23}: $\mathcal{K} = \sum f_n(v,w,x,z) s_{23}^n$. Expanding s_{23} according to (2.38)–(2.40) will provide a sum of terms of the form

$$\mathcal{K} = \sum_{m,n} f_{n,m}(v,w,x,z)\ u^m\,, \tag{2.42}$$

and the integral over the variable u gives a factor $\beta\big(\frac{d-3}{2}+m, \frac{d-3}{2}\big)$ for each term. The next steps depend on the diagram at hand. Consider the diagrams with $P_{7,8}$. In this case,

$$f_{n,m}(v,w,x,z) = v^a\,\bar{v}^b\,w^c\,\bar{w}^e\,x^f\,\bar{x}^g\,z^h\,\bar{z}^p\,(1-\bar{z}\bar{v})^q\,(1-z\bar{w})^r \tag{2.43}$$

for some $a,b,c,\ldots \in R$. The integral over x gives again a β-function: $\beta\big(\frac{d-2}{2}+f, \frac{d-2}{2}+g\big)$. Because of the $(1-\bar{z}\bar{v})^q$ and $(1-z\bar{w})^r$ factors, the next steps will introduce hypergeometric functions. The integral over v gives

$$\beta\left(d-2+a, \frac{d-2}{2}+e\right) {}_2F_1\left(-q, \frac{d-2}{2}+b; \frac{3d-6}{2}+a+b; \bar{z}\right)\,, \tag{2.44}$$

and the integral over w, gives:

$$\beta\left(\frac{d-2}{2}+c, \frac{d-2}{2}+e\right) {}_2F_1\left(-r, \frac{d-2}{2}+e; d-2+c+e; z\right)\,. \tag{2.45}$$

The next step is to expand around $\epsilon \to 0$ (with $d = 4-2\epsilon$). The expansion of hypergeometric functions is performed automatically by the package `HypExp` [61]. This will give finite results in the case of P_7, but $1/\epsilon$ poles in the case of P_8, corresponding to collinear divergences. The integration over the photon energy $z \in (0,\delta)$ can then be performed, also analytically, for all terms.

The case of loop diagrams is in principle more complicated, as the function $\mathcal{K}$ contains already a hypergeometric function. For instance, in the case of diagrams (i) with the photon *not* attaching to the quark loop, the variable s_{12} appears in the function $g(m_q) \sim {}_2F_1(\epsilon, 2; \frac{5}{2}; \frac{s_{12}}{4z_q})$ (cf. eq. (2.14)). However, by a suitable choice in the order of integration, analytic results can be obtained as before. In the case of diagrams such as (iii), the hypergeometric function depends on the triple invariant $s_{124} = s_{12}+s_{14}+s_{24}$, and the sequential-integration procedure described above does not seem to work up to finite order in ϵ. In this case we extract all the $1/\epsilon^2$ and $1/\epsilon$ poles analytically and leave the finite terms differential in one of the variables, which we integrate numerically afterwards. This is also the case for the diagrams where the photon couples to the charm loop, which are both UV and collinear finite. In general, for the loop contributions, some finite terms turn out to be complicated functions of δ and $z_c \equiv m_c^2/m_b^2$. We give these results as polynomial expansions in δ around the physical value $\delta = 0.316$. The coefficients of this expansion are presented as numerical interpolations in the variable z_c, reproducing the exact results to enough precision for all practical purposes. We have checked that the interpolated expressions in the appendix reproduce the exact results with high precision in the full range $z_c \in (0,1)$ for values of δ near 0.316.

JHEP01(2015)115

2.5 Renormalization

Tree-level four-body contributions from four-quark operators arise at LO in α_s and have been computed in ref. [50]. At NLO the corresponding counterterm contributions must be included, which cancel the UV divergences from the loop diagrams. One must consider the insertion of the bare operators $P_i^{(0)}$, $i = 1q, 2q, 3, \ldots, 6$, in the tree-level diagrams to the left of the cut, where:

$$\begin{aligned}\sum_{i=3,\ldots,6,1q,2q} \mathcal{C}_i\, P_i^{(0)} &= \sum_{\substack{i=3,\ldots,6,1q,2q\\ j=3,\ldots,6,1u,2u}} \mathcal{C}_i\, Z_{ij} P_j = \sum_{\substack{i=3,\ldots,6,1q,2q\\ j=3,\ldots,6,1u,2u}} \mathcal{C}_i \left(\delta_{ij} + \frac{1}{\epsilon}\frac{\alpha_s}{4\pi}\delta Z_{ij}\right) P_j \\ &= \sum_{i=3,\ldots,6,1u,2u} \mathcal{C}_i\, P_i + \frac{1}{\epsilon}\frac{\alpha_s}{4\pi} \sum_{\substack{i=3,\ldots,6,1q,2q\\ j=3,\ldots,6,1u,2u}} \mathcal{C}_i\, \delta Z_{ij} P_j \end{aligned} \tag{2.46}$$

The first term leads to the LO contributions in ref. [50], while the second term contributes to the NLO result and takes care of the UV divergences. For this we need, a priori, the tree level results with $P_{3,\ldots,6,1u,2u}$ including $\mathcal{O}(\epsilon)$ terms, and the renormalization factors δZ_{ij}.

The relevant renormalization factors are simple to compute. Using the relationships developed in section 2.1, and expressing the result in terms of tree-level matrix elements of four-quark operators, we find that:

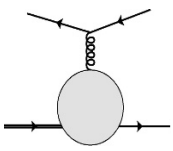

$$\begin{aligned} &= \left[\mathcal{C}_1^u - 6\,\mathcal{C}_2^u + \mathcal{C}_1^c - 6\,\mathcal{C}_2^c - 12\,\mathcal{C}_3 - 28\,\mathcal{C}_4 - 192\,\mathcal{C}_5 - 268\,\mathcal{C}_6\right] \\ &\quad \times \frac{1}{9}\frac{1}{\epsilon}\frac{\alpha_s}{4\pi}\langle P_4\rangle^{\text{tree}} + \mathcal{O}(\epsilon^0)\ . \end{aligned} \tag{2.47}$$

This fixes the renormalization factors needed in our calculation:

$$\begin{aligned} &\delta Z_{1u\,4} = -\tfrac{1}{9} \qquad \delta Z_{1c\,4} = -\tfrac{1}{9} \qquad \delta Z_{34} = \tfrac{4}{3} \qquad \delta Z_{44} = \tfrac{28}{9} \\ &\delta Z_{2u\,4} = \tfrac{2}{3} \qquad \delta Z_{2c\,4} = \tfrac{2}{3} \qquad \delta Z_{54} = \tfrac{64}{3} \qquad \delta Z_{64} = \tfrac{268}{9}\ . \end{aligned} \tag{2.48}$$

We also see that we need only tree level diagrams with insertion of P_4 to the left of the cut. All the diagrams needed are shown in figure 5.

For the operator insertions to the right of the cut we can (and must) use the 4D identities derived in section 2.1, noting that evanescent terms cancel in the renormalization process by virtue of eq. (2.27). This leads to exactly the same structure as eqs. (2.18), (2.19), (2.20) for the counterterm diagrams $\mathcal{D}^C_{(J)}$ (i.e. eq. (2.21)), with the corresponding matrix elements $\langle P_4\rangle^{I,C}_{(J)}$ given by:

$$\begin{aligned} \langle P_4\rangle^{I,C}_{(J)} &= \left[\mathcal{C}_1^u - 6\,\mathcal{C}_2^u + \mathcal{C}_1^c - 6\,\mathcal{C}_2^c - 12\,\mathcal{C}_3 - 28\,\mathcal{C}_4 - 192\,\mathcal{C}_5 - 268\,\mathcal{C}_6\right] \\ &\quad \times \begin{cases} Q_d \hat{\mathcal{F}}^{I,C}_{(J)}(\delta) & \text{for} \quad (I,J) = (s,i), (\times,i), (\times,ii) \\ \hat{\mathcal{F}}^{I,C}_{(J)}(\delta) & \text{for} \quad I = s,\times \ \text{ and } \ J = iii\ . \end{cases} \end{aligned} \tag{2.49}$$

JHEP01(2015)115

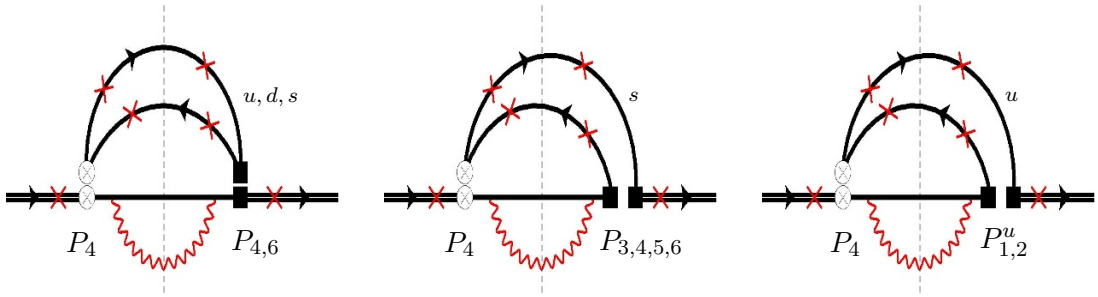

Figure 5. Tree-level counterterm diagrams. Crosses denote alternative insertions of the photon vertex (always one vertex at each side of the cut). These diagrams can be classified in types (i), (ii), (iii) as done for the loop diagrams.

Again, $\hat{\mathcal{F}}^{I,C}_{(J)} = \mathcal{F}^{I,C}_{(J)} + \mathcal{F}^{I,C}_{\mathrm{coll}(J)}$. The functions $\mathcal{F}^{I,C}_{(J)}, \mathcal{F}^{I,C}_{\mathrm{coll}(J)}$ are given in appendix A. One can check that all UV divergences cancel, as expected: $\langle P_4\rangle^{I,C}_{(J)} + \sum_k \langle P_4\rangle^{I,k}_{(J)} = \text{UV finite}$.

2.6 Collinear divergences and splitting functions

The region of phase space in which the photon is collinear to one of the light quarks gives rise to collinear divergences. These divergences are regulated dimensionally in our computation. However, these are just artifacts of the massless limit used for light quarks, and there is a more natural regulator: a physical cut-off given by the light meson masses. A suitable parametrization of such (near-) collinear effects consists in keeping the light quarks massive and perform a massive phase-space integration. This is quite complicated from the practical point of view, taking into account that the massless phase-space integrals computed here are already rather challenging.

Fortunately, one may resort to the factorization properties of the amplitudes in the quasi-collinear limit (see e.g. [50]). The idea is that close to the collinear region, the $b \to q_1\bar{q}_2 q_3\gamma$ amplitude may be expressed as a $b \to q_1\bar{q}_2 q_3$ amplitude times a *splitting function* f_i, describing the quasi-collinear emission of a photon from q_i, summed over $i = 1, 2, 3$. The splitting functions encode the collinear divergences, and can themselves be regulated by quark masses or in dimensional regularization. Both approaches are rather simple, since in this limit the four-body phase space factorizes into a convolution of the three-body phase space of the non-radiative process and the phase space of the radiative process alone: $d\Phi_4 = d\Phi_3 \otimes d\Phi$. By comparing the splitting functions regulated in these two different schemes, one can write a formula to switch from one to the other at the level of the decay rate [50]:

$$\frac{d\Gamma_{\mathrm{m}}}{dz} = \frac{d\Gamma_{\epsilon}}{dz} + \frac{d\Gamma_{\mathrm{shift}}}{dz} \tag{2.50}$$

where

$$\begin{aligned}\frac{d\Gamma_{\mathrm{shift}}}{dz} = \frac{1}{2m_b}\frac{1}{2N_c}\int dPS_3\, \mathcal{K}_3(s_{ij})\, \frac{\alpha_e}{2\pi\bar{z}} \Bigg\{ Q_1^2 \left[1 + \frac{(z-s_{23})^2}{(1-s_{23})^2}\right] \\ \times \left[\frac{1}{\epsilon} - 1 + 2\log\frac{(1-s_{23})\mu}{m_{q_1}(1-z)}\right]\Theta(z-s_{23}) + (\text{cyclic})\Bigg\}\ .\end{aligned} \tag{2.51}$$

Here $\mathcal{K}_3 = \sum |\mathcal{M}_3|^2$ is the spin-summed squared matrix element of the $b \to q_1\bar{q}_2 q_3$ decay obtained by evaluating the diagrams in figure 6, and dPS_3 is the three-particle phase-space

JHEP01(2015)115

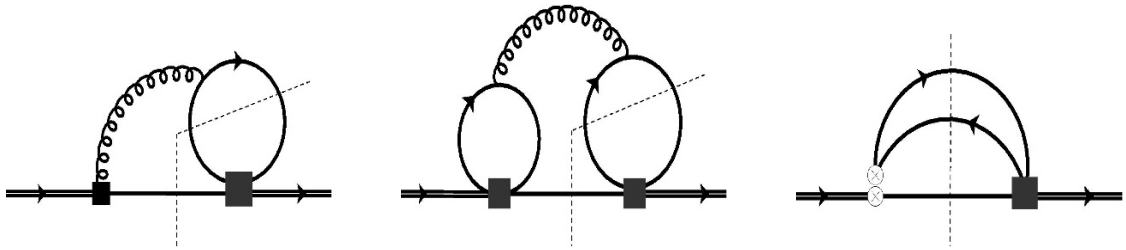

Figure 6. Three-particle-cut diagrams needed for the calculation of collinear terms.

measure in $d = 4 - 2\epsilon$ dimensions [59]:

$$dPS_3 = \tilde{\mu}^{4\epsilon}\, 2^{2-3d}\pi^{3-2d} m_b^{2d-6}\, (s_{12}s_{13}s_{23})^{\frac{d-4}{2}}\, \delta(1 - s_{12} - s_{13} - s_{23}) \\ \times d\Omega_{d-1} d\Omega_{d-2}\, ds_{12} ds_{13} ds_{23}\ . \tag{2.52}$$

Integrating eq. (2.51) over $z \in [0, \delta]$ provides the terms $\mathcal{F}_{\rm coll}$ contained in the functions $\hat{\mathcal{F}}$. The contributions from the chromomagnetic operator (figure 6, left) enter into eq. (2.22). The contributions from four-quark operators (figure 6, center) go into eqs. (2.23), (2.24) and (2.25). The counterterm contributions (figure 6, right), enter into eq. (2.49). The functions $\mathcal{F}_{\rm coll}(\delta)$ are collected in appendix A.

One can check that adding the collinear contribution removes the $1/\epsilon$ terms that survive the renormalization process, trading them for collinear logarithms of quark-mass ratios. These collinear logarithms are of the form $\log(m_q/m_b)$, with $q = u, d, s$. The quark masses are collinear regulators and it is difficult to relate them to physical masses. In our numerical analysis we will take a common constituent-quark mass $m_q \sim 100 - 250\,$MeV for all three light flavors, and use the notation $L_q = \log(m_q/m_b) \sim \log(m_u/m_b) \sim \log(m_d/m_b) \sim \log(m_s/m_b)$. This should provide a reasonable estimate of the effect of collinear logarithms.

3 Results

We write the four-body contribution to the $\bar{B} \to X_s\gamma$ rate as:

$$\Delta\Gamma(\bar{B} \to X_s\gamma)^{s\bar{q}q\gamma}_{E_\gamma > E_0} = \Gamma_0 \sum_{i,j} \mathcal{C}_i^{\rm eff}(\mu_b)^*\, \mathcal{C}_j^{\rm eff}(\mu_b)\, G_{ij}(\mu_b, \delta)\,, \tag{3.1}$$

where Γ_0 is the absolute normalization of the decay rate:

$$\Gamma_0 = \frac{G_F^2 \alpha_e m_b^5 |V_{ts}^* V_{tb}|^2}{32\pi^4}\ . \tag{3.2}$$

The sum runs over $i, j = 1u, 2u, 3, \ldots, 6, 1c, 2c, 7, 8$. The Wilson coefficients $\mathcal{C}_{3,\ldots,8}$ are real, but $\mathcal{C}_{1u,2u,1c,2c}$ contain CKM phases:

$$\mathcal{C}^{\rm eff}_{3,\ldots,6} = C_{3,\ldots,6}\,, \quad \mathcal{C}^{\rm eff}_{1u,2u} = -\frac{V_{us}^* V_{ub}}{V_{ts}^* V_{tb}} C_{1,2}\,, \quad \mathcal{C}^{\rm eff}_{1c,2c} = -\frac{V_{cs}^* V_{cb}}{V_{ts}^* V_{tb}} C_{1,2}\,, \\ \mathcal{C}^{\rm eff}_7 = C_7 - \frac{1}{3}C_3 - \frac{4}{3}C_4 - \frac{20}{3}C_5 - \frac{80}{9}C_6\,, \\ \mathcal{C}^{\rm eff}_8 = C_8 + C_3 - \frac{1}{6}C_4 + 20C_5 - \frac{10}{3}C_6\,, \tag{3.3}$$

JHEP01(2015)115

with C_i the Wilson coefficients in the notation of ref. [24]. They are needed here to NLO:

$$\mathcal{C}_i^{\rm eff}(\mu) = \mathcal{C}_i^{(0)\rm eff}(\mu) + \frac{\alpha_s(\mu)}{4\pi}\mathcal{C}_i^{(1)\rm eff}(\mu) + \mathcal{O}(\alpha_s^2), \tag{3.4}$$

their numerical values are given below.

The matrix elements $G_{ij}(\mu,\delta)$ depend on the renormalization scale and the photon-energy cut and can be split into LO and NLO components:

$$G_{ij}(\mu,\delta) = G_{ij}^{(0)}(\delta) + \frac{\alpha_s(\mu)}{4\pi}G_{ij}^{(1)}(\mu,\delta) + \mathcal{O}(\alpha_s^2)\ . \tag{3.5}$$

The LO matrix $G^{(0)}$ is real and symmetric and was computed in ref. [50]: we reproduce and confirm these results (after the 2014 update of that paper). We write (here $i,j = 1u, 2u, 3, \ldots, 6$):

$$G^{(0)}(\delta) = \begin{pmatrix} \frac{2}{9}T_2 & 0 & \frac{4}{9}T_2 & -\frac{2}{27}T_2 & \frac{64}{9}T_2 & -\frac{32}{27}T_2 \\ 0 & T_2 & \frac{1}{3}T_2 & \frac{4}{9}T_2 & \frac{16}{3}T_2 & \frac{64}{9}T_2 \\ \frac{4}{9}T_2 & \frac{1}{3}T_2 & T_1+T_3 & \frac{4}{3}T_3 & 10T_1+16T_3 & \frac{64}{3}T_3 \\ -\frac{2}{27}T_2 & \frac{4}{9}T_2 & \frac{4}{3}T_3 & \frac{2}{9}(T_1-T_3) & \frac{64}{3}T_3 & \frac{20}{9}T_1-\frac{32}{9}T_3 \\ \frac{64}{9}T_2 & \frac{16}{3}T_2 & 10T_1+16T_3 & \frac{64}{3}T_3 & 136T_1+256T_3 & \frac{1024}{3}T_3 \\ -\frac{32}{27}T_2 & \frac{64}{9}T_2 & \frac{64}{3}T_3 & \frac{20}{9}T_1-\frac{32}{9}T_3 & \frac{1024}{3}T_3 & \frac{272}{9}T_1-\frac{512}{9}T_3 \end{pmatrix} \tag{3.6}$$

where:

$$\begin{aligned} T_1(\delta) = {} & \frac{23\delta^4}{16} - \frac{1}{2}\delta^4\log(\delta) - \frac{191\delta^3}{108} + \frac{4}{9}\delta^3\log(\delta) + \frac{17\delta^2}{18} - \frac{1}{3}\delta^2\log(\delta) + \frac{109\delta}{18} \\ & -\frac{5}{3}\delta\log(\delta) + \frac{79}{18}\log(1-\delta) - \frac{5}{3}\log(1-\delta)\log(\delta) \\ & + \left[\delta^4 - \frac{8}{9}\delta^3 + \frac{2}{3}\delta^2 + \frac{10}{3}\delta + \frac{10}{3}\log(1-\delta)\right]\log\left(\frac{m_q}{m_b}\right) - \frac{5\mathrm{Li}_2(\delta)}{3}\,, \end{aligned} \tag{3.7}$$

$$\begin{aligned} T_2(\delta) = {} & \frac{1181\delta^4}{2592} - \frac{17}{108}\delta^4\log(\delta) - \frac{395\delta^3}{648} + \frac{4}{27}\delta^3\log(\delta) + \frac{7\delta^2}{18} - \frac{1}{9}\delta^2\log(\delta) + \frac{187\delta}{108} \\ & -\frac{1}{2}\delta\log(\delta) + \frac{133}{108}\log(1-\delta) - \frac{1}{2}\log(1-\delta)\log(\delta) \\ & + \left[\frac{17\delta^4}{54} - \frac{8\delta^3}{27} + \frac{2\delta^2}{9} + \delta + \log(1-\delta)\right]\log\left(\frac{m_q}{m_b}\right) - \frac{\mathrm{Li}_2(\delta)}{2}\,, \end{aligned} \tag{3.8}$$

$$\begin{aligned} T_3(\delta) = {} & \frac{341\delta^4}{7776} - \frac{5}{324}\delta^4\log(\delta) - \frac{89\delta^3}{1944} + \frac{1}{81}\delta^3\log(\delta) + \frac{\delta^2}{72} - \frac{1}{108}\delta^2\log(\delta) + \frac{35\delta}{162} \\ & -\frac{1}{18}\delta\log(\delta) + \frac{13}{81}\log(1-\delta) - \frac{1}{18}\log(1-\delta)\log(\delta) \\ & + \left[\frac{5\delta^4}{162} - \frac{2\delta^3}{81} + \frac{\delta^2}{54} + \frac{\delta}{9} + \frac{1}{9}\log(1-\delta)\right]\log\left(\frac{m_q}{m_b}\right) - \frac{\mathrm{Li}_2(\delta)}{18}\ . \end{aligned} \tag{3.9}$$

The NLO matrix $G^{(1)}$ contains perturbative strong phases from on-shell contributions from light quarks, as well as from charm quarks when the photon-energy cut is low enough. The

JHEP01(2015)115

matrix $G^{(1)}$ is the main result of this paper. It has the following structure:

$$G^{(1)}(\mu,\delta) = G_1(\delta)L_q L_\mu + G_2(\delta)L_\mu + G_3(z_c,\delta)L_q + G_4(z_c,\delta)\,, \tag{3.10}$$

where $L_\mu \equiv \log(\mu/m_b)$, $L_q \equiv \log(m_q/m_b)$ and $z_c \equiv m_c^2/m_b^2$. The explicit form of $G_{ij}^{(1)}$ is too complicated to be written down here. However, it can be constructed completely from the expressions in sections 2.2, 2.5 and appendix A: start from eq. (2.21), substitute the objects $\mathcal{D}_{(J)}$ from eqs. (2.18), (2.19), (2.20), then use eqs. (2.22)–(2.25) and (2.49) for the different matrix elements $\langle P_4\rangle_{(J)}$, and use the expressions in the appendix for the functions $\mathcal{F}_{(J)}$, $\mathcal{F}_{\mathrm{coll}(J)}$ and $\widetilde{\mathcal{F}}_{(J)}$, noting that $\hat{\mathcal{F}}_{(J)} \equiv \mathcal{F}_{(J)} + \mathcal{F}_{\mathrm{coll}(J)}$. Finally, perform the replacement $G^{(1)} \to G^{(1)} + G^{(1)\dagger}$ to account for the "mirror" contributions. For convenience, we provide the full matrices $G_{ij}^{(0)}$ and $G_{ij}^{(1)}$ in the file "`Gij.m`" attached to the arXiv submission of the present manuscript. The first is given by the 6×6 matrix "`GijLO`" $(i,j = 1u, 2u, 3, \ldots, 6)$ and the second by the 10×10 matrix "`GijNLO`" (with $i,j = 1u, 2u, 3, \ldots, 6, 1c, 2c, 7, 8$).

4 Numerical analysis

We briefly discuss here the numerical impact of the four-body contributions to the total $\bar{B} \to X_s\gamma$ rate. We consider for convenience the following quantity:

$$\widetilde{\Delta\Gamma} = \frac{\Delta\Gamma(\bar{B} \to X_s\gamma)^{s\bar{q}q\gamma}_{E_\gamma > E_0}}{\Gamma_0 \left|\mathcal{C}_7^{(0)\mathrm{eff}}\right|^2}, \tag{4.1}$$

given by eq. (3.1) and normalized to the leading contribution to the decay rate. The Wilson coefficients are given by:

$$\mathcal{C}_i^{\mathrm{eff}}(\mu) = \mathcal{C}_i^{(0)\mathrm{eff}}(\mu) + \frac{\alpha_s(\mu)}{4\pi}\mathcal{C}_i^{(1)\mathrm{eff}}(\mu) + \mathcal{O}(\alpha_s^2), \tag{4.2}$$

which are computed following ref. [17]. For the reference matching and renormalization scales $\mu_0 = 160\,\mathrm{GeV}$, $\mu = \mu_b = 2.5\,\mathrm{GeV}$, we have:[4]

$$\mathcal{C}_i^{(0)\mathrm{eff}} = (0.828\,\lambda_q, -1.063\,\lambda_q, -0.013, -0.125, 0.0012, 0.0027, -0.372, -0.172)\,, \tag{4.3}$$

$$\mathcal{C}_i^{(1)\mathrm{eff}} = (-15.32\,\lambda_q, 2.10\,\lambda_q, 0.097, -0.447, -0.021, -0.013, \mathrm{nn}, \mathrm{nn})\,, \tag{4.4}$$

for $i = 1q, 2q, 3, \ldots, 8$. However, the μ-dependence of the Wilson coefficients is important and we will analyze it here. In addition, $\lambda_q \equiv V_{qs}^* V_{qb}/V_{ts}^* V_{tb}$ denote the appropriate CKM factors, given by [62]:

$$\lambda_u = -0.0059 + 0.018i\,, \quad \lambda_c = -0.97\,. \tag{4.5}$$

The quantity $\widetilde{\Delta\Gamma}$ can be expanded in α_s:

$$\begin{aligned}\widetilde{\Delta\Gamma} = \widetilde{\Delta\Gamma}_{\mathrm{LO}} + \widetilde{\Delta\Gamma}_{\mathrm{NLO}} &= \sum_{\substack{i,j\,=\,1u,\,2u\\ 3,\ldots,6}} \frac{\mathcal{C}_i^{(0)*}\mathcal{C}_j^{(0)}}{\left|\mathcal{C}_7^{(0)\mathrm{eff}}\right|^2}\, G_{ij}^{(0)} \\ &+ \frac{\alpha_s(\mu)}{4\pi}\left[\sum_{\substack{i,j\,=\,1u,\,2u\\ 3,\ldots,6}} \frac{\mathcal{C}_i^{(1)*}\mathcal{C}_j^{(0)} + \mathcal{C}_i^{(0)*}\mathcal{C}_j^{(1)}}{\left|\mathcal{C}_7^{(0)\mathrm{eff}}\right|^2}\, G_{ij}^{(0)} + \sum_{i,j=all} \frac{\mathcal{C}_i^{(0)*}\mathcal{C}_j^{(0)}}{\left|\mathcal{C}_7^{(0)\mathrm{eff}}\right|^2}\, G_{ij}^{(1)}\right].\end{aligned} \tag{4.6}$$

[4]The NLO Wilson Coefficients $\mathcal{C}_{7,8}^{\mathrm{eff}}$ are not needed for our NLO results as $P_{7,8}$ do not contribute at LO.

JHEP01(2015)115

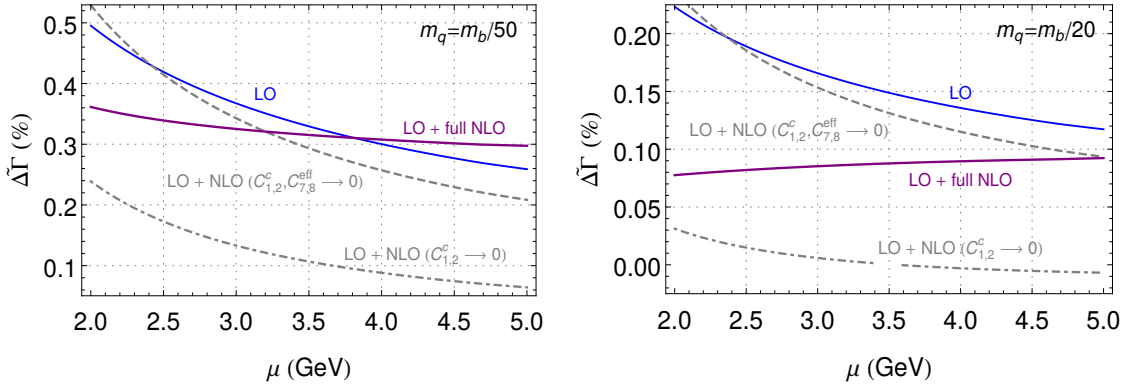

Figure 7. Renormalization-scale dependence of $\widetilde{\Delta\Gamma}$ in *percent units*. Here we have taken $\mu_0 = 160\,\text{GeV}$, $z_c = 0.07$, $\delta = 0.316$ and $L_q = -\log 50$ ($m_q \sim 100\,\text{MeV}$) [Left panel], or $L_q = -\log 20$ ($m_q \sim 250\,\text{MeV}$) [Right panel].

We begin with a discussion of the μ-dependence of our results. To leading order, the μ-dependence is given purely by the LL (leading-log) running in the effective theory. Note that to this order, only $\mathcal{C}^u_{1,2}$ and $\mathcal{C}_{3,4,5,6}$ contribute. At NLO, three new contributions arise: (i) the contribution from NLO Wilson coefficients, (ii) NLO matrix elements and (iii) contributions from $\mathcal{C}^c_{1,2}, \mathcal{C}_{7,8}$, absent at LO. The μ-dependence should cancel up to a residual scale-dependence from higher orders, and up to the neglected contributions shown in figure 1.f (note that the Z factors in eq. (2.48) are not the full renormalization constants).

In figure 7 we show the μ-dependence of the LO result, and LO+NLO excluding $\mathcal{C}^c_{1,2}, \mathcal{C}_{7,8}$, LO+NLO excluding $\mathcal{C}^c_{1,2}$ and LO+ full NLO. We also gauge the impact of collinear logarithms, showing the result for two different choices of L_q, corresponding to $m_q = m_b/50$ ($m_q \sim 100\,\text{MeV}$) and $m_q = m_b/20$ ($m_q \sim 250\,\text{MeV}$). Collinear logarithms are, as expected, numerically important.

Contributions from $P^c_{1,2}$ and $P_{7,8}$ arise only at NLO and therefore introduce at this order a novel μ-dependence. Although, as we will see, certain cancellations make the NLO contribution small, there is a considerable reduction in the renormalization-scale dependence of the full LO+NLO result as compared to the LO contribution alone. This is due to the fact that the main μ-dependence of the leading order contribution arises from the mixing of $P^c_{1,2}$ into penguin operators, which is compensated at NLO by the matrix elements of $P^c_{1,2}$. This can be seen in figure 7: the reduction in the μ-dependence is achieved only after including $\mathcal{C}^c_{1,2}$ contributions.

In the left plot of figure 7 one can see that for the value $\mu \simeq 4\,\text{GeV}$ strong cancellations make the NLO contribution very small. More concretely, for the inputs $\mu_0 = 160\,\text{GeV}$, $\mu = 4\,\text{GeV}$, $z_c = 0.07$, $\delta = 0.316$ and $m_q = m_b/50$, we have:

$$\begin{aligned}
\widetilde{\Delta\Gamma}(\%) &= (0.300)_{\text{LO}} + (0.044)_{\text{NLO WCs}} - (0.087)_{\text{NLO penguins}} - (0.169)_{\mathcal{C}^{\rm eff}_{7,8}} + (0.219)_{\mathcal{C}^c_{1,2}} \\
&= (0.300)_{\text{LO}} + (0.044)_{\text{NLO WCs}} - (0.036)_{\text{NLO MEs}} \\
&= (0.300)_{\text{LO}} - (0.007)_{\text{NLO}} \qquad (4.7)
\end{aligned}$$

JHEP01(2015)115

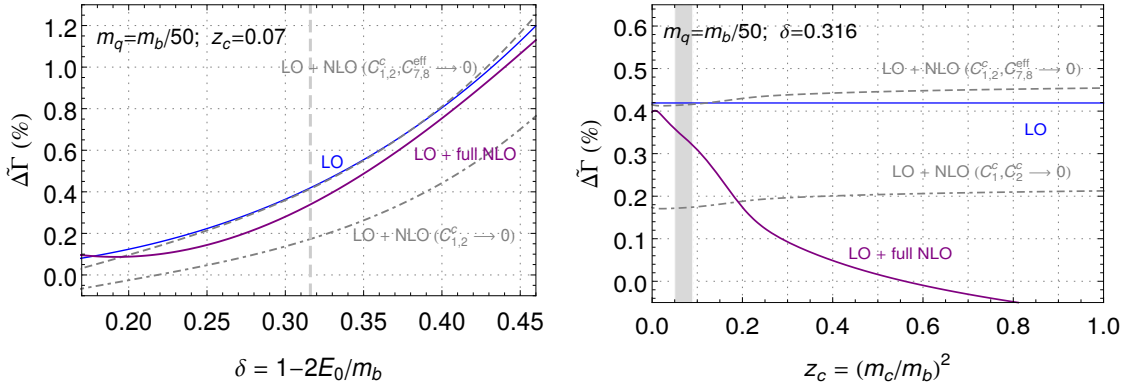

Figure 8. $\widetilde{\Delta\Gamma}$ in *percent units*. Left: dependence on the photon energy cut E_0. Right: dependence on the charm mass. We have fixed $\mu_0 = 160\,\text{GeV}$, $\mu = 2.5\,\text{GeV}$ and $L_q = -\log 50$ ($m_q \sim 100\,\text{MeV}$). The vertical dashed line in the left panel shows the benchmark point $\delta = 0.316$, while the vertical band in the right panel corresponds to the physical value $z_c = 0.07 \pm 0.02$.

where the term labeled 'NLO WCs' corresponds to the second term in eq. (4.6). This cancellation is very efficient for $\mu \simeq 3.8\,\text{GeV}$, but depends strongly on m_q and z_c. However, it is a general feature of our results that the contribution from $\mathcal{C}^c_{1,2}$ is of the same order as the rest of the NLO contribution, but with opposite sign, leading always to some level of cancellation. Note also that the (NLO) $\mathcal{C}^c_{1,2}$ contribution is also as large as the LO result.

In the following we fix the renormalization scale to $\mu = 2.5\,\text{GeV}$ and study the dependence on the charm mass and the photon-energy cut. This is shown in figure 8. In general the full LO+NLO result increases with δ and decreases with m_c, always remaining below the 1% level for $\delta \lesssim 0.45$. We note that these results are only valid for δ not far from 0.316 as some of the functions are expanded up to second order in $(\delta - 0.316)$.

Finally, we provide some results for two different values of E_0 of interest: $E_0 = 1.6\,\text{GeV}$, corresponding to $\delta = 0.316$, and $E_0 = 1.9\,\text{GeV}$, corresponding to $\delta = 0.188$. For the input parameters and their uncertainties we take: $\mu_0 = 160^{+90}_{-80}$, $\mu = 2.5^{+2.5}_{-0.5}$ and $z_c = 0.07 \pm 0.02$, which captures the different values for m_c within different schemes.

For $m_q = m_b/50 \sim 100\,\text{MeV}$, we find:

$$\begin{aligned}\widetilde{\Delta\Gamma}_{E_0=1.6\,\text{GeV}}\,[\%] &= (0.419)_{\text{LO}} - (0.080)_{\text{NLO}} \pm (0.028)_{\mu_0} \pm (0.032)_{\mu} \pm (0.019)_{z_c} \\ &= 0.34 \pm 0.05 \end{aligned} \tag{4.8}$$

$$\begin{aligned}\widetilde{\Delta\Gamma}_{E_0=1.9\,\text{GeV}}\,[\%] &= (0.105)_{\text{LO}} - (0.077)_{\text{NLO}} \pm (0.012)_{\mu_0} \pm (0.009)_{\mu} \pm (0.003)_{z_c} \\ &= 0.03 \pm 0.02 \end{aligned} \tag{4.9}$$

For $m_q = m_b/20 \sim 250\,\text{MeV}$:

$$\begin{aligned}\widetilde{\Delta\Gamma}_{E_0=1.6\,\text{GeV}}\,[\%] &= (0.189)_{\text{LO}} - (0.107)_{\text{NLO}} \pm (0.019)_{\mu_0} \pm (0.007)_{\mu} \pm (0.007)_{z_c} \\ &= 0.08 \pm 0.02 \end{aligned} \tag{4.10}$$

$$\begin{aligned}\widetilde{\Delta\Gamma}_{E_0=1.9\,\text{GeV}}\,[\%] &= (0.037)_{\text{LO}} - (0.081)_{\text{NLO}} \pm (0.009)_{\mu_0} \pm (0.020)_{\mu} \pm (0.001)_{z_c} \\ &= -0.04 \pm 0.02 \end{aligned} \tag{4.11}$$

JHEP01(2015)115

For the value $\delta = 0.188$ ($E_0 = 1.9\,\text{GeV}$) we have used the exact results (not the expanded ones), as for this value of δ the quadratic expansion is not expected to be accurate enough.

5 Conclusions

The inclusive radiative decay $\bar{B} \to X_s\gamma$ has beyond any doubt reached the era of precision physics, with the total uncertainties on both the experimental and theoretical side being at the $\pm 7\%$ level. The foreseen improvement in precision on the experimental side — the envisaged uncertainty with 50/ab at Belle II is of $\mathcal{O}(6\%)$ [63], although this might even be a conservative estimate — justifies every effort to reduce the theoretical error to at least the same level.

The present article aims at addressing a particular higher-order perturbative contribution, namely the four-body contributions $b \to sq\bar{q}\gamma$ to $\Gamma(\bar{B} \to X_s\gamma)$ at NLO. The smallness of the Wilson coefficients of penguin operators and CKM-suppression of current-current operators suggests that this contribution should be small. However, only an explicit calculation can turn this estimate into a firm statement. The calculation arises from tree and one-loop amplitudes, but it involves the four-body phase-space integration in dimensional regularization, which makes the calculation non-trivial owing to the appearance of higher transcendental functions. Moreover, the cancellation of poles in the dimensional regularization parameter ϵ is only achieved after proper UV and IR renormalization. The latter gives rise to logarithms $\ln(m_q/m_b)$ when turning the dimensional into a mass regulator. These logarithms stem from the phase space region of energetic collinear photon radiation off light quarks in the final state. They are computed with the splitting function technique and treated in the same way as in [50, 60].

We find indeed that the contribution of our four-body NLO correction to the total rate is below the 1% level, as expected. This statement even holds true once we vary the input parameters such as the charm mass m_c, the photon energy cut (parameterized by δ), the masses m_q of the light quarks, or the renormalization and matching scales, as can be seen by the numbers and the plots in section 4. We also confirm the LO results presented previously in ref. [50].

Yet the NLO calculation of $\bar{B} \to X_s\gamma$ is still not complete. There are certain yet unpublished three-particle cuts contributing to $\Gamma(b \to sg\gamma)$, mainly interferences of $P^u_{1,2}$ with $P^c_{1,2}$, which are also of the (A, B)-interference type. These contributions can be extracted from the results of ref. [32]. The only missing pieces are given by the diagrams in figure 1.f. These are NLO interferences of the type (B, B) and are expected to be negligible with respect to the (A, B) ones that we have calculated in a complete manner. While these contributions can be calculated with the techniques described in this paper, they are left for future work.

Acknowledgments

We thank Mikolaj Misiak for valuable correspondence and comments on the manuscript, and Dirk Seidel for useful discussions about penguins. This work has been funded by the

JHEP01(2015)115

Deutsche Forschungsgemeinschaft (DFG) within research unit FOR 1873 (QFET). M.P. acknowledges support by the National Science Centre (Poland) research project, decision DEC-2011/01/B/ST2/00438.

A Intermediate results

A.1 (P_7, P_i) interference

The functions $\mathcal{F}^{I,7}_{(J)}(\delta)$ are given by:

$$\mathcal{F}^{s,7}_{(i)}(\delta) = -6\,\mathcal{F}^{\times,7}_{(i)}(\delta)\ ; \tag{A.1}$$

$$\mathcal{F}^{\times,7}_{(i)}(\delta) = \frac{-18\delta + 33\delta^2 - 2\delta^3 - 13\delta^4 + 6\delta^3(2+\delta)\log(\delta)}{243(1-\delta)}\ ; \tag{A.2}$$

$$\mathcal{F}^{\times,7}_{(ii)}(\delta) = \frac{12\delta - 3\delta^2 - 8\delta^3 - \delta^4 + 6\delta^2(2+\delta)\log(\delta)}{54(1-\delta)}\ ; \tag{A.3}$$

A.2 (P_8, P_i) interference

Up to subleading terms in ϵ, we have always

$$\mathcal{F}^{s,8}(\delta) = -6\,(1+\epsilon)\,\mathcal{F}^{\times,8}(\delta)\ . \tag{A.4}$$

The functions $\mathcal{F}^{\times,8}(\delta)$ are given by:

$$\mathcal{F}^{\times,8}_{(i)}(\delta) = A_8(\delta)\left[\frac{1}{\epsilon} + 6L_\mu\right] + B_8(\delta)\ ; \tag{A.5}$$

$$\mathcal{F}^{\times,8}_{(ii)}(\delta) = B'_8(\delta)\ ; \qquad \mathcal{F}^{\times,8}_{\mathrm{coll}(ii)}(\delta) = 0\ ; \tag{A.6}$$

$$\mathcal{F}^{\times,8}_{(iii)}(\delta) = A''_8(\delta)\left[\frac{1}{\epsilon} + 6L_\mu\right] + B''_8(\delta)\ ; \tag{A.7}$$

$$\mathcal{F}^{\times,8}_{\mathrm{coll}(i)}(\delta) = -A_8(\delta)\left[\frac{1}{\epsilon} + 6L_\mu - 2L_q\right] + D_8(\delta)\ ; \tag{A.8}$$

$$\mathcal{F}^{\times,8}_{\mathrm{coll}(iii)}(\delta) = -A''_8(\delta)\left[\frac{1}{\epsilon} + 6L_\mu - 2L_q\right] + D''_8(\delta)\ ; \tag{A.9}$$

where $L_\mu = \log(\mu/m_b)$ and $L_q = \log(m_q/m_b)$, and:

$$A_8(\delta) = \frac{4\delta^3}{81} - \frac{\delta^2}{27} + \frac{4\delta}{27} + \frac{4}{27}\log(1-\delta)\ ; \tag{A.10}$$

$$A''_8(\delta) = -\frac{4\delta^3}{81} + \frac{10\delta^2}{27} + \frac{2\delta}{27} - \left(\frac{2\delta^2}{9} - \frac{4\delta}{9} - \frac{2}{27}\right)\log(1-\delta)\ ; \tag{A.11}$$

$$\begin{aligned} B_8(\delta) = {} & \frac{62\delta^3}{243} - \frac{17\delta^2}{162} + \frac{116\delta}{81} - \left(\frac{8\delta^3}{81} - \frac{2\delta^2}{27} + \frac{8\delta}{27}\right)\log\delta - \frac{8}{27}\log\delta\log(1-\delta) \\ & - \log(1-\delta)\left(\frac{8\delta^3}{81} - \frac{2\delta^2}{27} + \frac{8\delta}{27} - \frac{92}{81}\right) - \frac{4}{27}\log^2(1-\delta) - \frac{8\mathrm{Li}_2(\delta)}{27}\ ; \end{aligned} \tag{A.12}$$

JHEP01(2015)115

$$B_8'(\delta) = \frac{4\delta}{27} - \frac{\delta^2}{9} + \frac{2\delta^3}{81} + \frac{4\log(1-\delta)}{27} \; ; \tag{A.13}$$

$$\begin{aligned} B_8''(\delta) = & -\frac{8\delta^3}{27} + \frac{199\delta^2}{81} + \frac{119\delta}{81} + \left(\frac{8\delta^3}{81} - \frac{20\delta^2}{27} - \frac{4\delta}{27}\right)\log\delta \\ & + \left(\frac{8\delta^3}{81} - \frac{47\delta^2}{27} + \frac{50\delta}{27} + \frac{107}{81} + \frac{4\delta^2\log\delta}{9} - \frac{8\delta\log\delta}{9} - \frac{4\log\delta}{27}\right)\log(1-\delta) \\ & + \left(\frac{5\delta^2}{9} - \frac{10\delta}{9} + \frac{7}{27}\right)\log^2(1-\delta) + \left(\frac{4\delta^2}{9} - \frac{8\delta}{9} - \frac{4}{27}\right)\mathrm{Li}_2(\delta) \; ; \end{aligned} \tag{A.14}$$

$$\begin{aligned} D_8(\delta) = & -\frac{37\delta^3}{243} + \frac{\delta^2}{54} - \frac{8\delta}{9} + \log(1-\delta)\left(\frac{8\delta^3}{81} - \frac{2\delta^2}{27} + \frac{8\delta}{27} + \frac{4\log\delta}{27} - \frac{20}{27}\right) \\ & + \left(\frac{4\delta^3}{81} - \frac{\delta^2}{27} + \frac{4\delta}{27}\right)\log(\delta) + \frac{4}{27}\log^2(1-\delta) + \frac{4\mathrm{Li}_2(\delta)}{27} \; ; \end{aligned} \tag{A.15}$$

$$\begin{aligned} D_8''(\delta) = & +\frac{37\delta^3}{243} - \frac{35\delta^2}{27} - \frac{10\delta}{9} - \left(\frac{8\delta^3}{81} - \frac{32\delta^2}{27} + \frac{20\delta}{27} + \frac{28}{27}\right)\log(1-\delta) \\ & - \left(\frac{4\delta^3}{81} - \frac{10\delta^2}{27} - \frac{2\delta}{27}\right)\log\delta - \left(\frac{2\delta^2}{9} - \frac{4\delta}{9} - \frac{2}{27}\right)\log\delta\log(1-\delta) \\ & - \left(\frac{4\delta^2}{9} - \frac{8\delta}{9} + \frac{4}{27}\right)\log^2(1-\delta) - \left(\frac{2\delta^2}{9} - \frac{4\delta}{9} - \frac{2}{27}\right)\mathrm{Li}_2(\delta) \; ; \end{aligned} \tag{A.16}$$

A.3 (P_i, P_j) interference

For $\mathcal{F}^{I,1}_{(J)}(\delta)$ we give analytical results for m_c-independent functions, but the m_c-dependence is given as interpolated functions. Up to subleading terms in ϵ, we have always

$$\mathcal{F}^s(z_q,\delta) = -6\,(1+\epsilon+\epsilon^2)\,\mathcal{F}^\times(z_q,\delta) \; . \tag{A.17}$$

The functions $\mathcal{F}^\times(z_q,\delta)$ are given by:

$$\mathcal{F}^{\times,1}_{(i)}(z_q,\delta) = A(\delta)\left[\frac{1}{\epsilon^2} + \frac{1}{\epsilon}8L_\mu + 32L_\mu^2\right] + B(z_q,\delta)\left[\frac{1}{\epsilon} + 8L_\mu\right] + C(z_q,\delta) \; ; \tag{A.18}$$

$$\mathcal{F}^{\times,1}_{(ii)}(z_q,\delta) = B'(\delta)\left[\frac{1}{\epsilon} + 8L_\mu\right] + C'(z_q,\delta) \; ; \qquad \mathcal{F}^{\times,1}_{\mathrm{coll}(ii)}(z_q,\delta) = 0 \; ; \tag{A.19}$$

$$\mathcal{F}^{\times,1}_{(iii)}(z_q,\delta) = A''(\delta)\left[\frac{1}{\epsilon^2} + \frac{1}{\epsilon}8L_\mu + 32L_\mu^2\right] + B''(z_q,\delta)\left[\frac{1}{\epsilon} + 8L_\mu\right] + C''(z_q,\delta) \; ; \tag{A.20}$$

$$\begin{aligned} \mathcal{F}^{\times,1}_{\mathrm{coll}(i)}(z_q,\delta) = & -A(\delta)\left[\frac{1}{\epsilon^2} + \frac{1}{\epsilon}(8L_\mu - 2L_q) + 30L_\mu^2 - 12L_\mu L_q + 2L_\mu - 2L_q\right] \\ & -[B(z_q,\delta) + F(\delta) + H(\delta)]\left[\frac{1}{\epsilon} + 8L_\mu - 2L_q\right] + f(\delta)\,[L_\mu - L_q] + E(z_q,\delta); \end{aligned} \tag{A.21}$$

$$\begin{aligned} \mathcal{F}^{\times,1}_{\mathrm{coll}(iii)}(z_q,\delta) = & -A''(\delta)\left[\frac{1}{\epsilon^2} + \frac{1}{\epsilon}(8L_\mu - 2L_q) + 30L_\mu^2 - 12L_\mu L_q + 2L_\mu - 2L_q\right] \\ & -[B''(z_q,\delta) + F''(\delta) + H''(\delta)]\left[\frac{1}{\epsilon} + 8L_\mu - 2L_q\right] + f''(\delta)\,[L_\mu - L_q] + E''(z_q,\delta); \end{aligned} \tag{A.22}$$

JHEP01(2015)115

Counterterms are given by:

$$\mathcal{F}^{\times,C}_{(i)}(\delta) = -A(\delta)\left[\frac{1}{\epsilon^2}+\frac{1}{\epsilon}6L_\mu+18L_\mu^2\right]+F(\delta)\left[\frac{1}{\epsilon}+6L_\mu\right]+G(\delta)\ ; \tag{A.23}$$

$$\mathcal{F}^{\times,C}_{(ii)}(\delta) = -B'(\delta)\left[\frac{1}{\epsilon}+6L_\mu\right]+G'(\delta)\ ; \qquad \mathcal{F}^{\times,C}_{\mathrm{coll}(ii)}(z_q,\delta)=0\ ; \tag{A.24}$$

$$\mathcal{F}^{\times,C}_{(iii)}(\delta) = -A''(\delta)\left[\frac{1}{\epsilon^2}+\frac{1}{\epsilon}6L_\mu+18L_\mu^2\right]+F''(\delta)\left[\frac{1}{\epsilon}+6L_\mu\right]+G''(\delta)\ ; \tag{A.25}$$

$$\begin{aligned}\mathcal{F}^{\times,C}_{\mathrm{coll}(i)}(\delta) &= A(\delta)\left[\frac{1}{\epsilon^2}+\frac{1}{\epsilon}(6L_\mu-2L_q)+16L_\mu^2-8L_\mu L_q+2L_\mu-2L_q\right]\\ &\quad +H(\delta)\left[\frac{1}{\epsilon}+6L_\mu-2L_q\right]-f(\delta)\left[L_\mu-L_q\right]+I(\delta)\ ;\end{aligned} \tag{A.26}$$

$$\begin{aligned}\mathcal{F}^{\times,C}_{\mathrm{coll}(iii)}(\delta) &= A''(\delta)\left[\frac{1}{\epsilon^2}+\frac{1}{\epsilon}(6L_\mu-2L_q)+16L_\mu^2-8L_\mu L_q+2L_\mu-2L_q\right]\\ &\quad +H''(\delta)\left[\frac{1}{\epsilon}+6L_\mu-2L_q\right]-f''(\delta)\left[L_\mu-L_q\right]+I''(\delta)\ ;\end{aligned} \tag{A.27}$$

where again $L_\mu=\log(\mu/m_b)$ and $L_q=\log(m_q/m_b)$. From these expressions one can check the pattern of cancellation of UV and collinear divergences. The z_q-independent functions are given by (with the notation $\bar\delta\equiv 1-\delta$, $L_{\bar\delta}\equiv\log(1-\delta)$, $L_\delta\equiv\log\delta$),

$$A(\delta) = -\frac{\delta^4}{1458}-\frac{\delta}{243}-\frac{1}{243}L_{\bar\delta}\ ; \tag{A.28}$$

$$A''(\delta) = -\frac{2\delta^4}{729}+\frac{2\delta^3}{729}-\frac{\delta^2}{486}-\frac{2\delta}{243}-\frac{2}{243}L_{\bar\delta}\ ; \tag{A.29}$$

$$B'(\delta) = -\frac{2\delta^3}{2187}+\frac{2\delta^2}{729}-\frac{2\delta}{729}-\frac{2}{729}L_{\bar\delta}\ ; \tag{A.30}$$

$$f(\delta) = \left(\frac{4\delta^2}{243}-\frac{4\delta}{729}-\frac{1}{243}\right)L_{\bar\delta}+\frac{2}{243}L_{\bar\delta}^2+\frac{11\delta^4}{8748}+\frac{5\delta^3}{729}-\frac{23\delta^2}{1458}-\frac{\delta}{243}\ ; \tag{A.31}$$

$$f''(\delta) = \left(\frac{10\delta^2}{243}-\frac{16\delta}{729}-\frac{2}{729}\right)L_{\bar\delta}+\frac{4}{243}L_{\bar\delta}^2+\frac{11\delta^4}{2187}+\frac{34\delta^3}{2187}-\frac{29\delta^2}{729}-\frac{2\delta}{729}\ ; \tag{A.32}$$

$$\begin{aligned}F(\delta) &= -\left(\frac{2L_{\bar\delta}}{243}+\frac{\delta^4}{729}+\frac{2\delta}{243}\right)L_\delta-\left(\frac{\delta^4}{729}+\frac{2\delta}{243}-\frac{97}{2916}\right)L_{\bar\delta}-\frac{L_{\bar\delta}^2}{243}+\frac{53\delta^4}{17496}+\frac{4\delta^3}{2187}\\ &\quad +\frac{7\delta^2}{5832}+\frac{121\delta}{2916}-\frac{2\mathrm{Li}_2(\delta)}{243}\ ;\end{aligned} \tag{A.33}$$

$$\begin{aligned}F''(\delta) &= -\left(\frac{4L_{\bar\delta}}{243}+\frac{4\delta^4}{729}-\frac{4\delta^3}{729}+\frac{\delta^2}{243}+\frac{4\delta}{243}\right)L_\delta-\left(\frac{4\delta^4}{729}-\frac{4\delta^3}{729}+\frac{\delta^2}{243}+\frac{4\delta}{243}-\frac{47}{729}\right)L_{\bar\delta}\\ &\quad -\frac{2L_{\bar\delta}^2}{243}+\frac{71\delta^4}{4374}-\frac{38\delta^3}{2187}+\frac{49\delta^2}{2916}+\frac{59\delta}{729}-\frac{4\mathrm{Li}_2(\delta)}{243}\ ;\end{aligned} \tag{A.34}$$

$$\begin{aligned}G(\delta) &= \left(\frac{\delta^4}{729}+\frac{2\delta}{243}-\frac{97}{2916}\right)L_{\bar\delta}^2+\left(\frac{2L_{\bar\delta}}{243}+\frac{\delta^4}{729}+\frac{2\delta}{243}\right)L_\delta^2+\frac{2L_{\bar\delta}^3}{729}-\left(\frac{53\delta^4}{8748}+\frac{8\delta^3}{2187}\right.\\ &\quad \left.+\frac{7\delta^2}{2916}+\frac{121\delta}{1458}-\frac{4\mathrm{Li}_2(\delta)}{243}+\frac{7\pi^2}{972}-\frac{6901}{34992}\right)L_{\bar\delta}+\left(\frac{2\delta^4}{729}+\frac{4\delta}{243}-\frac{97}{1458}\right)L_\delta L_{\bar\delta}\end{aligned}$$

JHEP01(2015)115

$$+\left(\frac{4L_{\bar\delta}^2}{243}-\frac{53\delta^4}{8748}-\frac{8\delta^3}{2187}-\frac{7\delta^2}{2916}-\frac{121\delta}{1458}+\frac{4\mathrm{Li}_2(\delta)}{243}\right)L_\delta-\frac{13\pi^2\delta^4}{17496}+\frac{2233\delta^4}{209952}+\frac{\delta^3}{81}$$
$$+\frac{733\delta^2}{69984}-\frac{13\pi^2\delta}{2916}+\frac{9805\delta}{34992}-\frac{97\mathrm{Li}_2(\delta)}{1458}+\frac{4\mathrm{Li}_3(\bar\delta)}{243}-\frac{4\mathrm{Li}_3(\delta)}{243}-\frac{4\zeta(3)}{243}\ ; \tag{A.35}$$

$$G'(\delta)=-\left(\frac{4L_{\bar\delta}}{729}+\frac{4\delta^3}{2187}-\frac{4\delta^2}{729}+\frac{4\delta}{729}\right)L_\delta-\left(\frac{4\delta^3}{2187}-\frac{4\delta^2}{729}+\frac{4\delta}{729}-\frac{59}{2187}\right)L_{\bar\delta}-\frac{2L_{\bar\delta}^2}{729}$$
$$+\frac{5\delta^3}{729}-\frac{50\delta^2}{2187}+\frac{71\delta}{2187}-\frac{4\mathrm{Li}_2(\delta)}{729}\ ; \tag{A.36}$$

$$G''(\delta)=\left(\frac{4\delta^4}{729}-\frac{4\delta^3}{729}+\frac{\delta^2}{243}+\frac{4\delta}{243}-\frac{47}{729}\right)L_{\bar\delta}^2+\left(\frac{4L_{\bar\delta}}{243}+\frac{4\delta^4}{729}-\frac{4\delta^3}{729}+\frac{\delta^2}{243}+\frac{4\delta}{243}\right)L_\delta^2$$
$$+\frac{4}{729}L_{\bar\delta}^3-\left(\frac{71\delta^4}{2187}-\frac{76\delta^3}{2187}+\frac{49\delta^2}{1458}+\frac{118\delta}{729}-\frac{8\mathrm{Li}_2(\delta)}{243}+\frac{7\pi^2}{486}-\frac{1645}{4374}\right)L_{\bar\delta}$$
$$-L_\delta\left[\left(-\frac{8\delta^4}{729}+\frac{8\delta^3}{729}-\frac{2\delta^2}{243}-\frac{8\delta}{243}+\frac{94}{729}\right)L_{\bar\delta}-\frac{8L_{\bar\delta}^2}{243}+\frac{71\delta^4}{2187}-\frac{76\delta^3}{2187}+\frac{49\delta^2}{1458}\right.$$
$$\left.+\frac{118\delta}{729}-\frac{8\mathrm{Li}_2(\delta)}{243}\right]-\frac{13\pi^2\delta^4}{4374}+\frac{1877\delta^4}{26244}+\frac{13\pi^2\delta^3}{4374}-\frac{527\delta^3}{6561}-\frac{13\pi^2\delta^2}{5832}+\frac{1493\delta^2}{17496}$$
$$-\frac{13\pi^2\delta}{1458}+\frac{2353\delta}{4374}-\frac{94\mathrm{Li}_2(\delta)}{729}+\frac{8\mathrm{Li}_3(\bar\delta)}{243}-\frac{8\mathrm{Li}_3(\delta)}{243}-\frac{8\zeta(3)}{243}\ ; \tag{A.37}$$

$$H(\delta)=\left(\frac{L_{\bar\delta}}{243}+\frac{\delta^4}{1458}+\frac{\delta}{243}\right)L_\delta+\left(\frac{\delta^4}{729}+\frac{2\delta}{243}-\frac{7}{324}\right)L_{\bar\delta}+\frac{L_{\bar\delta}^2}{243}-\frac{5\delta^4}{3888}-\frac{19\delta^3}{8748}$$
$$-\frac{7\delta^2}{5832}-\frac{25\delta}{972}+\frac{\mathrm{Li}_2(\delta)}{243}\ ; \tag{A.38}$$

$$H''(\delta)=\left(\frac{2L_{\bar\delta}}{243}+\frac{2\delta^4}{729}-\frac{2\delta^3}{729}+\frac{\delta^2}{486}+\frac{2\delta}{243}\right)L_\delta+\left(\frac{4\delta^4}{729}-\frac{4\delta^3}{729}+\frac{\delta^2}{243}+\frac{4\delta}{243}-\frac{7}{162}\right)L_{\bar\delta}$$
$$+\frac{2L_{\bar\delta}^2}{243}-\frac{2\delta^4}{243}+\frac{29\delta^3}{4374}-\frac{8\delta^2}{729}-\frac{25\delta}{486}+\frac{2\mathrm{Li}_2(\delta)}{243}\ ; \tag{A.39}$$

$$I(\delta)=-\left(\frac{L_{\bar\delta}}{486}+\frac{\delta^4}{2916}+\frac{\delta}{486}\right)L_\delta^2-\left(\frac{\delta^4}{729}-\frac{2\delta^2}{243}+\frac{8\delta}{729}-\frac{23}{972}\right)L_{\bar\delta}^2+\left(\frac{5\delta^4}{1944}+\frac{19\delta^3}{4374}\right.$$
$$\left.+\frac{67\delta^2}{2916}+\frac{61\delta}{4374}+\frac{2\mathrm{Li}_2(\bar\delta)}{243}+\frac{\pi^2}{486}-\frac{809}{11664}\right)L_{\bar\delta}-L_\delta\left[\left(\frac{\delta^4}{729}+\frac{2\delta}{243}-\frac{7}{729}\right)L_{\bar\delta}\right.$$
$$\left.-\frac{5\delta^4}{3888}-\frac{19\delta^3}{8748}-\frac{7\delta^2}{5832}-\frac{25\delta}{972}+\frac{\mathrm{Li}_2(\delta)}{243}\right]+\frac{\pi^2\delta^4}{2916}-\frac{5\delta^4}{2916}+\frac{247\delta^3}{34992}-\frac{2461\delta^2}{69984}$$
$$+\frac{\pi^2\delta}{486}-\frac{1109\delta}{11664}-\frac{35\mathrm{Li}_2(\bar\delta)}{2916}+\frac{7\mathrm{Li}_2(\delta)}{729}-\frac{2\mathrm{Li}_3(\bar\delta)}{243}+\frac{\mathrm{Li}_3(\delta)}{243}+\frac{2\zeta(3)}{243}+\frac{35\pi^2}{17496}\ ; \tag{A.40}$$

$$I''(\delta)=-\left(\frac{4\delta^4}{729}-\frac{4\delta^3}{729}-\frac{4\delta^2}{243}+\frac{20\delta}{729}-\frac{73}{1458}\right)L_{\bar\delta}^2-\left(\frac{L_{\bar\delta}}{243}+\frac{\delta^4}{729}-\frac{\delta^3}{729}+\frac{\delta^2}{972}+\frac{\delta}{243}\right)L_\delta^2$$
$$+\left(\frac{4\delta^4}{243}-\frac{29\delta^3}{2187}+\frac{58\delta^2}{729}+\frac{5\delta}{2187}+\frac{4\mathrm{Li}_2(\bar\delta)}{243}+\frac{\pi^2}{243}-\frac{2215}{17496}\right)L_{\bar\delta}-L_\delta\left[\left(\frac{4\delta^4}{729}\right.\right.$$
$$\left.\left.-\frac{4\delta^3}{729}+\frac{\delta^2}{243}+\frac{4\delta}{243}-\frac{5}{243}\right)L_{\bar\delta}-\frac{2\delta^4}{243}+\frac{29\delta^3}{4374}-\frac{8\delta^2}{729}-\frac{25\delta}{486}+\frac{2\mathrm{Li}_2(\delta)}{243}\right]+\frac{\pi^2\delta^4}{729}$$
$$-\frac{383\delta^4}{23328}-\frac{\pi^2\delta^3}{729}+\frac{923\delta^3}{17496}+\frac{\pi^2\delta^2}{972}-\frac{1357\delta^2}{11664}+\frac{\pi^2\delta}{243}-\frac{3115\delta}{17496}-\frac{11\mathrm{Li}_2(\bar\delta)}{486}+\frac{5\mathrm{Li}_2(\delta)}{243}$$
$$-\frac{4\mathrm{Li}_3(\bar\delta)}{243}+\frac{2\mathrm{Li}_3(\delta)}{243}+\frac{4\zeta(3)}{243}+\frac{11\pi^2}{2916}\ ; \tag{A.41}$$

JHEP01(2015)115

$\{j\}$	$f^{(0)}_{B,\{j\}}$	$f^{(1)}_{B,\{j\}}$	$f^{(2)}_{B,\{j\}}$	$h^{(0)}_{B,\{j\}}$	$h^{(1)}_{B,\{j\}}$	$h^{(2)}_{B,\{j\}}$
{5}	2.6085e2	-2.3748e3	7.8427e2	-2.5964e0	-1.8780e1	-7.0839e1
{4}	5.5417e2	1.6248e2	8.9587e2	3.6935e0	2.6299e1	8.9418e1
{3}	-8.6141e0	1.2216e3	-2.0894e2	-1.6902e0	-1.1864e1	-3.5637e1
{2}	-1.5107e0	-9.2378e1	2.1731e1	3.2301e-1	2.2545e0	6.0307e0
{1}	1.1241e-1	5.4522e0	-1.3841e0	-2.6875e-2	-1.8840e-1	-4.5543e-1
{0}	3.2101e-3	2.0675e-2	4.0727e-2	8.0387e-4	5.7122e-3	1.2664e-2
{-1}	2.7478e1	2.4959e2	-3.5865e1	5.1543e0	-9.6139e0	-2.1925e1
{-2}	-6.5543e1	-4.3377e3	5.9242e2	-2.5093e2	-1.8937e2	-1.6101e2
{-3}	-9.6131e3	5.7863e4	-5.6283e3	1.7465e4	1.1349e4	1.1056e4
{-4}	2.2612e5	7.7096e4	2.1131e4	-4.3025e5	-2.3262e5	-1.5200e5
{-5}	1.6782e5	-2.0939e5	3.8351e4	4.3797e6	1.7123e6	7.2442e5

Table 1. Padé coefficients for $B(z_q, \delta)$.

While our calculation provides *exactly* all the functions $B^{(\prime\prime)}(z_q, \delta)$, $C^{(\prime,\prime\prime)}(z_q, \delta)$ and $E^{(\prime\prime)}(z_q, \delta)$, the corresponding expressions depend on z_q and the photon energy E_γ through complex functions of harmonic polylogarithms of various weights, which must be integrated in the region $2E_\gamma/m_B \in [1-\delta, 1]$. Solving these integrals analytically is highly non-trivial, and even the numerical integration is computationally demanding. We have performed a numerical evaluation of such integrals and find it more convenient to present the results as an expansion in δ around the value $\delta = 0.316$, and as an interpolation in z_q. These interpolations coincide with the exact results in the region $z \in [0, 1]$ to a very good precision. The relevant functions are written as:

$$\begin{aligned}\mathcal{G}(z_q, \delta) \,=\, & \left[f^{(0)}_{\mathcal{G}}(z_q) + i\, h^{(0)}_{\mathcal{G}}(z_q)\right] + \left[f^{(1)}_{\mathcal{G}}(z_q) + i\, h^{(1)}_{\mathcal{G}}(z_q)\right](\delta - 0.316) \\ & + \left[f^{(2)}_{\mathcal{G}}(z_q) + i\, h^{(2)}_{\mathcal{G}}(z_q)\right](\delta - 0.316)^2 + \cdots \end{aligned} \tag{A.42}$$

with $\mathcal{G} = B, B'', C, C', C'', E, E''$. The functions $f^{(i)}_{\mathcal{G}}(z_q)$, $h^{(i)}_{\mathcal{G}}(z_q)$ are fitted to padé approximants of order [5/5]:

$$f^{(i)}_{\mathcal{G}}(z_q) = \frac{f^{(i)}_{\mathcal{G},\{5\}} z_q^5 + f^{(i)}_{\mathcal{G},\{4\}} z_q^4 + f^{(i)}_{\mathcal{G},\{3\}} z_q^3 + f^{(i)}_{\mathcal{G},\{2\}} z_q^2 + f^{(i)}_{\mathcal{G},\{1\}} z_q + f^{(i)}_{\mathcal{G},\{0\}}}{f^{(i)}_{\mathcal{G},\{-5\}} z_q^5 + f^{(i)}_{\mathcal{G},\{-4\}} z_q^4 + f^{(i)}_{\mathcal{G},\{-3\}} z_q^3 + f^{(i)}_{\mathcal{G},\{-2\}} z_q^2 + f^{(i)}_{\mathcal{G},\{-1\}} z_q + 1} \tag{A.43}$$

and similar for $h^{(i)}_{\mathcal{G}}(z_q)$. The Padé coefficients $f^{(i)}_{\mathcal{G},\{j\}}, h^{(i)}_{\mathcal{G},\{j\}}$ are given in tables 1–7.

The functions $\widetilde{\mathcal{F}}(z_q, \delta)$ are UV finite and collinear safe. Again, we have the following relationship,

$$\widetilde{\mathcal{F}}^{s,1}_{(i)}(z_q, \delta) = -6\, \widetilde{\mathcal{F}}^{\times,1}_{(i)}(z_q, \delta)\ . \tag{A.44}$$

As before, the 'crossed' functions $\widetilde{\mathcal{F}}^{\times,1}_{(J)}(z_q, \delta)$ are known exactly but we provide here simplified expressions as an expansion in $(\delta - 0.316)$ and interpolated in z_q. We write:

$$\begin{aligned}\widetilde{\mathcal{F}}^{\times,1}_{(J)}(z_q, \delta) \,=\, & \left[\tilde{f}^{(0)}_{(J)}(z_q) + i\, \tilde{h}^{(0)}_{(J)}(z_q)\right] + \left[\tilde{f}^{(1)}_{(J)}(z_q) + i\, \tilde{h}^{(1)}_{(J)}(z_q)\right](\delta - 0.316) \\ & + \left[\tilde{f}^{(2)}_{(J)}(z_q) + i\, \tilde{h}^{(2)}_{(J)}(z_q)\right](\delta - 0.316)^2 + \cdots \end{aligned} \tag{A.45}$$

JHEP01(2015)115

$\{j\}$	$f^{(0)}_{B'',\{j\}}$	$f^{(1)}_{B'',\{j\}}$	$f^{(2)}_{B'',\{j\}}$	$h^{(0)}_{B'',\{j\}}$	$h^{(1)}_{B'',\{j\}}$	$h^{(2)}_{B'',\{j\}}$
{5}	-9.5739e-1	-9.6422e0	-2.8386e1	-7.9067e-2	-6.6893e-1	-2.9051e0
{4}	3.0239e0	2.7036e1	1.2991e2	1.9267e-1	1.6095e0	6.3544e0
{3}	-3.9058e-1	-6.8880e-1	2.3899e0	-1.7623e-1	-1.4512e0	-5.1486e0
{2}	3.7847e-3	-6.4972e-1	-4.0154e0	7.5813e-2	6.1479e-1	1.9516e0
{1}	-9.5759e-3	3.6265e-3	2.4684e-1	-1.5417e-2	-1.2304e-1	-3.5068e-1
{0}	3.9641e-3	3.0018e-2	7.5378e-2	1.1925e-3	9.3670e-3	2.4204e-2
{-1}	-4.6336e0	-2.3791e0	2.8343e-1	-7.6041e0	-6.7239e0	-5.9052e0
{-2}	3.1991e1	1.5265e1	-1.9554e0	5.0750e1	4.1512e1	2.0995e1
{-3}	-2.6083e2	-2.3013e2	-3.0385e2	-1.6999e2	-8.9622e1	2.8933e2
{-4}	1.1184e3	1.4088e3	2.6697e3	-2.6338e2	-7.5669e2	-4.3799e3
{-5}	-3.1470e2	-4.4778e2	-4.4635e2	3.2029e3	5.1645e3	1.9822e4

Table 2. Padé coefficients for $B''(z_q, \delta)$.

$\{j\}$	$f^{(0)}_{C,\{j\}}$	$f^{(1)}_{C,\{j\}}$	$f^{(2)}_{C,\{j\}}$	$h^{(0)}_{C,\{j\}}$	$h^{(1)}_{C,\{j\}}$	$h^{(2)}_{C,\{j\}}$
{5}	6.7269e2	4.9426e2	1.0451e3	-3.4512e1	-2.3670e2	-9.4447e2
{4}	3.3679e3	5.8344e3	3.4974e3	4.8342e1	3.2457e2	1.1315e3
{3}	2.3178e2	2.4369e2	-6.8258e2	-2.1749e1	-1.4292e2	-4.2386e2
{2}	-3.3437e1	-8.0765e1	7.0897e1	4.0984e0	2.6571e1	6.7645e1
{1}	1.7801e0	2.8034e0	-5.3246e0	-3.3765e-1	-2.1805e0	-4.8418e0
{0}	1.8570e-2	1.0740e-1	1.8133e-1	1.0040e-2	6.5154e-2	1.2819e-1
{-1}	7.1021e1	1.0292e1	-3.4108e1	9.6116e0	-8.1610e0	-2.2268e1
{-2}	-6.9880e2	-1.5360e2	5.3644e2	-6.8385e2	-3.9083e2	-2.5150e2
{-3}	-5.9528e3	-6.3499e3	-5.0770e3	3.0179e4	1.5933e4	1.3515e4
{-4}	3.3626e5	9.9501e4	2.0032e4	-6.1404e5	-2.6974e5	-1.6966e5
{-5}	1.9465e5	4.3193e4	3.0917e4	5.0960e6	1.7175e6	7.4113e5

Table 3. Padé coefficients for $C(z_q, \delta)$.

$\{j\}$	$f^{(0)}_{C',\{j\}}$	$f^{(1)}_{C',\{j\}}$	$f^{(2)}_{C',\{j\}}$	$h^{(0)}_{C',\{j\}}$	$h^{(1)}_{C',\{j\}}$	$h^{(2)}_{C',\{j\}}$
{5}	3.7841e2	5.9118e2	3.9056e2	-4.5121e-1	-6.0463e1	-2.1698e1
{4}	2.7044e2	4.8884e2	5.4690e2	7.9268e-1	8.8873e1	3.5043e1
{3}	-1.1579e2	-1.8312e2	-1.8791e2	-5.0952e-1	-3.9767e1	-1.8854e1
{2}	1.3594e1	1.9867e1	2.5682e1	1.5463e-1	5.9243e0	4.2454e0
{1}	3.0297e-2	-1.6165e-1	-1.7434e0	-2.2768e-2	-1.7640e-1	-4.0900e-1
{0}	5.8184e-3	3.5538e-2	5.7703e-2	1.3344e-3	8.5805e-3	1.5244e-2
{-1}	1.4953e0	-7.2811e0	-3.1995e1	1.1886e1	-8.8975e0	-2.7485e1
{-2}	2.4503e3	6.0955e2	4.7985e2	-5.2688e2	4.2689e2	3.3788e2
{-3}	-1.9815e4	-5.2682e3	-3.4156e3	5.3900e3	1.1219e4	-9.5618e2
{-4}	3.7632e4	1.1781e4	8.8305e3	-2.3444e4	-1.4783e5	-1.2086e4
{-5}	1.0249e5	2.6408e4	1.1136e4	3.8372e4	5.4497e5	8.0691e4

Table 4. Padé coefficients for $C'(z_q, \delta)$.

JHEP01(2015)115

$\{j\}$	$f^{(0)}_{C'',\{j\}}$	$f^{(1)}_{C'',\{j\}}$	$f^{(2)}_{C'',\{j\}}$	$h^{(0)}_{C'',\{j\}}$	$h^{(1)}_{C'',\{j\}}$	$h^{(2)}_{C'',\{j\}}$
{5}	-7.7072e0	-7.3684e1	-3.2672e2	-8.7364e-1	-6.3940e0	-3.5367e1
{4}	6.5728e0	3.6241e1	1.4444e2	2.0978e0	1.5469e1	7.3871e1
{3}	4.6807e0	7.0186e1	3.8320e2	-1.8917e0	-1.4054e1	-5.6847e1
{2}	-1.5486e0	-1.9670e1	-9.3766e1	8.0372e-1	6.0118e0	2.0476e1
{1}	1.0573e-1	1.6449e0	8.0166e0	-1.6179e-1	-1.2175e0	-3.5220e0
{0}	1.8873e-2	1.3658e-1	3.3186e-1	1.2423e-2	9.3960e-2	2.3583e-1
{-1}	-4.4964e-1	4.8147e0	1.4577e1	-6.6212e0	-4.6773e0	-2.9278e0
{-2}	-2.5309e0	-4.5104e1	-1.3130e2	2.2861e1	-8.8411e0	-7.8932e1
{-3}	-1.7756e2	-5.9658e1	1.1661e2	1.0154e2	4.6805e2	1.6895e3
{-4}	1.3958e3	1.8710e3	3.9334e3	-1.5110e3	-3.7935e3	-1.3934e4
{-5}	-1.0185e3	-1.5684e3	-3.2201e3	5.1086e3	1.1386e4	4.4771e4

Table 5. Padé coefficients for $C''(z_q, \delta)$.

$\{j\}$	$f^{(0)}_{E,\{j\}}$	$f^{(1)}_{E,\{j\}}$	$f^{(2)}_{E,\{j\}}$	$h^{(0)}_{E,\{j\}}$	$h^{(1)}_{E,\{j\}}$	$h^{(2)}_{E,\{j\}}$
{5}	6.4806e1	3.5981e2	1.2940e2	2.1801e1	1.5065e2	6.3214e2
{4}	-8.5279e2	-1.5483e3	-1.4843e3	-3.0643e1	-2.0732e2	-7.5761e2
{3}	-9.9349e1	-4.0637e2	2.2130e2	1.3820e1	9.1544e1	2.8342e2
{2}	1.2871e1	6.1243e1	-2.0763e1	-2.6077e0	-1.7054e1	-4.5145e1
{1}	-5.9578e-1	-2.2780e0	1.9360e0	2.1490e-1	1.4015e0	3.2245e0
{0}	-7.3348e-3	-4.1945e-2	-7.8462e-2	-6.3860e-3	-4.1912e-2	-8.5194e-2
{-1}	4.7343e1	2.3190e1	-3.2893e1	1.4649e1	-3.5937e0	-1.8952e1
{-2}	-1.4068e2	-3.0228e2	5.2625e2	-7.6567e2	-5.4265e2	-3.8314e2
{-3}	-1.3594e4	-7.1646e3	-5.3673e3	3.2909e4	1.9737e4	1.5799e4
{-4}	3.2738e5	1.3102e5	2.2555e4	-6.6974e5	-3.2807e5	-1.9062e5
{-5}	2.8262e5	4.3433e4	3.7019e4	5.6997e6	2.0888e6	8.2259e5

Table 6. Padé coefficients for $E(z_q, \delta)$.

$\{j\}$	$f^{(0)}_{E'',\{j\}}$	$f^{(1)}_{E'',\{j\}}$	$f^{(2)}_{E'',\{j\}}$	$h^{(0)}_{E'',\{j\}}$	$h^{(1)}_{E'',\{j\}}$	$h^{(2)}_{E'',\{j\}}$
{5}	-2.7046e1	-1.1652e2	-6.3378e3	4.8640e-1	3.9114e0	1.7243e1
{4}	-4.2392e2	-4.6203e3	-5.8000e4	-1.1720e0	-9.3898e0	-3.7292e1
{3}	1.3189e2	1.3432e3	1.5166e4	1.0609e0	8.4650e0	3.0070e1
{2}	-8.8744e0	-9.3948e1	-1.1660e3	-4.5251e-1	-3.5954e0	-1.1478e1
{1}	-1.4275e0	-1.2464e1	-8.5821e1	9.1466e-2	7.2362e-1	2.1083e0
{0}	-4.5677e-3	-3.6869e-2	-1.1199e-1	-7.0517e-3	-5.5554e-2	-1.5106e-1
{-1}	2.8279e2	3.0406e2	7.1445e2	-7.6394e0	-6.0846e0	-4.0315e0
{-2}	-1.2889e3	-9.3334e2	1.1757e3	3.3059e1	7.5335e0	-4.7914e1
{-3}	9.6814e3	7.3874e3	-7.4918e3	1.2448e1	2.7671e2	1.2068e3
{-4}	-7.8680e4	-8.4193e4	-1.9839e5	-1.0211e3	-2.5305e3	-1.0096e4
{-5}	2.9932e5	3.9930e5	1.7241e6	3.8601e3	7.8008e3	3.2678e4

Table 7. Padé coefficients for $E''(z_q, \delta)$.

JHEP01(2015)115

$\{j\}$	$\tilde{f}^{(0)}_{(i),\{j\}}$	$\tilde{f}^{(1)}_{(i),\{j\}}$	$\tilde{f}^{(2)}_{(i),\{j\}}$	$\tilde{f}^{(0)}_{(ii),\{j\}}$	$\tilde{f}^{(1)}_{(ii),\{j\}}$	$\tilde{f}^{(2)}_{(ii),\{j\}}$
{5}	-6.0396e1	-7.9313e2	-4.1781e2	8.5226e3	5.9559e4	6.0577e2
{4}	-4.3337e1	4.3943e1	1.7075e2	5.2397e2	-1.7693e3	-2.4607e2
{3}	2.7398e1	7.1810e1	-2.3013e1	-6.9260e2	-2.5828e3	4.0981e1
{2}	-4.9232e0	-1.6196e1	1.0162e0	1.3412e2	5.3783e2	-3.9970e0
{1}	1.9455e-1	6.9739e-1	-1.0853e-2	-3.4138e0	-1.4094e1	2.4014e-1
{0}	4.7105e-4	2.1302e-3	4.5410e-4	-1.5811e-3	-8.3330e-3	-5.1000e-3
{-1}	3.2507e2	2.5362e2	-6.7339e1	1.8946e3	1.4787e3	-3.6244e1
{-2}	-1.2129e3	-3.3619e3	2.9914e3	2.7983e4	1.4145e4	1.3530e3
{-3}	4.5871e4	3.7550e4	-6.7242e4	3.3450e5	-3.5081e4	-3.2312e4
{-4}	-2.7172e5	8.5735e4	7.6883e5	2.2367e6	7.2362e6	4.1425e5
{-5}	-3.6784e5	-2.6336e6	-4.2134e6	-4.8970e7	-7.8826e7	-2.5466e6
{-6}	4.8301e6	9.5241e6	8.8361e6	3.1279e8	4.0127e8	5.9475e6

Table 8. Padé coefficients for the real parts of $\widetilde{\mathcal{F}}^{\times,1}_{(J)}(z_q,\delta)$.

with $J = i, ii$. The functions $\tilde{f}^{(i)}_{(J)}(z_q)$ are again fitted to Padé approximants:

$$\tilde{f}^{(i)}_{(J)}(z_q) = \frac{\tilde{f}^{(i)}_{(J),\{5\}} z_q^5 + \tilde{f}^{(i)}_{(J),\{4\}} z_q^4 + \tilde{f}^{(i)}_{(J),\{3\}} z_q^3 + \tilde{f}^{(i)}_{(J),\{2\}} z_q^2 + \tilde{f}^{(i)}_{(J),\{1\}} z_q + \tilde{f}^{(i)}_{(J),\{0\}}}{\tilde{f}^{(i)}_{(J),\{-6\}} z_q^6 + \tilde{f}^{(i)}_{(J),\{-5\}} z_q^5 + \tilde{f}^{(i)}_{(J),\{-4\}} z_q^4 + \tilde{f}^{(i)}_{(J),\{-3\}} z_q^3 + \tilde{f}^{(i)}_{(J),\{-2\}} z_q^2 + \tilde{f}^{(i)}_{(J),\{-1\}} z_q + 1} \tag{A.46}$$

but a different parameterization for the functions $\tilde{h}^{(i)}_{(J)}(z_q)$ is found to reproduce the exact result more accurately. While for $\tilde{h}^{(0)}_{(J)}(z_q)$ and $\tilde{h}^{(1)}_{(J)}(z_q)$ we use

$$\tilde{h}^{(i)}_{(J)}(z_q) = z_q \exp\left[-\tilde{h}^{(i)}_{(J),\{e\}} z_q\right] \left(\frac{1}{4} - z_q\right)^2 \theta\left(\frac{1}{4} - z_q\right) \sum_{j=0}^{6} \tilde{h}^{(i)}_{(J),\{j\}} z_q^j \,, \tag{A.47}$$

we make the ansatz

$$\tilde{h}^{(2)}_{(J)}(z_q) = z_q \left(\frac{1}{4} - z_q\right)^2 \theta\left(\frac{1}{4} - z_q\right) \frac{\sum_{j=0}^{7} \tilde{h}^{(2)}_{(J),\{j\}} z_q^j}{1 + \sum_{j=1}^{7} \tilde{h}^{(2)}_{(J),\{j\}} z_q^j} \tag{A.48}$$

for $\tilde{h}^{(2)}_{(J)}(z_q)$. The coefficients $\tilde{f}^{(i)}_{(J),\{j\}}$ and $\tilde{h}^{(i)}_{(J),\{j\}}$ can be found in tables 8 and 9, respectively. Finally the functions $\widetilde{\mathcal{F}}^{I,4}_{(J)}(\delta)$ are given by

$$\widetilde{\mathcal{F}}^{s,4}_{(i)}(\delta) = -6\, \widetilde{\mathcal{F}}^{\times,4}_{(i)}(\delta) \tag{A.49}$$

and

$$\begin{aligned} \widetilde{\mathcal{F}}^{\times,4}_{(i)}(\delta) &= -0.0000513772 - 0.0003375398\,(\delta - 0.316) - 0.000532746\,(\delta - 0.316)^2 + \cdots \,, \\ \widetilde{\mathcal{F}}^{\times,4}_{(ii)}(\delta) &= -0.0001176336 - 0.0003362453\,(\delta - 0.316) + 0.001067501\,(\delta - 0.316)^2 + \cdots \,. \end{aligned} \tag{A.50}$$

JHEP01(2015)115

$\{j\}$	$\tilde{h}^{(0)}_{(i),\{j\}}$	$\tilde{h}^{(1)}_{(i),\{j\}}$	$\tilde{h}^{(0)}_{(ii),\{j\}}$	$\tilde{h}^{(1)}_{(ii),\{j\}}$
{6}	0	0	2.7269e9	3.0740e10
{5}	0	5.9601e5	-5.6512e8	-5.4396e9
{4}	-3.4279e4	-2.5773e5	5.1876e7	4.4076e8
{3}	5.4423e3	3.5916e4	-2.2643e6	-1.6493e7
{2}	-5.0377e2	-2.5068e3	5.7546e4	3.7561e5
{1}	9.7190e0	2.9523e1	-5.7810e2	-3.0581e3
{0}	-7.3742e-1	-2.5466e0	6.7661e0	3.4673e1
{e}	2.9801e1	2.3898e1	8.2260e1	9.3516e1

$\{j\}$	$\tilde{h}^{(2)}_{(i),\{j\}}$	$\tilde{h}^{(2)}_{(ii),\{j\}}$
{7}	1.9156e7	0
{6}	-1.2045e7	-4.0614e7
{5}	2.7691e6	2.8773e7
{4}	-2.4695e5	-9.2094e6
{3}	-1.3034e3	1.6547e6
{2}	1.5514e3	-1.5575e5
{1}	-8.3143e1	5.4749e3
{0}	1.1641e0	3.0407e1
{-1}	5.3853e1	1.0191e3
{-2}	-4.7202e3	5.4442e3
{-3}	1.2537e5	-6.7695e5
{-4}	-1.7062e6	1.0194e7
{-5}	1.2920e7	-4.8380e7
{-6}	-5.1347e7	-2.3921e7
{-7}	8.3239e7	4.9141e8

Table 9. Coefficients for the imaginary parts of $\widetilde{\mathcal{F}}^{\times,1}_{(J)}(z_q,\delta)$.

Open Access. This article is distributed under the terms of the Creative Commons Attribution License (CC-BY 4.0), which permits any use, distribution and reproduction in any medium, provided the original author(s) and source are credited.

References

[1] CLEO collaboration, S. Chen et al., *Branching fraction and photon energy spectrum for $b \to s\gamma$*, *Phys. Rev. Lett.* **87** (2001) 251807 [hep-ex/0108032] [INSPIRE].

[2] BELLE collaboration, K. Abe et al., *A Measurement of the branching fraction for the inclusive $B \to X_s\gamma$ decays with BELLE*, *Phys. Lett.* **B 511** (2001) 151 [hep-ex/0103042] [INSPIRE].

[3] BELLE collaboration, A. Limosani et al., *Measurement of Inclusive Radiative B-meson Decays with a Photon Energy Threshold of 1.7-GeV*, *Phys. Rev. Lett.* **103** (2009) 241801 [arXiv:0907.1384] [INSPIRE].

[4] BABAR collaboration, B. Aubert et al., *Measurement of the $B \to X_s\gamma$ branching fraction and photon energy spectrum using the recoil method*, *Phys. Rev.* **D 77** (2008) 051103 [arXiv:0711.4889] [INSPIRE].

[5] BABAR collaboration, J.P. Lees et al., *Exclusive Measurements of $b \to s\gamma$ Transition Rate and Photon Energy Spectrum*, *Phys. Rev.* **D 86** (2012) 052012 [arXiv:1207.2520] [INSPIRE].

[6] BABAR collaboration, J.P. Lees et al., *Measurement of $B(B \to X_s\gamma)$, the $B \to X_s\gamma$ photon energy spectrum and the direct CP asymmetry in $B \to X_{s+d}\gamma$ decays*, *Phys. Rev.* **D 86** (2012) 112008 [arXiv:1207.5772] [INSPIRE].

[7] BABAR collaboration, J.P. Lees et al., *Precision Measurement of the $B \to X_s\gamma$ Photon Energy Spectrum, Branching Fraction and Direct CP Asymmetry $A_{CP}(B \to X_{s+d}\gamma)$*, *Phys. Rev. Lett.* **109** (2012) 191801 [arXiv:1207.2690] [INSPIRE].

JHEP01(2015)115

[8] Heavy Flavor Averaging Group collaboration, Y. Amhis et al., *Averages of b-hadron, c-hadron and τ-lepton properties as of early 2012*, arXiv:1207.1158 [inSPIRE].

[9] Y. Sato, *Inclusive B decays and exclusive radiative decays by Belle*, arXiv:1411.3773 [inSPIRE].

[10] Belle collaboration, T. Saito et al., *Measurement of the $\bar{B} \to X_s\gamma$ Branching Fraction with a Sum of Exclusive Decays*, arXiv:1411.7198 [inSPIRE].

[11] M. Misiak et al., *Estimate of $B(\bar{B} \to X_s\gamma)$ at $O(\alpha_s^2)$*, Phys. Rev. Lett. **98** (2007) 022002 [hep-ph/0609232] [inSPIRE].

[12] K. Adel and Y.-P. Yao, *Exact α_s calculation of $b \to s + \gamma$ $b \to s + g$*, Phys. Rev. **D 49** (1994) 4945 [hep-ph/9308349] [inSPIRE].

[13] C. Greub and T. Hurth, *Two loop matching of the dipole operators for $b \to s\gamma$ and $b \to sg$*, Phys. Rev. **D 56** (1997) 2934 [hep-ph/9703349] [inSPIRE].

[14] A.J. Buras, A. Kwiatkowski and N. Pott, *Next-to-leading order matching for the magnetic photon penguin operator in the $B \to X_s\gamma$ decay*, Nucl. Phys. **B 517** (1998) 353 [hep-ph/9710336] [inSPIRE].

[15] M. Ciuchini, G. Degrassi, P. Gambino and G.F. Giudice, *Next-to-leading QCD corrections to $\bar{B} \to X_s\gamma$: Standard model and two Higgs doublet model*, Nucl. Phys. **B 527** (1998) 21 [hep-ph/9710335] [inSPIRE].

[16] C. Bobeth, M. Misiak and J. Urban, *Matching conditions for $b \to s\gamma$ and $b \to s$ gluon in extensions of the standard model*, Nucl. Phys. **B 567** (2000) 153 [hep-ph/9904413] [inSPIRE].

[17] C. Bobeth, M. Misiak and J. Urban, *Photonic penguins at two loops and m_t dependence of $BR[B \to X_s l^+ l^-]$*, Nucl. Phys. **B 574** (2000) 291 [hep-ph/9910220] [inSPIRE].

[18] P. Gambino and U. Haisch, *Electroweak effects in radiative B decays*, JHEP **09** (2000) 001 [hep-ph/0007259] [inSPIRE].

[19] P. Gambino and U. Haisch, *Complete electroweak matching for radiative B decays*, JHEP **10** (2001) 020 [hep-ph/0109058] [inSPIRE].

[20] M. Misiak and M. Steinhauser, *Three loop matching of the dipole operators for $b \to s\gamma$ and $b \to s\ g$*, Nucl. Phys. **B 683** (2004) 277 [hep-ph/0401041] [inSPIRE].

[21] A.J. Buras, M. Jamin, M.E. Lautenbacher and P.H. Weisz, *Two loop anomalous dimension matrix for $\Delta S = 1$ weak nonleptonic decays. 1. $O(\alpha_S^2)$*, Nucl. Phys. **B 400** (1993) 37 [hep-ph/9211304] [inSPIRE].

[22] M. Ciuchini, E. Franco, G. Martinelli and L. Reina, *The $\Delta S = 1$ effective Hamiltonian including next-to-leading order QCD and QED corrections*, Nucl. Phys. **B 415** (1994) 403 [hep-ph/9304257] [inSPIRE].

[23] M. Misiak and M. Münz, *Two loop mixing of dimension five flavor changing operators*, Phys. Lett. **B 344** (1995) 308 [hep-ph/9409454] [inSPIRE].

[24] K.G. Chetyrkin, M. Misiak and M. Münz, *Weak radiative B meson decay beyond leading logarithms*, Phys. Lett. **B 400** (1997) 206 [*Erratum ibid.* **B 425** (1998) 414] [hep-ph/9612313] [inSPIRE].

[25] K.G. Chetyrkin, M. Misiak and M. Münz, *$|\Delta F| = 1$ nonleptonic effective Hamiltonian in a simpler scheme*, Nucl. Phys. **B 520** (1998) 279 [hep-ph/9711280] [inSPIRE].

[26] K.G. Chetyrkin, M. Misiak and M. Münz, *β-functions and anomalous dimensions up to three loops*, Nucl. Phys. **B 518** (1998) 473 [hep-ph/9711266] [inSPIRE].

JHEP01(2015)115

[27] P. Gambino, M. Gorbahn and U. Haisch, *Anomalous dimension matrix for radiative and rare semileptonic B decays up to three loops*, Nucl. Phys. **B 673** (2003) 238 [hep-ph/0306079] [INSPIRE].

[28] M. Gorbahn and U. Haisch, *Effective Hamiltonian for non-leptonic $|\Delta F| = 1$ decays at NNLO in QCD*, Nucl. Phys. **B 713** (2005) 291 [hep-ph/0411071] [INSPIRE].

[29] M. Gorbahn, U. Haisch and M. Misiak, *Three-loop mixing of dipole operators*, Phys. Rev. Lett. **95** (2005) 102004 [hep-ph/0504194] [INSPIRE].

[30] M. Czakon, U. Haisch and M. Misiak, *Four-Loop Anomalous Dimensions for Radiative Flavour-Changing Decays*, JHEP **03** (2007) 008 [hep-ph/0612329] [INSPIRE].

[31] A. Ali and C. Greub, *Photon energy spectrum in $B \to X_s + \gamma$ and comparison with data*, Phys. Lett. **B 361** (1995) 146 [hep-ph/9506374] [INSPIRE].

[32] N. Pott, *Bremsstrahlung corrections to the decay $b \to s\gamma$*, Phys. Rev. **D 54** (1996) 938 [hep-ph/9512252] [INSPIRE].

[33] C. Greub, T. Hurth and D. Wyler, *Virtual corrections to the decay $b \to s + \gamma$*, Phys. Lett. **B 380** (1996) 385 [hep-ph/9602281] [INSPIRE].

[34] C. Greub, T. Hurth and D. Wyler, *Virtual $O(\alpha_s)$ corrections to the inclusive decay $b \to s\gamma$*, Phys. Rev. **D 54** (1996) 3350 [hep-ph/9603404] [INSPIRE].

[35] Z. Ligeti, M.E. Luke, A.V. Manohar and M.B. Wise, *The $\bar{B} \to X_s\gamma$ photon spectrum*, Phys. Rev. **D 60** (1999) 034019 [hep-ph/9903305] [INSPIRE].

[36] A.J. Buras, A. Czarnecki, M. Misiak and J. Urban, *Two loop matrix element of the current current operator in the decay $B \to X_s\gamma$*, Nucl. Phys. **B 611** (2001) 488 [hep-ph/0105160] [INSPIRE].

[37] A.J. Buras, A. Czarnecki, M. Misiak and J. Urban, *Completing the NLO QCD calculation of $\bar{B} \to X_s\gamma$*, Nucl. Phys. **B 631** (2002) 219 [hep-ph/0203135] [INSPIRE].

[38] K. Bieri, C. Greub and M. Steinhauser, *Fermionic NNLL corrections to $b \to s\gamma$*, Phys. Rev. **D 67** (2003) 114019 [hep-ph/0302051] [INSPIRE].

[39] K. Melnikov and A. Mitov, *The Photon energy spectrum in $\bar{B} \to X_s\gamma$ in perturbative QCD through $O(\alpha_s^2)$*, Phys. Lett. **B 620** (2005) 69 [hep-ph/0505097] [INSPIRE].

[40] I.R. Blokland, A. Czarnecki, M. Misiak, M. Ślusarczyk and F. Tkachov, *The Electromagnetic dipole operator effect on $\bar{B} \to X_s\gamma$ at $O(\alpha_s^2)$*, Phys. Rev. **D 72** (2005) 033014 [hep-ph/0506055] [INSPIRE].

[41] H.M. Asatrian et al., *NNLL QCD contribution of the electromagnetic dipole operator to $\Gamma(\bar{B} \to X_s\gamma)$*, Nucl. Phys. **B 749** (2006) 325 [hep-ph/0605009] [INSPIRE].

[42] H.M. Asatrian, T. Ewerth, A. Ferroglia, P. Gambino and C. Greub, *Magnetic dipole operator contributions to the photon energy spectrum in $\bar{B} \to X_s\gamma$ at $O(\alpha_s^2)$*, Nucl. Phys. **B 762** (2007) 212 [hep-ph/0607316] [INSPIRE].

[43] M. Misiak and M. Steinhauser, *NNLO QCD corrections to the $\bar{B} \to X_s\gamma$ matrix elements using interpolation in m_c*, Nucl. Phys. **B 764** (2007) 62 [hep-ph/0609241] [INSPIRE].

[44] R. Boughezal, M. Czakon and T. Schutzmeier, *NNLO fermionic corrections to the charm quark mass dependent matrix elements in $\bar{B} \to X_s\gamma$*, JHEP **09** (2007) 072 [arXiv:0707.3090] [INSPIRE].

[45] T. Ewerth, *Fermionic corrections to the interference of the electro- and chromomagnetic dipole operators in $\bar{B} \to X_s\gamma$ at $O(\alpha_s^2)$*, Phys. Lett. **B 669** (2008) 167 [arXiv:0805.3911] [INSPIRE].

JHEP01(2015)115

[46] M. Misiak and M. Steinhauser, *Large-m_c Asymptotic Behaviour of $O(\alpha_s^2)$ Corrections to $B \to X_s\gamma$*, *Nucl. Phys.* **B 840** (2010) 271 [arXiv:1005.1173] [INSPIRE].

[47] H.M. Asatrian, T. Ewerth, A. Ferroglia, C. Greub and G. Ossola, *Complete (O_7, O_8) contribution to $B \to X_s\gamma$ at $O(\alpha_s^2)$*, *Phys. Rev.* **D 82** (2010) 074006 [arXiv:1005.5587] [INSPIRE].

[48] A. Ferroglia and U. Haisch, *Chromomagnetic Dipole-Operator Corrections in $\bar{B} \to X_s\gamma$ at $O(\beta_0\alpha_s^2)$*, *Phys. Rev.* **D 82** (2010) 094012 [arXiv:1009.2144] [INSPIRE].

[49] M. Misiak and M. Poradzinski, *Completing the Calculation of BLM corrections to $\bar{-}B \to X_s\gamma$*, *Phys. Rev.* **D 83** (2011) 014024 [arXiv:1009.5685] [INSPIRE].

[50] M. Kaminski, M. Misiak and M. Poradzinski, *Tree-level contributions to $B \to X_s\gamma$*, *Phys. Rev.* **D 86** (2012) 094004 [arXiv:1209.0965] [INSPIRE].

[51] M. Czakon, P. Fiedler, T. Huber, M. Misiak, T. Schutzmeier and M. Steinhauser, *The $(Q_7, Q_{1,2})$ contribution to $\mathcal{B}(\bar{B} \to X_s\gamma)$ at $\mathcal{O}(\alpha_s^2)$*, in preparation.

[52] P. Gambino and M. Misiak, *Quark mass effects in $\bar{B} \to X_s\gamma$*, *Nucl. Phys.* **B 611** (2001) 338 [hep-ph/0104034] [INSPIRE].

[53] M. Benzke, S.J. Lee, M. Neubert and G. Paz, *Factorization at Subleading Power and Irreducible Uncertainties in $\bar{B} \to X_s\gamma$ Decay*, *JHEP* **08** (2010) 099 [arXiv:1003.5012] [INSPIRE].

[54] T. van Ritbergen, *The Second order QCD contribution to the semileptonic $b \to u$ decay rate*, *Phys. Lett.* **B 454** (1999) 353 [hep-ph/9903226] [INSPIRE].

[55] S. Catani and M.H. Seymour, *A General algorithm for calculating jet cross-sections in NLO QCD*, *Nucl. Phys.* **B 485** (1997) 291 [*Erratum ibid.* **B 510** (1998) 503] [hep-ph/9605323] [INSPIRE].

[56] S. Catani, S. Dittmaier and Z. Trócsányi, *One loop singular behavior of QCD and SUSY QCD amplitudes with massive partons*, *Phys. Lett.* **B 500** (2001) 149 [hep-ph/0011222] [INSPIRE].

[57] M. Cacciari and S. Catani, *Soft gluon resummation for the fragmentation of light and heavy quarks at large x*, *Nucl. Phys.* **B 617** (2001) 253 [hep-ph/0107138] [INSPIRE].

[58] M. Cacciari and E. Gardi, *Heavy quark fragmentation*, *Nucl. Phys.* **B 664** (2003) 299 [hep-ph/0301047] [INSPIRE].

[59] A. Gehrmann-De Ridder, T. Gehrmann and G. Heinrich, *Four particle phase space integrals in massless QCD*, *Nucl. Phys.* **B 682** (2004) 265 [hep-ph/0311276] [INSPIRE].

[60] T. Huber, E. Lunghi, M. Misiak and D. Wyler, *Electromagnetic logarithms in $\bar{B} \to X_s\ell^+\ell^-$*, *Nucl. Phys.* **B 740** (2006) 105 [hep-ph/0512066] [INSPIRE].

[61] T. Huber and D. Maître, *HypExp 2, Expanding Hypergeometric Functions about Half-Integer Parameters*, *Comput. Phys. Commun.* **178** (2008) 755 [arXiv:0708.2443] [INSPIRE].

[62] Particle Data Group collaboration, K.A. Olive et al., *Review of Particle Physics*, *Chin. Phys.* **C 38** (2014) 090001 [INSPIRE].

[63] Belle-II collaboration, T. Abe et al., *Belle II Technical Design Report*, arXiv:1011.0352 [INSPIRE].

JHEP01(2015)115

Published for SISSA by Springer

Received: March 11, 2015
Accepted: April 8, 2015
Published: April 29, 2015

The $(Q_7, Q_{1,2})$ contribution to $\bar{B} \to X_s\gamma$ at $\mathcal{O}\left(\alpha_s^2\right)$

Michał Czakon,[a] Paul Fiedler,[a] Tobias Huber,[b] Mikołaj Misiak,[c] Thomas Schutzmeier[d] and Matthias Steinhauser[e]

[a] *Institut für Theoretische Teilchenphysik und Kosmologie, RWTH Aachen University, D-52056 Aachen, Germany*

[b] *Theoretische Physik 1, Naturwissenschaftlich-Technische Fakultät, Universität Siegen, Walter-Flex-Straße 3, D-57068 Siegen, Germany*

[c] *Institute of Theoretical Physics, University of Warsaw, Pasteura 5, PL-02-093 Warsaw, Poland*

[d] *Physics Department, Florida State University, Tallahassee, FL, 32306-4350, U.S.A.*

[e] *Institut für Theoretische Teilchenphysik, Karlsruhe Institute of Technology (KIT), Wolfgang-Gaede Straße 1, D-76128 Karlsruhe, Germany*

E-mail: mczakon@physik.rwth-aachen.de, fiedler@physik.rwth-aachen.de, huber@physik.uni-siegen.de, mikolaj.misiak@fuw.edu.pl, tschutzmeier@gmail.com, matthias.steinhauser@kit.edu

Abstract: Interference between the photonic dipole operator Q_7 and the current-current operators $Q_{1,2}$ gives one of the most important QCD corrections to the $\bar{B} \to X_s\gamma$ decay rate. So far, the $\mathcal{O}\left(\alpha_s^2\right)$ part of this correction has been known in the heavy charm quark limit only ($m_c \gg m_b/2$). Here, we evaluate this part at $m_c = 0$, and use both limits in an updated phenomenological study. Our prediction for the CP- and isospin-averaged branching ratio in the Standard Model reads $\mathcal{B}_{s\gamma}^{\rm SM} = (3.36 \pm 0.23) \times 10^{-4}$ for $E_\gamma > 1.6$ GeV.

Keywords: Rare Decays, B-Physics, Standard Model, Beyond Standard Model

ArXiv ePrint: 1503.01791

Open Access, © The Authors.
Article funded by SCOAP[3].

doi:10.1007/JHEP04(2015)168

Contents

1 Introduction **1**

2 Calculation of $\widetilde{G}_{17}^{(2)}$ and $\widetilde{G}_{27}^{(2)}$ for $m_c = E_0 = 0$ **5**
2.1 The bare calculation 5
2.2 Renormalization 10

3 Impact of the NNLO corrections to $(Q_7, Q_{1,2})$ interferences on the branching ratio **12**

4 Evaluation of $\mathcal{B}_{s\gamma}$ in the SM **16**

5 Conclusions **20**

A Massless master integrals **20**
A.1 Results for the four-particle-cut master integrals 23
A.2 Results for the three-particle-cut master integrals 27

B Relation to ref. [43] **30**

C NLO results of relevance for section 3 **31**

D Input parameters **32**

1 Introduction

The inclusive weak radiative decay $\bar{B} \to X_s\gamma$ is known to provide valuable tests of the Standard Model (SM), as well as constraints on beyond-SM physics. Measurements of its CP- and isospin-averaged branching ratio $\mathcal{B}_{s\gamma}$ at the $\Upsilon(4S)$ experiments, namely CLEO [1], Belle [2, 3] and Babar [4–7], contribute to the following world average[1] [8]

$$\mathcal{B}_{s\gamma}^{\text{exp}} = (3.43 \pm 0.21 \pm 0.07) \times 10^{-4} \tag{1.1}$$

for $E_\gamma > E_0 = 1.6\,\text{GeV}$ in the B-meson rest frame. A significant suppression of the experimental error is expected once Belle II begins collecting data in a few years from now [10, 11].

Let us describe the relation of $\mathcal{B}_{s\gamma}$ to decay rates in an untagged measurement at $\Upsilon(4S)$. One begins with the CP-averaged decay rates

$$\Gamma_0 = \frac{\Gamma(\bar{B}^0 \to X_s\gamma) + \Gamma(B^0 \to X_{\bar{s}}\gamma)}{2}, \qquad \Gamma_\pm = \frac{\Gamma(B^- \to X_s\gamma) + \Gamma(B^+ \to X_{\bar{s}}\gamma)}{2}. \tag{1.2}$$

[1] The new semi-inclusive measurement by Belle [9] which supersedes [2] is not yet taken into account in this average.

JHEP04(2015)168

Their isospin average $\Gamma = (\Gamma_0 + \Gamma_\pm)/2$ and asymmetry $\Delta_{0\pm} = (\Gamma_0 - \Gamma_\pm)/(\Gamma_0 + \Gamma_\pm)$ are related to $\mathcal{B}_{s\gamma}$ as follows

$$\mathcal{B}_{s\gamma} = \tau_{B^0}\Gamma\left(\frac{1 + r_f r_\tau}{1 + r_f} + \Delta_{0\pm}\frac{1 - r_f r_\tau}{1 + r_f}\right). \tag{1.3}$$

Here, $r_\tau = \tau_{B^+}/\tau_{B^0} = 1.076 \pm 0.004$ [8] and $r_f = f^{+-}/f^{00} = 1.059 \pm 0.027$ [8] are the measured lifetime and production rate ratios of the charged and neutral B-mesons at $\Upsilon(4S)$. The term proportional to $\Delta_{0\pm}$ in eq. (1.3) contributes only at a permille level, which follows from the measured value of $\Delta_{0\pm} = -0.01 \pm 0.06$ (for $E_\gamma > 1.9\,\text{GeV}$) [7, 12, 13].

The final state strangeness in eq. (1.2) (-1 for X_s and $+1$ for $X_{\bar{s}}$) as well as the neutral B-meson flavours have been specified upon ignoring effects of the $B^0\bar{B}^0$ and $K^0\bar{K}^0$ mixing. Taking the $K^0\bar{K}^0$ mixing into account amounts to replacing X_s and $X_{\bar{s}}$ by $X_{|s|}$ with an unspecified strangeness sign, which leaves Γ_0 and $\Gamma_\pm$ invariant. Next, taking the $B^0\bar{B}^0$ mixing into account amounts to using in Γ_0 the time-integrated decay rates of mesons whose flavour is fixed at the production time. Such a change leaves Γ_0 practically unaffected because mass eigenstates in the $B^0\bar{B}^0$ system are very close to being orthogonal ($|p/q| = 1$) and having the same decay width [13]. In the following, we shall thus ignore the neutral meson mixing effects.

Theoretical calculations of the $\bar{B} \to X_s\gamma$ decay rate are based on the equality

$$\Gamma(\bar{B} \to X_s\gamma)_{E_\gamma > E_0} = \Gamma(b \to X_s^p\gamma)_{E_\gamma > E_0} + \delta\Gamma_{\text{nonp}}, \tag{1.4}$$

where the first term on the r.h.s. stands for the perturbatively calculable inclusive decay rate of the b quark into charmless partons $X_s^p = s, sg, sgg, sq\bar{q}, \ldots$ and the photon. For appropriately chosen E_0, the second term $\delta\Gamma_{\text{nonp}}$ becomes small, and is called a non-perturbative correction. For $E_0 = 1.6\,\text{GeV}$, the uncertainty due to poor knowledge of $\delta\Gamma_{\text{nonp}}$ has been estimated to remain below 5% of the decay rate [14]. The non-perturbative correction is partly correlated with the isospin asymmetry because $\delta\Gamma_{\text{nonp}}$ depends on whether $\bar{B} = \bar{B}^0$ or $\bar{B} = B^-$ [14].

As far as the perturbative contribution $\Gamma(b \to X_s^p\gamma)$ is concerned, its determination with an accuracy significantly better than 5% is what the ongoing calculations aim at. For this purpose, order $\mathcal{O}(\alpha_s^2)$ corrections need to be evaluated. Moreover, resummation of logarithmically enhanced terms like $\left(\alpha_s \ln(M_W^2/m_b^2)\right)^n$ is necessary at each order of the usual α_s-expansion.[2] Such a resummation is most conveniently performed in the framework of an effective theory that arises after decoupling of the electroweak-scale degrees of freedom. In the SM, which we restrict to in the present paper, one decouples the top quark, the Higgs boson and the gauge bosons $W^\pm$ and Z^0. Barring higher-order electroweak corrections, all the relevant interactions are then described by the following effective Lagrangian:

$$\mathcal{L}_{\text{eff}} = \mathcal{L}_{\text{QCD}\times\text{QED}}(u,d,s,c,b) + \frac{4G_F}{\sqrt{2}}\left[V_{ts}^* V_{tb}\sum_{i=1}^{8} C_i(\mu)Q_i + V_{us}^* V_{ub}\sum_{i=1}^{2} C_i(\mu)(Q_i - Q_i^u)\right], \tag{1.5}$$

[2] After the resummation, subsequent $\mathcal{O}(1)$, $\mathcal{O}(\alpha_s)$ and $\mathcal{O}(\alpha_s^2)$ terms in this expansion are called Leading Order (LO), Next-to-Leading Order (NLO) and Next-to-Next-to-Leading Order (NNLO).

JHEP04(2015)168

where G_F is the Fermi constant, and V_{ij} are the Cabibbo-Kobayashi-Maskawa (CKM) matrix elements. The operators $Q_i^{(u)}$ are given by

$$\begin{aligned}
Q_1^u &= (\bar{s}_L\gamma_\mu T^a u_L)(\bar{u}_L\gamma^\mu T^a b_L),\\
Q_2^u &= (\bar{s}_L\gamma_\mu u_L)(\bar{u}_L\gamma^\mu b_L),\\
Q_1 &= (\bar{s}_L\gamma_\mu T^a c_L)(\bar{c}_L\gamma^\mu T^a b_L),\\
Q_2 &= (\bar{s}_L\gamma_\mu c_L)(\bar{c}_L\gamma^\mu b_L),\\
Q_3 &= (\bar{s}_L\gamma_\mu b_L)\sum_q(\bar{q}\gamma^\mu q),\\
Q_4 &= (\bar{s}_L\gamma_\mu T^a b_L)\sum_q(\bar{q}\gamma^\mu T^a q),\\
Q_5 &= (\bar{s}_L\gamma_{\mu_1}\gamma_{\mu_2}\gamma_{\mu_3} b_L)\sum_q(\bar{q}\gamma^{\mu_1}\gamma^{\mu_2}\gamma^{\mu_3} q),\\
Q_6 &= (\bar{s}_L\gamma_{\mu_1}\gamma_{\mu_2}\gamma_{\mu_3} T^a b_L)\sum_q(\bar{q}\gamma^{\mu_1}\gamma^{\mu_2}\gamma^{\mu_3} T^a q),\\
Q_7 &= \frac{e}{16\pi^2} m_b(\bar{s}_L\sigma^{\mu\nu} b_R)F_{\mu\nu},\\
Q_8 &= \frac{g}{16\pi^2} m_b(\bar{s}_L\sigma^{\mu\nu} T^a b_R)G^a_{\mu\nu},
\end{aligned} \tag{1.6}$$

where the sums in $Q_{3,\ldots,6}$ go over all the active flavours $q = u, d, s, c, b$ in the effective theory.

Decoupling (matching) calculations give us values of the electroweak-scale Wilson coefficients $C_i(\mu_0)$, where $\mu_0 \sim (M_W, m_t)$. Next, renormalization group equations are used to evolve them down to the low-energy scale, i.e. to find $C_i(\mu_b)$, where $\mu_b \sim m_b/2$ is of order of the final hadronic state energy in the $\bar{B}$-meson rest frame. Determination of the Wilson coefficients $C_{1,\ldots,8}(\mu_b)$ up to $\mathcal{O}(\alpha_s^2)$ in the SM was completed in 2006 [15–19]. Matching calculations up to three loops [16] and anomalous dimension matrices up to four loops [19] were necessary for this purpose. The three-loop matching calculation has recently been extended to the Two-Higgs-Doublet-Model case [20]. Most of the final results have been presented for the so-called effective coefficients

$$C_i^{\rm eff}(\mu) = \begin{cases} C_i(\mu), & \text{for } i = 1,\ldots,6,\\ C_7(\mu) + \sum_{j=1}^6 y_j C_j(\mu), & \text{for } i = 7,\\ C_8(\mu) + \sum_{j=1}^6 z_j C_j(\mu), & \text{for } i = 8, \end{cases} \tag{1.7}$$

where the numbers y_j and z_j are such that the LO decay amplitudes for $b \to s\gamma$ and $b \to sg$ are proportional to the LO terms in $C_7^{\rm eff}(\mu_b)$ and $C_8^{\rm eff}(\mu_b)$, respectively [21]. In the $\overline{\rm MS}$ scheme with fully anticommuting γ_5, one finds $\vec{y} = (0, 0, -\frac{1}{3}, -\frac{4}{9}, -\frac{20}{3}, -\frac{80}{9})$ and $\vec{z} = (0, 0, 1, -\frac{1}{6}, 20, -\frac{10}{3})$ [22].

JHEP04(2015)168

Once the Wilson coefficients $C_i^{\rm eff}(\mu_b)$ have been found up to the NNLO, one proceeds to evaluating all the on-shell decay amplitudes that matter at this order for[3]

$$\Gamma(b\to X_s^p\gamma)_{E_\gamma>E_0} = \frac{G_F^2\alpha_{em}m_{b,\rm pole}^5}{32\pi^4}\,|V_{ts}^*V_{tb}|^2\sum_{i,j=1}^{8} C_i^{\rm eff}(\mu_b)\;C_j^{\rm eff}(\mu_b)\times$$
$$\times\left[\widetilde{G}_{ij}^{(0)}(E_0)+\frac{\alpha_{\rm s}}{4\pi}\,\widetilde{G}_{ij}^{(1)}(E_0,\mu_b)+\left(\frac{\alpha_{\rm s}}{4\pi}\right)^2\widetilde{G}_{ij}^{(2)}(E_0,\mu_b)+\mathcal{O}(\alpha_{\rm s}^3)\right]+\ldots\,, \qquad (1.8)$$

where ellipses stand for higher-order electroweak corrections. At the LO, the symmetric matrix $\widetilde{G}_{ij}^{(0)}$ takes the form

$$\widetilde{G}_{ij}^{(0)}(E_0)=\delta_{i7}\delta_{j7}+T_{ij}^{(0)}, \qquad (1.9)$$

where $T_{ij}^{(0)}$ describe small tree-level contributions to $b\to sq\bar{q}\gamma$ from $Q_{1,2}^u$ and $Q_{3,\ldots,6}$ [23, 24]. At the NLO and NNLO, numerically dominant effects come from $\widetilde{G}_{77}^{(n)}$, $\widetilde{G}_{17}^{(n)}$ and $\widetilde{G}_{27}^{(n)}$. While $\widetilde{G}_{77}^{(2)}$ is known in a complete manner [25–29], calculations of $\widetilde{G}_{17}^{(2)}$ and $\widetilde{G}_{27}^{(2)}$ are still in progress. Contributions from massless and massive fermion loops on the gluon lines have been found in refs. [30–32], and served as a basis for applying the Brodsky-Lepage-Mackenzie (BLM) approximation [33]. The remaining (non-BLM) parts of $\widetilde{G}_{(1,2)7}^{(2)}$ have been known so far in the heavy charm quark limit only ($m_c\gg m_b/2$) [34, 35].

In the present work, we evaluate the full $\widetilde{G}_{(1,2)7}^{(2)}$ for $m_c=E_0=0$. It is achieved by calculating imaginary parts of several hundreds four-loop propagator-type diagrams with massive internal lines. Next, both limits are used to interpolate in m_c those parts of the non-BLM contributions to $\widetilde{G}_{(1,2)7}^{(2)}$ whose exact m_c-dependence is not yet known. It will give us an estimate of their values at the measured value of m_c, and for non-vanishing E_0.

Our current approach differs in several aspects from the one in ref. [34] where interpolation in m_c was applied to a combined non-BLM effect from all the $\widetilde{G}_{ij}^{(2)}$ with $i,j\in\{1,2,7,8\}$.[4] In the present paper, the only interpolated quantities are the above-mentioned parts of $\widetilde{G}_{(1,2)7}^{(2)}$. Exact m_c-dependence of most of the other important non-BLM contributions to $\widetilde{G}_{ij}^{(2)}$ is now available thanks to calculations performed in refs. [29, 32, 36]. Last but not least, the current analysis includes the previously unknown m_c-independent part of $\widetilde{G}_{78}^{(2)}$ [37], all the relevant BLM corrections to $\widetilde{G}_{ij}^{(2)}$ with $i,j\neq 7$ [31, 38, 39], tree-level contributions $T_{ij}^{(0)}$ [23, 24], four-body NLO corrections [24], as well as the updated non-perturbative corrections [14, 40, 41]. The only contributions to $\widetilde{G}_{ij}^{(2)}$ with $i,j\in\{1,2,7,8\}$ that remain neglected are the unknown ($n\geq 3$)-body final state contributions to the non-BLM parts of $\widetilde{G}_{ij}^{(2)}$ with $i,j\neq 7$.

The article is organized as follows. In section 2, we describe the calculation of $\widetilde{G}_{(1,2)7}^{(2)}$ for $m_c=E_0=0$. A new phenomenological analysis begins in section 3 where m_c-dependence of the considered correction is discussed, and the corresponding uncertainty is estimated.

[3] Following the notation of ref. [25], we use tilde over G in the r.h.s. of eq. (1.8) to indicate the overall normalization to $m_{b,\rm pole}^5$.

[4] At the NNLO level, we neglect the small Wilson coefficients $C_3,\ldots,C_6$, and the CKM-suppressed effects from $Q_{1,2}^u$.

JHEP04(2015)168

In section 4, we evaluate our current prediction for $\mathcal{B}_{s\gamma}$ in the SM, which constitutes an update of the one given in ref. [42]. We conclude in section 5. Appendix A contains results for all the massless master integrals that were necessary for the calculation in section 2. Several relations to quantities encountered in ref. [43] are presented in appendix B. In appendix C, we collect some of the relevant NLO quantities. Appendix D contains a list of input parameters for our numerical analysis together with a correlation matrix for a subset of them.

2 Calculation of $\widetilde{G}_{17}^{(2)}$ and $\widetilde{G}_{27}^{(2)}$ for $m_c = E_0 = 0$

2.1 The bare calculation

Typical diagrams that had to be evaluated for the present project are shown in figure 1. They represent a subset of possible unitarity cut contributions to the b-quark self-energy due to the interference of various effective operators. At the highest loop level, i.e. four-loops, this interference involves the operators $Q_{1,2}$ and Q_7. We need to consider two-, three- and four-particle cuts. Possible five-particle cuts would necessarily involve real $c\bar{c}$ pairs originating from the $Q_{1,2}$ operator vertices, while open charm production is not included in $\bar{B} \to X_s\gamma$ by definition. For this reason, we skip the diagrams with five-particle cuts together with all the diagrams with real $c\bar{c}$ production or virtual charm loops on the gluon lines. In section 3, contributions from virtual charm loops on the gluon lines will be taken over from the $m_c \neq 0$ calculation of ref. [32], and added to the final result.

For efficiency reasons, we work directly with cut diagrams and employ the technique first proposed in [44]. The idea of the method is to represent cut propagators as

$$-2\pi i\delta(p^2 - m^2) = \frac{1}{p^2 - m^2 + i\varepsilon} - \frac{1}{p^2 - m^2 - i\varepsilon} \,. \tag{2.1}$$

As long as we perform only algebraic transformations on the integrands, there is no difference between the first and second terms on the r.h.s. of the above equation, and it is sufficient to work with one of them only. This is particularly convenient for the integration-by-parts (IBP) method for reduction of integrals [45]. The only difference in such an approach between complete integrals and cut integrals is that a given integral vanishes if the cut propagator disappears due to cancellation of numerators with denominators. This fact reduces the number of occurring integrals in comparison to a computation without cuts.

In practice, the calculation follows the standard procedure. Diagrams are generated with `DiaGen` [46], the Dirac algebra is performed with `FORM` [47], and the resulting scalar integrals are reduced using IBP identities with `IdSolver` [46]. The main challenge of this calculation begins after these steps. The amplitudes for the interference contributions are expressed in terms of a number of master integrals, most of them containing massive internal b-quark lines and a non-trivial phase space integration in $D = 4 - 2\epsilon$ spacetime dimensions, with up to four particles in the final state. A feeling for the size of the problem can be gained from table 1.

Having a large number of massive cut integrals, it is advantageous to devise a strategy to treat them in a uniform manner. It is clear that purely massless cut integrals are easier to

JHEP04(2015)168

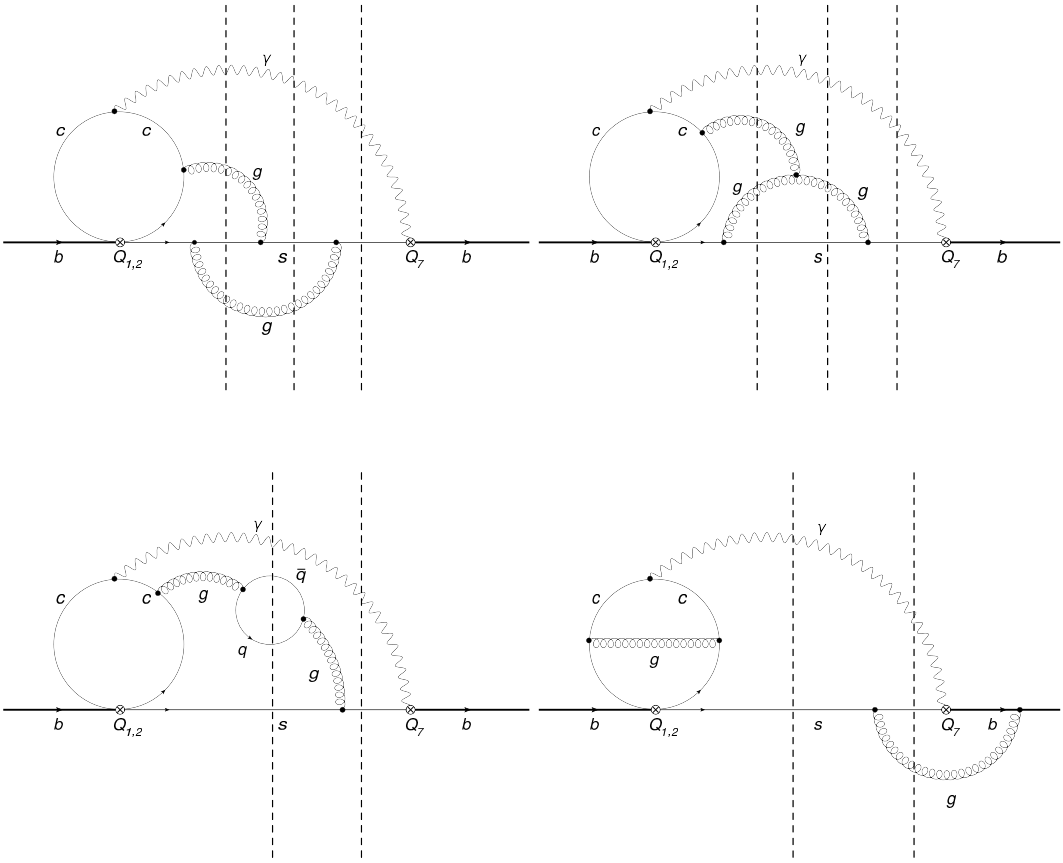

Figure 1. Sample diagrams for $\widetilde{G}^{(2)}_{(1,2)7}$ with some of the possible cuts indicated by the dashed lines.

	n_D	n_{OS}	n_{eff}	n_{massless}
two-particle cuts	292	92	143	9
three-particle cuts	267	54	110	11
four-particle cuts	292	17	37	7
total	851	163	290	27

Table 1. Number of diagrams n_D, number of massive on-shell master integrals n_{OS}, number of effectively computed massive master integrals n_{eff}, and number of massless master integrals n_{massless}. The last two columns are explained in the text.

calculate than massive ones. Therefore, we aim at replacing a calculation of massive propagator integrals by a calculation of massless ones. This can be achieved by extending the integral definitions. We assume, namely, that the external momentum squared p_b^2 is a free parameter, and treat coefficients $\mathcal{I}_i$ in the ϵ-expansion of the master integrals as functions of a single dimensionless variable $x = p_b^2/m_b^2$. IBP identities give us differential equations

$$\frac{d}{dx}\mathcal{I}_i(x) = \sum_j \mathcal{J}_{ij}(x)\mathcal{I}_j(x) \ , \tag{2.2}$$

JHEP04(2015)168

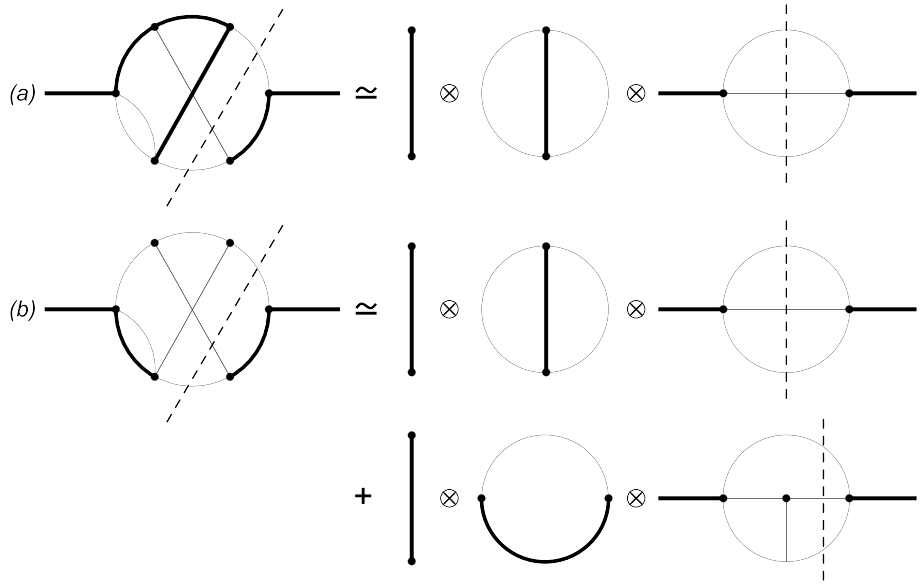

Figure 2. Diagrammatic representation of the asymptotic large mass expansion of two non-planar master integrals.Thick and thin lines represent massive and massless propagators, respectively, while dashed lines show the unitarity cuts.

with $\mathcal{J}_{ij}(x)$ being certain rational functions of x. Boundary conditions for these equations in the vicinity of $x = 0$ are given by asymptotic large-mass expansions, i.e. by power-log series in x. A few leading terms in the series for each $\mathcal{I}_i$ can be found by calculating products of massive tadpole integrals up to three loops and massless propagator ones up to four loops, as illustrated in figure 2. Next, higher-order terms can be determined from the differential equations themselves by substituting $\mathcal{I}_i$ in terms of power-log series in x. For our application it turns out that around 50 terms are sufficient to obtain the desired accuracy. This gives us high-precision boundary conditions at small but non-vanishing x for solving the differential equations (2.2) numerically.

On the way from the vicinity of $x = 0$ to the physical point at $x = 1$, one often encounters spurious singularities on the real axis. To bypass them, the differential equations are solved along ellipses in the complex x plane. Several such ellipses are usually considered to test whether the numerical solution is stable.

Naively, one might think that as long as there are no infinities at $x = 1$, the numerical solution could be continued up to that point. However, there is an essential singularity there, and the integrals behave as $(1-x)^n \ln^m(1-x)$, with $n, m > 0$ being some positive powers. Due to such a behaviour, the numerical solution has poor convergence, as the algorithms assume locally polynomial behaviour of the considered functions. In order to overcome this problem, we perform another power-log expansion around $x = 1$, and match it onto the numerical result. To determine the maximal power of the logarithms, we begin with observing that the highest poles in the cut diagrams could potentially be of order $1/\epsilon^6$, due to the presence of collinear and soft divergences. The coefficient of the leading singularity contains no $\ln(1-x)$ because logarithms are generated by expanding expressions

JHEP04(2015)168

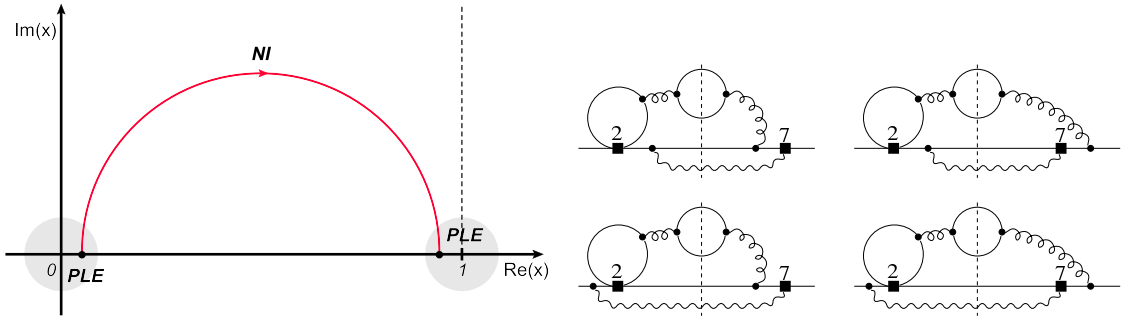

Figure 3. Left (a): integration contour in the complex x plane. The numerical integration (NI) is performed between the regions close to $x = 0$ and $x = 1$ that are accessible by power-log expansions (PLE). Right (b): diagrams that give the terms marked with κ in eq. (2.3).

of the form $(1-x)^{a\epsilon}/\epsilon^6$ (with a being some constant) in the framework of expansion by regions. Thus, finite parts of the master integral expansions may only contain $\ln^6(1-x)$. Higher powers may be needed due to the presence of spurious singularities, i.e. poles in the coefficients at the master integrals in the physical amplitude. In practice, we have used an ansatz with logarithm powers up to fifteen. Our numerical matching has shown that such high powers never occur in the considered problem, i.e. the respective expansion coefficients are consistent with zero to very high numerical precision. Using the matched series, we finally obtain the required values of the original master integrals at $x = 1$. The solution procedure is schematically represented in figure 3a.

Since the master integrals are considered for $x \neq 1$, their overall number n_{eff} is larger than it would be for $x = 1$, i.e. $n_{\text{eff}} > n_{OS}$. However, the massless integrals that are necessary to determine the boundary conditions near $x = 0$ are not only simpler, but also their number n_{massless} is much smaller than n_{OS}, as seen in table 1. All the massless integrals that we had to consider are depicted in appendix A, in figure 7 and table 3.

Using the above method, we have obtained the following bare NNLO results for the considered interferences in the Feynman-'t Hooft gauge:

$$
\begin{aligned}
\widetilde{G}_{17}^{(2)\text{bare}} &= -\frac{1}{6}\widetilde{G}_{27}^{(2)\text{bare}} + \frac{80}{81\,\epsilon^2} + \frac{1592+54\pi^2}{243\,\epsilon} + 42.0026519628, \\
\widetilde{G}_{27}^{(2)\text{bare}} &= -\frac{4}{3\,\epsilon^3} - \frac{30332+432\pi^2}{2187\,\epsilon^2} - \frac{67.66077706444119}{\epsilon} + 44.5070537274 \\
&\quad +\kappa\, n_l \left(\frac{32}{729\,\epsilon} + 0.6520676315\right) + n_l \left(\frac{352}{729\,\epsilon^2} + \frac{11624}{2187\,\epsilon} + \frac{228656}{6561} - \frac{188}{243}\pi^2\right) \\
&\quad +n_b \left(\frac{352}{729\,\epsilon^2} + \frac{5.17409838118169}{\epsilon} + 15.1790288135\right) + \mathcal{O}(\epsilon).
\end{aligned}
\tag{2.3}
$$

Here, n_l and n_b denote numbers of massless and massive ($m = m_b$) quark flavours, while $\kappa = 1$ marks contributions from the diagrams in figure 3b describing interferences involving four-body $sq\bar{q}\gamma$ final states and no $c\bar{c}\gamma$ couplings. The terms proportional to n_l and n_b but not marked by κ reproduce (after renormalization) the $m_c \to 0$ limits of what is already

JHEP04(2015)168

known for non-zero m_c [30–32]. For compactness, all the results in this subsection are given for $\mu^2 = e^\gamma m_b^2/(4\pi)$, where γ is the Euler-Mascheroni constant.

Some of the numbers in eq. (2.3) have been given in an exact form even though our calculation of the master integrals at $x = 1$ is purely numerical. However, the accuracy is very high (to around 14 decimals), so identification of simple rationals is possible. Moreover, renormalization gives us relations to lower-order results where more terms are known in an exact manner (see below). For the n_l-term, after verifying numerical agreement with refs. [30, 39], we have made use of the available exact expressions.[5] Several other numbers in this subsection that have been retained in a decimal form can actually be related to quantities encountered in ref. [43], as described in appendix B.

Let us now list all the lower-order bare contributions that are needed for renormalization. For this purpose, it is convenient to express eq. (1.8) in terms of C_i rather than $C_i^{\rm eff}$, and denote the corresponding interference terms by $\hat{G}_{ij}^{(n)}$ rather than $\widetilde{G}_{ij}^{(n)}$. All the necessary $\hat{G}_{i7}^{(0)}$ and $\hat{G}_{i7}^{(1)\rm bare}$ read[6]

$$
\begin{aligned}
\hat{G}_{77}^{(0)} &= \frac{\Gamma(2-\epsilon)\, e^{\gamma\epsilon}}{\Gamma(2-2\epsilon)}, \\
\hat{G}_{47}^{(0)} &= \frac{4}{3}\hat{G}_{37}^{(0)} \;=\; -\frac{4}{9}\,\Gamma(1+\epsilon)\, e^{\gamma\epsilon}\, \hat{G}_{77}^{(0)}, \\
\hat{G}_{67}^{(0)} &= \frac{4}{3}\hat{G}_{57}^{(0)} \;=\; 4\left(5-3\,\epsilon-\epsilon^2\right)\, \hat{G}_{47}^{(0)}, \\
\hat{G}_{27}^{(1)\rm bare} &= -6\,\hat{G}_{17}^{(1)\rm bare} \;=\; -\frac{92}{81\,\epsilon} - \frac{1978}{243} + \frac{777\pi^2-27185}{729}\,\epsilon + \mathcal{O}(\epsilon^2), \\
\hat{G}_{47}^{(1)\rm bare} &= \frac{16}{3\,\epsilon^2} + \frac{3674}{243\,\epsilon} + 43.76456245573869 + 94.9884724116\,\epsilon \\
&\quad +\kappa\, n_l\left(-\frac{16}{243} + \frac{44\pi^2-612}{243}\,\epsilon\right) + n_l\left(\frac{16}{81\,\epsilon} - \frac{4}{243} + \frac{264\pi^2-2186}{729}\,\epsilon\right) \\
&\quad +n_b\left(\frac{16}{81\,\epsilon} + 0.04680853247986 + 0.3194493123\,\epsilon\right) + \mathcal{O}(\epsilon^2), \\
\hat{G}_{77}^{(1)\rm bare} &= \frac{4}{3\,\epsilon} + \frac{124}{9} - \frac{16}{9}\pi^2 + \left(\frac{212}{3} - \frac{58}{9}\pi^2 - \frac{64}{3}\zeta_3\right)\epsilon + \mathcal{O}(\epsilon^2), \\
\hat{G}_{78}^{(1)\rm bare} &= \frac{16}{9\,\epsilon} + \frac{280}{27} - \frac{16}{27}\pi^2 + \left(\frac{382}{9} - \frac{16}{9}\pi^2 - \frac{160}{9}\zeta_3\right)\epsilon + \mathcal{O}(\epsilon^2), \\
\hat{G}_{7(12)}^{(1)\rm bare} &= -6\,\hat{G}_{7(11)}^{(1)\rm bare} \;=\; \frac{2096}{81} + \frac{39832}{243}\,\epsilon + \mathcal{O}(\epsilon^2).
\end{aligned}
\tag{2.4}
$$

The last line of the above equation describes contributions from the so-called evanescent operators that vanish in four spacetime dimensions

$$
Q_{11} = (\bar{s}_L\gamma_{\mu_1}\gamma_{\mu_2}\gamma_{\mu_3}T^a c_L)(\bar{c}_L\gamma^{\mu_1}\gamma^{\mu_2}\gamma^{\mu_3}T^a b_L) - 16Q_1,
$$

[5] In particular, for the function given in eq. (13) of ref. [39], we have $\lim_{m_c\to 0} h_{27}^{(2)}(\delta=1) = \frac{41}{27} - \frac{2}{9}\pi^2$.

[6] $\hat{G}_{i7}$ differ from $\widetilde{G}_{i7}$ only for $i = 3, 4, 5, 6$.

JHEP04(2015)168

$$Q_{12} = (\bar{s}_L\gamma_{\mu_1}\gamma_{\mu_2}\gamma_{\mu_3}c_L)(\bar{c}_L\gamma^{\mu_1}\gamma^{\mu_2}\gamma^{\mu_3}b_L) - 16Q_2. \tag{2.5}$$

In $\hat{G}^{(1)\text{bare}}_{(1,2)7}$, the three-particle-cut contributions alone ($b \to s\gamma g$) read

$$\hat{G}^{(1)3P}_{27} = -6\,\hat{G}^{(1)3P}_{17} = -\frac{4}{27} - \frac{106}{81}\,\epsilon + \mathcal{O}(\epsilon^2). \tag{2.6}$$

In addition, several interferences need to be calculated with the b-quark propagators squared, to account for the renormalization of m_b. We find

$$\begin{aligned}
\hat{G}^{(1)m}_{27} &= -6\,\hat{G}^{(1)m}_{17} = -\frac{1}{3\,\epsilon^2} - \frac{21+4\pi^2}{81\,\epsilon} + \frac{1085}{81} - \frac{161}{972}\pi^2 - \frac{40}{27}\zeta_3 \\
&\quad + \left(\frac{59071}{486} - \frac{1645}{2916}\pi^2 - \frac{65}{81}\zeta_3 - \frac{7}{81}\pi^4\right)\epsilon + \mathcal{O}(\epsilon^2), \\
\hat{G}^{(0)m}_{47} &= \frac{4}{3\epsilon} + 2 + \frac{50-2\pi^2}{9}\,\epsilon + \frac{94-3\pi^2-32\zeta_3}{9}\,\epsilon^2 + \mathcal{O}(\epsilon^3).
\end{aligned} \tag{2.7}$$

Our conventions for their global normalization will become clear through the way they enter the renormalized NNLO expression in eq. (2.10) below.

Some of the diagrams with Q_4 insertions contain b-quark tadpoles that are the only source of $1/\epsilon^2$ terms in $\hat{G}^{(1)\text{bare}}_{47}$, and $1/\epsilon$ terms in $\hat{G}^{(0)m}_{47}$. Such divergences are actually necessary to renormalize the $1/\epsilon^3$ poles in eq. (2.3). These tadpole diagrams have been skipped in the NLO calculation of ref. [43] because they give no contribution to the renormalized $\hat{G}^{(1)}_{47}$, i.e. they cancel out after renormalization of m_b.

Among all the bare interferences given in this section, not only the NNLO ones are entirely new, but also $\hat{G}^{(1)\text{bare}}_{7(12)}$, $\hat{G}^{(1)m}_{27}$ and $\hat{G}^{(0)m}_{47}$. The remaining LO and NLO results are extensions of the known ones by another power of ϵ, as necessary for the current calculation.[7]

2.2 Renormalization

Our results in the previous subsection contain no loop corrections on external legs in the interfered amplitudes. Such corrections are taken into account below, with the help of on-shell renormalization constants for the b-quark, s-quark and gluon fields

$$\begin{aligned}
Z_b^{\text{OS}} &= 1 - \frac{4}{3}\,\widetilde{\alpha}_{\text{s}}\,s^{\epsilon}\,e^{\gamma\epsilon}\,\Gamma(\epsilon)\,\frac{3-2\epsilon}{1-2\epsilon} + \mathcal{O}(\widetilde{\alpha}_{\text{s}}^2), \\
Z_s^{\text{OS}} &= 1 + \mathcal{O}(\widetilde{\alpha}_{\text{s}}^2), \\
Z_G^{\text{OS}} &= 1 - \frac{2}{3}\,n_b\,\widetilde{\alpha}_{\text{s}}\,s^{\epsilon}\,e^{\gamma\epsilon}\,\Gamma(\epsilon) + \mathcal{O}(\widetilde{\alpha}_{\text{s}}^2),
\end{aligned} \tag{2.8}$$

where $\widetilde{\alpha}_{\text{s}} = \frac{\alpha_{\text{s}}}{4\pi} = \frac{g_s^2}{16\pi^2}$ and $s = \frac{4\pi\mu^2}{m_b^2}e^{-\gamma}$. The QCD coupling g_s and the Wilson coefficients C_i are renormalized in the $\overline{\text{MS}}$ scheme: $g_s^{\text{bare}} = \bar{Z}_g g_s$, and $C_i^{\text{bare}} = \sum_j C_j \bar{Z}_{ji}$. The corresponding MS renormalization constants can be taken over from the literature (see, e.g.,

[7] Exceptions are $\hat{G}^{(0)\text{bare}}_{77}$ $\hat{G}^{(1)\text{bare}}_{77}$ and $\hat{G}^{(1)\text{bare}}_{78}$, for which sufficiently many terms in the ϵ expansions have been already found in refs. [25, 27, 37]. Our results agree with theirs, barring different conventions for the global $1+\mathcal{O}(\epsilon)$ normalization factor (see the end of subsection 2.2).

JHEP04(2015)168

refs. [17, 19])

$$
\begin{aligned}
Z_g &= 1 + \tfrac{\widetilde{\alpha}_s}{\epsilon}\left(-\tfrac{11}{2} + \tfrac{f}{3}\right) + \mathcal{O}(\widetilde{\alpha}_s^2), & Z_{77} &= 1 + \tfrac{16\,\widetilde{\alpha}_s}{3\,\epsilon} + \mathcal{O}(\widetilde{\alpha}_s^2),\\
Z_{11} &= 1 - \tfrac{2\,\widetilde{\alpha}_s}{\epsilon} + \mathcal{O}(\widetilde{\alpha}_s^2), & Z_{21} &= \tfrac{6\,\widetilde{\alpha}_s}{\epsilon} + \mathcal{O}(\widetilde{\alpha}_s^2),\\
Z_{12} &= \tfrac{4\,\widetilde{\alpha}_s}{3\,\epsilon} + \mathcal{O}(\widetilde{\alpha}_s^2), & Z_{22} &= 1 + \mathcal{O}(\widetilde{\alpha}_s^2),\\
Z_{13} &= \widetilde{\alpha}_s^2\left(\tfrac{10}{81\,\epsilon^2} - \tfrac{353}{243\,\epsilon}\right) + \mathcal{O}(\widetilde{\alpha}_s^3), & Z_{23} &= \widetilde{\alpha}_s^2\left(-\tfrac{20}{27\,\epsilon^2} - \tfrac{104}{81\,\epsilon}\right) + \mathcal{O}(\widetilde{\alpha}_s^3),\\
Z_{14} &= -\tfrac{1}{6}Z_{24} + \widetilde{\alpha}_s^2\left(\tfrac{1}{2\epsilon^2} - \tfrac{11}{12\,\epsilon}\right), & Z_{24} &= \tfrac{2\,\widetilde{\alpha}_s}{3\,\epsilon} + \widetilde{\alpha}_s^2\left(\tfrac{-188+12f}{27\,\epsilon^2} + \tfrac{338}{81\,\epsilon}\right) + \mathcal{O}(\widetilde{\alpha}_s^3),\\
Z_{15} &= \widetilde{\alpha}_s^2\left(-\tfrac{1}{81\,\epsilon^2} + \tfrac{67}{486\,\epsilon}\right) + \mathcal{O}(\widetilde{\alpha}_s^3), & Z_{25} &= \widetilde{\alpha}_s^2\left(\tfrac{2}{27\,\epsilon^2} + \tfrac{14}{81\,\epsilon}\right) + \mathcal{O}(\widetilde{\alpha}_s^3),\\
Z_{16} &= \widetilde{\alpha}_s^2\left(-\tfrac{5}{216\,\epsilon^2} - \tfrac{35}{648\,\epsilon}\right) + \mathcal{O}(\widetilde{\alpha}_s^3), & Z_{26} &= \widetilde{\alpha}_s^2\left(\tfrac{5}{36\,\epsilon^2} + \tfrac{35}{108\,\epsilon}\right) + \mathcal{O}(\widetilde{\alpha}_s^3),\\
Z_{17} &= -\tfrac{1}{6}Z_{27} + \widetilde{\alpha}_s^2\left(\tfrac{22}{81\,\epsilon^2} - \tfrac{332}{243\,\epsilon}\right), & Z_{27} &= \tfrac{116\,\widetilde{\alpha}_s}{81\,\epsilon} + \widetilde{\alpha}_s^2\left(\tfrac{-3556+744f}{2187\,\epsilon^2} + \tfrac{13610-44f}{2187\,\epsilon}\right) + \mathcal{O}(\widetilde{\alpha}_s^3),\\
Z_{18} &= \tfrac{167\,\widetilde{\alpha}_s}{648\,\epsilon} + \mathcal{O}(\widetilde{\alpha}_s^2), & Z_{28} &= \tfrac{19\,\widetilde{\alpha}_s}{27\,\epsilon} + \mathcal{O}(\widetilde{\alpha}_s^2),\\
Z_{1(11)} &= \tfrac{5\,\widetilde{\alpha}_s}{12\,\epsilon} + \mathcal{O}(\widetilde{\alpha}_s^2), & Z_{2(11)} &= \tfrac{\widetilde{\alpha}_s}{\epsilon} + \mathcal{O}(\widetilde{\alpha}_s^2),\\
Z_{1(12)} &= \tfrac{2\,\widetilde{\alpha}_s}{9\,\epsilon} + \mathcal{O}(\widetilde{\alpha}_s^2), & Z_{2(12)} &= \mathcal{O}(\widetilde{\alpha}_s^2),
\end{aligned}
\tag{2.9}
$$

where $f = n_l + n_b$ here, as we have skipped all the charm loops on the gluon lines. For the b-quark mass renormalization, we use the on-shell scheme everywhere ($Z_m^{\rm OS} = Z_b^{\rm OS} + \mathcal{O}(\widetilde{\alpha}_s^2)$), to get the overall $m_{b,\rm pole}^5$ in eq. (1.8).

With all the necessary ingredients at hand, we can now write an explicit formula for the renormalized interference terms up to the NNLO ($i = 1, 2$)[8]

$$
\begin{aligned}
\widetilde{\alpha}_s\,\widetilde{G}_{i7}^{(1)} + \widetilde{\alpha}_s^2\,\widetilde{G}_{i7}^{(2)} = Z_b^{\rm OS}\,Z_m^{\rm OS}\,\bar{Z}_{77}\Big\{&\widetilde{\alpha}_s^2\,s^{3\epsilon}\,\widetilde{G}_{i7}^{(2)\rm bare} + (Z_m^{\rm OS}-1)\,s^{\epsilon}\left[\bar{Z}_{i4}\,\hat{G}_{47}^{(0)m} + \widetilde{\alpha}_s\,s^{\epsilon}\,\hat{G}_{i7}^{(1)m}\right]\\
&+ \widetilde{\alpha}_s\,(Z_G^{\rm OS}-1)\,s^{2\epsilon}\,\hat{G}_{i7}^{(1)3P} + \bar{Z}_{i7}\,Z_m^{\rm OS}\left[\hat{G}_{77}^{(0)} + \widetilde{\alpha}_s\,s^{\epsilon}\,\hat{G}_{77}^{(1)\rm bare}\right] + \widetilde{\alpha}_s\,\bar{Z}_{i8}\,s^{\epsilon}\,\hat{G}_{78}^{(1)\rm bare}\\
&+ \sum_{j=1,\ldots,6,11,12} \bar{Z}_{ij}\,s^{\epsilon}\left[\hat{G}_{j7}^{(0)} + \widetilde{\alpha}_s\,s^{\epsilon}\,\bar{Z}_g^2\,\hat{G}_{j7}^{(1)\rm bare}\right]\Big\} + \mathcal{O}(\widetilde{\alpha}_s^3),
\end{aligned}
\tag{2.10}
$$

where $\hat{G}_{j7}^{(0)} = 0$ for $j = 1, 2, 11, 12$. Once the above expression is expanded in $\widetilde{\alpha}_s$, and $\mathcal{O}(\widetilde{\alpha}_s^3)$ terms are neglected, all the $1/\epsilon^n$ poles cancel out as they should. Our final renormalized results at $E_0 = m_c = 0$ read

$$
\widetilde{G}_{27}^{(1)} = -6\,\widetilde{G}_{17}^{(1)} = -\frac{1702}{243} - \frac{416}{81}\ln\frac{\mu}{m_b},
$$

$$
\widetilde{G}_{17}^{(2)} = -\frac{1}{6}\widetilde{G}_{27}^{(2)} + \frac{136}{27}\ln^2\frac{\mu}{m_b} + \frac{94+8\pi^2}{9}\ln\frac{\mu}{m_b} + 22.6049613485,
$$

[8] Obviously, the renormalized $\widetilde{G}_{i7}^{(n)}$ remain unchanged after replacing $\bar{Z}_g \to Z_g$, $\bar{Z}_{ij} \to Z_{ij}$ and $s \to \mu^2/m_b^2$ on the r.h.s. of eq. (2.10) and inside the on-shell constants (2.8).

JHEP04(2015)168

$$\widetilde{G}_{27}^{(2)} = \left(\frac{11792}{729} + \frac{800}{243}(n_l + n_b)\right)\ln^2\frac{\mu}{m_b} + \left(1.0460332197 + \frac{64}{729}\kappa\, n_l + \frac{2368}{243}n_l + 9.6604967166\, n_b\right)\ln\frac{\mu}{m_b} - 14.0663747289 + 0.1644478609\,\kappa\, n_l + \left(\frac{54170}{6561} + \frac{92}{729}\pi^2\right) n_l - 1.8324081161\, n_b. \tag{2.11}$$

They are, of course, insensitive to conventions for the global $1+\mathcal{O}(\epsilon)$ normalization factor in eqs. (2.3)–(2.7), so long as it is the same in all these equations. In particular, it does not matter that our $\hat{G}_{77}^{(0)}$ differs from the one in ref. [25] by an overall factor of $\Gamma(1+\epsilon)\, e^{\gamma\epsilon}$.

As already mentioned, the n_l terms not marked by κ in eq. (2.11) agree with the previous calculations where both $m_c \neq 0$ and $m_c = 0$ were considered. In the case of the n_b terms, the current result extends the published fit (eq. (3.3) of ref. [32]) down to $m_c = 0$. All the remaining terms are entirely new.

3 Impact of the NNLO corrections to $(Q_7, Q_{1,2})$ interferences on the branching ratio

In the description of our phenomenological analysis, we shall strictly follow the notation of ref. [34], where the relevant perturbative quantity

$$P(E_0) = \sum_{i,j=1}^{8} C_i^{\rm eff}(\mu_b)\, C_j^{\rm eff}(\mu_b)\, K_{ij}(E_0,\mu_b), \tag{3.1}$$

has been defined through

$$\frac{\Gamma[b\to X_s^p\gamma]_{E_\gamma>E_0}}{|V_{cb}/V_{ub}|^2\,\Gamma[b\to X_u^p e\bar{\nu}]} = \left|\frac{V_{ts}^* V_{tb}}{V_{cb}}\right|^2 \frac{6\alpha_{\rm em}}{\pi}\, P(E_0). \tag{3.2}$$

The relation between $\widetilde{G}_{i7}^{(n)}$ for $i=1,2$ and $K_{i7} = \widetilde{\alpha}_{\rm s} K_{i7}^{(1)} + \widetilde{\alpha}_{\rm s}^2 K_{i7}^{(2)} + \mathcal{O}(\widetilde{\alpha}_{\rm s}^3)$ is thus very simple

$$\widetilde{\alpha}_{\rm s} K_{i7}^{(1)} + \widetilde{\alpha}_{\rm s}^2 K_{i7}^{(2)} + \mathcal{O}(\widetilde{\alpha}_{\rm s}^3) = \frac{\widetilde{\alpha}_{\rm s}\,\widetilde{G}_{i7}^{(1)} + \widetilde{\alpha}_{\rm s}^2\,\widetilde{G}_{i7}^{(2)} + \mathcal{O}(\widetilde{\alpha}_{\rm s}^3)}{1 + \widetilde{\alpha}_{\rm s}(50-8\pi^2)/3 + \mathcal{O}(\widetilde{\alpha}_{\rm s}^2)}, \tag{3.3}$$

where the denominator comes from the NLO correction to the semileptonic $b\to X_u^p e\bar{\nu}$ decay rate.

In the following, we shall write expressions for $K_{i7}^{(2)}$ that are valid for arbitrary m_c and E_0 but incorporate information from our calculation in the previous section, where $E_0 = m_c = 0$ has been assumed. For this purpose, four functions

$$f_{NLO}(z,\delta) = {\rm Re}\, r_2^{(1)}(z) + 2\phi_{27}^{(1)}(z,\delta),$$
$$f_q(z,\delta) = {\rm Re}\, r_2^{(2)}(z) - \frac{4}{3}h_{27}^{(2)}(z,\delta),$$

JHEP04(2015)168

$$f_b(z) \simeq -1.836 + 2.608\,z + 0.8271\,z^2 - 2.441\,z\ln z,$$
$$f_c(z) \simeq 9.099 + 13.20\,z - 19.68\,z^2 + 25.71\,z\ln z, \tag{3.4}$$

of $z = m_c^2/m_b^2$ and $\delta = 1 - 2E_0/m_b$ are going to be useful. Explicit formulae for $r_2^{(1)}(z)$ and $\mathrm{Re}\, r_2^{(2)}(z)$ can be found in eq. (3.1) of ref. [43] and eq. (26) of ref. [30], respectively. For $h_{27}^{(2)}(z,\delta)$, we shall use a numerical fit from eq. (13) of ref. [39]. An analytical expression for $\phi_{27}^{(1)}(z,\delta)$ for $4z < 1-\delta$ (which is the phenomenologically relevant region) reads

$$\begin{aligned}\phi_{27}^{(1)}(z,\delta) &= -\frac{2}{27}\delta(3-3\delta+\delta^2) + \frac{4}{3}z\,\delta\,s_\delta\,L_\delta + \frac{12-8\pi^2}{9}z^2\delta + \frac{4}{3}z(1-2z)(s_0L_0 - s_\delta L_\delta)\\ &\quad + \frac{2\pi^2-7}{9}z\delta(2-\delta) - \frac{8}{9}z(6z^2-4z+1)(L_0^2 - L_\delta^2) - \frac{8}{9}z\delta(2-\delta-4z)L_\delta^2,\end{aligned} \tag{3.5}$$

with $s_\delta = \sqrt{(1-\delta)(1-\delta-4z)}$, $s_0 = \sqrt{1-4z}$, $L_\delta = \ln\frac{\sqrt{1-\delta}+\sqrt{1-\delta-4z}}{2\sqrt{z}}$ and $L_0 = \ln\frac{1+\sqrt{1-4z}}{2\sqrt{z}}$.

In the $\delta = 1$ case, $\phi_{27}^{(1)}$ and $h_{27}^{(2)}$ for $z < \frac{1}{4}$ are given by

$$\begin{aligned}\phi_{27}^{(1)}(z,1) &= -\frac{2}{27} + \frac{12-8\pi^2}{9}z^2 + \frac{4}{3}z(1-2z)s_0L_0 + \frac{2\pi^2-7}{9}z - \frac{8}{9}z(6z^2-4z+1)L_0^2 + \frac{4}{3}\pi^2z^3,\\ h_{27}^{(2)}(z,1) &\simeq \frac{41}{27} - \frac{2}{9}\pi^2 - 2.24\,z^{1/2} - 7.04\,z + 23.72\,z^{3/2} + (-9.86\,z + 31.28\,z^2)\ln z.\end{aligned} \tag{3.6}$$

The functions $f_b(z)$ and $f_c(z)$ in eq. (3.4) come from eqs. (3.3) and (3.4) of ref. [32], respectively. These numerical fits (in the range $z \in [0.017, 0.155]$) describe contributions from three-loop $b \to s\gamma$ amplitudes with massive b-quark and c-quark loops on the gluon lines.

The ratio $z = m_c^2/m_b^2$ is defined in terms of the $\overline{\mathrm{MS}}$-renormalized charm quark mass at an arbitrary scale μ_c. In practice, we shall use $\mu_c = 2.0\,\mathrm{GeV}$ as a central value. As far as the renormalization scheme for m_b is concerned, we assume the following relation to the on-shell scheme

$$\frac{m_{b,\mathrm{pole}}}{m_b} = 1 + \widetilde{\alpha}_\mathrm{s} x_m + \mathcal{O}(\widetilde{\alpha}_\mathrm{s}^2). \tag{3.7}$$

In the 1S and kinetic schemes, one finds $x_m = \frac{8}{9}\pi\alpha_\Upsilon$ and $x_m = \frac{64\mu_\mathrm{kin}}{9m_b}\left(1 + \frac{3\mu_\mathrm{kin}}{8m_b}\right)$, respectively. In our numerical analysis, the kinetic scheme is going to be used.

Complete expressions for the NNLO quantities $K_{17}^{(2)}$ and $K_{27}^{(2)}$ can now be written as follows

$$\begin{aligned}K_{17}^{(2)}(z,\delta) &= -\frac{1}{6}K_{27}^{(2)}(z,\delta) + A_1 + F_1(z,\delta) + \left(\frac{94}{81} - \frac{3}{2}K_{27}^{(1)} - \frac{3}{4}K_{78}^{(1)}\right)L_b - \frac{34}{27}L_b^2,\\ K_{27}^{(2)}(z,\delta) &= A_2 + F_2(z,\delta) - \frac{3}{2}\beta_0^{n_l=3}f_q(z,\delta) + f_b(z) + f_c(z) + \frac{4}{3}\phi_{27}^{(1)}(z,\delta)\ln z\\ &\quad + \left[(8L_c - 2x_m)\,z\frac{d}{dz} + (1-\delta)x_m\frac{d}{d\delta}\right]f_{NLO}(z,\delta) + \frac{416}{81}x_m\\ &\quad + \left(\frac{10}{3}K_{27}^{(1)} - \frac{2}{3}K_{47}^{(1)} - \frac{208}{81}K_{77}^{(1)} - \frac{35}{27}K_{78}^{(1)} - \frac{254}{81}\right)L_b - \frac{5948}{729}L_b^2,\end{aligned} \tag{3.8}$$

JHEP04(2015)168

where $\beta_0^{n_l=3} = 9$, $L_b = \ln(\mu_b^2/m_b^2)$ and $L_c = \ln(\mu_c^2/m_c^2)$, while the relevant $K_{ij}^{(1)}$ are collected in appendix C.

The expressions $A_i + F_i(z,\delta)$ contain all the contributions that are not yet known for the measured value of m_c. They correspond to those parts of the considered interference terms that are obtained by: *(i)* setting $\mu_b = m_b$, $\mu_c = m_c$ and $x_m = 0$, *(ii)* removing the BLM-extended contributions from quark loops on the gluon lines and from $b \to sq\bar{q}\gamma$ decays ($q = u, d, s$), except for those given in figure 3b.

We define the constants A_i by requiring that $F_i(0,1) = 0$. Then we evaluate A_i from eq. (2.11) by setting there $\mu = m_b$, $n_b = 0$ and $\kappa n_l = 3$. Next, a replacement $n_l \to n_l + \frac{3}{2}\beta_0^{n_l} = \frac{33}{2}$ is done in the remaining n_l-terms. Finally, eq. (3.3) is used to find

$$A_1 \simeq 22.605, \qquad A_2 \simeq 75.603. \tag{3.9}$$

These two numbers are the only outcome of our calculation in section 2 that is going to be used in the phenomenological analysis below.

Apart from the condition $F_i(0,1) = 0$, everything that is known at the moment about the functions $F_i(z,\delta)$ are their large-z asymptotic forms. They can be derived from the results of ref. [35].[9] Explicitly, we find

$$\begin{aligned}
F_1(z,\delta) &= \frac{70}{27}\ln^2 z + \left(\frac{119}{27} - \frac{2}{9}\pi^2 + \frac{3}{2}\phi_{78}^{(1)}(\delta)\right)\ln z - \frac{493}{2916} - \frac{5}{54}\pi^2 + \frac{232}{27}\zeta_3 + \frac{5}{8}\phi_{78}^{(1)}(\delta) \\
&\quad - A_1 + \mathcal{O}\left(\frac{1}{z}\right), \\
F_2(z,\delta) &= -\frac{4736}{729}\ln^2 z + \left\{-\frac{165385}{2187} + \frac{1186}{729}\pi^2 - \frac{2\pi}{9\sqrt{3}} + \frac{2}{3}Y_1 + \frac{4}{3}\phi_{47}^{(1)}(\delta) + \frac{832}{81}\phi_{77}^{(1)}(\delta)\right. \\
&\quad \left. + \frac{70}{27}\phi_{78}^{(1)}(\delta)\right\}(\ln z + 1) - \frac{956435}{19683} - \frac{2662}{2187}\pi^2 + \frac{20060}{243}\zeta_3 - \frac{1624}{243}\phi_{77}^{(1)}(\delta) \\
&\quad - \frac{293}{162}\phi_{78}^{(1)}(\delta) - A_2 + \mathcal{O}\left(\frac{1}{z}\right).
\end{aligned} \tag{3.10}$$

The constant Y_1 and the necessary $\phi_{ij}^{(1)}$ functions are given in appendices B and C, respectively.

Let $\Delta\mathcal{B}_{s\gamma}$ denote the contribution from $F_{1,2}(z,\delta)$ to $\mathcal{B}_{s\gamma}$. Then the relative effect is given by

$$\frac{\Delta\mathcal{B}_{s\gamma}}{\mathcal{B}_{s\gamma}} \simeq U(z,\delta) \equiv \frac{\alpha_s^2(\mu_b)}{8\pi^2}\,\frac{C_1^{(0)}(\mu_b)F_1(z,\delta) + \left(C_2^{(0)}(\mu_b) - \frac{1}{6}C_1^{(0)}(\mu_b)\right)F_2(z,\delta)}{C_7^{(0)\mathrm{eff}}(\mu_b)}. \tag{3.11}$$

For $\mu_b = 2.0\,\mathrm{GeV}$, we have $\alpha_s(\mu_b) \simeq 0.293$, $C_1^{(0)}(\mu_b) \simeq -0.902$, $C_2^{(0)}(\mu_b) \simeq 1.073$, and $C_7^{(0)\mathrm{eff}}(\mu_b) \simeq -0.385$.

[9] We supplement them now with the previously omitted large-m_c contributions from the diagrams in figure 1 in ref. [35] or, equivalently, figure 3b in the present paper. The effect of such a modification is numerically very small.

JHEP04(2015)168

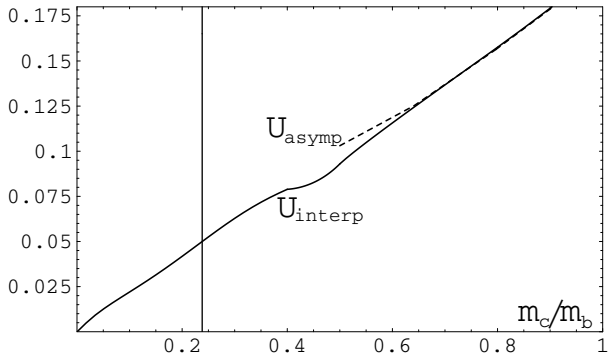

Figure 4. The interpolating function defined in eq. (3.12) (solid line) and asymptotic behaviour of the true function $U(z,1)$ for $m_c \gg m_b/2$ (dashed line). The vertical line corresponds to the measured value of m_c/m_b.

We shall estimate the contribution to $\mathcal{B}_{s\gamma}$ that comes from the unknown $U(z,\delta)$ by considering an interpolation model where $U(z,1)$ is given by the following linear combination

$$U_{\rm interp}(z,1) \;=\; x_1 \,+\, x_2\, f_q(z,1) \,+\, \left(x_3 \,+\, x_4\, z\frac{d}{dz}\right) f_{NLO}(z,1). \tag{3.12}$$

The numbers x_i are fixed by the condition $U(0,1)=0$ as well as by the large-z behaviour of $U(z,1)$ that follows from eq. (3.10). This determines x_i in a unique manner, namely $x_i \simeq (-0.0502,\ 0.0328,\ 0.0373,\ 0.0309)_i$. In figure 4, the function $U_{\rm interp}(z,1)$ is plotted with a solid line, while the dashed line shows $U_{\rm asymp}(z,1)$, i.e. asymptotic large-z behaviour of the true $U(z,1)$. Note that $\sqrt{z}=m_c/m_b$ rather than z is used on the horizontal axis. The vertical line corresponds to the measured value of this mass ratio. The plot involves some extra approximation in the region between $\sqrt{z}\simeq 0.4$ and $\sqrt{z}\simeq 0.8$ where we need to interpolate between the known small-z and large-z expansions of $\mathrm{Re}\, r_2^{(2)}(z)$ (see figure 1 of ref. [34]).

In refs. [34, 42] the uncertainty in $\mathcal{B}_{s\gamma}$ due to unknown m_c-dependence of the NNLO corrections has been estimated at the $\pm 3\%$ level. The size of the interpolated contribution in figure 4 implies that no reduction of this uncertainty is possible at the moment. One might wonder whether the uncertainty should not be enlarged. Our choice here is to leave it unchanged, for the following reasons:

(i) Our choice of functions for the linear combination in eq. (3.12) is dictated by the fact, that these very functions determine the dependence on z of the known parts of $K_{17}^{(2)}$ and $K_{27}^{(2)}$. The known parts are either those related to renormalization of the Wilson coefficients and quark masses (in the terms proportional to L_b and L_c) or the renormalization of α_s (the function f_q parametrizes the considered correction in the BLM approximation). It often happens in perturbation theory that higher-order corrections are dominated by renormalization effects. If this is the case here, the true $U(z,1)$ should have a similar shape to $U_{\rm interp}(z,1)$.

(ii) The growth of $U_{\rm interp}(z,1)$ for $m_c > m_b/2$ is perfectly understandable. In this region, logarithms of z from eq. (3.10) combine with L_b from eq. (3.8), and the asymptotic

JHEP04(2015)168

large-m_c behaviour of $K^{(2)}_{(1,2)7}$ is determined by $\ln(\mu_b/m_c)$ and $\ln(\mu_c/m_c)$ only (see eqs. (5.12) and (5.14) of ref. [35]). Thus, the growth of the correction for large z can be compensated by an appropriate choice of the renormalization scales, which means (not surprisingly) that the dangerous large logarithms can get resummed using renormalization group evolution of the Wilson coefficients, masses and α_s.

(iii) Our $\pm 3\%$ uncertainty is going to be combined in quadrature with the other ones, which means that it should be treated as a "theoretical 1σ error". To gain higher confidence levels, it would need to be enlarged.

(iv) In the considered interference terms K_{17} and K_{27}, the dependence on δ is very weak in the whole range $\delta \in [0,1]$, both at the NLO and in the BLM approximation for the NNLO corrections. Specifically, changing δ from 1 ($E_0 = 0$) to 0.295 ($E_0 = 1.6\,\mathrm{GeV}$) results in modifications of f_{NLO} by $+0.2\%$ and f_q by $+1.0\%$, respectively, for the measured value of m_c. The corresponding changes at $m_c = 0$ amount to -0.7% and -2.4% only. Thus, our estimates made for $\delta = 1$ are likely to be valid for arbitrary δ.

In the phenomenological analysis below, we shall take $K^{(2)}_{17}$ and $K^{(2)}_{27}$ as they stand in eq. (3.8), replace the unknown $F_i(z,\delta)$ by $F_i^{\mathrm{interp}}(z,1)$ interpolated analogously to eq. (3.12)

$$F_1^{\mathrm{interp}}(z,1) = -23.75 + \frac{35}{12} f_q(z,1) + \left(\frac{2129}{936} - \frac{9}{52}\pi^2 - 0.84\, z\frac{d}{dz}\right) f_{NLO}(z,1),$$
$$F_2^{\mathrm{interp}}(z,1) = -3.01 - \frac{592}{81} f_q(z,1) + \left(-10.34 - 9.55\, z\frac{d}{dz}\right) f_{NLO}(z,1), \tag{3.13}$$

and include a $\pm 3\%$ uncertainty in the branching ratio due to such an approximation.

4 Evaluation of $\mathcal{B}_{s\gamma}$ in the SM

In the present section, we include all the other corrections to $\mathcal{B}_{s\gamma}$ that have been evaluated after the analysis in refs. [34, 42]. Next, we update the SM prediction. To provide information on sizes of the subsequent corrections, the description is split into steps, and the corresponding modifications in the branching ratio central value are summarized in table 2. The steps are as follows:

1. We begin with performing the calculation precisely as it was described in ref. [34] but only shifting from $\mathcal{B}(\bar{B} \to X_s\gamma)$ to $\mathcal{B}_{s\gamma}$, which amounts to CP-averaging the perturbative decay widths. No directly CP-violating non-perturbative corrections to $\mathcal{B}(\bar{B} \to X_s\gamma)$ were considered in ref. [34]. It was not equivalent to neglecting them but rather to assuming that they have vanishing central values. A dedicated analysis in ref. [48] leads to an estimate of $0.4 \pm 1.7\%$ for such effects.

2. The input parameters are updated as outlined in appendix D. In particular, we use results of the very recent kinetic-scheme fit to the semileptonic B decay data [49].

JHEP04(2015)168

1	2	3	4	5	6	7	8	9	10	total
−0.6%	+1.0%	−0.2%	+2.0%	+1.0%	+1.6%	+2.1%	−0.5%	+0.2%	−0.4%	+6.4%

Table 2. Shifts in the central value of $\mathcal{B}_{s\gamma}$ for $E_0 = 1.6\,\text{GeV}$ at each step (see the text).

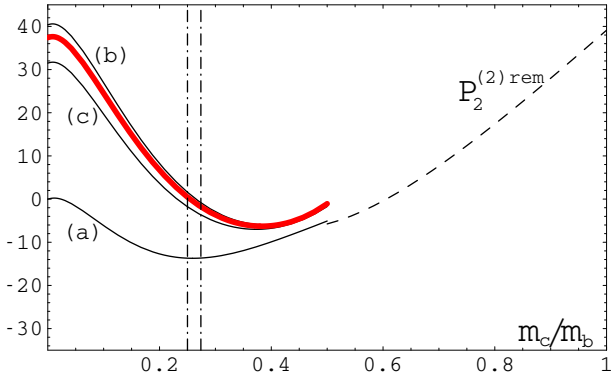

Figure 5. Interpolation of $P_2^{(2)\text{rem}}$ in m_c as in figure 2 of ref. [34] but with updated input parameters and with renormalization scales shifted to $(\mu_c, \mu_b) = (2, 2)\,\text{GeV}$. In addition, the thick solid (red) line shows the case with the presently known boundary condition at $m_c = 0$ imposed.

3. Central values of the renormalization scales (μ_c, μ_b) are shifted from $(1.5, 2.5)\,\text{GeV}$ to $(2, 2)\,\text{GeV}$. Both scales are then varied in the ranges $[1.25,\ 5]\,\text{GeV}$ to estimate the higher-order uncertainty. In the resulting range of $\mathcal{B}_{s\gamma}$, the value corresponding to the $(2, 2)\,\text{GeV}$ renormalization scales is more centrally located than the $(1.5, 2.5)\,\text{GeV}$ one, after performing all the updates 1-10 here. It is the main reason for shifting the default scales. The $(2, 2)\,\text{GeV}$ choice is also simpler (both scales are equal), and μ_c is exactly as in the fit from which we take $m_c(\mu_c)$ (appendix D). As far as μ_b is concerned, it should be of the same order as the energy transferred to the partonic system after the b-quark decay. For the leading $b \to s\gamma$ contribution from the photonic dipole operator P_7, this energy equals to $\frac{1}{2}m_b$ which gives 2.3 GeV when one substitutes $m_b = m_{b,kin}$ from appendix D.[10] Rounding 2.3 to either 2.5 or 2.0 for the default value is equally fine, given that the observed μ_b-dependence of $\mathcal{B}_{s\gamma}$ is weak (see figure 6), and our range for μ_b is $[1.25,\ 5]\,\text{GeV}$.

4. In the interpolation of $P_2^{(2)\text{rem}}$ (see ref. [34] for its definition), we shift to the so-called case (c) where the interpolated quantity at $m_c = 0$ was given by the (Q_7, Q_7) interference alone.

5. The $m_c = 0$ boundary for $P_2^{(2)\text{rem}}$ is updated to include all the relevant interferences, especially the ones evaluated in section 2. The thick solid (red) line in figure 5 shows the new $P_2^{(2)\text{rem}}$ in such a case, while the remaining lines are as in figure 2 of ref. [34] (somewhat shifted due to the parameter and scale modifications only).

[10] The measured photon spectra are also peaked at around 2.3 GeV, which confirms the leading role of the two-body partonic mode.

JHEP04(2015)168

6. At this point, we abandon the approach with m_c-interpolation applied to the *whole* non-BLM correction $P_2^{(2)\mathrm{rem}}$. As before, the penguin operators $Q_{3,\ldots,6}$ and the CKM-suppressed ones $Q^u_{1,2}$ are neglected at the NNLO level. The corrections $K^{(2)}_{17}$ and $K^{(2)}_{27}$ are treated as summarized at the end of the previous section. For $K^{(2)}_{78}$, the complete results from refs. [36, 37] are included. $K^{(2)}_{77}$ is made complete by taking into account its exact m_c-dependence [29, 50], in addition to the previously included terms. For the NNLO interferences among Q_1, Q_2 and Q_8, only the two-body final state contributions are present at this step. They are infrared-finite by themselves, and given by products of the well-known NLO amplitudes $r_i^{(1)}$ (see eq. (3.1) of ref. [43]) whose imaginary parts matter here, too.

7. Three- and four-body final state contributions to the NNLO interferences among Q_1, Q_2 and Q_8 are included in the BLM approximation, using the results of refs. [31, 38, 39]. Non-BLM corrections to these interferences remain neglected. The corresponding uncertainty is going to be absorbed below into the overall $\pm 3\%$ perturbative one.

8. Four-loop $Q_{1,\ldots,6} \to Q_8$ anomalous dimensions from ref. [19] are included in the renormalization group equations.

9. The LO and NLO contributions from four body final states are included [23, 24]. They are not yet formally complete, but the only neglected terms are the NLO ones that undergo double (quadratic) suppression either by the small Wilson coefficients $C_{3,\ldots,6}$ or by the small CKM element ratio $|V^*_{us}V_{ub}|\,/\,|V^*_{ts}V_{tb}|$. The uncertainty that results from neglecting such terms is below a permille in $\mathcal{B}_{s\gamma}$. As far as the CKM-suppressed two-body and three-body contributions are concerned, the two-body NLO one has already been taken into account in ref. [34]. The remaining NLO and NNLO ones (also those with double CKM suppression) are included at the present step. Their contribution to $\mathcal{B}_{s\gamma}$ is below a permille. However, the branching ratio $\mathcal{B}_{d\gamma}$ [51] receives around 2% enhancement from them.

10. We update our treatment of non-perturbative corrections. The $\mathcal{O}\left(\alpha_s\Lambda^2/m_b^2\right)$ correction to the (Q_7, Q_7) interference from ref. [40] replaces the previous approximate expression from ref. [52]. Moreover, we include a similar correction [41, 53] to the charmless semileptonic rate that is used for normalization in $[P(E_0)+N(E_0)]$ (see eqs. (D.2) and (D.4) in appendix D). In consequence, the previous (tiny) effect in $N(E_0)$ gets reduced by a factor of around 4. Finally, our treatment of non-perturbative effects in interferences other than (Q_7, Q_7) gets modified according to ref. [14]. A vanishing contribution to the branching ratio central value from such corrections is assumed, except for the leading $\mathcal{O}\left(\lambda_2/m_c^2\right)$ one [54] where m_c is fixed to 1.131 GeV. At the same time, a $\pm 5\%$ non-perturbative uncertainty in the branching ratio is assumed, as obtained in section 7.4 of ref. [14] by adding the relevant three uncertainties in a linear manner.[11]

[11] If their ranges were treated as 1σ ones and combined in quadrature, the uncertainty would go down to 3.3%.

JHEP04(2015)168

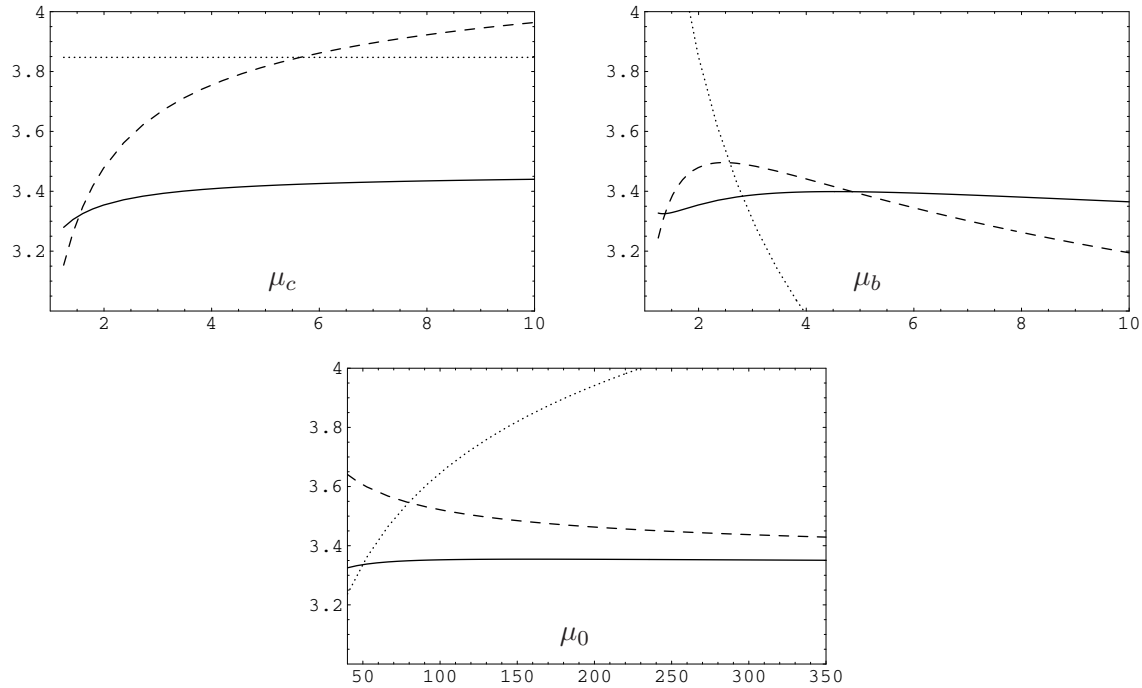

Figure 6. Renormalization scale dependence of $\mathcal{B}_{s\gamma}$ in units 10^{-4} at the LO (dotted lines), NLO (dashed lines) and NNLO (solid lines). The upper-left, upper-right and lower plots describe the dependence on μ_c, μ_b and μ_0 [GeV], respectively. When one of the scales is varied, the remaining ones are set to their default values.

Our final result reads

$$\mathcal{B}_{s\gamma}^{\rm SM} = (3.36 \pm 0.23) \times 10^{-4} \tag{4.1}$$

for $E_0 = 1.6\,\text{GeV}$, where four types of uncertainties have been combined in quadrature: $\pm 5\%$ non-perturbative (step 10 above), $\pm 3\%$ from our interpolation of $F_{1,2}(z,\delta)$ (section 3), $\pm 2.0\%$ parametric (appendix D), as well as $\pm 3\%$ from higher-order perturbative effects.

The latter uncertainty is assumed to account for approximations made at the NLO and NNLO levels, too. In the NLO case, it refers to the doubly suppressed terms mentioned in step 9 above. In the NNLO case, it refers to neglecting the penguin operators at this level, and using the BLM approximation in step 7 above. If we relied just on the renormalization-scale dependence in figure 6 (with $1.25\,\text{GeV} < \mu_c, \mu_b < 5\,\text{GeV}$), we could reduce this uncertainty to around $\pm 2.4\%$. However, apart from the scale-dependence, one needs to study how the perturbation series behaves, which is hard to judge before learning the actual contributions from $F_{1,2}(z,\delta)$. Thus, we leave the higher-order uncertainty unchanged with respect to refs. [34, 42]. Our treatment of the electroweak corrections [55] remains unchanged, too.

The central value in eq. (4.1) is about 6.4% higher than the previous estimate of 3.15×10^{-4} in refs. [34, 42]. Around half of this effect comes from improving the m_c-interpolation. As seen in figure 5, the currently known $m_c = 0$ boundary for the thick line is close to the edge of the previously assumed range between the curves (a) and (b). It is consistent with the fact that the corrections in steps 4 and 5 sum up to 3% being the

JHEP04(2015)168

previous "1σ" interpolation uncertainty. The $m_c = 0$ boundary has been the main worry in the past because estimating the range for its location was based on quite arbitrary assumptions. It is precisely the reason why no update of the SM prediction seemed to make sense until now, given moderate sizes of the other new corrections.

5 Conclusions

We evaluated $\mathcal{O}(\alpha_s^2)$ contributions to the perturbative $\Gamma(b \to X_s\gamma)$ decay rate that originate from the $(Q_7, Q_{1,2})$ interference for $m_c = E_0 = 0$. The calculation involved 163 four-loop massive on-shell propagator master integrals with unitarity cuts. Our updated prediction for the CP- and isospin-averaged branching ratio in the SM reads $\mathcal{B}_{s\gamma}^{\rm SM} = (3.36 \pm 0.23) \times 10^{-4}$. It includes all the perturbative and non-perturbative contributions that have been calculated to date. It agrees very well with the current experimental world average $\mathcal{B}_{s\gamma}^{\rm exp} = (3.43 \pm 0.21 \pm 0.07) \times 10^{-4}$. An extension of our analysis to the case of $\mathcal{B}_{d\gamma}$ and an update of bounds on the Two Higgs Doublet Model is going to be presented in a parallel article [51].

Acknowledgments

We would like to thank Ulrich Nierste for helpful discussions, and Paolo Gambino for extensive correspondence concerning non-perturbative corrections and input parameters, as well as for providing us with the semileptonic fit results in an unpublished option (see appendix D). We are grateful to Michał Poradziński and Abdur Rehman for performing several cross-checks of the three- and four-body contributions. The work of M.C., P.F. and M.S. has been supported by the Deutsche Forschungsgemeinschaft in the Sonderforschungsbereich Transregio 9 "Computational Particle Physics". T.H. acknowledges support from the Deutsche Forschungsgemeinschaft within research unit FOR 1873 (QFET). M.M. acknowledges partial support by the National Science Centre (Poland) research project, decision no DEC-2014/13/B/ST2/03969.

A Massless master integrals

In the course of this work, it has been necessary to compute a number of massless scalar integrals with various unitarity cuts. All of them are depicted in figure 7 and table 3. They occur after applying the large mass expansion for $p_b^2 \ll m_b^2$, as well as in the decay rate calculation itself. Apart from the four-loop diagrams with four-particle cuts, and the four-loop diagrams 4L3C1, 4L3C2 and 4L3C3 with three-particle cuts, values of all our master integrals can either be found in the literature [56–60] or obtained using standard techniques described, for instance, in ref. [64]. Let us note that the results for all the massless propagator four-loop master integrals in refs. [65, 66] are not sufficient here because they correspond to sums over all the possible cuts, while certain cuts need to be discarded in our case.

In the following, we explain our computation of the four-particle-cut master integrals in dimensional regularization with $D = 4-2\epsilon$. The total momentum is $q = p_1+p_2+p_3+p_4$, and we have $p_i^2 = 0$ for $i = 1, \ldots, 4$. Moreover, all the internal lines are massless. The

JHEP04(2015)168

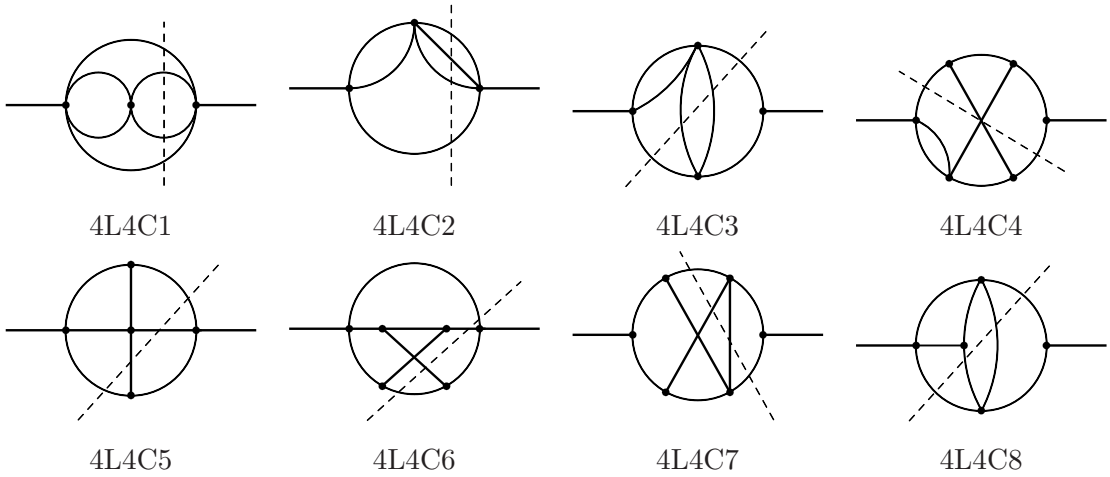

Figure 7. The massless four-particle-cut diagrams calculated in the course of this work.

momenta are in Minkowski space, and we tacitly assume that all the propagators below contain an infinitesimal $+i\eta$ with $\eta > 0$. We also define the invariants

$$s_{ijk\ldots} \equiv (p_i + p_j + p_k + \ldots)^2 \,. \tag{A.1}$$

We therefore have $s_{12}+s_{13}+s_{14}+s_{23}+s_{24}+s_{34} = q^2$ as a constraint from overall momentum conservation.

Our convention for the loop measure is

$$\int [dk] \equiv \int \frac{d^D k}{i\,(2\pi)^D} \,, \tag{A.2}$$

and we define the prefactor

$$S_\Gamma \equiv \frac{1}{(4\pi)^{D/2}\,\Gamma(1-\epsilon)} \,. \tag{A.3}$$

Note that our definition of S_Γ is different from the one in eq. (4.13) of ref. [57].

As far as integration over the four-particle massless phase space in $D = 4 - 2\epsilon$ dimensions is concerned, we closely follow ref. [57]. The phase space measure reads

$$dPS_4 = \frac{d^{D-1}p_1}{(2\pi)^{D-1}\,2E_1} \cdots \frac{d^{D-1}p_4}{(2\pi)^{D-1}\,2E_4}\,(2\pi)^D\,\delta^{(D)}(q - p_1 - p_2 - p_3 - p_4) \,. \tag{A.4}$$

It can be rewritten in terms of invariants and angular variables according to

$$\begin{aligned} dPS_4 = {} & (2\pi)^{4-3D}\left(q^2\right)^{1-\frac{D}{2}} 2^{1-\frac{D}{2}}\,(-\Delta_4)^{\frac{D-5}{2}}\,\theta(-\Delta_4)\,d\Omega_{D-1}\,d\Omega_{D-2}\,d\Omega_{D-3} \\ & \times\delta(q^2 - s_{12} - s_{13} - s_{14} - s_{23} - s_{24} - s_{34})\,ds_{12}\,ds_{13}\,ds_{14}\,ds_{23}\,ds_{24}\,ds_{34} \,, \end{aligned} \tag{A.5}$$

with the Gram determinant

$$\Delta_4 = \lambda(s_{12}s_{34}, s_{13}s_{24}, s_{14}s_{23}) \,, \qquad \lambda(x,y,z) = x^2 + y^2 + z^2 - 2xy - 2xz - 2yz \,. \tag{A.6}$$

JHEP04(2015)168

2PCuts		3PCuts		
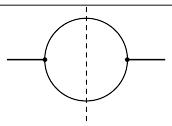 1L2C1				
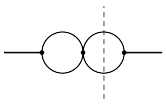 2L2C1		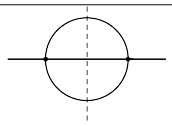 2L3C1		
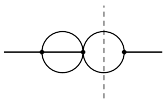 3L2C1		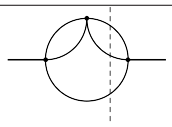 3L3C1		
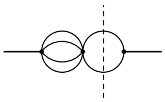 4L2C1	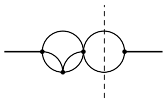 4L2C2	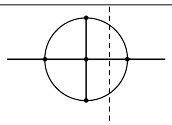 4L3C1	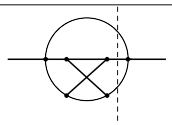 4L3C2	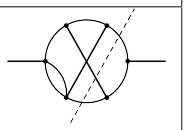 4L3C3
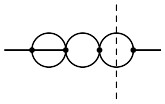 4L2C3	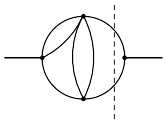 4L2C4	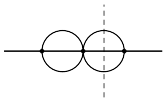 4L3C4	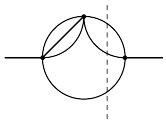 4L3C5	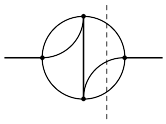 4L3C6
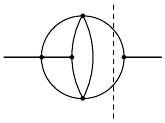 4L2C5	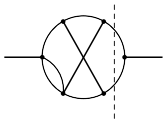 4L2C6	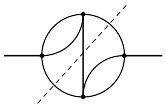 4L3C7	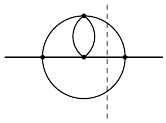 4L3C8	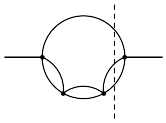 4L3C9

Table 3. The massless two- and three-particle-cut diagrams used in the course of this work.

It turns out that integration over angular variables is trivial in all the cases we encounter here, and we can use

$$\int d\Omega_D = \frac{2\pi^{D/2}}{\Gamma(D/2)} \,. \tag{A.7}$$

Performing the angular integration, and furthermore applying the steps explained in ref. [57] to factorize the phase space measure, we arrive at

$$\begin{aligned} dPS_4 = & \frac{2\pi \left(q^2\right)^{2-3\epsilon}}{(4\pi)^{\frac{3D}{2}}(1-2\epsilon)\Gamma(1-\epsilon)\Gamma^2(\frac{1}{2}-\epsilon)} \, dt\, dv\, d\chi\, dz_1\, dy_{134}\, dy_{1234}\, \delta(1-y_{1234}) \\ & t^{-\epsilon}\,(1-t)^{-\epsilon}\, v^{-\epsilon}\,(1-v)^{-\epsilon}\, \chi^{-\frac{1}{2}-\epsilon}\,(1-\chi)^{-\frac{1}{2}-\epsilon}\, z_1^{-\epsilon}\,(1-z_1)^{1-2\epsilon}\, y_{134}^{1-2\epsilon}\,(1-y_{134})^{1-2\epsilon}. \end{aligned} \tag{A.8}$$

JHEP04(2015)168

All the integration variables t, v, χ, z_1, y_{134}, and y_{1234} run from $0\ldots1$ and originate from

$$\begin{aligned}
s_{ijk\ldots} &= q^2\, y_{ijk\ldots}\,, & y_{13} &= (y_{13,\,b} - y_{13,\,a})\chi + y_{13,\,a}\,,\\
y_{12} &= \bar{y}_{134}\,\bar{z}_1\,\bar{t}\,, & y_{13,\,b/a} &= B \pm \sqrt{B^2 - C}\,,\\
y_{23} &= \bar{y}_{134}\,z_1\,, & B &= y_{134}\,(\bar{t}\,\bar{v} + v\,t\,z_1)\,,\\
y_{14} &= y_{134}\,\bar{z}_1\,v\,, & C &= y_{134}^2\,(\bar{t}\,\bar{v} - v\,t\,z_1)^2\,,\\
y_{24} &= \bar{y}_{134}\,\bar{z}_1\,t\,, & \sqrt{B^2 - C} &= 2\,y_{134}\,\sqrt{t}\,\sqrt{\bar{t}}\,\sqrt{v}\,\sqrt{\bar{v}}\,\sqrt{z_1}\,,\\
y_{124} &= \bar{z}_1\,(1 - y_{134}\bar{v})\,, & y_{13,\,b} - y_{13,\,a} &= 2\sqrt{B^2 - C}\,,
\end{aligned} \tag{A.9}$$

where $\bar{t} = 1 - t$, and analogously for all the other variables. The substitutions (A.9) should be done in the integrands, too.

A.1 Results for the four-particle-cut master integrals

We are now in position to present results for the four-particle-cut diagrams depicted in figure 7. Normalization factors are extracted according to

$$I_{4L4Ci} = 2\pi\, e^{i\pi\epsilon}\, S_\Gamma^4\, \left(q^2\right)^{a_i - 4\epsilon}\, \widetilde{I}_{4L4Ci}\,, \tag{A.10}$$

where the a_i follow from dimensional considerations. One finds $a_i = (2, 2, 1, -1, 0, -1, -1, 0)_i$ for $i = 1, \ldots, 8$.

We start with I_{4L4C1},

$$\begin{aligned}
I_{4L4C1} &= \int dPS_4 \int [dk]\, \frac{1}{k^2\,(k + p_1 + p_2)^2}\\
&= \frac{e^{i\pi\epsilon}\,\Gamma(\epsilon)\Gamma^2(1-\epsilon)}{(4\pi)^{D/2}\,\Gamma(2-2\epsilon)}\, \left(q^2\right)^{-\epsilon} \int dPS_4\, y_{12}^{-\epsilon}\,,
\end{aligned} \tag{A.11}$$

which yields

$$\widetilde{I}_{4L4C1} = \frac{\Gamma(\epsilon)\Gamma^9(1-\epsilon)\Gamma(1-2\epsilon)\Gamma(2-3\epsilon)}{\Gamma^2(2-2\epsilon)\Gamma(3-4\epsilon)\Gamma(4-5\epsilon)}\,. \tag{A.12}$$

The next integral to consider is I_{4L4C2},

$$\begin{aligned}
I_{4L4C2} &= \int dPS_4 \int [dk]\, \frac{1}{k^2\,(k + p_1 + p_2 + p_4)^2}\\
&= \frac{e^{i\pi\epsilon}\,\Gamma(\epsilon)\Gamma^2(1-\epsilon)}{(4\pi)^{D/2}\,\Gamma(2-2\epsilon)}\, \left(q^2\right)^{-\epsilon} \int dPS_4\, y_{134}^{-\epsilon}\,,
\end{aligned} \tag{A.13}$$

and we get

$$\widetilde{I}_{4L4C2} = \frac{\Gamma(\epsilon)\Gamma^{10}(1-\epsilon)\Gamma(2-3\epsilon)}{\Gamma^2(2-2\epsilon)\Gamma(3-3\epsilon)\Gamma(4-5\epsilon)}\,. \tag{A.14}$$

We proceed with I_{4L4C3},

$$I_{4L4C3} = \int dPS_4 \int [dk]\, \frac{1}{k^2\,(k + p_1 + p_3 + p_4)^2\,(p_1 + p_2 + p_4)^2}$$

JHEP04(2015)168

$$= \frac{e^{i\pi\epsilon}\,\Gamma(\epsilon)\Gamma^2(1-\epsilon)}{(4\pi)^{D/2}\,\Gamma(2-2\epsilon)}\,\left(q^2\right)^{-1-\epsilon}\int dPS_4\; y_{134}^{-\epsilon}\, y_{124}^{-1}\,, \tag{A.15}$$

and arrive at

$$\widetilde{I}_{4L4C3} = \frac{\Gamma(\epsilon)\Gamma^{10}(1-\epsilon)\Gamma(1-2\epsilon)}{\Gamma^3(2-2\epsilon)\Gamma(4-5\epsilon)}\;{}_3F_2(1,1-\epsilon,2-3\epsilon\,;\,2-2\epsilon,4-5\epsilon\,;\,1). \tag{A.16}$$

The expansion of $\widetilde{I}_{4L4C3}$ in ϵ is conveniently done with the package `HypExp` [68, 69],

$$\begin{aligned}\widetilde{I}_{4L4C3} = {}& \frac{1}{4\epsilon}+\left(\frac{37}{8}-\frac{\pi^2}{12}\right)+\left(\frac{809}{16}-\frac{35\pi^2}{24}-5\zeta_3\right)\epsilon+\left(\frac{13677}{32}-\frac{253\pi^2}{16}-\frac{29\pi^4}{144}-71\zeta_3\right)\epsilon^2\\ &+\left(\frac{198241}{64}-\frac{12995\pi^2}{96}-\frac{3521\pi^4}{1440}-\frac{1287}{2}\zeta_3+\frac{67}{6}\pi^2\zeta_3-\frac{315}{2}\zeta_5\right)\epsilon^3+\left(\frac{2597477}{128}\right.\\ &\left.-\frac{192175\pi^2}{192}-\frac{17519\pi^4}{960}-\frac{1481\pi^6}{6048}-\frac{19139}{4}\zeta_3+\frac{925}{6}\pi^2\zeta_3+170\zeta_3^2-2049\zeta_5\right)\epsilon^4\\ &+\mathcal{O}(\epsilon^5)\,.\end{aligned} \tag{A.17}$$

We now move to I_{4L4C4},

$$\begin{aligned}I_{4L4C4} &= \int dPS_4\int[dk]\;\frac{1}{k^2\,(k+p_1+p_3+p_4)^2\,(p_1+p_3)^2\,(p_1+p_2+p_4)^2\,(p_1+p_2)^2}\\ &= \frac{e^{i\pi\epsilon}\,\Gamma(\epsilon)\Gamma^2(1-\epsilon)}{(4\pi)^{D/2}\,\Gamma(2-2\epsilon)}\,\left(q^2\right)^{-3-\epsilon}\int dPS_4\; y_{134}^{-\epsilon}\, y_{124}^{-1}\, y_{13}^{-1}\, y_{12}^{-1}\,,\end{aligned} \tag{A.18}$$

which does not reveal a closed form since we cannot avoid y_{13} in the integrand. We therefore compute it from the following two-fold Mellin-Barnes representation [61–64, 67]

$$\begin{aligned}\widetilde{I}_{4L4C4} = {}& \frac{\Gamma(\epsilon)\Gamma^6(1-\epsilon)\Gamma(-\epsilon)\Gamma(1-3\epsilon)}{\Gamma(-2\epsilon)\Gamma^2(2-2\epsilon)}\int_{c_1-i\infty}^{c_1+i\infty}\frac{dz_1}{2\pi i}\int_{c_2-i\infty}^{c_2+i\infty}\frac{dz_2}{2\pi i}\,\Gamma(z_1+z_2-\epsilon)\Gamma(-\epsilon-z_1-z_2)\Gamma(z_1)\\ &\times\frac{\Gamma(1-z_1)\Gamma(1-2\epsilon-z_1)}{\Gamma(2-5\epsilon-z_1)}\,\frac{\Gamma(-z_2)\Gamma(1+z_2)\Gamma(-1-\epsilon-z_2)\Gamma(1-\epsilon+z_2)}{\Gamma(1-3\epsilon+z_2)\Gamma(-\epsilon-z_2)}\,.\end{aligned} \tag{A.19}$$

The integration contours in the complex plane can be chosen as straight lines parallel to the imaginary axis. The integral is then regulated [67] for $c_1 = 1/2$, $c_2 = -1/4$, and $\epsilon = -7/4$. We perform an analytic continuation to $\epsilon = 0$ with the package `MB.m` [67], which is also used for numerical cross checks. The expansion of $\widetilde{I}_{4L4C4}$ in ϵ reads

$$\begin{aligned}\widetilde{I}_{4L4C4} = {}& \frac{1}{4\epsilon^5}+\frac{1}{\epsilon^4}+\left(3-\frac{13\pi^2}{24}\right)\frac{1}{\epsilon^3}+\left(8-\frac{13\pi^2}{6}-\frac{33}{2}\zeta_3\right)\frac{1}{\epsilon^2}+\left(20-\frac{13\pi^2}{2}-\frac{397\pi^4}{1440}\right.\\ &\left.-66\zeta_3\right)\frac{1}{\epsilon}+\left(48-\frac{52\pi^2}{3}-\frac{397\pi^4}{360}-198\zeta_3+\frac{131}{4}\pi^2\zeta_3-\frac{687}{2}\zeta_5\right)\\ &+\left(112-\frac{130\pi^2}{3}-\frac{397\pi^4}{120}-\frac{24539\pi^6}{60480}-528\zeta_3+131\pi^2\zeta_3+\frac{897}{2}\zeta_3^2-1374\zeta_5\right)\epsilon\\ &+\mathcal{O}(\epsilon^2)\,.\end{aligned} \tag{A.20}$$

JHEP04(2015)168

The next integral, I_{4L4C5}, with

$$I_{4L4C5} = \int dPS_4 \int [dk] \, \frac{1}{k^2\,(k+p_4)^2\,(k+p_1+p_2+p_4)^2\,(p_2+p_3)^2} \tag{A.21}$$
$$= \frac{e^{i\pi\epsilon}\,\Gamma(1+\epsilon)\Gamma(-\epsilon)\Gamma(1-\epsilon)}{(4\pi)^{D/2}\,\Gamma(1-2\epsilon)}\,(q^2)^{-2-\epsilon} \int dPS_4 \int_0^1 dx \, \frac{1}{[y_{12}+x\,y_{14}+x\,y_{24}]^{1+\epsilon}\,y_{23}},$$

can again be expressed to all orders in ϵ. One first integrates over x, and finally finds

$$\widetilde{I}_{4L4C5} = -\frac{\Gamma(\epsilon)\Gamma^6(1-\epsilon)\Gamma^3(-\epsilon)}{\Gamma(2-5\epsilon)\Gamma(2-2\epsilon)} \left[\frac{\Gamma(1-\epsilon)}{\Gamma(2-2\epsilon)}\, {}_3F_2(1,1-\epsilon,1-2\epsilon\,;\,1+\epsilon,2-2\epsilon\,;\,1) \right.$$
$$\left. - \frac{\Gamma(1-3\epsilon)}{(1-3\epsilon)\Gamma(1-4\epsilon)}\, {}_3F_2(1,1-\epsilon,1-3\epsilon\,;\,1+\epsilon,2-3\epsilon\,;\,1) \right] . \tag{A.22}$$

The expansion of $\widetilde{I}_{4L4C5}$ in ϵ reads

$$\widetilde{I}_{4L4C5} = \frac{2\zeta_3}{\epsilon^2} + \left(14\zeta_3 + \frac{31\pi^4}{180}\right)\frac{1}{\epsilon} + \left(78\zeta_3 + \frac{217\pi^4}{180} - \frac{20}{3}\pi^2\zeta_3 + 114\zeta_5\right)$$
$$+ \left(406\zeta_3 + \frac{403\pi^4}{60} - \frac{140}{3}\pi^2\zeta_3 + 798\zeta_5 + \frac{799\pi^6}{7560} - 125\zeta_3^2\right)\epsilon + \mathcal{O}(\epsilon^2) . \tag{A.23}$$

Also the next integral, I_{4L4C6}, with

$$I_{4L4C6} = \int dPS_4 \int [dk] \, \frac{1}{k^2\,(k-p_2)^2\,(k+p_4)^2\,(k+p_1+p_4)^2\,(p_1+p_2)^2} \tag{A.24}$$
$$= \frac{e^{i\pi\epsilon}\,\Gamma(2+\epsilon)\Gamma^2(-\epsilon)}{(4\pi)^{D/2}\,\Gamma(-2\epsilon)}\,(q^2)^{-3-\epsilon} \int dPS_4 \int_0^1 dx \int_0^1 dy \, \frac{1}{[x\,y_{24}+y\,y_{14}+xy\,y_{12}]^{2+\epsilon}\,y_{12}},$$

reveals a closed form which, however, turns out to be more complicated. One first integrates over x and y, and finally finds

$$\widetilde{I}_{4L4C6} = \frac{\Gamma(\epsilon)\Gamma^6(1-\epsilon)\Gamma^2(-\epsilon)\Gamma(-1-3\epsilon)}{\Gamma(1-5\epsilon)\Gamma(2-2\epsilon)\Gamma(1-4\epsilon)} \left[-\frac{3}{2}\,\Gamma(1-2\epsilon)\Gamma(\epsilon) - 2\,\Gamma^2(1-2\epsilon)\Gamma(2\epsilon)\Gamma(1+\epsilon) \right.$$
$$-2\Gamma(1-2\epsilon)\Gamma(1+\epsilon)\left(\psi^{(0)}(1-\epsilon) - \psi^{(0)}(\epsilon) - \psi^{(0)}(1-4\epsilon) + 2\psi^{(0)}(1-2\epsilon) + \gamma\right)$$
$$-4\Gamma(-\epsilon)\,{}_3F_2(1,-\epsilon,-\epsilon\,;\,1+\epsilon,1-\epsilon\,;\,1) - \frac{4\Gamma^2(-2\epsilon)}{\Gamma(-3\epsilon)}\,{}_3F_2(-\epsilon,-\epsilon,-\epsilon\,;\,-3\epsilon,1-\epsilon\,;\,1)$$
$$+\frac{\Gamma^2(1-\epsilon)\Gamma(1-4\epsilon)}{(1+\epsilon)^2\Gamma(1-3\epsilon)\Gamma(-2\epsilon)}\,{}_4F_3(1,1-\epsilon,1-\epsilon,1+\epsilon\,;\,2+\epsilon,2+\epsilon,1-3\epsilon\,;\,1)$$
$$\left. -\frac{\Gamma^2(1-2\epsilon)\Gamma(1+\epsilon)}{\Gamma(-2\epsilon)}\,{}_4F_3(1,1,1-2\epsilon,1-2\epsilon\,;\,2,2,1-4\epsilon\,;\,1) \right] , \tag{A.25}$$

where $\psi^{(0)}(z) = \frac{d}{dz}\ln\Gamma(z)$. The expansion of $\widetilde{I}_{4L4C6}$ in ϵ reads

$$\widetilde{I}_{4L4C6} = \frac{5}{6\epsilon^5} - \frac{5}{6\epsilon^4} + \left(\frac{35}{6} - \frac{79\pi^2}{36}\right)\frac{1}{\epsilon^3} + \left(-\frac{65}{6} + \frac{79\pi^2}{36} - 58\zeta_3\right)\frac{1}{\epsilon^2} + \left(\frac{275}{6} - \frac{553\pi^2}{36}\right.$$

JHEP04(2015)168

$$+\frac{643\pi^4}{2160}+58\zeta_3\Big)\frac{1}{\epsilon}+\Big(-\frac{665}{6}+\frac{1027\pi^2}{36}-\frac{643\pi^4}{2160}-406\zeta_3+\frac{1301}{9}\pi^2\zeta_3-\frac{2590}{3}\zeta_5\Big)$$
$$+\Big(\frac{2315}{6}-\frac{4345\pi^2}{36}+\frac{4501\pi^4}{2160}+\frac{63229\pi^6}{272160}+754\zeta_3-\frac{1301}{9}\pi^2\zeta_3+1884\zeta_3^2+\frac{2590}{3}\zeta_5\Big)\epsilon$$
$$+\mathcal{O}(\epsilon^2)\,. \tag{A.26}$$

The next integral, I_{4L4C7}, has not been necessary for the actual calculation of $\widetilde{G}_{17}^{(2)}$ and $\widetilde{G}_{27}^{(2)}$ because it stems from diagrams where the charm quark loop is cut. However, we still give the result, as it is the most complicated integral, and might be useful for future computations of other interferences. The difficulty is due to the fact that one cannot avoid y_{13} in the integrand, and the resulting Mellin-Barnes representation is four-dimensional. Starting from

$$\begin{aligned}I_{4L4C7} &= \int dPS_4 \int [dk]\, \frac{1}{k^2\,(k-p_1)^2\,(k+p_2+p_3+p_4)^2\,(k+p_3+p_4)^2\,(p_1+p_2+p_3)^2}\\ &= \frac{e^{i\pi\epsilon}\,\Gamma(2+\epsilon)\Gamma^2(-\epsilon)}{(4\pi)^{D/2}\,\Gamma(-2\epsilon)}\left(q^2\right)^{-3-\epsilon}\\ &\quad\times\int dPS_4 \int_0^1 dx \int_0^1 dy\, \frac{1}{\left[y_{34}+x\,(y_{13}+y_{14})+y\,(y_{23}+y_{24})+xy\,y_{12}\right]^{2+\epsilon}\,y_{123}}\,,\end{aligned} \tag{A.27}$$

we first integrate over x and y, and find the following Mellin-Barnes representation.

$$\begin{aligned}\widetilde{I}_{4L4C7} &= \frac{\Gamma(\epsilon)\Gamma^5(1-\epsilon)\Gamma(-\epsilon)\Gamma(1-3\epsilon)}{\Gamma(-2\epsilon)\Gamma(2-2\epsilon)}\int_{c_1-i\infty}^{c_1+i\infty}\frac{dz_1}{2\pi i}\int_{c_2-i\infty}^{c_2+i\infty}\frac{dz_2}{2\pi i}\\ &\quad\times\frac{\Gamma(-\epsilon-z_1)\Gamma(1-\epsilon+z_1)\Gamma(1-3\epsilon+z_1-z_2)\Gamma(1-2\epsilon-z_2)\Gamma(-\epsilon-z_1+z_2)}{\Gamma(1-z_2-3\epsilon)\Gamma(1-z_2-4\epsilon)\Gamma(1+z_2-\epsilon)}\\ &\quad\times\frac{\Gamma(-z_1)\Gamma(1+z_1)\Gamma(-z_2)\Gamma(1+z_2)\Gamma(-z_2-\epsilon)\Gamma(z_2-\epsilon)}{\Gamma(1-z_1-3\epsilon)\Gamma(2+z_1-3\epsilon)}\\ &\quad-\frac{2\Gamma(\epsilon)\Gamma^5(1-\epsilon)\Gamma(-\epsilon)\Gamma^2(1-3\epsilon)}{\Gamma(1-5\epsilon)\Gamma(1-2\epsilon)\Gamma(-2\epsilon)\Gamma(2-2\epsilon)}\int_{c_1-i\infty}^{c_1+i\infty}\frac{dz_1}{2\pi i}\int_{c_2-i\infty}^{c_2+i\infty}\frac{dz_2}{2\pi i}\int_{c_3-i\infty}^{c_3+i\infty}\frac{dz_3}{2\pi i}\\ &\quad\times\frac{\Gamma(-z_1)\Gamma(1+z_1-z_3)\Gamma(-z_2)\Gamma(1+z_2)\Gamma(-z_1+z_3-\epsilon)\Gamma(z_2-\epsilon)\Gamma(-z_2-z_3-\epsilon)}{\Gamma(1-z_1+z_2+z_3-4\epsilon)\Gamma(2+z_1-z_3-3\epsilon)}\\ &\quad\times\frac{\Gamma(z_3)\Gamma(1-4\epsilon+z_2+z_3)\Gamma(1-2\epsilon+z_1)\Gamma(-z_1+z_2+z_3-\epsilon)\Gamma(1-\epsilon+z_1-z_3)}{\Gamma(1+z_3-3\epsilon)\Gamma(1+z_2-\epsilon)}\\ &\quad+\frac{\Gamma(\epsilon)\Gamma^5(1-\epsilon)\Gamma(-\epsilon)\Gamma(1-3\epsilon)}{\Gamma(1-5\epsilon)\Gamma(1-2\epsilon)\Gamma(-2\epsilon)\Gamma(2-2\epsilon)}\int_{c_1-i\infty}^{c_1+i\infty}\frac{dz_1}{2\pi i}\int_{c_2-i\infty}^{c_2+i\infty}\frac{dz_2}{2\pi i}\int_{c_3-i\infty}^{c_3+i\infty}\frac{dz_3}{2\pi i}\int_{c_4-i\infty}^{c_4+i\infty}\frac{dz_4}{2\pi i}\\ &\quad\times\frac{\Gamma(-z_3)\Gamma(z_3-z_1)\Gamma(-z_2)\Gamma(1+z_2)\Gamma(-z_4)\Gamma(1+z_1+z_4)\Gamma(z_2-\epsilon)}{\Gamma(1-z_1+z_2+z_3-z_4-4\epsilon)\Gamma(1+z_1-z_3-\epsilon)}\end{aligned}$$

JHEP04(2015)168

$$\times\frac{\Gamma(1-\epsilon+z_1)\Gamma(z_1-z_2-z_3-\epsilon)\Gamma(-z_1+z_3-z_4-\epsilon)\Gamma(-z_1+z_2+z_3-z_4-\epsilon)}{\Gamma(1+z_3-\epsilon)\Gamma(1+z_2-\epsilon)}$$
$$\times\Gamma(-z_1-2\epsilon)\Gamma(1+z_2+z_3-2\epsilon)\Gamma(1+z_1-z_3+z_4-\epsilon)\,. \tag{A.28}$$

The expansion of $\widetilde{I}_{4L4C7}$ in ϵ reads

$$\widetilde{I}_{4L4C7} = -\frac{2\pi^4}{45\epsilon} + \left(-\frac{16\pi^4}{45} + 2\pi^2\zeta_3 - 58\zeta_5\right) + \left(-\frac{104\pi^4}{45} + 16\pi^2\zeta_3 - 464\zeta_5 + 84\zeta_3^2 - \frac{1289\pi^6}{5670}\right)\epsilon + \mathcal{O}(\epsilon^2)\,. \tag{A.29}$$

We have also derived an alternative, seven-fold, Mellin-Barnes representation for $\widetilde{I}_{4L4C7}$ and used it to confirm (A.29) numerically with the help of the code `MB.m` [67].

The last integral, I_{4L4C8}, reads

$$I_{4L4C8} = \int dPS_4 \int [dk]\, \frac{1}{k^2\,(k+p_1+p_2+p_4)^2\,(k+p_1+p_2)^2\,(p_1+p_3+p_4)^2} \tag{A.30}$$
$$= \frac{e^{i\pi\epsilon}\,\Gamma(1+\epsilon)\Gamma(-\epsilon)\Gamma(1-\epsilon)}{(4\pi)^{D/2}\,\Gamma(1-2\epsilon)}\left(q^2\right)^{-2-\epsilon}\int dPS_4 \int_0^1 dx\, \frac{1}{\left[y_{12}+x\,y_{14}+x\,y_{24}\right]^{1+\epsilon}\,y_{134}}.$$

Again, one first integrates over x, and finally finds an expression involving a one-dimensional Feynman parameter integral

$$\widetilde{I}_{4L4C8} = \frac{\Gamma(1-3\epsilon)\Gamma(1-2\epsilon)\Gamma^4(1-\epsilon)\Gamma^4(-\epsilon)\Gamma(2\epsilon)\Gamma^3(1+\epsilon)}{\Gamma(2-5\epsilon)\Gamma(2-4\epsilon)\Gamma(2-2\epsilon)\Gamma(3\epsilon)}$$
$$+\frac{\Gamma^2(1-3\epsilon)\Gamma(1-2\epsilon)\Gamma^4(1-\epsilon)\Gamma^3(-\epsilon)\Gamma^2(1+\epsilon)\Gamma(2\epsilon)}{\Gamma(2-5\epsilon)\Gamma(2-4\epsilon)\Gamma(2-2\epsilon)}$$
$$-\frac{\Gamma(1-3\epsilon)\Gamma^5(1-\epsilon)\Gamma^4(-\epsilon)\Gamma(1+\epsilon)}{2\,\Gamma(2-5\epsilon)\Gamma(2-4\epsilon)\Gamma(2-2\epsilon)}\,{}_3F_2(1,1-\epsilon,2\epsilon\,;\,1+\epsilon,1+2\epsilon\,;\,1)$$
$$-\frac{\Gamma(1-3\epsilon)\Gamma^7(1-\epsilon)\Gamma^2(-\epsilon)\Gamma(\epsilon)}{2\,\Gamma(3-5\epsilon)\Gamma^2(2-2\epsilon)\Gamma(-2\epsilon)}$$
$$\times\int_0^1 dt\; t^{1-2\epsilon}\,(1-t)^{-\epsilon}\;{}_2F_1(1,2-4\epsilon\,;\,3-5\epsilon\,;\,t)\;{}_2F_1(1,1-\epsilon\,;\,2-2\epsilon\,;\,t)\,. \tag{A.31}$$

The expansion of $\widetilde{I}_{4L4C8}$ in ϵ reads

$$\widetilde{I}_{4L4C8} = -\frac{\zeta_3}{\epsilon} + \left(-11\zeta_3 - \frac{19\pi^4}{360}\right) + \left(-83\zeta_3 + \frac{23\pi^2\zeta_3}{6} - 36\zeta_5 - \frac{209\pi^4}{360}\right)\epsilon$$
$$+\left(-535\zeta_3 + \frac{253\pi^2\zeta_3}{6} + 70\zeta_3^2 - 396\zeta_5 - \frac{1577\pi^4}{360} + \frac{13\pi^6}{378}\right)\epsilon^2 + \mathcal{O}(\epsilon^3)\,. \tag{A.32}$$

A.2 Results for the three-particle-cut master integrals

In this section, we describe our computation of the three-particle-cut diagrams 4L3C1, 4L3C2 and 4L3C3. Similarly to eq. (A.10), we extract the normalization factors according to

$$I_{4L3Ci} = 2\pi\, e^{2\pi i\epsilon}\, S_\Gamma^4\, \left(q^2\right)^{b_i-4\epsilon}\, \widetilde{I}_{4L3Ci}\,, \tag{A.33}$$

JHEP04(2015)168

where the b_i again follow from dimensional considerations. One finds $b_1 = 0$ and $b_2 = -1$. For 4L3C3, we have used a different method, as explained below.

The kinematics and the phase space measure are much simpler in the three-particle case, compared to the four-particle one. The total momentum is $q = p_1 + p_2 + p_3$, and we have $p_i^2 = 0$ for $i = 1, \ldots, 3$. We define the invariants

$$s_{ijk\ldots} \equiv (p_i + p_j + p_k + \ldots)^2 \tag{A.34}$$

as before, and have $s_{12}+s_{13}+s_{23} = q^2$ as a constraint from overall momentum conservation. The phase space measure

$$dPS_3 = \frac{d^{D-1}p_1}{(2\pi)^{D-1}\,2E_1} \cdots \frac{d^{D-1}p_3}{(2\pi)^{D-1}\,2E_3}\,(2\pi)^D\,\delta^{(D)}(q - p_1 - p_2 - p_3) \tag{A.35}$$

is again taken over from ref. [57]. After integration over angular variables one finds

$$dPS_3 = \frac{2\pi\,S_\Gamma^2\,\Gamma^2(1-\epsilon)\,\left(q^2\right)^{1-2\epsilon}}{\Gamma(2-2\epsilon)}\,dy_{12}\,dy_{13}\,dy_{23}\,y_{12}^{-\epsilon}\,y_{13}^{-\epsilon}\,y_{23}^{-\epsilon}\,\delta(1 - y_{12} - y_{13} - y_{23}).$$

The integration variables y_{12}, y_{13}, and y_{23} run from $0 \ldots 1$, and originate from $s_{ij} = q^2\,y_{ij}$. The latter substitutions have to be made in the integrands, as well.

Our first three-particle-cut integral I_{4L3C1} reads

$$\begin{aligned} I_{4L3C1} &= \int dPS_3 \int [dk_1] \int [dk_2]\,\frac{1}{k_1^2\,(k_1+p_1)^2\,k_2^2\,(k_2+p_3)^2\,(k_1+k_2-p_2)^2} \\ &= \frac{e^{2\pi i\epsilon}\,S_\Gamma^2\,\Gamma^2(-\epsilon)\Gamma^3(1-\epsilon)\Gamma(1+2\epsilon)}{\Gamma(1-3\epsilon)}\left(q^2\right)^{-1-2\epsilon} \\ &\quad \times \int dPS_3 \int_0^1 dx \int_0^1 dy\,\frac{1}{[x\,y_{12} + x\,y\,y_{13} + y\,y_{23}]^{1+2\epsilon}}\,. \end{aligned} \tag{A.36}$$

It can be expressed in a closed form valid to all orders in ϵ. One first integrates over x, and finally finds

$$\begin{aligned} \widetilde{I}_{4L3C1} &= -\frac{3\,\Gamma(1-2\epsilon)\Gamma(-3\epsilon)\Gamma^2(-\epsilon)\Gamma(\epsilon)\Gamma(2\epsilon)\Gamma(2\epsilon+1)\Gamma^5(1-\epsilon)}{2\,\Gamma(2-5\epsilon)\Gamma(2-2\epsilon)} \\ &\quad + \frac{\Gamma^4(-\epsilon)\Gamma(2\epsilon)\Gamma^5(1-\epsilon)}{(2\epsilon-1)^2\,\Gamma(2-5\epsilon)\Gamma(-2\epsilon)}\;{}_3F_2(1, 1-\epsilon, 1-2\epsilon\,;\,2-2\epsilon, 1+\epsilon\,;\,1) \\ &\quad + \frac{\Gamma^2(1-2\epsilon)\Gamma^4(-\epsilon)\Gamma(1+\epsilon)\Gamma(2\epsilon)\Gamma^4(1-\epsilon)}{\Gamma(2-4\epsilon)\Gamma(1-3\epsilon)\Gamma(2-2\epsilon)}\;{}_3F_2(\epsilon, 1-2\epsilon, 1-2\epsilon\,;\,2-4\epsilon, 1+\epsilon\,;\,1) \\ &\quad - \frac{\Gamma(1-2\epsilon)\Gamma^5(-\epsilon)\Gamma(2\epsilon)\Gamma^5(1-\epsilon)}{4\,\Gamma(1-3\epsilon)\Gamma(2-3\epsilon)\Gamma(2-2\epsilon)\Gamma(-2\epsilon)}\;{}_4F_3(1, 2\epsilon, 1-\epsilon, 1-\epsilon\,;\,2-3\epsilon, 1+\epsilon, 1+2\epsilon\,;\,1)\,. \end{aligned} \tag{A.37}$$

The expansion of $\widetilde{I}_{4L3C1}$ in ϵ reads

$$\widetilde{I}_{4L3C1} = \frac{2\zeta_3}{\epsilon^2} + \left(14\zeta_3 + \frac{\pi^4}{9}\right)\frac{1}{\epsilon} + \left(78\zeta_3 + \frac{7\pi^4}{9} - 6\pi^2\zeta_3 + 78\zeta_5\right)$$

JHEP04(2015)168

$$+\left(406\zeta_3+\frac{13\pi^4}{3}-42\pi^2\zeta_3+546\zeta_5+\frac{5\pi^6}{63}-140\zeta_3^2\right)\epsilon+\mathcal{O}(\epsilon^2)\,. \quad \text{(A.38)}$$

The next three-particle-cut integral is I_{4L3C2},

$$I_{4L3C2}=\int dPS_3\int[dk_1]\int[dk_2]\,\frac{1}{(k_1+p_1+p_2)^2\,k_1^2\,(k_1-k_2+p_1)^2\,(k_1-k_2)^2\,(k_2+p_2)^2\,k_2^2}\,. \quad \text{(A.39)}$$

Despite the fact that p_3 does not appear in the integrand, the result of the integral is quite lengthy. In the end, we find the following expression that involves a one-dimensional Feynman parameter integral:

$$\begin{aligned}
\widetilde{I}_{4L3C2}=&\frac{\Gamma(-3\epsilon-1)\Gamma(-\epsilon)\Gamma(\epsilon)\Gamma^6(1-\epsilon)\Gamma^3(-2\epsilon)\Gamma^2(1+2\epsilon)}{\Gamma(1-5\epsilon)\Gamma(2-2\epsilon)\Gamma(-4\epsilon)}\\
&+\frac{\Gamma(-3\epsilon-1)\Gamma^2(-\epsilon)\Gamma(2\epsilon)\Gamma^7(1-\epsilon)\Gamma(-2\epsilon)}{\Gamma(1-5\epsilon)\Gamma(2-2\epsilon)\Gamma(1-4\epsilon)\Gamma(-3\epsilon)\Gamma(2+2\epsilon)}\,{}_3F_2(1,1,1-\epsilon\,;\,1-4\epsilon,2+2\epsilon\,;\,1)\\
&-\frac{\Gamma(-3\epsilon-1)\Gamma^3(-\epsilon)\Gamma^2(1+2\epsilon)\Gamma^7(1-\epsilon)\Gamma^2(-2\epsilon)}{\Gamma(1-5\epsilon)\Gamma(2-2\epsilon)\Gamma(1-2\epsilon)\Gamma^2(-3\epsilon)\Gamma(2+2\epsilon)}\,{}_3F_2(1,1,1-\epsilon\,;\,1-2\epsilon,2+2\epsilon\,;\,1)\\
&+\frac{\Gamma(-3\epsilon-1)\Gamma^2(-\epsilon)\Gamma(2\epsilon)\Gamma^6(1-\epsilon)\Gamma(-2\epsilon)}{\Gamma(1-5\epsilon)\Gamma(2-2\epsilon)\Gamma^2(-3\epsilon)\Gamma(2+2\epsilon)}\int_0^1 dt\;t^{-\epsilon}\;(1-t)^{-3\epsilon-1}\\
&\times\left[{}_2F_1(-2\epsilon,-2\epsilon\,;\,1-2\epsilon\,;\,1-t)-1\right]\,{}_2F_1(1,1\,;\,2+2\epsilon\,;\,t)\\
&-\frac{2\,\Gamma(-3\epsilon-1)\Gamma^2(-\epsilon)\Gamma^2(1+2\epsilon)\Gamma^6(1-\epsilon)\Gamma^2(-2\epsilon)}{\Gamma(1-5\epsilon)\Gamma(2-2\epsilon)\Gamma^2(-3\epsilon)\Gamma(2+2\epsilon)}\int_0^1 dt\;t^{-\epsilon}\;(1-t)^{-\epsilon-1}\\
&\times\left[{}_2F_1(-2\epsilon,-2\epsilon\,;\,-3\epsilon\,;\,1-t)-1\right]\,{}_2F_1(1,1\,;\,2+2\epsilon\,;\,t)\\
&+\frac{\Gamma(-3\epsilon-1)\Gamma^2(-\epsilon)\Gamma^2(1+2\epsilon)\Gamma^6(1-\epsilon)\Gamma(-2\epsilon)}{\Gamma(1-5\epsilon)\Gamma(2-2\epsilon)\Gamma^2(-3\epsilon)\Gamma^2(2+2\epsilon)}\int_0^1 dt\;t^{1+\epsilon}\;(1-t)^{-3\epsilon-1}\\
&\times\left[{}_2F_1(-2\epsilon,-2\epsilon\,;\,-3\epsilon\,;\,1-t)-1\right]\,\left[{}_2F_1(1,1\,;\,2+2\epsilon\,;\,t)\right]^2\,. \qquad \text{(A.40)}
\end{aligned}$$

The expansion of $\widetilde{I}_{4L3C2}$ in ϵ reads

$$\begin{aligned}
\widetilde{I}_{4L3C2}=&\frac{1}{3\epsilon^5}-\frac{1}{3\epsilon^4}+\left(\frac{7}{3}-\frac{13\pi^2}{18}\right)\frac{1}{\epsilon^3}+\left(\frac{13\pi^2}{18}-\frac{13}{3}-\frac{61}{3}\zeta_3\right)\frac{1}{\epsilon^2}+\left(\frac{55}{3}-\frac{91\pi^2}{18}-\frac{11\pi^4}{180}\right.\\
&\left.+\frac{61}{3}\zeta_3\right)\frac{1}{\epsilon}+\left(\frac{169\pi^2}{18}-\frac{133}{3}+\frac{11\pi^4}{180}-\frac{427}{3}\zeta_3+\frac{353}{9}\pi^2\zeta_3-233\zeta_5\right)\\
&+\left(\frac{463}{3}-\frac{715\pi^2}{18}-\frac{77\pi^4}{180}+\frac{17\pi^6}{140}+\frac{793}{3}\zeta_3-\frac{353}{9}\pi^2\zeta_3+\frac{1763}{3}\zeta_3^2+233\zeta_5\right)\epsilon\\
&+\mathcal{O}(\epsilon^2)\,. \qquad \text{(A.41)}
\end{aligned}$$

For the last integral I_{4L3C3}, we employ a different approach. Due to the structure of the integrand, it is not possible to find a regulated Mellin-Barnes representation. Therefore, we begin with evaluating an integral $I_{4L3C3'}$ defined as

$$I_{4L3C3'}=\int dPS_3\int[dk_1]\int[dk_2]\,\frac{1}{[(k_1+k_2)^2]^2\;(k_2+p_2)^2\,k_1^2\,(k_1+p_3)^2\,(k_1+p_1+p_3)^2\,s_{12}}$$

JHEP04(2015)168

$$= \frac{e^{2\pi i\epsilon}\, S_\Gamma^2\, \Gamma^2(-\epsilon)\Gamma^3(1-\epsilon)\Gamma(2+2\epsilon)\Gamma(-2\epsilon)}{\Gamma(1-2\epsilon)\Gamma(-3\epsilon)} \left(q^2\right)^{-3-2\epsilon}$$
$$\times \int dPS_3 \int_0^1 dx \int_0^1 dy\, \frac{y^\epsilon}{[x\, y\, y_{12} + x\, y_{13} + y\, y_{23}]^{2+2\epsilon}\; y_{12}} \,. \tag{A.42}$$

Again, we extract the normalization factor according to

$$I_{4L3C3'} = 2\pi\, e^{2\pi i\epsilon}\, S_\Gamma^4 \left(q^2\right)^{-2-4\epsilon}\, \widetilde{I}_{4L3C3'} \,, \tag{A.43}$$

The above quantity can be expressed in terms of a one-dimensional Feynman parameter integral as follows:

$$\begin{aligned}\widetilde{I}_{4L3C3'} = {} & \frac{3\,\Gamma^4(-\epsilon)\Gamma(2\epsilon)\Gamma^6(1-\epsilon)}{4\,\Gamma^2(1-3\epsilon)\Gamma(2-2\epsilon)} - \frac{5\,\Gamma^2(1-2\epsilon)\Gamma^5(1-\epsilon)\Gamma^3(-\epsilon)\Gamma^2(2\epsilon)\Gamma(1+\epsilon)}{2\,\Gamma(1-5\epsilon)\Gamma(2-2\epsilon)} \\ & + \frac{5\,\Gamma^4(1-\epsilon)\Gamma^5(-\epsilon)\Gamma(1+2\epsilon)}{2\,\Gamma(1-5\epsilon)\Gamma(2-2\epsilon)}\, {}_3F_2(1,-\epsilon,-\epsilon\,;\,1-\epsilon,1+\epsilon\,;\,1) \\ & + \frac{3\,\Gamma^6(1-\epsilon)\Gamma^3(-\epsilon)\Gamma(2\epsilon)}{2\,\Gamma(1-3\epsilon)\Gamma(1-2\epsilon)\Gamma(2-2\epsilon)} \int_0^1 dt\; t^{-2\epsilon}\, (1-t)^{-2\epsilon-1} \\ & \times \left[{}_2F_1(1,-5\epsilon\,;\,1-2\epsilon\,;\,1-t) - 1\right]\, {}_2F_1(-\epsilon,-2\epsilon\,;\,1-2\epsilon\,;\,t) \,.\end{aligned} \tag{A.44}$$

The expansion of $\widetilde{I}_{4L3C3'}$ in ϵ reads

$$\begin{aligned}\widetilde{I}_{4L3C3'} = \frac{1}{(1-2\epsilon)} \Bigg[& -\frac{3}{2\epsilon^5} + \frac{37\pi^2}{12\epsilon^3} + \frac{100\zeta_3}{\epsilon^2} + \frac{149\pi^4}{80\epsilon} + 1727\zeta_5 - \frac{505}{3}\pi^2\zeta_3 \\ & + \left(\frac{186493\pi^6}{90720} - 2680\zeta_3^2\right)\epsilon + \mathcal{O}(\epsilon^2)\Bigg] \,.\end{aligned} \tag{A.45}$$

The original integral I_{4L3C3} can then be obtained by relating it to $I_{4L3C3'}$ with the help of integration-by-parts identities.

B Relation to ref. [43]

Several decimal numbers in subsection 2.1 can be related to the quantities encountered in ref. [43] as follows. In the finite part of $\hat{G}_{47}^{(1)\text{bare}}$ in eq. (2.4), we have

$$\begin{aligned} 43.76456245573869 = Y_1 \;&\equiv\; \frac{19039}{486} + \frac{11}{27}\pi^2 - \frac{\pi}{9\sqrt{3}} - \frac{16}{27}X_b + \frac{1}{6}\mathrm{Re}[a(1) - 2b(1)], \\ 0.04680853247986 = Y_2 \;&\equiv\; 2\mathrm{Re}\, b(1) - \frac{4}{243}, \end{aligned} \tag{B.1}$$

where

$$\begin{aligned} X_b &= -\frac{9}{8} - \frac{\pi^2}{5} - \frac{2}{3}\zeta_3 + \frac{1}{10}\,\psi^{(1)}\left(\frac{1}{6}\right), \\ \mathrm{Re}\, a(1) &= \frac{16}{3} + \frac{164}{405}\pi^2 - \frac{16}{9}\zeta_3 - \frac{300\pi + 64\pi^3}{135\sqrt{3}} + \frac{32\pi\sqrt{3} - 72}{405}\,\psi^{(1)}\left(\frac{1}{6}\right), \end{aligned}$$

JHEP04(2015)168

$$\mathrm{Re}\, b(1) = \frac{320}{81} + \frac{632}{1215}\pi^2 - \frac{4\pi}{3\sqrt{3}} - \frac{8}{45}\,\psi^{(1)}\left(\frac{1}{6}\right), \tag{B.2}$$

and

$$\psi^{(1)}(z) = \frac{d^2}{dz^2}\ln\Gamma(z). \tag{B.3}$$

The above exact expressions for X_b and $\mathrm{Re}\, a(1)$ are new. They come from the three-fold Feynman parameter integrals in eqs. (3.2) and (3.3) of ref. [43].

In the $\frac{1}{\epsilon}$-part of $\widetilde{G}_{27}^{(2)\mathrm{bare}}$ in eq. (2.3), we have

$$\begin{aligned} -67.66077706444119 &= -\frac{2}{3}Y_1 - \frac{103762}{2187} + \frac{44}{27}\pi^2 - \frac{160}{27}\zeta_3, \\ 5.17409838118169 &= -\frac{2}{3}Y_2 + \frac{11384}{2187}. \end{aligned} \tag{B.4}$$

Finally, in the coefficients multiplying $\ln(\mu/m_b)$ in eq. (2.11), we have

$$\begin{aligned} 1.0460332197 &= -\frac{4}{3}Y_1 - \frac{37708}{729} + \frac{304}{27}\pi^2, \\ 9.6604967166 &= -\frac{4}{3}Y_2 + \frac{7088}{729}. \end{aligned} \tag{B.5}$$

C NLO results of relevance for section 3

The NLO quantities $K_{ij}^{(1)}$ that occur in eq. (3.8) are given by

$$\begin{aligned} K_{27}^{(1)} &= -6K_{17}^{(1)} = \mathrm{Re}\, r_2^{(1)} - \frac{208}{81}L_b + 2\phi_{27}^{(1)}(\delta), \\ K_{47}^{(1)} &= \mathrm{Re}\, r_4^{(1)} + \frac{76}{243}L_b + 2\phi_{47}^{(1)}(\delta), \\ K_{77}^{(1)} &= -\frac{182}{9} + \frac{8}{9}\pi^2 - \frac{32}{3}L_b + 4\,\phi_{77}^{(1)}(\delta), \\ K_{78}^{(1)} &= \frac{44}{9} - \frac{8}{27}\pi^2 + \frac{16}{9}L_b + 2\,\phi_{78}^{(1)}(\delta), \end{aligned} \tag{C.1}$$

where $r_2^{(1)}$ and $r_4^{(1)}$ can be found in eq. (3.1) of ref. [43]. The function $\phi_{27}^{(1)}$ has been already given in eq. (3.5) here. The remaining ones read

$$\begin{aligned} \phi_{77}^{(1)} &= -\frac{2}{3}\ln^2\delta - \frac{7}{3}\ln\delta - \frac{31}{9} + \frac{10}{3}\delta + \frac{1}{3}\delta^2 - \frac{2}{9}\delta^3 + \frac{1}{3}\delta(\delta-4)\ln\delta, \\ \phi_{78}^{(1)} &= \frac{8}{9}\left[\mathrm{Li}_2(1-\delta) - \frac{1}{6}\pi^2 - \delta\ln\delta + \frac{9}{4}\delta - \frac{1}{4}\delta^2 + \frac{1}{12}\delta^3\right], \\ \phi_{47}^{(1)}(\delta) &= \phi_{47}^{(1)A}(\delta) + \phi_{47}^{(1)B}(\delta), \end{aligned} \tag{C.2}$$

where[12]

$$\phi_{47}^{(1)A}(\delta) = \frac{1}{54}\pi\left(3\sqrt{3}-\pi\right) + \frac{1}{81}\delta^3 - \frac{25}{108}\delta^2 + \frac{5}{54}\delta + \frac{2}{9}\left(\delta^2+2\delta+3\right)\arctan^2\sqrt{\frac{1-\delta}{3+\delta}}$$

[12] Eq. (3.12) of ref. [34] gives $\phi_{47}^{(1)A}$ only, and contains a misprint in the coefficient at $\lim_{m_c\to m_b}$.

JHEP04(2015)168

$$-\frac{1}{3}\left(\delta^2+4\delta+3\right)\sqrt{\frac{1-\delta}{3+\delta}}\,\arctan\sqrt{\frac{1-\delta}{3+\delta}},$$

$$\phi_{47}^{(1)B}(\delta) = \frac{34\,\delta^2+59\,\delta-18}{486}\,\frac{\delta^2\ln\delta}{1-\delta} + \frac{433\,\delta^3+429\,\delta^2-720\,\delta}{2916}. \tag{C.3}$$

The latter function is a new result from ref. [24] that originates from $sq\bar{q}\gamma$ final states ($q = u, d, s$). Contributions to $b \to X_s^p\gamma$ from such final states at the NLO have been neglected in the previous literature because they are suppressed by phase space factors and the small Wilson coefficients $C_{3,\ldots,6}$.

D Input parameters

In this appendix, we collect numerical values of the parameters that matter for our branching ratio calculation in section 4. The photon energy cut is set to $E_0 = 1.6\,\text{GeV}$. Our central values for the renormalization scales are $\mu_b = \mu_c = 2.0$ GeV and $\mu_0 = 160$ GeV.

Masses of the b and c quarks together with the semileptonic $B \to X_c\ell\bar{\nu}$ branching ratio $\mathcal{B}_{c\ell\bar{\nu}}$ and several non-perturbative parameters are adopted from the very recent analysis in ref. [49].[13] In that work, fits to the measured semileptonic decay spectra have been performed with optional inclusion of constraints from the b-hadron spectroscopy, as well as from the quark mass determinations utilizing moments of $R(e^+e^- \to \text{hadrons})$ [71]. While m_c is $\overline{\text{MS}}$-renormalized, m_b and the non-perturbative parameters are treated in the kinetic scheme. We choose the option where both m_b and m_c are constrained by $R(e^+e^- \to \text{hadrons})$, and $m_c(2\,\text{GeV})$ is used in the fit. Once the parameters are ordered as $\{m_{b,\text{kin}},\ m_c(2\,\text{GeV}),\ \mu_\pi^2,\ \rho_D^3,\ \mu_G^2,\ \rho_{LS}^3,\ \mathcal{B}_{c\ell\bar{\nu}}\}$ (expressed in GeV raised to appropriate powers), their central values $\vec{x}$, uncertainties $\vec{\sigma}$, and the correlation matrix $\hat{R}$ read [53]

$$\vec{x} = \begin{pmatrix} 4.564 & 1.087 & 0.470 & 0.171 & 0.309 & -0.135 & 10.67 \end{pmatrix},$$

$$\vec{\sigma} = \begin{pmatrix} 0.017 & 0.013 & 0.067 & 0.039 & 0.058 & 0.095 & 0.16 \end{pmatrix},$$

$$\hat{R} = \begin{pmatrix} 1.000 & 0.461 & -0.087 & 0.114 & 0.542 & -0.157 & -0.061 \\ 0.461 & 1.000 & -0.002 & -0.020 & -0.125 & 0.036 & 0.029 \\ -0.087 & -0.002 & 1.000 & 0.724 & -0.024 & 0.049 & 0.153 \\ 0.114 & -0.020 & 0.724 & 1.000 & -0.101 & -0.135 & 0.076 \\ 0.542 & -0.125 & -0.024 & -0.101 & 1.000 & -0.011 & -0.009 \\ -0.157 & 0.036 & 0.049 & -0.135 & -0.011 & 1.000 & -0.023 \\ -0.061 & 0.029 & 0.153 & 0.076 & -0.009 & -0.023 & 1.000 \end{pmatrix}. \tag{D.1}$$

Apart from the above parameters, the analysis of ref. [49] serves us as a source of a numerical formula for the semileptonic phase-space factor

$$C = \left|\frac{V_{ub}}{V_{cb}}\right|^2 \frac{\Gamma[\bar{B} \to X_c e\bar{\nu}]}{\Gamma[\bar{B} \to X_u e\bar{\nu}]}, \tag{D.2}$$

[13] See also the previous version [70] where more details on the method are given.

JHEP04(2015)168

which reads [53]

$$C = g(z)\ \{0.903 - 0.588\,[\alpha_s(4.6\,\mathrm{GeV}) - 0.22] + 0.0650\,[m_{b,\mathrm{kin}} - 4.55] \\ - 0.1080\,[m_c(2\,\mathrm{GeV}) - 1.05] - 0.0122\,\mu_G^2 - 0.199\,\rho_D^3 + 0.004\,\rho_{LS}^3\}\,, \tag{D.3}$$

where $g(z) = 1 - 8z + 8z^3 - z^4 - 12z^2 \ln z$ and $z = m_c^2(2\,\mathrm{GeV})/m_{b,\mathrm{kin}}^2$. Next, we use C in the expression [72]

$$\mathcal{B}_{s\gamma}(E_\gamma > E_0) = \mathcal{B}_{c\ell\bar{\nu}} \left|\frac{V_{ts}^* V_{tb}}{V_{cb}}\right|^2 \frac{6\alpha_{\mathrm{em}}}{\pi\, C}\,[P(E_0) + N(E_0)]\,, \tag{D.4}$$

to determine the radiative branching ratio. Known contributions to the non-perturbative correction $N(E_0)$ are given in terms of μ_π^2, ρ_D^3, μ_G^2 and ρ_{LS}^3. The semileptonic branching ratio $\mathcal{B}_{c\ell\bar{\nu}}$ is CP- and isospin-averaged analogously to eq. (1.3), while the isospin asymmetry effects in both decay rates are negligible. Thus, neither the lifetimes nor the production rates need to be considered among our inputs.

The remaining parameters that are necessary to determine $P(E_0)$ and the overall factor in eq. (D.4) are as follows:

$$\alpha_{\mathrm{em}}(0) = 1/137.036, \qquad M_Z = 91.1876\ \mathrm{GeV}, \qquad M_W = 80.385\ \mathrm{GeV}\ [13],$$
$$\alpha_s(M_Z) = 0.1185 \pm 0.0006\ [13], \quad m_{t,\mathrm{pole}} = (173.21 \pm 0.51 \pm 0.71)\ \mathrm{GeV}\ [13],$$
$$\left|\frac{V_{ts}^* V_{tb}}{V_{cb}}\right|^2 = 0.9626 \pm 0.0012\ [73], \qquad \frac{m_b}{m_q} \in (10, 50). \tag{D.5}$$

For the electroweak and $\mathcal{O}(V_{ub})$ corrections to $P(E_0)$, we also need

$$\alpha_{\mathrm{em}}(M_Z) = 1/128.940, \qquad \sin^2\theta_W = 0.23126\ [13],$$
$$M_{\mathrm{Higgs}} = 125.7\mathrm{GeV}\ [13], \qquad \frac{V_{us}^* V_{ub}}{V_{ts}^* V_{tb}} = -0.0080 + 0.018\,i\ [73]. \tag{D.6}$$

The quark mass ratio m_b/m_q ($q = u, d, s$) in eq. (D.5) serves as a collinear regulator wherever necessary. Fortunately, the dominant contributions to $\Gamma(b \to X_s^p\gamma)$ are IR-safe, while all the quantities requiring such a collinear regulator contribute at a sub-percent level only. They undergo suppression by various multiplicative factors ($C_{3,\ldots,6}$, $Q_d^2\alpha_s/\pi$, etc.), and by phase-space restrictions following from the relatively high $E_0 \sim m_b/3$. Changing m_b/m_q from 10 to 50 affects the branching ratio by around 0.7% only. We include this effect in our parametric uncertainty even though the dependence on m_b/m_q is spurious, i.e. it should cancel out once the non-perturbative correction calculations are upgraded to take collinear photon emission into account (see refs. [38, 74, 75]). Thus, the parametric uncertainty due to m_b/m_q might alternatively be absorbed into the overall $\pm 5\%$ non-perturbative error [14]. Our range for m_b/m_q roughly corresponds to the range $[m_B/m_K, m_B/m_\pi]$, which is motivated by the fact that light hadron masses are the physical collinear regulators in our case.

All the uncertainties except for those in eq. (D.1) are treated as uncorrelated. One should remember though that the dependence of C on α_s is taken into account via eq. (D.3).

JHEP04(2015)168

Open Access. This article is distributed under the terms of the Creative Commons Attribution License (CC-BY 4.0), which permits any use, distribution and reproduction in any medium, provided the original author(s) and source are credited.

References

[1] CLEO collaboration, S. Chen et al., *Branching fraction and photon energy spectrum for $b \to s\gamma$*, *Phys. Rev. Lett.* **87** (2001) 251807 [hep-ex/0108032] [INSPIRE].

[2] Belle collaboration, K. Abe et al., *A measurement of the branching fraction for the inclusive $B \to X_s\gamma$ decays with BELLE*, *Phys. Lett.* **B 511** (2001) 151 [hep-ex/0103042] [INSPIRE].

[3] Belle collaboration, A. Limosani et al., *Measurement of inclusive radiative B-meson decays with a photon energy threshold of* 1.7 *GeV*, *Phys. Rev. Lett.* **103** (2009) 241801 [arXiv:0907.1384] [INSPIRE].

[4] BaBar collaboration, J.P. Lees et al., *Precision measurement of the $B \to X_s\gamma$ photon energy spectrum, branching fraction and direct CP asymmetry $A_{\rm CP}(B \to X_{s+d}\gamma)$*, *Phys. Rev. Lett.* **109** (2012) 191801 [arXiv:1207.2690] [INSPIRE].

[5] BaBar collaboration, J.P. Lees et al., *Measurement of $B(B \to X_s\gamma)$, the $B \to X_s\gamma$ photon energy spectrum and the direct CP asymmetry in $B \to X_{s+d}\gamma$ decays*, *Phys. Rev.* **D 86** (2012) 112008 [arXiv:1207.5772] [INSPIRE].

[6] BaBar collaboration, J.P. Lees et al., *Exclusive measurements of $b \to s\gamma$ transition rate and photon energy spectrum*, *Phys. Rev.* **D 86** (2012) 052012 [arXiv:1207.2520] [INSPIRE].

[7] BaBar collaboration, B. Aubert et al., *Measurement of the $B \to X_s\gamma$ branching fraction and photon energy spectrum using the recoil method*, *Phys. Rev.* **D 77** (2008) 051103 [arXiv:0711.4889] [INSPIRE].

[8] Heavy Flavor Averaging Group (HFAG) collaboration, Y. Amhis et al., *Averages of b-hadron, c-hadron and τ-lepton properties as of summer* 2014, arXiv:1412.7515 [INSPIRE].

[9] Belle collaboration, T. Saito et al., *Measurement of the $\bar{B} \to X_s\gamma$ branching fraction with a sum of exclusive decays*, *Phys. Rev.* **D 91** (2015) 052004 [arXiv:1411.7198] [INSPIRE].

[10] T. Aushev et al., *Physics at super B factory*, arXiv:1002.5012 [INSPIRE].

[11] Belle-II collaboration, T. Abe et al., *Belle II technical design report*, arXiv:1011.0352 [INSPIRE].

[12] BaBar collaboration, B. Aubert et al., *Measurements of the $B \to X_s\gamma$ branching fraction and photon spectrum from a sum of exclusive final states*, *Phys. Rev.* **D 72** (2005) 052004 [hep-ex/0508004] [INSPIRE].

[13] Particle Data Group collaboration, K.A. Olive et al., *Review of particle physics*, *Chin. Phys.* **C 38** (2014) 090001 [INSPIRE].

[14] M. Benzke, S.J. Lee, M. Neubert and G. Paz, *Factorization at subleading power and irreducible uncertainties in $\bar{B} \to X_s\gamma$ decay*, *JHEP* **08** (2010) 099 [arXiv:1003.5012] [INSPIRE].

[15] C. Bobeth, M. Misiak and J. Urban, *Photonic penguins at two loops and m_t dependence of $BR[B \to X_s\ell^+\ell^-]$*, *Nucl. Phys.* **B 574** (2000) 291 [hep-ph/9910220] [INSPIRE].

[16] M. Misiak and M. Steinhauser, *Three loop matching of the dipole operators for $b \to s\gamma$ and $b \to sg$*, *Nucl. Phys.* **B 683** (2004) 277 [hep-ph/0401041] [INSPIRE].

JHEP04(2015)168

[17] M. Gorbahn and U. Haisch, *Effective Hamiltonian for non-leptonic $|\Delta F| = 1$ decays at NNLO in QCD*, *Nucl. Phys.* **B 713** (2005) 291 [hep-ph/0411071] [INSPIRE].

[18] M. Gorbahn, U. Haisch and M. Misiak, *Three-loop mixing of dipole operators*, *Phys. Rev. Lett.* **95** (2005) 102004 [hep-ph/0504194] [INSPIRE].

[19] M. Czakon, U. Haisch and M. Misiak, *Four-loop anomalous dimensions for radiative flavour-changing decays*, *JHEP* **03** (2007) 008 [hep-ph/0612329] [INSPIRE].

[20] T. Hermann, M. Misiak and M. Steinhauser, *$\bar{B} \to X_s\gamma$ in the two Higgs doublet model up to next-to-next-to-leading order in QCD*, *JHEP* **11** (2012) 036 [arXiv:1208.2788] [INSPIRE].

[21] A.J. Buras, M. Misiak, M. Münz and S. Pokorski, *Theoretical uncertainties and phenomenological aspects of $B \to X_s\gamma$ decay*, *Nucl. Phys.* **B 424** (1994) 374 [hep-ph/9311345] [INSPIRE].

[22] K.G. Chetyrkin, M. Misiak and M. Münz, *Weak radiative B meson decay beyond leading logarithms*, *Phys. Lett.* **B 400** (1997) 206 [*Erratum ibid.* **B 425** (1998) 414] [hep-ph/9612313] [INSPIRE].

[23] M. Kamiński, M. Misiak and M. Poradziński, *Tree-level contributions to $B \to X_s\gamma$*, *Phys. Rev.* **D 86** (2012) 094004 [arXiv:1209.0965] [INSPIRE].

[24] T. Huber, M. Poradziński and J. Virto, *Four-body contributions to $\bar{B} \to X_s\gamma$ at NLO*, *JHEP* **01** (2015) 115 [arXiv:1411.7677] [INSPIRE].

[25] I.R. Blokland, A. Czarnecki, M. Misiak, M. Ślusarczyk and F. Tkachov, *The electromagnetic dipole operator effect on $\bar{B} \to X_s\gamma$ at $O(\alpha_s^2)$*, *Phys. Rev.* **D 72** (2005) 033014 [hep-ph/0506055] [INSPIRE].

[26] K. Melnikov and A. Mitov, *The photon energy spectrum in $B \to X_s + \gamma$ in perturbative QCD through $O(\alpha_s^2)$*, *Phys. Lett.* **B 620** (2005) 69 [hep-ph/0505097] [INSPIRE].

[27] H.M. Asatrian et al., *NNLL QCD contribution of the electromagnetic dipole operator to $\Gamma(\bar{B} \to X_s\gamma)$*, *Nucl. Phys.* **B 749** (2006) 325 [hep-ph/0605009] [INSPIRE].

[28] H.M. Asatrian, T. Ewerth, A. Ferroglia, P. Gambino and C. Greub, *Magnetic dipole operator contributions to the photon energy spectrum in $\bar{B} \to X_s\gamma$ at $O(\alpha_s^2)$*, *Nucl. Phys.* **B 762** (2007) 212 [hep-ph/0607316] [INSPIRE].

[29] H.M. Asatrian, T. Ewerth, H. Gabrielyan and C. Greub, *Charm quark mass dependence of the electromagnetic dipole operator contribution to $\bar{B} \to X_s\gamma$ at $O(\alpha_s^2)$*, *Phys. Lett.* **B 647** (2007) 173 [hep-ph/0611123] [INSPIRE].

[30] K. Bieri, C. Greub and M. Steinhauser, *Fermionic NNLL corrections to $b \to s\gamma$*, *Phys. Rev.* **D 67** (2003) 114019 [hep-ph/0302051] [INSPIRE].

[31] Z. Ligeti, M.E. Luke, A.V. Manohar and M.B. Wise, *The $\bar{B} \to X_s\gamma$ photon spectrum*, *Phys. Rev.* **D 60** (1999) 034019 [hep-ph/9903305] [INSPIRE].

[32] R. Boughezal, M. Czakon and T. Schutzmeier, *NNLO fermionic corrections to the charm quark mass dependent matrix elements in $\bar{B} \to X_s z\gamma$*, *JHEP* **09** (2007) 072 [arXiv:0707.3090] [INSPIRE].

[33] S.J. Brodsky, G.P. Lepage and P.B. Mackenzie, *On the elimination of scale ambiguities in perturbative quantum chromodynamics*, *Phys. Rev.* **D 28** (1983) 228 [INSPIRE].

[34] M. Misiak and M. Steinhauser, *NNLO QCD corrections to the $\bar{B} \to X_s\gamma$ matrix elements using interpolation in m_c*, *Nucl. Phys.* **B 764** (2007) 62 [hep-ph/0609241] [INSPIRE].

JHEP04(2015)168

[35] M. Misiak and M. Steinhauser, *Large-m_c asymptotic behaviour of $O(\alpha_s^2)$ corrections to $B \to X_s\gamma$*, *Nucl. Phys.* **B 840** (2010) 271 [arXiv:1005.1173] [INSPIRE].

[36] T. Ewerth, *Fermionic corrections to the interference of the electro- and chromomagnetic dipole operators in $\bar{B} \to X_s\gamma$ at $O(\alpha_s^2)$*, *Phys. Lett.* **B 669** (2008) 167 [arXiv:0805.3911] [INSPIRE].

[37] H.M. Asatrian, T. Ewerth, A. Ferroglia, C. Greub and G. Ossola, *Complete (O_7, O_8) contribution to $B \to X_s\gamma$ at order α_s^2*, *Phys. Rev.* **D 82** (2010) 074006 [arXiv:1005.5587] [INSPIRE].

[38] A. Ferroglia and U. Haisch, *Chromomagnetic dipole-operator corrections in $\bar{B} \to X_s\gamma$ at $O(\beta_0\alpha_s^2)$*, *Phys. Rev.* **D 82** (2010) 094012 [arXiv:1009.2144] [INSPIRE].

[39] M. Misiak and M. Poradziński, *Completing the calculation of BLM corrections to $\bar{B} \to X_s\gamma$*, *Phys. Rev.* **D 83** (2011) 014024 [arXiv:1009.5685] [INSPIRE].

[40] T. Ewerth, P. Gambino and S. Nandi, *Power suppressed effects in $\bar{B} \to X_s\gamma$ at $O(\alpha_s)$*, *Nucl. Phys.* **B 830** (2010) 278 [arXiv:0911.2175] [INSPIRE].

[41] A. Alberti, P. Gambino and S. Nandi, *Perturbative corrections to power suppressed effects in semileptonic B decays*, *JHEP* **01** (2014) 147 [arXiv:1311.7381] [INSPIRE].

[42] M. Misiak et al., *Estimate of $B(\bar{B} \to X_s\gamma)$ at $O(\alpha_s^2)$*, *Phys. Rev. Lett.* **98** (2007) 022002 [hep-ph/0609232] [INSPIRE].

[43] A.J. Buras, A. Czarnecki, M. Misiak and J. Urban, *Completing the NLO QCD calculation of $\bar{B} \to X_s\gamma$*, *Nucl. Phys.* **B 631** (2002) 219 [hep-ph/0203135] [INSPIRE].

[44] C. Anastasiou and K. Melnikov, *Higgs boson production at hadron colliders in NNLO QCD*, *Nucl. Phys.* **B 646** (2002) 220 [hep-ph/0207004] [INSPIRE].

[45] K.G. Chetyrkin and F.V. Tkachov, *Integration by parts: the algorithm to calculate β-functions in 4 loops*, *Nucl. Phys.* **B 192** (1981) 159 [INSPIRE].

[46] M. Czakon, `DiaGen/IdSolver`, unpublished.

[47] J. Kuipers, T. Ueda, J.A.M. Vermaseren and J. Vollinga, *FORM version* 4.0, *Comput. Phys. Commun.* **184** (2013) 1453 [arXiv:1203.6543] [INSPIRE].

[48] M. Benzke, S.J. Lee, M. Neubert and G. Paz, *Long-distance dominance of the CP asymmetry in $B \to X_{s,d} + \gamma$ decays*, *Phys. Rev. Lett.* **106** (2011) 141801 [arXiv:1012.3167] [INSPIRE].

[49] A. Alberti, P. Gambino, K.J. Healey and S. Nandi, *Precision determination of the Cabibbo-Kobayashi-Maskawa element V_{cb}*, *Phys. Rev. Lett.* **114** (2015) 061802 [arXiv:1411.6560] [INSPIRE].

[50] A. Pak and A. Czarnecki, *Mass effects in muon and semileptonic $b \to c$ decays*, *Phys. Rev. Lett.* **100** (2008) 241807 [arXiv:0803.0960] [INSPIRE].

[51] M. Misiak et al., *Updated NNLO QCD predictions for the weak radiative B-meson decays*, arXiv:1503.01789 [INSPIRE].

[52] M. Neubert, *Renormalization-group improved calculation of the $B \to X_s\gamma$ branching ratio*, *Eur. Phys. J.* **C 40** (2005) 165 [hep-ph/0408179] [INSPIRE].

[53] P. Gambino, private communication.

[54] G. Buchalla, G. Isidori and S.J. Rey, *Corrections of order $\Lambda_{\rm QCD}^2/m_c^2$ to inclusive rare B decays*, *Nucl. Phys.* **B 511** (1998) 594 [hep-ph/9705253] [INSPIRE].

[55] P. Gambino and U. Haisch, *Complete electroweak matching for radiative B decays*, *JHEP* **10** (2001) 020 [hep-ph/0109058] [INSPIRE].

JHEP04(2015)168

[56] T. Huber, *Master integrals for massless three-loop form factors*, PoS(RADCOR2009)038 [arXiv:1001.3132] [INSPIRE].

[57] A. Gehrmann-De Ridder, T. Gehrmann and G. Heinrich, *Four particle phase space integrals in massless QCD*, *Nucl. Phys.* **B 682** (2004) 265 [hep-ph/0311276] [INSPIRE].

[58] P.A. Baikov, K.G. Chetyrkin, A.V. Smirnov, V.A. Smirnov and M. Steinhauser, *Quark and gluon form factors to three loops*, *Phys. Rev. Lett.* **102** (2009) 212002 [arXiv:0902.3519] [INSPIRE].

[59] R.N. Lee, A.V. Smirnov and V.A. Smirnov, *Analytic results for massless three-loop form factors*, *JHEP* **04** (2010) 020 [arXiv:1001.2887] [INSPIRE].

[60] T. Gehrmann, E.W.N. Glover, T. Huber, N. Ikizlerli and C. Studerus, *Calculation of the quark and gluon form factors to three loops in QCD*, *JHEP* **06** (2010) 094 [arXiv:1004.3653] [INSPIRE].

[61] V.A. Smirnov, *Analytical result for dimensionally regularized massless on shell double box*, *Phys. Lett.* **B 460** (1999) 397 [hep-ph/9905323] [INSPIRE].

[62] J.B. Tausk, *Nonplanar massless two loop Feynman diagrams with four on-shell legs*, *Phys. Lett.* **B 469** (1999) 225 [hep-ph/9909506] [INSPIRE].

[63] C. Anastasiou and A. Daleo, *Numerical evaluation of loop integrals*, *JHEP* **10** (2006) 031 [hep-ph/0511176] [INSPIRE].

[64] V.A. Smirnov, *Evaluating Feynman integrals*, *Springer Tracts Mod. Phys.* **211** (2004) 1 [INSPIRE].

[65] P.A. Baikov and K.G. Chetyrkin, *Four loop massless propagators: an algebraic evaluation of all master integrals*, *Nucl. Phys.* **B 837** (2010) 186 [arXiv:1004.1153] [INSPIRE].

[66] A.V. Smirnov and M. Tentyukov, *Four loop massless propagators: a numerical evaluation of all master integrals*, *Nucl. Phys.* **B 837** (2010) 40 [arXiv:1004.1149] [INSPIRE].

[67] M. Czakon, *Automatized analytic continuation of Mellin-Barnes integrals*, *Comput. Phys. Commun.* **175** (2006) 559 [hep-ph/0511200] [INSPIRE].

[68] T. Huber and D. Maître, *HypExp: a Mathematica package for expanding hypergeometric functions around integer-valued parameters*, *Comput. Phys. Commun.* **175** (2006) 122 [hep-ph/0507094] [INSPIRE].

[69] T. Huber and D. Maître, *HypExp 2, expanding hypergeometric functions about half-integer parameters*, *Comput. Phys. Commun.* **178** (2008) 755 [arXiv:0708.2443] [INSPIRE].

[70] P. Gambino and C. Schwanda, *Inclusive semileptonic fits, heavy quark masses and V_{cb}*, *Phys. Rev.* **D 89** (2014) 014022 [arXiv:1307.4551] [INSPIRE].

[71] K.G. Chetyrkin et al., *Charm and bottom quark masses: an update*, *Phys. Rev.* **D 80** (2009) 074010 [arXiv:0907.2110] [INSPIRE].

[72] P. Gambino and M. Misiak, *Quark mass effects in $\bar{B} \to X_s\gamma$*, *Nucl. Phys.* **B 611** (2001) 338 [hep-ph/0104034] [INSPIRE].

[73] J. Charles et al., *Current status of the standard model CKM fit and constraints on $\Delta F = 2$ new physics*, *Phys. Rev.* **D 91** (2015) 073007 [arXiv:1501.05013] [INSPIRE].

[74] A. Kapustin, Z. Ligeti and H.D. Politzer, *Leading logarithms of the b quark mass in inclusive $B \to X_s\gamma$ decay*, *Phys. Lett.* **B 357** (1995) 653 [hep-ph/9507248] [INSPIRE].

[75] H.M. Asatrian and C. Greub, *Tree-level contribution to $\bar{B} \to X_d\gamma$ using fragmentation functions*, *Phys. Rev.* **D 88** (2013) 074014 [arXiv:1305.6464] [INSPIRE].

JHEP04(2015)168

Published for SISSA by Springer

Received: March 24, 2015
Accepted: June 8, 2015
Published: June 25, 2015

Inclusive $\bar{B} \to X_s \ell^+ \ell^-$: complete angular analysis and a thorough study of collinear photons

Tobias Huber,[a] **Tobias Hurth**[b] **and Enrico Lunghi**[c]

[a] *Theoretische Physik 1, Naturwissenschaftlich-Technische Fakultät, Universität Siegen, D-57068 Siegen, Germany*

[b] *PRISMA Cluster of Excellence and Institute for Physics (THEP), Johannes Gutenberg University, D-55099 Mainz, Germany*

[c] *Physics Department, Indiana University, Bloomington, IN 47405, U.S.A.*

E-mail: huber@physik.uni-siegen.de, hurth@uni-mainz.de, elunghi@indiana.edu

Abstract: We investigate logarithmically enhanced electromagnetic corrections of all angular observables in inclusive $\bar{B} \to X_s \ell^+ \ell^-$. We present analytical results, which are supplemented by a dedicated Monte Carlo study on the treatment of collinear photons in order to determine the size of the electromagnetic logarithms. We then give the Standard Model predictions of all observables, considering all available NNLO QCD, NLO QED and power corrections, and investigate their sensitivity to New Physics. Since the structure of the double differential decay rate is modified in the presence of QED corrections, we also propose new observables which vanish if only QCD corrections are taken into account. Moreover, we study the experimental sensitivity to these new observables at Belle II.

Keywords: Rare Decays, B-Physics, Beyond Standard Model

ArXiv ePrint: 1503.04849

Open Access, © The Authors.
Article funded by SCOAP[3].

doi:10.1007/JHEP06(2015)176

JHEP06(2015)176

Contents

1 Introduction **1**

2 Definition of the observables **5**

3 Log-enhanced QED corrections to the double differential decay rate **7**

4 Master formulas for the observables **14**

5 Phenomenological results **20**
- 5.1 $\mathcal{H}_T$ and $\mathcal{H}_L$ 23
- 5.2 $\mathcal{H}_A$ 24
- 5.3 $\mathcal{H}_3$ and $\mathcal{H}_4$ 25
- 5.4 Branching ratio, low-q^2 region 26
- 5.5 Branching ratio, high-q^2 region 26
- 5.6 The ratio $\mathcal{R}(s_0)$ 28

6 New physics sensitivities **28**

7 On the connection between theory and experiments **34**
- 7.1 Various experimental settings 34
- 7.2 Validation 35
- 7.3 Monte Carlo estimate of QED corrections to $\mathcal{H}_T$ and $\mathcal{H}_L$ 38

8 Conclusion **39**

A QED and QCD functions **41**
- A.1 QED functions for the double differential rate 41
- A.2 Functions for the QCD corrections to the $\mathcal{H}_I$ 43
- A.3 Functions for the QED corrections to the $\mathcal{H}_I$ 45

B New physics formulas **47**

1 Introduction

By now the LHC experiment has not discovered any new degrees of freedom beyond the Standard Model (SM). In particular, the measurements of the LHCb experiment and the B-physics experiments of ATLAS and CMS have confirmed the simple Cabibbo-Kobayashi-Maskawa (CKM) theory of the SM [1–3]. This corresponds to the general result of the

JHEP06(2015)176

B-factories [4, 5] and of the Tevatron B-physics experiments [6, 7] which have not indicated any sizable discrepancy from SM predictions in the B-meson sector (for reviews see refs. [8–10]).

However, recently the first measurement of new angular observables in the exclusive decay $B \to K^* \mu^+ \mu^-$ has shown a kind of anomaly [11]. Due to the large hadronic uncertainties it is not clear if this anomaly is a first sign for new physics beyond the SM, or a consequence of hadronic power corrections; but of course, it could turn out to just be a statistical fluctuation (see e.g. refs. [12–20]. The LHCb analysis based on the $3\,\mathrm{fb}^{-1}$ dataset is eagerly awaited to clarify the situation. More recently, another slight discrepancy occurred. The ratio $R_K = \mathrm{BR}(B^+ \to K^+ \mu^+ \mu^-)/\mathrm{BR}(B^+ \to K^+ e^+ e^-)$ in the low-q^2 region (q^2 being the di-lepton invariant mass) has been measured by LHCb showing a 2.6σ deviation from the SM prediction [21]. In contrast to the anomaly in the rare decay $B \to K^* \mu^+ \mu^-$ which is affected by unknown power corrections, the ratio R_K is theoretically rather clean. This might be a sign for lepton non-universality (see e.g. refs. [22–31]).

The inclusive decay mode $\bar{B} \to X_s \ell^+ \ell^-$ is one of the most important, theoretically clean modes of the indirect search for new physics via flavour observables (for a review and updates see refs. [32–34]); especially it allows for a nontrivial crosscheck of the recent LHCb data on the exclusive mode [18, 35].

The observables within this inclusive mode are dominated by perturbative contributions if the $c\bar{c}$ resonances that show up as large peaks in the dilepton invariant mass spectrum are removed by appropriate kinematic cuts — leading to so-called 'perturbative di-lepton invariant mass windows', namely the low di-lepton mass region $1\,\mathrm{GeV}^2 < s = q^2 = m_{\ell\ell}^2 < 6\,\mathrm{GeV}^2$, and also the high dilepton mass region with $q^2 > 14.4\,\mathrm{GeV}^2$ (or $q^2 > 14.2\,\mathrm{GeV}^2$). In these regions a theoretical precision of order 10% is in principle possible.

By now the branching fraction has been measured by Belle and BaBar using the sum-of-exclusive technique only. The latest published measurement of Belle [36] is based on a sample of 152×10^6 $B\bar{B}$ events only, which corresponds to less than 30% of the dataset available at the end of the Belle experiment. Babar has just recently presented an analysis based on the whole dataset of Babar using a sample of 471×10^6 $B\bar{B}$ events [37] which updated the former analysis of 2004 [38].

In the low- and high-dilepton invariant mass region the weighted averages of the experimental results read

$$\mathcal{B}(\bar{B} \to X_s \ell^+ \ell^-)^{\mathrm{exp}}_{\mathrm{low}} = (1.58 \pm 0.37) \times 10^{-6}\,, \tag{1.1}$$

$$\mathcal{B}(\bar{B} \to X_s \ell^+ \ell^-)^{\mathrm{exp}}_{\mathrm{high}} = (0.48 \pm 0.10) \times 10^{-6}\,. \tag{1.2}$$

All the measurements are still dominated by the statistical error. The expectation is that the final word of the present B factories leads to an experimental accuracy of $15 - 20\%$.

In addition, Belle has presented a first measurement of the forward-backward asymmetry [39] and Babar a measurement of the CP violation in this channel [37].

The super flavour factory Belle II at KEK will accumulate two orders of magnitude larger data samples [40]. Such data will push experimental precision to its limit. This is the main motivation for the present study to decrease the theoretical uncertainties accordingly.

JHEP06(2015)176

The theoretical precision has already reached a highly sophisticated level. Let us briefly review the previous analyses.

- Within the inclusive decay mode $\bar{B} \to X_s \ell^+ \ell^-$ the dominating perturbative QCD contributions are calculated up to NNLL precision. The complete NLL QCD contributions have been presented [41, 42]. For the NNLL calculation, many components were taken over from the NLL calculation of the $\bar{B} \to X_s \gamma$ mode. The additional components for the NNLL QCD precision have been calculated in refs. [43–55].

- If only the leading operator of the electroweak hamiltonian is considered, one is led to a local operator product expansion (OPE). In this case, the leading hadronic power corrections in the decay $\bar{B} \to X_s \ell^+ \ell^-$ scale with $1/m_b^2$ and $1/m_b^3$ only and have already been analysed [56–61]. Power correction that scale with $1/m_c^2$ [62] have also been considered. They can be calculated quite analogously to those in the decay $\bar{B} \to X_s \gamma$. A systematic and careful analysis of hadronic power corrections including all relevant operators has been performed in the case of the decay $\bar{B} \to X_s \gamma$ [63]. Such analysis goes beyond the local OPE. An additional uncertainty of $\pm 5\%$ has been identified. The analysis in the case of $\bar{B} \to X_s \ell^+ \ell^-$ is fully analogous and work in progress. There is no reason to expect any large deviation from the $\bar{B} \to X_s \gamma$ result.

  In the high-q^2 region, one encounters the breakdown of the heavy-mass expansion (HME) at the end point of the dilepton mass spectrum: whereas the partonic contribution vanishes, the $1/m_b^2$ and $1/m_b^3$ corrections tend towards a finite, non-zero value. Contrary to the end-point region of the photon-energy spectrum in the $\bar{B} \to X_s \gamma$ decay, no partial all-order resummation into a shape-function is possible. However, for the *integrated* high-q^2 spectrum an effective expansion is found in inverse powers of $m_b^{\rm eff} = m_b \times (1 - \sqrt{s_{\rm min}})$ instead of m_b [64, 65]. The expansion converges less rapidly, and the convergence behaviour depends on the lower dilepton-mass cut $s_{\rm min} = q^2_{\rm min}/m_b^2$ [53].

  The large theoretical uncertainties could be significantly reduced by normalizing the $\bar{B} \to X_s \ell^+ \ell^-$ decay rate to the semileptonic $\bar{B} \to X_u \ell \bar{\nu}$ decay rate with the same s cut [61]:

$$\mathcal{R}(s_0) = \int_{\hat{s}_0}^1 \mathrm{d}\hat{s}\, \frac{\mathrm{d}\Gamma(\bar{B} \to X_s \ell^+ \ell^-)}{\mathrm{d}\hat{s}} \Big/ \int_{\hat{s}_0}^1 \mathrm{d}\hat{s}\, \frac{\mathrm{d}\Gamma(\bar{B}^0 \to X_u \ell \nu)}{\mathrm{d}\hat{s}} \,. \tag{1.3}$$

  For example, the uncertainty due to the dominating $1/m_b^3$ term could be reduced from 19% to 9% [66].

- In the inclusive decay $\bar{B} \to X_s \ell^+ \ell^-$, the hadronic and dilepton invariant masses are independent kinematical quantities. A hadronic invariant-mass cut is imposed in the experiments. The high-dilepton-mass region is not affected by this cut, but in the low-dilepton mass region the kinematics with a jet-like X_s and $m_X^2 \leq m_b \Lambda$ implies the relevance of the shape function. A recent analysis in soft-collinear effective theory (SCET) shows that by using the universality of the shape function, a $10-30\%$ reduction in the dilepton-mass spectrum can be accurately computed. Nevertheless, the

JHEP06(2015)176

effects of subleading shape functions lead to an additional uncertainty of 5% [67, 68]. A more recent analysis [69] estimates the uncertainties due to subleading shape functions more conservatively. By scanning over a range of models of these functions, one finds corrections in the rates relative to the leading-order result to be between -10% to $+10\%$ with equally large uncertainties. In the future it may be possible to decrease such uncertainties significantly by constraining both the leading and subleading shape functions using the combined $\bar{B} \to X_s\gamma$, $\bar{B} \to X_u\ell\bar{\nu}$ and $\bar{B} \to X_s\ell^+\ell^-$ data [69, 70]. In [71], $\bar{B} \to X_s\ell^+\ell^-$ in the presence of a cut on m_{X_s} was analysed by performing the matching from QCD onto SCET at NNLO, and a prediction of the zero of the forward-backward asymmetry in this semi-inclusive channel was provided.

- As already discussed, the $c\bar{c}$ resonances can be removed by making appropriate kinematic cuts in the invariant mass spectrum. However, nonperturbative contributions away from the resonances within the perturbative windows are also important. In the KS approach [72, 73] one absorbs factorizable long-distance charm rescattering effects (in which the $\bar{B} \to X_s c\bar{c}r$ transition can be factorized into the product of $\bar{s}b$ and $c\bar{c}$ color-singlet currents) into the matrix element of the leading semileptonic operator $\mathcal{O}_9$. Following the inclusion of nonperturbative corrections scaling with $1/m_c^2$, the KS approach avoids double-counting. For the integrated branching fractions one finds an increase of $(1-2)\%$ in the low-q^2 region due to the KS effect, whereas in the high-q^2 region there is a decrease of $\sim 10\%$, which is still below the uncertainty due to the $1/m_b$ corrections.

- The integrated branching fraction is dominated by this resonance background which exceeds the nonresonant charm-loop contribution by two orders of magnitude. This feature should not be misinterpreted as a striking failure of global parton-hadron duality [74], which postulates that the sum over the hadronic final states, including resonances, should be well approximated by a quark-level calculation [75]. Crucially, the charm-resonance contributions to the decay $\bar{B} \to X_s\ell^+\ell^-$ are expressed in terms of a phase-space integral over the absolute square of a correlator. For such a quantity global quark-hadron duality is not expected to hold. Nevertheless, local quark-hadron duality (which, of course, also implies global duality) may be reestablished by resumming Coulomb-like interactions [74].

- Also electromagnetic perturbative corrections were calculated: NLL quantum electrodynamics (QED) two-loop corrections to the Wilson coefficients are of $\mathcal{O}(2\%)$ [55]. In the QED one-loop corrections to matrix elements, large collinear logarithms of the form $\log(m_b^2/m_\ell^2)$ survive integration over phase space if only a restricted part of the dilepton mass spectrum is considered. These collinear logarithms add another contribution of order $+2\%$ in the low-q^2 region of the dilepton mass spectrum in $\bar{B} \to X_s\mu^+\mu^-$ [76]. For the high-q^2 region, one finds -8% [66].

Based on all these scientific efforts of various groups, the latest theoretical predictions have been presented in ref. [66].

JHEP06(2015)176

In the present manuscript, we make the effort to provide all missing relevant perturbative contributions to all independent observables in the decay $\bar{B} \to X_s \ell^+ \ell^-$. As it is well-known, the angular decomposition of this inclusive decay rate provides three independent observables, H_T, H_A, H_L from which one can extract the short-distance electroweak Wilson coefficients that test for possible new physics [77]:

$$\frac{d^2\Gamma}{dq^2\, dz} = \frac{3}{8}\big[(1+z^2)H_T(q^2) + 2(1-z^2)H_L(q^2) + 2zH_A(q^2)\big]\,. \tag{1.4}$$

Here, $z = \cos\theta$, where θ is the angle between the ℓ^+ and B meson three momenta in the di-lepton rest frame, H_A is equivalent to the forward-backward asymmetry [78], and the q^2 spectrum is given by $H_T + H_L$. The observables dominantly depend on the effective Wilson coefficients corresponding to the operators $\mathcal{O}_7, \mathcal{O}_9$, and $\mathcal{O}_{10}$.

The paper is organized as follows. In section 2 we define the observables which we consider in the present analysis. In section 3 the derivation of the log-enhanced terms is presented. Master formulae for our observables are given in section 4, our phenomenological results in section 5. We briefly discuss the new physics sensitivity of our observables in section 6. Finally we explore the precise connection between experimental and theoretical quantities using Monte Carlo techniques in section 7. The latter analysis updates, and in parts supersedes, our previous statements in ref. [79]. We conclude in section 8. In the appendices we collect various functions that arise in the computation of QED and QCD corrections to the observables (appendix A), as well as formulas that parametrise the observables in terms of ratios of high-scale Wilson coefficients (appendix B).

2 Definition of the observables

The z dependence of the double differential decay distribution presented in eq. (1.4) is exact to all orders in QCD because it is controlled by the square of the leptonic current. The inclusion of QED bremsstrahlung modifies the simple second order polynomial structure and replaces it with a complicated analytical z dependence (see eqs. (3.28)–(3.33)). In particular this implies that, as long as QED effects are observably large, a simple fit to a quadratic polynomial will introduce non-negligible distorsions in the comparison between theory and experiment. In this section we explain the procedure that we adopt to construct various q^2 differential distributions and suggest that experimental analyses follow the same prescriptions.

The extraction of multiple differential distributions from eq. (1.4) is phenomenologically important because the various observables have different functional dependence on the Wilson coefficients. For instance, at next-to-leading order in QCD and without including any QED effect, the three H_I defined in eq. (1.4) are given by [77]:

$$H_T(q^2) = \frac{G_F^2 m_b^5 \,|V_{ts}^* V_{tb}|^2}{48\pi^3}\, 2\hat{s}(1-\hat{s})^2 \left[\left|C_9 + \frac{2}{\hat{s}}\, C_7\right|^2 + |C_{10}|^2\right], \tag{2.1}$$

$$H_L(q^2) = \frac{G_F^2 m_b^5 \,|V_{ts}^* V_{tb}|^2}{48\pi^3}\, (1-\hat{s})^2 \left[\left|C_9 + 2\, C_7\right|^2 + |C_{10}|^2\right], \tag{2.2}$$

$$H_A(q^2) = \frac{G_F^2 m_b^5 \,|V_{ts}^* V_{tb}|^2}{48\pi^3}\, (-4\hat{s})\,(1-\hat{s})^2\, \mathrm{Re}\left[C_{10}\left(C_9 + \frac{2}{\hat{s}}\, C_7\right)\right]. \tag{2.3}$$

JHEP06(2015)176

We decided to preserve the natural definitions of the differential decay width $d\Gamma/dq^2$ and of the forward-backward asymmetry $d\mathcal{A}_{\rm FB}/dq^2$:

$$\frac{d\Gamma}{dq^2} \equiv \int_{-1}^{+1} \frac{d^2\Gamma}{dq^2 dz} dz \,, \tag{2.4}$$

$$\frac{dA_{\rm FB}}{dq^2} \equiv \int_{-1}^{+1} \frac{d^2\Gamma}{dq^2 dz} {\rm sign}(z) dz \,, \tag{2.5}$$

with the understanding that $A_{\rm FB}$ does not coincide with the coefficient of the linear term in z in the Taylor expansion of $d^2\Gamma/dq^2dz$.

We extract other single-differential distributions by projecting the double-differential rate onto various Legendre polynomials, $P_n(z)$. These polynomials are orthogonal in the $[-1, 1]$ interval and are, therefore, ideally suited as angular projectors. In order to make connection with the existing literature we choose the first two projections in such a way to reproduce H_T and H_L in the limit of no QED radiation. For the higher order terms we simply adopt the corresponding Legendre polynomials. The observables are defined as

$$H_I(q^2) = \int_{-1}^{+1} \frac{d^2\Gamma}{dq^2 dz} W_I(z) dz \tag{2.6}$$

and the weights we use are:

$$\begin{aligned} W_T &= \frac{2}{3}\, P_0(z) + \frac{10}{3}\, P_2(z)\,, \qquad & W_3 &= P_3(z)\,, \\ W_L &= \frac{1}{3}\, P_0(z) - \frac{10}{3}\, P_2(z)\,, \qquad & W_4 &= P_4(z)\,, \\ W_A &= \frac{4}{3} {\rm sign}(z)\,. \end{aligned} \tag{2.7}$$

Note that $W_T + W_L = P_0(z) = 1$ implying that the relation $d\Gamma/dq^2 = H_T + H_L$ is exact.

The unnormalized (defined in eq. (2.5)) forward-backward asymmetry receives contributions form all odd powers of z in the Taylor expansion of the double differential rate and is given by

$$\frac{dA_{\rm FB}}{dq^2} = \frac{3}{4}\, H_A(q^2)\,. \tag{2.8}$$

In the literature the normalized differential and integrated forward-backward asymmetries are often considered (see for instance ref. [66]):

$$\frac{d\overline{A}_{\rm FB}}{dq^2} \equiv \frac{\displaystyle\int_{-1}^{+1} dz \frac{d^2\Gamma}{dq^2 dz} {\rm sign}(z)}{\displaystyle\int_{-1}^{+1} dz \frac{d^2\Gamma}{dq^2 dz}} = \frac{3}{4} \frac{H_A(q^2)}{H_T(q^2) + H_L(q^2)}\,, \tag{2.9}$$

$$\overline{A}_{\rm FB}[q_m^2, q_M^2] \equiv \frac{\displaystyle\int_{q_m^2}^{q_M^2} dq^2 \int_{-1}^{+1} dz \frac{d^2\Gamma}{dq^2 dz} {\rm sign}(z)}{\displaystyle\int_{q_m^2}^{q_M^2} dq^2 \int_{-1}^{+1} dz \frac{d^2\Gamma}{dq^2 dz}} = \frac{3}{4} \frac{\displaystyle\int_{q_m^2}^{q_M^2} dq^2 H_A(q^2)}{\displaystyle\int_{q_m^2}^{q_M^2} dq^2 \left[H_T(q^2) + H_L(q^2)\right]}\,. \tag{2.10}$$

JHEP06(2015)176

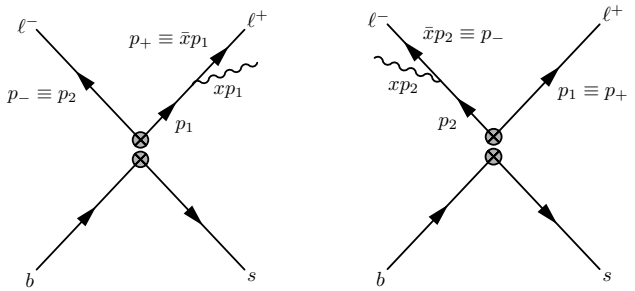

Figure 1. Kinematics of collinear photon radiation. The collinear photon is radiated off ℓ^+ (left panel) and ℓ^- (right panel), respectively. The crossed grey circles denote an operator insertion from the effective weak Hamiltonian. The arrows indicate momentum rather than fermion flow. x denotes the momentum fraction of the collinear photon.

The new observables H_3 and H_4 (obtained by employing the weights W_3 and W_4) vanish exactly in the limit of no QED radiation but are still potentially important for phenomenology because of their non trivial dependence on the Wilson coefficients. We find that projections with even higher Legendre polynomials are suppressed and will not be considered further.

Note that the expected statistical experimental uncertainties (at a given luminosity) are well understood in the total width $(H_T + H_L)$ and forward-backward asymmetry $(3/4\ H_A)$ cases. On the other hand, H_T, H_L, H_3 and H_4 are obtained by projecting the double differential rate with weights that (especially for W_3 and W_4) are essentially arbitrary. As a consequence a simple rescaling of these weights implies a corresponding rescaling of the central values we find. In section 6 we show how to use the squared weights (W_I^2) to assess the expected Belle II reach for each of these observables.

The experimental procedure that we recommend is to use the weights W_I to extract single-differential distributions and to refrain from attempting polynomial fits to the data.

3 Log-enhanced QED corrections to the double differential decay rate

In this section we work out the formulas for the logarithmically enhanced electromagnetic corrections of the double differential decay rate $d^2\Gamma/(dq^2\, dz)$. The operators and Wilson coefficients of the effective weak Hamiltonian are the same as in [66, 76]. The kinematics can be inferred from figure 1.

Let us first consider the case without photon radiation. The momenta of the quarks are labelled p_b and p_s, respectively. The momenta of ℓ^+ and ℓ^- are denoted by p_1 and p_2, respectively. From momentum conservation we arrive at $p_b = p_1 + p_2 + p_s$. We define the invariants

$$s_{ij} \equiv \frac{2p_i\, p_j}{m_b^2}\,, \qquad i \in \{1, 2, s, b\}\,. \tag{3.1}$$

Moreover, we define

$$y_1 \equiv \frac{2\, E_1}{m_b}\,, \qquad y_2 \equiv \frac{2\, E_2}{m_b}\,, \tag{3.2}$$

JHEP06(2015)176

where E_i $(i = 1, 2)$ is the zero-component of p_i when evaluated in the rest-frame of the decaying b-quark. From momentum conservation and by treating all final-state particles as massless, we obtain the relation $y_1 + y_2 = 1 + s_{12}$. This relation also implies

$$\begin{aligned} s_{1s} &= 1 - y_2 \,, \qquad s_{1b} = y_1 \,, \qquad s_{sb} = 1 - s_{12} \,, \\ s_{2s} &= 1 - y_1 \,, \qquad s_{2b} = y_2 \,. \end{aligned} \tag{3.3}$$

For the double differential decay rate we also need $z \equiv \cos\theta$, where θ is the angle between the b-quark and the positively charged lepton in the centre-of-mass system (c.m.s.) of the final-state lepton pair. Hence

$$z = \cos\theta = \frac{\vec{p}_1{}' \cdot \vec{p}_b{}'}{|\vec{p}_1{}'|\,|\vec{p}_b{}'|} \,, \tag{3.4}$$

where all primed momenta are taken in the c.m.s. of the final-state lepton pair. It turns out that z is simply given by [57]

$$z = \frac{y_2 - y_1}{1 - s_{12}} \,. \tag{3.5}$$

At this point we stress that the l.h.s. of this equation is evaluated in the lepton c.m.s., whereas its r.h.s. is evaluated in the rest-frame of the decaying b-quark. The connection between the angle θ and the leponic energy asymmetry has already been emphasized in [57].

We now switch on QED and consider the radiation of a collinear photon off a lepton leg as shown in figure 1. The momentum of the positively (negatively) charged lepton is denoted by p_1 (p_2) before radiation and by p_+ (p_-) thereafter. If the positively charged lepton radiates the photon (left panel of figure 1), its momentum p_+ after radiation is given by $p_+ = \bar{x} p_1$, where x denotes the momentum fraction of the collinear photon and $\bar{x} \equiv 1 - x$. In this case, the momentum of the negatively charged lepton remains unchanged and hence we have $p_- = p_2$. If the negatively charged lepton radiates the photon (right panel of figure 1), we obviously have $p_- = \bar{x} p_2$ and $p_+ = p_1$. In analogy to eq. (3.2), we define

$$y_\pm \equiv \frac{2\,E_\pm}{m_b} \,, \tag{3.6}$$

where $E_\pm$ is the zero-component of $p_\pm$, again evaluated in the rest-frame of the decaying b-quark. We will also need the definition

$$s_{+-} \equiv \bar{x}\, s_{12} \,. \tag{3.7}$$

As already discussed in refs. [66, 76], the logarithmically enhanced contributions stemming from collinear photon radiation are evaluated by

$$\frac{d^2\Gamma_{\rm coll}}{ds\,dz} = \frac{d^2\Gamma_{\rm coll,2}}{ds\,dz} - \frac{d^2\Gamma_{\rm coll,3}}{ds\,dz} \,, \tag{3.8}$$

where we stay differential in the double invariant $s_{+-} = (p_+ + p_-)^2 = \bar{x}\, s_{12}$ and the triple invariant $s_{12} = (p_+ + p_- + p_\gamma)^2 = (p_1 + p_2)^2$, respectively. We first consider the case of the triple invariant, where the formulae look exactly the same as in the case without QED, since we can lump the lepton and the collinear photon. We therefore arrive at

$$\begin{aligned} d\Gamma_{\rm coll,3} = {} & PF\, ds_{12}\, dy_1\, dy_2\, dx\, \delta(1 + s_{12} - y_1 - y_2)\, f_\gamma^{(m)}(x) \left[|\mathcal{A}|^2 (s_{12}, y_1, y_2) \right] \\ & \times \theta(y_1)\, \theta(1 - y_1)\, \theta(y_2)\, \theta(1 - y_2)\, \theta(s_{12})\, \theta(1 - s_{12})\, \theta(x)\, \theta(1 - x) \,. \end{aligned} \tag{3.9}$$

JHEP06(2015)176

Here θ denotes the heaviside step-function, PF is the pre-factor

$$PF = \frac{G_F^2 m_b |V_{tb} V_{ts}^*|^2}{32\pi^3} \,, \tag{3.10}$$

and $f_\gamma^{(m)}(x)$ is the mass-regularised splitting function for collinear photon radiation of which we only keep the logarithmically enhanced part ($\widetilde{\alpha}_\mathrm{e} = \alpha_e/(4\pi)$),

$$f_\gamma^{(m)}(x) = 4\,\widetilde{\alpha}_\mathrm{e}\,\frac{[1+(1-x)^2]}{x}\,\ln\!\left(\frac{m_b}{m_\ell}\right) \,. \tag{3.11}$$

The squared matrix elements $|\mathcal{A}|^2$ for the different operators read

$$\begin{aligned}
|\mathcal{A}|^2_{77}\,(s_{12},y_1,y_2) &= \frac{8m_b^4}{s_{12}}\,[(1-y_2)\,y_1 + (1-y_1)\,y_2]\,,\\
|\mathcal{A}|^2_{79}\,(s_{12},y_1,y_2) &= 4m_b^4\,(1-s_{12})\,,\\
|\mathcal{A}|^2_{99}\,(s_{12},y_1,y_2) &= 4m_b^4(1-y_1)(1-y_2) + 2m_b^4\,s_{12}\,(1-s_{12})\,,\\
|\mathcal{A}|^2_{710}\,(s_{12},y_1,y_2) &= 4m_b^4\,(y_1-y_2)\,,\\
|\mathcal{A}|^2_{910}\,(s_{12},y_1,y_2) &= 2m_b^4\,s_{12}\,(y_1-y_2)\,,\\
|\mathcal{A}|^2_{29}\,(s_{12},y_1,y_2) &= \widetilde{\alpha}_\mathrm{e}\,f_2(s_{12})\;|\mathcal{A}|^2_{99}\,(s_{12},y_1,y_2)\,,\\
|\mathcal{A}|^2_{27}\,(s_{12},y_1,y_2) &= \widetilde{\alpha}_\mathrm{e}\,f_2(s_{12})\;|\mathcal{A}|^2_{79}\,(s_{12},y_1,y_2)\,,\\
|\mathcal{A}|^2_{22}\,(s_{12},y_1,y_2) &= \widetilde{\alpha}_\mathrm{e}^2\,|f_2(s_{12})|^2\;|\mathcal{A}|^2_{99}\,(s_{12},y_1,y_2)\,,\\
|\mathcal{A}|^2_{210}\,(s_{12},y_1,y_2) &= \widetilde{\alpha}_\mathrm{e}\,f_2(s_{12})\;|\mathcal{A}|^2_{910}\,(s_{12},y_1,y_2)\,.
\end{aligned} \tag{3.12}$$

The function $f_2(s_{12})$ denotes the one-loop matrix element of P_2 and is given by

$$\begin{aligned}
f_2(s_{12}) = {}& \frac{8}{9}\ln\!\left(\frac{\mu}{m_c}\right) + \frac{8}{27} + \frac{4}{9}y_c \\
& - \frac{2}{9}(2+y_c)\sqrt{|1-y_c|}\begin{cases} \ln\left|\dfrac{1+\sqrt{1-y_c}}{1-\sqrt{1-y_c}}\right| - i\pi, & \text{when } y_c < 1\,,\\[2ex] 2\arctan\dfrac{1}{\sqrt{y_c-1}}, & \text{when } y_c \geq 1\,,\end{cases}
\end{aligned} \tag{3.13}$$

with $y_c = 4m_c^2/(m_b^2 s_{12})$. $f_2(s_{12})$ is a complex function and therefore the $|\mathcal{A}|^2_{2j}$ with $j \neq 2$ are complex. However, after taking into account the Wilson coefficients and adding the appropriate complex conjugate expression, the double differential rate turns out to be real, see eq. (3.28).

Let us now come back to the evaluation of (3.9). After integrating over the δ-function and changing variables according to eq. (3.5) we arrive at

$$\begin{aligned}
\frac{d^2\Gamma_{\mathrm{coll},3}}{ds_{12}\,dz} = {}& 2\,PF\int_0^1 dx\,f_\gamma^{(m)}(x)\left[|\mathcal{A}|^2\left(s_{12},\frac{1+s_{12}}{2}-\frac{1-s_{12}}{2}\,z,\frac{1+s_{12}}{2}+\frac{1-s_{12}}{2}\,z\right)\right]\\
& \times\frac{1-s_{12}}{2}\;\theta(1-z)\,\theta(1+z)\,\theta(s_{12})\,\theta(1-s_{12})\,.
\end{aligned} \tag{3.14}$$

JHEP06(2015)176

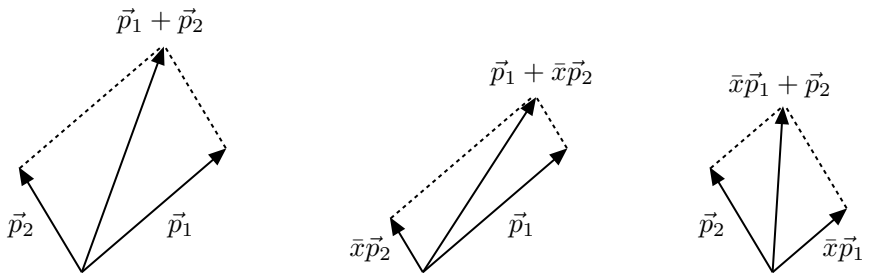

Figure 2. Boosts that have to be performed in order to translate the b rest-frame into the leptonic c.m.s. Left panel: without QED. Middle panel: radiation off ℓ^-. Right panel: radiation off ℓ^+.

The factor of two stems from the fact that both diagrams in figure 1 are relevant. Note that the integral in eq. (3.14) is divergent at $x = 0$. However, eq. (3.8) is well-behaved once all expressions on its r.h.s. are plugged in.

We now turn our attention to the more complicated case of the double invariant $d^2\Gamma_{\text{coll},2}/(ds\,dz)$, and first address radiation off ℓ^-. As can be seen from the middle panel of figure 2, the boost Λ from the b-quark rest-frame into the leptonic c.m.s. is determined by

$$\vec{p}_1 + \bar{x}\vec{p}_2 \xrightarrow{\Lambda} 0. \tag{3.15}$$

After the boost, we compute $z = \cos\theta$ via

$$z = \frac{\vec{p}_+{}' \cdot \vec{p}_b{}'}{|\vec{p}_+{}'|\;|\vec{p}_b{}'|} = \frac{\bar{x}y_2 - y_1}{\sqrt{(y_1 + \bar{x}y_2)^2 - 4\bar{x}s_{12}}}\,, \tag{3.16}$$

Again, the primed momenta are evaluated in the lepton c.m.s., whereas the r.h.s. of the equation is evaluated in the rest-frame of the b-quark. The differential decay width reads

$$\begin{aligned} d\Gamma^{\ell^-}_{\text{coll},2} = {} & PF\, ds_{12}\, dy_1\, dy_2\, dx\, \delta(1 + s_{12} - y_1 - y_2)\, f_\gamma^{(m)}(x) \left[|\mathcal{A}|^2\,(s_{12}, y_1, y_2)\right] \\ & \times\theta(y_1)\,\theta(1-y_1)\,\theta(y_2)\,\theta(1-y_2)\,\theta(s_{12})\,\theta(1-s_{12})\,\theta(x)\,\theta(1-x)\,. \end{aligned} \tag{3.17}$$

We first eliminate y_1 by integrating over the δ-function. Subsequently, we eliminate y_2 in favour of z according to eq. (3.16). This transformation reads

$$y_2^{(\pm)}(z) = \frac{(1+s_{12})(2 - x - xz^2) \pm 2z\sqrt{1-x}\sqrt{(1-s_{12})^2\bar{x} - s_{12}x^2(1-z^2)}}{x^2(1-z^2) + 4\bar{x}}\,. \tag{3.18}$$

It turns out that this in an injective mapping only for $s_{12} < \bar{x}$. For $s_{12} > \bar{x}$ we have to subdivide the y_2-interval into two pieces, so that we get a total of three contributions.

JHEP06(2015)176

After the additional variable substitution $s_{12} = s_{+-}/\bar{x}$ they read

$$\frac{d^2\Gamma^{\ell^-}_{\text{coll},2;\,1}}{ds_{+-}\,dz} = PF\int_0^{1-\sqrt{s_{+-}}} dx\;\frac{f_\gamma^{(m)}(x)}{\bar{x}}\left[\frac{\partial}{\partial z}y_2^{(+)}(z)\right]\left[|\mathcal{A}|^2\left(s_{12},1+s_{12}-y_2,y_2\right)\right]\Bigg|_{\substack{y_2=y_2^{(+)}(z)\\ s_{12}=s_{+-}/\bar{x}}} \times\theta(1-z)\,\theta(1+z)\,\theta(s_{+-})\,\theta(1-s_{+-})\,, \tag{3.19}$$

$$\frac{d^2\Gamma^{\ell^-}_{\text{coll},2;\,2/3}}{ds_{+-}\,dz} = \pm PF\int_{1-\sqrt{s_{+-}}}^{x_-} dx\;\frac{f_\gamma^{(m)}(x)}{\bar{x}}\left[\frac{\partial}{\partial z}y_2^{(\pm)}(z)\right]\left[|\mathcal{A}|^2\left(s_{12},1+s_{12}-y_2,y_2\right)\right]\Bigg|_{\substack{y_2=y_2^{(\pm)}(z)\\ s_{12}=s_{+-}/\bar{x}}} \times\theta(-z)\,\theta(1+z)\,\theta(s_{+-})\,\theta(1-s_{+-})\,, \tag{3.20}$$

where

$$x_\pm = \frac{1-s_{+-}}{1\mp\sqrt{(1-z^2)s_{+-}}}\,. \tag{3.21}$$

Once the photon is radiated off ℓ^+, we apply very similar steps. As can be seen from the right panel of figure 2, the boost Λ, from the b-quark rest-frame into the leptonic c.m.s., is determined by

$$\bar{x}\vec{p}_1 + \vec{p}_2 \xrightarrow{\Lambda} 0. \tag{3.22}$$

After the boost, we compute $z = \cos\theta$ by

$$z = \frac{\vec{p}_+{}'\cdot\vec{p}_b{}'}{|\vec{p}_+{}'|\;|\vec{p}_b{}'|} = \frac{y_2-\bar{x}y_1}{\sqrt{(\bar{x}y_1+y_2)^2-4\bar{x}s_{12}}}\,, \tag{3.23}$$

We now eliminate y_2 by integrating over the δ-function. Subsequently, we eliminate y_1 in favour of z according to eq. (3.23). This transformation reads

$$y_1^{(\pm)}(z) = \frac{(1+s_{12})(2-x-xz^2)\pm 2z\sqrt{1-x}\sqrt{(1-s_{12})^2\bar{x}-s_{12}x^2(1-z^2)}}{x^2(1-z^2)+4\bar{x}}\,. \tag{3.24}$$

As mentioned before, this is an injective mapping only for $s_{12} < \bar{x}$. For $s_{12} > \bar{x}$ we have to subdivide the y_1-interval into two pieces, so that in this case we also get a total of three

JHEP06(2015)176

contributions. After the additional variable substitution $s_{12} = s_{+-}/\bar{x}$ they read

$$\frac{d^2\Gamma^{\ell^+}_{\text{coll},2;\,1}}{ds_{+-}\,dz} = -PF \int_0^{1-\sqrt{s_{+-}}} dx\ \frac{f_\gamma^{(m)}(x)}{\bar{x}} \left[\frac{\partial}{\partial z} y_1^{(-)}(z)\right] \left[|\mathcal{A}|^2\,(s_{12}, y_1, 1+s_{12}-y_1)\right]\Bigg|_{\substack{y_1 = y_1^{(-)}(z)\\ s_{12} = s_{+-}/\bar{x}}} \times\theta(1-z)\,\theta(1+z)\,\theta(s_{+-})\,\theta(1-s_{+-})\,, \tag{3.25}$$

$$\frac{d^2\Gamma^{\ell^+}_{\text{coll},2;\,2/3}}{ds_{+-}\,dz} = \mp PF \int_{1-\sqrt{s_{+-}}}^{x_-} dx\ \frac{f_\gamma^{(m)}(x)}{\bar{x}} \left[\frac{\partial}{\partial z} y_1^{(\mp)}(z)\right] \left[|\mathcal{A}|^2\,(s_{12}, y_1, 1+s_{12}-y_1)\right]\Bigg|_{\substack{y_1 = y_1^{(\mp)}(z)\\ s_{12} = s_{+-}/\bar{x}}} \times\theta(z)\,\theta(1-z)\,\theta(s_{+-})\,\theta(1-s_{+-})\,. \tag{3.26}$$

The total contribution in case of the double invariant is now obtained by

$$\frac{d^2\Gamma_{\text{coll},2}}{ds_{+-}\,dz} = \sum_{i=1}^{3} \left[\frac{d^2\Gamma^{\ell^+}_{\text{coll},2;\,i}}{ds_{+-}\,dz} + \frac{d^2\Gamma^{\ell^-}_{\text{coll},2;\,i}}{ds_{+-}\,dz}\right]\,. \tag{3.27}$$

We finally identify $s_{12} \equiv s$ in eq. (3.14) and $s_{+-} \equiv s$ in eq. (3.27) and plug everything into eq. (3.8). This leads us to the following expression for the logarithmically enhanced collinear decay width

$$\begin{aligned}\frac{d^2\Gamma_{\text{coll}}}{ds\,dz} = \frac{G_F^2 m_b^5 |V_{tb}V_{ts}^*|^2}{32\pi^3}\,\widetilde{\alpha}_{\text{e}}\,\ln\!\left(\frac{m_b^2}{m_\ell^2}\right) \Big\{ &|C_9|^2\,\xi_{99}^{(\text{em})}(s,z) + |C_{10}|^2\,\xi_{99}^{(\text{em})}(s,z)\\ &+\widetilde{\alpha}_{\text{e}}^2\,|C_7^{\text{eff}}|^2\,\xi_{77}^{(\text{em})}(s,z) + \widetilde{\alpha}_{\text{e}}\,\text{Re}\left[C_7^{\text{eff}} C_9^*\right]\,\xi_{79}^{(\text{em})}(s,z) + \widetilde{\alpha}_{\text{e}}\,\text{Re}\left[C_7^{\text{eff}} C_{10}^*\right]\,\xi_{710}^{(\text{em})}(s,z)\\ &+\text{Re}\left[C_9 C_{10}^*\right]\,\xi_{910}^{(\text{em})}(s,z) + \widetilde{\alpha}_{\text{e}}^2\,\text{Re}\left[(C_2 + C_F C_1)\,C_7^{\text{eff}\,*}\,\xi_{27}^{(\text{em})}(s,z)\right]\\ &+\widetilde{\alpha}_{\text{e}}\,\text{Re}\left[(C_2 + C_F C_1) C_9^*\,\xi_{29}^{(\text{em})}(s,z)\right] + \widetilde{\alpha}_{\text{e}}\,\text{Re}\left[(C_2 + C_F C_1) C_{10}^*\,\xi_{210}^{(\text{em})}(s,z)\right]\\ &+\widetilde{\alpha}_{\text{e}}^2\,(C_2 + C_F C_1)^2\,\xi_{22}^{(\text{em})}(s,z)\Big\}\,,\end{aligned} \tag{3.28}$$

where we assumed that the Wilson coefficients C_1 and C_2 are real, and we neglected contributions from the penguin operators P_{3-6} due to their small Wilson coefficients. The functions $\xi_{ij}^{(\text{em})}(s,z)$ are given by

$$\begin{aligned}\xi_{77}^{(\text{em})}(s,z) = &-\frac{64\,p_1(s,z)\,\sqrt{s}\,\ln\!\left(\sqrt{\frac{s}{1-z^2}} - \sqrt{\frac{s}{1-z^2}-1}\right)}{(z^2-1)^3\,\sqrt{s+z^2-1}} + \frac{64\,z\,p_2(s,z)\,\ln\!\left(\frac{1-z}{z+1}\right)}{s(z^2-1)^3}\\ &+\frac{64\,p_3(s,z)\,\ln\!\left(\sqrt{\frac{1}{s(1-z^2)}} - \sqrt{\frac{1}{s(1-z^2)}-1}\right)}{s(z^2-1)^3\,(s\,(z^2-1)+1)^{3/2}} + \frac{16\,p_4(s,z)\,\ln(s)}{s(z^2-1)^3}\\ &+\frac{4\,p_5(s,z)}{3s\,(z^2-1)^2\,(s\,(z^2-1)+1)} - \frac{16(s-1)^2\,p_6(s,z)\,\ln\!\left(\frac{2(1-s)}{\sqrt{1-z^2}}\right)}{s}\,,\end{aligned} \tag{3.29}$$

JHEP06(2015)176

$$\xi_{99}^{(\mathrm{em})}(s,z) = -\frac{16\,s\,z\,p_7(s,z)\,\ln\left(\frac{1-z}{z+1}\right)}{(z^2-1)^4} + \frac{4\,s\,p_8(s,z)\,\ln(s)}{(z^2-1)^4}$$
$$+\frac{8\,s^{3/2}\,p_9(s,z)\,\ln\left(\sqrt{\frac{s}{1-z^2}}-\sqrt{\frac{s}{1-z^2}-1}\right)}{(z^2-1)^4\,(s+z^2-1)^{5/2}} + \frac{p_{10}(s,z)}{3(z^2-1)^3\,(s+z^2-1)^2}$$
$$+4(s-1)^2\left(sz^2+s-z^2+1\right)\ln\left(\frac{2(1-s)}{\sqrt{1-z^2}}\right)\,, \tag{3.30}$$

$$\xi_{79}^{(\mathrm{em})}(s,z) = -\frac{64\,z\,p_{11}(s,z)\,\ln\left(\frac{1-z}{z+1}\right)}{(z^2-1)^3} - \frac{32\,p_{12}(s,z)\,\ln(s)}{(z^2-1)^3}$$
$$-\frac{8\,p_{13}(s,z)}{(z^2-1)^2\,(s+z^2-1)} + \frac{64\sqrt{s}\,p_{14}(s,z)\,\ln\left(\sqrt{\frac{s}{1-z^2}}-\sqrt{\frac{s}{1-z^2}-1}\right)}{(z^2-1)^3\,(s+z^2-1)^{3/2}}$$
$$+32\,(s-1)^2\ln\left(\frac{2(1-s)}{\sqrt{1-z^2}}\right) + \frac{64\,p_{15}(s,z)\,\ln\left(\sqrt{\frac{1}{s(1-z^2)}}-\sqrt{\frac{1}{s(1-z^2)}-1}\right)}{(z^2-1)^2\,\sqrt{s\,(z^2-1)+1}} \tag{3.31}$$

$$\xi_{710}^{(\mathrm{em})}(s,z) = -\frac{64\,p_{15}(s,z)\,\mathrm{sign}(z)\ln\left(\frac{-\sqrt{s}(z^2-1)-\sqrt{z^2}\sqrt{s(z^2-1)+1}+1}{(\sqrt{s}+1)\sqrt{1-z^2}}\right)}{(z^2-1)^2\,\sqrt{s\,(z^2-1)+1}}$$
$$-\frac{64\,p_{16}(s,z)\,\sqrt{s}\,\mathrm{sign}(z)\ln\left(\frac{-\sqrt{z^2}\sqrt{s+z^2-1}+\sqrt{s}-z^2+1}{(\sqrt{s}+1)\sqrt{1-z^2}}\right)}{(z^2-1)^3\,(s+z^2-1)^{3/2}}$$
$$+\frac{32\,z\,p_{17}(s,z)\,\ln\left(\frac{1}{2}\left(\sqrt{s}+1\right)\sqrt{1-z^2}\right)}{(z^2-1)^3} + \frac{8\left(\sqrt{s}-1\right)^2 z\,p_{18}(s,z)}{(z^2-1)^2\,(s+z^2-1)}$$
$$-\frac{64\,s\,z\,\left(9sz^2+7s+4z^2-4\right)\ln(s)}{(z^2-1)^3} - 32(s-1)^2\,z\,\ln\left(1-\sqrt{s}\right)\,, \tag{3.32}$$

$$\xi_{910}^{(\mathrm{em})}(s,z) = -\frac{32\,s\,z\,p_{19}(s,z)\,\ln(s)}{(z^2-1)^4} + \frac{16\,s\,z\,p_{20}(s,z)\,\ln\left(\frac{1}{2}\left(\sqrt{s}+1\right)\sqrt{1-z^2}\right)}{(z^2-1)^4}$$
$$+\frac{4s\left(\sqrt{s}-1\right)^2 z\,p_{21}(s,z)}{(z^2-1)^3\,(s+z^2-1)^2} - \frac{16\,p_{22}(s,z)\,s^{3/2}\mathrm{sign}(z)\ln\left(\frac{-\sqrt{z^2}\sqrt{s+z^2-1}+\sqrt{s}-z^2+1}{(\sqrt{s}+1)\sqrt{1-z^2}}\right)}{(z^2-1)^4\,(s+z^2-1)^{5/2}}$$
$$-16(s-1)^2\,s\,z\,\ln\left(1-\sqrt{s}\right)\,. \tag{3.33}$$

The $p_i(s,z)$ are polynomials in s and z and are given in appendix A. In case of negative or complex arguments, the logarithms and square-roots are defined as

$$\sqrt{z} = \sqrt{|z|}\,e^{i/2\,\arg(z)}\,,$$
$$\ln(z) = \ln|z| + i\,\arg(z)\,,$$
$$\arg(z) \in (-\pi,\pi]\,. \tag{3.34}$$

The functions $\xi_{2x}^{(\mathrm{em})}(s,z)$ with $x = 2,7,9,10$ cannot be computed analytically since the squared matrix elements (see eq. (3.12)) are complicated functions of s_{12}. We therefore

JHEP06(2015)176

refrain from presenting their explicit expressions. They can easily be computed numerically by applying the steps outlined above.

A strong cross-check is done if we weight the $\xi_{ij}^{(\mathrm{em})}(s,z)$ by unity or by sign(z) and subsequently integrating over z. After proper normalisation one obtains the functions $\omega_{ij}^{(\mathrm{em})}(s)$ from [66, 76]. Note that this cross-check is non-trivial due to the fact that in our former work we computed the $\omega_{ij}^{(\mathrm{em})}(s)$ in a different way: since there was no need to introduce the variable z we performed the calculation entirely in terms of the rescaled energies y_i. Moreover, there was more freedom in choosing the order of integrations since we were not forced to perform the x-integration immediately after that over the δ-function. These two simplifications led to significantly simpler variable substitutions and shorter expressions. With the ability to reproduce them by the more complicated calculation can therefore be regarded as a non-trivial cross-check.

4 Master formulas for the observables

We start again from the double differential decay width

$$\frac{d^2\Gamma}{dz\,dq^2} = \frac{3}{8}\left[(1+z^2)H_T(q^2) + 2zH_A(q^2) + 2(1-z^2)H_L(q^2)\right], \tag{4.1}$$

where $z = \cos\theta$ and θ is the angle between the ℓ^+ and the B meson three momenta in the di-lepton rest frame. This formula is modified once QED corrections are taken into account (see sections 2 and 3) due to the appearance of higher powers of z. As stated in section 2, we project out the H_I $(I = T, A, L)$ by eq. (2.6) in this case. Then the H_I are functions of the dilepton-invariant mass $q^2 = m_{\ell\ell}^2$, but obviously not of z. H_A is proportional to the lepton forward-backward asymmetry; the q^2-spectrum is given by $H_T + H_L$,

$$\frac{d\Gamma}{dq^2} = \int_{-1}^{1} dz\,\frac{d^2\Gamma}{dz\,dq^2} = H_T(q^2) + H_L(q^2)\,, \tag{4.2}$$

$$\frac{d\mathcal{A}_{\mathrm{FB}}}{dq^2} = \int_{-1}^{1} dz\,\frac{d^2\Gamma}{dz\,dq^2}\,\mathrm{sign}(z) = \frac{3}{4}\,H_A(q^2)\,. \tag{4.3}$$

Each of the H_I can be expressed as follows ($\hat{s} = q^2/m_{b,\mathrm{pole}}^2$):

$$H_I(q^2) = \frac{G_F^2 m_{b,\mathrm{pole}}^5}{48\pi^3}\,|V_{ts}^* V_{tb}|^2\;\Phi_{\ell\ell}^I(\hat{s}), \tag{4.4}$$

where the dimensionless functions $\Phi_{\ell\ell}^I(\hat{s})$ include both perturbative and non-perturbative contributions. Moreover, we normalise the observables to the inclusive semi-leptonic $b \to X_c e\bar{\nu}$ decay. However, the normalisation proceeds in such a way that we insert the perturbative expansion of the inclusive semi-leptonic $b \to X_u e\bar{\nu}$ decay (including power-corrections), and also use the ratio [55, 80]

$$C = \left|\frac{V_{ub}}{V_{cb}}\right|^2 \frac{\Gamma(\bar{B} \to X_c e\bar{\nu})}{\Gamma(\bar{B} \to X_u e\bar{\nu})}\,, \tag{4.5}$$

JHEP06(2015)176

which was recently reanalysed in [81]. We therefore use $C = 0.574 \pm 0.019$ (see also table 1). Consequently, our expression of the normalised angular observables $\mathcal{H}_I$ reads

$$\mathcal{H}_I = \mathcal{B}(B \to X_c e\bar{\nu})_{\rm exp} \left|\frac{V_{ts}^* V_{tb}}{V_{cb}}\right|^2 \frac{4}{C} \frac{\Phi_{\ell\ell}^I(\hat{s})}{\Phi_u} , \tag{4.6}$$

where Φ_u is defined by [76]

$$\Gamma(B \to X_u e\bar{\nu}) = \frac{G_F^2 m_{b,\rm pole}^5}{192\pi^3} |V_{ub}|^2 \ \Phi_u . \tag{4.7}$$

The expansion of Φ_u is given by

$$\begin{aligned}
\Phi_u &= 1 + \widetilde{\alpha}_{\rm s}\varphi^{(1)} + \kappa\left[\frac{12}{23}\left(1-\eta^{-1}\right)\right] + \widetilde{\alpha}_{\rm s}^2\left[\varphi^{(2)} + 2\beta_0^{(5)}\varphi^{(1)}\ln\left(\frac{\mu_b}{m_b}\right)\right] + \frac{\lambda_1}{2m_b^2} - \frac{9\lambda_2}{2m_b^2} \\
&\quad + \mathcal{O}(\widetilde{\alpha}_{\rm s}^3, \kappa^2, \widetilde{\alpha}_{\rm s}\kappa, \widetilde{\alpha}_{\rm s}\Lambda^2/m_b^2, \Lambda^3/m_b^3) , \\
\varphi^{(1)} &= \frac{50}{3} - \frac{8\pi^2}{3} , \\
\varphi^{(2)} &= n_h\left(-\frac{2048\zeta_3}{9} + \frac{16987}{54} - \frac{340\pi^2}{81}\right) + n_l\left(\frac{256\zeta_3}{9} - \frac{1009}{27} + \frac{308\pi^2}{81}\right) \\
&\quad - \frac{41848\zeta_3}{81} + \frac{578\pi^4}{81} - \frac{104480\pi^2}{729} + \frac{1571095}{1458} - \frac{848}{27}\pi^2\ln(2) .
\end{aligned} \tag{4.8}$$

As explained in detail in [76], a consistent perturbative expansion in inclusive $\bar{B} \to X_s\ell^+\ell^-$ in the presence of QED corrections is done in $\widetilde{\alpha}_{\rm s} = \alpha_s(\mu_b)/(4\pi)$ and $\kappa = \alpha_e(\mu_b)/\alpha_s(\mu_b)$. We will also briefly sketch the structure of this expansion later below.

In the above equation, the $\mathcal{O}(\kappa)$ is taken from [82], with $\eta = \alpha_s(\mu_0)/\alpha_s(\mu_b)$. There also exist QED corrections at $\mathcal{O}(\widetilde{\alpha}_{\rm s}\kappa)$ which could be computed in principle. However, they are not logarithmically enhanced since the fully integrated $\bar{B} \to X_u e\bar{\nu}$ rate is an infrared safe observable with respect to collinear photon radiation. We therefore neglect this contribution, but include it lateron in the quantity $\mathcal{R}(s_0)$, where QED logs will be present in the normalisation.

The two-loop correction of $\mathcal{O}(\widetilde{\alpha}_{\rm s}^2)$ was taken from [83]. Here, n_h and n_l are the numbers of heavy and light quark flavours, respectively, and $\beta_0^{(5)} = 23/3$ is the one-loop QCD β-function for five active flavours. The coefficients λ_1 and λ_2 in the power-suppressed terms represent the matrix element of the kinetic energy and magnetic moment operator, respectively, and are defined as

$$\begin{aligned}
\lambda_1 &= \langle B|\bar{h}(iD)^2 h|B\rangle/(2M_B) , \\
\lambda_2 &= -\langle B|\bar{h}i\sigma^{\mu\nu}G_{\mu\nu}h|B\rangle/(12M_B) \approx \frac{1}{4}(M_{B^*}^2 - M_B^2) .
\end{aligned} \tag{4.9}$$

As far as the quantity $\Phi_{\ell\ell}^I(\hat{s})$ is concerned, we expand it in the following way in terms of products of the low-scale Wilson coefficients and various functions arising from the matrix elements,

$$\Phi_{\ell\ell}^I(\hat{s}) = \sum_{i\le j} {\rm Re}\left[C_i^{\rm eff}(\mu_b)\, C_j^{\rm eff*}(\mu_b)\, H_{ij}^I(\mu_b, \hat{s})\right] , \tag{4.10}$$

JHEP06(2015)176

where $C_i^{\rm eff}(\mu_b) \neq C_i(\mu_b)$ only for $i = 7, 8$. Here i and j run over all operators of eqs. (15) and (16) in [76]. Their low-scale Wilson coefficients are also given explicitly (analytically and numerically) in that paper. For $I = T, L$ the functions $H_{ij}^I(\mu_b, \hat{s})$ are given by

$$H_{ij}^I = \begin{cases} \sum\limits_{N=7,9,10} |M_i^N|^2\, S_{NN}^I + \mathrm{Re}(M_i^7 M_i^{9*})\, S_{79}^I + \Delta H_{ii}^I\,, & \text{for } i = j\,, \\ \sum\limits_{N=7,9,10} 2M_i^N M_j^{N*}\, S_{NN}^I + \left(M_i^7 M_j^{9*} + M_i^9 M_j^{7*}\right)\, S_{79}^I + \Delta H_{ij}^I\,, & \text{for } i \neq j\,. \end{cases} \tag{4.11}$$

For $I = A$ the formula is simpler,

$$H_{ij}^A = \begin{cases} 0\,, & \text{for } i = j\,, \\ \sum\limits_{N=7,9} \left(M_i^N M_j^{10*} + M_i^{10} M_j^{N*}\right)\, S_{N10}^A + \Delta H_{ij}^A\,, & \text{for } i \neq j\,. \end{cases} \tag{4.12}$$

The coefficients M_i^A are listed in table 6 of [76]. The building blocks S_{NM}^I have the following structure,

$$\mathrm{S}_{NM}^I = \sigma_{NM}^I(\hat{s}) \left\{1 + 8\,\widetilde{\alpha}_{\rm s}\, \omega_{NM,I}^{(1)}(\hat{s}) + 16\,\widetilde{\alpha}_{\rm s}^2\, \omega_{NM,I}^{(2)}(\hat{s})\right\} + \frac{\lambda_1}{m_b^2}\, \chi_{1,NM}^I(\hat{s}) + \frac{\lambda_2}{m_b^2}\, \chi_{2,NM}^I(\hat{s})\,. \tag{4.13}$$

From (4.11) and (4.12) we see that the possible combinations of indices are $NM = 77, 79, 99, 1010$ for $I = T, L$ and $NM = 710, 910$ for $I = A$. Moreover, we have $S_{99}^I = S_{1010}^I$ for $I = T, L$. Explicitly, the phase-space factors $\sigma_{NM}^I(\hat{s})$ read

$$\begin{aligned} &\sigma_{77}^T(\hat{s}) = 8(1-\hat{s})^2/\hat{s}\,, && \sigma_{77}^L(\hat{s}) = 4(1-\hat{s})^2\,, && \sigma_{710}^A(\hat{s}) = -8(1-\hat{s})^2\,, \\ &\sigma_{79}^T(\hat{s}) = 8(1-\hat{s})^2\,, && \sigma_{79}^L(\hat{s}) = 4(1-\hat{s})^2\,, && \sigma_{910}^A(\hat{s}) = -4\hat{s}(1-\hat{s})^2\,, \\ &\sigma_{99}^T(\hat{s}) = 2\hat{s}(1-\hat{s})^2\,, && \sigma_{99}^L(\hat{s}) = (1-\hat{s})^2\,. \end{aligned} \tag{4.14}$$

The one-loop QCD functions $\omega_{NM,I}^{(1)}(\hat{s})$ can be extracted from [50] and have already been given in [77]. The two-loop functions $\omega_{NM,I}^{(2)}(\hat{s})$ have so far only been available for the q^2-spectrum [84–87], but not for the double differential rate. Due to a recent calculation of the double differential rate of the inclusive semi-leptonic $b \to X_u \ell \bar{\nu}_\ell$ decay at two loops in QCD [88], they can be extracted for $NM = 99$, 1010 and $I = T, L$ as well as for $NM = 910$ and $I = A$. The data to extract these functions was kindly provided by the authors of [88, 89] and we can therefore present them here for the first time. All functions $\omega_{NM,I}^{(1,2)}(\hat{s})$ are rather lengthy and we therefore relegate their explicit expressions to appendix A.

The functions $\chi_{i,NM}^I(\hat{s})$ $(i = 1, 2)$ that accompany the non-perturbative $\mathcal{O}(\Lambda_{\rm QCD}^2/m_b^2)$ corrections can be obtained from [57] (see also [56, 59]) and were previously computed in [77]. We confirm their expressions,

$$\begin{aligned} &\chi_{1,77}^T(\hat{s}) = \frac{4}{3\hat{s}}\,(1-\hat{s})(5\hat{s}+3)\,, && \chi_{1,77}^L(\hat{s}) = \frac{2}{3}(\hat{s}-1)(3\hat{s}+13)\,, \\ &\chi_{1,79}^T(\hat{s}) = 4(1-\hat{s})^2\,, && \chi_{1,79}^L(\hat{s}) = 2(1-\hat{s})^2\,, \end{aligned}$$

JHEP06(2015)176

$$\chi^T_{1,99}(\hat{s}) = -\frac{\hat{s}}{3}(1-\hat{s})(3\hat{s}+5)\,, \qquad \chi^L_{1,99}(\hat{s}) = \frac{1}{6}(1-\hat{s})(13\hat{s}+3)\,,$$
$$\chi^A_{1,710}(\hat{s}) = -\frac{4}{3}\left(3\hat{s}^2+2\hat{s}+3\right)\,, \qquad \chi^A_{1,910}(\hat{s}) = -\frac{2}{3}\hat{s}\left(3\hat{s}^2+2\hat{s}+3\right)\,, \tag{4.15}$$
$$\chi^T_{2,77}(\hat{s}) = \frac{4}{\hat{s}}\left(3\hat{s}^2+2\hat{s}-9\right)\,, \qquad \chi^L_{2,77}(\hat{s}) = 2\left(15\hat{s}^2-6\hat{s}-13\right)\,,$$
$$\chi^T_{2,79}(\hat{s}) = 4\left(9\hat{s}^2-6\hat{s}-7\right)\,, \qquad \chi^L_{2,79}(\hat{s}) = 2\left(3\hat{s}^2-6\hat{s}-1\right)\,,$$
$$\chi^T_{2,99}(\hat{s}) = \hat{s}\left(15\hat{s}^2-14\hat{s}-5\right)\,, \qquad \chi^L_{2,99}(\hat{s}) = \frac{1}{2}\left(-17\hat{s}^2+10\hat{s}+3\right)\,,$$
$$\chi^A_{2,710}(\hat{s}) = -4\left(9\hat{s}^2-10\hat{s}-7\right)\,, \qquad \chi^A_{2,910}(\hat{s}) = -2\hat{s}\left(15\hat{s}^2-14\hat{s}-9\right)\,. \tag{4.16}$$

The quantities ΔH^I_{ij} can be further decomposed into

$$\Delta H^I_{ij} = b^I_{ij} + c^I_{ij} + e^I_{ij}\,. \tag{4.17}$$

Here the contributions b^I_{ij} represent finite bremsstrahlung corrections that appear at NNLO. They are known for the q^2-spectrum (i.e. $I = T + L$) [48] and the forward-backward asymmetry (equivalent to $I = A$) [51], but not for the double differential rate. Hence we only include them for these two cases, but not for H_T and H_L separately. This is still an excellent approximation since the effect of finite bremsstrahlung corrections is very small anyway. The explicit formulas can be found in [48, 51] and will therefore not be repeated.

The coefficients c^I_{ij} comprise non-perturbative $\mathcal{O}(\Lambda^2_{\rm QCD}/m_c^2)$ contributions and were calculated in ref. [62] for $I = T + L$ and $I = A$. Moreover, the coefficients of the double differential rate can be inferred from that paper. One obtains

$$\begin{aligned}
c^T_{2j} &= -\widetilde{\alpha}_{\rm s}\kappa\frac{8\lambda_2}{9m_c^2}\,(1-\hat{s})^2(1+3\hat{s})\,F(r)\left[\frac{1}{s}\,M_j^{7*}+\frac{1}{2}\,M_j^{9*}\right]\,, \qquad \text{for j} \neq 1,2\,,\\
c^T_{1j} &= -\frac{1}{6}\,c^T_{2j}\,, \qquad \text{for j} \neq 1,2\,,\\
c^T_{22} &= -\widetilde{\alpha}_{\rm s}\kappa\frac{8\lambda_2}{9m_c^2}\,(1-\hat{s})^2(1+3\hat{s})\,F(r)\left[\frac{1}{s}\,M_2^{7*}+\frac{1}{2}\,M_2^{9*}\right]\,,\\
c^T_{11} &= +\widetilde{\alpha}_{\rm s}\kappa\frac{4\lambda_2}{27m_c^2}\,(1-\hat{s})^2(1+3\hat{s})\,F(r)\left[\frac{1}{s}\,M_1^{7*}+\frac{1}{2}\,M_1^{9*}\right]\,,\\
c^T_{12} &= -\widetilde{\alpha}_{\rm s}\kappa\frac{8\lambda_2}{9m_c^2}\,(1-\hat{s})^2(1+3\hat{s})\left[F^*(r)\left(\frac{1}{s}\,M_1^{7}+\frac{1}{2}\,M_1^{9}\right)-\frac{1}{6}\,F(r)\left(\frac{1}{s}\,M_2^{7*}+\frac{1}{2}\,M_2^{9*}\right)\right]\,,\\
c^L_{2j} &= -\widetilde{\alpha}_{\rm s}\kappa\frac{8\lambda_2}{9m_c^2}\,(1-\hat{s})^2(3-\hat{s})\,F(r)\left[M_j^{7*}+\frac{1}{2}\,M_j^{9*}\right]\,, \qquad \text{for j} \neq 1,2\,,\\
c^L_{1j} &= -\frac{1}{6}\,c^L_{2j}\,, \qquad \text{for j} \neq 1,2\,,\\
c^L_{22} &= -\widetilde{\alpha}_{\rm s}\kappa\frac{8\lambda_2}{9m_c^2}\,(1-\hat{s})^2(3-\hat{s})\,F(r)\left[M_2^{7*}+\frac{1}{2}\,M_2^{9*}\right]\,,\\
c^L_{11} &= +\widetilde{\alpha}_{\rm s}\kappa\frac{4\lambda_2}{27m_c^2}\,(1-\hat{s})^2(3-\hat{s})\,F(r)\left[M_1^{7*}+\frac{1}{2}\,M_1^{9*}\right]\,,\\
c^L_{12} &= -\widetilde{\alpha}_{\rm s}\kappa\frac{8\lambda_2}{9m_c^2}\,(1-\hat{s})^2(3-\hat{s})\left[F^*(r)\left(M_1^{7}+\frac{1}{2}\,M_1^{9}\right)-\frac{1}{6}\,F(r)\left(M_2^{7*}+\frac{1}{2}\,M_2^{9*}\right)\right]\,,
\end{aligned}$$

JHEP06(2015)176

$$c_{210}^A = +\widetilde{\alpha}_s \kappa \frac{4\lambda_2}{9m_c^2}(1-\hat{s})^2(1+3\hat{s})\, F(r)\,,$$
$$c_{110}^A = -\frac{1}{6}\, c_{210}^A\,, \tag{4.18}$$

where $r = q^2/(4m_c^2)$. The function $F(r)$ can be found in the appendix of [76]. Moreover, we also include factorisable non-perturbative charm contributions which we implement by means of the Krüger-Sehgal approach [72, 73]. We elaborated extensively on this approach and also the formulas by means of which these corrections are taken into account in ref. [66]. Given their length we do not repeat these formulas here but refer the inclined reader to refs. [66, 72, 73] for all necessary details.

Finally, the coefficients e_{ij}^I collect the $\ln(m_b^2/m_\ell^2)$-enhanced electromagnetic corrections which we calculated in section 3 for the double differential rate. Their contribution to the H_I can be derived from (3.28) by applying the projections given in section 2. One finds

$$\begin{aligned}
e_{77}^I &= 8\,\widetilde{\alpha}_s^3\kappa^3\,\sigma_{77}^I(\hat{s})\,\omega_{77,I}^{(\mathrm{em})}(\hat{s})\,, & e_{29}^I &= 8\,\widetilde{\alpha}_s^2\kappa^2\,\sigma_{99}^I(\hat{s})\,\omega_{29,I}^{(\mathrm{em})}(\hat{s})\,,\\
e_{79}^I &= 8\,\widetilde{\alpha}_s^2\kappa^2\,\sigma_{79}^I(\hat{s})\,\omega_{79,I}^{(\mathrm{em})}(\hat{s})\,, & e_{22}^I &= 8\,\widetilde{\alpha}_s^3\kappa^3\,\sigma_{99}^I(\hat{s})\,\omega_{22,I}^{(\mathrm{em})}(\hat{s})\,,\\
e_{99}^I &= 8\,\widetilde{\alpha}_s\kappa\,\sigma_{99}^I(\hat{s})\,\omega_{99,I}^{(\mathrm{em})}(\hat{s})\,, & e_{11}^I &= \frac{16}{9}\,e_{22}^I\,,\\
e_{1010}^I &= e_{99}^I\,, & e_{12}^I &= \frac{8}{3}\,e_{22}^I\,,\\
e_{27}^I &= 8\,\widetilde{\alpha}_s^3\kappa^3\,\sigma_{79}^I(\hat{s})\,\omega_{27,I}^{(\mathrm{em})}(\hat{s})\,, & e_{1j}^I &= \frac{4}{3}e_{2j}^I, \qquad \text{for } j=7,9\,,
\end{aligned} \tag{4.19}$$

for $I = T, L$, while for $I = A$ one gets

$$\begin{aligned}
e_{710}^A &= 8\,\widetilde{\alpha}_s^2\kappa^2\,\sigma_{710}^A(\hat{s})\,\omega_{710,A}^{(\mathrm{em})}(\hat{s})\,, & e_{210}^A &= 8\,\widetilde{\alpha}_s^2\kappa^2\,\sigma_{910}^A(\hat{s})\,\omega_{210,A}^{(\mathrm{em})}(\hat{s})\,,\\
e_{910}^A &= 8\,\widetilde{\alpha}_s\kappa\,\sigma_{910}^A(\hat{s})\,\omega_{910,A}^{(\mathrm{em})}(\hat{s})\,, & e_{110}^A &= \frac{4}{3}e_{210}^A.
\end{aligned} \tag{4.20}$$

The functions $\omega_{ij,I}^{(\mathrm{em})}(\hat{s})$ have again been moved to appendix A.

We consider the observables H_I (or equivalently $\mathcal{H}_I$) in the low-q^2 region only, because their sensitivity to New Physics is highest in this region [77]. Besides, there are two more observables which we compute in the low-$\hat{s}$ region. First, there is the zero crossing q_0^2 of the forward-backward asymmetry, which we extract numerically from $\mathcal{H}_A$ by means of the formulas given above. Moreover, there is the branching ratio. In principle, it can be obtained by taking the sum of $\mathcal{H}_T$ and $\mathcal{H}_L$. Its master formula has already been given in [76]. We therefore only highlight two small pieces which are available for the branching ratio only, but not for $\mathcal{H}_T$ and $\mathcal{H}_L$ individually. These are only the finite bremsstrahlung contributions from [48] and the non-log enhanced terms of $\omega_{99}^{(\mathrm{em})}(\hat{s})$ (see eq. (94) of ref. [76]).

In the high-q^2 region we consider two observables. The first one is the branching ratio, where we include the same terms as in the low-q^2 region. As far as QED corrections are concerned, the functions $\omega_{99}^{(\mathrm{em})}(\hat{s})$, $\omega_{1010}^{(\mathrm{em})}(\hat{s})$, $\omega_{77}^{(\mathrm{em})}(\hat{s})$, and $\omega_{79}^{(\mathrm{em})}(\hat{s})$ (see eqs. (94) and (100) – (102) of [76]) are valid in the entire q^2-region, while the functions $\omega_{2x}^{(\mathrm{em})}(\hat{s})$ are again obtained from a numerical fit. To take into account our most recent input parameters (see

JHEP06(2015)176

table 1), we re-did the fits and collected the results in appendix A. In addition, the two-loop QCD matrix element functions $F^7_{1,2}(\hat{s})$ and $F^9_{1,2}(\hat{s})$, which were originally computed in [53], were given explicitly only in [54]. We implement these formulas in our numerical code. Moreover, non-perturbative $1/m_b^3$ corrections become sizable in the high-$\hat{s}$ region. They were originally computed in [60] and we implement the formulas of refs. [60, 61]. The second observable is the ratio $\mathcal{R}(s_0)$ which we have already mentioned in the introduction. It was proposed in [61][1] and is obtained by normalizing the $\bar{B} \to X_s \ell^+ \ell^-$ decay rate to the semileptonic $\bar{B}^0 \to X_u \ell \bar{\nu}$ rate *with the same cut in* q^2. In this way, large theoretical uncertainties that stem from poorly known parameters in the $1/m_b^2$ and $1/m_b^3$ power-corrections can be significantly reduced, as we will see in our numerical analysis in section 5. In terms of our perturbative quantities, it reads

$$\mathcal{R}(s_0) = \frac{\displaystyle\int_{\hat{s}_0}^1 \mathrm{d}\hat{s}\, \frac{\mathrm{d}\Gamma(\bar{B} \to X_s \ell^+ \ell^-)}{\mathrm{d}\hat{s}}}{\displaystyle\int_{\hat{s}_0}^1 \mathrm{d}\hat{s}\, \frac{\mathrm{d}\Gamma(\bar{B}^0 \to X_u \ell \nu)}{\mathrm{d}\hat{s}}} = 4 \left| \frac{V_{ts}^* V_{tb}}{V_{ub}} \right|^2 \frac{\int_{\hat{s}_0}^1 \mathrm{d}\hat{s}\, \Phi_{\ell\ell}(\hat{s})}{\int_{\hat{s}_0}^1 \mathrm{d}\hat{s}\, \Phi_u(\hat{s})} \,. \tag{4.21}$$

The quantity $\Phi_{\ell\ell}(\hat{s})$ is known from the branching ratio. The differential $\Phi_u(\hat{s})$ is given by

$$\frac{\mathrm{d}\Gamma(\bar{B}^0 \to X_u \ell \nu)}{\mathrm{d}\hat{s}} = \frac{G_F^2 \left|V_{ub}\right|^2 m_{b,\mathrm{pole}}^5}{192\pi^3}\, \Phi_u(\hat{s}) \,. \tag{4.22}$$

We elaborated extensively in ref. [66] about how to obtain the $\mathcal{O}(1, \widetilde{\alpha}_\mathrm{s}, \widetilde{\alpha}_\mathrm{s}^2, 1/m_b^2, 1/m_b^3)$ contributions to $\Phi_u(\hat{s})$, and will therefore not repeat these formulas. We would rather like to describe the $\mathcal{O}(\widetilde{\alpha}_\mathrm{s}\kappa)$ contribution to $\Phi_u(\hat{s})$, which we include in the present work and which was absent in [66]. Once the integration over $\hat{s}$ is restricted to the high-q^2 region, the corrections of $\mathcal{O}(\widetilde{\alpha}_\mathrm{s}\kappa)$ to $\Phi_u(\hat{s})$ contain residual terms logarithmically enhanced by $\ln(m_b^2/m_\ell^2)$. These must be proportional to $\omega_{99}^{(\mathrm{em})}(\hat{s})$. We take into account that we only have one charged lepton in the final state, and that the leptonic current is $V - A$. Moreover, we average over e and μ, and arrive at

$$\Phi_u(\hat{s})\big|_{\widetilde{\alpha}_\mathrm{s}\kappa} = 8\, \widetilde{\alpha}_\mathrm{s}\kappa\, (1-\hat{s})^2\, (1+2\hat{s})\, \omega_{99}^{(\mathrm{em})}(\hat{s})\Big|_{\ln\left(\frac{m_b^2}{m_\ell^2}\right) \longrightarrow \ln\left(\frac{m_b^2}{m_e m_\mu}\right)} \,. \tag{4.23}$$

As in our previous analysis [66] we do not include electromagnetic corrections of order $\mathcal{O}(\kappa)$ to $\Phi_u(\hat{s})$ because they are unknown.

Let us conclude this section by a few remarks on the renormalisation schemes for the quark masses, as well as on the expansion in $\widetilde{\alpha}_\mathrm{s}$ and κ. The pole masses of the b and c quark that are present in the definition of $\hat{s}$ and in several loop functions suffer from renormalon ambiguities [90, 91]. We therefore convert them analytically to short-distance schemes (1S and $\overline{\mathrm{MS}}$, respectively) before any numerical evaluation of the observables is carried out. In our numerical analysis we use the conversion formulas up to order $\mathcal{O}(\widetilde{\alpha}_\mathrm{s}^2)$ [92]. As far as the mass of the top quark is concerned we take the pole mass as input and convert it to the $\overline{\mathrm{MS}}$ scheme at order $\mathcal{O}(\widetilde{\alpha}_\mathrm{s}^3)$ using `RunDec` [93]. We also take into account electroweak

[1] Note that we use a different pre-factor here.

JHEP06(2015)176

corrections presented in eq. (31) of ref. [94], consistently to the other contributions. Turning our attention to the expansion in $\widetilde{\alpha}_s$ and κ, we observe that the amplitude has the structure

$$\begin{aligned}\mathcal{A} = \kappa \left[\mathcal{A}_{\rm LO} + \alpha_s\, \mathcal{A}_{\rm NLO} + \alpha_s^2\, \mathcal{A}_{\rm NNLO} + \mathcal{O}(\alpha_s^3)\right] \\ +\kappa^2 \left[\mathcal{A}^{em}_{\rm LO} + \alpha_s\, \mathcal{A}^{em}_{\rm NLO} + \alpha_s^2\, \mathcal{A}^{em}_{\rm NNLO} + \mathcal{O}(\alpha_s^3)\right] + \mathcal{O}(\kappa^3)\,,\end{aligned} \tag{4.24}$$

and that the ratio $\Phi^I_{\ell\ell}(\hat{s})/\Phi_u$ in (4.6) has a similar structure to that of the squared amplitude (up to bremsstrahlung and non-perturbative corrections),

$$\begin{aligned}\mathcal{A}^2 = \kappa^2 \Big[&\mathcal{A}^2_{\rm LO} + \alpha_s\, 2\mathcal{A}_{\rm LO}\mathcal{A}_{\rm NLO} + \alpha_s^2\, (\mathcal{A}^2_{\rm NLO} + 2\mathcal{A}_{\rm LO}\mathcal{A}_{\rm NNLO}) \\ &+\alpha_s^3\, 2(\mathcal{A}_{\rm NLO}\mathcal{A}_{\rm NNLO} + \ldots) + \mathcal{O}(\alpha_s^4)\Big] \\ +\kappa^3 \Big[&2\mathcal{A}_{\rm LO}\mathcal{A}^{em}_{\rm LO} + \alpha_s\, 2(\mathcal{A}_{\rm NLO}\mathcal{A}^{em}_{\rm LO} + \mathcal{A}_{\rm LO}\mathcal{A}^{em}_{\rm NLO}) \\ &+\alpha_s^2\, 2(\mathcal{A}_{\rm NLO}\mathcal{A}^{em}_{\rm NLO} + \mathcal{A}_{\rm NNLO}\mathcal{A}^{em}_{\rm LO} + \mathcal{A}_{\rm LO}\mathcal{A}^{em}_{\rm NNLO}) \\ &+\alpha_s^3\, 2(\mathcal{A}_{\rm NLO}\mathcal{A}^{em}_{\rm NNLO} + \mathcal{A}_{\rm NNLO}\mathcal{A}^{em}_{\rm NLO} + \ldots) + \mathcal{O}(\alpha_s^4)\Big] + \mathcal{O}(\kappa^4)\,.\end{aligned} \tag{4.25}$$

We already argued in refs. [66, 76] that an expansion of this kind up to and including $\mathcal{O}(\widetilde{\alpha}_s^3\kappa^3)$ also captures the dominant N^{3}LO QCD corrections, since the missing terms $\mathcal{A}_{\rm LO}\mathcal{A}_{N^3LO}$, $\mathcal{A}_{\rm LO}\mathcal{A}^{em}_{N^3LO}$, and $\mathcal{A}^{em}_{\rm LO}\mathcal{A}_{N^3LO}$ (represented by the dots) are small. It is therefore justified to refer to the accuracy of our calculations as *improved* NNLO. Hence we expand all products in eq. (4.6) (and in all other observables) in $\widetilde{\alpha}_s$ and κ up to the aforementioned order, and neglect all higher terms. The observables are also expanded in the power-correction parameters $\lambda_{1,2}, \rho_1, f_u^{0,\pm}, f_s$ up to linear terms. Higher powers as well as products of these parameters are dropped.

5 Phenomenological results

In this section we give the numerical results of our phenomenological analysis. We use the input parameters as given in table 1. For each variable we give the integral over bin 1 ($1\ \text{GeV}^2 < q^2 < 3.5\ \text{GeV}^2$), bin 2 ($3.5\ \text{GeV}^2 < q^2 < 6\ \text{GeV}^2$), and the entire low-$q^2$ region ($1\ \text{GeV}^2 < q^2 < 6\ \text{GeV}^2$). In the high-$q^2$ region we integrate over all $q^2 > 14.4\ \text{GeV}^2$. The respective q^2-interval is indicated by the argument of the observables. We give the numbers for electron and muon final state separately, and remind the reader that, depending on the channel and the experimental setup, our numbers have to be modified according to our Monte Carlo study in section 7.

The quoted uncertainties are the parametric and perturbative ones only. Additional uncertainties from subleading non-perturbative corrections are not included. In particular, the $\mathcal{O}(\alpha_s(\mu_b)\Lambda_{\rm QCD}/m_{c,b})$ non-perturbative corrections are estimated to be around $\sim 5\%$ in the low-q^2 region. The individual error bars are obtained by varying the parameters in the range indicated in table 1, where we assume the errors on C and m_c to be fully correlated. The total error is obtained by adding the individual ones in quadrature. By default we give two decimal digits. In case this leads to 0.00 we give the number up to the first significant digit.

JHEP06(2015)176

$\alpha_s(M_z) = 0.1184 \pm 0.0007$	$m_e = 0.51099892$ MeV
$\alpha_e(M_z) = 1/127.918$	$m_\mu = 105.658369$ MeV
$s_W^2 \equiv \sin^2\theta_W = 0.2312$	$m_\tau = 1.77699$ GeV
$\lvert V_{ts}^* V_{tb}/V_{cb}\rvert^2 = 0.9621 \pm 0.0027$ [95]	$m_c(m_c) = (1.275 \pm 0.025)$ GeV
$\lvert V_{ts}^* V_{tb}/V_{ub}\rvert^2 = 130.5 \pm 11.6$ [95]	$m_b^{1S} = (4.691 \pm 0.037)$ GeV [96, 97]
$BR(B \to X_c e\bar{\nu})_{\rm exp} = 0.1051 \pm 0.0013$ [96]	$m_{t,\rm pole} = (173.5 \pm 1.0)$ GeV
$M_Z = 91.1876$ GeV	$m_B = 5.2794$ GeV
$M_W = 80.385$ GeV	$C = 0.574 \pm 0.019$ [81]
$\mu_b = 5^{+5}_{-2.5}$ GeV	$\mu_0 = 120^{+120}_{-60}$ GeV
$\lambda_2^{\rm eff} = (0.12 \pm 0.02)$ GeV^2	$\rho_1 = (0.06 \pm 0.06)$ GeV^3 [98]
$\lambda_1^{\rm eff} = (-0.362 \pm 0.067)$ GeV^2 [96, 97]	$f_u^0 + f_s = (0 \pm 0.2)$ GeV^3 [61]
$f_u^0 - f_s = (0 \pm 0.04)$ GeV^3 [61]	$f_u^\pm = (0 \pm 0.4)$ GeV^3 [61]

Table 1. Numerical inputs used in the phenomenological analysis. Unless specified otherwise, they are taken from PDG [99].

Before presenting our actual results, we would like to comment on the size of QED corrections. In table 2 the first two columns in each of the three sections are, respectively, the observable at NNLL and its QED correction expressed as a percentage of the branching ratio integrated in the whole low-q^2 region ($\mathcal{B}[1,6]_{ee}$). The third column is the relative size of the QED correction with respect to each NNLL observable.

One can see immediately that the relative size of QED corrections to $\mathcal{H}_T$ is large, see third column in each section in table 2. Therefore, a few remarks on this observable are in order. It turns out that $\mathcal{H}_T$ is suppressed in the low-q^2 region. To see this, let us look at the tree-level dependence of H_T and H_L on the Wilson coefficients presented in eqs. (2.1) and (2.2). The phase space corresponding to $|C_9|^2$ is suppressed in H_T compared to H_L, whereas that associated to $|C_7|^2$ is enhanced. Surprisingly, this leads to a two-fold suppression of H_T. First, there is an additional factor of $2\hat{s}$ in the overall phase space w.r.t. H_L. Second, the factor $|C_9 + 2/\hat{s}\, C_7|^2$ is small in the low-q^2 region, and even vanishes at the position of the zero of H_A.

The QED corrections to the H_I, however, do not follow this pattern of suppression. In fact, from the inspection of the second columns in each section in table 2 we see that the absolute values of these corrections are natural in size and that all entries in these columns have the same order of magnitude. In the case of H_T the smallness of the NNLL

JHEP06(2015)176

	$q^2 \in [1,6]$ GeV^2			$q^2 \in [1,3.5]$ GeV^2			$q^2 \in [3.5,6]$ GeV^2		
	$\frac{O_{[1,6]}}{\mathcal{B}_{[1,6]}}$	$\frac{\Delta O_{[1,6]}}{\mathcal{B}_{[1,6]}}$	$\frac{\Delta O_{[1,6]}}{O_{[1,6]}}$	$\frac{O_{[1,3.5]}}{\mathcal{B}_{[1,6]}}$	$\frac{\Delta O_{[1,3.5]}}{\mathcal{B}_{[1,6]}}$	$\frac{\Delta O_{[1,3.5]}}{O_{[1,3.5]}}$	$\frac{O_{[3.5,6]}}{\mathcal{B}_{[1,6]}}$	$\frac{\Delta O_{[3.5,6]}}{\mathcal{B}_{[1,6]}}$	$\frac{\Delta O_{[3.5,6]}}{O_{[3.5,6]}}$
$\mathcal{B}$	100	5.1	5.1	54.6	3.7	6.8	45.4	1.4	3.1
$\mathcal{H}_T$	19.5	14.1	72.5	9.5	8.8	92.1	10.0	5.4	53.6
$\mathcal{H}_L$	80.0	-8.7	-10.9	44.7	-4.7	-10.6	35.3	-4.0	-11.3
$\mathcal{H}_A$	-3.3	1.4	-43.6	-7.2	0.8	-10.7	4.0	0.6	16.2

Table 2. Relative size of QED effects on $b \to se^+e^-$ at low-q^2 (the muon case can be easily obtained by rescaling). All entries are given in percent. For each of the three bins the first two columns are the integrated observable and its QED correction normalized to the total low-q^2 branching ratio, respectively ($\int_{s_1}^{s_2} O / \int_1^6 \mathcal{B}$ and $\int_{s_1}^{s_2} \Delta O / \int_1^6 \mathcal{B}$). The third column is the relative size of the QED correction ($\int_{s_1}^{s_2} \Delta O / \int_{s_1}^{s_2} O$). The sum of $\mathcal{H}_T$ and $\mathcal{H}_L$ does not exactly reproduce the branching ratio because in the latter we include finite bremsstrahlung and non-log enhanced QED corrections that are not available for the first two.

QCD result implies that their relative size is anomalously large (see the third columns in table 2). However, we emphasize here that this does *not* indicate a breakdown of the perturbative series because the large relative size of QED corrections is almost entirely due to the suppression of the tree-level plus QCD contribution, and not due to a large absolute value of the QED corrections. To support our analytical findings, we investigated the situation in a Monte Carlo study (for details, see section 7) and find exactly the same pattern once we use EVTGEN and PHOTOS, see figures 12 and 13 in section 7.3.

We can even turn the argument around and regard the relative size of QED corrections in $\mathcal{H}_T$ as a virtue rather than a drawback, because it offers a good opportunity to be sensitive to QED corrections even without the pure QED observables $\mathcal{H}_3$ and $\mathcal{H}_4$ defined in section 2.

Finally, let us point out that similar large effects on $\mathcal{H}_A$ (or, equivalently, the forward-backward asymmetry) integrated in the whole low-q^2 region are simply a due to the large cancellation between the integrated asymmetry in the two bins. This cancellation originates from the presence of a zero in the differential $\mathcal{H}_A$ spectrum and is not reproduced in the pattern of QED corrections. As we see in table 2, the latter imply a positive shift on $\mathcal{H}_A$ in both bins.

In the upper panel of figure 3 we show the differential distributions that we obtain for the various $\mathcal{H}_I$ in the electron channel; dashed lines are obtained by switching QED corrections off. In the lower panel of figure 3 we show the log-enhanced QED correction itself, i.e. the difference between solid and dashed lines in the upper panel.

JHEP06(2015)176

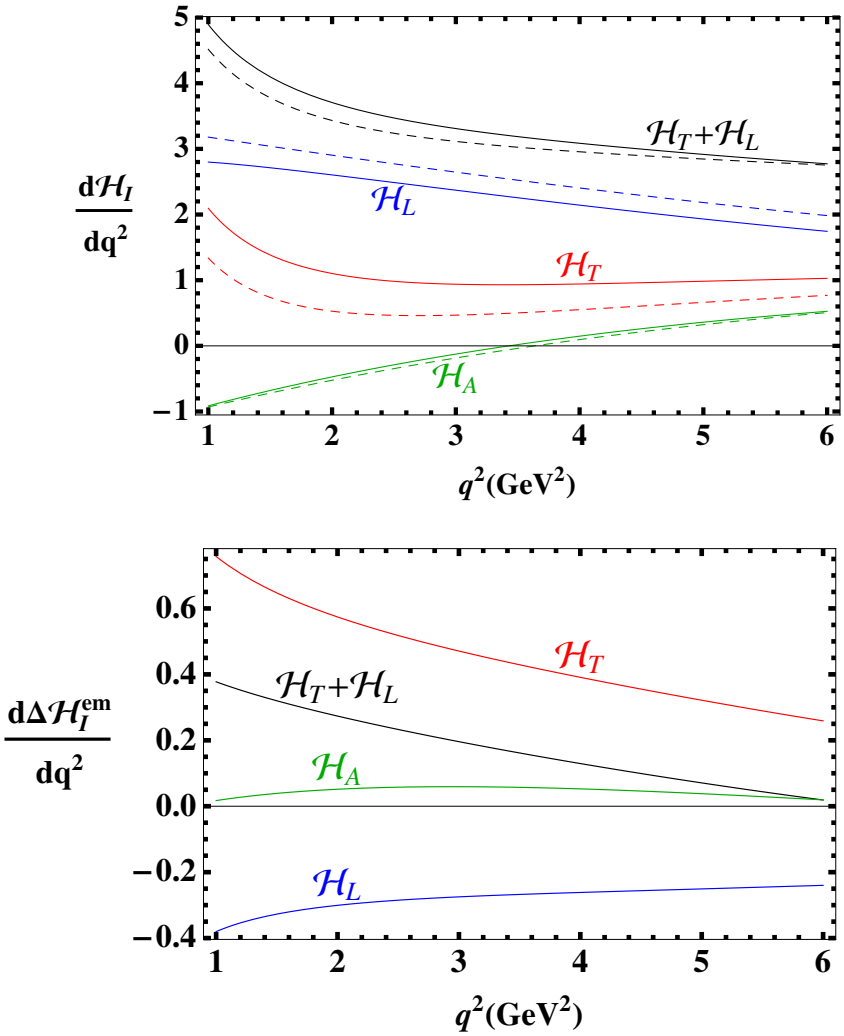

Figure 3. Differential distributions for the various observables (upper panel) and their respective log-enhanced QED correction (lower panel) in units of 10^{-7}. Dashed lines correspond to switching off all QED corrections. The integrals under the curves reproduce the results presented in section 5 for the electron channel.

5.1 $\mathcal{H}_T$ and $\mathcal{H}_L$

For the quantities $\mathcal{H}_T$ and $\mathcal{H}_L$ we find theoretical uncertainties of 6 to 9%. In this sense the QED corrections listed in table 2 are really significant.

$$\begin{aligned}
\mathcal{H}_T[1,3.5]_{ee} =&(2.91 \pm 0.16_{\text{scale}} \pm 0.03_{m_t} \pm 0.08_{C,m_c} \pm 0.02_{m_b} \\
&\pm 0.003_{\alpha_s} \pm 0.01_{\text{CKM}} \pm 0.04_{\text{BR}_{\text{sl}}}) \cdot 10^{-7} = (2.91 \pm 0.19) \cdot 10^{-7} \,, \\
\mathcal{H}_T[3.5,6]_{ee} =&(2.43 \pm 0.16_{\text{scale}} \pm 0.04_{m_t} \pm 0.08_{C,m_c} \pm 0.05_{m_b} \\
&\pm 0.01_{\alpha_s} \pm 0.01_{\text{CKM}} \pm 0.03_{\text{BR}_{\text{sl}}}) \cdot 10^{-7} = (2.43 \pm 0.20) \cdot 10^{-7} \,, \\
\mathcal{H}_T[1,6]_{ee} =&(5.34 \pm 0.33_{\text{scale}} \pm 0.07_{m_t} \pm 0.16_{C,m_c} \pm 0.06_{m_b} \\
&\pm 0.01_{\alpha_s} \pm 0.01_{\text{CKM}} \pm 0.06_{\text{BR}_{\text{sl}}}) \cdot 10^{-7} = (5.34 \pm 0.38) \cdot 10^{-7} \,. \qquad (5.1)
\end{aligned}$$

JHEP06(2015)176

$$
\begin{aligned}
\mathcal{H}_T[1,3.5]_{\mu\mu} =&(2.09 \pm 0.10_{\text{scale}} \pm 0.02_{m_t} \pm 0.06_{C,m_c} \pm 0.01_{m_b} \\
&\pm 0.01_{\alpha_s} \pm 0.01_{\text{CKM}} \pm 0.03_{\text{BR}_{\text{sl}}}) \cdot 10^{-7} = (2.09 \pm 0.12) \cdot 10^{-7} \,, \\
\mathcal{H}_T[3.5,6]_{\mu\mu} =&(1.94 \pm 0.13_{\text{scale}} \pm 0.03_{m_t} \pm 0.07_{C,m_c} \pm 0.05_{m_b} \\
&\pm 0.01_{\alpha_s} \pm 0.01_{\text{CKM}} \pm 0.02_{\text{BR}_{\text{sl}}}) \cdot 10^{-7} = (1.94 \pm 0.16) \cdot 10^{-7} \,, \\
\mathcal{H}_T[1,6]_{\mu\mu} =&(4.03 \pm 0.23_{\text{scale}} \pm 0.06_{m_t} \pm 0.12_{C,m_c} \pm 0.06_{m_b} \\
&\pm 0.002_{\alpha_s} \pm 0.01_{\text{CKM}} \pm 0.05_{\text{BR}_{\text{sl}}}) \cdot 10^{-7} = (4.03 \pm 0.28) \cdot 10^{-7} \,. \qquad (5.2)
\end{aligned}
$$

$$
\begin{aligned}
\mathcal{H}_L[1,3.5]_{ee} =&(6.35 \pm 0.23_{\text{scale}} \pm 0.08_{m_t} \pm 0.22_{C,m_c} \pm 0.08_{m_b} \\
&\pm 0.03_{\alpha_s} \pm 0.02_{\text{CKM}} \pm 0.08_{\text{BR}_{\text{sl}}}) \cdot 10^{-7} = (6.35 \pm 0.35) \cdot 10^{-7} \,, \\
\mathcal{H}_L[3.5,6]_{ee} =&(4.97 \pm 0.22_{\text{scale}} \pm 0.06_{m_t} \pm 0.17_{C,m_c} \pm 0.04_{m_b} \\
&\pm 0.02_{\alpha_s} \pm 0.01_{\text{CKM}} \pm 0.06_{\text{BR}_{\text{sl}}}) \cdot 10^{-7} = (4.97 \pm 0.29) \cdot 10^{-7} \,, \\
\mathcal{H}_L[1,6]_{ee} =&(1.13 \pm 0.04_{\text{scale}} \pm 0.01_{m_t} \pm 0.04_{C,m_c} \pm 0.01_{m_b} \\
&\pm 0.01_{\alpha_s} \pm 0.003_{\text{CKM}} \pm 0.01_{\text{BR}_{\text{sl}}}) \cdot 10^{-6} = (1.13 \pm 0.06) \cdot 10^{-6} \,. \qquad (5.3)
\end{aligned}
$$

$$
\begin{aligned}
\mathcal{H}_L[1,3.5]_{\mu\mu} =&(6.79 \pm 0.23_{\text{scale}} \pm 0.08_{m_t} \pm 0.23_{C,m_c} \pm 0.09_{m_b} \\
&\pm 0.03_{\alpha_s} \pm 0.02_{\text{CKM}} \pm 0.08_{\text{BR}_{\text{sl}}}) \cdot 10^{-7} = (6.79 \pm 0.36) \cdot 10^{-7} \,, \\
\mathcal{H}_L[3.5,6]_{\mu\mu} =&(5.34 \pm 0.23_{\text{scale}} \pm 0.06_{m_t} \pm 0.19_{C,m_c} \pm 0.04_{m_b} \\
&\pm 0.03_{\alpha_s} \pm 0.01_{\text{CKM}} \pm 0.07_{\text{BR}_{\text{sl}}}) \cdot 10^{-7} = (5.34 \pm 0.32) \cdot 10^{-7} \,, \\
\mathcal{H}_L[1,6]_{\mu\mu} =&(1.21 \pm 0.04_{\text{scale}} \pm 0.01_{m_t} \pm 0.04_{C,m_c} \pm 0.01_{m_b} \\
&\pm 0.01_{\alpha_s} \pm 0.003_{\text{CKM}} \pm 0.02_{\text{BR}_{\text{sl}}}) \cdot 10^{-6} = (1.21 \pm 0.07) \cdot 10^{-6} \,. \qquad (5.4)
\end{aligned}
$$

5.2 $\mathcal{H}_A$

For the zero-crossing q_0^2 of $\mathcal{H}_A$, which is equivalent to the zero of the forward-backward asymmetry due to equation (4.3), we find

$$
\begin{aligned}
(q_0^2)_{ee} =&(3.46 \pm 0.10_{\text{scale}} \pm 0.001_{m_t} \pm 0.02_{C,m_c} \pm 0.06_{m_b} \pm 0.02_{\alpha_s})\ \text{GeV}^2 \\
=&(3.46 \pm 0.11)\ \text{GeV}^2 \,, \qquad (5.5) \\
(q_0^2)_{\mu\mu} =&(3.58 \pm 0.10_{\text{scale}} \pm 0.001_{m_t} \pm 0.02_{C,m_c} \pm 0.06_{m_b} \pm 0.02_{\alpha_s})\ \text{GeV}^2 \\
=&(3.58 \pm 0.12)\ \text{GeV}^2 \,. \qquad (5.6)
\end{aligned}
$$

We observe that the inclusive zero is in the same region as the semi-inclusive one obtained in the presence of a cut on m_{X_s} [71], but considerably lower than in the exclusive $\bar{B} \to K^* \ell^+ \ell^-$ case [100]. The integrated $\mathcal{H}_A$ reads

$$
\begin{aligned}
\mathcal{H}_A[1,3.5]_{ee} =&(-1.03 \pm 0.04_{\text{scale}} \pm 0.01_{m_t} \pm 0.02_{C,m_c} \pm 0.02_{m_b} \\
&\pm 0.01_{\alpha_s} \pm 0.003_{\text{CKM}} \pm 0.01_{\text{BR}_{\text{sl}}}) \cdot 10^{-7} = (-1.03 \pm 0.05) \cdot 10^{-7} \,, \\
\mathcal{H}_A[3.5,6]_{ee} =&(+0.73 \pm 0.11_{\text{scale}} \pm 0.01_{m_t} \pm 0.04_{C,m_c} \pm 0.05_{m_b} \\
&\pm 0.02_{\alpha_s} \pm 0.002_{\text{CKM}} \pm 0.01_{\text{BR}_{\text{sl}}}) \cdot 10^{-7} = (+0.73 \pm 0.12) \cdot 10^{-7} \,,
\end{aligned}
$$

JHEP06(2015)176

$$\begin{aligned}\mathcal{H}_A[1,6]_{ee} =&(-0.29 \pm 0.14_{\text{scale}} \pm 0.002_{m_t} \pm 0.02_{C,m_c} \pm 0.06_{m_b} \\ &\pm 0.03_{\alpha_s} \pm 0.001_{\text{CKM}} \pm 0.004_{\text{BR}_{\text{sl}}}) \cdot 10^{-7} = (-0.29 \pm 0.16) \cdot 10^{-7} \,.\end{aligned} \tag{5.7}$$

$$\begin{aligned}\mathcal{H}_A[1,3.5]_{\mu\mu} =&(-1.10 \pm 0.03_{\text{scale}} \pm 0.01_{m_t} \pm 0.02_{C,m_c} \pm 0.02_{m_b} \\ &\pm 0.01_{\alpha_s} \pm 0.003_{\text{CKM}} \pm 0.01_{\text{BR}_{\text{sl}}}) \cdot 10^{-7} = (-1.10 \pm 0.05) \cdot 10^{-7} \,, \\ \mathcal{H}_A[3.5,6]_{\mu\mu} =&(+0.67 \pm 0.11_{\text{scale}} \pm 0.01_{m_t} \pm 0.04_{C,m_c} \pm 0.05_{m_b} \\ &\pm 0.02_{\alpha_s} \pm 0.002_{\text{CKM}} \pm 0.01_{\text{BR}_{\text{sl}}}) \cdot 10^{-7} = (+0.67 \pm 0.12) \cdot 10^{-7} \,, \\ \mathcal{H}_A[1,6]_{\mu\mu} =&(-0.42 \pm 0.14_{\text{scale}} \pm 0.003_{m_t} \pm 0.01_{C,m_c} \pm 0.06_{m_b} \\ &\pm 0.03_{\alpha_s} \pm 0.001_{\text{CKM}} \pm 0.01_{\text{BR}_{\text{sl}}}) \cdot 10^{-7} = (-0.42 \pm 0.16) \cdot 10^{-7} \,.\end{aligned} \tag{5.8}$$

As far as the total error is concerned, the single bins are much better behaved than the entire low-q^2 region. This is due to the large cancellation of the central values of bin 1 and bin 2, which is owed to the presence of the zero. The value of the latter happens to be almost exactly at the position where we subdivide the low-q^2 region into bin 1 and bin 2.

5.3 $\mathcal{H}_3$ and $\mathcal{H}_4$

For the observables $\mathcal{H}_3$ and $\mathcal{H}_4$, sensitive to QED corrections, we find

$$\begin{aligned}\mathcal{H}_3[1,3.5]_{ee} =&(4.04 \pm 0.64_{\text{scale}} \pm 0.04_{m_t} \pm 0.13_{C,m_c} \pm 0.10_{m_b} \\ &\pm 0.03_{\alpha_s} \pm 0.01_{\text{CKM}} \pm 0.05_{\text{BR}_{\text{sl}}}) \cdot 10^{-9} = (4.04 \pm 0.67) \cdot 10^{-9} \,, \\ \mathcal{H}_3[3.5,6]_{ee} =&(4.88 \pm 0.50_{\text{scale}} \pm 0.05_{m_t} \pm 0.16_{C,m_c} \pm 0.07_{m_b} \\ &\pm 0.02_{\alpha_s} \pm 0.01_{\text{CKM}} \pm 0.06_{\text{BR}_{\text{sl}}}) \cdot 10^{-9} = (4.88 \pm 0.54) \cdot 10^{-9} \,, \\ \mathcal{H}_3[1,6]_{ee} =&(8.92 \pm 1.14_{\text{scale}} \pm 0.10_{m_t} \pm 0.30_{C,m_c} \pm 0.16_{m_b} \\ &\pm 0.06_{\alpha_s} \pm 0.03_{\text{CKM}} \pm 0.11_{\text{BR}_{\text{sl}}}) \cdot 10^{-9} = (8.92 \pm 1.20) \cdot 10^{-9} \,.\end{aligned} \tag{5.9}$$

$$\begin{aligned}\mathcal{H}_3[1,3.5]_{\mu\mu} =&(1.68 \pm 0.26_{\text{scale}} \pm 0.02_{m_t} \pm 0.06_{C,m_c} \pm 0.04_{m_b} \\ &\pm 0.01_{\alpha_s} \pm 0.005_{\text{CKM}} \pm 0.02_{\text{BR}_{\text{sl}}}) \cdot 10^{-9} = (1.68 \pm 0.27) \cdot 10^{-9} \,, \\ \mathcal{H}_3[3.5,6]_{\mu\mu} =&(2.03 \pm 0.21_{\text{scale}} \pm 0.02_{m_t} \pm 0.07_{C,m_c} \pm 0.03_{m_b} \\ &\pm 0.01_{\alpha_s} \pm 0.006_{\text{CKM}} \pm 0.03_{\text{BR}_{\text{sl}}}) \cdot 10^{-9} = (2.03 \pm 0.22) \cdot 10^{-9} \,, \\ \mathcal{H}_3[1,6]_{\mu\mu} =&(3.71 \pm 0.47_{\text{scale}} \pm 0.04_{m_t} \pm 0.12_{C,m_c} \pm 0.06_{m_b} \\ &\pm 0.02_{\alpha_s} \pm 0.01_{\text{CKM}} \pm 0.05_{\text{BR}_{\text{sl}}}) \cdot 10^{-9} = (3.71 \pm 0.50) \cdot 10^{-9} \,.\end{aligned} \tag{5.10}$$

$$\begin{aligned}\mathcal{H}_4[1,3.5]_{ee} =&(6.23 \pm 0.55_{\text{scale}} \pm 0.07_{m_t} \pm 0.21_{C,m_c} \pm 0.01_{m_b} \\ &\pm 0.02_{\alpha_s} \pm 0.02_{\text{CKM}} \pm 0.08_{\text{BR}_{\text{sl}}}) \cdot 10^{-9} = (6.23 \pm 0.60) \cdot 10^{-9} \,, \\ \mathcal{H}_4[3.5,6]_{ee} =&(2.19 \pm 0.16_{\text{scale}} \pm 0.03_{m_t} \pm 0.07_{C,m_c} \pm 0.02_{m_b} \\ &\pm 0.006_{\alpha_s} \pm 0.006_{\text{CKM}} \pm 0.03_{\text{BR}_{\text{sl}}}) \cdot 10^{-9} = (2.19 \pm 0.18) \cdot 10^{-9} \,,\end{aligned}$$

JHEP06(2015)176

$$\mathcal{H}_4[1,6]_{ee} =(8.41 \pm 0.71_{\text{scale}} \pm 0.10_{m_t} \pm 0.28_{C,m_c} \pm 0.02_{m_b} \pm 0.02_{\alpha_s} \pm 0.02_{\text{CKM}} \pm 0.10_{\text{BR}_{\text{sl}}}) \cdot 10^{-9} = (8.41 \pm 0.78) \cdot 10^{-9} \,. \tag{5.11}$$

$$\mathcal{H}_4[1,3.5]_{\mu\mu} =(2.59 \pm 0.23_{\text{scale}} \pm 0.03_{m_t} \pm 0.09_{C,m_c} \pm 0.006_{m_b} \pm 0.007_{\alpha_s} \pm 0.007_{\text{CKM}} \pm 0.03_{\text{BR}_{\text{sl}}}) \cdot 10^{-9} = (2.59 \pm 0.25) \cdot 10^{-9} \,,$$

$$\mathcal{H}_4[3.5,6]_{\mu\mu} =(0.91 \pm 0.07_{\text{scale}} \pm 0.01_{m_t} \pm 0.03_{C,m_c} \pm 0.008_{m_b} \pm 0.002_{\alpha_s} \pm 0.003_{\text{CKM}} \pm 0.01_{\text{BR}_{\text{sl}}}) \cdot 10^{-9} = (0.91 \pm 0.075) \cdot 10^{-9} \,,$$

$$\mathcal{H}_4[1,6]_{\mu\mu} =(3.50 \pm 0.29_{\text{scale}} \pm 0.04_{m_t} \pm 0.12_{C,m_c} \pm 0.01_{m_b} \pm 0.01_{\alpha_s} \pm 0.01_{\text{CKM}} \pm 0.04_{\text{BR}_{\text{sl}}}) \cdot 10^{-9} = (3.50 \pm 0.32) \cdot 10^{-9} \,. \tag{5.12}$$

5.4 Branching ratio, low-q^2 region

The decay width is simply given by the sum of H_T and H_L and hence can in principle be derived by the numbers given in the previous subsections. However, we give the numbers explicitly here, for two reasons. First, the branching ratio is an important quantity, also experimentally. Second, there are two more contributions which are available only for the branching ratio, but not for $\mathcal{H}_T$ or $\mathcal{H}_L$ individually. These are the finite bremsstrahlung contributions from [48] and the non-log enhanced terms of $\omega_{99}^{(\text{em})}(\hat{s})$. Both give only a small correction, but we include them for the sake of completeness. This yields

$$\mathcal{B}[1,3.5]_{ee} =(9.26 \pm 0.34_{\text{scale}} \pm 0.11_{m_t} \pm 0.30_{C,m_c} \pm 0.10_{m_b} \pm 0.02_{\alpha_s} \pm 0.03_{\text{CKM}} \pm 0.11_{\text{BR}_{\text{sl}}}) \cdot 10^{-7} = (9.26 \pm 0.49) \cdot 10^{-7} \,,$$

$$\mathcal{B}[3.5,6]_{ee} =(7.44 \pm 0.37_{\text{scale}} \pm 0.10_{m_t} \pm 0.26_{C,m_c} \pm 0.08_{m_b} \pm 0.03_{\alpha_s} \pm 0.02_{\text{CKM}} \pm 0.09_{\text{BR}_{\text{sl}}}) \cdot 10^{-7} = (7.44 \pm 0.48) \cdot 10^{-7} \,,$$

$$\mathcal{B}[1,6]_{ee} =(1.67 \pm 0.07_{\text{scale}} \pm 0.02_{m_t} \pm 0.06_{C,m_c} \pm 0.02_{m_b} \pm 0.01_{\alpha_s} \pm 0.005_{\text{CKM}} \pm 0.02_{\text{BR}_{\text{sl}}}) \cdot 10^{-6} = (1.67 \pm 0.10) \cdot 10^{-6} \,. \tag{5.13}$$

$$\mathcal{B}[1,3.5]_{\mu\mu} =(8.88 \pm 0.31_{\text{scale}} \pm 0.11_{m_t} \pm 0.29_{C,m_c} \pm 0.10_{m_b} \pm 0.02_{\alpha_s} \pm 0.02_{\text{CKM}} \pm 0.11_{\text{BR}_{\text{sl}}}) \cdot 10^{-7} = (8.88 \pm 0.46) \cdot 10^{-7} \,,$$

$$\mathcal{B}[3.5,6]_{\mu\mu} =(7.31 \pm 0.36_{\text{scale}} \pm 0.09_{m_t} \pm 0.25_{C,m_c} \pm 0.09_{m_b} \pm 0.03_{\alpha_s} \pm 0.02_{\text{CKM}} \pm 0.09_{\text{BR}_{\text{sl}}}) \cdot 10^{-7} = (7.31 \pm 0.47) \cdot 10^{-7} \,,$$

$$\mathcal{B}[1,6]_{\mu\mu} =(1.62 \pm 0.07_{\text{scale}} \pm 0.02_{m_t} \pm 0.05_{C,m_c} \pm 0.02_{m_b} \pm 0.01_{\alpha_s} \pm 0.005_{\text{CKM}} \pm 0.02_{\text{BR}_{\text{sl}}}) \cdot 10^{-6} = (1.62 \pm 0.09) \cdot 10^{-6} \,. \tag{5.14}$$

The values are about 2% larger compared to our previous analysis [76]. This is due to updated input parameters and the inclusion of the Krüger-Sehgal corrections [72, 73].

5.5 Branching ratio, high-q^2 region

The branching ratio in the high-q^2 region suffers from large uncertainties stemming from hadronic input parameters in the $1/m_b^{2,3}$ power-corrections, which results in total error

JHEP06(2015)176

bars of $\mathcal{O}(30\%)$,

$$\begin{aligned}
\mathcal{B}[>14.4]_{ee} =&(2.20 \pm 0.30_{\text{scale}} \pm 0.03_{m_t} \pm 0.06_{C,m_c} \pm 0.16_{m_b} \pm 0.003_{\alpha_s} \\
&\pm 0.01_{\text{CKM}} \pm 0.03_{\text{BR}_{\text{sl}}} \pm 0.12_{\lambda_2} \pm 0.48_{\rho_1} \pm 0.36_{f_s} \pm 0.05_{f_u}) \cdot 10^{-7} \\
=&(2.20 \pm 0.70) \cdot 10^{-7} \,, \\
\mathcal{B}[>14.4]_{\mu\mu} =&(2.53 \pm 0.29_{\text{scale}} \pm 0.03_{m_t} \pm 0.07_{C,m_c} \pm 0.18_{m_b} \pm 0.003_{\alpha_s} \\
&\pm 0.01_{\text{CKM}} \pm 0.03_{\text{BR}_{\text{sl}}} \pm 0.12_{\lambda_2} \pm 0.48_{\rho_1} \pm 0.36_{f_s} \pm 0.05_{f_u}) \cdot 10^{-7} \\
=&(2.53 \pm 0.70) \cdot 10^{-7} \,.
\end{aligned} \tag{5.15}$$

Comparing these results to earlier analyses on the high-q^2 branching ratio shows that our numbers are considerably lower than the ones in [53, 54]. In the following, we show that this is the result of several effects which all give corrections in the same direction. Once we turn to the prescriptions given in [53, 54] we reproduce their results, as can be seen below.

We first perform the comparison to Greub et al. [54]. We start with the above numbers and first switch off the $\ln(m_b^2/m_\ell^2)$-enhanced QED corrections, which also removes the difference between the muon and the electron channel, and yields 2.74 (all numbers that follow are in units of 10^{-7}). Next, we turn off the finite bremsstrahlung contributions, which is only a minor effect and does not change the digits given before. Taking out the Krüger-Sehgal corrections, on the other hand, is a rather large effect in the high-q^2 region and results in 3.05. We also have to remove the $1/m_b^{2,3}$ and $1/m_c^2$ non-factorisable power-corrections which further increases the result to 3.36. Switching furthermore off those QED corrections which are not $\ln(m_b^2/m_\ell^2)$-enhanced, we get 3.56. This shift is rather large, but we remind the reader that some of these terms are enhanced by $m_t^2/(M_W^2 \sin^2\theta_W)$. Changing from four- to two-loop running for α_s has again only a minor impact and gives 3.55. We now switch off the change in renormalisation scheme for the quark masses, i.e. we use the pole mass for charm and bottom. Furthermore, we use the input parameters from [54]. Both effects taken together give 3.68. We now take into account that the integration interval in [54] is given in the variable $\hat{s} = q^2/m_b^2$. Hence a change in the value for m_b results in the modified lower integration limit $q^2_{\text{min}} = 13.824\ \text{GeV}^2$. This effect must not be underestimated because it brings the branching ratio up to 4.36. We now turn to the normalisation prescription given in [54], which instead of the factor C from eq. (4.5) and the perturbative expansion of $\Gamma(b \to u\, e\, \bar{\nu})$ makes direct use of the perturbative expansion of $\Gamma(b \to c\, e\, \bar{\nu})$, including charm-mass dependent phase-space factors and radiative corrections. This increases the branching ratio further to 4.57. Finally, we divide by the experimentally measured semileptonic $b \to c$ branching ratio (see table 1) and get 43, which is precisely the value of $R_{\text{high, pert}}$ in eq. (48) of [54].

The comparison to Ghinculov et al. in [53] proceeds along the same lines. The differences to the analysis by Greub et al. are the Krüger-Sehgal corrections and the $1/m_b^{2,3}$, $1/m_c^2$ power corrections, both are taken into account in [53]. Moreover, different input parameters are used and the lower integration limit is formulated in q^2 rather than in $\hat{s}$. To quantify these effects, we first switch off again $\ln(m_b^2/m_\ell^2)$-enhanced QED corrections and finite bremsstrahlung effects first and end up with 2.74. We then also remove those QED

JHEP06(2015)176

corrections that are not enhanced by $\ln(m_b^2/m_\ell^2)$, which gives 2.93. Changing from four- to two-loop running for α_s is again only a small effect and gives 2.92. The biggest effect comes from the change of input parameters and the removal of the renormalisation-scheme conversion for the quark masses, i.e. we now use the pole mass for charm and bottom. These two effects taken together result in 3.89. Finally, we switch to the normalisation that is used in [53] and get 4.02. This number coincides within a fraction of a percent with the value 4.04 from eq. (6.36) in [53]. The obtained level of accuracy shall be sufficient for the present check.

5.6 The ratio $\mathcal{R}(s_0)$

$$\begin{aligned}
\mathcal{R}(14.4)_{ee} =&(2.25 \pm 0.12_{\text{scale}} \pm 0.03_{m_t} \pm 0.02_{C,m_c} \pm 0.01_{m_b} \pm 0.01_{\alpha_s} \pm 0.20_{\text{CKM}} \\
&\pm 0.02_{\lambda_2} \pm 0.14_{\rho_1} \pm 0.08_{f_u^0+f_s} \pm 0.12_{f_u^0-f_s}) \cdot 10^{-3} \\
=&(2.25 \pm 0.31) \cdot 10^{-3} \,, \\
\mathcal{R}(14.4)_{\mu\mu} =&(2.62 \pm 0.09_{\text{scale}} \pm 0.03_{m_t} \pm 0.01_{C,m_c} \pm 0.01_{m_b} \pm 0.01_{\alpha_s} \pm 0.23_{\text{CKM}} \\
&\pm 0.0002_{\lambda_2} \pm 0.09_{\rho_1} \pm 0.04_{f_u^0+f_s} \pm 0.12_{f_u^0-f_s}) \cdot 10^{-3} \\
=&(2.62 \pm 0.30) \cdot 10^{-3} \,.
\end{aligned} \tag{5.16}$$

We clearly see a reduction of the total error bars from $\mathcal{O}(30\%)$ in the high-q^2 branching ratio to 14% and 11% in the electron and muon channel of $\mathcal{R}(s_0)$, respectively. Besides the uncertainties due to power corrections, also the scale uncertainty gets significantly reduced. The largest source of error are CKM elements (notably V_{ub}).

6 New physics sensitivities

In this section we present the constraints on the most relevant Wilson coefficients (C_9 and C_{10}) that we obtain using the current experimental results, and investigate the reach of Belle II with an expected final integrated luminosity of 50 ab^{-1}.

Previous model-independent new physics analyses [77, 101–103], as well as studies in specific models such as minimal-flavour-violation [104–106], two-Higgs doublet models [107, 108], and supersymmetry [102, 109–115] can be found in the literature.

The weighted averages for the low- and high-q^2 branching fractions have been presented in eq. (1.2). Here we need the results on the individual channels:

$$\mathcal{B}(\bar{B} \to X_s \ell^+\ell^-)^{\text{exp}}_{\text{low}} = \begin{cases} \left(1.493 \pm 0.504^{+0.411}_{-0.321}\right) \times 10^{-6} & (\text{Belle}, \ell\ell) \\ \left(1.93^{+0.47+0.21}_{-0.45-0.16} \pm 0.18\right) \times 10^{-6} & (\text{BaBar}, ee) \\ \left(0.66^{+0.82+0.30}_{-0.76-0.24} \pm 0.18\right) \times 10^{-6} & (\text{BaBar}, \mu\mu) \\ \left(1.6^{+0.41+0.17}_{-0.39-0.13} \pm 0.18\right) \times 10^{-6} & (\text{BaBar}, \ell\ell)\,, \end{cases} \tag{6.1}$$

$$\mathcal{B}(\bar{B} \to X_s \ell^+\ell^-)^{\text{exp}}_{\text{high}} = \begin{cases} \left(0.418 \pm 0.117^{+0.061}_{-0.068}\right) \times 10^{-6} & (\text{Belle}, \ell\ell) \\ \left(0.56^{+0.19+0.03}_{-0.18-0.03} \pm 0.00\right) \times 10^{-6} & (\text{BaBar}, ee) \\ \left(0.60^{+0.31+0.05}_{-0.29-0.04} \pm 0.00\right) \times 10^{-6} & (\text{BaBar}, \mu\mu\,) \\ \left(0.57^{+0.16+0.03}_{-0.15-0.02} \pm 0.00\right) \times 10^{-6} & (\text{BaBar}, \ell\ell)\,. \end{cases} \tag{6.2}$$

JHEP06(2015)176

In each result, the first error is statistical, the second systematics and the third model-depedent systematics which is included in case of Belle in the second error. Note that the high-q^2 region chosen by BaBar and Belle have a slightly different q^2 minimum (14.4 and 14.2 GeV^2 for Belle and BaBar, respectively).

In ref. [39] Belle presented a measurement of the normalized forward-backward asymmetry defined in eq. (2.10) in the low- and high-q^2 regions. The binning chosen to present the measurement (bin1 = [0.2,4.3] GeV^2 and bin2 = [4.3,7.3(8.1)] GeV^2 for electrons (muons)) differs from the one proposed in this work. In particular, the larger integration end-point in the second bin includes a region of the spectrum where sizable interference from the tail of the J/ψ is present. From ref. [39] we read:

$$\overline{A}_{\rm FB}^{\rm exp}(\bar{B} \to X_s \ell^+ \ell^-) = \begin{cases} 0.34 \pm 0.24 \pm 0.02 & \text{Belle, bin1} \\ 0.04 \pm 0.31 \pm 0.05 & \text{Belle, bin2.} \end{cases} \tag{6.3}$$

In order to preserve the cancellation of systematic uncertainties, Belle averaged the normalized asymmetries in the electron and muon channels; i.e.

$$\overline{A}_{\rm FB}(\bar{B} \to X_s \ell^+ \ell^-) = \left(\overline{A}_{\rm FB}(\bar{B} \to X_s e^+ e^-) + \overline{A}_{\rm FB}(\bar{B} \to X_s \mu^+ \mu^-)\right)/2\,. \tag{6.4}$$

We integrated our differential spectra in the above bins in order to investigate the impact that this measurement has on the Wilson coefficients, but we caution the reader that the uncertainties we quote could be underestimated. We find:

$$\overline{A}_{\rm FB}(\bar{B} \to X_s \ell^+ \ell^-) = \begin{cases} -0.0773 \pm 0.0057 & \text{bin1} \\ +0.049 \pm 0.018 & \text{bin2.} \end{cases} \tag{6.5}$$

We define the following ratios of high-scale Wilson coefficients (see [76] for the precise definitions of the Wilson coefficients),

$$R_{7,8} = \frac{C_{7,8}^{(00)\rm eff}(\mu_0)}{C_{7,8}^{(00)\rm eff,SM}(\mu_0)} \qquad \text{and} \qquad R_{9,10} = \frac{C_{9,10}^{(11)}(\mu_0)}{C_{9,10}^{(11)\rm SM}(\mu_0)}\,. \tag{6.6}$$

The numerical formulas for all observables in terms of the ratios R_i can be found in appendix B. We assume that the relative theoretical uncertainty on a given observable ($\delta O/O$) is mostly independent of the precise values of Wilson coefficients and that it can be extracted from the SM predictions presented in section 5.

We present the bounds on the ratios R_9 and R_{10} under the assumption of no new physics contributions to the magnetic and chromo-magnetic dipole operators ($R_{7,8} = 1$) in figure 4 (similar analyses were done, e.g., in [77, 101]). The contours are the 95% C.L. regions allowed by the experimental results in eqs. (6.1), (6.2) and (1.2); two sigma theoretical uncertainties are added linearly. In each plot we show the impact of the branching ratio measurement in the low-q^2 (red regions) and high-q^2 (green regions) and their overlap (black regions). The SM corresponds to the point $[R_9, R_{10}] = [1, 1]$. As we discuss below, the small yellow contours correspond to the Belle II estimated reach, assuming that the observed central values coincide with our predictions. The top left, top right and lower

JHEP06(2015)176

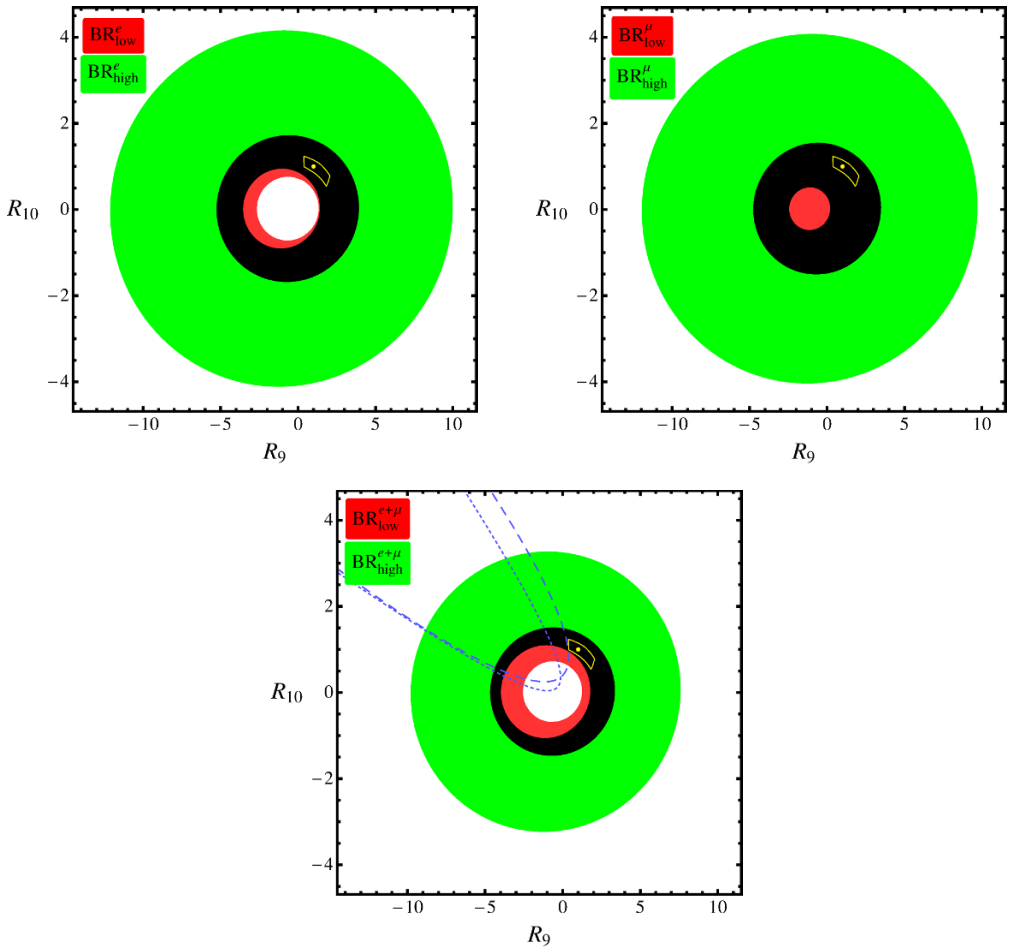

Figure 4. Constraints on the high-scale Wilson coefficient ratios $[R_9, R_{10}]$ that we obtain at 95% C.L. from the present BaBar and Belle experimental branching ratios measurements. In the upper left (upper right, lower) plot we show the constraints obtained from the measured branching ratios in the low-q^2 and high-q^2 region in the electron (muon, electron plus muon) channel. The red and green regions correspond to the low- and high-q^2 regions, respectively. The black region is the overlap of these two constraints. The dot is the SM expectation ($[R_9, R_{10}] = [1, 1]$). The yellow contour is the Belle II reach (see figures 5–7). The region outside the dashed (dotted) parabola shaped regions are allowed by the Belle measurement of the normalized forward-backward asymmetry in bin1 (bin2).

plot consider the $B \to X_s e^+ e^-$, $B \to X_s \mu^+ \mu^-$ and $B \to X_s \ell^+ \ell^-$ cases, respectively. In the lower plot in figure 4 we include also the 95% C.L. bounds from the Belle measurement of the normalized forward-backward asymmetry given in eq. (6.3); the region outside the dashed and dotted parabola shaped regions are allowed by the measurement in bin1 and bin2, respectively. The resulting picture is in overall agreement with the SM expectations at the 95% C.L.; though we should note that at the one sigma level there are some statistically insignificant tensions driven by a disagreement between low- and high-q^2 measurements in the muon channel.

In order to study the expected Belle II reach, we estimate the statistical uncertainties on the various observables using the squared weight method detailed in ref. [116]. Let us

JHEP06(2015)176

	$[1, 3.5]$	$[3.5, 6]$	$[1, 6]$	> 14.4
$\mathcal{B}$	3.7 %	4.0 %	3.0 %	4.1%
$\mathcal{H}_T$	24 %	21 %	16 %	—
$\mathcal{H}_L$	5.8 %	6.8 %	4.6 %	—
$\mathcal{H}_A$	37 %	44 %	200 %	—
$\mathcal{H}_3$	240 %	180 %	150 %	—
$\mathcal{H}_4$	140 %	360 %	140 %	—

Table 3. Statistical uncertainties that we expect at Belle II with 50 ab^{-1} of integrated luminosity. The first row gives the considered q^2 bin in GeV^2.

consider the following differential quantity:

$$\frac{d^2\mathcal{N}}{d\hat{s}dz} = \frac{\mathcal{L}\ \sigma_{\text{prod}}}{\Gamma_{\text{tot}}} \frac{d^2\Gamma}{d\hat{s}dz} \tag{6.7}$$

where the $\mathcal{L}$ is the integrated luminosity, σ_{prod} is the production cross section for $e^+e^- \to B\bar{B}$ at the B-factories' center of mass energy, Γ_{tot} is the total B decay width and $d^2\Gamma/d\hat{s}dz$ is the double differential $B \to X_s\ell^+\ell^-$ decay rate. The number of events that we expect to observe in a certain range of $\hat{s}$ and z is

$$\mathcal{N}_{\text{exp}} = \int \frac{d^2\mathcal{N}}{d\hat{s}dz} d\hat{s}\ dz\ , \tag{6.8}$$

$$\delta\mathcal{N}_{\text{exp}} = \sqrt{\mathcal{N}_{\text{exp}}} \tag{6.9}$$

where $\delta\mathcal{N}_{\text{exp}}$ is the expected statistical error. If instead of considering simple slices of the integration region we utilize a weight function $W[\hat{s}, z]$ to define an observable (that cannot be anymore interpreted in terms of "number of events"), the above equations generalize to

$$\mathcal{O}_{\text{exp}} = \int \frac{d^2\mathcal{N}}{d\hat{s}dz}\ W[\hat{s}, z]\ d\hat{s}\ dz\ , \tag{6.10}$$

$$\delta\mathcal{O}_{\text{exp}} = \left[\int \frac{d^2\mathcal{N}}{d\hat{s}dz}\ W[\hat{s}, z]^2\ d\hat{s}\ dz\right]^{\frac{1}{2}}\ . \tag{6.11}$$

Note that eq. (6.11) reproduces the correct uncertainties for the simple case in which the weight is a product of theta functions (i.e. the integral is restricted to a certain region of phase space) and that the relative uncertainty $\delta\mathcal{O}_{\text{exp}}/\mathcal{O}_{\text{exp}}$ is invariant under rescaling of the weight function.

In order to asses expected uncertainties on observables corresponding to the weights given in eq. (2.7) we start from the double differential rate given in eq. (1.4) and use the expressions for the H_I in eqs. (2.1)–(2.3) and use some reference value for the Wilson coefficients. Next we fix the normalization $\mathcal{L}\ \sigma_{\text{prod}}/\Gamma_{\text{tot}}$ in such a way to reproduce the $\sim 25\%$ statistical uncertainty that BaBar obtains with an integrated luminosity $\mathcal{L}_{\text{current}} =$

JHEP06(2015)176

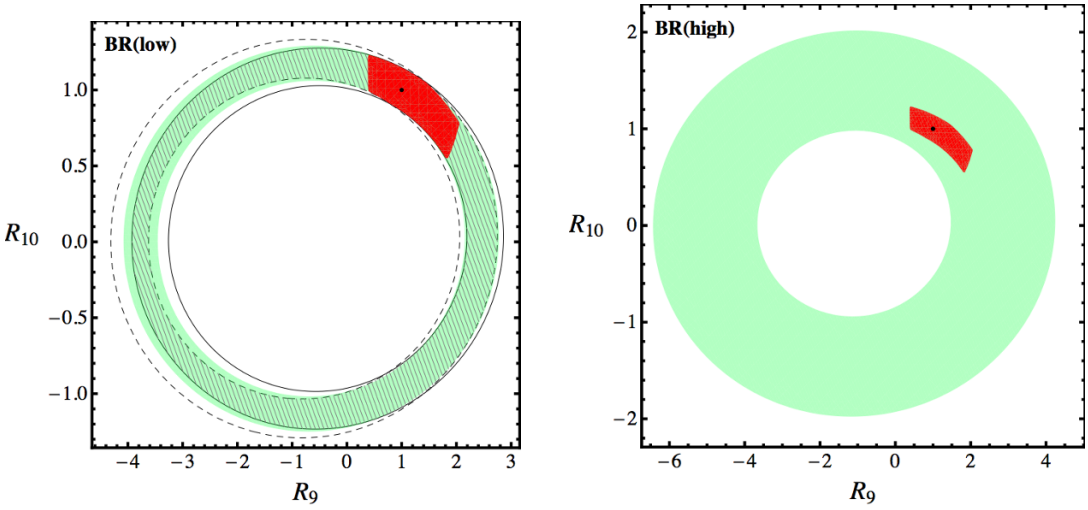

Figure 5. Constraints on $[R_9, R_{10}]$ that we expect at 95% C.L. from Belle II measurements of the branching ratio in the low-q^2 (left plot) and high-q^2 (right plot) regions with 50 ab^{-1} of integrated luminosity. For the low-q^2 case, the solid and dashed contours correspond to the branching ratio restricted to the low ($[1, 3.5]$ GeV^2) and high ($[3.5, 6]$ GeV^2) bin, respectively. The hashed region is the overlap of the expected constraints from these two bins. The shaded region is the constraint we obtain by considering the branching ratio integrated in the whole low-q^2 region. The black dot is the SM expectation. The solid red area is the overlap of all constraints we consider (it corresponds to the yellow contour in figure 4).

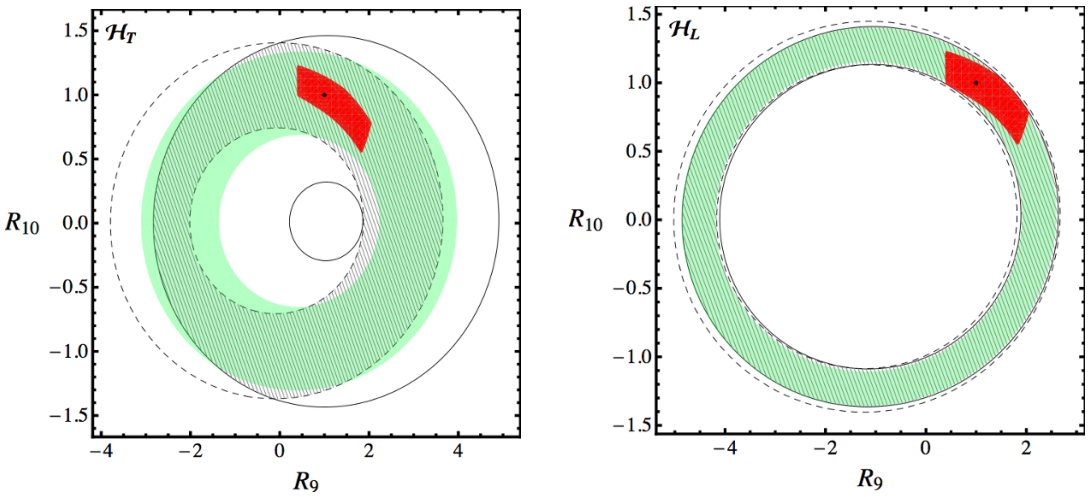

Figure 6. Constraints on $[R_9, R_{10}]$ that we expect at 95% C.L. from Belle II measurements of $\mathcal{H}_T$ (left plot) and $\mathcal{H}_L$ (right plot) in the low-q^2 region with 50 ab^{-1} of integrated luminosity. See figure 5 for further details.

0.4242 ab^{-1} [37]. Finally we rescale the normalization by the factor $\mathcal{L}_{\text{future}}/\mathcal{L}_{\text{current}}$ where $\mathcal{L}_{\text{future}} = 50$ ab^{-1} is the Belle II expected final integrated luminosity.

This procedure produces acceptable error estimates for $\mathcal{H}_T$, $\mathcal{H}_L$ and $\mathcal{H}_A$, while fails for $\mathcal{H}_3$ and $\mathcal{H}_4$. The reason is that the integral in eq. (6.10) vanishes when integrated the simple NLO formula given in eq. (1.4) against the weights $W_{3,4}$. We bypass this problem by

JHEP06(2015)176

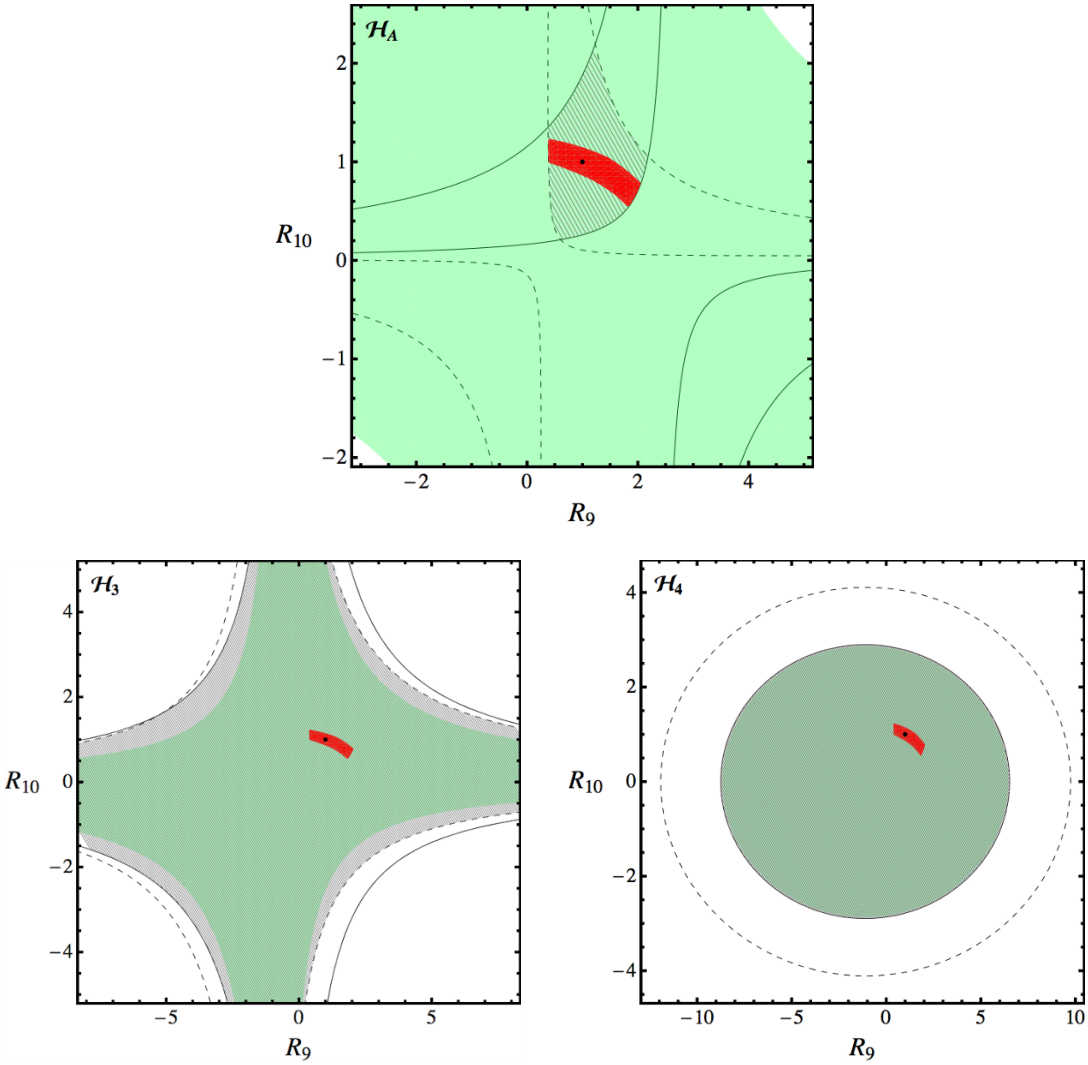

Figure 7. Constraints on $[R_9, R_{10}]$ that we expect at 95% C.L. from Belle II measurements of $\mathcal{H}_A$ (upper plot), $\mathcal{H}_3$ (lower left plot) and $\mathcal{H}_4$ (lower right plot) in the low-q^2 region with 50 ab^{-1} of integrated luminosity. See figure 5 for further details.

extracting $\mathcal{O}_{\rm exp}$ from the exact results presented in section 5 and using eq. (6.11) to calculate the error (in fact the weights $(W_{3,4})^2$ *do not* annihilate the NLO differential width).

Following the discussion summarized in section 5 of ref. [18], we add a flat 2% systematics to the projected statistical errors obtained with the squared weight method and obtain the low-q^2 uncertainties collected in table 3. The expected uncertainty on the high-q^2 branching ratio is taken directly from ref. [18]; in fact, near the end-point of the spectrum our method fails to take into account the improvement in the signal-to-background ratio.

In figures 5, 6 and 7 we show the expected impact of Belle II measurements on the various observables we consider in the $[R_9, R_{10}]$ plane. Each contour is drawn at 95% C.L. by combining linearly theoretical and experimental uncertainties. In the scenario we consider the strongest bounds on the Wilson coefficients are driven by measurements of the low-q^2 branching ratio and of $\mathcal{H}_A$ and $\mathcal{H}_T$ in the two bins. The latter statement is

JHEP06(2015)176

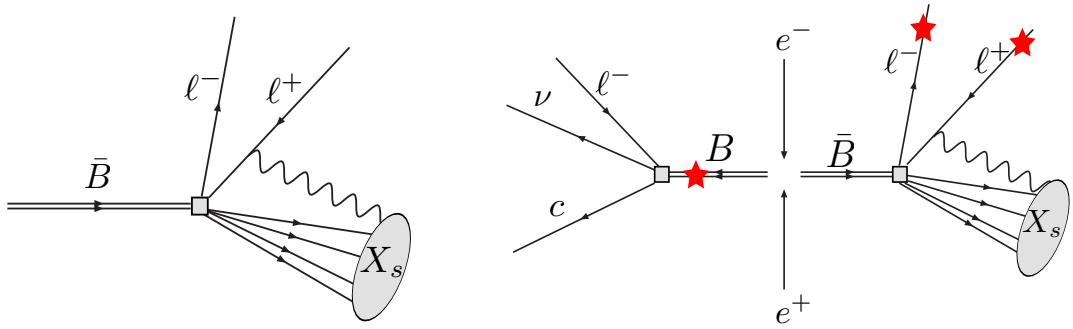

Figure 8. Pictorial descriptions of the theoretical definition (left) of $\bar{B} \to X_s \ell^+ \ell^-$ and of the experimental recoil technique.

driven by the assumption that the future experimental central values will coincide with the respective SM expectations. If deviations are seen, all observables become crucial to pin down the structure of new physics.

7 On the connection between theory and experiments

7.1 Various experimental settings

Here we discuss how to compare integrated low and high–q^2 observables, calculated with the inclusion of QED corrections, to quantities measured by BaBar, Belle and also by the future Belle II experiment. As we explain below, we find that our results can be directly compared to integrated observables measured at BaBar, Belle, and Belle II with the exception of the di-electron case at BaBar. In the latter case we have to increase our predictions for the integrated branching ratio in the low (high) q^2 region by 1.65% (6.8%), see eqs. (7.1) and (7.2).

From the theoretical standpoint the X_s system, in the inclusive $X_s \ell^+ \ell^-$ final state, contains all the electromagnetic radiation produced in the hard interaction, see the diagram on the left in figure 8. From the experimental point of view there are two distinct techniques to measure the inclusive $B \to X_s \ell^+ \ell^-$ rate: the recoil and sum-over-exclusive methods. In the recoil technique, whose luminosity requirement makes it viable only at super flavor factories, one of the B mesons produced in the e^+e^- hard interaction is tagged using a semileptonic or hadronic decay and the final state is identified by the two leptons only, see the diagram on the right in figure 8. In the sum-over-exclusive method, the recoling heavy meson is not looked at and the decaying B is fully reconstructed in final states with a $K^{(*)}$ and up to four pions. The fully inclusive rate is then reconstructed using JETSET [117].

The comparison between the measured branching ratio (BR) and the results of our inclusive calculations depends critically on the definition of q^2. If no photons are included in the definition of the di-lepton invariant mass (i.e. $q^2 \equiv (p_{\ell^+} + p_{\ell^-})^2$) our results can be used directly in the comparison with experiments. This is the case for the di-muon channel at both experiments [118, 119] and for the di-electron channel at Belle [118]. This will be exactly the case in a fully inclusive analysis using the recoil technique at Belle II. However,

JHEP06(2015)176

at BaBar photons that belong to a $B \to X_s e^+ e^-$ event and that are emitted in a cone of 35 mrad angular opening around either final state electron are included in the calculation of the q^2 [119].

In order to calculate the shift that the latter q^2 definition has on to the inclusive theory prediction we generate inclusive $B \to X_s \ell^+ \ell^-$ events using EVTGEN [120], hadronize them with JETSET and include electromagnetic radiation with PHOTOS [121, 122]. Following the BaBar and Belle procedure we build a fully inclusive sample in the whole q^2 and m_{X_s} phase space by fully inclusive events (parton level supplemented by a Fermi Motion Model [57]) for $m_{X_s} > 1.1$ GeV with exclusive $B \to K^{(*)} \ell^+ \ell^-$ events (to describe the low m_{X_s} region). Using this large event sample we were able to calculate the impact of including photons emitted in a 35 mrad cone around either electron in the q^2 calculation. We find:

$$\frac{\left[\mathcal{B}_{ee}^{\text{low}}\right]_{q=p_{e^+}+p_{e^-}+p_{\gamma_{\text{coll}}}}}{\left[\mathcal{B}_{ee}^{\text{low}}\right]_{q=p_{e^+}+p_{e^-}}} - 1 = 1.65\% \tag{7.1}$$

$$\frac{\left[\mathcal{B}_{ee}^{\text{high}}\right]_{q=p_{e^+}+p_{e^-}+p_{\gamma_{\text{coll}}}}}{\left[\mathcal{B}_{ee}^{\text{high}}\right]_{q=p_{e^+}+p_{e^-}}} - 1 = 6.8\% \,. \tag{7.2}$$

where the suffixes $q = p_{e^+} + p_{e^-}$ and $q = p_{e^+} + p_{e^-} + p_{\gamma_{\text{coll}}}$ refer to quantities we calculate and observables measured at BaBar, respectively.

7.2 Validation

The results presented in the previous subsection depend crucially on the reliability of using PHOTOS to model photon radiation in $b \to s\ell^+\ell^-$ decays. In this subsection we perform several checks to validate this approach; in particular we show that PHOTOS can be used to reproduce (to a good enough extent) the effects of QED radiation that we calculate analytically.

As discussed above, we generate inclusive $B \to X_s \ell^+ \ell^-$ events using EVTGEN, hadronize them with JETSET and include electromagnetic radiation with PHOTOS. In order to obtain a fully inclusive event set we combine K, K^* and $X_s(m_{X_s} > 1.1$ GeV) samples. The m_{X_s} and q^2 spectra that we obtain are presented in figure 9. The relative weights of the K and K^* samples with respect to the inclusive ($m_{X_s} > 1.1$ GeV) one have to be provided externally. The actual weights we adopt are extracted from experimental results for the exclusive and inclusive modes and their precise values do not impact much the shape of the q^2 spectrum. In fact, as we can see in the plot on the right of figure 9 only the very high di-lepton invariant mass region, $q^2 > 17$ GeV^2, is affected.

A point that is important to mention is that PHOTOS generates events with large photon multiplicity while analytic calculations are confined to a single photon emission. Obviously the vast majority of photons emitted are soft and/or collinear to the final state leptons; moreover, only relatively high energy collinear photons can impact the shape of the q^2 spectrum.

JHEP06(2015)176

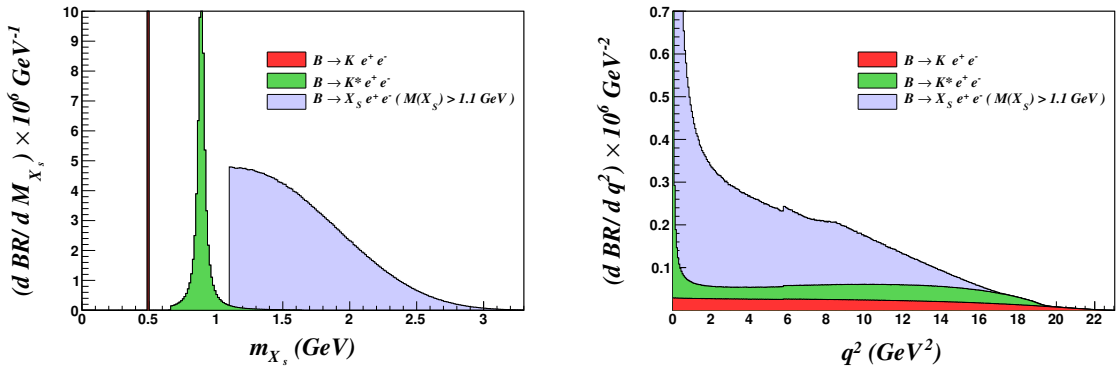

Figure 9. m_{X_s} and q^2 spectra that we obtain in a $B \to X_s \ell^+ \ell^-$ sample generated combining the exclusive $B \to K^{(*)} \ell^+ \ell^-$ modes with a pure inclusive calculation for $m_{X_s} > 1.1$ GeV.

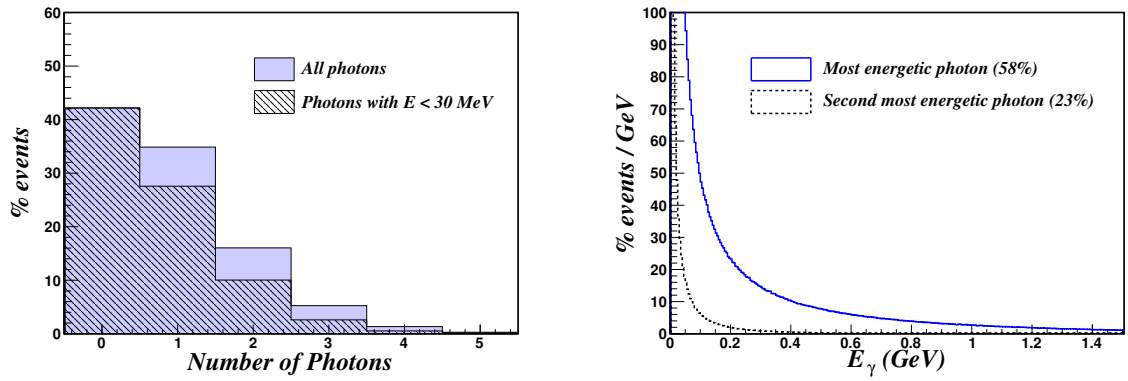

Figure 10. Left: distribution of events with $n_\gamma \leq 5$. Right: distribution of the most energetic and second most energetic photons.

In the left panel of figure 10 we show the photon multiplicity we observe in the generated events. The shaded area corresponds to events for which the most energetic photon has $E_\gamma < 30$ MeV and that, at the experimental level, are identified as purely hadronic $B \to X_s \ell^+ \ell^-$. As expected there is a very large multiplicity of soft photons. We find that only 17% of all events (this is the integral of the purple unshaded region) correspond to final states with at least one photon with energy larger than 30 MeV. These photons are resolved experimentally and need to be included in the hadronic (X_s) or leptonic ($\ell^+ \ell^-$) system least the event is rejected (cf. also the last paragraph of this subsection).

In the right panel of figure 10 we show the distribution of the most and second most energetic photon. The integral of the upper (lower) curve over a photon energy range $[E_{\gamma 1}, E_{\gamma 2}]$ yields the percentage of events in which the most (second-most) energetic photon has energy in that interval. The fraction of events with at least one (two) photons is 58% (23%), is given by the integral of these curves and can also be easily read off from the left panel of figure 10. Since the impact of including certain collinear photons in the definition of the q^2 is more pronounced for more energetic photons, we see that these effects are completely described by a single photon emission: the analytic calculation of QED radiation is, therefore, completely adequate to discuss this phenomenon.

JHEP06(2015)176

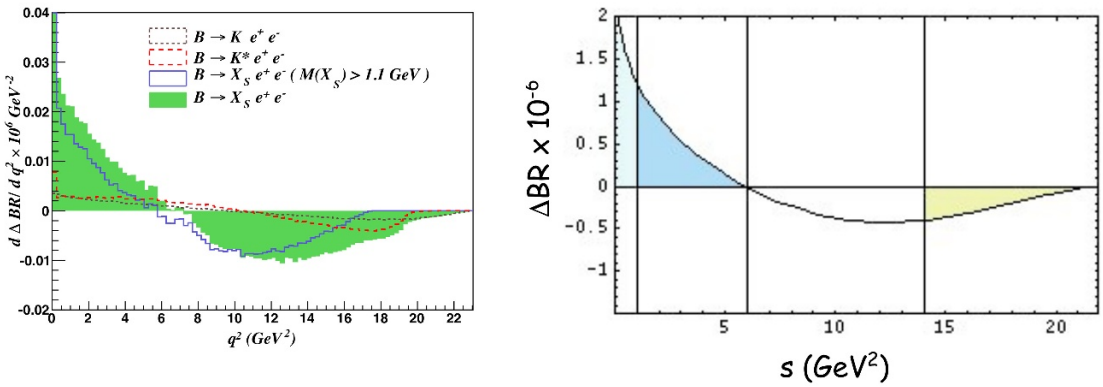

Figure 11. Effect of the inclusion of electromagnetic radiation calculated using EVTGEN + PHOTOS (left) and using analytical methods (right).

Finally, in order to verify whether PHOTOS correctly models photon radiation in this decay, we need to compare q^2 spectra calculated with and without the inclusion of QED radiation. Therefore, we generated a second set of events in which we switched PHOTOS off. The result of this analysis is presented in figure 11. In the left and right panels we show the Monte Carlo study and the result of our analytical calculation, respectively. Numerically, the relative shifts that we obtain for the branching ratio in the low and high–q^2 regions are (in round brackets we present the analytical results):

$$\delta\mathrm{BR}(B \to X_s\mu^+\mu^-) = \begin{cases} +1.5\%(+2.0\%) & \text{low } q^2 \\ -4.4\%(-6.8\%) & \text{high } q^2 \end{cases} \tag{7.3}$$

$$\delta\mathrm{BR}(B \to X_s e^+e^-) = \begin{cases} +3.6\%(+5.2\%) & \text{low } q^2 \\ -12.9\%(-17.6\%) & \text{high } q^2 \ . \end{cases} \tag{7.4}$$

Given the differences in the techniques used, the agreement is remarkable. We conclude that the PHOTOS description of electromagnetic radiation is sufficiently close to the exact calculation to be used to reliably calculate the shifts we presented in eqs. (7.1) and (7.2).

Before concluding this subsection, we would like to stress that validating the use of PHOTOS is important in its own right because experiments use it to estimate the impact of missing photons on their efficiencies. Legitimate $B \to X_s\ell^+\ell^-$ events might be rejected because of two possible reasons. First, if a large number of soft photons ($E_\gamma < 30$ MeV and 20 MeV for BaBar and Belle, respectively) is present, they might push the event out of the m_{ES},[2] and ΔE acceptance windows (see, for instance, refs. [36, 38] for a definition of these kinematical quantities). Second, if a photon with energy larger than 30 (20) MeV is not identified, most likely the event is discarded because the total momentum fails to reconstruct a decaying B meson. The latter effect can be quite substantial because, as we discussed above, about 17% (18%) of all $B \to X_s\ell^+\ell^-$ events have at least one photon with energy larger than 30 MeV (20 MeV). The fraction of events that is lost to these two mechanisms is taken into account, in the calculation of the efficiencies, using PHOTOS.

[2]Belle names this quantity m_{bc}.

JHEP06(2015)176

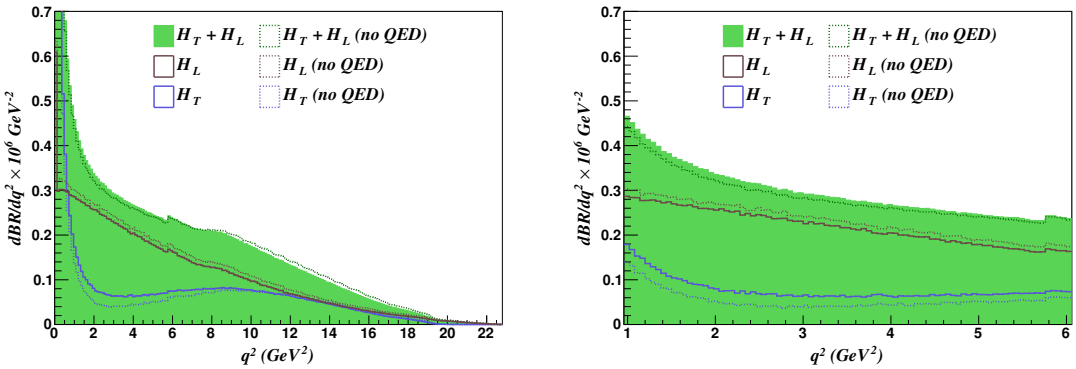

Figure 12. q^2-dependence of $\mathcal{H}_T$, $\mathcal{H}_L$ and branching ratio $(\mathcal{H}_T + \mathcal{H}_L)$ that we extract from a $B \to X_s \ell^+ \ell^-$ sample generated combining the exclusive $B \to K^{(*)} \ell^+ \ell^-$ modes with a pure inclusive calculation for $m_{X_s} > 1.1$ GeV. The dotted lines are obtained by switching off QED radiation.

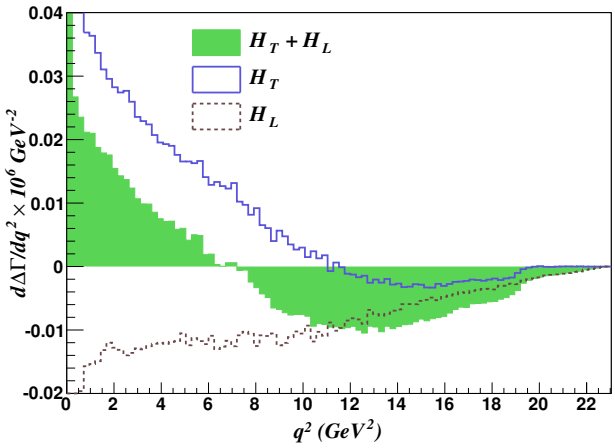

Figure 13. Differential q^2 distributions of the QED corrections to $\mathcal{H}_T$, $\mathcal{H}_L$ and branching ratio $(\mathcal{H}_T + \mathcal{H}_L)$ that we obtain in a $B \to X_s \ell^+ \ell^-$ sample generated using EVTGEN and PHOTOS and combining the exclusive $B \to K^{(*)} \ell^+ \ell^-$ modes with a pure inclusive calculation for $m_{X_s} > 1.1$ GeV.

7.3 Monte Carlo estimate of QED corrections to $\mathcal{H}_T$ and $\mathcal{H}_L$

The results presented in section 5.1 indicate that the relative size of QED corrections to $\mathcal{H}_T$ are about an order of magnitude larger than the corresponding corrections to $\mathcal{H}_L$ and to the branching ratio. In this section we show that this result is actually reproduced in our Monte Carlo study. As a first step we plot in figure 12 the q^2 spectra for $\mathcal{H}_T$, $\mathcal{H}_L$ and the branching ratio with (solid lines) and without (dotted lines) the inclusion of QED radiation.

Note that the absolute size of QED effects on $\mathcal{H}_T$, $\mathcal{H}_L$ and $\mathcal{H}_T + \mathcal{H}_L$ is very similar and natural in size; in particular, a small positive net contribution to the integrated branching ratio in the low-q^2 region is the sum of a small negative shift on $\mathcal{H}_L$ and a slightly larger positive shift on $\mathcal{H}_T$. We plot the actual QED corrections to the three observables in figure 13.

JHEP06(2015)176

	$q^2 \in [1,6]$ GeV^2			$q^2 \in [1,3.5]$ GeV^2			$q^2 \in [3.5,6]$ GeV^2		
	$\frac{O_{[1,6]}}{\mathcal{B}_{[1,6]}}$	$\frac{\Delta O_{[1,6]}}{\mathcal{B}_{[1,6]}}$	$\frac{\Delta O_{[1,6]}}{O_{[1,6]}}$	$\frac{O_{[1,3.5]}}{\mathcal{B}_{[1,6]}}$	$\frac{\Delta O_{[1,3.5]}}{\mathcal{B}_{[1,6]}}$	$\frac{\Delta O_{[1,3.5]}}{O_{[1,3.5]}}$	$\frac{O_{[3.5,6]}}{\mathcal{B}_{[1,6]}}$	$\frac{\Delta O_{[3.5,6]}}{\mathcal{B}_{[1,6]}}$	$\frac{\Delta O_{[3.5,6]}}{O_{[3.5,6]}}$
$\mathcal{B}$	100	3.5	3.5	56.5	2.5	4.5	43.5	1.0	2.5
$\mathcal{H}_T$	19.0	8.0	43.0	10.0	5.0	48.5	8.5	3.0	36.0
$\mathcal{H}_L$	81.0	-4.5	-5.5	46.5	-2.5	-5.0	35.0	-2.0	-6.0

Table 4. Relative size of QED effects at low-q^2 that we extract from our Monte Carlo $b \to se^+e^-$ sample (All entries are given in percent). For each of the three bins the two columns are the integrated observable and its QED correction normalized to the total low-q^2 branching ratio ($\int_{s_1}^{s_2} O / \int_1^6 \mathcal{B}$ and $\int_{s_1}^{s_2} \Delta O / \int_1^6 \mathcal{B}$). The third column is the relative size of the QED correction ($\int_{s_1}^{s_2} \Delta O / \int_{s_1}^{s_2} O$).

From inspection of the left plot in figure 12 we see that, in the low-q^2 region $\mathcal{H}_T$ is much smaller than $\mathcal{H}_L$. We can understand the origin of this effect by looking at the ratio $\mathcal{H}_T/\mathcal{H}_L$ at leading order:

$$\frac{\mathcal{H}_T}{\mathcal{H}_L} = 2\hat{s}\frac{C_{10}^2 + \left(C_9 + \frac{2C_7}{\hat{s}}\right)^2}{C_{10}^2 + (C_9 + 2C_7)^2} \,. \tag{7.5}$$

The suppression comes from the small $2\hat{s} \lesssim 1$ factor and from the accidental strong cancellation between C_9 and $2C_7/\hat{s}$ at low $\hat{s}$ (in fact, the combination $C_9 + 2C_7/\hat{s}$ vanishes for $\hat{s} \sim 0.15$). In the Standard Model C_7 is negative; if its sign was reversed we would obtain $C_9 + 2C_7/\hat{s} > C_9 + 2C_7$ and the integrated $\mathcal{H}_T$ and $\mathcal{H}_L$ observables at low-q^2 would assume very similar values.

In table 4 we present the results we obtain by integrating the Monte Carlo generated $b \to s\ell\ell$ histograms. For each bin ($[s_1, s_2]$) and for each observable O ($\mathcal{H}_T + \mathcal{H}_L$, $\mathcal{H}_T$ and $\mathcal{H}_L$) we show the total integrated observable ($\int_{s_1}^{s_2} O / \int_1^6 (\mathcal{H}_T + \mathcal{H}_L)$), the total integrated QED effect ($\int_{s_1}^{s_2} \Delta O / \int_1^6 (\mathcal{H}_T + \mathcal{H}_L)$) and the relative size of the QED correction ($\int_{s_1}^{s_2} \Delta O / \int_{s_1}^{s_2} O$). We see that the absolute size of QED corrections is very similar amongst the three observables (with the effect on $\mathcal{H}_T$ being only slightly larger) and that the suppression of $\mathcal{H}_T$ with respect to $\mathcal{H}_L$ is responsible for very large relative effects in the 30–50% range.

Finally we must point out that the numerical estimates presented in table 4 are affected by sizable uncertainties that are hard to quantify and that only the analytical results presented in table 2 should be utilized. The Monte Carlo study was nevertheless extremely valuable to build confidence in our study.

8 Conclusion

The inclusive decay $\bar{B} \to X_s \ell^+ \ell^-$ is one of the most important modes in the indirect search for new physics via quark flavour observables. It is theoretically clean, while the exclusive mode is affected by unknown power corrections. Thus, besides allowing for a

JHEP06(2015)176

nontrivial check of the recent LHCb data on the exclusive mode, it contains complementary information both in Standard Model predictions and in pinning down new physics. It is therefore a precious channel to be measured at Belle II, and might be accessible even at LHCb.

In the present article we perform a complete angular analysis of the inclusive decay $\bar{B} \to X_s \ell^+ \ell^-$ by taking into account all perturbative and power corrections that are available to date. We confirm the findings of ref. [77] that a separation of the double differential decay width into three observables $H_{T,A,L}(q^2)$, as well as subdivision of the low-q^2 region into two bins (see also [66]), provides significantly more information than the branching ratio or forward-backward asymmetry in the entire low-q^2 region alone.

We compute logarithmically enhanced QED corrections to these observables and find that they do not obey the simple second-order polynomial in $z = \cos(\theta)$ exhibited by the double differential decay width in the absence of QED corrections. We therefore propose to project out $H_{T,A,L}(q^2)$ using weight functions, and argue that the Legendre polynomials $P_n(z)$ are the optimal choice for the latter. Besides reproducing $H_T(q^2)$ and $H_L(q^2)$ in the absence of QED radiation, they allow to construct observables $H_{3,4}(q^2)$ (eq. (2.6)) that vanish if only QCD corrections are taken into account, and are therefore particular sensitive to QED effects. In view of the benefits of the Legendre weight functions we *urgently* recommend the experiments to use the weights (2.6) to extract single-differential distributions, and to refrain from attempting polynomial fits to the data.

The absolute values of the QED effects that we compute are natural in size. However, due to the phase-space and Wilson coefficient suppression of $H_T(q^2)$ the relative size of the QED corrections is large in this observable. We argue carefully that this does clearly not indicate a breakdown of perturbation theory. On the contrary, we can benefit from the fact that QED corrections lift the smallness of $H_T(q^2)$ to a certain extent, which makes it an observable that is particular sensitive to QED radiation.

To supplement our calculation we carry out a dedicated Monte Carlo study, whose main purpose is three-fold. First, we investigate how the electromagnetic logarithms are treated correctly in the presence of angular and energy cuts. We find that our analytical predictions can be directly applied, with the exception of the electron channel at BaBar, where our numbers have to be modified according to eqs. (7.1) and (7.2). Second, the size of the QED corrections, in particular their large relative size in $H_T(q^2)$, are confirmed by the Monte Carlo (cf. tables 2 and 4). Last but not least, it consitutes also a validation of PHOTOS, which is used by experiments to estimate QED effects in the calculation of efficiencies.

We update the Standard Model predictions for all angular observables integrated over two bins in the low-q^2 region. The branching ratio and the observable $\mathcal{R}(s_0)$ are also evaluated in the high-q^2 region. Moreover, we provide our prediction for the zero crossing of the forward-backward asymmetry (or, equivalently, $\mathcal{H}_A$). The parametric and perturbative uncertainties are in general in the $5 - 15\%$ range, exceptions are $\mathcal{H}_A[1,6]$ and the high-q^2 branching ratio, where the relative errors are much larger. In the former case the reason is the zero crossing of $\mathcal{H}_A$ which entails a cancellation between the central values of the two bins in the low-q^2 region. In the latter case we suffer from poorly known hadronic

JHEP06(2015)176

parameters in the $1/m_b^{2,3}$ power-corrections, a drawback that is circumvented in the ratio $\mathcal{R}(s_0)$, which normalizes the $\bar{B} \to X_s \ell^+ \ell^-$ rate to the inclusive $\bar{B}^0 \to X_u \ell \nu$ rate with the same cut in q^2 [61].

We also study the sensitivity of the $\bar{B} \to X_s \ell^+ \ell^-$ decay to new physics in a model-independent way. We give all observables in terms of ratios $R_{7,8,9,10}$ of high-scale Wilson coefficients, which we assume to be altered by the new interactions. We also study correlations between different observables, bins and channels in the $R_9 - R_{10}$ plane, and extrapolate to the final Belle II data set of 50 ab^{-1}. We find that $\mathcal{H}_T$ and $\mathcal{H}_A$ give the tightest constraints. On the other hand, if deviations from the Standard Model are seen, all observables become crucial to pin down the structure of new physics.

In view of the recent measurement by LHCb [21] which reports a value for $R_K = \mathrm{BR}(B^+ \to K^+ \mu^+ \mu^-)/\mathrm{BR}(B^+ \to K^+ e^+ e^-)$ in the low-q^2 region that is significantly different from unity, one might wonder whether this sign of lepton non-universality could be traced back to logarithmically enhanced QED corrections. LHCb uses the PHOTOS Monte Carlo to eliminate the impact of collinear photon emissions from the final state electrons. Therefore, the corrections calculated in this paper do not seem to apply to the ratio R_K. Given that the agreement between PHOTOS and our analytical calculations is not perfect (see e.g. tables 2 and 4), it would be advisable to correct for photon radiation using data-driven methods that do not rely on PHOTOS.

Acknowledgments

We would like to thank Javier Virto for useful discussions, and Kevin Flood, Chris Schilling and Owen Long for logistic and technical support that allowed the Monte Carlo study presented in section 7. We are indebted to Mathias Brucherseifer, Fabrizio Caola, and Kirill Melnikov for providing us with the data for the two-loop functions $\omega^{(2)}_{ij,I}(\hat{s})$, based on their studies [88, 89]. T. Huber acknowledges support from Deutsche Forschungsgemeinschaft within research unit FOR 1873 (QFET). T. Hurth thanks the CERN theory group for its hospitality during his regular visits to CERN. All authors are grateful to the Mainz Institute for Theoretical Physics (MITP) for its hospitality at the Capri-Institute in May 2014, where part of this work was done.

A QED and QCD functions

A.1 QED functions for the double differential rate

Here we list the polynomials that appear in the functions $\xi^{(\mathrm{em})}_{ij}(s,z)$ of the log-enhanced QED corrections to the double differential rate in eq. (3.28).

$$
\begin{aligned}
p_1(s,z) &= 2s^2\left(z^4+6z^2+1\right)+s\left(11z^4-8z^2-3\right)+\left(z^2-1\right)^2 \,, \\
p_2(s,z) &= 4s^3\left(z^2+1\right)+3s^2\left(z^2-1\right)-4s\left(z^2-1\right)-9z^2-7 \,, \\
p_3(s,z) &= s^3\left(z^2-1\right)^3+s^2\left(z^2-1\right)^2\left(19z^2+5\right) \\
&\quad +s\left(6z^6+37z^4-36z^2-7\right)+5z^4+24z^2+3 \,,
\end{aligned}
$$

JHEP06(2015)176

$$
\begin{aligned}
p_4(s,z) &= s^3\left(z^8-4z^6+2z^4-28z^2-3\right)-3s^2\left(z^8-4z^6+8z^4-4z^2-1\right)\\
&\quad +4s\left(z^6-5z^4+3z^2+1\right)-2\left(5z^4+24z^2+3\right)\ ,\\
p_5(s,z) &= s^4\left(13z^8-56z^6+210z^4-112z^2-55\right)\\
&\quad +s^3\left(-15z^8+31z^6-127z^4+149z^2+154\right)\\
&\quad +3s^2\left(5z^8-9z^6+55z^4-31z^2-84\right)\\
&\quad +s\left(-13z^8+65z^6-285z^4+355z^2+262\right)\\
&\quad -13z^6+37z^4-299z^2-109\ ,\\
p_6(s,z) &= s\left(z^2-1\right)-z^2-1\ ,\\
p_7(s,z) &= s^2\left(43z^4+106z^2+27\right)+24s\left(2z^4-z^2-1\right)+3\left(z^2-1\right)^2\ ,\\
p_8(s,z) &= s^2\left(-z^{10}+3z^8+32z^6+364z^4+289z^2+17\right)\\
&\quad +s\left(3z^{10}-19z^8+106z^6+102z^4-173z^2-19\right)\\
&\quad +2\left(-z^8+7z^6-9z^4+z^2+2\right)\ ,\\
p_9(s,z) &= 2s^4\left(17z^6+183z^4+143z^2+9\right)+s^3\left(77z^8+922z^6-92z^4-842z^2-65\right)\\
&\quad +s^2\left(z^2-1\right)^2\left(46z^6+889z^4+1030z^2+87\right)\\
&\quad +s\left(z^2-1\right)^3\left(256z^4+483z^2+51\right)+\left(z^2-1\right)^4\left(74z^2+11\right)\ ,\\
p_{10}(s,z) &= -s^5\left(13z^8-66z^6+1288z^4+2706z^2+283\right)\\
&\quad +s^4\left(-26z^{10}+173z^8-2504z^6-2098z^4+7690z^2+989\right)\\
&\quad +s^3\left(-13z^{12}+122z^{10}-1190z^8+830z^6+8809z^4-7288z^2-1270\right)\\
&\quad +s^2\left(z^2-1\right)^2\left(15z^8-18z^6+397z^4+3716z^2+706\right)\\
&\quad -s\left(z^2-1\right)^3\left(15z^6+19z^4-403z^2-143\right)+\left(z^2-1\right)^4\left(13z^4-22z^2+1\right)\ ,\\
p_{11}(s,z) &= s^2\left(5z^2+3\right)+z^2-1\ ,\\
p_{12}(s,z) &= s^2\left(z^6-6z^4-9z^2-2\right)-s\left(z^2-1\right)^3+z^4-1\ ,\\
p_{13}(s,z) &= s^3\left(z^4+22z^2+9\right)+s^2\left(z^6+11z^4-33z^2-11\right)\\
&\quad -s\left(2z^6+17z^4-24z^2+5\right)+\left(z^2-1\right)^2\left(z^2+7\right)\ ,\\
p_{14}(s,z) &= s^3\left(3z^4+12z^2+1\right)+s^2\left(4z^6+15z^4-18z^2-1\right)\\
&\quad +s\left(z^2-1\right)^2\left(7z^2-1\right)-\left(z^2-1\right)^3\ ,\\
p_{15}(s,z) &= s\left(z^2-1\right)+z^2+1\ ,\\
p_{16}(s,z) &= s^3\left(5z^4+24z^2+3\right)+s^2\left(6z^6+37z^4-36z^2-7\right)\\
&\quad +s\left(z^2-1\right)^2\left(19z^2+5\right)+\left(z^2-1\right)^3\ ,\\
p_{17}(s,z) &= s^2\left(z^6-3z^4+39z^2+27\right)-2s\left(z^6-3z^4-5z^2+7\right)+z^6-3z^4+7z^2-5\ ,\\
p_{18}(s,z) &= s^2\left(3z^4-18z^2-49\right)-2s^{3/2}\left(z^4-10z^2+9\right)+3s\left(z^6-6z^4-11z^2+16\right)\\
&\quad -2\sqrt{s}\left(z^2-5\right)\left(z^2-1\right)^2+\left(z^2-1\right)^2\left(3z^2-7\right)\ ,\\
p_{19}(s,z) &= s^2\left(37z^4+86z^2+21\right)+16s\left(2z^4-z^2-1\right)+\left(z^2-1\right)^2\ ,\\
p_{20}(s,z) &= s^2\left(z^8-4z^6+154z^4+340z^2+85\right)-2s\left(z^8-4z^6-58z^4+28z^2+33\right)\\
&\quad +\left(z^2-1\right)^2\left(z^4-2z^2+5\right)\ ,
\end{aligned}
$$

JHEP06(2015)176

$$
\begin{aligned}
p_{21}(s,z) = {} & s^3\left(3z^6-37z^4-359z^2-183\right)-2s^{5/2}\left(z^6-35z^4-5z^2+39\right) \\
& +s^2\left(6z^8-77z^6-613z^4+305z^2+379\right)-4s^{3/2}\left(z^2-1\right)^2\left(z^4-27z^2-34\right) \\
& +s\left(z^2-1\right)^2\left(3z^6-31z^4-323z^2-229\right)-2\sqrt{s}\left(z^2-1\right)^3\left(z^4-14z^2-29\right) \\
& +\left(z^2-1\right)^3\left(3z^4-10z^2-33\right)\ , \\
p_{22}(s,z) = {} & 2s^4\left(15z^6+153z^4+113z^2+7\right)+s^3\left(69z^8+754z^6-132z^4-642z^2-49\right) \\
& +s^2\left(z^2-1\right)^2\left(42z^6+717z^4+742z^2+63\right)+5s\left(z^2-1\right)^3\left(40z^4+63z^2+7\right) \\
& +\left(z^2-1\right)^4\left(38z^2+7\right)\ . \qquad \text{(A.1)}
\end{aligned}
$$

A.2 Functions for the QCD corrections to the $\mathcal{H}_I$

The one-loop QCD functions [50, 77] can be computed analytically,

$$
\begin{aligned}
\omega^{(1)}_{77,T}(\hat{s}) = {} & -\frac{8}{3}\log\left(\frac{\mu_b}{m_b}\right)-\frac{(\sqrt{\hat{s}}+1)^2(\hat{s}^{3/2}-10\hat{s}+13\sqrt{\hat{s}}-8)\mathrm{Li}_2(1-\hat{s})}{6(\hat{s}-1)^2} \\
& +\frac{2\sqrt{\hat{s}}(\hat{s}^2-6\hat{s}-3)\mathrm{Li}_2(1-\sqrt{\hat{s}})}{3(\hat{s}-1)^2}-\frac{\pi^2(3\hat{s}^{3/2}+22\hat{s}+23\sqrt{\hat{s}}+16)(\sqrt{\hat{s}}-1)^2}{36(\hat{s}-1)^2} \\
& +\frac{5\hat{s}^3-54\hat{s}^2+57\hat{s}-8}{18(\hat{s}-1)^2}-\log(1-\hat{s})+\frac{\hat{s}(5\hat{s}+1)\log(\hat{s})}{3(\hat{s}-1)^2}+\frac{2}{3}\log(1-\hat{s})\log(\hat{s})\,, \\
\omega^{(1)}_{79,T}(\hat{s}) = {} & -\frac{4}{3}\log\left(\frac{\mu_b}{m_b}\right)-\frac{2\sqrt{\hat{s}}(\hat{s}+3)\mathrm{Li}_2(1-\sqrt{\hat{s}})}{3(\hat{s}-1)^2}-\frac{\pi^2(16\hat{s}+29\sqrt{\hat{s}}+19)(\sqrt{\hat{s}}-1)^2}{36(\hat{s}-1)^2} \\
& +\frac{\hat{s}^2-6\hat{s}+5}{6(\hat{s}-1)^2}+\frac{(\sqrt{\hat{s}}+1)^2(8\hat{s}-15\sqrt{\hat{s}}+9)\mathrm{Li}_2(1-\hat{s})}{6(\hat{s}-1)^2} \\
& -\frac{(5\hat{s}+1)\log(1-\hat{s})}{6\hat{s}}+\frac{\hat{s}(3\hat{s}+1)\log(\hat{s})}{6(\hat{s}-1)^2}+\frac{2}{3}\log(1-\hat{s})\log(\hat{s})\,, \\
\omega^{(1)}_{99,T}(\hat{s}) = {} & \frac{(\sqrt{\hat{s}}+1)^2(8\hat{s}^{3/2}-15\hat{s}+4\sqrt{\hat{s}}-5)\mathrm{Li}_2(1-\hat{s})}{6(\hat{s}-1)^2\sqrt{\hat{s}}}-\frac{2(\hat{s}^2-12\hat{s}-5)\mathrm{Li}_2(1-\sqrt{\hat{s}})}{3(\hat{s}-1)^2\sqrt{\hat{s}}} \\
& -\frac{\pi^2(16\hat{s}^{3/2}+29\hat{s}+4\sqrt{\hat{s}}+15)(\sqrt{\hat{s}}-1)^2}{36(\hat{s}-1)^2\sqrt{\hat{s}}}+\frac{(2\hat{s}^2-7\hat{s}-5)\log(\hat{s})}{3(\hat{s}-1)^2} \\
& +\frac{\hat{s}^2+18\hat{s}-19}{6(\hat{s}-1)^2}-\frac{(2\hat{s}+1)\log(1-\hat{s})}{3\hat{s}}+\frac{2}{3}\log(1-\hat{s})\log(\hat{s})\,, \\
\omega^{(1)}_{710,A}(\hat{s}) = {} & -\frac{4}{3}\log\left(\frac{\mu_b}{m_b}\right)+\frac{2(4\hat{s}^2-13\hat{s}-1)\mathrm{Li}_2(1-\sqrt{\hat{s}})}{3(\hat{s}-1)^2}-\frac{(2\hat{s}^2-9\hat{s}-3)\mathrm{Li}_2(1-\hat{s})}{3(\hat{s}-1)^2} \\
& -\frac{(3\hat{s}^2-16\hat{s}+13)\log(1-\sqrt{\hat{s}})}{3(\hat{s}-1)^2}+\frac{(4\hat{s}^2-13\hat{s}-1)\log(1-\sqrt{\hat{s}})\log(\hat{s})}{3(\hat{s}-1)^2} \\
& -\frac{(2\hat{s}^2-9\hat{s}-3)\log(1-\hat{s})\log(\hat{s})}{3(\hat{s}-1)^2}+\frac{(\hat{s}^3-23\hat{s}^2+23\hat{s}-1)\log(1-\hat{s})}{6(\hat{s}-1)^2\hat{s}} \\
& +\frac{(\hat{s}-20\sqrt{\hat{s}}+5)(\sqrt{\hat{s}}-1)^2}{6(\hat{s}-1)^2}-\frac{\pi^2}{3}\,, \\
\omega^{(1)}_{910,A}(\hat{s}) = {} & -\frac{2(\hat{s}^2-3\hat{s}-1)\mathrm{Li}_2(1-\hat{s})}{3(\hat{s}-1)^2}-\frac{4(5-2\hat{s})\hat{s}\mathrm{Li}_2(1-\sqrt{\hat{s}})}{3(\hat{s}-1)^2}-\frac{(4\sqrt{\hat{s}}-3)(\sqrt{\hat{s}}-1)^2}{3(\hat{s}-1)^2}
\end{aligned}
$$

JHEP06(2015)176

$$
\begin{aligned}
&- \frac{2(2\hat{s}^2-7\hat{s}+5)\log(1-\sqrt{\hat{s}})}{3(\hat{s}-1)^2} - \frac{2(\hat{s}^2-3\hat{s}-1)\log(1-\hat{s})\log(\hat{s})}{3(\hat{s}-1)^2} \\
&+ \frac{(2\hat{s}^3-11\hat{s}^2+10\hat{s}-1)\log(1-\hat{s})}{3(\hat{s}-1)^2\hat{s}} + \frac{2\hat{s}(2\hat{s}-5)\log(1-\sqrt{\hat{s}})\log(\hat{s})}{3(\hat{s}-1)^2} - \frac{\pi^2}{3}\,, \\
\omega^{(1)}_{77,L}(\hat{s}) = &- \frac{8}{3}\log\left(\frac{\mu_b}{m_b}\right) + \frac{(\sqrt{\hat{s}}+1)^2(4\hat{s}^{3/2}-7\hat{s}+2\sqrt{\hat{s}}-3)\mathrm{Li}_2(1-\hat{s})}{3(\hat{s}-1)^2\sqrt{\hat{s}}} - \frac{9\hat{s}^2-38\hat{s}+29}{6(\hat{s}-1)^2} \\
&- \frac{4(\hat{s}^2-6\hat{s}-3)\mathrm{Li}_2(1-\sqrt{\hat{s}})}{3(\hat{s}-1)^2\sqrt{\hat{s}}} - \frac{\pi^2(8\hat{s}^{3/2}+13\hat{s}+2\sqrt{\hat{s}}+9)(\sqrt{\hat{s}}-1)^2}{18(\hat{s}-1)^2\sqrt{\hat{s}}} \\
&- \frac{(\hat{s}^3-3\hat{s}+2)\log(1-\hat{s})}{3(\hat{s}-1)^2\hat{s}} + \frac{2(\hat{s}^2-3\hat{s}-3)\log(\hat{s})}{3(\hat{s}-1)^2} + \frac{2}{3}\log(1-\hat{s})\log(\hat{s})\,, \\
\omega^{(1)}_{79,L}(\hat{s}) = &- \frac{4}{3}\log\left(\frac{\mu_b}{m_b}\right) + \frac{4\sqrt{\hat{s}}(\hat{s}+3)\mathrm{Li}_2(1-\sqrt{\hat{s}})}{3(\hat{s}-1)^2} + \frac{(\sqrt{\hat{s}}+1)^2(4\hat{s}-9\sqrt{\hat{s}}+3)\mathrm{Li}_2(1-\hat{s})}{3(\hat{s}-1)^2} \\
&+ \frac{7\hat{s}^2-2\hat{s}-5}{6(\hat{s}-1)^2} - \frac{\pi^2(8\hat{s}+19\sqrt{\hat{s}}+5)(\sqrt{\hat{s}}-1)^2}{18(\hat{s}-1)^2} - \frac{(2\hat{s}+1)\log(1-\hat{s})}{3\hat{s}} \\
&+ \frac{(\hat{s}-7)\hat{s}\log(\hat{s})}{3(\hat{s}-1)^2} + \frac{2}{3}\log(1-\hat{s})\log(\hat{s})\,, \\
\omega^{(1)}_{99,L}(\hat{s}) = &- \frac{(\sqrt{\hat{s}}+1)^2(\hat{s}^{3/2}-8\hat{s}+3\sqrt{\hat{s}}-4)\mathrm{Li}_2(1-\hat{s})}{3(\hat{s}-1)^2} + \frac{4\sqrt{\hat{s}}(\hat{s}^2-12\hat{s}-5)\mathrm{Li}_2(1-\sqrt{\hat{s}})}{3(\hat{s}-1)^2} \\
&- \frac{\pi^2(3\hat{s}^{3/2}+20\hat{s}+\sqrt{\hat{s}}+8)(\sqrt{\hat{s}}-1)^2}{18(\hat{s}-1)^2} + \frac{4\hat{s}^3-51\hat{s}^2+42\hat{s}+5}{6(\hat{s}-1)^2} - \log(1-\hat{s}) \\
&+ \frac{8\hat{s}(2\hat{s}+1)\log(\hat{s})}{3(\hat{s}-1)^2} + \frac{2}{3}\log(1-\hat{s})\log(\hat{s})\,. \qquad \text{(A.2)}
\end{aligned}
$$

The two-loop QCD functions [88, 89] are obtained from least-squares fits and are also valid for all q^2. The necessary data was kindly provided by the authors of [88, 89].

$$
\begin{aligned}
\omega^{(2)}_{99,T}(\hat{s}) &= \beta_0^{(5)}\log\left(\frac{\mu_b}{m_b}\right)\omega^{(1)}_{99,T}(\hat{s}) + 54.919(1-\hat{s})^4 - 136.374(1-\hat{s})^3 \\
&\quad + 119.344(1-\hat{s})^2 - 15.6175(1-\hat{s}) - 31.1706\,, \\
\omega^{(2)}_{910,A}(\hat{s}) &= \beta_0^{(5)}\log\left(\frac{\mu_b}{m_b}\right)\omega^{(1)}_{910,A}(\hat{s}) + 74.3717(1-\hat{s})^4 - 183.885(1-\hat{s})^3 \\
&\quad + 158.739(1-\hat{s})^2 - 29.0124(1-\hat{s}) - 30.8056\,, \\
\omega^{(2)}_{99,L}(\hat{s}) &= \beta_0^{(5)}\log\left(\frac{\mu_b}{m_b}\right)\omega^{(1)}_{99,L}(\hat{s}) - 5.95974(1-s)^3 + 11.7493(1-s)^2 \\
&\quad + 12.2293(1-s) - 38.6457\,. \qquad \text{(A.3)}
\end{aligned}
$$

They are given for $n_h = 2$ and $n_l = 3$. $\beta_0^{(5)} = 23/3$ denotes the one-loop QCD β-function for five active flavours.

JHEP06(2015)176

A.3 Functions for the QED corrections to the $\mathcal{H}_I$

The following functions are again obtained by least-squares fits. They are valid in the low-q^2 region ($1\ \mathrm{GeV}^2 < q^2 < 6\ \mathrm{GeV}^2$) only.

$$\omega^{(\mathrm{em})}_{77,T}(\hat{s}) = \ln\left(\frac{m_b^2}{m_\ell^2}\right) \frac{1.54986 - 1703.72\,\hat{s}^5 + 1653.38\,\hat{s}^4 - 683.608\,\hat{s}^3 + 179.279\,\hat{s}^2 - 35.5047\,\hat{s}}{8(1-\hat{s})^2},$$

$$\omega^{(\mathrm{em})}_{77,L}(\hat{s}) = \ln\left(\frac{m_b^2}{m_\ell^2}\right) \frac{9.73761 + 647.747\,\hat{s}^4 - 642.637\,\hat{s}^3 + 276.839\,\hat{s}^2 - 68.3562\,\hat{s} - \frac{1.6755}{\hat{s}}}{4(1-\hat{s})^2},$$

$$\omega^{(\mathrm{em})}_{99,T}(\hat{s}) = \ln\left(\frac{m_b^2}{m_\ell^2}\right) \frac{2.2596 + 157.984\,\hat{s}^4 - 141.281\,\hat{s}^3 + 52.8914\,\hat{s}^2 - 13.5377\,\hat{s} + \frac{0.0284049}{\hat{s}}}{2\hat{s}(1-\hat{s})^2},$$

$$\omega^{(\mathrm{em})}_{99,L}(\hat{s}) = \ln\left(\frac{m_b^2}{m_\ell^2}\right) \frac{-0.768521 - 80.8068\,\hat{s}^4 + 70.0821\,\hat{s}^3 - 21.2787\,\hat{s}^2 + 2.9335\,\hat{s} - \frac{0.0180809}{\hat{s}}}{(1-\hat{s})^2},$$

$$\omega^{(\mathrm{em})}_{79,T}(\hat{s}) = \ln\left(\frac{m_b^2}{m_\ell^2}\right) \frac{19.063 + 2158.03\hat{s}^4 - 2062.92\hat{s}^3 + 830.53\hat{s}^2 - 186.12\hat{s} + \frac{0.324236}{\hat{s}}}{8(1-\hat{s})^2},$$

$$\omega^{(\mathrm{em})}_{79,L}(\hat{s}) = \ln\left(\frac{m_b^2}{m_\ell^2}\right) \frac{-6.03641 - 896.643\hat{s}^4 + 807.349\hat{s}^3 - 278.559\hat{s}^2 + 47.6636\hat{s} - \frac{0.190701}{\hat{s}}}{4(1-\hat{s})^2},$$

$$\begin{aligned}\omega^{(\mathrm{em})}_{27,T}(\hat{s}) = \ln\left(\frac{m_b^2}{m_\ell^2}\right) \Bigg[&\frac{21.5291 + 3044.94\hat{s}^4 - 2563.05\hat{s}^3 + 874.074\hat{s}^2 - 175.874\hat{s} + \frac{0.121398}{\hat{s}}}{8(1-\hat{s})^2} \\ &+ i\,\frac{2.49475 + 598.376\hat{s}^4 - 456.831\hat{s}^3 + 117.683\hat{s}^2 - 9.90525\hat{s} - \frac{0.0116501}{\hat{s}}}{8(1-\hat{s})^2}\Bigg] \\ &+ \frac{8}{9}\,\omega^{(\mathrm{em})}_{79,T}(\hat{s})\,\ln\left(\frac{\mu_b}{5\mathrm{GeV}}\right),\end{aligned}$$

$$\begin{aligned}\omega^{(\mathrm{em})}_{27,L}(\hat{s}) = \ln\left(\frac{m_b^2}{m_\ell^2}\right) \Bigg[&\frac{-8.01684 - 1121.13\hat{s}^4 + 882.711\hat{s}^3 - 280.866\hat{s}^2 + 54.1943\hat{s} - \frac{0.128988}{\hat{s}}}{4(1-\hat{s})^2} \\ &+ i\,\frac{-2.14058 - 588.771\hat{s}^4 + 483.997\hat{s}^3 - 124.579\hat{s}^2 + 12.3282\hat{s} + \frac{0.0145059}{\hat{s}}}{4(1-\hat{s})^2}\Bigg] \\ &+ \frac{8}{9}\,\omega^{(\mathrm{em})}_{79,L}(\hat{s})\,\ln\left(\frac{\mu_b}{5\mathrm{GeV}}\right),\end{aligned}$$

$$\begin{aligned}\omega^{(\mathrm{em})}_{29,T}(\hat{s}) = \ln\left(\frac{m_b^2}{m_\ell^2}\right) \Bigg[&\frac{4.54727 + 330.182\hat{s}^4 - 258.194\hat{s}^3 + 79.8713\hat{s}^2 - 19.6855\hat{s} + \frac{0.0371348}{\hat{s}}}{2\hat{s}(1-\hat{s})^2} \\ &+ i\,\frac{73.9149\hat{s}^4 - 61.1338\hat{s}^3 + 14.6517\hat{s}^2 - 0.102331\hat{s} + 0.710037}{2\hat{s}(1-\hat{s})^2}\Bigg] \\ &+ \frac{16}{9}\,\omega^{(\mathrm{em})}_{99,T}(\hat{s})\,\ln\left(\frac{\mu_b}{5\mathrm{GeV}}\right),\end{aligned}$$

$$\begin{aligned}\omega^{(\mathrm{em})}_{29,L}(\hat{s}) = \ln\left(\frac{m_b^2}{m_\ell^2}\right) \Bigg[&\frac{-2.27221 - 298.369\hat{s}^4 + 224.662\hat{s}^3 - 65.1375\hat{s}^2 + 11.5686\hat{s} - \frac{0.0233098}{\hat{s}}}{(1-\hat{s})^2} \\ &+ i\,\frac{-0.666157 - 120.303\hat{s}^4 + 109.315\hat{s}^3 - 28.2734\hat{s}^2 + 2.44527\hat{s} + \frac{0.00279781}{\hat{s}}}{(1-\hat{s})^2}\Bigg] \\ &+ \frac{16}{9}\,\omega^{(\mathrm{em})}_{99,L}(\hat{s})\,\ln\left(\frac{\mu_b}{5\mathrm{GeV}}\right),\end{aligned}$$

JHEP06(2015)176

$$
\begin{aligned}
\omega_{22,T}^{(\mathrm{em})}(\hat{s}) &= \ln\left(\frac{m_b^2}{m_\ell^2}\right)\left[\frac{2.84257+269.974\hat{s}^4-194.443\hat{s}^3+48.4535\hat{s}^2-8.24929\hat{s}+\frac{0.0111118}{\hat{s}}}{2\hat{s}(1-\hat{s})^2}\right.\\
&\quad\left.+\ln\left(\frac{\mu_b}{5\mathrm{GeV}}\right)\frac{4(4.54727+330.182\hat{s}^4-258.194\hat{s}^3+79.8713\hat{s}^2-19.6855\hat{s}+\frac{0.0371348}{\hat{s}})}{9\hat{s}(1-\hat{s})^2}\right]\\
&\quad+\frac{64}{81}\,\omega_{99,T}^{(\mathrm{em})}(\hat{s})\,\ln^2\left(\frac{\mu_b}{5\mathrm{GeV}}\right)\,,\\
\omega_{22,L}^{(\mathrm{em})}(\hat{s}) &= \ln\left(\frac{m_b^2}{m_\ell^2}\right)\left[\frac{-1.71832-234.11\hat{s}^4+162.126\hat{s}^3-37.2361\hat{s}^2+6.29949\hat{s}-\frac{0.00810233}{\hat{s}}}{(1-\hat{s})^2}\right.\\
&\quad\left.+\ln\left(\frac{\mu_b}{5\mathrm{GeV}}\right)\frac{8(224.662\hat{s}^3-2.27221-298.369\hat{s}^4-65.1375\hat{s}^2+11.5686\hat{s}-\frac{0.0233098}{\hat{s}})}{9(1-\hat{s})^2}\right]\\
&\quad+\frac{64}{81}\,\omega_{99,L}^{(\mathrm{em})}(\hat{s})\,\ln^2\left(\frac{\mu_b}{5\mathrm{GeV}}\right)\,,\\
\omega_{710,A}^{(\mathrm{em})}(\hat{s}) &= \ln\left(\frac{m_b^2}{m_\ell^2}\right)\left[\frac{7-16\sqrt{\hat{s}}+9\,\hat{s}}{4\,(1-\hat{s})}+\ln(1-\sqrt{\hat{s}})+\frac{1+3\,\hat{s}}{1-\hat{s}}\,\ln\left(\frac{1+\sqrt{\hat{s}}}{2}\right)-\frac{\hat{s}\,\ln\hat{s}}{(1-\hat{s})}\right]\,,\\
\omega_{910,A}^{(\mathrm{em})}(\hat{s}) &= \ln\left(\frac{m_b^2}{m_\ell^2}\right)\left[\ln(1-\sqrt{\hat{s}})-\frac{5-16\sqrt{\hat{s}}+11\,\hat{s}}{4\,(1-\hat{s})}\right.\\
&\quad\left.+\frac{1-5\,\hat{s}}{1-\hat{s}}\,\ln\left(\frac{1+\sqrt{\hat{s}}}{2}\right)-\frac{(1-3\,\hat{s})\ln\hat{s}}{(1-\hat{s})}\right],\\
\omega_{210,A}^{(\mathrm{em})}(\hat{s}) &= \ln\left(\frac{m_b^2}{m_\ell^2}\right)\left[\frac{-351.322\hat{s}^4+378.173\hat{s}^3-160.158\hat{s}^2+24.2096\hat{s}+0.305176}{24\hat{s}(1-\hat{s})^2}\right.\\
&\quad\left.+i\,\frac{7.98625+238.507\,(\hat{s}-a)-766.869\,(\hat{s}-a)^2}{24\hat{s}(1-\hat{s})^2}\,(\hat{s}-a)^2\,\theta(\hat{s}-a)\right]\\
&\quad+\frac{8}{9}\,\omega_{910,A}^{(\mathrm{em})}(\hat{s})\,\ln\left(\frac{\mu_b}{5\mathrm{GeV}}\right)\,,
\end{aligned}
\tag{A.4}
$$

with $a=(4m_c^2/m_b^2)^2$.

The respective high-q^2 functions for the branching ratio that are obtained by a least-squares fit (for fixed values of m_b and m_c) read

$$
\omega_{29}^{(\mathrm{em})}(\hat{s}) = \ln\left(\frac{m_b^2}{m_\ell^2}\right)\left[\frac{\Sigma_4(\hat{s})+i\,\Sigma_4^I(\hat{s})}{8(1-\hat{s})^2(1+2\hat{s})}\right]+\frac{16}{9}\,\omega_{1010}^{(\mathrm{em})}(\hat{s})\,\ln\left(\frac{\mu_b}{5\mathrm{GeV}}\right)\,, \tag{A.5}
$$

$$
\begin{aligned}
\omega_{22}^{(\mathrm{em})}(\hat{s}) &= \ln\left(\frac{m_b^2}{m_\ell^2}\right)\left[\frac{\Sigma_5(\hat{s})}{8(1-\hat{s})^2(1+2\hat{s})}+\frac{\Sigma_4(\hat{s})}{9(1-\hat{s})^2(1+2\hat{s})}\ln\left(\frac{\mu_b}{5\mathrm{GeV}}\right)\right]\\
&\quad+\frac{64}{81}\,\omega_{1010}^{(\mathrm{em})}(\hat{s})\,\ln^2\left(\frac{\mu_b}{5\mathrm{GeV}}\right)\,,
\end{aligned}
\tag{A.6}
$$

$$
\omega_{27}^{(\mathrm{em})}(\hat{s}) = \ln\left(\frac{m_b^2}{m_\ell^2}\right)\left[\frac{\Sigma_6(\hat{s})+i\,\Sigma_6^I(\hat{s})}{96(1-\hat{s})^2}\right]+\frac{8}{9}\,\omega_{79}^{(\mathrm{em})}(\hat{s})\,\ln\left(\frac{\mu_b}{5\mathrm{GeV}}\right)\,. \tag{A.7}
$$

The functions Σ_i are polynomials in $\delta=1-\hat{s}$ and are valid for $\hat{s}>0.65$.

$$
\begin{aligned}
\Sigma_4(\hat{s}) &= -153.673\,\delta^2+498.823\,\delta^3-1146.74\,\delta^4+1138.81\,\delta^5\,,\\
\Sigma_4^I(\hat{s}) &= -255.712\,\delta^2+1139.10\,\delta^3-2414.21\,\delta^4+2379.91\,\delta^5\,,\\
\Sigma_5(\hat{s}) &= -220.101\,\delta^2+875.703\,\delta^3-1920.56\,\delta^4+1822.07\,\delta^5\,,\\
\Sigma_6(\hat{s}) &= -310.113\,\delta^2+834.253\,\delta^3-2181.94\,\delta^4+2133.78\,\delta^5\,,\\
\Sigma_6^I(\hat{s}) &= -518.180\,\delta^2+2047.18\,\delta^3-4470.04\,\delta^4+4827.74\,\delta^5\,.
\end{aligned}
\tag{A.8}
$$

JHEP06(2015)176

B New physics formulas

$$
\begin{aligned}
\mathcal{H}_T[1,3.5]_{ee} =& \big[0.0162226\,\mathcal{I}(R_7R_8^*) + 0.00186782\,\mathcal{I}(R_7R_9^*) + 0.00985919\,\mathcal{I}(R_8R_9^*) \\
&- 0.000201564\,\mathcal{I}(R_8R_{10}^*) + 0.0465868\,\mathcal{I}(R_7) - 0.00822885\,\mathcal{I}(R_8) \\
&- 0.0187815\,\mathcal{I}(R_9) + 0.000379966\,\mathcal{I}(R_{10}) + 0.393156\,\mathcal{R}(R_7) \\
&+ 0.0400072\,\mathcal{R}(R_8) + 0.0531851\,\mathcal{R}(R_9) - 0.0385002\,\mathcal{R}(R_{10}) \\
&+ 0.0458427\,\mathcal{R}(R_7R_8^*) - 0.369964\,\mathcal{R}(R_7R_9^*) + 0.00570607\,\mathcal{R}(R_7R_{10}^*) \\
&- 0.0369498\,\mathcal{R}(R_8R_9^*) + 0.000616422\,\mathcal{R}(R_8R_{10}^*) - 0.00978058\,\mathcal{R}(R_9R_{10}^*) \\
&+ 0.204994\,|R_7|^2 + 0.00230146\,|R_8|^2 + 0.244813\,|R_9|^2 \\
&+ 1.74294\,|R_{10}|^2 + 0.632156\big] \times 10^{-7}\,, \qquad \text{(B.1)}
\end{aligned}
$$

$$
\begin{aligned}
\mathcal{H}_T[3.5,6]_{ee} =& \big[0.00519889\,\mathcal{I}(R_7R_8^*) + 0.00141211\,\mathcal{I}(R_7R_9^*) + 0.00745377\,\mathcal{I}(R_8R_9^*) \\
&- 0.000152386\,\mathcal{I}(R_8R_{10}^*) + 0.0151043\,\mathcal{I}(R_7) + 0.00358335\,\mathcal{I}(R_8) \\
&- 0.0100672\,\mathcal{I}(R_9) + 0.000148662\,\mathcal{I}(R_{10}) - 0.138516\,\mathcal{R}(R_7) \\
&- 0.0131665\,\mathcal{R}(R_8) + 0.375959\,\mathcal{R}(R_9) - 0.074623\,\mathcal{R}(R_{10}) \\
&+ 0.0143568\,\mathcal{R}(R_7R_8^*) - 0.254325\,\mathcal{R}(R_7R_9^*) + 0.00431139\,\mathcal{R}(R_7R_{10}^*) \\
&- 0.0260943\,\mathcal{R}(R_8R_9^*) + 0.000467687\,\mathcal{R}(R_8R_{10}^*) - 0.0157259\,\mathcal{R}(R_9R_{10}^*) \\
&+ 0.0631028\,|R_7|^2 + 0.000727107\,|R_8|^2 + 0.273706\,|R_9|^2 \\
&+ 1.96638\,|R_{10}|^2 + 0.257773\big] \times 10^{-7}\,, \qquad \text{(B.2)}
\end{aligned}
$$

$$
\begin{aligned}
\mathcal{H}_T[1,6]_{ee} =& \big[0.0214215\,\mathcal{I}(R_7R_8^*) + 0.00327993\,\mathcal{I}(R_7R_9^*) + 0.017313\,\mathcal{I}(R_8R_9^*) \\
&- 0.000353949\,\mathcal{I}(R_8R_{10}^*) + 0.0616911\,\mathcal{I}(R_7) - 0.0046455\,\mathcal{I}(R_8) \\
&- 0.0288487\,\mathcal{I}(R_9) + 0.000528628\,\mathcal{I}(R_{10}) + 0.25464\,\mathcal{R}(R_7) \\
&+ 0.0268407\,\mathcal{R}(R_8) + 0.429144\,\mathcal{R}(R_9) - 0.113123\,\mathcal{R}(R_{10}) \\
&+ 0.0601994\,\mathcal{R}(R_7R_8^*) - 0.624289\,\mathcal{R}(R_7R_9^*) + 0.0100175\,\mathcal{R}(R_7R_{10}^*) \\
&- 0.0630441\,\mathcal{R}(R_8R_9^*) + 0.00108411\,\mathcal{R}(R_8R_{10}^*) - 0.0255065\,\mathcal{R}(R_9R_{10}^*) \\
&+ 0.268097\,|R_7|^2 + 0.00302857\,|R_8|^2 + 0.518519\,|R_9|^2 \\
&+ 3.70932\,|R_{10}|^2 + 0.889929\big] \times 10^{-7}\,, \qquad \text{(B.3)}
\end{aligned}
$$

$$
\begin{aligned}
\mathcal{H}_T[1,3.5]_{\mu\mu} =& \big[0.0162226\,\mathcal{I}(R_7R_8^*) + 0.00186782\,\mathcal{I}(R_7R_9^*) + 0.00985919\,\mathcal{I}(R_8R_9^*) \\
&- 0.000201564\,\mathcal{I}(R_8R_{10}^*) + 0.0478295\,\mathcal{I}(R_7) - 0.00813434\,\mathcal{I}(R_8) \\
&- 0.0247652\,\mathcal{I}(R_9) + 0.000379966\,\mathcal{I}(R_{10}) + 0.459563\,\mathcal{R}(R_7) \\
&+ 0.0451794\,\mathcal{R}(R_8) - 0.155638\,\mathcal{R}(R_9) - 0.0385002\,\mathcal{R}(R_{10}) \\
&+ 0.0460521\,\mathcal{R}(R_7R_8^*) - 0.337431\,\mathcal{R}(R_7R_9^*) + 0.00570607\,\mathcal{R}(R_7R_{10}^*) \\
&- 0.0344757\,\mathcal{R}(R_8R_9^*) + 0.000616422\,\mathcal{R}(R_8R_{10}^*) - 0.00978058\,\mathcal{R}(R_9R_{10}^*) \\
&+ 0.206371\,|R_7|^2 + 0.00230943\,|R_8|^2 + 0.179467\,|R_9|^2 \\
&+ 1.28881\,|R_{10}|^2 + 0.436438\big] \times 10^{-7}\,, \qquad \text{(B.4)}
\end{aligned}
$$

$$
\begin{aligned}
\mathcal{H}_T[3.5,6]_{\mu\mu} =& \big[0.00519889\,\mathcal{I}(R_7R_8^*) + 0.00141211\,\mathcal{I}(R_7R_9^*) + 0.00745377\,\mathcal{I}(R_8R_9^*) \\
&- 0.000152386\,\mathcal{I}(R_8R_{10}^*) + 0.0165184\,\mathcal{I}(R_7) + 0.00369089\,\mathcal{I}(R_8) \\
&- 0.0169196\,\mathcal{I}(R_9) + 0.000148662\,\mathcal{I}(R_{10}) - 0.112376\,\mathcal{R}(R_7)
\end{aligned}
$$

JHEP06(2015)176

$$
\begin{aligned}
&- 0.0111424\,\mathcal{R}(R_8) + 0.249027\,\mathcal{R}(R_9) - 0.074623\,\mathcal{R}(R_{10}) \\
&+ 0.0146547\,\mathcal{R}(R_7R_8^*) - 0.244671\,\mathcal{R}(R_7R_9^*) + 0.00431139\,\mathcal{R}(R_7R_{10}^*) \\
&- 0.0253601\,\mathcal{R}(R_8R_9^*) + 0.000467687\,\mathcal{R}(R_8R_{10}^*) - 0.0157259\,\mathcal{R}(R_9R_{10}^*) \\
&+ 0.0650616\,|R_7|^2 + 0.000738436\,|R_8|^2 + 0.239011\,|R_9|^2 \\
&+ 1.72527\,|R_{10}|^2 + 0.123204\big]\,\times\,10^{-7}\,, \qquad \text{(B.5)}
\end{aligned}
$$

$$
\begin{aligned}
\mathcal{H}_T[1,6]_{\mu\mu} =& \big[0.0214215\,\mathcal{I}(R_7R_8^*) + 0.00327993\,\mathcal{I}(R_7R_9^*) + 0.017313\,\mathcal{I}(R_8R_9^*) \\
&- 0.000353949\,\mathcal{I}(R_8R_{10}^*) + 0.0643479\,\mathcal{I}(R_7) - 0.00444346\,\mathcal{I}(R_8) \\
&- 0.0416848\,\mathcal{I}(R_9) + 0.000528628\,\mathcal{I}(R_{10}) + 0.347186\,\mathcal{R}(R_7) \\
&+ 0.034037\,\mathcal{R}(R_8) + 0.0933889\,\mathcal{R}(R_9) - 0.113123\,\mathcal{R}(R_{10}) \\
&+ 0.0607068\,\mathcal{R}(R_7R_8^*) - 0.582101\,\mathcal{R}(R_7R_9^*) + 0.0100175\,\mathcal{R}(R_7R_{10}^*) \\
&- 0.0598358\,\mathcal{R}(R_8R_9^*) + 0.00108411\,\mathcal{R}(R_8R_{10}^*) - 0.0255065\,\mathcal{R}(R_9R_{10}^*) \\
&+ 0.271433\,|R_7|^2 + 0.00304786\,|R_8|^2 + 0.418478\,|R_9|^2 \\
&+ 3.01408\,|R_{10}|^2 + 0.559642\big]\,\times\,10^{-7}\,, \qquad \text{(B.6)}
\end{aligned}
$$

$$
\begin{aligned}
\mathcal{H}_A[1,3.5]_{ee} =& \big[-0.0000761415\,\mathcal{I}(R_8R_9^*) + 0.0259112\,\mathcal{I}(R_8R_{10}^*) + 0.0031943\,\mathcal{I}(R_9R_{10}^*) \\
&- 0.000083788\,\mathcal{I}(R_8) + 0.00025712\,\mathcal{I}(R_9) - 0.112552\,\mathcal{I}(R_{10}) \\
&+ 0.0230277\,\mathcal{R}(R_7) + 0.00181543\,\mathcal{R}(R_8) - 0.0133235\,\mathcal{R}(R_9) \\
&- 0.826626\,\mathcal{R}(R_{10}) + 0.00214715\,\mathcal{R}(R_7R_9^*) - 0.849154\,\mathcal{R}(R_7R_{10}^*) \\
&+ 0.000222401\,\mathcal{R}(R_8R_9^*) - 0.0847389\,\mathcal{R}(R_8R_{10}^*) + 0.722934\,\mathcal{R}(R_9R_{10}^*) \\
&- 0.00174093\,|R_9|^2 - 0.0120987\,|R_{10}|^2 + 0.0121072\big]\,\times\,10^{-7}\,, \qquad \text{(B.7)}
\end{aligned}
$$

$$
\begin{aligned}
\mathcal{H}_A[3.5,6]_{ee} =& \big[-0.000057133\,\mathcal{I}(R_8R_9^*) + 0.0194427\,\mathcal{I}(R_8R_{10}^*) + 0.00509883\,\mathcal{I}(R_9R_{10}^*) \\
&- 0.000062727\,\mathcal{I}(R_8) + 0.000151953\,\mathcal{I}(R_9) - 0.0912157\,\mathcal{I}(R_{10}) \\
&+ 0.0172872\,\mathcal{R}(R_7) + 0.00136744\,\mathcal{R}(R_8) - 0.0259495\,\mathcal{R}(R_9) \\
&+ 0.356293\,\mathcal{R}(R_{10}) + 0.00160379\,\mathcal{R}(R_7R_9^*) - 0.605103\,\mathcal{R}(R_7R_{10}^*) \\
&+ 0.000169807\,\mathcal{R}(R_8R_9^*) - 0.0623319\,\mathcal{R}(R_8R_{10}^*) + 1.08406\,\mathcal{R}(R_9R_{10}^*) \\
&- 0.0027675\,|R_9|^2 - 0.0192329\,|R_{10}|^2 - 0.0115297\big]\,\times\,10^{-7}\,, \qquad \text{(B.8)}
\end{aligned}
$$

$$
\begin{aligned}
\mathcal{H}_A[1,6]_{ee} =& \big[-0.000133274\,\mathcal{I}(R_8R_9^*) + 0.0453539\,\mathcal{I}(R_8R_{10}^*) + 0.00829314\,\mathcal{I}(R_9R_{10}^*) \\
&- 0.000146515\,\mathcal{I}(R_8) + 0.000409073\,\mathcal{I}(R_9) - 0.203767\,\mathcal{I}(R_{10}) \\
&+ 0.0403149\,\mathcal{R}(R_7) + 0.00318287\,\mathcal{R}(R_8) - 0.0392731\,\mathcal{R}(R_9) \\
&- 0.470333\,\mathcal{R}(R_{10}) + 0.00375094\,\mathcal{R}(R_7R_9^*) - 1.45426\,\mathcal{R}(R_7R_{10}^*) \\
&+ 0.000392209\,\mathcal{R}(R_8R_9^*) - 0.147071\,\mathcal{R}(R_8R_{10}^*) + 1.80699\,\mathcal{R}(R_9R_{10}^*) \\
&- 0.00450843\,|R_9|^2 - 0.0313316\,|R_{10}|^2 + 0.000577448\big]\,\times\,10^{-7}\,, \qquad \text{(B.9)}
\end{aligned}
$$

$$
\begin{aligned}
\mathcal{H}_A[1,3.5]_{\mu\mu} =& \big[-0.0000761415\,\mathcal{I}(R_8R_9^*) + 0.0259112\,\mathcal{I}(R_8R_{10}^*) + 0.0031943\,\mathcal{I}(R_9R_{10}^*) \\
&- 0.000083788\,\mathcal{I}(R_8) + 0.00025712\,\mathcal{I}(R_9) - 0.112552\,\mathcal{I}(R_{10}) \\
&+ 0.0230277\,\mathcal{R}(R_7) + 0.00181543\,\mathcal{R}(R_8) - 0.0133235\,\mathcal{R}(R_9) \\
&- 0.875607\,\mathcal{R}(R_{10}) + 0.00214715\,\mathcal{R}(R_7R_9^*) - 0.845327\,\mathcal{R}(R_7R_{10}^*)
\end{aligned}
$$

JHEP06(2015)176

$$
\begin{aligned}
&+ 0.000222401\,\mathcal{R}(R_8R_9^*) - 0.0844478\,\mathcal{R}(R_8R_{10}^*) + 0.694542\,\mathcal{R}(R_9R_{10}^*)\\
&- 0.00174093\,|R_9|^2 - 0.0120987\,|R_{10}|^2 + 0.0131242\big]\,\times\,10^{-7}\,, \qquad \text{(B.10)}\\
\mathcal{H}_A[3.5,6]_{\mu\mu} =&\big[-0.000057133\,\mathcal{I}(R_8R_9^*) + 0.0194427\,\mathcal{I}(R_8R_{10}^*) + 0.00509883\,\mathcal{I}(R_9R_{10}^*)\\
&- 0.000062727\,\mathcal{I}(R_8) + 0.000151953\,\mathcal{I}(R_9) - 0.091289\,\mathcal{I}(R_{10})\\
&+ 0.0172872\,\mathcal{R}(R_7) + 0.00136744\,\mathcal{R}(R_8) - 0.0259495\,\mathcal{R}(R_9)\\
&+ 0.318008\,\mathcal{R}(R_{10}) + 0.00160379\,\mathcal{R}(R_7R_9^*) - 0.619516\,\mathcal{R}(R_7R_{10}^*)\\
&+ 0.000169807\,\mathcal{R}(R_8R_9^*) - 0.063428\,\mathcal{R}(R_8R_{10}^*) + 1.07786\,\mathcal{R}(R_9R_{10}^*)\\
&- 0.0027675\,|R_9|^2 - 0.0192329\,|R_{10}|^2 - 0.0113078\big]\,\times\,10^{-7}\,, \qquad \text{(B.11)}\\
\mathcal{H}_A[1,6]_{\mu\mu} =&\big[-0.000133274\,\mathcal{I}(R_8R_9^*) + 0.0453539\,\mathcal{I}(R_8R_{10}^*) + 0.00829314\,\mathcal{I}(R_9R_{10}^*)\\
&- 0.000146515\,\mathcal{I}(R_8) + 0.000409073\,\mathcal{I}(R_9) - 0.203841\,\mathcal{I}(R_{10})\\
&+ 0.0403149\,\mathcal{R}(R_7) + 0.00318287\,\mathcal{R}(R_8) - 0.0392731\,\mathcal{R}(R_9)\\
&- 0.557599\,\mathcal{R}(R_{10}) + 0.00375094\,\mathcal{R}(R_7R_9^*) - 1.46484\,\mathcal{R}(R_7R_{10}^*)\\
&+ 0.000392209\,\mathcal{R}(R_8R_9^*) - 0.147876\,\mathcal{R}(R_8R_{10}^*) + 1.77241\,\mathcal{R}(R_9R_{10}^*)\\
&- 0.00450843\,|R_9|^2 - 0.0313316\,|R_{10}|^2 + 0.00181642\big]\,\times\,10^{-7}\,, \qquad \text{(B.12)}\\
\mathcal{H}_3[1,3.5]_{ee} =&\big[0.0264036\,\mathcal{I}(R_{10}) + 3.07156\,\mathcal{R}(R_{10}) - 1.74043\,\mathcal{R}(R_7R_{10}^*)\\
&- 0.132357\,\mathcal{R}(R_8R_{10}^*) + 2.94364\,\mathcal{R}(R_9R_{10}^*) - 0.105444\big]\,\times\,10^{-9}\,, \qquad \text{(B.13)}\\
\mathcal{H}_3[3.5,6]_{ee} =&\big[0.132813\,\mathcal{I}(R_{10}) + 3.51904\,\mathcal{R}(R_{10}) - 0.913353\,\mathcal{R}(R_7R_{10}^*)\\
&- 0.0694587\,\mathcal{R}(R_8R_{10}^*) + 2.4359\,\mathcal{R}(R_9R_{10}^*) - 0.0872558\big]\,\times\,10^{-9}\,, \qquad \text{(B.14)}\\
\mathcal{H}_3[1,6]_{ee} =&\big[0.159216\,\mathcal{I}(R_{10}) + 6.5906\,\mathcal{R}(R_{10}) - 2.65379\,\mathcal{R}(R_7R_{10}^*)\\
&- 0.201815\,\mathcal{R}(R_8R_{10}^*) + 5.37954\,\mathcal{R}(R_9R_{10}^*) - 0.192699\big]\,\times\,10^{-9}\,, \qquad \text{(B.15)}\\
\mathcal{H}_3[1,3.5]_{\mu\mu} =&\big[0.010976\,\mathcal{I}(R_{10}) + 1.27946\,\mathcal{R}(R_{10}) - 0.723502\,\mathcal{R}(R_7R_{10}^*)\\
&-0.0550209\,\mathcal{R}(R_8R_{10}^*)+1.22368\,\mathcal{R}(R_9R_{10}^*)-0.0438331\big]\,\times\,10^{-9}\,, \qquad \text{(B.16)}\\
\mathcal{H}_3[3.5,6]_{\mu\mu} =&\big[0.0552105\,\mathcal{I}(R_{10}) + 1.46503\,\mathcal{R}(R_{10}) - 0.379682\,\mathcal{R}(R_7R_{10}^*)\\
&-0.0288741\,\mathcal{R}(R_8R_{10}^*) + 1.01261\,\mathcal{R}(R_9R_{10}^*) - 0.0362724\big]\,\times\,10^{-9}\,, \qquad \text{(B.17)}\\
\mathcal{H}_3[1,6]_{\mu\mu} =&\big[0.0661865\,\mathcal{I}(R_{10}) + 2.74449\,\mathcal{R}(R_{10}) - 1.10318\,\mathcal{R}(R_7R_{10}^*)\\
&- 0.083895\,\mathcal{R}(R_8R_{10}^*) + 2.23628\,\mathcal{R}(R_9R_{10}^*) - 0.0801055\big]\,\times\,10^{-9}\,, \qquad \text{(B.18)}\\
\mathcal{H}_4[1,3.5]_{ee} =&\big[-0.0412679\,\mathcal{I}(R_7) - 0.00313835\,\mathcal{I}(R_8) + 0.200198\,\mathcal{I}(R_9)\\
&- 0.430034\,\mathcal{R}(R_7) - 0.034058\,\mathcal{R}(R_8) + 1.46516\,\mathcal{R}(R_9)\\
&+ 0.0135748\,\mathcal{R}(R_7R_8^*) - 0.361104\,\mathcal{R}(R_7R_9^*) - 0.0274613\,\mathcal{R}(R_8R_9^*)\\
&+ 0.482688\,|R_9|^2 + 0.0892516\,|R_7|^2 + 0.00051617\,|R_8|^2\\
&+ 3.35446\,|R_{10}|^2 + 1.6742\big]\,\times\,10^{-9}\,, \qquad \text{(B.19)}\\
\mathcal{H}_4[3.5,6]_{ee} =&\big[-0.0257056\,\mathcal{I}(R_7) - 0.00195486\,\mathcal{I}(R_8) + 0.127314\,\mathcal{I}(R_9)\\
&- 0.17595\,\mathcal{R}(R_7) - 0.0138586\,\mathcal{R}(R_8) + 0.528054\,\mathcal{R}(R_9)\\
&+ 0.00348411\,\mathcal{R}(R_7R_8^*) - 0.127392\,\mathcal{R}(R_7R_9^*) - 0.00968792\,\mathcal{R}(R_8R_9^*)\\
&+ 0.179914\,|R_9|^2 + 0.0229073\,|R_7|^2 + 0.00013248\,|R_8|^2\\
&+ 1.25032\,|R_{10}|^2 + 0.529364\big]\,\times\,10^{-9}\,, \qquad \text{(B.20)}
\end{aligned}
$$

JHEP06(2015)176

$$
\begin{aligned}
\mathcal{H}_4[1,6]_{ee} =\big[& -0.0669735\,\mathcal{I}(R_7) - 0.0050932\,\mathcal{I}(R_8) + 0.327512\,\mathcal{I}(R_9) \\
& - 0.605984\,\mathcal{R}(R_7) - 0.0479166\,\mathcal{R}(R_8) + 1.99322\,\mathcal{R}(R_9) \\
& + 0.0170589\,\mathcal{R}(R_7R_8^*) - 0.488496\,\mathcal{R}(R_7R_9^*) - 0.0371492\,\mathcal{R}(R_8R_9^*) \\
& + 0.662601\,|R_9|^2 + 0.112159\,|R_7|^2 + 0.00064865\,|R_8|^2 \\
& + 4.60478\,|R_{10}|^2 + 2.20357\big] \times 10^{-9}\,, \qquad \text{(B.21)} \\
\mathcal{H}_4[1,3.5]_{\mu\mu} =\big[& -0.0171551\,\mathcal{I}(R_7) - 0.00130462\,\mathcal{I}(R_8) + 0.0832226\,\mathcal{I}(R_9) \\
& - 0.179086\,\mathcal{R}(R_7) - 0.0141823\,\mathcal{R}(R_8) + 0.609926\,\mathcal{R}(R_9) \\
& + 0.00564308\,\mathcal{R}(R_7R_8^*) - 0.150112\,\mathcal{R}(R_7R_9^*) - 0.0114157\,\mathcal{R}(R_8R_9^*) \\
& + 0.200654\,|R_9|^2 + 0.0371021\,|R_7|^2 + 0.000214573\,|R_8|^2 \\
& + 1.39446\,|R_{10}|^2 + 0.697498\big] \times 10^{-9}\,, \qquad \text{(B.22)} \\
\mathcal{H}_4[3.5,6]_{\mu\mu} =\big[& -0.0106858\,\mathcal{I}(R_7) - 0.000812638\,\mathcal{I}(R_8) + 0.0529245\,\mathcal{I}(R_9) \\
& - 0.0732557\,\mathcal{R}(R_7) - 0.00576964\,\mathcal{R}(R_8) + 0.219832\,\mathcal{R}(R_9) \\
& + 0.00144835\,\mathcal{R}(R_7R_8^*) - 0.0529571\,\mathcal{R}(R_7R_9^*) - 0.00402729\,\mathcal{R}(R_8R_9^*) \\
& + 0.0747905\,|R_9|^2 + 0.00952261\,|R_7|^2 + 0.0000550722\,|R_8|^2 \\
& + 0.51976\,|R_{10}|^2 + 0.22061\big] \times 10^{-9}\,, \qquad \text{(B.23)} \\
\mathcal{H}_4[1,6]_{\mu\mu} =\big[& -0.027841\,\mathcal{I}(R_7) - 0.00211725\,\mathcal{I}(R_8) + 0.136147\,\mathcal{I}(R_9) \\
& - 0.252341\,\mathcal{R}(R_7) - 0.0199519\,\mathcal{R}(R_8) + 0.829758\,\mathcal{R}(R_9) \\
& + 0.00709143\,\mathcal{R}(R_7R_8^*) - 0.203069\,\mathcal{R}(R_7R_9^*) - 0.015443\,\mathcal{R}(R_8R_9^*) \\
& + 0.275445\,|R_9|^2 + 0.0466247\,|R_7|^2 + 0.000269645\,|R_8|^2 \\
& + 1.91422\,|R_{10}|^2 + 0.918108\big] \times 10^{-9}\,, \qquad \text{(B.24)} \\
\mathcal{H}_L[1,3.5]_{ee} =\big[& 0.000741931\,\mathcal{I}(R_7R_8^*) + 0.000952641\,\mathcal{I}(R_7R_9^*) + 0.0050284\,\mathcal{I}(R_8R_9^*) \\
& - 0.000102803\,\mathcal{I}(R_8R_{10}^*) + 0.00124959\,\mathcal{I}(R_7) + 0.00594309\,\mathcal{I}(R_8) \\
& + 0.00735758\,\mathcal{I}(R_9) - 0.00113202\,\mathcal{I}(R_{10}) - 0.194866\,\mathcal{R}(R_7) \\
& - 0.0251935\,\mathcal{R}(R_8) + 1.42501\,\mathcal{R}(R_9) - 0.25154\,\mathcal{R}(R_{10}) \\
& + 0.00213751\,\mathcal{R}(R_7R_8^*) - 0.136283\,\mathcal{R}(R_7R_9^*) + 0.00300802\,\mathcal{R}(R_7R_{10}^*) \\
& - 0.0187453\,\mathcal{R}(R_8R_9^*) + 0.000402421\,\mathcal{R}(R_8R_{10}^*) - 0.0462841\,\mathcal{R}(R_9R_{10}^*) \\
& + 0.00589466\,|R_7|^2 + 0.000128527\,|R_8|^2 + 0.575967\,|R_9|^2 \\
& + 4.20578\,|R_{10}|^2 + 0.806915\big] \times 10^{-7}\,, \qquad \text{(B.25)} \\
\mathcal{H}_L[3.5,6]_{ee} =\big[& 0.000562052\,\mathcal{I}(R_7R_8^*) + 0.000724099\,\mathcal{I}(R_7R_9^*) + 0.00382208\,\mathcal{I}(R_8R_9^*) \\
& - 0.0000781401\,\mathcal{I}(R_8R_{10}^*) + 0.00223749\,\mathcal{I}(R_7) + 0.0047901\,\mathcal{I}(R_8) \\
& - 0.00211229\,\mathcal{I}(R_9) - 0.000740423\,\mathcal{I}(R_{10}) - 0.161117\,\mathcal{R}(R_7) \\
& - 0.0192094\,\mathcal{R}(R_8) + 1.14892\,\mathcal{R}(R_9) - 0.193345\,\mathcal{R}(R_{10}) \\
& + 0.0017624\,\mathcal{R}(R_7R_8^*) - 0.107501\,\mathcal{R}(R_7R_9^*) + 0.00228636\,\mathcal{R}(R_7R_{10}^*) \\
& - 0.0136079\,\mathcal{R}(R_8R_9^*) + 0.000286423\,\mathcal{R}(R_8R_{10}^*) - 0.0355109\,\mathcal{R}(R_9R_{10}^*) \\
& + 0.00631092\,|R_7|^2 + 0.0000975709\,|R_8|^2 + 0.439598\,|R_9|^2 \\
& + 3.20293\,|R_{10}|^2 + 0.701014\big] \times 10^{-7}\,, \qquad \text{(B.26)}
\end{aligned}
$$

JHEP06(2015)176

$$
\begin{aligned}
\mathcal{H}_L[1,6]_{ee} =& \big[0.00130398\,\mathcal{I}(R_7R_8^*) + 0.00167674\,\mathcal{I}(R_7R_9^*) + 0.00885049\,\mathcal{I}(R_8R_9^*) \\
&- 0.000180943\,\mathcal{I}(R_8R_{10}^*) + 0.00348707\,\mathcal{I}(R_7) + 0.0107332\,\mathcal{I}(R_8) \\
&+ 0.00524529\,\mathcal{I}(R_9) - 0.00187244\,\mathcal{I}(R_{10}) - 0.355982\,\mathcal{R}(R_7) \\
&- 0.0444029\,\mathcal{R}(R_8) + 2.57393\,\mathcal{R}(R_9) - 0.444885\,\mathcal{R}(R_{10}) \\
&+ 0.00389991\,\mathcal{R}(R_7R_8^*) - 0.243784\,\mathcal{R}(R_7R_9^*) + 0.00529438\,\mathcal{R}(R_7R_{10}^*) \\
&- 0.0323532\,\mathcal{R}(R_8R_9^*) + 0.000688843\,\mathcal{R}(R_8R_{10}^*) - 0.081795\,\mathcal{R}(R_9R_{10}^*) \\
&+ 0.0122056\,|R_7|^2 + 0.000226098\,|R_8|^2 + 1.01556\,|R_9|^2 \\
&+ 7.40871\,|R_{10}|^2 + 1.50793\big] \times 10^{-7}\,, \qquad \text{(B.27)}
\end{aligned}
$$

$$
\begin{aligned}
\mathcal{H}_L[1,3.5]_{\mu\mu} =& \big[0.000741931\,\mathcal{I}(R_7R_8^*) + 0.000952641\,\mathcal{I}(R_7R_9^*) + 0.0050284\,\mathcal{I}(R_8R_9^*) \\
&- 0.000102803\,\mathcal{I}(R_8R_{10}^*) + 0.000345511\,\mathcal{I}(R_7) + 0.00587433\,\mathcal{I}(R_8) \\
&+ 0.0117155\,\mathcal{I}(R_9) - 0.00113202\,\mathcal{I}(R_{10}) - 0.217245\,\mathcal{R}(R_7) \\
&- 0.0269584\,\mathcal{R}(R_8) + 1.53068\,\mathcal{R}(R_9) - 0.25154\,\mathcal{R}(R_{10}) \\
&+ 0.00260573\,\mathcal{R}(R_7R_8^*) - 0.153057\,\mathcal{R}(R_7R_9^*) + 0.00300802\,\mathcal{R}(R_7R_{10}^*) \\
&- 0.0200209\,\mathcal{R}(R_8R_9^*) + 0.000402421\,\mathcal{R}(R_8R_{10}^*) - 0.0462841\,\mathcal{R}(R_9R_{10}^*) \\
&+ 0.00897313\,|R_7|^2 + 0.000146331\,|R_8|^2 + 0.609248\,|R_9|^2 \\
&+ 4.43707\,|R_{10}|^2 + 0.914888\big] \times 10^{-7}\,, \qquad \text{(B.28)}
\end{aligned}
$$

$$
\begin{aligned}
\mathcal{H}_L[3.5,6]_{\mu\mu} =& \big[0.000562052\,\mathcal{I}(R_7R_8^*) + 0.000724099\,\mathcal{I}(R_7R_9^*) + 0.00382208\,\mathcal{I}(R_8R_9^*) \\
&- 0.0000781401\,\mathcal{I}(R_8R_{10}^*) + 0.00132426\,\mathcal{I}(R_7) + 0.00472065\,\mathcal{I}(R_8) \\
&+ 0.00235817\,\mathcal{I}(R_9) - 0.000740423\,\mathcal{I}(R_{10}) - 0.177392\,\mathcal{R}(R_7) \\
&- 0.0204867\,\mathcal{R}(R_8) + 1.23911\,\mathcal{R}(R_9) - 0.193345\,\mathcal{R}(R_{10}) \\
&+ 0.00194094\,\mathcal{R}(R_7R_8^*) - 0.118058\,\mathcal{R}(R_7R_9^*) + 0.00228636\,\mathcal{R}(R_7R_{10}^*) \\
&- 0.0144108\,\mathcal{R}(R_8R_9^*) + 0.000286423\,\mathcal{R}(R_8R_{10}^*) - 0.0355109\,\mathcal{R}(R_9R_{10}^*) \\
&+ 0.00748476\,|R_7|^2 + 0.00010436\,|R_8|^2 + 0.466941\,|R_9|^2 \\
&+ 3.39295\,|R_{10}|^2 + 0.791074\big] \times 10^{-7}\,, \qquad \text{(B.29)}
\end{aligned}
$$

$$
\begin{aligned}
\mathcal{H}_L[1,6]_{\mu\mu} =& \big[0.00130398\,\mathcal{I}(R_7R_8^*) + 0.00167674\,\mathcal{I}(R_7R_9^*) + 0.00885049\,\mathcal{I}(R_8R_9^*) \\
&- 0.000180943\,\mathcal{I}(R_8R_{10}^*) + 0.00166977\,\mathcal{I}(R_7) + 0.010595\,\mathcal{I}(R_8) \\
&+ 0.0140737\,\mathcal{I}(R_9) - 0.00187244\,\mathcal{I}(R_{10}) - 0.394638\,\mathcal{R}(R_7) \\
&- 0.0474451\,\mathcal{R}(R_8) + 2.76979\,\mathcal{R}(R_9) - 0.444885\,\mathcal{R}(R_{10}) \\
&+ 0.00454667\,\mathcal{R}(R_7R_8^*) - 0.271115\,\mathcal{R}(R_7R_9^*) + 0.00529438\,\mathcal{R}(R_7R_{10}^*) \\
&- 0.0344317\,\mathcal{R}(R_8R_9^*) + 0.000688843\,\mathcal{R}(R_8R_{10}^*) - 0.081795\,\mathcal{R}(R_9R_{10}^*) \\
&+ 0.0164579\,|R_7|^2 + 0.000250691\,|R_8|^2 + 1.07619\,|R_9|^2 \\
&+ 7.83003\,|R_{10}|^2 + 1.70596\big] \times 10^{-7}\,, \qquad \text{(B.30)}
\end{aligned}
$$

$$
\begin{aligned}
\mathcal{B}[1,3.5]_{ee} =& \big[0.0169646\,\mathcal{I}(R_7R_8^*) + 0.00282046\,\mathcal{I}(R_7R_9^*) + 0.0148876\,\mathcal{I}(R_8R_9^*) \\
&- 0.000304367\,\mathcal{I}(R_8R_{10}^*) + 0.0347138\,\mathcal{I}(R_7) - 0.00283044\,\mathcal{I}(R_8) \\
&+ 0.000660238\,\mathcal{I}(R_9) - 0.00100106\,\mathcal{I}(R_{10}) + 0.189792\,\mathcal{R}(R_7)
\end{aligned}
$$

JHEP06(2015)176

$$
\begin{aligned}
&+ 0.0139496\,\mathcal{R}(R_8) + 1.46271\,\mathcal{R}(R_9) - 0.290285\,\mathcal{R}(R_{10}) \\
&+ 0.0507378\,\mathcal{R}(R_7R_8^*) - 0.506251\,\mathcal{R}(R_7R_9^*) + 0.00871409\,\mathcal{R}(R_7R_{10}^*) \\
&- 0.0584716\,\mathcal{R}(R_8R_9^*) + 0.00107643\,\mathcal{R}(R_8R_{10}^*) - 0.0560647\,\mathcal{R}(R_9R_{10}^*) \\
&+ 0.210889\,|R_7|^2 + 0.0028916\,|R_8|^2 + 0.813297\,|R_9|^2 \\
&+ 5.94874\,|R_{10}|^2 + 1.46402\big]\ \times\ 10^{-7}\,, \qquad \text{(B.31)}
\end{aligned}
$$

$$
\begin{aligned}
\mathcal{B}[3.5,6]_{ee} =& \big[0.00576094\,\mathcal{I}(R_7R_8^*) + 0.00213621\,\mathcal{I}(R_7R_9^*) + 0.0112758\,\mathcal{I}(R_8R_9^*) \\
&- 0.000230526\,\mathcal{I}(R_8R_{10}^*) + 0.0117001\,\mathcal{I}(R_7) + 0.00792519\,\mathcal{I}(R_8) \\
&- 0.000973809\,\mathcal{I}(R_9) - 0.000822616\,\mathcal{I}(R_{10}) - 0.304197\,\mathcal{R}(R_7) \\
&- 0.0338418\,\mathcal{R}(R_8) + 1.538\,\mathcal{R}(R_9) - 0.268205\,\mathcal{R}(R_{10}) \\
&+ 0.0166482\,\mathcal{R}(R_7R_8^*) - 0.361825\,\mathcal{R}(R_7R_9^*) + 0.00659775\,\mathcal{R}(R_7R_{10}^*) \\
&- 0.0407383\,\mathcal{R}(R_8R_9^*) + 0.000775603\,\mathcal{R}(R_8R_{10}^*) - 0.0512368\,\mathcal{R}(R_9R_{10}^*) \\
&+ 0.0694138\,|R_7|^2 + 0.000881518\,|R_8|^2 + 0.714084\,|R_9|^2 \\
&+ 5.16931\,|R_{10}|^2 + 0.985134\big]\ \times\ 10^{-7}\,, \qquad \text{(B.32)}
\end{aligned}
$$

$$
\begin{aligned}
\mathcal{B}[1,6]_{ee} =& \big[0.0227255\,\mathcal{I}(R_7R_8^*) + 0.00495667\,\mathcal{I}(R_7R_9^*) + 0.0261634\,\mathcal{I}(R_8R_9^*) \\
&- 0.000534893\,\mathcal{I}(R_8R_{10}^*) + 0.0464139\,\mathcal{I}(R_7) + 0.00509475\,\mathcal{I}(R_8) \\
&- 0.000313571\,\mathcal{I}(R_9) - 0.00182368\,\mathcal{I}(R_{10}) - 0.114406\,\mathcal{R}(R_7) \\
&- 0.0198921\,\mathcal{R}(R_8) + 3.00071\,\mathcal{R}(R_9) - 0.55849\,\mathcal{R}(R_{10}) \\
&+ 0.067386\,\mathcal{R}(R_7R_8^*) - 0.868076\,\mathcal{R}(R_7R_9^*) + 0.0153118\,\mathcal{R}(R_7R_{10}^*) \\
&- 0.0992099\,\mathcal{R}(R_8R_9^*) + 0.00185203\,\mathcal{R}(R_8R_{10}^*) - 0.107301\,\mathcal{R}(R_9R_{10}^*) \\
&+ 0.280302\,|R_7|^2 + 0.00377311\,|R_8|^2 + 1.52738\,|R_9|^2 \\
&+ 11.1181\,|R_{10}|^2 + 2.44915\big]\ \times\ 10^{-7}\,, \qquad \text{(B.33)}
\end{aligned}
$$

$$
\begin{aligned}
\mathcal{B}[1,3.5]_{\mu\mu} =& \big[0.0169646\,\mathcal{I}(R_7R_8^*) + 0.00282046\,\mathcal{I}(R_7R_9^*) + 0.0148876\,\mathcal{I}(R_8R_9^*) \\
&- 0.000304367\,\mathcal{I}(R_8R_{10}^*) + 0.0350544\,\mathcal{I}(R_7) - 0.00280454\,\mathcal{I}(R_8) \\
&- 0.000975567\,\mathcal{I}(R_9) - 0.00100106\,\mathcal{I}(R_{10}) + 0.233832\,\mathcal{R}(R_7) \\
&+ 0.017358\,\mathcal{R}(R_8) + 1.35952\,\mathcal{R}(R_9) - 0.290285\,\mathcal{R}(R_{10}) \\
&+ 0.0514155\,\mathcal{R}(R_7R_8^*) - 0.490489\,\mathcal{R}(R_7R_9^*) + 0.00871409\,\mathcal{R}(R_7R_{10}^*) \\
&- 0.0572729\,\mathcal{R}(R_8R_9^*) + 0.00107643\,\mathcal{R}(R_8R_{10}^*) - 0.0560647\,\mathcal{R}(R_9R_{10}^*) \\
&+ 0.215344\,|R_7|^2 + 0.00291736\,|R_8|^2 + 0.78123\,|R_9|^2 \\
&+ 5.7259\,|R_{10}|^2 + 1.3762\big]\ \times\ 10^{-7}\,, \qquad \text{(B.34)}
\end{aligned}
$$

$$
\begin{aligned}
\mathcal{B}[3.5,6]_{\mu\mu} =& \big[0.00576094\,\mathcal{I}(R_7R_8^*) + 0.00213621\,\mathcal{I}(R_7R_9^*) + 0.0112758\,\mathcal{I}(R_8R_9^*) \\
&- 0.000230526\,\mathcal{I}(R_8R_{10}^*) + 0.0122024\,\mathcal{I}(R_7) + 0.00796339\,\mathcal{I}(R_8) \\
&- 0.00336638\,\mathcal{I}(R_9) - 0.000822616\,\mathcal{I}(R_{10}) - 0.29433\,\mathcal{R}(R_7) \\
&- 0.0330948\,\mathcal{R}(R_8) + 1.50123\,\mathcal{R}(R_9) - 0.268205\,\mathcal{R}(R_{10}) \\
&+ 0.0171247\,\mathcal{R}(R_7R_8^*) - 0.362728\,\mathcal{R}(R_7R_9^*) + 0.00659775\,\mathcal{R}(R_7R_{10}^*) \\
&- 0.040807\,\mathcal{R}(R_8R_9^*) + 0.000775603\,\mathcal{R}(R_8R_{10}^*) - 0.0512368\,\mathcal{R}(R_9R_{10}^*)
\end{aligned}
$$

JHEP06(2015)176

$$
\begin{aligned}
&+ 0.0725464\,|R_7|^2 + 0.000899635\,|R_8|^2 + 0.706733\,|R_9|^2 \\
&+ 5.11822\,|R_{10}|^2 + 0.940534\big]\ \times\ 10^{-7}\,, \qquad \text{(B.35)}\\
\mathcal{B}[1,6]_{\mu\mu} =&\big[0.0227255\,\mathcal{I}(R_7R_8^*) + 0.00495667\,\mathcal{I}(R_7R_9^*) + 0.0261634\,\mathcal{I}(R_8R_9^*) \\
&- 0.000534893\,\mathcal{I}(R_8R_{10}^*) + 0.0472568\,\mathcal{I}(R_7) + 0.00515885\,\mathcal{I}(R_8) \\
&- 0.00434195\,\mathcal{I}(R_9) - 0.00182368\,\mathcal{I}(R_{10}) - 0.0604983\,\mathcal{R}(R_7) \\
&- 0.0157368\,\mathcal{R}(R_8) + 2.86075\,\mathcal{R}(R_9) - 0.55849\,\mathcal{R}(R_{10}) \\
&+ 0.0685402\,\mathcal{R}(R_7R_8^*) - 0.853217\,\mathcal{R}(R_7R_9^*) + 0.0153118\,\mathcal{R}(R_7R_{10}^*) \\
&- 0.09808\,\mathcal{R}(R_8R_9^*) + 0.00185203\,\mathcal{R}(R_8R_{10}^*) - 0.107301\,\mathcal{R}(R_9R_{10}^*) \\
&+ 0.287891\,|R_7|^2 + 0.003817\,|R_8|^2 + 1.48796\,|R_9|^2 \\
&+ 10.8441\,|R_{10}|^2 + 2.31673\big]\ \times\ 10^{-7}\,, \qquad \text{(B.36)}\\
\mathcal{B}[>14.4]_{ee} =&\big[0.000264356\,\mathcal{I}(R_7R_8^*) + 0.000401975\,\mathcal{I}(R_7R_9^*) + 0.00161219\,\mathcal{I}(R_8R_9^*) \\
&- 0.0000328066\,\mathcal{I}(R_8R_{10}^*) - 0.0158129\,\mathcal{I}(R_7) + 0.000478008\,\mathcal{I}(R_8) \\
&+ 0.125395\,\mathcal{I}(R_9) - 0.00293188\,\mathcal{I}(R_{10}) - 0.0723471\,\mathcal{R}(R_7) \\
&- 0.00827793\,\mathcal{R}(R_8) + 0.511715\,\mathcal{R}(R_9) - 0.0806142\,\mathcal{R}(R_{10}) \\
&+ 0.000709678\,\mathcal{R}(R_7R_8^*) - 0.0516424\,\mathcal{R}(R_7R_9^*) + 0.00111614\,\mathcal{R}(R_7R_{10}^*) \\
&- 0.00651216\,\mathcal{R}(R_8R_9^*) + 0.000119004\,\mathcal{R}(R_8R_{10}^*) - 0.0168936\,\mathcal{R}(R_9R_{10}^*) \\
&+ 0.00287361\,|R_7|^2 + 0.0000373632\,|R_8|^2 + 0.211548\,|R_9|^2 \\
&+ 1.50748\,|R_{10}|^2 + 0.200589\big]\ \times\ 10^{-7}\,, \qquad \text{(B.37)}\\
\mathcal{B}[>14.4]_{\mu\mu} =&\big[0.000264356\,\mathcal{I}(R_7R_8^*) + 0.000401975\,\mathcal{I}(R_7R_9^*) + 0.00161219\,\mathcal{I}(R_8R_9^*) \\
&- 0.0000328066\,\mathcal{I}(R_8R_{10}^*) - 0.0175987\,\mathcal{I}(R_7) + 0.000342205\,\mathcal{I}(R_8) \\
&+ 0.134924\,\mathcal{I}(R_9) - 0.00293188\,\mathcal{I}(R_{10}) - 0.0871863\,\mathcal{R}(R_7) \\
&- 0.00943852\,\mathcal{R}(R_8) + 0.594393\,\mathcal{R}(R_9) - 0.0806142\,\mathcal{R}(R_{10}) \\
&+ 0.000835527\,\mathcal{R}(R_7R_8^*) - 0.0601984\,\mathcal{R}(R_7R_9^*) + 0.00111614\,\mathcal{R}(R_7R_{10}^*) \\
&- 0.00716282\,\mathcal{R}(R_8R_9^*) + 0.000119004\,\mathcal{R}(R_8R_{10}^*) - 0.0168936\,\mathcal{R}(R_9R_{10}^*) \\
&+ 0.00370104\,|R_7|^2 + 0.0000421485\,|R_8|^2 \\
&+ 0.234333\,|R_9|^2 + 1.66583\,|R_{10}|^2 + 0.292268\big]\ \times\ 10^{-7}\,, \qquad \text{(B.38)}\\
\mathcal{R}(14.4)_{ee} =&\big[0.000352294\,\mathcal{I}(R_7R_8^*) + 0.000544926\,\mathcal{I}(R_7R_9^*) + 0.00213997\,\mathcal{I}(R_8R_9^*) \\
&- 0.0000442492\,\mathcal{I}(R_8R_{10}^*) - 0.0160419\,\mathcal{I}(R_7) + 0.000523537\,\mathcal{I}(R_8) \\
&+ 0.130938\,\mathcal{I}(R_9) - 0.00323922\,\mathcal{I}(R_{10}) - 0.0669411\,\mathcal{R}(R_7) \\
&- 0.00821459\,\mathcal{R}(R_8) + 0.458105\,\mathcal{R}(R_9) - 0.0958901\,\mathcal{R}(R_{10}) \\
&+ 0.000807558\,\mathcal{R}(R_7R_8^*) - 0.054864\,\mathcal{R}(R_7R_9^*) + 0.00123432\,\mathcal{R}(R_7R_{10}^*) \\
&- 0.00734198\,\mathcal{R}(R_8R_9^*) + 0.000139543\,\mathcal{R}(R_8R_{10}^*) - 0.0189772\,\mathcal{R}(R_9R_{10}^*) \\
&+ 0.00293717\,|R_7|^2 + 0.0000444449\,|R_8|^2 + 0.228597\,|R_9|^2 \\
&+ 1.6322\,|R_{10}|^2 + 0.174573\big]\ \times\ 10^{-3}\,, \qquad \text{(B.39)}
\end{aligned}
$$

JHEP06(2015)176

$$
\begin{aligned}
\mathcal{R}(14.4)_{\mu\mu} = \big[& 0.000352294\,\mathcal{I}(R_7 R_8^*) + 0.000544926\,\mathcal{I}(R_7 R_9^*) + 0.00213997\,\mathcal{I}(R_8 R_9^*) \\
& - 0.0000442492\,\mathcal{I}(R_8 R_{10}^*) - 0.0181914\,\mathcal{I}(R_7) + 0.000360068\,\mathcal{I}(R_8) \\
& + 0.142407\,\mathcal{I}(R_9) - 0.00323922\,\mathcal{I}(R_{10}) - 0.0825154\,\mathcal{R}(R_7) \\
& - 0.00943762\,\mathcal{R}(R_8) + 0.54544\,\mathcal{R}(R_9) - 0.0958901\,\mathcal{R}(R_{10}) \\
& + 0.000959044\,\mathcal{R}(R_7 R_8^*) - 0.0651631\,\mathcal{R}(R_7 R_9^*) + 0.00123432\,\mathcal{R}(R_7 R_{10}^*) \\
& - 0.0081252\,\mathcal{R}(R_8 R_9^*) + 0.000139543\,\mathcal{R}(R_8 R_{10}^*) - 0.0189772\,\mathcal{R}(R_9 R_{10}^*) \\
& + 0.00393316\,|R_7|^2 + 0.000050205\,|R_8|^2 + 0.256024\,|R_9|^2 \\
& + 1.82281\,|R_{10}|^2 + 0.266662 \big] \times 10^{-3} \,. \qquad \text{(B.40)}
\end{aligned}
$$

Open Access. This article is distributed under the terms of the Creative Commons Attribution License (CC-BY 4.0), which permits any use, distribution and reproduction in any medium, provided the original author(s) and source are credited.

References

[1] LHCb collaboration, http://lhcb.web.cern.ch/lhcb/.

[2] https://twiki.cern.ch/twiki/bin/view/AtlasPublic/BPhysPublicResults.

[3] https://twiki.cern.ch/twiki/bin/view/CMSPublic/PhysicsResultsBPH.

[4] http://www.slac.stanford.edu/BFROOT/.

[5] http://belle.kek.jp/.

[6] http://www-cdf.fnal.gov/physics/new/bottom/bottom.html.

[7] http://www-d0.fnal.gov/Run2Physics/WWW/results/b.htm.

[8] G. Isidori, Y. Nir and G. Perez, *Flavor physics constraints for physics beyond the standard model*, *Ann. Rev. Nucl. Part. Sci.* **60** (2010) 355 [arXiv:1002.0900] [INSPIRE].

[9] T. Hurth and M. Nakao, *Radiative and electroweak penguin decays of B mesons*, *Ann. Rev. Nucl. Part. Sci.* **60** (2010) 645 [arXiv:1005.1224] [INSPIRE].

[10] T. Hurth and F. Mahmoudi, *Colloquium: new physics search with flavor in the LHC era*, *Rev. Mod. Phys.* **85** (2013) 795 [arXiv:1211.6453] [INSPIRE].

[11] LHCb collaboration, *Measurement of form-factor-independent observables in the decay* $B^0 \to K^{*0}\mu^+\mu^-$, *Phys. Rev. Lett.* **111** (2013) 191801 [arXiv:1308.1707] [INSPIRE].

[12] S. Descotes-Genon, J. Matias and J. Virto, *Understanding the* $B \to K * \mu^+\mu^-$ *anomaly*, *Phys. Rev.* **D 88** (2013) 074002 [arXiv:1307.5683] [INSPIRE].

[13] W. Altmannshofer and D.M. Straub, *New physics in* $B \to K^*\mu\mu$*?*, *Eur. Phys. J.* **C 73** (2013) 2646 [arXiv:1308.1501] [INSPIRE].

[14] F. Beaujean, C. Bobeth and D. van Dyk, *Comprehensive bayesian analysis of rare (semi)leptonic and radiative B decays*, *Eur. Phys. J.* **C 74** (2014) 2897 [arXiv:1310.2478] [INSPIRE].

[15] C. Hambrock, G. Hiller, S. Schacht and R. Zwicky, $B \to K^\star$ *form factors from flavor data to QCD and back*, *Phys. Rev.* **D 89** (2014) 074014 [arXiv:1308.4379] [INSPIRE].

JHEP06(2015)176

[16] R. Gauld, F. Goertz and U. Haisch, *On minimal Z' explanations of the $B \to K^* \mu^+ \mu^-$ anomaly*, Phys. Rev. **D 89** (2014) 015005 [arXiv:1308.1959] [INSPIRE].

[17] A.J. Buras, F. De Fazio and J. Girrbach, 331 *models facing new $b \to s\mu^+\mu^-$ data*, JHEP **02** (2014) 112 [arXiv:1311.6729] [INSPIRE].

[18] T. Hurth and F. Mahmoudi, *On the LHCb anomaly in $B \to K^* \ell^+ \ell^-$*, JHEP **04** (2014) 097 [arXiv:1312.5267] [INSPIRE].

[19] F. Mahmoudi, S. Neshatpour and J. Virto, *$B \to K^* \mu^+ \mu^-$ optimised observables in the MSSM*, Eur. Phys. J. **C 74** (2014) 2927 [arXiv:1401.2145] [INSPIRE].

[20] J. Lyon and R. Zwicky, *Resonances gone topsy turvy — The charm of QCD or new physics in $b \to s\ell^+\ell^-$?*, arXiv:1406.0566 [INSPIRE].

[21] LHCb collaboration, *Test of lepton universality using $B^+ \to K^+ \ell^+ \ell^-$ decays*, Phys. Rev. Lett. **113** (2014) 151601 [arXiv:1406.6482] [INSPIRE].

[22] R. Alonso, B. Grinstein and J. Martin Camalich, SU(2) $\times$ U(1) *gauge invariance and the shape of new physics in rare B decays*, Phys. Rev. Lett. **113** (2014) 241802 [arXiv:1407.7044] [INSPIRE].

[23] G. Hiller and M. Schmaltz, *R_K and future $b \to s\ell\ell$ physics beyond the standard model opportunities*, Phys. Rev. **D 90** (2014) 054014 [arXiv:1408.1627] [INSPIRE].

[24] D. Ghosh, M. Nardecchia and S.A. Renner, *Hint of lepton flavour non-universality in B meson decays*, JHEP **12** (2014) 131 [arXiv:1408.4097] [INSPIRE].

[25] S. Biswas, D. Chowdhury, S. Han and S.J. Lee, *Explaining the lepton non-universality at the LHCb and CMS within a unified framework*, JHEP **02** (2015) 142 [arXiv:1409.0882] [INSPIRE].

[26] D. Straub, *New Physics models facing $b \to s$ data*, talk given at the workshop *Implications of LHCb measurements and future prospects*, October 14–16, CERN, Switzerland (2014).

[27] T. Hurth, F. Mahmoudi and S. Neshatpour, *Global fits to $b \to s\ell\ell$ data and signs for lepton non-universality*, JHEP **12** (2014) 053 [arXiv:1410.4545] [INSPIRE].

[28] S.L. Glashow, D. Guadagnoli and K. Lane, *Lepton flavor violation in B decays?*, Phys. Rev. Lett. **114** (2015) 091801 [arXiv:1411.0565] [INSPIRE].

[29] W. Altmannshofer and D.M. Straub, *New physics in $b \to s$ transitions after LHC run 1*, arXiv:1411.3161 [INSPIRE].

[30] G. Hiller and M. Schmaltz, *Diagnosing lepton-nonuniversality in $b \to s\ell\ell$*, JHEP **02** (2015) 055 [arXiv:1411.4773] [INSPIRE].

[31] B. Bhattacharya, A. Datta, D. London and S. Shivashankara, *Simultaneous explanation of the R_K and $R(D^{(*)})$ puzzles*, Phys. Lett. **B 742** (2015) 370 [arXiv:1412.7164] [INSPIRE].

[32] M. Misiak, *Perturbative contributions to rare B-meson decays*, PoS(DIS2014)198 [INSPIRE].

[33] M. Misiak, *Rare B-meson decays*, arXiv:1112.5978 [INSPIRE].

[34] T. Hurth, *Present status of inclusive rare B decays*, Rev. Mod. Phys. **75** (2003) 1159 [hep-ph/0212304] [INSPIRE].

[35] T. Hurth and F. Mahmoudi, *Signs for new physics in the recent LHCb data?*, arXiv:1411.2786 [INSPIRE].

JHEP06(2015)176

[36] Belle collaboration, M. Iwasaki et al., *Improved measurement of the electroweak penguin process $B \to X_s \ell^+ \ell^-$*, Phys. Rev. **D 72** (2005) 092005 [hep-ex/0503044] [inSPIRE].

[37] BaBar collaboration, J.P. Lees et al., *Measurement of the $B \to X_s \ell^+ \ell^-$ branching fraction and search for direct CP-violation from a sum of exclusive final states*, Phys. Rev. Lett. **112** (2014) 211802 [arXiv:1312.5364] [inSPIRE].

[38] BaBar collaboration, B. Aubert et al., *Measurement of the $B \to X_s \ell^+ \ell^-$ branching fraction with a sum over exclusive modes*, Phys. Rev. Lett. **93** (2004) 081802 [hep-ex/0404006] [inSPIRE].

[39] Belle collaboration, Y. Sato et al., *Measurement of the lepton forward-backward asymmetry in $B \to X_s \ell^+ \ell^-$ decays with a sum of exclusive modes*, arXiv:1402.7134 [inSPIRE].

[40] Belle-II collaboration, T. Abe et al., *Belle II technical design report*, arXiv:1011.0352 [inSPIRE].

[41] M. Misiak, *The $b \to s e^+ e^-$ and $b \to s\gamma$ decays with next-to-leading logarithmic QCD corrections*, Nucl. Phys. **B 393** (1993) 23 [*Erratum ibid.* **B 439** (1995) 461] [inSPIRE].

[42] A.J. Buras and M. Münz, *Effective Hamiltonian for $B \to X_s e^+ e^-$ beyond leading logarithms in the NDR and HV schemes*, Phys. Rev. **D 52** (1995) 186 [hep-ph/9501281] [inSPIRE].

[43] C. Bobeth, M. Misiak and J. Urban, *Photonic penguins at two loops and $m(t)$ dependence of $BR[B \to X_s l^+ l^-]$*, Nucl. Phys. **B 574** (2000) 291 [hep-ph/9910220] [inSPIRE].

[44] P. Gambino, M. Gorbahn and U. Haisch, *Anomalous dimension matrix for radiative and rare semileptonic B decays up to three loops*, Nucl. Phys. **B 673** (2003) 238 [hep-ph/0306079] [inSPIRE].

[45] M. Gorbahn and U. Haisch, *Effective Hamiltonian for non-leptonic $|\Delta F| = 1$ decays at NNLO in QCD*, Nucl. Phys. **B 713** (2005) 291 [hep-ph/0411071] [inSPIRE].

[46] H.H. Asatryan, H.M. Asatrian, C. Greub and M. Walker, *Calculation of two loop virtual corrections to $b \to s \ell^+ \ell^-$ in the standard model*, Phys. Rev. **D 65** (2002) 074004 [hep-ph/0109140] [inSPIRE].

[47] H.H. Asatrian, H.M. Asatrian, C. Greub and M. Walker, *Two loop virtual corrections to $B \to X_s l^+ l^-$ in the standard model*, Phys. Lett. **B 507** (2001) 162 [hep-ph/0103087] [inSPIRE].

[48] H.H. Asatryan, H.M. Asatrian, C. Greub and M. Walker, *Complete gluon bremsstrahlung corrections to the process $b \to s \ell^+ \ell^-$*, Phys. Rev. **D 66** (2002) 034009 [hep-ph/0204341] [inSPIRE].

[49] A. Ghinculov, T. Hurth, G. Isidori and Y.P. Yao, *Forward backward asymmetry in $B \to X_s \ell^+ \ell^-$ at the NNLL level*, Nucl. Phys. **B 648** (2003) 254 [hep-ph/0208088] [inSPIRE].

[50] H.M. Asatrian, K. Bieri, C. Greub and A. Hovhannisyan, *NNLL corrections to the angular distribution and to the forward backward asymmetries in $b \to X_s \ell^+ \ell^-$*, Phys. Rev. **D 66** (2002) 094013 [hep-ph/0209006] [inSPIRE].

[51] H.M. Asatrian, H.H. Asatryan, A. Hovhannisyan and V. Poghosyan, *Complete bremsstrahlung corrections to the forward backward asymmetries in $b \to X_s \ell^+ \ell^-$*, Mod. Phys. Lett. **A 19** (2004) 603 [hep-ph/0311187] [inSPIRE].

JHEP06(2015)176

[52] A. Ghinculov, T. Hurth, G. Isidori and Y.P. Yao, *New NNLL results on the decay $B \to X_s \ell^+ \ell^-$*, *Eur. Phys. J.* **C 33** (2004) S288 [hep-ph/0310187] [INSPIRE].

[53] A. Ghinculov, T. Hurth, G. Isidori and Y.P. Yao, *The rare decay $B \to X_s \ell^+ \ell^-$ to NNLL precision for arbitrary dilepton invariant mass*, *Nucl. Phys.* **B 685** (2004) 351 [hep-ph/0312128] [INSPIRE].

[54] C. Greub, V. Pilipp and C. Schupbach, *Analytic calculation of two-loop QCD corrections to $b \to s\ell^+\ell^-$ in the high Q^2 region*, *JHEP* **12** (2008) 040 [arXiv:0810.4077] [INSPIRE].

[55] C. Bobeth, P. Gambino, M. Gorbahn and U. Haisch, *Complete NNLO QCD analysis of $\bar{B} \to X_s \ell^+ \ell^-$ and higher order electroweak effects*, *JHEP* **04** (2004) 071 [hep-ph/0312090] [INSPIRE].

[56] A.F. Falk, M.E. Luke and M.J. Savage, *Nonperturbative contributions to the inclusive rare decays $B \to X_s \gamma$ and $B \to X_s l^+ l^-$*, *Phys. Rev.* **D 49** (1994) 3367 [hep-ph/9308288] [INSPIRE].

[57] A. Ali, G. Hiller, L.T. Handoko and T. Morozumi, *Power corrections in the decay rate and distributions in $B \to X_s l^+ l^-$ in the standard model*, *Phys. Rev.* **D 55** (1997) 4105 [hep-ph/9609449] [INSPIRE].

[58] J.-W. Chen, G. Rupak and M.J. Savage, *Non $(1/m(b)^n)$ power suppressed contributions to inclusive $B \to X_s l^+ l^-$ decays*, *Phys. Lett.* **B 410** (1997) 285 [hep-ph/9705219] [INSPIRE].

[59] G. Buchalla and G. Isidori, *Nonperturbative effects in $\bar{B} \to X_s l^+ l^-$ for large dilepton invariant mass*, *Nucl. Phys.* **B 525** (1998) 333 [hep-ph/9801456] [INSPIRE].

[60] C.W. Bauer and C.N. Burrell, *Nonperturbative corrections to moments of the decay $B \to X_s \ell^+ \ell^-$*, *Phys. Rev.* **D 62** (2000) 114028 [hep-ph/9911404] [INSPIRE].

[61] Z. Ligeti and F.J. Tackmann, *Precise predictions for $B \to X_s \ell^+ \ell^-$ in the large Q^2 region*, *Phys. Lett.* **B 653** (2007) 404 [arXiv:0707.1694] [INSPIRE].

[62] G. Buchalla, G. Isidori and S.J. Rey, *Corrections of order $\Lambda^2_{\rm QCD}/m_c^2$ to inclusive rare B decays*, *Nucl. Phys.* **B 511** (1998) 594 [hep-ph/9705253] [INSPIRE].

[63] M. Benzke, S.J. Lee, M. Neubert and G. Paz, *Factorization at subleading power and irreducible uncertainties in $\bar{B} \to X_s \gamma$ decay*, *JHEP* **08** (2010) 099 [arXiv:1003.5012] [INSPIRE].

[64] M. Neubert, *On the inclusive determination of $|V(ub)|$ from the lepton invariant mass spectrum*, *JHEP* **07** (2000) 022 [hep-ph/0006068] [INSPIRE].

[65] C.W. Bauer, Z. Ligeti and M.E. Luke, *Precision determination of $|V(ub)|$ from inclusive decays*, *Phys. Rev.* **D 64** (2001) 113004 [hep-ph/0107074] [INSPIRE].

[66] T. Huber, T. Hurth and E. Lunghi, *Logarithmically enhanced corrections to the decay rate and forward backward asymmetry in $\bar{B} \to X_s \ell^+ \ell^-$*, *Nucl. Phys.* **B 802** (2008) 40 [arXiv:0712.3009] [INSPIRE].

[67] K.S.M. Lee and I.W. Stewart, *Shape-function effects and split matching in $B \to X_s \ell^+ \ell^-$*, *Phys. Rev.* **D 74** (2006) 014005 [hep-ph/0511334] [INSPIRE].

[68] K.S.M. Lee, Z. Ligeti, I.W. Stewart and F.J. Tackmann, *Universality and $m(X)$ cut effects in $B \to X_s \ell^+ \ell^-$*, *Phys. Rev.* **D 74** (2006) 011501 [hep-ph/0512191] [INSPIRE].

[69] K.S.M. Lee and F.J. Tackmann, *Nonperturbative $m(X)$ cut effects in $B \to X_s \ell^+ \ell^-$ observables*, *Phys. Rev.* **D 79** (2009) 114021 [arXiv:0812.0001] [INSPIRE].

JHEP06(2015)176

[70] F.U. Bernlochner et al., *Status of SIMBA*, arXiv:1101.3310 [INSPIRE].

[71] G. Bell, M. Beneke, T. Huber and X.-Q. Li, *Heavy-to-light currents at NNLO in SCET and semi-inclusive $\bar{B} \to X_s l^+ l^-$ decay*, Nucl. Phys. **B 843** (2011) 143 [arXiv:1007.3758] [INSPIRE].

[72] F. Krüger and L.M. Sehgal, *Lepton polarization in the decays $B \to X_s \mu^+ \mu^-$ and $B \to X_s \tau^+ \tau^-$*, Phys. Lett. **B 380** (1996) 199 [hep-ph/9603237] [INSPIRE].

[73] F. Krüger and L.M. Sehgal, *CP violation in the decay $B \to X_d e^+ e^-$*, Phys. Rev. **D 55** (1997) 2799 [hep-ph/9608361] [INSPIRE].

[74] M. Beneke, G. Buchalla, M. Neubert and C.T. Sachrajda, *Penguins with charm and quark-hadron duality*, Eur. Phys. J. **C 61** (2009) 439 [arXiv:0902.4446] [INSPIRE].

[75] E.C. Poggio, H.R. Quinn and S. Weinberg, *Smearing the quark model*, Phys. Rev. **D 13** (1976) 1958 [INSPIRE].

[76] T. Huber, E. Lunghi, M. Misiak and D. Wyler, *Electromagnetic logarithms in $\bar{B} \to X_s \ell^+ \ell^-$*, Nucl. Phys. **B 740** (2006) 105 [hep-ph/0512066] [INSPIRE].

[77] K.S.M. Lee, Z. Ligeti, I.W. Stewart and F.J. Tackmann, *Extracting short distance information from $B \to s\ell^+\ell^-$ effectively*, Phys. Rev. **D 75** (2007) 034016 [hep-ph/0612156] [INSPIRE].

[78] A. Ali, T. Mannel and T. Morozumi, *Forward backward asymmetry of dilepton angular distribution in the decay $B \to s\ell^+\ell^-$*, Phys. Lett. **B 273** (1991) 505 [INSPIRE].

[79] T. Huber, T. Hurth and E. Lunghi, *The role of collinear photons in the rare decay $\bar{B} \to X_s \ell^+ \ell^-$*, arXiv:0807.1940 [INSPIRE].

[80] P. Gambino and M. Misiak, *Quark mass effects in $\bar{B} \to X(s\gamma)$*, Nucl. Phys. **B 611** (2001) 338 [hep-ph/0104034] [INSPIRE].

[81] P. Gambino and C. Schwanda, *Inclusive semileptonic fits, heavy quark masses and V_{cb}*, Phys. Rev. **D 89** (2014) 014022 [arXiv:1307.4551] [INSPIRE].

[82] A. Sirlin, *Large $m(W)$, $m(Z)$ behavior of the $O(\alpha)$ corrections to semileptonic processes mediated by W*, Nucl. Phys. **B 196** (1982) 83 [INSPIRE].

[83] T. van Ritbergen, *The second order QCD contribution to the semileptonic $B \to u$ decay rate*, Phys. Lett. **B 454** (1999) 353 [hep-ph/9903226] [INSPIRE].

[84] K.G. Chetyrkin, R. Harlander, T. Seidensticker and M. Steinhauser, *Second order QCD corrections to $\Gamma(t \to Wb)$*, Phys. Rev. **D 60** (1999) 114015 [hep-ph/9906273] [INSPIRE].

[85] A. Czarnecki and K. Melnikov, *Semileptonic $b \to u$ decays: lepton invariant mass spectrum*, Phys. Rev. Lett. **88** (2002) 131801 [hep-ph/0112264] [INSPIRE].

[86] I.R. Blokland, A. Czarnecki, M. Ślusarczyk and F. Tkachov, *Heavy to light decays with a two loop accuracy*, Phys. Rev. Lett. **93** (2004) 062001 [hep-ph/0403221] [INSPIRE].

[87] I.R. Blokland, A. Czarnecki, M. Ślusarczyk and F. Tkachov, *Next-to-next-to-leading order calculations for heavy-to-light decays*, Phys. Rev. **D 71** (2005) 054004 [hep-ph/0503039] [INSPIRE].

[88] M. Brucherseifer, F. Caola and K. Melnikov, *On the $O(\alpha_s^2)$ corrections to $b \to X_u e \bar{\nu}$ inclusive decays*, Phys. Lett. **B 721** (2013) 107 [arXiv:1302.0444] [INSPIRE].

JHEP06(2015)176

[89] M. Brucherseifer, F. Caola and K. Melnikov, $O(\alpha_s^2)$ *corrections to fully-differential top quark decays*, *JHEP* **04** (2013) 059 [arXiv:1301.7133] [INSPIRE].

[90] M. Beneke, *Renormalons*, *Phys. Rept.* **317** (1999) 1 [hep-ph/9807443] [INSPIRE].

[91] A.H. Hoang, Z. Ligeti and A.V. Manohar, *B decays in the Upsilon expansion*, *Phys. Rev.* **D 59** (1999) 074017 [hep-ph/9811239] [INSPIRE].

[92] A.H. Hoang, *Bottom quark mass from Upsilon mesons: charm mass effects*, hep-ph/0008102 [INSPIRE].

[93] K.G. Chetyrkin, J.H. Kuhn and M. Steinhauser, *RunDec: a Mathematica package for running and decoupling of the strong coupling and quark masses*, *Comput. Phys. Commun.* **133** (2000) 43 [hep-ph/0004189] [INSPIRE].

[94] G. Buchalla and A.J. Buras, *Two loop large $m(t)$ electroweak corrections to $K \to \pi$ neutrino anti-neutrino for arbitrary Higgs boson mass*, *Phys. Rev.* **D 57** (1998) 216 [hep-ph/9707243] [INSPIRE].

[95] CKMFITTER GROUP collaboration, J. Charles et al., *CP violation and the CKM matrix: assessing the impact of the asymmetric B factories*, *Eur. Phys. J.* **C 41** (2005) 1 [hep-ph/0406184] [INSPIRE].

[96] HEAVY FLAVOR AVERAGING GROUP collaboration, Y. Amhis et al., *Averages of B-hadron, C-hadron and τ-lepton properties as of early 2012*, arXiv:1207.1158 [INSPIRE].

[97] C. Schwanda, *Determination of $|V_{cb}|$ from inclusive decays $B \to X_c \ell \nu$ using a global fit*, arXiv:1302.0294 [INSPIRE].

[98] C.W. Bauer, Z. Ligeti, M. Luke, A.V. Manohar and M. Trott, *Global analysis of inclusive B decays*, *Phys. Rev.* **D 70** (2004) 094017 [hep-ph/0408002] [INSPIRE].

[99] PARTICLE DATA GROUP collaboration, K.A. Olive et al., *Review of particle physics*, *Chin. Phys.* **C 38** (2014) 090001 [INSPIRE].

[100] M. Beneke, T. Feldmann and D. Seidel, *Systematic approach to exclusive $B \to V \ell^+ \ell^-$, $V\gamma$ decays*, *Nucl. Phys.* **B 612** (2001) 25 [hep-ph/0106067] [INSPIRE].

[101] A. Ali, E. Lunghi, C. Greub and G. Hiller, *Improved model independent analysis of semileptonic and radiative rare B decays*, *Phys. Rev.* **D 66** (2002) 034002 [hep-ph/0112300] [INSPIRE].

[102] Y.G. Kim, P. Ko and J.S. Lee, *Possible new physics signals in $b \to s\gamma$ and $b \to s\ell^+\ell^-$*, *Nucl. Phys.* **B 544** (1999) 64 [hep-ph/9810336] [INSPIRE].

[103] P. Gambino, U. Haisch and M. Misiak, *Determining the sign of the $b \to s\gamma$ amplitude*, *Phys. Rev. Lett.* **94** (2005) 061803 [hep-ph/0410155] [INSPIRE].

[104] C. Bobeth, M. Bona, A.J. Buras, T. Ewerth, M. Pierini et al., *Upper bounds on rare K and B decays from minimal flavor violation*, *Nucl. Phys.* **B 726** (2005) 252 [hep-ph/0505110] [INSPIRE].

[105] T. Hurth, G. Isidori, J.F. Kamenik and F. Mescia, *Constraints on new physics in MFV models: a model-independent analysis of $\Delta F = 1$ processes*, *Nucl. Phys.* **B 808** (2009) 326 [arXiv:0807.5039] [INSPIRE].

[106] T. Hurth and F. Mahmoudi, *The minimal flavour violation benchmark in view of the latest LHCb data*, *Nucl. Phys.* **B 865** (2012) 461 [arXiv:1207.0688] [INSPIRE].

JHEP06(2015)176

[107] S. Schilling, C. Greub, N. Salzmann and B. Toedtli, *QCD corrections to the Wilson coefficients C(9) and C(10) in two-Higgs doublet models*, Phys. Lett. **B 616** (2005) 93 [hep-ph/0407323] [INSPIRE].

[108] Z.-j. Xiao and L.-x. Lu, *$B \to X_s \ell^+ \ell^-$ decay in a top quark two-Higgs-doublet model*, Phys. Rev. **D 74** (2006) 034016 [hep-ph/0605076] [INSPIRE].

[109] S. Bertolini, F. Borzumati, A. Masiero and G. Ridolfi, *Effects of supergravity induced electroweak breaking on rare B decays and mixings*, Nucl. Phys. **B 353** (1991) 591 [INSPIRE].

[110] P.L. Cho, M. Misiak and D. Wyler, *$K(L) \to \pi^0 e^+ e^-$ and $B \to X_s l^+ l^-$ decay in the MSSM*, Phys. Rev. **D 54** (1996) 3329 [hep-ph/9601360] [INSPIRE].

[111] T. Goto, Y. Okada, Y. Shimizu and M. Tanaka, *$b \to s$ lepton anti-lepton in the minimal supergravity model*, Phys. Rev. **D 55** (1997) 4273 [*Erratum ibid.* **D 66** (2002) 019901] [hep-ph/9609512] [INSPIRE].

[112] J.L. Hewett and J.D. Wells, *Searching for supersymmetry in rare B decays*, Phys. Rev. **D 55** (1997) 5549 [hep-ph/9610323] [INSPIRE].

[113] C.-S. Huang, W. Liao and Q.-S. Yan, *The Promising process to distinguish supersymmetric models with large* $\tan\beta$ *from the standard model: $B \to X_s \mu^+ \mu^-$*, Phys. Rev. **D 59** (1999) 011701 [hep-ph/9803460] [INSPIRE].

[114] E. Lunghi, A. Masiero, I. Scimemi and L. Silvestrini, *$B \to X_s l^+ l^-$ decays in supersymmetry*, Nucl. Phys. **B 568** (2000) 120 [hep-ph/9906286] [INSPIRE].

[115] C. Bobeth, A.J. Buras and T. Ewerth, *$\bar{B} \to X_s \ell^+ \ell^-$ in the MSSM at NNLO*, Nucl. Phys. **B 713** (2005) 522 [hep-ph/0409293] [INSPIRE].

[116] G. Cowan, http://www.pp.rhul.ac.uk/∼cowan/stat/notes/weights.pdf

[117] T. Sjöstrand, *High-energy physics event generation with PYTHIA 5.7 and JETSET 7.4*, Comput. Phys. Commun. **82** (1994) 74 [INSPIRE].

[118] A. Ishikawa and M. Nakao, private communication.

[119] S. Playfer, G. Eigen and K. Flood, private communication.

[120] D.J. Lange, *The EvtGen particle decay simulation package*, Nucl. Instrum. Meth. **A 462** (2001) 152 [INSPIRE].

[121] E. Barberio, B. van Eijk and Z. Was, *PHOTOS: a universal Monte Carlo for QED radiative corrections in decays*, Comput. Phys. Commun. **66** (1991) 115 [INSPIRE].

[122] E. Barberio and Z. Was, *PHOTOS: a universal Monte Carlo for QED radiative corrections. Version 2.0*, Comput. Phys. Commun. **79** (1994) 291 [INSPIRE].

JHEP06(2015)176

Part II

Collider Physics

Published for SISSA by Springer

Received: May 12, 2010
Revised: June 8, 2010
Accepted: June 8, 2010
Published: June 25, 2010

JHEP06(2010)094

Calculation of the quark and gluon form factors to three loops in QCD

T. Gehrmann,[a] E.W.N. Glover,[b] T. Huber,[c] N. Ikizlerli[b] and C. Studerus[a]

[a] *Institut für Theoretische Physik, Universität Zürich, Winterthurerstrasse 190, CH-8057 Zürich, Switzerland*

[b] *Institute for Particle Physics Phenomenology, University of Durham, South Road, Durham DH1 3LE, England, U.K.*

[c] *Fachbereich 7, Universität Siegen, Walter-Flex-Strasse 3, D-57068 Siegen, Germany*

E-mail: thomas.gehrmann@physik.uzh.ch, e.w.n.glover@durham.ac.uk, huber@tp1.physik.uni-siegen.de, nehir.ikizlerli@durham.ac.uk, cedric@physik.uzh.ch

Abstract: We describe the calculation of the three-loop QCD corrections to quark and gluon form factors. The relevant three-loop Feynman diagrams are evaluated and the resulting three-loop Feynman integrals are reduced to a small set of known master integrals by using integration-by-parts relations. Our calculation confirms the recent results by Baikov et al. for the three-loop form factors. In addition, we derive the subleading $\mathcal{O}(\epsilon)$ terms for the fermion-loop type contributions to the three-loop form factors which are required for the extraction of the fermionic contributions to the four-loop quark and gluon collinear anomalous dimensions. The finite parts of the form factors are used to determine the hard matching coefficients for the Drell-Yan process and inclusive Higgs-production in soft-collinear effective theory.

Keywords: Higgs Physics, NLO Computations, QCD

ArXiv ePrint: 1004.3653

© SISSA 2010

doi:10.1007/JHEP06(2010)094

Contents

1 Introduction **1**

2 Quark and gluon form factors in perturbative QCD **3**
2.1 Results at one-loop 6
2.2 Results at two-loops 7

3 Calculation of the three-loop form factors **10**

4 Three-loop form factor master integrals **12**

5 Three-loop form factors **15**

6 Infrared pole structure **22**

7 Effective theory matching coefficients **24**

8 Conclusions **28**

A Master integrals for three-loop form factors **28**

B Form factors in terms of master integrals **34**

JHEP06(2010)094

1 Introduction

The form factors are basic vertex functions, and are as such fundamental ingredients for many precision calculations in QCD. They couple an external, colour-neutral off-shell current to a pair of partons: the quark form factor is the coupling of a virtual photon to a quark-antiquark pair, while the gluon form factor is the coupling of a Higgs boson to a pair of gluons through an effective Lagrangian. They appear as virtual higher-order corrections in coefficient functions for the inclusive Drell-Yan process [1–3] and the inclusive Higgs production cross section [3–12]. In these observables, the infrared poles of the form factors cancel with infrared singularities from real radiation corrections. Consequently, it is possible to relate the coefficients of the infrared poles of the form factors to the coefficients of large logarithmic terms in the corresponding real radiation processes [13–16]. A framework for combining the resummation of logarithmically enhanced terms at all orders with fixed-order results is provided in an effective field theory expansion [17] of QCD, which is systematized by soft-collinear effective theory [18–23]. In this context, the pole terms of the form factors yield the anomalous dimensions of the effective operators, while their finite terms determine the matching coefficients to a given order [24–27].

The form factors are actually the simplest QCD objects that display a non-trivial infrared pole structure. As such, their infrared pole coefficients can be used to extract fundamental constants: the cusp anomalous dimensions [28] which control the structure of soft divergences and the collinear quark and gluon anomalous dimensions. While the cusp anomalous dimensions were first obtained to three loops from the asymptotic behaviour of splitting functions [29, 30], it is the calculation [31, 32] of the pole terms of the three-loop form factors (and finite plus subleading terms in the two-loop and one-loop form factors [33–37]), which led to the derivation of the three-loop collinear anomalous dimensions [31, 38, 39]. An important observation is the agreement (up to an overall colour factor) of the cusp anomalous dimension for the quark and gluon, the so-called Casimir scaling [40]. Casimir scaling has been verified to three loops [29, 30], but it is an open question whether it holds at four loops and beyond [41]. From non-perturbative arguments, the Casimir scaling is expected to break down at some loop order [42].

Based on the observation that infrared singularities of massless on-shell amplitudes in QCD are related to ultraviolet singularities of operators in soft-collinear effective field theory [28, 43], the pole structure of these amplitudes can be analyzed using operator renormalization. The singularity structure of arbitrary multi-leg massless QCD amplitudes is determined by an anomalous dimension matrix. The terms allowed in this anomalous dimension matrix are strongly constrained by relations between soft and collinear terms, from non-abelian exponentiation and from soft and collinear factorization. Independently, Becher and Neubert [39] and Gardi and Magnea [44] have proposed a remarkable all-loops conjecture that describes the pole structure of massless on-shell multi-loop multi-leg QCD amplitudes (generalizing earlier results at two [45] and three loops [46]) in terms of the cusp anomalous dimensions and the collinear anomalous dimensions. In this conjecture, the colour matrix structure of the soft anomalous dimension generated by soft gluons is simply a sum over two-body interactions between hard partons, and thus the matrix structure at any loop order is the same as at one loop. This result builds on the earlier work of refs. [47, 48] which showed the colour matrix structure of the soft anomalous dimension at two loops is identical to that at one loop. There may be additional colour correlations at three loops or beyond, which cannot be excluded at present [49]. However strong arguments for the absence of these terms are given in refs. [39]. If the all-order conjecture [39, 44] holds, the calculation of the pole parts of the form factors to a given loop order (and of the finite and subleading parts at fewer loops) would be sufficient to determine the infrared poles of all massless on-shell QCD amplitudes to this order.

The calculation of the three-loop form factors requires two principal ingredients: the algebraic reduction of all three-loop integrals appearing in the relevant Feynman diagrams to master integrals, and the analytical calculation of these master integrals. The reduction of integrals to master integrals exploits linear relations among different integrals, and is done based on a lexicographic ordering of the integrals (the Laporta algorithm [50]). Several dedicated computer-algebra implementations of the Laporta algorithm are available [50–53]. The reduction of the integrals relevant to the three-loop form factors is among the most challenging applications of the Laporta algorithm to date: due to the very large number of interconnected integrals to be reduced, the linear systems to be solved are often containing tens of thousand equations with a similar number of unknowns.

JHEP06(2010)094

The master integrals in the three-loop form factors were identified already several years ago [54]. Their analytical calculation proved to be a major computational challenge, which was completed only in several steps. The one-loop bubble insertions into two-loop vertex integrals as well as the two-loop bubble insertions into one-loop vertex integrals were derived using standard Feynman parameter integrals [54], while the genuine three-loop integrals required an extensive use of Mellin-Barnes integration techniques [55–57].

A first calculation of the three-loop form factors (based in part on numerical results for some of the expansion coefficients of the master integrals) was accomplished by Baikov et al. [58] in 2009. The analytical calculation of the last remaining master integrals was only completed recently [57]. It is the purpose of this paper to validate the three-loop form factor results of ref. [57, 58] by an independent calculation, and to extend them in in part to a higher order in the expansion in the dimensional regularization parameter $\epsilon = 2 - d/2$. These further expansion terms will be needed for an extraction of the quark and gluon collinear anomalous dimensions from the single pole pieces of the four-loop form factors.

We define the quark and gluon form factors in section 2, where we also discuss their UV-renomalization and summarize existing results at one- and two-loops. The reduction of the form factors to master integrals is described in section 3, and the three-loop master integrals are discussed in section 4. Explicit analytical expressions for them are collected in appendix A. Our results for the three-loop form factors are presented in section 5, and supplemented by appendix B. The infrared structure of the QCD form factors up to four-loops is analyzed in section 6. The three-loop hard matching coefficients for Drell-Yan and Higgs production in soft-collinear effective theory are determined from the form factors in section 7. An outlook on future applications is contained in section 8.

2 Quark and gluon form factors in perturbative QCD

The form factors are the basic vertex functions of an external off-shell current (with virtuality $q^2 = s_{12}$) coupling to a pair of partons with on-shell momenta p_1 and p_2. One distinguishes time-like ($s_{12} > 0$, i.e. with partons both either in the initial or in the final state) and space-like ($s_{12} < 0$, i.e. with one parton in the initial and one in the final state) configurations. The form factors are described in terms of scalar functions by contracting the respective vertex functions (evaluated in dimensional regularization with $d = 4 - 2\epsilon$ dimensions) with projectors. For massless partons, the full vertex function is described with only a single form factor.

The quark form factor is obtained from the photon-quark-antiquark vertex $\Gamma^{\mu}_{q\bar{q}}$ by

$$\mathcal{F}^q = -\frac{1}{4(1-\epsilon)q^2}\,\mathrm{Tr}\left(\not{p}_2\Gamma^{\mu}_{q\bar{q}}\not{p}_1\gamma_\mu\right)\,, \tag{2.1}$$

while the gluon form factor relates to the effective Higgs-gluon-gluon vertex $\Gamma^{\mu\nu}_{gg}$ as

$$\mathcal{F}^g = \frac{p_1\cdot p_2\, g_{\mu\nu} - p_{1,\mu}p_{2,\nu} - p_{1,\nu}p_{2,\mu}}{2(1-\epsilon)}\,\Gamma^{\mu\nu}_{gg}\,. \tag{2.2}$$

The form factors are expanded in perturbative QCD in powers of the coupling constant, with each power corresponding to a virtual loop. We denote the unrenormalized form factors by $\mathcal{F}^a$ and the renormalized form factors by F^a with $a = q, g$.

JHEP06(2010)094

At tree level, the Higgs boson does not couple either to the gluon or to massless quarks. In higher orders in perturbation theory, heavy quark loops introduce a coupling between the Higgs boson and gluons. In the limit of infinitely massive quarks, these loops give rise to an effective Lagrangian [59–62] mediating the coupling between the scalar Higgs field and the gluon field strength tensor:

$$\mathcal{L}_{\text{int}} = -\frac{\lambda}{4} H F_a^{\mu\nu} F_{a,\mu\nu} \ . \tag{2.3}$$

The coupling λ has inverse mass dimension. It can be computed by matching [63–65] the effective theory to the full standard model cross sections [5–9].

Evaluation of the Feynman diagrams, contributing to the vertex functions at a given loop order yields the bare (unrenormalised) form factors,

$$\mathcal{F}_b^q(\alpha_s^b, s_{12}) = 1 + \sum_{n=1}^{\infty} \left(\frac{\alpha_s^b}{4\pi}\right)^n \left(\frac{-s_{12}}{\mu_0^2}\right)^{-n\epsilon} S_\epsilon^n \, \mathcal{F}_n^q, \tag{2.4}$$

$$\mathcal{F}_b^g(\alpha_s^b, s_{12}) = \lambda^b \left(1 + \sum_{n=1}^{\infty} \left(\frac{\alpha_s^b}{4\pi}\right)^n \left(\frac{-s_{12}}{\mu_0^2}\right)^{-n\epsilon} S_\epsilon^n \, \mathcal{F}_n^g\right), \tag{2.5}$$

where μ_0^2 is the mass parameter introduced in dimensional regularisation to maintain a dimensionless coupling in the bare Lagrangian density and where

$$S_\epsilon = e^{-\epsilon\gamma}(4\pi)^\epsilon, \qquad \text{with the Euler constant } \gamma = 0.5772\ldots \tag{2.6}$$

The renormalization of the form factor is carried out by replacing the bare coupling α^b with the renormalized coupling $\alpha_s \equiv \alpha_s(\mu^2)$ evaluated at the renormalization scale μ^2

$$\alpha_s^b \mu_0^{2\epsilon} = Z_{\alpha_s} \mu^{2\epsilon} \alpha_s(\mu^2). \tag{2.7}$$

For simplicity we set $\mu^2 = |s_{12}|$ so that in the $\overline{\text{MS}}$ scheme [66],

$$\begin{aligned} Z_{\alpha_s} = S_\epsilon^{-1} \Bigg[& 1 - \frac{\beta_0}{\epsilon}\left(\frac{\alpha_s}{4\pi}\right) + \left(\frac{\beta_0^2}{\epsilon^2} - \frac{\beta_1}{2\epsilon}\right)\left(\frac{\alpha_s}{4\pi}\right)^2 \\ & - \left(\frac{\beta_0^3}{\epsilon^3} - \frac{7}{6}\frac{\beta_1\beta_0}{\epsilon^2} + \frac{1}{3}\frac{\beta_2}{\epsilon}\right)\left(\frac{\alpha_s}{4\pi}\right)^3 + \mathcal{O}(\alpha_s^4) \Bigg], \end{aligned} \tag{2.8}$$

where β_0, β_1 and β_2 are [67–73]

$$\beta_0 = \frac{11 C_A}{3} - \frac{2 N_F}{3}, \tag{2.9}$$

$$\beta_1 = \frac{34 C_A^2}{3} - \frac{10 C_A N_F}{3} - 2 C_F N_F, \tag{2.10}$$

$$\beta_2 = \frac{2857 C_A^3}{54} + C_F^2 N_F - \frac{205 C_F C_A N_F}{18} - \frac{1415 C_A^2 N_F}{54} + \frac{11 C_F N_F^2}{9} + \frac{79 C_A N_F^2}{54}. \tag{2.11}$$

The renormalization relation for the effective coupling λ^b in the $\overline{\text{MS}}$ scheme is given by,

$$\lambda^b = Z_\lambda \lambda \tag{2.12}$$

JHEP06(2010)094

with

$$Z_\lambda = 1 - \frac{\beta_0}{\epsilon}\left(\frac{\alpha_s}{4\pi}\right) + \left(\frac{\beta_0^2}{\epsilon^2} - \frac{\beta_1}{\epsilon}\right)\left(\frac{\alpha_s}{4\pi}\right)^2 - \left(\frac{\beta_0^3}{\epsilon^3} - \frac{2\beta_1\beta_0}{\epsilon^2} + \frac{\beta_2}{\epsilon}\right)\left(\frac{\alpha_s}{4\pi}\right)^3 + \mathcal{O}(\alpha_s^4)\,. \tag{2.13}$$

The i-loop contribution to the unrenormalized coefficients is $\mathcal{F}_i^a$, while the renormalised coefficient is denoted by F_i^a where $a = q, g$. If s_{12} is space-like, the form factors are real, while they acquire imaginary parts for time-like s_{12}. These imaginary parts (and corresponding real parts) arise from the ϵ-expansion of

$$\Delta(s_{12}) = (-\mathrm{sgn}(s_{12}) - i0)^{-\epsilon} \tag{2.14}$$

so that the renormalized form factors are given by,

$$F^q(\alpha_s(\mu^2), s_{12}, \mu^2 = |s_{12}|) = 1 + \sum_{n=1}^{\infty}\left(\frac{\alpha_s(\mu^2)}{4\pi}\right)^n F_n^q, \tag{2.15}$$

$$F^g(\alpha_s(\mu^2), s_{12}, \mu^2 = |s_{12}|) = \lambda\left(1 + \sum_{n=1}^{\infty}\left(\frac{\alpha_s(\mu^2)}{4\pi}\right)^n F_n^g\right). \tag{2.16}$$

Up to three loops, the renormalized coefficients for the quark form factor (with $\mu^2 = |s_{12}|$) are then obtained as,

$$\begin{aligned} F_1^q &= \mathcal{F}_1^q \Delta(s_{12}), \\ F_2^q &= \mathcal{F}_2^q \left(\Delta(s_{12})\right)^2 - \frac{\beta_0}{\epsilon}\mathcal{F}_1^q \Delta(s_{12}), \\ F_3^q &= \mathcal{F}_3^q \left(\Delta(s_{12})\right)^3 - \frac{2\beta_0}{\epsilon}\mathcal{F}_2^q \left(\Delta(s_{12})\right)^2 - \left(\frac{\beta_1}{2\epsilon} - \frac{\beta_0^2}{\epsilon^2}\right)\mathcal{F}_1^q \Delta(s_{12}), \end{aligned} \tag{2.17}$$

while those for the gluon form factor are given by,

$$\begin{aligned} F_1^g &= \mathcal{F}_1^g \Delta(s_{12}) - \frac{\beta_0}{\epsilon}, \\ F_2^g &= \mathcal{F}_2^g \left(\Delta(s_{12})\right)^2 - \frac{2\beta_0}{\epsilon}\mathcal{F}_1^g \Delta(s_{12}) - \left(\frac{\beta_1}{\epsilon} - \frac{\beta_0^2}{\epsilon^2}\right), \\ F_3^g &= \mathcal{F}_3^g \left(\Delta(s_{12})\right)^3 - \frac{3\beta_0}{\epsilon}\mathcal{F}_2^g \left(\Delta(s_{12})\right)^2 - \left(\frac{3\beta_1}{2\epsilon} - \frac{3\beta_0^2}{\epsilon^2}\right)\mathcal{F}_1^g \Delta(s_{12}) - \left(\frac{\beta_2}{\epsilon} - \frac{2\beta_1\beta_0}{\epsilon^2} + \frac{\beta_0^3}{\epsilon^3}\right). \end{aligned} \tag{2.18}$$

Unless explicitly stated otherwise, the renormalized form factors are given in the space-like case in the following sections.

The one-loop and two-loop form factors were computed in many places in the literature [31–37]. All-order expressions in terms of one-loop and two-loop master integrals are given in [37], and are summarized below.

JHEP06(2010)094

2.1 Results at one-loop

Written in terms of the one-loop bubble integral, which is normalized to the factor

$$S_\Gamma = \frac{(4\pi)^\epsilon}{16\pi^2\Gamma(1-\epsilon)}, \tag{2.19}$$

the unrenormalised one-loop form factors are given by

$$\mathcal{F}_1^q/S_R = \; C_F\, B_{2,1}\left(\frac{4}{(D-4)} + D - 3\right), \tag{2.20}$$

$$\mathcal{F}_1^g/S_R = \; C_A\, B_{2,1}\left(\frac{4}{(D-4)} - \frac{4}{(D-2)} + 10 - D\right), \tag{2.21}$$

where

$$S_R = \frac{16\pi^2 S_\Gamma}{S_\epsilon} = \frac{\exp(\epsilon\gamma)}{\Gamma(1-\epsilon)}. \tag{2.22}$$

Eqs. (2.20) and (2.21) agree with eqs. (8) and (9) of ref. [37] respectively.

Inserting the expansion of the one-loop master integrals and keeping terms through to $\mathcal{O}(\epsilon^5)$, we find that

$$\begin{aligned}\mathcal{F}_1^q = C_F\Bigg[& -\frac{2}{\epsilon^2} - \frac{3}{\epsilon} + (\zeta_2 - 8) + \epsilon\left(\frac{3\zeta_2}{2} + \frac{14\zeta_3}{3} - 16\right) + \epsilon^2\left(\frac{47\zeta_2^2}{20} + 4\zeta_2 + 7\zeta_3 - 32\right) \\ & + \epsilon^3\left(\frac{141\zeta_2^2}{40} - \frac{7\zeta_2\zeta_3}{3} + 8\zeta_2 + \frac{56\zeta_3}{3} + \frac{62\zeta_5}{5} - 64\right) \\ & + \epsilon^4\left(\frac{949\zeta_2^3}{280} + \frac{47\zeta_2^2}{5} - \frac{7\zeta_2\zeta_3}{2} - \frac{49\zeta_3^2}{9} + 16\zeta_2 + \frac{112\zeta_3}{3} + \frac{93\zeta_5}{5} - 128\right) \\ & + \epsilon^5\Bigg(\frac{2847\zeta_2^3}{560} + \frac{94\zeta_2^2}{5} - \frac{329\zeta_2^2\zeta_3}{60} - \frac{28\zeta_2\zeta_3}{3} - \frac{31\zeta_2\zeta_5}{5} - \frac{49\zeta_3^2}{6} \\ & \qquad + 32\zeta_2 + \frac{224\zeta_3}{3} + \frac{248\zeta_5}{5} + \frac{254\zeta_7}{7} - 256\Bigg)\Bigg],\end{aligned} \tag{2.23}$$

$$\begin{aligned}\mathcal{F}_1^g = C_A\Bigg[& -\frac{2}{\epsilon^2} + \zeta_2 + \epsilon\left(\frac{14\zeta_3}{3} - 2\right) + \epsilon^2\left(\frac{47\zeta_2^2}{20} - 6\right) \\ & + \epsilon^3\left(-\frac{7\zeta_2\zeta_3}{3} + \zeta_2 + \frac{62\zeta_5}{5} - 14\right) + \epsilon^4\left(\frac{949\zeta_2^3}{280} - \frac{49\zeta_3^2}{9} + 3\zeta_2 + \frac{14\zeta_3}{3} - 30\right) \\ & + \epsilon^5\left(\frac{47\zeta_2^2}{20} - \frac{329\zeta_2^2\zeta_3}{60} - \frac{31\zeta_2\zeta_5}{5} + 7\zeta_2 + 14\zeta_3 + \frac{254\zeta_7}{7} - 62\right)\Bigg]\end{aligned} \tag{2.24}$$

where the gluon form factor agrees with eq. (7) of ref. [32] through to $\mathcal{O}(\epsilon^4)$. Note that at each order in ϵ, the terms of highest harmonic weight are the same for both quark and gluon form-factor. This is guaranteed by the equivalence of the coefficient of the leading pole in eqs. (2.20) and (2.21).

JHEP06(2010)094

2.2 Results at two-loops

Written in terms of the two-loop master integrals (listed in the appendix), the unrenormalised two-loop gluon form factor is given by

$$
\begin{aligned}
\mathcal{F}_2^q/S_R^2 = C_F^2 \Bigg[& B_{4,2}\left(\frac{16}{(D-4)^2}+\frac{8}{(D-4)}+D^2-6D+17\right) \\
& -C_{4,1}\left(\frac{7D^2}{8}-\frac{983D}{48}-\frac{565}{32(2D-7)}-\frac{20}{9(3D-8)}-\frac{28}{(D-4)}\right. \\
& \qquad \left.-\frac{40}{(D-4)^2}+\frac{10693}{288}\right) \\
& +B_{3,1}\left(\frac{27D^2}{8}-\frac{1293D}{16}+\frac{3955}{32(2D-7)}-\frac{17}{2(D-3)}-\frac{476}{(D-4)}\right. \\
& \qquad \left.-\frac{456}{(D-4)^2}-\frac{288}{(D-4)^3}+\frac{581}{32}\right) \\
& -C_{6,2}\frac{D^3-20D^2+104D-176}{8(2D-7)}\Bigg] \\
& +C_F C_A\Bigg[-C_{4,1}\left(\frac{D^2}{16}+\frac{77D}{32}+\frac{565}{64(2D-7)}+\frac{12}{5(3D-8)}+\frac{23}{15(D-1)}\right. \\
& \qquad \left.+\frac{8}{3(D-4)}+\frac{16}{(D-4)^2}+\frac{163}{64}\right) \\
& -B_{3,1}\left(\frac{75D^2}{16}-\frac{1837D}{32}+\frac{3955}{64(2D-7)}+\frac{3}{4(D-3)}-\frac{186}{(D-4)}\right. \\
& \qquad \left.-\frac{144}{(D-4)^2}-\frac{96}{(D-4)^3}+\frac{3845}{64}\right) \\
& +C_{6,2}\frac{D^3-20D^2+104D-176}{16(2D-7)}\Bigg] \\
& +C_F N_F\left[-C_{4,1}\frac{(D-2)(3D^3-31D^2+110D-128)}{(3D-8)(D-4)(D-1)}\right]
\end{aligned}
\tag{2.25}
$$

$$
\begin{aligned}
\mathcal{F}_2^g/S_R^2 = C_A^2 \Bigg[& B_{4,2}\left(D^2-20D-\frac{48}{(D-2)}+\frac{32}{(D-4)}+\frac{16}{(D-2)^2}\right. \\
& \qquad \left.+\frac{16}{(D-4)^2}+100\right) \\
& +C_{4,1}\left(\frac{27D}{2}+\frac{119}{48(2D-5)}+\frac{75}{16(2D-7)}+\frac{10}{3(D-1)}+\frac{80}{(D-2)}\right. \\
& \qquad \left.+\frac{103}{3(D-4)}-\frac{32}{(D-2)^2}+\frac{24}{(D-4)^2}-\frac{609}{8}\right) \\
& +B_{3,1}\left(24D+\frac{107}{144(2D-5)}+\frac{525}{16(2D-7)}+\frac{116}{9(D-1)}+\frac{96}{(D-2)}\right. \\
& \qquad \left.-\frac{2}{(D-3)}-\frac{1175}{3(D-4)}-\frac{32}{(D-2)^2}-\frac{1388}{3(D-4)^2}-\frac{192}{(D-4)^3}-\frac{1955}{8}\right)
\end{aligned}
$$

JHEP06(2010)094

$$
\begin{aligned}
&+C_{6,2}\frac{3(3D-8)(D-3)}{4(2D-5)(2D-7)}\Bigg] \\
&+C_A N_F\Bigg[C_{4,1}\left(\frac{7D}{8}+\frac{119}{12(2D-5)}+\frac{35}{48(2D-7)}+\frac{20}{3(D-1)}-\frac{40}{3(D-2)}\right. \\
&\qquad\left.-\frac{2}{(D-4)}-\frac{45}{16}\right) \\
&-B_{3,1}\left(\frac{19D}{8}-\frac{107}{36(2D-5)}-\frac{245}{48(2D-7)}-\frac{232}{9(D-1)}+\frac{40}{3(D-2)}\right. \\
&\qquad\left.-\frac{3}{2(D-3)}+\frac{8}{9(D-4)}-\frac{8}{(D-4)^2}-\frac{61}{16}\right) \\
&+C_{6,2}\frac{(2D^3-25D^2+94D-112)(D-4)}{8(D-2)(2D-5)(2D-7)}\Bigg] \\
&\quad+C_F N_F\Bigg[-C_{4,1}\frac{(46D^4-545D^3+2395D^2-4606D+3248)(D-6)}{2(2D-7)(2D-5)(D-4)(D-2)} \\
&+B_{3,1}\left(\frac{35D}{4}-\frac{107}{18(2D-5)}-\frac{245}{24(2D-7)}+\frac{8}{3(D-2)}-\frac{1}{(D-3)}\right. \\
&\qquad\left.-\frac{448}{9(D-4)}-\frac{112}{3(D-4)^2}-\frac{333}{8}\right) \\
&-C_{6,2}\frac{(2D^3-25D^2+94D-112)(D-4)}{4(D-2)(2D-5)(2D-7)}\Bigg]
\end{aligned}
\tag{2.26}
$$

which, after re-expressing in terms of N and N_F agrees with eqs. (10) and (11) of ref. [37].

Inserting the expansion of the two-loop master integrals and keeping terms through to $\mathcal{O}(\epsilon^3)$, we find that

$$
\begin{aligned}
\mathcal{F}_2^q = C_F^2\Bigg[&\frac{2}{\epsilon^4}+\frac{6}{\epsilon^3}-\frac{1}{\epsilon^2}\left(2\zeta_2-\frac{41}{2}\right)-\frac{1}{\epsilon}\left(\frac{64\zeta_3}{3}-\frac{221}{4}\right) \\
&-\left(13\zeta_2^2-\frac{17\zeta_2}{2}+58\zeta_3-\frac{1151}{8}\right) \\
&-\epsilon\left(\frac{171\zeta_2^2}{5}-\frac{112\zeta_2\zeta_3}{3}-\frac{213\zeta_2}{4}+\frac{839\zeta_3}{3}+\frac{184\zeta_5}{5}-\frac{5741}{16}\right) \\
&+\epsilon^2\left(\frac{223\zeta_2^3}{5}-\frac{3401\zeta_2^2}{20}+54\zeta_2\zeta_3+\frac{2608\zeta_3^2}{9}+\frac{1839\zeta_2}{8}\right. \\
&\qquad\left.-\frac{6989\zeta_3}{6}-\frac{462\zeta_5}{5}+\frac{27911}{32}\right) \\
&+\epsilon^3\left(\frac{768\zeta_2^3}{7}+\frac{5488\zeta_2^2\zeta_3}{15}-\frac{29157\zeta_2^2}{40}+\frac{757\zeta_2\zeta_3}{3}+\frac{184\zeta_2\zeta_5}{5}+\frac{2434\zeta_3^2}{3}\right. \\
&\qquad\left.+\frac{13773\zeta_2}{16}-\frac{58283\zeta_3}{12}-\frac{3251\zeta_5}{5}+\frac{8942\zeta_7}{7}+\frac{133781}{64}\right)\Bigg] \\
&+C_F C_A\Bigg[-\frac{11}{6\epsilon^3}+\frac{1}{\epsilon^2}\left(\zeta_2-\frac{83}{9}\right)-\frac{1}{\epsilon}\left(\frac{11\zeta_2}{6}-13\zeta_3+\frac{4129}{108}\right)
\end{aligned}
$$

JHEP06(2010)094

$$
\begin{aligned}
&+\left(\frac{44\zeta_2^2}{5}-\frac{119\zeta_2}{9}+\frac{467\zeta_3}{9}-\frac{89173}{648}\right)\\
&+\epsilon\left(\frac{1891\zeta_2^2}{60}-\frac{89\zeta_2\zeta_3}{3}-\frac{6505\zeta_2}{108}+\frac{6586\zeta_3}{27}+51\zeta_5-\frac{1775893}{3888}\right)\\
&-\epsilon^2\left(\frac{809\zeta_2^3}{70}-\frac{2639\zeta_2^2}{18}+\frac{397\zeta_2\zeta_3}{9}+\frac{569\zeta_3^2}{3}+\frac{146197\zeta_2}{648}\right.\\
&\qquad\left.-\frac{159949\zeta_3}{162}-\frac{3491\zeta_5}{15}+\frac{33912061}{23328}\right)\\
&+\epsilon^3\left(\frac{3817\zeta_2^3}{140}-\frac{7103\zeta_2^2\zeta_3}{30}+\frac{638441\zeta_2^2}{1080}-\frac{4358\zeta_2\zeta_3}{27}-\frac{497\zeta_2\zeta_5}{5}-\frac{16439\zeta_3^2}{27}\right.\\
&\qquad\left.\left.-\frac{2996725\zeta_2}{3888}+\frac{3709777\zeta_3}{972}+\frac{49786\zeta_5}{45}-372\zeta_7-\frac{632412901}{139968}\right)\right]\\
&+C_FN_F\left[\frac{1}{3\epsilon^3}+\frac{14}{9\epsilon^2}+\frac{1}{\epsilon}\left(\frac{\zeta_2}{3}+\frac{353}{54}\right)+\left(\frac{14\zeta_2}{9}-\frac{26\zeta_3}{9}+\frac{7541}{324}\right)\right.\\
&-\epsilon\left(\frac{41\zeta_2^2}{30}-\frac{353\zeta_2}{54}+\frac{364\zeta_3}{27}-\frac{150125}{1944}\right)\\
&-\epsilon^2\left(\frac{287\zeta_2^2}{45}+\frac{26\zeta_2\zeta_3}{9}-\frac{7541\zeta_2}{324}+\frac{4589\zeta_3}{81}+\frac{242\zeta_5}{15}-\frac{2877653}{11664}\right)\\
&+\epsilon^3\left(-\frac{127\zeta_2^3}{14}-\frac{14473\zeta_2^2}{540}-\frac{364\zeta_2\zeta_3}{27}+\frac{338\zeta_3^2}{27}\right.\\
&\qquad\left.\left.+\frac{150125\zeta_2}{1944}-\frac{98033\zeta_3}{486}-\frac{3388\zeta_5}{45}+\frac{53933309}{69984}\right)\right],
\end{aligned}
\tag{2.27}
$$

which agrees through to $\mathcal{O}(\epsilon^2)$ with eq. (3.6) of ref. [31] and provides the next term in the expansion.

Similarly we find that the two-loop expansion of the gluon form factor is given by

$$
\begin{aligned}
\mathcal{F}_2^g = C_A^2\Bigg[&\frac{2}{\epsilon^4}-\frac{11}{6\epsilon^3}-\frac{1}{\epsilon^2}\left(\zeta_2+\frac{67}{18}\right)+\frac{1}{\epsilon}\left(\frac{11\zeta_2}{2}-\frac{25\zeta_3}{3}+\frac{68}{27}\right)\\
&-\left(\frac{21\zeta_2^2}{5}-\frac{67\zeta_2}{6}-\frac{11\zeta_3}{9}-\frac{5861}{162}\right)\\
&-\epsilon\left(\frac{77\zeta_2^2}{60}-\frac{23\zeta_2\zeta_3}{3}-\frac{106\zeta_2}{9}+\frac{1139\zeta_3}{27}-\frac{71\zeta_5}{5}-\frac{158201}{972}\right)\\
&+\epsilon^2\left(\frac{2313\zeta_2^3}{70}-\frac{1943\zeta_2^2}{60}-\frac{55\zeta_2\zeta_3}{3}+\frac{901\zeta_3^2}{9}+\frac{481\zeta_2}{54}\right.\\
&\qquad\left.-\frac{26218\zeta_3}{81}+\frac{341\zeta_5}{15}+\frac{3484193}{5832}\right)\\
&+\epsilon^3\left(\frac{2057\zeta_2^3}{60}+\frac{1291\zeta_2^2\zeta_3}{10}-\frac{28826\zeta_2^2}{135}+\frac{335\zeta_2\zeta_3}{9}-\frac{313\zeta_2\zeta_5}{5}+\frac{5137\zeta_3^2}{27}\right.\\
&\qquad\left.\left.-\frac{4019\zeta_2}{324}-\frac{397460\zeta_3}{243}-\frac{5963\zeta_5}{45}+\frac{6338\zeta_7}{7}+\frac{70647113}{34992}\right)\right]
\end{aligned}
$$

JHEP06(2010)094

$$
\begin{aligned}
&+C_A N_F \Bigg[\frac{1}{3\epsilon^3} + \frac{5}{9\epsilon^2} - \frac{1}{\epsilon}\left(\zeta_2 + \frac{26}{27}\right) - \left(\frac{5\zeta_2}{3} + \frac{74\zeta_3}{9} + \frac{808}{81}\right) \\
&\quad -\epsilon\left(\frac{51\zeta_2^2}{10} + \frac{16\zeta_2}{9} + \frac{604\zeta_3}{27} + \frac{23131}{486}\right) \\
&\quad -\epsilon^2\left(\frac{257\zeta_2^2}{18} - \frac{50\zeta_2\zeta_3}{3} - \frac{28\zeta_2}{27} + \frac{3962\zeta_3}{81} + \frac{542\zeta_5}{15} + \frac{540805}{2916}\right) \\
&\quad +\epsilon^3\Bigg(-\frac{253\zeta_2^3}{210} - \frac{103\zeta_2^2}{3} + \frac{380\zeta_2\zeta_3}{9} + \frac{2306\zeta_3^2}{27} \\
&\qquad +\frac{3157\zeta_2}{162} - \frac{30568\zeta_3}{243} - \frac{854\zeta_5}{9} - \frac{11511241}{17496}\Bigg)\Bigg] \\
&+C_F N_F \Bigg[-\frac{1}{\epsilon} + \left(8\zeta_3 - \frac{67}{6}\right) + \epsilon\left(+\frac{16\zeta_2^2}{3} + \frac{7\zeta_2}{3} + \frac{92\zeta_3}{3} - \frac{2027}{36}\right) \\
&\quad +\epsilon^2\left(\frac{184\zeta_2^2}{9} - \frac{40\zeta_2\zeta_3}{3} + \frac{209\zeta_2}{18} + \frac{1124\zeta_3}{9} + 32\zeta_5 - \frac{47491}{216}\right) \\
&\quad +\epsilon^3\Bigg(-\frac{176\zeta_2^3}{35} + \frac{22147\zeta_2^2}{270} - \frac{460\zeta_2\zeta_3}{9} - 120\zeta_3^2 \\
&\qquad +\frac{4273\zeta_2}{108} + \frac{15284\zeta_3}{27} + \frac{368\zeta_5}{3} - \frac{987995}{1296}\Bigg)\Bigg],
\end{aligned}
\tag{2.28}
$$

which agrees through to $\mathcal{O}(\epsilon^2)$ with eq. (8) of ref. [32] and provides the next term in the expansion. Expressions for the renormalized one-loop and two-loop form factors, expanded to the appropriate order in ϵ, can be found in [37].

3 Calculation of the three-loop form factors

To compute the three-loop quark and gluon form factors, we evaluate the relevant three-loop vertex functions within dimensional regularisation. At this loop order, there are 244 Feynman diagrams contributing to the quark form factor, and 1586 diagrams contributing to the gluon form factor. We generated these diagrams using QGRAF [74]. After contraction with the projectors (2.1)–(2.2), each diagram can be expressed as a linear combination of (typically hundreds of) scalar three-loop Feynman integrals. The three-loop integrals appearing in the form factors have up to nine different propagators. The integrands can depend on the three loop momenta, and the two on-shell external momenta, such that 12 different scalar products involving loop momenta can be formed. Consequently, not all scalar products can be cancelled against combinations of denominators, and we are left with irreducible scalar products in the numerator of the integrand. We denote the number of different propagators in an integral by t, the total number of propagators by r and the total number of irreducible scalar products by s. The topology of each integral is fixed by specifying the set of t different propagators and subtopologies are obtained by removing one or more of the propagators.

JHEP06(2010)094

AuxTopo 1	AuxTopo 2	AuxTopo3
k_1^2	k_1^2	k_1^2
k_2^2	k_2^2	k_2^2
k_3^2	k_3^2	k_3^2
$(k_1-k_2)^2$	$(k_1-k_2)^2$	$(k_1-k_2)^2$
$(k_1-k_3)^2$	$(k_1-k_3)^2$	$(k_1-k_3)^2$
$(k_2-k_3)^2$	$(k_2-k_3)^2$	$(k_1-k_2-k_3)^2$
$(k_1-p_1)^2$	$(k_1-k_3-p_2)^2$	$(k_1-p_1)^2$
$(k_1-p_1-p_2)^2$	$(k_1-p_1-p_2)^2$	$(k_1-p_1-p_2)^2$
$(k_2-p_1)^2$	$(k_2-p_1)^2$	$(k_2-p_1)^2$
$(k_2-p_1-p_2)^2$	$(k_1-k_2-p_2)^2$	$(k_2-p_1-p_2)^2$
$(k_3-p_1)^2$	$(k_3-p_1)^2$	$(k_3-p_1)^2$
$(k_3-p_1-p_2)^2$	$(k_3-p_1-p_2)^2$	$(k_3-p_1-p_2)^2$

Table 1. Propagators in the three different auxiliary topologies used to represent all three-loop form factor integrals.

Using relations between different integrals based on integration-by-parts (IBP) [75] and Lorentz invariance (LI) [76], one can express the large number of different integrals in terms of a small number of so-called master integrals. These identities yield large linear systems of equations, which are solved in an iterative manner using lexicographic ordering [50]. To carry out the reduction in a systematic manner, we introduce so-called auxiliary topologies. Each auxiliary topology is a set of 12 linearly independent propagators. Within the auxiliary topology, the integrand of a three-loop form factor integral with (r, s, t) is expressed by r propagators (with exactly t different propagators) in the denominator, and s propagators (with at most 12-t different propagators) in the numerator. All three-loop form factor integrals can be cast into one of three auxiliary topologies, which are listed in table 1. The first auxiliary topology contains planar integrals only.

Three-loop integrals with $4 \leq t \leq 9$ and $t \leq r \leq 9$ appear in the form factors. These come with up to $s = 4$ irreducible scalar products for the quark form factor and up to $s = 5$ for the gluon form factor. For a fixed topology and given (r, s, t), there are in total

$$N_{r,s,t} = \binom{r-1}{t-1}\binom{11-t+s}{s}$$

different integrals.

To obtain a reduction, one has to solve very large systems of equations. Already for $s \leq 4$, the system for a given auxiliary topology contains 900000 equations, and its solution is feasible only with dedicated computer algebra tools. For this reduction, we used the Mathematica-based package FIRE [52] and the C++ package Reduze [53], which was developed most recently by one of us.

With Reduze, the reduction and its performance are as follows. The topologies with more than 4 propagators are reduced after inserting the results of the sub-topologies into the system. With increasing t the number of equations decrease as (in general) does the

JHEP06(2010)094

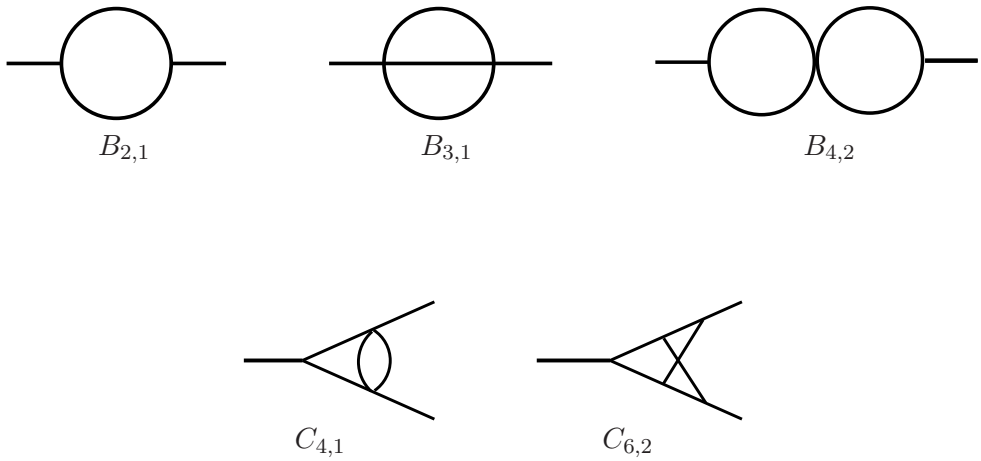

Figure 1. One and two-loop master integrals appearing in the quark and gluon form factors.

time taken to solve the system which is in the range of a few days to less than an hour with the program Reduze on a modern desktop computer. The total computing time for all the planar diagrams is more than 2 months. However, the parallelization of topologies with an equal number of propagators reduced the overall reduction time to a few weeks.

The three-loop form factors contain in total 22 master integrals, of which 14 are genuine three-loop vertex functions, 4 are three-loop propagator integrals and 4 are products of one-loop and two-loop integrals. They are described in detail in the following section.

4 Three-loop form factor master integrals

Our notation for the master integrals follows [54], and we distinguish three topological types of master integrals: genuine three-loop triangles ($A_{t,i}$-type), bubble integrals ($B_{t,i}$-type) and integrals that contain two-loop triangles ($C_{t,i}$-type). In this notation, the index t denotes the number of propagators, and i is simply enumerating the topologically different integrals with the same number of propagators.

The one-loop and two-loop master integrals appearing in the form factors at these loop orders are displayed in figure 1. Their expansions to finite order have been known for a long time, all-orders expressions were derived in [37], they can for example be expanded using HypExp [77]. $B_{t,i}$-type and $C_{t,i}$-type three-loop integrals are listed in figure 2. The $B_{t,i}$-type integrals were computed to finite order in [75, 78, 79], and supplemented by the higher order terms in [80]. Finally, the genuine three-loop vertex integrals are shown in figure 3, their expansions to finite order were derived in [54–57].

The calculation of the nine-line three-loop integrals was the last missing ingredient to the form factor calculation for a long time. The full result for $A_{9,1}$ and most of the pole parts of $A_{9,2}$ and $A_{9,4}$ were computed analytically in [56]. Analytical expressions for the remaining pieces of the latter two integrals were subsequently obtained in [57]. In [56], it was pointed out that for each of these three integrals one can find an integral from the same topology with an irreducible scalar product, which has homogeneous transcendentality.

JHEP06(2010)094

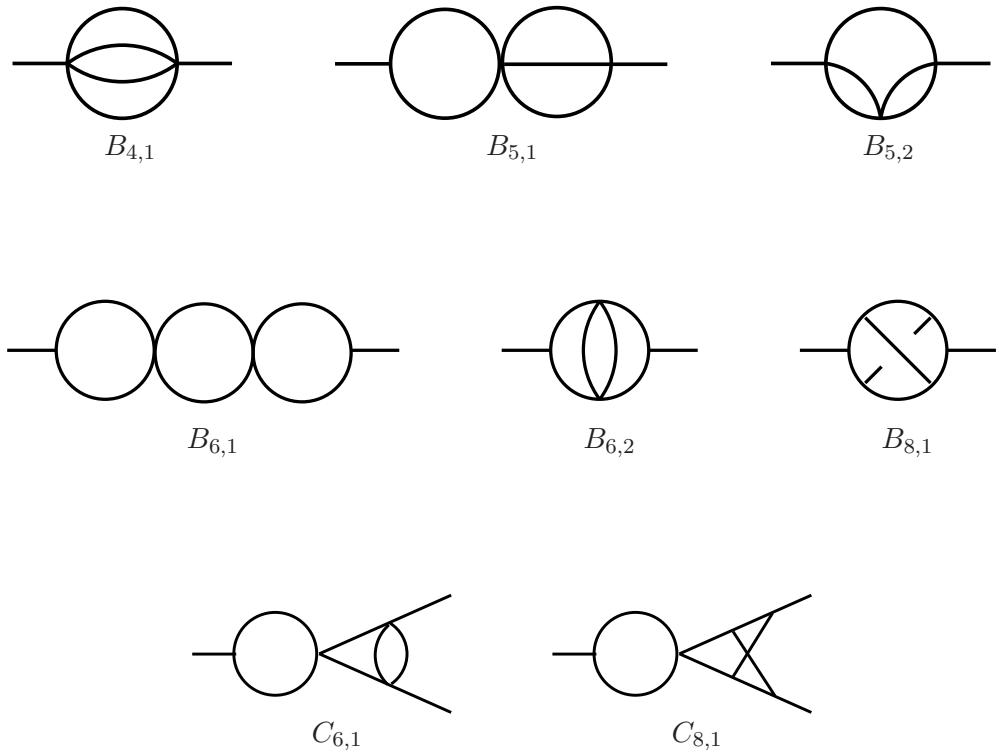

Figure 2. Three-loop two-point and factorizable three-point integrals.

JHEP06(2010)094

These integrals were named $A_{9,1n}$, $A_{9,2n}$ and $A_{9,4n}$, and are defined in [56]. Compared to [56] we increased the numerical precision of the remaining coefficients, both for $A_{9,2}$ and $A_{9,4}$, by means of conventional packages like `MB.m` [81]. We reproduce thirteen significant digits of the analytic result of [57] in the case of $A_{9,2}$, and fourteen in the case of $A_{9,4}$. We also converted our numerical results for these two integrals into the corresponding integrals of homogeneous transcendentality, $A_{9,2n}$ and $A_{9,4n}$. On the coefficients of these integrals, a PSLQ [82] determination was attempted. For the pole coefficients, the PSLQ algorithm converged to a unique solution in agreement with [57]. For the finite coefficients, the numerical precision that we obtained is yet insufficient for PSLQ to yield a unique solution.

An analytic result for $A_{9,2}$ and $A_{9,4}$, derived by purely analytic steps and without fitting rational coefficients to numerical values, is still a desirable task, and remains to be investigated in the future. This goal is definitely within reach in the case of $A_{9,4}$, whereas the situation is less clear for $A_{9,2}$.

Expansions of all master integrals to the order in ϵ where transcendentality six first appears are listed in the appendix.

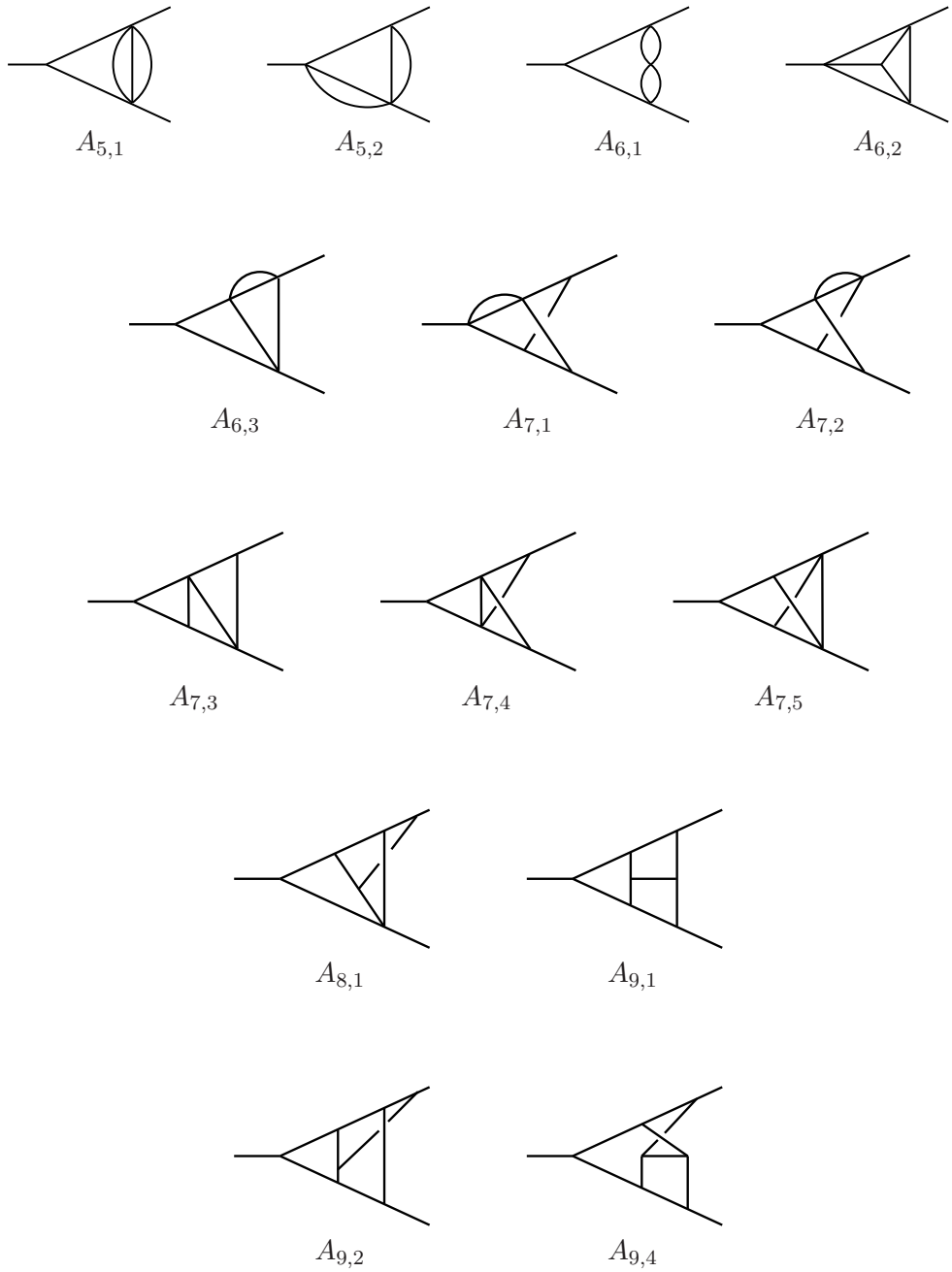

Figure 3. Three-point integrals listed in refs. [54–56].

JHEP06(2010)094

5 Three-loop form factors

The unrenormalised three-loop form factors can be decomposed into different colour structures as follows:

$$\mathcal{F}_3^q/S_R^3 = C_F^3\ X^q_{C_F^3} + C_F^2 C_A\ X^q_{C_F^2 C_A} + C_F C_A^2\ X^q_{C_F C_A^2} + C_F^2 N_F\ X^q_{C_F^2 N_F} + C_F C_A N_F\ X^q_{C_F C_A N_F} + C_F N_F^2\ X^q_{C_F N_F^2} + C_F N_{F,V} \left(\frac{N^2-4}{N}\right)\ X^q_{C_F N_{F,V}} \tag{5.1}$$

and

$$\mathcal{F}_3^g/S_R^3 = C_A^3\ X^g_{C_A^3} + C_A^2 N_F\ X^g_{C_A^2 N_F} + C_A C_F N_F\ X^g_{C_A C_F N_F} + C_F^2 N_F\ X^g_{C_F^2 N_F} + C_A N_F^2\ X^g_{C_A N_F^2} + C_F N_F^2\ X^g_{C_F N_F^2}\ , \tag{5.2}$$

where the last term in the quark form factor is generated by graphs where the virtual gauge boson does not couple directly to the final-state quarks. This contribution is denoted by $N_{F,V}$ and is proportional to the charge weighted sum of the quark flavours. In the case of purely electromagnetic interactions, we find,

$$N_{F,\gamma} = \frac{\sum_q e_q}{e_q}. \tag{5.3}$$

The coefficient of each colour structure is a linear combination of master integrals, resulting from the reduction of the integrals appearing in the Feynman diagrams. All coefficients are listed in appendix B.

Inserting the expansion of the three-loop master integrals and keeping terms through to $\mathcal{O}(\epsilon^0)$, we find that the three-loop coefficients are given by

$$\begin{aligned}
\mathcal{F}_3^q = C_F^3 \Bigg[& -\frac{4}{3\epsilon^6} - \frac{6}{\epsilon^5} + \frac{1}{\epsilon^4}(2\zeta_2 - 25) + \frac{1}{\epsilon^3}\left(-3\zeta_2 + \frac{100\zeta_3}{3} - 83\right) \\
& + \frac{1}{\epsilon^2}\left(\frac{213\zeta_2^2}{10} - \frac{77\zeta_2}{2} + 138\zeta_3 - \frac{515}{2}\right) \\
& + \frac{1}{\epsilon}\left(\frac{1461\zeta_2^2}{20} - \frac{214\zeta_2\zeta_3}{3} - \frac{467\zeta_2}{2} + \frac{2119\zeta_3}{3} + \frac{644\zeta_5}{5} - \frac{9073}{12}\right) \\
& + \Bigg(-\frac{53675}{24} - \frac{13001\zeta_2}{12} + \frac{12743\zeta_2^2}{40} - \frac{9095\zeta_2^3}{252} + 2669\zeta_3 + 61\zeta_3\zeta_2 \\
& \quad - \frac{1826\zeta_3^2}{3} + \frac{4238\zeta_5}{5}\Bigg)\Bigg] \\
+ C_F^2 C_A \Bigg[& \frac{11}{3\epsilon^5} + \frac{1}{\epsilon^4}\left(-2\zeta_2 + \frac{431}{18}\right) + \frac{1}{\epsilon^3}\left(-\frac{7\zeta_2}{6} - 26\zeta_3 + \frac{6415}{54}\right) \\
& + \frac{1}{\epsilon^2}\left(-\frac{83\zeta_2^2}{5} + \frac{1487\zeta_2}{36} - 210\zeta_3 + \frac{79277}{162}\right) \\
& + \frac{1}{\epsilon}\left(-\frac{9839\zeta_2^2}{72} + \frac{215\zeta_2\zeta_3}{3} + \frac{38623\zeta_2}{108} - \frac{6703\zeta_3}{6} - 142\zeta_5 + \frac{1773839}{972}\right)
\end{aligned}$$

JHEP06(2010)094

$$
\begin{aligned}
&+\left(\frac{37684115}{5832}+\frac{664325\zeta_2}{324}-\frac{1265467\zeta_2^2}{2160}-\frac{18619\zeta_2^3}{1260}\right.\\
&\qquad\left.-\frac{96715\zeta_3}{18}+\frac{46\zeta_2\zeta_3}{9}+\frac{1616\zeta_3^2}{3}-\frac{46594\zeta_5}{45}\right)\Bigg]\\
&+C_F C_A^2\left[-\frac{242}{81\epsilon^4}+\frac{1}{\epsilon^3}\left(\frac{88\zeta_2}{27}-\frac{6521}{243}\right)+\frac{1}{\epsilon^2}\left(-\frac{88\zeta_2^2}{45}-\frac{553\zeta_2}{81}+\frac{1672\zeta_3}{27}-\frac{40289}{243}\right)\right.\\
&\quad+\frac{1}{\epsilon}\left(\frac{802\zeta_2^2}{15}-\frac{88\zeta_2\zeta_3}{9}-\frac{68497\zeta_2}{486}+\frac{12106\zeta_3}{27}-\frac{136\zeta_5}{3}-\frac{1870564}{2187}\right)\\
&\quad+\left(-\frac{52268375}{13122}-\frac{767320\zeta_2}{729}+\frac{152059\zeta_2^2}{540}-\frac{6152\zeta_2^3}{189}\right.\\
&\qquad\left.\left.+\frac{1341553\zeta_3}{486}-\frac{710\zeta_2\zeta_3}{9}-\frac{1136\zeta_3^2}{9}+\frac{2932\zeta_5}{9}\right)\right]\\
&+C_F^2 N_F\left[-\frac{2}{3\epsilon^5}-\frac{37}{9\epsilon^4}+\frac{1}{\epsilon^3}\left(-\frac{\zeta_2}{3}-\frac{545}{27}\right)+\frac{1}{\epsilon^2}\left(-\frac{133\zeta_2}{18}+\frac{146\zeta_3}{9}-\frac{6499}{81}\right)\right.\\
&\quad+\frac{1}{\epsilon}\left(\frac{337\zeta_2^2}{36}-\frac{2849\zeta_2}{54}+\frac{2557\zeta_3}{27}-\frac{138865}{486}\right)\\
&\quad\left.+\left(\frac{8149\zeta_2^2}{216}-\frac{343\zeta_2\zeta_3}{9}-\frac{45235\zeta_2}{162}+\frac{51005\zeta_3}{81}+\frac{278\zeta_5}{45}-\frac{2732173}{2916}\right)\right]\\
&+C_F C_A N_F\left[\frac{88}{81\epsilon^4}+\frac{1}{\epsilon^3}\left(-\frac{16\zeta_2}{27}+\frac{2254}{243}\right)+\frac{1}{\epsilon^2}\left(\frac{316\zeta_2}{81}-\frac{256\zeta_3}{27}+\frac{13679}{243}\right)\right.\\
&\quad+\frac{1}{\epsilon}\left(-\frac{44\zeta_2^2}{5}+\frac{11027\zeta_2}{243}-\frac{6436\zeta_3}{81}+\frac{623987}{2187}\right)\\
&\quad\left.+\left(-\frac{1093\zeta_2^2}{27}+\frac{368\zeta_2\zeta_3}{9}+\frac{442961\zeta_2}{1458}-\frac{45074\zeta_3}{81}-\frac{208\zeta_5}{3}+\frac{8560052}{6561}\right)\right]\\
&+C_F N_F^2\left[-\frac{8}{81\epsilon^4}-\frac{188}{243\epsilon^3}+\frac{1}{\epsilon^2}\left(-\frac{4\zeta_2}{9}-\frac{124}{27}\right)+\frac{1}{\epsilon}\left(-\frac{94\zeta_2}{27}+\frac{136\zeta_3}{81}-\frac{49900}{2187}\right)\right.\\
&\quad\left.+\left(-\frac{83\zeta_2^2}{135}-\frac{62\zeta_2}{3}+\frac{3196\zeta_3}{243}-\frac{677716}{6561}\right)\right]\\
&+C_F N_{F,V}\left(\frac{N^2-4}{N}\right)\left[4-\frac{2\zeta_2^2}{5}+10\zeta_2+\frac{14\zeta_3}{3}-\frac{80\zeta_5}{3}\right]. \qquad (5.4)
\end{aligned}
$$

The pole contributions of $\mathcal{F}_3^q$ are given in eq. (3.7) of ref. [31] while the finite parts of the N_F^2, $C_A N_F$ and $C_F N_F$ contributions are given in eq. (6) of ref. [32]. The finite $N_{F,V}$ contribution can be obtained from the $\delta(1-x)$ contribution to the $d^{abc}d_{abc}$ colour factor in eq. (6.6) of ref. [83]. The remaining finite contributions are given in eqs. (8) and (9) of ref. [58].

JHEP06(2010)094

Similarly, the expansion of the gluon form factor at three-loops is given by

$$
\begin{aligned}
\mathcal{F}_3^g = C_A^3 \Bigg[& -\frac{4}{3\epsilon^6} + \frac{11}{3\epsilon^5} + \frac{361}{81\epsilon^4} + \frac{1}{\epsilon^3}\left(-\frac{517\zeta_2}{54} + \frac{22\zeta_3}{3} - \frac{3506}{243}\right) \\
& + \frac{1}{\epsilon^2}\left(\frac{247\zeta_2^2}{90} + \frac{481\zeta_2}{162} - \frac{209\zeta_3}{27} - \frac{17741}{243}\right) \\
& + \frac{1}{\epsilon}\left(-\frac{3751\zeta_2^2}{360} - \frac{85\zeta_2\zeta_3}{9} + \frac{20329\zeta_2}{243} + \frac{241\zeta_3}{9} - \frac{878\zeta_5}{15} - \frac{145219}{2187}\right) \\
& + \Bigg(\frac{14474131}{13122} + \frac{307057\zeta_2}{1458} + \frac{8459\zeta_2^2}{1080} - \frac{22523\zeta_2^3}{270} \\
& \quad - \frac{68590\zeta_3}{243} + \frac{77\zeta_2\zeta_3}{18} - \frac{1766\zeta_3^2}{9} + \frac{20911\zeta_5}{45}\Bigg)\Bigg] \\
+ C_A^2 N_F \Bigg[& -\frac{2}{3\epsilon^5} - \frac{2}{81\epsilon^4} + \frac{1}{\epsilon^3}\left(\frac{47\zeta_2}{27} + \frac{1534}{243}\right) + \frac{1}{\epsilon^2}\left(-\frac{425\zeta_2}{81} + \frac{518\zeta_3}{27} + \frac{4280}{243}\right) \\
& + \frac{1}{\epsilon}\left(\frac{2453\zeta_2^2}{180} - \frac{7561\zeta_2}{243} + \frac{1022\zeta_3}{81} - \frac{92449}{2187}\right) \\
& + \left(\frac{437\zeta_2^2}{60} - \frac{439\zeta_2\zeta_3}{9} - \frac{37868\zeta_2}{729} - \frac{754\zeta_3}{27} + \frac{3238\zeta_5}{45} - \frac{10021313}{13122}\right)\Bigg] \\
+ C_A C_F N_F \Bigg[& \frac{20}{9\epsilon^3} + \frac{1}{\epsilon^2}\left(-\frac{160\zeta_3}{9} + \frac{526}{27}\right) + \frac{1}{\epsilon}\left(-\frac{176\zeta_2^2}{15} - \frac{22\zeta_2}{3} - \frac{224\zeta_3}{27} + \frac{2783}{81}\right) \\
& + \left(-\frac{16\zeta_2^2}{5} + 48\zeta_2\zeta_3 - \frac{41\zeta_2}{3} + \frac{11792\zeta_3}{81} + \frac{32\zeta_5}{9} - \frac{155629}{486}\right)\Bigg] \\
+ C_F^2 N_F \Bigg[& \frac{2}{3\epsilon} + \left(\frac{296\zeta_3}{3} - 160\zeta_5 + \frac{304}{9}\right)\Bigg] \\
+ C_A N_F^2 \Bigg[& -\frac{8}{81\epsilon^4} - \frac{80}{243\epsilon^3} + \frac{1}{\epsilon^2}\left(\frac{20\zeta_2}{27} + \frac{8}{9}\right) + \frac{1}{\epsilon}\left(\frac{200\zeta_2}{81} + \frac{664\zeta_3}{81} + \frac{34097}{2187}\right) \\
& + \left(\frac{797\zeta_2^2}{135} + \frac{76\zeta_2}{27} + \frac{11824\zeta_3}{243} + \frac{1479109}{13122}\right)\Bigg] \\
+ C_F N_F^2 \Bigg[& \frac{8}{9\epsilon^2} + \frac{1}{\epsilon}\left(-\frac{32\zeta_3}{3} + \frac{424}{27}\right) + \left(-\frac{112\zeta_2^2}{15} - \frac{16\zeta_2}{3} - \frac{704\zeta_3}{9} + \frac{10562}{81}\right)\Bigg] . \qquad (5.5)
\end{aligned}
$$

The divergent parts agree with eq. (8) of ref. [32] while the finite contributions agree with eq. (10) of ref. [58].

Using our knowledge of the three-loop form factors, we can also write down the $\mathcal{O}(\epsilon)$ contributions to the N_F parts of the quark and gluon form factors. For the quark form-factor we find that,

$$
\mathcal{F}_3^q|_{N_F} = C_F N_F^2 \epsilon \left(-\frac{2913928}{6561} + \frac{2248}{135}\zeta_5 + \frac{2108}{27}\zeta_3 - \frac{24950}{243}\zeta_2 + \frac{68}{9}\zeta_2\zeta_3 - \frac{3901}{810}\zeta_2^2\right)
$$

JHEP06(2010)094

$$
\begin{aligned}
&+C_F C_A N_F \epsilon \left(\frac{24570881}{4374} - \frac{28156}{45}\zeta_5 - \frac{2418896}{729}\zeta_3 + \frac{10816}{27}\zeta_3^2 + \frac{7137385}{4374}\zeta_2 \right. \\
&\qquad \left. + \frac{2674}{27}\zeta_2\zeta_3 - \frac{352559}{1620}\zeta_2^2 + \frac{17324}{945}\zeta_2^3 \right) \\
&+C_F^2 N_F \epsilon \left(-\frac{50187205}{17496} + \frac{5863}{135}\zeta_5 + \frac{929587}{243}\zeta_3 - \frac{5771}{9}\zeta_3^2 - \frac{1263505}{972}\zeta_2 \right. \\
&\qquad \left. - \frac{8515}{54}\zeta_2\zeta_3 + \frac{821749}{3240}\zeta_2^2 - \frac{875381}{7560}\zeta_2^3 \right) \\
&+C_F N_{F,V} \left(\frac{N^2-4}{N} \right) \epsilon \left(\frac{170}{3} + \frac{752}{9}\zeta_5 + \frac{94}{9}\zeta_3 - \frac{344}{3}\zeta_3^2 + \frac{260}{3}\zeta_2 \right. \\
&\qquad \left. + 30\zeta_2\zeta_3 - \frac{196}{15}\zeta_2^2 - \frac{9728}{315}\zeta_2^3 \right) ,
\end{aligned}
\tag{5.6}
$$

and for the gluon form factor

$$
\begin{aligned}
\mathcal{F}_3^g|_{N_F} = \; & C_A N_F^2 \epsilon \left(\frac{16823771}{26244} + \frac{9368}{135}\zeta_5 + \frac{5440}{27}\zeta_3 - \frac{30283}{1458}\zeta_2 - \frac{988}{27}\zeta_2\zeta_3 + \frac{14018}{405}\zeta_2^2 \right) \\
&+C_A^2 N_F \epsilon \left(-\frac{48658741}{8748} - \frac{10066}{45}\zeta_5 + \frac{349918}{729}\zeta_3 - \frac{11657}{27}\zeta_3^2 + \frac{904045}{4374}\zeta_2 \right. \\
&\qquad \left. + \frac{791}{9}\zeta_2\zeta_3 - \frac{34931}{1620}\zeta_2^2 - \frac{52283}{1080}\zeta_2^3 \right) \\
&+C_F N_F^2 \epsilon \left(\frac{196900}{243} - \frac{800}{9}\zeta_5 - \frac{4208}{9}\zeta_3 - 54\zeta_2 + \frac{112}{3}\zeta_2\zeta_3 - \frac{2464}{45}\zeta_2^2 \right) \\
&+C_F C_A N_F \epsilon \left(-\frac{10508593}{2916} + \frac{17092}{27}\zeta_5 + \frac{240934}{243}\zeta_3 + \frac{4064}{9}\zeta_3^2 + \frac{8869}{54}\zeta_2 \right. \\
&\qquad \left. + \frac{640}{9}\zeta_2\zeta_3 + \frac{28823}{270}\zeta_2^2 + \frac{23624}{315}\zeta_2^3 \right) \\
&+C_F^2 N_F \epsilon \left(\frac{18613}{54} - \frac{3080}{3}\zeta_5 + \frac{10552}{9}\zeta_3 - 272\zeta_3^2 - \frac{74}{3}\zeta_2 \right. \\
&\qquad \left. - 16\zeta_2\zeta_3 + \frac{328}{5}\zeta_2^2 - \frac{35648}{315}\zeta_2^3 \right)
\end{aligned}
\tag{5.7}
$$

The UV-renormalization of the form factors is derived in section 2 above. Applying (2.17) and (2.19) yields the expansion coefficients of the renormalized form factors. These are in the space-like kinematics:

$$
F_3^q = C_F^3 \left[-\frac{4}{3\epsilon^6} - \frac{6}{\epsilon^5} + \frac{1}{\epsilon^4}\left(2\zeta_2 - 25\right) - \frac{1}{\epsilon^3}\left(3\zeta_2 - \frac{100\zeta_3}{3} + 83\right) \right.
$$

JHEP06(2010)094

$$
\begin{aligned}
&+\frac{1}{\epsilon^2}\left(\frac{213\zeta_2^2}{10}-\frac{77\zeta_2}{2}+138\zeta_3-\frac{515}{2}\right)\\
&+\frac{1}{\epsilon}\left(\frac{1461\zeta_2^2}{20}-\frac{214\zeta_2\zeta_3}{3}-\frac{467\zeta_2}{2}+\frac{2119\zeta_3}{3}+\frac{644\zeta_5}{5}-\frac{9073}{12}\right)\\
&+\left(-\frac{53675}{24}-\frac{13001\zeta_2}{12}+\frac{12743\zeta_2^2}{40}-\frac{9095\zeta_2^3}{252}+2669\zeta_3+61\zeta_3\zeta_2\right.\\
&\qquad\left.-\frac{1826\zeta_3^2}{3}+\frac{4238\zeta_5}{5}\right)\Bigg]\\
&+C_F^2C_A\left[-\frac{11}{\epsilon^5}-\frac{1}{\epsilon^4}\left(\frac{361}{18}+2\zeta_2\right)+\frac{1}{\epsilon^3}\left(-\frac{1703}{54}-26\zeta_3+\frac{27\zeta_2}{2}\right)\right.\\
&+\frac{1}{\epsilon^2}\left(\frac{6820}{81}-\frac{482\zeta_3}{9}+\frac{1487\zeta_2}{36}-\frac{83\zeta_2^2}{5}\right)\\
&+\frac{1}{\epsilon}\left(\frac{374149}{486}-142\zeta_5+\frac{215\zeta_3\zeta_2}{3}-\frac{4151\zeta_3}{6}+\frac{31891\zeta_2}{108}-\frac{2975\zeta_2^2}{72}\right)\\
&+\left(\frac{11169211}{2916}-\frac{6890\zeta_5}{9}-\frac{806\zeta_3\zeta_2}{3}-\frac{19933\zeta_3}{6}\right.\\
&\qquad\left.\left.+\frac{1616\zeta_3^2}{3}+\frac{537803\zeta_2}{324}-\frac{723739\zeta_2^2}{2160}-\frac{18619\zeta_2^3}{1260}\right)\right]\\
&+C_FC_A^2\left[-\frac{1331}{81\epsilon^4}+\frac{1}{\epsilon^3}\left(\frac{2866}{243}-\frac{110\zeta_2}{27}\right)+\frac{1}{\epsilon^2}\left(\frac{11669}{486}-\frac{902\zeta_3}{27}+\frac{1625\zeta_2}{81}-\frac{88\zeta_2^2}{45}\right)\right.\\
&+\frac{1}{\epsilon}\left(-\frac{139345}{8748}-\frac{136\zeta_5}{3}-\frac{88\zeta_3\zeta_2}{9}+\frac{3526\zeta_3}{27}-\frac{7163\zeta_2}{243}-\frac{166\zeta_2^2}{15}\right)\\
&+\left(-\frac{51082685}{52488}-\frac{434\zeta_5}{9}+\frac{416\zeta_3\zeta_2}{3}+\frac{505087\zeta_3}{486}\right.\\
&\qquad\left.\left.-\frac{1136\zeta_3^2}{9}-\frac{412315\zeta_2}{729}+\frac{22157\zeta_2^2}{270}-\frac{6152\zeta_2^3}{189}\right)\right]\\
&+C_F^2N_F\left[\frac{2}{\epsilon^5}+\frac{35}{9\epsilon^4}+\frac{1}{\epsilon^3}\left(\frac{139}{27}-3\zeta_2\right)+\frac{1}{\epsilon^2}\left(-\frac{775}{81}-\frac{110\zeta_3}{9}-\frac{133\zeta_2}{18}\right)\right.\\
&+\frac{1}{\epsilon}\left(-\frac{24761}{243}+\frac{469\zeta_3}{27}-\frac{2183\zeta_2}{54}-\frac{287\zeta_2^2}{36}\right)\\
&\left.+\left(-\frac{691883}{1458}-\frac{386\zeta_5}{9}+\frac{35\zeta_3\zeta_2}{3}+\frac{21179\zeta_3}{81}-\frac{16745\zeta_2}{81}-\frac{8503\zeta_2^2}{1080}\right)\right]\\
&+C_FC_AN_F\left[\frac{484}{81\epsilon^4}+\frac{1}{\epsilon^3}\left(-\frac{752}{243}+\frac{20\zeta_2}{27}\right)+\frac{1}{\epsilon^2}\left(-\frac{2068}{243}+\frac{212\zeta_3}{27}-\frac{476\zeta_2}{81}\right)\right.\\
&+\frac{1}{\epsilon}\left(-\frac{8659}{2187}-\frac{964\zeta_3}{81}+\frac{2594\zeta_2}{243}+\frac{44\zeta_2^2}{15}\right)\\
&\left.+\left(\frac{1700171}{6561}-\frac{4\zeta_5}{3}+\frac{4\zeta_3\zeta_2}{3}-\frac{4288\zeta_3}{27}+\frac{115555\zeta_2}{729}+\frac{2\zeta_2^2}{27}\right)\right]
\end{aligned}
$$

JHEP06(2010)094

$$
\begin{aligned}
&+C_F N_F^2\left[-\frac{44}{81\epsilon^4}-\frac{8}{243\epsilon^3}+\frac{1}{\epsilon^2}\left(\frac{46}{81}+\frac{4}{9}\zeta_2\right)+\frac{1}{\epsilon}\left(\frac{2417}{2187}-\frac{8}{81}\zeta_3-\frac{20}{27}\zeta_2\right)\right.\\
&\qquad\left.+\left(-\frac{190931}{13122}-\frac{416}{243}\zeta_3-\frac{824}{81}\zeta_2-\frac{188}{135}\zeta_2^2\right)\right]\\
&+C_F N_{F,V}\left(\frac{N^2-4}{N}\right)\left[4-\frac{2\zeta_2^2}{5}+10\zeta_2+\frac{14\zeta_3}{3}-\frac{80\zeta_5}{3}\right], \qquad (5.8)
\end{aligned}
$$

$$
\begin{aligned}
F_3^g = {} & C_A^3\left[-\frac{4}{3\epsilon^6}-\frac{55}{3\epsilon^5}-\frac{9079}{162\epsilon^4}+\frac{1}{\epsilon^3}\left(\frac{5453}{486}+\frac{22\zeta_3}{3}+\frac{77\zeta_2}{54}\right)\right.\\
&+\frac{1}{\epsilon^2}\left(-\frac{4277}{243}+\frac{2266\zeta_3}{27}-\frac{1393\zeta_2}{81}+\frac{247\zeta_2^2}{90}\right)\\
&+\frac{1}{\epsilon}\left(-\frac{1307704}{2187}-\frac{878\zeta_5}{15}-\frac{85\zeta_3\zeta_2}{9}+\frac{1814\zeta_3}{9}-\frac{27301\zeta_2}{486}+\frac{12881\zeta_2^2}{360}\right)\\
&+\left(-\frac{23496187}{26244}+\frac{13882\zeta_5}{45}-\frac{1441\zeta_3\zeta_2}{18}+\frac{24893\zeta_3}{243}\right.\\
&\qquad\left.\left.-\frac{1766\zeta_3^2}{9}+\frac{118165\zeta_2}{1458}+\frac{126071\zeta_2^2}{1080}-\frac{22523\zeta_2^3}{270}\right)\right]\\
&+C_A^2 N_F\left[\frac{10}{3\epsilon^5}+\frac{1780}{81\epsilon^4}+\frac{1}{\epsilon^3}\left(\frac{2344}{243}-\frac{7\zeta_2}{27}\right)+\frac{1}{\epsilon^2}\left(-\frac{1534}{243}+\frac{68\zeta_3}{27}+\frac{169\zeta_2}{81}\right)\right.\\
&+\frac{1}{\epsilon}\left(\frac{854467}{4374}+\frac{3002\zeta_3}{81}+\frac{3536\zeta_2}{243}+\frac{941\zeta_2^2}{180}\right)\\
&\left.+\left(\frac{2143537}{13122}+\frac{4516\zeta_5}{45}-\frac{301\zeta_3\zeta_2}{9}+\frac{1414\zeta_3}{9}-\frac{6440\zeta_2}{729}+\frac{527\zeta_2^2}{20}\right)\right]\\
&+C_A C_F N_F\left[-\frac{34}{9\epsilon^3}+\frac{1}{\epsilon^2}\left(\frac{427}{27}-\frac{160\zeta_3}{9}\right)+\frac{1}{\epsilon}\left(\frac{13655}{81}-\frac{2600\zeta_3}{27}-\frac{13\zeta_2}{3}-\frac{176\zeta_2^2}{15}\right)\right.\\
&\qquad\left.+\left(\frac{284929}{972}+\frac{32\zeta_5}{9}+48\zeta_3\zeta_2-\frac{14398\zeta_3}{81}-\frac{118\zeta_2}{3}-\frac{928\zeta_2^2}{15}\right)\right]\\
&+C_F^2 N_F\left[-\frac{1}{3\epsilon}+\left(\frac{304}{9}-160\zeta_5+\frac{296\zeta_3}{3}\right)\right]\\
&+C_A N_F^2\left[-\frac{170}{81\epsilon^4}-\frac{998}{243\epsilon^3}+\frac{1}{\epsilon^2}\left(\frac{92}{27}+\frac{2\zeta_2}{27}\right)+\frac{1}{\epsilon}\left(-\frac{37133}{4374}-\frac{164\zeta_3}{81}-\frac{70\zeta_2}{81}\right)\right.\\
&\qquad\left.+\left(\frac{125059}{13122}+\frac{952\zeta_3}{243}-\frac{20\zeta_2}{27}-\frac{157\zeta_2^2}{135}\right)\right]\\
&+C_F N_F^2\left[\frac{14}{9\epsilon^2}+\frac{1}{\epsilon}\left(-\frac{212}{27}+\frac{16\zeta_3}{3}\right)+\left(\frac{2881}{162}-\frac{152\zeta_3}{9}-\frac{2\zeta_2}{3}+\frac{16\zeta_2^2}{5}\right)\right]\\
&+N_F^3\left[\frac{8}{27\epsilon^3}\right] \qquad (5.9)
\end{aligned}
$$

JHEP06(2010)094

The $\mathcal{O}(\epsilon)$ contributions to the N_F parts of the UV-renormalized space-like quark and gluon form factors are given by,

$$
\begin{aligned}
F_3^q|_{N_F} = &+C_F N_F^2 \epsilon \left(-\frac{3769249}{26244} + \frac{88}{135}\zeta_5 + \frac{2632}{243}\zeta_3 - \frac{5515}{81}\zeta_2 + \frac{8}{3}\zeta_2\zeta_3 - \frac{952}{81}\zeta_2^2 \right) \\
&+C_F C_A N_F \epsilon \left(\frac{1552436}{729} - \frac{11596}{45}\zeta_5 - \frac{1214351}{729}\zeta_3 + \frac{3988}{27}\zeta_3^2 + \frac{4933141}{4374}\zeta_2 \right. \\
&\qquad \left. + \frac{1966}{27}\zeta_2\zeta_3 + \frac{4579}{405}\zeta_2^2 + \frac{2762}{945}\zeta_2^3 \right) \\
&+C_F^2 N_F \epsilon \left(-\frac{15199979}{8748} - \frac{10769}{135}\zeta_5 + \frac{553882}{243}\zeta_3 - \frac{6881}{27}\zeta_3^2 - \frac{961699}{972}\zeta_2 \right. \\
&\qquad \left. - \frac{4627}{54}\zeta_2\zeta_3 + \frac{94747}{3240}\zeta_2^2 - \frac{425813}{7560}\zeta_2^3 \right) \\
&+C_F N_{F,V} \left(\frac{N^2-4}{N} \right) \epsilon \left(\frac{170}{3} + \frac{752}{9}\zeta_5 + \frac{94}{9}\zeta_3 - \frac{344}{3}\zeta_3^2 + \frac{260}{3}\zeta_2 \right. \\
&\qquad \left. + 30\zeta_2\zeta_3 - \frac{196}{15}\zeta_2^2 - \frac{9728}{315}\zeta_2^3 \right) ,
\end{aligned}
\tag{5.10}
$$

and for the gluon form factor

$$
\begin{aligned}
F_3^g|_{N_F} = &+C_A N_F^2 \epsilon \left(\frac{6599393}{26244} + \frac{1844}{135}\zeta_5 + \frac{8396}{81}\zeta_3 - \frac{25315}{1458}\zeta_2 - \frac{172}{27}\zeta_2\zeta_3 + \frac{2453}{405}\zeta_2^2 \right) \\
&+C_A^2 N_F \epsilon \left(-\frac{18825781}{8748} + \frac{1682}{45}\zeta_5 + \frac{270232}{729}\zeta_3 - \frac{6251}{27}\zeta_3^2 + \frac{867919}{4374}\zeta_2 \right. \\
&\qquad \left. - \frac{881}{9}\zeta_2\zeta_3 + \frac{33403}{405}\zeta_2^2 + \frac{133627}{7560}\zeta_2^3 \right) \\
&+C_F N_F^2 \epsilon \left(\frac{360181}{972} - \frac{224}{9}\zeta_5 - \frac{1960}{9}\zeta_3 - \frac{277}{9}\zeta_2 + \frac{32}{3}\zeta_2\zeta_3 - \frac{208}{15}\zeta_2^2 \right) \\
&+C_F C_A N_F \epsilon \left(-\frac{7017335}{5832} + \frac{7588}{27}\zeta_5 - \frac{92894}{243}\zeta_3 + \frac{4064}{9}\zeta_3^2 + \frac{986}{54}\zeta_2 \right. \\
&\qquad \left. + \frac{1960}{9}\zeta_2\zeta_3 - \frac{59987}{540}\zeta_2^2 + \frac{23624}{315}\zeta_2^3 \right) \\
&+C_F^2 N_F \epsilon \left(\frac{18613}{54} - \frac{3080}{3}\zeta_5 + \frac{10552}{9}\zeta_3 - 272\zeta_3^2 - \frac{74}{3}\zeta_2 \right. \\
&\qquad \left. - 16\zeta_2\zeta_3 + \frac{328}{5}\zeta_2^2 - \frac{35648}{315}\zeta_2^3 \right).
\end{aligned}
\tag{5.11}
$$

JHEP06(2010)094

6 Infrared pole structure

According to ref. [28, 39], the general infrared pole structure of a renormalised QCD amplitude is related to the ultraviolet behaviour of an effective operator in soft-collinear effective theory. These poles can therefore be subtracted by means of a multiplicative renormalization factor $\mathbf{Z}$. This means that the finite remainders of a scattering amplitude $\mathbf{M^F}$ is obtained from the full amplitude $\mathbf{M}$ via the relation,

$$\mathbf{M^F} = \mathbf{Z}^{-1}\mathbf{M}. \tag{6.1}$$

In general, the scattering amplitude $\mathbf{M}$ and $\mathbf{Z}$ are matrices in colour space. However, in the context of the quark and gluon form factors, the colour matrix is trivial. The UV renormalised amplitudes M and M_F have perturbative expansions,

$$M = 1 + \sum_{i=1} \left(\frac{\alpha_s(\mu^2)}{4\pi}\right)^i M_i, \tag{6.2}$$

$$M^F = 1 + \sum_{i=1} \left(\frac{\alpha_s(\mu^2)}{4\pi}\right)^i M_i^F, \tag{6.3}$$

while

$$\log(Z) = \sum_{i=1} \left(\frac{\alpha_s(\mu^2)}{4\pi}\right)^i Z_i. \tag{6.4}$$

We can now solve eq. (6.1) order by order in the strong coupling,

$$\mathcal{P}oles(M_1) = Z_1, \tag{6.5}$$

$$\mathcal{P}oles(M_2) = Z_2 + \frac{M_1^2}{2}, \tag{6.6}$$

$$\mathcal{P}oles(M_3) = Z_3 - \frac{M_1^3}{3} + M_2 M_1, \tag{6.7}$$

$$\mathcal{P}oles(M_4) = Z_4 + \frac{M_1^4}{4} - M_1^2 M_2 + M_1 M_3 + \frac{M_2^2}{2}, \tag{6.8}$$

$$\mathcal{P}oles(M_5) = Z_5 - \frac{M_1^5}{5} + M_1^3 M_2 - M_1^2 M_3 - M_1 M_2^2 + M_1 M_4 + M_2 M_3. \tag{6.9}$$

The deepest infrared pole for the i-loop amplitude is ϵ^{-2i}. However, the deepest pole in the Z_i-factor is ϵ^{-i-1}. All of the deepest poles are obtained directly from the lower loop amplitudes - which must be known to an appropriately high order in ϵ. For example, to obtain the correct pole structure for M_i, one needs knowledge of M_1 through to $\mathcal{O}(\epsilon^{2i-3})$.

We find that the infrared pole structure of the renormalised form factors is given by

JHEP06(2010)094

($i = q, g$ and $C_q = C_F$, $C_g = C_A$ for the cusp anomalous dimension):

$$\mathcal{P}oles(F_1^i) = -\frac{C_i\gamma_0^{\rm cusp}}{2\epsilon^2} + \frac{\gamma_0^i}{\epsilon}\,, \tag{6.10}$$

$$\mathcal{P}oles(F_2^i) = \frac{3C_i\gamma_0^{\rm cusp}\beta_0}{8\epsilon^3} + \frac{1}{\epsilon^2}\left(-\frac{\beta_0\gamma_0^i}{2} - \frac{C_i\gamma_1^{\rm cusp}}{8}\right) + \frac{\gamma_1^i}{2\epsilon} + \frac{\left(F_1^i\right)^2}{2}\,, \tag{6.11}$$

$$\begin{aligned}\mathcal{P}oles(F_3^i) = &-\frac{11\beta_0^2 C_i\gamma_0^{\rm cusp}}{36\epsilon^4} + \frac{1}{\epsilon^3}\left(\frac{5\beta_0 C_i\gamma_1^{\rm cusp}}{36} + \frac{\beta_0^2\gamma_0^i}{3} + \frac{2C_i\gamma_0^{\rm cusp}\beta_1}{9}\right)\\ &+\frac{1}{\epsilon^2}\left(-\frac{\beta_0\gamma_1^i}{3} - \frac{C_i\gamma_2^{\rm cusp}}{18} - \frac{\beta_1\gamma_0^i}{3}\right) + \frac{\gamma_2^i}{3\epsilon} - \frac{\left(F_1^i\right)^3}{3} + F_2^q F_1^q\,.\end{aligned} \tag{6.12}$$

Note that the full (all-orders) expressions for F_i^q are recycled on the right-hand-side. The coefficients of the cusp soft anomalous dimension $\gamma_i^{\rm cusp}$ are known to three-loop order [31] and are given by:

$$\gamma_0^{\rm cusp} = 4\,, \tag{6.13}$$

$$\gamma_1^{\rm cusp} = C_A\left(\frac{268}{9} - \frac{4\pi^2}{3}\right) - \frac{40N_F}{9}\,, \tag{6.14}$$

$$\begin{aligned}\gamma_2^{\rm cusp} = &\,C_A^2\left(\frac{490}{3} - \frac{536\pi^2}{27} + \frac{44\pi^4}{45} + \frac{88\zeta_3}{3}\right) + C_A N_F\left(-\frac{836}{27} + \frac{80\pi^2}{27} - \frac{112\zeta_3}{3}\right)\\ &+C_F N_F\left(-\frac{110}{3} + 32\zeta_3\right) - \frac{16N_F^2}{27}\,.\end{aligned} \tag{6.15}$$

while the quark and gluon collinear anomalous dimensions γ_i^q and γ_i^g in the conventional dimensional regularisation scheme are also known to three-loop order [38, 39] and are given by:

$$\gamma_0^q = -3C_F\,, \tag{6.16}$$

$$\begin{aligned}\gamma_1^q = &\,C_F^2\left(-\frac{3}{2} + 2\pi^2 - 24\zeta_3\right) + C_F C_A\left(-\frac{961}{54} - \frac{11\pi^2}{6} + 26\zeta_3\right)\\ &+C_F N_F\left(\frac{65}{27} + \frac{\pi^2}{3}\right),\end{aligned} \tag{6.17}$$

$$\begin{aligned}\gamma_2^q = &\,C_F^2 N_F\left(\frac{2953}{54} - \frac{13\pi^2}{9} - \frac{14\pi^4}{27} + \frac{256\zeta_3}{9}\right) + C_F N_F^2\left(\frac{2417}{729} - \frac{10\pi^2}{27} - \frac{8\zeta_3}{27}\right)\\ &+C_F C_A N_F\left(-\frac{8659}{729} + \frac{1297\pi^2}{243} + \frac{11\pi^4}{45} - \frac{964\zeta_3}{27}\right)\\ &+C_F^3\left(-\frac{29}{2} - 3\pi^2 - \frac{8\pi^4}{5} - 68\zeta_3 + \frac{16\pi^2\zeta_3}{3} + 240\zeta_5\right)\\ &+C_A C_F^2\left(-\frac{151}{4} + \frac{205\pi^2}{9} + \frac{247\pi^4}{135} - \frac{844\zeta_3}{3} - \frac{8\pi^2\zeta_3}{3} - 120\zeta_5\right)\\ &+C_A^2 C_F\left(-\frac{139345}{2916} - \frac{7163\pi^2}{486} - \frac{83\pi^4}{90} + \frac{3526\zeta_3}{9} - \frac{44\pi^2\zeta_3}{9} - 136\zeta_5\right),\end{aligned} \tag{6.18}$$

$$\gamma_0^g = -\frac{11C_A}{3} + \frac{2N_F}{3}\,, \tag{6.19}$$

JHEP06(2010)094

$$\gamma_1^g = C_A^2\left(-\frac{692}{27}+\frac{11\pi^2}{18}+2\zeta_3\right)+C_AN_F\left(\frac{128}{27}-\frac{\pi^2}{9}\right)+2C_FN_F \tag{6.20}$$

$$\begin{aligned}\gamma_2^g = {} & C_A^3\left(-\frac{97186}{729}+\frac{6109\pi^2}{486}-\frac{319\pi^4}{270}+\frac{122\zeta_3}{3}-\frac{20\pi^2\zeta_3}{9}-16\zeta_5\right),\\ & +C_A^2N_F\left(\frac{30715}{1458}-\frac{599\pi^2}{243}+\frac{41\pi^4}{135}+\frac{356\zeta_3}{27}\right)\\ & +C_FC_AN_F\left(\frac{1217}{27}-\frac{\pi^2}{3}-\frac{4\pi^4}{45}-\frac{152\zeta_3}{9}\right)-C_F^2N_F\\ & +C_AN_F^2\left(-\frac{269}{1458}+\frac{10\pi^2}{81}-\frac{56\zeta_3}{27}\right)-\frac{11C_FN_F^2}{9}\,.\end{aligned} \tag{6.21}$$

Taking this one step further, we find that the pole structure of the renormalised four-loop quark form factor is given by

$$\begin{aligned}\mathcal{P}oles(F_4^i) = {} & \frac{25\beta_0^3C_i\gamma_0^{\rm cusp}}{96\epsilon^5}-\frac{\beta_0(24\beta_0^2\gamma_0^i+13\beta_0C_i\gamma_1^{\rm cusp}+40C_i\gamma_0^{\rm cusp}\beta_1)}{96\epsilon^4}\\ & +\frac{1}{\epsilon^3}\left(\frac{7\beta_0C_i\gamma_2^{\rm cusp}}{96}+\frac{3\beta_1C_i\gamma_1^{\rm cusp}}{32}+\frac{\beta_0^2\gamma_1^i}{4}+\frac{\beta_1\beta_0\gamma_0^i}{2}+\frac{5C_i\gamma_0^{\rm cusp}\beta_2}{32}\right)\\ & +\frac{1}{\epsilon^2}\left(-\frac{\beta_1\gamma_1^i}{4}-\frac{C_i\gamma_3^{\rm cusp}}{32}-\frac{\beta_0\gamma_2^i}{4}-\frac{\beta_2\gamma_0^i}{4}\right)+\frac{\gamma_3^i}{4\epsilon}\\ & +\frac{\left(F_1^i\right)^4}{4}+\left(F_1^i\right)^2F_2^i-\frac{\left(F_2^i\right)^2}{2}-F_1^iF_3^i\,.\end{aligned} \tag{6.22}$$

In this expression, we assume Casimir scaling of the cusp anomalous dimension to hold at four loops [39, 40], such that only a universal $\gamma_3^{\rm cusp}$ appears. If, contrary to expectations, Casimir scaling should be violated at this order, different $\gamma_3^{\rm cusp}$ would appear in the double pole terms of the quark and gluon form factors at four loops.

Eq. (6.22) shows that in order to make use of a calculation of the pole parts of the four-loop form factors to extract the cusp and collinear anomalous dimensions, one requires the finite parts of the three-loop form factor for $\gamma_3^{\rm cusp}$, and of the subleading $\mathcal{O}(\epsilon)$ parts for $\gamma_3^{q,g}$. For all colour-factor contributions proportional to N_F, these are provided in the previous section. The required subleading terms in higher orders in ϵ from the one-loop and two-loop form factors were summarized in section 2 above.

7 Effective theory matching coefficients

It is well known that fixed-order perturbation theory is not necessarily reliable for physical quantities involving several disparate scales. In such cases, higher-order corrections are enhanced by large logarithms of scale ratios. Experimentally relevant examples are the Drell-Yan and Higgs production processes in hadron-hadron colliders. When the phase space for soft gluon emission is constrained, large logarithmic threshold corrections appear of the form

$$\alpha_s^k\left[\frac{\ln^{m-1}(1-z)}{(1-z)}\right]_+, \qquad (m\le 2k), \tag{7.1}$$

JHEP06(2010)094

where $(1-z)$ is the fraction of centre-of-mass energy of the initial partons available for soft gluon radiation. These can spoil the convergence of the perturbative series. The resummation of these so-called Sudakov-logarithms has been accomplished to fourth logarithmic order [84–86], using the exponentiation properties of the coefficient functions in moment space [87–90].

An alternative resummation framework is provided by soft-collinear effective field theory (SCET), which is based on the idea to split the calculation into a series of single-scale problems by successively integrating out the physics associated with the largest remaining scale. The SCET framework [18–23] originated in the study of heavy quarks, and has been subsequently generalized to massless collider processes [91]. The infrared poles in the high energy theory (QCD) get transformed into ultraviolet poles in the effective theory [17, 28] and can then be resummed by renormalization-group (RG) evolution from the larger scales to the smaller ones. Of course the SCET must match precisely onto the high energy theory, and this is achieved by computing matrix elements in both the SCET and QCD and adjusting the Wilson coefficients so that they agree. If the matching is performed on-shell, then the matching coefficients relevant for Drell Yan and Higgs production can be obtained from the quark and gluon form factors respectively. Therefore, we can utilise the results presented in the previous sections to compute the matching conditions through to three-loops. Results up to two loops were obtained previously in [24–27].

The renormalised form-factors are infrared divergent. In the effective field theory, these infrared divergences are transformed into ultraviolet poles. The matching coefficient C^i $(i = q, g)$ is obtained by extracting the poles using a renormalisation factor such that,

$$C^i(\alpha_s(\mu^2), s_{12}, \mu^2) = \lim_{\epsilon\to 0} Z_i^{-1}(\epsilon, s_{12}, \mu) F^i(\epsilon, s_{12}, \mu^2). \tag{7.2}$$

The matching coefficients have the perturbative expansion,

$$C^i(\alpha_s(\mu^2), s_{12}, \mu^2) = 1 + \sum_{n=1}^{\infty} \left(\frac{\alpha_s(\mu^2)}{4\pi}\right)^n C_n^i(s_{12}, \mu^2). \tag{7.3}$$

They are are known to two loop order for Drell-Yan [24, 25] and Higgs [26, 27] production,

$$C_1^q = C_F\Big(- L^2 + 3L - 8 + \zeta_2\Big), \tag{7.4}$$

$$\begin{aligned} C_2^q = {} & C_F^2\Big(\frac{1}{2}L^4 - 3L^3 + \Big(\frac{25}{2} - \zeta_2\Big)L^2 + \Big(- \frac{45}{2} + 24\zeta_3 - 9\zeta_2\Big)L \\ & \qquad + \frac{255}{8} - 30\zeta_3 + 21\zeta_2 - \frac{83}{10}\zeta_2^2\Big) \\ & + C_F C_A\Big(\frac{11}{9}L^3 + \Big(- \frac{233}{18} + 2\zeta_2\Big)L^2 + \Big(\frac{2545}{54} - 26\zeta_3 + \frac{22}{3}\zeta_2\Big)L \\ & \qquad - \frac{51157}{648} + \frac{313}{9}\zeta_3 - \frac{337}{18}\zeta_2 + \frac{44}{5}\zeta_2^2\Big) \\ & + C_F N_F\Big(- \frac{2}{9}L^3 + \frac{19}{9}L^2 + \Big(- \frac{209}{27} - \frac{4}{3}\zeta_2\Big)L + \frac{4085}{324} + \frac{2}{9}\zeta_3 + \frac{23}{9}\zeta_2\Big), \end{aligned} \tag{7.5}$$

JHEP06(2010)094

$$C_1^g = C_A\Big(-L^2+\zeta_2\Big), \tag{7.6}$$

$$\begin{aligned}C_2^g = {} & C_A^2\Big(\frac{1}{2}L^4+\frac{11}{9}L^3+\Big(-\frac{67}{9}+\zeta_2\Big)L^2+\Big(\frac{80}{27}-2\zeta_3-\frac{22}{3}\zeta_2\Big)L \\ & \qquad +\frac{5105}{162}-\frac{143}{9}\zeta_3+\frac{67}{6}\zeta_2+\frac{1}{2}\zeta_2^2\Big) \\ & +C_AN_F\Big(-\frac{2}{9}L^3+\frac{10}{9}L^2+\Big(\frac{52}{27}+\frac{4}{3}\zeta_2\Big)L-\frac{916}{81}-\frac{46}{9}\zeta_3-\frac{5}{3}\zeta_2\Big) \\ & +C_FN_F\Big(2L-\frac{67}{6}+8\zeta_3\Big)\end{aligned} \tag{7.7}$$

where $L=\log(-s_{12}/\mu^2)$.

Exploiting the expressions for the renormalised quark and gluon form factors given in eqs. (5.8) and (5.9) respectively, we find that the three-loop matching coefficients are

$$\begin{aligned}C_3^q = {} & C_F^3\Big(-\frac{1}{6}L^6+\frac{3}{2}L^5+\Big(-\frac{17}{2}+\frac{1}{2}\zeta_2\Big)L^4+\Big(9\zeta_2+27-24\zeta_3\Big)L^3 \\ & \qquad +\Big(102\zeta_3-\frac{507}{8}-\frac{105}{2}\zeta_2+\frac{83}{10}\zeta_2^2\Big)L^2 \\ & \qquad +\Big(-214\zeta_3-240\zeta_5-8\zeta_2\zeta_3+\frac{357}{2}\zeta_2+\frac{207}{10}\zeta_2^2+\frac{785}{8}\Big)L \\ & \qquad -\frac{413}{5}\zeta_2^2+664\zeta_5-\frac{6451}{24}\zeta_2+\frac{37729}{630}\zeta_2^3-470\zeta_3+250\zeta_2\zeta_3-\frac{2539}{12}+16\zeta_3^2\Big) \\ & +C_F^2C_A\Big(-\frac{11}{9}L^5+\Big(\frac{299}{18}-2\zeta_2\Big)L^4+\Big(-\frac{2585}{27}+26\zeta_3-\frac{1}{9}\zeta_2\Big)L^3 \\ & \qquad +\Big(\frac{206317}{648}-\frac{1807}{9}\zeta_3+\frac{502}{9}\zeta_2-\frac{34}{5}\zeta_2^2\Big)L^2 \\ & \qquad +\Big(-\frac{13805}{24}+120\zeta_5+\frac{2441}{3}\zeta_3-\frac{11260}{27}\zeta_2-10\zeta_2\zeta_3+\frac{162}{5}\zeta_2^2\Big)L \\ & \qquad +\frac{415025}{648}-\frac{2756}{9}\zeta_5-\frac{18770}{27}\zeta_3+\frac{296}{3}\zeta_3^2+\frac{538835}{648}\zeta_2-\frac{3751}{9}\zeta_2\zeta_3 \\ & \qquad -\frac{4943}{270}\zeta_2^2-\frac{12676}{315}\zeta_2^3\Big) \\ & +C_F^2N_F\Big(\frac{2}{9}L^5-\frac{25}{9}L^4+\Big(\frac{410}{27}+\frac{10}{9}\zeta_2\Big)L^3+\Big(-\frac{12815}{324}+\frac{70}{9}\zeta_3-\frac{112}{9}\zeta_2\Big)L^2 \\ & \qquad +\Big(\frac{3121}{108}-\frac{610}{9}\zeta_3+\frac{1618}{27}\zeta_2+\frac{28}{5}\zeta_2^2\Big)L \\ & \qquad +\frac{41077}{972}-\frac{416}{9}\zeta_5+\frac{13184}{81}\zeta_3-\frac{31729}{324}\zeta_2-\frac{38}{9}\zeta_2\zeta_3-\frac{331}{27}\zeta_2^2\Big) \\ & +C_FC_A^2\Big(-\frac{121}{54}L^4+\Big(\frac{2869}{81}-\frac{44}{9}\zeta_2\Big)L^3+\Big(-\frac{18682}{81}+88\zeta_3+\frac{26}{9}\zeta_2-\frac{44}{5}\zeta_2^2\Big)L^2 \\ & \qquad +\Big(\frac{1045955}{1458}+136\zeta_5-\frac{17464}{27}\zeta_3+\frac{17366}{81}\zeta_2+\frac{88}{3}\zeta_2\zeta_3-\frac{94}{3}\zeta_2^2\Big)L \\ & \qquad -\frac{51082685}{52488}-\frac{434}{9}\zeta_5+\frac{505087}{486}\zeta_3-\frac{1136}{9}\zeta_3^2-\frac{412315}{729}\zeta_2+\frac{416}{3}\zeta_2\zeta_3\end{aligned}$$

JHEP06(2010)094

$$
\begin{aligned}
&\quad + \frac{22157}{270}\zeta_2^2 - \frac{6152}{189}\zeta_2^3\Big) \\
&+ C_F C_A N_F \Big(\frac{22}{27}L^4 + \Big(-\frac{974}{81} + \frac{8}{9}\zeta_2\Big)L^3 + \Big(\frac{5876}{81} - 8\zeta_3 + \frac{16}{3}\zeta_2\Big)L^2 \\
&\quad + \Big(-\frac{154919}{729} + \frac{724}{9}\zeta_3 - \frac{5864}{81}\zeta_2 + \frac{44}{15}\zeta_2^2\Big)L \\
&\quad + \frac{1700171}{6561} - \frac{4}{3}\zeta_5 - \frac{4288}{27}\zeta_3 + \frac{115555}{729}\zeta_2 + \frac{4}{3}\zeta_2\zeta_3 + \frac{2}{27}\zeta_2^2\Big) \\
&+ C_F N_F^2 \Big(-\frac{2}{27}L^4 + \frac{76}{81}L^3 + \Big(-\frac{406}{81} - \frac{8}{9}\zeta_2\Big)L^2 + \Big(\frac{9838}{729} + \frac{16}{27}\zeta_3 + \frac{152}{27}\zeta_2\Big)L \\
&\quad - \frac{190931}{13122} - \frac{416}{243}\zeta_3 - \frac{824}{81}\zeta_2 - \frac{188}{135}\zeta_2^2\Big) \\
&+ C_F N_{F,V}\Big(\frac{N^2-4}{N}\Big)\Big(4 - \frac{80}{3}\zeta_5 + \frac{14}{3}\zeta_3 + 10\zeta_2 - \frac{2}{5}\zeta_2^2\Big)
\end{aligned}
\tag{7.8}
$$

and,

$$
\begin{aligned}
C_3^g = C_A^3 \Big(&-\frac{1}{6}L^6 - \frac{11}{9}L^5 + \Big(\frac{281}{54} - \frac{3}{2}\zeta_2\Big)L^4 + \Big(\frac{11}{3}\zeta_2 + \frac{1540}{81} + 2\zeta_3\Big)L^3 \\
&+ \Big(\frac{143}{9}\zeta_3 - \frac{6740}{81} + \frac{685}{18}\zeta_2 - \frac{73}{10}\zeta_2^2\Big)L^2 \\
&+ \Big(\frac{2048}{27}\zeta_3 + 16\zeta_5 + \frac{34}{3}\zeta_2\zeta_3 - \frac{13420}{81}\zeta_2 + \frac{176}{5}\zeta_2^2 - \frac{373975}{1458}\Big)L \\
&- \frac{1939}{270}\zeta_2^2 + \frac{2222}{9}\zeta_5 + \frac{105617}{729}\zeta_2 - \frac{24389}{1890}\zeta_2^3 - \frac{152716}{243}\zeta_3 - \frac{605}{9}\zeta_2\zeta_3 \\
&+ \frac{29639273}{26244} - \frac{104}{9}\zeta_3^2\Big) \\
&+ C_A^2 N_F \Big(\frac{2}{9}L^5 - \frac{8}{27}L^4 + \Big(-\frac{734}{81} - \frac{2}{3}\zeta_2\Big)L^3 + \Big(\frac{377}{27} + \frac{118}{9}\zeta_3 - \frac{103}{9}\zeta_2\Big)L^2 \\
&\quad + \Big(\frac{133036}{729} + \frac{28}{9}\zeta_3 + \frac{3820}{81}\zeta_2 - \frac{48}{5}\zeta_2^2\Big)L \\
&\quad - \frac{3765007}{6561} + \frac{428}{9}\zeta_5 - \frac{460}{81}\zeta_3 - \frac{14189}{729}\zeta_2 - \frac{82}{9}\zeta_2\zeta_3 + \frac{73}{45}\zeta_2^2\Big) \\
&+ C_A N_F^2 \Big(-\frac{2}{27}L^4 + \frac{40}{81}L^3 + \Big(\frac{116}{81} + \frac{8}{9}\zeta_2\Big)L^2 + \Big(-\frac{14057}{729} - \frac{128}{27}\zeta_3 - \frac{80}{27}\zeta_2\Big)L \\
&\quad + \frac{611401}{13122} + \frac{4576}{243}\zeta_3 + \frac{4}{9}\zeta_2 + \frac{4}{27}\zeta_2^2\Big) \\
&+ C_F N_F^2 \Big(\frac{4}{3}L^2 + \Big(-\frac{52}{3} + \frac{32}{3}\zeta_3\Big)L + \frac{4481}{81} - \frac{112}{3}\zeta_3 - \frac{20}{9}\zeta_2 - \frac{16}{45}\zeta_2^2\Big) \\
&+ C_F C_A N_F \Big(-\frac{8}{3}L^3 + \Big(13 - 16\zeta_3\Big)L^2 + \Big(\frac{3833}{54} - \frac{376}{9}\zeta_3 + 6\zeta_2 + \frac{16}{5}\zeta_2^2\Big)L \\
&\quad - \frac{341219}{972} + \frac{608}{9}\zeta_5 + \frac{14564}{81}\zeta_3 - \frac{68}{9}\zeta_2 + \frac{64}{3}\zeta_2\zeta_3 - \frac{64}{45}\zeta_2^2\Big)
\end{aligned}
$$

JHEP06(2010)094

$$+C_F^2 N_F\left(-2L+\frac{304}{9}-160\zeta_5+\frac{296}{3}\zeta_3\right). \tag{7.9}$$

These matching coefficients allow to perform the three-loop matching of the SCET-based resummation onto the full QCD calculation.

8 Conclusions

In this paper, we described the calculation of the three-loop quark and gluon form factors in detail. Our results confirm earlier expressions obtained by Baikov et al. [58], which we extended by subleading terms in the fermionic corrections.

The form factors are the simplest QCD objects with non-trivial infrared structure. Recent findings on the relation between massless on-shell QCD amplitudes and operators in soft-collinear effective theory [43], combined with constraints from factorization, has led to the conjecture [39] that their pole terms at a given loop level contain all information needed to predict the pole structure of massless on-shell multi-leg amplitudes at the same loop order. In particular, the cusp anomalous dimension can be extracted from the double pole, and the collinear anomalous dimension from the single pole. At a given loop order, finite and subleading terms from lower loop orders are also required. In this respect, the finite terms presented here will be instrumental for the extraction of the four-loop cusp anomalous dimension, while the subleading terms contribute to the four-loop quark and gluon collinear anomalous dimension.

The three-loop form factors are key ingredients for the fourth order (N^3LO) corrections to the inclusive Drell-Yan and Higgs boson production cross sections. The calculation of these, at least in an improvement to the soft approximation [14–16, 25], could be envisaged in future work. In view of this application, we derived the hard matching coefficients of the SCET operators to this order. Inclusion of these corrections will lead to a further stabilization of the perturbative prediction under scale variations, and are thus important for precision physics at hadron colliders.

Acknowledgments

This research was supported in part by the Swiss National Science Foundation (SNF) under contract 200020-126691, by the Forschungskredit der Universität Zürich, the UK Science and Technology Facilities Council, by the European Commission's Marie-Curie Research Training Network under contract MRTN-CT-2006-035505 'Tools and Precision Calculations for Physics Discoveries at Colliders', and by the Helmholtz Alliance "Physics at the Terascale". EWNG gratefully acknowledges the support of the Wolfson Foundation and the Royal Society.

A Master integrals for three-loop form factors

In this appendix, we summarize the ϵ-expansions of all master integrals needed for the three-loop form factors. Our notation for the integrals follows [54], using a Minkowskian loop integration measure $\mathrm{d}^d k/(2\pi)^d$. All master integrals are defined in section 4 above.

JHEP06(2010)094

With the normalization S_Γ defined in (2.19), all M-loop integrals have an overall factor of

$$s_{12}^n \left(iS_\Gamma \left(-s_{12}-i0\right)^{-\epsilon}\right)^M \tag{A.1}$$

where n is fixed by dimensional arguments. Unlike refs. [54–56], there is no $(-1)^n$ factor. We expand to the required order for the three-loop form factors (which is typically the order where transcendentality 6 first appears).

The one-loop master integral is:

$$\begin{aligned} B_{2,1} = \; & \frac{1}{\epsilon} + 2 + 4\epsilon - \epsilon^2\left(2\zeta_3 - 8\right) - \epsilon^3\left(\frac{6\zeta_2^2}{5} + 4\zeta_3 - 16\right) \\ & -\epsilon^4\left(\frac{12\zeta_2^2}{5} + 8\zeta_3 + 6\zeta_5 - 32\right) \\ & -\epsilon^5\left(\frac{16\zeta_2^3}{7} + \frac{24\zeta_2^2}{5} - 2\zeta_3^2 + 16\zeta_3 + 12\zeta_5 \; - 64\right) \\ & +\epsilon^6\left(128 - 18\zeta_7 - 24\zeta_5 - 32\zeta_3 + 4\zeta_3^2 - \frac{48}{5}\zeta_2^2 + \frac{12}{5}\zeta_2^2\zeta_3 - \frac{32}{7}\zeta_2^3\right) + \mathcal{O}(\epsilon^7)\,. \end{aligned} \tag{A.2}$$

The two-loop two-point and three-point master integrals are:

$$\begin{aligned} B_{3,1} = \; & -\frac{1}{4\epsilon} - \frac{13}{8} - \frac{115\epsilon}{16} + \epsilon^2\left(\frac{5\zeta_3}{2} - \frac{865}{32}\right) + \epsilon^3\left(\frac{3\zeta_2^2}{2} + \frac{65\zeta_3}{4} - \frac{5971}{64}\right) \\ & +\epsilon^4\left(\frac{39\zeta_2^2}{4} + \frac{575\zeta_3}{8} + \frac{27\zeta_5}{2} - \frac{39193}{128}\right) \\ & +\epsilon^5\left(\frac{44\zeta_2^3}{7} + \frac{345\zeta_2^2}{8} - \frac{25\zeta_3^2}{2} + \frac{4325\zeta_3}{16} + \frac{351\zeta_5}{4} - \frac{249355}{256}\right) \\ & +\epsilon^6\left(-\frac{1555105}{512} + \frac{165}{2}\zeta_7 + \frac{3105}{8}\zeta_5 + \frac{29855}{32}\zeta_3 - \frac{325}{4}\zeta_3^2 + \frac{2595}{16}\zeta_2^2 - 15\zeta_2^2\zeta_3 + \frac{286}{7}\zeta_2^3\right) \\ & +\mathcal{O}(\epsilon^7)\,, \end{aligned} \tag{A.3}$$

$$\begin{aligned} B_{4,2} = \; & +\frac{1}{\epsilon^2} + \frac{4}{\epsilon} + 12 - \epsilon\left(4\zeta_3 - 32\right) - \epsilon^2\left(\frac{12\zeta_2^2}{5} + 16\zeta_3 - 80\right) \\ & -\epsilon^3\left(\frac{48\zeta_2^2}{5} + 48\zeta_3 + 12\zeta_5 - 192\right) \\ & -\epsilon^4\left(\frac{32\zeta_2^3}{7} + \frac{144\zeta_2^2}{5} - 8\zeta_3^2 + 128\zeta_3 + 48\zeta_5 - 448\right) \\ & +\epsilon^5\left(1024 - 36\zeta_7 - 144\zeta_5 - 320\zeta_3 + 32\zeta_3^2 - \frac{384}{5}\zeta_2^2 + \frac{48}{5}\zeta_2^2\zeta_3 - \frac{128}{7}\zeta_2^3\right) \\ & +\mathcal{O}(\epsilon^6)\,, \end{aligned} \tag{A.4}$$

$$\begin{aligned} C_{4,1} = \; & +\frac{1}{2\epsilon^2} + \frac{5}{2\epsilon} + \left(\zeta_2 + \frac{19}{2}\right) + \epsilon\left(5\zeta_2 - 4\zeta_3 + \frac{65}{2}\right) \\ & -\epsilon^2\left(\frac{6\zeta_2^2}{5} - 19\zeta_2 + 20\zeta_3 - \frac{211}{2}\right) \\ & -\epsilon^3\left(6\zeta_2^2 + 8\zeta_2\zeta_3 - 65\zeta_2 + 76\zeta_3 + 24\zeta_5 - \frac{665}{2}\right) \end{aligned}$$

JHEP06(2010)094

$$
\begin{aligned}
&-\epsilon^4\left(\frac{528\zeta_2^3}{35}+\frac{114\zeta_2^2}{5}+40\zeta_2\zeta_3-16\zeta_3^2-211\zeta_2+260\zeta_3+120\zeta_5-\frac{2059}{2}\right)\\
&+\epsilon^5\left(\frac{6305}{2}-156\zeta_7-456\zeta_5-844\zeta_3+80\zeta_3^2+665\zeta_2-48\zeta_2\zeta_5-152\zeta_2\zeta_3-78\zeta_2^2\right.\\
&\left.+\frac{48}{5}\zeta_2^2\zeta_3-\frac{528}{7}\zeta_2^3\right)+\mathcal{O}(\epsilon^6)\,, \qquad \text{(A.5)}\\
C_{6,2}=\;&+\frac{1}{\epsilon^4}-\frac{5\zeta_2}{\epsilon^2}-\frac{27\zeta_3}{\epsilon}-23\zeta_2^2+\epsilon\left(48\zeta_2\zeta_3-117\zeta_5\right)-\epsilon^2\left(\frac{456\zeta_2^3}{35}-267\zeta_3^2\right)\\
&+\epsilon^3\left(6\zeta_7+240\zeta_2\zeta_5+\frac{1962}{5}\zeta_2^2\zeta_3\right)+\mathcal{O}(\epsilon^4)\,. \qquad \text{(A.6)}
\end{aligned}
$$

The $B_{t,i}$-type and $C_{t,i}$-type master integrals read at three loops:

$$
\begin{aligned}
B_{4,1}=\;&\frac{1}{36\epsilon}+\frac{71}{216}+\frac{3115\epsilon}{1296}+\epsilon^2\left(-\frac{7\zeta_3}{9}+\frac{109403}{7776}\right)+\epsilon^3\left(-\frac{497\zeta_3}{54}-\frac{7\pi^4}{540}+\frac{3386467}{46656}\right)\\
&+\epsilon^4\left(-\frac{21805\zeta_3}{324}-7\zeta_5-\frac{497\pi^4}{3240}+\frac{96885467}{279936}\right)\\
&+\epsilon^5\left(-\frac{765821\zeta_3}{1944}-\frac{497\zeta_5}{6}-\frac{4361\pi^4}{3888}-\frac{4\pi^6}{243}+\frac{98\zeta_3^2}{9}+\frac{2631913075}{1679616}\right)\\
&+\mathcal{O}(\epsilon^6)\,, \qquad \text{(A.7)}\\
B_{5,1}=\;&-\frac{1}{4\epsilon^2}-\frac{17}{8\epsilon}-\frac{183}{16}+\epsilon\left(3\zeta_3-\frac{1597}{32}\right)+\epsilon^2\left(\frac{51\zeta_3}{2}+\frac{\pi^4}{20}-\frac{12359}{64}\right)\\
&+\epsilon^3\left(\frac{549\zeta_3}{4}+15\zeta_5+\frac{17\pi^4}{40}-\frac{88629}{128}\right)\\
&+\epsilon^4\left(\frac{4791\zeta_3}{8}+\frac{255\zeta_5}{2}+\frac{183\pi^4}{80}+\frac{2\pi^6}{63}-18\zeta_3^2-\frac{603871}{256}\right)+\mathcal{O}(\epsilon^5)\,, \qquad \text{(A.8)}\\
B_{5,2}=\;&-\frac{1}{3\epsilon^2}-\frac{10}{3\epsilon}-\frac{64}{3}+\epsilon\left(-112+\frac{22\zeta_3}{3}\right)+\epsilon^2\left(-528+\frac{220\zeta_3}{3}+\frac{11\pi^4}{90}\right)\\
&+\epsilon^3\left(-2336+\frac{1408\zeta_3}{3}+70\zeta_5+\frac{11\pi^4}{9}\right)\\
&+\epsilon^4\left(\frac{352\pi^4}{45}+2464\zeta_3+700\zeta_5-\frac{29824}{3}+\frac{94\pi^6}{567}-\frac{242\zeta_3^2}{3}\right)+\mathcal{O}(\epsilon^5)\,, \qquad \text{(A.9)}\\
B_{6,1}=\;&\frac{1}{\epsilon^3}+\frac{6}{\epsilon^2}+\frac{24}{\epsilon}+\left(80-6\zeta_3\right)+\epsilon\left(240-36\zeta_3-\frac{\pi^4}{10}\right)\\
&+\epsilon^2\left(672-144\zeta_3-18\zeta_5-\frac{3\pi^4}{5}\right)\\
&+\epsilon^3\left(1792-480\zeta_3-108\zeta_5-\frac{12\pi^4}{5}-\frac{2\pi^6}{63}+18\zeta_3^2\right)+\mathcal{O}(\epsilon^4)\,, \qquad \text{(A.10)}\\
B_{6,2}=\;&\frac{1}{3\epsilon^3}+\frac{7}{3\epsilon^2}+\frac{31}{3\epsilon}+\left(\frac{8\zeta_3}{3}+\frac{103}{3}\right)+\epsilon\left(\frac{235}{3}+\frac{56\zeta_3}{3}+\frac{2\pi^4}{45}\right)\\
&+\epsilon^2\left(\frac{19}{3}+120\zeta_5+\frac{320\zeta_3}{3}+\frac{14\pi^4}{45}\right)
\end{aligned}
$$

JHEP06(2010)094

$$+\epsilon^3\left(-\frac{3953}{3}+840\zeta_5+\frac{1832\zeta_3}{3}+\frac{16\pi^4}{9}+\frac{176\pi^6}{567}-\frac{292\zeta_3^2}{3}\right)+\mathcal{O}(\epsilon^4)\,, \tag{A.11}$$

$$\begin{aligned}B_{8,1} &= 20\zeta_5+\epsilon\left(68\zeta_3^2+40\zeta_5+\frac{10\pi^6}{189}\right)\\ &+\epsilon^2\left(136\zeta_3^2+\frac{34\pi^4\zeta_3}{15}+80\zeta_5+\frac{20\pi^6}{189}+450\zeta_7\right)\\ &+\mathcal{O}(\epsilon^3)\,,\end{aligned} \tag{A.12}$$

$$\begin{aligned}C_{6,1} &= \frac{1}{2\epsilon^3}+\frac{7}{2\epsilon^2}+\frac{1}{\epsilon}\left(\frac{\pi^2}{6}+\frac{33}{2}\right)+\left(\frac{7\pi^2}{6}-5\zeta_3+\frac{131}{2}\right)\\ &+\epsilon\left(\frac{11\pi^2}{2}-35\zeta_3-\frac{\pi^4}{20}+\frac{473}{2}\right)\\ &+\epsilon^2\left(\frac{131\pi^2}{6}-\frac{5\pi^2\zeta_3}{3}-165\zeta_3-27\zeta_5-\frac{7\pi^4}{20}+\frac{1611}{2}\right)\\ &+\epsilon^3\left(\frac{473\pi^2}{6}-\frac{35\pi^2\zeta_3}{3}-655\zeta_3-189\zeta_5-\frac{33\pi^4}{20}-\frac{61\pi^6}{756}+25\zeta_3^2+\frac{5281}{2}\right)\\ &+\mathcal{O}(\epsilon^4)\,,\end{aligned} \tag{A.13}$$

$$\begin{aligned}C_{8,1} &= \frac{1}{\epsilon^5}+\frac{2}{\epsilon^4}+\frac{1}{\epsilon^3}\left(-\frac{5\pi^2}{6}+4\right)+\frac{1}{\epsilon^2}\left(8-\frac{5\pi^2}{3}-29\zeta_3\right)\\ &+\frac{1}{\epsilon}\left(16-\frac{10\pi^2}{3}-58\zeta_3-\frac{121\pi^4}{180}\right)\\ &+\left(32-\frac{20\pi^2}{3}+\frac{29\pi^2\zeta_3}{3}-116\zeta_3-123\zeta_5-\frac{121\pi^4}{90}\right)\\ &+\epsilon\left(\frac{58\pi^2\zeta_3}{3}-232\zeta_3-246\zeta_5-\frac{40\pi^2}{3}+323\zeta_3^2-\frac{121\pi^4}{45}+64-\frac{163\pi^6}{3780}\right)\\ &+\mathcal{O}(\epsilon^2)\,.\end{aligned} \tag{A.14}$$

The genuine three-loop vertex integrals are:

$$\begin{aligned}A_{5,1} &= \frac{1}{24\epsilon^2}+\frac{19}{48\epsilon}+\left(\frac{233}{96}+\frac{\pi^2}{24}\right)+\epsilon\left(\frac{2363}{192}+\frac{19\pi^2}{48}-\frac{11\zeta_3}{12}\right)\\ &+\epsilon^2\left(\frac{7227}{128}+\frac{233\pi^2}{96}+\frac{\pi^4}{80}-\frac{209\zeta_3}{24}\right)\\ &+\epsilon^3\left(\frac{62641}{256}+\frac{2363\pi^2}{192}+\frac{19\pi^4}{160}-\frac{2563\zeta_3}{48}-\frac{11\pi^2\zeta_3}{12}-\frac{35\zeta_5}{4}\right)\\ &+\epsilon^4\left(\frac{1575481}{1536}+\frac{7227\pi^2}{128}+\frac{233\pi^4}{320}-\frac{919\pi^6}{45360}-\frac{25993\zeta_3}{96}\right.\\ &\left.-\frac{209\pi^2\zeta_3}{24}+\frac{121\zeta_3^2}{12}-\frac{665\zeta_5}{8}\right)\\ &+\mathcal{O}(\epsilon^5)\,,\end{aligned} \tag{A.15}$$

$$\begin{aligned}A_{5,2} &= -\frac{1}{6\epsilon^2}-\frac{5}{3\epsilon}+\left(-\frac{32}{3}-\frac{\pi^2}{12}\right)+\epsilon\left(-56-\frac{5\pi^2}{6}+\frac{11\zeta_3}{3}\right)\\ &+\epsilon^2\left(-264-\frac{16\pi^2}{3}+\frac{19\pi^4}{720}+\frac{110\zeta_3}{3}\right)\end{aligned}$$

JHEP06(2010)094

$$
\begin{aligned}
&+\epsilon^3\left(-1168-28\pi^2+\frac{19\pi^4}{72}+\frac{704\zeta_3}{3}+\frac{11\pi^2\zeta_3}{6}+35\zeta_5\right)\\
&+\epsilon^4\left(-\frac{14912}{3}-132\pi^2+\frac{76\pi^4}{45}+\frac{9011\pi^6}{90720}+1232\zeta_3+\frac{55\pi^2\zeta_3}{3}-\frac{121\zeta_3^2}{3}+350\zeta_5\right)\\
&+\mathcal{O}(\epsilon^5)\,, \qquad \text{(A.16)}\\
A_{6,1} =\ &\frac{1}{3\epsilon^3}+\frac{8}{3\epsilon^2}+\frac{1}{\epsilon}\left(\frac{44}{3}+\frac{\pi^2}{3}\right)+\left(\frac{8\pi^2}{3}+\frac{208}{3}-\frac{16\zeta_3}{3}\right)\\
&+\epsilon\left(304+\frac{44\pi^2}{3}+\frac{2\pi^4}{15}-\frac{128\zeta_3}{3}\right)\\
&+\epsilon^2\left(1280+\frac{208\pi^2}{3}+\frac{16\pi^4}{15}-\frac{704\zeta_3}{3}-\frac{16\pi^2\zeta_3}{3}-56\zeta_5\right)\\
&+\epsilon^3\left(\frac{15808}{3}+304\pi^2+\frac{88\pi^4}{15}-\frac{55\pi^6}{567}-\frac{3328\zeta_3}{3}-\frac{128\pi^2\zeta_3}{3}+\frac{128\zeta_3^2}{3}-448\zeta_5\right)\\
&+\mathcal{O}(\epsilon^4)\,, \qquad \text{(A.17)}\\
A_{6,2} =\ &\frac{2\zeta_3}{\epsilon}+\left(\frac{7\pi^4}{180}+18\zeta_3\right)\\
&+\epsilon\left(\frac{7\pi^4}{20}+122\zeta_3-\frac{2\pi^2\zeta_3}{3}+10\zeta_5\right)\\
&+\epsilon^2\left(\frac{427\pi^4}{180}-\frac{163\pi^6}{7560}+738\zeta_3-6\pi^2\zeta_3-76\zeta_3^2+90\zeta_5\right)+\mathcal{O}(\epsilon^3)\,, \qquad \text{(A.18)}\\
A_{6,3} =\ &\frac{1}{6\epsilon^3}+\frac{3}{2\epsilon^2}+\frac{1}{\epsilon}\left(\frac{55}{6}+\frac{\pi^2}{6}\right)+\left(\frac{3\pi^2}{2}+\frac{95}{2}-\frac{17\zeta_3}{3}\right)\\
&+\epsilon\left(\frac{1351}{6}+\frac{55\pi^2}{6}+\frac{\pi^4}{90}-51\zeta_3\right)\\
&+\epsilon^2\left(\frac{2023}{2}+\frac{95\pi^2}{2}+\frac{\pi^4}{10}-\frac{935\zeta_3}{3}-\frac{10\pi^2\zeta_3}{3}-65\zeta_5\right)\\
&+\epsilon^3\left(\frac{26335}{6}+\frac{1351\pi^2}{6}+\frac{11\pi^4}{18}-\frac{7\pi^6}{54}-1615\zeta_3-30\pi^2\zeta_3+\frac{268\zeta_3^2}{3}-585\zeta_5\right)\\
&+\mathcal{O}(\epsilon^4)\,, \qquad \text{(A.19)}\\
A_{7,1} =\ &\frac{1}{4\epsilon^5}+\frac{1}{2\epsilon^4}+\frac{1}{\epsilon^3}\left(1-\frac{\pi^2}{6}\right)+\frac{1}{\epsilon^2}\left(2-\frac{\pi^2}{3}-10\zeta_3\right)\\
&+\frac{1}{\epsilon}\left(4-\frac{2\pi^2}{3}-\frac{11\pi^4}{45}-20\zeta_3\right)\\
&+\left(-\frac{22\pi^4}{45}-\frac{4\pi^2}{3}+\frac{14\pi^2\zeta_3}{3}+8-40\zeta_3-88\zeta_5\right)\\
&+\epsilon\left(16-\frac{8\pi^2}{3}-\frac{44\pi^4}{45}-\frac{943\pi^6}{7560}-80\zeta_3+\frac{28\pi^2\zeta_3}{3}+196\zeta_3^2-176\zeta_5\right)\\
&+\mathcal{O}(\epsilon^2)\,, \qquad \text{(A.20)}\\
A_{7,2} =\ &\frac{\pi^2}{12\epsilon^3}+\frac{1}{\epsilon^2}\left(\frac{\pi^2}{6}+2\zeta_3\right)+\frac{1}{\epsilon}\left(\frac{\pi^2}{3}+\frac{83\pi^4}{720}+4\zeta_3\right)
\end{aligned}
$$

JHEP06(2010)094

$$
\begin{aligned}
&+\left(\frac{2\pi^2}{3}+\frac{83\pi^4}{360}+8\zeta_3-\frac{5\pi^2\zeta_3}{3}+15\zeta_5\right)\\
&+\epsilon\left(\frac{4\pi^2}{3}+\frac{83\pi^4}{180}+\frac{2741\pi^6}{90720}+16\zeta_3-\frac{10\pi^2\zeta_3}{3}-73\zeta_3^2+30\zeta_5\right)\\
&+\mathcal{O}(\epsilon^2)\,, \qquad \text{(A.21)}\\
A_{7,3} &= +\frac{1}{\epsilon}\left(-\frac{\pi^2\zeta_3}{6}-10\zeta_5\right)+\left(-\frac{119\pi^6}{2160}-\frac{31\zeta_3^2}{2}\right)+\mathcal{O}(\epsilon)\,, \qquad \text{(A.22)}\\
A_{7,4} &= \frac{6\zeta_3}{\epsilon^2}+\frac{1}{\epsilon}\left(\frac{11\pi^4}{90}+36\zeta_3\right)+\left(216\zeta_3-2\pi^2\zeta_3+\frac{11\pi^4}{15}+46\zeta_5\right)\\
&+\epsilon\left(\frac{22\pi^4}{5}-\frac{19\pi^6}{270}+1296\zeta_3-12\pi^2\zeta_3-282\zeta_3^2+276\zeta_5\right)+\mathcal{O}(\epsilon^2)\,, \qquad \text{(A.23)}\\
A_{7,5} &= +\left(2\pi^2\zeta_3+10\zeta_5\right)+\epsilon\left(\frac{11\pi^6}{162}+12\pi^2\zeta_3+18\zeta_3^2+60\zeta_5\right)+\mathcal{O}(\epsilon^2)\,, \qquad \text{(A.24)}\\
A_{8,1} &= -\frac{8\zeta_3}{3\epsilon^2}+\frac{1}{\epsilon}\left(-\frac{5\pi^4}{27}+8\zeta_3\right)+\left(\frac{5\pi^4}{9}-24\zeta_3+\frac{52\pi^2\zeta_3}{9}-\frac{352\zeta_5}{3}\right)\\
&+\epsilon\left(-\frac{5\pi^4}{3}-\frac{1709\pi^6}{8505}+72\zeta_3-\frac{52\pi^2\zeta_3}{3}+\frac{332\zeta_3^2}{3}+352\zeta_5\right)+\mathcal{O}(\epsilon^2)\,. \qquad \text{(A.25)}
\end{aligned}
$$

The most complicated three-loop vertex integrals are the nine-line master integrals [57]:

$$
\begin{aligned}
A_{9,1} &= -\frac{1}{18\epsilon^5}+\frac{1}{2\epsilon^4}+\frac{1}{\epsilon^3}\left(-\frac{53}{18}-\frac{4\pi^2}{27}\right)\\
&+\frac{1}{\epsilon^2}\left(\frac{29}{2}+\frac{22\pi^2}{27}-2\zeta_3\right)\\
&+\frac{1}{\epsilon}\left(-\frac{8\pi^2}{3}+\frac{158\zeta_3}{9}-\frac{20\pi^4}{81}-\frac{129}{2}\right)\\
&+\left(\frac{322\pi^4}{405}+6\pi^2-\frac{14\pi^2\zeta_3}{3}+\frac{537}{2}-\frac{578\zeta_3}{9}-\frac{238\zeta_5}{3}\right)\\
&+\epsilon\left(-\frac{2133}{2}-4\pi^2-\frac{302\pi^4}{135}-\frac{2398\pi^6}{5103}+158\zeta_3-\frac{26\pi^2\zeta_3}{3}-\frac{466\zeta_3^2}{3}+\frac{826\zeta_5}{3}\right)\\
&+\mathcal{O}(\epsilon^2)\,, \qquad \text{(A.26)}\\
A_{9,2} &= \frac{2}{9\epsilon^6}+\frac{5}{6\epsilon^5}+\frac{1}{\epsilon^4}\left(-\frac{20}{9}-\frac{7\pi^2}{27}\right)\\
&+\frac{1}{\epsilon^3}\left(\frac{50}{9}-\frac{17\pi^2}{27}-\frac{91\zeta_3}{9}\right)\\
&+\frac{1}{\epsilon^2}\left(\frac{4\pi^2}{3}-\frac{166\zeta_3}{9}-\frac{373\pi^4}{1080}-\frac{110}{9}\right)\\
&+\frac{1}{\epsilon}\left(\frac{494\zeta_3}{9}+\frac{179\pi^2\zeta_3}{27}-167\zeta_5-\frac{16\pi^2}{9}-\frac{187\pi^4}{540}+\frac{170}{9}\right)\\
&+\left(\frac{130}{9}-\frac{32\pi^2}{9}-\frac{1466\zeta_3}{9}+\frac{679\pi^4}{540}+\frac{682\pi^2\zeta_3}{27}-\frac{1390\zeta_5}{3}-\frac{59797\pi^6}{136080}+\frac{169\zeta_3^2}{9}\right)\\
&+\mathcal{O}(\epsilon)\,, \qquad \text{(A.27)}
\end{aligned}
$$

JHEP06(2010)094

$$
\begin{aligned}
A_{9,4} = & \frac{1}{9\epsilon^6} + \frac{8}{9\epsilon^5} + \frac{1}{\epsilon^4}\left(-1 - \frac{10\pi^2}{27}\right) \\
& + \frac{1}{\epsilon^3}\left(-\frac{14}{9} - \frac{47\pi^2}{27} - 12\zeta_3\right) \\
& + \frac{1}{\epsilon^2}\left(17 + \frac{71\pi^2}{27} - \frac{200\zeta_3}{3} - \frac{47\pi^4}{810}\right) \\
& + \frac{1}{\epsilon}\left(-84 - \pi^2 + \frac{940\zeta_3}{9} - \frac{671\pi^4}{540} + \frac{652\pi^2\zeta_3}{27} - \frac{692\zeta_5}{9}\right) \\
& + \left(339 - 15\pi^2 - \frac{448\zeta_3}{9} + \frac{2689\pi^4}{1620} + \frac{2188\pi^2\zeta_3}{27} - 524\zeta_5 + \frac{53563\pi^6}{102060} + \frac{4564\zeta_3^2}{9}\right) \\
& + \mathcal{O}(\epsilon)\,, \qquad \text{(A.28)}
\end{aligned}
$$

where the analytic expressions for $A_{9,1}$ and for the pole parts of $A_{9,2}$ and $A_{9,4}$ were obtained independently in [56]. For the corresponding integrals with homogeneous transcendentality, one finds:

$$
\begin{aligned}
A_{9,1n} = & \frac{1}{36\epsilon^6} + \frac{\pi^2}{18\epsilon^4} + \frac{14\zeta_3}{9\epsilon^3} + \frac{47\pi^4}{405\epsilon^2} \\
& + \left(\frac{85}{27}\pi^2\zeta_3 + 20\zeta_5\right)\frac{1}{\epsilon} + \frac{1160\pi^6}{5103} + \frac{137}{3}\zeta_3^2 + \mathcal{O}(\epsilon) \qquad \text{(A.29)} \\
A_{9,2n} = & \frac{2}{9\epsilon^6} - \frac{7\pi^2}{27\epsilon^4} - \frac{91\zeta_3}{9\epsilon^3} - \frac{373\pi^4}{1080\epsilon^2} \\
& + \left(\frac{179}{27}\pi^2\zeta_3 - 167\zeta_5\right)\frac{1}{\epsilon} - \frac{59797}{136080}\pi^6 + \frac{169}{9}\zeta_3^2 + \mathcal{O}(\epsilon) \qquad \text{(A.30)} \\
A_{9,4n} = & -\frac{1}{9\epsilon^6} + \frac{10\pi^2}{27\epsilon^4} + \frac{12\zeta_3}{\epsilon^3} + \frac{47\pi^4}{810\epsilon^2} \\
& + \left(-\frac{652}{27}\pi^2\zeta_3 + \frac{692}{9}\zeta_5\right)\frac{1}{\epsilon} - \frac{53563}{102060}\pi^6 - \frac{4564}{9}\zeta_3^2 + \mathcal{O}(\epsilon) \qquad \text{(A.31)}
\end{aligned}
$$

B Form factors in terms of master integrals

The unrenormalised three-loop form factors can be expressed as a linear combination of master integrals. In the colour factor decomposition as defined in (5.1) and (5.2), these coefficients read:

$$
\begin{aligned}
& X^q_{C_F^3} = \\
& -B_{4,1}\left(+\frac{489406D^3}{625} - \frac{43304589D^2}{3125} + \frac{615952127D}{7500} + \frac{34015}{4(2D-7)} - \frac{109222498}{75(2D-9)}\right. \\
& \quad + \frac{50720}{9(3D-10)} + \frac{6816654}{11(3D-14)} + \frac{89728}{25(D-2)} - \frac{12581}{12(D-3)} + \frac{6489724}{15(D-4)} \\
& \quad + \frac{19326056092}{7734375(5D-16)} - \frac{7186019918}{78125(5D-18)} + \frac{643118017984}{703125(5D-22)} - \frac{1024}{3(D-2)^2} - \frac{779}{12(D-3)^2} \\
& \quad \left. + \frac{884312}{5(D-4)^2} + \frac{1187096}{15(D-4)^3} + \frac{745376}{15(D-4)^4} + \frac{91648}{5(D-4)^5} - \frac{53258146831}{562500}\right)
\end{aligned}
$$

JHEP06(2010)094

$$
\begin{aligned}
&-A_{5,1}\Bigg(+\frac{54568D^3}{625}-\frac{16060301D^2}{9375}+\frac{135964099D}{11250}-\frac{7315}{2(2D-7)}-\frac{59657807}{1300(2D-9)}\\
&\quad-\frac{36208}{27(3D-10)}+\frac{142784}{75(D-2)}-\frac{106}{3(D-3)}+\frac{770008}{15(D-4)}+\frac{3481535536}{3046875(5D-16)}\\
&\quad+\frac{2887120096}{78125(5D-18)}-\frac{32265012416}{234375(5D-22)}+\frac{83104}{3(D-4)^2}+\frac{12800}{(D-4)^3}+\frac{26112}{5(D-4)^4}\\
&\quad-\frac{35332079719}{1687500}\Bigg)\\
&+A_{5,2}\Bigg(+\frac{87316D^3}{1875}-\frac{8532244D^2}{9375}+\frac{15436454D}{3125}+\frac{418}{(2D-7)}+\frac{3273151}{325(2D-9)}\\
&\quad+\frac{9920}{27(3D-10)}+\frac{2913100}{99(3D-14)}+\frac{400}{27(3D-8)}+\frac{152056}{225(D-2)}-\frac{70952}{15(D-4)}\\
&\quad-\frac{9365062376}{33515625(5D-16)}-\frac{368980436}{78125(5D-18)}-\frac{37325556352}{703125(5D-22)}-\frac{512}{3(D-2)^2}-\frac{97088}{15(D-4)^2}\\
&\quad-\frac{19392}{5(D-4)^3}-\frac{22016}{15(D-4)^4}-\frac{3578943149}{421875}\Bigg)\\
&-B_{5,1}\Bigg(+\frac{46827D^3}{5000}-\frac{7169631D^2}{50000}+\frac{221676243D}{100000}+\frac{177975}{64(2D-7)}-\frac{2274503}{130(2D-9)}\\
&\quad+\frac{9728}{15(D-2)}-\frac{151}{2(D-3)}+\frac{44476}{5(D-4)}-\frac{50689072}{3046875(5D-16)}+\frac{648026848}{78125(5D-18)}\\
&\quad+\frac{1055401984}{78125(5D-22)}+\frac{53792}{5(D-4)^2}+\frac{33824}{5(D-4)^3}+\frac{19072}{5(D-4)^4}-\frac{3774996391}{1000000}\Bigg)\\
&+B_{5,2}\Bigg(+\frac{105167D^3}{1875}-\frac{33225224D^2}{28125}+\frac{792891607D}{84375}-\frac{1654184}{65(2D-9)}-\frac{4912}{81(3D-10)}\\
&\quad+\frac{29696}{15(D-2)}+\frac{150868}{15(D-4)}+\frac{500415488}{3046875(5D-16)}+\frac{470084528}{78125(5D-18)}+\frac{3580901184}{78125(5D-22)}\\
&\quad+\frac{29936}{3(D-4)^2}+\frac{22112}{3(D-4)^3}+\frac{46592}{15(D-4)^4}-\frac{21148347004}{1265625}\Bigg)\\
&-A_{6,1}\Bigg(+\frac{2207D^3}{375}-\frac{7837D^2}{50}+\frac{62616143D}{56250}+\frac{291310}{297(3D-14)}+\frac{2252}{9(D-2)}\\
&\quad+\frac{23}{(D-3)}+\frac{3136}{15(D-4)}+\frac{1553908}{61875(5D-16)}-\frac{5323758}{15625(5D-18)}-\frac{74762464}{46875(5D-22)}\\
&\quad+\frac{496}{5(D-4)^2}+\frac{192}{5(D-4)^3}-\frac{183504334}{84375}\Bigg)\\
&+A_{6,2}\Bigg(+\frac{39857D^3}{3000}-\frac{4628009D^2}{15000}+\frac{22107268D}{9375}-\frac{627}{16(2D-7)}+\frac{235409}{600(2D-9)}\\
&\quad+\frac{98768}{225(D-2)}-\frac{4993}{280(D-3)}+\frac{1024}{15(D-4)}+\frac{36333448}{140625(5D-16)}+\frac{446887648}{984375(5D-22)}\\
&\quad+\frac{1024}{3(D-2)^2}+\frac{58}{3(D-3)^2}+\frac{256}{15(D-4)^2}-\frac{817543919}{150000}\Bigg)\\
&-A_{6,3}\Bigg(+\frac{3422D^3}{125}-\frac{2017249D^2}{3750}+\frac{835107683D}{225000}+\frac{1045}{8(2D-7)}+\frac{4880379}{5200(2D-9)}
\end{aligned}
$$

JHEP06(2010)094

$$
\begin{aligned}
&+\frac{80}{27(3D-8)}+\frac{28736}{25(D-2)}-\frac{161}{4(D-3)}+\frac{4336}{5(D-4)}+\frac{30753004}{203125(5D-16)}\\
&-\frac{1526704}{3125(5D-18)}-\frac{85442816}{15625(5D-22)}+\frac{576}{(D-4)^2}+\frac{3392}{15(D-4)^3}-\frac{10891722217}{1350000}\Bigg)\\
&+B_{6,1}\frac{(D^2-7D+16)^3}{(D-4)^3}\\
&-B_{6,2}\Bigg(+\frac{7D^3}{8}-\frac{1109D^2}{48}+\frac{29395D}{288}+\frac{8475}{64(2D-7)}+\frac{200}{27(3D-8)}\\
&-\frac{264}{(D-4)}-\frac{152}{(D-4)^2}-\frac{160}{(D-4)^3}-\frac{374753}{1728}\Bigg)\\
&-C_{6,1}\Bigg(+\frac{7D^3}{8}-\frac{1109D^2}{48}+\frac{29395D}{288}+\frac{8475}{64(2D-7)}+\frac{200}{27(3D-8)}\\
&-\frac{264}{(D-4)}-\frac{152}{(D-4)^2}-\frac{160}{(D-4)^3}-\frac{374753}{1728}\Bigg)\\
&-A_{7,1}\Bigg(+\frac{21D^3}{50}-\frac{5907D^2}{500}+\frac{523857D}{5000}-\frac{1213}{12(2D-7)}+\frac{29539}{624(2D-9)}\\
&+\frac{64}{3(D-2)}+\frac{80}{(D-4)}-\frac{655856}{121875(5D-16)}-\frac{388064}{9375(5D-18)}-\frac{2151447}{10000}\Bigg)\\
&+A_{7,2}\Bigg(+\frac{15D^3}{16}-\frac{733D^2}{32}+\frac{228267D}{1600}+\frac{42745}{288(2D-7)}+\frac{232399}{8320(2D-9)}\\
&+\frac{488}{45(D-2)}-\frac{128}{(D-4)}-\frac{2821088}{14625(5D-16)}+\frac{47928}{125(5D-18)}-\frac{4633049}{16000}\Bigg)\\
&+A_{7,3}\Bigg(+\frac{601D^3}{1250}-\frac{60199D^2}{6250}+\frac{760189D}{6250}-\frac{1213}{12(2D-7)}+\frac{29539}{2340(2D-9)}\\
&+\frac{496}{(D-2)}+\frac{8329}{210(D-3)}-\frac{909167104}{3046875(5D-16)}+\frac{101225984}{703125(5D-18)}-\frac{15661504}{546875(5D-22)}\\
&+\frac{21}{(D-3)^2}-\frac{8803773}{15625}\Bigg)\\
&-A_{7,4}\Bigg(+\frac{2489D^3}{5000}-\frac{686707D^2}{50000}+\frac{7042751D}{60000}+\frac{865}{72(2D-7)}+\frac{235409}{2880(2D-9)}\\
&+\frac{556}{45(D-2)}-\frac{4397}{420(D-3)}-\frac{16}{5(D-4)}+\frac{93131696}{703125(5D-16)}-\frac{9430916}{703125(5D-18)}\\
&-\frac{365471216}{4921875(5D-22)}+\frac{1}{3(D-3)^2}-\frac{277480707}{1000000}\Bigg)\\
&-A_{7,5}\Bigg(+\frac{2489D^3}{5000}-\frac{686707D^2}{50000}+\frac{7042751D}{60000}+\frac{865}{72(2D-7)}+\frac{235409}{2880(2D-9)}\\
&+\frac{556}{45(D-2)}-\frac{4397}{420(D-3)}-\frac{16}{5(D-4)}+\frac{93131696}{703125(5D-16)}-\frac{9430916}{703125(5D-18)}\\
&-\frac{365471216}{4921875(5D-22)}+\frac{1}{3(D-3)^2}-\frac{277480707}{1000000}\Bigg)\\
&+A_{8,1}\Bigg(+\frac{3411D^3}{80000}-\frac{758793D^2}{800000}+\frac{3243781D}{320000}+\frac{33573}{1024(2D-7)}+\frac{32}{(D-2)}
\end{aligned}
$$

JHEP06(2010)094

$$
\begin{aligned}
&-\frac{3015}{448(D-3)}+\frac{4}{5(D-4)}+\frac{3411716}{78125(5D-16)}-\frac{8269536}{78125(5D-18)}-\frac{1425936}{546875(5D-22)}\\
&+\frac{4389}{256(2D-7)^2}-\frac{663954073}{16000000}\Bigg)\\
&-B_{8,1}\frac{(D^3-20D^2+104D-176)(D^2-7D+16)}{8(2D-7)(D-4)}\\
&-C_{8,1}\frac{(D^3-20D^2+104D-176)(D^2-7D+16)}{8(2D-7)(D-4)}\\
&+A_{9,1}\Bigg(+\frac{243D^3}{1250}-\frac{14661D^2}{3125}+\frac{257769D}{6250}+\frac{256}{5(D-2)}-\frac{225}{14(D-3)}\\
&-\frac{48}{5(D-4)}+\frac{4083992}{78125(5D-16)}+\frac{6463488}{78125(5D-18)}+\frac{2127008}{546875(5D-22)}-\frac{4086513}{31250}\Bigg)\\
&-A_{9,2}\frac{3(3D-14)(D^6-41D^5+661D^4-4992D^3+19276D^2-37104D+28288)}{10(5D-16)(5D-18)(5D-22)(D-3)}\\
&-A_{9,4}\Bigg(+\frac{567D^3}{80000}-\frac{125091D^2}{800000}+\frac{1808937D}{1600000}+\frac{4067}{2304(2D-7)}+\frac{232399}{998400(2D-9)}\\
&-\frac{16}{75(D-2)}-\frac{225}{448(D-3)}+\frac{8388688}{3046875(5D-16)}-\frac{574016}{234375(5D-18)}-\frac{7557808}{4921875(5D-22)}\\
&-\frac{38866491}{16000000}\Bigg)
\end{aligned}
$$

$$
\begin{aligned}
X^q_{C_F^2C_A}=&\\
&+B_{4,1}\Bigg(+\frac{225717D^3}{250}-\frac{9995657D^2}{625}+\frac{893831341D}{9375}+\frac{45685}{24(2D-7)}-\frac{990312631}{975(2D-9)}\\
&+\frac{116080}{21(3D-10)}+\frac{707967}{(3D-14)}-\frac{371482}{6237(D-1)}+\frac{125032}{25(D-2)}-\frac{875}{4(D-3)}\\
&+\frac{172908907}{405(D-4)}-\frac{5622111978}{2234375(5D-16)}-\frac{345702357}{3125(5D-18)}-\frac{5032168544}{46875(5D-22)}-\frac{1280}{3(D-2)^2}\\
&+\frac{9}{4(D-3)^2}+\frac{22959056}{135(D-4)^2}+\frac{3875224}{45(D-4)^3}+\frac{2622656}{45(D-4)^4}+\frac{340096}{15(D-4)^5}\\
&-\frac{2728978211}{25000}\Bigg)\\
&+A_{5,1}\Bigg(+\frac{71304D^3}{625}-\frac{12785517D^2}{6250}+\frac{156484099D}{12500}-\frac{17815}{3(2D-7)}-\frac{97578701}{2600(2D-9)}\\
&-\frac{73232}{63(3D-10)}+\frac{2467480}{27027(D-1)}+\frac{108736}{75(D-2)}-\frac{1}{(D-3)}+\frac{6422264}{135(D-4)}\\
&+\frac{9290021216}{11171875(5D-16)}+\frac{26729196704}{1015625(5D-18)}-\frac{10782693376}{78125(5D-22)}+\frac{179840}{9(D-4)^2}+\frac{130816}{15(D-4)^3}\\
&+\frac{50176}{15(D-4)^4}-\frac{23118311953}{1125000}\Bigg)\\
&-A_{5,2}\Bigg(+\frac{25782D^3}{625}-\frac{24183202D^2}{28125}+\frac{437583827D}{84375}+\frac{2036}{3(2D-7)}+\frac{7969573}{650(2D-9)}\\
&+\frac{190048}{567(3D-10)}+\frac{100850}{3(3D-14)}+\frac{16}{(3D-8)}-\frac{2178524}{81081(D-1)}+\frac{71828}{75(D-2)}
\end{aligned}
$$

JHEP06(2010)094

$$
\begin{aligned}
&-\frac{1092208}{405(D-4)}-\frac{9583273136}{33515625(5D-16)}-\frac{4168502038}{1015625(5D-18)}-\frac{14910736064}{234375(5D-22)}-\frac{640}{3(D-2)^2}\\
&-\frac{523712}{135(D-4)^2}-\frac{90176}{45(D-4)^3}-\frac{35072}{45(D-4)^4}-\frac{21872512759}{2531250}\Bigg)\\
&+B_{5,1}\Bigg(+\frac{114279D^3}{10000}-\frac{22958287D^2}{100000}+\frac{448177891D}{200000}+\frac{177975}{128(2D-7)}-\frac{326249}{26(2D-9)}\\
&+\frac{6128}{15(D-2)}-\frac{2}{(D-3)}+\frac{35294}{5(D-4)}-\frac{25589872}{3046875(5D-16)}+\frac{831628448}{78125(5D-18)}\\
&-\frac{130364416}{78125(5D-22)}+\frac{7272}{(D-4)^2}+\frac{17696}{5(D-4)^3}+\frac{10624}{5(D-4)^4}-\frac{7313613927}{2000000}\Bigg)\\
&-B_{5,2}\Bigg(+\frac{44339D^3}{625}-\frac{4405736D^2}{3125}+\frac{287753909D}{28125}-\frac{237272}{13(2D-9)}+\frac{16}{27(3D-10)}\\
&+\frac{25456}{15(D-2)}+\frac{154624}{15(D-4)}-\frac{76140512}{3046875(5D-16)}+\frac{650239528}{78125(5D-18)}+\frac{1665432384}{78125(5D-22)}\\
&+\frac{47624}{5(D-4)^2}+\frac{32416}{5(D-4)^3}+\frac{41984}{15(D-4)^4}-\frac{7361965928}{421875}\Bigg)\\
&+A_{6,1}\Bigg(+\frac{4678D^3}{625}-\frac{609667D^2}{3125}+\frac{25888633D}{18750}+\frac{10085}{9(3D-14)}+\frac{545}{54(D-1)}\\
&+\frac{5366}{15(D-2)}+\frac{18}{(D-3)}+\frac{31492}{135(D-4)}+\frac{5042024}{78125(5D-16)}-\frac{23129849}{78125(5D-18)}\\
&-\frac{142238992}{78125(5D-22)}+\frac{1264}{9(D-4)^2}+\frac{512}{15(D-4)^3}-\frac{777739429}{281250}\Bigg)\\
&-A_{6,2}\Bigg(+\frac{9671D^3}{1200}-\frac{1150061D^2}{6000}+\frac{27382277D}{18000}-\frac{509}{8(2D-7)}+\frac{5481191}{15600(2D-9)}\\
&+\frac{728}{25(D-2)}-\frac{257261}{1680(D-3)}+\frac{3164}{15(D-4)}+\frac{92725544}{121875(5D-16)}+\frac{20493136}{65625(5D-22)}\\
&+\frac{1280}{3(D-2)^2}+\frac{1}{2(D-3)^2}+\frac{3952}{45(D-4)^2}-\frac{379243601}{112500}\Bigg)\\
&+A_{6,3}\Bigg(+\frac{60679D^3}{2500}-\frac{33322501D^2}{75000}+\frac{436696447D}{150000}+\frac{2545}{12(2D-7)}+\frac{14641137}{10400(2D-9)}\\
&+\frac{16}{5(3D-8)}-\frac{250462}{19305(D-1)}+\frac{37352}{75(D-2)}-\frac{1}{4(D-3)}+\frac{106784}{135(D-4)}\\
&+\frac{3533209912}{33515625(5D-16)}-\frac{433927224}{1015625(5D-18)}-\frac{487676544}{78125(5D-22)}+\frac{27568}{45(D-4)^2}+\frac{640}{3(D-4)^3}\\
&-\frac{2875843347}{500000}\Bigg)\\
&-B_{6,2}\Bigg(+\frac{D^3}{16}+\frac{71D^2}{32}-\frac{283D}{64}-\frac{8475}{128(2D-7)}-\frac{8}{(3D-8)}\\
&-\frac{46}{9(D-1)}+\frac{1000}{9(D-4)}+\frac{80}{3(D-4)^2}+\frac{64}{(D-4)^3}+\frac{1587}{128}\Bigg)\\
&-C_{6,1}\Bigg(+\frac{D^3}{16}+\frac{71D^2}{32}-\frac{283D}{64}-\frac{8475}{128(2D-7)}-\frac{8}{(3D-8)}
\end{aligned}
$$

JHEP06(2010)094

$$
\begin{aligned}
&\quad -\frac{46}{9(D-1)}+\frac{1000}{9(D-4)}+\frac{80}{3(D-4)^2}+\frac{64}{(D-4)^3}+\frac{1587}{128}\Bigg)\\
&+A_{7,1}\Bigg(+\frac{27D^3}{50}-\frac{7009D^2}{500}+\frac{584559D}{5000}-\frac{301}{6(2D-7)}+\frac{21185}{624(2D-9)}\\
&\quad +\frac{32}{(D-2)}+\frac{80}{(D-4)}-\frac{6069872}{121875(5D-16)}-\frac{827368}{9375(5D-18)}-\frac{2492249}{10000}\Bigg)\\
&-A_{7,2}\Bigg(+\frac{517D^3}{800}-\frac{142459D^2}{8000}+\frac{9023129D}{80000}+\frac{42745}{192(2D-7)}+\frac{697197}{16640(2D-9)}\\
&\quad -\frac{1124}{143(D-1)}-\frac{76}{15(D-2)}-\frac{112}{(D-4)}-\frac{106444064}{446875(5D-16)}+\frac{9644612}{40625(5D-18)}\\
&\quad -\frac{33226167}{160000}\Bigg)\\
&-A_{7,3}\Bigg(+\frac{601D^3}{1250}-\frac{29899D^2}{6250}+\frac{152417D}{3125}-\frac{301}{6(2D-7)}+\frac{4237}{468(2D-9)}\\
&\quad +\frac{544}{3(D-2)}+\frac{3683}{210(D-3)}+\frac{10424832}{1015625(5D-16)}+\frac{54045184}{703125(5D-18)}-\frac{12403904}{546875(5D-22)}\\
&\quad -\frac{3}{(D-3)^2}-\frac{15077947}{62500}\Bigg)\\
&+A_{7,4}\Bigg(+\frac{19D^3}{80}-\frac{458683D^2}{60000}+\frac{40603349D}{600000}-\frac{235}{32(2D-7)}+\frac{5481191}{74880(2D-9)}\\
&\quad +\frac{118}{15(D-2)}-\frac{26393}{840(D-3)}-\frac{24}{5(D-4)}+\frac{46026288}{203125(5D-16)}-\frac{501158}{140625(5D-18)}\\
&\quad -\frac{21760904}{328125(5D-22)}-\frac{62067409}{400000}\Bigg)\\
&+A_{7,5}\Bigg(+\frac{19D^3}{80}-\frac{458683D^2}{60000}+\frac{40603349D}{600000}-\frac{235}{32(2D-7)}+\frac{5481191}{74880(2D-9)}\\
&\quad +\frac{118}{15(D-2)}-\frac{26393}{840(D-3)}-\frac{24}{5(D-4)}+\frac{46026288}{203125(5D-16)}-\frac{501158}{140625(5D-18)}\\
&\quad -\frac{21760904}{328125(5D-22)}-\frac{62067409}{400000}\Bigg)\\
&-A_{8,1}\Bigg(+\frac{1197D^3}{160000}-\frac{979611D^2}{1600000}+\frac{8338443D}{640000}+\frac{29027}{2048(2D-7)}+\frac{160}{3(D-2)}\\
&\quad -\frac{13665}{896(D-3)}-\frac{34}{5(D-4)}+\frac{23109548}{234375(5D-16)}-\frac{3147936}{78125(5D-18)}-\frac{1018736}{546875(5D-22)}\\
&\quad +\frac{3563}{128(2D-7)^2}-\frac{2065843091}{32000000}\Bigg)\\
&+B_{8,1}\frac{(D^3-20D^2+104D-176)(D^2-7D+16)}{16(2D-7)(D-4)}\\
&+C_{8,1}\frac{(D^3-20D^2+104D-176)(D^2-7D+16)}{16(2D-7)(D-4)}\\
&-A_{9,1}\Bigg(+\frac{243D^3}{1250}-\frac{14661D^2}{3125}+\frac{257769D}{6250}+\frac{256}{5(D-2)}-\frac{225}{14(D-3)}
\end{aligned}
$$

JHEP06(2010)094

$$-\frac{48}{5(D-4)}+\frac{4083992}{78125(5D-16)}+\frac{6463488}{78125(5D-18)}+\frac{2127008}{546875(5D-22)}-\frac{4086513}{31250}\Bigg)$$

$$+A_{9,2}\frac{(3D-14)(3D^6-108D^5+1586D^4-11304D^3+41928D^2-78208D+57984)}{10(5D-16)(5D-18)(5D-22)(D-3)}$$

$$+A_{9,4}\Bigg(+\frac{1701D^3}{160000}-\frac{375273D^2}{1600000}+\frac{5426811D}{3200000}+\frac{4067}{1536(2D-7)}+\frac{232399}{665600(2D-9)}$$

$$-\frac{8}{25(D-2)}-\frac{675}{896(D-3)}+\frac{4194344}{1015625(5D-16)}-\frac{287008}{78125(5D-18)}-\frac{3778904}{1640625(5D-22)}$$

$$-\frac{116599473}{32000000}\Bigg)$$

$$X^q_{C_FC_A^2}=$$

$$-B_{4,1}\Bigg(+\frac{153701D^3}{625}-\frac{45111262D^2}{9375}+\frac{3307905503D}{112500}-\frac{7045}{6(2D-7)}-\frac{140183197}{975(2D-9)}$$

$$-\frac{2060}{27(3D-10)}+\frac{9383166}{55(3D-14)}-\frac{165455}{2673(D-1)}+\frac{44164}{25(D-2)}+\frac{659}{12(D-3)}$$

$$+\frac{416301857}{4860(D-4)}-\frac{138263099401}{402187500(5D-16)}-\frac{5093619454}{234375(5D-18)}$$

$$-\frac{144904142656}{703125(5D-22)}-\frac{128}{(D-2)^2}$$

$$+\frac{143}{12(D-3)^2}+\frac{8793673}{405(D-4)^2}+\frac{915068}{135(D-4)^3}+\frac{345128}{45(D-4)^4}+\frac{20864}{5(D-4)^5}$$

$$-\frac{31855488829}{843750}\Bigg)$$

$$-A_{5,1}\Bigg(+\frac{4277D^3}{125}-\frac{243647D^2}{375}+\frac{106547887D}{28125}-\frac{49315}{24(2D-7)}-\frac{18960447}{2600(2D-9)}$$

$$+\frac{357584}{1323(3D-10)}+\frac{7618840}{567567(D-1)}+\frac{10064}{25(D-2)}+\frac{10}{3(D-3)}+\frac{3703898}{405(D-4)}$$

$$+\frac{332977894}{1340625(5D-16)}+\frac{563608248}{203125(5D-18)}-\frac{1415791832}{46875(5D-22)}+\frac{3488}{189(D-1)^2}+\frac{81212}{45(D-4)^2}$$

$$+\frac{11584}{45(D-4)^3}+\frac{256}{3(D-4)^4}-\frac{452116231}{67500}\Bigg)$$

$$+A_{5,2}\Bigg(+\frac{20594D^3}{1875}-\frac{6630308D^2}{28125}+\frac{25700042D}{16875}+\frac{1409}{6(2D-7)}+\frac{2348211}{650(2D-9)}$$

$$-\frac{11944}{567(3D-10)}+\frac{801980}{99(3D-14)}-\frac{10360820}{243243(D-1)}+\frac{75128}{225(D-2)}-\frac{559813}{1215(D-4)}$$

$$-\frac{1022764469}{33515625(5D-16)}-\frac{1052157372}{1015625(5D-18)}-\frac{11705152928}{703125(5D-22)}$$

$$-\frac{64}{(D-2)^2}-\frac{306428}{405(D-4)^2}$$

$$-\frac{43696}{135(D-4)^3}-\frac{1408}{15(D-4)^4}-\frac{3344023858}{1265625}\Bigg)$$

$$-B_{5,1}\Bigg(+\frac{7497D^3}{1250}-\frac{394839D^2}{3125}+\frac{10983001D}{12500}-\frac{75999}{40(2D-9)}+\frac{1424}{15(D-2)}$$

JHEP06(2010)094

$$
\begin{aligned}
&-\frac{1}{(D-3)}+\frac{1055}{(D-4)}-\frac{712201}{234375(5D-16)}+\frac{200430972}{78125(5D-18)}-\frac{146129984}{78125(5D-22)}\\
&+\frac{4176}{5(D-4)^2}+\frac{296}{(D-4)^3}+\frac{1152}{5(D-4)^4}-\frac{189456643}{125000}\Big)\\
+B_{5,2}\Big(&+\frac{13666D^3}{625}-\frac{4406452D^2}{9375}+\frac{92206756D}{28125}-\frac{13818}{5(2D-9)}+\frac{320}{27(3D-10)}\\
&+\frac{2536}{5(D-2)}+\frac{10325}{6(D-4)}-\frac{3748279}{156250(5D-16)}+\frac{169244232}{78125(5D-18)}+\frac{122152296}{78125(5D-22)}\\
&+\frac{22774}{15(D-4)^2}+\frac{15736}{15(D-4)^3}+\frac{7552}{15(D-4)^4}-\frac{2504444962}{421875}\Big)\\
-A_{6,1}\Big(&+\frac{17033D^3}{7500}-\frac{1493603D^2}{25000}+\frac{95481487D}{225000}+\frac{80198}{297(3D-14)}+\frac{1711}{288(D-1)}\\
&+\frac{1090}{9(D-2)}+\frac{113}{32(D-3)}+\frac{479}{18(D-4)}+\frac{294544271}{15468750(5D-16)}-\frac{3011532}{78125(5D-18)}\\
&-\frac{104077288}{234375(5D-22)}+\frac{1853}{144(D-1)^2}+\frac{136}{9(D-4)^2}-\frac{64}{15(D-4)^3}-\frac{1505097247}{1687500}\Big)\\
+A_{6,2}\Big(&+\frac{4249D^3}{6000}-\frac{322949D^2}{15000}+\frac{61126331D}{300000}-\frac{1409}{64(2D-7)}+\frac{403479}{5200(2D-9)}\\
&-\frac{872}{297(D-1)}+\frac{5584}{225(D-2)}-\frac{117431}{1680(D-3)}+\frac{9704}{135(D-4)}+\frac{5192329489}{20109375(5D-16)}\\
&+\frac{41976608}{984375(5D-22)}+\frac{128}{(D-2)^2}-\frac{25}{12(D-3)^2}+\frac{176}{5(D-4)^2}-\frac{846754451}{1800000}\Big)\\
-A_{6,3}\Big(&+\frac{3073D^3}{625}-\frac{831416D^2}{9375}+\frac{41933917D}{75000}+\frac{7045}{96(2D-7)}+\frac{4880379}{10400(2D-9)}\\
&-\frac{13867}{429(D-1)}+\frac{9004}{75(D-2)}+\frac{13}{4(D-3)}+\frac{293}{30(D-4)}+\frac{1849361647}{67031250(5D-16)}\\
&-\frac{49983292}{1015625(5D-18)}-\frac{118945472}{78125(5D-22)}+\frac{236}{5(D-4)^2}+\frac{96}{5(D-4)^3}-\frac{51691069}{46875}\Big)\\
-A_{7,1}\Big(&+\frac{33D^3}{200}-\frac{8111D^2}{2000}+\frac{645261D}{20000}+\frac{3}{16(2D-7)}+\frac{329}{64(2D-9)}\\
&+\frac{32}{3(D-2)}+\frac{20}{(D-4)}-\frac{220844}{9375(5D-16)}-\frac{105556}{3125(5D-18)}-\frac{2833051}{40000}\Big)\\
+A_{7,2}\Big(&+\frac{71D^3}{800}-\frac{25417D^2}{8000}+\frac{1658227D}{80000}+\frac{42745}{576(2D-7)}+\frac{232399}{16640(2D-9)}\\
&-\frac{562}{143(D-1)}-\frac{236}{45(D-2)}-\frac{24}{(D-4)}-\frac{285048488}{4021875(5D-16)}+\frac{928156}{40625(5D-18)}\\
&-\frac{5030461}{160000}\Big)\\
-A_{7,3}\Big(&+\frac{3D^3}{625}-\frac{2023D^2}{12500}-\frac{41819D}{12500}-\frac{3}{16(2D-7)}-\frac{329}{240(2D-9)}\\
&-\frac{44}{3(D-2)}-\frac{263}{105(D-3)}-\frac{2204608}{234375(5D-16)}-\frac{33404}{78125(5D-18)}+\frac{2035336}{546875(5D-22)}
\end{aligned}
$$

JHEP06(2010)094

$$+\frac{7}{4(D-3)^2}+\frac{421802}{15625}\Bigg)$$
$$+A_{7,4}\Bigg(+\frac{57D^3}{10000}+\frac{116647D^2}{300000}-\frac{2694797D}{600000}+\frac{3845}{576(2D-7)}-\frac{134493}{8320(2D-9)}$$
$$-\frac{38}{45(D-2)}+\frac{1833}{140(D-3)}+\frac{8}{5(D-4)}-\frac{732913468}{9140625(5D-16)}-\frac{368278}{234375(5D-18)}$$
$$+\frac{71838976}{4921875(5D-22)}+\frac{1}{12(D-3)^2}+\frac{16428169}{2000000}\Bigg)$$
$$+A_{7,5}\Bigg(+\frac{57D^3}{10000}+\frac{116647D^2}{300000}-\frac{2694797D}{600000}+\frac{3845}{576(2D-7)}-\frac{134493}{8320(2D-9)}$$
$$-\frac{38}{45(D-2)}+\frac{1833}{140(D-3)}+\frac{8}{5(D-4)}-\frac{732913468}{9140625(5D-16)}-\frac{368278}{234375(5D-18)}$$
$$+\frac{71838976}{4921875(5D-22)}+\frac{1}{12(D-3)^2}+\frac{16428169}{2000000}\Bigg)$$
$$-A_{8,1}\Bigg(+\frac{1107D^3}{160000}+\frac{110409D^2}{1600000}-\frac{2547331D}{640000}+\frac{2273}{2048(2D-7)}-\frac{56}{3(D-2)}$$
$$+\frac{5325}{896(D-3)}+\frac{18}{5(D-4)}-\frac{8995987}{234375(5D-16)}-\frac{493416}{78125(5D-18)}+\frac{152884}{546875(5D-22)}$$
$$-\frac{9863}{1024(2D-7)^2}+\frac{700944509}{32000000}\Bigg)$$
$$+A_{9,1}\Bigg(+\frac{243D^3}{5000}-\frac{62289D^2}{50000}+\frac{283527D}{25000}+\frac{88}{5(D-2)}-\frac{285}{56(D-3)}$$
$$-\frac{2}{(D-4)}+\frac{1549163}{78125(5D-16)}+\frac{1250592}{78125(5D-18)}+\frac{406132}{546875(5D-22)}-\frac{4692843}{125000}\Bigg)$$
$$-A_{9,2}\frac{(3D-14)(3D^6-93D^5+1189D^4-7632D^3+26028D^2-45104D+31104)}{40(5D-16)(5D-18)(5D-22)(D-3)}$$
$$-A_{9,4}\Bigg(+\frac{567D^3}{160000}-\frac{125091D^2}{1600000}+\frac{1808937D}{3200000}+\frac{4067}{4608(2D-7)}+\frac{232399}{1996800(2D-9)}$$
$$-\frac{8}{75(D-2)}-\frac{225}{896(D-3)}+\frac{4194344}{3046875(5D-16)}-\frac{287008}{234375(5D-18)}-\frac{3778904}{4921875(5D-22)}$$
$$-\frac{38866491}{32000000}\Bigg)$$
$$X^q_{C_F^2N_F}=$$
$$+B_{4,1}\Bigg(+\frac{72D^2}{5}-\frac{11524D}{75}-\frac{37120}{63(3D-10)}-\frac{742964}{6237(D-1)}+\frac{4}{(D-3)}$$
$$+\frac{10576}{81(D-4)}+\frac{319872}{1375(5D-16)}-\frac{3088}{27(D-4)^2}+\frac{1024}{9(D-4)^3}+\frac{256}{3(D-4)^4}$$
$$+\frac{412948}{1125}\Bigg)$$
$$-A_{5,1}\Bigg(+\frac{1216D^2}{75}-\frac{83936D}{375}-\frac{512}{3(3D-10)}-\frac{2293120}{11583(D-1)}-\frac{19648}{81(D-4)}$$

JHEP06(2010)094

$$
\begin{aligned}
&\quad +\frac{297024}{6875(5D-16)}+\frac{3698688}{8125(5D-18)}-\frac{6272}{27(D-4)^2}-\frac{1024}{9(D-4)^3}+\frac{983968}{1875}\Bigg)\\
&-A_{5,2}\Bigg(+\frac{4D^2}{75}-\frac{78712D}{1125}-\frac{6656}{189(3D-10)}-\frac{32}{9(3D-8)}-\frac{4357048}{81081(D-1)}\\
&\quad -\frac{20464}{81(D-4)}+\frac{131376}{6875(5D-16)}+\frac{1585152}{8125(5D-18)}-\frac{5312}{27(D-4)^2}-\frac{1024}{9(D-4)^3}\\
&\quad +\frac{2009608}{16875}\Bigg)\\
&-A_{6,1}\frac{(D^2-7D+16)(6D^3-65D^2+238D-288)(D-2)}{2(D-3)(D-1)(D-4)^2}\\
&+A_{6,3}\Bigg(+\frac{28D^2}{25}-\frac{2868D}{125}-\frac{32}{45(3D-8)}-\frac{500924}{19305(D-1)}-\frac{400}{27(D-4)}\\
&\quad -\frac{39984}{6875(5D-16)}-\frac{176128}{8125(5D-18)}-\frac{128}{9(D-4)^2}+\frac{334516}{5625}\Bigg)\\
&-B_{6,2}\frac{(D^2-7D+16)(3D^3-31D^2+110D-128)(D-2)}{(D-1)(3D-8)(D-4)^2}\\
&-C_{6,1}\frac{(D^2-7D+16)(3D^3-31D^2+110D-128)(D-2)}{(D-1)(3D-8)(D-4)^2}\\
&-A_{7,2}\frac{8(D-2)(D^4-28D^3+220D^2-696D+784)}{(5D-18)(D-1)(5D-16)}
\end{aligned}
$$

$$
\begin{aligned}
X^q_{C_FC_AN_F} &=\\
&+B_{4,1}\Bigg(+\frac{24D^2}{5}-\frac{396D}{25}-\frac{250}{3(3D-10)}+\frac{330910}{2673(D-1)}-\frac{170}{3(D-2)}\\
&\quad +\frac{34408}{243(D-4)}+\frac{92064}{1375(5D-16)}+\frac{32}{3(D-2)^2}+\frac{14624}{81(D-4)^2}+\frac{3904}{27(D-4)^3}\\
&\quad +\frac{256}{9(D-4)^4}+\frac{4364}{125}\Bigg)\\
&+A_{5,1}\Bigg(+\frac{208D^2}{75}-\frac{3656D}{125}+\frac{25352}{441(3D-10)}-\frac{4990592}{63063(D-1)}+\frac{184}{3(D-2)}\\
&\quad -\frac{992}{9(D-4)}+\frac{148512}{6875(5D-16)}+\frac{1849344}{8125(5D-18)}-\frac{6976}{189(D-1)^2}-\frac{16}{(D-2)^2}\\
&\quad +\frac{256}{27(D-4)^2}-\frac{512}{9(D-4)^3}+\frac{205952}{5625}\Bigg)\\
&+A_{5,2}\Bigg(+\frac{84D^2}{25}-\frac{6984D}{125}+\frac{460}{63(3D-10)}-\frac{20721640}{243243(D-1)}+\frac{20}{(D-2)}\\
&\quad -\frac{24568}{243(D-4)}-\frac{24312}{6875(5D-16)}+\frac{792576}{8125(5D-18)}-\frac{16}{3(D-2)^2}-\frac{5024}{81(D-4)^2}\\
&\quad -\frac{1024}{27(D-4)^3}+\frac{700768}{5625}\Bigg)\\
&+A_{6,1}\Bigg(+\frac{3D^2}{2}-\frac{47D}{4}-\frac{3073}{72(D-1)}+\frac{86}{3(D-2)}+\frac{11}{8(D-3)}
\end{aligned}
$$

JHEP06(2010)094

$$+\frac{8}{9(D-4)}-\frac{109}{4(D-1)^2}-\frac{8}{(D-2)^2}+\frac{16}{3(D-4)^2}+\frac{133}{4}\Bigg)$$

$$+A_{6,2}\frac{90D^7-1803D^6+15301D^5-70848D^4+191676D^3-299024D^2+242976D-74880}{9(5D-16)(D-3)(D-2)^2(D-1)(D-4)}$$

$$-A_{6,3}\frac{42D^7-656D^6+3854D^5-11430D^4+24896D^3-65144D^2+134560D-113856}{3(D-1)(D-2)^2(5D-18)(5D-16)}$$

$$+A_{7,2}\frac{4(D-2)(D^4-28D^3+220D^2-696D+784)}{(5D-18)(D-1)(5D-16)}$$

$$X^q_{C_F N_F^2}=$$

$$+A_{6,1}\frac{(6D^3-65D^2+238D-288)(D-2)^2}{6(D-4)(D-3)(D-1)^2}$$

$$X^q_{C_F N_{F,V}}=$$

$$+B_{4,1}\Bigg(+\frac{119132D}{625}+\frac{380}{9(2D-7)}-\frac{50245888}{975(2D-9)}+\frac{280}{3(3D-10)}+\frac{9088443}{242(3D-14)}$$
$$+\frac{9269061200}{722007(D-1)}-\frac{4169543}{675(D-2)}+\frac{182}{3(D-3)}+\frac{1194157}{54(D-4)}-\frac{57818921783}{265443750(5D-16)}$$
$$+\frac{808885693}{243750(5D-18)}+\frac{221659776}{53125(5D-22)}+\frac{15748}{9(D-2)^2}+\frac{35}{3(D-3)^2}+\frac{750554}{45(D-4)^2}$$
$$-\frac{608}{3(D-2)^3}+\frac{25148}{3(D-4)^3}+\frac{2048}{(D-4)^4}+\frac{12730856}{9375}\Bigg)$$

$$+A_{5,1}\Bigg(+\frac{12243D}{625}+\frac{665}{9(2D-7)}-\frac{448624}{325(2D-9)}-\frac{56}{3(3D-10)}+\frac{92219200}{65637(D-1)}$$
$$-\frac{83479}{225(D-2)}+\frac{10}{3(D-3)}+\frac{148888}{135(D-4)}-\frac{14475728}{446875(5D-16)}-\frac{29074423}{40625(5D-18)}$$
$$-\frac{292095986}{53125(5D-22)}-\frac{1496}{3(D-2)^2}-\frac{14608}{45(D-4)^2}+\frac{256}{(D-2)^3}-\frac{2048}{15(D-4)^3}$$
$$-\frac{2436926}{9375}\Bigg)$$

$$-A_{5,2}\Bigg(+\frac{14644D}{1875}-\frac{76}{9(2D-7)}+\frac{40784}{325(2D-9)}+\frac{56}{9(3D-10)}+\frac{215775}{121(3D-14)}$$
$$+\frac{4075274240}{2166021(D-1)}-\frac{1082473}{675(D-2)}+\frac{34666}{405(D-4)}-\frac{176454986}{132721875(5D-16)}-\frac{831538}{40625(5D-18)}$$
$$-\frac{99059576}{53125(5D-22)}+\frac{8024}{9(D-2)^2}+\frac{17912}{135(D-4)^2}-\frac{640}{3(D-2)^3}+\frac{2176}{45(D-4)^3}$$
$$+\frac{2370412}{28125}\Bigg)$$

$$+B_{5,1}\Bigg(+\frac{3474D}{625}-\frac{196273}{325(2D-9)}-\frac{25123840}{65637(D-1)}+\frac{144542}{225(D-2)}-\frac{2}{(D-3)}$$
$$+\frac{93338}{135(D-4)}+\frac{1437614}{4021875(5D-16)}-\frac{9370564}{40625(5D-18)}-\frac{39796848}{53125(5D-22)}-\frac{1984}{3(D-2)^2}$$
$$+\frac{2900}{9(D-4)^2}+\frac{224}{(D-2)^3}+\frac{1664}{15(D-4)^3}+\frac{190269}{3125}\Bigg)$$

JHEP06(2010)094

$$
\begin{aligned}
&-B_{5,2}\Bigg(+\frac{37136D}{1875}-\frac{285488}{325(2D-9)}+\frac{80}{9(3D-10)}+\frac{28564480}{65637(D-1)}+\frac{163559}{450(D-2)}\\
&\quad+\frac{150403}{135(D-4)}-\frac{25678283}{4021875(5D-16)}-\frac{13477879}{81250(5D-18)}+\frac{10007466}{53125(5D-22)}-\frac{2972}{3(D-2)^2}\\
&\quad+\frac{32612}{45(D-4)^2}+\frac{480}{(D-2)^3}+\frac{3328}{15(D-4)^3}+\frac{4577488}{28125}\Bigg)\\
&-A_{6,1}\Bigg(+\frac{49D}{625}-\frac{14385}{242(3D-14)}-\frac{58221088}{722007(D-1)}+\frac{931}{18(D-2)}+\frac{1}{2(D-3)}\\
&\quad+\frac{418}{135(D-4)}-\frac{3759722}{3403125(5D-16)}-\frac{432134}{40625(5D-18)}+\frac{3537842}{53125(5D-22)}-\frac{16}{(D-2)^2}\\
&\quad-\frac{64}{45(D-4)^2}+\frac{100399}{18750}\Bigg)\\
&-A_{6,2}\Bigg(+\frac{17533D}{3000}+\frac{19}{24(2D-7)}+\frac{10196}{975(2D-9)}+\frac{1382570}{1683(D-1)}-\frac{411274}{675(D-2)}\\
&\quad-\frac{1623}{56(D-3)}+\frac{1088}{45(D-4)}+\frac{18324568}{2413125(5D-16)}+\frac{1024224}{74375(5D-22)}+\frac{3680}{9(D-2)^2}\\
&\quad-\frac{11}{6(D-3)^2}-\frac{256}{3(D-2)^3}+\frac{42883}{1875}\Bigg)\\
&+A_{6,3}\Bigg(+\frac{26253D}{2500}-\frac{95}{36(2D-7)}+\frac{41793584}{21879(D-1)}-\frac{13967}{9(D-2)}+\frac{3}{(D-3)}\\
&\quad+\frac{3548}{45(D-4)}-\frac{359662}{103125(5D-16)}+\frac{883413}{40625(5D-18)}-\frac{12129744}{53125(5D-22)}+\frac{2048}{3(D-2)^2}\\
&\quad+\frac{352}{15(D-4)^2}-\frac{64}{(D-2)^3}-\frac{243387}{12500}\Bigg)\\
&+A_{7,1}\Bigg(+\frac{9D}{100}+\frac{37}{18(2D-7)}+\frac{2549}{1560(2D-9)}+\frac{280}{143(D-1)}+\frac{37}{90(D-2)}\\
&\quad-\frac{144076}{160875(5D-16)}+\frac{6313}{9750(5D-18)}+\frac{4}{(D-2)^2}+\frac{3927}{1000}\Bigg)\\
&-A_{7,2}\frac{5D^6-93D^5+892D^4-4656D^3+12528D^2-15472D+6080}{(D-1)(D-2)^2(5D-18)(5D-16)}\\
&-A_{7,3}\Bigg(+\frac{211D}{625}+\frac{37}{18(2D-7)}+\frac{2549}{5850(2D-9)}-\frac{5424}{187(D-1)}+\frac{2566}{75(D-2)}\\
&\quad+\frac{2}{3(D-3)}+\frac{26995456}{4021875(5D-16)}-\frac{79688}{28125(5D-18)}-\frac{56582}{53125(5D-22)}-\frac{328}{3(D-2)^2}\\
&\quad-\frac{2}{(D-3)^2}+\frac{128}{(D-2)^3}+\frac{4576}{3125}\Bigg)\\
&+A_{7,4}\Bigg(+\frac{162D}{625}-\frac{37}{72(2D-7)}+\frac{2549}{1170(2D-9)}-\frac{22736}{2431(D-1)}+\frac{754}{45(D-2)}\\
&\quad-\frac{323}{84(D-3)}-\frac{2696828}{4021875(5D-16)}+\frac{97442}{365625(5D-18)}-\frac{1877744}{1115625(5D-22)}-\frac{8}{(D-2)^2}\\
&\quad-\frac{1}{12(D-3)^2}+\frac{273763}{75000}\Bigg)
\end{aligned}
$$

JHEP06(2010)094

$$+A_{7,5}\left(+\frac{162D}{625}-\frac{37}{72(2D-7)}+\frac{2549}{1170(2D-9)}-\frac{22736}{2431(D-1)}+\frac{754}{45(D-2)}\right.$$
$$-\frac{323}{84(D-3)}-\frac{2696828}{4021875(5D-16)}+\frac{97442}{365625(5D-18)}-\frac{1877744}{1115625(5D-22)}-\frac{8}{(D-2)^2}$$
$$\left.-\frac{1}{12(D-3)^2}+\frac{273763}{75000}\right)$$
$$+A_{8,1}\left(+\frac{1107D}{80000}+\frac{1643}{768(2D-7)}-\frac{8085}{884(D-1)}+\frac{349}{45(D-2)}+\frac{1305}{448(D-3)}\right.$$
$$+\frac{22363}{28125(5D-16)}-\frac{77484}{40625(5D-18)}+\frac{85352}{1115625(5D-22)}+\frac{133}{384(2D-7)^2}-\frac{8}{(D-2)^2}$$
$$\left.-\frac{1511991}{800000}\right)$$
$$-A_{9,1}\left(+\frac{243D}{5000}+\frac{24255}{884(D-1)}-\frac{24}{(D-2)}-\frac{75}{56(D-3)}-\frac{10076}{9375(5D-16)}\right.$$
$$\left.-\frac{83136}{40625(5D-18)}+\frac{252703}{1115625(5D-22)}+\frac{16}{(D-2)^2}+\frac{5103}{25000}\right)$$
$$+A_{9,2}\frac{3(3D-14)(D-4)(D^5+25D^4-290D^3+1036D^2-1560D+928)}{20(D-1)(D-2)(D-3)(5D-22)(5D-18)(5D-16)}$$

$$X^g_{C_A^3}=$$
$$+B_{4,1}\left(+\frac{141\,D^2}{2}-\frac{2592693\,D}{500}-\frac{1120}{D}-\frac{223915}{126\,(2D-7)}+\frac{11621367296}{16575\,(2D-9)}\right.$$
$$+\frac{26512}{21\,(3D-10)}-\frac{17781309}{110\,(3D-14)}+\frac{32}{5\,(3D-8)}-\frac{9391405657}{1216215\,(D-1)}+\frac{2004296}{225\,(D-2)}$$
$$+\frac{280}{3\,(D-3)}-\frac{158773009}{1215\,(D-4)}+\frac{360}{(D-6)}-\frac{7497336208}{30121875\,(5D-14)}+\frac{1340410849}{4021875\,(5D-16)}$$
$$-\frac{3469841417}{243750\,(5D-18)}-\frac{2529983456}{3125\,(5D-22)}-\frac{55039}{432\,(D-1)^2}-\frac{25736}{5\,(D-2)^2}-\frac{1787}{16\,(D-3)^2}$$
$$-\frac{32740532}{405\,(D-4)^2}+\frac{832}{(D-2)^3}-\frac{5426656}{135\,(D-4)^3}-\frac{89824}{9\,(D-4)^4}+\frac{512}{3\,(D-4)^5}$$
$$\left.+\frac{300276143}{18750}\right)$$
$$-A_{5,1}\left(+\frac{528664\,D}{375}+\frac{152}{5\,(2D-5)}+\frac{3380}{9\,(2D-7)}-\frac{103762208}{5525\,(2D-9)}-\frac{64048}{2205\,(3D-10)}\right.$$
$$-\frac{1621951952}{567567\,(D-1)}+\frac{2189086}{225\,(D-2)}+\frac{8}{(D-3)}+\frac{1487996}{81\,(D-4)}+\frac{1440}{7\,(D-6)}$$
$$+\frac{65552704}{4303125\,(5D-14)}+\frac{1985701772}{28153125\,(5D-16)}+\frac{194176682}{40625\,(5D-18)}$$
$$-\frac{140342384}{3125\,(5D-22)}-\frac{5504}{189\,(D-1)^2}$$
$$-\frac{23952}{5\,(D-2)^2}+\frac{40016}{3\,(D-4)^2}+\frac{768}{(D-2)^3}+\frac{315872}{45\,(D-4)^3}+\frac{5888}{3\,(D-4)^4}$$
$$\left.-\frac{248426212}{28125}\right)$$

JHEP06(2010)094

$$
\begin{aligned}
&-A_{5,2}\Bigg(+\frac{797251\,D}{2250}-\frac{144}{D}-\frac{9424}{1485\,(2D-5)}+\frac{2704}{63\,(2D-7)}-\frac{9432928}{5525\,(2D-9)}\\
&\quad-\frac{34088}{945\,(3D-10)}-\frac{253295}{33\,(3D-14)}+\frac{112}{15\,(3D-8)}-\frac{734044771}{810810\,(D-1)}+\frac{1047656}{225\,(D-2)}\\
&\quad+\frac{2009948}{1215\,(D-4)}+\frac{576}{7\,(D-6)}+\frac{857312704}{90365625\,(5D-14)}\\
&\quad+\frac{1909981852}{28153125\,(5D-16)}+\frac{402543587}{446875\,(5D-18)}\\
&\quad+\frac{35345856}{3125\,(5D-22)}-\frac{497}{54\,(D-1)^2}-\frac{3184}{(D-2)^2}+\frac{1267888}{405\,(D-4)^2}+\frac{768}{(D-2)^3}\\
&\quad+\frac{333248}{135\,(D-4)^3}+\frac{7040}{9\,(D-4)^4}-\frac{225667646}{84375}\Bigg)\\
&-B_{5,1}\Bigg(+51\,D^2-\frac{495373\,D}{1000}+\frac{5681}{288\,(2D-5)}+\frac{13125}{32\,(2D-7)}-\frac{45395966}{5525\,(2D-9)}\\
&\quad-\frac{317395}{162\,(D-1)}+\frac{235954}{75\,(D-2)}+\frac{5}{2\,(D-3)}+\frac{859702}{135\,(D-4)}+\frac{51714784}{4303125\,(5D-14)}\\
&\quad-\frac{103936}{40625\,(5D-16)}-\frac{3138226}{3125\,(5D-18)}+\frac{101873408}{9375\,(5D-22)}-\frac{9056}{5\,(D-2)^2}+\frac{47116}{5\,(D-4)^2}\\
&\quad+\frac{320}{(D-2)^3}+\frac{20464}{3\,(D-4)^3}+\frac{1920}{(D-4)^4}+\frac{14613393}{12500}\Bigg)\\
&+B_{5,2}\Bigg(+\frac{218919\,D}{250}+\frac{769576}{10395\,(2D-5)}-\frac{66030496}{5525\,(2D-9)}+\frac{4784}{105\,(3D-10)}+\frac{32}{5\,(3D-8)}\\
&\quad-\frac{1921435783}{810810\,(D-1)}+\frac{582929}{75\,(D-2)}+\frac{565904}{135\,(D-4)}+\frac{72}{7\,(D-6)}-\frac{24448544}{4303125\,(5D-14)}\\
&\quad+\frac{25102328}{1340625\,(5D-16)}-\frac{415352077}{446875\,(5D-18)}+\frac{81364304}{3125\,(5D-22)}+\frac{4267}{54\,(D-1)^2}-\frac{23272}{5\,(D-2)^2}\\
&\quad+\frac{791264}{135\,(D-4)^2}+\frac{960}{(D-2)^3}+\frac{33184}{9\,(D-4)^3}+\frac{2432}{3\,(D-4)^4}-\frac{45656086}{9375}\Bigg)\\
&-A_{6,1}\Bigg(+\frac{D^2}{4}+\frac{1581\,D}{125}+\frac{50659}{198\,(3D-14)}+\frac{593}{162\,(D-1)}+\frac{179}{3\,(D-2)}\\
&\quad+\frac{199}{3\,(D-4)}+\frac{1676696}{253125\,(5D-14)}-\frac{155971}{34375\,(5D-16)}-\frac{19461}{6250\,(5D-18)}-\frac{1262352}{3125\,(5D-22)}\\
&\quad-\frac{787}{36\,(D-1)^2}-\frac{96}{5\,(D-2)^2}+\frac{132}{5\,(D-4)^2}-\frac{5861159}{112500}\Bigg)\\
&+A_{6,2}\Bigg(+\frac{28093\,D}{225}-\frac{160}{D}-\frac{551}{42\,(2D-5)}+\frac{169}{42\,(2D-7)}+\frac{2358232}{16575\,(2D-9)}\\
&\quad-\frac{25856}{297\,(D-1)}+\frac{91264}{75\,(D-2)}+\frac{4136}{105\,(D-3)}-\frac{5894}{135\,(D-4)}-\frac{16}{7\,(D-6)}\\
&\quad-\frac{265141864}{2008125\,(5D-14)}-\frac{1316274}{625625\,(5D-16)}+\frac{960816}{4375\,(5D-22)}-\frac{832}{(D-2)^2}-\frac{10}{(D-3)^2}\\
&\quad-\frac{320}{9\,(D-4)^2}-\frac{3682658}{5625}\Bigg)
\end{aligned}
$$

JHEP06(2010)094

$$
\begin{aligned}
&-A_{6,3}\Bigg(+D^2+\frac{33372\,D}{125}-\frac{845}{63\,(2D-7)}+\frac{304}{15\,(3D-8)}+\frac{4688143}{38610\,(D-1)}\\
&\quad+\frac{131356}{45\,(D-2)}+\frac{25}{2\,(D-3)}+\frac{24319}{45\,(D-4)}-\frac{29688032}{590625\,(5D-14)}+\frac{2863027}{309375\,(5D-16)}\\
&\quad+\frac{19412}{40625\,(5D-18)}-\frac{4328064}{3125\,(5D-22)}-\frac{10688}{5\,(D-2)^2}+\frac{3124}{15\,(D-4)^2}+\frac{384}{(D-2)^3}\\
&\quad+\frac{32}{(D-4)^3}-\frac{18671174}{9375}\Bigg)\\
&-B_{6,1}\Bigg(+D^3-30\,D^2+300\,D+\frac{528}{(D-2)}-\frac{192}{(D-4)}\\
&\quad-\frac{288}{(D-2)^2}-\frac{192}{(D-4)^2}+\frac{64}{(D-2)^3}-\frac{64}{(D-4)^3}-1024\Bigg)\\
&-B_{6,2}\Bigg(+\frac{27\,D^2}{2}-\frac{1689\,D}{8}+\frac{2261}{288\,(2D-5)}+\frac{625}{32\,(2D-7)}-\frac{350}{9\,(D-1)}\\
&\quad-\frac{788}{(D-2)}-\frac{610}{3\,(D-4)}+\frac{512}{(D-2)^2}-\frac{700}{3\,(D-4)^2}-\frac{128}{(D-2)^3}\\
&\quad-\frac{96}{(D-4)^3}+\frac{1765}{2}\Bigg)\\
&-C_{6,1}\Bigg(+\frac{27\,D^2}{2}-\frac{1689\,D}{8}+\frac{2261}{288\,(2D-5)}+\frac{625}{32\,(2D-7)}-\frac{350}{9\,(D-1)}\\
&\quad-\frac{788}{(D-2)}-\frac{610}{3\,(D-4)}+\frac{512}{(D-2)^2}-\frac{700}{3\,(D-4)^2}-\frac{128}{(D-2)^3}\\
&\quad-\frac{96}{(D-4)^3}+\frac{1765}{2}\Bigg)\\
&-A_{7,1}\Bigg(+\frac{27\,D}{10}+\frac{76}{77\,(2D-5)}-\frac{1198}{63\,(2D-7)}+\frac{294779}{13260\,(2D-9)}-\frac{2268}{715\,(D-1)}\\
&\quad-\frac{349}{45\,(D-2)}+\frac{20}{(D-4)}+\frac{12}{35\,(D-6)}+\frac{72}{119\,(5D-14)}-\frac{56684}{32175\,(5D-16)}\\
&\quad+\frac{139433}{10725\,(5D-18)}+\frac{8}{(D-2)^2}+\frac{873}{100}\Bigg)\\
&+A_{7,2}\Bigg(+\frac{196\,D}{25}-\frac{3098}{715\,(D-1)}+\frac{26}{(D-2)}-\frac{40}{(D-4)}-\frac{48}{35\,(D-6)}\\
&\quad-\frac{176}{125\,(5D-14)}+\frac{5304}{1925\,(5D-16)}+\frac{122054}{1625\,(5D-18)}-\frac{16}{(D-2)^2}-\frac{4618}{125}\Bigg)\\
&+A_{7,3}\Bigg(+\frac{6516\,D}{125}+\frac{57}{(2D-5)}-\frac{1198}{63\,(2D-7)}+\frac{294779}{49725\,(2D-9)}-\frac{502}{(D-1)}\\
&\quad+\frac{361018}{225\,(D-2)}+\frac{4258}{35\,(D-3)}-\frac{14232368}{74375\,(5D-14)}-\frac{5003392}{73125\,(5D-16)}+\frac{176798}{5625\,(5D-18)}\\
&\quad-\frac{164176}{13125\,(5D-22)}-\frac{1840}{(D-2)^2}-\frac{10}{(D-3)^2}+\frac{512}{(D-2)^3}-\frac{328828}{625}\Bigg)\\
&-A_{7,4}\Bigg(+\frac{8401\,D}{1000}-\frac{19}{16\,(2D-5)}+\frac{599}{126\,(2D-7)}+\frac{294779}{9945\,(2D-9)}+\frac{43}{60\,(D-1)}
\end{aligned}
$$

JHEP06(2010)094

$$+\frac{1234}{45\,(D-2)}-\frac{717}{140\,(D-3)}-\frac{4}{5\,(D-6)}+\frac{11198396}{1115625\,(5D-14)}-\frac{1234996}{365625\,(5D-16)}$$
$$-\frac{119686}{28125\,(5D-18)}-\frac{1761496}{65625\,(5D-22)}-\frac{16}{(D-2)^2}+\frac{1}{4\,(D-3)^2}-\frac{1219407}{50000}\Bigg)$$
$$-A_{7,5}\Bigg(+\frac{8401\,D}{1000}-\frac{19}{16\,(2D-5)}+\frac{599}{126\,(2D-7)}+\frac{294779}{9945\,(2D-9)}+\frac{43}{60\,(D-1)}$$
$$+\frac{1234}{45\,(D-2)}-\frac{717}{140\,(D-3)}-\frac{4}{5\,(D-6)}+\frac{11198396}{1115625\,(5D-14)}-\frac{1234996}{365625\,(5D-16)}$$
$$-\frac{119686}{28125\,(5D-18)}-\frac{1761496}{65625\,(5D-22)}-\frac{16}{(D-2)^2}+\frac{1}{4\,(D-3)^2}-\frac{1219407}{50000}\Bigg)$$
$$-A_{8,1}\Bigg(+\frac{837\,D}{1000}-\frac{463}{84\,(2D-7)}+\frac{844}{45\,(D-2)}+\frac{15}{14\,(D-3)}-\frac{4}{(D-4)}$$
$$-\frac{79508}{21875\,(5D-14)}+\frac{112651}{28125\,(5D-16)}+\frac{95172}{3125\,(5D-18)}$$
$$+\frac{80068}{65625\,(5D-22)}+\frac{169}{96\,(2D-7)^2}$$
$$-\frac{16}{(D-2)^2}-\frac{807543}{100000}\Bigg)$$
$$-B_{8,1}\frac{3\,(D-3)\,(3D-8)\,(D^3-16\,D^2+68\,D-88)}{4\,(2D-5)\,(D-2)\,(2D-7)\,(D-4)}$$
$$-C_{8,1}\frac{3\,(D-3)\,(3D-8)\,(D^3-16\,D^2+68\,D-88)}{4\,(2D-5)\,(D-2)\,(2D-7)\,(D-4)}$$
$$+A_{9,1}\Bigg(+\frac{729\,D}{500}+\frac{132}{5\,(D-2)}+\frac{15}{28\,(D-3)}-\frac{2}{(D-4)}-\frac{16464}{3125\,(5D-14)}$$
$$+\frac{13794}{3125\,(5D-16)}+\frac{1872}{3125\,(5D-18)}+\frac{30056}{21875\,(5D-22)}-\frac{96}{5\,(D-2)^2}-\frac{156321}{12500}\Bigg)$$
$$-A_{9,2}\frac{3\,(3D-14)\,(75\,D^6-1048\,D^5+5956\,D^4-17776\,D^3+30208\,D^2-29440\,D+13952)}{10\,(D-2)\,(D-3)\,(5D-22)\,(5D-14)\,(5D-16)\,(5D-18)}$$

$$X^g_{C_A^2 N_F}=$$
$$-B_{4,1}\Bigg(+\frac{37168\,D^2}{125}-\frac{5809119\,D}{1250}+\frac{2240}{3\,D}+\frac{34925}{126\,(2D-7)}+\frac{104123558}{3315\,(2D-9)}$$
$$+\frac{11162}{21\,(3D-10)}-\frac{2318004}{385\,(3D-14)}+\frac{64}{45\,(3D-8)}+\frac{77206856351}{4864860\,(D-1)}-\frac{657533}{90\,(D-2)}$$
$$-\frac{41}{12\,(D-3)}-\frac{8729134}{1215\,(D-4)}+\frac{180}{(D-6)}-\frac{563997052}{6024375\,(5D-14)}+\frac{538277353}{4021875\,(5D-16)}$$
$$+\frac{16666937}{81250\,(5D-18)}-\frac{1207808264}{28125\,(5D-22)}+\frac{7637}{36\,(D-1)^2}+\frac{6740}{3\,(D-2)^2}-\frac{151}{4\,(D-3)^2}$$
$$+\frac{783268}{405\,(D-4)^2}-\frac{896}{3\,(D-2)^3}+\frac{313448}{135\,(D-4)^3}+\frac{29312}{45\,(D-4)^4}+\frac{27982342}{5625}\Bigg)$$
$$-A_{5,1}\Bigg(+\frac{6881\,D^2}{125}-\frac{7596253\,D}{11250}+\frac{608}{5\,(2D-5)}+\frac{1075}{18\,(2D-7)}+\frac{27315013}{22100\,(2D-9)}$$
$$-\frac{212536}{6615\,(3D-10)}-\frac{3290734688}{567567\,(D-1)}+\frac{239912}{75\,(D-2)}+\frac{8}{(D-3)}-\frac{3016}{3\,(D-4)}$$

JHEP06(2010)094

$$
\begin{aligned}
&-\frac{720}{7\,(D-6)}-\frac{19049176}{4303125\,(5D-14)}-\frac{160235632}{5630625\,(5D-16)}\\
&+\frac{67577636}{40625\,(5D-18)}+\frac{10234588}{9375\,(5D-22)}\\
&-\frac{11008}{189\,(D-1)^2}-\frac{4928}{3\,(D-2)^2}-\frac{62704}{135\,(D-4)^2}+\frac{256}{(D-2)^3}-\frac{19264}{45\,(D-4)^3}\\
&+\frac{183292489}{67500}\Bigg)\\
+A_{5,2}\Bigg(&+\frac{7688\,D^2}{375}-\frac{822412\,D}{1875}+\frac{96}{D}+\frac{37696}{1485\,(2D-5)}-\frac{430}{63\,(2D-7)}\\
&-\frac{2489693}{5525\,(2D-9)}-\frac{20648}{945\,(3D-10)}-\frac{66040}{231\,(3D-14)}+\frac{224}{135\,(3D-8)}+\frac{247020002}{135135\,(D-1)}\\
&-\frac{111043}{75\,(D-2)}+\frac{377408}{1215\,(D-4)}+\frac{288}{7\,(D-6)}+\frac{67345168}{3614625\,(5D-14)}+\frac{73779424}{9384375\,(5D-16)}\\
&-\frac{137313893}{446875\,(5D-18)}+\frac{19692512}{28125\,(5D-22)}+\frac{994}{27\,(D-1)^2}+\frac{504}{(D-2)^2}+\frac{125248}{405\,(D-4)^2}\\
&-\frac{256}{3\,(D-2)^3}+\frac{4480}{27\,(D-4)^3}+\frac{3858677}{3375}\Bigg)\\
+B_{5,1}\Bigg(&+\frac{1397\,D^2}{1000}+\frac{646933\,D}{10000}-\frac{5681}{72\,(2D-5)}-\frac{6125}{96\,(2D-7)}-\frac{2169937}{5525\,(2D-9)}\\
&+\frac{317395}{81\,(D-1)}-\frac{541766}{225\,(D-2)}-\frac{1}{2\,(D-3)}-\frac{1862}{45\,(D-4)}+\frac{49642912}{4303125\,(5D-14)}\\
&-\frac{488704}{365625\,(5D-16)}+\frac{1246}{125\,(5D-18)}+\frac{14295008}{9375\,(5D-22)}+\frac{3136}{3\,(D-2)^2}+\frac{3136}{45\,(D-4)^2}\\
&-\frac{128}{(D-2)^3}+\frac{1312}{15\,(D-4)^3}-\frac{11790061}{20000}\Bigg)\\
+B_{5,2}\Bigg(&+\frac{871\,D^2}{75}-\frac{1716962\,D}{5625}+\frac{3078304}{10395\,(2D-5)}+\frac{3156272}{5525\,(2D-9)}-\frac{256}{945\,(3D-10)}\\
&-\frac{64}{45\,(3D-8)}-\frac{1836706258}{405405\,(D-1)}+\frac{1384157}{450\,(D-2)}-\frac{15388}{405\,(D-4)}-\frac{36}{7\,(D-6)}\\
&+\frac{1683416}{53125\,(5D-14)}+\frac{137885032}{28153125\,(5D-16)}\\
&+\frac{88774237}{893750\,(5D-18)}-\frac{6784148}{3125\,(5D-22)}+\frac{502}{3\,(D-1)^2}\\
&-\frac{5348}{3\,(D-2)^2}-\frac{21104}{135\,(D-4)^2}+\frac{224}{(D-2)^3}-\frac{4672}{45\,(D-4)^3}+\frac{18770368}{16875}\Bigg)\\
-A_{6,1}\Bigg(&+\frac{197\,D^2}{50}-\frac{2993\,D}{50}-\frac{6604}{693\,(3D-14)}-\frac{4333}{81\,(D-1)}-\frac{159}{5\,(D-2)}\\
&+\frac{44}{45\,(D-4)}-\frac{3850072}{354375\,(5D-14)}+\frac{4564}{4125\,(5D-16)}-\frac{11563}{625\,(5D-18)}+\frac{17696}{1875\,(5D-22)}\\
&-\frac{443}{9\,(D-1)^2}-\frac{8}{(D-4)^2}+\frac{1203449}{5625}\Bigg)
\end{aligned}
$$

JHEP06(2010)094

$$
\begin{aligned}
&+A_{6,2}\Bigg(+\frac{119\,D^2}{50}-\frac{84531\,D}{1000}-\frac{320}{3\,D}-\frac{1102}{21\,(2D-5)}+\frac{215}{336\,(2D-7)}\\
&\quad-\frac{93023}{7800\,(2D-9)}-\frac{51712}{297\,(D-1)}-\frac{19264}{75\,(D-2)}-\frac{4183}{210\,(D-3)}-\frac{1084}{135\,(D-4)}\\
&\quad+\frac{8}{7\,(D-6)}+\frac{38037128}{118125\,(5D-14)}-\frac{161431412}{5630625\,(5D-16)}-\frac{331172}{39375\,(5D-22)}+\frac{272}{3\,(D-2)^2}\\
&\quad+\frac{4}{(D-3)^2}-\frac{64}{3\,(D-2)^3}+\frac{40336667}{90000}\Bigg)\\
&-A_{6,3}\Bigg(+\frac{921\,D^2}{100}-\frac{1571239\,D}{9000}-\frac{1075}{504\,(2D-7)}-\frac{4757193}{88400\,(2D-9)}-\frac{608}{135\,(3D-8)}\\
&\quad+\frac{4688143}{19305\,(D-1)}-\frac{116434}{225\,(D-2)}-\frac{3}{(D-3)}+\frac{112}{45\,(D-4)}+\frac{139041824}{2008125\,(5D-14)}\\
&\quad-\frac{1488052}{804375\,(5D-16)}-\frac{2138}{1625\,(5D-18)}+\frac{20224}{625\,(5D-22)}+\frac{32}{(D-2)^2}-\frac{24}{5\,(D-4)^2}\\
&\quad+\frac{128}{(D-2)^3}+\frac{182032831}{270000}\Bigg)\\
&-B_{6,2}\Bigg(+\frac{7\,D^2}{8}-\frac{185\,D}{16}+\frac{2261}{72\,(2D-5)}+\frac{875}{288\,(2D-7)}-\frac{700}{9\,(D-1)}\\
&\quad+\frac{592}{9\,(D-2)}+\frac{62}{9\,(D-4)}-\frac{160}{3\,(D-2)^2}+\frac{8}{(D-4)^2}+\frac{793}{32}\Bigg)\\
&-C_{6,1}\Bigg(+\frac{7\,D^2}{8}-\frac{185\,D}{16}+\frac{2261}{72\,(2D-5)}+\frac{875}{288\,(2D-7)}-\frac{700}{9\,(D-1)}\\
&\quad+\frac{592}{9\,(D-2)}+\frac{62}{9\,(D-4)}-\frac{160}{3\,(D-2)^2}+\frac{8}{(D-4)^2}+\frac{793}{32}\Bigg)\\
&-A_{7,1}\Bigg(+\frac{4\,D^2}{25}-\frac{1437\,D}{500}+\frac{304}{77\,(2D-5)}-\frac{451}{126\,(2D-7)}-\frac{28181}{26520\,(2D-9)}\\
&\quad-\frac{9248}{2145\,(D-1)}-\frac{263}{30\,(D-2)}-\frac{6}{35\,(D-6)}+\frac{2253164}{223125\,(5D-14)}+\frac{38046376}{5630625\,(5D-16)}\\
&\quad-\frac{7073303}{536250\,(5D-18)}-\frac{20}{3\,(D-2)^2}+\frac{10761}{1000}\Bigg)\\
&+A_{7,2}\Bigg(+\frac{17\,D^2}{80}-\frac{2237\,D}{400}-\frac{71585}{8064\,(2D-7)}-\frac{226533}{141440\,(2D-9)}-\frac{6196}{715\,(D-1)}\\
&\quad+\frac{142}{45\,(D-2)}+\frac{24}{35\,(D-6)}+\frac{63088}{14875\,(5D-14)}+\frac{105104}{375375\,(5D-16)}+\frac{55686}{1625\,(5D-18)}\\
&\quad-\frac{32}{3\,(D-2)^2}+\frac{35181}{1600}\Bigg)\\
&+A_{7,3}\Bigg(+\frac{11\,D^2}{125}-\frac{4966\,D}{625}+\frac{228}{(2D-5)}-\frac{451}{126\,(2D-7)}-\frac{28181}{99450\,(2D-9)}\\
&\quad-\frac{1004}{(D-1)}+\frac{141554}{225\,(D-2)}-\frac{202}{5\,(D-3)}+\frac{63075448}{371875\,(5D-14)}+\frac{1714432}{73125\,(5D-16)}\\
&\quad+\frac{129298}{28125\,(5D-18)}+\frac{2948}{9375\,(5D-22)}-\frac{480}{(D-2)^2}+\frac{2}{(D-3)^2}+\frac{128}{(D-2)^3}
\end{aligned}
$$

JHEP06(2010)094

$$+\frac{52438}{625}\Bigg)$$

$$-A_{7,4}\Bigg(+\frac{21\,D^2}{1000}-\frac{15043\,D}{5000}-\frac{19}{4\,(2D-5)}+\frac{6805}{4032\,(2D-7)}-\frac{93023}{37440\,(2D-9)}$$
$$+\frac{43}{30\,(D-1)}-\frac{779}{45\,(D-2)}+\frac{467}{210\,(D-3)}+\frac{2}{5\,(D-6)}+\frac{1100828}{65625\,(5D-14)}$$
$$-\frac{2621912}{365625\,(5D-16)}-\frac{4403}{5625\,(5D-18)}+\frac{393514}{196875\,(5D-22)}+\frac{1}{4\,(D-3)^2}+\frac{916069}{60000}\Bigg)$$

$$-A_{7,5}\Bigg(+\frac{21\,D^2}{1000}-\frac{15043\,D}{5000}-\frac{19}{4\,(2D-5)}+\frac{6805}{4032\,(2D-7)}-\frac{93023}{37440\,(2D-9)}$$
$$+\frac{43}{30\,(D-1)}-\frac{779}{45\,(D-2)}+\frac{467}{210\,(D-3)}+\frac{2}{5\,(D-6)}+\frac{1100828}{65625\,(5D-14)}$$
$$-\frac{2621912}{365625\,(5D-16)}-\frac{4403}{5625\,(5D-18)}+\frac{393514}{196875\,(5D-22)}+\frac{1}{4\,(D-3)^2}+\frac{916069}{60000}\Bigg)$$

$$-A_{8,1}\Bigg(+\frac{113787\,D}{80000}-\frac{2377}{1792\,(2D-7)}+\frac{712}{45\,(D-2)}-\frac{45}{28\,(D-3)}-\frac{169858}{21875\,(5D-14)}$$
$$+\frac{105754}{28125\,(5D-16)}+\frac{12804}{3125\,(5D-18)}-\frac{3356}{65625\,(5D-22)}+\frac{215}{768\,(2D-7)^2}-\frac{920019}{80000}\Bigg)$$

$$-B_{8,1}\frac{(2\,D^3-25\,D^2+94\,D-112)\,(D^3-16\,D^2+68\,D-88)}{8\,(2D-7)\,(D-2)^2\,(2D-5)}$$

$$-C_{8,1}\frac{(2\,D^3-25\,D^2+94\,D-112)\,(D^3-16\,D^2+68\,D-88)}{8\,(2D-7)\,(D-2)^2\,(2D-5)}$$

$$+A_{9,1}\Bigg(+\frac{81\,D^2}{1000}-\frac{9369\,D}{5000}-\frac{44}{3\,(D-2)}+\frac{45}{56\,(D-3)}+\frac{8232}{625\,(5D-14)}$$
$$-\frac{40172}{9375\,(5D-16)}+\frac{2928}{3125\,(5D-18)}+\frac{3106}{65625\,(5D-22)}+\frac{54801}{5000}\Bigg)$$

$$+A_{9,2}\frac{(3D-14)\,(D-4)\,(135\,D^5-2200\,D^4+15156\,D^3-54336\,D^2+99776\,D-74112)}{20\,(D-3)\,(5D-22)\,(5D-14)\,(5D-16)\,(5D-18)\,(D-2)}$$

$$-A_{9,4}\Bigg(+\frac{81\,D^2}{16000}-\frac{513\,D}{10000}-\frac{973}{9216\,(2D-7)}-\frac{75511}{5657600\,(2D-9)}-\frac{4}{75\,(D-2)}$$
$$+\frac{756}{10625\,(5D-14)}-\frac{14036}{121875\,(5D-16)}+\frac{1168}{3125\,(5D-18)}+\frac{2234}{28125\,(5D-22)}+\frac{36117}{320000}\Bigg)$$

$$X^g_{C_A C_F N_F}=$$

$$+B_{4,1}\Bigg(+\frac{169208\,D^2}{125}-\frac{28533686\,D}{1875}-\frac{1120}{3\,D}+\frac{4465}{7\,(2D-7)}+\frac{1070886586}{16575\,(2D-9)}$$
$$-\frac{56648}{63\,(3D-10)}+\frac{18168111}{770\,(3D-14)}-\frac{1664}{45\,(3D-8)}+\frac{19856072}{405405\,(D-1)}-\frac{3342712}{675\,(D-2)}$$
$$-\frac{1138}{3\,(D-3)}+\frac{480653}{135\,(D-4)}+\frac{2161801556}{30121875\,(5D-14)}$$
$$+\frac{868101691}{2413125\,(5D-16)}+\frac{669068729}{48750\,(5D-18)}$$

JHEP06(2010)094

$$-\frac{1607924552}{9375\,(5D-22)}+\frac{13376}{9\,(D-2)^2}-\frac{19}{3\,(D-3)^2}+\frac{554888}{15\,(D-4)^2}+\frac{471544}{15\,(D-4)^3}$$
$$+\frac{46784}{5\,(D-4)^4}+\frac{876803866}{28125}\Bigg)$$
$$+A_{5,1}\Bigg(+\frac{25803\,D^2}{125}-\frac{21754033\,D}{11250}+\frac{1216}{5\,(2D-5)}+\frac{2390}{9\,(2D-7)}+\frac{64410511}{22100\,(2D-9)}$$
$$-\frac{63976}{945\,(3D-10)}-\frac{13760}{567\,(D-1)}+\frac{295132}{225\,(D-2)}+\frac{40}{3\,(D-3)}-\frac{711848}{405\,(D-4)}$$
$$-\frac{11375744}{478125\,(5D-14)}+\frac{6633272}{73125\,(5D-16)}+\frac{9607724}{3125\,(5D-18)}-\frac{7186816}{3125\,(5D-22)}-\frac{3712}{3\,(D-2)^2}$$
$$-\frac{5776}{135\,(D-4)^2}-\frac{19328}{45\,(D-4)^3}+\frac{1255139429}{337500}\Bigg)$$
$$-A_{5,2}\Bigg(+\frac{27472\,D^2}{375}-\frac{6814294\,D}{5625}-\frac{48}{D}+\frac{75392}{1485\,(2D-5)}-\frac{1912}{63\,(2D-7)}$$
$$-\frac{7070567}{5525\,(2D-9)}-\frac{27436}{945\,(3D-10)}+\frac{258805}{231\,(3D-14)}-\frac{992}{27\,(3D-8)}-\frac{2189468}{81081\,(D-1)}$$
$$-\frac{1407278}{675\,(D-2)}+\frac{1712}{(D-4)}+\frac{1146502544}{30121875\,(5D-14)}$$
$$-\frac{482461664}{12065625\,(5D-16)}-\frac{464255741}{446875\,(5D-18)}$$
$$-\frac{10192}{375\,(5D-22)}+\frac{6544}{9\,(D-2)^2}+\frac{71776}{45\,(D-4)^2}+\frac{10496}{15\,(D-4)^3}+\frac{124446769}{28125}\Bigg)$$
$$+B_{5,1}\Bigg(+\frac{7331\,D^2}{500}+\frac{205803\,D}{5000}+\frac{5681}{36\,(2D-5)}+\frac{6125}{48\,(2D-7)}+\frac{270116}{325\,(2D-9)}$$
$$+\frac{40704}{25\,(D-2)}+\frac{19}{(D-3)}+\frac{10708}{15\,(D-4)}-\frac{31328}{5625\,(5D-14)}-\frac{10336}{40625\,(5D-16)}$$
$$-\frac{3005968}{3125\,(5D-18)}-\frac{11927552}{1875\,(5D-22)}-\frac{928}{(D-2)^2}-\frac{224}{3\,(D-4)^2}-\frac{192}{5\,(D-4)^3}$$
$$-\frac{52885663}{50000}\Bigg)$$
$$-B_{5,2}\Bigg(+\frac{7409\,D^2}{75}-\frac{5308534\,D}{5625}+\frac{6156608}{10395\,(2D-5)}+\frac{392896}{325\,(2D-9)}+\frac{28528}{945\,(3D-10)}$$
$$+\frac{16}{9\,(3D-8)}+\frac{1921904}{27027\,(D-1)}+\frac{423956}{225\,(D-2)}+\frac{129704}{81\,(D-4)}+\frac{13379128}{253125\,(5D-14)}$$
$$+\frac{1042664096}{28153125\,(5D-16)}-\frac{184123036}{446875\,(5D-18)}-\frac{4877264}{625\,(5D-22)}-\frac{5344}{3\,(D-2)^2}+\frac{118976}{135\,(D-4)^2}$$
$$+\frac{10624}{45\,(D-4)^3}+\frac{112377904}{84375}\Bigg)$$
$$+A_{6,1}\Bigg(+\frac{5321\,D^2}{375}-\frac{340129\,D}{1875}+\frac{51761}{1386\,(3D-14)}-\frac{430}{27\,(D-1)}-\frac{2273}{15\,(D-2)}$$
$$+\frac{178}{3\,(D-4)}-\frac{1645052}{590625\,(5D-14)}-\frac{823378}{103125\,(5D-16)}-\frac{121841}{6250\,(5D-18)}-\frac{148988}{3125\,(5D-22)}$$

JHEP06(2010)094

$$+\frac{272}{15\,(D-4)^2}+\frac{17076368}{28125}\Bigg)$$

$$-A_{6,2}\Bigg(+\frac{1489\,D^2}{100}-\frac{334171\,D}{1500}+\frac{160}{3\,D}-\frac{2204}{21\,(2D-5)}+\frac{239}{84\,(2D-7)}$$
$$-\frac{3947149}{132600\,(2D-9)}-\frac{461624}{675\,(D-2)}+\frac{8131}{210\,(D-3)}+\frac{304}{9\,(D-4)}+\frac{169118132}{669375\,(5D-14)}$$
$$-\frac{123983528}{1535625\,(5D-16)}-\frac{232964}{13125\,(5D-22)}+\frac{544}{9\,(D-2)^2}+\frac{5}{12\,(D-3)^2}+\frac{14824063}{15000}\Bigg)$$

$$+A_{6,3}\Bigg(+\frac{24791\,D^2}{500}-\frac{26566007\,D}{45000}-\frac{1195}{126\,(2D-7)}-\frac{14271579}{88400\,(2D-9)}+\frac{1520}{27\,(3D-8)}$$
$$-\frac{91192}{225\,(D-2)}-\frac{2}{(D-3)}+\frac{13466}{45\,(D-4)}-\frac{146291696}{3346875\,(5D-14)}+\frac{4052666}{365625\,(5D-16)}$$
$$+\frac{200184}{3125\,(5D-18)}-\frac{510816}{3125\,(5D-22)}+\frac{1552}{15\,(D-4)^2}+\frac{2491573703}{1350000}\Bigg)$$

$$+B_{6,2}\Bigg(+\frac{23\,D^2}{4}-\frac{729\,D}{8}+\frac{2261}{36\,(2D-5)}+\frac{875}{144\,(2D-7)}-\frac{1264}{9\,(D-2)}$$
$$+\frac{380}{9\,(D-4)}-\frac{32}{3\,(D-2)^2}+\frac{80}{3\,(D-4)^2}+\frac{5401}{16}\Bigg)$$

$$+C_{6,1}\Bigg(+\frac{23\,D^2}{4}-\frac{729\,D}{8}+\frac{2261}{36\,(2D-5)}+\frac{875}{144\,(2D-7)}-\frac{1264}{9\,(D-2)}$$
$$+\frac{380}{9\,(D-4)}-\frac{32}{3\,(D-2)^2}+\frac{80}{3\,(D-4)^2}+\frac{5401}{16}\Bigg)$$

$$+A_{7,1}\Bigg(+\frac{16\,D^2}{25}-\frac{771\,D}{125}+\frac{608}{77\,(2D-5)}-\frac{139}{21\,(2D-7)}-\frac{877}{390\,(2D-9)}$$
$$+\frac{1744}{429\,(D-1)}-\frac{1192}{45\,(D-2)}+\frac{10112}{525\,(5D-14)}+\frac{72675488}{5630625\,(5D-16)}-\frac{9210328}{268125\,(5D-18)}$$
$$-\frac{32}{3\,(D-2)^2}+\frac{21831}{1250}\Bigg)$$

$$-A_{7,2}\Bigg(+\frac{83\,D^2}{80}-\frac{1307\,D}{80}-\frac{71585}{2688\,(2D-7)}-\frac{679599}{141440\,(2D-9)}-\frac{246}{5\,(D-2)}$$
$$+\frac{226392}{14875\,(5D-14)}+\frac{7712}{4875\,(5D-16)}+\frac{12886}{125\,(5D-18)}+\frac{645603}{8000}\Bigg)$$

$$-A_{7,3}\Bigg(+\frac{169\,D^2}{125}-\frac{24\,D}{5}+\frac{456}{(2D-5)}-\frac{139}{21\,(2D-7)}-\frac{1754}{2925\,(2D-9)}$$
$$+\frac{15704}{225\,(D-2)}+\frac{472}{15\,(D-3)}+\frac{1432656}{21875\,(5D-14)}-\frac{7709696}{365625\,(5D-16)}+\frac{47912}{5625\,(5D-18)}$$
$$+\frac{176}{1875\,(5D-22)}-\frac{1792}{3\,(D-2)^2}+\frac{1}{(D-3)^2}-\frac{238436}{3125}\Bigg)$$

$$+A_{7,4}\Bigg(+\frac{313\,D^2}{1000}-\frac{10751\,D}{3000}-\frac{19}{2\,(2D-5)}+\frac{1807}{448\,(2D-7)}-\frac{3947149}{636480\,(2D-9)}$$
$$-\frac{1681}{45\,(D-2)}+\frac{1817}{420\,(D-3)}+\frac{12096842}{371875\,(5D-14)}-\frac{6605536}{365625\,(5D-16)}-\frac{57247}{28125\,(5D-18)}$$

JHEP06(2010)094

$$+\frac{111166}{21875\,(5D-22)}+\frac{32}{3\,(D-2)^2}+\frac{5}{12\,(D-3)^2}+\frac{5654087}{300000}\Bigg)$$

$$+A_{7,5}\Bigg(+\frac{313\,D^2}{1000}-\frac{10751\,D}{3000}-\frac{19}{2\,(2D-5)}+\frac{1807}{448\,(2D-7)}-\frac{3947149}{636480\,(2D-9)}$$

$$-\frac{1681}{45\,(D-2)}+\frac{1817}{420\,(D-3)}+\frac{12096842}{371875\,(5D-14)}-\frac{6605536}{365625\,(5D-16)}-\frac{57247}{28125\,(5D-18)}$$

$$+\frac{111166}{21875\,(5D-22)}+\frac{32}{3\,(D-2)^2}+\frac{5}{12\,(D-3)^2}+\frac{5654087}{300000}\Bigg)$$

$$+A_{8,1}\Bigg(+\frac{37071\,D}{20000}-\frac{1853}{448\,(2D-7)}+\frac{1132}{45\,(D-2)}-\frac{15}{7\,(D-3)}-\frac{368628}{21875\,(5D-14)}$$

$$+\frac{202312}{28125\,(5D-16)}+\frac{31416}{3125\,(5D-18)}-\frac{1468}{13125\,(5D-22)}+\frac{239}{192\,(2D-7)^2}-\frac{1622997}{100000}\Bigg)$$

$$+B_{8,1}\frac{(2\,D^3-25\,D^2+94\,D-112)\,(D^3-16\,D^2+68\,D-88)}{4\,(2D-7)\,(D-2)^2\,(2D-5)}$$

$$+C_{8,1}\frac{(2\,D^3-25\,D^2+94\,D-112)\,(D^3-16\,D^2+68\,D-88)}{4\,(2D-7)\,(D-2)^2\,(2D-5)}$$

$$-A_{9,1}\Bigg(+\frac{81\,D^2}{250}-\frac{6939\,D}{1250}-\frac{144}{5\,(D-2)}+\frac{15}{14\,(D-3)}+\frac{49392}{3125\,(5D-14)}$$

$$-\frac{5808}{3125\,(5D-16)}-\frac{12864}{3125\,(5D-18)}+\frac{1752}{4375\,(5D-22)}+\frac{175239}{6250}\Bigg)$$

$$+A_{9,2}\frac{3\,(D-4)\,(3D-14)\,(15\,D^5-266\,D^4+1708\,D^3-5016\,D^2+6624\,D-2944)}{5\,(D-3)\,(5D-22)\,(5D-14)\,(5D-16)\,(5D-18)\,(D-2)}$$

$$+A_{9,4}\Bigg(+\frac{243\,D^2}{16000}-\frac{1539\,D}{10000}-\frac{973}{3072\,(2D-7)}-\frac{226533}{5657600\,(2D-9)}-\frac{4}{25\,(D-2)}$$

$$+\frac{2268}{10625\,(5D-14)}-\frac{14036}{40625\,(5D-16)}+\frac{3504}{3125\,(5D-18)}+\frac{2234}{9375\,(5D-22)}+\frac{108351}{320000}\Bigg)$$

$$X^{g}_{C_F^2 N_F}=$$

$$-B_{4,1}\Bigg(+\frac{188119\,D^2}{125}-\frac{61815901\,D}{3750}-\frac{23257388}{5525\,(2D-9)}-\frac{280}{9\,(3D-10)}+\frac{13405743}{385\,(3D-14)}$$

$$-\frac{160}{9\,(3D-8)}-\frac{23276}{25\,(D-2)}-\frac{499}{6\,(D-3)}+\frac{773374}{45\,(D-4)}-\frac{1533843736}{3346875\,(5D-14)}$$

$$+\frac{4855107866}{4021875\,(5D-16)}+\frac{79707397}{9375\,(5D-18)}-\frac{2286575824}{28125\,(5D-22)}+\frac{64}{(D-2)^2}-\frac{53}{6\,(D-3)^2}$$

$$+\frac{573968}{15\,(D-4)^2}+\frac{135408}{5\,(D-4)^3}+\frac{36096}{5\,(D-4)^4}+\frac{296368802}{9375}\Bigg)$$

$$-A_{5,1}\Bigg(+\frac{27082\,D^2}{125}-\frac{1697483\,D}{625}+\frac{7475589}{11050\,(2D-9)}+\frac{56}{9\,(3D-10)}-\frac{89768}{75\,(D-2)}$$

$$-\frac{32}{3\,(D-3)}+\frac{282832}{135\,(D-4)}-\frac{16480952}{286875\,(5D-14)}+\frac{1500528}{40625\,(5D-16)}+\frac{2180808}{3125\,(5D-18)}$$

$$-\frac{48975472}{9375\,(5D-22)}+\frac{94688}{45\,(D-4)^2}+\frac{8704}{15\,(D-4)^3}+\frac{87298177}{11250}\Bigg)$$

JHEP06(2010)094

$$+A_{5,2}\left(+\frac{21317\,D^2}{375}-\frac{1283138\,D}{1875}-\frac{4077594}{5525\,(2D-9)}-\frac{344}{27\,(3D-10)}+\frac{127310}{77\,(3D-14)}\right.$$
$$-\frac{400}{27\,(3D-8)}-\frac{46972}{225\,(D-2)}+\frac{29872}{45\,(D-4)}+\frac{141597536}{3346875\,(5D-14)}+\frac{73031344}{1340625\,(5D-16)}$$
$$-\frac{1607982}{3125\,(5D-18)}-\frac{6282976}{5625\,(5D-22)}+\frac{32}{(D-2)^2}+\frac{8576}{15\,(D-4)^2}+\frac{256}{(D-4)^3}$$
$$\left.+\frac{152810662}{84375}\right)$$
$$-B_{5,1}\left(+\frac{7239\,D^2}{125}-\frac{446671\,D}{625}-\frac{1784}{5\,(D-2)}-\frac{11}{(D-3)}+\frac{184976}{135\,(D-4)}\right.$$
$$-\frac{2031568}{84375\,(5D-14)}+\frac{2576}{3125\,(5D-16)}-\frac{1879752}{3125\,(5D-18)}-\frac{2550912}{625\,(5D-22)}+\frac{37696}{45\,(D-4)^2}$$
$$\left.+\frac{4736}{15\,(D-4)^3}+\frac{6406811}{3125}\right)$$
$$+B_{5,2}\left(+\frac{11609\,D^2}{75}-\frac{726482\,D}{375}-\frac{728}{27\,(3D-10)}-\frac{400}{27\,(3D-8)}-\frac{4948}{5\,(D-2)}\right.$$
$$+\frac{55288}{27\,(D-4)}+\frac{117104}{3375\,(5D-14)}+\frac{12584}{625\,(5D-16)}-\frac{133092}{625\,(5D-18)}-\frac{515088}{125\,(5D-22)}$$
$$\left.+\frac{13280}{9\,(D-4)^2}+\frac{6272}{15\,(D-4)^3}+\frac{3837572}{675}\right)$$
$$-A_{6,1}\left(+\frac{4732\,D^2}{375}-\frac{300428\,D}{1875}+\frac{12731}{231\,(3D-14)}-\frac{5458}{45\,(D-2)}+\frac{2524}{45\,(D-4)}\right.$$
$$-\frac{1669664}{196875\,(5D-14)}-\frac{289948}{61875\,(5D-16)}-\frac{733}{125\,(5D-18)}-\frac{665896}{9375\,(5D-22)}+\frac{64}{3\,(D-4)^2}$$
$$\left.+\frac{4892596}{9375}\right)$$
$$+A_{6,2}\left(+\frac{1013\,D^2}{50}-\frac{215473\,D}{750}-\frac{226533}{22100\,(2D-9)}-\frac{154016}{225\,(D-2)}+\frac{98}{3\,(D-3)}\right.$$
$$+\frac{208}{15\,(D-4)}+\frac{1662152}{6375\,(5D-14)}-\frac{5141248}{73125\,(5D-16)}+\frac{8936}{5625\,(5D-22)}-\frac{64}{(D-2)^2}$$
$$\left.-\frac{5}{6\,(D-3)^2}+\frac{8774231}{7500}\right)$$
$$-A_{6,3}\left(+\frac{14331\,D^2}{250}-\frac{1856633\,D}{2500}-\frac{4757193}{44200\,(2D-9)}-\frac{60536}{75\,(D-2)}+\frac{9}{(D-3)}\right.$$
$$+\frac{4396}{15\,(D-4)}+\frac{2026304}{159375\,(5D-14)}+\frac{56236}{24375\,(5D-16)}+\frac{33752}{625\,(5D-18)}-\frac{761024}{3125\,(5D-22)}$$
$$\left.+\frac{512}{5\,(D-4)^2}+\frac{64132247}{25000}\right)$$
$$-A_{7,1}\frac{16\,(D-3)\,(D^2-7\,D+16)\,(5\,D^3-62\,D^2+236\,D-288)}{(D-2)\,(5D-14)\,(5D-16)\,(5D-18)}$$
$$+A_{7,2}\left(+\frac{49\,D^2}{40}-\frac{3181\,D}{200}-\frac{71585}{4032\,(2D-7)}-\frac{226533}{70720\,(2D-9)}-\frac{1556}{45\,(D-2)}\right.$$

JHEP06(2010)094

$$+\frac{215664}{14875\,(5D-14)}+\frac{2752}{2925\,(5D-16)}+\frac{6548}{125\,(5D-18)}+\frac{50413}{800}\Big)$$

$$+A_{7,3}\Big(+\frac{419\,D^2}{125}-\frac{33136\,D}{625}-\frac{328}{(D-2)}+\frac{1126}{105\,(D-3)}+\frac{1169616}{3125\,(5D-14)}$$

$$+\frac{60416}{3125\,(5D-16)}-\frac{16616}{9375\,(5D-18)}-\frac{3504}{4375\,(5D-22)}-\frac{7}{(D-3)^2}+\frac{787461}{3125}\Big)$$

$$-A_{7,4}\Big(+\frac{271\,D^2}{500}-\frac{48887\,D}{7500}+\frac{3197}{2016\,(2D-7)}-\frac{75511}{35360\,(2D-9)}-\frac{622}{45\,(D-2)}$$

$$+\frac{3}{(D-3)}-\frac{694636}{74375\,(5D-14)}-\frac{2925056}{365625\,(5D-16)}-\frac{1314}{3125\,(5D-18)}+\frac{49148}{28125\,(5D-22)}$$

$$-\frac{1}{3\,(D-3)^2}+\frac{47263}{2000}\Big)$$

$$-A_{7,5}\Big(+\frac{271\,D^2}{500}-\frac{48887\,D}{7500}+\frac{3197}{2016\,(2D-7)}-\frac{75511}{35360\,(2D-9)}-\frac{622}{45\,(D-2)}$$

$$+\frac{3}{(D-3)}-\frac{694636}{74375\,(5D-14)}-\frac{2925056}{365625\,(5D-16)}-\frac{1314}{3125\,(5D-18)}+\frac{49148}{28125\,(5D-22)}$$

$$-\frac{1}{3\,(D-3)^2}+\frac{47263}{2000}\Big)$$

$$+A_{9,1}\Big(+\frac{81\,D^2}{250}-\frac{6939\,D}{1250}-\frac{144}{5\,(D-2)}+\frac{15}{14\,(D-3)}+\frac{49392}{3125\,(5D-14)}$$

$$-\frac{5808}{3125\,(5D-16)}-\frac{12864}{3125\,(5D-18)}+\frac{1752}{4375\,(5D-22)}+\frac{175239}{6250}\Big)$$

$$-A_{9,4}\Big(+\frac{81\,D^2}{8000}-\frac{513\,D}{5000}-\frac{973}{4608\,(2D-7)}-\frac{75511}{2828800\,(2D-9)}-\frac{8}{75\,(D-2)}$$

$$+\frac{1512}{10625\,(5D-14)}-\frac{28072}{121875\,(5D-16)}+\frac{2336}{3125\,(5D-18)}+\frac{4468}{28125\,(5D-22)}+\frac{36117}{160000}\Big)$$

$$X^{g}_{C_A N_F^2}=$$

$$+B_{4,1}\Big(+\frac{968\,D}{25}+\frac{715}{21\,(3D-10)}-\frac{1693529}{162162\,(D-1)}-\frac{55}{3\,(D-2)}-\frac{37}{6\,(D-3)}$$

$$-\frac{12496}{81\,(D-4)}+\frac{12056}{3375\,(5D-14)}+\frac{20832}{1375\,(5D-16)}+\frac{299376}{1625\,(5D-18)}+\frac{9217}{108\,(D-1)^2}$$

$$+\frac{4}{(D-2)^2}+\frac{1}{4\,(D-3)^2}-\frac{1504}{9\,(D-4)^2}-\frac{896}{9\,(D-4)^3}-\frac{46756}{375}\Big)$$

$$-A_{5,2}\Big(+\frac{238\,D}{75}-\frac{68}{63\,(3D-10)}-\frac{2806094}{81081\,(D-1)}+\frac{80}{3\,(D-2)}-\frac{256}{81\,(D-4)}$$

$$+\frac{21296}{10125\,(5D-14)}-\frac{2496}{1375\,(5D-16)}-\frac{23328}{1625\,(5D-18)}-\frac{994}{27\,(D-1)^2}-\frac{8}{(D-2)^2}$$

$$-\frac{256}{27\,(D-4)^2}-\frac{4096}{1125}\Big)$$

$$+B_{5,2}\Big(+\frac{154\,D}{75}-\frac{32}{63\,(3D-10)}-\frac{278326}{81081\,(D-1)}-\frac{128}{81\,(D-4)}-\frac{17072}{10125\,(5D-14)}$$

JHEP06(2010)094

$$-\frac{2208}{1375\,(5D-16)}-\frac{11664}{1625\,(5D-18)}+\frac{502}{27\,(D-1)^2}-\frac{128}{27\,(D-4)^2}-\frac{10408}{1125}\Bigg)$$

$$+A_{6,1}\frac{(5D-16)\,(D-4)}{3\,(D-1)^2\,(D-2)^2}$$

$$-A_{7,1}\frac{8\,(D-3)\,(D-4)\,(5\,D^3-62\,D^2+236\,D-288)}{(D-1)\,(5D-14)\,(5D-16)\,(5D-18)}$$

$$X^g_{C_F N_F^2}=$$

$$-B_{4,1}\Bigg(+\frac{2336\,D}{25}-\frac{1360}{21\,(3D-10)}-\frac{64}{15\,(3D-8)}+\frac{20262752}{135135\,(D-1)}-\frac{4256}{9\,(D-4)}$$

$$+\frac{24112}{3375\,(5D-14)}+\frac{41664}{1375\,(5D-16)}+\frac{598752}{1625\,(5D-18)}-\frac{576}{(D-4)^2}-\frac{256}{(D-4)^3}$$

$$-\frac{158512}{375}\Bigg)$$

$$+A_{5,2}\Bigg(+\frac{1976\,D}{75}+\frac{160}{63\,(3D-10)}-\frac{32}{9\,(3D-8)}+\frac{4378936}{81081\,(D-1)}-\frac{1024}{27\,(D-4)}$$

$$+\frac{42592}{10125\,(5D-14)}-\frac{4992}{1375\,(5D-16)}-\frac{46656}{1625\,(5D-18)}-\frac{256}{9\,(D-4)^2}-\frac{49064}{375}\Bigg)$$

$$-B_{5,2}\Bigg(+\frac{136\,D}{25}+\frac{160}{63\,(3D-10)}+\frac{32}{9\,(3D-8)}+\frac{1481384}{81081\,(D-1)}-\frac{512}{27\,(D-4)}$$

$$-\frac{34144}{10125\,(5D-14)}-\frac{4416}{1375\,(5D-16)}-\frac{23328}{1625\,(5D-18)}-\frac{128}{9\,(D-4)^2}-\frac{35816}{1125}\Bigg)$$

$$+A_{7,1}\frac{16\,(D-3)\,(D-4)\,(5\,D^3-62\,D^2+236\,D-288)}{(D-1)\,(5D-14)\,(5D-16)\,(5D-18)}$$

JHEP06(2010)094

References

[1] G. Altarelli, R.K. Ellis and G. Martinelli, *Large perturbative corrections to the Drell-Yan process in QCD*, *Nucl. Phys.* **B 157** (1979) 461 [SPIRES].

[2] R. Hamberg, W.L. van Neerven and T. Matsuura, *A Complete calculation of the order α_s^2 correction to the Drell-Yan K factor*, *Nucl. Phys.* **B 359** (1991) 343 [*Erratum ibid.* **B 644** (2002) 403] [SPIRES].

[3] R.V. Harlander and W.B. Kilgore, *Next-to-next-to-leading order Higgs production at hadron colliders*, *Phys. Rev. Lett.* **88** (2002) 201801 [hep-ph/0201206] [SPIRES].

[4] S. Dawson, *Radiative corrections to Higgs boson production*, *Nucl. Phys.* **B 359** (1991) 283 [SPIRES].

[5] D. Graudenz, M. Spira and P.M. Zerwas, *QCD corrections to Higgs boson production at proton proton colliders*, *Phys. Rev. Lett.* **70** (1993) 1372 [SPIRES].

[6] M. Spira, A. Djouadi, D. Graudenz and P.M. Zerwas, *Higgs boson production at the LHC*, *Nucl. Phys.* **B 453** (1995) 17 [hep-ph/9504378] [SPIRES].

[7] A. Djouadi, M. Spira and P.M. Zerwas, *QCD corrections to hadronic Higgs decays*, *Z. Phys.* **C 70** (1996) 427 [hep-ph/9511344] [SPIRES].

[8] M. Spira, *QCD effects in Higgs physics*, *Fortsch. Phys.* **46** (1998) 203 [hep-ph/9705337] [SPIRES].

[9] R. Harlander and P. Kant, *Higgs production and decay: analytic results at next-to-leading order QCD*, *JHEP* **12** (2005) 015 [hep-ph/0509189] [SPIRES].

[10] S. Catani, D. de Florian and M. Grazzini, *Higgs production in hadron collisions: Soft and virtual QCD corrections at NNLO*, *JHEP* **05** (2001) 025 [hep-ph/0102227] [SPIRES].

[11] C. Anastasiou and K. Melnikov, *Higgs boson production at hadron colliders in NNLO QCD*, *Nucl. Phys.* **B 646** (2002) 220 [hep-ph/0207004] [SPIRES].

[12] V. Ravindran, J. Smith and W.L. van Neerven, *NNLO corrections to the total cross section for Higgs boson production in hadron hadron collisions*, *Nucl. Phys.* **B 665** (2003) 325 [*Erratum ibid.* **704** (2005) 332] [hep-ph/0302135] [SPIRES].

[13] L. Magnea and G. Sterman, *Analytic continuation of the Sudakov form-factor in QCD*, *Phys. Rev.* **D 42** (1990) 4222 [SPIRES].

[14] S. Moch and A. Vogt, *Higher-order soft corrections to lepton pair and Higgs boson production*, *Phys. Lett.* **B 631** (2005) 48 [hep-ph/0508265] [SPIRES].

[15] E. Laenen and L. Magnea, *Threshold resummation for electroweak annihilation from DIS data*, *Phys. Lett.* **B 632** (2006) 270 [hep-ph/0508284] [SPIRES].

[16] V. Ravindran, *On Sudakov and soft resummations in QCD*, *Nucl. Phys.* **B 746** (2006) 58 [hep-ph/0512249] [SPIRES].

[17] G.P. Korchemsky, *Double logarithmic asymptotics in QCD*, *Phys. Lett.* **B 217** (1989) 330 [SPIRES].

[18] C.W. Bauer, S. Fleming and M.E. Luke, *Summing Sudakov logarithms in $B \to X/s$ gamma in effective field theory*, *Phys. Rev.* **D 63** (2000) 014006 [hep-ph/0005275] [SPIRES].

[19] C.W. Bauer, S. Fleming, D. Pirjol and I.W. Stewart, *An effective field theory for collinear and soft gluons: heavy to light decays*, *Phys. Rev.* **D 63** (2001) 114020 [hep-ph/0011336] [SPIRES].

[20] C.W. Bauer and I.W. Stewart, *Invariant operators in collinear effective theory*, *Phys. Lett.* **B 516** (2001) 134 [hep-ph/0107001] [SPIRES].

[21] C.W. Bauer, D. Pirjol and I.W. Stewart, *Soft-collinear factorization in effective field theory*, *Phys. Rev.* **D 65** (2002) 054022 [hep-ph/0109045] [SPIRES].

[22] M. Beneke, A.P. Chapovsky, M. Diehl and T. Feldmann, *Soft-collinear effective theory and heavy-to-light currents beyond leading power*, *Nucl. Phys.* **B 643** (2002) 431 [hep-ph/0206152] [SPIRES].

[23] M. Beneke and T. Feldmann, *Multipole-expanded soft-collinear effective theory with non-abelian gauge symmetry*, *Phys. Lett.* **B 553** (2003) 267 [hep-ph/0211358] [SPIRES].

[24] A. Idilbi and X.-d. Ji, *Threshold resummation for Drell-Yan process in soft-collinear effective theory*, *Phys. Rev.* **D 72** (2005) 054016 [hep-ph/0501006] [SPIRES].

[25] A. Idilbi, X.-d. Ji and F. Yuan, *Resummation of threshold logarithms in effective field theory for DIS, Drell-Yan and Higgs production*, *Nucl. Phys.* **B 753** (2006) 42 [hep-ph/0605068] [SPIRES].

[26] A. Idilbi, X.-d. Ji, J.-P. Ma and F. Yuan, *Threshold resummation for Higgs production in effective field theory*, *Phys. Rev.* **D 73** (2006) 077501 [hep-ph/0509294] [SPIRES].

JHEP06(2010)094

[27] V. Ahrens, T. Becher, M. Neubert and L.L. Yang, *Renormalization-group improved prediction for Higgs production at hadron colliders*, *Eur. Phys. J.* **C 62** (2009) 333 [arXiv:0809.4283] [SPIRES].

[28] G.P. Korchemsky and A.V. Radyushkin, *Loop space formalism and renormalization group for the infrared asymptotics of QCD*, *Phys. Lett.* **B 171** (1986) 459 [SPIRES]. G.P. Korchemsky and A.V. Radyushkin, *Renormalization of the Wilson loops beyond the leading order*, *Nucl. Phys.* **B 283** (1987) 342 [SPIRES].

[29] S. Moch, J.A.M. Vermaseren and A. Vogt, *The three-loop splitting functions in QCD: the non-singlet case*, *Nucl. Phys.* **B 688** (2004) 101 [hep-ph/0403192] [SPIRES].

[30] A. Vogt, S. Moch and J.A.M. Vermaseren, *The three-loop splitting functions in QCD: the singlet case*, *Nucl. Phys.* **B 691** (2004) 129 [hep-ph/0404111] [SPIRES].

[31] S. Moch, J.A.M. Vermaseren and A. Vogt, *The quark form factor at higher orders*, *JHEP* **08** (2005) 049 [hep-ph/0507039] [SPIRES].

[32] S. Moch, J.A.M. Vermaseren and A. Vogt, *Three-loop results for quark and gluon form factors*, *Phys. Lett.* **B 625** (2005) 245 [hep-ph/0508055] [SPIRES].

[33] G. Kramer and B. Lampe, *Two Jet Cross-Section in e^+e^- Annihilation*, *Z. Phys.* **C 34** (1987) 497 [*Erratum ibid.* **42** (1989) 504] [SPIRES].

[34] T. Matsuura and W.L. van Neerven, *Second order logarithmic corrections to the Drell-Yan cross-section*, *Z. Phys.* **C 38** (1988) 623 [SPIRES].

[35] T. Matsuura, S.C. van der Marck and W.L. van Neerven, *The calculation of the second order soft and virtual contributions to the Drell-Yan cross-section*, *Nucl. Phys.* **B 319** (1989) 570 [SPIRES].

[36] R.V. Harlander, *Virtual corrections to $gg \to H$ to two loops in the heavy top limit*, *Phys. Lett.* **B 492** (2000) 74 [hep-ph/0007289] [SPIRES].

[37] T. Gehrmann, T. Huber and D. Maître, *Two-loop quark and gluon form factors in dimensional regularisation*, *Phys. Lett.* **B 622** (2005) 295 [hep-ph/0507061] [SPIRES].

[38] T. Becher, M. Neubert and B.D. Pecjak, *Factorization and momentum-space resummation in deep-inelastic scattering*, *JHEP* **01** (2007) 076 [hep-ph/0607228] [SPIRES].

[39] T. Becher and M. Neubert, *On the structure of infrared singularities of Gauge-theory amplitudes*, *JHEP* **06** (2009) 081 [arXiv:0903.1126] [SPIRES].

[40] G.P. Korchemsky, *Asymptotics of the Altarelli-Parisi-Lipatov evolution kernels of parton distributions*, *Mod. Phys. Lett.* **A 4** (1989) 1257 [SPIRES].

[41] L.F. Alday and J.M. Maldacena, *Comments on operators with large spin*, *JHEP* **11** (2007) 019 [arXiv:0708.0672] [SPIRES].

[42] J. Frenkel and J.C. Taylor, *Nonabelian eikonal exponentiation*, *Nucl. Phys.* **B 246** (1984) 231 [SPIRES].

[43] T. Becher and M. Neubert, *Infrared singularities of scattering amplitudes in perturbative QCD*, *Phys. Rev. Lett.* **102** (2009) 162001 [arXiv:0901.0722] [SPIRES].

[44] E. Gardi and L. Magnea, *Factorization constraints for soft anomalous dimensions in QCD scattering amplitudes*, *JHEP* **03** (2009) 079 [arXiv:0901.1091] [SPIRES].

[45] S. Catani, *The singular behaviour of QCD amplitudes at two-loop order*, *Phys. Lett.* **B 427** (1998) 161 [hep-ph/9802439] [SPIRES].

JHEP06(2010)094

[46] G. Sterman and M.E. Tejeda-Yeomans, *Multi-loop amplitudes and resummation*, *Phys. Lett.* **B 552** (2003) 48 [hep-ph/0210130] [SPIRES].

[47] S.M. Aybat, L.J. Dixon and G. Sterman, *The two-loop soft anomalous dimension matrix and resummation at next-to-next-to leading pole*, *Phys. Rev.* **D 74** (2006) 074004 [hep-ph/0607309] [SPIRES].

[48] S.M. Aybat, L.J. Dixon and G. Sterman, *The two-loop anomalous dimension matrix for soft gluon exchange*, *Phys. Rev. Lett.* **97** (2006) 072001 [hep-ph/0606254] [SPIRES].

[49] L.J. Dixon, E. Gardi and L. Magnea, *On soft singularities at three loops and beyond*, *JHEP* **02** (2010) 081 [arXiv:0910.3653] [SPIRES].

[50] S. Laporta, *High-precision calculation of multi-loop Feynman integrals by difference equations*, *Int. J. Mod. Phys.* **A 15** (2000) 5087 [hep-ph/0102033] [SPIRES].

[51] C. Anastasiou and A. Lazopoulos, *Automatic integral reduction for higher order perturbative calculations*, *JHEP* **07** (2004) 046 [hep-ph/0404258] [SPIRES].

[52] A.V. Smirnov, *Algorithm FIRE – Feynman Integral REduction*, *JHEP* **10** (2008) 107 [arXiv:0807.3243] [SPIRES].

[53] C. Studerus, *Reduze - Feynman integral reduction in C++*, *Comput. Phys. Commun.* **181** (2010) 1293 [arXiv:0912.2546] [SPIRES].

[54] T. Gehrmann, G. Heinrich, T. Huber and C. Studerus, *Master integrals for massless three-loop form factors: One-loop and two-loop insertions*, *Phys. Lett.* **B 640** (2006) 252 [hep-ph/0607185] [SPIRES].

[55] G. Heinrich, T. Huber and D. Maître, *Master integrals for fermionic contributions to massless three-loop form factors*, *Phys. Lett.* **B 662** (2008) 344 [arXiv:0711.3590] [SPIRES].

[56] G. Heinrich, T. Huber, D.A. Kosower and V.A. Smirnov, *Nine-propagator master integrals for massless three-loop form factors*, *Phys. Lett.* **B 678** (2009) 359 [arXiv:0902.3512] [SPIRES].

[57] R.N. Lee, A.V. Smirnov and V.A. Smirnov, *Analytic results for massless three-loop form factors*, *JHEP* **04** (2010) 020 [arXiv:1001.2887] [SPIRES].

[58] P.A. Baikov, K.G. Chetyrkin, A.V. Smirnov, V.A. Smirnov and M. Steinhauser, *Quark and gluon form factors to three loops*, *Phys. Rev. Lett.* **102** (2009) 212002 [arXiv:0902.3519] [SPIRES].

[59] F. Wilczek, *Decays of heavy vector mesons into higgs particles*, *Phys. Rev. Lett.* **39** (1977) 1304 [SPIRES].

[60] M.A. Shifman, A.I. Vainshtein and V.I. Zakharov, *Remarks on Higgs boson interactions with nucleons*, *Phys. Lett.* **B 78** (1978) 443 [SPIRES].

[61] J.R. Ellis, M.K. Gaillard, D.V. Nanopoulos and C.T. Sachrajda, *Is the mass of the Higgs boson about 10 GeV?*, *Phys. Lett.* **B 83** (1979) 339 [SPIRES].

[62] T. Inami, T. Kubota and Y. Okada, *Effective gauge theory and the effect of heavy quarks in Higgs boson decays*, *Z. Phys.* **C 18** (1983) 69 [SPIRES].

[63] K.G. Chetyrkin, B.A. Kniehl and M. Steinhauser, *Hadronic Higgs decay to order* α_s^4, *Phys. Rev. Lett.* **79** (1997) 353 [hep-ph/9705240] [SPIRES].

JHEP06(2010)094

[64] B.A. Kniehl and M. Spira, *Low-energy theorems in Higgs physics*, *Z. Phys.* **C 69** (1995) 77 [hep-ph/9505225] [SPIRES].

[65] K.G. Chetyrkin, B.A. Kniehl and M. Steinhauser, *Decoupling relations to $O(\alpha_s^3)$ and their connection to low-energy theorems*, *Nucl. Phys.* **B 510** (1998) 61 [hep-ph/9708255] [SPIRES].

[66] W.A. Bardeen, A.J. Buras, D.W. Duke and T. Muta, *Deep inelastic scattering beyond the leading order in asymptotically free gauge theories*, *Phys. Rev.* **D 18** (1978) 3998 [SPIRES].

[67] D.J. Gross and F. Wilczek, *Ultraviolet behavior of non-abelian gauge theories*, *Phys. Rev. Lett.* **30** (1973) 1343 [SPIRES].

[68] H.D. Politzer, *Reliable perturbative results for strong interactions?*, *Phys. Rev. Lett.* **30** (1973) 1346 [SPIRES].

[69] W.E. Caswell, *Asymptotic behavior of nonabelian gauge theories to two loop order*, *Phys. Rev. Lett.* **33** (1974) 244 [SPIRES].

[70] D.R.T. Jones, *Two loop diagrams in Yang-Mills theory*, *Nucl. Phys.* **B 75** (1974) 531 [SPIRES].

[71] E. Egorian and O.V. Tarasov, *Two loop renormalization of the qcd in an arbitrary gauge*, *Teor. Mat. Fiz.* **41** (1979) 26 [*Theor. Math. Phys.* **41** (1979) 863] [SPIRES].

[72] O.V. Tarasov, A.A. Vladimirov and A.Y. Zharkov, *The Gell-Mann-Low function of QCD in the three loop approximation*, *Phys. Lett.* **B 93** (1980) 429 [SPIRES].

[73] S.A. Larin and J.A.M. Vermaseren, *The three loop QCD β-function and anomalous dimensions*, *Phys. Lett.* **B 303** (1993) 334 [hep-ph/9302208] [SPIRES].

[74] P. Nogueira, *Automatic Feynman graph generation*, *J. Comput. Phys.* **105** (1993) 279 [SPIRES].

[75] K.G. Chetyrkin and F.V. Tkachov, *Integration by parts: the algorithm to calculate β-functions in 4 loops*, *Nucl. Phys.* **B 192** (1981) 159 [SPIRES].

[76] T. Gehrmann and E. Remiddi, *Differential equations for two-loop four-point functions*, *Nucl. Phys.* **B 580** (2000) 485 [hep-ph/9912329] [SPIRES].

[77] T. Huber and D. Maître, *HypExp, a Mathematica package for expanding hypergeometric functions around integer-valued parameters*, *Comput. Phys. Commun.* **175** (2006) 122 [hep-ph/0507094] [SPIRES].

[78] S.G. Gorishnii, S.A. Larin, L.R. Surguladze and F.V. Tkachov, *Mincer: program for multiloop calculations in quantum field theory for the schoonschip system*, *Comput. Phys. Commun.* **55** (1989) 381 [SPIRES].

[79] S.A. Larin, F.V. Tkachov and J.A.M. Vermaseren, *The form version of mincer*, NIKHEF-H-91-18.

[80] S. Bekavac, *Calculation of massless Feynman integrals using harmonic sums*, *Comput. Phys. Commun.* **175** (2006) 180 [hep-ph/0505174] [SPIRES].

[81] M. Czakon, *Automatized analytic continuation of Mellin-Barnes integrals*, *Comput. Phys. Commun.* **175** (2006) 559 [hep-ph/0511200] [SPIRES].

[82] H.R.P. Ferguson, D.H. Bailey and S. Arno, *Analysis of PSLQ, an integer relation finding algorithm*, *Math. Comput.* **68** (1999) 351, *NASA-Ames Technical Report, NAS-96-005.*

JHEP06(2010)094

[83] J.A.M. Vermaseren, A. Vogt and S. Moch, *The third-order QCD corrections to deep-inelastic scattering by photon exchange*, *Nucl. Phys.* **B 724** (2005) 3 [hep-ph/0504242] [SPIRES].

[84] A. Vogt, *Next-to-next-to-leading logarithmic threshold resummation for deep-inelastic scattering and the Drell-Yan process*, *Phys. Lett.* **B 497** (2001) 228 [hep-ph/0010146] [SPIRES].

[85] S. Catani, D. de Florian, M. Grazzini and P. Nason, *Soft-gluon resummation for Higgs boson production at hadron colliders*, *JHEP* **07** (2003) 028 [hep-ph/0306211] [SPIRES].

[86] S. Moch, J.A.M. Vermaseren and A. Vogt, *Higher-order corrections in threshold resummation*, *Nucl. Phys.* **B 726** (2005) 317 [hep-ph/0506288] [SPIRES].

[87] G. Sterman, *Summation of large corrections to short distance hadronic cross-sections*, *Nucl. Phys.* **B 281** (1987) 310 [SPIRES].

[88] S. Catani and L. Trentadue, *Resummation of the QCD perturbative series for hard processes*, *Nucl. Phys.* **B 327** (1989) 323 [SPIRES]. S. Catani and L. Trentadue, *Comment on QCD exponentiation at large x*, *Nucl. Phys.* **B 353** (1991) 183 [SPIRES].

[89] S. Catani, M.L. Mangano, P. Nason and L. Trentadue, *The resummation of soft gluon in hadronic collisions*, *Nucl. Phys.* **B 478** (1996) 273 [hep-ph/9604351] [SPIRES].

[90] H. Contopanagos, E. Laenen and G. Sterman, *Sudakov factorization and resummation*, *Nucl. Phys.* **B 484** (1997) 303 [hep-ph/9604313] [SPIRES].

[91] C.W. Bauer, S. Fleming, D. Pirjol, I.Z. Rothstein and I.W. Stewart, *Hard scattering factorization from effective field theory*, *Phys. Rev.* **D 66** (2002) 014017 [hep-ph/0202088] [SPIRES].

JHEP06(2010)094

Published for SISSA by Springer

Received: October 25, 2010
Accepted: November 9, 2010
Published: November 23, 2010

The quark and gluon form factors to three loops in QCD through to $\mathcal{O}(\epsilon^2)$

T. Gehrmann,[a] E.W.N. Glover,[b] T. Huber,[c] N. Ikizlerli[b] and C. Studerus[a,d]

[a] *Institut für Theoretische Physik, Universität Zürich, Winterthurerstrasse 190, CH-8057 Zürich, Switzerland*

[b] *Institute for Particle Physics Phenomenology, University of Durham, South Road, Durham DH1 3LE, U.K.*

[c] *Fachbereich 7, Universität Siegen, Walter-Flex-Strasse 3, D-57068 Siegen, Germany*

[d] *Faculty of Physics, University of Bielefeld, D-33501 Bielefeld, Germany*

E-mail: thomas.gehrmann@physik.uzh.ch, e.w.n.glover@durham.ac.uk, huber@tp1.physik.uni-siegen.de, nehir.ikizlerli@durham.ac.uk, cedric@physik.uni-bielefeld.de

Abstract: We give explicit formulae for the $\mathcal{O}(\epsilon)$ and $\mathcal{O}(\epsilon^2)$ contributions to the unrenormalised three loop QCD corrections to quark and gluon form factors. These contributions have at most transcendentality weight eight. The $\mathcal{O}(\epsilon)$ terms of the three-loop form factors are required for the extraction of the four-loop quark and gluon collinear anomalous dimensions. The $\mathcal{O}(\epsilon^2)$ terms represent an irreducible contribution to the finite part of the form factors at four-loops. For the sake of completeness, we also give the contributions to the one and two loop form factors to the same transcendentality weight eight.

Keywords: NLO Computations, QCD

ArXiv ePrint: 1010.4478

© SISSA 2010

doi:10.1007/JHEP11(2010)102

JHEP11(2010)102

The form factors are fundamental ingredients for many precision calculations in QCD. These basic building blocks describe the coupling of an external, colour-neutral off-shell particle to a pair of partons: the quark form factor is the coupling of a virtual photon to a quark-antiquark pair, while the gluon form factor is the coupling of a Higgs boson to a pair of gluons through an effective Lagrangian.

The form factors are phenomenologically important and appear directly as virtual higher-order corrections in coefficient functions for the inclusive Drell-Yan process [1–3] and the inclusive Higgs production cross section [3–13]. The form factors also display a non-trivial infrared pole structure which is determined by the infrared factorisation formula. This implies that their infrared pole coefficients can be used to extract fundamental constants such as the cusp anomalous dimensions which control the structure of soft divergences and the collinear quark and gluon anomalous dimensions. In fact, the cusp anomalous dimensions were first obtained to three loops from the asymptotic behaviour of splitting functions [14, 15]. However, it was the calculation [16, 17] of the pole terms of the three-loop form factors (and finite plus subleading terms in the two-loop and one-loop form factors [18–22]), which led to the derivation of the three-loop collinear anomalous dimensions [16, 23, 24].

The infrared factorisation formula for a given form factor (or more generally for a given multi-leg amplitude) at a certain number of loops involves infrared singularity operators acting on the form factor evaluated with a lower number of loops. These infrared singularity operators contain explicit infrared poles $1/\epsilon^2$ and $1/\epsilon$. Therefore, the computation of the finite contribution to any n-loop form factor relies on contributions from $(n-m)$-loops evaluated to $\mathcal{O}(\epsilon^{2m})$.

At present, the state of the art is at the three-loop level for the massless quark and gluon form factors. There are 22 master integrals shown in figure 1, of which 14 are genuine three-loop vertex functions ($A_{t,i}$-type), 4 are three-loop propagator integrals ($B_{t,i}$-type) and 4 are products of one-loop and two-loop integrals ($C_{t,i}$-type). In this notation, the index t denotes the number of propagators, and i is simply enumerating the topologically different integrals with the same number of propagators. Expressions for the form factors in terms of the 22 independent master integrals, and valid for any value of the dimension D, are given in ref. [25]. The $B_{t,i}$-type integrals were computed to finite order in [26–28] and supplemented by the higher order terms in [29]. Explicit expansions of the $A_{t,i}$-type integrals were obtained in refs. [30–33] using Mellin-Barnes techniques. They enabled the evaluation of the three-loop form factors up to and including the finite contributions [25, 33, 34]. The deepest pole contribution is of $\mathcal{O}(1/\epsilon^6)$. Correspondingly, the finite terms are of at most transcendentality weight six, that is terms such as π^6 (ζ_2^3) or ζ_3^2.

More recently [35], 20 of the three-loop master integrals have been re-evaluated up to transcendentality weight eight using dimensional recurrence relations [36, 37] and analytic properties of Feynman integrals (the DRA method [38]). Expressions for the two remaining integrals, $B_{8,1}$ and $C_{8,1}$, can be obtained from refs. [38] and [22] respectively. Once the same normalisation and basis set of multiple zeta values is used, ref. [35] confirms the earlier result of ref. [39] for $A_{6,2}$. On the other hand, we confirm a certain subset of master integrals ($B_{6,2}$, $B_{8,1}$, $A_{7,3}$, $A_{7,5}$, $A_{8,1}$, $A_{9,1}$, $A_{9,2}$, $A_{9,4}$) from [35, 38] up to coefficients corresponding

JHEP11(2010)102

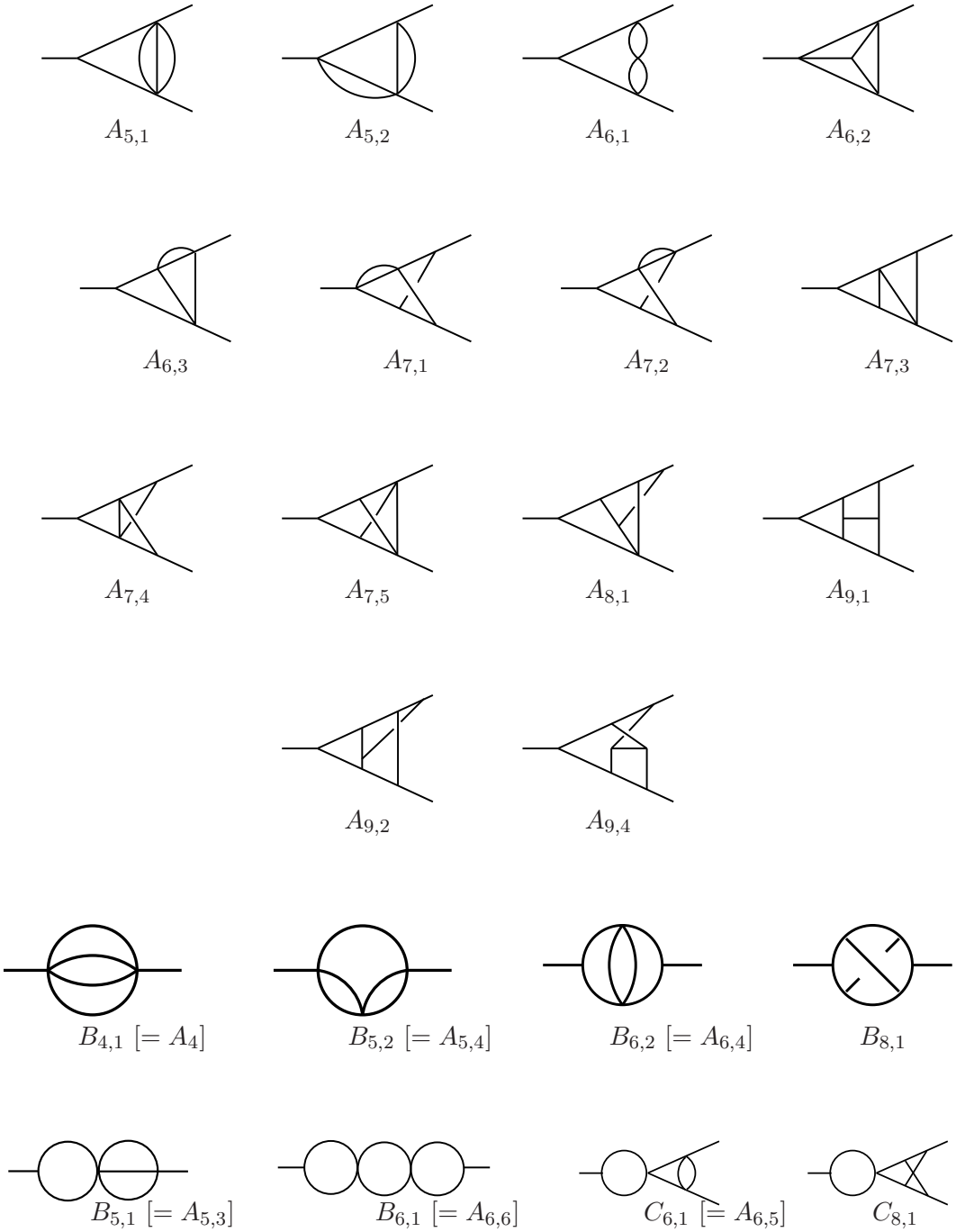

Figure 1. Master integrals for the three-loop form factors. Labels in brackets indicate the naming convention of ref. [35].

to weight eight numerically to a precision of one per-mille or better using `MB.m` [40] and `FIESTA` [41, 42]. All other of the 22 master integrals we even confirm analytically through to weight eight by expanding the closed form in terms of hypergeometric functions given in [30, 31] using the `HypExp` package [43].

JHEP11(2010)102

All master integrals are therefore known up to transcendentality weight eight i.e. terms including π^8 (ζ_2^4), $\zeta_2\zeta_3^2$, $\zeta_3\zeta_5$ as well as the multiple zeta value $\zeta_{5,3}$ (or equivalently $\zeta_{-6,-2}$). The multiple zeta values are defined by (see e.g. [44] and references therein)

$$\zeta(m_1,\ldots,m_k) = \sum_{i_1=1}^{\infty}\sum_{i_2=1}^{i_1-1}\cdots\sum_{i_k=1}^{i_{k-1}-1}\prod_{j=1}^{k}\frac{\mathrm{sgn}(m_j)^{i_j}}{i_j^{|m_j|}}\,. \tag{1}$$

Specifically, $\zeta_{-6,-2}$ is related to $\zeta_{5,3}$ by [44, 45]

$$\zeta_{-6,-2} = \frac{9}{20}\zeta_{5,3} - \frac{3}{2}\zeta_5\zeta_3 + \frac{781}{4032000}\pi^8. \tag{2}$$

The numerical values of the transcendental constants up to weight eight are:

$$\zeta_3 = 1.2020569031595942854\ldots\,, \qquad \zeta_5 = 1.0369277551433699263\ldots\,,$$
$$\zeta_7 = 1.0083492773819228268\ldots\,, \qquad \zeta_{5,3} = 0.03770767298484754401 1\ldots\,.$$

The new results on the higher order terms in the master integrals enable the computation of the three-loop form factors through to $\mathcal{O}(\epsilon^2)$ which is an intrinsic component for the four-loop evaluation of the form factors. This is the topic of this Letter and we give explicit formulae for the $\mathcal{O}(\epsilon)$ and $\mathcal{O}(\epsilon^2)$ contributions to the unrenormalised three loop form factors.

The form factors are the basic vertex functions of an external off-shell current (with virtuality $q^2 = s_{12}$) coupling to a pair of partons with on-shell momenta p_1 and p_2. One distinguishes time-like ($s_{12} > 0$, i.e. with partons both either in the initial or in the final state) and space-like ($s_{12} < 0$, i.e. with one parton in the initial and one in the final state) configurations. The form factors are described in terms of scalar functions by contracting the respective vertex functions (evaluated in dimensional regularization with $D = 4 - 2\epsilon$ dimensions) with projectors. For massless partons, the full vertex function is described with only a single form factor.

The quark form factor is obtained from the photon-quark-antiquark vertex $\Gamma^{\mu}_{q\bar{q}}$ by

$$\mathcal{F}^q = -\frac{1}{4(1-\epsilon)q^2}\,\mathrm{Tr}\left(\not{p}_2\Gamma^{\mu}_{q\bar{q}}\not{p}_1\gamma_\mu\right)\,, \tag{3}$$

while the gluon form factor relates to the effective Higgs-gluon-gluon vertex $\Gamma^{\mu\nu}_{gg}$ as

$$\mathcal{F}^g = \frac{p_1\cdot p_2\, g_{\mu\nu} - p_{1,\mu}p_{2,\nu} - p_{1,\nu}p_{2,\mu}}{2(1-\epsilon)}\,\Gamma^{\mu\nu}_{gg}\,. \tag{4}$$

The form factors are expanded in perturbative QCD in powers of the coupling constant, with each power corresponding to a virtual loop. We denote the unrenormalized form factors by $\mathcal{F}^a$ and the renormalized form factors by F^a with $a = q, g$.

At tree level, the Higgs boson does not couple either to the gluon or to massless quarks. In higher orders in perturbation theory, heavy quark loops introduce a coupling between the Higgs boson and gluons. In the limit of infinitely massive quarks, these loops give rise to an effective Lagrangian [46–49] mediating the coupling between the scalar Higgs field and the gluon field strength tensor:

$$\mathcal{L}_{\mathrm{int}} = -\frac{\lambda}{4}HF_a^{\mu\nu}F_{a,\mu\nu}\,. \tag{5}$$

JHEP11(2010)102

The coupling λ has inverse mass dimension. It can be computed by matching [50–52] the effective theory to the full standard model cross sections [5–9].

Direct evaluation of the Feynman diagrams at the appropriate loop order yields the bare (unrenormalised) form factors,

$$\mathcal{F}_b^q(\alpha_s^b, s_{12}) = 1 + \sum_{n=1}^{\infty} \left(\frac{\alpha_s^b}{4\pi}\right)^n \left(\frac{-s_{12}}{\mu_0^2}\right)^{-n\epsilon} S_\epsilon^n \, \mathcal{F}_n^q, \tag{6}$$

$$\mathcal{F}_b^g(\alpha_s^b, s_{12}) = \lambda^b \left(1 + \sum_{n=1}^{\infty} \left(\frac{\alpha_s^b}{4\pi}\right)^n \left(\frac{-s_{12}}{\mu_0^2}\right)^{-n\epsilon} S_\epsilon^n \, \mathcal{F}_n^g\right), \tag{7}$$

where μ_0^2 is the mass parameter introduced in dimensional regularisation to maintain a dimensionless coupling in the bare Lagrangian density and where

$$S_\epsilon = e^{-\epsilon\gamma}(4\pi)^\epsilon, \qquad \text{with the Euler constant } \gamma = 0.5772\ldots \tag{8}$$

The one-loop and two-loop form factors were computed in many places in the literature [16–22]. All-order expressions in terms of one-loop and two-loop master integrals are given in [22]. Explicit expressions for the one- and two-loop form factors through to $\mathrm{O}(\epsilon^5)$ and $\mathrm{O}(\epsilon^3)$ respectively are given already in [25]. To determine the finite piece at the four-loop level, these form factors are needed to one higher power in ϵ, and for the sake of completeness, we quote them here. At one-loop,

$$\begin{aligned}
\mathcal{F}_1^q &= \mathcal{F}_1^q|_{\frac{1}{\epsilon^2}} + \cdots + \mathcal{F}_1^q|_{\epsilon^5} \\
&\quad + C_F \Bigg[\epsilon^6 \Bigg(-512 + \frac{381\zeta_7}{7} + \frac{496\zeta_5}{5} + \frac{448\zeta_3}{3} - \frac{434\zeta_3\zeta_5}{15} - \frac{196\zeta_3^2}{9} + 64\zeta_2 \\
&\qquad - \frac{93\zeta_2\zeta_5}{10} - \frac{56\zeta_2\zeta_3}{3} + \frac{49\zeta_2\zeta_3^2}{18} + \frac{188\zeta_2^2}{5} - \frac{329\zeta_2^2\zeta_3}{40} + \frac{949\zeta_2^3}{70} + \frac{55779\zeta_2^4}{11200}\Bigg)\Bigg] \\
\mathcal{F}_1^g &= \mathcal{F}_1^g|_{\frac{1}{\epsilon^2}} + \cdots + \mathcal{F}_1^g|_{\epsilon^5} \\
&\quad + C_A \Bigg[\epsilon^6 \Bigg(-126 + \frac{62\zeta_5}{5} + \frac{98\zeta_3}{3} - \frac{434\zeta_3\zeta_5}{15} + 15\zeta_2 - \frac{7\zeta_2\zeta_3}{3} + \frac{49\zeta_2\zeta_3^2}{18} \\
&\qquad + \frac{141\zeta_2^2}{20} + \frac{55779\zeta_2^4}{11200}\Bigg)\Bigg]
\end{aligned} \tag{9}$$

and at two-loops

$$\begin{aligned}
\mathcal{F}_2^q &= \mathcal{F}_2^q|_{\frac{1}{\epsilon^4}} + \cdots + \mathcal{F}_2^q|_{\epsilon^3} \\
&\quad + C_F^2 \Bigg[\epsilon^4 \Bigg(+\frac{637631}{128} - 528\zeta_{5,3} + \frac{27204\zeta_7}{7} - \frac{34001\zeta_5}{10} - \frac{481913\zeta_3}{24} + \frac{33248\zeta_3\zeta_5}{15} \\
&\qquad + \frac{36359\zeta_3^2}{9} + \frac{95559\zeta_2}{32} - 198\zeta_2\zeta_5 + \frac{2257\zeta_2\zeta_3}{2} - \frac{4576\zeta_2\zeta_3^2}{9} - \frac{248023\zeta_2^2}{80} \\
&\qquad + \frac{5109\zeta_2^2\zeta_3}{5} + \frac{55623\zeta_2^3}{140} + \frac{653901\zeta_2^4}{700}\Bigg)\Bigg]
\end{aligned}$$

JHEP11(2010)102

$$
\begin{aligned}
&+C_F C_A\Bigg[\epsilon^4\Bigg(-\frac{11630115085}{839808}+264\zeta_{5,3}-\frac{11980\zeta_7}{21}+\frac{1214029\zeta_5}{270}+\frac{84520897\zeta_3}{5832}\\
&\qquad-\frac{8266\zeta_3\zeta_5}{5}-\frac{229042\zeta_3^2}{81}-\frac{58499773\zeta_2}{23328}-\frac{829\zeta_2\zeta_5}{15}-\frac{94931\zeta_2\zeta_3}{162}+\frac{3029\zeta_2\zeta_3^2}{9}\\
&\qquad+\frac{14915741\zeta_2^2}{6480}-\frac{66379\zeta_2^2\zeta_3}{90}+\frac{4843\zeta_2^3}{30}-\frac{75242\zeta_2^4}{175}\Bigg)\Bigg]\\
&+C_F N_F\Bigg[\epsilon^4\Bigg(+\frac{996726245}{419904}-\frac{2186\zeta_7}{21}-\frac{42713\zeta_5}{135}-\frac{1951625\zeta_3}{2916}+\frac{4732\zeta_3^2}{81}+\frac{2877653\zeta_2}{11664}\\
&\qquad-\frac{242\zeta_2\zeta_5}{15}-\frac{4589\zeta_2\zeta_3}{81}-\frac{309181\zeta_2^2}{3240}+\frac{533\zeta_2^2\zeta_3}{45}-\frac{127\zeta_2^3}{3}\Bigg)\Bigg]\\
\mathcal{F}_2^g &= \mathcal{F}_2^g|_{\frac{1}{\epsilon^4}}+\cdots+\mathcal{F}_2^g|_{\epsilon^3}\\
&+C_A^2\Bigg[\epsilon^4\Bigg(+\frac{1371828689}{209952}-264\zeta_{5,3}+\frac{56155\zeta_7}{42}-\frac{161266\zeta_5}{135}-\frac{5108944\zeta_3}{729}+\frac{1690\zeta_3\zeta_5}{3}\\
&\qquad+\frac{85559\zeta_3^2}{81}-\frac{219275\zeta_2}{1944}-\frac{1001\zeta_2\zeta_5}{5}+\frac{11858\zeta_2\zeta_3}{27}-\frac{1547\zeta_2\zeta_3^2}{9}-\frac{187733\zeta_2^2}{180}\\
&\qquad+\frac{22781\zeta_2^2\zeta_3}{90}+\frac{123079\zeta_2^3}{1260}+\frac{50419\zeta_2^4}{100}\Bigg)\Bigg]\\
&+C_A N_F\Bigg[\epsilon^4\Bigg(-\frac{232282297}{104976}+\frac{229\zeta_7}{21}-\frac{24518\zeta_5}{135}-\frac{301886\zeta_3}{729}+\frac{22060\zeta_3^2}{81}\\
&\qquad+\frac{98791\zeta_2}{972}+\frac{342\zeta_2\zeta_5}{5}+\frac{2978\zeta_2\zeta_3}{27}-\frac{40148\zeta_2^2}{405}+\frac{517\zeta_2^2\zeta_3}{5}+\frac{2167\zeta_2^3}{630}\Bigg)\Bigg]\\
&+C_F N_F\Bigg[\epsilon^4\Bigg(-\frac{19296691}{7776}-254\zeta_7+\frac{22948\zeta_5}{45}+\frac{192068\zeta_3}{81}-460\zeta_3^2+\frac{75305\zeta_2}{648}\\
&\qquad-32\zeta_2\zeta_5-\frac{5716\zeta_2\zeta_3}{27}+\frac{585929\zeta_2^2}{1620}-\frac{6724\zeta_2^2\zeta_3}{45}-\frac{2024\zeta_2^3}{105}\Bigg)\Bigg]
\end{aligned}
\tag{10}
$$

The unrenormalised three-loop quark form factor $\mathcal{F}_3^q$ through to (and including) $\mathcal{O}(\epsilon^0)$ is given in eq. (5.4) of ref. [25]. The pole contributions of $\mathcal{F}_3^q$ are also given in eq. (3.7) of ref. [16] while the finite parts of the N_F^2, $C_A N_F$ and $C_F N_F$ contributions are given in eq. (6) of ref. [17]. The finite $N_{F,V}$ contribution could already be inferred from [53]. The remaining finite contributions are also given in eqs. (8) and (9) of ref. [34]. The $\mathcal{O}(\epsilon^1)$ and $\mathcal{O}(\epsilon^2)$ contributions are given by,

$$
\begin{aligned}
\mathcal{F}_3^q &= \mathcal{F}_3^q|_{\frac{1}{\epsilon^6}}+\cdots+\mathcal{F}_3^q|_{\epsilon^0}\\
&+C_F^3\Bigg[+\epsilon\Bigg(-\frac{343393}{48}-\frac{11896\zeta_7}{7}+\frac{22349\zeta_5}{3}+\frac{40835\zeta_3}{6}-1203\zeta_3^2-\frac{105553\zeta_2}{24}\\
&\qquad-\frac{7858\zeta_2\zeta_5}{15}+\frac{6083\zeta_2\zeta_3}{6}+\frac{36693\zeta_2^2}{40}-\frac{3931\zeta_2^2\zeta_3}{6}+\frac{321227\zeta_2^3}{840}\Bigg)
\end{aligned}
$$

JHEP11(2010)102

$$+\epsilon^2\Bigg(-\frac{2512115}{96}+\frac{4160\zeta_{5,3}}{3}+\frac{45168\zeta_7}{7}+\frac{716537\zeta_5}{15}-\frac{137417\zeta_3}{12}$$
$$-\frac{33148\zeta_3\zeta_5}{3}+\frac{12749\zeta_3^2}{6}-\frac{797995\zeta_2}{48}-\frac{12361\zeta_2\zeta_5}{5}+\frac{18469\zeta_2\zeta_3}{2}$$
$$+1985\zeta_2\zeta_3^2+\frac{7653\zeta_2^2}{80}-\frac{15491\zeta_2^2\zeta_3}{20}+\frac{1147979\zeta_2^3}{240}-\frac{74208727\zeta_2^4}{50400}\Bigg)\Bigg]$$
$$+C_F^2C_A\Bigg[+\epsilon\Bigg(+\frac{783459131}{34992}-1349\zeta_7-\frac{1894909\zeta_5}{270}-\frac{1259477\zeta_3}{54}+\frac{85649\zeta_3^2}{18}$$
$$+\frac{19394303\zeta_2}{1944}+\frac{4851\zeta_2\zeta_5}{5}-\frac{195175\zeta_2\zeta_3}{108}-\frac{15062939\zeta_2^2}{6480}$$
$$+\frac{9751\zeta_2^2\zeta_3}{20}-\frac{1811231\zeta_2^3}{15120}\Bigg)$$
$$+\epsilon^2\Bigg(+\frac{16308475427}{209952}-\frac{15472\zeta_{5,3}}{15}+\frac{415489\zeta_7}{42}-\frac{7913725\zeta_5}{162}-\frac{27356135\zeta_3}{324}$$
$$+\frac{72904\zeta_3\zeta_5}{15}+\frac{2174933\zeta_3^2}{108}+\frac{521534243\zeta_2}{11664}+\frac{53128\zeta_2\zeta_5}{15}-\frac{5620115\zeta_2\zeta_3}{324}$$
$$-1425\zeta_2\zeta_3^2-\frac{161423233\zeta_2^2}{19440}+\frac{1083953\zeta_2^2\zeta_3}{180}-\frac{211343621\zeta_2^3}{90720}$$
$$-\frac{22796551\zeta_2^4}{63000}\Bigg)\Bigg]$$
$$+C_FC_A^2\Bigg[+\epsilon\Bigg(-\frac{458292965}{26244}-\frac{211\zeta_7}{18}+\frac{15601\zeta_5}{5}+\frac{42813461\zeta_3}{2916}-\frac{71734\zeta_3^2}{27}$$
$$-\frac{52068575\zeta_2}{8748}-\frac{1568\zeta_2\zeta_5}{9}+\frac{13139\zeta_2\zeta_3}{27}+\frac{4467743\zeta_2^2}{3240}-\frac{4408\zeta_2^2\zeta_3}{45}$$
$$-\frac{8009\zeta_2^3}{945}\Bigg)$$
$$+\epsilon^2\Bigg(-\frac{34868838031}{472392}-\frac{3592\zeta_{5,3}}{45}-\frac{176495\zeta_7}{36}+\frac{18727307\zeta_5}{810}+\frac{405838949\zeta_3}{5832}$$
$$+\frac{568\zeta_3\zeta_5}{3}-\frac{820579\zeta_3^2}{54}-\frac{1546106255\zeta_2}{52488}-\frac{23456\zeta_2\zeta_5}{15}+\frac{2116327\zeta_2\zeta_3}{324}$$
$$+\frac{2896\zeta_2\zeta_3^2}{9}+\frac{167549\zeta_2^2}{27}-3805\zeta_2^2\zeta_3+\frac{201469\zeta_2^3}{216}+\frac{6341548\zeta_2^4}{23625}\Bigg)\Bigg]$$
$$+C_F^2N_F\Bigg[+\epsilon\Bigg(-\frac{50187205}{17496}+\frac{5863\zeta_5}{135}+\frac{929587\zeta_3}{243}-\frac{5771\zeta_3^2}{9}-\frac{1263505\zeta_2}{972}$$
$$-\frac{8515\zeta_2\zeta_3}{54}+\frac{821749\zeta_2^2}{3240}-\frac{875381\zeta_2^3}{7560}\Bigg)$$
$$+\epsilon^2\Bigg(-\frac{861740653}{104976}-\frac{294430\zeta_7}{63}+\frac{167299\zeta_5}{81}+\frac{32307433\zeta_3}{1458}-\frac{208487\zeta_3^2}{54}$$
$$-\frac{32868205\zeta_2}{5832}+\frac{953\zeta_2\zeta_5}{15}-\frac{152867\zeta_2\zeta_3}{162}+\frac{17061119\zeta_2^2}{9720}-\frac{172799\zeta_2^2\zeta_3}{180}$$

JHEP11(2010)102

$$
\begin{aligned}
&\quad -\frac{4769039\zeta_2^3}{6480}\Bigg)\Bigg] \\
&+C_F C_A N_F\Bigg[+\epsilon\Bigg(+\frac{24570881}{4374}-\frac{28156\zeta_5}{45}-\frac{2418896\zeta_3}{729}+\frac{10816\zeta_3^2}{27}+\frac{7137385\zeta_2}{4374} \\
&\quad +\frac{2674\zeta_2\zeta_3}{27}-\frac{352559\zeta_2^2}{1620}+\frac{17324\zeta_2^3}{945}\Bigg) \\
&+\epsilon^2\Bigg(+\frac{5509319623}{236196}+1170\zeta_7-\frac{622178\zeta_5}{135}-\frac{79031137\zeta_3}{4374}+\frac{218296\zeta_3^2}{81} \\
&\quad +\frac{102669593\zeta_2}{13122}+\frac{3272\zeta_2\zeta_5}{15}+\frac{11939\zeta_2\zeta_3}{81}-\frac{3829919\zeta_2^2}{3240}+\frac{9572\zeta_2^2\zeta_3}{15} \\
&\quad +\frac{74461\zeta_2^3}{5670}\Bigg)\Bigg] \\
&+C_F N_F^2\Bigg[+\epsilon\Bigg(-\frac{2913928}{6561}+\frac{2248\zeta_5}{135}+\frac{2108\zeta_3}{27}-\frac{24950\zeta_2}{243}+\frac{68\zeta_2\zeta_3}{9}-\frac{3901\zeta_2^2}{810}\Bigg) \\
&+\epsilon^2\Bigg(-\frac{109448624}{59049}+\frac{52828\zeta_5}{405}+\frac{848300\zeta_3}{2187}-\frac{1156\zeta_3^2}{81}-\frac{338858\zeta_2}{729} \\
&\quad +\frac{1598\zeta_2\zeta_3}{27}-\frac{2573\zeta_2^2}{90}+\frac{44651\zeta_2^3}{5670}\Bigg)\Bigg] \\
&+C_F N_{F,V}\left(\frac{N^2-4}{N}\right)\times \\
&\times\Bigg[+\epsilon\Bigg(+\frac{170}{3}+\frac{752\zeta_5}{9}+\frac{94\zeta_3}{9}-\frac{344\zeta_3^2}{3}+\frac{260\zeta_2}{3}+30\zeta_2\zeta_3-\frac{196\zeta_2^2}{15}-\frac{9728\zeta_2^3}{315}\Bigg) \\
&+\epsilon^2\Bigg(+\frac{1460}{3}-\frac{4271\zeta_7}{3}+\frac{12970\zeta_5}{27}+\frac{2501\zeta_3}{27}-\frac{748\zeta_3^2}{9}+\frac{4345\zeta_2}{9} \\
&\quad -\frac{256\zeta_2\zeta_5}{3}+\frac{239\zeta_2\zeta_3}{3}-\frac{3677\zeta_2^2}{45}-\frac{392\zeta_2^2\zeta_3}{3}+\frac{85244\zeta_2^3}{945}\Bigg)\Bigg]
\end{aligned}
\tag{11}
$$

Note that last colour factor is generated by graphs where the virtual gauge boson does not couple directly to the final-state quarks. This contribution is denoted by $N_{F,V}$ and is proportional to the charge weighted sum of the quark flavours. In the case of purely electromagnetic interactions, we find,

$$
N_{F,\gamma} = \frac{\sum_q e_q}{e_q}. \tag{12}
$$

The unrenormalised three-loop gluon form factor through to (and including) $\mathcal{O}(\epsilon^0)$ is given in eq. (5.5) of ref. [25]. The divergent parts are also given in eq. (8) of ref. [17] while the finite contributions are given in eq. (10) of ref. [34]. The $\mathcal{O}(\epsilon^1)$ and $\mathcal{O}(\epsilon^2)$ contributions for $\mathcal{F}_3^g$ are given by,

$$
\mathcal{F}_3^g = \mathcal{F}_3^g|_{\frac{1}{\epsilon^6}} + \cdots + \mathcal{F}_3^g|_{\epsilon^0}
$$

JHEP11(2010)102

$$
\begin{aligned}
&+C_A^3\Bigg[+\epsilon\Bigg(+\frac{270573319}{26244}-\frac{385579\zeta_7}{126}+\frac{389159\zeta_5}{135}-\frac{3601570\zeta_3}{729}+\frac{74899\zeta_3^2}{54}\\
&\qquad-\frac{446863\zeta_2}{4374}+\frac{2449\zeta_2\zeta_5}{9}-\frac{34093\zeta_2\zeta_3}{54}-\frac{40819\zeta_2^2}{180}-\frac{47803\zeta_2^2\zeta_3}{180}\\
&\qquad+\frac{7200127\zeta_2^3}{15120}\Bigg)\\
&+\epsilon^2\Bigg(+\frac{30151577675}{472392}+\frac{12392\zeta_{5,3}}{45}+\frac{2169431\zeta_7}{126}+\frac{3101341\zeta_5}{405}-\frac{59902487\zeta_3}{1458}\\
&\qquad-\frac{89996\zeta_3\zeta_5}{15}+\frac{16453\zeta_3^2}{2}-\frac{108299125\zeta_2}{26244}-\frac{6897\zeta_2\zeta_5}{10}-\frac{80255\zeta_2\zeta_3}{27}\\
&\qquad+\frac{7936\zeta_2\zeta_3^2}{9}-\frac{34875497\zeta_2^2}{9720}+\frac{714109\zeta_2^2\zeta_3}{360}+\frac{12226469\zeta_2^3}{5040}-\frac{1183759981\zeta_2^4}{756000}\Bigg)\Bigg]\\
&+C_A^2N_F\Bigg[+\epsilon\Bigg(-\frac{48658741}{8748}-\frac{10066\zeta_5}{45}+\frac{349918\zeta_3}{729}-\frac{11657\zeta_3^2}{27}+\frac{904045\zeta_2}{4374}\\
&\qquad+\frac{791\zeta_2\zeta_3}{9}-\frac{34931\zeta_2^2}{1620}-\frac{52283\zeta_2^3}{1080}\Bigg)\\
&+\epsilon^2\Bigg(-\frac{15039308929}{472392}-\frac{14271\zeta_7}{7}-\frac{391564\zeta_5}{405}+\frac{13422322\zeta_3}{2187}-\frac{76349\zeta_3^2}{81}\\
&\qquad+\frac{66386911\zeta_2}{26244}+\frac{307\zeta_2\zeta_5}{5}+\frac{31849\zeta_2\zeta_3}{81}+\frac{373234\zeta_2^2}{1215}-\frac{104327\zeta_2^2\zeta_3}{180}\\
&\qquad-\frac{6878021\zeta_2^3}{22680}\Bigg)\Bigg]\\
&+C_AC_FN_F\Bigg[+\epsilon\Bigg(-\frac{10508593}{2916}+\frac{17092\zeta_5}{27}+\frac{240934\zeta_3}{243}+\frac{4064\zeta_3^2}{9}+\frac{8869\zeta_2}{54}\\
&\qquad+\frac{640\zeta_2\zeta_3}{9}+\frac{28823\zeta_2^2}{270}+\frac{23624\zeta_2^3}{315}\Bigg)\\
&+\epsilon^2\Bigg(-\frac{418631245}{17496}+\frac{16658\zeta_7}{9}+\frac{386102\zeta_5}{81}+\frac{4492979\zeta_3}{729}+\frac{17176\zeta_3^2}{27}\\
&\qquad+\frac{163523\zeta_2}{108}-496\zeta_2\zeta_5+\frac{3500\zeta_2\zeta_3}{9}+\frac{437599\zeta_2^2}{540}+\frac{3148\zeta_2^2\zeta_3}{5}\\
&\qquad+\frac{157424\zeta_2^3}{315}\Bigg)\Bigg]\\
&+C_F^2N_F\Bigg[+\epsilon\Bigg(+\frac{18613}{54}-\frac{3080\zeta_5}{3}+\frac{10552\zeta_3}{9}-272\zeta_3^2-\frac{74\zeta_2}{3}-16\zeta_2\zeta_3+\frac{328\zeta_2^2}{5}-\frac{35648\zeta_2^3}{315}\Bigg)\\
&+\epsilon^2\Bigg(+\frac{383765}{162}-\frac{8828\zeta_7}{3}-\frac{35956\zeta_5}{9}+\frac{229772\zeta_3}{27}-\frac{6400\zeta_3^2}{3}-\frac{4109\zeta_2}{18}\\
&\qquad+560\zeta_2\zeta_5-276\zeta_2\zeta_3+764\zeta_2^2-\frac{1232\zeta_2^2\zeta_3}{3}-\frac{796168\zeta_2^3}{945}\Bigg)\Bigg]
\end{aligned}
$$

JHEP11(2010)102

$$
\begin{aligned}
&+C_A N_F^2 \Bigg[+\epsilon\left(+\frac{16823771}{26244}+\frac{9368\zeta_5}{135}+\frac{5440\zeta_3}{27}-\frac{30283\zeta_2}{1458}-\frac{988\zeta_2\zeta_3}{27}+\frac{14018\zeta_2^2}{405}\right)\\
&+\epsilon^2\Bigg(+\frac{1534229129}{472392}+\frac{33136\zeta_5}{81}+\frac{1698929\zeta_3}{2187}-\frac{17908\zeta_3^2}{81}-\frac{1822421\zeta_2}{8748}\\
&\qquad -\frac{15928\zeta_2\zeta_3}{81}+\frac{20009\zeta_2^2}{135}+\frac{12851\zeta_2^3}{5670}\Bigg)\Bigg]\\
&+C_F N_F^2 \Bigg[+\epsilon\left(+\frac{196900}{243}-\frac{800\zeta_5}{9}-\frac{4208\zeta_3}{9}-54\zeta_2+\frac{112\zeta_2\zeta_3}{3}-\frac{2464\zeta_2^2}{45}\right)\\
&+\epsilon^2\Bigg(+\frac{6322579}{1458}-\frac{17600\zeta_5}{27}-\frac{223756\zeta_3}{81}+\frac{3232\zeta_3^2}{9}-\frac{9626\zeta_2}{27}+\frac{2464\zeta_2\zeta_3}{9}\\
&\qquad -\frac{4913\zeta_2^2}{15}+\frac{248\zeta_2^3}{63}\Bigg)\Bigg]
\end{aligned}
\tag{13}
$$

The renormalised form factors are directly related to the unrenormalised form factors and details on how to extract the renormalised form factors to this order are given in section 2 of ref. [25].

In this letter, we computed the three-loop quark and gluon form factors through to $\mathrm{O}(\epsilon^2)$ in the dimensional regularisation parameter. These contributions are relevant in the study of the infrared singularity structure at four loops. In particular, the $\mathcal{O}(\epsilon)$ terms of the three-loop form factors are required for the extraction of the four-loop quark and gluon collinear anomalous dimensions. The $\mathcal{O}(\epsilon^2)$ terms contribute to the finite part of the infrared-subtraction of the form factors at four loops. It is this infrared-subtracted finite part which is relevant for the study of the next-to-next-to-next-to-next-to-leading ($\mathrm{N^4LO}$) Drell-Yan and Higgs production processes. In particular, the $\mathcal{O}(\epsilon^2)$ three-loop contributions represent a finite ingredient to these processes at four-loops.

Acknowledgments

We thank Daniel Maître and Volodya Smirnov for useful comments regarding the conversion of $\zeta_{-6,-2}$ to $\zeta_{5,3}$. This research was supported in part by the Swiss National Science Foundation (SNF) under contract 200020-126691, by the Forschungskredit der Universität Zürich, the UK Science and Technology Facilities Council, by the European Commission's Marie-Curie Research Training Network under contract MRTN-CT-2006-035505 'Tools and Precision Calculations for Physics Discoveries at Colliders', by the Helmholtz Alliance "Physics at the Terascale", and by Deutsche Forschungsgemeinschaft (DFG SCHR 993/2-1). EWNG gratefully acknowledges the support of the Wolfson Foundation and the Royal Society.

References

[1] G. Altarelli, R.K. Ellis and G. Martinelli, *Large perturbative corrections to the Drell-Yan process in QCD*, *Nucl. Phys.* **B 157** (1979) 461 [SPIRES].

JHEP11(2010)102

[2] R. Hamberg, W.L. van Neerven and T. Matsuura, *A complete calculation of the order α_s^2 correction to the Drell-Yan K factor*, *Nucl. Phys.* **B 359** (1991) 343 [*Erratum ibid.* **B 644** (2002) 403] [SPIRES].

[3] R.V. Harlander and W.B. Kilgore, *Next-to-next-to-leading order Higgs production at hadron colliders*, *Phys. Rev. Lett.* **88** (2002) 201801 [hep-ph/0201206] [SPIRES].

[4] S. Dawson, *Radiative corrections to Higgs boson production*, *Nucl. Phys.* **B 359** (1991) 283 [SPIRES].

[5] D. Graudenz, M. Spira and P.M. Zerwas, *QCD corrections to Higgs boson production at proton proton colliders*, *Phys. Rev. Lett.* **70** (1993) 1372 [SPIRES].

[6] M. Spira, A. Djouadi, D. Graudenz and P.M. Zerwas, *Higgs boson production at the LHC*, *Nucl. Phys.* **B 453** (1995) 17 [hep-ph/9504378] [SPIRES].

[7] A. Djouadi, M. Spira and P.M. Zerwas, *QCD corrections to hadronic Higgs decays*, *Z. Phys.* **C 70** (1996) 427 [hep-ph/9511344] [SPIRES].

[8] M. Spira, *QCD effects in Higgs physics*, *Fortsch. Phys.* **46** (1998) 203 [hep-ph/9705337] [SPIRES].

[9] R. Harlander and P. Kant, *Higgs production and decay: analytic results at next-to-leading order QCD*, *JHEP* **12** (2005) 015 [hep-ph/0509189] [SPIRES].

[10] S. Catani, D. de Florian and M. Grazzini, *Higgs production in hadron collisions: soft and virtual QCD corrections at NNLO*, *JHEP* **05** (2001) 025 [hep-ph/0102227] [SPIRES].

[11] C. Anastasiou and K. Melnikov, *Higgs boson production at hadron colliders in NNLO QCD*, *Nucl. Phys.* **B 646** (2002) 220 [hep-ph/0207004] [SPIRES].

[12] V. Ravindran, J. Smith and W.L. van Neerven, *NNLO corrections to the total cross section for Higgs boson production in hadron hadron collisions*, *Nucl. Phys.* **B 665** (2003) 325 [hep-ph/0302135] [SPIRES].

[13] V. Ravindran, J. Smith and W.L. van Neerven, *Two-loop corrections to Higgs boson production*, *Nucl. Phys.* **B 704** (2005) 332 [hep-ph/0408315] [SPIRES].

[14] S. Moch, J.A.M. Vermaseren and A. Vogt, *The three-loop splitting functions in QCD: the non-singlet case*, *Nucl. Phys.* **B 688** (2004) 101 [hep-ph/0403192] [SPIRES].

[15] A. Vogt, S. Moch and J.A.M. Vermaseren, *The three-loop splitting functions in QCD: the singlet case*, *Nucl. Phys.* **B 691** (2004) 129 [hep-ph/0404111] [SPIRES].

[16] S. Moch, J.A.M. Vermaseren and A. Vogt, *The quark form factor at higher orders*, *JHEP* **08** (2005) 049 [hep-ph/0507039] [SPIRES].

[17] S. Moch, J.A.M. Vermaseren and A. Vogt, *Three-loop results for quark and gluon form factors*, *Phys. Lett.* **B 625** (2005) 245 [hep-ph/0508055] [SPIRES].

[18] G. Kramer and B. Lampe, *Two jet cross-section in e^+e^- annihilation*, *Z. Phys.* **C 34** (1987) 497 [*Erratum ibid.* **C 42** (1989) 504] [SPIRES].

[19] T. Matsuura and W.L. van Neerven, *Second order logarithmic corrections to the Drell-Yan cross-section*, *Z. Phys.* **C 38** (1988) 623 [SPIRES].

[20] T. Matsuura, S.C. van der Marck and W.L. van Neerven, *The calculation of the second order soft and virtual contributions to the Drell-Yan cross-section*, *Nucl. Phys.* **B 319** (1989) 570 [SPIRES].

JHEP11(2010)102

[21] R.V. Harlander, *Virtual corrections to $gg \to H$ to two loops in the heavy top limit*, *Phys. Lett.* **B 492** (2000) 74 [hep-ph/0007289] [SPIRES].

[22] T. Gehrmann, T. Huber and D. Maître, *Two-loop quark and gluon form factors in dimensional regularisation*, *Phys. Lett.* **B 622** (2005) 295 [hep-ph/0507061] [SPIRES].

[23] T. Becher, M. Neubert and B.D. Pecjak, *Factorization and momentum-space resummation in deep-inelastic scattering*, *JHEP* **01** (2007) 076 [hep-ph/0607228] [SPIRES].

[24] T. Becher and M. Neubert, *On the structure of infrared singularities of gauge-theory amplitudes*, *JHEP* **06** (2009) 081 [arXiv:0903.1126] [SPIRES].

[25] T. Gehrmann, E.W.N. Glover, T. Huber, N. Ikizlerli and C. Studerus, *Calculation of the quark and gluon form factors to three loops in QCD*, *JHEP* **06** (2010) 094 [arXiv:1004.3653] [SPIRES].

[26] K.G. Chetyrkin and F.V. Tkachov, *Integration by parts: the algorithm to calculate β-functions in 4 loops*, *Nucl. Phys.* **B 192** (1981) 159 [SPIRES].

[27] S.G. Gorishnii, S.A. Larin, L.R. Surguladze and F.V. Tkachov, *Mincer: program for multiloop calculations in quantum field theory for the SCHOONSCHIP system*, *Comput. Phys. Commun.* **55** (1989) 381 [SPIRES].

[28] S.A. Larin, F.V. Tkachov and J.A.M. Vermaseren, *The form version of Mincer*, NIKHEF-H-91-18, NIKHEF, Amsterdam The Netherlands (1991) [SPIRES].

[29] S. Bekavac, *Calculation of massless Feynman integrals using harmonic sums*, *Comput. Phys. Commun.* **175** (2006) 180 [hep-ph/0505174] [SPIRES].

[30] T. Gehrmann, G. Heinrich, T. Huber and C. Studerus, *Master integrals for massless three-loop form factors: one-loop and two-loop insertions*, *Phys. Lett.* **B 640** (2006) 252 [hep-ph/0607185] [SPIRES].

[31] G. Heinrich, T. Huber and D. Maître, *Master integrals for fermionic contributions to massless three-loop form factors*, *Phys. Lett.* **B 662** (2008) 344 [arXiv:0711.3590] [SPIRES].

[32] G. Heinrich, T. Huber, D.A. Kosower and V.A. Smirnov, *Nine-propagator master integrals for massless three-loop form factors*, *Phys. Lett.* **B 678** (2009) 359 [arXiv:0902.3512] [SPIRES].

[33] R.N. Lee, A.V. Smirnov and V.A. Smirnov, *Analytic results for massless three-loop form factors*, *JHEP* **04** (2010) 020 [arXiv:1001.2887] [SPIRES].

[34] P.A. Baikov, K.G. Chetyrkin, A.V. Smirnov, V.A. Smirnov and M. Steinhauser, *Quark and gluon form factors to three loops*, *Phys. Rev. Lett.* **102** (2009) 212002 [arXiv:0902.3519] [SPIRES].

[35] R.N. Lee and V.A. Smirnov, *Analytic ϵ-expansions of master integrals corresponding to massless three-loop form factors and three-loop g-2 up to four-loop transcendentality weight*, arXiv:1010.1334 [SPIRES].

[36] O.V. Tarasov, *Connection between Feynman integrals having different values of the space-time dimension*, *Phys. Rev.* **D 54** (1996) 6479 [hep-th/9606018] [SPIRES].

[37] R.N. Lee, *Space-time dimensionality D as complex variable: calculating loop integrals using dimensional recurrence relation and analytical properties with respect to D*, *Nucl. Phys.* **B 830** (2010) 474 [arXiv:0911.0252] [SPIRES].

JHEP11(2010)102

[38] R.N. Lee, A.V. Smirnov and V.A. Smirnov, *Dimensional recurrence relations: an easy way to evaluate higher orders of expansion in ϵ*, arXiv:1005.0362 [SPIRES].

[39] T. Huber and D. Maître, *HypExp 2, expanding hypergeometric functions about half-integer parameters*, *Comput. Phys. Commun.* **178** (2008) 755 [arXiv:0708.2443] [SPIRES].

[40] M. Czakon, *Automatized analytic continuation of Mellin-Barnes integrals*, *Comput. Phys. Commun.* **175** (2006) 559 [hep-ph/0511200] [SPIRES].

[41] A.V. Smirnov and M.N. Tentyukov, *Feynman Integral Evaluation by a Sector decomposiTion Approach (FIESTA)*, *Comput. Phys. Commun.* **180** (2009) 735 [arXiv:0807.4129] [SPIRES].

[42] A.V. Smirnov, V.A. Smirnov and M. Tentyukov, *FIESTA 2: parallelizeable multiloop numerical calculations*, arXiv:0912.0158 [SPIRES].

[43] T. Huber and D. Maître, *HypExp, a Mathematica package for expanding hypergeometric functions around integer-valued parameters*, *Comput. Phys. Commun.* **175** (2006) 122 [hep-ph/0507094] [SPIRES].

[44] J. Blumlein, D.J. Broadhurst and J.A.M. Vermaseren, *The multiple zeta value data mine*, *Comput. Phys. Commun.* **181** (2010) 582 [arXiv:0907.2557] [SPIRES].

[45] D. Maître, *HPL, a Mathematica implementation of the harmonic polylogarithms*, *Comput. Phys. Commun.* **174** (2006) 222 [hep-ph/0507152] [SPIRES].

[46] F. Wilczek, *Decays of heavy vector mesons into Higgs particles*, *Phys. Rev. Lett.* **39** (1977) 1304 [SPIRES].

[47] M.A. Shifman, A.I. Vainshtein and V.I. Zakharov, *Remarks on Higgs boson interactions with nucleons*, *Phys. Lett.* **B 78** (1978) 443 [SPIRES].

[48] J.R. Ellis, M.K. Gaillard, D.V. Nanopoulos and C.T. Sachrajda, *Is the mass of the Higgs boson about* 10 *GeV?*, *Phys. Lett.* **B 83** (1979) 339 [SPIRES].

[49] T. Inami, T. Kubota and Y. Okada, *Effective gauge theory and the effect of heavy quarks in Higgs boson decays*, *Z. Phys.* **C 18** (1983) 69 [SPIRES].

[50] K.G. Chetyrkin, B.A. Kniehl and M. Steinhauser, *Hadronic Higgs decay to order α_s^4*, *Phys. Rev. Lett.* **79** (1997) 353 [hep-ph/9705240] [SPIRES].

[51] B.A. Kniehl and M. Spira, *Low-energy theorems in Higgs physics*, *Z. Phys.* **C 69** (1995) 77 [hep-ph/9505225] [SPIRES].

[52] K.G. Chetyrkin, B.A. Kniehl and M. Steinhauser, *Decoupling relations to $O(\alpha_s^3)$ and their connection to low-energy theorems*, *Nucl. Phys.* **B 510** (1998) 61 [hep-ph/9708255] [SPIRES].

[53] J.A.M. Vermaseren, A. Vogt and S. Moch, *The third-order QCD corrections to deep-inelastic scattering by photon exchange*, *Nucl. Phys.* **B 724** (2005) 3 [hep-ph/0504242] [SPIRES].

JHEP11(2010)102

Part III

Supersymmetric Gauge Theories

Published for SISSA by Springer

Received: *January 20, 2012*
Accepted: *March 9, 2012*
Published: *March 30, 2012*

The three-loop form factor in $\mathcal{N} = 4$ super Yang-Mills

Thomas Gehrmann,[a,b] **Johannes M. Henn**[b,c,d] **and Tobias Huber**[b,e]

[a] *Institut für Theoretische Physik, Universität Zürich, Winterthurerstrasse 190, CH-8057 Zürich, Switzerland*

[b] *Kavli Institute for Theoretical Physics, University of California, Santa Barbara, CA 93106, U.S.A.*

[c] *Institut für Physik, Humboldt-Universität zu Berlin, Newtonstraße15, D-12489 Berlin, Germany*

[d] *Institute for Advanced Study, Princeton, NJ 08540, U.S.A.*

[e] *Theoretische Physik 1, Naturwissenschaftlich-Technische Fakultät, Universität Siegen, Walter-Flex-Strasse 3, D-57068 Siegen, Germany*

E-mail: thomas.gehrmann@uzh.ch, jmhenn@ias.edu, huber@tp1.physik.uni-siegen.de

Abstract: In this paper we study the Sudakov form factor in $\mathcal{N} = 4$ super Yang-Mills theory to the three-loop order. The latter is expressed in terms of planar and non-planar loop integrals. We show that it is possible to choose a representation in which each loop integral has uniform transcendentality. We verify analytically the expected exponentiation of the infrared divergences with the correct values of the three-loop cusp and collinear anomalous dimensions in dimensional regularisation. We find that the form factor in $\mathcal{N} = 4$ super Yang-Mills can be related to the leading transcendentality part of the quark and gluon form factors in QCD. We also study the ultraviolet properties of the form factor in $D > 4$ dimensions, and find unexpected cancellations, resulting in an improved ultraviolet behaviour.

Keywords: Supersymmetric gauge theory, Scattering Amplitudes

ArXiv ePrint: 1112.4524

© SISSA 2012

doi:10.1007/JHEP03(2012)101

JHEP03(2012)101

Contents

1 Introduction **1**

2 Form factor to two loops **4**

3 Momentum routing invariances of integrals **7**

4 Form factor to three loops from unitarity cuts **10**
- 4.1 One-loop form factor from unitarity cuts 11
- 4.2 Two-loop form factor from unitarity cuts 12
- 4.3 Three-loop form factor from unitarity cuts 13

5 Final result for the form factor at three loops **15**

6 Logarithm of the form factor **17**

7 Ultraviolet divergences in higher dimensions **18**

8 Discussion and conclusion **21**

A Explicit results of integrals **23**

B Form factor in terms of master integrals **28**

C Four-point amplitude to two loops **29**

JHEP03(2012)101

1 Introduction

In this paper we study the Sudakov form factor in $\mathcal{N} = 4$ super Yang-Mills (SYM) with gauge group SU(N). Following van Neerven [1], we study the vacuum expectation value of an operator built from two scalars, inserted into two on-shell states. The operator belongs to the stress-energy supermultiplet, which contains the conserved currents of $\mathcal{N} = 4$ SYM, and has zero anomalous dimension. Together with the vanishing β function of $\mathcal{N} = 4$ SYM this means that the form factor is ultraviolet (UV) finite in four dimensions. Therefore only infrared (IR) divergences associated to the on-shell states appear, which we regularise using dimensional regularisation.

Generalisations of the Sudakov form factor to the case of different composite operators, and more external on-shell legs, have been discussed recently in refs. [2–5]. Form factors have also been studied within the AdS/CFT correspondence in the dual AdS description, see refs. [6, 7]. Here we will focus on the perturbative expansion of the form factor of ref. [1].

Form factors are closely related to scattering amplitudes. For example, planar amplitudes can be factorised into an infrared divergent part, given by a product of form factors, and an infrared finite remainder (a 'hard' function in QCD terminology), see e.g. ref. [8] and references therein. The infrared divergent part exponentiates and has a simple universal form. In fact, for four- and five-point scattering amplitudes the exponentiation property of the divergent part carries over to the finite part as well [8, 9]. This is a consequence of a hidden dual conformal symmetry of planar scattering amplitudes. The latter relates the finite part to the infrared divergent part through a Ward identity [10, 11]. The relation to form factors makes it possible to give an operator definition of the finite remainder. The scheme independence of the latter was recently checked in a two-loop computation using dimensional and massive regularisations [12].

Scattering amplitudes in $\mathcal{N} = 4$ SYM have many special properties, and it is interesting to ask how much of this simplicity carries over to the form factors. For both the planar four-particle amplitude and the form factor, the general form of the result is known in principle. For the former, this is due to dual conformal symmetry, and for the latter it is due to the exponentiation of infrared divergences. However it is quite non-trivial to obtain these a priori known results from explicit perturbative calculations, evaluating loop integrals. The simplicity of the final results suggests that there should be more structure hidden in the loop integral expressions, and by studying them further one might gain insights into better ways of evaluating them, which is of more general interest.

One might expect that the evaluation of form factors should be simpler than that of scattering amplitudes, as the former have a trivial scale dependence only, whereas the latter are functions of ratios of Mandelstam variables, e.g. s/t in the four-point case. Given this, it is somewhat surprising that less is known about the loop expansion of form factors in $\mathcal{N} = 4$ SYM than about scattering amplitudes. For example, while the planar four-point amplitude was evaluated to the four-loop order (in part numerically) [13–15], the form factor has only been computed to the two-loop order in ref. [1], in a calculation that dates back to 1986. In the present paper, we extend the calculation of ref. [1] to three loops, and study which of the properties that have been observed for scattering amplitudes are present.

One fact which makes form factors technically challenging compared to planar amplitudes, however also more interesting, is the following. At leading order in the 't Hooft limit $N \to \infty$, where the coupling $\lambda = g^2 N$ is kept fixed, both planar as well as non-planar integrals appear in the form factor. This is easily understood by the fact that the operator insertion is a colour-singlet. It is interesting to note that the non-planar diagrams appearing in the form factor are related, through the unitarity technique, to a priori subleading double trace terms in the four-particle scattering amplitude. Therefore, the form factor at leading order in N contains information about non-planar corrections to the four-particle amplitude. The first non-planar diagram, the crossed ladder, appears at the two-loop level. At three loops, we find five different non-planar diagrams that contribute, i.e. that have non-vanishing coefficient.

It is an observed, albeit unproven fact that results for scattering amplitudes in $\mathcal{N} = 4$ super Yang-Mills have uniform transcendentality (UT), i.e. can be expressed as linear combinations of polylogarithmic functions of uniform degree $2L$, where L is the loop order,

JHEP03(2012)101

with constant coefficients. In ϵ-expansions of dimensionally regularised quantities which depend only on a single scale, the coefficients of the Laurent expansion in ϵ are real constants which are in general of increasing transcendentality in the Riemann ζ-function. In this context uniform transcendentality refers to homogeneity in the degree of transcendentality (DT), where the latter is defined as

$$\begin{aligned} DT(r) &= 0 \quad \text{for rational } r \\ DT(\pi^k) &= DT(\zeta_k) = k \\ DT(x \cdot y) &= DT(x) + DT(y) \ . \end{aligned}$$

In the planar case, the property of UT is even true for individual loop integrals, at least when they are expressed in an appropriate basis of dual conformal integrals [16, 17]. Incidentally, this also has practical advantages, as these integrals are easier to evaluate [17, 18] than those in other representations. Dual conformal symmetry is only expected in the planar case, but what can be said about the transcendentality properties of non-planar integrals? At four points, the non-planar double ladder integral is not of uniform transcendentality. However, if defined with an appropriate loop-dependent numerator factor, it does have this property [19, 20]. Changing to a basis involving the latter integral allows one to understand the UT property of four-point non-planar $\mathcal{N} = 4$ SYM amplitudes [21] and $\mathcal{N} = 8$ supergravity amplitudes [22, 23]. It also raises the interesting question whether this is a generic feature.

All planar and non-planar master integrals for form factors in dimensional regularisation at three loops are known from the computation of the form factor in QCD [24–33], and some of them have UT, while others do not. It has been observed that some of the integrals do have UT if they are defined with certain (loop-dependent) numerator factors [19]. The latter resemble the numerator factors required by dual conformal symmetry in the planar case [34]. In this paper, we find similar numerator factors for all topologies with $7, 8, 9$ propagators, such that the integrals have UT. Moreover, we find that the complete three-loop form factor can be written solely in terms of UT integrals.

Finding a representation that has this property required using certain identities for non-planar form factor integrals that are based on reparametrisation invariances, which we found as a by-product of our analysis. They generalise an identity found by Davydychev and Usyukina [35].

As was already mentioned, in $\mathcal{N} = 4$ SYM, scattering amplitudes and the form factors studied here are UV finite in four dimensions. It is interesting to ask in what dimension, called critical dimension D_c, they first develop UV divergences. This question is of theoretical interest in the context of the discussion of possible finiteness of $\mathcal{N} = 8$ supergravity, see e.g. [36–38] and references therein. There are also speculations that maximal SYM in five dimensions might have better UV behaviour than naïvely expected [39]. More practically, bounds on the critical UV dimension at a given loop order can also be a useful cross-check of computations, or constrain the types of loop integrals that can appear. Ultraviolet power counting, based on the existence of $\mathcal{N} = 3$ off-shell superspace [40], provides a lower bound for the critical dimension. We analyse the UV properties of the form factor to three loops

JHEP03(2012)101

and find that at each loop order, the critical dimension is $D_c = 6$. This is consistent with the bound obtained from superspace power counting. We find that the latter bound is saturated at two loops, while it is too conservative at three loops, where the ultraviolet behaviour is better than suggested by the bound. This is the result of a cancellation between different loop integrals. We find a representation where the UV behaviour is manifest.

This paper is organised as follows. We review the known expression for the form factor to two loops in section 2. We then discuss identities for non-planar integrals to three loops in section 3. In section 4, using the unitarity-based method, we derive an expression for the three-loop form factor in terms of loop integrals. We then evaluate the latter in section 5 and verify the exponentiation of infrared divergences in section 6. We then analyse the ultraviolet properties of the form factor to three loops in section 7. We conclude in section 8. There are several appendices. Appendix A contains the analytic expressions of the ϵ expansion of the integrals used in the paper, while appendix B contains the expression of the form factor in terms of conventionally used master integrals. Finally, appendix C reviews the on-shell four-point amplitude to two loops that is used in the unitarity calculation in the main text.

2 Form factor to two loops

In order to define the scalar form factor in $\mathcal{N} = 4$ SYM, we start by introducing the bilinear operator

$$\mathcal{O} = \mathrm{Tr}(\phi_{12}\phi_{12}) \,, \tag{2.1}$$

where the scalars ϕ_{AB} are in the representation **6** of SU(4), and $\phi_{AB} = \phi^a_{AB} T_a$, with T_a being the generators of SU(N) in the fundamental representation, normalised according to $\mathrm{Tr}(T^a T^b) = \delta^{ab}$. This operator is a particular component of the stress-energy supermultiplet of $\mathcal{N} = 4$ SYM, and has zero anomalous dimension. We then define the form factor as the vacuum expectation value of $\mathcal{O}$ inserted into two on-shell states in the adjoint representation,

$$\mathcal{F}_{\mathcal{S}} = \langle \phi^a_{34}(p_1)\phi^b_{34}(p_2)\,\mathcal{O}\rangle \,, \tag{2.2}$$

with the convention that momentum is outgoing.

Since $\mathcal{O}$ is a colour singlet, the form factor must be proportional to $\mathrm{Tr}(T^a T^b)$,

$$\mathcal{F}_{\mathcal{S}} = \mathrm{Tr}(T^a T^b) F_{\mathcal{S}} \,. \tag{2.3}$$

We work in dimensional regularisation with $D = 4 - 2\epsilon$ dimensions in order to regulate IR divergences associated with the on-shell legs. We write the form factor as an expansion in the 't Hooft coupling [8]

$$a = \frac{g^2 N}{8\pi^2} (4\pi)^\epsilon \, e^{-\epsilon\gamma_E} \,, \tag{2.4}$$

according to

$$F_S = 1 + a\, x^\epsilon\, F_S^{(1)} + a^2\, x^{2\epsilon}\, F_S^{(2)} + a^3\, x^{3\epsilon}\, F_S^{(3)} + \mathcal{O}(a^4) \,. \tag{2.5}$$

JHEP03(2012)101

Here γ_E is the Euler-Mascheroni constant, $\gamma_E \approx 0.5772$. We normalized the tree-level contribution to unity and introduced

$$x = \frac{\mu^2}{-q^2 - i\eta}\,, \tag{2.6}$$

with the infinitesimal quantity $\eta > 0$.

We remark that the dependence on the number of colours N in equation (2.5) is exact. In order to see this, let us show that the three-loop contribution to the form factor must be proportional to N^3 (a similar analysis trivially holds at one and two loops).

The reasoning is as follows. Imagine a generic Feynman diagram contributing to $\mathcal{F}_{\mathcal{S}}$. Without loss of generality, suppose that it is built from three-point vertices, whose colour dependence is given by the structure constants $f^{a_1a_2a_3}$. For each internal line, there is a sum over adjoint colour indices, with the result being proportional to $\mathrm{Tr}(T^aT^b)$, as stated in equation (2.3). Our goal is to determine the proportionality factor. In order to do this, it is convenient to sum also over the free indices a and b,

$$\sum_{a,b} \delta^{ab}\mathrm{Tr}(T^aT^b) = N^2 - 1\,. \tag{2.7}$$

We can then represent each Feynman diagram as a circle with inscribed lines. There are three inequivalent structures that can appear,

$$\begin{aligned} A &= f^{abg} f^{bcg} f^{cdh} f^{edi} f^{efi} f^{fah}\,, \\ B &= f^{abg} f^{bch} f^{cdg} f^{dei} f^{eif} f^{fha}\,, \\ C &= f^{abg} f^{bch} f^{cdi} f^{deg} f^{ehf} f^{fia}\,, \end{aligned} \tag{2.8}$$

which correspond to the case of zero, one, or two intersections of the inscribed lines, respectively. Sums over repeated indices are implicit. In order to carry out the sums, it is convenient to write the structure constants as

$$f^{abc} = -i/\sqrt{2}\left(\mathrm{Tr}[T^aT^bT^c] - \mathrm{Tr}[T^aT^cT^b]\right)\,. \tag{2.9}$$

Using the SU(N) Fierz identities,

$$\sum_a \mathrm{Tr}(AT^a)\mathrm{Tr}(BT^a) = \mathrm{Tr}(AB) - 1/N\,\mathrm{Tr}(A)\,\mathrm{Tr}(B)\,, \tag{2.10}$$

$$\sum_a \mathrm{Tr}(AT^aBT^a) = \mathrm{Tr}(A)\,\mathrm{Tr}(B) - 1/N\,\mathrm{Tr}(AB)\,, \tag{2.11}$$

one easily finds

$$A = (N^2-1)N^3\,, \qquad B = -\frac{1}{2}(N^2-1)N^3\,, \qquad C = 0\,. \tag{2.12}$$

Taking into account equation (2.7), we see that F_S at three loops is proportional to N^3, as claimed.

JHEP03(2012)101

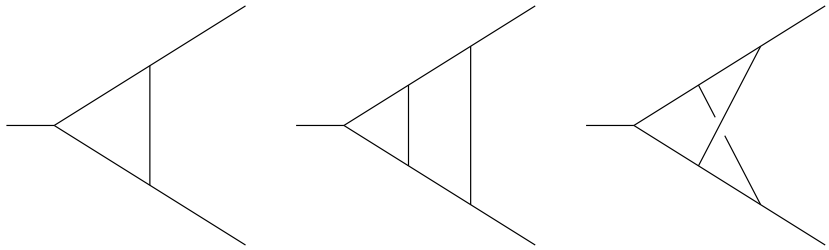

D_1 E_1 E_2

Figure 1. Diagrams that contribute to the one-loop and two-loop form factors $\mathcal{F}_S^{(1)}$ and $\mathcal{F}_S^{(2)}$ in $\mathcal{N}=4$ SYM. All internal lines are massless. The incoming momentum is $q=p_1+p_2$, outgoing lines are massless and on-shell, i. e. $p_1^2=p_2^2=0$. All diagrams displayed have unit numerator and exhibit uniform transcendentality (UT) in their Laurent expansion in $\epsilon=(4-D)/2$.

Note that beginning from four loops there can be more than one colour structure, and in particular the quartic Casimir can appear. An explicit example of this is the four-loop contribution to the QCD β function [41]. An interesting related question has to do with the colour dependence of infrared divergences in gauge theories, see e.g. [42], and references therein.

The form factor to two loops was computed a long time ago [1]. It contains as building blocks the diagrams displayed in figure 1 and reads

$$\begin{aligned} F_S &= 1 + g^2\, N\, \mu^{2\epsilon}\cdot(-q^2)\cdot 2\, D_1 + g^4\, N^2\, \mu^{4\epsilon}\cdot(-q^2)^2\cdot[4\, E_1 + E_2] + \mathcal{O}(g^6) \\ &= 1 + a\, x^\epsilon\, R_\epsilon\cdot 2\, D_1^{\rm exp} + a^2\, x^{2\epsilon}\, R_\epsilon^2\cdot[4\, E_1^{\rm exp} + E_2^{\rm exp}] + \mathcal{O}(a^3)\ , \end{aligned} \tag{2.13}$$

with

$$R_\epsilon \equiv \frac{e^{\epsilon\gamma_E}}{2\,\Gamma(1-\epsilon)}\ . \tag{2.14}$$

The expressions for D_1, $D_1^{\rm exp}$, E_i, and $E_i^{\rm exp}$ are given explicitly in appendix A and result in

$$\begin{aligned} F_S^{(1)} &= R_\epsilon\cdot 2\, D_1^{\rm exp} \\ &= -\frac{1}{\epsilon^2} + \frac{\pi^2}{12} + \frac{7\zeta_3}{3}\,\epsilon + \frac{47\pi^4}{1440}\,\epsilon^2 + \epsilon^3\left(\frac{31\zeta_5}{5} - \frac{7\pi^2\zeta_3}{36}\right) + \epsilon^4\left(\frac{949\pi^6}{120960} - \frac{49\zeta_3^2}{18}\right) \\ &\quad + \epsilon^5\left(-\frac{329\pi^4\zeta_3}{4320} - \frac{31\pi^2\zeta_5}{60} + \frac{127\zeta_7}{7}\right) + \epsilon^6\left(\frac{49\pi^2\zeta_3^2}{216} - \frac{217\zeta_3\zeta_5}{15} + \frac{18593\pi^8}{9676800}\right) \\ &\quad + \mathcal{O}(\epsilon^7)\ , \end{aligned} \tag{2.15}$$

$$\begin{aligned} F_S^{(2)} &= R_\epsilon^2\cdot[4\, E_1^{\rm exp} + E_2^{\rm exp}] \\ &= +\frac{1}{2\epsilon^4} - \frac{\pi^2}{24\epsilon^2} - \frac{25\zeta_3}{12\epsilon} - \frac{7\pi^4}{240} + \epsilon\left(\frac{23\pi^2\zeta_3}{72} + \frac{71\zeta_5}{20}\right) + \epsilon^2\left(\frac{901\zeta_3^2}{36} + \frac{257\pi^6}{6720}\right) \\ &\quad + \epsilon^3\left(\frac{1291\pi^4\zeta_3}{1440} - \frac{313\pi^2\zeta_5}{120} + \frac{3169\zeta_7}{14}\right) \\ &\quad + \epsilon^4\left(-66\zeta_{5,3} + \frac{845\zeta_3\zeta_5}{6} - \frac{1547\pi^2\zeta_3^2}{216} + \frac{50419\pi^8}{518400}\right) + \mathcal{O}(\epsilon^5)\ . \end{aligned} \tag{2.16}$$

JHEP03(2012)101

The multiple zeta values $\zeta_{m_1,\ldots,m_k}$ are defined by (see e.g. [43] and references therein)

$$\zeta_{m_1,\ldots,m_k} = \sum_{i_1=1}^{\infty}\sum_{i_2=1}^{i_1-1}\cdots\sum_{i_k=1}^{i_{k-1}-1}\prod_{j=1}^{k}\frac{\mathrm{sgn}(m_j)^{i_j}}{i_j^{|m_j|}} \,. \tag{2.17}$$

The numerical values of the transcendental constants up to weight eight are:

$$\zeta_3 = 1.2020569031595942854\ldots\,, \qquad \zeta_5 = 1.0369277551433699263\ldots\,,$$
$$\zeta_7 = 1.0083492773819228268\ldots\,, \qquad \zeta_{5,3} = 0.03770767298484754401 1\ldots\,.$$

We remark that in order to obtain all finite pieces of the logarithm of the form factor in section 6 we need the ϵ-expansion through terms of transcendental weight six, i.e. to order $\mathcal{O}(\epsilon^4)$ at one loop, $\mathcal{O}(\epsilon^2)$ at two loops, and $\mathcal{O}(\epsilon^0)$ later on at three loops. We emphasize that our expressions contain two more orders in ϵ and therefore contain already all information required for exponentiation at four loops.

3 Momentum routing invariances of integrals

Before we proceed to calculate the $\mathcal{N}=4$ SYM form factor to three loops via unitarity cuts, we want to investigate some of the occurring topologies more closely. In particular, we will derive identities that relate integrals without uniform transcendentality (UT) to integrals that do have this property. Since the diagrams that we will obtain from the unitarity method do not individually have UT, the following relations will be very useful later on for switching to an integral basis for the form factor in which each building block has UT.

We start with topology F_3^*, see figure 2. We label its incoming momentum with $q = p_1 + p_2$, and the outgoing ones with p_1 and p_2, respectively. The latter are massless and on-shell, i.e. $p_1^2 = p_2^2 = 0$. The topology can be parametrised according to

$$\{k_1 - k_2\,,\, k_1 - k_3\,,\, k_1 - k_2 - k_3\,,\, k_2\,,\, k_3\,,\, k_1 - q\,,\, k_2 - q\,,\, k_3 - q\,,\, k_2 - p_1\}\ , \tag{3.1}$$

where k_i are the loop momenta. It can be seen from figure 2 how the momenta are distributed among the lines of the diagram F_3^*. It turns out that the following reparametrization of loop momenta,

$$\begin{aligned} k_1 &\to q + k_2 - k_1 \\ k_2 &\to k_2 \\ k_3 &\to q - k_3\ , \end{aligned}$$

does not only leave the value of the integral invariant, but even its *integrand*. We can now apply this transformation to the integral F_3 which carries the factor $(k_2 - k_3)^2$ as an irreducible scalar product in its numerator. This yields

$$\begin{aligned} (k_2 - k_3)^2 &\to (k_2 + k_3 - q)^2 \\ &= k_2^2 + k_3^2 + (k_2 - q)^2 + (k_3 - q)^2 - (k_2 - k_3)^2 - q^2\ . \end{aligned} \tag{3.2}$$

JHEP03(2012)101

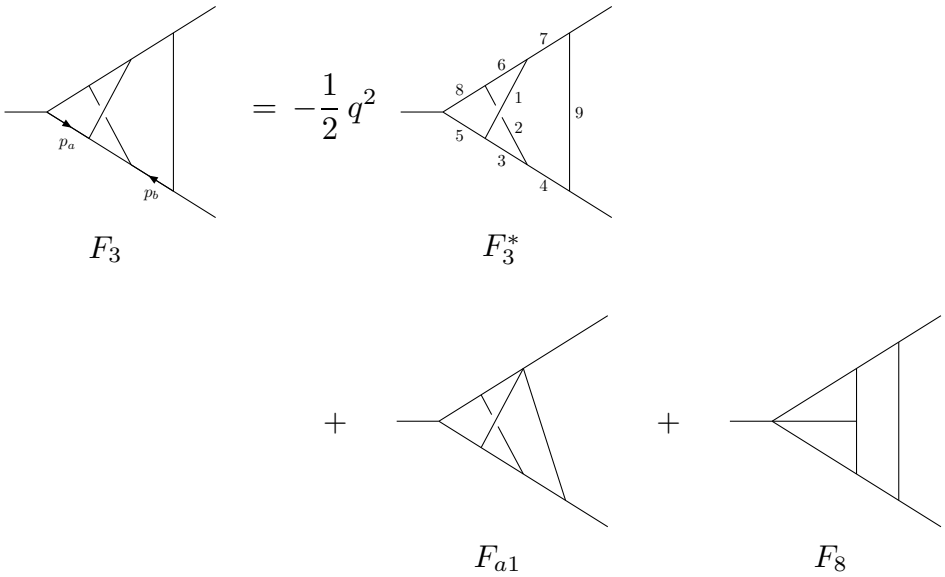

Figure 2. Diagrammatic representation of eq. (3.3). The internal lines of all diagrams are massless. The incoming momentum is $q = p_1 + p_2$, outgoing lines are massless and on-shell, i.e. $p_1^2 = p_2^2 = 0$. Diagrams with labels p_a and p_b on arrow lines have an irreducible scalar product $(p_a + p_b)^2$ in their numerator (diagrams that lack these labels have unit numerator). The numbers in F_3^* indicate the position of the entries in eq. (3.1). Diagrams F_3 and F_8 have UT, contrary to F_3^* and F_{a1}.

We can now solve this equation for $(k_2 - k_3)^2$ and get the following relation between integrals,

$$F_3 = -\frac{1}{2}\, q^2\, F_3^* + F_{a1} + F_8 \,, \tag{3.3}$$

which is diagrammatically shown in figure 2. We have now decomposed the integral F_3^*, which does not have UT in its Laurent expansion, into two integrals (F_3 and F_8) which indeed do have this property, and the auxiliary integral F_{a1}, which again does not have homogeneous transcendental weight, but which will be cancelled later on.

We can apply analogous steps to topology F_4^*, see figure 3. The topology can be parametrised according to

$$\{k_1\,,\, k_2\,,\, k_3\,,\, k_1 - k_2\,,\, k_1 - k_3\,,\, k_1 - q\,,\, k_1 - k_2 - p_2\,,\, k_3 - q\,,\, k_2 - p_1\} \;, \tag{3.4}$$

and the distribution of the momenta among the lines can be seen from figure 3. The integrand remains invariant under

$$\begin{aligned} k_1 &\to q - k_1 \\ k_2 &\to p_1 - k_2 \\ k_3 &\to q - k_3 \,, \end{aligned}$$

We now apply this transformation to the numerator $(k_1 - p_1)^2$ of the integral F_4. This yields

$$\begin{aligned} (k_1 - p_1)^2 &\to (k_1 - p_2)^2 \\ &= k_1^2 + (k_1 - q)^2 - (k_1 - p_1)^2 - q^2 \,. \end{aligned} \tag{3.5}$$

JHEP03(2012)101

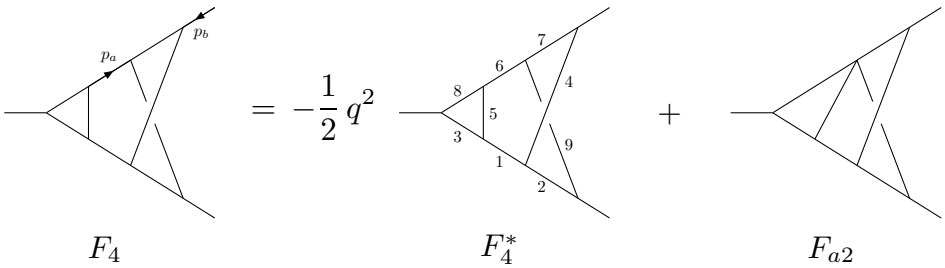

Figure 3. Diagrammatic representation of eq. (3.6). All symbols have the same meaning as in figure 2. The numbers in F_4^* indicate the position of the entries in eq. (3.4). Diagram F_4 has UT, contrary to F_4^* and F_{a2}.

We can now solve this equation for $(k_1 - p_1)^2$ and get

$$F_4 = -\frac{1}{2}\, q^2\, F_4^* + F_{a2}\ , \tag{3.6}$$

which is diagrammatically shown in figure 3. Again we decomposed the non-homogeneous integral F_4^* into the homogeneous integral F_4 and yet another non-homogeneous auxiliary integral (F_{a2}) which will be cancelled later on.

We can also decompose the topology F_5^*, see figure 4. In this case we cannot find a relation between integrals which is based on a momentum routing invariance, but a relation which is simply based on momentum conservation. The topology can be parametrised according to

$$\{k_1 - k_2\,,\, k_1 - k_3\,,\, k_1 - k_2 - k_3\,,\, k_2\,,\, k_3\,,\, k_1 - q\,,\, k_2 - q\,,\, k_1 - p_1\,,\, k_3 - p_1\}\ , \tag{3.7}$$

and we refer to figure 4 for their distributions among the lines. From momentum conservation we get

$$(k_2 - p_1)^2 = (k_1 - k_2)^2 - k_1^2 + k_2^2 + (k_1 - p_1)^2 - (k_1 - k_2 - p_1)^2\ , \tag{3.8}$$

which results in

$$F_5^* = F_{a1} + F_{a2} + F_9 - F_5 - F_6\ . \tag{3.9}$$

Hence we decomposed F_5^* into the homogeneous-weight diagrams F_5, F_6, and F_9, as well as the same non-homogeneous diagrams F_{a1}, and F_{a2} which already appeared above.

We see from eqs. (3.3), (3.6), and (3.9) that only two auxiliary diagrams of non-homogeneous weight, namely F_{a1}, and F_{a2} appear in all these relations. It turns out that the coefficients obtained from unitarity are precisely such that these integrals cancel in the expression for the form factor.

We checked all relations between integrals also at the level of their integration-by-parts (IBP) reduction [44, 45] to master integrals using the implementation of the Laporta algorithm [46] in the REDUZE [47] code. We find that all relations obtained from momentum routing invariance in this section can actually be reproduced from solving IBP relations, which is a priori not guaranteed for a general Feynman integral topology. The ϵ-expansions of all integrals can be found in appendix A.

JHEP03(2012)101

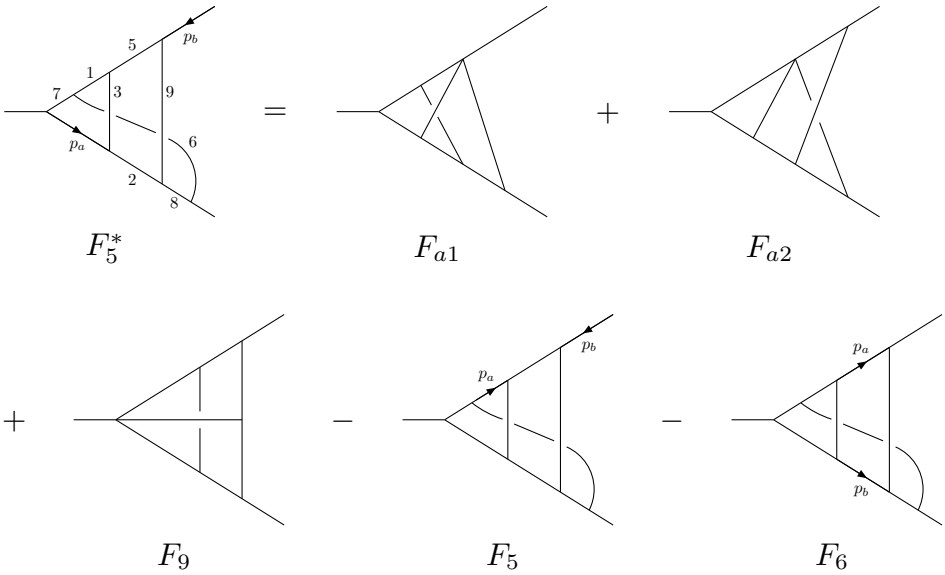

Figure 4. Diagrammatic representation of eq. (3.9). All symbols have the same meaning as in figure 2. The numbers in F_5^* indicate the position of the entries in eq. (3.7). Diagrams F_5, F_6, and F_9 have UT, contrary to F_5^*, F_{a1}, and F_{a2}.

4 Form factor to three loops from unitarity cuts

Here we use unitarity cuts to derive an expression for the three-loop form factor in terms of the integrals discussed in the previous section. We will compute the form factor in a perturbative expansion in the Yang-Mills coupling g, and denote the contribution at order g^0, g^2, g^4, g^6 by $\mathcal{F}_S^{\text{tree}}, \mathcal{F}_S^{1-\text{loop}}, \mathcal{F}_S^{2-\text{loop}}, \mathcal{F}_S^{3-\text{loop}}$, respectively, and similarly for F_S. Note that this notation, convenient for the unitarity calculations, differs from the one used in eq. (2.5).

The essential features of the unitarity-based method [48, 49] that we are going to use are reviewed in the recent paper [50]. We will employ two-particle cuts, as well as generalised cuts. The two-particle cuts are very easy to evaluate, and we show an explicit example below.

In order to evaluate more complicated cuts, with many intermediate state sums to be carried out, it is extremely useful to employ a formalism that makes supersymmetry manifest. This can be done by arranging the on-shell states of $\mathcal{N} = 4$ SYM into an on-shell supermultiplet [51]. The main advantage is that intermediate state sums appearing in the cuts become simple Grassmann integrals that can be carried out trivially [52–55]. In this way, following the Lorentz-covariant approach of [52] it is easy to obain compact analytical expressions for the cuts. In particular, unlike the MHV vertex expansion, the results do not depend on arbitrary reference spinors.

We follow the notations for unitarity cuts of ref. [56]. We start by reviewing the one- and two-loop cases as examples.

JHEP03(2012)101

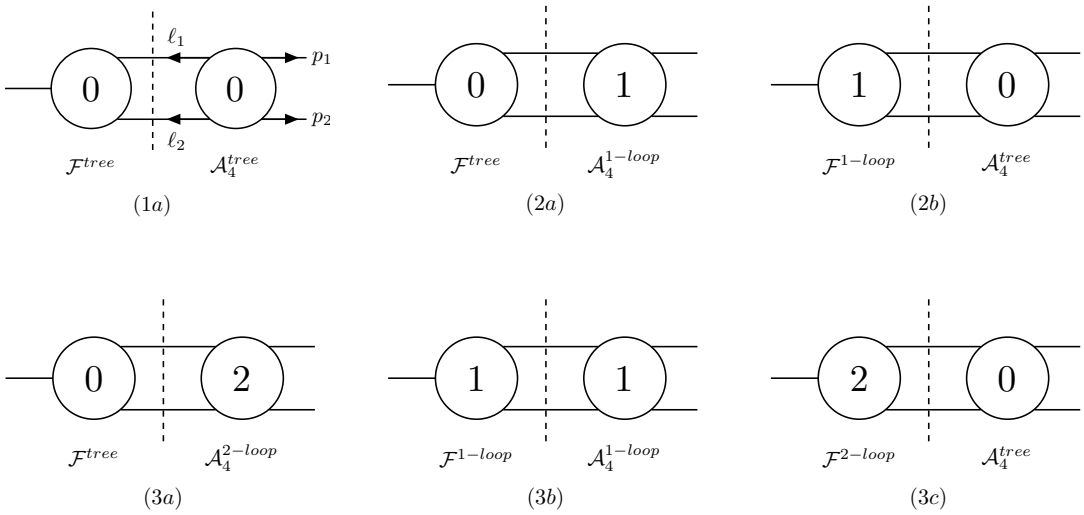

Figure 5. Two-particle cuts of form factors up to three loops.

4.1 One-loop form factor from unitarity cuts

As a simple warmup exercise, we rederive the one-loop result from unitarity cuts, see also ref. [2]. Let us compute the two-particle cut (1a) shown in figure 5. It is given by

$$\mathcal{F}_S^{1-\text{loop}}\Big|_{\text{cut(1a)}} = \int \sum_{P_1,P_2} \frac{d^D k}{(2\pi)^D} \frac{i}{\ell_2^2} \mathcal{F}_S^{\text{tree}}(-\ell_1,-\ell_2) \frac{i}{\ell_1^2} \mathcal{A}_4^{\text{tree}}(\ell_2,\ell_1,p_1,p_2)\Big|_{\ell_1^2=\ell_2^2=0}, \tag{4.1}$$

where ℓ_1 and ℓ_2 are the momenta of the cut legs, and the sum runs over all possible particles across the cut. We may use the on-shell condition $\ell_1^2 = \ell_2^2 = 0$ in the integrand (but not on the cut propagators), since any terms proportional to such numerator factors would vanish in the cut. The four-particle tree ampliutde $\mathcal{A}_4^{\text{tree}}(\ell_2,\ell_1,p_1,p_2)$ is given in appendix C. We use the convention that all momenta are defined as outgoing.

When computing the cut of a form factor (as opposed to a colour-ordered amplitude), one has to be careful about the overall normalisation, since the possible exchange of external legs p_1 and p_2 leads to a factor of 2 in the cuts. When comparing cuts of the form factor to cuts of integrals, this factor cancels out. In the following we count such contributions only once.

The two-particle cuts are particularly simple to evaluate. With our choice of external states, only scalars can appear as intermediate particles, and we therefore do not need to use the spinor helicity formalism. The tree-level form factor is simply given by

$$\mathcal{F}_S^{\text{tree}}(-\ell_1,-\ell_2) = \text{Tr}(T^a T^b)\,. \tag{4.2}$$

The necessary four-particle amplitudes are given in appendix C. The colour algebra across the cut is carried out using the SU(N) Fierz identities, see eqs. (2.10) and (2.11). It is easy

JHEP03(2012)101

to see that (4.1) becomes

$$\mathcal{F}_S^{1-\text{loop}}\Big|_{\text{cut (1a)}} = g^2\mu^{2\epsilon}\, N\, s_{12}\, \text{Tr}(T^aT^b) \int \frac{d^Dk}{(2\pi)^D}\, \frac{i}{\ell_2^2}\, \frac{i}{\ell_1^2} \left(\frac{-i}{(p_1+\ell_1)^2} + \frac{-i}{(p_2+\ell_2)^2} \right) \Big|_{\ell_1^2=\ell_2^2=0}$$
$$= -2\, g^2\mu^{2\epsilon}\, N\, s_{12}\, \text{Tr}(T^aT^b) \int \frac{d^Dk}{i(2\pi)^D} \frac{1}{k^2(k+p_1)^2(k-p_2)^2}\Big|_{\text{cut (1a)}}\,, \tag{4.3}$$

where $s_{ij} := (p_i+p_j)^2$, and where we have identified the cut of the one-loop form factor with the cut of the one-loop triangle integral D_1, see figure 1,

$$D_1 = \int \frac{d^Dk}{i(2\pi)^D} \frac{1}{k^2(k+p_1)^2(k-p_2)^2}\,. \tag{4.4}$$

We can now argue that this result is exact, i.e. that we can remove the "cut (1a)" in eq. (4.3). In order to do that, we have to make sure that no terms with vanishing cuts are missed. Such terms having no cuts in four dimensions can be detected in D dimensions. The two-particle cut calculation we just presented would have gone through unchanged in D dimensions, since all required amplitudes were those of scalars, and no spinor helicity identities intrinsic to four dimensions were used. A similar argument was given in ref. [56]. Therefore we conclude that in D dimensions,

$$F_S^{1-\text{loop}} = g^2 N \mu^{2\epsilon}(-q^2) 2 D_1\,. \tag{4.5}$$

4.2 Two-loop form factor from unitarity cuts

We recall that at two loops, the result for the form factor is given by [1],

$$F_S^{2-\text{loop}} = g^4 N^2 \mu^{4\epsilon}(-q^2)^2 \big[4E_1 + E_2\big]\,, \tag{4.6}$$

where the planar and non-planar ladder diagrams E_1 and E_2 are shown in figure 1.

Let us now understand this result from unitarity cuts. The unitarity cut (2b) of figure 5 detects the presence of the planar integral E_1 only. The calculation is identical to that of the one-loop case, with the exception that the one-loop form factor as opposed to the tree-level form factor is inserted on the l.h.s. of the cut.

The unitarity cut (2a) of figure 5 reveals a new feature, that was already mentioned in the introduction. On the r.h.s. of the cut we now insert the full one-loop four-point amplitude $\mathcal{A}_4^{1-\text{loop}}$, given explicitly in eq. (C.2), which in addition to single trace terms also contains double trace terms. The latter would ordinarily be subleading in the expansion of powers of N, e.g. when computing a four-point amplitude at leading colour using unitarity cuts. Here, however the colour algebra gives rise to another factor of N for those terms, so that they can contribute to the form factor at the same order as the single trace terms. This explains why the non-planar integral E_2 can appear in the form factor.

In principle, new terms could appear in the three-particle cut, but this is not the case. For example, the diagram E_3 shown in figure 6 has no two-particle cuts. The absence of this diagram can be understood by the fact that it has worse UV properties compared to E_1 and E_2, as we discuss in section 7. For the same reason, diagrams F_7 and F_{10} from

JHEP03(2012)101

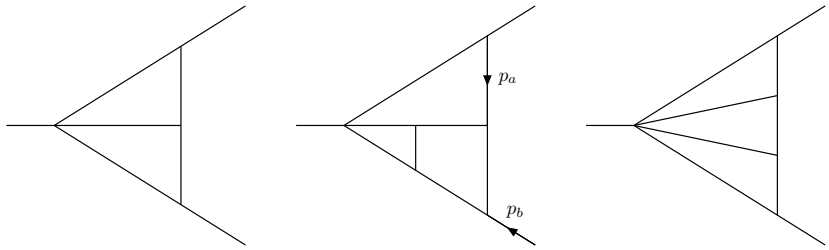

E_3 F_7 F_{10}

Figure 6. Diagrams that do not contribute to the form factor at two (E_3) and three loops (F_7 and F_{10}), respectively. They have worse UV properties compared to the integrals that do appear in the form factor. The labels p_a and p_b on F_7 indicate an irreducible scalar product $(p_a + p_b)^2$ in its numerator. The other two diagrams have unit numerator.

figure 6, the latter of which at has no three-particle cuts, will not contribute to the form factor at three loops, as we will see below.

We have also evaluated the three-particle and a generalised cut, with the result being in perfect agreement with eq. (4.6). We found it useful to employ a manifestly supersymmetric version of the unitarity method [52]. The necessary tree-level amplitudes for the local operator of eq. (2.1) inserted into three on-shell states were computed in refs. [2, 3]. The analytical calculation is straightforward to perform. We refrain from presenting the details since it would require introducing spinor helicity and superspace. We refer the interested reader to refs. [50, 52] for related instructive examples.

4.3 Three-loop form factor from unitarity cuts

We again begin by studying two-particle cuts, which are shown in the second line of figure 5. Again, all results for the form factors and four-point amplitudes appearing in the unitarity cuts are explicitly known, with the result for the four-point amplitudes summarized in appendix C.

When evaluating the cuts, one has a certain freedom in rewriting the answer to a given cut due to the on-shell conditions. Of course, eventually such ambiguities are fixed by the requirement that the answer must satisfy all cuts. In order to find such an expression that manifestly satisfies all cuts it is very useful to have an idea about the kind of integrals that should appear in the answer. We expect that the form factor can be expressed in terms of the integrals that have UT that were discussed in section 3. This turns out to be a very useful guiding principle.

The calculation is completely analogous to that at one and two loops. Let us start with the simplest cut (3c) from figure 5. It is given by

$$\mathcal{F}_S^{3-\text{loop}}\Big|_{\text{cut(3c)}} = \int \sum_{P_1,P_2} \frac{d^D k}{(2\pi)^D} \frac{i}{\ell_2^2} \mathcal{F}_S^{2-\text{loop}}(-\ell_1,-\ell_2) \frac{i}{\ell_1^2} \mathcal{A}_4^{\text{tree}}(\ell_2,\ell_1,p_1,p_2)\Big|_{\ell_1^2=\ell_2^2=0}, \quad (4.7)$$

The evaluation of the cut is exactly as that considered at one loop, with the difference that we now insert the two-loop expression for the form factor into the cut, as opposed to the

JHEP03(2012)101

tree-level one. One immediately finds

$$\mathcal{F}_S^{3-\text{loop}}\Big|_{\text{cut(3c)}} = g^6\,\mu^{6\epsilon}\,N^3\,(-q^2)^3\big[8\,F_1 + 2\,F_3^*\big]\Big|_{\text{cut(3c)}}\,, \tag{4.8}$$

where F_1 is the three-loop ladder integral shown in figure 7, and F_3^* is related to F_3 in the same figure via the identity (3.3). In fact, we know from section 3 that F_3^* does not have uniform transcendentality. Since we do expect the final result to have this property, use eq. (3.3) to eliminate F_3^*. When doing so, we note that the contribution of F_{a1} in that equation drops out on the cut (3c), and we have

$$F_S^{3-\text{loop}}\Big|_{\text{cut(3c)}} = g^6\,\mu^{6\epsilon}\,N^3\,(-q^2)^2\big[8\,(-q^2)\,F_1 + 4\,F_3 - 4\,F_8\big]\Big|_{\text{cut(3c)}}\,, \tag{4.9}$$

i.e. we have succeeded in writing the two-particle cut (3c) in terms of integrals having UT only.

Similarly, one can show that the two-particle cut (3b) of figure 5 can be written as

$$F_S^{3-\text{loop}}\Big|_{\text{cut(3b)}} = g^6\,\mu^{6\epsilon}\,N^3\,(-q^2)^2\big[8\,(-q^2)\,F_1 + 4\,F_4\big]\Big|_{\text{cut(3b)}}\,. \tag{4.10}$$

This confirms the coefficient of F_1, and introduces a new integral F_4, invisible to cut (3c).

Finally, the most interesting two-particle cut is (3a), as it uses the double trace terms present in $\mathcal{A}_4^{2-\text{loop}}$, see appendix C. Using the identities derived in section 3, we find

$$F_S^{3-\text{loop}}\Big|_{\text{cut(3a)}} = g^6\,\mu^{6\epsilon}\,N^3\,(-q^2)^2\big[8\,(-q^2)\,F_1 - 2\,F_2 + 4\,F_3 + 4\,F_4 - 4\,F_5 - 4\,F_6\big]\Big|_{\text{cut(3a)}}\,. \tag{4.11}$$

Comparing equations (4.9), (4.10), and (4.11) with each other, we see that they are manifestly consistent with each other, which suggests that we are indeed working with an appropriate integral basis to describe this problem. We find that the following expression is in agreement with all two-particle cuts,

$$\begin{aligned} &F_S^{3-\text{loop}}\Big|_{2-\text{part. cut}} \\ &\quad = g^6\,\mu^{6\epsilon}\,N^3\,(-q^2)^2\big[8\,(-q^2)\,F_1 - 2\,F_2 + 4\,F_3 + 4\,F_4 - 4\,F_5 - 4\,F_6 - 4\,F_8\big]\Big|_{2-\text{part. cut}}\,. \end{aligned} \tag{4.12}$$

It is quite remarkable that to three loops the coefficients of all integrals are small integer numbers.

We could proceed by evaluating three- and four-particle cuts, but we find it technically simpler to study generalised cuts. To begin with, we perform a cross-check on the two-particle cut calculation above by evaluating maximal cuts where nine propagators are cut. We find perfect agreement between the two calculations. Next, we release one cut constraint to detect integrals having only eight propagators. There are several ways in which this can be done. For example, cutting all eight propagators present in integral F_9 detects this integral, as well as integrals F_5 and F_6. Another eight-propagator cut detects integrals F_2, F_5, F_6 and F_7. The latter integral (see figure 6) turns out to have coefficient zero, i.e. it does not appear.

JHEP03(2012)101

We again find perfect agreement with the contributions already known from the two-particle cuts, and find further contributions not having any two-particle cuts, like F_9. The following expression satisfies all cuts that we have evaluated,

$$F_S^{3-\text{loop}} = g^6\,\mu^{6\epsilon}\,N^3\,(-q^2)^2\left[8\,(-q^2)\,F_1 - 2\,F_2 + 4\,F_3 + 4\,F_4 - 4\,F_5 - 4\,F_6 - 4\,F_8 + 2\,F_9\right]. \tag{4.13}$$

We will now argue that eq. (4.13) is the complete result for the three-loop form factor. In fact, potential corrections to equation (4.13) can come only from seven-propagator integrals that have vanishing two-particle cuts. An example of such an integral is F_{10} shown in figure 6. As we will see in section 7, the appearance of such integrals is highly unlikely due to their bad UV behaviour, violating a bound based on supersymmetry power counting.

Moreover, in section 6, we will perform an even more stringent check on eq. (4.13) by verifying the correct exponentiation of infrared divergences. In particular, this means that any potentially missing terms in equation (4.13) would have to be IR and UV finite, and vanish in all unitarity cuts that we considered.

5 Final result for the form factor at three loops

In the previous section we obtained the extension of eq. (2.13) to three loops,

$$\begin{aligned}
F_S &= 1 + g^2\,N\,\mu^{2\epsilon}\cdot(-q^2)\cdot 2\,D_1 + g^4\,N^2\,\mu^{4\epsilon}\cdot(-q^2)^2\cdot[4\,E_1 + E_2] \\
&\quad + g^6\,N^3\,\mu^{6\epsilon}\cdot(-q^2)^2\cdot\left[8\,(-q^2)\,F_1 - 2\,F_2 + 4\,F_3 + 4\,F_4 - 4\,F_5 - 4\,F_6 - 4\,F_8 + 2\,F_9\right] \\
&\quad + \mathcal{O}(g^8) \\
&= 1 + a\,x^{\epsilon}\,R_\epsilon\cdot 2\,D_1^{\text{exp}} + a^2\,x^{2\epsilon}\,R_\epsilon^2\cdot[4\,E_1^{\text{exp}} + E_2^{\text{exp}}] \\
&\quad + a^3\,x^{3\epsilon}\,R_\epsilon^3\cdot[8\,F_1^{\text{exp}} - 2\,F_2^{\text{exp}} + 4\,F_3^{\text{exp}} + 4\,F_4^{\text{exp}} - 4\,F_5^{\text{exp}} - 4\,F_6^{\text{exp}} - 4\,F_8^{\text{exp}} + 2\,F_9^{\text{exp}}] \\
&\quad + \mathcal{O}(a^4)\,.
\end{aligned} \tag{5.1}$$

The expressions for F_i, and F_i^{exp} are again given in appendix A. All diagrams are displayed in figure 7. This yields

$$\begin{aligned}
F_S^{(3)} &= R_\epsilon^3\cdot[8\,F_1^{\text{exp}} - 2\,F_2^{\text{exp}} + 4\,F_3^{\text{exp}} + 4\,F_4^{\text{exp}} - 4\,F_5^{\text{exp}} - 4\,F_6^{\text{exp}} - 4\,F_8^{\text{exp}} + 2\,F_9^{\text{exp}}] \\
&= -\frac{1}{6\epsilon^6} + \frac{11\zeta_3}{12\epsilon^3} + \frac{247\pi^4}{25920\epsilon^2} + \frac{1}{\epsilon}\left(-\frac{85\pi^2\zeta_3}{432} - \frac{439\zeta_5}{60}\right) \\
&\quad - \frac{883\zeta_3^2}{36} - \frac{22523\pi^6}{466560} + \epsilon\left(-\frac{47803\pi^4\zeta_3}{51840} + \frac{2449\pi^2\zeta_5}{432} - \frac{385579\zeta_7}{1008}\right) \\
&\quad + \epsilon^2\left(\frac{1549}{45}\zeta_{5,3} - \frac{22499\zeta_3\zeta_5}{30} + \frac{496\pi^2\zeta_3^2}{27} - \frac{1183759981\pi^8}{7838208000}\right) + \mathcal{O}(\epsilon^3)\,.
\end{aligned} \tag{5.2}$$

We can make a very interesting observation here. For anomalous dimensions of twist two operators, there is a heuristic leading transcendentality principle [57–59], which relates the $\mathcal{N} = 4$ SYM result to the leading transcendental part of the QCD result. We can investigate whether a similar property holds for the form factor.

JHEP03(2012)101

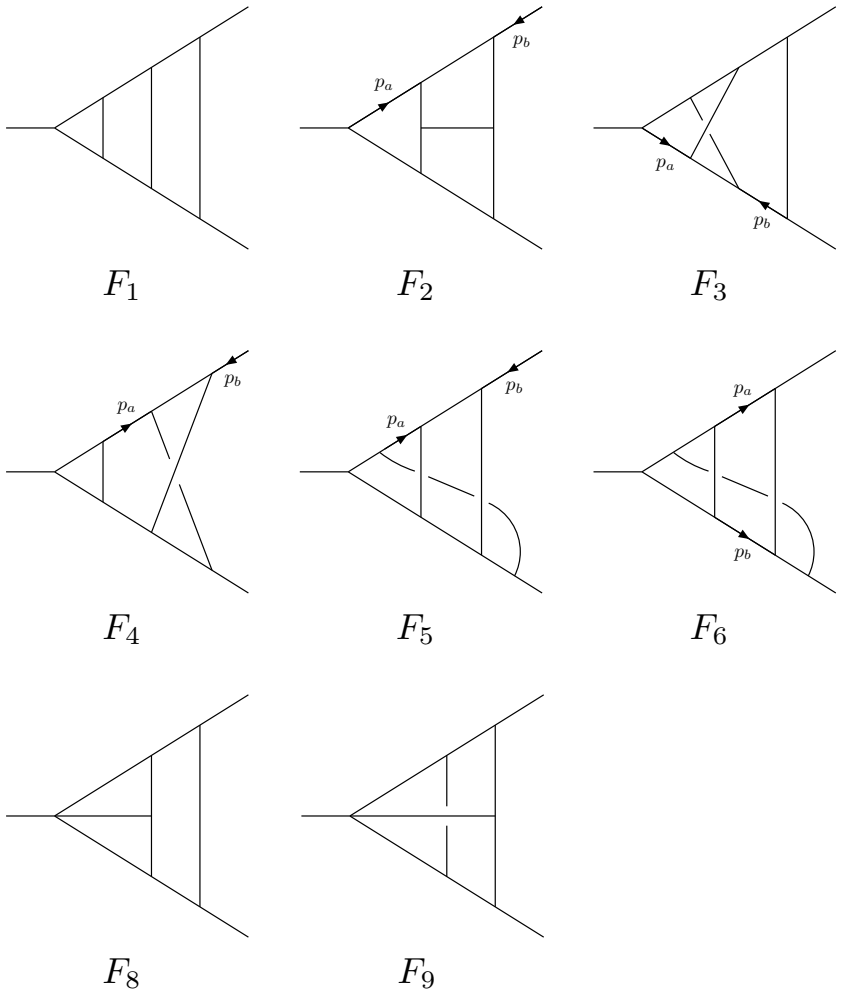

Figure 7. Diagrams of which the three-loop form factor $F_S^{(3)}$ in $\mathcal{N}=4$ SYM is built. All internal lines are massless. The incoming momentum is $q = p_1 + p_2$, outgoing lines are massless and on-shell, i.e. $p_1^2 = p_2^2 = 0$. Diagrams with labels p_a and p_b on arrow lines have an irreducible scalar product $(p_a + p_b)^2$ in their numerator (diagrams that lack these labels have unit numerator). All diagrams displayed exhibit uniform transcendentality (UT) in their Laurent expansion in $\epsilon = (4-D)/2$.

For the comparison, we specify the QCD quark and gluon form factor to a supersymmetric Yang-Mills theory containing a bosonic and fermionic degree of freedom in the same colour representation, which is achieved by setting $C_A = C_F = 2\,T_F$ and $n_f = 1$ in the QCD result [27]. It turns out that with this adjustment the leading transcendentality pieces of the quark and gluon form factor become equal at one, two, and three loops in all coefficients up to transcendental weight eight, i.e. $\mathcal{O}(\epsilon^6)$, $\mathcal{O}(\epsilon^4)$, and $\mathcal{O}(\epsilon^2)$ at one, two, and three loops, respectively. Moreover, the leading transcendentality pieces of the quark and gluon form factor coincide — up to a factor of 2^L (L is the number of loops) which is due to normalisation — with the coefficients of the scalar form factor in $\mathcal{N}=4$ SYM computed in the present work. This again holds true at one, two, and three loops and for all coefficients up to weight eight, and serves as an important check of our result.

JHEP03(2012)101

The question arises if the leading transcendentality principle [57–59] between QCD and $\mathcal{N}=4$ SYM carries over to more general quantities like scattering amplitudes, or if it is a special feature of form factors since they have only two external partons.

In fact, there are counterexamples in the case of scattering amplitudes [19]. For instance, the $\mathcal{N}=1$ supersymmetric one-loop four-point amplitudes [60] have a leading transcendentality piece which is not of the $\mathcal{N}=4$ SYM form, because it has $1/u$ power-law factors. This makes the property we have found for the form factor even more surprising.

6 Logarithm of the form factor

The logarithm of the form factor is given by

$$\begin{aligned}\ln(F_S) &= \ln\left(1 + a\,x^{\epsilon}\,F_S^{(1)} + a^2\,x^{2\epsilon}\,F_S^{(2)} + a^3\,x^{3\epsilon}\,F_S^{(3)} + \mathcal{O}(a^4)\right)\\ &= a\,x^{\epsilon}\,F_S^{(1)} + a^2\,x^{2\epsilon}\left[F_S^{(2)} - \frac{1}{2}\left(F_S^{(1)}\right)^2\right] + a^3\,x^{3\epsilon}\left[F_S^{(3)} - F_S^{(1)}F_S^{(2)} + \frac{1}{3}\left(F_S^{(1)}\right)^3\right]\\ &\quad + \mathcal{O}(a^4)\,, \end{aligned} \tag{6.1}$$

where

$$\begin{aligned}F_S^{(1)} &= -\frac{1}{\epsilon^2} + \frac{\pi^2}{12} + \frac{7\zeta_3}{3}\,\epsilon + \frac{47\pi^4}{1440}\,\epsilon^2 + \epsilon^3\left(\frac{31\zeta_5}{5} - \frac{7\pi^2\zeta_3}{36}\right)\\ &\quad + \epsilon^4\left(\frac{949\pi^6}{120960} - \frac{49\zeta_3^2}{18}\right) + \epsilon^5\left(\frac{127\zeta_7}{7} - \frac{329\pi^4\zeta_3}{4320} - \frac{31\pi^2\zeta_5}{60}\right)\\ &\quad + \epsilon^6\left(\frac{49\pi^2\zeta_3^2}{216} - \frac{217\zeta_3\zeta_5}{15} + \frac{18593\pi^8}{9676800}\right) + \mathcal{O}(\epsilon^7)\,, \end{aligned} \tag{6.2}$$

$$\begin{aligned}F_S^{(2)} - \frac{1}{2}\left(F_S^{(1)}\right)^2 &= \frac{\pi^2}{24\epsilon^2} + \frac{\zeta_3}{4\epsilon} + \epsilon\left(\frac{39\zeta_5}{4} - \frac{5\pi^2\zeta_3}{72}\right) + \epsilon^2\left(\frac{235\zeta_3^2}{12} + \frac{2623\pi^6}{60480}\right)\\ &\quad + \epsilon^3\left(\frac{73\pi^4\zeta_3}{96} - \frac{437\pi^2\zeta_5}{120} + \frac{489\zeta_7}{2}\right)\\ &\quad + \epsilon^4\left(-66\zeta_{5,3} + \frac{1119\zeta_3\zeta_5}{10} - \frac{1351\pi^2\zeta_3^2}{216} + \frac{127\pi^8}{1296}\right) + \mathcal{O}(\epsilon^5)\,, \end{aligned} \tag{6.3}$$

$$\begin{aligned}F_S^{(3)} - F_S^{(1)}F_S^{(2)} + \frac{1}{3}\left(F_S^{(1)}\right)^3 &= -\frac{11\pi^4}{1620\epsilon^2} + \frac{1}{\epsilon}\left(-\frac{5\pi^2\zeta_3}{54} - \frac{2\zeta_5}{3}\right) - \frac{13\zeta_3^2}{9} - \frac{193\pi^6}{25515}\\ &\quad + \epsilon\left(-\frac{107\pi^4\zeta_3}{1620} + \frac{187\pi^2\zeta_5}{108} - \frac{21181\zeta_7}{144}\right)\\ &\quad + \epsilon^2\left(-\frac{1421}{45}\zeta_{5,3} - \frac{1922\zeta_3\zeta_5}{3} + \frac{1057\pi^2\zeta_3^2}{108} - \frac{994807\pi^8}{17496000}\right)\\ &\quad + \mathcal{O}(\epsilon^3)\,. \end{aligned} \tag{6.4}$$

The poles of the logarithm of the form factor have the generic structure [61]

$$\ln(F_S) = \sum_{L=1}^{\infty} a^L\,x^{L\epsilon}\left[-\frac{\gamma^{(L)}}{4(L\epsilon)^2} - \frac{\mathcal{G}_0^{(L)}}{2L\epsilon}\right] + \mathcal{O}(\epsilon^0)\,, \tag{6.5}$$

JHEP03(2012)101

with the L-loop cusp $\gamma^{(L)}$ and collinear $\mathcal{G}_0^{(L)}$ anomalous dimensions [62] given by

$$\gamma(a) = \sum_{L=1}^{\infty} a^L \gamma^{(L)} = 4a - 4\zeta_2 a^2 + 22\zeta_4 a^3 + \mathcal{O}(a^4) \,, \tag{6.6}$$

$$\mathcal{G}_0(a) = \sum_{L=1}^{\infty} a^L \mathcal{G}_0^{(L)} = -\zeta_3 a^2 + \left(4\zeta_5 + \frac{10}{3}\zeta_2\zeta_3\right) a^3 + \mathcal{O}(a^4) \,. \tag{6.7}$$

We observe that the vanishing of the $\mathcal{O}(\epsilon^0)$-term in the logarithm of the two-loop form factor [1] appears to be a coincidence, which does not reproduce at three loops. The finite part of the $\mathcal{N} = 4$ form factor does therefore not exponentiate, as could have been conjectured from the two-loop result.

7 Ultraviolet divergences in higher dimensions

Scattering amplitudes and form factors in $\mathcal{N} = 4$ super Yang-Mills are ultraviolet (UV) finite in four dimensions. It is interesting to ask in what dimension, called critical dimension D_c, they first develop UV divergences. This question is of theoretical interest in the context of the discussion of possible finiteness of $\mathcal{N} = 8$ supergravity, see e.g. [38] and references therein. More practically, bounds on the critical UV dimension at a given loop order can also be a useful cross-check of computations, or constrain the types of loop integrals that can appear.

There is a bound on the critical dimension based on power counting for supergraphs and the background field method. The one-loop case is special due to some technical issue with ghosts, but there is a bound for $L > 1$ loops [63, 64],

$$D_c(L) \geq 4 + \frac{2(\mathcal{N}-1)}{L} \,, \qquad L > 1 \,, \tag{7.1}$$

such that for $D < D_c$ the theory is UV finite. The bound (7.1) depends on the number $\mathcal{N}$ of supersymmetries that can be realized off-shell. The maximal amount of supersymmetry can be realised using an $\mathcal{N} = 3$ harmonic superspace action for $\mathcal{N} = 4$ super Yang-Mills [40]. Taking thus $\mathcal{N} = 3$ in (7.1) we have

$$D_c(L) \geq 4 + \frac{4}{L} \,, \qquad L > 1 \,. \tag{7.2}$$

Equation (7.1) is a lower bound for D_c, and in some cases it can be too conservative. For example, in the case of scattering amplitudes, studying and excluding potential counterterms bounds on the critical dimension can sometimes be improved, see the reviews [65, 66]. Investigations of UV properties of four-particle scattering amplitudes have shown that their ultraviolet behaviour is better than expected [67]. Their critical dimension at two and three loops was shown to be 7 and 6, respectively, suggesting the improved bound $D_c(L) \geq 4 + 6/L$. The one-loop case is exceptional, but for completeness we note that $D_c(L = 1) = 8$ for the four-particle scattering amplitude.

We can now study the UV properties for $D > 4$ of the form factor that we have computed. There is no statement from eq. (7.2) for the one-loop case, but one can easily

JHEP03(2012)101

see that $D_c(L=1)=6$. For the two-loop form factor, the bound (7.2) is actually saturated since the two-loop form factor develops its first ultraviolet divergence at $D_c(L=2)=6$. Moreover, it turns out that in $D=6-2\epsilon$ dimensions the leading $1/\epsilon^2$ UV-pole is given by the leading UV-pole of the two-loop planar ladder diagram E_1, and that E_2 has only a simple $1/\epsilon$ pole.

At three loops, eq. (7.2) becomes $D_c \geq 16/3$. First of all, we see by power counting that diagrams F_7 and F_{10} (see figure 6) both have a UV divergence in $D=14/3$ dimensions, which would violate the supersymmetry bound (7.2). This comes close to explaining why their coefficients are zero, and why other integrals having seven or fewer propagators do not appear. A small caveat is that it may not always be possible to write the answer in a form such that the UV properties are manifest: one could have a linear combination of integrals that individually have worse UV properties than expected, but with appropriate UV behaviour of the linear combination. However, as we will see presently, we can make the UV properties of the three-loop form factor completely manifest.

At two loops we found that the bound from superspace counting was saturated. We can ask whether the same happens at three loops, i.e. do we have $D_c(L=3)=16/3$? It turns out that the three-loop form factor is better behaved in the UV than suggested by this equation. It is finite in $D=16/3$ and only develops a UV divergence at $D_c(L=3)=6$. In order to see this, we take the three-loop expression (4.13) and trade F_3, F_4 and F_5 for the non-UT integrals F_3^*, F_4^* and F_5^* by means of eqs. (3.3), (3.6), and (3.9), respectively, which leads to

$$F_S^{3-\text{loop}} \propto (-q^2)\,[8\,F_1 + 2\,F_3^* + 2\,F_4^*] - 2\,F_2 + 4\,F_5^* - 2\,F_9\,. \tag{7.3}$$

Counting numerators as propagators with negative powers, we see that the three integrals in the bracket have nine propagators each, whereas the last three integrals have only eight propagators. Since there are no sub-divergences in $D=16/3$ we can calculate the leading UV pole by simply giving all propagators (and also all numerators[1]) a common mass m and by setting the external momenta $p_1=p_2=0$. Then the first three integrals are finite by naïve power counting, and the last three integrals become equal, and cancel due to their pre-factors. This renders the three-loop form factor finite in $D=16/3$ dimensions. One can see the UV finiteness of the $\mathcal{N}=4$ SYM form factor in $D=16/3$ also in another, more elegant way. We start again from eq. (7.3), and add zero in the disguise of

$$+\,2\,F_7^* \;-\; 2\,F_7^*\,, \tag{7.4}$$

where F_7^* is F_7 (see figure 6) with unit numerator. This choice is particularly convenient since F_7^* is a subtopology of both, F_2 and F_5^*. It is obtained from F_2 by shrinking the line labelled p_a in figure 7. Alternatively, F_7^* is obtained from F_5^* by shrinking line number 7 in figure 4. In both cases one subsequently has to set the respective numerator to unity. Hence we can rewrite (7.3) as

$$F_S^{3-\text{loop}} \propto (-q^2)\,[8\,F_1 + 2\,F_3^* + 2\,F_4^*] - 2\,(F_2 - F_7^*) + 2\,(2\,F_5^* - F_7^* - F_9)\,. \tag{7.5}$$

[1]Whether or not we give a mass to the numerators changes the expressions only by integrals with nine propagators each. The latter are finite in $D=16/3$ by naïve power counting.

JHEP03(2012)101

If we adopt for F_2 the parametrisation

$$\{k_1\,,\,k_1+p_1\,,\,k_2\,,\,k_2+p_2\,,\,k_3-p_2\,,\,k_3+p_1\,,\,k_1+k_2\,,\,k_1-k_3\,,\,k_2+k_3\}\ , \tag{7.6}$$

and write $(F_2 - F_7^*)$ on a common denominator, the numerator of the latter expression reads

$$k_3^2 - (k_3 - p_2)^2 \tag{7.7}$$

and hence vanishes in the aforementioned UV limit. In complete analogy, we take the parametrisation (3.7) for F_5^* and write $(2\,F_5^* - F_7^* - F_9)$ on a common denominator, whose numerator becomes

$$\Big[(k_2-p_1)^2 - k_2^2\Big] + \Big[(k_2-p_1)^2 - (k_2-p_1-p_2)^2\Big]\ , \tag{7.8}$$

which clearly also vanishes upon taking the UV limit. Hence eqs. (7.3) and (7.5) make the UV properties of the form factor manifest. This is very similar to how the UV properties of four-particle amplitudes can be made manifest, see e.g. ref. [67].

It is now interesting to investigate the UV properties of the form factor in $D = 6 - 2\epsilon$ dimensions. Since the vanishing of $(F_2 - F_7^*)$ and $(2\,F_5^* - F_7^* - F_9)$ should be independent of the number of dimensions, we can simply look at the expression

$$8\,F_1 + 2\,F_3^* + 2\,F_4^*\,, \tag{7.9}$$

and the corresponding integrals at one and two loops. Introducing a common propagator mass and neglecting external momenta one finds

$$\begin{aligned}
2D_1^{\rm UV} &\overset{D=6-2\epsilon}{=} S_\Gamma\,[m^2]^{-\epsilon}\left\{-\frac{1}{\epsilon} - \frac{\pi^2}{6}\,\epsilon - \frac{7\pi^4}{360}\,\epsilon^3 + \mathcal{O}(\epsilon^5)\right\}\ ,\\
4E_1^{\rm UV} + E_2^{\rm UV} &\overset{D=6-2\epsilon}{=} S_\Gamma^2\,[m^2]^{-2\epsilon}\left\{\frac{1}{2\epsilon^2} + \frac{1}{2\epsilon} + \left[\frac{1}{2} + \frac{\pi^2}{6} - \frac{1}{5}\,a_\Phi\right] + \mathcal{O}(\epsilon)\right\}\ ,\\
8F_1^{\rm UV} + 2F_3^{*\,\rm UV} + 2F_4^{*\,\rm UV} &\overset{D=6-2\epsilon}{=} S_\Gamma^3\,[m^2]^{-3\epsilon}\left\{-\frac{1}{6\epsilon^3} - \frac{1}{2\epsilon^2}\right.\\
&\qquad\left. + \frac{1}{\epsilon}\left[\frac{\zeta_3}{3} - \frac{\pi^2}{12} - \frac{13}{9} + \frac{1}{5}\,a_\Phi\right] + \mathcal{O}(\epsilon^0)\right\}\ ,
\end{aligned} \tag{7.10}$$

where S_Γ is defined in appendix A, and (see e.g. [68])

$$a_\Phi = \Phi(-\tfrac{1}{3},2,\tfrac{1}{2}) + \frac{\pi\ln(3)}{\sqrt{3}}\ , \tag{7.11}$$

$$\Phi(z,s,a) = \sum_{k=0}^{\infty}\frac{z^k}{[(k+a)^2]^{s/2}}\ , \tag{7.12}$$

$$\Phi(-\tfrac{1}{3},2,\tfrac{1}{2}) = 4\sqrt{3}\,{\rm Im}\Big[{\rm Li}_2\Big(\tfrac{i}{\sqrt{3}}\Big)\Big] = -\frac{\pi\ln(3)}{\sqrt{3}} + \frac{10}{\sqrt{3}}\,{\rm Cl}_2\Big(\frac{\pi}{3}\Big)\ , \tag{7.13}$$

and ${\rm Cl}_2$ is the Clausen function. Hence we find that up to three loops the form factor at each loop-order has $D_c = 6$. Moreover, it turns out that for $D = 6 - 2\epsilon$ the leading $1/\epsilon^L$ UV-pole is at each loop order given by the leading UV-pole of the respective L-loop

JHEP03(2012)101

planar ladder diagram. Since at $D = 6 - 2\epsilon$ there might be issues due to the presence of sub-divergences, we also computed the UV divergences using a different regulator. After having taken the soft limit, we re-insert some external momentum into the graph to serve as IR regulator, instead of the mass (essentially, one nullifies one of the p_i and takes the other one off-shell). In this way one obtains massless propagator type integrals which lead to the following result

$$\begin{aligned} 2D_1^{\rm UV} &\overset{D=6-2\epsilon}{=} S_\Gamma \left(-q^2\right)^{-\epsilon} \left\{-\frac{1}{\epsilon} - 2 - 4\,\epsilon + (2\zeta_3 - 8)\,\epsilon^2 + \mathcal{O}(\epsilon^3)\right\}\,, \\ 4E_1^{\rm UV} + E_2^{\rm UV} &\overset{D=6-2\epsilon}{=} S_\Gamma^2 \left(-q^2\right)^{-2\epsilon} \left\{\frac{1}{2\epsilon^2} + \frac{5}{2\epsilon} + \left[\frac{53}{6} - \zeta_3\right] + \mathcal{O}(\epsilon)\right\}\,, \\ 8F_1^{\rm UV} + 2F_3^{*\,\rm UV} + 2F_4^{*\,\rm UV} &\overset{D=6-2\epsilon}{=} S_\Gamma^3 \left(-q^2\right)^{-3\epsilon} \left\{-\frac{1}{6\epsilon^3} - \frac{3}{2\epsilon^2} + \frac{1}{\epsilon}\left[\frac{4\zeta_3}{3} - \frac{79}{9}\right] + \mathcal{O}(\epsilon^0)\right\}\,. \end{aligned} \tag{7.14}$$

As expected, the leading ϵ^{-L} divergence at L loops is independent of the regulator, while the subleading terms are not. However, when considering $\log(F_{\mathcal{S}})$ in the UV limit there are only simple $1/\epsilon$ poles up to three loops. Moreover, these poles are identical in both regularisation schemes (7.10) and (7.14), and read

$$\ln(F_{\mathcal{S}}^{\rm UV}) \overset{D=6-2\epsilon}{=} -\frac{\alpha}{\epsilon} + \frac{\alpha^2}{\epsilon}\frac{1}{2} + \frac{\alpha^3}{\epsilon}\left(\frac{\zeta_3}{3} - \frac{17}{18}\right) + \mathcal{O}(\alpha^4, \epsilon^0)\,, \quad \text{with } \alpha = -q^2\frac{g^2 N}{(4\pi)^3}\,. \tag{7.15}$$

Let us now discuss this result.

Despite the fact that the form factor is better behaved in the UV than expected, one may wonder why the four-particle amplitudes at one- and two loops are even better behaved in the UV than the form factor. This is due to the fact that there are specific counterterms for the local composite operator $\mathcal{O}(x)$ in higher dimensions. Another way of saying this is in terms of operator mixing. We note that in D dimensions, the coupling constant g has dimension $(4 - D)/2$. Therefore, in $D = 6$, the operator $\mathrm{tr}\,(\phi^2)$ can mix at one loop with the operator $g^2\,\Box\,\mathrm{tr}\,(\phi^2)$, and other operators having the same quantum numbers (we have dropped SU(4) indices for simplicity). Another reason for the better UV behaviour of the four-point amplitudes, at least in the planar limit, is the fact that amplitudes have a dual conformal symmetry, which implies that the difference between the number of propagator factors and numerator factors is four for any loop, whereas form factors are not dual conformal invariant and therefore can have fewer propagators per loop.

8 Discussion and conclusion

In this paper, we extended the calculation of the two-particle form factor in $\mathcal{N} = 4$ SYM of ref. [1] to the three-loop order. We employed the unitarity-based method to obtain the answer in terms of loop integrals. The result contains both planar and non-planar integrals.

The form factor can be expressed in several ways in terms of loop integrals that make different properties manifest. One way of writing it, eq. (4.13) is in terms of integrals all having uniform transcendentality (UT). Other forms, eqs. (7.3) and (7.5), do not have this property, but in turn have the advantage of making the ultraviolet properties of the form

JHEP03(2012)101

factor manifest. In order to see the connection between the two representations, we derived identities between non-planar integrals based on reparametrisation invariances.

We evaluated the form factor in dimensional regularisation by reexpressing the integrals appearing in it in terms of conventionally used master integrals, c.f. eq. (B.1), whose ϵ expansion is known. This allowed us to evaluate the form factor to $\mathcal{O}(\epsilon^2)$. We verified the expected exponentiation of infrared divergences, with the correct values at three loops of the cusp and collinear anomalous dimensions.

We observed that the heuristic leading transcendentality principle that relates anomalous dimensions in QCD with those in $\mathcal{N} = 4$ SYM holds also for the form factor. We checked this principle to three loops, up to and including terms of transcendental weight eight.

We also studied the ultraviolet (UV) properties of the form factor in higher dimensions. We found that at three loops the UV behaviour is better than suggested by a supersymmetry argument. Based on power counting one would expect three-loop integrals having 8 propagators (or nine propagators, and one loop-dependent numerator factor) to diverge in $D = 16/3$ dimensions. However, we find that the particular linear combinations of integrals appearing in the form factor is in fact finite in this dimension, and diverges only in $D = 6$. We found a form, eqs. (7.3) and (7.5), where this is manifest, and computed the leading UV divergence of $\log(F_{\mathcal{S}})$ in $D = 6 - 2\epsilon$ dimensions.

There are a number of interesting further directions.

It is interesting to compare the UV behaviour of the form factor to that of four-particle scattering amplitudes. While there are differences due to specific counterterms allowed for composite operators, they both share the property of having better UV behaviour than expected. It would be interesting if one could understand the UV behaviour of the form factor a priori, perhaps based on the absence of potential counterterms, or from string theory arguments.

We remark that the representations of the form factor in terms of UT integrals, eq. (4.13), or those making its ultraviolet properties manifest, eq. (7.5), are simpler than that in terms of conventionally used master integrals. This may indicate that, even beyond $\mathcal{N} = 4$ SYM, there exists a basis of integrals in terms of which the result looks simpler. Similar observations about the simplicity of loop integrands and integrals in the case of planar scattering amplitudes were also made in refs. [69] and [17].

A further extension of this work could be to investigate generalised form factors with more on-shell external legs. At one-loop even all-multiplicity results could be envisaged [2–5]. At two loops, at least the three-particle form factors should be computable in a relatively straightforward manner, since the relevant integrals (two-loop four-point functions with one external leg off-shell, [70, 71]) are known from the calculation of QCD amplitudes for the $1 \to 3$ decay kinematics [72–74].

The form factor studied in this paper has a very rich structure, similar to that of scattering amplitudes. Planar loop integrands of scattering amplitudes, just like tree amplitudes, satisfy powerful recursion relations [69]. It would be extremely interesting to extend the applicability of recursion relations to the non-planar case, and the form factor studied here is perhaps the simplest case of this type where non-planar integrals appear.

JHEP03(2012)101

Acknowledgments

It is a pleasure to thank L. Dixon for many stimulating discussions and for sharing his insights on the transcendentality properties of non-planar loop integrals with us. We would also like to thank Z. Bern, H. Johansson, S. Naculich, R. Roiban, and E. Sokatchev for useful discussions. This project was started during the "Harmony of Scattering Amplitudes" program at the KITP Santa Barbara, whose hospitality and support we gratefully acknowledge. This research was supported in part by the National Science Foundation under Grant No. PHY05-51164. The work of TG was supported by the Swiss National Science Foundation (SNF) under grant 200020-138206, JMH was supported in part by the Department of Energy grant DE-FG02-90ER40542, TH is supported by the Helmholtz Alliance "Physics at the Terascale". Diagrams were drawn with axodraw [75].

A Explicit results of integrals

In this appendix we list explicit expressions of the integrals that appear as building blocks of the form factor. Our integration measure per loop reads

$$\int \frac{d^D k}{i(2\pi)^D} \,, \tag{A.1}$$

and we define the pre-factor

$$S_\Gamma = \frac{1}{(4\pi)^{D/2}\,\Gamma(1-\epsilon)} \,. \tag{A.2}$$

A generic integral I can be decomposed according to

$$I = S_\Gamma^L \left[-q^2 - i\eta\right]^{n-L\epsilon} \cdot I^{\rm exp} \,, \tag{A.3}$$

where L is the number of loops, and the integer n is fixed by dimensional arguments. $I^{\rm exp}$ contains the Laurent expansion about $\epsilon = 0$.

We start with the one-loop integral

$$\begin{aligned} D_1 &= S_\Gamma \left[-q^2 - i\eta\right]^{-1-\epsilon} \cdot D_1^{\rm exp} \,, \\ D_1^{\rm exp} &= -\frac{\Gamma^2(-\epsilon)\Gamma(1-\epsilon)\Gamma(1+\epsilon)}{\Gamma(1-2\epsilon)} \,. \end{aligned} \tag{A.4}$$

At two loops the integrals read

$$\begin{aligned} E_1 &= S_\Gamma^2 \left[-q^2 - i\eta\right]^{-2-2\epsilon} \cdot E_1^{\rm exp} \,, \\ E_1^{\rm exp} &= \frac{\Gamma^2(1-\epsilon)\Gamma^2(\epsilon+1)\Gamma^4(-\epsilon)}{\Gamma^2(1-2\epsilon)} - \frac{3\Gamma(1-\epsilon)\Gamma(2\epsilon+1)\Gamma^4(-\epsilon)}{2\Gamma(1-3\epsilon)} \\ &\quad + \frac{3\Gamma(1-2\epsilon)\Gamma(\epsilon+1)\Gamma(2\epsilon+1)\Gamma^4(-\epsilon)}{4\Gamma(1-3\epsilon)} \,. \end{aligned} \tag{A.5}$$

JHEP03(2012)101

An all-order expression for E_2 can be found in [76]. The expansion in ϵ reads

$$\begin{aligned}
E_2 &= S_\Gamma^2 \left[-q^2 - i\eta\right]^{-2-2\epsilon} \cdot E_2^{\text{exp}}\,, \\
E_2^{\text{exp}} &= +\frac{1}{\epsilon^4} - \frac{5\pi^2}{6\epsilon^2} - \frac{27\zeta_3}{\epsilon} - \frac{23\pi^4}{36} + \epsilon\left(8\pi^2\zeta_3 - 117\zeta_5\right) + \epsilon^2\left(267\zeta_3^2 - \frac{19\pi^6}{315}\right) \\
&\quad + \epsilon^3\left(\frac{109\pi^4\zeta_3}{10} + 40\pi^2\zeta_5 + 6\zeta_7\right) + \epsilon^4\left(-264\zeta_{5,3} + 2466\zeta_3\zeta_5 - 44\pi^2\zeta_3^2 + \frac{1073\pi^8}{3024}\right) \\
&\quad + \mathcal{O}(\epsilon^5)\,. \qquad \text{(A.6)}
\end{aligned}$$

At three loops the integrals with uniform transcendentality (UT) are shown in figures 6 and 7 and read

$$\begin{aligned}
F_1 &= S_\Gamma^3 \left[-q^2 - i\eta\right]^{-3-3\epsilon} \cdot F_1^{\text{exp}}\,, \\
F_1^{\text{exp}} &= -\frac{1}{36\epsilon^6} - \frac{\pi^2}{12\epsilon^4} - \frac{31\zeta_3}{18\epsilon^3} - \frac{23\pi^4}{216\epsilon^2} + \frac{1}{\epsilon}\left(-\frac{5\pi^2\zeta_3}{6} - \frac{49\zeta_5}{2}\right) \\
&\quad - \frac{43\zeta_3^2}{18} - \frac{5657\pi^6}{68040} + \epsilon\left(\frac{227\pi^4\zeta_3}{540} - \frac{7\pi^2\zeta_5}{6} - \frac{139\zeta_7}{3}\right) \\
&\quad + \epsilon^2\left(-192\zeta_{5,3} + 3\zeta_3\zeta_5 + \frac{47\pi^2\zeta_3^2}{2} + \frac{959\pi^8}{12960}\right) + \mathcal{O}(\epsilon^3)\,. \qquad \text{(A.7)}
\end{aligned}$$

The integral F_2 is just $A_{9,1}^{(n)}$ from [26],

$$\begin{aligned}
F_2 &= S_\Gamma^3 \left[-q^2 - i\eta\right]^{-2-3\epsilon} \cdot F_2^{\text{exp}}\,, \\
F_2^{\text{exp}} &= +\frac{1}{36\epsilon^6} + \frac{\pi^2}{18\epsilon^4} + \frac{14\zeta_3}{9\epsilon^3} + \frac{47\pi^4}{405\epsilon^2} + \frac{1}{\epsilon}\left(\frac{85\pi^2\zeta_3}{27} + 20\zeta_5\right) \\
&\quad + \frac{137\zeta_3^2}{3} + \frac{1160\pi^6}{5103} + \epsilon\left(\frac{829\pi^4\zeta_3}{405} + \frac{719\pi^2\zeta_5}{27} + \frac{6451\zeta_7}{9}\right) \\
&\quad + \epsilon^2\left(-\frac{1184}{9}\zeta_{5,3} + 1250\zeta_3\zeta_5 - \frac{712\pi^2\zeta_3^2}{9} + \frac{593749\pi^8}{1224720}\right) + \mathcal{O}(\epsilon^3)\,. \qquad \text{(A.8)}
\end{aligned}$$

Moreover, we have

$$\begin{aligned}
F_3 &= S_\Gamma^3 \left[-q^2 - i\eta\right]^{-2-3\epsilon} \cdot F_3^{\text{exp}}\,, \\
F_3^{\text{exp}} &= -\frac{1}{36\epsilon^6} + \frac{\pi^2}{9\epsilon^4} + \frac{37\zeta_3}{9\epsilon^3} + \frac{131\pi^4}{540\epsilon^2} + \frac{1}{\epsilon}\left(\frac{145\zeta_5}{3} - \frac{4\pi^2\zeta_3}{9}\right) \\
&\quad - \frac{1352\zeta_3^2}{9} + \frac{173\pi^6}{1215} + \epsilon\left(-\frac{253\pi^4\zeta_3}{27} - \frac{62\pi^2\zeta_5}{3} - \frac{525\zeta_7}{2}\right) \\
&\quad + \epsilon^2\left(\frac{6272}{5}\zeta_{5,3} - \frac{4696\zeta_3\zeta_5}{3} - \frac{712\pi^2\zeta_3^2}{9} - \frac{1301609\pi^8}{1701000}\right) + \mathcal{O}(\epsilon^3)\,, \qquad \text{(A.9)}
\end{aligned}$$

$$\begin{aligned}
F_4 &= S_\Gamma^3 \left[-q^2 - i\eta\right]^{-2-3\epsilon} \cdot F_4^{\text{exp}}\,, \\
F_4^{\text{exp}} &= -\frac{1}{36\epsilon^6} - \frac{\pi^2}{12\epsilon^4} - \frac{55\zeta_3}{18\epsilon^3} - \frac{11\pi^4}{216\epsilon^2} + \frac{1}{\epsilon}\left(\frac{43\pi^2\zeta_3}{6} - \frac{599\zeta_5}{6}\right) \\
&\quad - \frac{307\zeta_3^2}{18} - \frac{18797\pi^6}{68040} + \epsilon\left(-\frac{149\pi^4\zeta_3}{108} + \frac{239\pi^2\zeta_5}{2} - \frac{21253\zeta_7}{6}\right) \\
&\quad + \epsilon^2\left(\frac{8268}{5}\zeta_{5,3} + \frac{5569\zeta_3\zeta_5}{3} - \frac{439\pi^2\zeta_3^2}{6} - \frac{184873\pi^8}{108000}\right) + \mathcal{O}(\epsilon^3)\,, \qquad \text{(A.10)}
\end{aligned}$$

JHEP03(2012)101

$$
\begin{aligned}
F_5 &= S_\Gamma^3 \left[-q^2 - i\eta\right]^{-2-3\epsilon} \cdot F_5^{\text{exp}}\,, \\
F_5^{\text{exp}} &= +\frac{1}{12\epsilon^6} + \frac{\pi^2}{27\epsilon^4} + \frac{17\zeta_3}{9\epsilon^3} + \frac{71\pi^4}{540\epsilon^2} + \frac{1}{\epsilon}\left(\frac{71\pi^2\zeta_3}{54} + \frac{13\zeta_5}{3}\right) \\
&\quad -\frac{679\zeta_3^2}{6} + \frac{3991\pi^6}{136080} + \epsilon\left(-\frac{2837\pi^4\zeta_3}{540} + \frac{205\pi^2\zeta_5}{9} - \frac{25135\zeta_7}{24}\right) \\
&\quad +\epsilon^2\left(\frac{4006}{3}\zeta_{5,3} - 59\zeta_3\zeta_5 - \frac{10\pi^2\zeta_3^2}{27} - \frac{14156063\pi^8}{16329600}\right) + \mathcal{O}(\epsilon^3)\,. \qquad \text{(A.11)}
\end{aligned}
$$

The integral F_6 is just $A_{9,2}^{(n)}$ from [26],

$$
\begin{aligned}
F_6 &= S_\Gamma^3 \left[-q^2 - i\eta\right]^{-2-3\epsilon} \cdot F_6^{\text{exp}}\,, \\
F_6^{\text{exp}} &= +\frac{2}{9\epsilon^6} - \frac{7\pi^2}{27\epsilon^4} - \frac{91\zeta_3}{9\epsilon^3} - \frac{373\pi^4}{1080\epsilon^2} + \frac{1}{\epsilon}\left(\frac{179\pi^2\zeta_3}{27} - 167\zeta_5\right) \\
&\quad +\frac{169\zeta_3^2}{9} - \frac{59797\pi^6}{136080} + \epsilon\left(\frac{7\pi^4\zeta_3}{30} + \frac{850\pi^2\zeta_5}{9} - \frac{18569\zeta_7}{6}\right) \\
&\quad +\epsilon^2\left(\frac{5188}{5}\zeta_{5,3} + \frac{9362\zeta_3\zeta_5}{3} - \frac{4436\pi^2\zeta_3^2}{27} - \frac{107881603\pi^8}{81648000}\right) + \mathcal{O}(\epsilon^3)\,. \qquad \text{(A.12)}
\end{aligned}
$$

Moreover, we have

$$
\begin{aligned}
F_7 &= S_\Gamma^3 \left[-q^2 - i\eta\right]^{-1-3\epsilon} \cdot F_7^{\text{exp}}\,, \\
F_7^{\text{exp}} &= -\frac{1}{36\epsilon^6} - \frac{\pi^2}{27\epsilon^4} - \frac{7\zeta_3}{9\epsilon^3} - \frac{\pi^4}{36\epsilon^2} + \frac{1}{\epsilon}\left(\frac{20\pi^2\zeta_3}{27} - \frac{13\zeta_5}{3}\right) \\
&\quad +\frac{226\zeta_3^2}{9} - \frac{233\pi^6}{34020} + \epsilon\left(\frac{151\pi^4\zeta_3}{135} + \frac{70\pi^2\zeta_5}{9} - \frac{229\zeta_7}{6}\right) \\
&\quad +\epsilon^2\left(\frac{248}{15}\zeta_{5,3} + \frac{1244\zeta_3\zeta_5}{3} - \frac{176\pi^2\zeta_3^2}{27} + \frac{207311\pi^8}{20412000}\right) + \mathcal{O}(\epsilon^3)\,, \qquad \text{(A.13)}
\end{aligned}
$$

$$
\begin{aligned}
F_8 &= S_\Gamma^3 \left[-q^2 - i\eta\right]^{-2-3\epsilon} \cdot F_8^{\text{exp}}\,, \\
F_8^{\text{exp}} &= +\frac{1}{36\epsilon^6} + \frac{\pi^2}{27\epsilon^4} - \frac{5\zeta_3}{9\epsilon^3} + \frac{\pi^4}{108\epsilon^2} + \frac{1}{\epsilon}\left(\frac{37\zeta_5}{3} - \frac{32\pi^2\zeta_3}{27}\right) \\
&\quad +\frac{98\zeta_3^2}{9} + \frac{26\pi^6}{8505} + \epsilon\left(-\frac{4\pi^4\zeta_3}{15} - \frac{70\pi^2\zeta_5}{9} + \frac{835\zeta_7}{6}\right) \\
&\quad +\epsilon^2\left(\frac{248}{3}\zeta_{5,3} + \frac{124\zeta_3\zeta_5}{3} + \frac{572\pi^2\zeta_3^2}{27} - \frac{16159\pi^8}{1020600}\right) + \mathcal{O}(\epsilon^3)\,, \qquad \text{(A.14)}
\end{aligned}
$$

$$
\begin{aligned}
F_9 &= S_\Gamma^3 \left[-q^2 - i\eta\right]^{-2-3\epsilon} \cdot F_9^{\text{exp}}\,, \\
F_9^{\text{exp}} &= +\frac{1}{4\epsilon^6} - \frac{11\pi^2}{54\epsilon^4} - \frac{74\zeta_3}{9\epsilon^3} - \frac{43\pi^4}{180\epsilon^2} - \frac{1}{\epsilon}\left(\frac{328\zeta_5}{3} - \frac{176\pi^2\zeta_3}{27}\right) \\
&\quad +128\zeta_3^2 - \frac{2951\pi^6}{17010} - \epsilon\left(-\frac{1021\pi^4\zeta_3}{135} - \frac{610\pi^2\zeta_5}{9} + \frac{6149\zeta_7}{6}\right) \\
&\quad -\epsilon^2\left(\frac{392}{3}\zeta_{5,3} - \frac{11504\zeta_3\zeta_5}{3} + \frac{2876\pi^2\zeta_3^2}{27} - \frac{85171\pi^8}{1020600}\right) + \mathcal{O}(\epsilon^3)\,, \qquad \text{(A.15)}
\end{aligned}
$$

JHEP03(2012)101

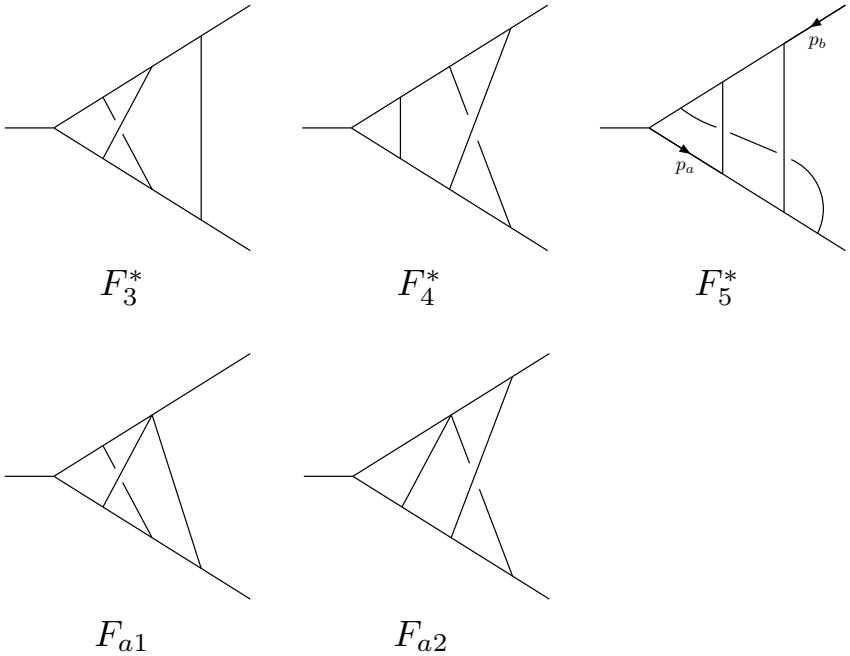

Figure 8. Diagrams which do *not* have uniform transcendentality. As before, labels p_a and p_b on arrow lines indicate an irreducible scalar product $(p_a + p_b)^2$ in the respective numerator, and diagrams that lack these labels have unit numerator.

$$
\begin{aligned}
F_{10} &= S_\Gamma^3 \left[-q^2 - i\eta\right]^{-1-3\epsilon} \cdot F_{10}^{\text{exp}}\,, \\
F_{10}^{\text{exp}} &= \frac{\Gamma(1-\epsilon)^2\Gamma(-\epsilon)^5\Gamma(3\epsilon)}{12\Gamma(1-4\epsilon)}\,.
\end{aligned}
\tag{A.16}
$$

The integrals *without* homogeneous transcendental weight are collected in figure 8 and read

$$
\begin{aligned}
F_3^* &= S_\Gamma^3 \left[-q^2 - i\eta\right]^{-3-3\epsilon} \cdot F_3^{*\,\text{exp}}\,, \\
F_3^{*\,\text{exp}} &= -\frac{1}{9\epsilon^6} + \frac{4\pi^2}{27\epsilon^4} + \frac{1}{\epsilon^3}\left(\frac{28\zeta_3}{3} + \frac{2\pi^2}{9}\right) + \frac{1}{\epsilon^2}\left(\frac{44\zeta_3}{3} - \frac{8\pi^2}{9} + \frac{7\pi^4}{15}\right) \\
&\quad + \frac{1}{\epsilon}\left(-\frac{176\zeta_3}{3} + \frac{40\pi^2\zeta_3}{27} + 72\zeta_5 + \frac{32\pi^2}{9} + \frac{8\pi^4}{15}\right) - \frac{236\zeta_5}{3} - \frac{2900\zeta_3^2}{9} + \frac{56\pi^2\zeta_3}{9} \\
&\quad + \frac{704\zeta_3}{3} + \frac{158\pi^6}{567} - \frac{32\pi^4}{15} - \frac{128\pi^2}{9} + \epsilon\left(-\frac{2816\zeta_3}{3} - \frac{224\pi^2\zeta_3}{9} - \frac{2458\pi^4\zeta_3}{135}\right. \\
&\quad \left. - \frac{1936\zeta_3^2}{3} + \frac{944\zeta_5}{3} - \frac{232\pi^2\zeta_5}{9} - \frac{2410\zeta_7}{3} + \frac{512\pi^2}{9} + \frac{128\pi^4}{15} - \frac{262\pi^6}{945}\right) \\
&\quad + \epsilon^2\left(\frac{35152}{15}\zeta_{5,3} - \frac{16082\zeta_7}{3} - \frac{9640\zeta_3\zeta_5}{3} - \frac{352\pi^2\zeta_5}{3} - \frac{3776\zeta_5}{3} - \frac{5416\pi^2\zeta_3^2}{27} - \frac{512\pi^4}{15}\right. \\
&\quad \left. + \frac{7744\zeta_3^2}{3} - \frac{224\pi^4\zeta_3}{9} + \frac{896\pi^2\zeta_3}{9} + \frac{11264\zeta_3}{3} - \frac{956008\pi^8}{637875} + \frac{1048\pi^6}{945} - \frac{2048\pi^2}{9}\right) \\
&\quad + \mathcal{O}(\epsilon^3)\,,
\end{aligned}
\tag{A.17}
$$

JHEP03(2012)101

$$
\begin{aligned}
F_4^* &= S_\Gamma^3\left[-q^2-i\eta\right]^{-3-3\epsilon}\cdot F_4^{*\,\mathrm{exp}}\,,\\
F_4^{*\,\mathrm{exp}} &= -\frac{1}{18\epsilon^6}+\frac{5}{18\epsilon^5}+\frac{1}{\epsilon^4}\left(-\frac{10}{9}-\frac{\pi^2}{6}\right)+\frac{1}{\epsilon^3}\left(-\frac{55\zeta_3}{9}+\frac{40}{9}-\frac{7\pi^2}{9}\right)\\
&\quad+\frac{1}{\epsilon^2}\left(-\frac{136\zeta_3}{9}-\frac{160}{9}+\frac{28\pi^2}{9}-\frac{11\pi^4}{108}\right)+\frac{1}{\epsilon}\left(\frac{544\zeta_3}{9}+\frac{43\pi^2\zeta_3}{3}-\frac{599\zeta_5}{3}\right.\\
&\quad\left.+\frac{640}{9}-\frac{112\pi^2}{9}-\frac{17\pi^4}{54}\right)-\frac{1108\zeta_5}{3}-\frac{307\zeta_3^2}{9}+\frac{88\pi^2\zeta_3}{9}-\frac{2176\zeta_3}{9}-\frac{18797\pi^6}{34020}\\
&\quad+\frac{34\pi^4}{27}+\frac{448\pi^2}{9}-\frac{2560}{9}+\epsilon\left(\frac{8704\zeta_3}{9}-\frac{352\pi^2\zeta_3}{9}-\frac{149\pi^4\zeta_3}{54}-\frac{7360\zeta_3^2}{9}+\frac{4432\zeta_5}{3}\right.\\
&\quad\left.+239\pi^2\zeta_5-\frac{21253\zeta_7}{3}+\frac{10240}{9}-\frac{1792\pi^2}{9}-\frac{136\pi^4}{27}-\frac{3055\pi^6}{1701}\right)+\epsilon^2\left(\frac{16536}{5}\zeta_{5,3}\right.\\
&\quad-17273\zeta_7+\frac{11138\zeta_3\zeta_5}{3}+180\pi^2\zeta_5-\frac{17728\zeta_5}{3}-\frac{439\pi^2\zeta_3^2}{3}+\frac{29440\zeta_3^2}{9}-\frac{4846\pi^4\zeta_3}{135}\\
&\quad\left.+\frac{1408\pi^2\zeta_3}{9}-\frac{34816\zeta_3}{9}-\frac{184873\pi^8}{54000}+\frac{12220\pi^6}{1701}+\frac{544\pi^4}{27}+\frac{7168\pi^2}{9}-\frac{40960}{9}\right)\\
&\quad+\mathcal{O}(\epsilon^3)\,,
\end{aligned}
\tag{A.18}
$$

$$
\begin{aligned}
F_5^* &= S_\Gamma^3\left[-q^2-i\eta\right]^{-2-3\epsilon}\cdot F_5^{*\,\mathrm{exp}}\,,\\
F_5^{*\,\mathrm{exp}} &= -\frac{1}{18\epsilon^6}-\frac{5}{36\epsilon^5}+\frac{1}{\epsilon^4}\left(\frac{5}{9}+\frac{\pi^2}{54}\right)+\frac{1}{\epsilon^3}\left(\frac{5\pi^2}{18}-\frac{20}{9}\right)\\
&\quad+\frac{1}{\epsilon^2}\left(\frac{2\zeta_3}{9}+\frac{80}{9}-\frac{10\pi^2}{9}-\frac{\pi^4}{40}\right)+\frac{1}{\epsilon}\left(-\frac{8\zeta_3}{9}-\frac{77\pi^2\zeta_3}{54}+\frac{160\zeta_5}{3}\right.\\
&\quad\left.-\frac{320}{9}+\frac{40\pi^2}{9}-\frac{59\pi^4}{540}\right)+224\zeta_5+\frac{4003\zeta_3^2}{18}-8\pi^2\zeta_3+\frac{32\zeta_3}{9}+\frac{16099\pi^6}{68040}\\
&\quad+\frac{59\pi^4}{135}-\frac{160\pi^2}{9}+\frac{1280}{9}+\epsilon\left(-\frac{128\zeta_3}{9}+32\pi^2\zeta_3+\frac{151\pi^4\zeta_3}{12}+\frac{6584\zeta_3^2}{9}-896\zeta_5\right.\\
&\quad\left.-\frac{445\pi^2\zeta_5}{9}+\frac{74815\zeta_7}{24}-\frac{5120}{9}+\frac{640\pi^2}{9}-\frac{236\pi^4}{135}+\frac{2519\pi^6}{2430}\right)+\epsilon^2\left(-\frac{12518}{5}\zeta_{5,3}\right.\\
&\quad+\frac{67901\zeta_7}{6}+773\zeta_3\zeta_5-\frac{94\pi^2\zeta_5}{3}+3584\zeta_5+\frac{1570\pi^2\zeta_3^2}{27}-\frac{26336\zeta_3^2}{9}+\frac{4103\pi^4\zeta_3}{135}\\
&\quad\left.-128\pi^2\zeta_3+\frac{512\zeta_3}{9}+\frac{13248257\pi^8}{5832000}-\frac{5038\pi^6}{1215}+\frac{944\pi^4}{135}-\frac{2560\pi^2}{9}+\frac{20480}{9}\right)\\
&\quad+\mathcal{O}(\epsilon^3)\,,
\end{aligned}
\tag{A.19}
$$

$$
\begin{aligned}
F_{a1} &= S_\Gamma^3\left[-q^2-i\eta\right]^{-2-3\epsilon}\cdot F_{a1}^{\mathrm{exp}}\,,\\
F_{a1}^{\mathrm{exp}} &= -\frac{\pi^2}{9\epsilon^3}+\frac{1}{\epsilon^2}\left(\frac{4\pi^2}{9}-\frac{22\zeta_3}{3}\right)+\frac{1}{\epsilon}\left(\frac{88\zeta_3}{3}-\frac{16\pi^2}{9}-\frac{4\pi^4}{15}\right)+\frac{118\zeta_5}{3}-\frac{28\pi^2\zeta_3}{9}\\
&\quad-\frac{352\zeta_3}{3}+\frac{16\pi^4}{15}+\frac{64\pi^2}{9}+\epsilon\left(\frac{1408\zeta_3}{3}+\frac{112\pi^2\zeta_3}{9}+\frac{968\zeta_3^2}{3}-\frac{472\zeta_5}{3}-\frac{256\pi^2}{9}\right.\\
&\quad\left.-\frac{64\pi^4}{15}+\frac{131\pi^6}{945}\right)+\epsilon^2\left(-\frac{5632\zeta_3}{3}-\frac{448\pi^2\zeta_3}{9}+\frac{112\pi^4\zeta_3}{9}-\frac{3872\zeta_3^2}{3}+\frac{1888\zeta_5}{3}\right.\\
&\quad\left.+\frac{176\pi^2\zeta_5}{3}+\frac{8041\zeta_7}{3}+\frac{1024\pi^2}{9}+\frac{256\pi^4}{15}-\frac{524\pi^6}{945}\right)+\mathcal{O}(\epsilon^3)\,,
\end{aligned}
\tag{A.20}
$$

JHEP03(2012)101

$$
\begin{aligned}
F_{a2} &= S_\Gamma^3 \left[-q^2 - i\eta\right]^{-2-3\epsilon} \cdot F_{a2}^{\text{exp}}\,, \\
F_{a2}^{\text{exp}} &= -\frac{5}{36\epsilon^5} + \frac{5}{9\epsilon^4} + \frac{1}{\epsilon^3}\left(\frac{7\pi^2}{18} - \frac{20}{9}\right) + \frac{1}{\epsilon^2}\left(\frac{68\zeta_3}{9} + \frac{80}{9} - \frac{14\pi^2}{9}\right) + \frac{1}{\epsilon}\left(-\frac{272\zeta_3}{9} - \frac{320}{9}\right. \\
&\quad \left. + \frac{56\pi^2}{9} + \frac{17\pi^4}{108}\right) + \frac{554\zeta_5}{3} - \frac{44\pi^2\zeta_3}{9} + \frac{1088\zeta_3}{9} - \frac{17\pi^4}{27} - \frac{224\pi^2}{9} + \frac{1280}{9} \\
&\quad + \epsilon\left(\frac{176\pi^2\zeta_3}{9} - \frac{4352\zeta_3}{9} + \frac{3680\zeta_3^2}{9} - \frac{2216\zeta_5}{3} - \frac{5120}{9} + \frac{896\pi^2}{9} + \frac{68\pi^4}{27} + \frac{3055\pi^6}{3402}\right) \\
&\quad + \epsilon^2\left(\frac{17408\zeta_3}{9} - \frac{704\pi^2\zeta_3}{9} + \frac{2423\pi^4\zeta_3}{135} - \frac{14720\zeta_3^2}{9} + \frac{8864\zeta_5}{3} - 90\pi^2\zeta_5 + \frac{17273\zeta_7}{2}\right. \\
&\quad \left. + \frac{20480}{9} - \frac{3584\pi^2}{9} - \frac{272\pi^4}{27} - \frac{6110\pi^6}{1701}\right) + \mathcal{O}(\epsilon^3)\,. \qquad \text{(A.21)}
\end{aligned}
$$

At three loops we also cross-checked the major part of the integrals with the sector decomposition program FIESTA [77, 78].

B Form factor in terms of master integrals

Just as in QCD, the three-loop scalar form factor in $\mathcal{N} = 4$ can be reduced to master integrals by means of the Laporta algorithm [46], for which we used the program REDUZE [47]. One obtains

$$
\begin{aligned}
F_S^{(3)} &= R_\epsilon^3 \left[+ \frac{(3D-14)^2}{(D-4)(5D-22)} A_{9,1} - \frac{2(3D-14)}{5D-22} A_{9,2} - \frac{4(2D-9)(3D-14)}{(D-4)(5D-22)} A_{8,1} \right. \\
&\quad - \frac{20(3D-13)(D-3)}{(D-4)(2D-9)} A_{7,1} - \frac{40(D-3)}{D-4} A_{7,2} + \frac{8(D-4)}{(2D-9)(5D-22)} A_{7,3} \\
&\quad - \frac{16(3D-13)(3D-11)}{(2D-9)(5D-22)} A_{7,4} - \frac{16(3D-13)(3D-11)}{(2D-9)(5D-22)} A_{7,5} \\
&\quad - \frac{128(2D-7)(D-3)^2}{3(D-4)(3D-14)(5D-22)} A_{6,1} \\
&\quad - \frac{16(2D-7)(5D-18)\left(52D^2-485D+1128\right)}{9(D-4)^2(2D-9)(5D-22)} A_{6,2} \\
&\quad - \frac{16(2D-7)(3D-14)(3D-10)(D-3)}{(D-4)^3(5D-22)} A_{6,3} \\
&\quad - \frac{128(2D-7)(3D-8)\left(91D^2-821D+1851\right)(D-3)^2}{3(D-4)^4(2D-9)(5D-22)} A_{5,1} \\
&\quad - \frac{128(2D-7)\left(1497D^3-20423D^2+92824D-140556\right)(D-3)^3}{9(D-4)^4(2D-9)(3D-14)(5D-22)} A_{5,2} \\
&\quad + \frac{4(D-3)}{D-4} B_{8,1} + \frac{64(D-3)^3}{(D-4)^3} B_{6,1} + \frac{48(3D-10)(D-3)^2}{(D-4)^3} B_{6,2} \\
&\quad - \frac{16(3D-10)(3D-8)\left(144D^2-1285D+2866\right)(D-3)^2}{(D-4)^4(2D-9)(5D-22)} B_{5,1} \\
&\quad + \frac{128(2D-7)\left(177D^2-1584D+3542\right)(D-3)^3}{3(D-4)^4(2D-9)(5D-22)} B_{5,2}
\end{aligned}
$$

JHEP03(2012)101

$$
\begin{aligned}
&+\frac{64(2D-5)(3D-8)(D-3)}{9(D-4)^5(2D-9)(3D-14)(5D-22)} \\
&\quad\times\left(2502D^5-51273D^4+419539D^3-1713688D^2+3495112D-2848104\right)B_{4,1} \\
&+\frac{4(D-3)}{D-4}C_{8,1}+\frac{48(3D-10)(D-3)^2}{(D-4)^3}C_{6,1}\Bigg] \,. \qquad \text{(B.1)}
\end{aligned}
$$

R_ϵ is given in eq. (2.14). In order to arrive at eq. (5.2) we have to plug in $D = 4 - 2\epsilon$ and the ϵ-expansions for the master integrals from eqs. (A.7) – (A.27) of [30], together with their higher order ϵ-terms from [32].

C Four-point amplitude to two loops

Here we summarise the known four-point amplitude in $\mathcal{N} = 4$ super Yang-Mills to two loop order. As we have seen in the main text, both leading and subleading terms in colour are required when computing the form factor at leading colour using unitarity.

We consider four-point amplitudes in SU(N) gauge theories with all particles in the adjoint representation. Let us review the decomposition of the latter into a trace basis with partial amplitudes as coefficients [79, 80].

At tree-level, we have

$$
\mathcal{A}_4^{\text{tree}} = g^2\mu^{2\epsilon}\sum_{\sigma\in S_4/Z_4}\text{Tr}(T^{a_{\sigma(1)}}T^{a_{\sigma(2)}}T^{a_{\sigma(3)}}T^{a_{\sigma(4)}})A^{\text{tree}}_{4;1;1}(\sigma(1),\sigma(2),\sigma(3),\sigma(4))\,, \qquad \text{(C.1)}
$$

where sum goes over the six non-cyclic permutations of (1234), i.e. $S_4/Z_4 = \{(1234), (2134), (1243), (2314), (3241), (3214)\}$. The $A^{\text{tree}}_{4;1;1}$ are 'partial amplitudes'. The arguments of $\mathcal{A}$ and A in eq. (C.1) are abbreviations, i.e. 1 stands for a given particle (gluon, fermion, or scalar) of a given helicity and momentum p_1^μ. The T^a are the (N^2-1) matrices in the fundamental representation of SU(N).

At loop level, double trace terms are present as well. Other possible trace terms vanish since $\text{Tr}(T^a) = 0$ for SU(N). We have, at one loop

$$
\begin{aligned}
\mathcal{A}_4^{1-\text{loop}} &= g^4\mu^{4\epsilon}\sum_{\sigma\in S_4/Z_4} N\,\text{Tr}(T^{a_{\sigma(1)}}T^{a_{\sigma(2)}}T^{a_{\sigma(3)}}T^{a_{\sigma(4)}})A^{1-\text{loop}}_{4;1,1}(\sigma(1),\sigma(2),\sigma(3),\sigma(4)) \qquad \text{(C.2)}\\
&\quad+g^4\mu^{4\epsilon}\sum_{\sigma\in S_4/Z_2^3}\text{Tr}(T^{a_{\sigma(1)}}T^{a_{\sigma(2)}})\text{Tr}(T^{a_{\sigma(3)}}T^{a_{\sigma(4)}})A^{1-\text{loop}}_{4;1,3}(\sigma(1),\sigma(2),\sigma(3),\sigma(4))\,,
\end{aligned}
$$

and two loops [56],

$$
\begin{aligned}
\mathcal{A}_4^{2-\text{loop}} &= g^6\mu^{6\epsilon}\sum_{\sigma\in S_4/Z_4}\text{Tr}(T^{a_{\sigma(1)}}T^{a_{\sigma(2)}}T^{a_{\sigma(3)}}T^{a_{\sigma(4)}})\times \qquad \text{(C.3)}\\
&\quad\times\Big(N^2\,A^{2-\text{loop},LC}_{4;1,1}(\sigma(1),\sigma(2),\sigma(3),\sigma(4))+A^{2-\text{loop},SC}_{4;1,1}(\sigma(1),\sigma(2),\sigma(3),\sigma(4))\Big)\\
&\quad+g^6\mu^{6\epsilon}\sum_{\sigma\in S_4/Z_2^3} N\,\text{Tr}(T^{a_{\sigma(1)}}T^{a_{\sigma(2)}})\text{Tr}(T^{a_{\sigma(3)}}T^{a_{\sigma(4)}})A^{2-\text{loop}}_{4;1,3}(\sigma(1),\sigma(2),\sigma(3),\sigma(4))\,.
\end{aligned}
$$

JHEP03(2012)101

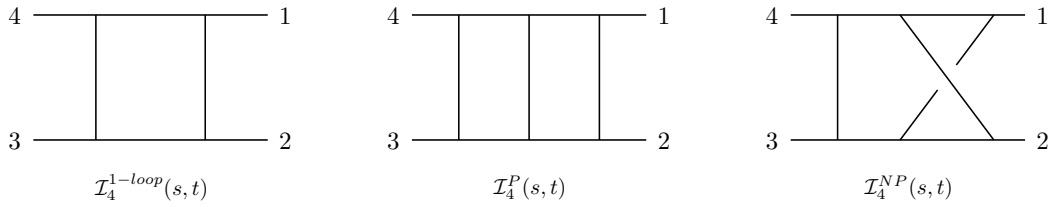

Figure 9. Scalar box integrals appearing in four-particle amplitudes to two loops.

Here $S_4/Z_2^3 = \{(1234),(1324),(1423)\}$. The double trace terms are subleading in the expansion in powers of N. At the two-loop order, we also have the appearence of subleading-in-N terms in the single trace terms, denoted by the superscript SC, while the leading-in-N terms have superscript LC.

$\mathcal{N}=4$ supersymmetric Ward identities imply that for MHV amplitudes the loop-level amplitudes are proportional to the tree-level ones, for any choice of external particles and helicities. We have

$$A_{4;1,1}^{1-\text{loop}}(1,2,3,4) = -st\, A_{4;1,1}^{\text{tree}}(1,2,3,4)\, \mathcal{I}_4^{1-\text{loop}}(s,t)\,, \tag{C.4}$$

where[2]

$$\mathcal{I}_4^{1-\text{loop}}(s,t) = \int \frac{d^Dk}{i(2\pi)^D} \frac{1}{k^2(k-p_1)^2(k-p_1-p_2)^2(k+p_4)^2}\,, \tag{C.5}$$

is the one-loop scalar box integral, see figure 9. The remaining subleading colour amplitudes at one loop are all equal and given by

$$A_{4;1,3}^{1-\text{loop}} = \sum_{\sigma\in S_4/Z_4} A_{4;1,1}^{1-\text{loop}}(\sigma(1),\sigma(2),\sigma(3),\sigma(4))\,, \tag{C.6}$$

which is the consequence of a U(1) decoupling identity [79].

At two loops, the partial amplitudes leading in N are given by [56]

$$A_{4;1,1}^{2-\text{loop},LC}(1,2,3,4) = +st\, A_{4;1,1}^{\text{tree}}(1,2,3,4)\, \left(s\mathcal{I}_4^P(s,t) + st\mathcal{I}_4^P(t,s)\right)\,, \tag{C.7}$$

where $\mathcal{I}_4^P(s,t)$ is the planar double box integral, see figure 9.

The partial amplitudes subleading in N are given by [56]

$$\begin{aligned} A_{4;1,1}^{2-\text{loop},SC}(1,2,3,4) &= 2A_4^P(1,2;3,4) + 2A_4^P(3,4;2,1) + 2A_4^P(1,4;2,3) + 2A_4^P(2,3;4,1) \\ &- 4A_4^P(1,3;2,4) - 4A_4^P(2,4;3,1) + 2A_4^{NP}(1;2;3,4) + 2A_4^{NP}(3;4;2,1) \\ &+ 2A_4^{NP}(1;4;2,3) + 2A_4^{NP}(2;3;4,1) - 4A_4^{NP}(1;3;2,4) - 4A_4^{NP}(2;4;3,1)\,, \end{aligned} \tag{C.8}$$

and

$$\begin{aligned} A_{4;1,3}^{2-\text{loop}}(1;2;3,4) &= 6A_4^P(1,2;3,4) + 6A_4^P(1,2;4,3) + 4A_4^{NP}(1;2;3,4) + 4A_4^{NP}(3;4;2,1) \\ &- 2A_4^{NP}(1;4;2,3) - 2A_4^{NP}(2;3;4,1) - 2A_4^{NP}(1;3;2,4) - 2A_4^{NP}(2;4;3,1)\,, \end{aligned} \tag{C.9}$$

[2]Note that our convention of defining loop integrals differs from that of ref. [56] by a factor of i per loop order, cf. eq. (A.1).

JHEP03(2012)101

where

$$A_4^P(1,2;3,4) \equiv s_{12}^2 s_{23}\, A_{4;1,1}^{\text{tree}}(1,2,3,4)\, \mathcal{I}_4^P(s_{12},s_{23})\,, \tag{C.10}$$

$$A_4^{NP}(1;2;3,4) \equiv s_{12}^2 s_{23}\, A_{4;1,1}^{\text{tree}}(1,2,3,4)\, \mathcal{I}_4^{NP}(s_{12},s_{23})\,, \tag{C.11}$$

and where $\mathcal{I}_4^P$ and $\mathcal{I}_4^{NP}$ are the planar and non-planar double box integral, respectively, see figure 9.

We remark that the expression for the double trace terms $A_{4;1,3}^{2-\text{loop}}$ can be obtained from the single trace terms using identities derived from group theory [80, 81].

The tree-level amplitude we need has external scalars only. It is given by

$$A_{4;1,1}^{\text{tree}}(\phi_{12}(1),\phi_{12}(2),\phi_{34}(3),\phi_{34}(4)) = -i\,\frac{s_{12}}{s_{23}}\,. \tag{C.12}$$

References

[1] W.L. van Neerven, *Infrared behavior of on-shell form-factors in a $N = 4$ supersymmetric Yang-mills field theory*, *Z. Phys.* **C 30** (1986) 595.

[2] A. Brandhuber, B. Spence, G. Travaglini and G. Yang, *Form factors in mathcal $N = 4$ super Yang-Mills and periodic Wilson loops*, *JHEP* **01** (2011) 134 [arXiv:1011.1899] [INSPIRE].

[3] A. Brandhuber, Ö. Gürdoğan, R. Mooney, G. Travaglini and G. Yang, *Harmony of super form factors*, *JHEP* **10** (2011) 046 [arXiv:1107.5067] [INSPIRE].

[4] L.V. Bork, D.I. Kazakov and G.S. Vartanov, *On form factors in $N = 4$ SYM*, *JHEP* **02** (2011) 063 [arXiv:1011.2440] [INSPIRE].

[5] L.V. Bork, D.I. Kazakov and G.S. Vartanov, *On MHV form factors in superspace for $N = 4$ SYM theory*, *JHEP* **10** (2011) 133 [arXiv:1107.5551] [INSPIRE].

[6] L.F. Alday and J. Maldacena, *Comments on gluon scattering amplitudes via AdS/CFT*, *JHEP* **11** (2007) 068 [arXiv:0710.1060] [INSPIRE].

[7] J. Maldacena and A. Zhiboedov, *Form factors at strong coupling via a Y-system*, *JHEP* **11** (2010) 104 [arXiv:1009.1139] [INSPIRE].

[8] Z. Bern, L.J. Dixon and V.A. Smirnov, *Iteration of planar amplitudes in maximally supersymmetric Yang-Mills theory at three loops and beyond*, *Phys. Rev.* **D 72** (2005) 085001 [hep-th/0505205] [INSPIRE].

[9] C. Anastasiou, L. Dixon, Z. Bern and D.A. Kosower, *Planar Amplitudes in Maximally Supersymmetric Yang-Mills Theory*, *Phys. Rev. Lett.* **91** (2003) 251602 [hep-th/0309040] [INSPIRE].

[10] J.M. Drummond, J. Henn, G.P. Korchemsky and E. Sokatchev, *On planar gluon amplitudes/Wilson loops duality*, *Nucl. Phys* **B 795** (2008) 52 [arXiv:0709.2368] [INSPIRE].

[11] J.M. Drummond, J. Henn, G.P. Korchemsky and E. Sokatchev, *Conformal Ward identities for Wilson loops and a test of the duality with gluon amplitudes*, *Nucl. Phys.* **B 826** (2010) 337 [arXiv:0712.1223] [INSPIRE].

[12] J.M. Henn, S. Moch and S.G. Naculich, *Form factors and scattering amplitudes in $N = 4$ SYM in dimensional and massive regularizations*, *JHEP* **12** (2011) 024 [arXiv:1109.5057] [INSPIRE].

JHEP03(2012)101

[13] Z. Bern, M. Czakon, L.J. Dixon, D.A. Kosower and V.A. Smirnov, *Four-loop planar amplitude and cusp anomalous dimension in maximally supersymmetric Yang-Mills theory*, *Phys. Rev.* **D 75** (2007) 085010 [hep-th/0610248] [INSPIRE].

[14] F. Cachazo, M. Spradlin and A. Volovich, *Four-loop cusp anomalous dimension from obstructions*, *Phys. Rev.* **D 75** (2007) 105011 [hep-th/0612309] [INSPIRE].

[15] J.M. Henn, S.G. Naculich, H.J. Schnitzer and M. Spradlin, *More loops and legs in Higgs-regulated $N = 4$ SYM amplitudes*, *JHEP* **08** (2010) 002 [arXiv:1004.5381] [INSPIRE].

[16] N. Arkani-Hamed, J.L. Bourjaily, F. Cachazo and J. Trnka, *Local integrals for planar scattering amplitudes*, arXiv:1012.6032 [INSPIRE].

[17] J.M. Drummond and J.M. Henn, *Simple loop integrals and amplitudes in $N = 4$ SYM*, *JHEP* **05** (2011) 105 [arXiv:1008.2965] [INSPIRE].

[18] J.M. Drummond, J.M. Henn and J. Trnka, *New differential equations for on-shell loop integrals*, *JHEP* **04** (2011) 083 [arXiv:1010.3679] [INSPIRE].

[19] L.J. Dixon, private communication.

[20] J.B. Tausk, *Non-planar massless two-loop Feynman diagram with four on-shell legs*, *Phys. Lett.* **B 469** (1999) 225 [hep-ph/9909506] [INSPIRE].

[21] S.G. Naculich, H. Nastase and H.J. Schnitzer, *Subleading-color contributions to gluon-gluon scattering in $N = 4$ SYM theory and relations to $N = 8$ supergravity*, *JHEP* **11** (2008) 018 [arXiv:0809.0376] [INSPIRE].

[22] S.G. Naculich, H. Nastase and H.J. Schnitzer, *Two-loop graviton scattering relation and IR behavior in $N = 8$ supergravity*, *Nucl. Phys.* **B 805** (2008) 40 [arXiv:0805.2347] [INSPIRE].

[23] A. Brandhuber, P. Heslop, A. Nasti, B. Spence and G. Travaglini, *Four-point amplitudes in $N = 8$ supergravity and Wilson loops*, *Nucl. Phys.* **B 807** (2009) 290 [arXiv:0805.2763] [INSPIRE].

[24] T. Gehrmann, G. Heinrich, T. Huber and C. Studerus, *Master integrals for massless three-loop form factors: One-loop and two-loop insertions*, *Phys. Lett.* **B 640** (2006) 252 [hep-ph/0607185] [INSPIRE].

[25] G. Heinrich, T. Huber and D. Maître, *Master integrals for fermionic contributions to massless three-loop form factors*, *Phys. Lett.* **B 662** (2008) 344 [arXiv:0711.3590] [INSPIRE].

[26] G. Heinrich, T. Huber, D.A. Kosower and V.A. Smirnov, *Nine-propagator master integrals for massless three-loop form factors*, *Phys. Lett.* **B 678** (2009) 359 [arXiv:0902.3512] [INSPIRE].

[27] P.A. Baikov, K.G. Chetyrkin, A.V. Smirnov, V.A. Smirnov and M. Steinhauser, *Quark and Gluon Form Factors to Three Loops*, *Phys. Rev. Lett.* **102** (2009) 212002 [arXiv:0902.3519] [INSPIRE].

[28] R.N. Lee, A.V. Smirnov and V.A. Smirnov, *Analytic results for massless three-loop form factors*, *JHEP* **04** (2010) 020 [arXiv:1001.2887] [INSPIRE].

[29] T. Huber, *Master integrals for massless three-loop form factors*, PoS(RADCOR2009)038 [arXiv:1001.3132] [INSPIRE].

JHEP03(2012)101

[30] T. Gehrmann, E.W.N. Glover, T. Huber, N. Ikizlerli and C. Studerus, *Calculation of the quark and gluon form factors to three loops in QCD*, *JHEP* **06** (2010) 094 [arXiv:1004.3653] [INSPIRE].

[31] R.N. Lee, A.V. Smirnov and V.A. Smirnov, *Dimensional recurrence relations: an easy way to evaluate higher orders of expansion in ϵ*, *Nucl. Phys. Proc. Suppl.* **205** (2010) 308 [arXiv:1005.0362] [INSPIRE].

[32] R.N. Lee and V.A. Smirnov, *Analytic ϵ-expansion of three-loop on-shell master integrals up to four-loop transcendentality weight*, *JHEP* **02** (2011) 102 [arXiv:1010.1334] [INSPIRE].

[33] T. Gehrmann, E.W.N. Glover, T. Huber, N. Ikizlerli and C. Studerus, *The quark and gluon form factors to three loops in QCD through to $\mathcal{O}(\epsilon^2)$*, *JHEP* **11** (2010) 102 [arXiv:1010.4478] [INSPIRE].

[34] J.M. Drummond, J. Henn, V.A. Smirnov and E. Sokatchev, *Magic identities for conformal four-point integrals*, *JHEP* **01** (2007) 064 [hep-th/0607160] [INSPIRE].

[35] N.I. Ussyukina and A.I. Davydychev, *Two-loop three-point diagrams with irreducible numerators*, *Phys. Lett.* **B 348** (1995) 503 [hep-ph/9412356] [INSPIRE].

[36] Z. Bern, J.J. Carrasco, L.J. Dixon, H. Johansson, D.A. Kosower and R. Roiban, *Cancellations Beyond Finiteness in $N = 8$ Supergravity at Three Loops*, *Phys. Rev. Lett.* **98** (2007) 161303 [hep-th/0702112] [INSPIRE].

[37] K. Stelle, *Supergravity: Finite after all?*, *Nature Phys.* **3** (2007) 448.

[38] Z. Bern, J.J.M. Carrasco, L.J. Dixon, H. Johansson and R. Roiban, *Ultraviolet Behavior of $N = 8$ Supergravity at Four Loops*, *Phys. Rev. Lett.* **103** (2009) 081301 [arXiv:0905.2326] [INSPIRE].

[39] M.R. Douglas, *On $D = 5$ super Yang-Mills theory and $(2, 0)$ theory*, *JHEP* **02** (2011) 011 [arXiv:1012.2880] [INSPIRE].

[40] A.S. Galperin, E.A. Ivanov, V.I. Ogievetsky and E.S. Sokatchev, *Harmonic superspace*, Cambridge University Press, Cambridge U.K. (2001), pg. 306.

[41] T. van Ritbergen, J.A.M. Vermaseren and S.A. Larin, *The four-loop β-function in quantum chromodynamics*, *Phys. Lett.* **B 400** (1997) 379 [hep-ph/9701390] [INSPIRE].

[42] T. Becher and M. Neubert, *On the structure of infrared singularities of gauge-theory amplitudes*, *JHEP* **06** (2009) 081 [arXiv:0903.1126] [INSPIRE].

[43] J. Blümlein, D.J. Broadhurst and J.A.M. Vermaseren, *The Multiple Zeta Value data mine*, *Comput. Phys. Commun.* **181** (2010) 582 [arXiv:0907.2557] [INSPIRE].

[44] F.V. Tkachov, *A theorem on analytical calculability of 4-loop renormalization group functions*, *Phys. Lett.* **B 100** (1981) 65.

[45] K.G. Chetyrkin and F.V. Tkachov, *Integration by parts: The algorithm to calculate β-functions in 4 loops*, *Nucl. Phys.* **B 192** (1981) 159.

[46] S. Laporta, *High-Precision Calculation of Multiloop Feynman Integrals by Difference Equations*, *Int. J. Mod. Phys.* **A 15** (2000) 5087 [hep-ph/0102033] [INSPIRE].

[47] C. Studerus, *Reduze-Feynman integral reduction in C++*, *Comput. Phys. Commun.* **181** (2010) 1293 [arXiv:0912.2546] [INSPIRE].

JHEP03(2012)101

[48] Z. Bern, L. Dixon, D.C. Dunbar and D.A. Kosower, *One-loop n-point gauge theory amplitudes, unitarity and collinear limits*, *Nucl. Phys.* **B 425** (1994) 217 [hep-ph/9403226] [INSPIRE].

[49] R. Britto, F. Cachazo and B. Feng, *Generalized unitarity and one-loop amplitudes in $N = 4$ super-Yang-Mills*, *Nucl. Phys.* **B 725** (2005) 275 [hep-th/0412103] [INSPIRE].

[50] J.J.M. Carrasco and H. Johansson, *Generic multiloop methods and application to $N = 4$ super-Yang-Mills*, *J. Phys.* **A 44** (2011) 4004 [arXiv:1103.3298] [INSPIRE].

[51] V.P. Nair, *A current algebra for some gauge theory amplitudes*, *Phys. Lett.* **B 214** (1988) 215.

[52] J.M. Drummond, J. Henn, G.P. Korchemsky and E. Sokatchev, *Generalized unitarity for $N = 4$ super-amplitudes*, arXiv:0808.0491 [INSPIRE].

[53] Z. Bern, J.J.M. Carrasco, H. Ita, H. Johansson and R. Roiban, *Structure of supersymmetric sums in multiloop unitarity cuts*, *Phys. Rev.* **D 80** (2009) 065029 [arXiv:0903.5348] [INSPIRE].

[54] H. Elvang, D.Z. Freedman and M. Kiermaier, *Recursion relations, generating functions and unitarity sums in Script $N = 4$ SYM theory*, *JHEP* **04** (2009) 009 [arXiv:0808.1720] [INSPIRE].

[55] M. Bianchi, H. Elvang and D.Z. Freedman, *Generating tree amplitudes in $N = 4$ SYM and $N = 8$ SG*, *JHEP* **09** (2008) 063 [arXiv:0805.0757] [INSPIRE].

[56] Z. Bern, J.S. Rozowsky and B. Yan, *Two-loop four-gluon amplitudes in $N = 4$ super-Yang-Mills*, *Phys. Lett.* **B 401** (1997) 273 [hep-ph/9702424] [INSPIRE].

[57] A.V. Kotikov and L.N. Lipatov, *DGLAP and BFKL evolution equations in the $N = 4$ supersymmetric gauge theory*, hep-ph/0112346 [INSPIRE].

[58] A.V. Kotikov, L.N. Lipatov, A.I. Onishchenko and V.N. Velizhanin, *Three-loop universal anomalous dimension of the Wilson operators in $N = 4$ SUSY Yang-Mills model*, *Phys. Lett.* **B 595** (2004) 521 [hep-th/0404092] [INSPIRE].

[59] A.V. Kotikov and L.N. Lipatov, *On the highest transcendentality in $N = 4$ SUSY*, *Nucl. Phys.* **B 769** (2007) 217 [hep-th/0611204] [INSPIRE].

[60] Z. Kunszt, A. Signer and Z. Trócsányi, *One-loop helicity amplitudes for all $2 \to 2$ processes in QCD and $N = 1$ supersymmetric Yang-Mills theory*, *Nucl. Phys.* **B 411** (1994) 397 [hep-ph/9305239] [INSPIRE].

[61] L. Magnea and G.F. Sterman, *Analytic continuation of the Sudakov form-factor in QCD*, *Phys. Rev.* **D 42** (1990) 4222.

[62] I.A. Korchemskaya and G.P. Korchemsky, *On lightlike Wilson loops*, *Phys. Lett.* **B 287** (1992) 169 [INSPIRE].

[63] M.T. Grisaru and W. Siegel, *Supergraphity. 2. Manifestly covariant rules and higher loop finiteness*, *Nucl. Phys.* **B 201** (1982) 292.

[64] N. Marcus and A. Sagnotti, *The ultraviolet behavior of $N = 4$ Yang-mills and the power counting of extended superspace*, *Nucl. Phys.* **B 256** (1985) 77.

[65] P.S. Howe and K.S. Stelle, *The ultraviolet properties of supersymmetric field theories*, *Int. J. Mod. Phys.* **A 4** (1989) 1871.

JHEP03(2012)101

[66] G. Bossard, P.S. Howe and K.S. Stelle, *The ultra-violet question in maximally supersymmetric field theories*, *Gen. Rel. Grav.* **41** (2009) 919 [arXiv:0901.4661] [INSPIRE].

[67] Z. Bern, J.J.M. Carrasco, L.J. Dixon, H. Johansson and R. Roiban, *Complete four-loop four-point amplitude in $N = 4$ super-Yang-Mills theory*, *Phys. Rev.* **D 82** (2010) 125040 [arXiv:1008.3327] [INSPIRE].

[68] T. Huber, *On a two-loop crossed six-line master integral with two massive lines*, *JHEP* **03** (2009) 024 [arXiv:0901.2133] [INSPIRE].

[69] N. Arkani-Hamed, J. Bourjaily, F. Cachazo, S. Caron-Huot and J. Trnka, *The all-loop integrand for scattering amplitudes in planar $N = 4$ SYM*, *JHEP* **01** (2011) 041 [arXiv:1008.2958] [INSPIRE].

[70] T. Gehrmann and E. Remiddi, *Two-loop master integrals for $\gamma^* \to 3$ jets: the planar topologies*, *Nucl. Phys.* **B 601** (2001) 248 [hep-ph/0008287] [INSPIRE].

[71] T. Gehrmann and E. Remiddi, *Two-loop master integrals for $\gamma^* \to 3$ jets: the non-planar topologies*, *Nucl. Phys.* **B 601** (2001) 287 [hep-ph/0101124] [INSPIRE].

[72] L.W. Garland, T. Gehrmann, E.W.N. Glover, A. Koukoutsakis and E. Remiddi, *The two-loop QCD matrix element for $e^+e^- \to 3$ jets*, *Nucl. Phys.* **B 627** (2002) 107 [hep-ph/0112081] [INSPIRE].

[73] L.W. Garland, T. Gehrmann, E.W.N. Glover, A. Koukoutsakis and E. Remiddi, *Two-loop QCD helicity amplitudes for $e^+e^- \to 3$ jets*, *Nucl. Phys.* **B 642** (2002) 227 [hep-ph/0206067] [INSPIRE].

[74] T. Gehrmann, M. Jaquier, E.W.N. Glover and A. Koukoutsakis, *Two-loop QCD corrections to the helicity amplitudes for $H \to 3$ partons*, *JHEP* **02** (2012) 056 [arXiv:1112.3554] [INSPIRE].

[75] J.A.M. Vermaseren, *Axodraw*, *Comput. Phys. Commun.* **83** (1994) 45.

[76] T. Gehrmann, T. Huber and D. Maître, *Two-loop quark and gluon form factors in dimensional regularisation*, *Phys. Lett.* **B 622** (2005) 295 [hep-ph/0507061] [INSPIRE].

[77] A.V. Smirnov and M.N. Tentyukov, *Feynman Integral Evaluation by a Sector decomposiTion Approach (FIESTA)*, *Comput. Phys. Commun.* **180** (2009) 735 [arXiv:0807.4129] [INSPIRE].

[78] A.V. Smirnov, V.A. Smirnov and M. Tentyukov, *FIESTA 2: Parallelizeable multiloop numerical calculations*, *Comput. Phys. Commun.* **182** (2011) 790 [arXiv:0912.0158] [INSPIRE].

[79] Z. Bern and D.A. Kosower, *Color decomposition of one loop amplitudes in gauge theories*, *Nucl. Phys.* **B 362** (1991) 389.

[80] Z. Bern, A. DeFreitas and L. Dixon, *two-loop helicity amplitudes for gluon-gluon scattering in QCD and supersymmetric Yang-Mills theory*, *JHEP* **03** (2002) 018 [hep-ph/0201161] [INSPIRE].

[81] S.G. Naculich, *All-loop group-theory constraints for color-ordered* SU(N) *gauge-theory amplitudes*, *Phys. Lett.* **B 707** (2012) 191 [arXiv:1110.1859] [INSPIRE].

JHEP03(2012)101

Published for SISSA by Springer

Received: *August 6, 2012*
Accepted: *October 10, 2012*
Published: *November 12, 2012*

Systematics of the cusp anomalous dimension

Johannes M. Henn[a] **and Tobias Huber**[b]

[a] *Institute for Advanced Study, Princeton, NJ 08540, U.S.A.*

[b] *Theoretische Physik 1, Naturwissenschaftlich-Technische Fakultät, Universität Siegen, Walter-Flex-Strasse 3, D-57068 Siegen, Germany*

E-mail: jmhenn@ias.edu, huber@tp1.physik.uni-siegen.de

Abstract: We study the velocity-dependent cusp anomalous dimension in supersymmetric Yang-Mills theory. In a paper by Correa, Maldacena, Sever, and one of the present authors, a scaling limit was identified in which the ladder diagrams are dominant and are mapped onto a Schrödinger problem. We show how to solve the latter in perturbation theory and provide an algorithm to compute the solution at any loop order. The answer is written in terms of harmonic polylogarithms. Moreover, we give evidence for two curious properties of the result. Firstly, we observe that the result can be written using a subset of harmonic polylogarithms only, at least up to six loops. Secondly, we show that in a light-like limit, only single zeta values appear in the asymptotic expansion, again up to six loops. We then extend the analysis of the scaling limit to systematically include subleading terms. This leads to a Schrödinger-type equation, but with an inhomogeneous term. We show how its solution can be computed in perturbation theory, in a way similar to the leading order case. Finally, we analyze the strong coupling limit of these subleading contributions and compare them to the string theory answer. We find agreement between the two calculations.

Keywords: Supersymmetric gauge theory, Scattering Amplitudes, Strong Coupling Expansion

ArXiv ePrint: 1207.2161

© SISSA 2012

doi:10.1007/JHEP11(2012)058

JHEP11(2012)058

Contents

1 Introduction **1**

2 General structure of the Bethe-Salpeter equations at LO and NLO **4**

3 Solution to the scaling limit at leading order **6**
- 3.1 Setup 6
- 3.2 Iterative solution 7
- 3.3 Structure of the perturbative result 8
- 3.4 Rewriting the expressions for Ω_0 in terms of HPLs 9
- 3.5 Explicit new results, and further surprises 11
- 3.6 Simplifications in the $x \to 0$ limit 13

4 NLO terms in large ξ limit **14**
- 4.1 Triangle-ladder diagrams (b) 14
- 4.2 H-exchange diagrams (c) 17

5 Strong coupling limit at LO and NLO **18**
- 5.1 Strong coupling limit of Bethe-Salpeter equation 19
- 5.2 Scaling limit of the string theory result 20

6 Discussion and conclusion **20**

A Differential equations for two-loop integral h **22**

B Details of the strong coupling calculation **23**

C Relation between integrals for four-particle scattering amplitude and cusp anomalous dimension **24**

D The six-loop function $\Omega_0^{(6)}$ **25**

1 Introduction

The cusp anomalous dimension $\Gamma_{\text{cusp}}(\phi)$ was originally introduced in [1] as the ultraviolet (UV) divergence of a Wilson loop with a cusp with Euclidean angle ϕ. It describes a wide range of interesting physical situations. It was computed in QCD to the two-loop order in ref. [2] and rederived and simplified in ref. [3].

JHEP11(2012)058

In supersymmetric Yang-Mills theories such as $\mathcal{N} = 4$ super Yang-Mills, one can define a Wilson loop operator that couples to scalars in addition to the gauge field [4, 5]. It is natural to consider a loop where the coupling to the scalars is different on the two segments of the cusp (but constant along each segment). The jump in the internal coupling to the scalars is characterized by an angle θ. The perturbative calculation of this supersymmetric cusp anomalous dimension $\Gamma_{\text{cusp}}(\phi, \theta)$ is similar to the QCD case. It has been performed to two loops in refs. [6, 7]. At strong coupling, it is known to second order in the strong coupling expansion [7].

Recently, there has been a lot of progress in understanding $\Gamma_{\text{cusp}}(\phi, \theta)$, in various domains.

In a small angle limit, an exact result was found in [8], based on localization techniques. The exact formula is in perfect agreement with perturbative results and the result at strong coupling. The same exact formula has also been obtained in [9].

In ref. [10], a relation of the cusp anomalous dimension to the Regge limit of massive scattering amplitudes was exploited to compute its three-loop value. The relation to scattering amplitudes [11], which is valid in the planar limit, implies in particular that the integrand needed to compute the cusp anomalous dimension can be deduced from the (in principle known) integrand for planar four-particle scattering amplitudes [12–14], when appropriately extended to the massive case [11, 15].

Very recently, Thermodynamic Bethe Ansatz (TBA) equations have been derived for the cusp anomalous dimensions [16, 17], and passed highly non-trivial consistency checks at the three-loop level [16].

In [10] a new scaling limit involving the complexified angle θ was introduced,

$$i\theta \gg 1, \qquad \lambda \ll 1\,, \qquad \text{with} \qquad \hat{\lambda} = \lambda e^{i\theta}/4 \quad \text{finite}\,. \tag{1.1}$$

Here $\lambda = g^2 N$ is the 't Hooft coupling. In this limit, the coupling of the loop to the scalars becomes dominant, and the leading order (LO) contribution is given by simple ladder diagrams, where the rungs of the ladder are scalar exchanges. It is important to realize that this is a gauge-invariant statement. The ladder diagrams can be described conveniently using Bethe-Salpeter equations. The latter are very convenient, since they provide a simple description. They can be solved exactly in the small angle limit, and it is easy to extract their strong coupling behaviour, finding agreement with the corresponding string theory calculation.

In this paper, we continue the analysis of the scaling limit of [10] and initiate a systematic study of the subleading contributions. A first question that one faces when computing $\Gamma_{\text{cusp}}(\phi, \theta)$ in perturbation theory is what functions the result can be expressed in. It is easy to see that the θ dependence is very simple, and to describe the ϕ dependence the variable $x = e^{i\phi}$ is useful. Experience shows that in that variable one obtains certain polylogarithms, multiplied by rational prefactors. In general, it is not known what class of polylogarithms, or more generally what class of iterated integrals, is sufficient to describe a given problem.

Similar questions are of great current interest in the understanding of the structure of scattering amplitudes, a problem that is closely related. To phrase the question in

JHEP11(2012)058

that language, given a loop integral depending on n space-time points, what is the set of functions describing it? On the one hand, one could argue that with increasing loop order, integrals with some number of external points "know about" lower-loop integrals with more external points that they contain as subdiagrams (which may e.g. contain elliptic integrals), making them very complicated, and perhaps requiring a larger functional basis at higher loops. On the other hand, one might argue that the set of functions should ultimately be determined by the external kinematics of the problem. An argument in favour of this point of view is that integrals are determined to a great part by their singularities, and the location of the latter is intimately tied to the external data. These questions are also of enormous practical importance, as they sometimes allow to make an ansatz for a given problem within a restricted class of functions, see [18–20] for recent examples.

In the present case of a single scale problem, it was observed in [10] that all functions occurring to the three-loop order could be expressed in terms of harmonic polylogarithms, i.e. in terms of iterated integrals with integration kernels $1/x, 1/(1+x), 1/(1-x)$. The fact that this was possible not only for the final answer, but also for individual loop integrals, and in fact also for all integrals of this type found in the literature, seems to suggest that this is a more general feature. Can this be proven rigorously? In this paper, we make a first step into this direction. We show that this property holds for the LO term of Γ_{cusp} in the scaling limit (1.1), and for one of the two contributions at NLO, at any loop order.

We also present an algorithm that determines Γ_{cusp} at LO in the scaling limit at any loop order in terms of harmonic polylogarithms. As an application, we verified the result of [10] at three loops, and evaluated the four-, five-, and six-loop results, which are new.

These results suggest two further properties. First, we find that at least up to six loops, one can express the result in terms of harmonic polylogarithms (HPLs) [21] of argument x^2 and indices $0, 1$ only. Second, in the $x \to 0$ limit we find that, again up to six loops, single zeta values and products thereof are sufficient to describe the coefficients of the asymptotic expansion.

We then discuss NLO terms in the scaling limit. We show that there are two classes of diagrams that satisfy a slightly modified Bethe-Salpeter equation. For one of the two classes of integrals, we show how to construct the solution in terms of HPLs at any loop order. For the second class of integrals, we compute the non-trivial integration kernel, which allows to express the result in terms of iterated integrals having the correct degree. We leave the question of whether the latter can be expressed in terms of HPLs to future work.

We also discuss the strong coupling limit of the Bethe-Salpeter equations, and compute the scaling limit of the corresponding string theory result. Under certain assumptions, we find perfect agreement between the two calculations.

This paper is organized as follows. We begin by reviewing the definition of the cusp anomalous dimension and the scaling limit in section 2. Then, in section 3, we present the perturbative solution at leading order in the scaling limit to any loop order. We prove that the result can be written in terms of HPLs, and make further observations about their structure. In section 4, we discuss the NLO Bethe-Salpeter equations. In section 5, we take the strong coupling limit of the equations, and compare them to the corresponding string theory calculation. There are several appendices containing technical details.

JHEP11(2012)058

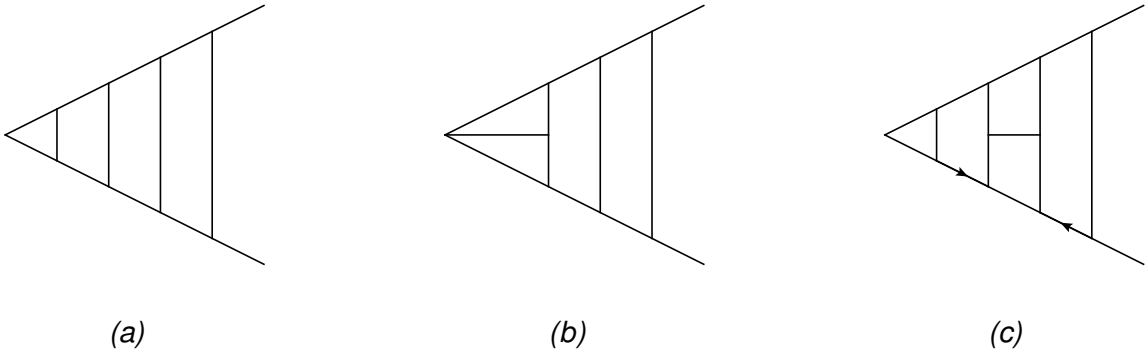

Figure 1. Classes of loop integrals contribution to LO (diagram (a)) and NLO (diagram (b) and (c)) in the scaling limit (1.1). Each class can have an arbitrary number of rungs. The arrows in (c) denote a numerator factor $(p+q)^2$, where p^μ and q^μ are the momenta along the arrows.

2 General structure of the Bethe-Salpeter equations at LO and NLO

Here we discuss the general structure of the Bethe-Salpeter equations at leading order (LO) and next-to-leading order (NLO) in the scaling limit. The LO equations were already discussed in [10]. They are a natural generalization of the equations for the quark-antiquark potential [22]. Here we briefly review the main points.

We recall the definition of the locally supersymmetric Wilson loop operator in $\mathcal{N}=4$ super Yang-Mills,

$$W \sim \mathrm{Tr}[Pe^{i\oint A\cdot dx+\oint |dx|\vec{n}\cdot\vec{\Phi}}]\,, \tag{2.1}$$

where $\vec{n}$ is a point on S^5. The contour we consider consists of two (infinite) segments forming a cusp of Euclidean angle ϕ. We take the coupling to the scalars to be constant along each segment, but with a jump of angle θ at the cusp, i.e. $\cos\theta = \vec{n}\cdot\vec{n}'$, where $\vec{n}$ and $\vec{n}'$ are the directions of the two segments. Such a cusped Wilson loop in general has a logarithmic divergence that takes the form

$$\langle W\rangle \sim e^{-\Gamma_{\rm cusp}(\phi,\theta)\log\frac{\Lambda_{\rm UV}}{\Lambda_{\rm IR}}}\,, \tag{2.2}$$

where $\Lambda_{\rm IR/UV}$ are infrared and ultraviolet cutoffs, respectively. This defines the cusp anomalous dimension $\Gamma_{\rm cusp}(\phi,\theta)$.[1]

In the scaling limit (1.1), the scalar coupling of the loop becomes dominant. At leading order (LO) in the limit, the segments of the Wilson loop couple to conjugate scalars, and we need to consider scalar exchange diagrams only. At next-to-leading order (NLO), we have mostly scalar exchanges, plus one-loop interaction diagrams.

An analysis of the integrals contributing to the cusp anomalous dimension allows one to see that the effective diagrams shown in figure 1 are needed at LO and NLO in the scaling limit. Since only one-loop internal graphs are allowed at NLO order, one can deduce the all-loop structure of these corrections already from the known three-loop expression. The fact that one has effective diagrams that arise after cancellations between

[1] Of course, $\Gamma_{\rm cusp}$ is also a function of the 't Hooft coupling g^2N, and the number of colours N.

JHEP11(2012)058

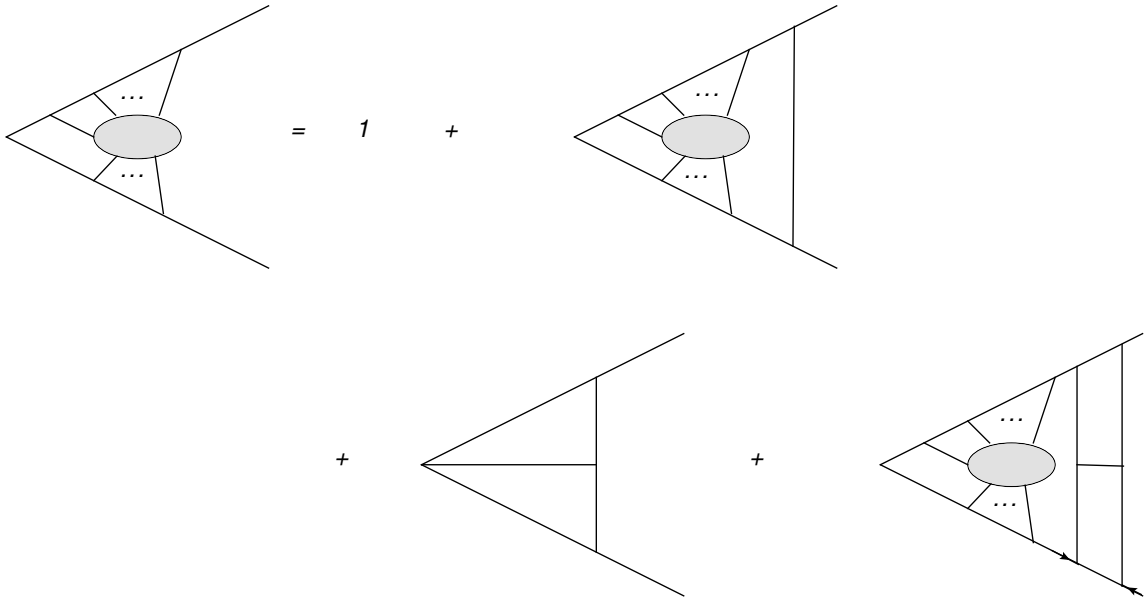

Figure 2. Bethe-Salpeter equation at LO and NLO. The arrows denote a numerator factor $(p+q)^2$, with p^μ, q^μ being the momenta flowing along the arrows (in momentum space).

various gauge-dependent Feynman diagrams[2] is intimately related to the similar diagrams appearing in scattering amplitudes. We illustrate this relation at the level of the loop integrals/integrands in appendix C.

It is easy to see that the integrals of figure 1 are described by a Bethe-Salpeter equation. The latter is shown (schematically) in figure 2. This equation sums the diagrams to all orders in the coupling. At LO in the scaling limit, only the first line contributes, as the second lines gives contributions of order $\alpha = \lambda/\hat{\lambda}$ and higher. At NLO, we keep the terms in the second line and compute the answer linear in α. Note that there are also higher-order terms in α contained in this equation that will only become relevant once we include all NNLO and higher terms.

We can see that there are two new features w.r.t. LO. First, the first term of the second line of figure 2 is the starting point for the new infinite class of diagrams shown in figure 1(b). These terms are absent in the quark-antiquark potential [23]. Second, there is a new interaction term that is a higher-loop generalization of the simple scalar exchange at LO.

Let us illustrate the usefulness of the Bethe-Salpether equation by reviewing the LO case. We denote the sum of the ladder diagrams by $F(s,t)$, where $-sp^\mu$ and tq^μ are positions on the cusp formed by the momenta p^μ and q^μ. Let us normalize $p^2 = q^2 = 1$ for convenience. Note that F also depends on the angle ϕ defined by $\cos\phi = p \cdot q$. Then F satisfies the Bethe-Salpeter equation

$$F(S,T) = 1 + \int_0^S ds \int_0^T dt\, F(s,t)\, P(s,t)\,, \tag{2.3}$$

[2]In ref. [23], this one-loop calculation was explicitly performed (for the quark-antiquark potential, corresponding to $\phi \to \pi$), in agreement with the result here. Integral class (b) discussed here follows from a boundary term at the cusp that is absent for the quark-antiquark potential.

JHEP11(2012)058

where

$$P(s,t) = \frac{\hat{\lambda}}{4\pi^2} \frac{1}{s^2 + t^2 + 2st\cos\phi} \tag{2.4}$$

is the propagator corresponding to a scalar exchange. Changing variables according to $s = e^{\sigma}, t = e^{\tau}$, this becomes

$$F(\sigma,\tau) = 1 + \int_{-\infty}^{\sigma} d\sigma_1 \int_{-\infty}^{\tau} d\tau_1\, F(\sigma_1,\tau_1)\, P(\sigma_1,\tau_1)\,, \tag{2.5}$$

where

$$P(\tau,\sigma) = \frac{\hat{\lambda}}{8\pi^2} \frac{1}{\cosh(\tau-\sigma) + \cos\phi}\,. \tag{2.6}$$

Differentiating eq. (2.5), we obtain,

$$\partial_\tau \partial_\sigma F(\sigma,\tau) = F(\sigma,\tau) P(\sigma,\tau)\,. \tag{2.7}$$

Let us change variables $y_1 = \tau - \sigma$ and $y_2 = (\tau+\sigma)/2$. We can extract Γ_{cusp} from the large y_2 behaviour of F, due to the equivalence of IR and UV divergences, see eq. (2.2).

For large y_2, we can make an ansatz

$$F = \sum_n e^{-\Omega_n y_2} \Psi_n(y_1)\,. \tag{2.8}$$

We are interested in the leading term, corresponding to the lowest eigen-energy Ω_0. Using the ansatz (2.8), one finds [10]

$$\left[-\partial_{y_1}^2 - \frac{\hat{\lambda}}{8\pi^2} \frac{1}{(\cosh y_1 + \cos\phi)} + \frac{\Omega^2(\phi)}{4} \right] \Psi(y_1,\phi) = 0\,. \tag{2.9}$$

This is a one-dimensional Schrödinger problem. The ground state energy Ω_0 is related to the cusp anomalous dimension in the scaling limit through $\Gamma_{\text{cusp}} = -\Omega_0$.

In summary, the Bethe-Salpeter equation has allowed us to conveniently sum an infinite class of diagrams. As a result, extracting the remaining overall logarithmic divergence could be done in a simple way, and the remaining calculation does not require any regulator. Moreover, the structure of the equation allowed us to rewrite the problem in terms of a linear differential equation.

We will now solve this equation in perturbation theory. In section 4, we will discuss the effects of the two new features that appear at NLO.

3 Solution to the scaling limit at leading order

3.1 Setup

To obtain the perturbative solution of (2.9), we follow [10] and perform the change of variables

$$\Psi(y_1) = \eta(y_1) e^{-\Omega_0 y_1/2} \tag{3.1}$$

JHEP11(2012)058

The exponential factor gives the correct solution as $y_1 \to \infty$, and we can normalize $\eta(y_1 = \infty) = 1$. We can determine Ω_0 from η thanks to the boundary condition

$$\partial_{y_1} \Psi(y_1)|_{y_1=0} = 0\,, \tag{3.2}$$

which follows from the $y_1 \to -y_1$ symmetry of the problem. Defining a new variable $w = e^{-y_1}$, and $x = e^{i\phi}$, the boundary condition (3.2) becomes

$$\Omega_0(x) = -2w\partial_w \log \eta(w,x)|_{w=1}\,, \tag{3.3}$$

and the Schrödinger equation (2.9) reads

$$\partial_w w \partial_w \eta = -\Omega_0(x)\partial_w \eta + \hat{\kappa}\left[\frac{1}{w+x^{-1}} - \frac{1}{w+x}\right]\eta\,, \qquad \hat{\kappa} = \frac{\hat{\lambda}\,x}{4\pi^2(1-x^2)} \tag{3.4}$$

The wavefunction η can be obtained by integrating the Schrödinger equation iteratively in the coupling, $\Omega_0 = \hat{\kappa}\Omega_0^{(1)} + \hat{\kappa}^2\Omega_0^{(2)} + \ldots$, and $\eta = 1 + \hat{\kappa}\eta^{(1)} + \ldots$. Let us now analyze in detail the perturbative solution for η and Ω.

3.2 Iterative solution

It is convenient to introduce an abbreviation for the nested integrals that one encounters in this problem. In analogy to two-dimensional harmonic polylogarithms (2dHPLs), we are going to use the self-explanatory notation

$$H_V(w,x) = \int_0^1 dw' \left[\frac{1}{w'+1/(wx)} - \frac{1}{w'+x/w}\right]\,, \tag{3.5}$$

and

$$H_{V,\vec{b}}(w,x) = \int_0^1 dw' \left[\frac{1}{w'+1/(wx)} - \frac{1}{w'+x/w}\right] H_{\vec{b}}(w'w,x)\,, \tag{3.6}$$

$$H_{0,\vec{b}}(w,x) = \int_0^1 \frac{dw'}{w'} H_{\vec{b}}(w'w,x)\,. \tag{3.7}$$

In the following we will sometimes drop the arguments (w,x) for brevity. So in general we will have $H_{\vec{b}}$, where the weight vector $\vec{b}$ has entries V and 0, with 0 not appearing in the last entry.

It is straightforward to write the perturbative answer for η in terms of these integrals. We find

$$\eta^{(1)} = H_{0,V} \tag{3.8}$$

$$\eta^{(2)} = H_{0,V,0,V} - H_{0,0,V}\Omega_0^{(1)}\,, \tag{3.9}$$

and so on. Using eq. (3.3) we find

$$\Omega_0^{(1)} = -2H_V\,, \tag{3.10}$$

$$\Omega_0^{(2)} = -2H_V H_{0,V} - 2H_{V,0,V}\,, \tag{3.11}$$

$$\begin{aligned}\Omega_0^{(3)} = &-2H_V H_{0,V}^2 - 4H_V^2 H_{0,0,V} - 2H_{0,V}H_{V,0,V} \\ &- 2H_V H_{0,V,0,V} - 4H_V H_{V,0,0,V} - 2H_{V,0,V,0,V}\,,\end{aligned} \tag{3.12}$$

JHEP11(2012)058

etc. These last relations are understood at $w = 1$.

In principle, eqs. (3.10), (3.11), (3.12), and their higher-order analogues, together with $\Gamma = -\Omega_0$, provide formulas for Γ. However, this representation is clearly not an optimal one. In the following, we will simplify it by converting it to a more appropriate and simpler class of iterated integrals. This will also allow us to make further observations regarding the structure of the result.

3.3 Structure of the perturbative result

Here, we first show certain properties of η and Ω_0, and then outline an algorithm for expressing Ω_0 in terms of harmonic polylogarithms.

As we show presently, the total differential of η at any loop order is of the form

$$\begin{aligned} d\eta^{(L)} &= f_1\, d\log x + f_2\, d\log(1+x) + f_3\, d\log(1-x) \\ &\quad + f_4\, d\log(w+x) + f_5\, d\log(w+1/x)\,, \end{aligned} \tag{3.13}$$

with the f_i being functions of the same type as $\eta^{(L)}$, but of degree (i.e. number of iterated integrals) lowered by one. From equations (3.13) and (3.3) it immediately follows that

$$d\Omega^{(L)} = g_1\, d\log x + g_2\, d\log(1+x) + g_3\, d\log(1-x)\,, \tag{3.14}$$

with g_i being functions of degree lowered by one, and satisfying the same property. This, implies that at any loop order L, $\Omega^{(L)}$ can be expressed in terms of harmonic polylogarithms (HPLs) of degree $(2L-1)$.

The latter are defined iteratively by

$$H_{a_1,a_2,\ldots,a_n}(x) = \int_0^x f_{a_1}(t) H_{a_2,\ldots,a_n}(t)\, dt\,, \tag{3.15}$$

where the integration kernels are

$$f_1(x) = \frac{1}{1-x}\,, \qquad f_0(x) = \frac{1}{x}\,, \qquad f_{-1}(x) = \frac{1}{1+x}\,. \tag{3.16}$$

The degree-one functions needed to start the recursion are defined as

$$H_1(x) = -\log(1-x)\,, \qquad H_0(x) = \log(x)\,, \qquad H_{-1}(x) = \log(1+x)\,. \tag{3.17}$$

The subscript of H is called the weight vector. A common abbreviation is to replace occurrences of m zeros to the left of ± 1 by $\pm(m+1)$. For example, $H_{0,0,1,0,-1}(x) = H_{3,-2}(x)$.

Note that a corollary of equations (3.13) and (3.14) is that the symbol [24, 25] of η is constructed from a five-letter alphabet consisting of $x, 1 \pm x, w + x, w + 1/x$. Similarly, the symbol of Ω_0 is constructed from the three-letter alphabet $x, 1 \pm x$. Of course, knowing the full differential provides us with much more information than just the symbol.

In order to prove the above statements, let us point out a relation of the $H_{\vec{b}}(w, x)$ to a known, albeit more general class of functions, the Goncharov polylogarithms [26],

$$G(a_1, \ldots a_n; z) = \int_0^z \frac{dt}{t - a_1} G(a_2, \ldots, a_n; t)\,, \tag{3.18}$$

JHEP11(2012)058

with

$$G(a_1;z) = \int_0^z \frac{dt}{t-a_1}\,. \tag{3.19}$$

In our case, the a_i are taken from $\{0,-x,-1/x\}$ and $z=w$. For example, we have

$$H_V(w,x) = G(-1/x;w) - G(-x;w)\,, \tag{3.20}$$

$$H_{0,V}(w,x) = G(0,-1/x;w) - G(0,-x;w)\,, \tag{3.21}$$

$$\begin{aligned} H_{V,0,V}(w,x) = {} & G(-1/x,0,-1/x;w) - G(-1/x,0,-x;w) \\ & + G(-x,0,-x;w) - G(-x,0,-1/x;w)\,, \end{aligned} \tag{3.22}$$

and so on. The total differential of a general Goncharov polylogarithm is

$$\begin{aligned} dG(a_1,\ldots a_n;z) = {} & G(\hat{a}_1,a_2,\ldots a_n;z)\,d\log\frac{z-a_1}{a_1-a_2} \\ & + G(a_1,\hat{a}_2,a_3,\ldots,a_n;z)\,d\log\frac{a_1-a_2}{a_2-a_3} + \ldots + \\ & + G(a_1,\ldots,a_{n-1},\hat{a}_n;z)\,d\log\frac{a_{n-1}-a_n}{a_n}\,, \end{aligned} \tag{3.23}$$

where $\hat{a}$ means that this element is omitted.

Given the possible values of the a_i in our case, it is straightforward to verify eq. (3.13).

3.4 Rewriting the expressions for Ω_0 in terms of HPLs

We have proven that Ω_0 can be written in terms of HPLs. Let us now explain how to find explicit results in terms of HPLs. We will begin by a simple example, and then outline an algorithm for doing so in general.

We observed that eq. (3.23), when applied to any function $H_{\vec{b}}(w=1,x)$ gives a result of the form (3.14). Iterating this procedure for the lower degree functions g_i in that equation, together with the fact that at any order we have a boundary condition at $w=1$, gives us the complete information for that function, in a form that makes contact with the definition of HPLs, see eq. (3.15).

As an example, let us write $H_{0,V}(1,x)$ in terms of HPLs. According to eq. (3.21), we need to rewrite $G(0,-x;1)$ and $G(0,-1/x;1)$ in terms of HPLs. Specializing (3.23) to the present case we have

$$\begin{aligned} d\,G(0,-x;1) &= -G(-x;1)\,d\log x \\ &= -\log((1+x)/x)\,d\log x \\ &= -\left[H_{-1}(x) - H_0(x)\right]\,d\log x\,. \end{aligned} \tag{3.24}$$

The integration can be done using the definition (3.15),

$$G(0,-x;1) = -H_{0,-1}(x) + H_{0,0}(x) + C\,. \tag{3.25}$$

It is convenient to relate C to the value at $x=1$,

$$G(0,-x;1) = -H_{0,-1}(x) + H_{0,0}(x) + \frac{1}{2}\zeta_2 + G(0,-1;1)\,, \tag{3.26}$$

where we used that $H_{0,-1}(1) = 1/2\zeta_2$.

JHEP11(2012)058

Similarly, we find

$$G(0,-1/x;1) = H_{0,-1}(x) - \tfrac{1}{2}\zeta_2 + G(0,-1;1)\,. \tag{3.27}$$

Combining eqs. (3.26) and (3.27) we find

$$H_{0,V}(1,x) = 2H_{0,-1}(x) - H_{0,0}(x) - \zeta_2\,. \tag{3.28}$$

By construction, $H_{0,V}(1,1) = 0$.

In summary, from this example it becomes clear how to rewrite any of the functions occurring in our problem in terms of HPLs, using the following steps:

1. Express the functions in terms of Goncharov polylogarithms
2. Use eq. (3.23) in order to compute their (total) differential; since all other variables are constants, this gives the derivative in x.
3. By iteration, that differential is of the form (3.14), with the g_i appearing there being HPLs. It can therefore be integrated in terms of HPLs, using (3.15).
4. Integrate the equation with the boundary term at $x = 1$.
5. Add up all terms; the boundary Goncharov polylogarithms at $x = 1$ do not necessarily drop out, but they are simple since they correspond to harmonic polylogarithms evaluated at $x = 1$.

Using this algorithm, we find e.g. the following expressions that are required to the three-loop order,

$$H_V(1,x) = H_0(x)\,, \tag{3.29}$$

$$H_{V,0,V}(1,x) = -4H_{-3}(x) - \zeta_2 H_0(x) + 2H_{-2,0}(x) - 4H_{2,0}(x) - H_{0,0,0}(x) - 2\zeta_3\,, \tag{3.30}$$

$$H_{0,0,0,V}(1,x) = -\frac{7\pi^4}{360} + 2H_{-4}(x) - \zeta_2 H_{0,0}(x) - H_{0,0,0,0}(x)\,, \tag{3.31}$$

$$\begin{aligned} H_{0,V,0,V}(1,x) = {} & \frac{19\pi^4}{360} - 14H_{-4}(x) - \pi^2 H_{-2}(x) + \frac{2}{3}\pi^2 H_2(x) + 8H_{-3,-1}(x) - 4H_{-3,0}(x) \\ & + 12H_{-2,-2}(x) + \frac{1}{6}\pi^2 H_{0,0}(x) - 8H_{2,-2}(x) - 6H_{-2,0,0}(x) \\ & + 4H_{2,0,0}(x) + H_{0,0,0,0}(x) + 2H_0(x)\zeta_3\,, \end{aligned} \tag{3.32}$$

$$\begin{aligned} H_{V,0,V,0,V}(1,x) = {} & 40H_{-5}(x) - \frac{2\pi^2}{3}H_{-3}(x) + \frac{19\pi^4}{360}H_0(x) + \frac{4\pi^2}{3}H_3(x) + 24H_{-4,-1}(x) \\ & - 38H_{-4,0}(x) - 16H_{-3,-2}(x) - 24H_{-2,-3}(x) - \pi^2 H_{-2,0}(x) + 32H_{2,-3}(x) \\ & + \frac{4\pi^2}{3}H_{2,0}(x) + 32H_{3,-2}(x) + 52H_{4,0}(x) + 8H_{-3,-1,0}(x) - 4H_{-3,0,0}(x) \\ & - 16H_{-3,1,0}(x) + 12H_{-2,-2,0}(x) - 24H_{-2,2,0}(x) + \frac{\pi^2}{6}H_{0,0,0}(x) \\ & - 16H_{2,-2,0}(x) + 32H_{2,2,0}(x) - 16H_{3,-1,0}(x) + 8H_{3,0,0}(x) + 32H_{3,1,0}(x) \\ & - 6H_{-2,0,0,0}(x) + 8H_{2,0,0,0}(x) + H_{0,0,0,0,0}(x) + \frac{\pi^2\zeta_3}{3} - 12\zeta_3 H_{-2}(x) \\ & + 16\zeta_3 H_2(x) + 2\zeta_3 H_{0,0}(x) + 6\zeta_5\,. \end{aligned} \tag{3.33}$$

JHEP11(2012)058

Plugging these formulas into eq. (3.12), we find perfect agreement with the three-loop result of ref. [10].

In the next section, we show explicit new results that we obtained using this algorithm.

3.5 Explicit new results, and further surprises

Using the method described in the previous section, we explicitly determined $\Omega_0^{(1)}(x)$ — $\Omega_0^{(6)}(x)$ in terms of HPLs. We will show these formulas below.

When analyzing the resulting formulas, in fact we found a further simplification, that was already noticed in [10] up to the three-loop level. Although results for individual integrals contain in general HPLs with all possible indices $0, \pm 1$, we observe that, at least up to six loops, it is possible to write the final result in terms of HPLs having indices $0, 1$ only, provided that we use x^2 as argument instead of x. That property is manifest in the following formulas. Up to three loops, one finds

$$\Omega_0^{(1)}(x) = -H_0 \,, \tag{3.34}$$

$$\Omega_0^{(2)}(x) = 4\,\zeta_3 + 2\,\zeta_2\,H_0 + 2\,H_{2,0} + H_{0,0,0} \,, \tag{3.35}$$

$$\begin{aligned}\Omega_0^{(3)}(x) = &-8\,\zeta_2\,\zeta_3 - 12\,\zeta_5 - 12\,\zeta_4\,H_0 - 16\,\zeta_3\,H_2 - 8\,\zeta_2\,H_3 - 4\,\zeta_3\,H_{0,0} - 8\,\zeta_2\,H_{2,0} \\ &- 8\,H_{4,0} - 8\,\zeta_2\,H_{0,0,0} - 8\,H_{2,2,0} - 4\,H_{3,0,0} - 8\,H_{3,1,0} - 4\,H_{2,0,0,0} - 6\,H_{0,0,0,0,0} \,.\end{aligned} \tag{3.36}$$

Our result at four loops reads

$$\begin{aligned}\Omega_0^{(4)}(x) = &\,48\,\zeta_3\,\zeta_4 + 24\,\zeta_2\,\zeta_5 + 36\,\zeta_7 + 8\,\zeta_3^2\,H_0 + 51\,\zeta_6\,H_0 + 48\,\zeta_2\,\zeta_3\,H_2 + 72\,\zeta_5\,H_2 \\ &+ 96\,\zeta_4\,H_3 + 88\,\zeta_3\,H_4 + 80\,\zeta_2\,H_5 + 32\,\zeta_2\,\zeta_3\,H_{0,0} + 20\,\zeta_5\,H_{0,0} + 72\,\zeta_4\,H_{2,0} \\ &+ 96\,\zeta_3\,H_{2,2} + 48\,\zeta_2\,H_{2,3} + 32\,\zeta_3\,H_{3,0} + 128\,\zeta_3\,H_{3,1} + 64\,\zeta_2\,H_{3,2} + 80\,\zeta_2\,H_{4,0} \\ &+ 48\,\zeta_2\,H_{4,1} + 92\,H_{6,0} + 114\,\zeta_4\,H_{0,0,0} + 24\,\zeta_3\,H_{2,0,0} + 48\,\zeta_2\,H_{2,2,0} + 48\,H_{2,4,0} \\ &+ 64\,\zeta_2\,H_{3,0,0} + 64\,\zeta_2\,H_{3,1,0} + 64\,H_{3,3,0} + 80\,H_{4,2,0} + 80\,H_{5,0,0} + 80\,H_{5,1,0} \\ &+ 24\,\zeta_3\,H_{0,0,0,0} + 48\,\zeta_2\,H_{2,0,0,0} + 48\,H_{2,2,2,0} + 24\,H_{2,3,0,0} + 48\,H_{2,3,1,0} + 64\,H_{3,1,2,0} \\ &+ 32\,H_{3,2,0,0} + 64\,H_{3,2,1,0} + 64\,H_{4,0,0,0} + 24\,H_{4,1,0,0} + 48\,H_{4,1,1,0} + 92\,\zeta_2\,H_{0,0,0,0,0} \\ &+ 24\,H_{2,2,0,0,0} + 48\,H_{3,0,0,0,0} + 32\,H_{3,1,0,0,0} + 36\,H_{2,0,0,0,0,0} + 92\,H_{0,0,0,0,0,0,0} \,.\end{aligned} \tag{3.37}$$

At five loops we obtain

$$\begin{aligned}\Omega_0^{(5)}(x) = &-\frac{32}{3}\,\zeta_3^3 - 144\,\zeta_4\,\zeta_5 - 204\,\zeta_3\,\zeta_6 - 72\,\zeta_2\,\zeta_7 - \frac{340}{3}\,\zeta_9 - 64\,\zeta_2\,\zeta_3^2\,H_0 - 80\,\zeta_3\,\zeta_5\,H_0 \\ &- \frac{620}{3}\,\zeta_8\,H_0 - 384\,\zeta_3\,\zeta_4\,H_2 - 192\,\zeta_2\,\zeta_5\,H_2 - 288\,\zeta_7\,H_2 - 96\,\zeta_3^2\,H_3 - 612\,\zeta_6\,H_3 \\ &- 576\,\zeta_2\,\zeta_3\,H_4 - 528\,\zeta_5\,H_4 - 1776\,\zeta_4\,H_5 - 1216\,\zeta_3\,H_6 - 1568\,\zeta_2\,H_7 - 456\,\zeta_3\,\zeta_4\,H_{0,0} \\ &- 144\,\zeta_2\,\zeta_5\,H_{0,0} - 84\,\zeta_7\,H_{0,0} - 64\,\zeta_3^2\,H_{2,0} - 408\,\zeta_6\,H_{2,0} - 384\,\zeta_2\,\zeta_3\,H_{2,2} - 576\,\zeta_5\,H_{2,2} \\ &- 768\,\zeta_4\,H_{2,3} - 704\,\zeta_3\,H_{2,4} - 640\,\zeta_2\,H_{2,5} - 384\,\zeta_2\,\zeta_3\,H_{3,0} - 240\,\zeta_5\,H_{3,0} - 576\,\zeta_2\,\zeta_3\,H_{3,1}\end{aligned}$$

JHEP11(2012)058

$$
\begin{aligned}
&- 864\,\zeta_5\,H_{3,1} - 1152\,\zeta_4\,H_{3,2} - 1056\,\zeta_3\,H_{3,3} - 960\,\zeta_2\,H_{3,4} - 1656\,\zeta_4\,H_{4,0} - 1152\,\zeta_4\,H_{4,1} \\
&- 1440\,\zeta_3\,H_{4,2} - 1152\,\zeta_2\,H_{4,3} - 704\,\zeta_3\,H_{5,0} - 1856\,\zeta_3\,H_{5,1} - 1216\,\zeta_2\,H_{5,2} - 1808\,\zeta_2\,H_{6,0} \\
&- 960\,\zeta_2\,H_{6,1} - 2144\,H_{8,0} - 48\,\zeta_3^2\,H_{0,0,0} - 948\,\zeta_6\,H_{0,0,0} - 256\,\zeta_2\,\zeta_3\,H_{2,0,0} - 160\,\zeta_5\,H_{2,0,0} \\
&- 576\,\zeta_4\,H_{2,2,0} - 768\,\zeta_3\,H_{2,2,2} - 384\,\zeta_2\,H_{2,2,3} - 256\,\zeta_3\,H_{2,3,0} - 1024\,\zeta_3\,H_{2,3,1} \\
&- 512\,\zeta_2\,H_{2,3,2} - 640\,\zeta_2\,H_{2,4,0} - 384\,\zeta_2\,H_{2,4,1} - 736\,H_{2,6,0} - 1368\,\zeta_4\,H_{3,0,0} \\
&- 864\,\zeta_4\,H_{3,1,0} - 1152\,\zeta_3\,H_{3,1,2} - 576\,\zeta_2\,H_{3,1,3} - 384\,\zeta_3\,H_{3,2,0} - 1536\,\zeta_3\,H_{3,2,1} \\
&- 768\,\zeta_2\,H_{3,2,2} - 960\,\zeta_2\,H_{3,3,0} - 576\,\zeta_2\,H_{3,3,1} - 1104\,H_{3,5,0} - 448\,\zeta_3\,H_{4,0,0} \\
&- 384\,\zeta_3\,H_{4,1,0} - 1536\,\zeta_3\,H_{4,1,1} - 768\,\zeta_2\,H_{4,1,2} - 1152\,\zeta_2\,H_{4,2,0} - 576\,\zeta_2\,H_{4,2,1} \\
&- 1392\,H_{4,4,0} - 1648\,\zeta_2\,H_{5,0,0} - 1216\,\zeta_2\,H_{5,1,0} - 384\,\zeta_2\,H_{5,1,1} - 1648\,H_{5,3,0} \\
&- 1808\,H_{6,2,0} - 2352\,H_{7,0,0} - 1568\,H_{7,1,0} - 368\,\zeta_2\,\zeta_3\,H_{0,0,0,0} - 152\,\zeta_5\,H_{0,0,0,0} \\
&- 912\,\zeta_4\,H_{2,0,0,0} - 192\,\zeta_3\,H_{2,2,0,0} - 384\,\zeta_2\,H_{2,2,2,0} - 384\,H_{2,2,4,0} - 512\,\zeta_2\,H_{2,3,0,0} \\
&- 512\,\zeta_2\,H_{2,3,1,0} - 512\,H_{2,3,3,0} - 640\,H_{2,4,2,0} - 640\,H_{2,5,0,0} - 640\,H_{2,5,1,0} \\
&- 288\,\zeta_3\,H_{3,0,0,0} - 288\,\zeta_3\,H_{3,1,0,0} - 576\,\zeta_2\,H_{3,1,2,0} - 576\,H_{3,1,4,0} - 768\,\zeta_2\,H_{3,2,0,0} \\
&- 768\,\zeta_2\,H_{3,2,1,0} - 768\,H_{3,2,3,0} - 960\,H_{3,3,2,0} - 960\,H_{3,4,0,0} - 960\,H_{3,4,1,0} \\
&- 1392\,\zeta_2\,H_{4,0,0,0} - 768\,\zeta_2\,H_{4,1,0,0} - 768\,\zeta_2\,H_{4,1,1,0} - 768\,H_{4,1,3,0} - 1152\,H_{4,2,2,0} \\
&- 1184\,H_{4,3,0,0} - 1152\,H_{4,3,1,0} - 1216\,H_{5,1,2,0} - 1376\,H_{5,2,0,0} - 1216\,H_{5,2,1,0} \\
&- 2080\,H_{6,0,0,0} - 1440\,H_{6,1,0,0} - 960\,H_{6,1,1,0} - 2172\,\zeta_4\,H_{0,0,0,0,0} - 192\,\zeta_3\,H_{2,0,0,0,0} \\
&- 384\,\zeta_2\,H_{2,2,0,0,0} - 384\,H_{2,2,2,2,0} - 192\,H_{2,2,3,0,0} - 384\,H_{2,2,3,1,0} - 512\,H_{2,3,1,2,0} \\
&- 256\,H_{2,3,2,0,0} - 512\,H_{2,3,2,1,0} - 512\,H_{2,4,0,0,0} - 192\,H_{2,4,1,0,0} - 384\,H_{2,4,1,1,0} \\
&- 1104\,\zeta_2\,H_{3,0,0,0,0} - 576\,\zeta_2\,H_{3,1,0,0,0} - 576\,H_{3,1,2,2,0} - 288\,H_{3,1,3,0,0} - 576\,H_{3,1,3,1,0} \\
&- 768\,H_{3,2,1,2,0} - 384\,H_{3,2,2,0,0} - 768\,H_{3,2,2,1,0} - 768\,H_{3,3,0,0,0} - 288\,H_{3,3,1,0,0} \\
&- 576\,H_{3,3,1,1,0} - 768\,H_{4,1,1,2,0} - 384\,H_{4,1,2,0,0} - 768\,H_{4,1,2,1,0} - 960\,H_{4,2,0,0,0} \\
&- 288\,H_{4,2,1,0,0} - 576\,H_{4,2,1,1,0} - 1728\,H_{5,0,0,0,0} - 1136\,H_{5,1,0,0,0} - 192\,H_{5,1,1,0,0} \\
&- 384\,H_{5,1,1,1,0} - 368\,\zeta_3\,H_{0,0,0,0,0,0} - 736\,\zeta_2\,H_{2,0,0,0,0,0} - 192\,H_{2,2,2,0,0,0} - 384\,H_{2,3,0,0,0,0} \\
&- 256\,H_{2,3,1,0,0,0} - 288\,H_{3,1,2,0,0,0} - 576\,H_{3,2,0,0,0,0} - 384\,H_{3,2,1,0,0,0} - 1408\,H_{4,0,0,0,0,0} \\
&- 576\,H_{4,1,0,0,0,0} - 384\,H_{4,1,1,0,0,0} - 2144\,\zeta_2\,H_{0,0,0,0,0,0,0} - 288\,H_{2,2,0,0,0,0,0} \\
&- 1104\,H_{3,0,0,0,0,0,0} - 432\,H_{3,1,0,0,0,0,0} - 736\,H_{2,0,0,0,0,0,0,0} - 2680\,H_{0,0,0,0,0,0,0,0,0}\,.
\end{aligned}
\tag{3.38}
$$

The six-loop result fills several pages and is therefore relegated to appendix D. All HPLs are understood to have argument x^2. Note that all indices are positive, in other words only the basic indices 0 and 1 appear. This is remarkable, and such a rewriting is in general not possible for individual terms contributing to (3.34) – (3.38) and (D.1).

It is very remarkable that within each of the equations (3.34) – (3.38) and (D.1) all terms have the same sign, and the common sign is alternating as the loop order increases. In fact, there is a sign constraint from the fact that the loop integrals leading to Ω_0 should be positive, at least in the Euclidean region $0 < x < 1$. Noting that the ladder diagrams appear with a factor of $(-1)^L$ per loop order, this implies that $(-1)^L \Omega_0^{(L)}$ is positive for any $0 < x < 1$. However, the fact that *all* signs within each of the above expressions are identical seems to be a less trivial statement.

JHEP11(2012)058

One more check that can be performed on the $\Omega_0^{(i)}$ is the limit $\phi \to 0$, corresponding to $x \to 1$. In this limit the contribution of the ladders to the cusp anomalous dimension was derived to all loop orders and to second order in ϕ in [10] and reads

$$\begin{aligned}\Gamma^{\rm lad} &= \frac{1-\sqrt{\kappa+1}}{2} - \frac{\phi^2}{16}\,\kappa\left(\frac{1+\sqrt{\kappa+1}}{1+\kappa+2\sqrt{\kappa+1}}\right) + \mathcal{O}(\phi^4) \\ &= \kappa\left[-\frac{1}{4}-\frac{\phi^2}{24}\right] + \kappa^2\left[\frac{1}{16}+\frac{5\phi^2}{288}\right] + \kappa^3\left[-\frac{1}{32}-\frac{43\phi^2}{3456}\right] + \kappa^4\left[\frac{5}{256}+\frac{211\phi^2}{20736}\right] \\ &\quad + \kappa^5\left[-\frac{7}{512}-\frac{4387\phi^2}{497664}\right] + \kappa^6\left[\frac{21}{2048}+\frac{23545\phi^2}{2985984}\right] + \mathcal{O}(\kappa^7,\phi^4)\,, \end{aligned} \tag{3.39}$$

with $\kappa = \hat{\lambda}/\pi^2$. In order to verify this expansion we note that the ladder contribution to the cusp anomalous dimension is given by

$$\Gamma^{\rm lad} = -\sum_{L\geq 1}\left(\frac{\lambda}{8\pi^2}\right)^L\left(-\frac{\xi}{2}\right)^L \Omega_0^{(L)}\,, \tag{3.40}$$

and that in the limit we are interested in

$$\frac{\lambda}{8\pi^2}\,\xi \to \frac{x}{2\,(x^2-1)}\,\kappa\,. \tag{3.41}$$

Taking into account that $x = e^{i\phi}$ we expand (3.40) to second order in ϕ and find perfect agreement with (3.39) through to six loops. In the next section, we will discuss the limit $x \to 0$.

3.6 Simplifications in the $x \to 0$ limit

The limit $x \to 0$ is interesting because it connects the velocity-dependent cusp anomalous dimension discussed here with the light-like cusp anomalous dimension.[3]

At four loops, taking the $x \to 0$ limit of eq. (3.37) leads to

$$\begin{aligned}\Omega_0^{(4)}(x) \overset{x\to 0}{=} \frac{736}{315}\log^7 x + \frac{184\pi^2}{45}\log^5 x + 16\zeta_3\log^4 x + \frac{76\pi^4}{45}\log^3 x + \left(\frac{32}{3}\pi^2\zeta_3 + 40\zeta_5\right)\log^2 x \\ + \left(\frac{34\pi^6}{315} + 16\zeta_3^2\right)\log x + \left(\frac{8}{15}\pi^4\zeta_3 + 4\pi^2\zeta_5 + 36\zeta_7\right) + \mathcal{O}(x)\,. \end{aligned} \tag{3.42}$$

At five loops, we find

$$\begin{aligned}\Omega_0^{(5)}(x) \overset{x\to 0}{=} & -\frac{2144}{567}\log^9 x - \frac{17152}{315}\zeta_2\log^7 x - \frac{1472}{45}\zeta_3\log^6 x - \frac{2896}{5}\zeta_4\log^5 x \\ & - \left(\frac{736}{3}\zeta_2\zeta_3 + \frac{304}{3}\zeta_5\right)\log^4 x - (64\,\zeta_3^2 + 1264\,\zeta_6)\log^3 x \\ & - (912\,\zeta_3\zeta_4 + 288\,\zeta_2\zeta_5 + 168\,\zeta_7)\log^2 x \\ & - \left(128\,\zeta_2\zeta_3^2 + 160\,\zeta_3\zeta_5 + \frac{1240}{3}\zeta_8\right)\log x \\ & - \frac{32}{3}\zeta_3^3 - 144\,\zeta_4\zeta_5 - 204\,\zeta_3\zeta_6 - 72\,\zeta_2\zeta_7 - \frac{340}{3}\zeta_9 + \mathcal{O}(x)\,. \end{aligned} \tag{3.43}$$

[3] Since we have taken the scaling limit we only have a subset of the usual diagrams. However, it is still interesting to discuss their behaviour.

JHEP11(2012)058

Finally, at six loops, one obtains

$$\begin{aligned}
\Omega_0^{(6)}(x) \overset{x\to 0}{=} & \frac{339008}{51975}\log^{11}x + \frac{339008}{2835}\zeta_2\log^9 x + \frac{4288}{63}\zeta_3\log^8 x \\
& + \frac{12800}{7}\zeta_4\log^7 x + \left(\frac{34304}{45}\zeta_2\zeta_3 + \frac{10688}{45}\zeta_5\right)\log^6 x \\
& + \left(\frac{2944}{15}\zeta_3^2 + \frac{110944}{15}\zeta_6\right)\log^5 x + (5792\,\zeta_3\zeta_4 + 1376\,\zeta_2\zeta_5 + 528\,\zeta_7)\log^4 x \\
& + \left(\frac{2944}{3}\zeta_2\zeta_3^2 + \frac{2432}{3}\zeta_3\zeta_5 + \frac{80048}{9}\zeta_8\right)\log^3 x \\
& + (128\,\zeta_3^3 + 3792\,\zeta_4\zeta_5 + 7584\,\zeta_3\zeta_6 + 1152\,\zeta_2\zeta_7 + 664\,\zeta_9)\log^2 x \\
& + (1824\,\zeta_3^2\zeta_4 + 1152\,\zeta_2\zeta_3\zeta_5 + 336\,\zeta_5^2 + 672\,\zeta_3\zeta_7 + \frac{8292}{5}\zeta_{10})\log x \\
& + \frac{256}{3}\zeta_2\zeta_3^3 + 160\,\zeta_3^2\zeta_5 + 612\,\zeta_5\zeta_6 + 432\,\zeta_4\zeta_7 + \frac{2480}{3}\zeta_3\zeta_8 \\
& + \frac{680}{3}\zeta_2\zeta_9 + 372\,\zeta_{11} + \mathcal{O}(x)\,. \qquad (3.44)
\end{aligned}$$

It is worth noting that in (3.42) – (3.44) certain transcendental constants which correspond to Multiple Zeta Values [27] having negative indices — such as $\log(2)$ or $\mathrm{Li}_4(\frac{1}{2})$ — do not appear. This becomes obvious from eqs. (3.37), (3.38), and (D.1) at four, five, and six loops, respectively. Moreover, eqs. (3.42) – (3.44) contain only single zeta values and products thereof. No Multiple Zeta Values of depth 2 or higher appear up to six loops, although constants like $\zeta_{5,3}$ would be allowed in principle.

We would like to mention that there is a shortcut for obtaining the asymptotic limit, without having to use the algorithm presented above. It suffices to notice that to logarithmic accuracy as $x \to 0$, we can make the following replacement of the integration kernel appearing e.g. in eq. (3.6),

$$\frac{1}{w'+1/x} - \frac{1}{w'+x} \longrightarrow -\frac{1}{w'+x}\,. \qquad (3.45)$$

Next, rescaling all integration variables by x, we see that one can write the result in the small x limit at any loop order in terms of HPLs with indices $0, -1$, and argument $1/x$. The latter can be rewritten in terms of HPLs of argument x, and their small x asymptotic behaviour can be made manifest using algorithms implemented in [28].

4 NLO terms in large ξ limit

4.1 Triangle-ladder diagrams (b)

We now wish to study the sum of the triangle-ladder diagrams shown in figure 1(b) in a similar way to LO. Let F now denote the sum of the diagrams of figures 1(a,b), starting with 1 (as at LO). Then F satisfies the Bethe-Salpeter equation of figure 2, with the last term omitted. (The last term will be discussed in the following section.)

Proceeding as at LO, we obtain the differential equation

$$\partial_\sigma\partial_\tau F(\sigma,\tau) = Q(\sigma,\tau) + F(\sigma,\tau)P(\sigma,\tau)\,. \qquad (4.1)$$

JHEP11(2012)058

Here the essential new feature is the appearance of $Q(\sigma,\tau)$. It arises from the first term in the second line of the r.h.s. of the equation shown in figure 2. It is given by the one-loop integral

$$Q(\sigma,\tau) = c\,\lambda\hat{\lambda}\,e^{(\sigma+\tau)} \int \frac{d^4x_1}{i\pi^2}\frac{1}{x_1^2(x_1-z_1)^2(x_1-z_2)^2} = c\,\lambda\hat{\lambda}\,\frac{e^{(\sigma+\tau)}}{z_{12}^2}\Phi^{(1)}\left(\frac{z_1^2}{z_{12}^2},\frac{z_2^2}{z_{12}^2}\right), \quad (4.2)$$

where $z_1^\mu = e^\sigma p^\mu$ and $z_2^\mu = -e^\tau q^\mu$ are points along the Wilson line, and $c = 2/(8\pi^2)^2$. The function $\Phi^{(1)}$ is known analytically, and we will give a useful form for it later in this section. Plugging in the expressions for z_1^μ, z_2^μ, we have

$$Q(\tau,\sigma) = c\,\lambda\hat{\lambda}\,\frac{1}{\cosh(\tau-\sigma)+\cos\phi}\,\Phi^{(1)}\left(\frac{e^{\tau-\sigma}/2}{\cosh(\tau-\sigma)+\cos\phi},\frac{e^{\sigma-\tau}/2}{\cosh(\tau-\sigma)+\cos\phi}\right). \quad (4.3)$$

Making the same ansatz as at LO, $F = \sum_n e^{-\Omega_n(\phi)y_2}\Psi_n(y_1,\phi)$, we obtain

$$\left[-\partial_{y_1}^2 - \frac{\hat{\lambda}}{8\pi^2}\frac{1}{(\cosh y_1+\cos\phi)} + \frac{\Omega^2(\phi)}{4}\right]\Psi(y_1,\phi) = \\ = c\,\frac{\lambda\,\hat{\lambda}}{(\cosh y_1+\cos\phi)}\,\Phi^{(1)}\left(\frac{e^{y_1}/2}{\cosh y_1+\cos\phi},\frac{e^{-y_1}/2}{\cosh y_1+\cos\phi}\right). \quad (4.4)$$

We see that the essential new feature w.r.t. the LO case is the appearance of an inhomogeneous term. It is important to realize that we would like to solve this equation to all orders in $\hat{\lambda}$, but only to linear order in $\alpha = \lambda/\hat{\lambda}$, corresponding to the NLO case.

For simplicity of notation, let us abbreviate the potential by $-\hat{\lambda}V$ and the inhomogeneous term by $\alpha\hat{\lambda}^2\tilde{Q}$. Then we have

$$\left[-\partial_{y_1}^2 - \hat{\lambda}V(y_1,\phi) + \frac{\Omega^2(\phi)}{4}\right]\Psi(y_1,\phi) = \alpha\,\hat{\lambda}^2\tilde{Q}\,. \quad (4.5)$$

Proceeding as in the homogeneous case and setting $\Psi = e^{-\Omega/2y_1}\eta$ we have

$$-\partial_{y_1}^2\eta + \Omega\partial_{y_1}\eta - \hat{\lambda}V\eta = \alpha\,e^{+\Omega/2\,y_1}\,\hat{\lambda}^2\,\tilde{Q}\,. \quad (4.6)$$

Recall that at $\alpha = 0$, this is just the equation for the ladder diagrams, which we already solved. We need the solution to order α. We can expand

$$\eta = \eta_{\text{ladders}} + \alpha\,\eta_\alpha\,, \quad \Omega = \Omega_{\text{ladders}} + \alpha\,\Omega_\alpha\,, \quad (4.7)$$

to obtain, at order α,

$$-\partial_{y_1}^2\eta_\alpha + \Omega_{\text{ladders}}\partial_{y_1}\eta_\alpha - \hat{\lambda}V\eta_\alpha = e^{y_1\Omega_{\text{ladders}}/2}\hat{\lambda}^2\tilde{Q} - \Omega_\alpha\eta'_{\text{ladders}}\,. \quad (4.8)$$

As before, Ω is obtained by requiring that $\Psi'(y_1)$ vanishes at $y_1 = 0$. Therefore we have

$$\Omega = 2\partial_{y_1}\log\eta|_{y_1=0}\,. \quad (4.9)$$

JHEP11(2012)058

At order α, this gives

$$\Omega_\alpha = 2\partial_{y_1}\left(\frac{\eta_\alpha}{\eta_{\text{ladders}}}\right)|_{y_1=0}\,. \tag{4.10}$$

In summary, we have arrived at a differential equation, eq. (4.8), together with (4.10), for the contribution of the triangle-ladder diagrams shown in figure 1(b).

We will now explain how to solve these equations to any order in $\hat{\lambda}$. First of all, it is clear that we can integrate order by oder in $\hat{\lambda}$ just as we did at LO. The main question is whether we can express the resulting wavefunction at each order in terms of the same set of iterated integrals as in the previous section. We will now show that this is indeed the case, and in fact is true also for a more general class of diagrams.

The new feature of eq. (4.8) is the appearance of $\tilde{Q}$, so we need to analyze whether integrals over $\tilde{Q}$ will be of the same form as at LO. An example will suffice to see that this is indeed the case. Consider expanding to order $\hat{\lambda}^2$. Then $\eta^{(1)\prime}(w,x)$ is given by an integral of the form

$$\int_{-\log w}^{\infty}\frac{dy_1}{(\cosh y_1+\cos\phi)}\,\Phi^{(1)}\left(\frac{e^{y_1}/2}{\cosh y_1+\cos\phi},\frac{e^{-y_1}/2}{\cosh y_1+\cos\phi}\right)\,. \tag{4.11}$$

We will now make use of the fact that $\Phi^{(1)}$ is a function with very special properties. In fact, this allows us to immediately make a generalization where $\Phi^{(1)}$ is replaced by $\Phi^{(n)}$. This function is given by a beautiful formula [29],

$$\Phi^{(n)}(x,y) = \frac{1}{\sqrt{(1-x-y)^2-4xy}}\,\tilde{\Phi}^{(n)}(x,y)\,, \tag{4.12}$$

where

$$\tilde{\Phi}^{(L)}(x,y) = \sum_{f=0}^{L}\frac{(-1)^f(2L-f)!}{L!f!(L-f)!}\log^f(z_1z_2)\left[\text{Li}_{2L-f}(z_1)-\text{Li}_{2L-f}(z_2)\right]\,, \tag{4.13}$$

and

$$x = z_1z_2\,,\qquad y=(1-z_1)(1-z_2)\,. \tag{4.14}$$

Changing variables to $w'=e^{-y_1}$ and $x=e^{i\phi}$, eq. (4.11) becomes, up to a trivial normalization factor,

$$\int_0^w\frac{dw'}{w'}\,\tilde{\Phi}^{(1)}\left(\frac{1}{w'^2+2w'\cos\phi+1},\frac{w'^2}{w'^2+2w'\cos\phi+1}\right)\,. \tag{4.15}$$

Inspection shows that the variables defined in (4.14) are given by

$$z_1=\frac{x}{x+w'}\,,\qquad z_2=\frac{1}{1+xw'}\,. \tag{4.16}$$

Furthermore, the functions above can be defined using only iterative integrals corresponding to symbols $z_1, z_2, 1-z_1, 1-z_2$. It is easy to verify that the latter factorize over $x, w, w+x, 1+$

JHEP11(2012)058

wx, and hence are contained in the function class discussed in the previous section. This implies that we can again perform all iterated integrals within the set of polylogarithms defined by the same integration kernels/symbols as in the homogeneous case, and therefore allowing for an algorithmic solution of this problem.

We note that there is an obvious generalization to a class of diagrams where $\Phi^{(1)}$ is replaced by $\Phi^{(n)}$, see appendix A of ref. [10]. The perturbative solution for that class of diagrams can be done in the same way as explained above.

4.2 H-exchange diagrams (c)

The diagrams with H-exchange of figure 1(c) were analyzed in ref. [23] for the quark-antiquark potential. It was found that the Bethe-Salpeter equation in that case contains a new term of the form

$$\int_0^\infty du \int_0^\infty dv\, e^{-\frac{\Omega_0}{2}(u+v)}\, f(u,v;y_1)\Psi(y_1-u+v)\,, \tag{4.17}$$

so that one has a linear integro-differential equation for Ψ. Their analysis can be adapted to the present case of general ϕ, with f now depending on ϕ.

Although such an equation may seem complicated, it simplifies considerably when solving it in the small $\alpha = \lambda/\hat{\lambda}$ limit. The reason is that the kernel, the H-exchange diagram is already of order α, so that we only need the wavefunction at order α^0. In other words, the problem reduces to a differential equation for the wavefunction at order α, with an inhomogeneous term. This is exactly the case we studied in the previous section.

Having said this, the main difficulty lies in the computation of the H insertion, and in integrating it when iteratively solving for the wavefunction. From the discussion above it is clear that we need to understand how to carry out the H-shaped and similar integrals. Let us therefore start with the basic three-loop integral, which has one H-exchange, and no additional rungs. It is given by

$$\int_0^\infty ds_2 \int_0^{s_2} ds_1 \int_0^\infty dt_2 \int_0^{t_2} dt_1\, f(-s_1p^\mu, t_1q^\mu; t_2q^\mu, -s_2p^\mu)\,. \tag{4.18}$$

Note that strictly speaking we should introduce IR and UV regulators for this integral, but since we are only interested in extracting the overall divergence, the details of the cutoffs are not very important. For the same reason, the H-shaped subintegral can be defined in exactly four dimensions,

$$f(x_1,x_2,x_3,x_4) = (\partial_1+\partial_4)^2\, h(x_1,x_2;x_3,x_4)\,, \tag{4.19}$$

$$h(x_1,x_2;x_3,x_4) = \int \frac{d^4x_5 d^4x_6}{(i\pi^2)^2}\, \frac{1}{x_{15}^2 x_{25}^2 x_{36}^2 x_{46}^2 x_{56}^2}\,. \tag{4.20}$$

Eq. (4.19) defines the function f. Although this is a two-loop integral, f reduces to one-loop integrals thanks to differential equations it satisfies. We review these differential equations

JHEP11(2012)058

in appendix A. Remarkably, they allow us to express f in terms of the one-loop function $\Phi^{(1)}$, the same function that appeared already in integral class (b). Explicitly, we have

$$\begin{aligned}\tilde{f} = {} & x_{24}^2(x_{12}^2+x_{23}^2-x_{31}^2)\,\Phi^{(1)}\left(\frac{x_{12}^2}{x_{13}^2},\frac{x_{23}^2}{x_{13}^2}\right)+x_{13}^2(x_{12}^2+x_{14}^2-x_{24}^2)\,\Phi^{(1)}\left(\frac{x_{12}^2}{x_{24}^2},\frac{x_{14}^2}{x_{24}^2}\right)\\ & +x_{24}^2(x_{14}^2+x_{34}^2-x_{13}^2)\,\Phi^{(1)}\left(\frac{x_{34}^2}{x_{13}^2},\frac{x_{14}^2}{x_{13}^2}\right)+x_{13}^2(x_{23}^2+x_{34}^2-x_{24}^2)\,\Phi^{(1)}\left(\frac{x_{34}^2}{x_{24}^2},\frac{x_{23}^2}{x_{24}^2}\right)\\ & +(x_{13}^2x_{24}^2-x_{14}^2x_{23}^2-x_{12}^2x_{34}^2)\,\Phi^{(1)}\left(\frac{x_{12}^2x_{34}^2}{x_{13}^2x_{24}^2},\frac{x_{14}^2x_{23}^2}{x_{13}^2x_{24}^2}\right)\,,\end{aligned} \tag{4.21}$$

where $\tilde{f} = (x_{12}^2x_{13}^2x_{24}^2x_{34}^2)f$. This formula will be very convenient when discussing the strong coupling limit.

After this digression on h, we can proceed to extract the overall UV divergence and compute the H-exchange integral. Changing variables according to $s_1 = x_1s_2, t_1 = x_2t_2$, and $s_2 = z\rho, t_2 = \rho\bar{z}$, where $\bar{z} = 1-z$, and using that h scales as $1/x^4$, we find

$$\int_0^\infty \frac{d\rho}{\rho}\,H^{(3)}\,, \tag{4.22}$$

where

$$H^{(3)} = \int_0^1 dz\,dx_1\,dx_2\,z\bar{z}f(-x_1zp^\mu,-zp^\mu;x_2\bar{z}q^\mu,\bar{z}q^\mu)\,. \tag{4.23}$$

Note that by assumption $H^{(3)}$ is finite (if combined with exponentiated contributions from lower loops). However, when carrying out the integration in (4.23), care is required, because the finiteness is not necessarily true for individual terms appearing in (4.21). This small problem can be avoided by introducing an auxiliary regulator. With the above parametrization, we have

$$x_1^\mu = -x_1zp^\mu\,,\quad x_2^\mu = x_2\bar{z}q^\mu\,,\quad x_3^\mu = \bar{z}q^\mu\,,\quad x_4^\mu = -zp^\mu\,, \tag{4.24}$$

and using $p^2 = q^2 = 1\,, p\cdot q = \cos\phi$, we have

$$x_{14}^2 = \bar{x}_1^2z^2\,,\quad x_{24}^2 = z^2+x_2^2\bar{z}^2+x_2z\bar{z}2\cos\phi\,, \tag{4.25}$$

and so on.

In summary, we found a parameter integral, where the number of integrations equals the expected degree of the function. Just as for integral class (b), higher orders can be obtained by iteration. However, it is not yet clear that the same class of functions will be sufficient to evaluate these integrals. Explicit results at three loops motivate that it might be. We leave this question for future work, and close this section by remarking that formula (4.13) will certainly be very useful when trying to evaluate this integral and similar integrals appearing in the iterative solution.

5 Strong coupling limit at LO and NLO

Here we discuss the strong coupling limit of the Bether-Salpeter equations. In this limit, the calculation of the ground state energy becomes almost trivial. It is straightforward to extend the analysis of ref. [23], which was done in the anti-parallel lines limit $\phi \to \pi$, to any angle.

JHEP11(2012)058

5.1 Strong coupling limit of Bethe-Salpeter equation

Let us start by discussing diagrams of type (c). First of all, we notice that as in [23], the Bethe-Salpeter equation for this class of diagrams simplifies dramatically in the strong coupling limit. The reason is that for $\Omega_0 \sim \sqrt{\lambda} \gg 1$, the region of small u, v will give the dominant contribution to the integral in eq. (4.17). This implies that the wavefunction $\Psi(y_1)$ can be pulled out of the integral, with the coefficient being an effective potential. This argument also works for the angle-dependent cusp Wilson loop.

We therefore need to compute the effective potential for general angles. Although the function h is not known analytically, its derivative f is known, as we saw in the previous section.

We need the function $f(x_1, x_2; x_3, x_4)$ in the limit where $x_1 \to x_4$ and $x_2 \to x_3$. Let us parametrize this limit by $x_{14}^2 = u^2, x_{23}^2 = v^2, x_{12}^2 = x_{24}^2 = x_{13}^2 = x_{34}^2 = 2\cosh y_1 + 2\cos\phi$, with u, v small. Plugging these values into eq. (4.21), it turns out we only need the following limit of $\Phi^{(1)}$,

$$\Phi^{(1)}(1, \epsilon) = -\log\epsilon + 2 + \mathcal{O}(\epsilon)\,. \tag{5.1}$$

Using this limit, we obtain

$$f \longrightarrow -4\frac{u^2\log u + v^2\log v}{(2\cosh y_1 + 2\cos\phi)^3} + \mathcal{O}(u^2, v^2)\,. \tag{5.2}$$

We see that this is a generalization of eq. (5.2) of [23] to general angles. One could also use eq. (4.21) to compute higher order terms in the expansion.

This means that the correct effective potential for the general angle case is obtained by replacing each (x^2+1) terms in (5.3) of [23] by $(2\cosh y_1 + 2\cos\phi)$ for the cusped Wilson loop. Then we have a Schrödinger equation

$$\left[-\partial_{y_1}^2 + V_{\text{eff}}(y_1) + \frac{\Omega^2}{4}\right]\Psi(y_1) = 0 \tag{5.3}$$

where the correction to the effective potential comes from the integral

$$V_{\text{eff}}|_{\lambda\hat{\lambda}^2} \sim \int_0^\infty \int_0^\infty du\, dv\, e^{-\frac{\Omega}{2}(u+v)}\, f(u, v)\,. \tag{5.4}$$

Explicitly, we have

$$V_{\text{eff}} = -\frac{\hat{\lambda}}{4\pi^2(2\cosh y_1 + 2\cos\phi)} + \frac{\lambda\hat{\lambda}^2\log\Omega}{2\pi^6\Omega^4(2\cosh y_1 + 2\cos\phi)^3}\,. \tag{5.5}$$

At strong coupling, we can focus on $\hat{\lambda} \gg 1, y_1 \ll 1$, with $\hat{\lambda}(y_1)^{1/4}$ fixed. In that regime the leading term of the Schrödinger equation is

$$V_{\text{eff}}(y_1 = 0) + \frac{\Omega_0^2}{4} = 0\,. \tag{5.6}$$

JHEP11(2012)058

From this we obtain for the ground state energy,

$$\Gamma^{(a)+(c)} = -\Omega_0 = -\frac{\sqrt{\hat{\lambda}}}{2\pi\cos\frac{\phi}{2}}\left[1 - \frac{1}{2}\frac{\lambda}{\hat{\lambda}}\log\frac{\hat{\lambda}}{\lambda} + \mathcal{O}\left(\frac{\lambda}{\hat{\lambda}}\right)\right] \tag{5.7}$$

Here the superscript indicates that this is the contribution from the integrals shown in figures 1(a), (c).

Let us now discuss the integrals of figure 1(b). Here we obtained a Schrödinger equation with an inhomogeneous term (note that there $\alpha = \lambda/\hat{\lambda}$) that is not multiplied by the wave function. The latter fact suggests to us that the contribution of this class of diagrams at strong coupling will not be given by an exponential factor of the type seen for integral classes (a) and (c). If one assumes the absence of contributions of integral class (b) at strong coupling, as we will do in the following, then (5.7) is the full answer at LO and NLO in the scaling limit.

Let us now compare this against the corresponding quantity computed in string theory.

5.2 Scaling limit of the string theory result

The leading term (and first subleading term as well) in the $1/\sqrt{\lambda}$ expansion at strong coupling has been computed using string theory in ref. [7]. It is straightforward to expand their result in the large $\hat{\lambda}$ limit that we are interested in. For the LO, this was already done in ref. [10].

It is easy to take the scaling limit of the formula for Γ given in ref. [7]. The details of this calculation are presented in appendix B. We find

$$\Gamma = -\frac{\sqrt{\hat{\lambda}}}{2\pi\cos\frac{\phi}{2}}\left[1 - \frac{1}{2}\frac{\lambda}{\hat{\lambda}}\log\frac{\hat{\lambda}}{\lambda} + \mathcal{O}\left(\frac{\lambda}{\hat{\lambda}}\right)\right]. \tag{5.8}$$

As a consistency check, we can take the limit $\phi = \pi - \delta$, $\delta \to 0$, where we expect to find the quark-antiquark potential V. More precisely, $\Gamma \sim -1/\delta V$, and indeed we find agreement with eq. (5.4) of [23].

Let us compare eq. (5.8) to the diagram calculation performed in the previous subsection. Comparing to eq. (5.7), we find perfect agreement. Recall that in principle there could also be a contribution from integrals of type (b) not accounted for in eq. (5.7), but we argued that this is not the case based on the structure of the Bethe-Salpeter equation for these integrals. Under this assumption, we see that there is a perfect match between the field theory calculation in the scaling limit, and the string theory calculation. As pointed out in [10], this agreement was not guaranteed due to potential order of limits issues.

6 Discussion and conclusion

In this paper we further studied the scaling limit of the cusp anomalous dimension introduced in [10], in several ways.

In the first part of the paper, working at LO we showed that the perturbative solution at weak coupling can be expressed at any loop order in terms of harmonic polylogarithms,

JHEP11(2012)058

and outlined a corresponding algorithm. As illustration, we reproduced the three-loop result of [10] and computed the four-, five-, and six-loop results, which are new. We also provide a shortcut for obtaining the $x \to 0$ asymptotics, which corresponds to the light-like limit of the edges of the Wilson loop.

We observed interesting features of these results. We find that, at least up to six loops, they can be written in terms of a reduced class of harmonic polylogarithms, with indices 0 and 1 only, when choosing x^2 as argument (this feature was already noted in [10] up to three loops.). Moreover, in the $x \to 0$ limit, again up to six loops, we find that the resulting asymptotic expansion can be expressed in terms of linear combinations of products of single zeta values only. Other constants such as $\log(2)$, or multiple zeta values of higher depth were not needed. This is especially interesting in the context of the BES equation for the closely related light-like cusp anomalous dimension, which has the same property [30].

It would be very interesting if one could prove these properties. Such a proof would likely shed more light on the structure of the cusp anomalous dimension.

In the second part of the paper, we extended the analysis of [10] to NLO order. The new feature of the equations is the appearance of an inhomogeneous term. (A similar analysis was recently done for the quark-antiquark potential [23]). This term does not alter the perturbative solution, however, and we were able to apply the same strategy as at LO. We showed how to compute these contributions systematically in perturbation theory. For one class of integrals, we provided an algorithmic solution at any loop order in terms of harmonic polylogarithms. For the second class of integrals, we showed how to obtain the solution in terms of iterated integrals of simple functions. We left the question of whether the latter can be expressed in terms of HPLs for future work.

Finally, we discussed the strong coupling limit of the equations. We computed the logarithmically enhanced terms at NLO, and found agreement between the field theory and the string theory calculation. This generalizes the calculation of [23] to any angle. Using our formulas, it should be possible to compute the non-logarithmic terms at NLO as well. We leave this for future work as well.

In ref. [10] the zero angle case was studied, where the Schrödinger potential becomes the exactly solvable Pöschl-Teller potential. It would be interesting to extend this analysis to NLO, where the equation is modified by an inhomogeneous term, as discussed in the present paper.

Our approach also suggests a general strategy for the computation of the cusp anomalous dimension, or related quantities. At a given loop order, there are two sets of contributions. First, there are a number of integrals that have an overall UV divergence. These diagrams are the "seed" of the Bethe-Salpeter equations and have to be computed. They correspond to the most complicated part of the calculation. However, the fact that they have no subdivergences allows one to extract the overall divergence easily, so that one is left with the calculation of a finite quantity. The latter is sometimes related to four-dimensional integrals. This observation allowed for example for the computation of an infinite class of integrals contributing to the cusp anomalous dimension in ref. [10]. Second, there are diagrams that do have subdivergences. For these contributions, the resummation technique via the Bethe-Salpeter equation is very useful, as it automatically takes into account the

JHEP11(2012)058

non-Abelian exponentiation. Although these contributions typically give the most complicated contributions as far as the functions involved are concerned [10], the latter have their origin in simple iterations of diagrams of the first type.

Although our analysis did not rely on the planar limit, non-planar contributions to Γ_{cusp} appear only at four loops, or at higher subleading terms in the scaling limit. It would be very interesting to compute the first non-planar corrections. We expect that many observations about the calculation of loop integrals, especially the comments for extracting overall divergences and using four-dimensional integrals, will be useful in related problems as well, e.g. as the non-planar integrals discussed in ref. [31].

Our approach can also be extended beyond the NLO. We remark that this does not require any Feynman graph calculations, as the integrand for the planar Wilson loop can be obtained from a soft limit of the integrand of a four-particle scattering amplitude [10, 11]. The latter can be obtained through on-shell recursion relations in principle to any loop order. We give examples of this procedure in appendix C. We hope that this all-loop knowledge of the Wilson loop integrand gives a good starting point for analyzing further the properties that we have observed in this paper.

Finally, the scaling limit discussed here might be useful for simplifying the TBA equations of refs. [16, 17]. It would also be interesting if those equation could shed light on some of the observations about the perturbative properties of Γ_{cusp} that we have made here.

Acknowledgments

It is a pleasure to thank N. Arkani-Hamed, F. Brown, S. Caron-Huot, A. Sever, and A. Zhiboedov for helpful conversations. JMH was supported in part by the Department of Energy grant DE-FG02-90ER40542. TH is supported by the Helmholtz Alliance "Physics at the Terascale".

A Differential equations for two-loop integral h

Here we give the differential equations for the two-loop integral h of eq. (4.20).

The non-trivial differential equation has been written down in ref. [32] and in eq. (A.7) of ref. [33]. The differential operator we have can be related to the one of eq. (A.7) of [33] by using translational invariance ($\sum_{i=1}^4 \partial_i = 0$), up to trivial pieces proportional to $\Box_i$, where we can use the Laplace equation. Note that all occurring terms can be written in terms of $\Phi^{(1)}$, thanks to eq. (A.5) below.

More explicitly, we have

$$2(\partial_1+\partial_4)^2 = -(\partial_1-\partial_2)\cdot(\partial_3-\partial_4) - (\partial_1+\partial_2)^2 + \Box_1 + \Box_2 + \Box_3 + \Box_4\,. \tag{A.1}$$

We have, using eq. (A.7) of ref. [33], up to overall factors,

$$\begin{aligned}-(\partial_1-\partial_2)\cdot(\partial_3-\partial_4)h = \frac{1}{x_{12}^2 x_{34}^2}\Big[&(x_{13}^2x_{24}^2 - x_{14}^2x_{23}^2)X_{1234} + (x_{14}^2 - x_{13}^2)X_{134}\\ &- (x_{24}^2 - x_{23}^2)X_{234} + (x_{32}^2 - x_{31}^2)X_{312} - (x_{42}^2 - x_{41}^2)X_{412}\Big]\,.\end{aligned} \tag{A.2}$$

JHEP11(2012)058

and, from the Laplace equation,

$$\left[-(\partial_1+\partial_2)^2+\Box_1+\Box_2+\Box_3+\Box_4\right] h = -X_{1234}+\frac{1}{x_{12}^2}(X_{134}+X_{234})+\frac{1}{x_{34}^2}(X_{123}+X_{124}), \tag{A.3}$$

where

$$X_{1234} = \int \frac{d^4x_i}{i\pi^2}\frac{1}{x_{1i}^2x_{2i}^2x_{3i}^2x_{4i}^2} = \frac{1}{x_{13}^2x_{24}^2}\Phi^{(1)}\left(\frac{x_{12}^2x_{34}^2}{x_{13}^2x_{24}^2},\frac{x_{14}^2x_{23}^2}{x_{13}^2x_{24}^2}\right), \tag{A.4}$$

$$X_{123} = \int \frac{d^4x_i}{i\pi^2}\frac{1}{x_{1i}^2x_{2i}^2x_{3i}^2} = \frac{1}{x_{13}^2}\Phi^{(1)}\left(\frac{x_{12}^2}{x_{13}^2},\frac{x_{23}^2}{x_{13}^2}\right). \tag{A.5}$$

Combining differential equations (A.2) and (A.3), and plugging in (A.4) and (A.5), we find eq. (4.21) given in the main text.

B Details of the strong coupling calculation

Here we show the details of the expansion of the string theory answer for Γ in the scaling limit. The result of [7] for Γ is parametrized by two parameters p and $q = -ir\,, r > 0$, which are implicitly defined through the angles ϕ and θ, in the following way

$$\theta = \frac{2bq}{\sqrt{b^4+p^2}}K(k^2), \tag{B.1}$$

$$\phi = \pi - 2\frac{p^2}{b\sqrt{b^4+p^2}}\left[\Pi\left(\frac{b^4}{b^4+p^2},k^2\right)-K(k^2)\right], \tag{B.2}$$

where

$$b^2 = \frac{1}{2}\left(p^2-q^2+\sqrt{(p^2-q^2)^2+4p^2}\right), \tag{B.3}$$

$$k^2 = \frac{b^2(b^2-p^2)}{b^4+p^2}. \tag{B.4}$$

In terms of these variables, we have

$$\Gamma = \frac{\sqrt{\lambda}}{2\pi}\frac{2\sqrt{b^4+p^2}}{bp}\left[\frac{(b^2+1)p^2}{b^4+p^2}K(k^2)-E(k^2)\right], \tag{B.5}$$

where E, K and Π are complete elliptic integrals,

$$E(k^2) = \int_0^{\frac{\pi}{2}} dt\frac{1}{\sqrt{1-k^2\sin^2 t}}, \tag{B.6}$$

$$K(k^2) = \int_0^{\frac{\pi}{2}} dt\sqrt{1-k^2\sin^2 t}, \tag{B.7}$$

$$\Pi(a^2,b^2) = \int_0^{\frac{\pi}{2}} dt\frac{1}{(1-a^2\sin^2 t)\sqrt{1-b^2\sin^2 t}}. \tag{B.8}$$

JHEP11(2012)058

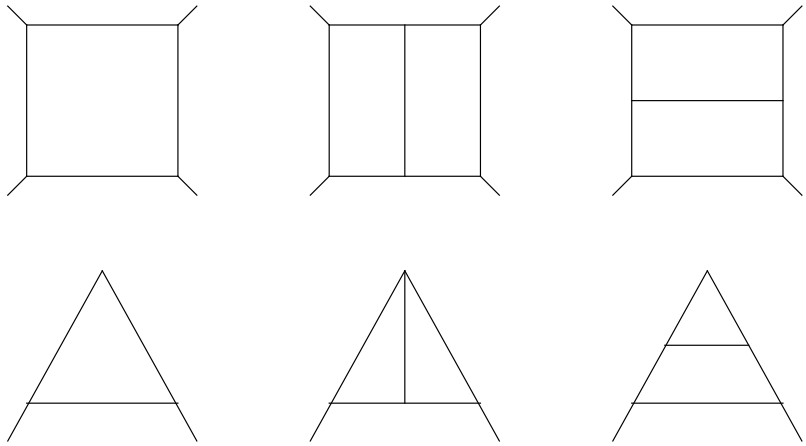

Figure 3. Relation between integrals of the four-point amplitude (first line) and Wilson line integrals (second line) at one and two loops.

The scaling limit $i\theta \gg 1$ is reached by letting $p \to 0$. We see that we require the leading and subleading divergences of Π in the limit where

$$\lim_{\epsilon\to 0} \Pi(1-a\epsilon, 1-\epsilon b) = \frac{1}{\epsilon}\frac{\pi - 2\arcsin\frac{\sqrt{a}}{\sqrt{b}}}{2\sqrt{a}\sqrt{b-a}} - \frac{1}{4}\log(\epsilon) - \frac{\sqrt{a}\left(\pi - 2\arcsin\frac{\sqrt{a}}{\sqrt{b}}\right)}{4\sqrt{b-a}} - \frac{1}{4}\log(b) + \frac{1}{4} + \log(2) + \mathcal{O}(\epsilon)\,. \tag{B.9}$$

In this way, we obtain, at leading order in $\sqrt{\lambda} \gg 1$,

$$\Gamma = -\frac{r\sqrt{\lambda}}{\pi p}\left[1 + p^2 \log p \frac{(1+r^2)}{2r^4}\right] + \mathcal{O}(p) \tag{B.10}$$

We now convert r and p to their expressions in terms of θ and ϕ. So we need the expansions of the latter to the necessary order in p. We find

$$e^{i\theta/2} = \frac{1}{p}\,4\frac{r^2}{\sqrt{1+r^2}} + p\log p\,\frac{3+r^2}{r^2\sqrt{1+r^2}} + \mathcal{O}(p)\,, \tag{B.11}$$

$$\phi = 2\arcsin\frac{1}{\sqrt{1+r^2}} - \frac{1}{r^3}p^2\log p + \mathcal{O}(p^2)\,, \tag{B.12}$$

We can see that this is in agreement with equation (5.8) quoted in the main text.

C Relation between integrals for four-particle scattering amplitude and cusp anomalous dimension

In figures 3 and 4 we illustrate the relation between the integrals contributing to the four-particle scattering amplitude (odd lines) and the integrals contributing to the cusp anomalous dimension (even lines) to three loops. The integrals occurring at one and two loops are shown in figure 3. The three-loop integrals are shown in figure 4. The reason for this relation [10, 11] is essentially exact dual conformal symmetry [15], together with the fact that massive scattering amplitudes in soft limits are related to Wilson loops [34].

JHEP11(2012)058

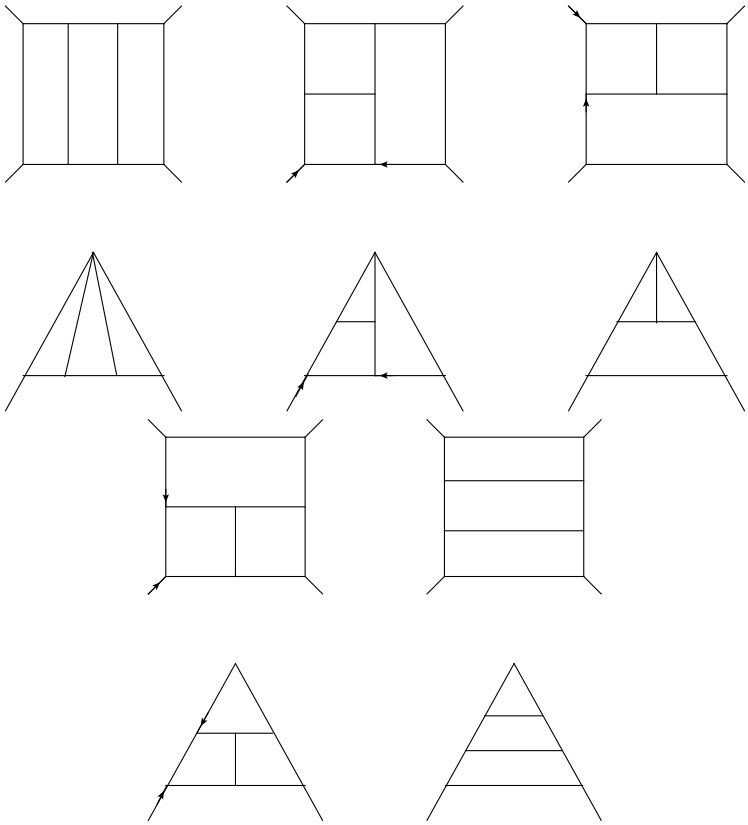

Figure 4. Relation between integrals of the four-point amplitude (first and third line) and Wilson line integrals (second and fourth line) at three loops. Arrows denote internal numerator factors $(p^\mu + q^\mu)^2$, where p^μ and q^μ are the momenta flowing along the lines with arrows.

D The six-loop function $\Omega_0^{(6)}$

Here we present the six-loop result $\Omega_0^{(6)}$ which we relegated from the main text to this appendix. Again, all HPLs are understood to have argument x^2.

$$
\begin{aligned}
\Omega_0^{(6)}(x) = {} & \frac{256}{3}\,\zeta_2\,\zeta_3^3 + 160\,\zeta_3^2\,\zeta_5 + 612\,\zeta_5\,\zeta_6 + 432\,\zeta_4\,\zeta_7 + \frac{2480}{3}\,\zeta_3\,\zeta_8 + \frac{680}{3}\,\zeta_2\,\zeta_9 + 372\,\zeta_{11} \\
& + 912\,\zeta_3^2\,\zeta_4\,H_0 + 576\,\zeta_2\,\zeta_3\,\zeta_5\,H_0 + 168\,\zeta_5^2\,H_0 + 336\,\zeta_3\,\zeta_7\,H_0 + \frac{4146}{5}\,\zeta_{10}\,H_0 \\
& + \frac{320}{3}\,\zeta_3^3\,H_2 + 1440\,\zeta_4\,\zeta_5\,H_2 + 2040\,\zeta_3\,\zeta_6\,H_2 + 720\,\zeta_2\,\zeta_7\,H_2 + \frac{3400}{3}\,\zeta_9\,H_2 \\
& + 1024\,\zeta_2\,\zeta_3^2\,H_3 + 1280\,\zeta_3\,\zeta_5\,H_3 + \frac{9920}{3}\,\zeta_8\,H_3 + 9744\,\zeta_3\,\zeta_4\,H_4 + 3360\,\zeta_2\,\zeta_5\,H_4 \\
& + 2664\,\zeta_7\,H_4 + 2176\,\zeta_3^2\,H_5 + 20472\,\zeta_6\,H_5 + 14688\,\zeta_2\,\zeta_3\,H_6 + 8592\,\zeta_5\,H_6 \\
& + 55776\,\zeta_4\,H_7 + 31936\,\zeta_3\,H_8 + 52928\,\zeta_2\,H_9 + 64\,\zeta_3^3\,H_{0,0} + 1896\,\zeta_4\,\zeta_5\,H_{0,0} \\
& + 3792\,\zeta_3\,\zeta_6\,H_{0,0} + 576\,\zeta_2\,\zeta_7\,H_{0,0} + 332\,\zeta_9\,H_{0,0} + 640\,\zeta_2\,\zeta_3^2\,H_{2,0} + 800\,\zeta_3\,\zeta_5\,H_{2,0} \\
& + \frac{6200}{3}\,\zeta_8\,H_{2,0} + 3840\,\zeta_3\,\zeta_4\,H_{2,2} + 1920\,\zeta_2\,\zeta_5\,H_{2,2} + 2880\,\zeta_7\,H_{2,2} + 960\,\zeta_3^2\,H_{2,3} \\
& + 6120\,\zeta_6\,H_{2,3} + 5760\,\zeta_2\,\zeta_3\,H_{2,4} + 5280\,\zeta_5\,H_{2,4} + 17760\,\zeta_4\,H_{2,5} + 12160\,\zeta_3\,H_{2,6}
\end{aligned}
$$

JHEP11(2012)058

$$
\begin{aligned}
&+ 15680\,\zeta_2\,H_{2,7} + 7296\,\zeta_3\,\zeta_4\,H_{3,0} + 2304\,\zeta_2\,\zeta_5\,H_{3,0} + 1344\,\zeta_7\,H_{3,0} + 6144\,\zeta_3\,\zeta_4\,H_{3,1}\\
&+ 3072\,\zeta_2\,\zeta_5\,H_{3,1} + 4608\,\zeta_7\,H_{3,1} + 1536\,\zeta_3^2\,H_{3,2} + 9792\,\zeta_6\,H_{3,2} + 9216\,\zeta_2\,\zeta_3\,H_{3,3}\\
&+ 8448\,\zeta_5\,H_{3,3} + 28416\,\zeta_4\,H_{3,4} + 19456\,\zeta_3\,H_{3,5} + 25088\,\zeta_2\,H_{3,6} + 1280\,\zeta_3^2\,H_{4,0}\\
&+ 18696\,\zeta_6\,H_{4,0} + 1728\,\zeta_3^2\,H_{4,1} + 11016\,\zeta_6\,H_{4,1} + 11904\,\zeta_2\,\zeta_3\,H_{4,2} + 11808\,\zeta_5\,H_{4,2}\\
&+ 35040\,\zeta_4\,H_{4,3} + 25664\,\zeta_3\,H_{4,4} + 31744\,\zeta_2\,H_{4,5} + 10944\,\zeta_2\,\zeta_3\,H_{5,0} + 5376\,\zeta_5\,H_{5,0}\\
&+ 14208\,\zeta_2\,\zeta_3\,H_{5,1} + 15936\,\zeta_5\,H_{5,1} + 38400\,\zeta_4\,H_{5,2} + 32064\,\zeta_3\,H_{5,3} + 36864\,\zeta_2\,H_{5,4}\\
&+ 56232\,\zeta_4\,H_{6,0} + 36960\,\zeta_4\,H_{6,1} + 38976\,\zeta_3\,H_{6,2} + 40128\,\zeta_2\,H_{6,3} + 22400\,\zeta_3\,H_{7,0}\\
&+ 45248\,\zeta_3\,H_{7,1} + 39424\,\zeta_2\,H_{7,2} + 67712\,\zeta_2\,H_{8,0} + 29568\,\zeta_2\,H_{8,1} + 84752\,H_{10,0}\\
&+ 736\,\zeta_2\,\zeta_3^2\,H_{0,0,0} + 608\,\zeta_3\,\zeta_5\,H_{0,0,0} + \frac{20012}{3}\,\zeta_8\,H_{0,0,0} + 4560\,\zeta_3\,\zeta_4\,H_{2,0,0}\\
&+ 1440\,\zeta_2\,\zeta_5\,H_{2,0,0} + 840\,\zeta_7\,H_{2,0,0} + 640\,\zeta_3^2\,H_{2,2,0} + 4080\,\zeta_6\,H_{2,2,0} + 3840\,\zeta_2\,\zeta_3\,H_{2,2,2}\\
&+ 5760\,\zeta_5\,H_{2,2,2} + 7680\,\zeta_4\,H_{2,2,3} + 7040\,\zeta_3\,H_{2,2,4} + 6400\,\zeta_2\,H_{2,2,5} + 3840\,\zeta_2\,\zeta_3\,H_{2,3,0}\\
&+ 2400\,\zeta_5\,H_{2,3,0} + 5760\,\zeta_2\,\zeta_3\,H_{2,3,1} + 8640\,\zeta_5\,H_{2,3,1} + 11520\,\zeta_4\,H_{2,3,2}\\
&+ 10560\,\zeta_3\,H_{2,3,3} + 9600\,\zeta_2\,H_{2,3,4} + 16560\,\zeta_4\,H_{2,4,0} + 11520\,\zeta_4\,H_{2,4,1}\\
&+ 14400\,\zeta_3\,H_{2,4,2} + 11520\,\zeta_2\,H_{2,4,3} + 7040\,\zeta_3\,H_{2,5,0} + 18560\,\zeta_3\,H_{2,5,1}\\
&+ 12160\,\zeta_2\,H_{2,5,2} + 18080\,\zeta_2\,H_{2,6,0} + 9600\,\zeta_2\,H_{2,6,1} + 21440\,H_{2,8,0}\\
&+ 768\,\zeta_3^2\,H_{3,0,0} + 15168\,\zeta_6\,H_{3,0,0} + 1024\,\zeta_3^2\,H_{3,1,0} + 6528\,\zeta_6\,H_{3,1,0}\\
&+ 6144\,\zeta_2\,\zeta_3\,H_{3,1,2} + 9216\,\zeta_5\,H_{3,1,2} + 12288\,\zeta_4\,H_{3,1,3} + 11264\,\zeta_3\,H_{3,1,4}\\
&+ 10240\,\zeta_2\,H_{3,1,5} + 6144\,\zeta_2\,\zeta_3\,H_{3,2,0} + 3840\,\zeta_5\,H_{3,2,0} + 9216\,\zeta_2\,\zeta_3\,H_{3,2,1}\\
&+ 13824\,\zeta_5\,H_{3,2,1} + 18432\,\zeta_4\,H_{3,2,2} + 16896\,\zeta_3\,H_{3,2,3} + 15360\,\zeta_2\,H_{3,2,4}\\
&+ 26496\,\zeta_4\,H_{3,3,0} + 18432\,\zeta_4\,H_{3,3,1} + 23040\,\zeta_3\,H_{3,3,2} + 18432\,\zeta_2\,H_{3,3,3}\\
&+ 11264\,\zeta_3\,H_{3,4,0} + 29696\,\zeta_3\,H_{3,4,1} + 19456\,\zeta_2\,H_{3,4,2} + 28928\,\zeta_2\,H_{3,5,0}\\
&+ 15360\,\zeta_2\,H_{3,5,1} + 34304\,H_{3,7,0} + 8128\,\zeta_2\,\zeta_3\,H_{4,0,0} + 3616\,\zeta_5\,H_{4,0,0}\\
&+ 6912\,\zeta_2\,\zeta_3\,H_{4,1,0} + 4320\,\zeta_5\,H_{4,1,0} + 10368\,\zeta_2\,\zeta_3\,H_{4,1,1} + 15552\,\zeta_5\,H_{4,1,1}\\
&+ 20736\,\zeta_4\,H_{4,1,2} + 19008\,\zeta_3\,H_{4,1,3} + 17280\,\zeta_2\,H_{4,1,4} + 32112\,\zeta_4\,H_{4,2,0}\\
&+ 20736\,\zeta_4\,H_{4,2,1} + 28992\,\zeta_3\,H_{4,2,2} + 22272\,\zeta_2\,H_{4,2,3} + 14656\,\zeta_3\,H_{4,3,0}\\
&+ 37504\,\zeta_3\,H_{4,3,1} + 23936\,\zeta_2\,H_{4,3,2} + 36544\,\zeta_2\,H_{4,4,0} + 18816\,\zeta_2\,H_{4,4,1}\\
&+ 43936\,H_{4,6,0} + 51360\,\zeta_4\,H_{5,0,0} + 33984\,\zeta_4\,H_{5,1,0} + 18432\,\zeta_4\,H_{5,1,1}\\
&+ 33024\,\zeta_3\,H_{5,1,2} + 23424\,\zeta_2\,H_{5,1,3} + 18048\,\zeta_3\,H_{5,2,0} + 43008\,\zeta_3\,H_{5,2,1}\\
&+ 26112\,\zeta_2\,H_{5,2,2} + 42432\,\zeta_2\,H_{5,3,0} + 20352\,\zeta_2\,H_{5,3,1} + 52512\,H_{5,5,0}\\
&+ 15776\,\zeta_3\,H_{6,0,0} + 21120\,\zeta_3\,H_{6,1,0} + 44160\,\zeta_3\,H_{6,1,1} + 24960\,\zeta_2\,H_{6,1,2}\\
&+ 46368\,\zeta_2\,H_{6,2,0} + 19200\,\zeta_2\,H_{6,2,1} + 60576\,H_{6,4,0} + 66976\,\zeta_2\,H_{7,0,0}\\
&+ 46144\,\zeta_2\,H_{7,1,0} + 13440\,\zeta_2\,H_{7,1,1} + 66976\,H_{7,3,0} + 67712\,H_{8,2,0}\\
&+ 105856\,H_{9,0,0} + 52928\,H_{9,1,0} + 8688\,\zeta_3\,\zeta_4\,H_{0,0,0,0} + 2064\,\zeta_2\,\zeta_5\,H_{0,0,0,0}\\
&+ 792\,\zeta_7\,H_{0,0,0,0} + 480\,\zeta_3^2\,H_{2,0,0,0} + 9480\,\zeta_6\,H_{2,0,0,0} + 2560\,\zeta_2\,\zeta_3\,H_{2,2,0,0}\\
&+ 1600\,\zeta_5\,H_{2,2,0,0} + 5760\,\zeta_4\,H_{2,2,2,0} + 7680\,\zeta_3\,H_{2,2,2,2} + 3840\,\zeta_2\,H_{2,2,2,3}\\
&+ 2560\,\zeta_3\,H_{2,2,3,0} + 10240\,\zeta_3\,H_{2,2,3,1} + 5120\,\zeta_2\,H_{2,2,3,2} + 6400\,\zeta_2\,H_{2,2,4,0}\\
&+ 3840\,\zeta_2\,H_{2,2,4,1} + 7360\,H_{2,2,6,0} + 13680\,\zeta_4\,H_{2,3,0,0} + 8640\,\zeta_4\,H_{2,3,1,0}\\
&+ 11520\,\zeta_3\,H_{2,3,1,2} + 5760\,\zeta_2\,H_{2,3,1,3} + 3840\,\zeta_3\,H_{2,3,2,0} + 15360\,\zeta_3\,H_{2,3,2,1}\\
&+ 7680\,\zeta_2\,H_{2,3,2,2} + 9600\,\zeta_2\,H_{2,3,3,0} + 5760\,\zeta_2\,H_{2,3,3,1} + 11040\,H_{2,3,5,0}
\end{aligned}
$$

JHEP11(2012)058

$$
\begin{aligned}
&+ 4480\,\zeta_3\,H_{2,4,0,0} + 3840\,\zeta_3\,H_{2,4,1,0} + 15360\,\zeta_3\,H_{2,4,1,1} + 7680\,\zeta_2\,H_{2,4,1,2}\\
&+ 11520\,\zeta_2\,H_{2,4,2,0} + 5760\,\zeta_2\,H_{2,4,2,1} + 13920\,H_{2,4,4,0} + 16480\,\zeta_2\,H_{2,5,0,0}\\
&+ 12160\,\zeta_2\,H_{2,5,1,0} + 3840\,\zeta_2\,H_{2,5,1,1} + 16480\,H_{2,5,3,0} + 18080\,H_{2,6,2,0}\\
&+ 23520\,H_{2,7,0,0} + 15680\,H_{2,7,1,0} + 5888\,\zeta_2\,\zeta_3\,H_{3,0,0,0} + 2432\,\zeta_5\,H_{3,0,0,0}\\
&+ 4096\,\zeta_2\,\zeta_3\,H_{3,1,0,0} + 2560\,\zeta_5\,H_{3,1,0,0} + 9216\,\zeta_4\,H_{3,1,2,0} + 12288\,\zeta_3\,H_{3,1,2,2}\\
&+ 6144\,\zeta_2\,H_{3,1,2,3} + 4096\,\zeta_3\,H_{3,1,3,0} + 16384\,\zeta_3\,H_{3,1,3,1} + 8192\,\zeta_2\,H_{3,1,3,2}\\
&+ 10240\,\zeta_2\,H_{3,1,4,0} + 6144\,\zeta_2\,H_{3,1,4,1} + 11776\,H_{3,1,6,0} + 21888\,\zeta_4\,H_{3,2,0,0}\\
&+ 13824\,\zeta_4\,H_{3,2,1,0} + 18432\,\zeta_3\,H_{3,2,1,2} + 9216\,\zeta_2\,H_{3,2,1,3} + 6144\,\zeta_3\,H_{3,2,2,0}\\
&+ 24576\,\zeta_3\,H_{3,2,2,1} + 12288\,\zeta_2\,H_{3,2,2,2} + 15360\,\zeta_2\,H_{3,2,3,0} + 9216\,\zeta_2\,H_{3,2,3,1}\\
&+ 17664\,H_{3,2,5,0} + 7168\,\zeta_3\,H_{3,3,0,0} + 6144\,\zeta_3\,H_{3,3,1,0} + 24576\,\zeta_3\,H_{3,3,1,1}\\
&+ 12288\,\zeta_2\,H_{3,3,1,2} + 18432\,\zeta_2\,H_{3,3,2,0} + 9216\,\zeta_2\,H_{3,3,2,1} + 22272\,H_{3,3,4,0}\\
&+ 26368\,\zeta_2\,H_{3,4,0,0} + 19456\,\zeta_2\,H_{3,4,1,0} + 6144\,\zeta_2\,H_{3,4,1,1} + 26368\,H_{3,4,3,0}\\
&+ 28928\,H_{3,5,2,0} + 37632\,H_{3,6,0,0} + 25088\,H_{3,6,1,0} + 44064\,\zeta_4\,H_{4,0,0,0}\\
&+ 24624\,\zeta_4\,H_{4,1,0,0} + 15552\,\zeta_4\,H_{4,1,1,0} + 20736\,\zeta_3\,H_{4,1,1,2} + 10368\,\zeta_2\,H_{4,1,1,3}\\
&+ 6912\,\zeta_3\,H_{4,1,2,0} + 27648\,\zeta_3\,H_{4,1,2,1} + 13824\,\zeta_2\,H_{4,1,2,2} + 17280\,\zeta_2\,H_{4,1,3,0}\\
&+ 10368\,\zeta_2\,H_{4,1,3,1} + 19872\,H_{4,1,5,0} + 9472\,\zeta_3\,H_{4,2,0,0} + 6912\,\zeta_3\,H_{4,2,1,0}\\
&+ 27648\,\zeta_3\,H_{4,2,1,1} + 13824\,\zeta_2\,H_{4,2,1,2} + 22272\,\zeta_2\,H_{4,2,2,0} + 10368\,\zeta_2\,H_{4,2,2,1}\\
&+ 27552\,H_{4,2,4,0} + 33152\,\zeta_2\,H_{4,3,0,0} + 23936\,\zeta_2\,H_{4,3,1,0} + 6912\,\zeta_2\,H_{4,3,1,1}\\
&+ 33152\,H_{4,3,3,0} + 36544\,H_{4,4,2,0} + 47936\,H_{4,5,0,0} + 31744\,H_{4,5,1,0}\\
&+ 11264\,\zeta_3\,H_{5,0,0,0} + 11968\,\zeta_3\,H_{5,1,0,0} + 6144\,\zeta_3\,H_{5,1,1,0} + 24576\,\zeta_3\,H_{5,1,1,1}\\
&+ 12288\,\zeta_2\,H_{5,1,1,2} + 23424\,\zeta_2\,H_{5,1,2,0} + 9216\,\zeta_2\,H_{5,1,2,1} + 30720\,H_{5,1,4,0}\\
&+ 38208\,\zeta_2\,H_{5,2,0,0} + 26112\,\zeta_2\,H_{5,2,1,0} + 6144\,\zeta_2\,H_{5,2,1,1} + 38208\,H_{5,2,3,0}\\
&+ 42432\,H_{5,3,2,0} + 56896\,H_{5,4,0,0} + 36864\,H_{5,4,1,0} + 60576\,\zeta_2\,H_{6,0,0,0}\\
&+ 40800\,\zeta_2\,H_{6,1,0,0} + 24960\,\zeta_2\,H_{6,1,1,0} + 3840\,\zeta_2\,H_{6,1,1,1} + 40800\,H_{6,1,3,0}\\
&+ 46368\,H_{6,2,2,0} + 65248\,H_{6,3,0,0} + 40128\,H_{6,3,1,0} + 46144\,H_{7,1,2,0}\\
&+ 72128\,H_{7,2,0,0} + 39424\,H_{7,2,1,0} + 102640\,H_{8,0,0,0} + 73920\,H_{8,1,0,0}\\
&+ 29568\,H_{8,1,1,0} + 736\,\zeta_3^2\,H_{0,0,0,0,0} + 27736\,\zeta_6\,H_{0,0,0,0,0} + 3680\,\zeta_2\,\zeta_3\,H_{2,0,0,0,0}\\
&+ 1520\,\zeta_5\,H_{2,0,0,0,0} + 9120\,\zeta_4\,H_{2,2,0,0,0} + 1920\,\zeta_3\,H_{2,2,2,0,0} + 3840\,\zeta_2\,H_{2,2,2,2,0}\\
&+ 3840\,H_{2,2,2,4,0} + 5120\,\zeta_2\,H_{2,2,3,0,0} + 5120\,\zeta_2\,H_{2,2,3,1,0} + 5120\,H_{2,2,3,3,0}\\
&+ 6400\,H_{2,2,4,2,0} + 6400\,H_{2,2,5,0,0} + 6400\,H_{2,2,5,1,0} + 2880\,\zeta_3\,H_{2,3,0,0,0}\\
&+ 2880\,\zeta_3\,H_{2,3,1,0,0} + 5760\,\zeta_2\,H_{2,3,1,2,0} + 5760\,H_{2,3,1,4,0} + 7680\,\zeta_2\,H_{2,3,2,0,0}\\
&+ 7680\,\zeta_2\,H_{2,3,2,1,0} + 7680\,H_{2,3,2,3,0} + 9600\,H_{2,3,3,2,0} + 9600\,H_{2,3,4,0,0}\\
&+ 9600\,H_{2,3,4,1,0} + 13920\,\zeta_2\,H_{2,4,0,0,0} + 7680\,\zeta_2\,H_{2,4,1,0,0} + 7680\,\zeta_2\,H_{2,4,1,1,0}\\
&+ 7680\,H_{2,4,1,3,0} + 11520\,H_{2,4,2,2,0} + 11840\,H_{2,4,3,0,0} + 11520\,H_{2,4,3,1,0}\\
&+ 12160\,H_{2,5,1,2,0} + 13760\,H_{2,5,2,0,0} + 12160\,H_{2,5,2,1,0} + 20800\,H_{2,6,0,0,0}\\
&+ 14400\,H_{2,6,1,0,0} + 9600\,H_{2,6,1,1,0} + 34752\,\zeta_4\,H_{3,0,0,0,0} + 14592\,\zeta_4\,H_{3,1,0,0,0}\\
&+ 3072\,\zeta_3\,H_{3,1,2,0,0} + 6144\,\zeta_2\,H_{3,1,2,2,0} + 6144\,H_{3,1,2,4,0} + 8192\,\zeta_2\,H_{3,1,3,0,0}\\
&+ 8192\,\zeta_2\,H_{3,1,3,1,0} + 8192\,H_{3,1,3,3,0} + 10240\,H_{3,1,4,2,0} + 10240\,H_{3,1,5,0,0}\\
&+ 10240\,H_{3,1,5,1,0} + 4608\,\zeta_3\,H_{3,2,0,0,0} + 4608\,\zeta_3\,H_{3,2,1,0,0} + 9216\,\zeta_2\,H_{3,2,1,2,0}
\end{aligned}
$$

JHEP11(2012)058

$$+ 9216\, H_{3,2,1,4,0} + 12288\, \zeta_2\, H_{3,2,2,0,0} + 12288\, \zeta_2\, H_{3,2,2,1,0} + 12288\, H_{3,2,2,3,0}$$
$$+ 15360\, H_{3,2,3,2,0} + 15360\, H_{3,2,4,0,0} + 15360\, H_{3,2,4,1,0} + 22272\, \zeta_2\, H_{3,3,0,0,0}$$
$$+ 12288\, \zeta_2\, H_{3,3,1,0,0} + 12288\, \zeta_2\, H_{3,3,1,1,0} + 12288\, H_{3,3,1,3,0} + 18432\, H_{3,3,2,2,0}$$
$$+ 18944\, H_{3,3,3,0,0} + 18432\, H_{3,3,3,1,0} + 19456\, H_{3,4,1,2,0} + 22016\, H_{3,4,2,0,0}$$
$$+ 19456\, H_{3,4,2,1,0} + 33280\, H_{3,5,0,0,0} + 23040\, H_{3,5,1,0,0} + 15360\, H_{3,5,1,1,0}$$
$$+ 8192\, \zeta_3\, H_{4,0,0,0,0} + 5184\, \zeta_3\, H_{4,1,0,0,0} + 5184\, \zeta_3\, H_{4,1,1,0,0} + 10368\, \zeta_2\, H_{4,1,1,2,0}$$
$$+ 10368\, H_{4,1,1,4,0} + 13824\, \zeta_2\, H_{4,1,2,0,0} + 13824\, \zeta_2\, H_{4,1,2,1,0} + 13824\, H_{4,1,2,3,0}$$
$$+ 17280\, H_{4,1,3,2,0} + 17280\, H_{4,1,4,0,0} + 17280\, H_{4,1,4,1,0} + 27552\, \zeta_2\, H_{4,2,0,0,0}$$
$$+ 13824\, \zeta_2\, H_{4,2,1,0,0} + 13824\, \zeta_2\, H_{4,2,1,1,0} + 13824\, H_{4,2,1,3,0} + 22272\, H_{4,2,2,2,0}$$
$$+ 23360\, H_{4,2,3,0,0} + 22272\, H_{4,2,3,1,0} + 23936\, H_{4,3,1,2,0} + 27712\, H_{4,3,2,0,0}$$
$$+ 23936\, H_{4,3,2,1,0} + 42368\, H_{4,4,0,0,0} + 28608\, H_{4,4,1,0,0} + 18816\, H_{4,4,1,1,0}$$
$$+ 52512\, \zeta_2\, H_{5,0,0,0,0} + 30720\, \zeta_2\, H_{5,1,0,0,0} + 12288\, \zeta_2\, H_{5,1,1,0,0} + 12288\, \zeta_2\, H_{5,1,1,1,0}$$
$$+ 12288\, H_{5,1,1,3,0} + 23424\, H_{5,1,2,2,0} + 26048\, H_{5,1,3,0,0} + 23424\, H_{5,1,3,1,0}$$
$$+ 26112\, H_{5,2,1,2,0} + 32256\, H_{5,2,2,0,0} + 26112\, H_{5,2,2,1,0} + 50304\, H_{5,3,0,0,0}$$
$$+ 32448\, H_{5,3,1,0,0} + 20352\, H_{5,3,1,1,0} + 24960\, H_{6,1,1,2,0} + 35520\, H_{6,1,2,0,0}$$
$$+ 24960\, H_{6,1,2,1,0} + 57792\, H_{6,2,0,0,0} + 34560\, H_{6,2,1,0,0} + 19200\, H_{6,2,1,1,0}$$
$$+ 91392\, H_{7,0,0,0,0} + 64064\, H_{7,1,0,0,0} + 33600\, H_{7,1,1,0,0} + 13440\, H_{7,1,1,1,0}$$
$$+ 8576\, \zeta_2\, \zeta_3\, H_{0,0,0,0,0,0} + 2672\, \zeta_5\, H_{0,0,0,0,0,0} + 21720\, \zeta_4\, H_{2,0,0,0,0,0}$$
$$+ 3840\, \zeta_2\, H_{2,2,2,0,0,0} + 3840\, H_{2,2,2,2,2,0} + 1920\, H_{2,2,2,3,0,0} + 3840\, H_{2,2,2,3,1,0}$$
$$+ 5120\, H_{2,2,3,1,2,0} + 2560\, H_{2,2,3,2,0,0} + 5120\, H_{2,2,3,2,1,0} + 5120\, H_{2,2,4,0,0,0}$$
$$+ 1920\, H_{2,2,4,1,0,0} + 3840\, H_{2,2,4,1,1,0} + 11040\, \zeta_2\, H_{2,3,0,0,0,0} + 5760\, \zeta_2\, H_{2,3,1,0,0,0}$$
$$+ 1920\, \zeta_3\, H_{2,2,0,0,0,0} + 5760\, H_{2,3,1,2,2,0} + 2880\, H_{2,3,1,3,0,0} + 5760\, H_{2,3,1,3,1,0}$$
$$+ 7680\, H_{2,3,2,1,2,0} + 3840\, H_{2,3,2,2,0,0} + 7680\, H_{2,3,2,2,1,0} + 7680\, H_{2,3,3,0,0,0}$$
$$+ 2880\, H_{2,3,3,1,0,0} + 5760\, H_{2,3,3,1,1,0} + 7680\, H_{2,4,1,1,2,0} + 3840\, H_{2,4,1,2,0,0}$$
$$+ 7680\, H_{2,4,1,2,1,0} + 9600\, H_{2,4,2,0,0,0} + 2880\, H_{2,4,2,1,0,0} + 5760\, H_{2,4,2,1,1,0}$$
$$+ 17280\, H_{2,5,0,0,0,0} + 11360\, H_{2,5,1,0,0,0} + 1920\, H_{2,5,1,1,0,0} + 3840\, H_{2,5,1,1,1,0}$$
$$+ 5888\, \zeta_3\, H_{3,0,0,0,0,0} + 3072\, \zeta_3\, H_{3,1,0,0,0,0} + 6144\, \zeta_2\, H_{3,1,2,0,0,0} + 6144\, H_{3,1,2,2,2,0}$$
$$+ 3072\, H_{3,1,2,3,0,0} + 6144\, H_{3,1,2,3,1,0} + 8192\, H_{3,1,3,1,2,0} + 4096\, H_{3,1,3,2,0,0}$$
$$+ 8192\, H_{3,1,3,2,1,0} + 8192\, H_{3,1,4,0,0,0} + 3072\, H_{3,1,4,1,0,0} + 6144\, H_{3,1,4,1,1,0}$$
$$+ 17664\, \zeta_2\, H_{3,2,0,0,0,0} + 9216\, \zeta_2\, H_{3,2,1,0,0,0} + 9216\, H_{3,2,1,2,2,0} + 4608\, H_{3,2,1,3,0,0}$$
$$+ 9216\, H_{3,2,1,3,1,0} + 12288\, H_{3,2,2,1,2,0} + 6144\, H_{3,2,2,2,0,0} + 12288\, H_{3,2,2,2,1,0}$$
$$+ 12288\, H_{3,2,3,0,0,0} + 4608\, H_{3,2,3,1,0,0} + 9216\, H_{3,2,3,1,1,0} + 12288\, H_{3,3,1,1,2,0}$$
$$+ 6144\, H_{3,3,1,2,0,0} + 12288\, H_{3,3,1,2,1,0} + 15360\, H_{3,3,2,0,0,0} + 4608\, H_{3,3,2,1,0,0}$$
$$+ 9216\, H_{3,3,2,1,1,0} + 27648\, H_{3,4,0,0,0,0} + 18176\, H_{3,4,1,0,0,0} + 3072\, H_{3,4,1,1,0,0}$$
$$+ 6144\, H_{3,4,1,1,1,0} + 43936\, \zeta_2\, H_{4,0,0,0,0,0} + 19872\, \zeta_2\, H_{4,1,0,0,0,0} + 10368\, \zeta_2\, H_{4,1,1,0,0,0}$$
$$+ 10368\, H_{4,1,1,2,2,0} + 5184\, H_{4,1,1,3,0,0} + 10368\, H_{4,1,1,3,1,0} + 13824\, H_{4,1,2,1,2,0}$$
$$+ 6912\, H_{4,1,2,2,0,0} + 13824\, H_{4,1,2,2,1,0} + 13824\, H_{4,1,3,0,0,0} + 5184\, H_{4,1,3,1,0,0}$$
$$+ 10368\, H_{4,1,3,1,1,0} + 13824\, H_{4,2,1,1,2,0} + 6912\, H_{4,2,1,2,0,0} + 13824\, H_{4,2,1,2,1,0}$$
$$+ 19008\, H_{4,2,2,0,0,0} + 5184\, H_{4,2,2,1,0,0} + 10368\, H_{4,2,2,1,1,0} + 35040\, H_{4,3,0,0,0,0}$$

JHEP11(2012)058

$$
\begin{aligned}
&+ 22912\, H_{4,3,1,0,0,0} + 3456\, H_{4,3,1,1,0,0} + 6912\, H_{4,3,1,1,1,0} + 12288\, H_{5,1,1,1,2,0} \\
&+ 6144\, H_{5,1,1,2,0,0} + 12288\, H_{5,1,1,2,1,0} + 21312\, H_{5,1,2,0,0,0} + 4608\, H_{5,1,2,1,0,0} \\
&+ 9216\, H_{5,1,2,1,1,0} + 41280\, H_{5,2,0,0,0,0} + 26688\, H_{5,2,1,0,0,0} + 3072\, H_{5,2,1,1,0,0} \\
&+ 6144\, H_{5,2,1,1,1,0} + 78656\, H_{6,0,0,0,0,0} + 46080\, H_{6,1,0,0,0,0} + 29280\, H_{6,1,1,0,0,0} \\
&+ 1920\, H_{6,1,1,1,0,0} + 3840\, H_{6,1,1,1,1,0} + 72000\, \zeta_4\, H_{0,0,0,0,0,0,0} + 3680\, \zeta_3\, H_{2,0,0,0,0,0,0} \\
&+ 7360\, \zeta_2\, H_{2,2,0,0,0,0,0} + 1920\, H_{2,2,2,2,0,0,0} + 3840\, H_{2,2,3,0,0,0,0} + 2560\, H_{2,2,3,1,0,0,0} \\
&+ 2880\, H_{2,3,1,2,0,0,0} + 5760\, H_{2,3,2,0,0,0,0} + 3840\, H_{2,3,2,1,0,0,0} + 14080\, H_{2,4,0,0,0,0,0} \\
&+ 5760\, H_{2,4,1,0,0,0,0} + 3840\, H_{2,4,1,1,0,0,0} + 34304\, \zeta_2\, H_{3,0,0,0,0,0,0} + 11776\, \zeta_2\, H_{3,1,0,0,0,0,0} \\
&+ 3072\, H_{3,1,2,2,0,0,0} + 6144\, H_{3,1,3,0,0,0,0} + 4096\, H_{3,1,3,1,0,0,0} + 4608\, H_{3,2,1,2,0,0,0} \\
&+ 9216\, H_{3,2,2,0,0,0,0} + 6144\, H_{3,2,2,1,0,0,0} + 22528\, H_{3,3,0,0,0,0,0} + 9216\, H_{3,3,1,0,0,0,0} \\
&+ 6144\, H_{3,3,1,1,0,0,0} + 5184\, H_{4,1,1,2,0,0,0} + 10368\, H_{4,1,2,0,0,0,0} + 6912\, H_{4,1,2,1,0,0,0} \\
&+ 28096\, H_{4,2,0,0,0,0,0} + 10368\, H_{4,2,1,0,0,0,0} + 6912\, H_{4,2,1,1,0,0,0} + 66560\, H_{5,0,0,0,0,0,0} \\
&+ 32032\, H_{5,1,0,0,0,0,0} + 9216\, H_{5,1,1,0,0,0,0} + 6144\, H_{5,1,1,1,0,0,0} \\
&+ 10720\, \zeta_3\, H_{0,0,0,0,0,0,0,0} + 21440\, \zeta_2\, H_{2,0,0,0,0,0,0,0} + 2880\, H_{2,2,2,0,0,0,0,0} \\
&+ 11040\, H_{2,3,0,0,0,0,0,0} + 4320\, H_{2,3,1,0,0,0,0,0} + 4608\, H_{3,1,2,0,0,0,0,0} \\
&+ 17664\, H_{3,2,0,0,0,0,0,0} + 6912\, H_{3,2,1,0,0,0,0,0} + 55104\, H_{4,0,0,0,0,0,0,0} \\
&+ 19872\, H_{4,1,0,0,0,0,0,0} + 7776\, H_{4,1,1,0,0,0,0,0} + 84752\, \zeta_2\, H_{0,0,0,0,0,0,0,0,0} \\
&+ 7360\, H_{2,2,0,0,0,0,0,0,0} + 42880\, H_{3,0,0,0,0,0,0,0,0} + 11776\, H_{3,1,0,0,0,0,0,0,0} \\
&+ 26800\, H_{2,0,0,0,0,0,0,0,0,0} + 127128\, H_{0,0,0,0,0,0,0,0,0,0,0} \,. \qquad \text{(D.1)}
\end{aligned}
$$

References

[1] A.M. Polyakov, *Gauge fields as rings of glue*, *Nucl. Phys.* **B 164** (1980) 171 [INSPIRE].

[2] G. Korchemsky and A. Radyushkin, *Renormalization of the Wilson loops beyond the leading order*, *Nucl. Phys.* **B 283** (1987) 342 [INSPIRE].

[3] N. Kidonakis, *Two-loop soft anomalous dimensions and NNLL resummation for heavy quark production*, *Phys. Rev. Lett.* **102** (2009) 232003 [arXiv:0903.2561] [INSPIRE].

[4] J.M. Maldacena, *Wilson loops in large-N field theories*, *Phys. Rev. Lett.* **80** (1998) 4859 [hep-th/9803002] [INSPIRE].

[5] S.-J. Rey and J.-T. Yee, *Macroscopic strings as heavy quarks in large-N gauge theory and Anti-de Sitter supergravity*, *Eur. Phys. J.* **C 22** (2001) 379 [hep-th/9803001] [INSPIRE].

[6] Y. Makeenko, P. Olesen and G.W. Semenoff, *Cusped SYM Wilson loop at two loops and beyond*, *Nucl. Phys.* **B 748** (2006) 170 [hep-th/0602100] [INSPIRE].

[7] N. Drukker and V. Forini, *Generalized quark-antiquark potential at weak and strong coupling*, *JHEP* **06** (2011) 131 [arXiv:1105.5144] [INSPIRE].

[8] D. Correa, J. Henn, J. Maldacena and A. Sever, *An exact formula for the radiation of a moving quark in $N = 4$ super Yang-Mills*, *JHEP* **06** (2012) 048 [arXiv:1202.4455] [INSPIRE].

[9] B. Fiol, B. Garolera and A. Lewkowycz, *Exact results for static and radiative fields of a quark in $N = 4$ super Yang-Mills*, *JHEP* **05** (2012) 093 [arXiv:1202.5292] [INSPIRE].

JHEP11(2012)058

[10] D. Correa, J. Henn, J. Maldacena and A. Sever, *The cusp anomalous dimension at three loops and beyond*, *JHEP* **05** (2012) 098 [arXiv:1203.1019] [INSPIRE].

[11] J.M. Henn, S.G. Naculich, H.J. Schnitzer and M. Spradlin, *Higgs-regularized three-loop four-gluon amplitude in $N = 4$ SYM: exponentiation and Regge limits*, *JHEP* **04** (2010) 038 [arXiv:1001.1358] [INSPIRE].

[12] N. Arkani-Hamed, J.L. Bourjaily, F. Cachazo, S. Caron-Huot and J. Trnka, *The all-loop integrand for scattering amplitudes in planar $N = 4$ SYM*, *JHEP* **01** (2011) 041 [arXiv:1008.2958] [INSPIRE].

[13] J.L. Bourjaily, A. DiRe, A. Shaikh, M. Spradlin and A. Volovich, *The soft-collinear bootstrap: $N = 4$ Yang-Mills amplitudes at six and seven loops*, *JHEP* **03** (2012) 032 [arXiv:1112.6432] [INSPIRE].

[14] B. Eden, P. Heslop, G.P. Korchemsky and E. Sokatchev, *Constructing the correlation function of four stress-tensor multiplets and the four-particle amplitude in $N = 4$ SYM*, *Nucl. Phys.* **B 862** (2012) 450 [arXiv:1201.5329] [INSPIRE].

[15] L.F. Alday, J.M. Henn, J. Plefka and T. Schuster, *Scattering into the fifth dimension of $N = 4$ super Yang-Mills*, *JHEP* **01** (2010) 077 [arXiv:0908.0684] [INSPIRE].

[16] D. Correa, J. Maldacena and A. Sever, *The quark anti-quark potential and the cusp anomalous dimension from a TBA equation*, *JHEP* **08** (2012) 134 [arXiv:1203.1913] [INSPIRE].

[17] N. Drukker, *Integrable Wilson loops*, arXiv:1203.1617 [INSPIRE].

[18] L.J. Dixon, J.M. Drummond and J.M. Henn, *Bootstrapping the three-loop hexagon*, *JHEP* **11** (2011) 023 [arXiv:1108.4461] [INSPIRE].

[19] S. Caron-Huot and S. He, *Jumpstarting the all-loop S-matrix of planar $N = 4$ super Yang-Mills*, *JHEP* **07** (2012) 174 [arXiv:1112.1060] [INSPIRE].

[20] L.J. Dixon, C. Duhr and J. Pennington, *Single-valued harmonic polylogarithms and the multi-Regge limit*, *JHEP* **10** (2012) 074 [arXiv:1207.0186] [INSPIRE].

[21] E. Remiddi and J. Vermaseren, *Harmonic polylogarithms*, *Int. J. Mod. Phys.* **A 15** (2000) 725 [hep-ph/9905237] [INSPIRE].

[22] J. Erickson, G. Semenoff, R. Szabo and K. Zarembo, *Static potential in $N = 4$ supersymmetric Yang-Mills theory*, *Phys. Rev.* **D 61** (2000) 105006 [hep-th/9911088] [INSPIRE].

[23] D. Bykov, K. Zarembo and K. Zarembo, *Ladders for Wilson loops beyond leading order*, *JHEP* **09** (2012) 057 [arXiv:1206.7117] [INSPIRE].

[24] F.C.S. Brown, *Multiple zeta values and periods of moduli spaces $\mathfrak{M}_{0,n}$*, math/0606419.

[25] A.B. Goncharov, *A simple construction of grassmannian polylogarithms*, arXiv:0908.2238.

[26] A.B. Goncharov, *Multiple polylogarithms, cyclotomy and modular complexes*, *Math. Res. Lett.* **5** (1998) 497.

[27] J. Blumlein, D. Broadhurst and J. Vermaseren, *The multiple zeta value data mine*, *Comput. Phys. Commun.* **181** (2010) 582 [arXiv:0907.2557] [INSPIRE].

[28] D. Maître, *HPL, a Mathematica implementation of the harmonic polylogarithms*, *Comput. Phys. Commun.* **174** (2006) 222 [hep-ph/0507152] [INSPIRE].

JHEP11(2012)058

[29] A. Isaev, *Multiloop Feynman integrals and conformal quantum mechanics*, *Nucl. Phys.* **B 662** (2003) 461 [hep-th/0303056] [INSPIRE].

[30] N. Beisert, B. Eden and M. Staudacher, *Transcendentality and crossing*, *J. Stat. Mech.* **0701** (2007) P01021 [hep-th/0610251] [INSPIRE].

[31] L.J. Dixon, E. Gardi and L. Magnea, *On soft singularities at three loops and beyond*, *JHEP* **02** (2010) 081 [arXiv:0910.3653] [INSPIRE].

[32] B. Eden, P.S. Howe, C. Schubert, E. Sokatchev and P.C. West, *Simplifications of four point functions in $N = 4$ supersymmetric Yang-Mills theory at two loops*, *Phys. Lett.* **B 466** (1999) 20 [hep-th/9906051] [INSPIRE].

[33] N. Beisert, C. Kristjansen, J. Plefka, G. Semenoff and M. Staudacher, *BMN correlators and operator mixing in $N = 4$ super Yang-Mills theory*, *Nucl. Phys.* **B 650** (2003) 125 [hep-th/0208178] [INSPIRE].

[34] G. Korchemsky and A. Radyushkin, *Infrared factorization, Wilson lines and the heavy quark limit*, *Phys. Lett.* **B 279** (1992) 359 [hep-ph/9203222] [INSPIRE].

JHEP11(2012)058

Published for SISSA by Springer

Received: June 16, 2013
Revised: September 2, 2013
Accepted: September 3, 2013
Published: September 26, 2013

The four-loop cusp anomalous dimension in $\mathcal{N} = 4$ super Yang-Mills and analytic integration techniques for Wilson line integrals

Johannes M. Henn[a] **and Tobias Huber**[b]

[a] *Institute for Advanced Study, Princeton, NJ 08540, U.S.A.*

[b] *Theoretische Physik 1, Naturwissenschaftlich-Technische Fakultät, Universität Siegen, Walter-Flex-Strasse 3, D-57068 Siegen, Germany*

E-mail: jmhenn@ias.edu, huber@tp1.physik.uni-siegen.de

Abstract: Correlation functions of Wilson lines are relevant for describing the infrared structure of scattering amplitudes. We develop a new method for evaluating a wide class of such Wilson line integrals, and apply it to the calculation of the velocity-dependent cusp anomalous dimension in maximally supersymmetric Yang-Mills theory. We compute the four-loop non-planar correction in a recently introduced scaling limit. Moreover, we derive the full planar four-loop result by means of an ansatz which is based on the structure of known analytic results. We determine the coefficients in this ansatz by making use of a relationship to massive scattering amplitudes. As a corollary, our analytical result confirms the four-loop value of the light-like cusp anomalous dimension. Finally, we use the available perturbative data, as well as insight from AdS/CFT, in order to extrapolate the leading order values at strong coupling. The latter agree within two per cent with the corresponding string theory result, over a wide range of parameters.

Keywords: Supersymmetric gauge theory, Scattering Amplitudes, Strong Coupling Expansion

ArXiv ePrint: 1304.6418

© SISSA 2013

doi:10.1007/JHEP09(2013)147

JHEP09(2013)147

Contents

1 Introduction **1**

2 Color structure to four loops **4**

3 Kinematics and integral functions **6**
3.1 Kinematical structure 6
3.2 Harmonic polylogarithms and symbols 7

4 Iterated Wilson line integrals, and non-planar result in scaling limit **8**
4.1 'd-log' forms for Wilson line integrals 8
4.2 Non-planar contribution to scaling limit 10

5 Planar calculation from massive scattering amplitude **13**
5.1 Assumptions and classification of HPLs 14
5.2 Asymptotic limit of Mellin-Barnes integrals 15
5.3 Planar result to four loops 16

6 Comparison to strong coupling via AdS/CFT **20**

7 Conclusion and outlook **21**

A Four-loop integrals and generalized cuts / leading singularities **23**

B Analytic continuation of Γ_{cusp} **24**

JHEP09(2013)147

1 Introduction

Wilson loops are very fundamental and important quantities in gauge theories. In this paper, our main focus will be on their relevance to the description of the infrared (IR) behavior of scattering amplitudes. We will consider the general massive case, from which the massless one can be obtained as a limit.

The appearance of Wilson loops in this problem is easy to understand. The infrared divergences in scattering amplitudes originate from soft regions of loop integration, for which one can employ the eikonal approximation. In this way, one finds that infrared divergences of a scattering process are given by a correlation function of Wilson lines, where the lines in position space point along the momenta of the scattered particles. However, in taking the eikonal limit, additional ultraviolet (UV) divergences are introduced. They are equivalent, up to a sign, to the original IR divergences. This allows one to regard the former as the UV anomalous dimension of Wilson line operators, whose renormalization properties are well understood [1–3]. Note that the latter depends on the color representation of the external particles and is in general a matrix in color space. It is known analytically to two

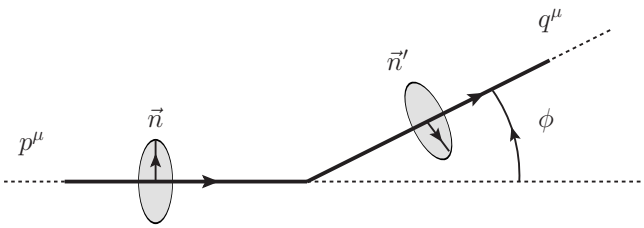

Figure 1. A Wilson line that makes a turn by an angle ϕ in Euclidean space. The two segments go along p^μ and q^μ, respectively. The vectors $\vec{n}$ and $\vec{n}'$ are internal vectors that determine the coupling to the six scalars $\vec{\Phi}$, see eq. (1.1).

loops [4]. The analysis of the general structure of this soft anomalous dimension matrix is of great interest, with recent studies involving the massless [5–9] and massive [10] case.

In the planar limit, the matrix factorizes into Wilson lines consisting of two segments. The cusp anomalous dimension associated to two Wilson lines is known in QCD to two loops [11], and in $\mathcal{N} = 4$ supersymmetric Yang-Mills (SYM) to three loops [12]. In this paper, we extend the calculation in planar $\mathcal{N} = 4$ SYM to four loops, and, in addition, compute the non-planar four-loop value in a special scaling limit.

The aim of this paper is to develop methods for the computation of such Wilson line correlators, planar and non-planar, and to deepen the understanding of the functions involved. This is closely related to ideas being discussed for understanding the loop corrections to scattering amplitudes. The functions that are typically encountered can be described by certain classes of iterated integrals. A key problem is to identify which specific class of functions is required to describe a given scattering process. It was found that integrals for scattering amplitudes or Wilson loops can be put into a 'd-log' form [13–15], where one can pull out an overall normalization factor, and the remaining integrand is a differential form. Moreover, such a representation suggests the existence of simple differential equations for the integrals. The latter also help to make the transcendentality properties of the integrals manifest. Recently, evidence was presented that integrals having such simple properties are not limited to supersymmetric theories, but can be present in generic $D = 4 - 2\epsilon$ dimensional integrals [16]. The Wilson line integrals considered in this paper can be considered as a special, simplifying limit of the more general scattering amplitude integrals. We will derive 'd-log' representations for a wide class of Wilson line integrals, relevant to the physical problems discussed above, and show how to compute them using differential equations.

The $\mathcal{N} = 4$ supersymmetric Yang-Mills (SYM) theory is a good testing ground for exploring such Wilson loops. For the specific Wilson loops studied in this paper, results can be obtained from various methods such as supersymmetric localization techniques or, in the planar case, integrability [17, 18]. The AdS/CFT conjecture also allows to compute Wilson loops at strong coupling.

In $\mathcal{N} = 4$ SYM, it is natural to define the locally supersymmetric Wilson loop operator [19, 20]

$$W \sim \mathrm{Tr}\left[P \exp\left(i \oint A^\mu \dot{x}_\mu + \oint |dx| \vec{n} \cdot \vec{\Phi}\right)\right] , \tag{1.1}$$

JHEP09(2013)147

where $\vec{n}$ is a vector on S^5. It parametrizes the coupling of the Wilson loop to the six scalars $\vec{\Phi}$. We consider as the integration contour a cusp formed by two segments along directions (momenta) p^μ and q^μ, and allow the two segments to couple to the scalars through $\vec{n}$ and $\vec{n}'$, see figure 1. Then, the vacuum expectation value $\langle W \rangle$ of the Wilson loop will depend on the angles

$$\cos\phi = \frac{p \cdot q}{\sqrt{p^2 q^2}}\,, \qquad \cos\theta = \vec{n} \cdot \vec{n}'\,, \tag{1.2}$$

as well as on the 't Hooft coupling $\lambda = g^2 N$, and the number of colors N.

If $\Lambda_{\rm UV}$ and $\Lambda_{\rm IR}$ are short and long distance cutoffs, respectively, then the divergent part of the vacuum expectation value of the Wilson loop takes the form [1, 2]

$$\langle W \rangle \sim \exp\left[-\log\frac{\Lambda_{\rm UV}}{\Lambda_{\rm IR}}\,\Gamma_{\rm cusp} + \ldots\right]. \tag{1.3}$$

This defines the cusp anomalous dimension $\Gamma_{\rm cusp}(\phi, \theta, \lambda, N)$.

Note that the dependence of $\Gamma_{\rm cusp}$ on θ is simple. It can only occur through Wick contractions of scalars, and because of SO(6) invariance it appears only through $\vec{n} \cdot \vec{n}' = \cos\theta$. Therefore, at L loops, $\Gamma_{\rm cusp}$ is a polynomial in $\cos\theta$, of maximal degree L. Having made this observation, we find it convenient to introduce the variable

$$\xi = \frac{\cos\theta - \cos\phi}{i\sin\phi}\,, \tag{1.4}$$

where the denominator was chosen for future convenience. When the geometric angle ϕ and internal angle θ satisfy $\phi = \pm\theta$, which corresponds to $\xi \to 0$, the anomalous dimension vanishes. Thus we expect the following structure in perturbation theory,

$$\Gamma_{\rm cusp}(\phi, \theta, \lambda, N) = \sum_{L=1}^{\infty}\left(\frac{\lambda}{8\pi^2}\right)^L \sum_{r=1}^{L} \xi^r\, \Gamma^{(L;r)}(\phi, 1/N^2)\,, \tag{1.5}$$

where $\lambda = g^2 N$ is the 't Hooft coupling, and g the Yang-Mills coupling. The sum over ξ^r starts from $r = 1$, since $\xi = 0$ corresponds to a supersymmetric configuration, for which $\Gamma_{\rm cusp}$ vanishes.

Note that $\Gamma_{\rm cusp}$ has non-planar corrections starting from four loops. We will discuss the full structure of the color dependence to four loops in sections 2 and 4.

The $r = 1$ term is known to all loop orders, including the non-planar corrections [21]. In this paper, we will compute the full planar result at four loops, for $\theta = 0$, as well as the non-planar contribution to $\Gamma^{(4;4)}$, which is the leading term in the scaling limit $\xi \to \infty$. This is done by analytically continuing θ and keeping ϕ as a free parameter. This scaling limit was introduced in ref. [21] and it was shown that it allows to describe the planar ladder diagrams in a simple way. This was further developed in [22, 23].

This paper is organized as follows. In section 2 we review the color dependence of $\Gamma_{\rm cusp}$ to four loops. In section 3 we explain the kinematics and give an overview of the functions that will appear in $\Gamma_{\rm cusp}$. In section 4 we discuss the structure of a class of Wilson line integrals and propose a systematic way of evaluating them. We then apply this to the

JHEP09(2013)147

non-planar correction to Γ_{cusp} in the scaling limit. In section 5 we give details on how we compute the planar Γ_{cusp} from a massive scattering amplitude, and give the result for the four-loop cusp anomalous dimension in the planar limit. In section 6 we compare our results to those at strong coupling. We conclude in section 7. There are two appendices. In appendix A we collect the contributing diagrams from the scattering amplitude and discuss their structure, while appendix B contains the analytic continuation of Γ_{cusp} to values beyond threshold.

2 Color structure to four loops

Here we discuss the color dependence of Γ_{cusp} to four loops. It is best understood using results from non-Abelian eikonal exponentiation [24, 25].

We start by setting up our conventions, following [26]. We consider a classical Lie-group with Lie-commutator

$$[T^a, T^b] = i f^{abc} T^c \,, \tag{2.1}$$

where the generators

$$T^a \,, \qquad a = 1, \ldots, N_A \tag{2.2}$$

are taken in the fundamental representation. f^{abc} are the structure constants of the Lie-algebra, and N_A is the number of generators of the group. The quadratic Casimir operators of the fundamental and adjoint representation of the Lie-algebra are

$$[T^a T^a]_{ij} = C_F \delta_{ij} \,, \qquad i, j = 1, \ldots, N_F \tag{2.3}$$

$$f^{acd} f^{bcd} = C_A \delta^{ab} \,, \tag{2.4}$$

respectively, where N_F is the dimension of the fundamental represenation. The fundamental generators are normalized by $\text{Tr}(T^a T^b) = T_F \delta^{ab}$.

The computation of color factors requires the evaluation of traces over products of generators. Up to three loops, at most six generators appear in the traces. Using the above equations, their result can be entirely expressed in terms of C_F and C_A (we normalize all color factors by $\text{Tr}[1_F] = N_F$), e.g. [26]

$$\text{Tr}(T^a T^b T^a T^b)/N_F = C_F (C_F - C_A/2) \,, \tag{2.5}$$

$$\text{Tr}(T^a T^b T^c T^a T^b T^c)/N_F = C_F (C_F - C_A)(C_F - C_A/2) \,. \tag{2.6}$$

At four loops the trace over a product of eight generators can — in general — not be expressed solely in terms of C_F and C_A, but higher group invariants are required. They can be expressed in terms of the following fully symmetrical tensors,

$$\begin{aligned} d_R^{abcd} = & \frac{1}{6} \text{Tr}[T_R^a T_R^b T_R^c T_R^d + T_R^a T_R^b T_R^d T_R^c + T_R^a T_R^c T_R^b T_R^d \\ & + T_R^a T_R^c T_R^d T_R^b + T_R^a T_R^d T_R^b T_R^c + T_R^a T_R^d T_R^c T_R^b] \,. \end{aligned} \tag{2.7}$$

JHEP09(2013)147

Here R can be either F or A for the fundamental and adjoint representation, respectively, with $[T_F^a]_{ij} \equiv [T^a]_{ij}$ and $[T_A^a]_{bc} = -if^{abc}$.

Using the Lie-commutator one can show that up to terms proportional to powers of C_F and C_A, $\mathrm{Tr}(T^aT^bT^cT^dT^aT^bT^cT^d)$ is given by $\mathrm{Tr}(T^aT^bT^cT^d)\mathrm{Tr}(T_A^aT_A^dT_A^cT_A^b)$, which in turn is related to $d_F^{abcd}d_A^{abcd}$, see table 11 of [26]. Explicitly, we have

$$\mathrm{Tr}(T^aT^bT^cT^dT^aT^bT^cT^d)/N_F = \frac{d_F^{abcd}d_A^{abcd}}{N_F} + C_F\left[C_F^3 - 3C_F^2C_A + \frac{11}{4}C_FC_A^2 - \frac{19}{24}C_A^3\right], \tag{2.8}$$

$$\frac{d_F^{abcd}d_A^{abcd}}{N_F} = \mathrm{Tr}(T^aT^bT^cT^d)\mathrm{Tr}(T_A^aT_A^dT_A^cT_A^b)/N_F - \frac{1}{12}C_FC_A^3\,. \tag{2.9}$$

For a general Lie-group the traces over four generators in eq. (2.9) cannot be expressed in terms of shorter traces which would lead to powers of C_F and/or C_A. Hence we can consider C_F, C_A and the quartic Casimir operator $d_F^{abcd}d_A^{abcd}/N_F$ as independent color structures at four loops, see ref. [27].

From [24, 25] it follows that Abelian-like terms containing powers of C_F cancel in Γ_{cusp}, thanks to the logarithm in its definition, see eq. (1.3). Moreover, an analysis of the possible color diagrams reveals that the result for Γ_{cusp} at one, two, and three loops is proportional to $C_F, C_FC_A, C_FC_A^2$, respectively. At four loops, two structures appear, which we choose to be $C_FC_A^3$ and the quartic Casimir operator $d_F^{abcd}d_A^{abcd}/N_F$.

In summary, we have, to four loops

$$\log\langle W\rangle = g^2C_Fw_1 + g^4C_FC_Aw_2 + g^6C_FC_A^2w_3 + g^8\left[C_FC_A^3w_{4a} + \frac{d_F^{abcd}d_A^{abcd}}{N_F}w_{4b}\right], \tag{2.10}$$

where we have chosen the normalization $\langle W\rangle = 1 + \mathcal{O}(g^2)$. We emphasize that hitherto all relations are group-independent and apply to any of the classical Lie-groups.

The *webs* w_i in (2.10) correspond to linear combinations of Feynman diagrams. The explicit expressions are easily obtained by the method of [24, 25]. One advantage of this formulation is that one can directly compute the logarithm of the Wilson loop correlator, and that each web only has an overall divergence.[1] The latter is easy to remove, so that in practice one can define Γ_{cusp} in terms of finite integrals.

We now specialize the Lie-group to SU(N), where all results can be explicitly written in terms of their dependence on N. With the standard normalization for the fundamental generators, we have $N_F = N$ and

$$T_F = \frac{1}{2}\,, \quad C_A = N\,, \quad C_F = \frac{N^2-1}{2N}\,, \quad N_A = N^2-1\,, \quad \frac{d_F^{abcd}d_A^{abcd}}{N_F} = \frac{(N^2-1)(N^2+6)}{48}\,. \tag{2.11}$$

Using eq. (2.11), we make the dependence on N of eq. (2.10) manifest. As discussed above, we have exactly one color structure up to three loops, and two contributions at four loops,

[1] We tacitly assume that the intrinsic renormalization of the bare parameters of the Lagrangian has already been carried out.

JHEP09(2013)147

which can now be distinguished thanks to their different dependence on N,

$$\log\langle W\rangle = g^2\frac{N^2-1}{2N}\left[w_1 + g^2 N w_2 + g^4 N^2 w_3 + g^6 N^3\left(w_{4a} + \frac{1}{24}w_{4b}\right) + g^6 N\frac{1}{4}w_{4b}\right]. \tag{2.12}$$

We see that in the large N limit, keeping $\lambda = g^2 N$ fixed, only the contribution $g^6 N\frac{1}{4}w_{4b}$ disappears from the R.H.S. of eq. (2.12). In other words, to three loops, it is sufficient to know the planar result for the Wilson loop in order to restore the full result in eq. (2.10). At four loops, an additional computation of the diagrams contributing to w_{4b} is required. In the remainder of this paper, we compute the non-planar contribution w_{4b} in a recently-introduced scaling limit, as well as the full planar result to four loops.

3 Kinematics and integral functions

As explained in the introduction, we will mainly be interested in the ϕ dependence of Γ_{cusp}. Here we discuss a convenient kinematical variable, and different physical regions. We also introduce a class of functions that we find appropriate to express the answer in, and discuss the branch cut structure of the latter.

3.1 Kinematical structure

It is convenient to introduce a new variable $x = e^{i\phi}$, which in general is complex. The computation we are considering is invariant under $\phi \to -\phi$. This corresponds to an inversion symmetry in x.

There are three different kinematical regions that we would like to discuss. It is useful to recall the relationship of Γ_{cusp} to IR divergences of scattering processes involving massive particles, such as $e^+(p) \to \gamma^* e^+(q)$, which have the same analytical structure. (See e.g. refs. [28, 29].) With the on-shell conditions $p^2 = q^2 = m^2$ (in the mostly-minus metric $+-\ldots-$), this process is naturally described using the variable s/m^2, where $s = (p-q)^2$. It is related to x via

$$x = \frac{\sqrt{1-4m^2/s}-1}{\sqrt{1-4m^2/s}+1}. \tag{3.1}$$

There we distinguish three kinematical regions, above threshold $s > 4m^2$, below threshold, $0 < s < 4m^2$, and finally the space-like region $s < 0$. They correspond to regions III, I , and II, respectively, that we now discuss from the Wilson loop viewpoint.

Region I: the first region corresponds to real ϕ, $\phi \in [0, \pi]$. This means that the absolute value of x is 1. In this case we have a cusp in Euclidean space, and Γ_{cusp} is real. The two limiting cases are the following: for $\phi = 0$ the contour is a straight line, and Γ_{cusp} vanishes (for $\theta = 0$). The first correction $\sim \phi^2$ in this small angle limit is known exactly in λ and N [21, 30]. The opposite limit $\phi \to \pi$ is related to the quark-antiquark potential. This limit is subtle and requires a resummation of certain diagrams, see [12, 22, 31–33]. One may also view the Wilson loop as the eikonal approximation to a form factor of massive quarks. In that case, this region corresponds to the region below the two-particle threshold.

JHEP09(2013)147

Region II: we can analytically continue ϕ to Minkowskian angles. In that case, x is real and positive. Because of the inversion symmetry $x \to 1/x$, it is sufficient to take $x \in [0,1]$. The second endpoint, $x = 1$, again corresponds to the case of a straight line discussed above. Near the endpoint $x \to 0$, on the other hand, the cusp anomalous dimension diverges linearly in $\log(x)$, to all orders in the coupling constant [11]. The coefficient of the linear divergence is the well-studied light-like cusp anomalous dimension; the latter can also be obtained from the anomalous dimension of high spin operators [34–36]. We may remark that the Wilson loop approach considered here is a very efficient way of computing this quantity.

Region III: finally, we have the region above the threshold of creating two massive particles. This region corresponds to x being real and negative. As before, it suffices to take $x \in [-1,0]$, because of the inversion symmetry in x. Γ_{cusp} has a branch cut along the negative real axis, and the $i0$ prescription in the propagators implies that x has a small imaginary part. For the mostly minus Minkowski-space metric that we are using, the position-space propagator connecting two segments of the Wilson loop is proportional to $(s^2 + t^2 + st(x + 1/x) - i0)^{-1+\epsilon}$, where the line parameters s and t are positive, and hence for $x \in [-1,0]$ we should add a small positive imaginary part to x. In this region, Γ_{cusp} has an imaginary part.

3.2 Harmonic polylogarithms and symbols

What are the functions needed to describe Γ_{cusp}? Results at lower loop orders and for related scattering processes suggest that the class of functions we are seeking are the harmonic polylogarithms (HPL) [37]. They are generalizations of ordinary polylogarithms, and appear naturally e.g. within the differential equation technique to evaluate loop integrals, see e.g. [28, 29]. They are also natural from the point of view of the singularity and branch cut structure described in the previous paragraph, with $x = 0, \pm 1$ being special points. They are defined iteratively by

$$H_{a_1,a_2,\ldots,a_n}(x) = \int_0^x f_{a_1}(t) H_{a_2,\ldots,a_n}(t)\, dt\,, \quad \{a_1, a_2, \ldots a_n\} \neq \{0, 0, \ldots 0\}\,, \tag{3.2}$$

where the integration kernels are defined as

$$f_1(x) = (1-x)^{-1}\,, \qquad f_0(x) = x^{-1}\,, \qquad f_{-1}(x) = (1+x)^{-1}\,. \tag{3.3}$$

The degree (or weight) 1 functions needed to start the recursion are defined as

$$H_1(x) = -\log(1-x)\,, \qquad H_0(x) = \log(x)\,, \qquad H_{-1}(x) = \log(1+x)\,. \tag{3.4}$$

There is a special case when all indices are zero, $H_{\underbrace{0,\ldots,0}_{n}}(x) = \frac{1}{n!}\log^n(x)$. The subscript of H is called the weight vector. A common abbreviation is to replace occurrences of m zeros to the left of ± 1 by $\pm(m+1)$. For example, $H_{0,0,1,0,-1}(x) = H_{3,-2}(x)$.

HPLs have simple properties under certain argument transformations, and one can use their algebraic properties to make their asymptotic behavior manifest. We refer the

JHEP09(2013)147

interested reader to ref. [37]. A very useful computer algebraic implementation has been given in refs. [38, 39]. For fast numerical evaluation, especially at complex arguments of the HPLs, we found the C++ implementation in GiNaC [40] very helpful.

As we will describe in the section 5, we compute the planar Γ_{cusp} from a massive scattering amplitude, where at each loop order a certain number of individual integrals appears. It turns out that each of these integrals can be expressed as a linear combination of HPLs of argument x where in general all possible weight vectors appear at a given degree. In the total result, however, we find the simplification that the result can be written in a compact form when using HPLs of argument $1-x^2$, and weight vectors with indices $0, 1$ only! The latter property is also present in the four-loop non-planar correction in the scaling limit, and becomes manifest from the formulas in sections 4 and 5.3.

In the context of the iterated integrals and differential equations studied in section 4, the notion of the symbol of a transcendental function [41–43] is very useful. It can be derived recursively for any function $f_w(x_1, \ldots, x_n)$ of weight w whose total differential assumes the form

$$df_w = \sum_i f_{i,w-1}\, d\log R_i\,, \tag{3.5}$$

where the $f_{i,w-1}$ are of weight $w-1$ and the R_i are algebraic functions. The symbol $\mathcal{S}(f_w)$ is then defined recursively via

$$\mathcal{S}(f_w) = \sum_i \mathcal{S}(f_{i,w-1}) \otimes R_i\,, \tag{3.6}$$

which involves a tensor product over the group of algebraic functions. We emphasize that eqs. (3.5) and (3.6) make the close connection between the 'd-log'-representations (to be discussed in the next section) and the symbol of a function manifest. We also note that symbols of the HPLs discussed above are built from the alphabet $\{x, 1 \pm x\}$. As a specific example, we have

$$\mathcal{S}(H_n(x)) = \mathcal{S}(\text{Li}_n(x)) = -(1-x) \otimes \underbrace{x \otimes \cdots \otimes x}_{n-1 \text{ terms}}\,. \tag{3.7}$$

4 Iterated Wilson line integrals, and non-planar result in scaling limit

Here we discuss a general method for computing Wilson line integrals in position space. We then apply it to the computation of the non-planar cusp anomalous dimension in the scaling limit.

4.1 'd-log' forms for Wilson line integrals

In this section we elaborate on 'd-log' forms for integrals, which were introduced in the context of scattering amplitudes in [13–15]. As an instructive example, let us discuss the diagram shown in Fig 2. The corresponding integral over the line parameters s and t can be written as

$$\int_\Lambda \frac{ds \wedge dt}{s^2 + t^2 + st(x + 1/x)} = \frac{x}{1-x^2} \int_\Lambda d\log(s + tx) \wedge d\log(t + sx)\,, \tag{4.1}$$

JHEP09(2013)147

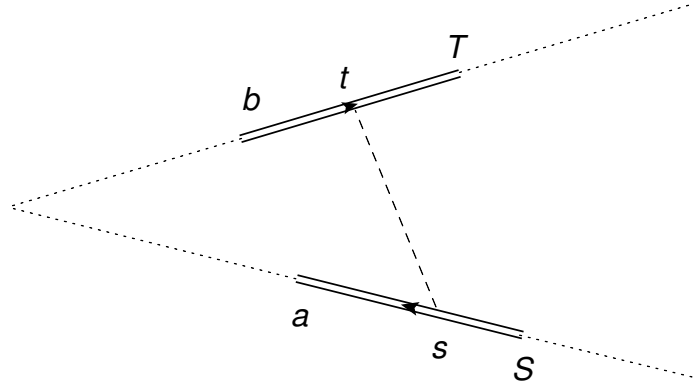

Figure 2. Propagator-type integral discussed in the main text.

where on the r.h.s. we have dropped differentials involving dx because they do not contribute to the integral, and where the integration region Λ is $s \in [a, S]$ and $t \in [b, T]$.

What is gained from writing the integral in this way? We see that a natural normalization factor, $x/(1-x^2)$, has been pulled out of the integral. Together with trivial prefactors originating from the Feynman rules, this constitutes the normalization of the diagram. The remaining integral will give a (generalized) polylogarithmic function, which, in the present example, has degree 2. It depends on the variables a, b, S, T and x,

$$f(a, b, S, T, x) = \int_\Lambda d\log(s + tx) \wedge d\log(t + sx)\,. \tag{4.2}$$

Integrals of this type satisfy simple differential equations, as we explain below. Let us first focus on one of the two integration variables, say s, and rewrite the integral in a more convenient form thanks to the identity [44]

$$d\log(s+\alpha) \wedge d\log(s+\beta) = d\log\frac{s+\alpha}{s+\beta} \wedge d\log(\alpha-\beta)\,. \tag{4.3}$$

A simple generalization of this identity holds for n-forms. Then, we perform one integration at a time, in this case starting with the one over s. The main point is that one will always have an integral of the form

$$G(\alpha, \beta_i) := \int_{\Lambda_y} d\log(y+\alpha) F(y, \beta_i)\,, \tag{4.4}$$

where y is the integration variable, and α and β_i are parameters, and F is some function. Then the algorithm outlined in appendix A of ref. [44] can be used to determine the differential of G. It can be expressed in terms of quantities appearing in the differential of F. In our example, a short calculation gives

$$\begin{aligned} d\,f(a,b,S,T,x) = {} & d\log b\,\log\frac{(b+ax)(S+bx)}{(a+bx)(b+Sx)} + d\log a\,\log\frac{(T+ax)(a+bx)}{(b+ax)(a+Tx)} \\ & + d\log S\,\log\frac{(b+Sx)(S+Tx)}{(S+bx)(T+Sx)} + d\log T\,\log\frac{(T+Sx)(a+Tx)}{(S+Tx)(T+ax)} \\ & + d\log x\,\log\frac{(T+ax)(S+bx)(b+Sx)(a+Tx)}{(b+ax)(a+bx)(T+Sx)(S+Tx)}\,. \end{aligned} \tag{4.5}$$

JHEP09(2013)147

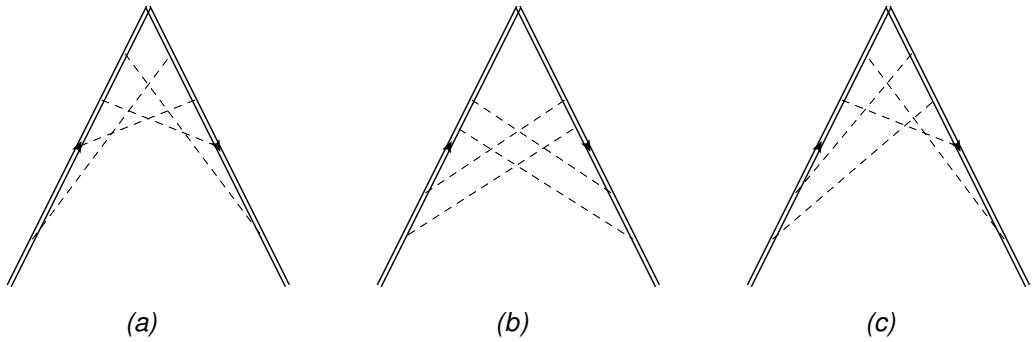

Figure 3. All diagrams contributing to the quartic Casimir terms at four loops, in the scaling limit.

This equation determines f up to an integration constant. The latter can be determined, for example, from the boundary condition that f vanishes at $a = S$. Note that it is trivial to read off the symbol of f from eq. (4.5).

In the present example, one can also directly integrate eq. (4.5). The answer obtained can be written in terms of dilogarithms,

$$f(a,b,S,T,x) = \mathrm{Li}_2\left(-\frac{T}{S}x\right) - \mathrm{Li}_2\left(-\frac{T}{S}\frac{1}{x}\right) - \mathrm{Li}_2\left(-\frac{T}{a}x\right) + \mathrm{Li}_2\left(-\frac{T}{a}\frac{1}{x}\right) \\ - \mathrm{Li}_2\left(-\frac{b}{S}x\right) + \mathrm{Li}_2\left(-\frac{b}{S}\frac{1}{x}\right) + \mathrm{Li}_2\left(-\frac{b}{a}x\right) - \mathrm{Li}_2\left(-\frac{b}{a}\frac{1}{x}\right) . \tag{4.6}$$

This agrees with ref. [45].

In summary, we see that one can always compute the symbol of integrals that are of the type (4.1), and for generalizations with more propagators, and polylogarithmic functions inserted into the integrand. In particular, any ladder integral appearing in Γ_{cusp} can be computed in this way. Preliminary results suggest that the generalization to graphs with interaction vertices is possible. For example, in ref. [23], for two classes of diagrams the internal integration associated to the interaction vertex could be computed analytically, with the remaining integral of the form (4.4).

We used this method to compute the non-planar ladder integrals appearing in Γ_{cusp} to four loops. In the next subsection, we discuss which integrals are required, and in the following subsection the results are reported.

4.2 Non-planar contribution to scaling limit

Here we compute the integrals contributing to w_{4b} of eq. (2.10) in the scaling limit. Thanks to the scaling limit, we only need to keep ladder diagrams with four rungs between the two Wilson line segments. Moreover, only diagrams containing the color factor $d_F^{abcd} d_A^{abcd}/N_F$ are required.[2]

[2]Recall that the color dependence of a general four-loop diagram can be expressed in terms of C_F, C_A, and $d_F^{abcd} d_A^{abcd}/N_F$. With our choice of color-basis in section 2, all terms with powers of C_F higher than one cancel in $\log\langle W\rangle$, as per eq. (2.10).

JHEP09(2013)147

It is easy to see that the only ladder type diagrams containing the quartic Casimir operator are the ones shown in figure 3. Denoting their color factors by $\mathcal{C}_i$ and the integral functions by $\mathcal{I}_i$, with $i = a, b, c$ we have

$$\log\langle W\rangle_{g^8} \sim \mathcal{C}_a\,\mathcal{I}_a + \mathcal{C}_b\,\mathcal{I}_b + 2\,\mathcal{C}_c\,\mathcal{I}_c + \dots\,, \tag{4.7}$$

where the dots represent other diagrams with color factors involving only C_F and C_A, and the 2 is a combinatorial factor, due to the fact that figure 3(c) also appears with the two Wilson lines interchanged. The color factors of these diagrams contain a trace over eight generators, e.g. $\mathrm{Tr}(T^aT^bT^cT^dT^aT^bT^cT^d)$ in figure 3(a), and similarly for the other two diagrams. Using the Lie commutator (2.1) one sees that the color factors of the three diagrams in figure 3 are related. One finds

$$\mathcal{C}_a = \mathrm{Tr}(T^aT^bT^cT^dT^aT^bT^cT^d)/N_F\,, \tag{4.8}$$

$$\mathcal{C}_c = \mathcal{C}_a + \frac{1}{2}C_FC_A(C_F - C_A/2)(C_F - C_A)\,, \tag{4.9}$$

$$\mathcal{C}_b = \mathcal{C}_a + \frac{1}{2}C_FC_A(C_F - C_A/2)(2C_F - 3/2C_A)\,, \tag{4.10}$$

where we normalize again all color factors by $\mathrm{Tr}[1_F] = N_F$. From (4.8) – (4.10) we conclude that the three diagrams contribute equally to the color factor $d_F^{abcd}d_A^{abcd}/N_F$, see eq. (2.8). Taking this into account, we find that in the scaling limit the term proportional to $d_F^{abcd}d_A^{abcd}/N_F$ is given by

$$w_{4b} \sim \mathcal{I}_a + \mathcal{I}_b + 2\,\mathcal{I}_c\,. \tag{4.11}$$

Let us discuss the definition of the integrals. They are line integrals of the type considered in section 4.1. Here a comment on the regularization of the Wilson loop operator is due. Naively, it has both infrared as well as ultraviolet divergences. We are interested in the ultraviolet divergences. Γ_{cusp} is defined as the coefficient of the ultraviolet divergence. Since $\log\langle W\rangle$ only has an overall divergence, it is easy to see how different regularization procedures are related. The position space calculations above can be formulated e.g. in cut-off regularization for both IR and UV divergences. Another possibility is to treat the integrals as in heavy-quark effective theory (HQET), with dimensional regularization.

In both cases, one can make the logarithmic divergence transparent by changing variables. Let us denote the line parameters on the two lines by s_i and t_i, with $i = 1, \dots 4$, respectively. After rescaling all variables $s_i = \rho\tilde{s}_i, t_i = \rho\tilde{t}_i$, with $\sum_{i=1}^4(\tilde{s}_i + \tilde{t}_i) = 1$, the ρ integral contains the divergence. When working with cutoffs, this integral takes the form

$$\int_{\Lambda_{\mathrm{UV}}}^{\Lambda_{\mathrm{IR}}} \frac{d\rho}{\rho} = \log\frac{\Lambda_{\mathrm{IR}}}{\Lambda_{\mathrm{UV}}}\,. \tag{4.12}$$

On the other hand, in HQET with dimensional regularization, one obtains

$$\int_0^\infty \frac{d\rho}{\rho^{1-L\epsilon}}e^{-\rho} = \frac{1}{L\epsilon} + \mathcal{O}(\epsilon^0)\,. \tag{4.13}$$

JHEP09(2013)147

In both cases, the coefficient of the ρ integral is the contribution to the cusp anomalous dimension that we wish to compute, and it is given by convergent integrals.

For concreteness, let us choose the cutoff version of the calculation. In that case, taking into account the discussion above and writing the integrals in d-log form as in section 4.1, we have

$$\mathcal{I}_i = \log \frac{\Lambda_{\rm IR}}{\Lambda_{\rm UV}} \left(\frac{x}{1-x^2}\right)^4 \tilde{\mathcal{I}}_i \,, \quad i = a, b, c \,. \tag{4.14}$$

Next, we can use the algorithm of section 4.1 to derive iterative differential equations for $\tilde{\mathcal{I}}_i$. From these equations, we can immediately determine the symbol of these functions as a corollary. We find that they are given by symbols composed from the alphabet $x, 1-x^2$. This implies that they can be expressed in terms of a subset of the HPLs discussed in section 3, namely those with indices drawn from $0, 1$, if we choose x^2 or $1-x^2$ as argument of the HPLs.

In order to determine the full functions from the differential equations, we have to complement them by boundary conditions. The kinematical point $x = 1$, or equivalently $\phi = 0$, is a good boundary condition, where the Feynman integrals are expected to be regular. However, the prefactor $(x/(1-x^2))^4$ in (4.14) diverges in this limit, and hence the functions $\tilde{I}_i$ must have corresponding zeros. We find it likely that a careful investigation of the iterative differential equations would reveal that this boundary condition fixes all undetermined constants. We found that simply using the condition of regularity of eq. (4.14) at $x = 1$ determined most coefficients, and we computed the remaining ones by considering asymptotic limits $x \to 0$, which we evaluated using standard Mellin-Barnes techniques. For more details on such methods, see section 5. In this way, we found

$$\begin{aligned}
\tilde{\mathcal{I}}_a = &- 6\pi^2 H_{1,1,1,2} + 48 H_{1,1,1,4} - 8\pi^2 H_{1,1,2,1} + 64 H_{1,1,2,3} + 64 H_{1,1,3,2} \\
&- 6\pi^2 H_{1,2,1,1} + 48 H_{1,2,1,3} + 48 H_{1,2,2,2} - 10\pi^2 H_{1,1,1,1,1} + 80 H_{1,1,1,1,3} \\
&+ 80 H_{1,1,1,2,2} + 24 H_{1,1,1,3,1} + 64 H_{1,1,2,1,2} + 32 H_{1,1,2,2,1} + 32 H_{1,1,3,1,1} \\
&+ 48 H_{1,2,1,1,2} + 24 H_{1,2,1,2,1} + 24 H_{1,2,2,1,1} + 62 H_{1,1,1,1,1,2} + 40 H_{1,1,1,1,2,1} \\
&+ 22 H_{1,1,1,2,1,1} + 8 H_{1,1,2,1,1,1} + 6 H_{1,2,1,1,1,1} + H_{1,1,1,1,1,1,1} \,,
\end{aligned} \tag{4.15}$$

$$\begin{aligned}
\tilde{\mathcal{I}}_b = &- 4\pi^2 H_{1,1,1,2} - \frac{16}{3}\pi^2 H_{1,1,2,1} + 16 H_{1,1,2,3} + 32 H_{1,1,3,2} - 4\pi^2 H_{1,2,1,1} \\
&+ 16 H_{1,2,1,3} + 16 H_{1,2,2,2} - \frac{20}{3}\pi^2 H_{1,1,1,1,1} + 16 H_{1,1,1,1,3} + 24 H_{1,1,1,2,2} \\
&+ 24 H_{1,1,2,1,2} + 8 H_{1,1,2,2,1} + 16 H_{1,1,3,1,1} + 16 H_{1,2,1,1,2} + 8 H_{1,2,1,2,1} \\
&+ 8 H_{1,2,2,1,1} + 40 H_{1,1,1,1,1,2} + 24 H_{1,1,1,1,2,1} - 8 H_{1,1,2,1,1,1} - 8 H_{1,2,1,1,1,1} \\
&+ 4 H_{1,1,1,1,1,1,1} + 48 \zeta_3 H_{1,1,1,1} \,,
\end{aligned} \tag{4.16}$$

JHEP09(2013)147

$$
\begin{aligned}
\tilde{\mathcal{I}}_c = &+ 4\pi^2 H_{1,1,1,2} - 12 H_{1,1,1,4} + \frac{16}{3}\pi^2 H_{1,1,2,1} - 28 H_{1,1,2,3} - 40 H_{1,1,3,2} \\
&+ 4\pi^2 H_{1,2,1,1} - 24 H_{1,2,1,3} - 24 H_{1,2,2,2} + \frac{20}{3}\pi^2 H_{1,1,1,1,1} - 32 H_{1,1,1,1,3} \\
&- 38 H_{1,1,1,2,2} - 6 H_{1,1,1,3,1} - 34 H_{1,1,2,1,2} - 14 H_{1,1,2,2,1} - 20 H_{1,1,3,1,1} \\
&- 24 H_{1,2,1,1,2} - 12 H_{1,2,1,2,1} - 12 H_{1,2,2,1,1} - 38 H_{1,1,1,1,1,2} - 22 H_{1,1,1,1,2,1} \\
&- 4 H_{1,1,1,2,1,1} + 2 H_{1,1,2,1,1,1} + 2 H_{1,2,1,1,1,1} + 2 H_{1,1,1,1,1,1,1} - 24\zeta_3 H_{1,1,1,1}\,. \qquad (4.17)
\end{aligned}
$$

Here we use the abbreviation $H_w = H_w(1-x^2)$. Recalling eqs. (4.14) and (4.11), this determines w_{4b} in the scaling limit.

We performed several consistency checks. First, using this algorithm, we reproduced the analytical result for the three-loop crossed ladder diagram computed in [12]. Moreover, we performed numerical checks on the above results using the explicit line integral representation of the integrals. Starting from the rescaled variables $\tilde{s}_i$ and $\tilde{t}_i$ above, we set

$$
\tilde{s}_1 = x_1 x_2 x_3 z\,, \qquad \tilde{s}_2 = x_1 x_2 z\,, \qquad \tilde{s}_3 = x_1 z\,, \qquad \tilde{s}_4 = z\,, \qquad (4.18)
$$

$$
\tilde{t}_1 = y_1 y_2 y_3 \bar{z}\,, \qquad \tilde{t}_2 = y_1 y_2 \bar{z}\,, \qquad \tilde{t}_3 = y_1 \bar{z}\,, \qquad \tilde{t}_4 = \bar{z}\,, \qquad (4.19)
$$

where $\bar{z} := 1 - z$, and with Jacobian $z^3 \bar{z}^3 x_1^2 x_2 y_1^2 y_2$. Then we have, e.g.

$$
\begin{aligned}
\tilde{I}_a = &\frac{(1-x^2)^4}{x^4} \int_0^1 dz \prod_{i=1}^{3} (dx_i dy_i)\, z^3 \bar{z}^3 x_1^2 x_2 y_1^2 y_2 \times \\
&\times P(\tilde{s}_1, \tilde{t}_4; x) P(\tilde{s}_2, \tilde{t}_3; x) P(\tilde{s}_3, \tilde{t}_2; x) P(\tilde{s}_4, \tilde{t}_1; x)\,, \qquad (4.20)
\end{aligned}
$$

where $P(s,t;x) := 1/(s^2 + t^2 + st(x + 1/x))$. We used this formula (and corresponding ones for $\tilde{I}_b$ and $\tilde{I}_c$) to check (4.15) – (4.17) numerically at the sub-per mille level for several values of x. Analytic checks can be done e.g. by switching to a Mellin-Barnes representation.

5 Planar calculation from massive scattering amplitude

It was shown in ref. [46] that the Regge limit $s/m^2 \gg 1$ of the planar Coulomb branch amplitude $M(s/m^2, t/m^2)$ is governed by the cusp anomalous dimension. This connection was used in [12] to compute the three-loop value of Γ_{cusp}.

The advantage of this approach is that an expression for the integrand of $M(s/m^2, t/m^2)$ is already known. It is in the form of a small number of scalar integrals, each of which results from many Feynman diagrams. This simple integrand was obtained by using generalized unitarity, in conjunction with (extended) dual conformal symmetry [47, 48]. It has been pointed out that the limit relating the amplitude and Γ_{cusp} also works at the level of the integrand [23]. This implies that one can obtain an efficient integral representation for Γ_{cusp} in this way.

Here we wish to extend the work of [12] to four loops and determine the planar part of Γ_{cusp} from the four-loop scattering amplitude. As a starting point, convenient Mellin-Barnes representations for the eight contributing integrals are available from [48]. The

JHEP09(2013)147

strategy of our calculation is the following: First, we use generalized cuts to determine the power of ξ to which each scattering amplitude integral contributes. Details of this procedure can be found in appendix A. Next, based on experience from lower loop orders and the structure observed for the ladder diagrams [23], we make an ansatz subject to certain assumptions, which we will specify below. This reduces the calculation to the determination of a certain number of undetermined coefficients. In order to determine the latter, we analyze both the Mellin-Barnes representations and the ansatz in various limits, such as $x \to 0$ and $x \to 1$. In this way, we obtain (more than) enough algebraic equations to determine all coefficients. Moreover, this provides consistency checks for the ansatz.

5.1 Assumptions and classification of HPLs

An analysis of the cuts of the integrals contributing to the scattering amplitude suggests that the four-loop result for $\theta = 0$, where we have $\xi = (1-x)/(1+x)$, has the structure

$$\Gamma_{\text{cusp}}|_{\lambda^4/(8\pi^2)^4} = \sum_{r=1}^{4} \left(\frac{1-x}{1+x}\right)^r \Gamma^{(4;r)}(x) + \mathcal{O}(1/N^2)\,, \tag{5.1}$$

where the $\Gamma^{(4;r)}(x)$ are certain transcendental functions. What can we assume about their structure? Looking at the results up to three loops we may make a number of observations.

- all results for Γ_{cusp} can be written in terms of harmonic polylogarithms
- the degree of transcendentality of the functions involved is uniformly $(2L-1)$, where L is the loop order
- the subset of HPLs with indices $0, 1$ only and argument $1-x^2$ is sufficient to describe the answer. In terms of the symbol, this means that only letters $x, 1-x^2$ are required.

In the case of ladder integrals, the first two items can be proved, and the third item is true at least up to six loops [23]. As we showed in section 4, it is also true in the non-planar case. We find it reasonable to assume that these properties hold true for the full result at four loops.

If this assumption is correct, the calculation is reduced to the determination of the precise linear combination of the allowed functions. Our starting point will be all functions $H_w(1-x^2)$ of weight seven, where the weight vector w is build from entries $0, 1$. We also allow transcendental constants such as $\zeta_i, \zeta_i\zeta_j$, possibly multiplying lower degree functions to construct a term of total degree seven.

We can restrict and classify these functions according to their symmetry properties. In fact, Γ_{cusp} has to be symmetric under the inversion $x \to 1/x$. This follows from the definition $\cos\phi = 1/2(x + 1/x)$. As a result, $\Gamma^{(4;r)}(x)$ has to be odd/even under this symmetry for r odd/even. In this way, we find 51 even and 50 odd functions under this symmetry.

Another simple condition we can impose is that $\Gamma^{(4;r)}(x)$ should have at least r zeros as $x \to 1$. The reason is that it is multiplied by the factor ξ^r, which for $\theta = \pi/2$ has a degree r pole at $x = 1$. But $x = 1$ corresponds to the straight line case, and this should be finite for each integral contributing to Γ_{cusp}. We will also verify this behavior by expanding integrals near $x \to 1$.

JHEP09(2013)147

In order to further restrict the number of functions, we make two additional observations about the results at lower loops $L \leq 3$, eqs. (5.4)–(5.9). Inspecting them one sees that in these cases the number of 0's in the weight vector of the functions $\Gamma^{(L;r)}(x)$ is always smaller than r. We will assume this to hold true also at four loops. Moreover, $\Gamma^{(L;r)}(x)$ vanishes for $L > 1$ at $x = -1$.[3] This is required in order to obtain the correct leading order behavior at $x \to -1$, which corresponds to the quark antiquark potential limit. This limit will be discussed in more detail at the end of this section.

Imposing all these conditions our ansatz becomes, in summary,

- 12 functions for $\Gamma^{(4;2)}(x)$, of degree 7, indices 0, 1, even under $x \to 1/x$, at most one 0 entry in weight vector, and vanishing as $(1-x)^2$ as $x \to 1$ and as $(1+x)^1$ as $x \to -1$.
- 21 functions for $\Gamma^{(4;3)}(x)$, of degree 7, indices 0, 1, odd under $x \to 1/x$, at most two 0 entries in weight vector, and vanishing as $(1-x)^3$ as $x \to 1$ and as $(1+x)^1$ as $x \to -1$.

The terms $\Gamma^{(4;1)}$ and $\Gamma^{(4;4)}$ were already computed in refs. [21] and [23], respectively.

5.2 Asymptotic limit of Mellin-Barnes integrals

Let us now explain how to determine the coefficients of the ansatz. By means of the Mathematica packages `MB.m` [49] and `MBasymptotics.m` [50] we perform the asymptotic expansions of the Mellin-Barnes representations, first about the point $x = 0$. The expansion parameter appears in the form $x^p \log^q(x)$, and each of these terms is accompanied by one or several transcendental constants. For $p > 0$ these constants are in general not of homogeneous weight, but the highest transcendentality is always $7 - q$.[4] We determine these constants analytically for $p = 0, \ldots, 6$ and $q = 3, \ldots, 7$. For $p = 0$ we also include $q = 2$. It is interesting to note that at most two-dimensional Mellin-Barnes integrals are required for this calculation at $q > 2$, and three-dimensional ones at $q = 2$. After we computed all relevant constants in this way, we perform the series expansion of our ansatz to the respective orders in x and $\log(x)$, and solve the resulting algebraic equations for the unknown coefficients appearing in our ansatz. As an illustrating example, take

$$\left[\frac{22}{9} + \frac{2\pi^2}{3}\right] x \log^5(x) \stackrel{!}{=} \left[\left(-\frac{8}{27}\, a_1 + \frac{28}{9}\, a_2\right) + \pi^2 \left(-\frac{1}{6}\, a_1 + \frac{1}{3}\, a_2\right)\right] x \log^5(x)\,, \tag{5.2}$$

where the l.h.s. stems from the solution of the Mellin-Barnes integrals at a particular power in x and $\log(x)$, and the r.h.s. stands for the expansion of the ansatz to the same order. Assuming 1 and π^2 to be linearly independent we obtain two *algebraic* equations, yielding $a_1 = -3$ and $a_2 = 1/2$.

Since some coefficients in our ansatz appear only at powers $q = 1$ or $q = 0$, the above procedure does yield most, but not all coefficients. In order to determine the remaining ones we expand the Mellin-Barnes representations about the point $x = 1$. In this limit the

[3] In this case one has to rewrite $\Gamma^{(L;r)}(x)$ in terms of HPLs of argument x. We will discuss the analytic continuation of Γ_{cusp} in the next section and in appendix B.

[4] Except for $q = 6$, where it is zero.

JHEP09(2013)147

expansion is purely of the form $(x-1)^s$, without any logarithms. We include all terms with $s \leq 4$ and determine the coefficients in the same way as above. However, this time we have to solve Mellin-Barnes integrals that are up to seven-dimensional.

We emphasize that the number of equations this procedure yields is much larger than the number of undetermined coefficients in our ansatz, such that our system of equations is largely overconstrained. As a rule of thumb we have about twice as many equations compared to the number of coefficients. This property is of utmost importance since otherwise potential inconsistencies in our ansatz could not be revealed.

We also do numerical checks, but only after the application of `MBasymptotics.m`, i.e. we check numerically all analogues of the x-independent part of the l.h.s. of eq. (5.2). Performing numerical checks on the unexpanded expressions is not well suited here since by construction the integral and the ansatz agree to high powers in x and $(x-1)$. Hence the ansatz obtained in this way will agree very well numerically with the integral we are computing, even if the ansatz was incomplete.

Last but not least we have the algebraic cross-check that the final answer does only diverge linearly in $\log(x)$ as $x \to 0$, see eq. (5.14). This cross-check is non-trivial since it connects different powers of ξ, each of which diverges with the seventh power of $\log(x)$.

5.3 Planar result to four loops

We are now in the position to present the results for the cusp anomalous dimension up to four loops in the planar limit. We have

$$\Gamma_{\text{cusp}}(x, \theta = 0, \lambda, N) = \sum_{L=1}^{4} \left(\frac{\lambda}{8\pi^2}\right)^L \sum_{r=1}^{L} \left(\frac{1-x}{1+x}\right)^r \Gamma^{(L;r)}(x) + \mathcal{O}(\lambda^5, 1/N^2)\,, \tag{5.3}$$

where

$$\Gamma^{(1;1)} = \frac{1}{2} H_1\,, \tag{5.4}$$

$$\Gamma^{(2;1)} = -\frac{1}{4} H_{1,1,1} - \frac{1}{6}\pi^2 H_1\,, \tag{5.5}$$

$$\Gamma^{(2;2)} = \frac{1}{2} H_{1,2} + \frac{1}{4} H_{1,1,1} \tag{5.6}$$

at one and two loops [11, 51–53],

$$\Gamma^{(3;1)} = \frac{1}{4}\pi^2 H_{1,1,1} + \frac{5}{8} H_{1,1,1,1,1} + \frac{\pi^4}{12} H_1\,, \tag{5.7}$$

$$\begin{aligned}\Gamma^{(3;2)} = &-\frac{3}{2}\zeta_3 H_{1,1} - \frac{1}{6}\pi^2 H_{1,2} - \frac{1}{3}\pi^2 H_{2,1} - \frac{1}{4}\pi^2 H_{1,1,1} - H_{1,1,1,2} - \frac{3}{4} H_{1,2,1,1} \\ &- H_{2,1,1,1} - \frac{11}{8} H_{1,1,1,1,1}\,,\end{aligned} \tag{5.8}$$

$$\Gamma^{(3;3)} = H_{1,1,3} + H_{1,2,2} + H_{1,1,1,2} + \frac{1}{2} H_{1,1,2,1} + \frac{1}{2} H_{1,2,1,1} + \frac{3}{4} H_{1,1,1,1,1} \tag{5.9}$$

JHEP09(2013)147

at three loops [12], and

$$\Gamma^{(4;1)} = -\frac{1}{5}\pi^4 H_{1,1,1} - \pi^2 H_{1,1,1,1,1} - \frac{7}{2}H_{1,1,1,1,1,1,1} - \frac{2}{45}\pi^6 H_1\,, \tag{5.10}$$

$$\begin{aligned}\Gamma^{(4;2)} = {} & \frac{45}{4}\zeta_5 H_{1,1} + \frac{2}{3}\pi^2\zeta_3 H_{1,1} + 5\zeta_3 H_{1,1,1,1} + \frac{1}{12}\pi^4 H_{1,2} + \frac{5}{18}\pi^4 H_{2,1} + \frac{13}{72}\pi^4 H_{1,1,1} \\ & + \pi^2 H_{1,1,1,2} + \pi^2 H_{1,1,2,1} + \frac{3}{4}\pi^2 H_{1,2,1,1} + \frac{5}{3}\pi^2 H_{2,1,1,1} + \frac{53}{24}\pi^2 H_{1,1,1,1,1} \\ & + 5H_{1,1,1,1,1,2} + \frac{7}{2}H_{1,1,1,1,2,1} + \frac{9}{2}H_{1,1,1,2,1,1} + 3H_{1,1,2,1,1,1} + \frac{25}{8}H_{1,2,1,1,1,1} \\ & + \frac{25}{4}H_{2,1,1,1,1,1} + \frac{203}{16}H_{1,1,1,1,1,1,1}\,,\end{aligned} \tag{5.11}$$

$$\begin{aligned}\Gamma^{(4;3)} = {} & -3\zeta_3 H_{1,1,2} - 4\zeta_3 H_{1,2,1} - 3\zeta_3 H_{2,1,1} - 5\zeta_3 H_{1,1,1,1} - \frac{1}{120}\pi^4 H_{1,1,1} - \frac{2}{3}\pi^2 H_{1,1,3} \\ & - \frac{2}{3}\pi^2 H_{1,2,2} - \pi^2 H_{1,3,1} - \pi^2 H_{2,1,2} - \pi^2 H_{2,2,1} - \frac{7}{6}\pi^2 H_{1,1,1,2} - \frac{4}{3}\pi^2 H_{1,1,2,1} \\ & - \frac{5}{6}\pi^2 H_{1,2,1,1} - \pi^2 H_{2,1,1,1} - \frac{29}{24}\pi^2 H_{1,1,1,1,1} - 5H_{1,1,1,1,3} - \frac{7}{2}H_{1,1,1,2,2} \\ & - 3H_{1,1,2,1,2} - 2H_{1,1,2,2,1} - 3H_{1,1,3,1,1} - 5H_{1,2,1,1,2} - 4H_{1,2,1,2,1} - \frac{9}{2}H_{1,2,2,1,1} \\ & - 3H_{1,3,1,1,1} - 5H_{2,1,1,1,2} - 6H_{2,1,1,2,1} - 5H_{2,1,2,1,1} - 3H_{2,2,1,1,1} - \frac{43}{4}H_{1,1,1,1,1,2} \\ & - \frac{17}{2}H_{1,1,1,1,2,1} - 8H_{1,1,1,2,1,1} - 7H_{1,1,2,1,1,1} - \frac{33}{4}H_{1,2,1,1,1,1} - \frac{19}{2}H_{2,1,1,1,1,1} \\ & - \frac{239}{16}H_{1,1,1,1,1,1,1}\,,\end{aligned} \tag{5.12}$$

$$\begin{aligned}\Gamma^{(4;4)} = {} & 3H_{1,1,1,4} + 4H_{1,1,2,3} + 4H_{1,1,3,2} + 3H_{1,2,1,3} + 3H_{1,2,2,2} + 5H_{1,1,1,1,3} + 5H_{1,1,1,2,2} \\ & + \frac{3}{2}H_{1,1,1,3,1} + 4H_{1,1,2,1,2} + 2H_{1,1,2,2,1} + 2H_{1,1,3,1,1} + 3H_{1,2,1,1,2} + \frac{3}{2}H_{1,2,1,2,1} \\ & + \frac{3}{2}H_{1,2,2,1,1} + \frac{23}{4}H_{1,1,1,1,1,2} + 5H_{1,1,1,1,2,1} + 4H_{1,1,1,2,1,1} + 3H_{1,1,2,1,1,1} \\ & + \frac{9}{4}H_{1,2,1,1,1,1} + \frac{23}{4}H_{1,1,1,1,1,1,1}\end{aligned} \tag{5.13}$$

at four loops. As mentioned above, the terms $\Gamma^{(4;1)}$ and $\Gamma^{(4;4)}$ were already computed in refs. [21] and [23], respectively. The remaining terms $\Gamma^{(4;2)}$ and $\Gamma^{(4;3)}$ are new. We derived them analytically, subject to the assumptions discussed in the previous section.

In the above equations $H_w := H_w(1-x^2)$, and $x = e^{i\phi}$. The perturbative results given in this section and in section 4 can be straightforwardly evaluated numerically in the region II, i.e. $0 < x < 1$. Other regions can be reached by analytical continuation, respecting the branch cut properties discussed in section 3. We collect the relevant formulas in appendix B.

A curious feature of the result up to four loops, already remarked upon in [23], is that once the result is written in terms of HPLs with argument $1 - x^2$ as above, all HPLs in $(-1)^{(r+L)}\Gamma^{(L;r)}$ come with non-negative coefficients.

In figures 4 and 5 we plot the cusp anomalous dimension in Regions II and I, respectively. From the plots one can see the properties discussed below and in section 3.

We now consider various limits of Γ_{cusp}. First, we can use the above results to analytically compute the light-like cusp anomalous dimension. It is obtained by taking the limit

JHEP09(2013)147

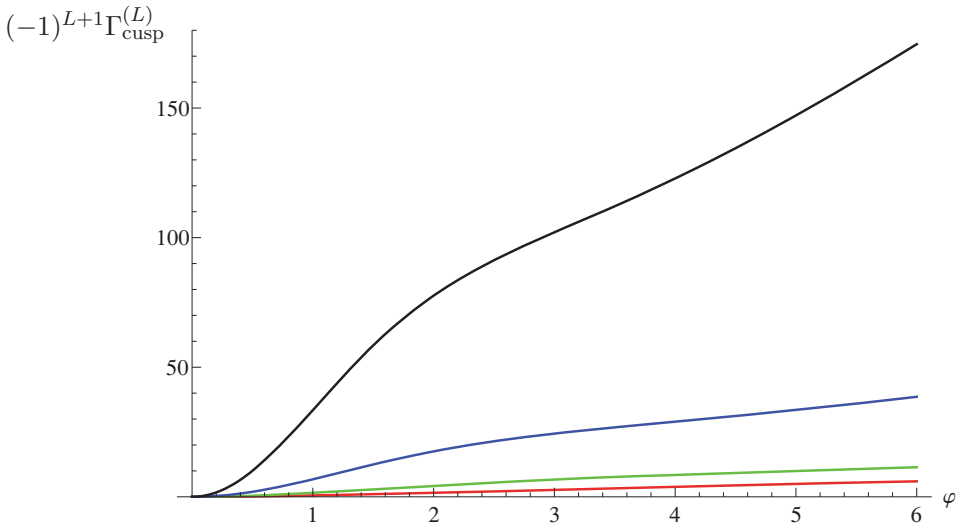

Figure 4. Plot of $(-1)^{L+1}\Gamma^{(L)}_{\text{cusp}}$ as a function of $\varphi = -\log(x)$ with $x \in [0,1]$, i.e. Region II. From bottom to top the plot shows $L = 1,2,3,4$. The small and large φ behavior is known to all loop orders: For small φ the first term is quadratic, with the coefficient given by the Bremsstrahlung function. At large φ, Γ_{cusp} grows linearly, with the coefficient determined by the light-like cusp anomalous dimension.

$x \to 0$, where Γ_{cusp} diverges logarithmically,

$$\lim_{x\to 0} \Gamma_{\text{cusp}} = -\frac{1}{2}\log(x)\,\Gamma^{\infty} + \mathcal{G}_0 + \mathcal{O}(x)\,. \tag{5.14}$$

We find

$$\Gamma^{\infty} = 2\left(\frac{\lambda}{8\pi^2}\right) - \frac{\pi^2}{3}\left(\frac{\lambda}{8\pi^2}\right)^2 + \frac{11\pi^4}{90}\left(\frac{\lambda}{8\pi^2}\right)^3 + \left(-2\zeta_3^2 - \frac{73\pi^6}{1260}\right)\left(\frac{\lambda}{8\pi^2}\right)^4 + \mathcal{O}(\lambda^5)\,. \tag{5.15}$$

This agrees with previous numerical results at four loops [47, 48, 54, 55], and with the spin chain prediction from ref. [56]. The behaviour (5.14) can also be seen from figure 4, where the curves grow linearly for large values of $\varphi = -\log(x)$. For $\mathcal{G}_0$ we find

$$\begin{aligned}\mathcal{G}_0 = &-\zeta_3\left(\frac{\lambda}{8\pi^2}\right)^2 + \left(\frac{9\zeta_5}{2} - \frac{\pi^2\zeta_3}{6}\right)\left(\frac{\lambda}{8\pi^2}\right)^3 + \left(\frac{\pi^4\zeta_3}{10} + \frac{11\pi^2\zeta_5}{12} - \frac{85\zeta_7}{4}\right)\left(\frac{\lambda}{8\pi^2}\right)^4 \\ &+ \mathcal{O}(\lambda^5, \lambda^4/N^2)\end{aligned} \tag{5.16}$$

$\mathcal{G}_0$ is related to the collinear anomalous dimension for mass-regulated scattering amplitudes [46]. Unlike Γ^{∞}, this quantity depends on the regularization scheme and takes a different value in dimensional regularization [57].

Next we consider $\phi \to 0$, corresponding to $x = e^{i\phi} \to 1$, where we find

$$\Gamma_{\text{cusp}} = \phi^2\left[-\frac{1}{2}\left(\frac{\lambda}{8\pi^2}\right) + \frac{\pi^2}{6}\left(\frac{\lambda}{8\pi^2}\right)^2 - \frac{\pi^4}{12}\left(\frac{\lambda}{8\pi^2}\right)^3 + \frac{2\pi^6}{45}\left(\frac{\lambda}{8\pi^2}\right)^4\right] + \mathcal{O}(\phi^3)\,. \tag{5.17}$$

JHEP09(2013)147

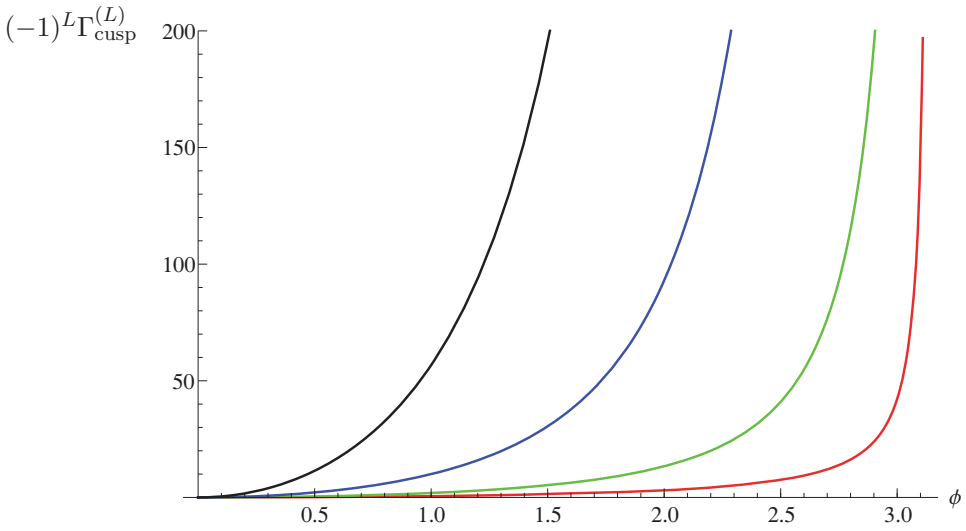

Figure 5. The functions $(-1)^L\Gamma^{(L)}_{\rm cusp}$ in the interval $\phi \in [0,\pi]$, i.e. Region I. From bottom to top the plot shows $L = 1, 2, 3, 4$.

This behaviour can be seen from figures 4 and 5, where all curves start quadratically from the respective origin. The expansion in (5.17) is in perfect agreement with the four-loop expansion of the exact result in [21, 30].

The third limit to consider is $x \to -1$, which we parameterize by $x = e^{i\phi}$, $\phi = \pi - \delta$, and $\delta \to 0$. We find

$$\xi\,\Gamma^{(1;1)} = -\frac{2\pi}{\delta} + \mathcal{O}(\delta^0)\,, \tag{5.18}$$

$$\xi\,\Gamma^{(2;1)} = \mathcal{O}(\delta^0)\,, \tag{5.19}$$

$$\xi^2\,\Gamma^{(2;2)} = -\frac{8\pi}{\delta}\,L_\delta + \mathcal{O}(\delta^0)\,, \tag{5.20}$$

$$\xi\,\Gamma^{(3;1)} = \mathcal{O}(\delta^0)\,, \tag{5.21}$$

$$\xi^2\,\Gamma^{(3;2)} = -\frac{\pi}{\delta}\left[\frac{16\pi^2}{3}\,L_\delta + 36\zeta_3 + \frac{16\pi^2}{3}\right] + \mathcal{O}(\delta^0)\,, \tag{5.22}$$

$$\xi^3\,\Gamma^{(3;3)} = -\frac{8\pi^4}{3\delta^2} - \frac{\pi}{\delta}\left[16\,L_\delta^2 + 16\,L_\delta - 4\pi^2 - 24\right] + \mathcal{O}(\delta^0)\,, \tag{5.23}$$

$$\xi\,\Gamma^{(4;1)} = \mathcal{O}(\delta^0)\,, \tag{5.24}$$

$$\xi^2\,\Gamma^{(4;2)} = -\frac{\pi}{\delta}\left[32\pi^2\zeta_3 - 190\zeta_5\right] + \mathcal{O}(\delta^0)\,, \tag{5.25}$$

$$\xi^3\,\Gamma^{(4;3)} = -\frac{16\pi^6}{9\delta^2} - \frac{\pi}{\delta}\left[\frac{64\pi^2}{3}\,L_\delta^2 + \left(96\zeta_3 + \frac{272\pi^2}{3}\right)L_\delta - \frac{8\pi^4}{3} + 48\zeta_3 - \frac{208\pi^2}{3}\right] + \mathcal{O}(\delta^0)\,, \tag{5.26}$$

JHEP09(2013)147

$$\xi^4\,\Gamma^{(4;4)} = 32\zeta_3\,\frac{\pi^3}{\delta^3} - \frac{\pi^2}{\delta^2}\left[\frac{64\pi^2}{3}\,L_\delta^2 + 64\zeta_3 + \frac{16\pi^2}{3}\right] - \frac{\pi}{\delta}\left[\frac{64}{3}\,L_\delta^3 + 64\,L_\delta^2 + \left(-\frac{112\pi^2}{3} - 32\right)L_\delta + \frac{32}{3}\,\pi^2\zeta_3 + 96\zeta_3 + \frac{16\pi^2}{9} - \frac{512}{3}\right] + \mathcal{O}(\delta^0)\,, \tag{5.27}$$

with $L_\delta = \ln(2\delta/e)$. Figure 5 shows the divergences as $\phi \to \pi$.

The limit $x \to -1$ is related to the quark antiquark potential. This limit is subtle. Due to ultrasoft effects, a resummation is required. This is done by matching fixed order calculations against an effective field theory calculation. In the context of $\mathcal{N} = 4$ SYM, this was discussed in ref. [32], and more recently in [33].

We close this section with two remarks. First, note that for $\theta = 0$, we have $\xi = (1-x)/(1+x)$. It is natural to expect that the full θ dependence can be obtained by replacing $((1-x)/(1+x))^r$ in eq. (5.3) by ξ^r, see section 1.

Our second remark concerns the regularization scheme dependence. The above method assumed a supersymmetric regularization scheme, and therefore we expect our result for Γ_{cusp} to be valid in that scheme. The transition to other schemes, such as $\overline{\text{MS}}$, is discussed in ref. [58], and has been explicitly worked out there to two loops.

6 Comparison to strong coupling via AdS/CFT

Can we compare the fixed order perturbative results of section 5.3 to the results available at strong coupling via the AdS/CFT correspondence? The authors of ref. [59] proposed such a procedure in the case of the light-like cusp anomalous dimension. They combined perturbative data with the string theory insight that the strong coupling expansion takes the form

$$\Gamma_{\text{cusp}} = c\sqrt{\lambda} + \dots\,, \tag{6.1}$$

where c is negative, and we work in the planar limit. In order to incorporate this behavior they proposed the following ansatz $f(\lambda)$ for Γ_{cusp}

$$\lambda^n = \sum_{r=n}^{2n} C_r\,[f(\lambda)]^r\,, \tag{6.2}$$

where n is connected to the loop order L via $n = L-1$. The constants C_r can be fixed using perturbative information. Of course, one can also use strong coupling data, as in [47], in order to gain insights on weak coupling. Here we will use the perturbative two-, three-, and four-loop results for Γ_{cusp} in order to determine the coefficient of $\sqrt{\lambda}$ at strong coupling.

Let us give more details about this ansatz in the simplest case, i.e. $n = 1$. Here the extrapolation is based on the two-loop perturbative information, i.e.

$$\Gamma_{\text{cusp}} = v_1\lambda + v_2\lambda^2 + \mathcal{O}(\lambda^3)\,. \tag{6.3}$$

Then one can determine the coefficients in eq. (6.2) to be $C_1 = 1/v_1, C_2 = -v_2/v_1^3$. The latter equation then implies that the ansatz for the interpolation function is

$$f(\lambda) = -\frac{v_1^2}{2v_2}\left[-1 + \sqrt{1 - 4\lambda\frac{v_2}{v_1}}\right]\,. \tag{6.4}$$

JHEP09(2013)147

which at strong coupling gives $-\sqrt{\lambda}\sqrt{-\frac{v_1^3}{v_2}}+\ldots$. This procedure can be generalized to higher loops, where eq. (6.2) implies that one has to solve equations of higher degree, which can be done numerically.

We then compare this extrapolation to results obtained via the AdS/CFT correspondence. At strong coupling, i.e. $\lambda \gg 1$, Wilson loops are described by minimal surfaces [19]. We have the expansion (6.1), and focus on the case $\theta = 0$. The result for c for region I, i.e. real angles, is available through implicit equations involving Elliptic integrals from [60]. In the case of region II, we can use the formulas of [61]. The first subleading coefficient in the expansion (6.1) is also known [62]. Let us discuss the results of the comparison for the two regions in turn.

Extrapolation for region I: we used the ansatz of eq. (6.2) in order to extrapolate the strong-coupling coefficient c in eq. (6.1) from the knowledge of the four-loop data. We found that the extrapolations based on our four loop results and the $\sqrt{\lambda}$ behavior give a leading order strong coupling answer that agrees to within 2 per cent for the range of $\phi \in [0.1, 2.5]$. However, for $\phi > 2.5$ the relative error grows significantly. This is not surprising since there one approaches the quark-antiquark limit $\phi \to \pi$.

Extrapolation for region II: here we find very good agreement between the extrapolation based on the four-loop perturbative data, and the strong coupling answer. It is interesting to note that the relative error to the strong coupling value goes down from approximately 25%, 3% and under 1.6%, when using two-loop, three-loop and four-loop data as input, respectively. It is also remarkable that this relative error stays small for all data points analyzed in the interval $x \in [0, 1]$, despite the fact that the leading coefficient (in front of $\sqrt{\lambda}$) at strong coupling varies by several orders of magnitude.

Let us comment on the radius of convergence of the expansions. It is known for the $x \to 1$ and $x \to 0$ limits, respectively. The former is described by the Bremsstrahlung function [21], whose perturbative series has a radius of convergence of $\lambda_c \approx 14.7$. The latter is governed by the light-like cusp anomalous dimension, where the radius of convergence [56] is $\lambda_c = \pi^2$.

7 Conclusion and outlook

We computed the velocity-dependent cusp anomalous dimension in maximally supersymmetric Yang-Mills theory to four-loop order. The result can be expressed in terms of harmonic polylogarithms of degree seven, with argument $1 - x^2$ and non-negative indices only. We determine the non-planar correction at four loops in the scaling limit, which involves quartic Casimir invariants as color factors. The method of 'd-log'-representations for iterated Wilson line integrals turns out to be extremely powerful for this purpose. It allows one to compute the symbol of such functions. If the symbols correspond to a known class of functions, HPLs in our case, one can integrate back using boundary conditions.

Moreover, we determine the full planar four-loop result from massive scattering amplitudes, where we use asymptotic expansions of Mellin-Barnes integrals to analytically pin down the coefficients of a well-motivated ansatz. Our analytical result gives the correct

JHEP09(2013)147

values of the four-loop light-like cusp anomalous dimension that was previously calculated only numerically [47, 48, 54, 55].

We also compare our perturbative result to strong coupling, and find that our extrapolation agrees to better than two per cent with the corresponding string theory result, over a wide range of parameters.

Taken together, the only pieces missing to obtain the full — planar and non-planar — result of the velocity-dependent cusp anomalous dimension to four loops are the non-planar terms proportional to ξ^2 and ξ^3. The light-like limit of the non-planar cusp anomalous dimension is also envisaged in [63] by means of the on-shell form factor. However, we emphasize that the present approach allows to obtain the full x-dependence, and not just the light-like limit.

The results we have derived here shed light on the structure of the planar four-particle amplitude on the Coulomb branch of $\mathcal{N} = 4$ super Yang-Mills. The latter is an infrared finite function $M(s/m^2, t/m^2)$. Kinematically it is very similar to light-by-light scattering via massive particles. It is an interesting open question what class of two-variable functions describe such processes beyond the one-loop order. The integrals we have computed determine the asymptotic limit of this amplitude as $s/m^2 \gg 1$.

There are several generalizations to the 'd-log'-approach discussed in section 4. The first generalization concerns the Wilson loop contour. While we have focused on a contour formed by two segments in this paper, it is clear that the technique applies equally to contours formed by n segments meeting in a point. This is relevant for the description of infrared divergences of massive scattering amplitudes at the non-planar level, see e.g. [4, 64, 65]. We also wish to emphasize that massless results can be obtained as a corollary.

Another obvious generalization of the applicability of this technique has to do with the regularization. On physical grounds, at least in principle, one can always choose combinations of diagrams that only have a superficial UV divergence. For such quantities, one can easily switch between regulators. Our method is very naturally formulated in a cut-off scheme, however it is equally possible to use dimensional regularization. This is straightforward for integrals that only have a superficial UV divergence. For other integrals, one first has to identify the integration regions that lead to divergences and perform subtractions.

Finally, whereas we focussed in the present paper on scalar and gluon exchanges, preliminary results suggest that the generalization to graphs with interaction vertices is possible [23].

Acknowledgments

It is a pleasure to thank Dirk Seidel and Simon Caron-Huot for very useful correspondence. We thank R. Britto, L. Dixon, E. Gardi, G. Korchemsky, L. Magnea, J. Maldacena, M. Neubert, D. Simmons-Duffins, and A. Sever for useful discussions. J.M.H. is grateful to the ECT* Trento for hospitality during part of this work, and wishes to thank the organizers of "Periods and Motives", Paris 2012, where part of this work was presented, for their invitation. J.M.H. was supported in part by the Department of Energy grant DE-FG02-90ER40542, and the IAS AMIAS fund. The work of T.H. was partially supported by the Helmholtz Alliance "Physics at the Terascale".

JHEP09(2013)147

A Four-loop integrals and generalized cuts / leading singularities

The velocity-dependent cusp anomalous dimension $\Gamma_{\text{cusp}}(\phi)$ can be obtained from the Regge limit of massive amplitudes in $\mathcal{N}=4$ super Yang-Mills [46, 48]. At the four-loop level, there are eight contributing diagrams, which are depicted in figure 1 of [48]. The corresponding amplitude is given by eq. (2.8) of that reference. In the Regge limit $s \to \infty$ the logarithm of the amplitude is given by[5]

$$\log \mathcal{M} \stackrel{s\to\infty}{\longrightarrow} \log(-m^2/s)\,\Gamma_{\text{cusp}}(-m^2/t)\,, \tag{A.1}$$

where t is related to x via $-m^2/t = x/(1-x)^2$.

We now study the systematics of the Regge limit at the four-loop level [48] by considering the integrals contributing to the four-loop amplitude. We expect them to have the general structure

$$I = I_0 \times \tilde{I}\,, \tag{A.2}$$

where I_0 is an algebraic normalization factor, and $\tilde{I}$ is a function having degree of transcendentality eight. In the literature, such functions are sometimes referred to as pure functions.

Generalized cuts or leading singularities are useful in order to test whether (A.2) holds, and to determine the normalization factor I_0.

For example, for the massive box integral at one loop, normalized by st, we have

$$I_0 \sim 1/\sqrt{1-4m^2/s-4m^2/t}\,. \tag{A.3}$$

Notice that in the Regge limit, this factor becomes proportional to ξ.

Likewise, we computed the maximal cuts of all integrals up to four loops. The result is consistent with eq. (A.2), and we find the following behavior of the prefactors as $s \to \infty$ (the superscript "r" means that the integral is rotated, i.e. $s \leftrightarrow t$)

$$\begin{aligned}
I_{4a} &\sim \xi, & I^r_{4a} &\sim \xi^4\\
I_{4b} &\sim \xi^2, & I^r_{4b} &\sim \xi\\
I_{4c} &\sim \xi, & I^r_{4c} &\sim \xi^3\\
I_{4d} &\sim \xi, & I^r_{4d} &\sim \xi^3\\
I_{4e} &\sim \xi, & I^r_{4e} &\sim \xi^2\\
I_{4f} &\sim \xi, & I^r_{4f} &\sim \xi^2\\
I_{4d2} &\sim \xi, & I^r_{4d2} &\sim \xi^2\\
I_{4f2} &\sim \xi^2, & I^r_{4f2} &\sim \xi^2\,.
\end{aligned} \tag{A.4}$$

Notice that due to exponentiation, the maximal power of Regge logarithms that a given integral has is bounded by the power of ξ. Comparing to appendix A of [48], we find that this is in agreement with the above ξ dependence.

We see that we can classify the contribution of the integrals to Γ_{cusp} according to which power of ξ that they are normalized by. This is a very useful feature, as it allows to compute the contributions to different powers of ξ independently.

[5] Note that refs. [46, 48] use different metric conventions.

JHEP09(2013)147

B Analytic continuation of Γ_{cusp}

In order to analytically continue Γ_{cusp} to regions I and III it is sufficient to apply the argument transformation $1-x^2 \to x^2$ to the HPLs in section 5.3 and subsequently extract the logarithms explicitly. This gives

$$\Gamma^{(1;1)} = -\log(x)\,, \tag{B.1}$$

$$\Gamma^{(2;1)} = +\frac{1}{3}\log^3(x) + \frac{\pi^2}{3}\log(x)\,, \tag{B.2}$$

$$\Gamma^{(2;2)} = -\frac{1}{3}\log^3(x) - \frac{\pi^2}{6}\log(x) - \log(x)\,H_2(x^2) + H_3(x^2) - \zeta_3 \tag{B.3}$$

at one and two loops,

$$\Gamma^{(3;1)} = -\frac{1}{6}\log^5(x) - \frac{\pi^2}{3}\log^3(x) - \frac{\pi^4}{6}\log(x)\,, \tag{B.4}$$

$$\begin{aligned}\Gamma^{(3;2)} = &-6H_5(x^2) + \frac{2}{3}\log^4(x)H_1(x^2) - \frac{1}{3}\log^3(x)H_2(x^2) + \frac{2\pi^2}{3}\log^2(x)H_1(x^2)\\ &-\log^2(x)H_3(x^2) - \frac{\pi^2}{3}\log(x)H_2(x^2) + \frac{9}{2}\log(x)H_4(x^2) + \zeta_3\log^2(x)\\ &+\frac{11}{30}\log^5(x) + \frac{5\pi^2}{9}\log^3(x) + \frac{5\pi^4}{36}\log(x) + 6\zeta_5\,,\end{aligned} \tag{B.5}$$

$$\begin{aligned}\Gamma^{(3;3)} = &-2\zeta_3 H_2(x^2) + \frac{\pi^2}{6}H_3(x^2) + 3H_5(x^2) + 2H_{2,3}(x^2) + 3H_{3,2}(x^2) + 3H_{4,1}(x^2)\\ &-\frac{2}{3}\log^3(x)H_2(x^2) + \log^2(x)H_3(x^2) - \frac{\pi^2}{3}\log(x)H_2(x^2) - 2\log(x)H_4(x^2)\\ &-2\log(x)H_{2,2}(x^2) - 2\log(x)H_{3,1}(x^2) - \zeta_3\log^2(x) - \frac{1}{5}\log^5(x) - \frac{2\pi^2}{9}\log^3(x)\\ &-\frac{\pi^4}{30}\log(x) - \frac{3}{2}\zeta_5 - \frac{\pi^2}{6}\zeta_3\end{aligned} \tag{B.6}$$

at three loops, and

$$\Gamma^{(4;1)} = +\frac{4}{45}\log^7(x) + \frac{4\pi^2}{15}\log^5(x) + \frac{4\pi^4}{15}\log^3(x) + \frac{4\pi^6}{45}\log(x)\,, \tag{B.7}$$

$$\begin{aligned}\Gamma^{(4;2)} = &-\frac{29}{90}\log^7(x) - \frac{5}{9}H_1(x^2)\log^6(x) + \frac{5}{6}H_2(x^2)\log^5(x) - \frac{73}{90}\pi^2\log^5(x)\\ &-\frac{10}{9}\pi^2 H_1(x^2)\log^4(x) - 2H_3(x^2)\log^4(x) - \zeta_3\log^4(x) + \frac{11}{9}\pi^2 H_2(x^2)\log^3(x)\\ &+\frac{11}{6}H_4(x^2)\log^3(x) - \frac{161}{270}\pi^4\log^3(x) - \frac{5}{9}\pi^4 H_1(x^2)\log^2(x) - \frac{7}{3}\pi^2 H_3(x^2)\log^2(x)\\ &+\frac{11}{2}H_5(x^2)\log^2(x) - \frac{11}{2}\zeta_5\log^2(x) - \frac{2}{3}\pi^2\zeta_3\log^2(x) + \frac{7}{18}\pi^4 H_2(x^2)\log(x)\\ &+\frac{17}{6}\pi^2 H_4(x^2)\log(x) - \frac{95}{4}H_6(x^2)\log(x) - \frac{353\pi^6}{3780}\log(x) - \frac{1}{9}\pi^4 H_3(x^2)\\ &-\frac{2}{3}\pi^2 H_5(x^2) + 35H_7(x^2) - 35\zeta_7 + \frac{2\pi^2\zeta_5}{3} + \frac{\pi^4\zeta_3}{9}\,,\end{aligned} \tag{B.8}$$

JHEP09(2013)147

$$
\begin{aligned}
\Gamma^{(4;3)} = &+ \frac{239}{630}\log^7(x) + \frac{38}{45}H_1(x^2)\log^6(x) - \frac{1}{3}H_2(x^2)\log^5(x) + \frac{4}{5}\pi^2\log^5(x) \\
&+ \frac{11}{9}\pi^2 H_1(x^2)\log^4(x) + 2H_{1,2}(x^2)\log^4(x) + 2H_{2,1}(x^2)\log^4(x) + 2\zeta_3\log^4(x) \\
&- \frac{2}{9}\pi^2 H_2(x^2)\log^3(x) + 3H_4(x^2)\log^3(x) - \frac{4}{3}H_{1,3}(x^2)\log^3(x) - 2H_{2,2}(x^2)\log^3(x) \\
&- 4H_{3,1}(x^2)\log^3(x) + \frac{4}{3}H_1(x^2)\zeta_3\log^3(x) + \frac{47}{108}\pi^4\log^3(x) + \frac{17}{45}\pi^4 H_1(x^2)\log^2(x) \\
&+ \frac{2}{3}\pi^2 H_3(x^2)\log^2(x) - 10H_5(x^2)\log^2(x) + 2\pi^2 H_{1,2}(x^2)\log^2(x) + 9H_4(x^2)\zeta_3 \\
&+ 2\pi^2 H_{2,1}(x^2)\log^2(x) - 2H_{2,3}(x^2)\log^2(x) - 2H_{3,2}(x^2)\log^2(x) + 8\zeta_5\log^2(x) \\
&+ 2H_2(x^2)\zeta_3\log^2(x) + \frac{4}{3}\pi^2\zeta_3\log^2(x) + \frac{1}{90}\pi^4 H_2(x^2)\log(x) - \frac{7}{6}\pi^2 H_4(x^2)\log(x) \\
&+ 20H_6(x^2)\log(x) - 2\pi^2 H_{1,3}(x^2)\log(x) - 2H_{1,5}(x^2)\log(x) - \frac{8}{3}\pi^2 H_{2,2}(x^2)\log(x) \\
&+ 7H_{2,4}(x^2)\log(x) - \frac{8}{3}\pi^2 H_{3,1}(x^2)\log(x) + 10H_{3,3}(x^2)\log(x) + 16H_{4,2}(x^2)\log(x) \\
&+ 22H_{5,1}(x^2)\log(x) + 2H_1(x^2)\zeta_5\log(x) + 2\zeta_3^2\log(x) + 2\pi^2 H_1(x^2)\zeta_3\log(x) \\
&- 4H_3(x^2)\zeta_3\log(x) + \frac{38}{945}\pi^6\log(x) - \frac{1}{45}\pi^4 H_3(x^2) - 32H_7(x^2) + \frac{2}{3}\pi^2 H_{2,3}(x^2) \\
&- 10H_{2,5}(x^2) + \pi^2 H_{3,2}(x^2) - 13H_{3,4}(x^2) + \pi^2 H_{4,1}(x^2) - 18H_{4,3}(x^2) - 28H_{5,2}(x^2) \\
&- 40H_{6,1}(x^2) + 16\zeta_7 + 10H_2(x^2)\zeta_5 + \frac{\pi^2}{2}\zeta_5 - \frac{2}{3}\pi^2 H_2(x^2)\zeta_3 + \frac{\pi^4\zeta_3}{45}\,, \qquad \text{(B.9)} \\
\Gamma^{(4;4)} = &- \frac{46}{315}\log^7(x) - \frac{3}{5}H_2(x^2)\log^5(x) - \frac{23}{90}\pi^2\log^5(x) + H_3(x^2)\log^4(x) - \zeta_3\log^4(x) \\
&- \frac{2}{3}\pi^2 H_2(x^2)\log^3(x) - \frac{7}{3}H_4(x^2)\log^3(x) - 2H_{2,2}(x^2)\log^3(x) - \frac{8}{3}H_{3,1}(x^2)\log^3(x) \\
&- \frac{19}{180}\pi^4\log^3(x) + \frac{2}{3}\pi^2 H_3(x^2)\log^2(x) + 4H_5(x^2)\log^2(x) + 3H_{2,3}(x^2)\log^2(x) \\
&+ 6H_{3,2}(x^2)\log^2(x) + 9H_{4,1}(x^2)\log^2(x) - \frac{5}{2}\zeta_5\log^2(x) - 3H_2(x^2)\zeta_3\log^2(x) \\
&- \frac{2}{3}\pi^2\zeta_3\log^2(x) - \frac{1}{10}\pi^4 H_2(x^2)\log(x) - \frac{2}{3}\pi^2 H_4(x^2)\log(x) - 4H_6(x^2)\log(x) \\
&- \pi^2 H_{2,2}(x^2)\log(x) - 6H_{2,4}(x^2)\log(x) - \frac{4}{3}\pi^2 H_{3,1}(x^2)\log(x) - 10H_{3,3}(x^2)\log(x) \\
&- 16H_{4,2}(x^2)\log(x) - 22H_{5,1}(x^2)\log(x) - 6H_{2,2,2}(x^2)\log(x) - 6H_{2,3,1}(x^2)\log(x) \\
&- 8H_{3,1,2}(x^2)\log(x) - 8H_{3,2,1}(x^2)\log(x) - 6H_{4,1,1}(x^2)\log(x) - \zeta_3^2\log(x) \\
&+ 2H_3(x^2)\zeta_3\log(x) - \frac{17\pi^6}{2520}\log(x) + \frac{1}{30}\pi^4 H_3(x^2) + \frac{1}{2}\pi^2 H_5(x^2) + 8H_7(x^2) \\
&+ \frac{1}{2}\pi^2 H_{2,3}(x^2) + 9H_{2,5}(x^2) + \pi^2 H_{3,2}(x^2) + 14H_{3,4}(x^2) + \frac{3}{2}\pi^2 H_{4,1}(x^2) \\
&+ 19H_{4,3}(x^2) + 25H_{5,2}(x^2) + 30H_{6,1}(x^2) + 6H_{2,2,3}(x^2) + 9H_{2,3,2}(x^2) + 9H_{2,4,1}(x^2)
\end{aligned}
$$

JHEP09(2013)147

$$
\begin{aligned}
&+ 8H_{3,1,3}(x^2) + 14H_{3,2,2}(x^2) + 14H_{3,3,1}(x^2) + 15H_{4,1,2}(x^2) + 15H_{4,2,1}(x^2) \\
&+ 12H_{5,1,1}(x^2) - \frac{9\zeta_7}{4} - \frac{9}{2}H_2(x^2)\zeta_5 - \frac{\pi^2\zeta_5}{4} - \frac{1}{2}\pi^2 H_2(x^2)\zeta_3 - 4H_4(x^2)\zeta_3 \\
&- 6H_{2,2}(x^2)\zeta_3 - 8H_{3,1}(x^2)\zeta_3 - \frac{\pi^4}{30}\zeta_3
\end{aligned} \tag{B.10}
$$

at four loops. In region III, i.e. $x \in [-1, 0]$, the logarithms are the only source of imaginary parts. Together with the $i0$-prescription from section 3 the imaginary part can therefore be extracted explicitly in this region.

References

[1] A.M. Polyakov, *Gauge fields as rings of glue*, *Nucl. Phys.* **B 164** (1980) 171 [INSPIRE].

[2] R.A. Brandt, F. Neri and M.-a. Sato, *Renormalization of loop functions for all loops*, *Phys. Rev.* **D 24** (1981) 879 [INSPIRE].

[3] G. Korchemsky and A. Radyushkin, *Loop space formalism and renormalization group for the infrared asymptotics of QCD*, *Phys. Lett.* **B 171** (1986) 459 [INSPIRE].

[4] A. Ferroglia, M. Neubert, B.D. Pecjak and L.L. Yang, *Two-loop divergences of massive scattering amplitudes in non-abelian gauge theories*, *JHEP* **11** (2009) 062 [arXiv:0908.3676] [INSPIRE].

[5] E. Gardi and L. Magnea, *Factorization constraints for soft anomalous dimensions in QCD scattering amplitudes*, *JHEP* **03** (2009) 079 [arXiv:0901.1091] [INSPIRE].

[6] L.J. Dixon, *Matter dependence of the three-loop soft anomalous dimension matrix*, *Phys. Rev.* **D 79** (2009) 091501 [arXiv:0901.3414] [INSPIRE].

[7] T. Becher and M. Neubert, *On the structure of infrared singularities of gauge-theory amplitudes*, *JHEP* **06** (2009) 081 [arXiv:0903.1126] [INSPIRE].

[8] L.J. Dixon, E. Gardi and L. Magnea, *On soft singularities at three loops and beyond*, *JHEP* **02** (2010) 081 [arXiv:0910.3653] [INSPIRE].

[9] V. Ahrens, M. Neubert and L. Vernazza, *Structure of infrared singularities of gauge-theory amplitudes at three and four loops*, *JHEP* **09** (2012) 138 [arXiv:1208.4847] [INSPIRE].

[10] T. Becher and M. Neubert, *Infrared singularities of QCD amplitudes with massive partons*, *Phys. Rev.* **D 79** (2009) 125004 [*Erratum ibid.* **D 80** (2009) 109901] [arXiv:0904.1021] [INSPIRE].

[11] G. Korchemsky and A. Radyushkin, *Renormalization of the Wilson loops beyond the leading order*, *Nucl. Phys.* **B 283** (1987) 342 [INSPIRE].

[12] D. Correa, J. Henn, J. Maldacena and A. Sever, *The cusp anomalous dimension at three loops and beyond*, *JHEP* **05** (2012) 098 [arXiv:1203.1019] [INSPIRE].

[13] S. Caron-Huot, *Loops in spacetime*, talk given at *Scattering amplitudes: from QCD to maximally supersymmetric Yang-Mills theory and back*, July 16–20, Trento, Italy (2012).

[14] N. Arkani-Hamed et al., *Scattering amplitudes and the positive grassmannian*, arXiv:1212.5605 [INSPIRE].

[15] A.E. Lipstein and L. Mason, *From the holomorphic Wilson loop to 'd log' loop-integrands for super-Yang-Mills amplitudes*, *JHEP* **05** (2013) 106 [arXiv:1212.6228] [INSPIRE].

JHEP09(2013)147

[16] J.M. Henn, *Multiloop integrals in dimensional regularization made simple*, *Phys. Rev. Lett.* **110** (2013) 251601 [arXiv:1304.1806] [INSPIRE].

[17] D. Correa, J. Maldacena and A. Sever, *The quark anti-quark potential and the cusp anomalous dimension from a TBA equation*, *JHEP* **08** (2012) 134 [arXiv:1203.1913] [INSPIRE].

[18] N. Drukker, *Integrable Wilson loops*, arXiv:1203.1617 [INSPIRE].

[19] J.M. Maldacena, *Wilson loops in large-N field theories*, *Phys. Rev. Lett.* **80** (1998) 4859 [hep-th/9803002] [INSPIRE].

[20] S.-J. Rey and J.-T. Yee, *Macroscopic strings as heavy quarks in large-N gauge theory and Anti-de Sitter supergravity*, *Eur. Phys. J.* **C 22** (2001) 379 [hep-th/9803001] [INSPIRE].

[21] D. Correa, J. Henn, J. Maldacena and A. Sever, *An exact formula for the radiation of a moving quark in $N = 4$ super Yang-Mills*, *JHEP* **06** (2012) 048 [arXiv:1202.4455] [INSPIRE].

[22] D. Bykov and K. Zarembo, *Ladders for Wilson loops beyond leading order*, *JHEP* **09** (2012) 057 [arXiv:1206.7117] [INSPIRE].

[23] J.M. Henn and T. Huber, *Systematics of the cusp anomalous dimension*, *JHEP* **11** (2012) 058 [arXiv:1207.2161] [INSPIRE].

[24] J. Gatheral, *Exponentiation of eikonal cross-sections in nonabelian gauge theories*, *Phys. Lett.* **B 133** (1983) 90 [INSPIRE].

[25] J. Frenkel and J. Taylor, *Nonabelian eikonal exponentiation*, *Nucl. Phys.* **B 246** (1984) 231 [INSPIRE].

[26] T. van Ritbergen, A. Schellekens and J. Vermaseren, *Group theory factors for Feynman diagrams*, *Int. J. Mod. Phys.* **A 14** (1999) 41 [hep-ph/9802376] [INSPIRE].

[27] T. van Ritbergen, J. Vermaseren and S. Larin, *The four loop β-function in quantum chromodynamics*, *Phys. Lett.* **B 400** (1997) 379 [hep-ph/9701390] [INSPIRE].

[28] M. Czakon, J. Gluza and T. Riemann, *Master integrals for massive two-loop bhabha scattering in QED*, *Phys. Rev.* **D 71** (2005) 073009 [hep-ph/0412164] [INSPIRE].

[29] C. Anastasiou, S. Beerli, S. Bucherer, A. Daleo and Z. Kunszt, *Two-loop amplitudes and master integrals for the production of a Higgs boson via a massive quark and a scalar-quark loop*, *JHEP* **01** (2007) 082 [hep-ph/0611236] [INSPIRE].

[30] B. Fiol, B. Garolera and A. Lewkowycz, *Exact results for static and radiative fields of a quark in $N = 4$ super Yang-Mills*, *JHEP* **05** (2012) 093 [arXiv:1202.5292] [INSPIRE].

[31] J. Erickson, G. Semenoff, R. Szabo and K. Zarembo, *Static potential in $N = 4$ supersymmetric Yang-Mills theory*, *Phys. Rev.* **D 61** (2000) 105006 [hep-th/9911088] [INSPIRE].

[32] A. Pineda, *The static potential in $N = 4$ supersymmetric Yang-Mills at weak coupling*, *Phys. Rev.* **D 77** (2008) 021701 [arXiv:0709.2876] [INSPIRE].

[33] M. Stahlhofen, *NLL resummation for the static potential in $N = 4$ SYM theory*, *JHEP* **11** (2012) 155 [arXiv:1209.2122] [INSPIRE].

[34] G. Korchemsky, *Asymptotics of the Altarelli-Parisi-Lipatov evolution kernels of parton distributions*, *Mod. Phys. Lett.* **A 4** (1989) 1257 [INSPIRE].

JHEP09(2013)147

[35] G. Korchemsky and G. Marchesini, *Structure function for large x and renormalization of Wilson loop*, *Nucl. Phys.* **B 406** (1993) 225 [hep-ph/9210281] [INSPIRE].

[36] L.F. Alday and J.M. Maldacena, *Comments on operators with large spin*, *JHEP* **11** (2007) 019 [arXiv:0708.0672] [INSPIRE].

[37] E. Remiddi and J. Vermaseren, *Harmonic polylogarithms*, *Int. J. Mod. Phys.* **A 15** (2000) 725 [hep-ph/9905237] [INSPIRE].

[38] D. Maître, *HPL, a Mathematica implementation of the harmonic polylogarithms*, *Comput. Phys. Commun.* **174** (2006) 222 [hep-ph/0507152] [INSPIRE].

[39] D. Maître, *Extension of HPL to complex arguments*, *Comput. Phys. Commun.* **183** (2012) 846 [hep-ph/0703052] [INSPIRE].

[40] C.W. Bauer, A. Frink and R. Kreckel, *Introduction to the GiNaC framework for symbolic computation within the C++ programming language*, *J. Symb. Comput.* **33** (2002) 1 [cs/0004015].

[41] F.C. Brown, *Multiple zeta values and periods of moduli spaces $M_{0,n}$*, *Annales Sci. Ecole Norm. Sup.* **42** (2009) 371 [math/0606419] [INSPIRE].

[42] G. A.B., *A simple construction of Grassmannian polylogarithms*, arXiv:0908.2238 [INSPIRE].

[43] A.B. Goncharov, M. Spradlin, C. Vergu and A. Volovich, *Classical polylogarithms for amplitudes and Wilson loops*, *Phys. Rev. Lett.* **105** (2010) 151605 [arXiv:1006.5703] [INSPIRE].

[44] S. Caron-Huot and S. He, *Jumpstarting the all-loop S-matrix of planar $N = 4$ super Yang-Mills*, *JHEP* **07** (2012) 174 [arXiv:1112.1060] [INSPIRE].

[45] Y. Makeenko, *Topics in cusped/lightcone Wilson loops*, *Acta Phys. Polon.* **B 39** (2008) 3047 [arXiv:0810.2183] [INSPIRE].

[46] J.M. Henn, S.G. Naculich, H.J. Schnitzer and M. Spradlin, *Higgs-regularized three-loop four-gluon amplitude in $N = 4$ SYM: exponentiation and Regge limits*, *JHEP* **04** (2010) 038 [arXiv:1001.1358] [INSPIRE].

[47] Z. Bern, M. Czakon, L.J. Dixon, D.A. Kosower and V.A. Smirnov, *The four-loop planar amplitude and cusp anomalous dimension in maximally supersymmetric Yang-Mills theory*, *Phys. Rev.* **D 75** (2007) 085010 [hep-th/0610248] [INSPIRE].

[48] J.M. Henn, S.G. Naculich, H.J. Schnitzer and M. Spradlin, *More loops and legs in Higgs-regulated $N = 4$ SYM amplitudes*, *JHEP* **08** (2010) 002 [arXiv:1004.5381] [INSPIRE].

[49] M. Czakon, *Automatized analytic continuation of Mellin-Barnes integrals*, *Comput. Phys. Commun.* **175** (2006) 559 [hep-ph/0511200] [INSPIRE].

[50] M. Czakon, http://mbtools.hepforge.org/.

[51] Y. Makeenko, P. Olesen and G.W. Semenoff, *Cusped SYM Wilson loop at two loops and beyond*, *Nucl. Phys.* **B 748** (2006) 170 [hep-th/0602100] [INSPIRE].

[52] N. Kidonakis, *Two-loop soft anomalous dimensions and NNLL resummation for heavy quark production*, *Phys. Rev. Lett.* **102** (2009) 232003 [arXiv:0903.2561] [INSPIRE].

[53] N. Drukker and V. Forini, *Generalized quark-antiquark potential at weak and strong coupling*, *JHEP* **06** (2011) 131 [arXiv:1105.5144] [INSPIRE].

JHEP09(2013)147

[54] Z. Bern, L.J. Dixon and V.A. Smirnov, *Iteration of planar amplitudes in maximally supersymmetric Yang-Mills theory at three loops and beyond*, *Phys. Rev.* **D 72** (2005) 085001 [hep-th/0505205] [INSPIRE].

[55] F. Cachazo, M. Spradlin and A. Volovich, *Four-loop cusp anomalous dimension from obstructions*, *Phys. Rev.* **D 75** (2007) 105011 [hep-th/0612309] [INSPIRE].

[56] N. Beisert, B. Eden and M. Staudacher, *Transcendentality and crossing*, *J. Stat. Mech.* **0701** (2007) P01021 [hep-th/0610251] [INSPIRE].

[57] F. Cachazo, M. Spradlin and A. Volovich, *Four-loop collinear anomalous dimension in $N = 4$ Yang-Mills theory*, *Phys. Rev.* **D 76** (2007) 106004 [arXiv:0707.1903] [INSPIRE].

[58] A.V. Belitsky, A. Gorsky and G. Korchemsky, *Gauge/string duality for QCD conformal operators*, *Nucl. Phys.* **B 667** (2003) 3 [hep-th/0304028] [INSPIRE].

[59] A. Kotikov, L. Lipatov and V. Velizhanin, *Anomalous dimensions of Wilson operators in $N = 4$ SYM theory*, *Phys. Lett.* **B 557** (2003) 114 [hep-ph/0301021] [INSPIRE].

[60] N. Drukker, D.J. Gross and H. Ooguri, *Wilson loops and minimal surfaces*, *Phys. Rev.* **D 60** (1999) 125006 [hep-th/9904191] [INSPIRE].

[61] M. Kruczenski, *A note on twist two operators in $N = 4$ SYM and Wilson loops in Minkowski signature*, *JHEP* **12** (2002) 024 [hep-th/0210115] [INSPIRE].

[62] V. Forini, *Quark-antiquark potential in AdS at one loop*, *JHEP* **11** (2010) 079 [arXiv:1009.3939] [INSPIRE].

[63] R.H. Boels, B.A. Kniehl, O.V. Tarasov and G. Yang, *Color-kinematic duality for form factors*, *JHEP* **02** (2013) 063 [arXiv:1211.7028] [INSPIRE].

[64] A. Mitov, G.F. Sterman and I. Sung, *The massive soft anomalous dimension matrix at two loops*, *Phys. Rev.* **D 79** (2009) 094015 [arXiv:0903.3241] [INSPIRE].

[65] Y.-T. Chien, M.D. Schwartz, D. Simmons-Duffin and I.W. Stewart, *Jet physics from static charges in AdS*, *Phys. Rev.* **D 85** (2012) 045010 [arXiv:1109.6010] [INSPIRE].

JHEP09(2013)147

Acknowledgments

In theoretical high energy physics it has become standard practice to pursue and publish scientific projects in small groups. It is therefore my extraordinary pleasure to thank the collaborators of the publications accumulated in the present habilitation thesis. The collaborations and scientific discussions were most enjoyable, and broadened as well as deepened my understanding of theoretical physics in general and of high energy physics in particular.

No lesser thank goes to the staff members of the TP1 institute here at Siegen University, notably Thomas Mannel, Thorsten Feldmann, Wolfgang Kilian, Alexander Khodjamirian, Guido Bell, and Björn O. Lange. Without their continuous support in scientific, organisational, administrative and private matters, the completion of the present thesis would not have been possible.

I would also like to thank Siegen University, the Helmholtz Alliance "Physics at the Terascale", and Deutsche Forschungsgemeinschaft (DFG) for financial support. The DFG-funded members Javier Virto and Susanne Kränkl constitute an essential part of my group and collaborating with them is most enjoyable and rewarding.

A special thank goes to Sven Faller and the TP1 computer admins for support in computer and other technical issues.

Last but not least I would like to thank my family for their never-ending love and care. My wife Cornelia has supported me and my professional career with unprecedented dedication, although she and our children Jana, Philipp, and Aaron had to spare me many times.